GEOLOGICAL SURVEY RESEARCH 1980

GEOLOGICAL SURVEY PROFESSIONAL PAPER 1175

A summary of recent significant scientific and economic results accompanied by a list of geologic, hydrologic, and cartographic investigations in progress

UNITED STATES GOVERNMENT PRINTING OFFICE, WASHINGTON, D.C.: 1980

UNITED STATES DEPARTMENT OF THE INTERIOR

JAMES G. WATT, *Secretary*

GEOLOGICAL SURVEY

Doyle G. Frederick, *Acting Director*

Library of Congress catalog-card No. 68-46150

For sale by the Superintendent of Documents, U.S. Government Printing Office
Washington, D.C. 20402

CONTENTS

	Page
Abbreviations	VII
SI units and inch-pound system equivalents	VIII
Mineral-resource investigations	1
United States and world mineral-resources assessments	1
Mineral-resource assessments of land areas	1
Geologic studies of mineral districts and mineral-bearing regions	6
Geochemical and geophysical techniques in resource assessments	13
Geochemical reconnaissance results	13
Geochemical processes	15
Hydrogeochemical prospecting	15
Remote sensing applied to geochemical exploration	16
Volatile gases useful in geochemical exploration	16
Sample media useful in geochemical exploration	16
Analytical methodology useful in geochemical exploration	17
Analysis of linear features	17
Methodology in exploration geophysics	18
Resource information systems and analysis	19
Resource information systems	19
Resource analysis	20
Chemical resources	22
Phosphorite	22
Lithium	22
Mineral-fuel investigations	24
Coal analysis	24
Global studies	24
Eastern coal	25
Stratigraphy	25
Resources and quality	25
Western and Alaskan coals	26
Geochemistry	28
Laboratory and field analytical techniques	30
Oil and gas resources	31
National Petroleum Reserve in Alaska	31
Offshore Alaska	32
Rocky Mountains and Great Plains	33
Great Basin and California	37
Gulf of Mexico and Florida	37
Appalachian Basin	38
Other areas	40
New exploration and production techniques	40
Nuclear-fuel resources	41
Geothermal resources	59
Regional geologic investigations	61
New England	61
Igneous rocks and geochemistry	61
Tectonics and stratigraphy	61
Glacier geology	63
Appalachian Highlands and the Coastal Plains	66
Carolinas, Tennessee	66

	Page
Regional geologic investigations—Continued	
Appalachian Highlands and the Coastal Plains—Continued	
Delmarva Peninsula	67
New Jersey	67
Pennsylvania	67
South Carolina, Georgia, and Alabama	68
Southeast Coastal Plain	70
Virginia	71
Central region	74
Tectonics and stratigraphy	74
Mineral resources	76
Rocky Mountains and the Great Plains	76
Economic geology	76
Environmental geology	76
Stratigraphy	77
Igneous rocks	79
Precambrian rocks	81
Tectonics	82
Basin and Range region	87
Mineral-resource studies	87
Stratigraphic and structural studies	87
Igneous rocks	91
Geochronologic studies	91
Pacific coast region	92
Oregon	92
Western United States	92
Washington	92
California	96
Alaska	101
Statewide	102
Northern	104
West-central	106
East-central	106
Southern	109
Southwestern	111
Southeastern	111
Geologic maps	114
Water-resource investigations	115
Northeastern region	116
Connecticut	117
Delaware	117
Illinois	117
Indiana	118
Maryland	119
Michigan	119
Minnesota	120
New Jersey	122
New York	122
Ohio	124
Pennsylvania	124
Rhode Island	124

	Page
Water-resource investigations—Continued	
Northeastern region—Continued	
Virginia	124
Wisconsin	125
Southeastern region	126
Alabama	126
Florida	127
Georgia	130
Kentucky	131
Mississippi	132
North Carolina	132
South Carolina	132
Tennessee	132
Central region	133
Kansas	135
Louisiana	135
Montana	136
Montana	136
New Mexico	137
North Dakota	137
Oklahoma	138
South Dakota	139
Texas	139
Utah	140
Wyoming	141
Western region	142
Arizona	142
California	143
Idaho	144
Nevada	144
Oregon	145
Washington	146
Special water-resource programs	146
Data coordination, acquisition, and storage	146
Office of Water Data Coordination	146
National Water Data Exchange	147
Water data storage system	148
Urban water programs	148
Water use	150
Regional Aquifer-System Analysis Program	150
Marine geology and coastal hydrology	152
Coastal and marine geology	152
Continental margin hazards and geologic environment of the seafloor	152
Continental margin geologic framework and resource studies	159
Deep sea geology and resources	163
Coastal and limnological studies	164
Estuarine and coastal hydrology	167
Atlantic and gulf coast	167
Pacific coast	170
Management of natural resources on Federal and Indian lands	175
Classification and evaluation of mineral lands	175
Classified land	175
Known Geologic Structures of producing oil and gas fields	175
Known Geothermal Resource Areas	176
Known Recoverable Coal Resource Areas	176
Coal Resource Occurrence/Coal Development Potential reports	176
Known leasing areas for potassium, phosphate, and sodium	176
Waterpower classification—preservation of resource sites	176

	Page
Management of natural resources on Federal and Indian lands—Continued	
Management of mineral leases on Federal and Indian lands	177
Management of oil and gas leases on the Outer Continental Shelf	178
Cooperation with other Federal agencies	179
Geologic and hydologic principles, processes, and techniques	180
Geophysics	180
Rock magnetism	180
Geomagnetism	181
Petrophysics	183
Applied geophysics	186
Geochemistry, mineralogy, and petrology	189
Experimental and theoretical geochemistry	189
Mineralogic studies in crystal chemistry	191
Volcanic rocks and processes	192
Hawaiian volcano studies	192
Icelandic studies	195
Columbia River Plateau studies	196
Evolution of silicic magma chambers	196
Cascade volcanism	198
Volcanic rocks in Eastern United States	198
Plutonic rocks and magnetic processes	199
Metamorphic rocks and processes	201
Geochemistry of water and sediments	201
Statistical geochemistry and petrology	203
Isotope and nuclear chemistry	203
Isotope tracer studies	203
Stable isotopes	205
Advances in geochronometry	205
Geothermal systems	208
Sedimentology	217
Variability of sediment yields	217
Stream morphology	217
Sediment transport	218
Instrumentation	219
Glaciology	219
Climate	219
Ground-water hydrology	224
Aquifer-model studies	225
Miscellaneous studies	225
Recharge studies	226
Surface-water hydrology	227
Paleontology	229
Mesozoic and Cenozoic studies	229
Paleozoic studies	232
Plant ecology	233
Chemical, physical, and biological properties of water	234
Chemical and biological quality of surface water	234
Chemical and biological quality of ground water	235
Surface-water-quality models and processes	237
Ground-water-quality models and processes	238
Areawide chemical loading	238
Relation between surface water and ground water	238
Evaporation and transpiration	239
Limnology and potamology	240
New hydrologic instruments and techniques	242
Sea-ice studies	242

Page

Geologic and hydrologic principles, processes, and techniques—Continued
Analytical methods 244
Analytical chemistry 244
Optical spectroscopy 244
X-ray spectroscopy 244
Radiochemistry 244
Trace elements in planetary materials by activation analysis 245
Analysis of water 245
Geology and hydrology applied to hazard assessment and environment 247
Earthquake studies 247
Seismicity 247
Seismology 249
Earthquake precursors 252
Tectonophysics 254
Earthquake hazard studies 256
Tectonic framework and fault investigations 256
Ground-failure investigations 263
Seismicity investigations 264
Ground-motion investigations 265
Stochastic modeling of faulting 266
Engineering geology 266
Landslides 267
Reactor hazards 268
Environmental aspects of energy 272
Hydrologic aspects of energy 274
Geology and hydrology related to national security 277
Relation of radioactive wastes to the geologic and hydrologic environments 278
Studies of low-level radioactive waste disposal sites 279
Regional studies 280
Nevada Test Site and vicinity 280
Waste isolation pilot plant site, southeastern New Mexico 281
Idaho National Engineering Laboratory 281
Geophysics 282
Geochemistry 283
Floods 283
Outstanding floods 283
Flood-frequency studies 285
Flood mapping 286
Effects of pollutants on water quality 287
Surface-water pollution 287
Ground-water pollution 287
Environmental geochemistry 289
Land subsidence 291
Hazards information and warnings 293
Astrogeology 295
Planetary studies 295
Galilean satellites 295
General geology 295
Cartography 295
Pioneer Venus radar 295
Martian geologic investigations from Viking data 295
Results from the surface landers 295
Global and broad-scale results 296
Martian channels 296
Glacier and polar features of Mars 297
Eolian landforms of Mars 297
Martian volcanism 298
Impact craters 298

Page

Astrogeology—Continued
Lunar investigations 299
Impact basins 299
Lunar sample investigations 299
Uranium-thorium-lead systematics of chondritic meteorites 300
Remote sensing and advanced techniques 301
Earth Resources Observation Systems Office 301
Cartographic applications 301
Geologic applications 302
Hydrologic applications 303
Techniques in processing Landsat image data 305
Land resource applications 306
Applications to geologic studies 308
Applications to hydrologic studies 311
Land use and environment impact 313
Multidisciplinary studies in support of land-use planning and decisionmaking 313
San Francisco Bay regional studies 313
Multidisciplinary studies in other areas 314
Land-use and land-cover maps and other geographic studies 315
Development of automated techniques for land-use mapping 315
Mapping land cover in northern Alaska with Landsat digital data 317
Land-use pattern analysis 317
Assessment of accuracy of land-use and land-cover maps produced from Landsat digital imagery 317
Updating land-use and land-cover maps 317
National wetland classification system 318
Land-use climatology 318
Environmetal impact studies 319
Resource and land investigations 321
Environmental statistics and indicators 321
Western coal planning assistance project 321
Conflict management research 322
Outer Continental Shelf oil and gas information program 322
International cooperation in the earth sciences 324
International resources assessment program 324
Resource data systems 326
Technical assistance and participant training 326
Technical assistance to developing countries 326
Training and scientist exchange 327
Scientific cooperation and research 331
International commissions and representation 336
International hydrological program and related activities 336
Activities related to other international organizations 338
International commissions 339
Representative activities in selected countries 339
Argentina 339
Botswana 339
Brazil 339
British Indian Ocean Territory 339
Canada 340
Caribbean area 340
Egypt 340
El Salvador 341
German Federal Republic 341
Hungary 341
Indonesia 341
Italy 342
Jordan 342
Korea, Republic of 342
Mexico 342

	Page
International cooperation in the earth sciences—Continued	
Representative activities in selected countries—Continued	
Morocco	342
Nigeria	343
Oman	343
People's Republic of China	344
Philippines	344
Poland	344
Portugal	345
Saudi Arabia	345
Thailand	347
Tunisia	347
Turkey	347
Venezuela	347
Yemen	348
Yugoslavia	348
Antarctic programs	348
Hydrologic studies	350
Arctic regions	351
Topographic surveys and mapping	352
Field surveys	352
Doppler translocation positioning	352
Inertial surveying	352
Aerial Profiling of Terrain system	352
Photogrammetry	353
Horizontal map acccuracy testing	353
Resolution targets	353
Satellite applications	354
Mapsat	354
Map projections for satellite applications	354
Landsat	354
Heat Capacity Mapping Mission	355
Topographic surveys and mapping—Continued	
Satellite applications—Continued	
Seasat	355
Satellite image map	355
Digital cartography	355
Interactive compilation and editing	355
Offline compilation	356
Special map digitizing	356
Voice terminal	356
Coordinate Transformation System	357
Computer-assisted map symbol placement	357
Gestalt Photo Mapper II software developments	357
Publications technology	357
Color proofing	357
Screenless printing	357
Experimental satellite-image map of the Grand Canyon	358
Computer resources and technology	360
Data communications	360
Batch computing	360
Interactive computing	361
ADP training	361
U.S. Geological Survey publications	362
Publications program	362
Publications issued	363
How to obtain publications	364
Over the counter	364
By mail	364
References cited	366
Investigations in progress	380
Indexes	418
Subject index	418
Investigator index	453

ILLUSTRATIONS

	Page
FIGURE 1. -Index map of the conterminous United States showing areal subdivisions used in the discussion of water resources	116
FIGURE 2. --Land-use and land-cover and associated maps on open file as of January 1, 1980	316

TABLES

	Page
TABLE 1. -Mineral production, value, and royalty for calendar year 1979	177
TABLE 2. -OCS oil and gas lease sales for calendar year 1979	178
TABLE 3. --Technical assistance to other countries provided by the USGS during FY 1979	327
TABLE 4. --Technical and administrative documents issued during the period October 1978 through October 1979 as a result of USGS technical and scientific cooperation programs	331

ABBREVIATIONS

A ____ angstrom
ABAG ____ Association of Bay Area Governments
ac ____ alternating current
A.D. ____ anno Domini
ADP ____ automatic data processing
AESOP ____ Automatic Surface Observation Platforms
AGID ____ Association of Geoscientists for International Development
AGWAT ____ Ministry of Agriculture and Water
AID ____ Agency for International Development
AIDJEX ____ Arctic Ice Dynamics Joint Experiment
AMRAP ____ Alaska Mineral Resource Assessment Program
ANCSA ____ Alaska Native Claims Settlement Act
AOCS ____ Atlantic Outer Continental Shelf
APD ____ antiphase domain
ARPA ____ Advanced Research Projects Agency
ASL ____ Albuquerque Seismological Laboratory
ASRO ____ Advanced Seismological Research Observatories
atm ____ atmosphere

b ____ barn (area)
bbl ____ barrel
BIA ____ Bureau of Indian Affairs
BLM ____ Bureau of Land Management
BOD ____ biochemical oxygen demand
B.P. ____ before present
Btu ____ British thermal unit
b.y. ____ billion years

*C ____ degrees Celsius
CAI ____ color alteration index
cal ____ calorie
CARETS ____ Central Atlantic Regional Ecological Test Site project
CCD ____ Computer Center Division
CCOP ____ U.N. Committee for Coordination of Joint Prospecting for Mineral Resources in Asian Offshore Areas
CCT ____ computer-compatible tape
C/DCP ____ convertible data-collection platforms
CDP ____ common depth point
CENTO ____ Central Treaty Organization
CEQ ____ Council on Environmental Quality
CFRUC ____ Colorado Front Range Urban Corridor Project
CGIS ____ Canada Geographic Information System
cgs ____ centimeter-gram-second
Ci ____ curie
cm ____ centimeter
COD ____ chemical oxygen demand
COM ____ computer-oriented microform
COST ____ Continent Offshore Stratigraphic Test Group
cps ____ counts per second
CPU ____ central processing unit
CRIB ____ Computerized Resource Information Bank
CV ____ characteristic value

d ____ day
D ____ Darcy
dc ____ direct current
DCAP ____ Digital Cartographic Applications Program
DCS ____ data-collection system
DEROCS ____ Development of Energy Resources of the Outer Continental Shelf
DMA ____ Defense Mapping Agency
DNPM ____ Departmento Nacional da Producão Mineral
DO ____ dissolved oxygen
DOD ____ Department of Defense
DOE ____ Department of Energy
DOI ____ Department of the Interior
DOMES ____ Deep Ocean Mining Environmental Study
DSDP ____ Deep Sea Drilling Project
dyn ____ dyne

Eh ____ oxidation reduction potential
EIA ____ Environmental Impact Analysis
EIS ____ environmental impact statement
EM ____ electromagnetic (soundings)
EMRIA ____ Energy Mineral Rehabilitation Inventory and Analysis
emu ____ electromagnetic unit
EPA ____ Environmental Protection Agency
ERDA ____ Energy Research and Development Administration
EROS ____ Earth Resources Observation System
ERTS ____ Earth Resources Technology Satellite
ESCAP ____ Economic and Social Commission for Asia and the Pacific Committee on Natural Resources
eV ____ electronvolt

FAO ____ Food and Agriculture Organization
ft ____ foot
f.l. ____ focal length
FLD ____ Fraunhofer line discriminator
FY ____ fiscal year

g ____ gram
GHz ____ gigahertz
GIPSY ____ General Information Processing System
GIRAS ____ Geographic Information Research and Analysis System
G.M.T. ____ Greenwich mean time
GOES ____ Geostationary Operational Environmental Satellite
GPa ____ gigapascal
GRASP ____ Geologic Retrieval and Synopsis Program

h ____ hour
H ____ Henry
ha ____ hectare
HFU ____ heat-flow unit
HIPLEX ____ High Plains Cooperative Program
hm ____ hectometer
HUD ____ Department of Housing and Urban Development
Hz ____ hertz

IAH ____ International Association of Hydrogeologists
IAHS ____ International Association of Hydrological Scientists
ICAT ____ Inorganic Chemical Analysis Team
IDB ____ Inter-American Development Bank
IDIMS ____ Interactive Display Image Manipulation System
IDOE ____ International Decade of Ocean Exploration
IGCP ____ International Geological Correlation Program
IGU ____ International Geographical Union
IHD ____ International Hydrological Decade
IHP ____ International Hydrological Program
IMW ____ International Map of thw World
in. ____ inch
IR ____ infrared
ISAM ____ Index Sequential Access Method
ISO ____ International Standardization Organization
IUGS ____ International Union of Geologic Sciences

J ____ joule
JECAR ____ Joint Commission of Economic Cooperation
JPL ____ Jet Propulsion Laboratory
JTU ____ Jackson turbidity unit

K ____ kelvin
kbar ____ kilobar
KCLA ____ Known Coal Leasing Area
KeV ____ kiloelectronvolt
kg ____ kilogram
KGRA ____ Known Geothermal Resources Area
KGS ____ Known Geologic Structure
kHz ____ kilohertz
km ____ kilometer
kn ____ knot
KRCRA ____ Known Recoverable Coal Resource Area
KREEP ____ potassium-rare-earth element-phosphorus
kWh ____ kilowatt-hour

L ____ liter
lb ____ pound
LARS ____ Laboratory for Application of Remote Sensing
lat ____ latitude
LMF ____ lithic matrix fragments
long ____ longitude

m ____ meter
M ____ magnitude (earthquake)
m_b ____ magnitude from body waves
M_L ____ Richter magnitude
M_s ____ magnitude from surface waves
mcal ____ millicalorie
MEF ____ maximum evident flood
mg ____ milligram
mGal ____ milligal
mi ____ mile
min ____ minute
ml ____ milliliter
mm ____ millimeter
MM ____ Modified Mercalli intensity
MN ____ meganewton
mo ____ month
mol ____ mole
MPa ____ megapascal
MSS ____ multispectral scanner
mV ____ millivolt
MW ____ megawatt
MWe ____ megawatts electrical
m.y. ____ million years
μ ____ micron
μcal ____ microcalorie
μg ____ microgram
μGal ____ microgal
μm ____ micrometer
μmho ____ micromho
μrad ____ microradian
μstrain/yr ____ engineering shear

NASA ____ National Aeronautics and Space Administration
NASQAN ____ National Stream Quality Accounting Network
NAWDEX ____ National Water Data Exchange
NCRDS ____ National Coal Resources Data System
NEIS ____ National Earthquake Information Service
NEPA ____ National Environmental Policy Act
ng ____ nanogram
NLCR ____ nonlinear complex resistivity
nm ____ nanometer
NOAA ____ National Oceanic and Atmospheric Administration
NOS ____ National Ocean Survey
NPRA ____ Naval Petroleum Reserve in Alaska
NRA ____ National Resources Agency
NRA ____ Nuclear Regulatory Agency
nT ____ nanotesla
NTIS ____ National Technical Information Service
NTS ____ Nevada Test Site
NWS ____ National Weather Service

OAS ____ Organization of American States
OCS ____ Outer Continental Shelf
OE ____ Oersted
ohm-m ____ ohm-meter
OIA ____ Office of International Activities
OME ____ Office of Minerals Exploration
ORNL ____ Oak Ridge National Laboratory
OWDC ____ Office of Water-Data Coordination
Ω ____ ohm

PAIGH ____ Pan American Institute of Geography and History
PCB ____ polychlorinated biphenyls
pCi ____ picocurie
ppb ____ part per billion
ppm ____ part per million
PSRV ____ pseudorelative velocity

R ---range
rad ---radian
RASS ---Rock Analysis Storage System
RBV ---return beam vidicon
REE ---rare-earth element
RF ---radio frequency
rms ---root mean square
rmse ---root mean square error
R/V ---research vessel

s ---second
SFBRS ---San Francisco Bay Region Environment and Resources Planning Study
SIP ---strongly implicit procedure
SLAR ---side-looking airborne radar
SMS ---Synchronous Meteorological Satellite
SOM ---Space Oblique Mercator
SP ---self potential
SRO ---Seismic Research Observatory

t ---tonne
T ---Tesla
TEM ---transmission electron microscopy
TIU ---Thermal-inertia unit
TL ---thermoluminescence
TVA ---Tennessee Valley Authority

UNDP ---U.N. Development Program
UNESCO ---United Nations Educational, Scientific and Cultural Organization
USAID ---U.S. Agency for International Development
USBM ---U.S. Bureau of Mines
USDA ---U.S. Department of Agriculture
USGS ---U.S. Geological Survey
USPHS ---U.S. Public Health Service
U.S.S.R. ---Union of Soviet Socialist Republics
UTM ---Universal Transverse Mercator

V ---volt
VDETS ---Voice Data Entry Terminal System
VES ---vertical electric soundings
VHRR ---very high resolution radiometer
VLF ---very low frequency

W ---watt
WHO ---World Health Organization
WMO ---World Meteorological Organization
WRC ---Water Resources Council
WRDD ---Water Resources Development Department
wt ---weight
WWSSN Worldwide Standardized Seismograph Network

yr ---year

SI UNITS AND INCH-POUND SYSTEM EQUIVALENTS

[SI, International System of Units, a modernized metric system of measurement. All values have been rounded to four significant digits except 0.01 bar, which is the exact equivalent of 1 kPa. Use of hectare (ha) as an alternative name for square hectometer (hm^2) is restricted to measurement of land or water areas. Use of liter (L) as a special name for cubic decimeter (dm^3) is restricted to the measurement of liquids and gases; no prefix other than milli should be used with liter. Metric ton (t) as a name for megagram (Mg) should be restricted to commercial usage, and no prefixes should be used with it. Note that the style of meter^2 rather than square meter has been used for convenience in finding units in this table. Where the units are spelled out in text, Survey style is to use square meter]

SI unit		Inch-Pound equivalent	
Length			
millimeter (mm)	=	0.039 37	inch (in)
meter (m)	=	3.281	feet (ft)
	=	1.094	yards (yd)
kilometer (km)	=	0.621 4	mile (mi)
	=	0.540 0	mile, nautical (nmi)
Area			
centimeter^2 (cm^2)	=	0.155 0	inch^2 (in^2)
meter^2 (m^2)	=	10.76	feet^2 (ft^2)
	=	1.196	yards^2 (yd^2)
	=	0.000 247 1	acre
hectometer^2 (hm^2)	=	2.471	acres
	=	0.003 861	section (640 acres or 1 mi^2)
kilometer^2 (km^2)	=	0.386 1	mile^2 (mi^2)
Volume			
centimeter^3 (cm^3)	=	0.061 02	inch^3 (in^3)
decimeter^3 (dm^3)	=	61.02	inches^3 (in^3)
	=	2.113	pints (pt)
	=	1.057	quarts (qt)
	=	0.264 2	gallon (gal)
	=	0.035 31	foot^3 (ft^3)
meter^3 (m^3)	=	35.31	feet^3 (ft^3)
	=	1.308	yards^3 (yd^3)
	=	264.2	gallons (gal)
	=	6.290	barrels (bbl) (petroleum, 1 bbl=42 gal)
	=	0.000 810 7	acre-foot (acre-ft)
hectometer^3 (hm^3)	=	810.7	acre-feet (acre-ft)
kilometer^3 (km^3)	=	0.239 9	mile^3 (mi^3)
Volume per unit time (includes flow)			
decimeter^3 per second (dm^3/s)	=	0.035 31	foot^3 per second (ft^3/s)
	=	2.119	feet^3 per minute (ft^3/min)
decimeter^3 per second (dm^3/s)	=	15.85	gallons per minute (gal/min)
	=	543.4	barrels per day (bbl/d) (petroleum, 1 bbl=42 gal)
meter^3 per second (m^3/s)	=	35.31	feet^3 per second (ft^3/s)
	=	15 850	gallons per minute (gal/min)
Mass			
gram (g)	=	0.035 27	ounce avoirdupois (oz avdp)
kilogram (kg)	=	2.205	pounds avoirdupois (lb avdp)
megagram (Mg)	=	1.102	tons, short (2 000 lb)
	=	0.984 2	ton, long (2 240 lb)
Mass per unit volume (includes density)			
kilogram per meter^3 (kg/m^3)	=	0.062 43	pound per foot^3 (lb/ft^3)
Pressure			
kilopascal (kPa)	=	0.145 0	pound-force per inch^2 (lbf/in^2)
	=	0.009 869	atmosphere, standard (atm)
	=	0.01	bar
	=	0.296 1	inch of mercury at 60°F (in Hg)
Temperature			
temp kelvin (K)	=	[temp deg Fahrenheit (°F) + 459.67]/1.8	
temp deg Celsius (°C)	=	[temp deg Fahrenheit (°F) − 32]/1.8	

MINERAL-RESOURCE INVESTIGATIONS

UNITED STATES AND WORLD MINERAL-RESOURCE ASSESSMENTS

Kaolin in the Macon-Gordon district, Georgia

Based on geologic mapping and work done jointly with other geologists (Buie and others, 1979), S. H. Patterson estimated that the kaolin resources in the Macon-Gordon district, Georgia, are probably 1.5 billion to 2 billion tonnes. The categories of resources in these estimates, in millions of metric tonnes, are as follows: reserves, more than 100; subeconomic resources, 700 to 900; and undiscovered resources, at least 700 to 1,000. The kaolin deposits occur in Upper Cretaceous beds and in a formation of middle Eocene age. Cretaceous kaolin, with few exceptions, has different physical properties than the Eocene clay. This difference in properties permits selective mining to meet varying product specifications.

Peat resources in Maine

C. C. Cameron estimates that a total of 25 million t of air-dried peat suitable for agricultural and horticultural purposes is contained in 57 peat deposits that she measured and sampled during 1979 in Penobscot, Aroostook, and Piscataquis Counties, northern Maine. One acre-foot of peat[1] is considered equivalent to 181 t of air-dried peat in deposits having a minimum thickness of 1.5 m with an ash content not exceeding 25 percent.

Initial BTU analysis of the samples from the same peat deposits sent to the DOE Pittsburgh Laboratory indicates a range of calorific values from 8,966 BTU/lb (20,855 kJ/kg) to 10,679 BTU/lb (24,839 kJ/kg) on a moisture-free basis for all samples with less than 10 percent ash content. Preliminary statistical analysis suggests that 95 percent of the peat deposits containing less than 10 percent ash content can be expected to have calorific values in the range of 8,748 BTU/lb (20,348 kJ/kg) to 10,548 BTU/lb (24,535 kJ/kg) moisture free. Qualitative estimates at this time suggest that approximately two-thirds of the commercial quality peat reserves in the area would contain less than 10 percent ash. Also at this time, experiments on fuel use of peat indicate that deposits preferably should be at least 1.5 m thick, contain an ash content not exceeding 15 percent, and have a calorific value of at least 8,000 BTU/lb (18,600 kJ/kg) to be of commercial value.

[1] Customary units are used here because there are no equivalent SI units for this description.

MINERAL-RESOURCE ASSESSMENTS OF LAND AREAS

Gravity studies in Montana indicate hydrocarbon potential

A notable anomaly detected during gravity studies conducted by D. M. Wilson and M. D. Kleinkopf of the disturbed belt in northwestern Montana is a 40-mGal negative feature located along the eastern edge of the overthrust belt just north of lat 48°N. The anomaly is coincident with an area of stacked Paleozoic thrust sheets of the Sawtooth Range and could indicate a thicker section of less dense rocks that may have had an influence on the potential for hydrocarbons.

In addition, a preliminary gravity map of the Choteau 2° quadrangle shows further definition of northeasterly trends parallel to the Scapegoat-Bannatyne trend (Kleinkopf and Mudge, 1972) and suggests additional similar trends to the north. These trends may indicate discontinuities in the crystalline basement such as fracture zones or warping that may have influenced sedimentation patterns and the potential for hydrocarbon accumulation. New gravity information that defined a 30-mGal positive anomaly near Brown Sandstone Peak also added to definition of the Brown Sandstone Peak–Brady trend.

Zinc and coal recoverable from coal mine refuse

J. C. Cobb (Illinois Geological Survey) reports that sphalerite-bearing bituminous coals in the Interior province contain approximately 0.1 percent zinc and 0.01 percent cadmium. The coals are restricted to certain areas in Oklahoma, Kansas, Missouri, Iowa, and Illinois. The majority of these coals are subjected to cleaning procedures, which concentrate much of the sulfide material including sphalerite into slurry and gob refuse, before shipping to market. Analyses of slurry and gob show up to 2.4 percent zinc in some gob samples and an average of 0.3 percent zinc in slurry, with a maximum of 2 percent. Both coal and sphalerite can be recovered

from these wastes by physical and (or) chemical separation techniques.

Aeromagnetic studies of the Square Butte Wilderness Area, Choteau County, Montana

Studies by M. D. Kleinkopf of the large dipole magnetic anomaly across Square Butte indicate that the igneous intrusion that forms Square Butte is a tabular body and probably is a laccolith, along the lines of the classical definition of a laccolith (American Geological Institute, 1972) and as described by Weed (1901). If one assumes that remanent magnetism plays an important role and if one places the bottom of the intrusion at the 1,250-m level observed in the field, then the intrusion can be modeled (Henderson and Allingham, 1964) to produce a theoretical magnetic anomaly that closely resembles the observed anomaly.

There is little direct evidence in the magnetic data to suggest conditions favorable for localization of mineral resources, with two possible exceptions. The assumption that the intrusion has a nominally flat bottom provides a contact zone beneath the intrusion that might be of interest for either contact or replacement mineralization. Secondly, along the northeastern side of the positive anomaly, a slight negative nosing, as evidenced by the southwest bowing of the isogamma contours, could reflect a zone of alteration (destruction of magnetite) that might be related to mineralization. The nosing is assumed to be valid because the values are consistent along two adjacent flight lines. However, it more likely represents magnetic reversals in the group of dikes and sills that have been mapped in this location.

Geophysical studies in the Big Snowy Mountains Wilderness Area, Fergus and Golden Valley Counties, Montana

Gravity and magnetic studies by C. L. Long provided new information about the structure and distribution of lithologies in the Big Snowy Mountains area, Montana. Major gravity anomalies are probably due to the density contrast between the Paleozoic and Mesozoic sedimentary rocks and the Belt Supergroup of Proterozoic Y age. A steep gravity gradient of 20 mGal reflects a major reverse fault mapped by Lindsey (personal commun., 1979) with the downthrown block on the south side of the Big Snowy anticline. In the same area, gravity maxima on the north side of the fault may correspond to near-surface or surface exposures of Precambrian rocks, and gravity minima on the south side are representative of a thickening sedimentary cover of Paleozoic and Mesozoic rocks over the downthrown block and the Wheatland syncline.

Magnetic anomalies in the Big Snowy Mountains area are part of a large circular magnetic high to the south (Zietz and others, 1971). This anomaly covers part of the Cat Creek–Hinsdale block, which was structurally and topographically low before Late Jurassic time, and is probably related to a post-Laramide igneous intrusive and to additional magnetic rock that may have intruded a basement weakness under the Cat Creek–Hinsdale block. A magnetic low bounding the north side of the area is in the same region as the east-west magnetic lineaments mentioned by Zietz and others (1971) and may be indicative of deep-seated fundamental shear zone.

The gravity trends of steep gradients associated with near-surface features and gentle magnetic gradients reflect magnetic susceptibility contrasts at depths of about 15 to 20 km. This is additional evidence to support the suggestion that the Big Snowy anticline is an en echelon drag fold related to the left lateral shear zones of the Cat Creek and Lake Basin–Lewis and Clark Line Zone.

Geophysical studies in the Never Summer Wilderness Area, Colorado

The geophysical data (gravity and magnetics) in the Never Summer Wilderness Area generally delineate two intrusive bodies of rock lying partly within the designated wilderness area, according to V. J. Flanigan. The first, a granodiorite porphyry, is distinctive because of its magnetic signature. To the south of the granodiorite body lies a rhyolite porphyry intrusive slightly less magnetic in character and less dense than the granodiorite as evidenced by a 5- to 10- mGal gravity low. Current mining activity (drilling) and past mining have generally been within or near the southern contact of the rhyolite porphyry body south of the boundary of the Never Summer area. This area contains some of the silver mines of the Teller City boom of the 1850's. The inferred northern and western contact of the rhyolite porphyry lies within the Never Summer Wilderness Area, and, if this is indeed the case, the contact area may represent an area of increased mineral potential.

Gravity studies in the Sierra Ancha Wilderness Area, Gila County, Arizona

Preliminary gravity results show several circular gravity features around the margins of the uplifted central block of the Sierra Ancha area. Gravity studies by D. M. Wilson indicate the presence of two lows of 10 and 14 mGal relief along the western border of the wilderness area. The presence of the lows, in concert with the magnetic and geochemical data, suggests possible blind intrusions that may be altered and, thus, have potential for mineralization.

Aerial radiometric and magnetic survey of the Sierra Ancha Wilderness Area and vicinity, Gila County, Arizona

The interpretation of radiometric and magnetic data by J. S. Duval and J. A. Pitkin from an aerial survey of the Sierra Ancha Wilderness Area and vicinity, Gila County, Ariz., shows that these data accurately reflect the location of almost all the known uranium and asbestos-iron mineralization. The known deposits were utilized to establish criteria that were used to make a map of areas where uranium or asbestos-iron mineralization may occur. Many of the known and possible mineralized sites lie within or near the wilderness area.

The radiometric data also show that large areas of diabase have significantly different radiometric values compared to most of the diabase within the survey area. This result suggests that some of the diabase may have a different chemical and physical origin than most of the mapped diabase.

A large pattern of lower magnetic intensity, coupled with low gravity value, and high geochemical values for a number of elements suggest the existence of a buried pluton that could be mineralized. The suspected location of this pluton lies to the west of the wilderness area.

Hydrothermal alteration in the Pioneer Mountains, Beaverhead County, Montana

Three bodies of deeply weathered and inconspicuous hydrothermally altered rocks in the central Pioneer Mountains, Mont., have characteristics that suggest they formed from large hydrothermal systems similar to a deposit being developed for molybdenum at Cannivan Gulch and to others being explored elsewhere in the range. The altered zones being studied by R. C. Pearson and B. R. Berger are in the Pioneer batholith and are associated with numerous small bodies of quartz porphyry. Desultory prospecting was done in the altered zones, primarily many decades ago when mining was active in the Elkhorn mining district 2 to 4 km away. The alteration is characterized by potassium-silicate assemblages, pyrite is widespread, and molybdenite has been found at several places. In two of the bodies, a vuggy greisenlike rock consisting largely of muscovite and quartz to a great extent replaced the original rock. In addition, potassium feldspar and limonite after pyrite (or rarely pyrite itself) are abundant locally. In the third altered zone, intersecting quartz-pyrite veinlets and disseminated pyrite are in fresh-appearing rock. Magnetite and potassium feldspar and disseminated biotite and muscovite are also common in the veinlets. Geochemically, the altered zones are anomalous in silver, arsenic, lead, zinc, tin, and molybdenum.

Plutonic rocks of the Ten Mile Creek RARE II Area, central Idaho

A variety of plutonic rocks in the Ten Mile Creek RARE II Area west of and contiguous to the Sawtooth Wilderness Area, central Idaho, has been mapped by T. H. Kiilsgaard. At least six and possibly seven varieties of plutonic rocks have been differentiated in the area, which previously was considered underlain by granitic rocks of the Idaho batholith. Oldest of the differentiated rocks is a foliated granodiorite to quartz diorite exposed along the North Fork of the Boise River, apparently as a pendent in biotite quartz monzonite of the Idaho batholith. In addition, xenoliths of foliated dioritic rock are found elsewhere in the biotite quartz monzonite of the Idaho batholith, which is the predominate plutonic rock in the Ten Mile Creek area and which has been described in nearby localities by Anderson (1939), Reid (1963), and Kiilsgaard and others (1970). Idaho batholith quartz monzonite is intruded by nonporphyritic medium-grained leucocratic quartz monzonite. More than 26 km^2 of leucocratic quartz monzonite is exposed in the headwaters area of Ten Mile Creek, where the base of the leucocratic pluton is inclined east at a low angle. Intrusive into the leucocratic quartz monzonite locally, but underlying it elsewhere, is pink granite of the Sawtooth batholith. The granite is characterized by abundant potassium feldspar and a rather coarse texture generally. A stock of granite in the Sawtooth Formation underlies Goat Mountain. The stock, which is exposed in cirques and stream heads on the mountain sides, has a rather flat top that is capped by fine-textured leucocratic quartz monzonite. The leucocratic capping thins near the border of the stock and pinches out at the western flank, where the stock contact is inclined steeply. Leucocratic cap rock on Goat Mountain appears to be related to intrusion of the Sawtooth granite, whereas, elsewhere, leucocratic rocks are intruded by the Sawtooth granite. Thus, there may be two varieties and even two ages of leucocratic rocks.

Intrusive into the Sawtooth granite is a plug of hornblende andesite, cut by dikes of biotite-hornblende quartz monzonite that are offshoots from a nearby stock. A larger stock of the biotite-hornblende quartz monzonite is exposed conspicuously on Jackson Peak. The rock is distinctive and is characterized by abundant rather closely set phenocrysts of feldspar in a pink fine-textured matrix. In many respects, the rock resembles some of the Tertiary quartz monzonite in Boise Basin (Anderson, 1947, p. 121–144).

Data are not available on ages of the plutonic rocks in the Ten Mile Creek area. Armstrong (1975) compiled the ages of various rocks in Idaho and presented geochronometric data indicating a wide range in age for rocks con-

sidered to be parts of the Idaho batholith. Included in his compilation are samples of adamellite-granodiorite from localities north of Boise and from Bear Valley Mountain. Potassium-argon ages of these rocks range from about 64 m.y. to about 71 m.y. Rocks in the two localities are considered to be parts of the Idaho batholith, and, megascopically, they are comparable to rocks mapped as Idaho batholith in the Ten Mile Creek area. Thus, it is reasonable to consider that Ten Mile rocks may be of comparable age, and the dioritic rocks intruded by Ten Mile rocks of the Idaho batholith are older. Armstrong (1975, p. 28) gives ages of three granite samples of the Sawtooth, one of which was collected by Kiilsgaard from a locality a few miles east of the Ten Mile Creek area. Potassium-argon ages of the three samples range from 43.7 m.y. to 44.4 m.y. Granite mapped as Sawtooth in the Ten Mile Creek area is identical to Sawtooth granite in the contiguous Sawtooth Wilderness Area; thus, Sawtooth rocks in the two localities are considered to be of the same age. The hornblende andesite plug that intrudes Sawtooth granite has to be younger and the intrusive biotite-hornblende quartz monzonite of Jackson Peak the youngest known plutonic rock in the Ten Mile Creek area.

A magnetic tectonic feature in southern Arizona

A quasi-linear and semicontinuous megascale aeromagnetic feature traverses southern Arizona from about lat 33°52′ N. at the Nevada border to the Arizona–New Mexico–Mexico junction. Studies by D. P. Klein show that at least three major ore districts and numerous lesser deposits correlate with the edges of this feature making it a possible regional guide in mineral exploration. The feature is expressed on a residual magnetic map (Sauck and Sumners, 1970) as a broad normally polarized anomaly of 300 gammas amplitude and 50 to 70 km wavelength. A discontinuity in this feature in the Papago area at about long 112° W. is possibly thermally induced demagnetization rather than a structural break. There are numerous geothermal indicators correlating well with the width of the magnetic anomaly attenuation. Geologically, the features correlate roughly with the known outcrop trend of upper Mesozoic and lower Cenozoic igneous rocks. Geophysically, the aeromagnetic pattern is consistent with a coherent volcanointrusive zone or an overthrust plate having basic crustal material displaced over less magnetic rocks. In either case, there is the implication of mobilization of metals from the deep crust or subcrustal region.

Diamond potential of Missouri Breaks diatremes, Montana

Eocene diatremes and dikes of the Missouri River Breaks area, Montana, have been produced by mantle-derived magmas of alkalic ultramafic composition (alnoite and monticellite peridotite) that show chemical affinities to kimberlite. Thus, the diatremes could have diamond potential, according to B. C. Hearn, Jr. (1979). Of the 32 diatremes, only 4 contain xenoliths derived from the lower crust, and only 6 contain xenoliths or xenocrysts derived from the upper mantle. Diamonds have not been found yet. If any diatremes contain diamonds, the most likely is the Williams group, which are true kimberlite, on the basis of megacrysts and xenocrysts of chromian garnet, chromian diopside, and magnesian ilmenite and xenoliths of garnet peridotite, the deepest upper mantle material. Calculated temperatures and pressures of equilibration of pyroxenes in garnet peridotite xenoliths outline a steep geothermal gradient that lies above or below, but close to, the graphite-diamond stability curve, depending on the method of pyroxene calculation. Thus, diamonds could have been stable in the source region of the kimberlite. Heavy mineral sampling of stream sediments and magnetic surveys may be useful techniques for locating additional diatremes, two of which show 200- to 600-gamma positive magnetic anomalies.

Mineral-resource assessment of the Charlotte 2° quadrangle, North Carolina and South Carolina

Sampling by J. W. Whitlow and J. P. D'Agostino in an unmined area in the midsouthwestern part of the Charlotte quadrangle has revealed a zone rich in tin and monazite. This zone is at least 20 km long and 5 km wide. Abundant amounts of coarse cassiterite have been found in concentrates of stream sediment. The cassiterite occurs as mostly dark water-worn poorly sorted grains 0.25 to 1.0 cm in diameter. Individual grains are black, dark brown to pale tan, and greenish gray to gray white. Monazite occurs mostly as coarse grains and large crystals 0.05 to 0.3 cm in diameter. The monazite is commonly lime green to yellow green.

Grid sampling has shown the crucial importance of drainage characteristics in locating alluvial concentrations of cassiterite and monazite. The cassiterite grains become foliated, flake easily, and are disintegrated and dispersed within short distances downstream from their source. The monazite grains, because of their small size, also are dispersed easily in alluvium a short distance downstream from their source. The coarse-grained cassiterite is concentrated in alluvium in only a small

vertical range in the upper reaches of headwater tributaries. The monazite is concentrated in a small vertical range adjacent to and below the cassiterite.

The bedrock source of the cassiterite and monazite has not been identified. Bedrock is Proterozoic to Paleozoic gneiss and schist bearing pegmatitelike lenses and pods concordant with bedrock foliation. These rocks are intruded by bodies and stringers of the Ordovician Toluca Quartz Monzonite.

Coarse native gold is present in quartz in the South Mountains area in the western part of the quadrangle. The quartz occurs as recently deposited horizontal to gently inclined sheets that nearly parallel the present topography. The quartz sheets are found near the surface in saprolite generally as a white massive tough layer 5 to 15 cm thick.

As a part of this mineral-resource study, the location and description of 650 metallic and nonmetallic mines, quarries, pits, prospects, and mineral occurrences in the Charlotte 2° quadrangle have been entered into the CRIB file. The information is available as a computer-printed map or text.

Gravity studies of mineralized features, Silver City quadrangle, Arizona and New Mexico

Gravity surveys by J. C. Wynn have identified two features in the Silver City quadrangle that have a relatively high potential for mineralization. One of these features is a largely buried ridge of Cretaceous rocks that, in terms of current exploration models in the Southwest, is a prime target for further exploration for a porphyry copper. The other feature is a probable caldera that was suspected, but not confirmed, from geologic mapping. Gravity data indicate closure of the feature where it is covered by valley fill.

Magnetic studies in the Belt Basin, Montana and Idaho

Sixty audiomagnetotelluric soundings were made by C. L. Long and M. D. Kleinkopf across the northwestern part of the Wallace 2° quadrangle to study the regional electrical properties of the Prichard Formation (lower part of the Belt Supergroup), particularly where it is intruded by plutonic rocks of Cretaceous age. These intrusions have striking magnetic positive anomalies associated with them and may be of interest in evaluating the mineral-resource potential of the area.

A 7.5-Hz scalar apparent resistivity map shows broad areas of low resistivity associated with the intrusions at Thompson Falls, Dixie Peak, Wallace, and Trout Creek. Some of the low resistivity areas probably represent low resistivity zones within the intrusions. Away from the intrusions, a low resistivity horizon within the Prichard Formation is inferred from the soundings.

Structure, stratigraphy, and intrusive rocks of part of the Sapphire Wilderness Study Area, Montana

The Sapphire Wilderness Study Area is located in the west part of the Sapphire thrust system. According to C. A. Wallace, the structural pattern of the area is dominated by a system of imbricate anastomosing thrust faults and broad open folds that are associated with thrust faults. Northwest-trending steep faults of small stratigraphic separation cut thrust faults. The country rocks are more intensely deformed by small-scale folds near intrusive bodies.

Rocks of the Proterozoic Y Belt Supergroup are the major formations in the study area. The Wallace, Snowslip(?), and Mount Shields Formations, the Bonner Quartzite, and the McNamara Formation have been mapped in the eastern part of the study area. These Proterozoic Y rocks have been metamorphosed by nearby intrusive rocks.

Silicic intrusive rocks occupy most of the east part of the study area. The intrusive mass is a complex of individual plutons, most of which are medium- and coarse-grained granite and quartz monzonite. Borders of individual plutons are gradational, and the plutons have little internal structure. Field relations suggest that these plutons may have differentiated from the same parent magma and that the intrusive bodies were emplaced within the same period. Because intrusive rocks truncate thrust faults and later steep faults, the Belt rocks were faulted into their present locations before the intrusive event occurred.

Mineral-resource assessment of the Big Frog Wilderness Study Area, Tennessee and Georgia

Reconnaissance geologic mapping and geochemical sampling have been done by J. F. Slack, assisted by E. R. Force, Andrew Grosz, and R. H. Ketelle, in the 18.2-km^2 Big Frog Wilderness Study Area of southeastern Tennessee and northern Georgia. Rocks of the area are in the Ocoee Supergroup of Proterozoic Y and (or) Z age. More than 200 samples of rock, soil, and stream sediment were analyzed spectrographically and by atomic absorption and fire assay methods for 31 major, minor, and trace elements. In many places, silty and sandy rocks contain 5 to 10 percent sulfides, chiefly pyrite and pyrrhotite. Locally, tiny grains of chalcopyrite and sphalerite intergrown with the iron sulfides provide minor concentrations of copper, zinc, and arsenic slightly higher than background

geochemical values, but no significant metal anomalies were found. The disseminated base-metal sulfides are not sufficiently concentrated to be of current economic interest, and no metallic mineral resources are known within the proposed wilderness. Nonmetallic resources such as slate, phyllite, stone, and sand and gravel are present, but they are not now of economic interest because similar materials exist closer to markets outside the study area.

Hypothetical submarginal kyanite resource, Craggy Mountain Wilderness Study Area, North Carolina

Reconnaissance geologic and geochemical studies by F. G. Lesure and Andrew Grosz (U.S. Geological Survey) and B. B. Williams and G. C. Gazdik (U.S. Bureau of Mines) have shown that the Craggy Mountain Wilderness Study Area and RARE II Extension contain moderately large hypothetical submarginal kyanite and accessory garnet resources. The kyanite and garnet resources are in alumina-rich schists containing 5 to 20 percent kyanite, partly altered to sillimanite, and 10 to 30 percent garnet, a mixture of three-fourths almandine and one-fourth pyrope. Some of the alumina-rich schist also contains 1 percent or more pyrite but has only a trace of base and precious metals. Most of the rock types are suitable for use as crushed stone or rough building stone; however, adequate resources of stone are available in the general area in more favorable locations.

Extension of Iron River–Crystal Falls basin, Michigan and Wisconsin

The Iron River–Crystal Falls basin in northern Michigan contains the Proterozoic X Paint River Group, for many years a source of iron ore and a potential host for uranium and base-metal mineralization. The basin was previously thought to terminate on the west as the keel of an east-plunging syncline near the city of Iron River. However, new gravity studies by W. F. Cannon suggest that the syncline reverses plunge near Iron River and opens into another basin to the west in an area with no outcrops. The iron-rich sedimentary rocks in the Iron River–Crystal Falls basin cause a very pronounced gravity high with steep gradients rising from an encircling belt of basaltic volcanic rocks. West of Iron River, this anomaly with its characteristic steep gradients continues for about 25 km and is as much as 10 km wide. Both north and south of the anomaly, basalt is exposed, so the rock body causing the anomaly must be substantially more dense than basalt, and it seems likely that the anomaly is caused by the iron-rich sedimentary rocks of the Paint River Group.

GEOLOGIC STUDIES OF MINERAL DISTRICTS AND MINERAL-BEARING REGIONS

Lineated granitic rocks mark early faults in the Beaver Creek area, western St. Lawrence County, New York

C. E. Brown reports that two of the northeast-trending curvilinear faults that separate areas of rocks in the Grenville Complex into large structurally and stratigraphically distinct lens-shaped panels (Brown, 1973) appear to be much older than others. These old faults are marked by lenses of strongly lineated and crushed granitic rocks that are mainly about a kilometer in length, with a few as much as 8 km long. They appear to have been intruded early into the zone of movement.

The Beaver Creek lineament that can be traced as much as 48 km has seven steeply dipping alined biotite granite bodies that are adjacent on the west side of the topographic lineament in the Beaver Creek area. More bodies probably exist along the lineament beyond the area of study. The microcline, oligoclase, quartz-biotite granite is foliated and has strongly lineated quartz. Locally, it also displays prominent feldspar augen. Enveloping these bodies of deformed granite is a thin rind, about 30 m thick, of fine-grained leucocratic granite composed of albite, microcline, and quartz with disseminated small, 1 to 2 mm, clear brownish-red garnets. The rind does not show the strong internal deformation shown by the biotite granite. Other rocks along the Beaver Creek fault also are lineated strongly parallel to the steeply dipping structure and have variable low plunges either to the southwest or northeast.

Another fault whose trace is marked by granitic bodies is the thrust that forms the sole of the North Gouverneur nappe that occupies the area southeast of Beaver Creek. These bodies also are microcline, oligoclase, quartz granite having less biotite than the granite along Beaver Creek and lacking the rind of different composition and texture. The rock is characterized by strongly lineated quartz and fine grain size that, at places, gives it a flinty mylonitic texture.

This fault is known to be an early structural feature as it is sharply folded by later deformation. In fact, the longest lineated granite body outlines a large isoclinal fold. Another linear zone of similar fine-grained lineated leucocratic granite in a zone of mixed metasediments and amphibolites in the upper limb of the nappe suggests a third early fault that was not recognized from other geologic relations.

Other northeast-trending faults such as the Pleasant Lake fault (Brown, 1973) appear to be younger because they are not folded but do have numerous pegmatite

bodies along their trace, indicating that initial movement was deep in the Earth's crust. Such faults also appear to have had late recurring movement at a level that allowed brittle deformation because brecciated and locally silicified rock exists along these faults.

Recognition of the intrusive rocks related to faulting enables a sequence of geologic events to be worked out. Isotopic geochronologic work is hindered by the widespread 0.9 b.y. to 1 b.y. overprinted age in rocks of the Grenville Complex. Identifying rock units related to certain events in the local Precambrian history provides targets for detailed geochronologic studies that might help in resolving that history.

Ore bodies at Great Gosaan Lead, Virginia

According to J. E. Gair, some wall rocks in contact with sulfide ore bodies at Great Gossan Lead, Va., and Ducktown, Tenn., both of which are in Blue Ridge province flysch-type rift-facies metasedimentary rocks, contain high percentages of either untwinned sodic plagioclase or biotite/chlorite. Such rocks evidently are absent or exceedingly rare in country rocks away from the ore deposits. Their origin, as yet unexplained, is probably related to metamorphic reactions between sulfide bodies and country rocks or to chemical deposition or alterations connected with the ore-forming process itself.

Subvolcanic hydrothermal mineral deposits in the Carolina volcanic slate belt

Significant new subvolcanic hydrothermal deposits may be present in the Eastern United States in such areas as the Carolina volcanic slate belt, which is a thick island-arc sequence. The slate belt rocks are known to include many small plutons, but surprisingly few volcanic intrusive rocks have been reported. Widespread deep saprolitic weathering has hindered identification of small felsic porphyry bodies surrounded by felsic volcanic rocks, which can be identified only by large-scale geologic mapping.

On the basis of volcanic and volcanoclastic rock suites, it should be possible to classify most areas in the Carolina volcanic slate belt as having formed near, at an intermediate distance, or far from volcanic sources. Assuming that porphyry copper alteration and mineralization systems form in or near areas of eruption, the slate belt areas with coarse pyroclastic rocks and felsic flows would have formed closest to felsic volcanic centers and would be the most favorable prospecting areas. Therefore, the nature of the volcanic rocks themselves is a guide to the most favorable areas. Reconnaissance of many old prospects and mineral occurrences in the region has resulted in the identification of four previously undescribed small porphyry bodies near the old Brewer gold mine near Jefferson, S.C., and several near Asheboro, N.C.

Tourmaline associated with New England massive sulfide deposits

Preliminary field examination, literature study, and petrography by J. F. Slack indicate that tourmaline may be a common accessory mineral in metamorphosed base-metal massive sulfide deposits. Tourmaline appears to be particularly abundant in proximal sediment-hosted deposits (Sullivan mine, British Columbia; Black Hawk mine, coastal Maine) and in environments of mixed sedimentary and mafic volcanic rocks (Elizabeth mine, Vermont copper belt).

Metamorphism has a pronounced effect on tourmaline and commonly results in extensive recrystallization and remobilization. Metamorphically recrystallized tourmaline shows preferential intergrowths with pyrrhotite and chalcopyrite, the most mobile sulfides in iron-copper-zinc deposits. Reconnaissance field work at the Elizabeth mine, Orange County, Vt., suggests that the tourmaline associated with deformed and metamorphosed sulfide ore there has been remobilized for distances of at least 10 m laterally away from the ore zone. Syn(?)-metamorphic fractures that crosscut the southern part of the orebody are filled with tourmaline-sulfide crusts and patches. Recrystallized tourmaline, therefore, may be useful as a prospecting guide for hidden massive sulfide deposits. In addition, this research suggests that boron anomalies in rock, soil, and (or) stream sediments may form a diagnostic geochemical halo surrounding some metamorphosed sulfide orebodies.

Cumulate and supercumulate nelsonite, central Virginia

Nelsonite (ilmenite-apatite rock, formerly mined as ilmenite ore) bodies of the Roseland district of central Virginia have cumulate affinities and are related to a regional titanium-phosphorus-zirconium-rich ferrodiorite, the Roses Mill pluton. Norman Herz and E. R. Force found that cumulate nelsonite in place in ferrodiorite is banded and has settled textures. Nelsonite veins in rock units under ferrodiorite are more common; presumably, they were cumulates that continued movement in response to gravity as some sort of solid.

Recovering rutile from porphyry copper deposits

The United States could become independent from imported rutile and improve its trade balance by $85 million a year if rutile were systematically recovered from its porphyry copper ores. E. R. Force, G. K. Czamanske, and W. J. Moore found that Bingham ore, for example, averages about 0.3 percent rutile in grains averaging about 0.03 by 0.06 mm. The potential supply

based on present mining rates of this deposit alone is more than 20 percent of domestic rutile consumption. The rutile in porphyry deposits is secondary and forms by alteration of primary sphene, ilmenite, and titanium-biotite.

Resource potential of bedded iron deposits in the Tobacco Root Mountains, Montana

Studies by H. L. James show that metamorphosed iron-formation forms distinctive units in the Archean metasedimentary sequences of southwest Montana. In the Tobacco Root Mountains, the principal bed occurs in a tightly folded northerly trending belt on the western side of the range, interbedded with dolomite marble and various gneisses and schists. The thickest and most continuous occurrence is in the Copper Mountain area, where the iron-formation averages 30 to 60 m in outcrop width along the limbs and axis of a tight anticlinal buckle within a major syncline. The rock is of excellent quality for use as a taconite ore (the iron content is about 35 percent, most of which is in the form of magnetite), but the quantity is less than that currently required for installation of a modern operation. The gross available tonnage in this belt, to a depth of 100 m, is estimated to be 59,000 t.

Structural control of rhyolite volcanism associated with uranium deposits, Western United States

Geologic mapping by J. J. Rytuba has defined the southern margin of a major early Miocene structure termed the Orovada rift, which strikes northwest and extends 150 km from the Santa Rosa Range in Nevada to the Pueblo Mountains in Oregon. Paleozoic and Mesozoic rocks occur to the south of the rift and are absent in the graben,which is filled with alkali basalts. The faults that constitute the rift in the McDermitt caldera complex were zones of weakness along which the rhyolites in the complex were emplaced for a period of 5 m.y. After volcanic activity ceased in the McDermitt area, the locus of rhyolitic volcanism proceeded westward along the rift. Uranium deposits within the McDermitt caldera complex are closely associated in time and space with the youngest comendites that were erupted from a strongly zoned magma chamber highly enriched in uranium, thorium, and zirconium and depleted in barium and strontium. The recognition of the Orovada rift as the locus of zoned magma chambers defines a large terrain of peralkaline rhyolites potentially important as host for the other uranium deposits similar to those in the McDermitt caldera complex.

Mineralization in the Spirit Lake quadrangle, southern Cascade Range, Washington

The Spirit Lake quadrangle includes three hydrothermally altered areas, all associated with a composite pluton of Tertiary age that crops out over an area of about 100 km^2, according to R. P. Ashley. One area is a porphyry copper prospect that includes biotite-potassic, quartz-sericite-pyrite-tourmaline, and pyritic propylitic zones arranged concentrically around closely spaced fractures. Propylitic alteration dominates the outer parts of this area and is the only alteration type seen in most of the scarce natural exposures of these altered rocks. The core of the area, dominated by quartz-sericite and potassic alteration, contains significant chalcopyrite mineralization. The other two altered areas are dominated by pyritic argillized rocks, locally with intensely leached silicified rocks but with little tourmalization. Small Cu-Pb-Zn-Au-Ag-bearing quartz veins with narrow alteration halos occur elsewhere in the pluton but not closely associated with any of the three altered areas described above. Work continues on the relations between the vein deposits, porphyry mineralization and associated alteration, and argillization.

Chromite and nickel, western Cordillera

A study by J. P. Albers was aimed at developing a geological-geophysical technique for detecting hidden podiform chromite deposits in the Josephine ultramafic mass, Del Norte County, Calif., disseminated chromite deposits in northern Siskiyou County, Calif., and the possible occurrence of large deposits of this type in the western Cordillera of the United States. Another objective was appraising the potential of nickeliferous laterites developed on the ultramafic rocks.

The geological results suggest that, in the Low Plateau area of Del Norte County, podiform chromite occurs sporadically along foliation trends in the peridotite. However, the geologic control for any particular chromite occurrence remains obscure, other than that chromite deposits always occur in dunite. This suggests that the foliation trend is a primary foliation developed perhaps when the ultramafic rock crystallized rather than during a later metamorphic event.

The geophysical results show that no single geophysical method gives unequivocal identification of hidden or buried podiform chromite, but that a combination of gravity, magnetics, seismics, and complex resistivity could be used to explore successfully if used in a systematic fashion. Some of the geophysical signatures appear to be secondary or associative in nature, raising the possibility that a specific method or combination of methods might be site specific and might fall in an area other than where it was developed.

The disseminated chromite deposits in the Seriad Creek and McGuffy Creek districts, Siskiyou County, are estimated to contain 300,000 t of rock containing an average of 8 percent Cr_2O_3. Individual deposits range in size from 200 to 135,000 t and consist of thin parallel layers on linear lenses of chromite in dunite. Individual

deposits and lenses of chromite are elongated parallel to flatly plunging lineations in the foliated peridotites. The chromite contains 54 to 59 percent Cr_2O_3 with a chromium to iron ratio of 2.2 to 2.8.

In addition to the economically important nickel laterite at Riddle, Oreg., nickel laterites overlie fresh to moderately serpentinized Jurassic or Cretaceous peridotite elsewhere in scattered areas in Tertiary erosion surfaces in southwestern Oregon, northwestern California, and the western Sierra Nevada, Calif. It is estimated that these undeveloped deposits have a resource potential of 96,000,000 t of laterite and saprolite containing 0.7 to 1.2 percent nickel and 0.05 to 0.08 percent cobalt.

Arizona molybdenum mineral associations as keys to ore deposit metallogenic types

A comprehensive literature survey by J. C. Wilt and S. B. Keith (Arizona Bureau of Geology and Mineral Technology) has located some 300 occurrences of molydenum in Arizona, the world's third largest molybdenum producer. In Arizona, molybdenum occurs in four major geologic habitats: (1) as molybdenite (also as lindgrenite and ferrimolybdite oxidation products) in the potassic cores of lower Tertiary porphyry copper sulfide systems, (2) as wulfenite in the oxide zone of Upper Cretaceous and middle Tertiary lead-silver-zinc deposits, (3) as powellite and molybdenite associated with scheelite and wolframite in tungsten fissure vein deposits, and (4) as ilsemannite, umohoite, and jordisite associated with uranium and vanadium oxysalts in sandstone uranium deposits on the Colorado Plateau.

In Arizona's Basin and Range province, the first two occurrence types are almost mutually exclusive. Molybdenite usually occurs in the potassic cores of porphyry copper sulfide systems near the center of the district zoning. Little or no wulfenite is found anywhere in those sulfide systems. In contrast, much larger amounts of wulfenite are found in the oxidized portions of lead-silver-zinc districts. None of these districts has produced more copper than lead plus zinc. Also, wulfenite-bearing districts consistently lack molybdenite, contain more lead than zinc, and are associated with more potassic igneous rocks than those districts that contain porphyry copper mineralization. Thus, the occurrence of large amounts of wulfenite is a guide to lead-silver-zinc districts but not to porphyry copper districts.

The unoxidized zones of wulfenite-bearing lead-silver-zinc deposits contain no reported molybdenum minerals or anomalous molybdenum contents. This fact, combined with the late paragenetic occurrence of wulfenite (generally after cerussite crystallization), suggests that molybdenum in the oxide zones of lead-silver-zinc deposits is exotic in character and was transported to the sites of oxidizing lead-silver-zinc deposits by meteoric ground waters, where it reacted with the oxidized lead minerals to form wulfenite.

Greenstone in the Havallah Formation, Nevada

Geologic mapping by D. H. Whitebread and M. L. Sorensen in the southern East Humbolt Range, Nev., has disclosed several large units of greenstone in the Havallah Formation of late Paleozoic age. The greenstones are of particular interest because of their potential for the occurrence of massive sulfide deposits. Locally, the greenstones contain small siliceous manganese deposits and copper-bearing quartz veins, but no disseminated sulfides or their gossans have been found.

Initial strontium ratios of plutonic rocks along the "Uinta trend," northwestern Utah

W. J. Moore and R. A. Armin report that initial strontium ratios for Upper Cretaceous and Tertiary plutonic rocks increase systematically westward from the Park City area (~0.7060), through the Bingham mining district (~0.7085), to the Gold Hill district (~0.7010) on the Utah-Nevada border, a distance of over 200 km. These igneous centers lie along an inferred westward prolongation of the Uinta arch commonly termed the Uinta trend; emplacement of the plutons was apparently guided by a deep-seated zone of crustal instability.

More than one source or mechanism of generation is necessary to explain the westward increase. For instance, the magmas may have been derived from progressively shallower source regions westward from the Park City area or from a lower crustal source and differentially contaminated by sedimentary rocks enriched in radiogenic strontium. "Hot spots" in the belt of metamorphic core complexes along the Utah-Nevada border may have enabled a more efficient scavenging of radiogenic strontium during magma generation.

Massive copper sulfide deposit of syngenetic- epigenetic origin, north-central Nevada

Sulfur isotopes and textures in sulfide minerals at the Big Mike mine, Pershing County, north-central Nevada, have been investigated by R. O. Rye and R. J. Roberts. The sulfides are of two contrasting textural and isotopic types: early fine-grained laminated framboidal pyrite with a $\delta^{34}S$ value of -22.3 per mil and later coarse-grained pyrite and chalcopyrite with $\delta^{34}S$ values ranging from -6.36 to $+5.54$ per mil. Coarsely crystalline pyrite-chalcopyrite pairs in equilibrium apparently formed at temperatures between 250° and 310°C.

These data are compatible with the formation of the early framboidal pyrite syngenetically on the sea floor in

a euxinic environment and of the coarse-grained pyrite and chalcopyrite epigenetically after burial beneath sedimentary and volcanic rocks. Djurleite replaces part of the chalcopyrite and probably formed at a temperature of <93°C during the latest part of the epigenetic stage or early in the supergene stage. Digenite and covellite also were precipitated in the deposit during supergene metallization, increasing the grade of the deposit from an estimated 2 to 3 percent copper to 10.5 percent. The deposit yielded more than 90,700 t of direct shipping ore in 1970.

Geochemical comparison of mineralized and barren stocks, Arizona

A comparison by S. C. Creasey of the major elements chemistry of barren and mineralized Laramide stocks in the Globe-Miami and Ray porphyry copper districts and the porphyry at nearby Granite Basin and Tea Cup Granodiorite indicates that the stocks related to ore deposits have a $Si/Fe^{+3}+Fe^{+2}+Mg+Ca+Si$ greater then 0.9 and a $K/Fe^{+3}+Fe^{+2}+Mg+Ca+K$ greater than 0.36. In contrast, the minor elements showed no consistent relations to either the barren or mineralized stocks indicated above.

The REE were obtained for the Schultze Granite (mineralized stock, Globe-Miami district), Tea Cup Granodiorite (weakly mineralized), and the porphyry at Granite Basin (unmineralized). The normalized abundance curves of all three rocks were distinctive, and all three indicate strong fractionation relative to meteoritic REE abundances. There was nothing in the REE data for the Schultze Granite to indicate that it had undergone any fractionation that the other two stocks had not. Therefore, REE data do not support the model that porphyry copper mineralization results from fractionation of a high level magma.

Stream sediment geochemical survey, southwestern Rawah Range, northern Colorado

M. E. McCallum reports that the southwestern flank of the Rawah Range is characterized by a system of arcuate and converging radial faults that cut granitic rocks of the Rawah batholith along with associated xenoliths of metaigneous and metasedimentary units. The fault pattern is similar to that observed in some mineralized districts underlain by shallow plutons. A reconnaissance stream sediment sampling program was undertaken to evaluate the area for potential geochemical anomalies. Samples were analyzed by the 6-step D.C. arc spectrographic method for 31 elements; copper, silver, and molybdenum also were determined by atomic absorption, and uranium determined fluorimetrically. No highly significant base metal anomalies were recorded. Gold and zinc were not detected. Silver concentrations did not exceed 0.15 ppm. Copper and lead levels ranged to 50 and 70 ppm respectively, and molybdenum, although detected in most samples, rarely exceeded 1.5 ppm (maximum value 4 ppm). Anomalous levels of uranium (as much as 73 ppm) were recorded at several localities, and the highest values appear to be related directly to sample site proximity to fault zones. Elevated uranium concentrations in fault zones may result from leaching of uranium from the host granite at Rawah Range, which averages approximately 23 ppm of uranium in the area.

Uranium potential of newly recognized caldera near Manhattan, Nevada

According to D. R. Shawe, a newly recognized caldera about 13 km across and filled with Miocene (25-m.y.-old) volcanic rocks is situated between Manhattan and Round Mountain, Nye County, Nev. Gold mineralization at Round Mountain occurred at the time of caldera formation (25 m.y. ago). Gold mineralization at Manhattan was younger (16 m.y. old) and possibly occurred at the time of intrusion of undated rhyolite plugs just south of Manhattan that are surrounded by an area of fluorite mineralization.

Two metal-mineralized samples collected from hydrothermally altered Paleozoic rocks near Manhattan at the south margin of the caldera contain anomalously high (0.05–0.1 percent) uranium. The presence of anomalous uranium near the caldera, both near Manhattan and, as previously known, near Round Mountain, suggests that the caldera structure and its contained volcanic rocks should be explored thoroughly for possible uranium deposits.

Stratabound Precambrian sulfide and gahnite deposits in the Pearl area, Colorado and Wyoming

Recent field investigations by W. H. Raymond and D. M. Sheridan in the vicinity of the old mining camp of Pearl in Jackson County, Colo., have indicated the presence of numerous stratabound Precambrian copper-zinc sulfide deposits in a northeast-trending area at least 12 km long and 9 km wide, overlapping into the adjacent part of Carbon County, Wyo. Host rocks at the deposits consist of intimately interlayered rocks of several types that are found typically as the hosts of numerous Precambrian sulfide deposits elsewhere in Colorado: garnetiferous and sillimanitic gneisses, calc-silicate and hornblende gneisses, and amphibolites containing layers rich in anthophyllite. Occurrences of the zinc spinel gahnite are numerous and widespread. In one area lying between sulfide deposits, gahnite occurs in noteworthy amounts in a sillimanitic quartz-mica gneiss that is 30 m thick and traceable for at least 0.5 km along the strike. Mineralized shear zones, principally of the copper-bearing type, are present also in the Pearl area but prob-

ably have less economic potential than the deposits of the strata-bound type.

Intrusion and mineralization in Moccasin Mountains, Montana

Mapping of the North and South Moccasin Mountains of central Montana by D. A. Lindsey and radiometric dating by R. F. Marvin, C. W. Naeser, and Lindsey have outlined the history of magmatism and mineralization of two intrusive complexes. The intrusive cores of both mountains were emplaced as laccoliths of calc-alkalic syenite about 65 m.y. ago; the South Moccasin Mountains were intruded by quartz monzonite soon after. Minor(?) base metal mineralization accompanied or closely followed intrusion. Then, both intrusive and mineralized rocks were penetrated by breccia pipes that extended more than 1 km vertically and may have reached the surface. Major gold mineralization, possibly about 45 m.y. to 50 m.y. ago, followed igneous activity in the North Moccasin Mountains.

Cretaceous volcanism and plutonism, Montana

The structural environment and controls of Cretaceous volcanism and plutonism in the Boulder batholith region, Montana, have been studied by W. R. Greenwood, C. A. Wallace, and J. E. Selverstone. Isopach maps show that the Boulder batholith occupies the site of an Early Cretaceous foreland rise. The rise lay east of an active magmatic arc in Idaho, a thrust belt in western Montana, and a foreland basin in west-central Montana. The foreland rise probably resulted from a rise of hot mantle material into the crust, perhaps in isostatic response to loading in the thrust belt and foreland basin. Doming and major erosion in the Boulder batholith region probably were produced by dilation resulting from anatectic melting and formation of a magma chamber(s) above the mantle rise just before Late Cretaceous volcanism (81 m.y.–77 m.y. ago). Doming was accompanied by thrusts west of dome and by large-scale folds and reverse faults on the east. These structures and the dome have east vergence. In mid-volcanic time, regional shortening waned, and thick welded tuff units were deposited in a major half graben over the present batholith and in several adjoining cauldrons to the east. Regional extension and volcanic withdrawal triggered emplacement of the batholith at its present level by hydraulic transfer of magma from a deep chamber(s) up along the steep eastern-bounding fault of the graben to form a tabular body with a subhorizontal roof and gently eastward-dipping floor. Room for the batholith was provided by subsidence of the floor as magma was withdrawn from the chamber below. A low-pressure hydraulic system supported a roof (2–3 km thick) largely composed of contemporaneous pyroclastic deposits produced by intermittent venting of the batholith.

Granodiorite augen gneiss-tonalite-metagabbro—the earliest magma series in the Cretaceous Idaho batholith

Reconnaissance field studies by W. R. Greenwood west of the Bitterroot lobe of the Idaho batholith suggest new interpretations of the orogenic history of the area. Granodiorite augen gneiss, which contains zircon dated by lead methods at about 1,450 m.y. (Reid and others, 1979), grades into tonalite gneiss near Elk City, Idaho. Similar tonalite gneiss cuts interbedded white and dark-gray marble and pyritiferous metagraywacke on U.S. Route 12, just west of Syringa, Idaho. These metasedimentary rocks are lithologically similar to rocks of the Paleozoic or Mesozoic Squaw Creek Schist of Myers (1969) near Harpster, Idaho, 15 km south-southwest and along strike with the Syringa rocks. These contact relations indicate that the augen gneiss and tonalite gneiss are no older than Mesozoic in age. These igneous rocks, along with metagabbro, appear to constitute the earliest magma suite of the Cretaceous Idaho batholith. This magma suite intruded the structural contact of Mesozoic oceanic and island-arc facies on the west with Precambrian metasedimentary rocks on the east, probably during or shortly after the juxtaposition of these rocks.

Model for the origin of hydrothermal uranium deposits near Marysvale, Utah

Studies by T. A. Steven show that hydrothermal uranium deposits are localized in veins that cut granitic and volcanic rocks near Marysvale, Utah. The deposits are in the eastern source area of the Mount Belknap Volcanics where shallow cupolas were progressively emplaced over a larger magma chamber between 21 m.y. and 16 m.y. ago. Most veins are in an elongate area 500 by 1,300 m across, at the center of a fracture pattern that reflects local distention imposed on regional late Cenozoic basin-range deformation. The principal ore minerals in the veins are uraninite, coffinite, jordisite, and umohoite, which occur in a matrix of fluorite, quartz, and minor pyrite. Fluorine-rich hydrothermal fluids, at 150°C and low pH and oxygen fugacity, reacted with the wall rocks to form kaolinite alteration products and to deposit the ore minerals. The fluids were progressively oxidized closer to the surface, sooty pitchblende and fluorite were deposited, and the wall rocks were altered to an oxidized hematite-bearing assemblage. The structural and chemical patterns are believed related to an unexposed epizonal stock that potentially may localize a porphyry-type molybdenum deposit.

Gravity features related to location of mineral deposits in North Carolina

The preliminary Bouguer gravity map of the Charlotte 2° quadrangle prepared by F. A. Wilson and D. L.

Daniels closely reflects the lithotectonic belts of the Piedmont of the Carolinas. Most of the 400 mines, prospects, and mineral localities in the quadrangle are spatially related to major gravity anomalies. This relation is most clearly expressed in the Kings Mountain belt. Iron deposits are located along the east side of the elliptical −26 mGal maximum gravity high in eastern Catawba County, iron sulfide deposits occur along the west side of the elliptical −38 mGal maximum high that crosses the boundary of Lincoln and Gaston Counties, and tin and spodumene deposits in west-central Gaston County coincide with the expansion of the narrow gravity gradient along the Kings Mountain shear zone, the Kings Mountain–Inner Piedmont boundary. A new alluvial tin deposit, in a previously unmined area, reported by J. W. Whitlow and J. P. D'Agostino is located at the southeast end of a northwest-southeast −52 mGal minimum gravity low along the eastern border of Cherokee County, S.C., and Cleveland County, N.C. This anomaly probably reflects a particular rock type of structure. Such a relation may be a clue to other discoveries of tin.

Massive sulfide deposits in ophiolitic terrain, northern Klamath Mountains, Oregon and California

Field work by R. A. Koski and R. E. Derkey in the northern Klamath Mountains near Takilma, Oreg., indicates that iron-copper-zinc sulfide deposits are part of an ophiolitic melange terrain previously assigned to the Applegate Group. Discontinuous layers and lenses of massive pyrite and (or) pyrrhotite with subordinate chalcopyrite and sphalerite are distributed along a north-south-trending contact between a greenschist-facies diabase-basalt complex and serpentinized peridotite and also are related spatially to large mafic xenoliths within serpentinite. Pyrite is the dominate sulfide phase in the diabase-basalt complex; pyrrhotite is dominant in mafic xenoliths and in sulfide pods in serpentinite. No stockwork or stringer mineralization has been observed. The composition and configuration of the deposits suggest that a once continuous or nearly continuous zone of sulfide mineralization in the mafic igneous complex was severely fragmented during accretion of the ophiolitic terrain and subsequent emplacement of serpentinized ultramafic rocks.

Possible hydrothermal signature in Belt stratabound copper deposits, Montana

J. J. Connor reports that stratabound copper-silver mineralization in quartzites of the Spokane Formation of the Ravalli Group (Belt Supergroup) in the Rogers Pass area, Montana, appears to exhibit a distinct trace element signature where the quartzites occur close to known outcrops of Tertiary plutons. Seven samples from outcrops of stratabound occurrences located within 4 km of the intrusions averaged 1.5 ppm of antimony, 3 ppm of arsenic, and 0.7 ppm of mercury compared to 0.2 ppm of antimony, 0.8 ppm of arsenic, and 0.1 ppm of mercury in 17 samples collected from occurrences more than 6 km away. As most of these occurrences are generally viewed as early postdepositional in origin, the patterns in these volatile metals may be reflecting a hydrothermally induced overlay signature on those occurrences near plutons.

Deep exploration target at Red Mountain stockwork, Yellow Pine, Idaho

The Red Mountain stockwork presents a target for deep exploration for tungsten, molybdenum, and other metals. Red Mountain is 8 km north-northeast of Yellow Pine settlement, Valley County, Idaho, in secs. 2, 3, 10, and 11, T. 19 N., R. 8 E. (Boise Meridian). The area is being mapped and studied by B. F. Leonard III.

The stockwork, about 1.5 km in diameter, is part of a major silicified zone in the outer ring fracture zone of the Thunder Mountain cauldron. The stockwork consists of myriad quartz veinlets and thin quartz veins in sheared and fractured granodiorite of the Idaho batholith. The stockwork envelops a quartz core that strikes north-northwest and is 430 m long by 120 m wide. Small dikes of Tertiary rhyolite and latite cut both core and stockwork. Some dikes strike east-northeast; others radiate from points in and near the core. Small faults radiate from some of the intrusive centers, and a radial fault pattern centered on the core is recognizable on the 1:48,000-scale map of the northwest half of the stockwork. Suites of alteration products typical of the propylitic, argillic, and phyllic alteration zones that accompany porphyry molybdenum and copper deposits have been identified in a few preliminary samples from Red Mountain. These samples show a systematic distribution of kaolinite-sericite, sericite, and chlorite-epidote-calcite outward from the quartz core. Pyrite is widespread as sparse minute crystals. Other sulfides are rarely seen. Molybdenite, not previously reported from the area, is present in a sample collected from the dump of a long adit whose portal is near the outer edge of the stockwork and 500 m lower than the apex of the quartz core. Scheelite and gold were found as float so long ago that the exact location of the discoveries on Red Mountain is uncertain. The conjunction of quartz-cored stockwork, radial dikes, and radial faults in a large crudely circular area affected by pyritic, propylitic, argillic, and phyllic alteration suggests that one or more Tertiary stocks lie at depth beneath Red Mountain. Though surface indications of metallization are weak, they may be a clue to the existence of disseminated

deposits of tungsten, molybdenum, and other metals within the inferred stocks.

Domestic minerals exploration program

Three successive programs of financial assistance to private industry to stimulate exploration for domestic mineral reserves have been provided by the DOI since 1950 (see table). These were the Defense Minerals Administration, 1950–51, and the Defense Minerals Exploration Administration, (DMEA) 1951–58, programs, both authorized under the Defense Production Act of 1950, as amended. The present Office of Minerals Exploration (OME), authorized under Public Law 85–701, August 21, 1958, was originally an independent agency in the DOI. On June 30, 1965, it was transferred to the USGS. Activities within OME have not been funded since 1974.

Travertine at Poncha Hot Springs, Chaffee County, Colorado

Travertine deposits at Poncha Hot Springs, Chaffee County, Colo., a known geothermal resource area (Barrett and others, 1976) contain calcite, opal, fluorite, and tungsten-bearing manganese oxides. The deposits are at an elevation of 2,425 m in SW¼ sec. 15, T. 49 N., R. 8 E. They formed downslope from north- and west-trending major fault zones that are extensively mineralized with fluorspar. The north-trending fault zone is part of the Rio Grande rift system, which extends from New Mexico to Wyoming (Tweto, 1979). Travertine occurs here chiefly as two aprons in gullies that slope northwest along the north face of Poncha Mountain. The deposits rest on reddish colluvium overlying Precambrian gneiss.

The travertine is largely fine-grained, porous, partly cemented, crudely layered, calcareous and manganiferous, black, gray, buff, and white tufa. A semiquantitative spectrographic analysis showed Ca, Mn, Ba, Si, W, and rare earths. A separate analysis for fluorine showed 3.35 percent, corresponding to 6.9 percent fluorite. Samples tested with a scintillometer were found to be radioactive; analyses showed 0.001 percent uranium and radium. The manganese oxides contain 30 percent manganese and are a mixture of pyrolusite and romanechite, Ba, $Mn^{+2}Mn_8^{+4}O_{16}(OH)_4$, the crystalline form of psilomelane.

The alkaline hot spring water is high in sodium, silica, bicarbonate, sulfate, and fluorine (12 ppm) and is saturated with respect to fluorite at its temperature of 76°C.

Mountain, saline water, and hot water forms of diatoms in the travertine were studied by G. W. Andrews, who found that the species and varieties identified in these collections are all recorded in Holocene deposits and that the absence of any extinct species or varieties suggests that the hot spring deposits at Poncha Springs are either late Pleistocene or Holocene in age.

The association of the hot springs with fluorite-bearing major tensional fault zones indicates continued deep hydrothermal circulation from underlying thermal zones. Many continental rifts like the Rio Grande rift system are associated with major fluorspar districts throughout the world (Van Alstine, 1976).

GEOCHEMICAL AND GEOPHYSICAL TECHNIQUES IN RESOURCE ASSESSMENTS

GEOCHEMICAL RECONNAISSANCE RESULTS

Regional geochemical studies, Patagonia Mountains, Arizona

In the Patagonia Mountains, Santa Cruz County, Ariz., M. A. Chaffee, R. H. Hill, S. J. Sutley, and J. R. Watterson collected 300 stream sediment samples along drainages and analyzed them for 32 elements. In spite of the variety of rock types present throughout the Patagonia Mountains, background lead and tellurium concentrations throughout this range generally were found to be well above regional background concentrations determined for these elements in southern Arizona.

High concentrations of gold, tellurium, and boron and low concentrations of manganese occur in north-northwest-trending zones that transect the range roughly parallel to the major north-northwest structures and to the west of Red Mountain. Lead and silver anomalies correlate with each other throughout the Patagonias; copper anomalies do not coincide with those of molybdenum or any of the other elements studied.

The Red Mountain porphyry copper system is best delineated by high concentrations of molybdenum, lead, and tellurium coincident with low concentrations of manganese. The coincidence of this combination of elements elsewhere in the range suggests the presence of other blind porphyry systems.

Potential uranium mineralization, Mineral Mountains, Utah

In the Mineral Mountains area of the Richfield 2° quadrangle, Utah, W. R. Miller interpreted the results of uranium analysis and *Q*-mode factor analysis of 30 water and 29 stream sediment samples to indicate the potential for uranium deposits in the area. The most favorable areas are in a granitic pluton near its contacts with sedimentary and metamorphic rocks. The uranium anomalies most likely are derived from uraninite-bearing veins along faults and fractures within the pluton.

Summary of OME and DMEA programs from 1958 to 1979

[Values are in millions of dollars]

	8-21-58 to 6-30-65 (DOI)	7-1-65 to 10-1-79 (USGS)	Total	Royalties received			Losses written off		
				FY 1979	Prior to FY 1979	Total	FY 1979	Prior to FY 1979	Total
OME:									
Number of contracts executed	101	110	211	---	---	---	---	---	---
Certified discoveries	13	44	57	---	---	---	---	---	---
Total contract value	$6.7	$6.6	$13.3	---	---	---	---	---	---
Government's share	$2.5	$2.4	$4.9	---	---	---	---	---	---
Disbursements for contract work	$1.5	$3.4	$4.9	---	---	---	---	---	---
Values of reserves	$16.0	$147.0	$163.0	---	---	---	---	---	---
Fiscal data	[1]	[1]	[1]	0	[2]$0.484	[2]$0.484	$0.5	$3.0	$3.5
DMEA, fiscal data	---	---	---	$26.0	$7,175.000	$7,201.000	$435.0	$15,146.0	$15,581.0

[1] Not reported until August 31, 1966.

[2] Distribution to principal and interest not available.

Gold and sapphires in Tertiary gravels, Sapphire Range, Montana

In the Butte 1°×2° quadrangle, Montana, J. C. Antweiler found gold distributed through thicknesses of 10 to 30 m or more in a veneer of Tertiary gravels that blanketed parts of the Sapphire Range. These gravels previously have not been prospected extensively because they are commonly on the flanks of forested ridges where no water is available. Some of these gravels were found to contain sapphires (C. A. Wallace, G. K. Lee, and J. C. Antweiler, oral commun., 1979).

Cassiterite and columbite, Charlotte 2° quadrangle, North Carolina

In the Charlotte 2° quadrangle, North Carolina, W. R. Griffitts found cassiterite and columbite in the granites at Brown Mountain and south of Salisbury, in the Cherryville pluton southwest of Kings Mountain, and in the well-known pegmatite belt that passes through King Mountain. Cassiterite also was found nearly 15 km west of the Cherryville pluton, as well as within it.

Lead and zinc, Choteau 2° quadrangle, Montana

During lead-zinc investigations in the Choteau 2° quadrangle, Montana, D. J. Grimes and R. W. Leinz used an oxalic acid leach of a banded Cambrian unit, the Flathead Sandstone, to locate several occurrences of lead-zinc mineralization in carbonate host rocks that were spatially related to the Flathead Sandstone. This relation suggests that the permeable sandstone was a channelway for mineralizing solutions. The separation of the limonitic fraction of the sandstone by an oxalic acid leach followed by multielement emission spectrographic analysis proved a useful geochemical technique for defining favorable areas for lead-zinc mineralization as well as for yielding information important in ore genesis studies.

Geochemical definition of mineral province, Alaska Range, Alaska

A regional study by G. C. Curtin and W. D. Crim of heavy-mineral concentrate and stream sediment data suggests that a gold-, silver-, tin-, and tungsten-rich belt paralleled the Alaska Range for a distance of more than 450 km. This belt, which is present along the southeast flank of the Alaska Range in the Talkeetna and Talkeetna Mountains 1:250,000-scale quadrangles, Central Alaska Range, cuts across the Alaska Range to the south and is present in the western part of the Lake Clark quadrangle. The belt follows a thick sequence of argillite, graywacke, and phyllite that had been intruded by a number of plutons that ranged in composition from granite to peridotite in the Talkeetna and Talkeetna Mountains quadrangles.

Geochemical definition of mineral province, Brooks Range, Alaska

In the Survey Pass quadrangle, Central Brooks Range, Alaska, J. B. Cathrall showed that mineralization in the quadrangle includes a diverse suite of elements and that areas of mineral occurrences are substantial in size. The most important mineralized areas are: (1) a zone rich in copper, lead, and zinc of stratiform volcanogenic origin, with lesser amounts of silver, antimony, and molybdenum, in the "schist belt" along the south-central flank of the Brooks Range, (2) tin-bearing granite bodies in the Arigetch-Igikpak area, (3) polymetallic contact metamorphic mineralization around the Arigetch-Igikpak plutons, and (4) copper, lead, and zinc sulfide mineralization in the northwest part of the quadrangle.

Geochemical evidence for mineral deposits, Petersburg and Port Alexander quadrangles, Alaska

Preliminary synthesis of chemical data on stream sediment samples and heavy-mineral concentrates from the

Petersburg and Port Alexander quadrangles, Alaska, by J. B. Cathrall indicates that the suite of Cu, Pb, Zn, and Ba outline a possible massive volcanogenic sulfide trend and that the additional suite of Cu, Ag, Sn, W, and Mo indicate areas of potential polymetallic contact metamorphic mineralization. Likewise, suites of elements associated with thorium, molybdenum, and lanthanum suggest a potential for uranium.

Geochemical lineament, Iron River 2° quadrangle, Michigan and Wisconsin

In the Iron River 2° quadrangle, Michigan and Wisconsin, H. V. Alminas interpreted chemical data from samples of B-horizon soils that delineate a set of northeast- and northwest-trending geochemical lineaments. These geochemical trends generally transect the predominant geologic fabric within this quadrangle and are independent of the soil types occurring along them. A high correlation between the lineaments based on Landsat imagery and gravity data and the geochemical lineaments is evident. Lineament intersection areas as well as areas of lineament-favorable rock unit intersections are frequently anomalous in copper content.

Geochemical features, Pinaleno Mountains, Arizona

K. C. Watts identified a geochemically enriched area in the southern Pinaleno Mountains of Arizona measuring approximately 235 km^2. This area is situated on and adjacent to a major regional tectonic feature, but mines do not exist in the area, and prospects are few. Much of the area contains dispersed metallization, but the magnitude of many of the analytical values (using enhancement techniques) suggests that local concentrations of metal of ore grade are possible. Leakage along dike-host rock contacts within the many rhyodacite dike swarms in the area appears to be the mode of metal dispersion. The major regional tectonic feature, the Stockton Pass fault, trends northwesterly, and displacement is left-lateral. This fault also appears to have localized metallization because geochemical anomalies in Mo, Bi, W, Ag, Au, As, and the mineral fluorite show close spatial relation to the zone, which is approximately 1.6 km in width. The fault zone not only appears to have localized metal concentrations, but also it may control the occurrence of a volcanic center south of it that contains geochemical anomalies of the same metals, most prominently molybdenum and bismuth.

Geochemical reconnaissance studies, Papago Indian Reservation, Arizona

Using reconnaissance studies on the Papago Indian Reservation, Ariz., J. H. McCarthy, Jr., observed significant variations between concentrate fractions of stream sediment samples. The higher concentration of many elements in the nonmagnetic (sulfide) fraction reflects the dominant physical weathering in this arid environment and indicates that geochemical dispersion patterns are more easily detected and followed using these media. Geochemical zoning patterns in bedrock samples reveal both regional and local trends that indicate areas of high potential for both base and precious metal deposits. These data provide a base for evaluating the effectiveness of geochemical exploration in this part of the Basin and Range province.

GEOCHEMICAL PROCESSES

Movement of trace elements in weathering environment

Studies by B. R. Berger on processes that control the movement of trace elements in the weathering environment indicate that streams in southwestern Montana draining areas where there is no significant mineralization reach a steady state with respect to chemical speciation. The results show that about 80 percent of the trace elements were transported as silicates or oxides and that most of the remainder were complexed by organics. Where significant mineralization occurs, the steady state was disrupted at the point of entry of the metals into the stream, and most of the trace metals were complexed by organic matter. Downstream from the metal source, the speciation moved systematically back towards the steady-state condition of dominantly silicate and oxide complexing. The amount of metal also decreased downstream. The rate at which the metal anomaly disappeared was a function of the mineralogy of the metal complexes entering the streams. Organic complexes appeared to flourish on a carbonate substrate, removing metals more quickly than either sulfides or oxides.

HYDROGEOCHEMICAL PROSPECTING

Arsenic, copper, and molybdenum, Baboquivari Mountains, Arizona

G. A. Nowlan extended a hydrogeochemical study of well waters that he reported last year to include all of the Baboquivari Mountains both on and off the Papago Indian Reservation. The extended study shows definite areal patterns of arsenic, copper, and molybdenum. Some of the patterns are related to various bedrock units within the mountain range, but one of the patterns, which was made up of anomalous molybdenum in the center, anomalous copper on one side, and anomalous arsenic on the opposite side, appears to be related to mineralization. The area of anomalous molybdenum contains old tungsten mines, and the area of anomalous copper is an old precious- and base-metal mining district.

Geochemical study of water and sediment, Rio Tanama district, Puerto Rico

According to R. E. Learned, T. T. Chao, and R. F. Sanzolone, who conducted a comparative geochemical study of water and sediment in streams of the Rio Tanama porphyry copper district, Puerto Rico, water has become a more practical sampling medium for geochemical exploration since the recent development of instrumentation that allows direct determination of submicrogram amounts of metals in a few milliliters of water. Determinations of the trace metals Cu, Mo, Pb, and Zn in stream water and sediment were performed to ascertain their relative effectiveness as geochemical exploration media. Sulfate determinations also were made on water. The results indicate that copper is the most useful trace element in both water and sediment in terms of optimal anomaly-to-background ratios and delineation of the known deposits. However, the "easily extractable" copper in sediment yielded appreciably higher ratios than did the "total" copper in sediment or the dissolved copper in water. Sulfate in water is an especially useful geochemical indicator because it facilitates the detection of the extent of hydrothermal alteration (which was a much broader target than the extent of copper mineralization) and because it has a downstream dispersion train much longer than that of any of the metals in either sediment or water.

REMOTE SENSING APPLIED TO GEOCHEMICAL EXPLORATION

Remote detection of geochemical soil anomalies

The feasibility of aerial detection of geochemically stressed vegetation associated with concealed sulfide deposits using a specially designed spectroradiometer (Chieu and Collins, 1978) and by computerized waveform analysis was confirmed at a higher confidence level by F. C. Canney and G. L. Raines (USGS) and William Collins (NASA and Columbia University). At Cotter Basin, Mont., where a mineralized zone is concealed by thick soil and vegetation, the areas of anomalous spectral reflectance in the forest canopy mapped in 1978 agree quite well with the location of the mineral zone and also match, within acceptable limits, the anomalous spectral areas detected in 1976. The spectral region that appears most altered is between 550 nm and 750 nm, and the most diagnostic spectral variation appears specifically to be on the wings of the red chlorophyll *a* band centered at about 680 nm. The spectral differences are subtle, but the high resolution (1.4 nm) of the spectroradiometer and of the sophisticated waveform analysis techniques employed permits their detection.

VOLATILE GASES USEFUL IN GEOCHEMICAL EXPLORATION

Helium and sulfur, Poorman fault, Colorado

M. E. Hinkle collected soil samples along the Poorman fault west of Boulder, Colo., and analyzed them for helium and sulfur. Average concentrations of helium in soils are higher along the fault than away from it. Concentrations of helium in soils are below average over a mineralized part of the fault. Concentrations of sulfur compounds are higher along the fault than away from it and are highest over the mineralized part of the fault.

Spectral investigation of sulfur dioxide

Using a ratiometer, R. C. Bigelow measured the differential absorption of 100 ppm of sulfur dioxide in nitrogen at wavelengths between 298.2 and 300.7 nm. A relative maximum of absorption was found at 300.2 nm and a relative minimum at 299.6 nm. In a 0.5-m-long tube, the difference in absorption was 12 percent in a mixture of 100 ppm SO_2 in nitrogen. In a 20 ppm mixture, the difference dropped to approximately 2 percent – the limits of reproducible detectability with the ratiometer.

SAMPLE MEDIA USEFUL IN GEOCHEMICAL EXPLORATION

Iron and manganese oxides, Pinos Altos district, New Mexico

R. H. Carpenter, T. T. Chao, and R. F. Sanzolone evaluated metal relations in iron-manganese oxide coatings on joints as a geochemical exploration tool, in the Pinos Altos district, New Mexico. Forty-eight samples were collected that contained an exposed coating of iron-manganese oxides at an average sample density of one sample per 1.5 km^2. The samples were treated with 3 percent oxalic acid, and the resulting solutions were evaporated to dryness. The residual oxalic acid was oxidized with 30 percent H_2O_2, and the solutions were again evaporated to dryness. The residue was analyzed for Fe, Mn, Cu, Zn, Pb, Cd, Bi, Mo, As, and Ag. The data were normalized to ratios in which metal:(Fe+Mn) is considered to represent an intensity factor and metal:metal (for example: Cu:Zn, Zn:Pb, and so forth) is considered to represent a metal zoning factor.

Intensity factors reveal higher metal concentrations in joints in the northern one-half of the Pinos Altos stock and adjacent country rocks. Zinc anomalies occur in the vicinity of the larger zinc-replacement deposits, but the buried copper-zinc skarn deposit was not indicated. Superposition of contoured metal:(Fe+Mn) maps reveals a semicircular metal distribution pattern

centered in the northwestern portion of the Pinos Altos stock. From the center outward, the general succession is Mo, Mo-Cu, Cu-Zn, and Pb-As-Zn.

The most pronounced trend in metal:metal ratios is a northwest-trending linear zone extending from the east-central boundary of the Pinos Altos stock through the northwestern boundary of the stock into adacent sedimentary rocks. This trend, which is well defined by CU:(Zn+Pb) and Fe:Mn, includes several known metal occurrences.

ANALYTICAL METHODOLOGY USEFUL IN GEOCHEMICAL EXPLORATION

Liquid ion exchange technique

Using liquid ion exchange and concomittant solvent extraction, J. G. Viets (USGS) and J. R. Clark (Colorado School of Mines) developed a system for separation and multielement determination of 18 different elements of interest in geochemical exploration. The organic separation isolated and concentrated the elements of interest away from possible major element interferences such as iron, manganese, and calcium in the sample digestion solution of rocks, soils, and stream sediments. The metals and metalloids in the organic phase were determined by flame or graphite furnace atomic absorption spectroscopy to near or below crustal abundance levels.

Induction-coupled plasma spectroscopy

Using an induction-coupled plasma optical emission spectrograph, J. M. Motooka and S. J. Sutley directly nebulized an oxalic acid leach of stream sediment and soil samples into the plasma to achieve a precise, low-detection limit, simultaneous multielement analysis of major and minor constituents. Preliminary investigations using this technique confirmed geochemical anomalies previously identified by heavy-mineral concentrates of stream sediment.

Atomic absorption method for arsenic

Using electrothermal atomization after hydride generation, R. F. Sanzolone, T. T. Chao, and E. P. Welsch developed an atomic absorption method for determining the presence of as little as 1 ppm of arsenic in rock, soil, or stream sediment samples. There were no significant interferences from Fe, Mn, Bi, Co, Cr, Cu, Ni, Pb, Sb, Se, or Te in the samples. Good results were obtained for geochemical reference samples.

Sensitive method for gold analysis

Using a flameless atomic absorption method, A. L. Meier detected as little as 0.002 ppm of gold in geologic materials. Gold in rock, soil, or sediment samples was dissolved using a solution of hydrobromic acid and bromine, extracted with methyl isobutyl ketone, and detemined with an atomic-absorption spectrophotometer equipped with a graphite furnace atomizer. The higher sensitivity of the method allowed acquisition of useful data about the distribution of gold at or below its crustal abundance.

ANALYSIS OF LINEAR FEATURES

Ajo 2° quadrangle, Arizona

Preliminary analysis of the Landsat data for the Ajo 2° quadrangle by G. L. Raines has resulted in the definition of regional tectonic features and regional mapping of limonite, both of which were related to areas of hydrothermal alteration and mineralization. On the basis of these data, several areas were visited in the field, and all contained at least minor mineralization. Using these data combined with data from geochemistry and geophysics, several areas have been selected as having high mineral potential.

Rio Grande Rift zone, central New Mexico

In the San Juan Basin, G. L. Raines and D. H. Knepper, Jr., note that a preliminary analysis of linear features, mapped from computer-enhanced Landsat images of the region, suggests that major northeast- and northwest-trending lineaments defined by concentrations of linear features along the Rio Grande Rift zone, New Mexico (Knepper, 1978), extends across the San Juan Basin. Along the rift, the lineaments are clearly expressed in available magnetic and gravity maps, indicating that they represent discontinuities in the Precambrian basement. In the San Juan Basin area to the west, the lineaments are reflected by thickness changes in Paleozoic sedimentary strata, occurrences of silicic volcanic rocks of Precambrian age, young volcanic cones and vents, and mapped geologic structures. Of particular interest are two northwest-trending lineaments: one along the linear trend of gas production southeast of Farmington, N. Mex., and the second along the linear trend of uranium mineralization between Laguna and Gallup, N. Mex.

Southern Utah

A preliminary lineament analysis of Utah south of lat 40° N. by G. L. Raines and D. H. Knepper, Jr., showed that (1) the northeast-trending lineaments of Arizona and New Mexico with a 50-km spacing are continuous onto the Colorado Plateau, (2) these northeast-trending lineaments are coincident with Precambrian-age fault zones previously mapped in northwestern Arizona and

into Utah, and (3) the 38th parallel lineament in Nevada continues across Utah into Colorado.

Powder River Basin, Wyoming

In the Powder River Basin, Wyo., block tectonics as defined by G. L. Raines and D. H. Knepper, Jr., from the analysis of lineaments and some field data appeared from analysis of Landsat 5 to 6 ratio images to be a primary controlling factor in definition of paleoenvironments and the resulting lithofacies. Uranium deposits were observed to be associated with particular environments defined by tectonics and lithofacies in this analysis. In addition, several new areas with uranium favorability were defined.

METHODOLOGY IN EXPLORATION GEOPHYSICS

Massive sulfide bodies in Colorado

Using airborne and ground geophysical surveys over known highly metamorphosed massive sulfide bodies in Colorado, F. S. Butterfield and B. D. Smith demonstrated that standard electrical geophysical methods produced, at best, only weak anomalies directly associated with the mineralization. However, careful interpretation of standard geophysical data can indirectly indicate favorable areas for massive sulfide mineralization.

Chromite in northern California

J. C. Wynn used a combination of refraction seismic, ground magnetic, and complex resistivity methods to identify podiform chromite deposits in northern California. All of these methods may be site specific. However, Landsat imagery can be used to distinguish the ophiolite peridotite host rock from the surrounding metasedimentary rocks.

Gold in South Carolina

In northern South Carolina, J. C. Wynn found that combined very long frequency (VLF) electromagnetic studies were effective in stratigraphic mapping, which is essential in exploration for gold. Gold-bearing strata show distinctive VLF resistivity highs. Triassic dikes, intruded along faults which displaced lithologic units, are readily mapped by ground magnetometer measurements. In the area studied, bedrock is completely obscured by a thick cover of weathered and altered material; the geophysical results were correlated with drill hole and other subsurface data.

Magnetite deposit, Minarets Wilderness Area, California

A ground magnetic survey by H. W. Oliver of Iron Mountain Minarets Wilderness Area, Calif. (at an elevation of about 3,100 m above sea level), revealed a magnetic high of about 80,000 γ (unit of density of magnetic field) located directly over an exposed elongate deposit of magnetite. The magnetic high extends both to the north and south of the exposed deposit and serves to trace the buried iron ore 300 m south of the outcrop.

An aeromagnetic survey of the area flown about 1,000 m above the Iron Mountain magnetite deposit revealed an associated broad anomaly of about 450 γ that was significantly larger and broader than expected from upward contribution of the ground level anomaly. This feature implies an additional magnetic source or combination of sources. These additional sources are probably a complex of subsurface small veins of magnetite throughout the metavolcanic country rock.

Residual Bouguer gravity maps

R. C. Jachens has written a program to generate residual Bouguer gravity anomaly maps by removing the long wavelength gravity anomalies caused by variations in crustal thickness. The basic assumption was that Airy-Heiskanen-type isostatic compensation prevailed and was a major cause of long wavelength anomalies. The model parameters selected for California based on coastal seismic results are sea level crustal thickness, 25 km; density of crust above sea level, 2.67 g/cm^3; and density contrast between crust and upper mantle, 0.40 g/cm^3. The program used digitized elevation data to determine the configuration of the bottom of the crust and then computed the gravity effect of the compensating layer.

This procedure has been applied to the gravity data in a number of wilderness areas including the Marble Mountains Wilderness Area in northern California and the Golden Trout and Domelands Wilderness Areas in the Sierra Nevada. The major effect has been to remove or greatly subdue the strong gravity gradients associated with the change from oceanic to continental crust and those associated with the root of the Sierra Nevada. The residual gravity maps revealed some features that were masked by the strong gradients and, in general, showed a more obvious correlation between surface geology and gravity than was apparent on the original maps.

Big Craggies ultramafic body, Oregon

New aeromagnetic data were used by R. J. Blakely to help define the structure of ultramafic bodies in the area of Big Craggies in southwestern Oregon. The edge of the anomalies, linear in the north-south direction, coincides with mapped contacts of the ultramafic rocks and the less magnetic rocks of the Dothan Formation. These

data are particularly useful as a geologic mapping tool in areas where the contacts were inaccessible.

Profiles across several of these anomalies were modeled with a computer program that assumed that the causative bodies were two dimensional. Results show that the bodies are tabular, very thin (<500 m), and strongly magnetic (~2 A:m). These results support geologic observations that these bodies were emplaced as thin tectonic slices.

Simultaneous interpretation of geophysical well logs

J. J. Daniels developed a computer-assisted interpretation technique for several geophysical well logs. Products and ratios of well logs combined physical property responses that were characteristic of a particular lithology. This procedure enables the geoscientist to utilize all of the physical properties that characterize a particular rock type and to make a consistent and comprehensive interpretation of the rocks associated with coal deposition. The geophysical well log responses have been found to be useful for interpreting the association of rock types with coal. (1) Coal is characterized by a low density, a low natural gamma ray count rate, and a high induced polarization response. (2) The density and gamma ray responses of black shale are slightly higher than those of coal. (3) Limestone conglomerate and sandstone both had high resistivity and neutron responses and low gamma ray responses. (4) The induced polarization well log can be used to distinguish the clays with a high cation exchange capacity from those with a low cation exchange capacity.

Hole-to-hole electrical measurements have proven effective in detecting physical properties changes between drill holes. Field tests in western Kentucky have shown that hole-to-hole dc-resistivity measurements can be used to locate voids in coal seams caused by previous mining activity.

RESOURCE INFORMATION SYSTEMS AND ANALYSIS

RESOURCE INFORMATION SYSTEMS

Computerized Resources Information Bank

At the end of 1978, the CRIB master file contained 46,300 records. New cooperative agreements were started this year with the states of Oregon, Idaho, Alabama, Michigan, and Virginia. Co-ops continue with the Bureau of Land Management, the State Department, and South Dakota and Tennessee.

New in-house data sources this year include Maine (R. G. Schmidt) and Michigan (W. F. Cannon); statewide inventories for California, Utah, Arizona, Nevada, and Oregon remain in progress. A commodity data source for nickel was commenced by M. P. Foose.

The Mineral Data System (MDS) Advisory Committee, which began operation 1 yr ago, under the direction of J. A. Calkins, has provided new ideas, direction, a distribution of work tasks, a working policy, and a platform for communication. The MDS will be comprised of a family of mineral resource files, of which CRIB is the principal component.

CRIB file management is gradually being transferred to the University of Oklahoma under a new contract signed this year.

Geothermal resources file

The GEOTHERM file is a fully operational data base on geothermal resources developed by J. A. Swanson. A new bibliographic file on references for data in the file was added this year. The file is being used for research and assessment and as a record of status of geothermal resource information. Much of the data is being entered by State geological surveys through contracts with the DOE and is being used to produce maps showing low-temperature geothermal resources. Presently, the file contains over 500 field-, 500 well-, and 6,000 chemical-analysis records.

National Coal Resources Data System

Seven data base files of specialized coal information now are established for interactive use with the PACER retrieval system. Data are continuously input from USGS and external sources, such as State and Federal cooperative programs, to provide a basis for national coal resource assessments. The files are managed by A. L. Medlin.

GARNET, a system of computer programs, has been developed by A. C. Olson to aid the commodity geologist in analyzing, evaluating, and mapping resources when dealing with irregularly spaced, point-located field data. These data are processed by the program to produce resource maps and contour maps of other relevant characteristics and to compute resource tonnages for each reliability category. Although developed for coal, the system is equally applicable to other commodities.

A significant revision of the boundary-handling procedure and the algorithm for logically combining boundary sets has made the system more efficient and has made its operation much easier for the user. Boundaries may be entered into the data set by means of a digitizer and may be created at the display terminal by means of the cursor. Boundaries can be generated by the software as a single contour level, and they may be generated from the logical combination of different types of constraining boundary conditions. From these boundaries,

resource maps are created, and tonnages are computed based on the standard reliability category distances from the field observation points.

Oil shale and saline mineral data system

The oil shale and saline mineral data storage and retrieval system prepared by J. K. Pitman makes available baseline data for determining geographic areas of greatest potential economic interest for evaluating areas under litigation, for evaluating sites suitable for specific methods of recovery, and for providing other data that can be used to study statistical and mineralogical trends in oil shale and other organic-rich deposits.

Geologic Retrieval and Synopsis Program

The Geologic Retrieval and Synopsis Program (GRASP), developed by R. W. Bowen, is a system for the storage, retrieval, and manipulation of computer storable data. This year, an automatic file linkage capability, which allows a more compact representation of historically structured data, was added to GRASP, and a new command (OUTPUT) was implemented, which may be used for backup files in GRASP. OUTPUT can also be used to restructure and (or) update GRASP data bases.

GRASP was implemented on the HP21MX computer at the Woods Hole office of Marine Geology. This implementation permits the scientists at Woods Hole to access and manipulate their data in time-share mode and will result in a more efficient use of their computer. The HP21MX implementation represents the first internal (to USGS) minicomputer (16 bit) GRASP installation. GRASP was also installed on the Tektronix 4081 Graphics Computer leased by the Office of Resource Analysis in Reston.

The GRASP system source code was distributed to nine requesting organizations in Canada, Australia, Spain, Brazil, West Germany, Denmark, Switzerland, and the United States.

Computer applications of resource data files

The following computerized data files were made operational by N. A. Wright on Honeywell MULTICS time-sharing: (1) the Scripps Institution of Oceanography file on manganese nodules, (2) Petroconsultants file of oil and gas fields exclusive of the United States and Canada, (3) Otter Creek and Cohutta Wilderness Areas geochemical data, and (4) the Cobb file of reference data for Alaskan mineral deposits and occurrences.

RESOURCE ANALYSIS

Dynamic modeling of mineral resources

M. E. Slade developed a model for longrun price movements of nonrenewable natural resource commodities that suggests a U-shaped time path for relative (deflated) prices. The model has been tested for all the major metals and fuels and has been found to be statistically significant in 10 out of 11 cases. It was found that a linear trend model underestimates relative prices in the last few years of the period of analysis (1870–1978) for every commodity studied and that, even though relative prices of some commodities have been falling during most of the last century, prices of every commodity have passed the minimum point on the U-shaped curve and have begun trending upwards.

Worth of geophysical and geological data and mineral supply

Analysis of past production statistics of mined strippable coal deposits and characteristics of unmined strippable coal deposits in Illinois indicates predictable regularity in the mining process, according to E. D. Attanasi. In general, the quality and costs associated with prospects that have been mined are superior and of lower mining cost than the unmined prospects. Estimation of costs associated with remaining prospective areas indicates that future costs of strip mining will be progressively higher in Illinois than in the past, and it is unlikely that production will exceed the peak production level attained in 1967. Economic analysis of characteristics of unmined deposits indicated that geologic data on seam thickness and overburden depth are of little value for estimating future costs of mining strippable coal deposits, unless these data are associated with data on the areal extent or size of potential reserve blocks.

Coal resource model studies

The Energy Minerals Rehabilitation Inventory and Analysis (EMRIA) reclamation and resource studies are based on core drilling programs of BLM. The program, managed by G. B. Schneider, provides samples of coal and associated rocks for quality assessment, data for evaluation of reclamation potential, and predictive information on possible mining and environmental hazards. The study areas are selected so as to be representative of large areas that are most likely to be involved in leasing activities in the near future. The detailed geologic and resource information developed in the study areas forms a vital part, by transfer value, of USGS resource assessment activities.

Mineral and energy resource system for Navajo Tribe

The Navajo Tribe currently has access to a pilot computer-based mineral and energy resource system built by J. D. Bliss on the Reston Honeywell computer. Members of the Navajo Tribe's Minerals Department have direct access to the system via a time-share net and are able to examine data files containing information on mineral and coal resources of the Navajo Reservation. Other files give information on geological maps on tribal land in New Mexico and Arizona. Literature applicable to tribal land and resource problems is currently being computerized by the Minerals Department and USGS.

Production statistics applied to resource estimation

D. H. Root and S. M. Cargill have found that the grade of mercury ores has declined in Spain, the United States, and Yugoslavia in such a way as to remain roughly proportional to the $-\frac{2}{3}$ power of the cumulative ore mined.

In the United States, the grade of mercury ores has declined from 36 percent in the middle of the 19th century to 0.5 percent at the recently opened McDermitt mine in Nevada. Extrapolating past trends in ore grades is one way to estimate what grades of ore will be available for mining in the future. The estimate from the extrapolation of the amount of mercury that can be produced in the United States after 1977 from ores having grades no lower than 0.1 percent is 53×10^6 kg.

Estimation of world phosphate resources

Asia and the Pacific region are generally thought to be deficient in phosphate rock, the raw material of phosphate fertilizer. However, analysis by R. P. Sheldon of phosphate resources of the region indicates otherwise. The collection of data on the occurrence of phosphate deposits shows that phosphate occurs throughout the region, and geologic analyses of the region show that much phosphate remains to be discovered. Although much of this resource is low grade, advances in manufacturing technology give hope that low-grade deposits can be utilized as a fertilizer raw material in the future.

The empirically determined episodicity of phosphate deposition in the geologic past can be explained by an hypothesis relating deep ocean circulation to global climatic cycles. The deep ocean serves as a geochemical sink for phosphorus that builds up in times of slow circulation and equitable global climate but is depleted by phosphorite deposition during times of colder polar climates and rapid circulation. A particularly favorable condition for phosphorite deposition occurs in equatorial regions as a result of equatorial upwelling, thus, phosphorus paleo-oceanographic reconstructions may be helpful in exploration for phosphate deposits in the unexplored parts of the world.

Petroleum resource appraisal and discovery process modeling

L. J. Drew determined that the step function form of the aggregate petroleum discovery rate curve can be explained as a consequence of the extreme size distribution of oil and gas fields and of the order in which these fields are discovered. This analysis resolved a debate that has been going on for more than a decade.

A technique was developed to allow the use of discovery process models to predict the future rates of discovery of oil and gas in regions when the discovery process has been constrained by government leasing policies, water depth, availability of pipelines, and other factors. The basic element in this technique is a reordering of past discoveries by computer simulation to remove discontinuities introduced into the discovery time series by constraining factors.

Results of estimating marginal finding and developing costs for undiscovered deposits in the Permian basin indicate that, even at $40 per barrel oil equivalent, total oil and gas from future discoveries will account for little more than 3 years of production at the 1974 production rate. Update of the forecast of the date of peak world oil production indicates that, if present trends continue, the date of peak production will occur before 1993.

Mineral-resource assessment

An analysis of the characteristics of porphyry copper deposits by D. A. Singer demonstrates that, within a geologic setting, the larger deposits tend to be found earlier. This suggests that grade-tonnage models developed in partially explored regions are probably biased estimates of the remaining deposits of the region. A comparison of average grade versus tonnage by deposit with the Lasky relationship shows that the methods do not contradict each other and that both methods are incapable of estimating resources at grades much below observed grades.

One approach to assessing the mineral resources of a region used by D. A. Singer is to delineate tracts as permissive for the occurrence of deposits by type; to estimate relevant characteristics, such as grade and tonnage or contained metal of each deposit type; and to estimate the number of deposits of each type that is likely to occur within the tracts. W. D. Menzie II applied the method to the regional assessment of mineral resources in Alaska and pointed out that a major limitation was the absence of adequate deposit characteristic models of vein- and stratiform-type deposits. New deposit characteristic models, for epithermal precious metal vein deposits, replacement lead-zinc deposits, and lead-

zinc deposits associated with sedimentary and minor volcanic and (or) volcanoclastic rocks, increase the applicability of the method.

D. A. Singer and J. H. DeYoung, Jr., show that a lognormal distribution closely approximates observed distributions of "ore" tonnage, contained metal, and average grade from copper, nickel, molybdenum, and tungsten deposits that are grouped by geologic deposit type. Correlations between "ore" tonnage and grade for the nine deposit types and two mixtures of deposit types (copper and nickel) are negative for five types, not significantly different from zero for five types, and positive for one type. Neither strength nor sign of the correlation has any bearing on accuracy of correlation cumulative tonnage versus grade regressions (the Lasky relationship); between 81 and 99 percent of the variability in grade is explained by cumulative tonnage in the Lasky regressions by deposit type. Projection of the Lasky relationships and the grade-versus-tonnage regressions to crustal grades or to crustal weights demonstrates that both methods are incapable of estimating resources at grades much below observed grades. Slopes of the grade-versus-tonnage regression lines are significantly different than would be expected if there were continuity of grade-tonnage relations to crustal weight, which brings into question the validity of assuming continuity in resource assessments. Regardless of deposit type, tonnage of "ore" and contained metal are highly correlated, and 10 percent of the largest deposits (ordered by metal content) typically accounts for 50 percent of total known metal. Greater precision in resource estimates might be achieved by concentrating on estimating the tonnage of the few largest deposits of each type.

Uranium resource analysis

Geologic decision analysis originally developed by R. B. McCammon as a computer-based method for determining the mineral deposits based on geologic, geophysical, and geochemical data has been expanded to provide for the generation of resource estimates of undiscovered deposits. Estimates of the size and grade of undiscovered deposits are generated by combining the measure of favorability determined in an area for a particular deposit model with size and grade data obtained from known deposits in geologically similar areas. By systematically weighting the various factors used to determine favorability differently, a range of estimates rather than a single estimate of the undiscovered resources can be obtained.

CHEMICAL RESOURCES

PHOSPHORITE

California phosphorite

Geologic mapping, trenching, and sampling by A. E. Roberts (1979) provided a thorough stratigraphic and geochemical study of the upper Miocene strata of the phosphatic mudstone members of the Santa Margarita Formation near New Cuyama, Santa Barbara County, Calif. This study determined the phosphate content of each stratigraphic unit in an area of complex stratigraphy and structure. Detailed petrology with chemical analyses of each unit and paleontological analyses of units containing a fauna were made. The chemical data indicated that the marine apatite (carbonate fluorapatite) is of variable composition. Faunal assemblages and sedimentary structures suggested deposition of phosphatic mudstone members of the Santa Margarita Formation in an offshore mud-shelf environment.

LITHIUM

Identification of domestic lithium resources

Various lithium-bearing smectite clays, low-grade lithium brine from Great Salt Lake, high-grade lithium brines from oil-field waters such as the Smackover brine of the gulf coast, and geothermal brines of the Imperial Valley, Calif., may need to be considered as domestic resources if increase in demand exceeds the abilities of existing domestic lithium producers. J. D. Vine reported that such an increase in demand could lead to the dependence of the United States on Canadian pegmatites and Chilean and Bolivian brines for lithium.

Test drilling of playa lake sediments in the Southwest has recovered anomalous concentrations of lithium in clays from Eureka Valley and Alkali Valley, Calif., and at Willcox Playa, Ariz. However, such drilling has encountered no commercial concentrations of lithium-rich brine such as found at Clayton Valley, Nev. Such results suggest that increased need for domestic lithium resources may require utilization of presently subeconomic resources.

Evaporative model of lithium brine generation

One of the largest lithium deposits in the United States occurs in Clayton Valley, Nev., where lithium is extracted from a sodium chloride brine pumped from beneath the playa. Study of the Quaternary sediments and geomorphology by J. R. Davis has shown that a

shallow pluvial lake existed in Clayton Valley during glacial periods. His hydrologic budget for pluvial periods suggested that the lake water might have been evaporatively concentrated many times. A simple geochemical model showed that evaporation of the lake waters and precipitation of calcite, halite, and silicate phases could produce the lithium-enriched brine.

Lithium—a new guide element for uranium

Lithium is generally associated with uranium occurrences and deposits in anomalous concentrations not only with, but also peripheral to, uranium-enriched rocks. R. K. Glanzman and J. K. Otton reported this association in altered tuffaceous sedimentary rocks of Tertiary age in the McDermitt caldera complex of Nevada and Oregon, at Spor Mountain, Utah, in the Date Creek Basin, Ariz., and in the Kramer Basin, Calif. Lithium occurs with uranium in the Morrison Formation of Jurassic age in the Henry Mountains, Utah. The two elements are associated also in a contact-metasomatic zone between syenite and dolomite at the Hope Mine near Amboy, Calif. The association is genetic in that both elements are transported in the same fluid from the same source. Both elements are lithophilic and are late-stage magmatic differentiation products. Lithium is transported farther from its source than is uranium because it forms very soluble chemical compounds, is not directly affected by oxidation potential, and has the lowest exchange capacity of common ions. These characteristics indicate that lithium is a new guide element for uranium exploration.

MINERAL-FUEL INVESTIGATIONS

COAL ANALYSIS

The Coal Resources Investigations Program of the Geologic Division classifies the Nation's remaining coal into resource- and reserve-base categories based on geographic and geologic distribution and physical and chemical characteristics. As part of this effort, personnel of the Division in 1979 mapped and assessed coal-bearing lands in Alabama, Alaska, Arizona, Colorado, Georgia, Montana, New Mexico, Pennsylvania, Utah, Virginia, West Virginia, and Wyoming. Included in these field investigations were studies conducted on the following Indian reservations: Blackfoot, Crow, and Fort Peck, in Montana; Ramah, Canoncito, and Acoma, in New Mexico; and Navaho, in New Mexico and Arizona. About 27,000 m of air and core drilling was completed in coordination with the field investigations in the coal basins of the Rocky Mountains, the Great Plains, and the Colorado Plateau to assess the quantity and quality of buried coal and to provide stratigraphic information. Nearly 1,150 channel and bench samples of coal were collected for chemical and physical analyses from 17 States, in cooperation with 15 State Geological Surveys, the Conservation Division of the USGS, the BLM, and the USBM.

Computerization of the Nation's coal resources

The National Coal Resources Data System (NCRDS) continues to grow in size and use under the direction of M. D. Carter and M. A. Carey. During 1979, approximately 7,000 records of coal resources, stratigraphy, and chemical analyses were added to the system raising the total to nearly 100,000. The data base includes 33,000 coal-resource tonnage records and 53,000 records of USBM proximate and ultimate analyses, largely reported by coal bed on a State and county basis. The NCRDS also contains 4,000 geodetically located records of proximate, ultimate, major-, and trace-element analyses and associated data provided by the USGS coal geochemical program and 5,000 stratigraphic records and drill hole records. The NCRDS has cooperative agreements with 13 State Geological Surveys for the collection, correlation, transmission, entry, retrieval, manipulation, and display of drill hole, chemical analyses, and other relevant coal-resources-related data.

Participation in the interagency Energy Minerals Rehabilitation Inventory and Analysis Program

The USGS is providing geological support to the Energy Minerals Rehabilitation Inventory and Analysis Program (EMRIA), BLM, by selecting representative reclamation study sites within several coal basins. USGS personnel obtain and examine samples of coal and other sedimentary rocks from cores drilled by BLM contractors and appraise coal quantity and quality, evaluate reclamation potential, and predict possible mining and environmental hazards. Studies were completed in 1979 in the following reclamation study areas: Emery Creek, Sevier and Emery Counties, Utah; Beulah Trench, Mercer County, N. Dak.; Ojo Encino, McKinley County, N. Mex.; Rattlesnake Butte, Stark County, N. Dak.; Prairie Dog Creek, Powder River County, Mont.; Lay Creek, Moffat County, Colo.; McCallum, Jackson County, Colo.; Arkoma Basin, eastern Oklahoma; and Warrior Basin, northern Alabama.

GLOBAL STUDIES

World coal resources

G. H. Wood, Jr. (USGS), and J. A. Simon (Illinois Geological Survey) calculated the world's coal resources to be 18.360 trillion t, of which 9.800 trillion t has been identified; the remainder lies in geologically favorable areas as yet not systematically explored. About 97 percent of this resource occurs in the U.S.S.R., the United States, People's Republic of China, United Kingdom, Australia, West Germany, Canada, and the Union of South Africa. The remaining 3 percent, about 0.550 trillion t, is dispersed among 90 other countries.

Wood and Simon also calcuated that, out of the above-cited resource, about 0.744 trillion t currently is minable from beds containing 1.550 trillion t of coal. They predict that minable coal in the future could reach a potential of 5.270 trillion t in coal beds containing 10.310 trillion t. The difference between coal in place and minable coal indicates how much coal is left in place and lost during conventional mining.

Intercontinental correlation of the Pennsylvanian System

Paleobotanical studies by W. H. Gillespie (USGS) and H.W. Pfefferkorn (University of Pennsylvania) for the Pennsylvania System stratotype in Virginia and West

Virginia have demonstrated that the first occurrences of new forms of flora in the stratotype's section correlate closely with first occurrences of the same flora in Pennsylvania strata elsewhere in North America and Western Europe. A comparison with the general European sequence indicates that (1) the Upper Mississippian rocks of the stratotype section correspond to the Namurian A of that continent, (2) the Lower Pennsylvania Series extends from Namurian B into the lower Westphalian B, (3) the Middle Pennsylvanian Series extends from the lower part of the Westphalian B into the Westphalian D, and (4) the Upper Pennsylvania Series ranges from the Westphalian D through the Stephanian Stage.

EASTERN COAL

STRATIGRAPHY

Tectonic subsidence in eastern Kentucky

Differential subsidence in the Appalachian Basin in eastern Kentucky during Early and Middle Pennsylvanian time produced a heretofore unrecognized hinge line that extends from the Kermit 7½-min quadrangle on the West Virginia border to the Oneida North 7½-min quadrangle on the Tennessee border, parallel to the strike of the Pine Mountain thrust fault. C. L. Rice considers that subsidence southeast of this hinge line is an important factor in the distribution of coarse clastic deposits as well as of some thin marine units. Southwestward-prograding distributary systems apparently occupied the subsiding trough for most of Early to Middle Pennsylvanian time, although marine waters transgressed the area during brief periods when subsidence exceeded supply of sediments. Recognition of the hinge line has allowed clarification of coal beds and associated rock correlations that previously were vague.

Resin rods in Upper Pennsylvanian coal beds

Resin rods and woody rodlike structures were found by P. C. Lyons and J. F. Windolph, Jr., in fusain partings in coal beds of the Conemaugh and Monongahela Formations and in the Dunkard Group in the vicinity of Charleston, W. Va. The resin rods lie in coalified wood and as isolated randomly oriented aggregates in fusain. The woody structures, as examined under the scanning electron microscope by R. B. Finkelman, consist of xylem tissue that shows both pitted and nonpitted cell walls.

RESOURCES AND QUALITY

Coal quality in the Pocahontas field, Virginia and West Virginia

Physical and chemical analyses made by the DOE and the USGS of 12 channel samples collected from Pennsylvanian coal beds in southwestern Virginia and southern West Virginia indicate that 11 of the coals are of high metallurgical quality, according to V. A. Trent. The coal beds are of medium-volatile bituminous rank and contain less than 1 percent sulfur, less than 7 percent ash, and no anomolous quantities of trace elements. The densities of the coals are directly proportional to the ash contents, and their heat or calorific values are inversely proportional to their ash contents. Coal densities do not vary serially with stratigraphic position or with metamorphic rank. The chemical elements found in the ash of the 12 samples do not detract from the value of the analyzed coals for metallurgical purposes.

A low percentage of iron and very low percentages of magnesia, soda, and potash in the coal ash suggest that the formation of scale deposits in boiler pipes and tubing during combustion or in coal conversion processes will be minimal. The analytical results correspond with and substantiate the known high quality of these West Virginia and Virginia coals.

Rank of coal in the Narragansett Basin, Rhode Island

Compilation of 149 analyses by P. C. Lyons and H. B. Chase, Jr. (1979), from coal samples collected in the Narragansett Basin indicates that the coal is mainly anthracite and, to a lesser extent, semianthracite and meta-anthracite. The coal generally has a high to very high ash content, averaging 22 percent, and a low sulfur content, averaging 0.4 percent. The mean heating value on an as-received basis is 23,167 kJ/kg or very low compared to 29,424 kJ/kg per pound for anthracite and semianthracite of the Southern Anthracite field of Pennsylvania (Wood and others, 1969). Sinkfloat tests of coal from the Narragansett Basin (Skehan and Murray, 1978) show that most ash can be removed to yield a product comparable in heating value to coal from the Southern Anthracite field.

Resources in Carbon County, Pennsylvania

Geologic analysis by G. H. Wood, Jr., of the Nesquehoning 7½-min quadrangle, Carbon County, Pa., indicates that the 11.7 km² of coal-bearing rocks contained an original anthracite resource of 534 t in seven minable beds. The content of coal averaged 46 million t/km² in an average thickness of 33 m of coal. About 243 million t was mined from 1769 to the present. Approximately 272 million t remains unmined and is considered to be the resource base, 136± million t of which probably is still recoverable by underground mining or by exceptionally deep strip mining.

Exploitation of thin coals in Georgia

T. J. Crawford reports that coking-quality coal beds as thin as 25 cm are being strip mined in Georgia. Coals

this thin, unless mined, are not included in national resource estimates.

WESTERN AND ALASKAN COALS

Predictive model for Cretaceous deltaic coals of Utah

After a detailed stratigraphic study and a paleoenvironmental analysis of the Ferron Sandstone Member of the Mancos Shale in central Utah, T. A. Ryer developed a model for deltaic coals of Cretaceous age in that region. In the Emery coal field, a clear relation exists between the geometries of the thick coal beds and the geometries of the associated delta-front sandstone lenses. In the five delta cycles recognized in the Ferron, the thickest coal beds are in belts, each about 10 km wide, lying immediately westward of the landward pinchout of an associated delta-front sandstone. The relation provides a predictable element in exploring for coal in this part of Utah, but superimposed are nonpredictable elements - the erosion resulting from fluvial channels cutting the original peat swamps and, to a lesser extent, fluvial channels postdating peat accumulation. Despite these unpredictable elements, the model is particularly valuable in guiding the early stages of coal exploratory drilling programs. Combined with data obtained from studies of outcrops, the model can be used to predict areas of highest probability of finding thick coal beds within the ancient delta system.

Wasatch Plateau coal field, Utah

Measured stratigraphic sections of the Upper Cretaceous Star Point Sandstone and the overlying coal-bearing Blackhawk Formation revealed that the coal bed geometry of the formation was strongly influenced by paleodepositional processes. For example, preliminary data established by J. D. Sanchez indicate that tongues of the delta-front Star Point pinching out landward were responsible for determining the seaward extent of coal beds and, thus, controlled the stratigraphy in the lower part of the Blackhawk over the entire central and southern part of the Wasatch Plateau coal field. The superb exposures of Cretaceous strata in this area provided a setting for detailed study of coal beds, their lateral continuity, and reconstruction of the paleoenvironments in which the original peats accumulated. The study should help in the determination of target areas for coal exploration and drilling.

Coal in the Mesaverde Formation, Wind River Indian Reservation

The basal sandstones of the Mesaverde Formation in the Wind River Indian Reservation, Wyo., intertongue with underlying Cody Shale, indicating a regression of the Cretaceous sea. J. F. Windolph, Jr., N. L. Hickling, and R. C. Warlow identified sedimentary structures in the lower sandstones of the Mesaverde that are characteristic of a delta front, including baymouth bars, point bars, and distributary-channel fillings. As the sea regressed southeastward in latest Cody and earliest Mesaverde time, protective barriers and widespread swampy platforms developed where accumulating vegetation was preserved to form peat. Most resulting coal beds in the lower part of the Mesaverde are thin, lenticular, and irregularly distributed and probably are related to crevasse splays and distributary channels.

A thicker widespread coal bed overlies the lenticular coal beds and appears to have formed in a stable back-bay swamp. About 300 m of interbedded lenticular sandstone, siltstone, gray shale, carbonaceous shale, thin coal beds, and thin beds of freshwater limestone rests conformably on this widespread coal bed. This sequence probably was deposited on an upper delta plain. The uppermost unit of the Mesaverde Formation is a white coarse- to medium-grained blanket sandstone containing several thin carbonaceous shales characterized by an absence of coal beds.

Development of thick coal beds in the eastern Powder River Basin

The stratigraphic framework of coal and sandstone underlying a 2,500-km^2 area in the western part of the Recluse 1° quadrangle, Wyoming, was resolved by B. H. Kent through construction of north-south and east-west interlocking lines of sections set to sea level datum. The framework outlined is on the east flank of the Powder River Basin, Wyo. The regional dip of coal beds within the area is about ½° west or southwest toward the depositional axis of the basin, about 50 km west of the study area.

Examination of the three-dimensional aspects of the grid indicates that two or more succeeding coal beds in the coal-bearing sequence commonly merge locally on broadly depressed surfaces to form roughly north-trending belts of thick coal and that succeeding belts of thick coal are offset westward toward the depositional axis of the basin. The areal extent of the offsets of succeeding belts of thick coal is bracketed by five Paleocene (Fort Union) coals that merge locally along the east margin of the basin to form the north-trending 35-m-thick Wyodak coal bed and by the five or more Eocene (Wasatch) coal beds that merge locally near the depositional axis of the basin to form the similarly north-trending 60-m-thick Lake deSmet coal bed.

The structural relief of all coal beds along east-west lines is directly related to progressively increasing westward subsidence of the basin during late Paleocene and early Eocene time. The north-trending belts of thick coal, thus, were the result of coalescing interconnected

paleoswamps that remained stable for extended periods of time, with optimum rates of subsidence maintained.

The current consensus is that coal deposition on the east flank of the Powder River Basin is associated with ancient deltas that prograded eastward away from the Big Horn uplift, about 80 km west of the mapped area. The westward offset pattern of succeeding belts of thick coal suggests that the clastic units between the belts of coal prograded westward during the late Paleocene and early Eocene time. The westward prograding is supported by observed paleocurrent directions in Eocene fluvial sandstone on the east flank of the basin (Seeland, 1976). The anomaly suggests that the Black Hills uplift, only about 40 km east of the mapped area, contributed a significant volume of detritus during late Paleocene and early Eocene time (Shapiro, 1971). The westward offset of succeeding belts of thick coal and the westward prograding sandstone bodies require resolution as to whether coal deposits in this area are associated with ancient fluvial-dominated environments and west-flowing drainage systems or with ancient delta-dominated environments and east-flowing drainage systems. Analysis of the sandstone depositional patterns does not supply an answer because eastwardly prograding delta drainage systems bifurcate downstream to the east (that is, by crevasse splays and associated features), whereas westwardly fluvial drainage systems would bifurcate upstream. Whether ancient delta systems were involved can be ascertained only by confirming that the ancient sandstone units are crevasse splays.

The Aspen Shale–Frontier Formation contact

At Cumberland Gap, western Wyoming, the marine Aspen Shale and the overlying nonmarine coal-bearing Frontier Formation appear to interfinger, according to J.W. M'Gonigle, whereas the contact appears to be conformable in other exposures to the north and to the south. Throughout the Hams Fork region, the Frontier lacks any substantial progradational beach sandstone at its basal contact with the Aspen Shale, in contrast to other contacts of Cretaceous marine and nonmarine units in the region, including a similar contact stratigraphically higher in the Frontier.

Coal in the Tongue River Member of the Fort Union Formation

Thick laterally persistent coal accumulations were mapped by R. M. Flores in the lower 300 m of the Tongue River Member of the Fort Union Formation in southeastern Montana. The coal beds are associated with a fluvial channel-dominated facies, are as much as 10 m thick, extend about 20 km laterally along a northeast-southwest line of section, are interbedded with small amounts of carbonaceous shale, and have a moderately low ash content. The facies developed as slowly subsiding interchannel flood basins, and abandoned channel ridges formed vast expanses of poorly drained backswamps that accumulated thicker-than-normal peats. As indicated by the preserved coal, swamp vegetation consisting of wood and herbaceous plants grew on hummocks and in hollows, with the woody plants preferentially growing on the hummocks. The hummocks and hollows alternately replaced each other through time as the ground-water table rose, resulting in unusually thick accumulations of peat. Occasional autocyclic shifts of major channels into topographically low parts of the backswamps and moderate overbank-crevasse splay sedimentation interrupted and produced splitting or merging peat beds. At other times, the backswamps were invaded by moderate influxes of flood waters containing suspended sediments that were deposited and formed carbonaceous shale. The stabilized nature of the backswamps and their moderate overbank sedimentation may have been controlled by well-developed levees along major channels.

Lignite in the Fort Peck Indian Reservation

The eastern part of the Fort Peck Indian Reservation, in northeastern Montana, is known to contain potentially recoverable lignite in several places. Preliminary evaluation of 1979 exploratory drilling by H. H. Arndt indicates that coal beds of Tertiary age in the Fort Union Formation may be more widespread than previously believed. The correlation of previously known potentially recoverable lignite beds was not well established before drilling, and final correlations cannot be made without further drilling and geologic mapping.

Coal in the central and east-central part of the San Juan Basin

A beach-shore facies predominates in the Pictured Cliffs Sandstone and Cliff House Sandstone, of Late Cretaceous age, where examined by J. W. Mytton in the central and east-central part of the San Juan Basin, N. Mex. Heavily bioturbated sandy units and trace fossils, including *Ophiomorpha,* are common and indicative of the middle to lower shore facies.

In the central part of the basin, the Fruitland Formation, which overlies the Pictured Cliffs Sandstone, contains coal beds of poor quality that gradually thin eastward across the basin. South of Cuba, N. Mex., coal is essentially absent, and the Fruitland seems indistinguishable from the overlying Kirtland Shale. Coal beds of the Menefee Formation, which intertongue with and underlie the Cliff House Sandstone, are thin, are of poor quality, and grade eastward into carbonaceous shale.

Northern Alaskan coals

According to H.W. Roehler and G. D. Stricker (1979), the Cretaceous coal-bearing strata in the western part of the National Petroleum Reserve, Alaska, were deposited as part of a large fluvial-dominated birdfoot delta named the Corwin Delta (Ahlbrandt and others, 1979). The most numerous, thickest, and laterally persistent coal beds were formed from interchannel, abandoned-channel, and interdistributary-bay peats that accumulated in a middle delta-plain environment. The maximum thickness of coal beds is 7 m.

GEOCHEMISTRY

Constitution of humic substances from aquatic and terrestrial sources

Proton and carbon-13 nuclear-magnetic resonance (NMR) techniques have been used to study the constitution and structural characteristics of humic substances, including fulvic acids, humic acids, and humin, in sediments of both terrestrial and aquatic origin. P. G. Hatcher and I. A. Breger confirmed that fulvic acid isolates from marine sediments contain high proportions of polysaccharides that are rich in uronic acids and that are probably of bacterial origin. Humic acids from terrestrial and aquatic sources are composed of complex aliphatic structures with varying amounts of aromatic moieties, the terrestrial humic acids being more highly aromatic than the aquatic humic acids (Hatcher and others, 1980). The proportion of aromatic character is measurable quantitatively and is used to identify either a terrestrial or an aquatic source for a particular humic acid. Humins of Holocene sediments have been examined by newly devised solid-state NMR techniques (Hatcher and others, 1980) that also allow source discrimination based on the quantifiable aromaticity of each humin.

Zinc and cadmium content of coal in the Interior coal province

Trace element analyses of more than 800 coal samples collected from drill cores and mines in the Interior coal province outline areas where coal beds of Pennsylvanian age contain more than 500 ppm of zinc and 10 ppm of cadmium, with maximum values reaching as much as 11,500 ppm of zinc and 60 ppm of cadmium. According to J. R. Hatch, these areas are in northwest, northeast, and southeast Illinois (Illinois Basin); in southeast Iowa; northeast, north-central, and southwest Missouri; southeast Kansas; northeast Oklahoma; and southeast Nebraska (Forest City and Arkoma Basins). Within these areas, the content of zinc and cadmium in coal beds is distributed irregularly and differs by as much as three orders of magnitude between beds that are closely related stratigraphically or laterally within a given bed. Zinc and cadmium occur in sphalerite (ZnS) along cleats and fractures in the coal beds; these openings also contain calcite, pyrite, kaolinite, barite, and quartz. Coal beds high in zinc and cadmium also contain relatively high contents of lead, nickel, cobalt, molybdenum, and silver.

The geographic distribution of these high zinc and cadmium areas appears related to the 38th parallel lineament and to the major positive structural features of the midcontinent area, such as the LaSalle anticlinal belt, the Mississippi River arch–Lincoln anticline, and the Nemaha anticline. Many of the areas are near mining districts containing Mississippi Valley-type lead-zinc-barite-flourite ores. The proximity and similarity in mineralogy suggest a common origin.

Chalcophile elements and uranium in coal

R. B. Finkelman reports that substantial quantities of the chalcophile elements in coal are distributed as discrete micron-sized mineral grains enmeshed in macerals. Because of this mode of occurrence, as much as 98 percent of the copper, 94 percent of the lead, 86 percent of the zinc, and comparable proportions of cadmium and selenium in the Waynesburg coal are in the lightest (<1.50 specific gravity) fractions of the examined specimens. Arsenic and mercury generally are in solid solution in the pyrite and are removed much more readily from the coal than are the micron-sized mineral grains. The mode of occurrence of uranium is variable. In Appalachian coals, at least 80 percent of the uranium is organically bound, and the remainder is in accessory minerals, primarily zircon. In contrast, all the uranium in a Missouri coal is in micron-sized grains of uraninite, whereas virtually all the uranium in a subbituminous coal from Wyoming appears to be organically bound.

The foregoing data suggest that the behavior of these chalcophile elements and uranium can be anticipated during the cleaning, conversion, combustion, weathering, or leaching of a coal.

Sulfur accumulation in coal

A principal factor controlling the content of sulfur in coal is believed to be the pH prevailing in ancestral peat-forming environments. C. B. Cecil and his associates postulate that coals derived from peats formed in highly acidic environments (pH<4.5) are low in sulfur (less than 1 percent), whereas coals derived from peats formed in less acidic environments (pH 4.5–7.5) tend to have a higher sulfur content (more than 1 percent) (Cecil, Renton, Stanton, and Dulong, 1979; Cecil, Renton, Stanton, and Finkelman, 1979).

The sulfur content in coal beds of the Appalachian Basin can be related to differences in pH in peat-forming paleoenvironmments. According to the Cecil postulate, high sulfur coals (1) are associated with calcareous sedimentary sequences (marine and (or) nonmarine), (2) have a relatively high calcium carbonate content, and (3) have a low kaolinite to illite ratio. The converse is true for low-sulfur coals. Exploration for low-sulfur coal should focus on coal-bearing sequences containing a paucity of calcareous sediments.

Distribution and genesis of primary pyrite in coal

Understanding the origin and distribution of sulfur in coal is obscured by a lack of knowledge concerning postdepositional mobilization of sulfur crystallization of pyrite in coal. Z. S. Altschuler, C. C. Silber, and M. M. Schnepfe determined the patterns and forms of sulfur distribution in the Everglades peat basin, Florida, by detailed analysis of peat cores in a regional cross section. The dominant form of sulfur in the cross section is organically bonded sulfur with free sulfate in moderate amounts and pyrite in trace quantities. Interpretation of analytical data indicates that, as the peat is buried and degraded, the pyrite content increases at the expense of organic sulfur. Contrary to most published speculation, inorganic sulfate does not participate in the formation of pyrite. In the regional pattern of sulfide (FeS_2) distribution, pyrite sulfur comprises from 1 to 5 percent of the total sulfur in the uppermost 70 to 80 cm of each core, but it increases to 10 to 25 percent of the total sulfur in the lowermost 20 to 30 cm of each core. The increase is accompanied by a comparable decrease in inorganic sulfur. In contrast, the content of sulfate sulfur varies irregularly throughout each core and does not systematically change in relation to pyrite or organic sulfur.

The described relation suggests that bacterial generation of hydrogen sulfide (H_2S) leading to pyrite formation by reaction with ubiquitous iron is based on utilization of some organic sulfur. The organic sulfur may be in two major forms in the vegetational mass of the peat: ester sulfur as organically bonded oxysulfur radicals, -C-O-S-O-, and carbon-bonded sulfides such as -C-S, -C-S-, or -C-S-S-.

The most likely pathway of sulfur reduction is anaerobic reduction of ester sulfate linked to bacterial degradation of plant matter, as opposed to autotropic reduction of ambient sulfate ions. Accordingly, analyses were performed for the determination of reducible sulfur from which carbon-bonded and ester sulfur can be derived. The analyses were conducted on peat derived from two distinctive environments: freshwater saw grass and water lily swamps of the interior Everglades and brackish to hypersaline mangrove swamps of the coastal zone. In both environments, the analyses revealed a clear relation between the onset and increase in pyrite content and the reduction of ester sulfate content, showing the dependence of pyrite formation on the bacterial utilization of ester sulfate in the Everglades. As a result of this relation, Altschuler and his colleagues suggest that anaerobic reduction of ester sulfate linked to bacterial degradation of plant matter is the major pathway for the initial genesis of pyrite in all coal. They further suggest that it may be the principal pathway for generation of pyrite in any organic-rich sediments in which the organic matter is mainly plant derived. Many pyritic black shales fall into this category.

Mobilization of elements resulting from use of coal

Using geometric means calculated for about 4,800 U.S. coal samples, the following metric tonnages of elements considered to be environmentally deleterious were mobilized as the result of coal usage in 1978 or will be mobilized between 1979 and 2000, according to Peter Zubovic, J. R. Hatch, and J. H. Medlin (1979). The metric tonnages of these elements were contained in the 590×10^6 t of coal produced in 1978 in the United States and $3{,}300 \times 10^6$ in the world; cumulative world production of coal from 1979 through 2000 is predicted to reach $137{,}000 \times 10^6$ t (Wood and Simon, pers.commun., 1979).

From the estimates below it is obvious that, unless entrapment and disposal methods are adopted on a worldwide scale, a deterioration of the worldwide environment could result from large-scale consumption

Element	U.S. 1978	World 1978	Cumulative world production, 1979–2000
As	3,000	17,000	700,000
Be	830	4,600	190,000
Cd	83	460	19,000
Co	2,100	12,000	480,000
Cr	5,500	31,000	1,300,000
Cu	7,100	39,000	1,600,000
F	38,000	210,000	8,800,000
Hg	54	300	13,000
Li	4,900	27,000	1,200,000
Mn	15,000	83,000	3,400,000
Mo	1,100	5,900	240,000
Ni	4,300	24,000	1,000,000
Pb	4,200	23,000	910,000
Sb	340	1,900	80,000
Se	1,000	5,600	230,000
U	770	4,300	180,000
V	8,900	49,000	2,100,000
Zn	8,300	46,000	1,900,000
S	6.66×10^6	37.1×10^6	$1{,}540 \times 10^6$

over a period of years. Serious environmental deterioration could result from the release of the large quantities of volatile elements, including arsenic, fluorine, mercury, selenium, and sulfur. Locally, the nonvolatile elements could cause environmental degradation either as components of airborne fine-particulate ash that cannot be entrapped or as contaminants in ground waters near disposal sites for the coarser ash and other refuse resulting from coal usage.

LABORATORY AND FIELD ANALYTICAL TECHNIQUES

Application of automatic image analysis to coal petrography

E. C. T. Chao, J. A. Minkin, and C. L. Thompson (1979) have developed and are currently evaluating a procedure, based on the use of an automatic image analysis system (AIAS), for relatively rapid accurate determination of volume percentages of maceral and mineral constituents present in coal samples. Megascopic examination using the AIAS, combined with selected specific gravity determinations on a given drill core or columnar block sample, delineates the lithologies present. Distinctive mixed lithologies (lithotypes and microlithotype assemblages) are designated for preparation of polished blocks and (or) polished thin sections for microscopic examination. After calibration, the AIAS can analyze a given field of view (megascopic or microscopic), consisting of five phases, in about 3 minutes. A "VEIM" notation system was adopted for presenting the quantitative data obtained. In VEIM notation, lithologies analyzed megascopically are described (with volume percentages indicated in subscripts) in terms of (V) for vitrite or vitrain, (E) for liptite, (I) for inertite or fusain, and (M) for mineral components. For microscopic analyses of mixed lithologies, V represents vitrinite group macerals; E, exinite; I, inertinite; and M, mineral components. For example, $(V)_{20}(V_{80}E_{10}I_5M_5)_{80}$ indicates an assemblage of 20 volume percent of vitrite and 80 percent of a microlithotype assemblage with composition $V_{80}E_{10}I_5M_5$. The term "clarain," conventionally used to describe such an assemblage, by comparison conveys only a vague indication of modal composition.

This method of modal analysis is not independent of the operator of the AIAS. The quality of an analysis is dependent on the judgment of a petrographer to identify the coal components; that is, to assign the range of gray tones associated with each coal constituent displayed on the TV screen. However, a major advantage of the AIAS is that, after selecting the gray level ranges, no futher judgmental uncertainties enter into an analysis.

Chao, Minkin, and Thompson are using the AIAS and the VEIM notation system to obtain rapidly maximum quantitative information on a large number of samples. The data they develop are being used for petrologic investigations of geologic processes in coal genesis and for prediction of coal quantity and quality changes laterally and stratigraphically.

Electrolytic oxidation of coal

Although the oxidation of anthracite by chemical techniques is extremely difficult, F. E. Senftle, A. N. Thorpe, and C. C. Alexander have devised an electrolytic method that oxidizes anthracite and some high-ash bituminous coals in several minutes. The oxidized products are humic and subhumic acids. The mechanism of electrolytic oxidation differs from that of chemical oxidation and is not understood clearly yet. Oxygen formed at the anode, probably in the form of O_2- or HO_2-, must be in close contact with the coal surfaces for effective oxidation. Therefore, it appears possible to electrolytically oxidize in situ coal beds where mining is not feasible or where an exceedingly high ash content renders a coal unsuitable as a fuel.

In situ capture gamma-ray analysis of coal in oversized boreholes

F. E. Senftle, A. B. Tanner, P. W. Philbin, G. R. Boynton, and C. W. Schram (1978) reported accurate in situ capture gamma-ray analysis of a coal bed using a high resolution gamma-ray spectrometer in a close-fitting drill hole. A check to determine the accuracy of the method was conducted in 1979 under adverse conditions. Similar measurements were made in the Pittsburgh coal bed, Green County, Pa., using a small-diameter sonde in an oversized drill hole. The hole was five times the diameter of the sonde, a ratio that substantially increased the contribution of water (hydrogen) to the total spectral count and reduced the size of the sample measured by the detector. The total natural count, the potassium-40 count, and the intensities of capture gamma rays from silicon, calcium, hydrogen, and aluminum were determined as a function of depth above, through, and below the coal bed. From these logs, the depth to the top and base of the coal bed, the thickness of the bed, and the location of the partings in the bed were determined. Spectra were allowed to accumulate in the coal bed for 1-h periods by using neutron sources of different strengths. Spectra obtained from several californium-252 neutron sources of different sizes allowed determination of the ultimate elemental composition of the coal and of its ash content. The analytical results were not as accurate as those obtained in a close-fitting drill hole. However, the accuracy of the results did improve with successively larger source-to-detector distances, that is, as the count contribution due to hydrogen in the water decreased. It was concluded

that in situ analyses should be made in relatively close-fitting drill holes.

OIL AND GAS RESOURCES

NATIONAL PETROLEUM RESERVE IN ALASKA

Depositional history and reservoir development of Nanushuk Group

The Nanushuk Group of Cretaceous (Albian to Cenomanian) age is a passive-margin deltaic deposit, as much as 3,500 m thick, that underlies much of the NPRA and adjacent areas of Alaska. Foreset dip directions in the underlying Torok Formation, as displayed on seismic sections, indicate that the delta prograded from west-southwest to east-northeast across the subsiding Colville basin (Bird and Andrews, 1979). Two distinct source areas are interpreted: one to the southwest in the area of the present Chukchi Sea and the other in the ancestral Brooks Range, which bounded the south side of the Colville basin.

Subsurface seismic-stratigraphic studies by C. M. Molenaar have added some interesting quantitative data on basin geometry and depositional history of the Nanushuk Group and associated strata. These data may relate to the delineation of areas of better development of sandstone reservoirs. Seismic data indicate that the Nanushuk is laterally equivalent to and prograded over shelf, slope, and basinal deposits of the Torok Formation. Measurements of these features indicate that (1) the prodelta shelf was 75 to 150 km wide, (2) the basin slope angle generally steepened from less than 2° on the west to as much as 6° on the east, and (3) the basinal or bottomset beds were deposited in water depths of 450 to 900 m. The foreset and bottomset beds in the Torok downlap onto or near the Neocomian pebble shale unit in the northern part of the NPRA. The thin intervening interval represents part of Neocomian time, all of Aptian time, and a large part of Albian time. Thus, a hydrocarbon migration path from mature source rocks in lower shales of the Torok or the underlying pebble shale unit to updip reservoirs in the Nanushuk could be provided by sandy zones along some of the foreset beds of the Torok.

The total incremental stratigraphic rise (a measure of relative sea level rise and (or) basin subsidence) of the base of the Nanushuk from the Tunalik well on the west to the Atigaru Point well on the east, a distance of 350 km, is about 2,100 m. However, subsidence was not uniform throughout the basin as indicated by less and (or) later subsidence of the Barrow arch, a passive high on the north side of the basin.

Because of increased subsidence on the south side of the asymmetrical basin, the southern-source deltas probably did not extend very far northward into the subsurface. However, the growth of the Umiat delta southeast of the NPRA coincided with the presence of the prodelta shelf of the larger eastward-prograding western delta; as a result, the southerly derived clastic deposits were distributed along the north-northwest-trending shoreline and shelf, probably by longshore currents. It is postulated that during late Nanushuk time, marine energy (that is, wave action and longshore currents) increased because of the more open marine conditions that prevailed after the Barrow arch subsided enough to lose its silling effect on the Colville basin. It is further postulated that marine circulation was restricted somewhat in the Colville basin prior to that time. This restriction would account for the low marine energy and relative paucity of open-marine faunas in much of the Nanushuk in the western part of the NPRA.

Thus, the eastern part of the NPRA, along the alinement of the Umiat, Inigok, and Simpson wells, has better development of sandstone. In addition, the sand contribution from the Umiat delta is relatively richer in quartz content, especially farther north where labile constituents are more likely to have been removed by winnowing and abrasion. Because the northeastern part of the NPRA has been less deeply buried than areas to the south and southwest, as indicated by velocity logs, the most favorable area for sandstone reservoirs is considered to be the northern part of the area of better sandstone.

Two types of oil on North Slope

Forty oil samples from the North Slope of Alaska have been analyzed by the USBM and USGS. Results of these analyses suggest two generally distinct types of oil, according to L. B. Magoon and G. E. Claypool. The first type, that of the Simpson-Umiat, occurs in reservoir rocks of Cretaceous to Quaternary ages and includes oils from seeps in the Skull Cliff, Cape Simpson, Manning Point, and Ungoon Point areas; the Wolf Creek Test Well No. 3; and the Umiat oil field. These oils have higher gravity, low sulfur content, no or only slight predominance of odd-numbered *n*-alkanes, and pristane-to-phytane ratios of greater than 1.5. The second type, that of the Barrow-Prudhoe, occurs in reservoir rocks of Carboniferous to Tertiary age and includes oils from South Barrow gas field, Prudhoe Bay oil field, and the Fish Creek Test Well No. 1. Physical properties of Barrow-Prudhoe oils are varied, but, in general, the oils are medium-gravity high-sulfur oils with a slight even-numbered *n*-alkane predominance and pristane-to-phytane ratios of less than 1.5. The two types are believed to originate from different source rocks. The

Barrow-Prudhoe oil type may have originated from a carbonate rock or other iron-deficient source rock. Geographic distribution of the two oil types indicates at least two exploration fairways. The fairway for the Barrow-Prudhoe oil type is along the Barrow arch, and the fairway for the Simpson-Umiat oil type is the area of the best reservoir development for the Nanushuk Group, as discussed by C. M. Molenaar.

Geochemical prospecting for petroleum, Simpson Peninsula

A helium survey was conducted by A. A. Roberts and K. I. Cunningham on the Simpson Peninsula to determine the concentrations of helium in near-surface soil gas. Past work in other areas had suggested that microseepage from petroleum reservoirs often results in detectable high helium concentrations. Frozen soil samples were collected at two depths, at 0.1 m in the active zone and at 0.5 m in the permafrost. These samples then were analyzed for helium content in the laboratory. The permafrost sample analysis revealed a strong helium anomaly that has been interpreted to be in a halo pattern around a possible petroleum prospect in the center of the peninsula. This possibility is supported by an aeromagnetic survey performed by T. J. Donovan, A. A. Roberts, and J. D. Hendricks, who observed a near-surface high-frequency magnetic anomaly around the same area outlined by the helium survey. The magnetic source is believed to be diagenetic magnetite that is formed by the reduction of ferric oxides in the reducing environment caused by microseepage of hydrocarbons from a buried petroleum reservoir. In contrast to the permafrost surveys, the helium survey of the active zone showed no discernible pattern of anomalously high concentrations. This indicates that sampling must be performed in the permafrost beneath the active layer to obtain meaningful results.

High-frequency aeromagnetic anomalies associated with hydrocarbon microseepage

Approximately 8,000 km of low-level total field aeromagnetic lines were surveyed in the NPRA during June and July 1979. The survey was conducted in areas of known and suspected hydrocarbon accumulations to identify areas of high frequency (near-surface) anomalies suspected to occur in association with hydrocarbon microseepage (Donovan and others, 1979). Preliminary results of the survey suggest to J. D. Hendricks that an excellent correlation exists between known surface-seep areas and high frequency magnetic anomalies. Regional lines flown across the reserve indicate that most magnetic variations result from changes in the deep (~5 km) magnetic basement rock; such variations produce very low frequency anomalies. The high frequency anomalies are quite distinctive and are easily separated from these longer wave length anomalies. Areas having high frequency variations but devoid of surface seepage also were noted. These areas warrant further exploration for oil and gas deposits.

OFFSHORE ALASKA

Petroleum potential of Norton basin, Outer Continental Shelf

Interpretation of carbon isotopic compositions of gas from the Norton basin marine gas seep south of Nome, Alaska, suggests that the ultimate source of the gas may be sedimentary source rocks at a subseafloor depth of about 2.5 km, according to T. H. McCulloh, M. L. Holmes, B. D. Ruppel, and R. J. Lantz. Nonsedimentary basement rocks beneath the seep area occur at depths of only 0.85 to 1.45 km, suggesting that the seeping gas originated to the south in the deeper central trough of the basin. Seismic refraction data indicate that the average depth to basement along the main basin axis is about 2.5 km, sufficient to account for the observed carbon isotopic compositions of the migrated hydrocarbon gases. Two areas where sedimentary rocks plunge to depths as great as 5 km have been defined by seismic refraction surveys northwest of the Yukon River Delta and far to the southeast of the offshore gas seep.

On the basis of regional geology and the character of seismic reflections, much of the fill in the Norton basin was interpreted by M. A. Fisher to be of nonmarine or deltaic origin. The oldest rocks in the basin may be Late Cretaceous or Paleocene. Preliminary assessment of the hydrocarbon resources showed that the Norton basin is deep enough to generate hydrocarbons.

Petroleum potential of Upper Cretaceous rocks, Cook Inlet

A section of Upper Cretaceous (Maestrichtian) nonmarine sandstone, conglomerate, siltstone, and coal, exposed near Saddle Mountain on the northwest flank of the Cook Inlet basin, Alaska, was studied by L. B. Magoon, F. R. Griesbach, and R. M. Egbert. This is the only known surface exposure of nonmarine Upper Cretaceous rocks in the Cook Inlet area. The section is at least 83.3 m thick and is unconformably overlain by lower Tertiary rocks of the West Foreland Formation. Palynology and petrography indicate that the studied Upper Cretaceous rocks correlate with the second or deeper interval of nonmarine Upper Cretaceous rocks penetrated in the lower Cook Inlet COST Well No. 1. The Upper Cretaceous rocks are important potential petroleum reservoirs in the lower Cook Inlet and Shelikof Strait.

ROCKY MOUNTAINS AND GREAT PLAINS

Origin and accumulation of biogenic gas in the Rocky Mountains

Shallow gas fields in the Rocky Mountains, documented by D. D. Rice to contain gas of biogenic origin, occur within marine sequences. The methane-rich gas was generated as a result of degradation of organic matter by anaerobic micro-organisms in accumulating sediments. Biogenic gas was produced by a succession of metabolic processes and organisms established in the sediment and water column, with organisms less efficient in producing biogenic gas occurring at greater depths. After the supply of oxygen was depleted, probably at some depth below the sediment-water interface, sulfate reduction became the dominant form of respiration. Methane generation began only when the high concentration of sulfate in seawater was greatly reduced. The most efficient mechanism of methane generation is CO_2 reduction. The major limiting factors of biogenic gas production after burial are anoxic environment, sulfate-free environment, temperature, abundance and complexity of organic matter, grain size of sediments, space, and rate of sedimentation.

In marine sediments, initially formed biogenic gas is generally dissolved in pore waters because of the limited amount that is generated and because of the hydrostatic pressure resulting from the sediment and water column. This dissolution acts as a holding mechanism until a free gas phase develops, the sediments are compacted, and traps and seals are formed. Free gas occurs either when the solubility minimum is exceeded or when exsolution results from a reduction in hydrostatic pressure. Possible trapping and sealing mechanisms are early carbonate cement resulting from reduction of CO_2, low-permeability reservoirs, bentonite deposits, hydrate deposits, and subnormal pressures.

Seismic models of stratigraphically controlled oil fields and gas fields in Rocky Mountain basins

Two-dimensional normal-incidence ray-theory seismic models were generated by R. T. Ryder for 15 stratigraphically trapped oil and gas accumulations in the Rocky Mountains. The investigation was a feasibility study to determine the seismic character of moderately thick (6–30 m) lenticular sandstone reservoirs in Rocky Mountain basins. The models are noise free and do not include all the complexities of the seismic phenomenon, but they do provide a reasonable indication of the anomaly to be expected for a specific problem and the quality of seismic data required to solve it. The fields modeled include Bell Creek, Dillinger Ranch, Pine Lodge, Raven Creek, Red Bird, Rozet, South Glenrock, Well Draw, and West Salt Creek in the Powder River Basin; Adena, Holster–Third Creek, and Peoria in the Denver Basin; Desert Springs and Patrick Draw in the greater Green River Basin; and Horseshoe in the San Juan Basin. Many of the 15 fields appear to have a reasonable chance of being detected by conventional seismic data. Several of the documented anomalies are very subtle. The seismic anomalies generally are manifested as amplitude increases due either to marked acoustic contrasts at the boundaries of a stratigraphic unit or to the constructive interference of waveforms interacting with adjacent stratigraphic horizons (that is, tuning).

Distribution and diagenetic history of possible reservoir beds in Madison Group, disturbed belt, Montana

Dolomitized crinoidal grainstone units locally form a recognizable unit in the upper part of the Mississippian Madison Group, which unconformably underlies Jurassic strata in the disturbed belt, northwestern Montana. These grainstone units on surface exposures exhibit a significant vuggy and intercrystalline porosity (4–12 percent) and permeability (6–12 md); many of the pores are filled with dead oil. The crinoidal grainstone unit has been interpreted by K. M. Nichols to have undergone eogenetic secondary dolomitization, probably in Late Mississippian time and prior to any significant erosional events. Porosity most likely resulted from solution effects during erosion and, hence, was fully developed prior to deposition of overlying Jurassic strata. Phreatic calcite cement partially occludes some of the pore space and developed after migration of liquid hydrocarbons into the grainstone unit.

Variations in thickness of the grainstone unit result mainly from pre-Jurassic erosion. In places, the grainstone units are eroded completely beneath the Jurassic rocks, but, where present, they thicken to more than 100 m, as observed in a north-south direction along the strike of imbricate thrust slices of the pre-Tertiary section. These thickness changes may have resulted either from broad warping of the Mississippian strata followed by planar erosional truncation or from erosional relief on the Jurassic erosion surface carved into unfolded Mississippian strata. It is also possible that the changes resulted from some combination of these two effects, which may have different geographic trends. Mapping of the thickness changes should be an aid to petroleum exploration in the adjacent subsurface of northwestern Montana.

Reservoir characteristics of gas-bearing Eagle Sandstone, Bearpaw Mountains, Montana

The Upper Cretaceous Eagle Sandstone in the Bearpaw Mountains area of Montana is an important reservoir for shallow isotopically light methane gas. D. L.

Gautier found that the formation is composed of sandstone and lesser amounts of mudstone. The sandstone is composed mainly of quartz (50 percent), plagioclase (25 percent), potassium-feldspar (5–10 percent), and various rock fragments (15–20 percent). The mudstone is composed mainly of highly expansible mixed-layer clay and coarser grained minerals similar to those of associated sandstone. The source area for the Eagle Sandstone lay to the west and was a mixed terrane of Precambrian metasedimentary rocks, Paleozoic sedimentary rocks, and volcanic rocks of probable Cretaceous age.

Although many lines of evidence indicate that the Eagle Sandstone and associated gas source rocks have not undergone thermal maturation sufficient for the generation of oil or thermogenic gas, diagenesis has, nevertheless, been important in determining the reservoir properties of the sandstone. Localized calcite precipitation began shortly after deposition. Compaction and minor quartz cementation occurred as burial depths increased. Then, extensive precipitation of isotopically light sparry calcite tightly sealed many intergranular pores and selectively replaced plagioclase. Siderite developed locally, usually because of increased iron activities associated with altering biotite. Dissolution of calcite provided space for precipitation of authigenic clays. The present distribution of calcite-cemented layers limits vertical permeability and compartmentalizes the reservoirs. Early diagenetic carbonate minerals may have acted as gas-trapping seals, particularly in lower permeability reservoirs to the east. Fluid-sensitive authigenic clays and iron carbonate minerals may cause reservoir damage if not considered during the development of gas recovery methods.

Paleogeography and petroleum resources of Tyler Formation, central Montana

The Lower Pennsylvanian Tyler Formation in central Montana is a deltaic complex, and its Bear Gulch Limestone Member of Norton (1956) has been interpreted by E. K. Maughan to represent brackish marine-bay deposits at the delta margin. The delta formed as the Early Pennsylvanian sea transgressed into the central Montana trough. This trough may have been an incipient aulacogen that developed between the Cordilleran geosyncline and the intracratonic Williston basin. The Stonehouse Canyon Member of the Tyler comprises mainly streamchannel sandstone and lacustrine humic-mudstone deposits. Norton's Bear Gulch is made up of thin-bedded argillaceous limestone. The Cameron Creek Member of the Tyler contains red beds, chiefly mudstones, which lie above the two other members and were deposited as the environment changed from paralic to littoral. The Tyler Formation lies with considerable erosional relief above the Upper Mississippian Heath Formation, and the organic-rich mudstones in the Heath were probably the source of the petroleum that is found in the streamchannel sandstone deposits of the Stonehouse Canyon Member of the Tyler.

Potential petroleum reservoir rocks in southwestern Montana

In both the Medicine Lodge and Tendoy allochthons east of the Deadman normal fault in the Edie Ranch quadrangle, Idaho and Montana (Skipp and Hait, 1977), potential petroleum reservoir rocks of late Paleozoic and Triassic age contain conodonts that locally have conodont CAI values of 1 to 2, according to A. L. Skipp. These low values indicate that the rocks have not been subjected to temperatures greater than 100°C, and, thus, are in the temperature range for oil generation (Epstein and others, 1977). In contrast, upper Paleozoic carbonate rocks of the overlying Beaverhead allochthon west of the Deadman fault have CAI values of 4 to 5½, indicating temperatures around 300°C, which are too high for petroleum generation.

Source-rock potential of some Upper Cretaceous shale, northeastern Wyoming

Shale in some lower Upper Cretaceous formations of northeastern Wyoming has been studied by E. A. Merewether and G. E. Claypool to identify possible source rocks and to evaluate their petroleum potential. Cores of lower Upper Cretaceous strata were obtained from boreholes in Weston County on the eastern margin of the Powder River Basin, in Converse County near the axis of the basin, and in Johnson County on the western flank of the basin. In Weston County, the studied core is from depths of less than 270 m and represents, in ascending order, the upper part of the Belle Fourche Shale, the Greenhorn Limestone, and the Carlile Shale. The Carlile comprises, from base to top, the Pool Creek, Turner Sandy, and Sage Breaks Members. Except for the Turner, these members and formations were deposited in offshore open-marine environments and consist largely of calcareous and noncalcareous shale. In Converse County, the studied core is from the upper part of the Frontier Formation and the lower part of the overlying Cody Shale, at depths of about 3,781 to 3,880 m. Core of the Frontier and the lower part of the Cody Shale was obtained also from Johnson County at depths of less than 320 m. The sampled beds in Converse and Johnson Counties were deposited in nearshore marine environments and consist mostly of noncalcareous shale.

Samples from the three localities were analyzed for their organic-carbon content, total pyrolytic hydrocarbon yield, and volatile hydrocarbon content. The temperature of maximum pyrolytic yield and the vitrinite reflectance also were determined. These

analyses indicate that the amount and character of the organic matter in the sampled rocks are related to the content of calcium carbonate, the depositional environment, and the burial depth of the strata. On the east flank of the Powder River Basin, calcareous shale of offshore marine origin contains abundant hydrogen-rich organic matter, which was derived mainly from aquatic plants. Noncalcareous shale of largely nearshore marine origin on the west flank of the basin locally contains a significant amount of hydrogen-poor organic matter, which was derived mostly from land plants. The noncalcareous nearshore marine shale in the middle of the basin probably contained similar amounts of hydrogen-deficient organic matter prior to deep burial and thermal alteration.

The calcareous shale in Weston County is a potentially rich source of oil and gas, but it is thermally immature and in a very early stage of the hydrocarbon-generation process. The noncalcareous shale in Johnson County is a potential source rock for gas, but it also is in an early stage of thermal alteration. The sampled beds in Converse County are thermally mature and have generated hydrocarbons. The extent of this contribution of hydrocarbons to the commercial petroleum occurrences of the area can be inferred from the composition of the original organic matter in the beds. Furthermore, the degree of thermal alteration of the organic matter at these localities indicates that the depth of the sampled strata was never as great on the flanks of the Powder River Basin as in the middle of the basin.

Biogeochemical and airborne geochemical prospecting of Recluse oil field, Wyoming

Biogeochemical measurements by Mary Dalziel and T. J. Donovan of anomalous Mn:Fe in pine needles and sage leaves from the Recluse oil field, Wyoming, suggested the effects on plants of microseepage from buried petroleum deposits. Soil and rock chemical and isotopic data also supported this conclusion. Hydrocarbons provide reducing conditions sufficient to enable divalent iron and manganese to be organically complexed or adsorbed on solids in the soils. Plants readily assimilate these bound or adsorped elements in the divalent state for their essential use. The magnitude of the plant anomalies, combined with the supportive isotopic and chemical evidence confirming petroleum leakage, makes a strong case for measurements of Mn:Fe as a biogeochemical prospecting tool.

Airborne geochemical prospecting studies by T. J. Donovan, A. A. Roberts, and Mary Dalziel suggested that particulates, captured by airborne collectors at low altitude over the Recluse oil field, Wyoming, chemically approximate the Mn:Fe found in the pine needles and sage leaves over and around the field. Particulates bearing anomalous Mn:Fe concentrations are shed by leaf surfaces and wafted into the air by thermal convection and other processes. These preliminary results suggest that airborne geochemical prospecting also may be a useful reconnaissance exploration tool.

Porosity of oil reservoirs in Bighorn Basin, Wyoming

Interval density and porosity profiles determined from borehole gravity surveys in the Garland, Gebo, and Big Polecat oil fields in the Bighorn Basin, Wyo., were compared with gamma-gamma density logs, neutron porosity logs, and density and porosity measurements of core samples by L. A. Beyer and F. G. Clutsom. Certain discrepancies between the density and porosity methods arise because borehole gravity, owing to its large radius of investigation, measures an average porosity that includes the irregularly distributed component (for example, vugular porosity of reservoir rocks in the Mississippian Madison Limestone at Garland), which is less effectively evaluated by conventional shallow-penetration logs or core samples. Variations in the contribution of fracture porosity to total porosity in the mainly Pennsylvanian Tensleep Sandstone reservoir at Gebo are masked by much larger fluctuations in intergranular porosity caused by differences in the cementation and abundance of dolomite. In any case, the magnitude of fracture porosity probably is below the threshold of detection by borehole gravity surveys. High-porosity (>15 percent) and (or) gas-filled sandstone units, principally in the Cretaceous Frontier Formation, were detected easily behind casing in the three oil fields studied. An abrupt (and possibly widespread) downward increase in porosity in the upper part of the Frontier may have exploration significance and probably reflects lithologic and mineralogic variations resulting from changes in the depositional environment (Beyer, 1979).

Petroleum source rocks in Chesterian strata, northwestern Wyoming

Strata of Late Mississippian (Chesterian) age that are similar in lithology and age to the Heath Formation of central Montana are present in northwestern Wyoming. E. K. Maughan has found these strata to be rich in sapropelic organic carbon. At an exposure in Teton County, 20 km northwest of Togwotee Pass, weight percentage of the organic carbon ranges from 9 percent in the noncalcareous claystone beds to about 1 percent in argillaceous limestone beds. The high amount of organic carbon and the petroliferous odor of these beds suggest that they are petroleum source rocks. They lie unconformably beneath the Lower Pennsylvanian Horseshoe Shale Member of the Amsden Formation, which provides a seal against upward migration of petroleum, and they are underlain by littoral and dune-sand deposits, which may provide good petroleum reservoirs. The area of distribution of these possible

petroleum source beds is limited, however, because erosion that preceded deposition of the Horseshoe removed them everywhere east of Togwotee Pass and from some places in Teton County.

Petrology and reservoir characteristics of Mesaverde Group, Washakie Basin, Wyoming

A petrographic study of core samples from hydrocarbon reservoirs in the Upper Cretaceous Mesaverde Group, Washakie Basin, Wyo., was conducted by J. C. Webb. This study showed that the amount and distribution of porosity and permeability in sandstones having similar grain size and sorting are related to the original composition of the sediments and to the response of these sediments to diagenetic alteration. Diagenetic alteration is responsible both for the reduction and enhancement of porosity by the precipitation of cements and for the dissolution of authigenic minerals and framework grains.

Quartzose sandstones are well cemented by overgrowths of quartz, authigenic illite, mixed-layer illite-smectite of low expansibility, minor kaolinite, and, locally, by dolomite. The porosity of quartzose sandstones decreases throughout diagenesis. In contrast, feldspathic sandstones contain a smaller volume of quartz cement and show evidence of extensive cementation by calcite of dolomite; precipitation of large amounts of kaolinite, minor amounts of mixed-layer illite-smectite of low expansibility, and illite; and dissolution of carbonate cement and silicate framework grains. During diagenesis, porosity in feldspathic rocks decreased due to cementation by quartz and carbonate minerals, increased due to dissolution of calcite and feldspars, and decreased, locally, by the subsequent precipitation of kaolinite mixed-layer illite-smectite and illite.

Permeability of quartzose and feldspathic sandstones is affected also by the diagenetic changes in porosity distribution and by the morphology and mode of occurrence of clay-mineral cements. Illite commonly occurs in pore throats of quartzose sandstone that has been constricted previously by overgrowths on surrounding quartz grains. The net effect is a further reduction in permeability, with little effect on porosity. Kaolinite commonly occurs as fillings in grain molds and intergranular pores in feldspathic sandstone. It is associated commonly with relicts of calcite cement, which was at the time more extensive. Kaolinite reduces both porosity and permeability, but, because it is associated with the development of secondary porosity, it does not reduce effective permeability of the arkosic sandstone. Conclusions of this study are that (1) porosity of quartzose rocks is preserved primary porosity, with the exception of intergranular porosity in chert grains, (2) porosity of feldspathic rocks is largely of secondary origin, (3) porosity and permeability of feldspathic rocks is greater than porosity and permeability of quartzose rocks of similar grain size and sorting, and (4) clay-mineral assemblages dominated by kaolinite are associated with higher porosity and permeability than those dominated by illite and mixed-layer illite-smectite.

Overpressuring and fracture development in low-permeability rocks, Green River Basin, Wyoming

Studies of subsurface temperature and pressure gradients and organic matter characterization in the Pacific Creek area of the northeastern Green River Basin, Wyo., have provided evidence indicating that the active (dynamic) process of thermal gas generation is the main cause of overpressuring (Law and others, 1980). Examination of highly fractured core from similar thermally mature overpressured rocks by B. E. Law, J. C. Webb, and D. J. Markochick in the Belco (Inexco) Al WASP well, sec. 28, T. 36 N., R. 112 W., northern Green River Basin indicates that at least some of the fractures may have resulted from internally generated stresses rather than from tectonic or overburden stresses. Fractures developed as a result of overpressuring caused by gas generation would have the overall effect of enhancing permeability in otherwise low-permeability reservoirs.

Mineralogy and diagenesis of gas-bearing reservoirs in Niobrara Chalk

The Upper Cretaceous Niobrara Chalk recently has been shown to be a widely distributed high-potential gas reservoir in a large area of the Western Interior. The main process controlling porosity reduction in chalk has been demonstrated to be pressure solution and reprecipitation of calcium carbonate caused by increases in lithostatic pressure during burial.

Preliminary mineralogical analysis of the chalk and associated sediments from core and well cutting samples of the Niobrara Chalk by R. M. Pollastro has suggested the occurrence of depth-diagenetic clay-mineral transformations similar to those known in shale, sandstone, and volcanogenic sedimentary rocks. However, differences apparently exist in the transformations of these clay minerals in the chalk. The changes may occur at much shallower depths than those recorded in studies of noncarbonate sedimentary rocks. This occurrence suggests that characteristics of the chalk environment, such as chemical composition, organic content, and type and amount of insoluble material, as well as the pressure-solution process, are important factors influencing these transformations and, hence, the resulting reservoir quality of the rock.

X-ray diffraction and scanning electron microscope analyses of numerous samples also have identified the

presence of authigenic kaolinite, commonly pelletal, which appears to develop in relatively large pore spaces, such as in the tests of forams. In many cases, this authigenic kaolinite appears to be associated with diagenetic pyrite.

GREAT BASIN AND CALIFORNIA

Sedimentation rates and timing of Antler orogenic events determined from conodont zonation, Western United States

The rates of sedimentation of Upper Devonian and Lower Mississippian petroleum source rocks and reservoir rocks in the eastern Great Basin and overthrust belt and the timing of early events of the Antler orogeny have been determined by C. A. Sandberg, using timespans of conodont zones for measurement. The methodology has been discussed by Sandberg and Poole (1977) and Sandberg and Gutschick (1979). The rock types and their rates of sedimentation in meters per million years are transgressive lag deposits, 1–3; organic-rich starved-basin phosphatic shale and micrite, 4½–9; micritic slope limestone, 26–30; bioclastic carbonate-platform rocks, 40–240; organic-rich nonphosphatic basinal mudstone, 55; protoflysch siltstone and silty limestone, 32–160; and Antler calcareous flysch, 267–400.

Antler orogenic events were timed in relation to the Devonian-Carboniferous boundary, which has been variously dated radiometrically as 345 m.y. B.P., 350 m.y. B.P., or 360 m.y. B.P. The following conodont-dated succession of events and their duration are internally consistent, regardless of any fluctuation in the radiometric dating of the boundary. Times are given in million years before (−) or after (+) the time of the boundary (0): (1) start of Antler orogeny and of Taghanic marine onlap of craton, −16; (2) end of predominantly carbonate depositional cycle, −5; (3) continent-wide erosion, −5 to −4; (4) minor orogenic pulse resulting in minor marine onlap of craton, −4; (5) major orogenic pulse resulting in major marine onlap of craton, −2½; (6) start of Roberts Mountains thrusting, −2; (7) orogenic quiescence resulting in marine regression, −1½ to 0; (8) episode of continental stability with only minor marine onlaps, 0 to +4; (9) renewed orogenic activity and thrusting resulting in major marine onlap, +4½; (10) end of Roberts Mountains thrusting, +6; and (11) deposition of overlap assemblage of Antler calcareous flysch on top of thrust, +6 to +9.

The most important single fact demonstrated by the above tabulation is that emplacement of the Roberts Mountains thrust took 8 m.y., spanning the Devonian-Carboniferous boundary between events 6 and 10.

Diagenesis of reservoir rocks of the Monterey Shale, Santa Barbara coast, California

Lateral differences in strata of the Monterey Shale along the Santa Barbara coast indicated to C. M. Isaacs (1979) that diagenesis increases toward the west. Silica alters westward from biogenic amorphous opal (in diatom frustules) to diagenetic opal-CT (cristobalite) and then to diagenetic quartz. Continuous exposure for 50 km, simple homoclinal structure, paleogeographic setting, and detailed analysis of 14 stratigraphic sections together show that the strata originally were continuous depositionally. Distinctive stratigraphic differences in sediment composition within the five informal members of the Monterey are also laterally age constant. Because silica phases differ in rocks of the same age, depositional environment, and composition, the differences must reflect postdepositional conditions. Overburden thicknesses and thermal changes in organic matter indicate that diagenesis increases westward owing to greater burial temperature.

Porosity of Miocene siliceous shale, Midway-Sunset oil field, California

Study of conventional core samples of siliceous shale from the Midway-Sunset oil field, California, indicated to L. A. Beyer and C. M. Isaacs (1979) that porosity is strongly influenced by silica phase and clay content. Diatomaceous shales, which contain silica as opal-A (amorphous opal), have high porosities (45–65 percent or more), whereas shales that contain silica as opal-CT (cristobalite) have distinctly lower porosities (25–45 percent). When silica is transformed from opal-A to opal-CT, 5 to 20 percent porosity is lost over a depth interval of less than 50 m. Porosity variations among diatomaceous shales and among opal-CT rocks and, hence, the magnitude of the porosity change across the phase boundary are governed primarily by variations in the clay content of the core samples. As clay content increases, porosity decreases, and the porosity change associated with the phase boundary is diminished. Although not yet confirmed by measurements, it is thought that permeability is affected by silica phase and clay content in the same manner as porosity.

GULF OF MEXICO AND FLORIDA

Possible effects on coral growth of offshore petroleum drilling, Gulf of Mexico

Large heads of the coral *Montastrea annularis* were cored by J. H. Hudson, D. M. Robbin, and E. A. Shinn at East Flower Gardens Reef in 22 m of water off the Texas coast to determine the annual coral growth rates since the turn of the century and the presence of components of drilling mud (mainly barium, bentonite, and chromium) in that portion of the coral skeleton

representing time of nearby offshore petroleum drilling activity. Analyses showed that background levels of barium during and after drilling were the same as those in coral skeletons prior to drilling; bentonite and chromium were not detected. Annual coral growth-rate studies, however, showed a drastic reduction (from 8 mm average to 6 mm average) starting in 1954 and continuing to about 5 yr. Cause of the growth-rate reduction is not known, but the following factors are being evaluated: (1) rapid increase in the use of otter trawls by the shrimp industry, (2) rapid increase in offshore drilling, although not in this area, (3) increase in use of chlorinated hydrocarbons, such as DDT, (4) chemical waste dumping in the Gulf of Mexico, and (5) air pollution resulting in reduced light levels.

Helium anomaly—possible indicator of petroleum in southern Florida

Surveys of helium concentrations in soil gases were conducted by J. G. Palacas and A. A. Roberts in two areas of southern Florida to further test their utility in petroleum exploration. In the first survey, a small but positive helium anomaly (40–60 ppb above background) was detected over the Sunniland oil field, indicating an association between the anomalous helium concentrations and the petroleum reservoir of Early Cretaceous age. The second survey discovered a relatively strong helium anomaly (40–140 ppb above background) in an area east of the town of Immokalee, Fla. This anomaly also may reflect oil accumulations in Lower Cretaceous carbonate rocks. The presence of apparently adequate source rocks and of significant oil shows in the "Fredericksburg 'B'" unit and Sunniland Limestone in nearby boreholes lends strong support to possible oil accumulations in these two formations. However, the anomaly alternatively may be related to helium produced during radioactive decay of uranium in a shallow enriched ore deposit or to helium produced in an upper Tertiary phosphate deposit containing small amounts of dispersed uranium that has been brought close to the surface by a domal or anticlinal structure. Regardless of whether petroleum, enriched uranium ore, or uraniferous phosphate is the cause of the anomaly, the area merits further investigation because all three possible anomaly causes have economic significance.

Reservoir characteristics of Sunniland Limestone (Lower Cretaceous), southern Florida

Porosity and permeability of the Sunniland Limestone were affected adversely by burial diagenesis, according to R. B. Halley. Burial diagenesis often has been considered unimportant in limestones such as the Sunniland, but the processes and products resulting from deep burial of this formation have been well documented. The processes include compaction (both mechanical and chemical) and cementation by calcite, dolomite, and anhydrite. The result may be that the Sunniland has lost original reservoir potential. The Sunniland Limestone illustrates that burial diagenesis can be as significant a factor as original sedimentary facies patterns or early diagenetic history in reservoir destruction.

APPALACHIAN BASIN

Origin of hydrocarbons in Devonian shale

Small amounts of methane were formed in Devonian black shale during early low-temperature stages of diagenesis, but most of the natural gas was generated by thermochemical conversion of solid and liquid organic matter during later higher temperature stages, according to G. E. Claypool. At any given locality, the amount of methane generated in Devonian shale is determined by the amount of organic matter originally present and by the extent of the transformation process, which, in turn, is determined by the maximum depth of burial and subsurface temperature to which the rock was subjected. This transformation process was halted in its early stages in rocks of the western part of the basin but approached completion in the east. The degree of transformation is indicated by systematic west-to-east changes in the geochemistry of gas ($\delta^{13}C$ of methane changes from -55 to -25 per mil), extractable organic matter (saturated hydrocarbons evolve from an immature to an incipiently metamorphosed assemblage), and solid organic matter (atomic H:C changes from 1.1 to 0.4).

Oils derived from Devonian shale exhibit systematic variation in hydrocarbon geochemistry. On the basis of correlations with Devonian source rocks, oils on the western margin of the basin in the Mississippian Berea Sandstone must have been generated in and migrated from shale located about 100 km to the east. In contrast, the easternmost oil occurrences in lenticular sandstones were products of very local migration from adjacent shale. In the eastern part of the basin, the advanced stage of thermal maturity of both oils and extractable hydrocarbons in adjacent source rocks suggests that hydrocarbons, both in reservoir and source rocks, underwent parallel thermal maturation after migration and emplacement of oil.

Distribution of organic matter in Devonian shale

The distribution of organic matter in Devonian shale of the western Appalachian Basin has been characterized by J. W. Schmoker using quantitative organic-content data derived from formation-density and gamma-ray wire-line logs. The boundary between organic-rich and organic-poor facies is arbitrarily taken

as 2-percent organic content by volume, a value that corresponds to the lower limit of organic content required for significant generation of hydrocarbons and for a decrease in the ratio of movable-gas content to organic content. (Conventional studies of source rocks, however, use a lower cutoff of 0.5 percent organic carbon.) Organic-rich facies defined by color have a lower boundary of about 5-percent organic content by volume, whereas those defined by gamma-ray intensity have boundaries ranging between 1 and 10 percent that vary as a function of location. The thickness of organic-rich facies defined by the 2 percent criterion ranges from 61 to 305 m and is significantly greater than that based on sample color over most of the region. The average organic content (volume percent) of organic-rich facies increases from 5 percent in the middle of the basin to 16 percent in central Kentucky. The net thickness of organic matter (the product of volume-percent organic content and facies thickness) ranges between 6.1 and 24.4 m, with local thickness highs centered in Martin County, Ky., and eastern Pike County and northern Ashland County, Ohio.

Potential siltstone and sandstone gas reservoirs in Devonian shale

Black shale of Devonian age generally has been considered the reservoir rock as well as the source rock for Devonian gas in the Appalachian Basin. Past production records are incomplete, however, and identification of the reservoir rock as black shale is not always possible. Currently, the USGS, together with State surveys and universities, is cooperating with the DOE to characterize the shale to increase production from gas-bearing Devonian black shale.

Interpretation by J. B. Roen and R. C. Kepferle of sediment distribution patterns and facies relations of Devonian black shale and interbedded very fine grained sandstone and siltstone tongues of the distal part of the Catskill delta has suggested that gas from organic-rich black shale may be trapped in the coarser clastic rocks. The sandstone and siltstone are considerably more porous and permeable than the black shale and locally may act as reservoirs for gas generated in the black shale.

Recent studies by R. C. Kepferle (USGS) and R. F. Broadhead and P. E. Potter (University of Cincinnati) have indicated that coarser clastic rocks are potential reservoirs in an area along Lake Erie in northern Ohio. The study of available cores, production records, and drillers' reports of gas shows from this area has related lithostratigraphic units to potential reservoirs. Shows and production in this area are concentrated in units of the Three Lick Bed of the Ohio Shale and in units of the Chagrin Shale. These units contain abundant thick moderately quartzose siltstone beds and have more gas shows than interbedded claystone of the Chagrin Shale and black shale of the Huron Member of the Ohio Shale. This finding agrees with the findings of Patchen (1977, p. 4) and Patchen and others (1979, p. 1246), who reported that sandstone units in the Hampshire and Chemung Formations of Late Devonian age in north-central West Virginia and siltstones and very fine grained sandstone units of equivalent rocks in western Pennsylvania produce gas that is considered by Roen and Kepferle to have been generated from black shale source rocks.

The concentration of gas shows and production from siltstone and very fine sandstone interbeds within the black shale sequence in eastern Ohio, western Pennsylvania, and north-central and western West Virginia supports a suggestion by Roen of tectonic control of the deposition of potential siltstone and sandstone reservoir rocks in these areas in Late Devonian time.

Surface joint patterns as a guide to fracture reservoirs

Attitude, orientation, spacing, and other characteristics have been measured for more than 12,000 joints in a wide variety of rock types at 500 localities in the Appalachian Basin. Preliminary analysis by W. J. Perry, Jr., and G. W. Colton indicated that the most consistent regional patterns are exhibited by Devonian black shale units and Pennsylvanian coal beds. Fresh exposures of black shale and coal beds exhibit joint intensities and orientations that appear to be related to their tectonic setting. For example, coal cleat patterns are affected strongly by proximity to the front of the Pine Mountain thrust in southeastern Kentucky and by large steeply dipping basement faults of the Rome trough in western West Virginia. Recognition that these surface joint patterns may reflect accurately a sensitivity to regional tectonic features suggests that they may be used as guides to assess the possibility of fracture reservoirs in the subsurface of parts of the Appalachian Basin.

Possible subsurface extension of Appalachian Basin natural gas province

A recent seismic reflection survey beginning in the Valley and Ridge province near Jacob, Tenn., and trending about 115 km southeastward across parts of the Blue Ridge and Piedmont provinces in North Carolina has been interpreted by L. D. Harris. It shows that low-angle thrust faults are not limited to sedimentary sequences of the eastern overthrust belt but also occur within the crystalline rocks of the Blue Ridge and Piedmont. Approximately 290 km of westward movement of crystalline rocks of the Blue Ridge and Piedmont above a low-angle thrust has buried a large section of sedimentary rocks of the eastern overthrust belt. In Tennessee

and North Carolina, where seismic data are concentrated, this buried segment ranges from 3,050 m to more than 6,100 m thick. It extends eastward in the subsurface beneath the Blue Ridge and Piedmont about 115 km to the end of the seismic data. Additional seismic reflection data about 250 km southwest of the USGS line in the Piedmont of Georgia suggest that the sedimentary rocks of the eastern overthrust belt may extend in the subsurface completely across the Piedmont. Because the buried part of the eastern overthrust belt is about as wide as the exposed part of the belt, the area for possible natural gas exploration in the southern Appalachians may be about doubled.

Extension of St. Clair bedding-plane thrust in Virginia

Abundant conodonts from two windows through the St. Clair thrust on the crest of Bane dome, Giles County, Va., have been studied by W. J. Perry, Jr., and J. E. Repetski. These conodonts are the same age as conodonts previously obtained from cuttings of the Strader well No. 1, which indicated the presence of Lower Ordovician dolomite beneath Lower Cambrian shale, 15 km behind the leading edge of the Saint Clair thrust. The new evidence suggests that the Saint Clair is a major bedding-plane thrust for much of its width and further refutes the concept of active basement tectonics in its type area.

OTHER AREAS

Petroleum resources of Outer Continental Shelf areas

Geologic assessments of undiscovered resources of oil and natural gas have been completed for several areas of the OCS that have been proposed for leasing. The areas assessed by a team composed of G. L. Dolton, S. E. Frezon, A. B. Coury, K. L. Varnes, R. S. Pike, R. B. Powers, E. W. Scott, R. W. Allen, and A. S. Khan include the Lower Cook Inlet–Shelikof Strait (Alaska), Norton basin, mid-Atlantic shelf and slope, South Atlantic (shelf and deep), St. George basin, and seven other OCS areas. The assessments suggest that significant quantities of undiscovered recoverable oil and gas may be in these areas. The Navarin Basin of the Bering Shelf is considered to have the greatest potential of these areas; its unconditional undiscovered recoverable resources are estimated to be between 0 and 11.8 billion barrels of oil and between 0 and 38.3 trillion ft^3 of gas at the 95 percent and 5 percent probabilities of occurrence, respectively. This area was closely followed in potential by the Beaufort Shelf area (Alaska). Considered to have the least potential of the newly assessed areas is the Gulf of Alaska.

Petroleum geology of Volga-Ural petroleum province

The Volga-Ural petroleum province is an example of a preserved continental shelf or platform margin that has remained relatively undisturbed since the end of marine deposition in Late Permian time. According to J. A. Peterson and J. W. Clarke (University of Montana), the province contains more than 600 oil and gas fields producing from a wide variety of structural and stratigraphic traps in a Middle Devonian to Permian marine clastic, carbonate, and evaporite sequence. The 135-billion-barrel Melekess tar deposits occur in stratigraphic-paleostructural traps in Permian carbonate and clastic rocks near the center of the province. Several unusual geological phenomena are recognized in the province, including the structural-stratigraphic origin of the Kamsk-Kinel deepwater trough system located on the platform, an extensive and thick (500–>1,500 m) Devonian and Lower Carboniferous reef system closely confined to paleostructures of the platform and adjacent eugeosyncline, a thick narrow platform-edge Permian reef belt about 2,000 km long, and large oil accumulations trapped in drape structures over nonproductive reefs. The Volga-Ural petroleum province also appears to be a remarkable example of close association among paleostructures, transgressive-regressive marine depositional cycles, and development of petroleum-reservoir and source-rock facies.

NEW EXPLORATION AND PRODUCTION TECHNIQUES

Economic implications of the solubility of crude oil in methane

Extensive data have been gathered by L. C. Price and L. L. Rumen concerning the aqueous solubility of methane in NaCl brines at elevated temperatures and pressures. These data strongly suggest that the geopressured geothermal resource, as currently conceived, is not economically feasible.

However, limited data gathered on the solubility of crude oil in a methane gas phase at elevated conditions suggest that methane has a high carrying capacity for crude oil. These data could have important implications for primary petroleum migration and for the economic feasibility of the geopressured geothermal resource under restricted conditions.

Reduction of sandstone permeability through shale dewatering

Preliminary petrographic and scanning electron microscope studies show that sandstone cementation is related to the expulsion of ion-charged water from dewatering shale into adjacent sandstone bodies. The greatest sandstone cementation occurs within a few meters of the upper or lower contact with an adjacent shale. In areas where this type of cementation is active,

sandstone bodies less than 15 m thick are commonly cemented throughout by authigenic clay and quartz. For deep sea sandstones, the economic implication of heavy cementation in thin sandstone beds is that outer fan, levee, and overbank deposits may be too tightly cemented to serve as petroleum reservoirs.

Estimation of sulfur reserves using borehole gravimetry

J. W. Schmoker has interpreted borehole gravity surveys from four exploratory wells penetrating the native sulfur deposit at the Duval Culberson property, Culberson County, Tex. (The borehole gravity meter has a depth of investigation comparable to the recovery radius of the Frasch process for mining sulfur.) Mineralized zones are treated as three-component systems, comprising bioepigenetic limestone, interstitial sulfur, and water-filled pores. A ternary diagram relating combinations of these three components to borehole gravity densities and empirical data relating sulfur content and water-filled porosity are used together to estimate sulfur volumes from borehole gravity data. Estimated sulfur contents range from 0 to 33 percent. Comparisons between cores and cuttings from the four wells surveyed and from those of surrounding wells show the positive effects of the large range of investigation of the borehole gravity meter and also the negative effects of relying solely on formation density as a measure of sulfur volume.

Significance of submarine slides on intercanyon continental margin slopes

Small-scale submarine slides (10 m thick by 500 m wide) were suggested by H. E. Cook (1979) to be more abundant than previously recognized on intercanyon continental margin slopes. A model was developed simulating the various stages of deformation that a submarine slide undergoes from its initial movement until its complete remolding into a conglomeratic debris and turbidity-current flow. This remolding begins at the basal shear zone and thin tapered margins of the slide. The rupture strength of submarine slides probably is exceeded due to strain, mechanical shock, and incorporation of water.

Small-scale submarine slides can be important in several ways: (1) slides can transport sediment downslope as coherent units or they can remold into debris and turbidity-current flows capable of traveling long distances into basinal settings, (2) slide-generated mass-flow deposits within intercanyon slope or adjacent basins could form petroleum reservoirs, and (3) small-scale slides on modern intercanyon slopes could pose geologic hazards.

Little published data exist on small-scale slides and mass-flow deposits on modern intercanyon slopes. This may be due to the paucity of such events, but more likely it is because they are difficult to detect with much of the seismic equipment used and because submarine canyons on slopes have received more attention than intercanyon slopes.

Production of hydrocarbons and alteration of sedimentary structures through compaction

Experiments conducted by E. A. Shinn, R. B. Halley, B. H. Lidz, J. H. Hudson, and D. M. Robbin in compaction of modern sediments under loads representing 300–3,000 m of overburden have led to these results: (1) destruction of characteristic birdseye voids in tidal flat sediments (implication: birdseye voids in ancient limestones indicate early cementation), (2) destruction of pellets in soft muds, but preservation of slightly cemented pellets (implication: ancient pelletal limestones indicate early cementation or hardening of pellets), (3) production of organic pseudostylolites that could be precursors of true solution-compaction stylolites, and (4) production at moderate temperatures (100°C) of hydrocarbons that may be precursors of oil (Shinn and others, 1977).

NUCLEAR-FUEL RESOURCES

In FY 1979, USGS studies related to nuclear-fuel resources in the United States and the world continued under three separately funded and interrelated programs. Geological, geochemical, geophysical, and resource-assessment investigations were conducted with funding from the USGS, DOE, and BIA.

The program funded by the USGS involved studies of uranium and thorium habitat and resources in nine regions of the United States, including the Colorado Plateau, Basin and Range province, Wyoming Tertiary basins, Texas coastal plain, Alaska, Front Range of Colorado, the North-Central States, and the Northeastern States. Fifty-eight projects, including several university contract and grant projects, were active under this program, which had a total expenditure of about $6.6 million.

Contract studies by the USGS for the DOE-sponsored National Uranium Resource Evaluation (NURE) Program were conducted in 23 National Topographic Map Series 1°×2° quadrangles covering uranium environments in the Colorado Plateau, Wyoming Tertiary basins, Basin and Range province, and Colorado Front Range. NURE quadrangle evaluations, designed to aid DOE uranium-resource assessment, were closely coordinated with USGS investigations in the same areas. Quadrangle evaluation studies by the USGS will be completed in fiscal year 1980. Also included under the

NURE Program were contract studies of "world class" uranium deposits. Several areas believed to be geologically similar to foreign terranes containing major unconformity vein-type and quartz-pebble conglomerate uranium deposits in Canada and Australia were studied or surveyed during the year. The total NURE expenditure was approximately $3.6 million.

Studies leading to a uranium-resource inventory of the Navajo Reservation in New Mexico, Arizona, and Utah and on Great Lakes region Indian lands were initiated during the fiscal year under funding by the BIA amounting to about $600,000. The objective of the program is the delineation and geologic characterization of areas and formations favorable for uranium deposits. An additional objective of the Navajo project is the training of Navajo Indians in geologic field methods and resource-assessment technology. The Navajo project is coordinated with USGS uranium studies in the San Juan Basin and adjacent parts of the Colorado Plateau. The following short reports summarize the most significant results of nuclear fuels-related research for fiscal year 1979.

Large thorium reserves in disseminated deposits

Recent thorium-reserve studies by M. H. Staatz, M. R. Brock, and J. C. Olson indicate that the largest resource of thorium occurs in disseminated deposits. Three disseminated deposits located in Wyoming, Illinois, and Colorado have 117,000 t of ThO_2 in indicated reserves and 815,000 t of ThO_2 in inferred reserves. These deposits tend to be multiproduct, and rare earths are commonly abundant. Other deposits that contain important thorium resources include carbonatites, veins, and beach placers in northern Florida and stream placers in Idaho.

Alkaline intrusive complexes, Wet Mountains, Colorado

Concentrations of rubidium, strontium, and REE and strontium-isotopic ratios in rocks of the Cambrian alkalline complexes in the Wet Mountains area, Colorado, define and delineate petrologic characteristics of these intrusions, according to T. J. Armbrustmacher and C. E. Hedge. Subsolvus nepheline syenite and hornblende-biotite syenite from the McClure Mountain Complex (530 m.y. $\pm$ 5 m.y.) are older than hypersolvus quartz-normative syenitic rocks from the complex at Democrat Creek (511 m.y. $\pm$ 8 m.y.). REE data indicate that the nepheline syenite cannot be derived from the hornblende-biotite syenite that it intrudes or from the associated mafic-ultramafic rocks. REE data also indicate that mafic-ultramafic rocks at McClure Mountain have a source distinct from that of the mafic-ultramafic rocks at Democrat Creek. In the McClure Mountain Complex, initial $^{87}Sr/^{86}Sr$ for the mafic-ultramafic rocks (0.7046 ± 0.0002) are similar to those of the hornblende-biotite syenite (0.7045), whereas the ratios for carbonatites (0.7038) and mafic nepheline-clinopyroxene rocks (0.7037) are similar to those of nepheline syenite (0.7038). At Democrat Creek, syenitic rocks (0.7032) and mafic-ultramafic rocks (0.7028) are unlike corresponding rocks at McClure Mountain. Combined data on minor-element concentrations and strontium-isotopic ratios show that the rocks of the alkaline complexes have not formed through a simple process of fractionation of a single magma but represent the end products of a variety of magmas generated from different source materials.

Uranium occurrence at Pajaro Azul, east-central Arizona

In view of the increased interest in caldera-related uranium occurrences, C. S. Bromfield and C. T. Pierson visited the Pajaro Azul prospect near the New Mexico State line in east-central Arizona. The uranium occurrence, in dense Tertiary rhyolite, lies near the hypothetical Mule Creek caldera, one of many interpreted calderas in southern New Mexico. They found that the low-grade uranium mineralization occurs in a northeast-trending fault zone in the rhyolite and that the rhyolite is part of a protrusive dome erupted onto a basement of Tertiary andesitic volcaniclastic rocks and flows. The rhyolite is extensively autobrecciated. Evidence for the presence of the caldera appears weak.

Fluorine, beryllium, and uranium mineralization in Thomas Range, western Utah

According to D. A. Lindsey, fluorine, beryllium, and uranium mineralization in the Thomas Range of western Utah took place during basin-range faulting and contemporaneous alkali rhyolite volcanism instead of during earlier caldera-related volcanism. Volcanism began about 42 m.y. ago with eruption of intermediate-composition flows, breccias, and tuffs from small central volcanoes; it culminated with the eruption of intermediate-composition ash flows and collapse of the Thomas caldera about 39 m.y. ago. Intermediate-composition volcanism was accompanied by base- and precious-metal mineralization, including development of porphyry-copper centers. Following collapse of the Thomas caldera, rhyolitic ash flows erupted 38 m.y. to 32 m.y. ago and largely filled the Thomas caldera. Eruption was accompanied by collapse of the Dugway Valley cauldron; apparently no mineralization was associated with the eruptions. Alkali-rhyolite volcanism, basin-range faulting, and fluorine-beryllium-uranium mineralization began about 21 m.y. ago, at least 11 m.y. after the last cauldron collapse. Most faulting and mineralization had ended by 6 m.y. to 7 m.y. ago when voluminous alkali rhyolite was erupted in the Thomas

Range, although minor hydrothermal activity persisted after these eruptions.

Fluorine, beryllium, and uranium were derived from alkali-rhyolite magma that was rich in these metals. Basin-range faults tapped such magma as early as 21 m.y. ago. Hydrothermal fluids rose along the faults and pervaded adjacent beds of dolomite-rich tuff interleaved between relatively impermeable strata. There, beryllium and uranium fluoride complexes dissociated as fluorite replaced dolomite, depositing disseminated beryllium (as bertrandite) and uranium in the structure of fluorite, opal, and, perhaps, other minerals. Uranium in hydrothermally mineralized tuff has been remobilized by ground water to form secondary concentrations of uranium in tuff.

Uranium in the Lakeview area, Oregon

Work in the Lakeview uranium area of Oregon by G. W. Walker has established a regionally extensive Cenozoic volcanic stratigraphic framework and identified at least three principal episodes of peraluminous silicic intrusive activity. Of the three episodes of intrusive activity, uranium (and other metal) mineralization appears to be restricted to the two younger episodes. Petrochemical studies indicate that (1) the abundance and distribution of minor elements, including uranium, are similar to those found in other rhyolitic rocks of the Western United States, (2) both uranium and thorium abundances tend to increase with differentiation index, and (3) rocks depleted in barium and strontium and, hence, in feldspar are generally highest in content of uranium and thorium. Abundances of other metals (As, Mo, Hg, Sb, and so forth) present in the uranium deposits appear to follow separate differentiation and fractionation patterns.

Supergene uranium deposits in fracture zones associated with Laramide upthrusts

Recent descriptions of uranium deposits at Copper Mountain, Wyo. (Yellich and others, 1978), and the Pitch mine, Colo. (Nash, 1979), indicate important structural control by zones of crushed and brecciated rock along major Laramide uplift structures. The Copper Mountain deposit is in brecciated Precambrian rocks of the frontal lobe above the Owl Creek thrust. The frontal lobe contains antithetic faults caused by extension during arching of the upper thrust plate. Brecciated Leadville Dolomite in the footwall of the Chester fault zone is the most important control on uranium distribution at the Pitch mine. The Chester fault appears to be composed of several strands that together have a concave downward profile. As is characteristic of upthrust faults or fold-thrust faults, the strands are steep at depth and flatten at the top. According to J. T. Nash, the structural permeability in these uranium deposits can be explained by brittle behavior in low pressure deformation characteristic of Laramide uplifts (termed "forced folding and faulting" by Stearns, 1978). Dolomite, quartzite, granite gneiss, and crystalline volcanic rocks behave as brittle materials that fracture rather than fold at depths less than about 6 km. Brittle rocks such as these develop abundant fractures and faults in two characteristic structural positions in basement upthrusts: the frontal lobe of the upper plate, high in the upthrust structure, as at Copper Mountain, and the lower plate, particularly where folded or overturned below the upthrust, as at the Pitch mine. Fracturing of brittle upper-plate rocks appears to be most intense where the upthrust arches as dips decrease to less than 45°. Fracturing in the lower plate appears to be greatest deep in the upthrust structure where the fault dips about 65° and cuts a thick section (hundreds of meters) of brittle sedimentary rocks that overlie the basement. These structural settings can create wide zones of fractured and brecciated rocks with geometry suitable for mass mining if mineralized and exposed near the surface.

Petrology and deformation of Leadville Dolomite, Pitch uranium mine

Leadville Dolomite in the Pitch mine area is about 130 m thick and is composed predominantly of non-fossiliferous dolomicrite. In the Pitch mine, the Leadville is bounded by faults, and the maximum known thickness is about 17 m. Mud texture, paucity of fossils and other allochems, thin laminations, and probable algal mat structures suggest sedimentation in a tidal-flat (possibly supratidal) environment. Preservation of mud texture and lack of replacement features indicate that dolomitization was an early prelithification process such as that which occurs in modern tidal flats. These processes produced a chemically and texturally uniform rock over tens of meters with relatively few limestone beds surviving diagenesis. According to J. T. Nash (1979), this sedimentary and diagenetic environment had two important consequences: unusual amounts of iron and sulfur accumulated as pyrite and marcasite (sulfide ions later were important as reductants for uranium) and the massive, weakly bedded, very fine grained, and dolomitic nature of the Leadville made it deform as a brittle material over many meters to form permeable breccia zones below the Chester upthrust, a favored site of uranium mineralization.

Possible hot-spring origin for Front Range uranium veins

Petrographic and field examinations of several vein uranium deposits in the Foothills belt of the Colorado Front Range by A. R. Wallace (1979) suggest that the deposits were formed in a carbonate-dominated hot-

spring environment. Wallrock alteration of the Precambrian gneisses chiefly involved carbonatization of mafic wallrock minerals, with lesser sericitization and chloritization. The veins are filled with uranium-stage pitchblende, coffinite, and adularia and with post-uranium iron dolomite, adularia, calcite, and sulfides. Transport of uranium was in a carbonate complex, and precipitation was caused by CO_2 removal by boiling or effervescence. Hematite in the wallrocks and gangue was formed by the oxidation, after boiling, of iron-bearing carbonate rocks. Uranium mineralization occurred during or after the early Tertiary uplift of the Front Range foothills. The source of the uranium has not yet been determined, but the correlation between carbonate-dominated fault systems and calc-silicate gneisses suggests that much of the carbonate was derived from the gneisses.

Uranium, gold, and thorium potential of Sierra Madre and Medicine Bow Mountains, Wyoming

Continued geologic, radiometric, and geochemical studies of pyritic, quartz-pebble conglomerate of Precambrian age in southeastern Wyoming by R. S. Houston and K. E. Karlstrom (University of Wyoming) show that the radioactive conglomerate that occurs at the base of the "Phantom Lake" metamorphic suite and "Deep Lake Group" is quite variable in above background radioactivity and probably in heavy-mineral content. Analytical results, although limited, show that gold values range from below the detection limit of the atomic absorption method for most samples to as much as 10 ppm in the Dexter Peak area of the Sierra Madre. Uranium values range from 0.5 to 150 ppm with a mean value of 17 ppm for 41 grab samples from 9 localities in the Sierra Madre and Medicine Bow Mountains; thorium values for these same localities have a mean value of 112 ppm and range from 5 to 1,087 ppm. In contrast, five samples of radioactive conglomerate from cores of the One Mile Creek locality of the Medicine Bow Mountains average 495 ppm uranium and 1,123 ppm thorium. Surface samples from this same locality average 130 ppm uranium and 616 ppm thorium. All One Mile Creek samples are biased toward the most radioactive zones and so are not typical of the grade, but they clearly show an increase in uranium values for unoxidized core samples.

It is too early to make definitive statements on the economic potential of these conglomerates because of the potentially large area that could be underlain by radioactive conglomerate in both the Sierra Madre and Medicine Bow Mountains and because of the limited number of outcrops that can be investigated on the surface. However, preliminary studies suggest that uranium values are not as high as nor are they as consistent as values in similar conglomerate beds of the Blind River area of Canada or Witwatersrand of South Africa.

Limitations on genesis of Midnite mine uranium ores

Uranium lead-ages for uranium minerals at the Midnite mine in northeastern Washington (Ludwig and others, 1978; Nash and Ludwig, 1979) specify that the deposits, as presently observed, formed at 50 m.y. and 52 m.y. ago, or about 25 m.y. after the adjacent pluton was emplaced. J. T. Nash and K. R. Ludwig believe that the deposits formed at the time of Eocene volcanism and that volcanic activity probably mildly heated ore-forming fluids. The preferred hypothesis is that the deposits formed below the Sanpoil Volcanics from near-surface partially oxidized fluids containing sulfide and metastable sulfur species capable of reducing uranium. The Eocene event redistributed uranium from the Cretaceous pluton and metamorphic aureole in the Togo Formation, but relatively little uranium was present in the volcanic rocks.

Uranium studies in Alaska

Rhyolite intrusive bodies with a high background radioactivity have been found by T. P. Miller in a calc-alkaline volcanic pile of Late Cretaceous and early Tertiary age in the northeastern corner of the Medfra quadrangle near Sischu Creek. Individual rhyolite bodies are up to 13 km^2 in area and generally occur within 1.5 to 3.0 km of each other. Background radioactivity ranges from 400 to 650 cps (total count). The association of high background radioactivity, red hematitic alteration, and purple fluorite suggests that this is a favorable area for uranium enrichment.

Possible low-grade uranium resources in graphitic slate, northern Michigan

Black slate that locally contains appreciable quantities of radioactive material and that could conceivably be a large-tonnage low-grade resource of uranium has been reported associated with sedimentary iron formation in the abandoned iron-mining districts of Gwinn and Iron River, Mich. (Barrett, 1952). Recent reconnaissance by M. R. Brock of waste piles of several dumps in these districts confirmed the presence of anomalously radioactive graphite-rich slate. Aerial geophysical traverses of a large area northeast of the Iron River district tend to confirm that such an association is regional in extent. B. D. Smith (oral commun., 1979) reports the occurrence of a highly conductive zone, probably graphitic slate, closely associated with a magnetic horizon. These anomalies probably reflect the same iron formation and graphite slate as noted in the Iron River mining district. Unfortunately, the units are concealed beneath a

persistent mantle of glacial till, and evaluation as a uranium resource will have to await drilling.

Potential unconformity-type uranium deposits, northern Michigan

According to J. O. Kalliokoski (Michigan Technological University), the Proterozoic Y Jacobsville Sandstone in the Upper Peninsula of Michigan was deposited in meandering and braided streams of a complex fluvial depositional system. Paleocurrent directions indicate that streams extended westward beyond the trace of the Keweenaw fault. Hence, the existing Jacobsville is a residual part of a former much larger body of the arkosic sandstone. A uranium model of the Jacobsville shows all of the favorable characteristics of the Athabasca Sandstone that at one time unconformably overlay several large unconformity-type uranium deposits in northern Saskatchewan and that contributed to their formation. The sedimentary basin that contained the Jacobsville Sandstone is believed to have been smaller than the Athabasca basin. The Jacobsville is about 0.5 b.y. younger than the 1.6-b.y.-old Athabasca. Accumulating evidence indicates that the physical and chemical composition of the Jacobsville Sandstone, the nature and extent of the basal unconformity, and the structure and composition of the underlying Archean rocks are similar to the Athabasca basin. The Jacobsville basin is considered by Kalliokoski to be a favorable geologic environment for the generation of one or more major deposits of the unconformity-type similar to those discovered in northern Saskatchewan. Several of the known uranium occurrences in the study area best fit the Athabasca genetic model.

Lake Superior region favorable for quartz-pebble-type uranium deposits

Paleocurrent studies by R. W. Ojakangas (University of Minnesota) in the lower exposed sequence of Proterozoic Y rocks in northern Michigan continue to confirm the accumulation of sediment eroded from granitic terrane having anomalously high uranium content. These data, coupled with regional structural data, strongly suggest that quartz-pebble uranium deposits may occur in the east-west-trending 161-km-wide foldbelt that underlies the study area. This foldbelt is a westward extension of the structural zone that harbors the large uranium deposits in the Elliot Lake–Blind River area, southern Ontario, about 320 km to the east of the study area.

An early Proterozoic Y orogeny caused erosion of uraniferous regolithic granite debris and its deposition in west-trending and northwest-trending fault-controlled basins in Ontario (J. A. Robertson, Ontario Division of Mines, oral commun., 1979). Disturbances in the Archean basement also created a similar, and possibly contemporary, sedimentary environment within the terrane of the Lake Superior region. If such uranium-bearing conglomerates are present in the area, M. R. Brock postulates that the most favorable sites for their preservation are in the lowermost Proterozoic Y strata in the troughs of the deeper synclines.

Trace-element patterns in spatially related plutonic differentiation suites

According to E. L. Boudette, trace-element distribution patterns in calc-alkalic plutonic rocks compared with spatially related peraluminous plutonic rocks (two-mica granite) in New Hampshire present some apparent contrasts. The baseline for this comparison is four differentiation suites used previously in geochronologic studies by Lyons and Livingstone (1977) to erect strontium-rubidium isochrons to establish an age sequence in rocks assigned traditionally to the New Hampshire Plutonic Suite. Although the name "New Hampshire" was a convenient interim vehicle, the name should be abandoned for modern purposes because the entire New Hampshire Plutonic Suite is not a differentiation suite, is not geochemically consanguineous, and is not made up of coeval components. There remains, however, the possibility that the incidence of calc-alkalic rock is about five times higher than in two-mica granite. The most scatter in data occurs in the rocks of its migmatitic Bethlehem Gneiss, and one sample is anomalously high in uranium (84 ppm), which probably weights the average unrealistically. If the data from the Bethlehem are ignored, the uranium abundance in the other calc-alkalic suites is only about half that of two-mica granite. K_2O enrichment is erratic in two-mica granite but increases with differentiation in calc-alkalic rocks.

The detailed data permit some speculations that may apply to similar rocks elsewhere: (1) uranium abundance closely follows that of REE in two-mica granite but is erratic in calc-alkalic rocks, (2) REE distribution is most even in two-mica granite, and abundance diminishes linearly with differentiation in calc-alkalic rocks, and (3) REE and uranium maxima appear both early and late in two-mica granite, probably indicative of two major periods of accessory-mineral crystallization.

Canadian, Australian, and United States uranium deposits compared

Field inspections of uranium deposits in the Athabasca region of Canada and the Alligator Rivers and Rum Jungle regions of Australia have led to the interpretation by R. I. Grauch that protoliths of host rocks for the Canadian, Australian, and possibly the Reading Prong region of southern New York–northern New Jersey deposits are in similar, albeit temporally different, stratigraphic envelopes. The protoliths in all areas are

nearshore marine sediments, including carbonaceous pelite, carbonate, and some evaporite deposits. It is hypothesized that a primary concentration of uranium occurred during or soon after deposition of the sediments, that a secondary concentration took place during regional metamorphism, and that a tertiary concentration was somehow related to the unconformable deposition of quartz sandstone over the metamorphites. Unfortunately, the tertiary concentrating event apparently did not occur in the Reading Prong region.

Nature of uranium occurrences in the northern Reading Prong

Comparative studies by R. I. Grauch and C. J. Nutt of three uranium occurrences (Ringwood and Upper Greenwood Lake, N.J., and Camp Smith, N.Y.) in the northern Reading Prong indicate that the host rocks in the three areas are similar. Uranium is spatially related to stratabound magnetite deposits that are hosted in a bimodal suite of melanocratic and leucocratic high-grade metamorphite rocks. The protoliths of the metamorphite rocks are interpreted as belonging to a nearshore (shallow water?) marine sequence of carbonaceous pelite, carbonate, and some evaporite deposits containing a substantial volcaniclastic component. In general, the mode of uranium occurrence in the three areas is similar in that the primary uranium phase is uraninite that occurs either as irregular grains or as near-spherical inclusions in silicates and iron-titanium oxides. In detail, however, there are significant differences in the silicate and iron-titanium oxide phases that are in contact with uraninite. At Camp Smith, uraninite is included in or is in contact with pyroxene, amphibole, magnetite, and (or) ilmenite, whereas, at Ringwood and Upper Greenwood Lake, it is in contact with or included in pyroxene, sphene, and (or) hematite. These differences are thought to be manifestations of variations in the original bulk compositions of the host rocks and in the metamorphic systems variables P, T, f_{O_2}, and f_{S_2}.

Proterozoic quartzite and conglomerate of central and northern Idaho unfavorable for quartz-pebble-conglomerate-type uranium deposits

Work by F. A. Hills has shown that the boundary zone separating the Archean Superior and Wyoming provinces from the Proterozoic Central United States province is characterized by a series of basins or synclinoria filled by Proterozoic X sedimentary rocks. Basal or near-basal formations in several of these basins or synclinoria contain uraniferous quartz-pebble conglomerates; the best known of these is in Huronian strata near Elliot Lake, Ontario. Others have recently been discovered in the Black Hills of South Dakota, the central Laramie Mountains, the Medicine Bow Mountains, and the Sierra Madre of Wyoming. The boundary zone is poorly located west of the Sierra Madre, Wyo., but, apparently, it passes south of the Uinta Mountains and south of the Wasatch Range in Utah before turning north into Idaho. The Yellowjacket Formation and other unnamed quartzite and conglomerate in central and northern Idaho are at least 1,500 m.y. old, lie in or near the probable location of the boundary zone, and have been considered to be possible host rocks for quartz-pebble-conglomerate uranium deposits.

The Yellowjacket Formation consists primarily of very fine grained quartzite and siltstone with many beds and zones of gray mudstone. Magnetite appears to be the predominant iron mineral found in streaks of heavy-mineral concentrates. Pyrite has not been recognized as detrital grains and is not present in heavy-mineral streaks. The only radioactivity anomalies detected in the formation were associated with numerous thorite veins in the vicinity of Lemhi Pass in Idaho. The low-energy environment of deposition, indicated by the fine sediment size, and the young age (relative to the hypothetical 2.2 b.y. oxyatmoversion), indicated by the presence of magnetite rather than pyrite in the heavy-mineral suite, suggest that the Yellowjacket Formation is not a suitable habitat for Elliot Lake-type uraniferous quartz-pebble conglomerate.

Quartzite and conglomerate that are at least 1,500 m.y. old occur in the metamorphic terrain near Lowell, Idaho, in the vicinity of the Idaho batholith. The conglomerate contains well-sorted layers consisting almost entirely of quartz, suggesting a high degree of sedimentologic maturity. Pyrite, though not abundant, is present in some beds. Pebbles are highly stretched and granulated, and it is not known whether they were originally quartz pebbles or quartzite pebbles. Pyrite occurs as scattered cubes and as coatings on fracture surfaces; its significance is problematic. No anomalous radioactivity was detected. The lack of radioactivity anomalies in the conglomerate suggests that, if age and sedimentologic conditions were appropriate, radioactive minerals were probably lacking in the provenance area. The conglomerate holds little promise as host rock for Elliot Lake-type uranium deposits.

Geologic factors in evolution of unconformity-type uranium deposits

Unconformity-type vein deposits in Northern Territory, Australia, and northern Saskatchewan, Canada, containing more than 450,000 t of uranium have many features in common that suggest a similar polystage genesis. When stages are skipped, deposits tend to be smaller in grade and tonnage. Some preliminary interpretations by J. T. Nash follow. (1) Initial uranium accumulation to tens of parts per million was in marginal marine mud and carbonate deposits, under reducing conditions associated with algal growth and decay. (2)

Proterozoic X sedimentary rocks are most favorable because they formed during the first period of oxidation and uranium transport in solutions, but this age is not unique because younger marginal marine sedimentary rocks are enriched in uranium (that is, African Copperbelt, Swedish Kolm, Chattanooga Shale). (3) The association with magnesium-calcium carbonate rocks reflects the sedimentary environment of uranium accumulation; these rocks are favorable for creation of karst-type structures and uranium-carbonate complexes. The magnesium metasomatism seems symptomatic of an alkaline hydrothermal environment and probably is not a geochemical requirement. (4) Hydrothermal enrichment of uranium is suggested by the proximity of deposits to mantled gneiss domes, late orogenic granite, and zones of retrograde metasomatism. The example of Shinkolowbwe, Zaire, also suggests that the characteristic pitchblende-magnesite-chlorite association forms under metamorphic-hydrothermal conditions. (5) Most deposits were enriched at least twice in the Proterozoic X; economic deposits of at least small size can form without unconformity-related processes acting. (6) Supraunconformity deposits in covering sandstone, as at Midwest Lake and Collins Bay, Saskatchewan, probably are redistributed from the basement, possibly under the influence of radiogenic heat. Postunconformity enrichment of basement deposits by oxidizing meteoric fluids is important but probably hampers geologic understanding by destroying evidence of earlier stages.

Early Permian depositional systems and paleogeography, Uncompahgre Basin

Studies by J. A. Campbell of depositional systems of the Cutler Formation, predominantly of Wolfcampian age, in the Uncompahgre (Paradox) Basin in Colorado and Utah have defined five fluvial, two marine, and associated eolian facies. The Cutler facies include proximal-braided, which consists of a fan-building sequence and a very coarse grained fan-head sequence, medial-braided, distal-braided, and 50 and 100-percent meandering sequences. The distribution of braided facies defines three large, 40- to 60-km-radius, fluvial or wet fans: the Gateway fan in the northern part of the basin developed to the southwest of the Uncompahgre highland, the San Miguel fan in the central part of the basin formed south off the southern end of the Uncompahgre highland, and the Piedra fan in the southeastern part of the basin developed west from the San Luis highland.

The marine and eolian facies occur only in the northern part of the basin around the Gateway fan. Transition of the streams from distal braided to coarse-grained meandering occurred at the toe of the fan, which was near sea level. Westward of the toe, meandering became more common. A marine transgression occurred early during fan development, resulting in deposition of the limestone and shale of the Rico Formation. In a later marine transgression from the southwest in Utah, "Elephant Canyon" limestone, sandstone, and shale were deposited that are lateral equivalents of the Cedar Mesa Sandstone Member of the Cutler Formation. The eolian facies are closely related stratigraphically and geographically to the marine facies and are, thus, considered deposits of a coastal dune field.

The San Miguel and Piedra fluvial systems coalesced approximately along the present course of the Animas River. Transition of both systems from distal braided to coarse-grained meandering occurred along their southwest flanks and may occur also along their northeast flanks, but accurate data are lacking.

Uranium is found in the Permian in this basin only in the northern part around the toe of the Gateway fan where fluvial meandering sequences are interbedded with the shallow-marine sequences.

Mudstone as uranium exploration guide

Sedimentologic and palynologic studies by Fred Peterson, R. H. Tschudy, and S. D. Van Loenen in the Henry basin, Utah, indicate that a particular type of mudstone can be used as an exploration guide to uranium deposits in nearby sandstone beds. Most mudstone in the Salt Wash Sandstone bears no relation to the ore deposits and consists of nonorganic red or green mudstone deposited in overbank environments on a flood plain. Other unfavorable but organic-rich gray mudstone contains carbonized wood fragments up to about 1 cm long, palynomorphs including the alga *Botryococcus,* powdery carbonaceous material, and structureless blebs of organic matter. The mudstone lacks swelling clay, is moderately to highly calcareous, and is associated with thin limestone. Most of the mudstone was deposited in shallow and relatively large lakes at least several kilometers wide and several tens of kilometers long.

Favorable organic-rich gray mudstone that lies near uraniferous sandstone contains minute carbonized wood particles less than about 0.5 mm long, a palynomorph suite lacking *Botryococcus,* cutinous and epidermal tissue, pyrite, and swelling clays. The mudstone is noncalcareous to slightly calcareous and rarely contains limestone. Favorable mudstone occurs just above or below uranium-bearing sandstone or interfingers with sandstone that contains uranium anomalies within several hundred meters of the mudstone. The mudstone is associated with distal-braided-stream sandstone and was deposited in small shallow lakes or ponds up to several square kilometers in area lying between stream courses or in abandoned stream channels. The mudstone

lies in structural lows that were active during deposition and tends to occur in the part of the low where fluvial sedimentation was least active. Prospecting strategies based on these observations should include searching for favorable mudstone in tectonic lows in strata deposited by distal-braided streams.

A regional disconformity in Jurassic rocks of the San Juan Basin

Using bore-hole geophysical logs, R. D. Lupe has identified a regionally extensive disconformity at the base of the Morrison Formation and its facies equivalents in the San Juan Basin, Colo., N. Mex., and Utah. This disconformity, which corresponds to the A–B disconformity identified in the outcrop by Green (1975) in the Gallup-Laguna area, apparently represents a time of abrupt change in deposition. Its recognition allows correlation of overlying units that previously have not been correlated with certainty in outcrops around the basin. The change in deposition generally is represented by the surface between overlying thick sandstone bodies of variously named units and the thinly bedded mudstone and siltstone of the Summerville Formation. The sandstone above the disconformity, which now appears to be largely time equivalent, is that of the Junction Creek Sandstone in the northern part of the basin, the upper part of the Bluff Sandstone in the northwest and all of the Bluff in the southeast, the upper part of the Cow Springs Sandstone in the south and northwest, and, in addition, local sandy facies at the base of the Recapture Shale and Salt Wash Sandstone Members of the Morrison Formation scattered throughout the basin. Relief at the disconformity is locally more than 10 m, judging from changes in the thickness of strata between the disconformity and marker beds in the underlying Summerville. This disconformity appears to represent a geologically short period of time and may be central to resolving long-standing uncertainties in Jurassic stratigraphy that exist at the outcrop.

Salt Wash depositional environments and uranium

Study by A. C. Huffman, Jr., A. R. Kirk, and R. J. Corken has shown that uranium deposits in the Salt Wash Sandstone Member of the Morrison Formation in the Carrizo Mountains area of Colorado are closely related to depositional facies. In the vicinity of the Eastside mines, southeastern Carrizo Mountains, the Salt Wash consists of a lower part (9–15 m thick) and an upper part (55–60 m thick), which is further divisible into two stratigraphic units. The lower part or distal-fan facies is predominantly mudstone and silty sandstone interpreted as overbank and partially abandoned channel-fill deposits. It also contains a few large lenticular channel sandstones deposited by braided and possibly meandering streams. Uranium deposits are uncommon in the lower part.

The upper part or midfan facies of the Salt Wash contains a much greater percentage of braided-stream-deposited channel sandstone, much of which coalesces to form prominent continuous ledges. Fine-grained low-energy deposits are limited in extent; they are commonly less than 200 m long, 20 m wide, and 2 m thick and have a lenticular cross section and a scoured base. They consist of interbedded mudstone, claystone, and sandstone and are interpreted as abandoned and partially abandoned channel fills. Scouring of these beds resulted in clay-clast conglomerate that was incorporated as lag deposits in the bases of overlying channel sandstone. Detrital organic debris is present in some channel-lag deposits, as well as in some of the bedded mudstone and parallel-bedded sandstone. Uranium deposits in the Carrizo Mountains area are associated with channel-sandstone systems that have scoured into abandoned and partially abandoned channel-fill deposits in the lower midfan facies of the Salt Wash.

Probable reactivated basement faults east of Defiance uplift

According to R. E. Thaden, the general sigmoidal offsets of the principal monocline on the east side of the Defiance uplift in the vicinity of Window Rock, Ariz., are characterized by steep eastward dips on north-south sections of the monocline, shallow dips on the transverse (east-west) sections, and extremely rapid changes of dip and orientation, together with brecciation, at the west end of the transverse section. These characteristics suggest that the offsets were produced by draping of the sedimentary rocks over north-northwest-trending vertical en echelon faults in the basement rocks that are displaced down on the west side. Furthermore, because the orientations of the sigmoidal offsets seem to require fault orientations at reasonably large angles to the gross trend of the monocline and because the sedimentary beds are not cut by the faults, it seems necessary to assume that the faults existed before formation of the Defiance uplift but were reactivated during or after the uplift.

Preservation of uranium deposits in the Mariano Lake mine, New Mexico

Preliminary observation by J. F. Robertson suggests that the uranium ore bodies in the Mariano Lake mine, McKinley County, N. Mex., are residual deposits. The ore bodies lie within the Poison Canyon-type arkosic sandstone of fluvial origin in the Brushy Basin Shale Member of the Upper Jurassic Morrison Formation, near the west end of the Smith Lake–Mariano Lake ore trend, and consist of black carbon-rich primary uranium

ore. They occur both below the ground-water table in the trough of the west-trending Mariano Lake syncline and above the water table to the north on the flank of the adjoining anticline. The margins of the deposits are leached and altered in varying degrees to low-grade dark-brown to gray ore that grades outward into barren oxidized limonitic brown to orange and buff sandstone. Mapping clearly shows that the ore bodies are appreciably more oxidized in the trough of the syncline but gradually less so updip on the flank of the anticline. The peripheral alteration and its distribution indicate that the deposits have been attacked by oxidizing ground water, probably during Tertiary to Holocene time, but the ground-water table apparently reached only part way up the flank of the anticline. It is reasoned that the deposits have been preserved largely because the movement of ground water was inhibited by the anticline, which acted as a barrier to the northerly regional flow. Restricted flow and consequent stagnation of ground water reduced its capacity to oxidize, thus averting massive dissolution of the uranium deposits locally along the Smith Lake–Mariano Lake trend.

Uranium mineralization at the Dennison-Bunn claim, Sandoval County, New Mexico

Uranium at the Dennison-Bunn claim, south of Cuba, N. Mex., on the east side of the San Juan Basin, occurs in fluvial channel sandstone of the Westwater Canyon Sandstone Member of the Upper Jurassic Morrison Formation. J. L. Ridgley believes the uranium deposit represents the remnant of an original roll-type deposit. He hypothesizes that the uranium was deposited from oxidizing uraniferous ground water along oxidation-reduction boundaries some time prior to middle early Eocene. Subsequent ground-water movement through the host rock has modified the original deposit configuration. Uranium has been remobilized and reconcentrated along the margins of numerous smaller tongues of oxidized rock in a configuration also indicative of roll-type uranium deposits. The uranium concentration in the mineralized rock at the outcrop ranges from 0.0001 to 0.07 percent U_3O_8.

Meeker uranium district projected

Based on field reconnaissance and information from preceding studies, L. C. Craig has projected an area favorable for the occurrence of uranium deposits in the Salt Wash Sandstone Member of the Morrison Formation (Upper Jurassic), trending northeastward from the known uranium-producing Meeker district, Colorado.

The uranium deposits in the Salt Wash of the Meeker district appear confined to a distal lobe of sandstone deposited from relatively high-energy streams. Sandstone beds in the Salt Wash lateral to the district are fine grained and lack the conspicuous trough cross-stratification and conglomerate beds that are observed in the host rock of the Meeker district. Both regional studies and past and current local studies indicate that this relatively permeable high-energy sandstone trends northeastward from the known mining area. This allows the projection of an area favorable for uranium deposits in this direction.

Probable origin of uranium in the Browns Park Formation (Miocene) of the Sand Wash Basin, Moffat County, Colorado

Reconnaissance studies by S. J. Luft of the Browns Park Formation (Miocene) in the Sand Wash Basin of northwestern Colorado suggest that the most probable source of uranium in deposits present in some sandstone and conglomerate beds was volcanic ash present in the upper part (and elsewhere) of the formation. Uranium was probably leached from ashy beds of low uranium content during their devitrification, crystallization, and lithification. As postulated by Bergin (1957), the ground water of Browns Park in later time became enriched in leached uranium and traveled down gradient to structurally low areas and (or) local traps along faults.

In the absence of organic matter and other obvious reductants in the Browns Park, the close spatial association of many deposits with known high-angle cross faults is particularly fortuitous. According to De Voto (1978, fig. 26), reducing gases, such as hydrogen sulfide and methane, can be introduced into the ground-water system by lateral and upward flow along faults and permeable beds and can concentrate and precipitate uranium along and near those faults and favorable beds. Favorable source beds for accumulations of such gases are present in earlier Tertiary rocks underlying the Browns Park of the Sand Wash Basin. These genetic models appear at this time to be valid for the Browns Park and will be the subject of further investigations.

Uranium in the Oligocene Antero Formation, Park County, Colorado

The Oligocene Antero Formation contains substantial uranium resources in Park County, Colo. The Formation is composed of a lacustrine and an ash-flow tuff facies. According to K. A. Dickinson, the ash-flow tuff facies, in part called the Badger Creek Tuff, dammed the fault-controlled valleys to form lake basins and later partly filled the lake basins, ripping up portions of lake bed that became inclusions in the tuff. The lacustrine facies consists of varved and thin-bedded mudstone and claystone and fine-grained tuffaceous sandstone containing carbonaceous debris. The lacustrine facies contains fossil ostracodes, mollusks, and algae. The upper part of the lacustrine facies is partly oxidized, and the lower part is reduced.

Uranium mineralization occurred in both the upper and lower parts of the lacustrine facies and may be associated with silicification. The uranium apparently was altered by one or more episodes of oxidation after deposition. In general, the uranium is absent from the tuff facies. The uranium precipitation probably was caused by the carbonaceous material in the lacustrine facies.

Formation of tabular uranium deposits in the Powder River Basin

Tabular concentrations of uranium occur in some near-surface deposits in the Powder River Basin. The distribution of iron oxides and uranium ore in these deposits suggests to E. S. Santos that these are remnants of roll-front deposits that have been highly modified by recent oxidation in the vadose zone. He proposes that tabular uranium deposits could be formed, under some conditions, by oxidation and redistribution of roll-front deposits below the water table as well as in the near-surface deposits.

Stratigraphic analysis of Western Interior Cretaceous uranium basins

Extended isopach studies by H. W. Dodge, Jr., of the uranium-bearing Fox Hills Formation in Crook and Weston Counties, northeastern Wyoming, show prominent northeasterly directed erosional features that cut into underlying marginal marine sedimentary rocks. These "channels" lead into areas of known uranium concentration. Studies of new cores bridging these concentrations suggest that the most favorable estuarine subenvironments include swash bars, ebb spits, estuarine channels, and rip-up deposits from subtidal estuary sediments.

Age of uranium host rocks in the Date Creek basin, west-central Arizona

The Artillery and Chapin Wash Formations are the principal uranium host rocks in the Date Creek basin. Potassium-argon dating of interbedded volcanic rocks in various parts of the basin area has allowed J. K. Otton to place approximate age limits on these units and their equivalent units. In the eastern part of the basin area, units correlating with the Artillery and the Chapin Wash rest unconformably on older volcanic rocks informally named the McClendon volcanics (W. E. Brooks, oral commun., 1979). These volcanic rocks have been dated at 25.7 ± 0.7 m.y. by potassium-argon dating on plagioclase in rhyodacite (N. H. Suneson and Brooks, oral commun., 1978). A series of andesite flows that separate the Artillery from Chapin Wash-equivalent units yielded an age of 19.2 ± 0.7 m.y. (potassium-argon whole rocks, R. F. Marvin, written commun., 1979). A basalt flow that overlies Chapin Wash-equivalent units at the Anderson mine has been dated at 13.2 ± 0.3 m.y. (potassium-argon whole rock, Scarborough and Wilt, 1979). In the western part of the basin area, a welded ash-flow tuff near the base of the Artillery Formation has yielded an age of 19.9 ± 0.5 m.y. (potassium-argon whole rock, Scarborough and Wilt, 1979). These data suggest that the age of the Artillery is best placed at 25 m.y. to 20 m.y. and the Chapin Wash at 20 m.y. to 13 m.y. These age limits are compatible with a Hemingfordian land mammal age (21 m.y.–17 m.y. absolute age) assigned to Chapin Wash alluvial-lacustrine rocks at the Anderson mine and a potassium-argon whole rock age of 15.9 ± 0.3 m.y. on basalt interbedded with alluvial-lacustrine Chapin Wash rocks in the western end of the basin (Shackelford, 1976).

A model for sedimentation at the Anderson mine, west-central Arizona

Uraniferous tuffaceous lacustrine sediments found in surface exposures at the Anderson mine are believed by J. K. Otton to be deposited largely by storm-induced debris flows and turbidity currents in a shallow lake. The sequence (lowermost exposures upward) consists of (1) thin (20–40 cm) cyclic graded beds, characterized by tuffaceous mud clasts, shell fragments, and rip-up clasts at the base grading upwards to micaceous tuffaceous carbonaceous siltstone, (2) thicker (30–60 cm) tuffaceous beds with abundant small silicified plant twigs and stems draped by a thin layer of tuff, (3) thick (90–150 cm) "fossil hash" beds composed of tuff debris and large silicified twigs and stems, (4) thinly laminated silicified carbonaceous tuffaceous siltstone commonly with well-preserved palm leaves, palm log fragments, and coniferous shrub stem fragments, (5) a thick (4.2 m) air-fall ash bed, and (6) calcareous tuff, limestone, and chert. This sequence is interpreted as basal distal-lacustrine turbidite deposits (1) that change upwards to proximal turbidite beds (2,3) and quiet nearshore sedimentation (4), followed by a period of sediment starvation where ash-fall material and chemical precipitation predominated (5,6).

Uranium in Monterey Formation

A preliminary investigation by D. L. Durham (1979) of uranium occurrences in diatomite and porcelanite of the Miocene Monterey Formation in the Temblor Range, Kern and San Luis Obispo Counties, Calif., indicates that the uranium was derived from sea water when highly organic siliceous sediment accumulated under anaerobic conditions on the seaward side of a marine embayment. Later dissolution and redistribution of uranium by ground water formed local concentrations of secondary uranium minerals in the Monterey. The

uranium content of the formation is considerably higher than it is for most rocks, suggesting that the Monterey is a possible source of low-grade uranium ore and may be an important and previously unrecognized source terrane for uranium.

Uraniferous phosphate occurrence on Kupreanof Island, southeast Alaska

An occurrence of uraniferous phosphate was found near Big John Bay and Hamilton Creek on Kupreanof Island in southeastern Alaska. Three samples were collected by K. A. Dickinson from a road-metal pit located near the center of the south half of sec. 6, T. 58 S., R. 75 E., in the Petersburg D–5 quadrangle. Although the area is unmapped, the samples were collected from a carbonate sequence that appears to be a facies of the Permian Cannery Formation (Muffler, 1966).

The dominant rock type at the pit is gray limestone with white calcite veins. The samples consist of fine-grained light- to dark-gray silty laminated apatitic dolomite that contains white calcite veins and quartz. Fragments of laminated phosphatic rock are suspended in white calcite. According to J. B. Cathcart (written commun., 1979), "The apatite mineral, judging from the X-ray diffractograms, is a rather typical carbonate fluorapatite–the mineral of all marine phosphate deposits." A beta eU measurement from one sample indicated 80 ± 24 ppm uranium. The uranium is apparently contained in the apatite. In the three samples studied, a direct relation exists between the height of the X-ray diffractogram peaks of apatite and the alpha-count of the X-ray sample. In addition to apatite, the samples contain dolomite, calcite, and quartz.

The bed from which the samples were taken is poorly exposed, but, judging from the dimensions of the radioactive anomaly that reached a maximum of about 20 times background, it is no more than 0.5 m in thickness. Its lateral extent was not determined.

This report is based on a very brief field visit, and it does not establish the existence of commercial-sized phosphate deposits in the area. It suggests, however, that further work could prove fruitful. The only other known occurrence of phosphate rocks in Alaska is in Mississippian and Triassic rocks along the northern margin of the Brooks Range (Patton and Matzko, 1959).

Porous media model computer and field studies of sandstone-type uranium deposits

Results of porous media model studies, conducted to date by D. K. Sunada and F. G. Ethridge (Colorado State University), reveal a close similarity between the modeled deposits and actual uranium deposits in the Colorado Plateau area, suggesting that model studies might provide valuable data for predicting the size and shape of tabular ore bodies and the relation between these bodies and ground-water flow patterns. Numerical model studies that have been verified for a homogeneous porous media suggest that, with additional research, this type of approach might be useful in predicting the location of actual uranium deposits.

Field studies have confirmed that the uraniferous Salt Wash Sandstone Member of the Morrison Formation in the Slick Rock district, Colorado, was deposited in a fine-grained meander-belt system and that this type of depositional model should be used as an exploration guide in the search for uranium in the Uravan mineral belt.

Organic geochemistry and uranium in the Grants mineral belt

Organic material is intimately associated with the primary uranium deposits of the Grants mineral belt. This organic material is insoluble and nonvolatile, and most of it is lacking in physical structure. The mixture of organic matter and uranium coats sand grains and fills interstices, which seems to indicate that both the organic matter and the uranium were introduced as soluble materials after sedimentation. The relation of organic matter and uranium can be shown physically, chemically, and statistically.

Pyrolysis-gas chromatography, mass spectrometry, and elemental analysis have been used by J. S. Leventhal to examine the organic matter from several ore deposits. The results show carbon-rich materials that have been severely degraded by radiation from uranium and daughter products. The organic material now resembles amorphous carbon, having lost most of its hydrogen and oxygen. From the uranium content and approximate age, the radiation dose is calculated to be 10^{11} rads. The radiation damage also has produced an interesting new carbon-isotope fractionation effect; that is, the carbon associated with ore is enriched in carbon-13 relative to the nonore carbon.

From model experiments and laboratory work on samples from the Grants district, two hypotheses are made. First, the soluble organic matter (of unknown origin) coated or precipitated on the mineral grains; subsequently, the uranium (probably as uranyl cation or carbonate anion complex) is concentrated in and on this organic matter by ion exchange and chelation with functional groups. This cycle of organic coating and uranium concentration could have been episodic or continuous but must have lasted at least 10^6 yr based on calculations using assumed porosity, permeability, hydraulic gradient, uranium content of water, and organic concentration factors. Second, after 10^8 yr, the radiation damage has created an amorphous carbon material that is deficient in hydrogen and oxygen but helps to protect the ore from mobilization due to its chemical inertness.

Experimental studies on uranyl ion reduction by H_2S reveal a marked pH dependence

Although reduction of uranyl ion is the most commonly cited mechanism of uranium localization, experimental studies of this process were lacking. Accordingly, studies were made by D. M. Updegraff (Colorado School of Mines) on the kinetics of reduction of uranyl ion to uranium (IV) oxide by hydrogen sulfide at 50°C (in collaboration with Ali Muhaggahi). The rate of this reaction increased markedly with pH between pH 4 and 7. At the lower pH, the initial product is soluble uranium (V), which subsequently disproportionates to uranium (IV) and uranium (VI). The initial sulfur oxidation product at this lower pH is elemental sulfur. As the pH of reaction is raised, the initial sulfur oxidation product is thiosulfate, and uranium reduction proceeds directly to uranium (IV).

Uranium (VI) sorption by iron oxides

Preliminary sorption data generated by Donald Langmuir (Colorado School of Mines) show strong chemical bonding between positively charged uranyl species and the ferric oxides in the pH range of about 4 to 8. Preliminary sorption data also indicate that the release of uranium from the ferric oxides is favored by an increase in the concentration of uranyl carbonate complexes in solution.

Dissolved free oxygen and the genesis of sandstone-type uranium deposits

According to H. C. Granger, one factor that distinguishes the genesis of roll-type uranium deposits from that of deposits in the Uravan mineral belt and other sandstone-type uranium deposits may be the presence and concentration of dissolved free oxygen in the ore-forming solutions. Although dissolved oxygen is a necessary prerequisite for the formation of roll-type deposits, it is proposed that a lack of dissolved oxygen is a prerequisite for the Uravan deposits.

Solutions that formed both types of deposits probably had a supergene origin and originated as meteoric water in approximate equilibrium with atmospheric oxygen. Roll-type deposits were formed where the oxidation-reduction potential (Eh) dropped abruptly following consumption of the oxygen by iron-sulfide minerals and creation of kinetically active sulfur species that could reduce uranium. The solutions that formed the Uravan deposits, however, probably first equilibrated with sulfide-free ferrous-ferric detrital minerals and fossil organic matter in the host rock; that is, the uraniferous solutions lost their oxygen without lowering their Eh enough to precipitate uranium. Without oxygen, they then became incapable of oxidizing iron-sulfide minerals. Subsequent localization and formation of ore bodies from these oxygen-depleted solutions, therefore, was not necessarily dependent on large reducing capacities.

Genetic geochemistry of Uravan mineral belt deposits—a new proposal

Uranium within unoxidized uranium-vanadium ore layers in the Deremo mine, San Miguel County, Colo., does not correlate with either organic matter or sulfide minerals. Neither of these constituents is consistently concentrated in or near ore layers. Uranium (IV), principally as coffinite, and both vanadium (III) and vanadium (IV), principally as vanadium alumino-silicates and oxides, are the dominant primary minerals. Because of the paucity of sulfide minerals and organic matter within the ore, it is difficult to explain either the source or fate of the reducing agent.

These observations have led to a novel proposal to explain ore localization. It is suggested by H. C. Granger that minor H_2S and organic acids derived from decomposing plant matter destroyed detrital magnetite grains, precipitated pyrite, and complexed the vanadium (III) that is generally contained in magnetite deposits. Into this relatively stagnant pore solution, a supergene solution containing uranium (VI) was introduced. This solution flowed through the most permeable conduits in the host rock, and, where it contacted the connate waters, uranium (VI) was reduced principally by the vanadium (III) in the organic acid complexes. This reduction reaction thereby permitted precipitation of uranium (IV) and vanadium (IV) minerals such as coffinite, vanadium clays, and doloresite. Excess vanadium (III) formed roscoelite and montroseite. Aluminum and silicon also were carried in the connate solution as organic-acid complexes and contributed to the formation of ore minerals. Upon destruction of the complexes, the organic acids remained in solution and were largely removed.

The novelty of this concept lies principally in the proposed oxidation-reduction reaction between uranium and vanadium rather than reduction of oxidized phases of both these elements by a separate reducing agent, as most earlier concepts have inferred.

Presence of ore-stage marcasite and formation of roll-type deposits

Study by M. B. Goldhaber of five roll-type uranium deposits (three in Texas and two in Wyoming), in collaboration with R. L. Reynolds, has resulted in the recognition of ore-stage marcasite in each deposit. Ore-stage marcasite is identified by its close association with uranium- and vanadium-bearing phases in the ore zones, by its close association with ferroselite at and near the redox boundary in some deposits, by its abundance and

distribution across deposits, and by its textural relation with identifiable preore iron-disulfide minerals (primarily pyrite). In deposits that are essentially devoid of fossil vegetal debris, marcasite is the dominant ore-stage sulfide and occurs in a large volume of rock beyond the ore zones. In deposits that contain organic matter, ore-stage pyrite is at least as abundant as ore-stage marcasite (Goldhaber and Reynolds, 1979). Many factors and processes may lead to the formation of either marcasite or pyrite as an ore-stage mineral in roll-type deposits. One of the dominant factors is the complex interrelation of pH and sulfur species that are precursors of iron-disulfide minerals. Experimental work and study of geochemical environments analogous to those governing the formation of roll-type deposits indicate that relatively low pH (less than about 6) and the presence of elemental sulfur favor marcasite, whereas higher pH and the presence of polysulfide ions favor pyrite. Conditions that favor marcasite as the dominant ore-stage iron disulfide are likely to arise during uranium deposition in the host rock without fossil vegetal matter. In host rock containing carbonaceous debris, the presence of polysulfide ions and pH buffering, combined with any anaerobic bacterial metabolic processes, apparently leads to the formation of ore-stage pyrite.

Geochemical studies of a tabular uranium ore body

Research by M. B. Goldhaber, in collaboration with D. J. Carpenter, on the geochemistry of the Tony M mine, a Colorado Plateau lenticular ore body in Garfield County, Utah, has placed strong constraints upon the mechanism of formation. The deposit, which, on the basis of uranium-lead ratio data, formed very early in the depositional history of the Salt Wash Sandstone Member of the Morrison Formation, developed at an interface between flowing ground water containing the ore elements in solution and underlying stagnant ground water containing reducing agents. The ground-water flow path was delineated on the basis of marked depletions in sodium, potassium, and magnesium, indicating leaching of these elements from the host rock. The interface between uranium ore and this ground-water transport zone is extremely sharp. The ore zone is characterized by a vertical element zonation in the sequence selenium, uranium plus vanadium, and molybdenum with vertical distance below the interface. Vanadium, in contrast to uranium, precipitated in the ground-water transport zone as well as in the ore zone. The vanadium in the transport zone occurs as vanadium (IV) clay, whereas vanadium in the uranium ore zone occurs as the trivalent oxide.

Pyrite and marcasite in roll-type uranium deposits

Study of roll-type uranium deposits by R. L. Reynolds and M. B. Goldhaber has shown that iron-disulfide (FeS_2) minerals in host rocks that contain organic matter differ in abundance, distribution, texture, and sulfur isotopic composition from FeS_2 minerals in host rocks that do not contain organic matter. In deposits without organic matter, preore FeS_2 is dominantly euhedral pyrite that is isotopically heavy and that formed from isotopically heavy fault-derived H_2S. In these deposits, ore-stage FeS_2 is dominantly marcasite that occurs as far as 400 m downdip from the altered tongue. In deposits that contain organic matter, preore FeS_2 is also dominantly pyrite, but it occurs commonly as framboids and as replacements of plant fragments. This preore pyrite is formed by bacterial sulfate reduction during early diagenesis and is isotopically lighter than pyrite formed from fault-derived H_2S. Ore-stage FeS_2 in these deposits is primarily pyrite. Consideration of geochemical conditions that favor pyrite formation suggests a biogenic origin for the ore-stage pyrite in deposits that contain organic matter. In contrast, formation of ore-stage marcasite in deposits that do not contain organic matter involved abiologic sulfur transformations. The contrasting origins of ore-stage FeS_2 minerals in host rocks with and without organic matter suggest that previously proposed biogenic and inorganic origins for roll-type deposits are both valid.

Uranium adsorption onto montmorillonite

Studies by G. W. Brindley (Pennsylvania State University) of uranium adsorption onto montmorillonite previously saturated with calcium have shown that adsorption occurs as a divalent ion, the uranyl ion UO_2^{2+}. The selectivity coefficient for this exchange is less than one, implying that the proportion of uranyl ion in solution is greater than that on the clay. The kinetics of this exchange are rapid, although there is an as yet unresolved minor time-dependence aspect, perhaps implying some additional mechanism of uranium interaction with the clay. In experiments designed to imitate a dynamic flow system in which uranium-bearing solution comes into contact with a static clay phase, there was a progressive increase of uranium on the clay, eventually building up to the full exchange capacity.

Oxygen isotope studies of uranium source rocks

The granite of Lankin Dome in the Granite Mountains, Wyo., has been identified as a probable source rock for uranium in three mining districts that surround the range (Rosholt and others, 1973; Stuckless and Nkomo, 1978). Preliminary investigations by David Wenner and

J. S. Stuckless of O^{18} values for whole-rock samples of the granite of Lankin dome have yielded results that are typical of I-type granite (Chappell and White, 1974). This classification contrasts with the S-type classification, indicated by chemical and radio-isotope data, which suggests that this uranium source rock had a mode of origin that may be different from most granite.

Sites of labile uranium in granitic rocks

Uranium, thorium, and lead concentrations and lead-isotopic compositions of minerals separated from two granite samples from the Granite Mountains, Wyo., suggest to J. S. Stuckless that nearly all the uranium and thorium are associated with minor and trace minerals (Stuckless and Nkomo, 1980). In a deep drill-core sample (which contains approximately equilibrium amounts of uranium and radiogenic lead and is, therefore, judged to be unleached), biotite and epidote account for more than 60 percent of the uranium and more than 70 percent of the thorium. In a surface sample (which is more than 50 percent deficient in uranium relative to radiogenic lead and is, therefore, judged to be leached), biotite and epidote still account for more than 70 percent of the thorium but only 35 percent of the uranium. These facts and the excess radiogenic lead in both minerals from the surface sample suggest that uranium loss from the surface samples (Rosholt and others, 1973; Stuckless and Nkomo, 1978) is a function of leaching of biotite and epidote.

Use of uranium-lead isotope systematics to date uraniferous opals

Uraniferous opals, containing several tens of thousands parts per million of uranium, occur in association with beryllium, fluorine, and uranium mineral concentrations at Spor Mountain, Utah. The timing of mineralization with respect to the volcanic host rocks of several different generations was unclear, however, until uranium-lead isotope investigations of the uraniferous opals were undertaken by K. R. Ludwig. The results of these investigations show that uraniferous opals indeed can be used for precision uranium-lead isotope geochronology, because of an often low common-lead content and good uranium-daughter retentivity characteristics. Data from both massive-nodule and fracture-filling opal in host rhyolite of several different ages give mostly concordant $^{206}Pb/^{238}U$ and $^{207}Pb/^{235}U$ ages that show that uraniferous opal formation began as early as 21 m.y. ago, probably during cooling of the host (21-m.y.-old topaz rhyolite), and continued either continuously or episodically until at least as late as 3.5 m.y. ago. Limiting requirements for the technique are probably at least 10 ppm uranium in the opal and an age for higher uranium opal of at least 1 m.y., making such opals among the youngest materials datable by the uranium-lead technique. In addition to age information, the lead-isotope systematics preserve a record of the initial $^{234}U/^{238}U$ of the fluids from which the opal formed—an important geochemical parameter unobtainable by any other means.

Geochemical uranium, fluorite, and beryllium ore controls at Spor Mountain

Uraniferous beryllium and fluorite ores are mined in the Spor Mountain area of Juab County, Utah. Fluorite ores occur principally in breccia pipes in Paleozoic limestone. Beryllium ores occur principally in Tertiary tuff, the beryllium member of the Spor Mountain Formation.

Multivariate factor analysis by R. A. Cadigan was computed on abundance data for 32 elements in 235 samples from drill holes in the Spor Mountain–Thomas Range area. The results suggest that six major geochemical processes account for 73 percent of the variation in the occurrence of the elements.

The first factor, interpreted to be a hydrothermal process, affects the occurrence principally of As, Ag, Mo, Sn, Co, Ni, Sc, and Pb, in that order. The second factor, also hydrothermal, affects the occurrence principally of F, Be, Y, Li, Nb, Cs, U, and W. The third and fourth factors, interpreted as epigenetic solution activity, affect the occurrence principally of Ca, Sr, V, Na, B, and Sb, with Na in negative relation to Ca, Sr, and V. The fifth factor, interpreted to be a lithic factor, affects the occurrence principally of La, Al, Zr, and Mn. The sixth factor, also hydrothermal, affects the occurrence principally of Zn, Cr, Fe, and Cu and secondarily of Pb, Ni, Co, and Ti.

The second factor group of elements corresponds to the suite of elements that compose the fluorite and beryllium ores at Spor Mountain. The ores contain economically important uranium values. Although the main fluorite deposits have been attributed to the hydrothermal mineralization of the limestone breccia pipes, the origin of the beryllium in the tuffs has been attributed by some investigators to the deposition of a beryllium-rich tuff. The high degree of association of the beryllium with fluorine, as indicated by the factor grouping that accounts for 72 percent of the variation of occurrence of beryllium, is strong evidence that fluorine mineralization and beryllium mineralization have a common hydrothermal origin. This mathematically demonstrated fluorine-beryllium relation is not compatible with the theory of a beryllium-tuff origin for the beryllium.

Uranium occurrences are affected positively by the fluorine-beryllium mineralization process to the extent that this mineralization accounts for 34 percent of uranium variation in the rocks. The epigenetic solution

effects on uranium occurrences are negative, accounting for 19 percent of uranium variation. The zinc-chromium mineralization effects are also negative, accounting for 10 percent of uranium variation. Negative effects mean that, as the measurable intensity of effects of a process at a site increase, the amount of uranium present at the site tends to be less because of the difference in geochemical environment.

The presence of the arsenic-silver factor and its highest intensity at the south end of the Thomas Range and west of the Spor Mountain suggest the possible presence of other economic mineral targets in these areas.

Uraniferous silica—conditions of formation

Uraniferous opal and (or) chalcedony are observed as cement, nodules, or veinlets in tuffaceous sedimentary rocks or as veins in silicic igneous rocks. Experiments by R. A. Zielinski were performed to define the conditions most favorable for incorporation of dissolved uranium by these authigenic silica-gel precipitates. Results set limits on the chemistry and uranium concentration of formation waters and, thus, provide vital information for uranium exploration. Silica gel was precipitated by adding NaCl to solutions of uranium (1 ppm), and colloidal silica and the uranium concentrations of the separated gel and liquid phases were determined. Partitioning of uranium was expressed as an enrichment factor (E.F.) defined as concentrate(d) (U) dried gel/concentrate(d) (U) liquid. Measured values of E.F. ranged from <1 to 3,000. Values of E.F. in carbonate-free solutions increased abruptly from 50 to 3,000 between pH 4.5 and 6.5, then decreased to 600 ± 200 at pH >7.5. Addition of carbonate to an alkaline solution of pH 8.3 caused E.F. to decrease from 800 to 500 ($CO_2 = 0.001$ to 0.01 molal) and from 500 to <1 ($CO_2 = 0.01$ to 0.15 molal). Values for E.F. for pH 8.3 and fixed total-carbonate concentration (0.001 molal) were insensitive to changes in initial dissolved-uranium concentration (1–10 ppm), NaCl concentration (0.05–0.5 molal), and solid-liquid weight ratio (0.057–0.135). Identical experiments performed without colloidal silica showed no evidence of uranium precipitation. Uraniferous hydrous silica gel was observed to re-equilibrate with new volumes of reaction solution, but dehydrated gels did not. For typical ground water of pH 7.0–8.5 and $CO_2 = 0.001$–0.01 molal, the results indicate that dried silica-gel precipitates will have 400 to 1,000 times the uranium concentration of the original coexisting solution.

Distribution and mobility of uranium in glassy and zeolitized tuff, Keg Mountain area, Utah

The distribution and mobility of uranium in a diagenetically altered 8-m.y.-old tuff in the Keg Mountain area, Utah, were modeled in studies by R. A. Zielinski. The modeling represents an improvement over similar earlier studies in that it (1) considers a large number of samples (76) collected with good geologic control that exhibit a wide range of alteration, (2) includes radiometric data for Th, K, and RaeU, as well as U, (3) considers mineralogic and trace-element data for the same samples, and (4) analyzes the mineral and chemical covariation by multivariate statistical methods.

The variation of uranium in the tuff is controlled mainly by its primary abundance in glass and by the relative abundance of nonuraniferous detritus and uraniferous accessory minerals. Alteration of glass to zeolite, even though extensive, caused no large or systematic change in the bulk concentration of uranium in the tuff. Some redistribution of uranium during diagenesis is indicated by association of uranium with minor alteration products such as opal and hydrous iron-manganese oxide minerals. Isotopic studies indicate that the zeolitized tuff has been open to migration of uranium decay products during the last 800,000 yr.

The tuff of Keg Mountain has not lost a statistically detectable fraction of its original uranium, even though it has a high (9-ppm) trace uranium content and has been extensively altered to zeolite. Similar studies in a variety of geological environments are required to identify the particular combination of conditions favorable for liberation and migration of uranium from tuff.

Uranium leachability from freshly erupted volcanic ash of basaltic and dacitic composition

An experimental leaching study by D. B. Smith and R. A. Zielinski of 30 freshly erupted basaltic and dacitic air-fall ash samples, unaffected by rain, shows that diagenetic alteration of glass is the dominant process by which uranium is mobilized from air-fall volcanic ash. Gaseous transfer followed by fixation of soluble uranium species on volcanic ash particles is not an important process affecting uranium mobility.

Ash samples collected from the active Guatemalan volcanoes Fuego and Pacaya (high-aluminum basalts) and Santiaguito (hornblende-hypersthene dacite) were subjected to three successive leaches with a constant water-to-ash weight ratio of 4:1. The diameter of the ash particles ranged from approximately 1 mm to submicron in size, with the mean diameter near 0.03 mm. The ash was leached by (1) distilled deionized water (pH 5.5) at room temperature for 24 h, which removed water-soluble gases and salts adsorbed to ash during eruption, (2) dilute HCl solution (pH 3.5–4.0) at room temperature for 24 h, which continued the attack initiated by the water (HCl also attacks acid-soluble sulfides and oxides), and (3) a solution of 0.05 molal in both Na_2CO_3 and $NaHCO_3$ (pH 10) at 800°C for 1 week, which selectively

dissolved volcanic glass. The first two leaches mimic interaction of ash with rain produced in the vicinity of the active eruption. The third leach accelerates the effect of prolonged contact of a pile of volcanic ash with alkaline ground waters present during ash diagenesis. The leachates were analyzed for uranium by a fission-track method; for B, Ba, Be, Ca, Cd, Co, Cu, Fe, Li, Mg, Mn, Mo, Na, Pb, Si, Sr, V, and Zn by inductively coupled plasma-optical emission spectroscopy; and for Cl and F by specific-ion-electrode techniques. Approximately 0.1 percent of the total uranium in the ash was removed by the water and acid leaches and about 1 percent by the carbonate-bicarbonate leach. Silicon, lithium, and vanadium were mobilized preferentially by the alkaline leach.

Geochemical maps of uranium, thorium, and thorium-uranium in granites of the Basin and Range province

J. M. McNeal, D. E. Lee, and H. T. Millard, Jr., examined the uranium and thorium concentration of granites from several areas of the Basin and Range province according to an analysis-of-variance design. Geochemical maps of uranium, thorium, and thorium-uranium were produced for use in predicting the possible location of secondary uranium occurrences where the uranium was derived by the weathering of granite. The thorium-uranium map is probably the most useful because uranium, but not thorium, is leached by chemical weathering. Consequently, high thorium-uranium ratios suggest a possible loss of uranium and possibly a greater potential for secondary uranium occurrences to be found in the area. The highest thorium-uranium values trend northeastward from the southern portions of California, through southern and southeastern Nevada, and into southwestern Utah.

Radioactivity in water wells, Pueblo County, Colorado

Radium, uranium, and radon concentrations in water from 37 wells tapping the aquifer system of the Dakota Sandstone and Purgatoire Formation in southwestern Pueblo County, Colo., have a wide range of values and define several areas of high radioactivity in the ground water, according to J. K. Felmlee and R. A. Cadigan. Maximum values are 420 pCi/L radium, 180 μg/L uranium, and 27,000 pCi/L radon.

Multivariate statistical analysis of data on the radioactive elements and 28 other geochemical parameters revealed 5 major influences on water chemistry: short-term solution reactions, oxidation reactions, hydrolysis reactions, uranium distribution, and long-term solution reactions. The radioactive elements are affected variously by oxidation reactions and uranium distribution in the rocks. Therefore, high concentrations of radioactive elements in the water are related to selective leaching of uranium-bearing minerals and metal sulfides by either oxidizing or reducing water along stratigraphic horizons or in fault zones.

A precipitation mechanism for hydrothermal vein-type uranium deposits

According to a theory proposed by C. S. Spirakis, the kinetics of sulfate reduction may have an important influence on the chemistry of a cooling hydrothermal solution. It is well known that sulfate is an active oxidizing agent at high temperatures. However, as a sulfate-bearing hydrothermal solution cools to less than about 200°C, kinetic factors prevent sulfate from entering into oxidation-reduction reactions. Consequently, the reducing effect of H_2S (and other reducing agents) is not balanced with the oxidizing effect of sulfate to the same extent as at higher temperatures. The result is a lower effective oxidation-reduction potential (Eh) of the system. This decrease in the effective Eh due to a slowing of the rate of sulfate reduction with cooling could cause the reduction and precipitation of uranium from hydrothermal solutions. The same mechanism may apply to other types of hydrothermal deposits. The temperature at which hydrothermal uranium deposits form and the paragenesis observed in these deposits are consistent with this model.

Uranium concentration by moss and algae from surface water

Samples collected from various locations in the Western United States show a marked difference between capacities of algae and moss to remove and concentrate uranium from water. Moss growing in water containing 5.1 μg/L uranium have concentrated uranium up to 1,500 ppm, whereas algae in waters containing as much as 70 μg/L uranium contained only 8 ppm uranium. Concentration differences were not so pronounced for most other trace elements.

According to K. J. Wenrich-Verbeek, there is a significant positive correlation between uranium in moss and uranium in coexisting water. Uranium in algae, however, shows no significant correlation with uranium in water. Differences in uranium content could be due to either adsorption (as moss has both a greater surface area-volume ratio and a longer life cycle than algae) or adsorption (perhaps by lignin, which is present in some mosses but not in algae).

Uranium in moss also shows a significant positive correlation with uranium in the coexisting stream sediments, suggesting mechanical entrapment by moss of fine particles of uranium-bearing minerals. Nevertheless, correlation coefficients between uranium and other elements indicate that only a minor amount of uranium in the moss is tied up in detrital minerals. Of the various elements forming detrital uranium-bearing

minerals, only yttrium shows a significant positive correlation with uranium. Yet, organic-carbon content shows a greater positive correlation, suggesting that the more organic-rich (less detrital) the sediment, the greater the uranium concentration in moss.

Helium detection for uranium exploration

A helium and radon analysis of well waters was conducted by C. G. Bowles and G. M. Reimer in the vicinity of a south Texas roll-front uranium deposit. The helium and radon concentrations were both anomalously high in the waters from the host-rock formation taken at the deposit. The helium concentration dropped by a factor of 3 for host-rock formation waters taken several kilometers from the deposit but still remained anomalous. Radon concentrations, however, dropped by a factor of 100 within the same distance and were not anomalous. This information suggests that helium may indicate whether a particular formation is a favorable target for uranium exploration and, in addition, may provide a guide to the distance from the sample to the deposit (within several kilometers). Radon analyses would then have the value of further refining distance from the deposit (within several tens of meters). Helium and radon analyses of waters are an important addition to any geochemical exploration program. Helium data alone can reveal information that otherwise would be overlooked in exploring for uranium.

Application of high resolution gamma-ray spectrometry to uranium prospecting

The depletion of uranium resources has increased the need for new techniques to detect and quantify low-level uranium deposits in new locations. High resolution gamma-ray spectrometry has been successfully applied to low-level uranium exploration (Tanner and others, 1977). F. E. Senftle has inferred concentrations of uranium by comparison to a standard ore whose radionuclei are assumed to be in radioactive equilibrium. A method to determine uranium concentrations independent of equilibrium considerations has been developed. This was accomplished using lines from the decay of bismuth-214 and lead-216 to supply information about the gamma-ray attenuation and density of the sandstone. Once the sandstone is characterized, the protactinium-234 line is used to determine the uranium-238 concentration.

Uranium occurrence in southern Wah Wah Range, Utah

Anomalous radioactivity up to 10 times local background was found by C. S. Bromfield and L. M. Osmonson in the southern Wah Wah Range of the Richfield 1°×2° quadrangle, associated with porous lapilli tuff and tuff breccia, probably of rhyolitic composition. The rocks are part of a sequence of rhyolitic volcaniclastic, epiclastic, and flow rocks that overlie the Needles Range Formation (29 m.y.) and locally the Isom Formation (22–26 m.y.). The flow rocks, which are dense flow-banded topaz-bearing rhyolite sequences, may be related in age, as well as composition, to the 21-m.y.-old topaz-bearing alkalic rhyolite plug at the nearby Staatz fluorite-uranium mine. Surface exposures suggest that high radioactivity is concentrated in hematite-stained tuff on or adjacent to steep north-northwest-striking fractures or joints.

Stratigraphic control of solutions that deposited uranium in Cretaceous rocks, Catron County, New Mexico

Field investigations made by C. T. Pierson as part of USGS work in the Socorro 1°×2° quadrangle, New Mexico, suggest that several small uranium deposits found in the Crevasse Canyon Formation of Late Cretaceous age in the McPhaul Ranch–Red Basin area (Bachman and others, 1957) in the southwest part of the Socorro quadrangle, probably were formed by precipitation of uranium from ground water that descended through sandstone of the overlying Baca Formation of Eocene(?) age. The ground water may have derived its uranium content by leaching of silicic tuffaceous rocks known to be present in the Datil Formation that overlies the Baca (Chapin and others, 1979; Willard, 1959). Precipitation was probably by organic material common in the Cretaceous strata.

Evidence supporting the postulated downward movement of mineralizing solutions consists of (1) the observation (Griggs, 1954, p. 5) that, in the Crevasse Canyon Formation, the "uranium minerals are generally localized at the contact of beds of sandstone and shale, and the highest grade material lies in the basal parts of those sandstone beds that lie directly above the shale beds" and (2) the fact that all of the known occurrences in the relatively untransmissive Crevasse Canyon Formation are found in the uppermost part of the formation stratigraphically just below beds of the relatively transmissive Baca Formation.

A possible relation between subsidence and uranium mineralization

The Cameron uranium district and the Holbrook–St. Johns uranium district in the Flagstaff 1°×2° quadrangle, Arizona, are the only places where significant mineralization has been found in the Petrified Forest Member of the Chinle Formation. Both of these districts occur in areas that were subsiding along with sedimentation. It is suggested by C. S. Spirakis that subsidence kept organic material below the water table much of the time and, thus, protected it from atmospheric oxidation. This organic material (which was

preserved by subsidence) was available to reduce uranium from the mineralizing solutions. This suggested link between subsidence and the localization of the ore may be used to predict the subsurface extensions of the Cameron and Holbrook–St. Johns uranium districts and might be useful in finding other mineralized areas.

Uranium mineralization in the Hopi Buttes of the Flagstaff and Gallup 1°×2° quadrangles, Arizona

The Hopi Buttes are remnants of diatremes approximately 5 m.y. in age that erupted into the Pliocene Bidahochi Lake. The volcanic rocks of the diatremes are monchiquitic lamprophyres distinct from normal alkalic basalts of the Colorado Plateau in their extreme silica undersaturation, high water, TiO_2, P_2O_5, and relatively high K_2O contents. Studies by K. J. Wenrich-Verbeek have shown that many trace elements are also unusually high, most notably Zr, Ba, Nb, Ce, and U (average value of about 4 ppm, as compared to the average value of 1 ppm for continental basalts). Many of these diatremes later were filled with localized lakes believed to have been fed by rising thermal solutions. Limestone beds deposited in these lakes resemble travertine deposits and contain high concentrations of phosphate, sulfate, Ba, Sr, and As, elements commonly occurring in hot-spring deposits, as well as U and Se. Areas of high selenium content are recognizable in the Hopi Buttes by the abundance of *Astragalus pattersoni*.

Approximately 300 diatremes or maars comprise the Hopi Buttes; of 79 studied during the past year, 35 contain hydrothermal lake-bed deposits, all with radioactivity exceeding background levels. Scintillometer traverses have shown 20 of these diatremes with radioactivity exceeding 5 times background. An aerial gamma-ray survey shows sharp-peaked anomalies above any of these 20 buttes crossed by the flight lines, as well as some new occurrences. Hydrogeochemical sampling in the area also revealed anomalous concentrations of uranium in spring and well waters from the Hopi Buttes area. Uranium ore was removed during the 1950's from the Morale claim, located on the margin of a small diatreme northeast of Indian Wells. Production records show the average grade of the ore was 0.15 percent U_3O_8 for 169 t. Selected samples from the old adit contain up to 0.5 percent U_3O_8. Extensive drilling into the Morale claim diatreme in October 1979 revealed intervals within the interbedded limestones and siltstones up to 6 m thick and 150 by 90 m in area containing an average of 0.015 percent U_3O_8. The potential for uranium in the Hopi Buttes is for low-grade deposits within 15 m of the surface containing on the order of 90 t of U_3O_8 per butte.

Unconformity-related uranium occurrences in the Precambrian basement in the upper basin of the Arkansas River, Colorado

Many uranium occurrences in the extensively fractured Precambrian crystalline basement of the Pueblo 1°×2° quadrangle were examined by M. R. Brock and are believed related to an ancient erosional surface in the vicinity of the Arkansas River canyon and southern Wet Mountains in south-central Colorado. A thick sequence of Oligocene sedimentary and volcanic rocks was deposited on the extensive pediment surface, and uranium leached from these rocks is believed to have been transported downward by ground water and redeposited in porous basement fractures. Erosion since has stripped the Oligocene rocks from large areas of the pediment during incisement by the Arkansas River and its major tributaries. A few hundred square kilometers of the ancient pediment is now exposed. Except for several small occurrences of uranium in pegmatites and schlieren zones, most concentrations of the metal are contained in fracture zones in the crystalline basement. These supergene concentrations contain pitchblende, autunite, and other labile secondary uranium minerals. Most such concentrations are entrapped in encrustations and films of red and brown iron oxide on fracture surfaces, an association that tends to preserve the uranium that otherwise would have been leached and transported to greater depth by surface water. These surface occurrences are generally limited to a few square meters or less in size but are considered significant because of the likelihood that, in some cases, they may be surface expressions of much larger unleached deposits at depth. The Schwartzwalter uranium mine in the Front Range of the Colorado Rocky Mountains, which has produced in excess of 5 million kg of U_3O_8, was discovered beneath a surface anomaly of a few square meters and a maximum radioactivity of only twice background. The two Jabiluka ore bodies in Australia resulted from subsurface exploration of ground under small surface occurrences that registered maximum surface radioactivity of 6½ times background. These two deposits contain more than 200 million kg of U_3O_8. Thus, the labile nature of uranium within faulted or heavily fractured terrane is a factor to be given serious consideration in assessing surface anomalies in similar geologic settings.

Numerous thorium veins of Early Cambrian age are exposed within the southeastern periphery of the upper Arkansas River basin on the flank of the southern Wet Mountains. Although most thorium veins contain only trace quantities of uranium, several veins within and near the pediment contain between 0.01 and 0.15 percent uranium. Reexamination and selective sampling show that the anomalous uranium values are restricted to earthy hematite veins that penetrate the earlier

thorium-bearing rock. This uranium now is considered to be of supergene origin and to have been derived from the previously overlying Oligocene clastic and volcanic rocks. It is conceivable that one or more large deposits of uranium may be concealed within the sheared basement beneath the ancient pediment surface.

Colorado uranium deposits as ancient geothermal systems

Deep vein systems containing major uranium deposits occur in an elongate north-south belt along the eastern Front Range foothills in the Denver 1° × 2° quadrangle. Studies by A. R. Wallace are in progress at several of the deposits to determine alteration and fluid geochemistry. Additional work is being done on the host breccia faults to put them, and the deposits, in a regional framework.

Wallrock alteration and vein mineralization studies show that the depositional environment was alkaline and dominated by carbonate. Siderite and ankerite replace primary mafic minerals in the wallrocks, and carbonate deposits and adularia fill open spaces in the veins. Under these conditions, the uranium would have been transported in a carbonate complex. Deposition of vein carbonate, adularia, and uranium probably was controlled by boiling of the hydrothermal solution. Work on the breccia faults shows that carbonate breccia filling is present only where the faults are in proximity to carbonate-rich hornblende gneisses, suggesting that at least the carbonate was derived from those rocks. The entire system is similar to deep modern hot springs in New Zealand and California.

Source of the uranium-bearing sandstone of the southern Powder River Basin

Major valleys traversing the Laramie Mountains of the Torrington 1° × 2° quadrangle were found by David Seeland to be alined with major uranium-bearing channel-sand bodies in the Powder River Basin, suggesting that Eocene streams carried granitic debris from an eastern Granite Mountains source through the Shirley Basin and northward across the Laramie Mountains into the Powder River Basin. By analogy with other Wyoming mountain ranges where it was found that major present-day valleys have existed since the Eocene, it seems probable that the major stream valleys of the northern Laramie Mountains are also as old as Eocene. The stream pattern of the Laramie Mountains is markedly asymmetric; many of the streams head from south and west of the axis of the range or flow completely across the range. Although this pattern could be the result of superposition, as has been suggested for the origin of the Big Horn River canyon through the Owl Creek Mountains, it most likely is not. Eocene rocks are present in some of the valleys, and the volume of granitic rocks eroded from the Laramie Range seems inadequate to account for the volume of arkosic sand.

This source hypothesis has important implications in the search for roll-type deposits in the Eocene sandstone of the Powder River Basin. It also suggests that unconformity-related deposits may exist in fractures and faults in the Precambrian rocks along the courses of the transmountain Eocene river.

GEOTHERMAL RESOURCES

Hydrothermal alteration in Yellowstone geyser basins

K. E. Bargar and M. H. Beeson studied Y–2, a USGS research diamond drill hole located in Lower Geyser Basin, Yellowstone National Park, Wyo. The drill hole penetrated interbedded siliceous sinter and travertine from the surface to 10.2 m, glacial sediments of Pinedale age with interlayered pumiceous tuff from 10.2 to 31.6 m, and rhyolite and related volcaniclastic rocks of the Elephant Back flow and the flow in the Mallard Lake Member of the Plateau Rhyolite of late Pleistocene age down to the bottom of the hole at 157.4 m. Hydrothermal alteration is pervasive and varied throughout most of the nearly continuous drill core.

Occurrences of kaolinite coincide with breaks in formations at three separate locations above 38.1 m, suggesting that the surface conditions in the past may have been somewhat variable and probably were different than those of today. Kaolinite typically forms in a near-surface acid-altered environment but also can occur as an alteration product of glass (Browne and Ellis, 1970).

Hydrothermal minerals containing sodium or potassium as the dominant cation are, as would be expected, plentiful in the drill core, and magnesium minerals are entirely absent. However, several calcium- and iron-rich hydrothermal minerals do occur in Y–2, and zones of calcium minerals alternate with minerals containing sodium or potassium. The alternating calcium-rich and sodium- and potassium-rich zones in the drill core are not coincident with changes in lithology and, thus, do not appear to have resulted from differences in composition of the starting minerals. Calcium and iron enrichment appears to be due to extraction of these elements from the circulating thermal waters, the composition of which may have varied with depth.

Hydrothermal alteration at Mount Hood, Oregon

M. H. Beeson, T. E. C. Keith, and K. E. Bargar found that secondary minerals present in the largely andesitic rocks that make up and surround Mount Hood volcano

may result from vapor-phase crystallization, fumarolic activity, or hydrothermal alteration. Vapor-phase tridymite, iron oxides, and iron hydroxides are found in virtually all the extrusive rocks but appear to be more plentiful along cooling joints in the andesites. Fumarolic alteration is limited to vent areas near the summit of Mount Hood, where acid-sulfate leaching is still actively altering the rocks and depositing silica minerals, native sulfur, sulfate minerals, iron oxides, and iron hydroxides. Hydrothermal alteration is limited largely to lower Pliocene andesitic rocks and volcanic and volcaniclastic rocks of the upper Miocene Rhododendron Member of the Sardine Formation. The area of most intense alteration forms a northwest-trending zone from Iron Creek across the southwest flank of Mount Hood into Old Maid Flat but is buried over much of the southern flank by a younger block and ash flow. This trend is presumably a broad fault zone containing many approximately N. 10° W.-trending minor faults that control much of the alteration. The dominant hydrothermal minerals in the lower Pliocene andesite are quartz, pyrite, epidote, iron oxides, and hydroxides. Hydrothermal minerals with only minor occurrences include calcite, adularia, galena, sphalerite, dolomite, illite, and cerussite. The Rhododendron Member of the Sardine Formation has been subjected largely to zeolitic alteration consisting of laumontite, stilbite, heulandite, chabazite, and mordenite. Where the upper Miocene and lower Pliocene rocks occur in contact with the Laurel Hill and Still Creek intrusions, they are altered propylitically and contain epidote, chlorite, quartz, apatite, and tourmaline, as well as the zeolites. Coatings of opal and iron oxides and iron hydroxides are found in stream gravels and morainal deposits. These come largely from the summit area of Mount Hood.

Alaska Peninsula volcanoes

Geologic mapping and petrologic mapping studies by T. P. Miller on Peulik, Kialagvik, Chiginagak, and Yantarni Volcanoes showed that they are generally similar systems consisting of relatively small stratovolcanoes with associated dacite domes and block-and-ash flows. All have had Holocene and (or) historic activity. The Chiginagak stratovolcano edifice is built on a much larger older volcanic complex that appears to range in composition from basalt to rhyodacite. All four volcanoes are considered to have geothermal potential; Chiginagak Volcano was thought previously to have little potential, and Yantarni was discovered only this year.

Seismic reflection survey in the Raft River Geothermal Area, Idaho

H. D. Ackermann interpreted approximately 35 km of vibroseis 24-fold seismic-reflection line data acquired and processed by contract in the Raft River Geothermal Area, southern Idaho. Data quality ranged from fair to good. Inspection of the processed sections showed the structure within the Tertiary sedimentary pile to be highly complex, with numerous faults, tight folds, and a highly varying velocity distribution. The basement complex appears unaffected by these overlying structures.

Improved methods for seismic refraction interpretation

H. D. Ackermann wrote an interactive computer program that interprets seismic refraction data in terms of both depth to refracting horizons and lateral velocity changes. This program is used now on a routine basis in the interpretation of all the refraction data obtained by the Regional Geophysics Branch. Correlation of results with drill-hole data is very satisfactory.

Vitrinite reflectance geothermometry in the Cerro Prieto geothermal system, Baja California, Mexico

C. E. Barker and N. H. Bostick studied vitrinite reflectance in samples of hydrothermally altered mudstone from four wells in the Cerro Prieto geothermal field. Their studies indicate that organic matter is a sensitive recorder of the maximum temperature reached in the reservoir rocks. Measurements of temperature in these wells are of varying precision because of variations in the conditions in the wells prior to logging and because of the extreme conditions encountered in the wells. However, the mean or median values of reflectance, plotted as a function of temperature, fall along smooth curves, of exponential form, with correlation coefficients in excess of 0.80. An empirical correlation of vitrinite reflectance and rock temperature is based on the best temperature data in the Cerro Prieto field. This relation allows prediction of stable reservoir temperatures in new wells in the Cerro Prieto system based on reflectance data with no need to wait for restoration of thermal equilibrium.

The approximate equivalence of temperatures from logging and from fluid inclusion and oxygen isotope geothermometry and the absence of retrograde mineral assemblages indicate that the sediments penetrated are now at the highest temperature they have yet experienced. By fitting these maximum temperatures and the vitrinite reflectance data into a time-temperature-rank model, the duration of heating in the Cerro Prieto system can be estimated. The duration, from several available models, is 10^6 yr or more—greater than that from other information by one or two orders of magnitude. This suggests that (1) maturation of the vitrinite proceeds faster in this system than in normal sedimentary basins, (2) the time-temperature-rank models should be changed for short durations (of great importance in prediction of petroleum occurrence in young offshore basins), or (3) temperatures in the Cerro Prieto geothermal system were formerly higher than at present.

REGIONAL GEOLOGIC INVESTIGATIONS

NEW ENGLAND

IGNEOUS ROCKS AND GEOCHEMISTRY

"Monson Gneiss," eastern Connecticut

R. P. Wintsch (Indiana University) and N. K. Grant (Miami University, Ohio) sampled and analyzed plagioclase gneisses from portions of the Killingworth dome, Monson anticline, and the upper and lower limbs of the Seldon Neck dome to test their correlation as a single stratigraphic unit. Major-element and rare-earth analyses show sufficiently significant variations to separate the Killingworth dome from the Monson anticline and from the Seldon Neck dome. Strontium-isotopic analyses show (with two sigma errors):

	Apparent age (million years)	$^{87}Sr^{86}$ initial date
Monson anticline	236±86	0.708718±0.001698
Killingworth dome	338±30	0.706792±0.000678
Upper limb of Seldon Neck dome	394±56	0.705752±0.000602
Lower limb of Seldon Neck dome	595±226	0.704092±0.001906

The authors believe that the apparent age of the Killingworth dome could reflect the crystallization age of undeformed tonalite but that the other apparent ages have been variably reset by intense ductile deformation culminating in the late Paleozoic.

Multiple intrusion of the Norridgewock pluton, Maine

The Norridgewock pluton of central Maine has been shown by P. H. Osberg to consist of three different intrusive bodies. The easternmost and largest body consists of light-gray coarse-grained inequigranular-seriate biotite granite. This body has an elliptical map pattern with its long axis parallel to the general trend of the regional foliation. The westernmost pluton has an oval map pattern and consists of light-gray coarse-grained inequigranular-hiatal muscovite-bearing granite. The muscovite forms large diamond-shaped books. A screen of country rocks separates the biotite granite and the muscovite-bearing granite. The third pluton is a small oval-shaped body that intrudes the south margin of the muscovite-bearing pluton and consists of light-gray medium-grained binary granite containing numerous garnets. A well-developed contact aureole at the northern margin of the plutonic complex at Norridgewock merges to the south with the regional metamorphism.

TECTONICS AND STRATIGRAPHY

Basement-cover rock relations, southeastern Connecticut

Upper Proterozoic basement in southeastern Connecticut has been remobilized and deformed along with its lower to middle Paleozoic cover rocks during Taconic to Alleghanian orogenies, according to Richard Goldsmith. Isoclinal recumbent folding, the formation of axial-plane foliation in both basement and cover rocks, and the intrusion of granite in the cover rocks were followed by pervasive southward- to eastward-verging folding and local formation of new foliation in the basement rocks. Forelimbs of folds are highly attenuated or sheared off. In the basement, antiforms are mostly granite-cored and tend to be broad and doubly plunging; synforms tend to be narrow and to lack obvious hinge lines. In places, lineations and axial planes of earlier formed folds are rotated into zones of shear or flow. Vertical adjustments have produced a complex interference pattern of domes and basins. In the cover rocks, the style of folding has been partly obscured by later deformation. Deformation during the preceding stages took place at a maximum sillimanite to sillimanite-orthoclase grade of metamorphism in the basement and staurolite to sillimanite-orthoclase grade in the cover rocks. Ages of intrusive rocks into the cover sequence indicate that the latest and most pervasive regional metamorphism and the thermal peak were Acadian but that some plutonism and probably some metamorphism were Taconic. Pervasive ductile deformation in the basement ceased before emplacement of Permian granite. After the thermal maximum, strain was concentrated in a ductile fault system along the basement-cover interface, and the cover rocks were deformed largely independently of the already deformed basement. Ductile deformation along the major basement detachment zone ceased prior to tensional faulting of Triassic and Jurassic age and was probably Alleghanian.

Correlation of Oakdale and Paxton Formations of east-central Massachusetts with stratigraphy in eastern Connecticut

The Oakdale and Paxton Formations of the Worcester area, Massachusetts, have been traced into Connecticut and correlated by M. H. Pease, Jr., with the Scotland Schist and Hebron and Southbridge Formations. The Oakdale Formation is a metasiltstone on strike with and lithologically similar to the eastern part of the Hebron Formation, as originally mapped east of the Willimantic dome and south to the Honey Hill fault. Much of the strata formerly mapped as Scotland Schist, and considered younger than the Hebron in the axis of a recumbent fold, is now included within the Oakdale. The Scotland Schist is retained only for the conspicuous belt of highly micaceous schist extending from the Fitchville quadrangle north to the southeast corner of the Hampton quadrangle in east-central Connecticut, where it is reduced in rank to Scotland Member and assigned to the Oakdale.

The Paxton Formation, which apparently conformably overlies the Oakdale in Massachusetts, is on strike with and stratigraphically equivalent to the Hebron and Southbridge Formations, as mapped in the Eastford quadrangle, Connecticut, and extends into the Webster area, Massachusetts. The Southbridge appears to stratigraphically overlie the Hebron, though the two formations are separated by a fault in Connecticut.

Fault-basin origin of Boston Basin, Massachusetts

The Boston Basin, studied by C. A. Kaye, appears to have originated as a fault-block basin in Proterozoic Z time and to have persisted into at least Late Cambrian time. Deposits filling the basin are terrigenous sediments and volcanic and pyroclastic rocks. The distribution of basin fill was controlled largely by fault-block movement, with coarse sediment-forming fans around the upthrown blocks and the finer sedimentbeing deposited in the deeper parts of the downfaulted areas. Volcanic centers appear to have been localized along the active faults. Among the depositional facies in the basins are true red beds, hypersaline beds, ash, lime zones (including pure algal limestone), turbidites and rhythmites, subaqueous slide deposits, spilitic pillow lavas, and various other types of volcanic rocks. Orogenic deformation consists of a broad general arching with some localized compressional folds that are generally overturned to the south.

Physical characteristics of faults, northeastern Massachusetts

A. F. Shride reports that fault zones of northeastern Massachusetts vary greatly in their characteristics. Some of the principal faults (that is, strike-slip faults of regional extent with displacements measurable in kilometers to tens of kilometers) are marked by zones that are narrow along lengths of many kilometers and are composed of cohesive mylonitic materials; these faults give way abruptly to bordering rocks that exhibit little cataclasis. Other regional faults are characterized by central zones whose widths are variable but approach 1 km, bordered by zones of pervasively shattered rock measuring hundreds of meters wide. Some central zones are dominantly mylonite or ultramylonite, whereas, in others, breccias make up considerable parts. Some of the weak and, therefore, rarely exposed fault zones are made up of thinly sheeted highly friable rock parted along innumerable slickensided shear surfaces; incoherent gouge, apparently, is a rare constituent. The cataclastic zones of secondary faults, those with displacements of no more than 1 to 2 km, are mostly only a few meters wide and sharply defined; a few exceptional zones are more than 250 m in width. Breccias seemingly are more characteristic of secondary faults than of faults of regional extent.

Stratigraphic modifications, eastern New Hampshire

An area of about 1,000 km^2 of metasedimentary gneisses and schists in eastern New Hampshire northeast from Crawford Notch to the Maine State line has previously been mapped as the Lower Devonian Littleton Formation (Billings, 1956). Preliminary interpretation of 1979 mapping in the Presidential Range in the western part of this area by N. L. Hatch, Jr., indicates that, although the gneiss unit may prove impossible to subdivide, Billings' schist unit can be subdivided into at least two stratigraphic units. The uppermost schist unit is lithically identical to and apparently correlative with the Lower Devonian Seboomook Formation to the northeast in Maine; the Seboomook is probably correlative with the type Littleton in New Hampshire. The lower schist unit, however, differs from typical Seboomook-Littleton schists in that it contains no carbonaceous material and has abundant lenses of coticule. A correlation with one of the Silurian units, such as the Perry Mountain Formation to the northeast, is suggested. The gneiss unit of Billings appears to underlie stratigraphically all of the schist units, but, because of the correlation of the lower schist unit, the gneiss is probably pre-Early Devonian in age, also. Finally, calc-silicate rocks mapped by Billings as "Boott Member of the Littleton Formation" appear to occupy more than one stratigraphic position, each of which is believed to be stratigraphically well below the Seboomook–Littleton-like rocks and, thus, is also probably pre-Early Devonian in age. Additional mapping in the area may

further clarify some of these preliminary stratigraphic revisions.

GLACIAL GEOLOGY

Deglaciation, eastern Connecticut

Recessional moraines representing stillstands and possibly slight readvances of active ice, according to Richard Goldsmith and J. P. Schafer, record the early stages of ice retreat on the gently seaward-sloping surface of southeastern Connecticut, north of and parallel to the terminal moraines of Long Island. In the larger valleys, the moraines are somewhat lobate. Spacing of the recessional moraines at 4- to 6-km intervals over a belt at least 20 km wide may indicate periodicity of the ice regimen. These moraines are alined discontinuous deposits of ablation till and some water-laid material, generally about 100 m wide and 3 to 6 m high. Their surfaces may be smooth without boulders, hummocky with many boulders, or irregular with accumulations of boulders lacking interstitial material. Heading at, or near, the moraines are ice-contact deposits laid down by streams draining the zone of stagnant ice that remained after the active ice front had retreated to a new position.

Deglaciation of central Connecticut and the "Middletown readvance"

The late Wisconsinan depositional chronology of glaciolacustrine deltas and lake bottom sediments in the northern part of the Middletown quadrangle, central Connecticut, is complicated by scattered evidence of a local glacial readvance, the so-called "Middletown readvance." Detailed surficial mapping by E. B. H. London has revealed several exposures of basal till overlying lake clays in the Mattabesset River valley. Younger glacial deltas, graded to the same ice-marginal lake in which the clays were deposited, show no evidence of glacial overriding. Traditionally, all lake-bottom sediments have been included in one unit, the "Berlin clay." The detailed mapping shows that the lake-bottom sediments are physically discontinuous and vary in composition. Differentiation of the "Berlin clay" with regard to depositional environment and age will help to delineate the extent of the readvance and its chronologic relation to the damming of glacial Lake Hitchcock in the Connecticut River valley to the north.

Saprolitic clay preserved in limestone solution depressions near East Canaan, Connecticut

Saprolitic clay is exposed in a marble quarry near East Canaan, Conn. The red to variegated clay, according to W. B. Thompson, is believed to be a pre-Quaternary deposit. It escaped total removal by glacial erosion because of its presence in solution depressions on the surface of the marble. One pocket of clay is approximately 15 m thick. The marble itself has been disintegrated partly by weathering and is penetrated by clastic dikes derived from the overlying till. Pieces of the saprolite have been incorporated into the till and smeared out, giving the till matrix a mottled red color.

Ice-shove structures in end moraines, northwest Connecticut

A group of end moraines (a rare type of glacial deposit in Connecticut) has been mapped by W. B. Thompson in the valleys of the Hollenbeck River and Wangum Lake Brook, north-flowing tributaries of the Housatonic River. The end moraines were deposited in glacial Lake Hollenbeck. They are stratified, and at least two of them are partly deltaic (and were mapped as deltas by previous investigators). Recent excavation in one of the moraines revealed spectacular ice-shove structures that were formed by active ice on the proximal side of the moraine ridge. The height of the moraines locally exceeds 30 m. They are oriented transversely with respect to the narrow valleys and terminate against the valley walls.

Small glacial lakes in the Housatonic River valley

A continuous succession of water-laid deposits occurs within the narrow Housatonic River valley, according to W. B. Thompson. Regional compilation of the surficial geology of this valley reveals that a series of small glacial lakes developed as the ice withdrew. The outlines of some of the lakes are not apparent because they were obliterated by prograding outwash deposits. The lake levels were controlled in some cases by spillways on bedrock and in others by drift dams composed of glacial sediments and (or) stagnant ice that temporarily obstructed the Housatonic River valley. Ice-contact deposits (especially kame terraces) are very common in the valley and occur as sequences that were graded to lake levels or outwash deposits to the south.

Deglaciation, ice lobation, and marine incursion, eastern Massachusetts

B. D. Stone and J. D. Peper, compiling the surficial geology of the northeastern and southeastern parts of Massachusetts, respectively, report that a broad lobe of the late Wisconsinan Laurentide ice sheet was confined by uplands to the west as its margin retreated across eastern Massachusetts. Alined heads of outwash deposits, local dispersal patterns of erratics, and drumlin orientations attest to a former northwest trend for the lobe margin along the edge of the upland near Uxbridge, Holden, Fitchburg, and Leominster. During the early phases of ice retreat, the lobe margin abutted against a more vigorous Cape Cod Bay lobe to the east,

and the resulting interlobate area retreated gradually in a north-northwest-trending belt from Sagamore to Kingston. The lobe of the southeast coastal zone is known as the Buzzards Bay–Narragansett Bay lobe. Heads of outwash deposits, moraine segments, and high-level kames marking successive positions of the edge of the lobe are alined east-northeast and are spaced at 5- to 10-km intervals from Buzzards Bay northward to the middle of the Taunton Basin. Spacing of retreat positions increases westward from the interlobate area and indicates more rapid retreat of the western part of the lobe.

As deglaciation continued, ice in the northeastern Massachusetts coastal area streamed vigorously east to east-southeast following calving and rapid erosion of ice that fronted against deep marine waters in the Gulf of Maine to the east. Because of this rapid wastage of ice, marine waters flooded the isostatically depressed crust north of the Boston area. Glaciomarine deltas with topset-foreset contacts at elevations of 16.5 m in Ipswich, 28.3 m in Newburyport, and 31.4 m at the New Hampshire State line define the maximum glaciomarine water plane in the northeast coastal zone. Postglacial crustal rebound tilted the glaciomarine water plane 0.65 m/km upward to the north.

Deglaciation of the Connecticut Valley, Massachusetts

F. D. Larsen, mapping and compiling the surficial geology of the Connecticut Valley area of Massachusetts, reports that during deglaciation in the Woodfordian Substage of the Wisconsinan Stage an ice lobe filled the valley. The form of the lobe is shown by a radial pattern of striations, defining a vector of due west on the west side of the valley to S. 73°E. on the east side. From Greenfield to Longmeadow, a north-south distance of 62 km, erratics of Triassic and Jurassic arkosic rocks have been carried both southeast and southwest onto the higher crystalline uplands. Erratics transported to the southeast could have been transported during the main advance of the ice sheet, which moved S. 10° E. across the valley; those transported southwest must have been carried by ice in the lobe. In addition, kames, kame terraces, kame deltas, and till ridges define arcuate ice margins that can be extrapolated across the valley. Deposits of stratified drift with north-south-trending ice-contact slopes indicate that tributary valleys were clear of ice while the main valley was filled with ice. Successively lower morphosequences formed in the side valleys as the lobe melted away from the valley wall. At Chicopee, the ice margin oscillated, producing at least two readvance tills. Evidence for the "Chicopee readvance" is found at nine localities within an area of approximately 80 km. Readvance localities also are found in the vicinity of Easthampton and Northampton.

The activity of ice during deglaciation in the Connecticut Valley is in marked contrast to the glacial history of the nearby Swift River–Quabbin Reservoir valley, the next major south-trending valley east of the Connecticut Valley. There, mapped striations lie in the sector S. 10° E. to S. 10° W. where no evidence of readvance has yet been found.

Deglaciation of the Westfield and Connecticut Valleys, Massachusetts

At one time during the last deglaciation of Massachusetts, tongues of glacier ice occupied the Westfield and Connecticut Valleys. C. R. Warren reports evidence at four places that records the relative levels of the ice in these tongues.

The structures, textures, and field relations of a deposit about 1 km south of the site of the Knightville flood-control dam on the Westfield River show that it is a kame delta, deposited at the front of ice that stood against a lake. The lake was dammed by ice at the site of Woronoco, some 13 km to the south; the Woronoco ice must have stood at about the same level as the ice at the Knightville delta. The ice at Woronoco was the terminus of a sublobe that came up the Westfield Valley, sloping northwest from the main ice tongue in the Connecticut Valley, and the ice in the Connecticut Valley east of Woronoco must have stood considerably higher than the termini at Woronoco and Knightville. At the latitude of Knightville, farther north, the Connecticut Valley ice must have been higher still.

Farther up the Westfield Valley, however, the ice of the Westfield ice tongue stood higher than that in the Connecticut Valley east of it. Approximately 6 km up the valley from the Knightville delta and about 240 m above it, a gravel ridge leads east to a saddle in the ridge that forms the divide between the Westfield and Connecticut Rivers. The gravel is an ice-channel deposit, laid down by a stream that may have been in a crevasse that was open to the sky but more probably was flowing in a tunnel under the ice. The position of this gravel ridge, leading east to the saddle, shows that the meltwater stream that deposited it was flowing east across the divide. The ice east of the divide must have been lower than that on the west to provide an outfall for the stream.

In the Goshen quadrangle, at two locations farther north, eskers lead up to saddles in the divide between the Westfield and Connecticut Rivers. At both places, the ice of the Westfield Valley ice tongue must have stood higher than that in the Connecticut Valley to the east.

Thus, at points 6 km and more north of the latitude of

the Knightville kame delta terminus, the Westfield Valley ice stood higher than that in the Connecticut Valley to the east. Yet the Connecticut Valley ice at that time must have extended tens of kilometers farther south, well below the latitude of Woronoco. Thus, the surface slope of the Westfield Valley ice tongue was much steeper than that of the Connecticut Valley ice. This steeper slope is to be expected because the Westfield Valley is narrower than the Connecticut Valley (5 km wide, instead of more than 30 km) and because the ice in it was thinner (the floor of Westfield Valley stands 100–300 m higher than that of the Connecticut Valley).

The regional relations indicate that the ice of the Westfield Valley ice tongue came from the Champlain-Hudson lowland to the west. This evidence, therefore, provides a valuable correlation between the deglaciation chronology in the Hudson Valley and that in the Connecticut Valley.

First bare ground in western Massachusetts

At one time during the last deglaciation of western Massachusetts, near the end of the Woodfordian Substage of the Wisconsinan Stage, melt water poured down Sandy Brook from ice that covered the site of South Sandisfield. The ice at South Sandisfield came from the northwest from the Champlain-Hudson lowland, and the direction of movement of the ice shows that it must have covered all of Massachusetts west of South Sandisfield at the time. The stream in Sandy Brook carried debris southeast into a lake at North Colebrook, Conn., that was dammed by ice that came south-southwest from the Connecticut Valley. To be able to reach the dam site, the Connecticut Valley ice must have covered the area of Massachusetts east of New Boston. The two ice sheets must have met at or near New Boston, and the only ice-free area of Massachusetts at that time was southwest of New Boston, in the town of Sandisfield near the Connecticut border. These relations, noted by C. R. Warren in mapping the surficial geology of western Massachusetts, establish a date correlation between the deglaciation chronologies of the ice tongues in the Connecticut and Hudson Valleys. No comparable correlation between the two chronologies has been known previously.

Stratigraphy and structure of the Sankaty Head Cliffs, Nantucket Island

R. N. Oldale reports that the Sankaty Head Cliffs along the southeastern shore of Nantucket Island, Mass., contain an exposed section of pre-Sangamonian drift, marine beds of Sangamonian Age and, possibly, of early Wisconsinan Age, drift of possible early Wisconsinan Age, and drift of late Wisconsinan Age. The oldest drift is composed of basal till, flow till, and glaciofluvial and glaciolacustrine deposits. In general, the strata dip gently southward. This drift is unconformably overlain by a continuous sequence of marine deposits that includes a basal conglomerate, current-bedded sand, a bioturbated silty sand that is represented by a red clay facies and a delta sand facies to the north, a bed composed mostly of worm tubes, and the "lower Sankaty beds," composed mostly of clam and oyster shells in place.

The ostracode assemblage of the "lower Sankaty beds" indicates a climate as warm as or warmer than that of today and a probable Sangamonian Age (T. M. Cronin, written commun., 1979). The "lower Sankaty" marine sequence appears to indicate a progressive submergence of the Continental Shelf. The "lower Sankaty beds" are unconformably overlain by the "upper Sankaty beds," a shelly marine gravel. The "upper Sankaty" ostracode assemblage suggests a climate significantly colder than that of today and a late Sangamonian or middle Wisconsinan Age (T. M. Cronin, written commun., 1979). Convolution of the "upper Sankaty beds" and the upper part of the "lower Sankaty" sequence indicates very cold subaerial conditions and emergence of the shelf. A ventifact horizon caps the "upper Sankaty beds."

The Wisconsinan section unconformably overlies the "upper Sankaty beds" and is dominated by a thick unit (12–15 m) composed mostly of current-bedded medium to fine sand. The age of this unit is not known and may be early or late Wisconsinan. The medium to fine sand is unconformably overlain by fluvially bedded medium to very coarse sand and gravel thought to be of late Wisconsinan Age. These glaciofluvial deposits are overlain by a discontinuous till layer. The sand, gravel, and capping till make up the surficial drift on Nantucket. The degree of erosion and weathering of these deposits is similar to that of the upper Wisconsinan drift on Martha's Vineyard and Cape Cod and suggests a similar age.

Glacial stratigraphy of Cape Cod, Nantucket, and Martha's Vineyard, Massachusetts

Studies by R. N. Oldale along the eastern shore of Nantucket show that glacial drift of pre-Wisconsinan Age crops out at the base of the Sankaty Head Cliffs. It occurs below shell beds of Sangamonian Age and, possibly, of early Wisconsinan Age. On Martha's Vineyard, a number of glacial and interglacial deposits of possible pre-Wisconsinan Age have been identified, but this stratigraphy remains to be proved. A till, deformed within the western Martha's Vineyard moraine and lithologically similar to the Montauk Till Member of the Manhasset Formation of Block Island, R.I., and Long Island, N.Y., has been considered to be of

Illinoian Age (Kay, 1964) but is more likely to be of early Wisconsinan Age, the age assigned to the Montauk by most recent investigators. The rest of the drift on the islands and on Cape Cod makes up the broad outwash plains and moraines and is most likely late Wisconsinan in age. A radiocarbon date indicated that this drift on Cape Cod is no older than about 26,000 yr. On Martha's Vineyard, a date of about 15,000 yr on tundra leaves overlain by till and outwash shows that the youngest drift is late Wisconsinan in age. There are no useful radiocarbon dates from Nantucket; however, the amount of erosion of the drift and the depth of weathering are similar to the upper Wisconsinan drift on Cape Cod and Martha's Vineyard and suggest a similar age. The end moraines and ice-contact heads of outwash mark positions of the late Wisconsinan ice front during its retreat from southeasternmost Massachusetts.

Discovery of upper Wisconsinan glacial till on the Continental Shelf off southeastern New England

M. H. Bothner reports that glacial till was identified in a sediment core 6 m long collected 69 km southeast of Nantucket Island at a water depth of 49 m. This is the first sample of till collected on the Outer Continental Shelf off the northeastern United States. The carbon-14 age of the total organic carbon in these sediments ranges between $19,500 \pm 450$ and $34,500 \pm 1,100$ yr. Because dates obtained for total organic carbon could be older than those for the sediments they are found in, it is possible that the till was deposited during the late Wisconsin Glaciation. This supports the heavily debated hypothesis that an extensive Laurentide ice sheet extended to the northern side of Georges Bank.

APPALACHIAN HIGHLANDS AND THE COASTAL PLAINS

CAROLINAS, TENNESSEE

Turbidite beds in the Albemarle Group, Carolina slate belt

Primary sedimentary features are well preserved in the only slightly metamorphosed Albemarle Group near the type locality in North Carolina, according to D. J. Milton and Juergen Reinhardt. Its Tillery Formation, the basal unit, is composed of laminated siltstone and mudstone. These may be pelagic sediments but more likely were deposited from low-density low-velocity turbidity currents (Bouma D or E divisions). Its overlying Cid Formation is characterized by 10- to 40-cm-thick beds, each composed of a lower part that consists of ripple-cross-stratified siltstone and of an upper laminated part in which the stratification is similar to the Tillery; these are interpreted, respectively, as Bouma C and D divisions, deposited from distal turbidity currents. Beds in the overlying siltstone of the Floyd Church Member of its Millingport Formation are typically 20 to 50 cm thick. Each has a basal unit that has planar bedding and commonly minor (<1 cm relief) channeling at the base (Bouma B division), has an overlying cross-stratified unit (C division), and may or may not have a thin poorly laminated upper unit (D division). The upward increase in energy of the depositional processes apparently continues into its highest unit, the graywacke of the Yadkin Member of its Millingport Formation as suggested by the coarser grain size, although its sedimentary features have not been examined yet.

A detrital heavy-mineral assemblage of zircon, tourmaline, kyanite, and rutile in the Floyd Church siltstone indicates a continental source. Orientation of crossbedding suggests transport from the west, although only a few observations have been made. Tuff beds are found throughout the section where debris from volcanic centers locally and briefly flooded the basin, but the volcanic component within the Albemarle Group may be less dominant than has been stated.

Shear zones associated with the Kings Mountain belt in the Piedmont of the Carolinas

Three major northeast-trending shear zones in and flanking the Kings Mountain belt were identified by J. W. Horton, Jr., near the North Carolina–South Carolina State line. From west to east, they are informally named the Kings Mountain, Kings Creek, and Boogertown shear zones. The Kings Mountain shear zone marks the boundary between the Inner Piedmont and Kings Mountain belts and truncates well-defined rock units of both belts. Relation of deformation to dated pegmatites suggests that the major mylonitic deformation was Late Devonian in age. The Boogertown shear zone marks the boundary between the Kings Mountain and Charlotte belts. The Kings Creek shear zone lies within the Kings Mountain belt. In addition to their regional tectonic significance, these shear zones have important implications for locating and understanding certain mineral deposits. Stresses associated with the Kings Mountain shear zone influenced the location of a belt of lithium-bearing pegmatites that has been called the most important source of lithium in the world (Kunosz, 1976). Metallic sulfide deposits are concentrated along both the Boogertown and Kings Creek zones.

Diverse types of garnets in metasedimentary rocks of the Great Smoky Group, North Carolina and Tennessee

Garnets are common accessory minerals of metasedimentary rocks of the Proterozoic Z Great Smoky Group (Ocoee Supergroup) of eastern Tennessee and western North Carolina. Mineral-resource investigations of the Citico Creek Wilderness Study Area (Slack and others, 1979) and the Joyce Kilmer–Slickrock

Wilderness (Lesure and others, 1977) identified garnets in both stream sediment concentrates (as detrital grains) and pelitic metasedimentary rocks. Mineralogical studies by J. F. Slack, L. B. Wiggins, and Andrew Grosz have documented two types of detrital garnets, euhedral cinnamon-brown zoned spessartine ($Py_{1-4}Al_{18-41}Sp_{34-55}Gr_{19-32}$) and anhedral pink magnesium-rich ($Py_{10-32}Al_{60-79}Sp_{2-7}Gr_{3-9}$) almandine. Both detrital garnets occur in streams draining only chlorite- or biotite-grade rocks. In contrast, in situ rock garnets are well-zoned magnesium-poor almandine ($Py_{4-7}Al_{43-71}Sp_{9-37}Gr_{8-23}$). The pyrope-rich detrital almandines are incompatible with the low metamorphic grade of the local area and are interpreted to be second-cycle garnets inherited from higher-grade Proterozoic source rocks of the Ocoee Supergroup.

DELMARVA PENINSULA

Paleomagnetic investigation of Pleistocene sediments of the Delmarva Peninsula, central Atlantic Coastal Plain

R. B. Mixon (USGS) and J. C. Liddicoat (Lamont-Doherty Geological Observatory, Columbia University) reported the first attempts to use magnetostratigraphy in the Chesapeake Bay area. Unconsolidated sand, silt, and clay of marginal marine origin, herein called the "Accomack" deposits, record a major transgression of the sea in the southern Delmarva area in Pleistocene time. The paleomagnetic studies were initiated to help evaluate widely varying absolute ages obtained for the "Accomack" deposits by different laboratory dating techniques.

Outcrop samples and fully oriented brass-Shelby-tube cores (7-cm diameter) from several localities in the central upland west of Chincoteague, Va., have magnetization of normal paleomagnetic polarity. Two coring sites, Nash (T's) Corner and Mathews' Field, are of particular interest because the section includes shell beds studied by radiocarbon, uranium-series, and amino-acid-racemization dating methods. At the coring sites, samples of dark-gray clayey silt at depths of 7.75 m (Nash Corner) and 8.42 m (Mathews' Field) have nearly identical paleomagnetic directions following demagnetization in a 200-Oe-peak alternating field. The lithology, the virtual lack of change in paleomagnetic direction during demagnetization, and the demagnetization spectra (median destructive field is 150 Oe) show no evidence for a stable secondary magnetization. Samples from three nearby outcrops were demagnetized the same way and gave similar results. Therefore, on the basis of the paleomagnetic data and stratigraphic relations to adjacent rock units of late Pleistocene age, Mixon and Liddicoat consider the "Accomack" deposits to be of Brunhes age. These studies provide an independent test of other dating techniques now being evaluated.

NEW JERSEY

Tectonic shortening in late Alleghanian time

Detailed structural mapping in the Kittatinny Valley of New Jersey by P. T. Lyttle and A. A. Drake, Jr., supports the hypothesis that, during late Alleghanian time, a series of far-traveled thrust sheets formed a complex imbricate stack. Evidence for this consists of numerous repeated sections, windows through higher thrusts to the next one below, remnants (klippen) of eroded thrust sheets (mainly Allentown Dolomite of Cambrian and Ordovician age(?) sitting in cleavage troughs of the Ordovician Martinsburg Formation), zones of tectonic melange, and exposed fault planes. The importance of this late Alleghanian thrusting is becoming more apparent both here and in the Great Valley of Pennsylvania. It is very likely that moderately to steeply dipping thrusts there become more gently dipping at depth and join one or more major décollements that are recognized by recent seismic surveys. Late open mostly upright folds of large wavelength that trend roughly east-west may be the surface expression of these listric thrust faults. Therefore, in late Alleghanian time, a great deal of tectonic shortening was accomplished by large- and small-scale thrusting and folding. In predominantly carbonate terranes, most shortening is parallel to bedding with ramps cutting through bedding, whereas, in slate terranes, shearing is common along bedding, as well as along more than one cleavage.

PENNSYLVANIA

A plate tectonic model for the Hamburg klippe, eastern Pennsylvania

G. G. Lash reported that the eastern end of the Hamburg klippe in Pennsylvania consists of two distinct allochthonous slices emplaced by imbricate thrust faulting. The lower Greenwich slice contains a sequence of middle fan turbidite and grain flow deposits of Middle Ordovician (Llandeilian) age, as well as numerous lenticular erratic fragments of variegated shale, chert, and limestone of Early Ordovician (Arenigian) age. These rocks are pervasively deformed and fragmented but lack the penetrative slaty cleavage typical of the Jacksonburg Limestone and Martinsburg Formation of the parautochthonous Lehigh Valley sequence. The upper Richmond slice contains a telescoped sequence of slope and toe-of-slope carbonate rocks and mudstone of uncertain age that were deposited basinward of a northwest-facing bank.

The Hamburg klippe is thought to result from the aborted subduction of a continental margin in which the allochthons were emplaced as wedge-shaped slices onto the shelf. The proposed model involves (1) Proterozoic Z rifting of a microcontinent from the North American

craton, (2) subduction of the North American craton accompanied by late Whiterockian foundering of the shelf, (3) Chazyan to early Blackriveran trench sedimentation and deformation evidenced by the Greenwich slice, (4) emplacement of allochthons onto the shelf accompanied by late Blackriveran to early Rocklandian isostatic uplift of the orogenic zone (Black River hiatus) and development of an exogeosyncline to the northwest, and (5) late Middle Ordovician foreland-directed subaqueous gravity sliding of the allochthons from the orogenic welt into the deepest part of the exogeosyncline.

SOUTH CAROLINA, GEORGIA, AND ALABAMA

Thrust plates in the Blue Ridge

Geologic mapping by A. E. Nelson indicates the Hayesville-Fries fault (Rankin, 1975; Hatcher, 1978), a premetamorphic folded thrust fault, separates two crystalline thrust plates; the Great Smoky plate to the northwest was overthrust by the Hayesville plate from the southeast. From the Hayesville-Fries thrust, the Hayesville plate extends for about 30 km southeast where it is juxtaposed to a distinctly different rock assemblage, here informally called the "Helen" sequence, along a northeast-trending fault near Lake Burton. Some "Helen" rocks resemble Ocoee Supergroup rock types, and the "Helen" sequence is tentatively assigned to the Ocoee. If this correlation is correct, then the east-bordering fault of the Hayesville plate probably represents the Hayesville-Fries fault as it emerges from under the Hayesville plate to expose a window or half window of Ocoee rocks.

The "Helen" sequence extends southwesterly from the Lake Burton area to just east of Dahlonega and beyond. It has a variable width and is exposed in a zone about 3 km wide lying between the Hayesville plate on the northwest and a broad terrane underlain by the Tallulah Falls Quartzite of Galpin (1915) on the southeast. The "Helen" sequence generally contains lower grade metamorphic rocks than those on either of its sides. Reconnaissance shows that, near Dahlonega, the "Helen" sequence underlies a series of prominent northeast-trending topographic lineaments and that locally cataclastic rocks are present. An aeromagnetic map of the same area also shows some magnetic lineaments, and cataclastic rocks suggest the "Helen" sequence may be in a large fault zone. This probable fault zone may be fairly extensive. It is on strike with several discontinuous faults and shear zones shown on the geologic map of Georgia (Pickering, 1976) between Dahlonega and the Allatona Reservoir area, approximately 80 km southwest.

Cenozoic tectonics and regional stratigraphy, Georgia

An isolated pod of Cenozoic sediment, immediately north of Pine Mountain and west of Warm Springs, Ga., has been extensively augered and trenched in a study conducted by D. C. Prowell, Juergen Reinhardt, H. W. Markewich, and R. A. Christopher to gain an understanding of how these sediments relate to the continuous wedge of coastal plain sediment more than 75 km to the south and to evaluate faulting in these sediments with respect to closely associated Piedmont structures and to Cenozoic regional tectonics.

The basal sedimentary sequence (locally as much as 60 m thick) is composed of well-sorted quartz sand and bauxitic kaolin, deposited in a throughgoing meandering stream flood plain complex. Well-preserved pollen assemblages indicate a Paleocene (early Wilcoxian) age for this part of the section.

The post-Paleocene sedimentary record north of Pine Mountain is very incomplete. Overlying the Paleocene fluvial sediments are locally derived alluvium and colluvium composed of poorly sorted gravelly sand that probably ranges in age from late Miocene to late Pliocene. The oldest sediments in the post-Paleocene sequence are typically the most angular and are the most extensive areally. These sediments and the underlying Paleocene sand and bauxitic clay have been offset 3 to 10 m along several high-angle reverse faults that trend N. 25–45° E. and N. 10° W.

The faulted section is overlain by as much as 5 m of colluvium and alluvium derived from the north slope of Pine Mountain. The youngest surficial deposits are unaffected by any of the faults mapped to date. Hence, the latest fault movement is clearly pre-Pleistocene and may be pre-Pliocene.

Tertiary stratigraphy, eastern Alabama and western Georgia

Stratigraphic studies by T. G. Gibson show the presence of five Paleocene to middle Eocene transgressive units in Tertiary deposits of eastern Alabama and western Georgia. The lithologies of these units vary from predominantly carbonate deposited during times of low clastic influx to predominantly carbonaceous clay, silt, and sand deposited during times of higher clastic supply. As much as 152 m of topographic relief in the Chattahoochee River drainage area provides an unusually long north-south sequence of exposures in an area in which the strata generally dip 10 to 15 m/km southward. Partly preserved sedimentary sequences indicate transition from nonmarine or marginal marine to marine strata. Fluvial and marginal marine deposits that consist of kaolinitic clay, crossbedded fine to medium sand, and poorly sorted coarse clastic material grade downdip into calcareous and glauconitic sand, silt,

and silty clay containing abundant invertebrate macrofossils. The lower marginal marine to marine parts of the transgressive sequences consist of fine to coarse sand and generally are preserved; the upper regressive phases commonly are not.

Greatest northward Cenozoic marine transgression in this area is exhibited by the Clayton Formation of early Paleocene (Danian) age. During the Clayton encroachment, Cretaceous sand was reworked into the basal part of the formation; this was followed by carbonate deposits and calcareous sand deposits, marking a period of low clastic influx into the basin. These limestone units thicken rapidly downdip. Marginal marine deposits are limited to thin clay beds in the northernmost part of the outcrop belt.

Two transgressive sequences are found in the upper Paleocene deposits. The basal part of the Nanafalia Formation consists of crossbedded medium to coarse clastic deposits that are present in channels containing abundant carbonaceous debris; overlying are glauconitic shelly sands. The Nanafalia grades downdip through largely kaolinitic clays, locally bauxitic, of fluvial to marginal marine origin into abundantly fossiliferous glauconitic and marine sand and clay beds.

The overlying Tuscahoma Formation rapidly thickens downdip. The basal transgressive glauconitic coarse sand of the Tuscahoma is overlain by a thick sequence of laminated silt and carbonaceous clay. These sediments were deposited in restricted marine to shallow marine environments.

The glauconitic sand and clay beds of the Bashi Marl Member of the Hatchitigbee Formation represent an extensive transgression during the earliest Eocene. In contrast to the other units, the Bashi thins downdip, suggesting a restricted sediment supply. The upper part of the Hatchitigbee Formation is not present in this area.

The Tallahatta Formation of early middle Eocene age unconformably overlies the Bashi. At its base, coarse sand and gravel deposits are found in channels incised into the Bashi. Downdip, most of the lower part of the Tallahatta is composed of calcareous sand and limestone.

Stratigraphy of the Atlanta area, Georgia

Geologic mapping by M. W. Higgins has defined the presence of 12 newly recognized formations in the Atlanta area southeast of the Brevard Zone. These rocks define a large, doubly plunging synform, here called the Newnan-Tucker synform. From closure to closure, the synform is more than 90 km long and is more than 40 km wide at its widest point. The synform is modified locally by several generations of later folding. Some of the stratigraphic units have been mapped for more than 200 km along strike around the synform. Another stratigraphic unit, the Lithonia Gneiss, is apparently in nappe or thrust contact with the units of the Newnan-Tucker synform east of Atlanta. Both the Lithonia Gneiss and some of the units in the Newnan-Tucker synform are overlain by a stratigraphic unit of amphibolite, schist, and quartzite that is underlain by either an unconformity or a thrust fault. The exact age of all of these rocks is unknown, but they are younger than 1,100-m.y.-old detrital zircons in a quartzite and older than 325-m.y.-old zircons in the granitic rocks that cut them.

Pleistocene and Holocene valley fill in coastal plain streams, eastern Alabama

Field mapping by H. W. Markewich of fluvial deposits along Uphapee Creek in eastern Alabama has delineated three distinct terraces of Pleistocene and Holocene age. The intermediate terrace is the most extensive and grades downstream to a broad terrace along the Tallapoosa River. Radiocarbon ages from wood contained in the alluvium underlying this terrace give Holocene ages that range from 5,400 to 7,500 yr B.P. Pollen from carbonaceous clay lenses that yielded the dated wood fragments suggests that deposition took place during warm-temperate climatic conditions. A carbon-14 age of 27,000 yr B.P. on wood fragments from a reworked pod of carbonaceous clay suggests a period of fluvial deposition during the middle Wisconsinan. The middle Holocene age and middle Wisconsinan Age are consistent with data on high stands of sea level and midcontinent soil formation. Weathering and pedogenic profiles developed in alluvium underlying the highest terrace, 20 m above creek level, suggest a Pleistocene age, not the expected Tertiary age. No evidence was found of Tertiary age fluvial deposits in the valley of Uphapee Creek; field investigations are still proceeding along the Tallapoosa River.

Geology of the Mississippian and Pennsylvanian of north-central Alabama

S. P. Schweinfurth reports that identification of fossils collected from the lower part of the Parkwood Formation in north-central Alabama (the Haleyville $1° \times ½°$ area) indicates that the formation in this area is somewhat younger than previously thought. Recent field work in the same area has shown that the Parkwood is much more extensive and that the area is far more complex, structurally, than had been reported previously.

Fossil plants, identified by W. H. Gillespie, and a species of goniatite, identified as *Bilinguites* n. sp. by Mackenzie Gordon, Jr., and T. W. Henry, indicate an age of late Early Pennsylvanian for the Parkwood

rather than an age of Mississippian and Pennsylvanian.

The Parkwood Formation rests on the Bangor Limestone, which has been reported to be of probable Late Mississippian (Chesterian) age, and was thought to be conformable with it. The new fossil evidence, however, indicates that a large hiatus separates the two formations, and evidence from fieldwork suggests that the relation is actually unconformable. In addition, it was found that the Parkwood overlies the Bangor throughout a belt of outcrops that extends from west to east across the entire Haleyville area. It had been reported previously that the Parkwood Formation was restricted to only the southwesternmost part of the area.

At least one anomalous structure has been found in the area during the course of recent fieldwork, and there are indications of others to the east and west of it. This structure, which is superimposed on a regional homocline dipping to the south-southwest at approximately 9m/km, has the shape of an anticlinal nose plunging to the south-southwest. The nose has a structural relief of approximately 30 m, based on elevations on the top of the Bangor Limestone, and is cut by at least one normal fault (other faults are suspected but have not yet been proven). The fault strikes approximately N. 60° W. and is downthrown approximately 30 m to the south-southwest. This structure seems to have been the product of several periods (perhaps as many as three) of recurrent vertical movement, which possibly began in the Late Mississippian or Early Pennsylvanian. This observation is based on evidence of differential erosion of the Parkwood Formation, and possibly also of the Bangor Limestone, and slight upwarping over the structure of the Boyles Sandstone Member, the basal unit of the Pottsville Formation. This structure overlies large positive gravity and magnetic anomalies, and, although there is no direct evidence of basement involvement in the structural deformation described above, the pattern of recurrent movement, the regional tilt to the south-southwest, and the normal faulting might signal some basement influence on the structural grain of the area. This possibility, as well as others, will be studied further.

SOUTHEAST COASTAL PLAIN

Application of radiometry to coastal plain formations

Comparative radiometric studies on a variety of calcareous materials were conducted in the Cape Fear area and Charleston, to the south, and in Delmarva, to the north. Basically, the study was designed to test the reliability of ages and reproducibility of these ages determined by the acid racemization technique within mapped units over a broad region.

Two laboratories (at the University of Delaware and the University of Texas) analyzed paired shells from several formations. The data obtained from both laboratories showed considerable scatter when compared to each other. J. P. Owens suggests that independent ages obtained from a few sample sites on corals using the uranium disequilibrium technique and faunas show the kinetic model used to obtain the amino-acid ages was probably incorrect.

Late Cenozoic marine deposition, Southeastern United States

B. W. Blackwelder reports that major hiatuses in upper Cenozoic marine deposits in the U.S. Atlantic Coastal Plain can be recognized on the basis of molluscan faunal changes at erosional unconformities. These hiatuses generally coincided with periods of global cooling and ice sheet formation. Major hiatuses are recognized within the early Miocene (23 m.y.–20 m.y. ago), at the end of the middle Miocene (11 m.y.–10 m.y. ago), at the end of the early Pliocene (4.0 m.y.–2.5 m.y. ago), at the end of the Pliocene (1.9 m.y.or 1.8 m.y. ago), within the Pleistocene (1.6 m.y.–0.5 m.y. ago), and several times within the last 0.4 m.y.

Marine deposition from the Miocene to the present in the Atlantic Coastal Plain took place during global warming or Northern Hemisphere warming. Initiation of Miocene deposition in the Salisbury embayment corresponds to a warming in Antarctica about 19 m.y. ago. Late Miocene marine deposition began during a warming in the Antarctic about 8 m.y. ago. Deposition of the Yorktown Formation, which is found as far inland as the Fall Line, took place during extreme warming in the Antarctic in the early Pliocene. Late Pliocene and early Pleistocene deposition took place during periods of global warming. Deposition of the Canepatch Formation in South Carolina and the Bermont Formation in Florida apparently took place during a warming trend in the Antarctic. Other upper Pleistocene deposits appear to correlate with warm Northern Hemisphere intervals. Elevations of past sea levels, based on published estimates of early Pliocene and Pleistocene ice volumes, correspond to shoreline elevations in the Atlantic Coastal Plain of Georgia. However, early Pliocene shorelines in the Cape Fear arch area have been uplifted about 57 m.

Aeromagnetic study of subsurface pre-Cretaceous rocks, Georgia and South Carolina coastal plains

Aeromagnetic studies by D. L. Daniels have delineated a subsurface basin of probable Triassic and Jurassic age centered on the town of Riddleville in eastern Georgia. This basin is on the northern edge of an inferred extensive series of interconnected Mesozoic rift basins that lie beneath the coastal plain of Alabama, northern Florida, Georgia, and South Carolina. The

basin at Riddleville, which was originally inferred from aeromagnetic maps and recently proven by drilling, is about 30 km wide and trends east-west. Measurements of the depth to magnetic sources have shown that the north edge of the basin is sharp and defined by an aeromagnetic lineament of 140 km length, while the south boundary appears less steep and rises up in a series of steps to a ridge interpreted as crystalline basement. The apparent minimum thickness of the basin near Riddleville is 1.7 km (beneath 0.4 km of coastal plain sediments), while south of the ridge, where the major rift basin lies, a thickness of at least 3.5 km is indicated. Magnetic depths indicate a similar structure for the subsurface Dunbarton basin in South Carolina.

VIRGINIA

Mineralogical, chemical, and physical properties of regolith over crystalline rocks, Fairfax County

Undisturbed cores of regolith extending from the surface to unweathered bedrock have been obtained using a combination of Shelby tubes, Denison sampler, and modified diamond core drilling. The regolith is subdivided into zones of weathered rock, saprolite, massive material, and soil. The principal purpose of the study by M. J. Pavich, G. W. Leo, and S. F. Obermeier is to attempt to correlate variations in chemistry, mineralogy, and texture with engineering properties throughout the weathering profile. Coring sites were chosen to obtain a maximum depth of weathering on diverse lithologies. Investigated rocks include schists, metagraywacke, granite, and diabase. Four to twelve samples were selected per core, depending on weathering profile zonation and thickness (from about 1 m in serpentinite to over 30 m in pelitic schist), for analysis of their petrology, texture, clay mineralogy, and major element chemistry. Shear strength and compressibility were determined on corresponding segments of core. Standard penetration tests were performed adjacent to coring sites to evaluate engineering properties in situ.

Geochemical changes of each rock type follow predictable trends from fresh rock to soil profile, with relative increases in Si, Ti, Al, Fe^{3+}, and H_2O; variable K; and relative loss of Fe^{2+}, Mg, Ca, and Na. Halloysite and kaolinite are the predominant clay minerals in saprolite developed on granite, schist, and metagraywacke. Soil clays include dioctahedral vermiculite and rare occurrences of gibbsite.

Standard penetration test data for the upper 7 m of saprolite over schist and metagraywacke show alternations between stronger and weaker horizons due to textural and mineralogical foliation of the parent rock. Penetration tests of granite saprolite indicate lower strength than in the metasediment regolith. Shear strength increases fairly regularly downward in the granite weathering profile. The engineering behavior of diabase regolith is controlled by a dense plastic near-surface clay layer (montmorillonite and koalinite) overlying gruslike weathered rock. Engineering properties of serpentinite regolith are highly variable due to a very thin weathering profile.

Paleozoic events in the Piedmont near Fredericksburg

Several suites of plutonic rocks have been recognized by geologic mapping by Louis Pavlides in the polydeformed and metamorphosed (amphibolite-grade) Piedmont near Fredericksburg, Va. Two of these suites were dated by uranium-lead (zircons) and rubidium-strontium (whole-rock) methods by T. W. Stern, J. G. Arth, K. G. Muth, and M. F. Newell.

The oldest suite is the Falls Run Granite Gneiss, a coarse-grained, strongly foliated, and highly metamorphosed rock that ranges in composition from adamellite to monzonite. The chief mass of Falls Run Granite Gneiss (formerly called the Berea pluton) is intrusive into the Holly Corner Gneiss of Cambrian(?) age. Both of these gneisses are allochthonous remnants of the inverted limb of a recumbent fold; subsequent deformation formed a type II interference fold. Uranium-lead and rubidium-strontium studies indicate that the Falls Run is 410 m.y. old and has an initial $^{87}Sr/^{86}Sr$ of 0.707.

Younger granitoid plutons, dikes, and sills are assigned to the Falmouth Intrusive Suite and are widespread in the area. These plutons are abundant in the eastern part of the area but are rare west of the Quantico Formation. Rocks of the Falmouth consist of strongly to weakly foliated (a) biotite adamellite and granodiorite having a rubidium-strontium ratio of less than 0.2 and (b) muscovite-biotite adamellite and granite having a rubidium-strontium ratio of greater than 0.4. Concordant zircon ages and two whole-rock isochrons indicate that both groups are 300 m.y. to 330 m.y. old.

The initial $^{87}Sr/^{86}Sr$ of group (a) is 0.704, which suggests a lower crust or mantle source, whereas that of group (b) is 0.709 and suggests crustal involvement in the magma generation. Recently reported ages from North and South Carolina are similar to those of the Falmouth. Thus, an extensive belt of 300-m.y.-old to 330-m.y.-old plutons is present in the eastern Piedmont.

Structural and stratigraphic relations, Chopawamsic Formation and subjacent rocks

A. R. Bobyarchick reports that in the Joplin quadrangle, Virginia, the contact between the Cambrian(?) Chopawamsic Formation and a massive body of diamictic conglomerate seems characterized by fine-grained layered mica schist and quartzose gneiss (quartzite?) that could be either an epiclastic facies of the

Chopawamsic or a nonconglomeratic facies of the diamictite. The type section of the Chopawamsic Formation along Chopawamsic Creek in the Joplin quadrangle contains minor epiclastic material. Most inclusions in the diamictite are vein quartz and biotite schist with minor amounts of biotite gneiss and granitic gneiss; few inclusions are similar to rock types in the Chopawamsic. A similar relation was recognized to the southeast by Louis Pavlides. The source for the diamictic conglomerate is presently uncertain.

Metamorphosed interlayered feldspathic graywacke and micaceous schist, locally containing small bodies of ultramafic/mafic igneous rocks, occur west of the diamictite in the Joplin and Independent Hill quadrangles. These rocks lie on strike with phyllite and mica schist of uncertain association to the southwest.

Metavolcanic rocks near the eastern border of the diamictite locally are folded intensely. The diamictite–quartzose gneiss–Chopawamsic contacts are regionally folded in the vicinity of the Breckenridge Reservoir on the U.S. Marine base. Within this structure, minor shear folds and kink bands indicate a dextral shear component, but it is unknown whether the small folds are contemporaneous with the larger structure.

Ordovician age of the Quantico Formation reaffirmed

The age of the Quantico Formation of the northern Virginia Piedmont, considered to be of Late Ordovician age on the basis of a fossil collection made by Watson and Powell (1911) and dated by R. S. Bassler, recently has been in dispute. The original fossil collection is lost, and the fossil locality along Powells Creek apparently is under road fill of Interstate 95. The Ordovician age of the Quantico was questioned when Seiders and others (1975) reported that fossil-like inorganic impressions were found in the Quantico 4.8 km north of Powells Creek. Because similar inorganic objects may have been incorrectly identified as fossils, they suggest that Bassler's determinations of the Quantico fossils may have been erroneous and should not be a "factor bearing on the age of the Quantico" (Seiders and others, 1975). Furthermore, the dioritic Dale City pluton in Dale City, Va., with a discordant zircon age of about 560 m.y., was reported to intrude the Quantico Formation (Seiders and others, 1975). Therefore, it was concluded that the Quantico predated the Dale City pluton and was no younger than Early Cambrian. Seiders and others (1975) also considered the Quantico to be in conformable and gradational contact with the underlying metavolcanic Chopawamsic Formation, also considered to be about 550 m.y. old on the basis of discordant zircon ages obtained from felsic metavolcanic rocks within it. However, the Chopawamsic-Quantico contact in the region to the south is an unconformity, with the Quantico containing a quartzitic zone at its base that is discontinuous but locally as much as 182 m thick (Pavlides, 1973, 1976).

The debate that followed concerning the age of the Quantico eventually focused on the reliability of zircon ages in dating the Dale City pluton and the adamellite (Higgins, 1976) in the nearby Occoquan Granite and (or) whether most zircon ages from the Piedmont were reliable for establishing ages of crystalline rocks (Higgins and others, 1977; Seiders, 1978; and Zartman, 1978).

Recently, Louis Pavlides reexamined the Dale City pluton and its contact with the Quantico Formation near the site of zircon sample 5 of Seiders and others (1975, fig. 1). The contact here is in saprolitized rock and was dug out and clearly exposed at several places along one large outcrop. Sandy, fine- to medium-grained saprolite (quartzite) about 2 m thick, which is the basal unit of the Quantico Formation, grades upward imperceptibly into slate typical of the Quantico. The quartzite (sandy saprolite) rests with sharp contact on saprolite of the plutonic rocks, which clearly lack any features that would suggest contact chilling. Also, contact metamorphic effects are absent in the overlying sand and slate saprolite. Joints within the plutonic rock terminate abruptly at the contact. A canvas peel coat across the contact, made by Juergen Reinhardt, clearly demonstrates the local channel-like character of the sand and, in places, its well-layered to crossbedded character, as well as the termination of a joint in the pluton at the contact. Clearly, this is an unconformity (nonconformity) and not an intrusive contact and is considered to be the same unconformity as that recognized by Pavlides in the Fredericksburg area.

During the initial search for and partial excavation of the contact, A. R. Bobyarchick discovered pelmatozoan fossils in slate exposures of the Quantico Formation about 50 m northeast of the Dale City Quartz Monzonite–Quantico contact. The initial collection was enlarged subsequently by Pavlides and a team of paleontologists from the National Museum. While splitting the slabs for study, John Pojeta, Jr., recognized a cephalopod in the collection, which Mackenzie Gordon, Jr., has identified as an actinoceroid probably of Ordovician to Silurian age. R. L. Parsley (Tulane University) has examined the pelmatozoa from this collection and concludes they are crinoids with star-shaped lumens, a morphological development recognized at present only in crinoids of Ordovician or younger age. The age of the fossil assemblage at Dale City, therefore, is Ordovician or younger. In addition, the lithologic and stratigraphic similarity of the Quantico Formation with the Arvonia Slate of Middle to Late Ordovician age in the central Virginia Piedmont (Pavlides, 1980) reaffirms the

original Ordovician age assigned to the Quantico. This confirms the authenticity of the original Powells Creek fossil collection made by Watson and Powell and the identification by Bassler of *Pterinea demissa* of Late Ordovician age from this collection.

Furthermore, because an unconformity separates the Quantico from the Dale City pluton, the approximately 560-m.y. zircon age for the Dale City pluton is no longer inconsistent with the geologic field relations. The Dale City pluton and its associated pre-Quantico rocks, therefore, are exposed within the strike belt of the Quantico Formation probably along a formerly unrecognized anticline.

Spotsylvania lineament

Reconnaissance and detailed mapping in Spotsylvania and Carolina Counties, Va., by Louis Pavlides, A. R. Bobyarchick, and K. E. Wier has concentrated on a controversial geophysical anomaly, the Spotsylvania lineament. Neuschel (1970) and Pavlides (1980) have discussed the contrasting aeromagnetic and aeroradiometric anomalies between amphibolitic rocks west of the lineament (Ta River Metamorphic Suite) and dominantly biotite gneiss east of the lineament (Po River Metamorphic Suite). Both terranes include abundant granitoid gneiss and granite of various ages and origins. Neuschel and Pavlides have suggested that the Spotsylvania lineament represents a fault or system of faults, to explain its remarkable regional linearity and the juxtaposition of contrasting lithologies on either side of it.

South of the James River, the western boundary fault of the Triassic and Jurassic(?) Farmville basin lies on strike with the Spotsylvania lineament. Bourland and Glover (1976) described late-metamorphic to postmetamorphic mylonites in the same area and also east of the Farmville basin. Cretaceous and Tertiary age faults in the coastal plain near Fredericksburg, Va., lie roughly along strike of the lineament (Mixon and Newell, 1977). Several silicified breccia zones occur just east of and parallel to the lineament in the Lake Anna East and Spotsylvania 7½-min quadrangles.

Detailed mapping and thin-section petrography along the northeastern segment of the Spotsylvania lineament have not revealed a pervasive nor extensive postmetamorphic mylonite zone near the lineament, nor has a zone of retrograde metamorphism, characteristic of such mylonites, been identified. Brittle faulting in this area does not appear to be of sufficient magnitude or extent to cause the lineament. One possible interpretation is that the lineament represents the trace of a fault that was initiated prior to regional prograde metamorphism. Regional relations suggest that early faulting could be at least as old as Cambrian(?) but not younger than the late Paleozoic regional metamorphism. Postmetamorphic ductile mylonitization and Mesozoic brittle faults were superimposed on the lineament south of the James River.

Although the Spotsylvania lineament is associated locally with Mesozoic and Cenozoic faults, its earlier history is obscure. It probably represents the trace of an old fault or possibly even an ancient crustal boundary along which later fault movement has occurred at different times and places.

Scarp degradation and morphological modification of fluvial terraces along the Rappahannock River

The morphology of fluvial terraces, mapped by W. L. Newell, along the Rappahannock River in Virginia was studied by S. M. Colman to determine rates of landform modification and scarp degradation. Such rates have important implications related to the degree of preservation of morphologic features, including possible fault scarps, and the ages of such features in the Eastern United States. The lowest terrace is thought to correlate with the high sea stand of the last interglaciation (Sangamonian), about 125,000 yr ago. Terrace surface measurements that yield the best relation to age are drainage density, density of first order streams, area to perimeter ratio (a measure of degree of dissection where, as dissection proceeds, terrace remnant perimeters become comparatively longer), and ratio of present area to reconstructed original area. Constructional morphology, such as meander scrolls and ridge-and-swale topography, is clearly recognizable on the Sangamonian terrace but not on older terraces. The degree of degradation of scarps between the terraces increases with age. Slope angles of the scarps depend to a considerable degree on scarp height and on position relative to former river meanders. In general, scarps ~5 m high, formed when the river occupied the Sangamonian terrace, have slopes of ~10 percent, and scarps more than 20 m high have slopes of as much as 38 percent. Scarps <5 m high related to the next older terrace have slopes of ~5 percent. Scarps related to the highest terrace are severely degraded but locally have slopes of as much as 7 percent. These data indicate that small-scale topographic features, including scarps <5 m high, are clearly preserved for more than 100,000 yr in a humid temperate climate.

Soil stratigraphy on fluvial terraces of the Potomac and Rappahannock Rivers

Cooperative investigations by the USGS and the Soil Conservation Service (USDA) have been made on numerous measured sections of soil profiles developed on river terraces ranging from late Pleistocene to Pliocene in age. M. J. Pavich and H. W. Markewich

(1979) report that the studies reveal time-related changes in soil characteristics. Soil parameters analyzed include B-horizon thickness and clay content, clay mineralogy, and iron-oxyhydroxide mineralogy. Mineralogical and chemical methods allow for quantification of some of these time-related factors.

Age comparison of soils and the surfaces on which they have developed is a potentially powerful tool for the establishment of stratigraphic relations and geomorphic evolution of various parts of an eroding landscape. In the absence of other methods of dating, soil stratigraphy may serve as the best method of estimating residence time of surficial materials.

Pine Mountain–Russell Fork–Richlands overthrust fault system

Geologic mapping of the Honaker 7½-min quadrangle of southwestern Virginia by C. R. Meissner and R. L. Miller indicates that the east-northeast-trending Richlands overthrust fault is part of a major surface of décollement along which northwestward movement of the Cumberland overthrust block occurred. Other elements that help to define this surface include, to the west, the northwest-striking Russell Fork fault along which as much as 6.5 km of right-lateral displacement has been shown by Englund (1971) and, to the northwest, the east-northeast-trending Pine Mountain overthrust fault. For emphasis, these three structural elements are combined into a single fault system, the Pine Mountain–Russell Fork–Richlands overthrust fault system (Meissner and Miller, 1979).

Middle and Late Devonian ashfall beds in Devonian shale

Previously unknown ashfall localities within the Devonian black shale sequence in the Appalachian Basin have been found by J. B. Roen. At least four ashfall (bentonite) beds of significant areal extent are now known within Middle and Upper Devonian black shale: the Tioga, the "Belpre," and the Center Hill and an unnamed inferred ashfall bed in the Cleveland Member of the Ohio Shale. The Tioga lies at or near the base of the Middle Devonian Marcellus Shale and has the greatest areal extent.

An ashfall bed near the base of the equivalent of the Upper Devonian Rhinestreet Shale Member of the West Falls Formation in southwestern Virginia, Tennessee, and Kentucky had been miscorrelated with the older Tioga by previous workers. From the discovery of additional ashfall localities and stratigraphic and paleontologic studies, the ashfall bed within the Rhinestreet equivalent is known to be younger and less extensive than the Tioga. Now it is correlated with the "Belpre bentonite" in eastern Ohio, which was documented and named by Collins (1979).

An ashfall bed found in association with black shale of the Pipe Creek Shale Member of the Java Formation in New York is of limited areal extent. Except for a few subsurface localities in Tennessee, Virginia, and West Virginia, the distribution of this ashfall bed or its equivalent is not well known. At present it is tentatively correlated with the Center Hill Bentonite Bed of the Dowelltown Member of the Chattanooga Shale of central and eastern Tennessee.

Recently, Jane Negus-deWys (University of West Virginia) (oral commun., 1979) reported the presence of biotite flakes in cuttings from wells in Lawrence and Martin Counties in the eastern Kentucky gas field. The biotite is interpreted as indicative of an ashfall in the lower part of the Cleveland Member of the Ohio Shale. The presence of an ashfall bed within the Cleveland Member has not been reported as yet in other areas. This is understandable because thin ashfalls are as difficult to recognize in drill cuttings as in outcrop and core material. To date, the known areal extent of this unnamed inferred ashfall is limited to only a few counties in eastern Kentucky.

Recognition of the areal distribution of these four ashfalls indicates that Middle and Late Devonian volcanism in eastern North America was more prevalent than previously considered. The stratigraphic record suggests a direct cyclic paleotectonic relation between volcanism and low-energy black shale sedimentation. The black shale–ashfall association does not, however, absolutely preclude continuous volcanism during Middle and Late Devonian time. The extremely thin ashfalls, which are yet to be found in the intervening mudstone and siltstone, may not have been preserved in relatively higher energy depositional environments.

CENTRAL REGION

TECTONICS AND STRATIGRAPHY

Upland gravel, northeastern Arkansas

The age and environment of deposition of an extensive layer of upland gravel in the eastern Ozark region of northeastern Arkansas have been reappraised by E. E. Glick in the light of new data and of the findings of earlier workers (Stephenson and Crider, 1916; Miser, 1922). Geologists generally agree that the major sources of this gravel are the sequences of cherty carbonate rock of Ordovician and Mississippian age that crop out across the Ozarks, but they are less inclined to agree on how and when the material was transported toward and partly into the Mississippi embayment.

Locally, the layer of gravel overlies Paleocene limestone or its silicified equivalent, but generally it rests on unconsolidated Upper Cretaceous sand and clay as a result of subgravel solution of most of the limestone. Soil and Pleistocene loess rest on and around remnants of the layer of gravel. Evidence from the stratigraphic sequence, therefore, indicates only that the gravel is of Tertiary or Quaternary age; other methods must be employed to determine a more exact age.

This upland gravel was transported by streams flowing southeastward from the Ozark source area toward the shoreline of the Mississippi embayment. Alluvial fans or beach ridges of gravel piled up at the edge of the sea, and part of the material from these nearshore deposits was reworked and transported southwestward by longshore currents. Reasonably strong marine currents were required to transport the material southwestward across a distance of at least 50 km without any loss of altitude, from the delta of the ancestral White River (the southernmost stream that transported chert gravel in this area) to the estuary of the ancestral Little Red River (a stream that did not cross cherty terrain). The late Paleocene sea probably was the last one in the embayment with sufficient depth to develop strong longshore currents.

Gravel from this layer is found near the crest of an uplift above the deeply buried Newport pluton, in the area between the ancestral White and Little Red Rivers. The gravel was deposited there prior to the development of the uplift, which is thought to have taken place no later than early Eocene time. On the basis of these various types of indirect evidence, the upland gravel appears to have been deposited during late Paleocene time. Probably, it was a major source of some of the younger stream-transported gravels that extend well out into the Mississippi embayment.

Earthquake localities and surficial and buried faults correspondence, Kentucky

Nineteen historic earthquakes MM=IV and greater were reported by Seay (1979) for 12 scattered localities in west-central to eastern Kentucky (exclusive of the western seismic zone of the New Madrid area). These localities, determinable only to the nearest tenth of a degree of latitude and longitude, were plotted on structure contour maps compiled for the region by D. F. B. Black from 1:24,000-scale geologic maps completed during the USGS–Kentucky Geological Survey (KGS) cooperative mapping project and on aeromagnetic maps prepared by the Tennessee Valley Authority, in part for the USGS–KGS project and in part for the KGS.

Many lineaments, expressed on the structure maps by moderate-displacement surface faults and by linear drape folds in Paleozoic strata and on the aeromagnetic maps by linear magnetic gradients and by boundaries between areas of different magnetic fabric, are known to correspond with subsurface faults, some of which have hundreds of meters of vertical displacement. Lateral displacements along certain faults are also indicated by offsets of lineaments.

Although it is probable that the earthquake localities are not exact, they plot (with perhaps one exception) along or sufficiently close to lineaments on either the structural or magnetic maps or both, suggesting a relation with these rather widely dispersed structures. It is suggested that minor movements are still occurring along some faults.

Basement control of Proterozoic X Penokean orogen

The Penokean orogen, a linear belt of deformed and metamorphosed Proterozoic X and Archean rocks extending from central Minnesota through Wisconsin and Michigan into Ontario at least to the Grenville front, coincides geographically with lower Archean basement gneisses. Its northern margin is approximately at the boundary between the Archean gneiss terrane and the upper Archean greenstone-granite terrane (Morey and Sims, 1976) to the north, which constitutes the southern part of the Superior province of the Canadian Shield.

Several events recorded in the Proterozoic X rocks in the Lake Superior region indicate that the boundary zone (suture?) between the two basement terranes was the locus of both extension and compression, according to P. K. Sims. Initially (~2,200 m.y. B.P.), crustal foundering accompanied by high-angle faulting approximately alined parallel to the boundary provided sites for deposition of the Marquette Range Supergroup and equivalent strata in Minnesota. Faulting in the boundary zone and downwarping to the south continued during accumulation, resulting in a marked thickening of the successions southward. During deposition, extension subparallel to the boundary provided sites for abundant mafic dikes, which probably were coeval with effusive volcanism in and south of the boundary zone. Subsequent deformation and metamorphism (Penokean orogeny) mimicked the sedimentation pattern, being intense in the thicker more eugeoclinal part of the accumulation. Rocks in the zone of intense deformation were intruded by numerous ~1,850-m.y.-old tonalite-granite plutons.

The Penokean orogen is interpreted by Sims as a cratonic feature developed within the Archean craton on the mobile Archean basement gneiss. The gneiss was deformed, together with the overlying supracrustal Proterozoic X rocks, resulting in severe disturbance of isotopic systems. The gneiss terrane did not stabilize until ~1,600 m.y. ago, nearly 1,000 m.y. after the Archean greenstone-granite terrane to the north had stabilized.

MINERAL RESOURCES

Sulfides in the Duluth Complex, Minnesota

Continued studies in part of the Duluth Complex, northeast Minnesota, by M. P. Foose reveal a complex history of intrusive events accompanied by faulting. The first intrusive episode involved a sulfur-saturated mafic to ultramafic magma that was emplaced during a period of active faulting. The next episode involved a sulfur-unsaturated mafic magma that was injected during a period of little fault activity. Locally, both the sulfur-rich and sulfur-poor rocks have been cut by a third mafic intrusion. Early faults were reactivated at a later time when most rocks were consolidated and broke the intrusive sequences into numerous blocks. The recognition of early "growth" faults that developed along with emplacement of a sulfur-rich magma provides a valuable guide to exploration, as fault-bounded troughs make ideal traps to concentrate magmatic sulfide deposits.

ROCKY MOUNTAINS AND THE GREAT PLAINS

ECONOMIC GEOLOGY

Pleistocene gravel in southeastern Montana

Thick deposits of Pleistocene sand and gravel occur along the Yellowstone River and its tributaries, the Powder River, and O'Fallon Creek at altitudes of as much as 110 to 120 m above present stream levels. R. B. Colton, who has mapped these deposits as part of the Williston Basin Energy Lands study, estimates their volume to be about 7 billion m^3. They constitute a major resource in the area.

Alton and Kolob coal fields, Cedar City 1°×2° quadrangle, Utah

Commercial quantities of subbituminous to bituminous coal are found in the Straight Cliffs Formation, Tropic Shale, and Dakota Formation in the Cedar City 1°×2° quadrangle, studied by K. A. Sargent. In the eastern part of the quadrangle (part of the Kaiparowits coal field), the coal is in the Straight Cliffs Formation; in the central part of the quadrangle (the Alton field), the coal is in the Dakota Formation; and in the western part (the Kolob field), it is in strata probably equivalent to the Straight Cliffs Formation and in strata probably equivalent to the Dakota Formation. The Alton and Kolob fields contain about 1.227 billion t of measured reserves and about 1.97 billion t of inferred reserves. Reserve figures for that part of the Kaiparowits field that lies within the quadrangle have not yet been estimated. About 180 million t of strippable coal occurs in the Alton field.

Gold in Oligocene conglomerate, southeast margin of Wind River Mountains, Wyoming

Gold-bearing Oligocene conglomerate, chiefly of clasts of Precambrian rocks, unconformably overlaps Precambrian and gently dipping Paleozoic and Mesozoic rocks along the southeast margin of the Wind River Mountains, about 16 km northeast of the South Pass–Atlantic City gold district. Topography and paleodrainage patterns make it unlikely that this district was the source of the placer gold. The Oligocene conglomerate is generally 30 m or more in thickness. Gold was found by J. C. Antweiler and J. D. Love in pan concentrates in an area of about 40 km^2 but probably is present in a much larger area.

ENVIRONMENTAL GEOLOGY

Seismic risk on the Rexburg fault, Idaho

The Rexburg fault, which forms part of the eastern boundary of the Snake River Plain, passes through Rexburg, Idaho, and may pose seismic risks to the residents of the town. Data from domestic water wells suggest that the fault has offset the 2-m.y.-old Huckleberry Ridge Tuff at least 100 m, indicating major amounts of movement along the fault during the Pleistocene. E. J. Williams (Ricks College) and G. F. Embree (Ricks College) have excavated and examined a trench across the Rexburg fault 2.8 km south of Rexburg. In the trench area, the fault strikes N. 5° W. and dips about 85° W.; faulting there has produced normal displacement totaling about 1.5 m in upper Pleistocene (post-Huckleberry Tuff) Snake River flood-plain deposits that are overlain unconformably by younger Pleistocene (or Holocene?) alluvial deposits, which are not offset by the fault.

Evidence for icecap in West Pioneer Mountains, Montana

Glacial striations and polished rock surfaces were observed by E-an Zen on Precambrian quartzite just below the summit of Stine Mountain, which, at 2,893 m, is the highest peak in the West Pioneer range. The striations strike east-west and are abruptly cut off by the upper lip of the headwall of a large cirque that encloses the Grouse Lakes. Similar relations are found at least at one other peak in this range. The relations indicate that a substantial thickness of ice covered the highest peak (so that polishing and grooving could occur) and imply the existence of an icecap prior to the development of the cirque glaciers. This history is closely parallel to that previously deduced for the East Pioneer Mountains (Alden, 1953; Zen, unpublished data). No local absolute age for the glacial chronology is available, but Zen identified several likely periglacial lake deposits suitable for attempts to obtain organic material for carbon dating.

Geologic maps of possible sites for proposed coal-fired powerplants, central Utah

A series of coal-fired powerplants are to be built throughout central Utah, and many of the sites being considered fall within the confines of the Price 1°×2° quadrangle, Utah. In an effort to be certain that all involved—power company officials and State and local planning agencies—consider the geologic as well as the social and economic factors involved in the siting of such plants, a series of multicolored geologic maps by I. J. Witkind of several possible sites have been prepared for publication. These maps, at a scale of 1:24,000, are designed to give an overview of the general geology of the area in which a plant may be located. Maps showing more detail and focusing on the engineering geology will be needed for the final sites selected.

Radioactive rocks and water, Yellowstone National Park, Wyoming

Radioactive hot springs, flowing 3 to 5 Mgal/d of water with temperatures of 50° to 74°C, were sampled for uranium and radium along the southeast margin of the Pitchstone Plateau in southwestern Yellowstone National Park. The springs emerge along faults cutting the Lewis Canyon Rhyolite (900,000 yr old). Modern gopher bones and annual plants that were sufficiently radioactive to produce autoradiographs were sampled on the Pitchstone Plateau rhyolite flow in the Plateau Rhyolite (70,000 yr old) 8.8 km north-northwest of these hot springs. Data from these sites and from adjacent radioactive rocks and thermal water (Love and others, 1975; Diem and Kennington, 1979) suggest that effects of the radioactivity on nearby plants and animals warrant investigation.

STRATIGRAPHY

Correlation of Cambrian formations in southwestern Montana

According to E-an Zen, the Phanerozoic rocks of the Pioneer Mountains begin with quartzite conglomerate, >500 m thick, that grades up into rocks mapped as the Silver Hill Formation, named in the Philipsburg area by Emmons and Calkins (1913). In the Pioneer Mountains, the Silver Hill has two informal members, each about 30 to 50 m thick. The upper member consists of silty limestone, calcareous sandstone, calcareous siltstone, and dolostone. The lower member consists of thin-bedded siliceous argillite, siltstone, and ferruginous sandstone; mudcracks, loadcasts, slumps, ripple marks, crossbeds, and scour grooves are common. Near the top of the lower member is a zone of bioturbation in which trace fossils and an *Albertella* was found (Zen and others, 1979). The Silver Hill passes up into about 500 m of supratidal to intertidal sugary dolostone, the Hasmark Formation, containing peloidal beds, oolites, pisolites, algal mats, intraformational conglomerates, and so forth.

At type Silver Hill, the equivalent of Zen's upper member is divided by Emmons and Calkins into a middle limestone member and an upper limy shale member; from the middle member, *Glossopleura* had been found. *Albertella* has been found elsewhere in the Silver Hill of the Garnet Range (Kauffman, 1965), in the Alberton area (Wells, 1974), and in the Gordon Shale of the thrust belt (Deiss, 1939), among other places. *Glossopleura* has been found in the lower part of the Wolsey Shale of the cratonic area to the east (Hanson, 1952). The Meagher Limestone of the latter area, which overlies the Wolsey and is homotaxial with the lower part of the Hasmark, contains younger trilobite faunas.

These relations show that the conventional correlation of Cambrian strata suggested by Emmons and Calkins (lower part of Silver Hill = Wolsey, middle part of Silver Hill = Meagher, upper part of Silver Hill = Park, Hasmark = Pilgrim) is untenable. Better correlations are the entire Silver Hill with the Wolsey (lower member equivalent to the Flathead Sandstone because of the eastward (craton-ward) onlap of basal Phanerozoic strata) and the Hasmark (with its middle silty member) with the Meagher-Park-Pilgrim sequence. Such a correlation also would obviate the need to thin the pre-Pilgrim rocks of the craton about fivefold westward to the Philipsburg–Pioneer Mountains area and a concomitant converse thickening of the Pilgrim by the same ratio.

Depositional environment of the Groat Sandstone Bed in the northern Black Hills, Montana

The Groat Sandstone Bed of the Gammon Member of the Pierre Shale (Campanian) crops out on the north flank of the Black Hills, Mont. Subsurface studies by G. W. Shurr in Carter County, Mont., show that this sandstone underlies an area of 3,900 km^2 and is locally more than 23 m thick. Two small elongate lenses in T. 6 and 7 S., R. 54 and 55, trend northwest and are about 16 km long and 6 km wide. In adjacent outcrops, sandstone grades downward and laterally northeastward into siltstone and then to shale. Sandstone units are less than 15 m thick; near the base they are fine grained and mottled with clay. They grade upward into bioturbated medium- to fine-grained sandstone and then to medium- to coarse-grained sandstone in large-scale open-trough crossbeds.

The Groat Sandstone Bed was probably deposited 322 km from the strandline near an outer shelf margin. This interpretation is based upon published strandline positions and upon regional isopach maps of subsurface units within the Pierre Shale. Local thickening of shale marks the position of the shelf margin. The elongate

northwest-trending lenses of sandstone are similar in size and shape to modern sand ridges, and the large area of sandstone may have been the site of closely spaced sand ridges.

Tertiary gravels, Little Belt Mountains, Montana

Remnants of high-level gravels of postmiddle Eocene age have been mapped in the east-central part of the Little Belt Mountains, Mont., by M. W. Reynolds. The gravels are composed primarily of lower and middle Paleozoic carbonate clasts but also contain clasts of Jurassic and Cretaceous sedimentary rocks, not now exposed across the mountains, and clasts of middle Eocene plutonic rocks derived from the north-central part of the range. Both the high topographic position of the gravel remnants and the pattern of incision by streams in the mountains suggest that the mountains have been uplifted in postmiddle Eocene time; if so, the uplift would be younger than heretofore suspected and the youngest identified in central Montana.

Basin-fill deposits of Beaver Valley, southwestern Utah

The Beaver Valley basin is a tectonic depression west of the Tushar Mountains containing deposits that accumulated in a bolson environment during Miocene(?) through middle Quaternary time. The deposits include local coarse-grained fanglomerate, piedmont-slope, and shallow-water facies and a thick lacustrine sequence. Mapping by M. N. Machette, following preliminary work by R. E. Anderson, indicates that the basin may be underlain by a shallow north-trending horst. The northern end of the basin is bounded by Miocene rhyolites, and the western side is bounded by the Mineral Mountains batholith of probable early Miocene age.

Early Quaternary (1 m.y.–2 m.y.) tectonism resulted in the formation of an extensively faulted north-trending antiform centered over the postulated subsurface horst. This feature was completely eroded about 0.5 m.y. ago during the integration of the Beaver River with the Sevier Desert to the west. The resulting pediment, Last Chance Bench, is the oldest erosional feature in the basin. Renewed deformation later produced another surface antiform, although the individual fault displacements range from only 3 to 10 m. The upper Quaternary deposits consist of three phases of terrace and piedmont-slope deposits and a widespread Holocene flood-plain deposit. All but the Holocene deposits are cut by faults, many of which are recurrent growth faults.

Early Eocene streams of the Bighorn Basin, Wyoming

A study of the crossbedding in the lower Eocene Willwood Formation of the Bighorn Basin in northwestern Wyoming by Sarah Andrews and D. A. Seeland indicates that paleostream flow was dominantly to the northwest but had many local variations. On the eastern side of the basin, the paleostream pattern indicates flow parallel to the trend of the Bighorn Mountains. This suggests that the rocks that should occur on the eastern margin of the basin, and that should record streams flowing southwest toward the axis of the basin, have been eroded away. On the west side of the Powder River Basin, this belt of rocks does exist and contains coarse conglomerates. This is additional evidence that erosion rather than nondeposition is the best explanation for the lack of basin-margin rocks on the east side of the Bighorn Basin.

Crossbedding in the Bighorn Basin seems more variable than in the Powder River or Wind River Basins. This variability, along with the relatively smaller proportion of sandstone and conglomerate, indicates the dominance of low-gradient highly sinuous streams in the Bighorn Basin.

Stratigraphic relations and volcanic history of Eocene rocks, eastern Absaroka Range, Wyoming

The volcaniclastic Aycross and Tepee Trail Formations, largely of middle Eocene age, have been traced by T. M. Bown from their type areas in the northwest Wind River basin of Wyoming into the eastern Absaroka Range, bordering the Bighorn Basin. They are present as far north as the north flank of Carter Mountain in Park County, where they were earlier included in the Pitchfork Formation. Farther north, they intertongue with and are supplanted by igneous rocks and lahars of the Wapiti Formation.

The Aycross, Tepee Trail, and Wapiti Formations are overlain unconformably by the Trout Peak Trachyandesite. Aycross and Tepee Trail rocks of the eastern Absaroka Range occur in a series of strongly folded anticlines and synclines that were breached shortly before deposition of the Trout Peak Trachyandesite. Folding and truncation are such that, in the synclines, the Trout Peak overlies the Tepee Trail Formation, and, in the anticlines, it overlies the Aycross Formation with angular unconformity. The Trout Peak Trachyandesite may be regarded either as a formation or as the basal unit of the Wiggins Formation; it is younger than Tepee Trail rocks of the eastern Absaroka Range. Some basaltic rocks previously included in the base of the Trout Peak actually lie beneath the angular unconformity and belong in the Tepee Trail Formation.

Folding and erosion of Aycross and Tepee Trail rocks record significant tectonic activity preceding expansion of the Absaroka volcanic field to the south and east in Wiggins time. In the eastern part of the Absaroka Range, this expansion was reflected by outpouring of basaltic lavas of the Trout Peak Trachyandesite (48.2 m.y. $\pm$ 0.7 m.y.).

IGNEOUS ROCKS

Basaltic rocks of the Springerville volcanic field, Arizona

The basaltic volcanic field west of Springerville, Ariz. is on the southern margin of the Colorado Plateau in east-central Arizona. On the basis of field examination, C. D. Condit, L. S. Crumpler, and J. C. Aubele have found that olivine-phyric basalts are the most abundant type; other types include quartz-bearing olivine basalt, pyroxene-olivine-plagioclase-phyric basalt, hornblende-plagioclase andesite(?), and a variety of aphyric and microcrystalline lavas that may include hawaiite, mugearite, and benmoreite. The mapped lavas range in age from late Tertiary to late Quaternary (Holocene?). On the basis of freshness of eruptive surface features, the youngest basaltic vent and its flows, approximately 13 km northwest of Springerville, are estimated to have occurred within the last 10,000 yr.

Buried Pliocene calderas of the eastern Snake River Plain, Idaho

Geologic mapping and related studies by H. J. Prostka (Colorado State University) of rhyolites exposed along the margins of the eastern Snake River Plain between American Falls and Island Park, Idaho, reveal six major densely welded ash-flow sheets that range in age from 4 m.y. to 10 m.y. Distribution patterns of the ash flows suggest that some basin-and-range structures were present as northwest-trending barriers across the plain during eruptions. An unconformity in the rhyolite sequences along both margins of the eastern Snake River Plain is approximately dated at 4 m.y. to 5 m.y. Flow lineations and lithologic variations combined with geophysical data suggest that the tuffs were erupted from four buried caldera complexes. Especially hot phenocryst-poor very densely welded ash flows were erupted from a source between Big Southern Butte and the Lost River sinks. A 3,159-m-deep geothermal well drilled in this area near the Idaho National Engineering Laboratory in early 1979 penetrated 2,414 m of rhyolitic rocks consisting of 15 welded ash-flow sheets and interlayered nonwelded tuffaceous rocks interpreted as caldera fill. This caldera is surrounded on the south, east, and northeast by older (7 m.y.–10 m.y.) and younger (4 m.y.–5 m.y.) sources of cooler more phenocrystic less densely welded tuffs. These eruptions did not progress uniformly northeastward up the eastern Snake River Plain as most models suggest.

Petrogenetic possibilities for late two-mica granites, Pioneer Mountains, Montana

The genetic relations between Upper Cretaceous calc-alkalic granitic rocks and lower Tertiary (65 m.y. by K-Ar determinations on biotite separates) two-mica granite in the East Pioneer Mountains have been studied by E-an Zen. According to experimental data, the upper limit of stability of stoichiometric muscovite + quartz intersects the minimum melt curve of the haplogranite only in a narrow temperature range at a pressure above about 5 kbars. The Cretaceous intrusive rocks, however, give evidence that the pressure was no more than 1 kbar (miarolite, stratigraphic reconstruction, andalusite-cordierite-biotite contact-metamorphic assemblage).

If the increase in pressure is real, a hypothesis of increased rock burden, presumably by thrust loading, would be needed. Other possible explanations include (1) the departure of composition of the muscovite, which by textural evidence appears to be magmatic, from stoichiometry was enough to make the experimental data inapplicable, (2) the liquidus was depressed by presence of fugitive components not now recognized in the mineralogical and chemical data, and (3) the muscovite crystallized at a deeper part of the magma chamber through progressive cooling of the roof, was bodily brought to the higher level of intrusion, and was frozen in place before it had a chance to react to the lower pressure environment. It is doubtful that minor amounts of other components (mainly titanium and iron) are enough to stabilize muscovite to a pressure region 3 kbar below that for the stoichiometric muscovite. Other components than H_2O undoubtedly existed in the magma, as the coexisting biotite has fluorine (but no chlorine), even though the muscovite is free of both halogens. Late pegmatites associated with the calc-alkalic granite show garnet, tourmaline, muscovite, and rarely beryl. These minerals seem to be closely associated with roof rock of Precambrian quartzite and, thus, may reflect contamination near the contact and not something that permeated the magma.

The third explanation is attractive because it offers a natural way to evolve one rock type into another (and thus allow its general application), provided there is a way to evolve peraluminous magma from calc-alkali magma at the pressure ranges concerned. One possible hypothesis is that the "saussurite reaction" operated: anorthitic component of plagioclase + K-spar + H_2O = zoisite + muscovite component + quartz. If zoisite should crystallize and separate itself, the residual liquid would have muscovite as an actual and positive component. Thermochemical data on epidote is lacking, but, at pressures of 2 to 3 kbar, data of Haas and others (1979) and unpublished data show that zoisite might be favored under a full head of steam at temperature of about 500° to 600°C. This would be true especially if the magma is undersaturated with respect to the muscovite component. Liou's (1973) and Holdaway's (1972) experimental data show that epidote is stable at its own composition up to temperatures well above the granite

minimum-melting curve at pressures exceeding 2 to 3 kbar. Naney's (1977) experimental data on melts of granodiorite composition show epidote can be present in the melting interval. Thus, on the basis of available data, this mechanism might be feasible as a way to get from calc-alkalic to peraluminous granites.

Two suites of Cretaceous granitic rocks from the Pioneer batholith, Montana

In the East Pioneer Mountains, two suites of uppermost Cretaceous intrusive rocks (median K-Ar ages on biotite and (or) hornblende 71.5 m.y.), marked by distinct initial strontium isotope ratios, have been mapped by E-an Zen and studied mineralogically and isotopically by Zen, J. G. Arth, B. R. Doe, J. M. Hammarstrom, R. F. Marvin, and J. R. O'Neil. One suite of granite and granodiorite has a ratio of 0.7131 to 0.7138. The other volumetrically more important suite of quartz diorite, tonalite, and granodiorite has a ratio of about 0.7113 to 0.7119.

The two suites of rocks, having the same age, must have evolved in magma chambers that existed side by side. Local cross-cutting relations on individual outcrops show that, at a given locality, the high initial ratio rocks are younger. Over much of the area, however, the contact between granodiorite and granite of the two suites is indistinct and not readily mappable; the zone of gradation is as much as 1 km wide. Toward this zone from the granodiorite (low initial ratio) side, the rocks contain clean, nearly inclusion-free pink potassic fieldspar phenocrysts that are typical of the granite suite. Concomitantly, large anhedral megacrysts of potassic feldspar were found that contain the matrix minerals as inclusions in the same size and textural arrangement that occur elsewhere only in low initial ratio rocks. These megacrysts clearly are later than the main stage of crystallization of the granodiorite and may be secondary, related to the intrusion of the granite.

Rocks from the intermediate zone are also chemically intermediate. They have alkali contents resembling granites of the high initial ratio suite but otherwise are comparable to the low initial ratio rocks of the same silica content. The rocks may have been from simultaneous and independently evolving magma bodies (derived ultimately, perhaps, by partial melting of a gneiss-amphibolite terrane by admixture of different proportions of these two components) that locally broke through the partition between the chambers, and the phenocryst-laden melts mixed to produce the hybrid rock.

Volcanic rocks of Eocene age from the Pioneer Mountains, Montana

Eocene volcanic rocks from the Pioneer Mountains, Mont., studied by E-an Zen and J. M. Hammarstrom, have been dated by whole-rock potassium-argon methods at between 47 m.y. and 50 m.y. old. They are subaerial flows showing columnar joints and have an uppermost rubble zone that includes partially resedimented material. Phenocrysts in rocks having less than 57 percent silica are mostly olivine and augite and, less commonly, hypersthene. In more siliceous rocks, the phenocrysts are augite-hypersthene-pigeonite. Quench augite in the groundmass is common, and glass is ubiquitous. The compositions of the phenocrysts indicate temperatures of about 1,050°C; this temperature estimate is supported by available laboratory determination of 2 kbar liquidus for appropriate compositions (Naney, 1977). The presence of magnesium-rich olivine shows the pressure not in excess of 3 to 4 kbars, so the laboratory data are applicable. The absence of amphibole, even as relics, reflects dry magmas. Initial strontium ratios for the rocks are in the range of 0.7058 to 0.7083 ± 0.0002, and the magmas, thus, have a significant lower crust or upper mantle source component. Rare-earth element data for the rocks are compatible with partial melting controlled by pyroxene or amphibole.

Apparently, coexisting with magmas that formed this typical continental volcanic suite were highly differentiated siliceous magmas that now form shallow intrusions (volcanic necks?) and ash deposits of biotite-rich vitrophyre. The intrusions and ash deposits are not distinguishable from the Lowland Creek Volcanics of the Butte area, which are the same age (50 m.y.) and have the same initial strontium ratios. The ash is locally interbedded with the flow rocks. The genesis of these different magma bodies and their ability to maintain their discrete plumbing systems at the same time and place remain problems to be solved.

Caldera source of Miocene Osiris Tuff, southwestern Utah

The Osiris Tuff is the most widespread ash-flow sheet derived from the Marysvale volcanic field. It largely overlies thick sequences of dacitic to andesitic lava flows, flow breccia, and volcanic mudflow breccia that make up most of the volume of the field. The tuff covers an area that has a diameter of about 100 km. It locally is more than 100 m thick, although in most places it is less than 15 m thick. It consists of tan, orange, and gray densely welded ash-flow tuff containing about 15 percent crystals of plagioclase and subordinate sanidine and minor biotite, pyroxene, and iron-titanium oxides. The sheet has received potassium-argon ages of about 22 m.y. (Fleck and others, 1975).

On the basis of regional relations noted in mapping the eastern edge of the Marysvale field, P. L. Williams predicted that the caldera source was in the Marysvale Peak area of the central Sevier Plateau, in the center of

the distribution of the Osiris Tuff (Williams and Hackman, 1971). Recent mapping of the Richfield 1°×2° quadrangle, Utah, by P. D. Rowley, T. A. Steven, P. L. Williams, J. J. Anderson, and C. G. Cunningham confirmed that the caldera occurs in this area. Specifically, it is cut by and exposed along the main frontal Sevier fault zone at the western edge of the Sevier Plateau between Monroe Canyon and Manning Creek; here the caldera has a maximum north-south diameter of about 14 km. The western part is downthrown and largely underlies valley fill; the eastern part is largely overlain by younger high-sanidine rhyodacitic lava flows. The structural margin of the caldera, and probably the topographic wall, is exposed in only a few localities in the Monroe Creek and Manning Creek areas. The caldera fill of Osiris Tuff is slightly to intensely altered, alunitized, and perhaps weakly mineralized because it has been engulfed by a monzonite porphyry batholith, dated by H. H. Mehnert by potassium-argon determinations as 21.5 m.y. old. Cupolas from this batholith locally breached the surface at the margins of the caldera and produced the overlying high-sanidine lava flows and related craters and domes. The caldera does not appear to be significantly resurgent, but the caldera fill is broken by numerous faults related to caldera activity.

Mafic flows in the Cedar Breaks–Panguitch Lake area, Utah

Mafic and intermediate lava flows in the northeastern part of the Cedar City 1°×2° quadrangle, Utah, have been studied by K. A. Sargent. Most of the flows are olivine basalts and pyroxene andesites; a few of the most recent flows south of Panguitch Lake appear to be less mafic hornblende andesites. Field investigations indicate the oldest flows are olivine basalts. Successively younger flows are pyroxene andesites, pyroxene-hornblende andesites, and hornblende andesites. The older flows are probably no older than Pleistocene, and the youngest may be Holocene. Lava extrusion combined with faulting has led to interruptions and readjustments of drainage, as at Panguitch Lake where drainage now is diverted from easterly to northerly. Elsewhere, flows into the Duck Creek drainage have formed Navajo Lake and diverted at least part of its outflow from Sevier River interior drainage to the Virgin River drainage basin (Wilson and Thomas, 1964).

PRECAMBRIAN ROCKS

Age of Yellowjacket Formation, Idaho

Uranium-thorium-lead analyses of zircons by R. E. Zartman from porphyritic adamellite bodies within the Salmon and Leesburg (Idaho) quadrangles indicate a Precambrian age of intrusion, as suggested by Armstrong (1975). Least-magnetic size splits of cogenetic zircons all fall nearly on concordia, yet have lead-lead ages spanning approximately 100 m.y., with ages increasing systematically as size decreases. This trend applies to all three plutons analyzed thus far whose lead-lead age spans are 1,377 m.y.–1,430 m.y., 1,367 m.y.–1,476 m.y., and 1,367 m.y.–1,473 m.y. These results indicate that the upper part of the Yellowjacket Formation, which is cut by the plutons, is at least 1,367 m.y. old and possibly as old as 1,476 m.y.

Comparison of Precambrian rocks of the Hartville uplift, eastern Wyoming, and of the Black Hills, western South Dakota

G. L. Snyder, who has studied the geology of the Hartville uplift, eastern Wyoming, and J. J. Norton and J. A. Redden, who have studied the geology of the Black Hills, western South Dakota, compared the Precambrian rocks of these areas in a 5-d field conference in the fall of 1979. They found the similarities to be so far outweighed by differences between the geology of the two areas that a useful correlation scheme cannot be suggested.

Both areas have thick supracrustal metasedimentary and metavolcanic rocks. At Hartville, these are believed to be older than an Archean granite (2.6 b.y.), but in the Black Hills they probably are mostly younger than granite of similar age. Both areas have metashale, graphitic metashale, metagraywacke, pillowed metabasalt, and quartzite, but the relative abundances of these rocks and their stratigraphic sequences are different. Furthermore, algal dolomite is a dominant sedimentary rock at Hartville, but dolomite is rare in the Black Hills. Large units of quartzite-pebble conglomerate in the Black Hills have no counterpart at Hartville. Iron deposits of the Hartville region are in a massive partly secondary hematitic iron formation, which is unlike the several units of cummingtonite and magnetite banded iron formation of the Black Hills.

According to unpublished data of G. E. Peterman, two ages (2.6 b.y. and 1.7 b.y.) of granite in the Hartville uplift are about the same as the two ages in the Black Hills (Zartman and Stern, 1967; Ratté and Zartman, 1970; and Riley, 1970). The older age is represented by similar gneissic granites at Little Elk Creek in the Black Hills and in the Rawhide Buttes of the Hartsville uplift. The 1.7-b.y. Harney Peak Granite of the Black Hills is a pegmatitic rock. It is a multiple intrusion containing many schist screens and is at the center of a dome. The wall rocks contain about 20,000 unzoned pegmatites and about 200 zoned pegmatites, many of which have been important commercial deposits. The 1.7-b.y. granite of the Haystack Range in the Hartville uplift has ordinary medium- to coarse-grained granitic texture. It has a few metasedimentary inclusions and a generally simple ver-

tical planar contact with the wall rocks. Pegmatites of unproved age occur nearby, but only a few are zoned, and none have been economically significant.

Newly recognized Precambrian metasedimentary and metavolcanic rocks in the Seminoe Mountains, Wyoming

Mapping by H. R. Dixon shows that metamorphic rocks increase in thickness in the western half of the Seminoe Mountains and have a maximum thickness of about 2,000 m at the western edge of the Seminoe Dam quadrangle. The northern 1,300 m of this sequence consists primarily of mafic metavolcanic rocks, mainly amphibolite and amphibole schists and gneiss, lesser amounts of interlayered mica schist, epidote quartzite, calc-silicate gneiss, and a few thin layers (about 0.5 m thick) of iron formation. The amphibole gneiss has been serpentinized along shear zones subparallel to the Seminoe fault along the north side of the mountain range. Along the southern edge of the metamorphic sequence is a layered granitic gneiss, which has a maximum thickness of about 700 m at the western edge of the Seminoe Dam quadrangle and thins to the east. The gneiss is dark gray to white and contains layers from a few millimeters to a few centimeters thick. The dark layers, commonly thinner than the light felsic layers, are either biotite gneiss or amphibolite. This granitic gneiss was included with the massive unfoliated granite south of granite gneiss in the adjacent Bradley Peak quadrangle (Bayley, 1968). This granitic gneiss likely represents original felsic volcanic rocks.

Two ages of mafic intrusive rocks are found in the Seminoe Mountains. The older rocks are megagabbros, occurring along the western edge of the Seminoe Dam quadrangle and, more abundantly, in the adjacent Bradley Peak quadrangle. The metagabbros are now massive to strongly foliated amphibolite. The younger mafic rocks are gabbro to diabase dikes that are commonly altered but not metamorphosed. Many dikes are less than a meter thick and are indicated by one or two exposures, although some can be traced for as much as 3 km. A few are as much as 150 m thick and are gabbroic, though they commonly have diabasic borders. One such gabbroic dike was traced for about 7 km completely across the range. The mafic dikes cut all other rocks of the area. They are cataclastically deformed along the Seminoe fault and sheared along other fault zones within the mountains.

Reconnaissance in the Pedro Mountains indicates the rocks are the same granite as that immediately north of the Seminoe fault and establishes the continuity of this granite with the granite of Lankin dome of Peterman and Hildreth (1978). For the most part, this granite is massive and unfoliated, but, in a few localities, it has a conspicuous flow foliation and contains inclusions of metamorphic rocks, mostly biotite gneiss and amphibolite.

TECTONICS

Tectonism in the San Francisco volcanic field and southern Colorado Plateau, Arizona

Mapping and related studies by E. W. Wolfe, G. E. Ulrich, and L. D. Nealey show that tectonism related to volcanism on the southern Colorado Plateau is expressed by extensive high-angle normal faulting known to involve basalts as young as 0.5 m.y. old. Monoclinal folding has occurred along the same structural trends, but it preceded the onset of volcanism. Northeast faults are few in number, and the largest of them represent ancient and deep-seated systems that are strongly reflected by aeromagnetic and Bouger gravity anomalies (Sauck and Sumner, 1970; West and Sumner, 1973). Seismicity is still occurring along some of these trends. Northwest faults are the most common modifiers of topography, and their density increases markedly toward the edge of the Colorado Plateau. They are approximately parallel to the trend of the plateau margin, the Arizona Transition Zone, and related structural basins (for example, Verde Valley, Chino Valley). North-south faults or fractures have provided the main access to the surface for lavas as reflected by lines of vents and elongated vents, although the other trends have also provided access. To the north in the Grand Canyon and possibly southward toward the Transition Zone, some of these north-south faults show, in their earlier history, reversed movement from their present displacement.

A well-developed northeasterly grain in the aeromagnetic and gravity data characterizes the region northeast of the Transition Zone. Superposed on and locally truncating this pattern is a pronounced northwest grain that approximately coincides with the Arizona Transition Zone, supporting a younger age for that structural province.

Uplift studies in the Front Range, Colorado

Fission-track ages of apatite determined by C. W. Naeser from samples collected by B. H. Bryant at altitudes ranging from 2,400 to 4,300 m from within a fault block in the Mount Evans area of the central part of the Front Range of Colorado indicate that the 100° isotherm during Late Cretaceous time is now at an altitude of 3,500 m. Assuming a geothermal gradient of 25°/km and inferring 2.5 km of Jurassic and Cretaceous sedimentary rocks above the Precambrian basement, the projected level of the latest Cretaceous sea floor is at an altitude of about 7.5 km, about 3.2 km above the top of Mount Evans. The total structural relief between the

Front Range uplift in the Mount Evans area and the deepest part of the Denver Basin to the east is about 6.5 km.

Precambrian basement rocks in South Park on the west margin of the Front Range uplift are thrust over Paleocene basin fill along the Elkhorn fault, which has an apparent stratigraphic displacement of as much as 5.5 km. Fission-track ages of apatite from Precambrian rocks in the overblock are older than the time of basin filling and faulting. Thus, these rocks were not buried at depths of 3 to 4 km at the end of the Paleocene when sedimentation ceased. To explain the apatite ages in the area of maximum stratigraphic displacement, the Elkhorn fault must have a shallow dip, as suggested by Salwatzky (1967), and the margin of the Paleocene basin must have been rather abrupt and not many kilometers east of the fault.

Allochthonous Paleozoic sedimentary rocks, central Idaho

Mapping in the Boulder Mountains in the southern part of the Challis quadrangle, Idaho, south of the Salmon River, by W. E. Hall, J. N. Batchelder, and H. C. Winsor has demonstrated that all the outcropping Paleozoic rocks are allochthonous. The structurally lowest allochthon, named informally the Salmon River sequence by Nilsen (1977), consists of 2,000 m of dark-gray carbonaceous argillite, siltite, and micritic limestone turbidite deposits of Late Mississippian age. This is overlain by the Wood River allochthon of Pennsylvanian and Early Permian age that, in turn, is overlain by 2,000 m of dark-gray carbonaceous siltites, limy sandstones, and fine-grained quartzites of Leonardian-Roadcanyonian age (middle and late Leonardian, B. R. Wardlaw, written commun., 1979). This latter sequence is characterized by graded bedding, abundant crossbedding, conspicuous banding, and soft-sediment deformation. It is here named informally the Pole Creek allochthon.

The Salmon River and Pole Creek allochthons were mapped from the south end of the Challis $1° \times 2°$ quadrangle at Washington Basin northward 30 km to the Salmon River. S. W. Hobbs mapped windows of these allochthons north of the Salmon River for approximately 12 km between the Yankee Fork of the Salmon River on the west and Thompson Creek on the east.

The Wood River allochthon does not extend north of Washington Basin. It overlies the south end of the Salmon River allochthon and extends northeast about 9 km to the White Clouds area. The Wood River allochthon extends to the south about 100 km in the Wood River area (Dover, 1969; Hall and others, 1974; Tschanz and others, 1974; and Dover and others, 1976).

Recognition of the thrust faults has an important economic significance. Most of the metalliferous deposits in the Boulder Mountains in the Challis quadrangle, except uranium, are in or near the thrust-fault zone at the top of the Salmon River allochthon. This thrust-fault zone was intruded by numerous plutons of biotite granodiorite and granite, was bleached and contact metamorphosed over a thickness as much as 300 m, and, subsequently, was invaded by mineralizing fluids that deposited Ag, Mo, Pb, Zn, W, and Sn minerals and formed significant economic deposits.

Geologic framework along the Idaho Falls–Blackfoot corridor, east flank of the Snake River Plain, Idaho

Geologic mapping by J. F. Karlo (Central Michigan University) along the Idaho Falls–Blackfoot portion of the Snake River Plain boundary reveals that the Tertiary volcanic stratigraphy is divisible into two sequences. The early sequence is a blanket deposit that predated basin-and-range uplift; the later sequence consists of local deposits strongly controlled by basin-and-range topography. Potassium-argon dating of the youngest unit that clearly predates uplift and the oldest unit that demonstrably postdates uplift gives a range of 9.6 m.y. to 6.0 m.y. B.P. for major deformation. All Tertiary units are cut by northeast-trending en echelon scissor and normal faults parallel to the margin of the plain with downdrop and rotation of fault blocks toward the plain. Structural styles change somewhat with the stratigraphic units involved. The oldest units and structures are clearly truncated at the margin of the plain, and the youngest units continue across the boundary. Mapping of Bouguer gravity yielded a similar pattern for identifiable anomalies. The pattern is interpreted as indicating a progressive downfaulting at the boundary of the plain, postdating the major basin-and-range uplift and continuing after deposition of the youngest unit 4.5 m.y. B.P. Identifiable structural patterns across the boundary within the Quaternary basalts of the plain were not found to be correlatable with structures in the Tertiary highlands.

Post-Early Triassic structures in the North Hansel Mountains, Idaho

Geologic mapping by R. W. Allmendinger of the North Hansel Mountains during the summer field season of 1979 resulted in a sevenfold subdivision of the Pennsylvanian and Permian Oquirrh Group. These new units have enabled the identification of thrust plates within the stack of Oquirrh and have facilitated the mapping of several sets of high-angle faults.

The North Hansel Mountains are comprised of three major allochthons. The structurally lowest of these plates is represented by limited exposures of highly deformed Manning Canyon Shale of Mississippian and Pennsylvanian age. The intermediate plate covers most of the mountain range and is composed of Atokan to

Leonardian parts of the Oquirrh. Large-scale folds, though rare, are present, and, in one place, an overturned, west-dipping fold limb has been preserved in a Cenozoic fault block. The east-verging asymmetry of all of the folds indicates approximately west- to east-transport of the middle allochthon. The structurally highest plate is composed of Oquirrh of Virgilian age. It rests tectonically on Des Moinesian and Virgilian rocks of the middle plate at the crest of the mountain range. The upper plate also may be thrust directly on the lower plate at one locality. There are striking differences in facies of equivalent-age rocks in the upper and middle plates, indicating a significant distance of transport of one plate relative to the other. All of these plates display younger-over-older thrust geometry, which coincides with observations from elsewhere in southern Idaho (Oriel and Platt, 1979; Allmendinger and others, 1979). Although the age of these allochthons cannot be determined from exposures in the North Hansel Mountains, they are probably post-Early Triassic and pre-Cenozoic.

Five sets of high-angle faults of probable Cenozoic age have been mapped. Their trends, in order from oldest to youngest, are north-south, northeast, east-west, north-south to north-northwest, and northeast. The three oldest sets of faults are found only in the interior of the mountain range. The second youngest set is found in the range and as range-front faults on the west side, now covered by Quaternary deposits. The youngest fault set probably cuts level shoreline deposits of the Bonneville and Provo Formations of Quaternary Lake Bonneville. The region is the locus of intense seismic activity; thus, the youngest fault set may be active.

Ordovician plutonism in Idaho and Montana

Radiometric (K-Ar) ages on hornblende and biotite obtained from a meladiorite associated with syenite on the Black Mountain thrust plate in the southern Beaverhead Mountains, Idaho (Skipp and others, 1979), were determined by R. F. Marvin to be 467 m.y. ± 16 m.y. and 482 m.y. ± 16 m.y., respectively. These concordant ages are similar to the potassium-argon age (441 ± m.y.) reported by Ramspott and Scholten (1964) for the Beaverhead pluton and substantiate a period of Middle to Late Ordovician plutonism in allochthonous rocks now present in the central and southern Beaverhead Mountains of Idaho and Montana. Metamorphism of a similar age is present in southeastern British Columbia (A. V. Okulitch, Geological Survey of Canada, oral commun., 1979), indicating that a large part of the western margin of North America was affected by an early Paleozoic orogenic event (Taconic?) prior to the Antler orogeny. This early Paleozoic plutonism in the Beaverhead Mountains is spatially associated with thin lower Paleozoic sequences attributed to a Paleozoic high variously referred to as the Lemhi arch (Sloss, 1954; Ruppel, 1978), Tendoy dome (Scholten, 1957), and the southern Beaverhead Mountains uplift (Sandberg, 1975).

Neotectonics in Kansas

Geologic mapping by G. A. Izett, T. M. Bown, and J. G. Honey combined with detailed stratigraphic-paleontologic, tephrochronologic, and isotopic age studies along the trace of the northeast-trending Crooked Creek fault zone (Pleistocene) in Meade County, Kans., reveals a complex history of fault movement and related deposition of sediments in late Cenozoic time. An early period of northeast-trending faulting (50-m throw, east side down) of pre-Ogallala Formation (upper Miocene) is shown by study of geophysical logs of oil and gas wells in the area. Following deposition of the Ogallala Formation (upper Miocene, 10 m.y.–5 m.y.), recurrent movements along the Crooked Creek fault zone resulted in about 30 m of throw, west side down. Sandstone and claystone of the Rexroad Formation (Pliocene, 4.5 m.y.–2.5 m.y.), which are well-dated by fossil vertebrates, were deposited west of the fault zone. Recurrent movements along the Crooked Creek fault zone deformed the Rexroad sediments about 2.2 m.y.–2.5 m.y. ago. A thin sheet of clean-washed sandy gravels and associated overbank silts of the Stump Arroyo Member of the Crooked Creek Formation was laid down by the ancestral Arkansas River over wide areas in Meade County about 2.1 m.y. ago. Renewed movements along the fault zone offset the Stump Arroyo (about 20 m throw, east side down) and the lower part of the Crooked Creek Formation containing the Type B "Pearlette ash" and the Borchers fauna (2.0 m.y.). The latest movements along the Crooked Creek fault occurred following the deposition of the upper part of the Crooked Creek Formation (Pleistocene, 1.4 m.y.–0.6 m.y.).

Basement controls on steep faults, southwestern Montana and east-central Idaho

The steep normal and reverse faults of southwestern Montana and east-central Idaho, according to E. T. Ruppel, all appear to have formed as a result of dominantly vertical movements on basement blocks first defined in Precambrian time rather than as a result of alternating episodes of crustal compression and extension—the conventional explanation. The division of the region into two tectonic provinces, one of basement tectonics and one of compressive extensional tectonics, thus, is artificial, and the apparent differences reflect instead only the thicker sedimentary cover in the western part of the region. The faults that bound the basement blocks also appear to have been the primary structural control on

the emplacement of small stocks and related metallic mineral deposits, suggesting that mineral deposits most likely are to be found more or less above known or inferred block edges. Conversely, mineral deposits much less likely are to be found away from the basement-block edges, and, thus, not in the interior parts of most of the present mountain ranges or beneath the intervening valleys, a conclusion of critical importance in any estimate of the total mineral-resource potential of the region.

Eastern edge of the Sapphire thrust system, Montana

Part of the eastern edge of the Sapphire thrust system (as defined by C. A. Wallace and M. R. Klepper) has been mapped by R. G. Schmidt in the vicinity of Elliston, Mont. In that area, the thrust system is marked by juxtaposed slabs of deformed Proterozoic Y, Paleozoic, and Mesozoic rocks that have ridden eastward over a younger sequence of north-striking Paleozoic and Mesozoic rocks that forms the western limb of the Black Mountain syncline. The thrust slabs appear to be detached and rootless, and the rocks that form them constitute a stratigraphic sequence that contrasts sharply with the sequence in the western limb of the Black Mountain syncline. Each of the thrust slabs is characterized by a unique stratigraphy, which implies that they have moved considerable distances relative to one another. The faults between the slabs are low-angle thrusts. Because these faults cut across folded beds in the slabs, at some places older strata are shoved over younger strata, and at other places younger strata are shoved over older strata along the thrust surfaces. This distinctive style of deformation is similar to the structural pattern mapped by C. A. Wallace and A. B. French along the northern margin of the Sapphire thrust system in the Garnet Range west of the Elliston area.

Facies changes and structural belts in the Proterozoic Y rocks of Glacier National Park, Montana

Preliminary results of geologic studies by R. L. Earhart in Glacier National Park suggest rapid facies changes in the lower part of the Belt Supergroup (Proterozoic Y) rocks from east to west. These facies changes are related to crustal shortening due to thrust faulting, changes of sediment sources, and the configuration of the Belt depositional basin. The Park may be divided into three structural belts that trend north to northwesterly. The eastern belt contains thrust faults and tight folds associated with the Lewis thrust fault. Strata in the central belt are gently dipping and form broad open folds. The western belt contains low-angle thrusts that cut abruptly upsection along the leading edges and high-angle normal faults that were displaced as much as several thousand meters.

Thrusting faults in Belt terrane in Montana

A large triangle of Belt terrane that has an apex in Canada is bounded on the east by the Montana disturbed belt, on the west by major thrusts and the Okanagan dome of eastern Washington, and on the south by the Lewis and Clark line (a zone of high-angle and tear faults that stretches about 300 km from Spokane to Helena). Although many thrust faults have been mapped within the apex of the triangle between the east- and west-boundary thrust zones in Canada, the apparent lack of major disturbance within the portion of the triangle located in the United States most commonly explained by an assumption that Belt terrane was largely autochthonous or parautochthonous except perhaps for the Montana disturbed belt, which might represent a special case of thrusting differing from the foreland fold and thrust belt of Canada. Summaries of Belt paleogeography and sedimentation have also largely assumed that Belt terrane was essentially autochthonous.

New geologic mapping on the Kalispell 1°×2° quadrangle, Montana, by J. E. Harrison and field revision on the Wallace 1°×2° quadrangle, Montana, by Harrison and J. D. Wells have revealed a dozen previously unmapped thrusts. Some thrusts bound major plates with significant tectonic transport as shown by the unusual abrupt changes and facies across them. The new geological data plus reinterpretation of previous geologic maps suggest that Belt terrane in the base of the triangle consists of at least six major plates ranging in width from about 40 to 70 km. Internal thrusting within major plates ranges from intense to sparse. In general, intense thrusting is near the sole, whereas the upper and distal parts of the plates show broad open folds.

Some thrusts are almost horizontal, but most dip 45° or more. They are cut by abundant horst-and-graben (basin-and-range) faults. Thus, the thrusts are highly segmented and difficult to trace in many areas, which may explain the sparsity and scattered short thrusts shown on existing maps. Some of the steeper, probably listric, thrusts previously have been interpreted as high-angle faults that have reverse drag. Increase in stratigraphic knowledge now shows significant changes across some such faults and supports reinterpretation of them as listric thrusts.

The patterns of faulting that emerge in the base of the triangle are much more compatible than previously thought with those patterns found in the apex of the triangle in Canada, and they seem to eliminate any need for a special case solution to thrusting in the Montana disturbed belt. Apparent significant tectonic transport also suggests the need for reevaluation of prior concepts of Belt paleogeography and sedimentation.

Southern extension of the Sapphire thrust system, Montana

Geologic mapping by C. A. Wallace in the southern part of the Sapphire and Flint Creek Ranges and in the northern part of the Anaconda Range has resulted in extension of the Sapphire thrust system to the south boundary of the Butte quadrangle, Montana. In the Anaconda area and to the west, Paleozoic and Mesozoic rocks are complexly folded and intensely thrust faulted. The pattern of structural deformation in this area is related to the Garnet Range thrust subsystem. West of the Georgetown Lake area, Precambrian and Paleozoic rocks are cut by imbricate thrust faults; the thrust faults are not closely spaced and the folds are broad, gently plunging structures. The structural pattern suggests that the southern part of the Sapphire Mountains and the western part of the Anaconda Range belong to the Rock Creek thrust subsystem.

In the Bitterroot Divide area of the southern Sapphire Mountains, new lithofacies of the McNamara and Wallace Formations have been mapped. The McNamara is a quartzite that contains red and green chert clasts in the Divide area. The conspicuous argillite component that typifies this unit to the north and east is absent, as are chert beds. The Wallace has become more argillaceous and sandy in the upper part where this unit is exposed in the Bitterroot Divide area. Red argillite beds present in this area have not been noted in the Wallace north or east of the Divide.

Concurrent regional faulting and silicic volcanism, Sangre de Cristo Mountains, New Mexico

A Miocene volcano plutonic complex, studied by P. W. Lipman, is associated with large-scale molybdenum mineralization and a major fossil geothermal system near Questa, N. Mex. The regional volcano-plutonic complex includes a large-volume silicic ash-flow sheet that has yielded preliminary potassium-argon and fission-track ages of 22 m.y. to 23 m.y., several petrologically diverse granitic intrusions that have yielded similar radiometric ages, and diverse older and younger lavas and volcaniclastic sedimentary rocks. A caldera-like structural depression formed during eruption of the ash-flow tuffs, which ponded to a thickness of greater than 2 km within the downdropped area. The granitic rocks largely represent crystallized late phases of the magma chamber that underlay the ash-flow caldera.

Relations between volcanic and plutonic suites are well exposed along a major north-south boundary fault between the Sangre de Cristo Mountains and the Rio Grande rift zone to the west. The caldera and adjacent areas of the volcanic field within the Sangre de Cristo Mountains also have been disrupted extensively by extreme listric antithetic faulting, causing rotation of much of the intercaldera sequence to near-vertical orientations. The fault patterns, typical of late Cenozoic extensional structures elsewhere in the Western United States, indicate a close interrelation between extension of the Rio Grande rift zone, silicic volcanism, and caldera formation in this area. This faulting occurred at the time of ash-flow eruption, as indicated both by development of extreme secondary flow structures in the ash-flow tuffs where draped across fault scarps and by paleomagnetic data obtained by J. T. Hagstrum and D. P. Elston that indicate that cogenetic granitic rocks were not rotated or extensively faulted. The Questa mine of the Molybdenum Corporation of America has mineralized rock along the margin of a granitic pluton, one of three alined along the south margin of the caldera. The entire south margin of the caldera is mineralized to some degree and appears to mark a major fossil geothermal system.

An alternative explanation for some "orogenies" in central Utah

Recent work by I. J. Witkind in central Utah along the west flank of the Wasatch Plateau has suggested that some of the angular unconformities and thrusts so common in that area may be due to movement of the evaporite-rich Arapien Formation (Jurassic) rather than reflecting localized orogenies. Former workers in the area have postulated at least a dozen separate episodes of structural unrest ranging in age from Late Jurassic into the late Tertiary. Much of the evidence, confined chiefly to the area between Manti and Salina where the Arapien Formation is best exposed, suggests that the deformation was very local. The evaporite deposits in the Arapien apparently have been moving sporadically ever since they were deposited, presumably as a result of static load or compressional forces. In this interpretation, the apparent unconformities and thrust planes could be intrusive contacts between, for example, the steeply upturned Green River Formation (Paleocene and Eocene) and the underlying Arapien Formation—the intrusive agent. Elsewhere, striking angular unconformities between near-vertical Upper Cretaceous beds and overlying near-horizontal lower Tertiary strata also may be due to the movement of the evaporite deposits. Here, upward flowage of the Arapien evaporite deposits may have bowed up the overlying Cretaceous beds. These, after beveling, were buried beneath Tertiary strata. Exhumation of this angular unconformity could be interpreted as evidence of a Late Cretaceous–early Tertiary orogenic episode. The fact that the deformation is localized and is most intense near the Arapien outcrops suggests that the evaporites, and not tectonic forces, are the cause of these "orogenies."

Gravity fault klippen of volcanic rocks, northwest Wyoming

Mapping investigations by T. M. Bown in 1977 and 1978 recorded more than 100 detachment klippen of intensely deformed Eocene volcanic rocks along the east-facing scarp of the Absaroka Range, northwest Wyoming. Mapping in 1979 increased this number to more than 150 and enlarged their area of distribution from about 1,200 km² to nearly 2,000 km². The thickest klippen are about 350 m thick.

Source rocks for most of the klippen have been identified in the middle and upper parts of the Tepee Trail Formation and in the lower part of the Wiggins Formation of middle and late Eocene age. These rocks are in place west of the klippen field where they crop out on the east-facing scarp of the Absaroka Range at elevations of 50 to 1,000 m above the field. Topographic, geomorphic, and stratigraphic relations in the southeast Absaroka Range and southwest Bighorn Basin indicate a late Neogene age for much of the gravity faulting, but this does not preclude the possibility of several earlier episodes of faulting, some perhaps as old as Eocene.

BASIN AND RANGE REGION

MINERAL-RESOURCE STUDIES

Massive zunyite rock in north-central Nevada

Massive monomineralic zunyite (hydroxy-fluoro-chloro-silicate of aluminum) rock has been reported by R. R. Coats, J. J. Consul, and S. T. Neil in northwestern Elko County, Nev. (loc. 1). The zunyite lode occurs in altered dacitic tuff of probable Tertiary age. The cryptocrystalline rock forms a N. 80° W.-trending ridge about 370 m long and as much as 10 m wide. Most of the lode consists of rock ranging in volumetric composition from 75 to 100 percent zunyite with subordinate quartz slightly coarser than the zunyite. This discovery of massive zunyite in Nevada may be the first large volume occurrence known in North America. According to Meyer and Hemley (1967), zunyite is a mineral formed during intense argillic alteration. Alunite (hydrous sulfate of aluminum) and zunyite commonly are associated, and their regional distribution is similar to that of high-fluorine felsic volcanic rocks. In addition, zunyite is associated with some porphyry copper and fluorite deposits. Although the economic significance of zunyite is unclear, it may be an important guide to economic mineralization. Signs of metallic mineralization were not seen near the zunyite lode.

STRATIGRAPHIC AND STRUCTURAL STUDIES

Metamorphic terrane in Pilot Range of Nevada and Utah

Geologic mapping by D. M. Miller in the Pilot Range of Elko County, Utah (loc. 2), has revealed an extensive terrane of moderately metamorphosed upper Precambrian and Cambrian strata that are deformed by large folds and low-angle faults. This terrane resembles parts of nearby metamorphic core complexes exposed in the Raft River and Grouse Creek Mountains in northwesternmost Utah, Albion Mountains in south-central Idaho, Ruby and East Humboldt Ranges and Wood Hills in northeastern Nevada, southern Deep Creek Mountains in west-central Utah, and northern Snake Range in east-central Nevada.

Metamorphosed strata in the Pilot Range include the Proterozoic Z McCoy Creek Group as used by Woodward (1967), Proterozoic Z and Cambrian Prospect Mountain Quartzite, and impure to pure marble sequences assigned to the Lower and Middle Cambrian. These metamorphic rocks crop out in the central part of the range in a large window (125 km²) through a décollement whose upper plate consists of unmetamorphosed Upper Cambrian through Permian strata.

Low-angle faults subparallel to bedding that eliminate section are common near the upper and lower boundaries of the Prospect Mountain Quartzite. These faults are folded along with strata into southeast vergent open

overturned folds with wavelengths of several kilometers. Small folds in low-angle fault zones are similar to the large folds, indicating that movement on low-angle faults and subsequent large-scale folding were parts of a single tectonic event with southeast-directed transport. Metamorphic fabrics were developed in association with this event, and metamorphic grades locally were as high as the staurolite zone of amphibolite facies. Strain was low in thick quartzite units, as indicated by little-deformed quartz pebbles. Pronounced deformational fabrics in pelitic and carbonaceous rocks support the hypothesis that these units locally underwent large strains.

North-trending folds and associated reverse and thrust faults related to middle(?) Tertiary plutonism and uplift of the range locally were intensely developed, and metamorphic rocks were pervasively retrogressed, suggesting that lower greenschist facies conditions were present in the deeper rocks during middle(?) Tertiary time.

Early Palezoic symmetry across southern North America

Recent detailed geologic mapping by K. B. Ketner of allochthonous lower Paleozoic eugeosynclinal rocks in the Independence Mountains and Adobe Range, Elko County, Nev. (loc. 3), and synthesis of published data from elsewhere in northern Nevada indicate that many stratigraphic units are similar to correlative allochthonous formations in the Marathon area of Texas and in the Ouchita Mountains of Arkansas. Similarities include the following: (1) Lower and Middle Ordovician quartzites in the Valmy Formation of Nevada are nearly exact counterparts of sandstones in the contemporaneous Crystal Mountain and Blakely Sandstones of Arkansas, (2) upper Middle and Upper Ordovician sequences of shale overlain by bedded chert in the Vinini Formation of Nevada are counterparts of the correlative Woods Hollow Shale overlain by the Maravillas Chert in the Marathon area, Texas, and of the Womble Shale overlain by the Bigfork Chert in the Ouachitas, of Arkansas and Oklahoma, (3) novaculite concordantly overlying Upper Ordovician chert in Nevada is the lithic and apparently temporal counterpart of the lower part of the Caballos Novaculite of the Marathon area, Texas, (4) Silurian micaceous feldspathic sandstone such as the Elder Sandstone in Nevada is the lithic counterpart of the Silurian Blaylock Sandstone of the Ouachitas, of Arkansas and Oklahoma, and (5) Devonian rocks are characteristically cherty in both Nevada and the Marathon area.

Such remarkable stratigraphic symmetry across the continent is interpreted to mean that the allochthonous rocks on both sides of the southern part of the North American continent are not randomly accreted melanges transported of converging plates from a variety of distant sources but, instead, belong to Paleozoic North America and were deposited on, or close to, the continental margin under similar environmental conditions.

Lower Paleozoic rock fragments in Antler flysch, northern Nevada

According to F. G. Poole and K. B. Ketner, unsorted subrounded to well-rounded pebbles, cobbles, and boulders of chert, argillite, siltite, fine- to coarse-grained quartzite, grit, pebbly and gritty quartzite, limestone, dolomite, and vesicular greenstone occur in a widespread mudstone and siltstone debris flow in the Lower and Upper Mississippian Chainman Shale in the northern Piñon Range in southwestern Elko County, Nev. (loc. 4). The most common clasts are chert, argillite, siltite, fine-grained quartzite, carbonate rock, and greenstone resembling lower Paleozoic formations in the Roberts Mountains allochthon to the west. One unique type of clast is gritty and pebbly quartzite containing numerous grains of feldspar, and another is limestone containing oncolites (*Girvanella*?) of probable shallow-water origin. The arkosic quartzite clasts represent the Cambrian Harmony Formation exposed in the western part of the Roberts Mountains allochthon. The source of the oncolitic limestone clasts, however, is more difficult to explain in terms of regional tectonic framework. In view of their association with Harmony clasts, they probably represent eroded Cambrian and Ordovician outer carbonate-shelf rocks exposed in Early Mississippian time in uplifted lower-plate rocks of the Antler orogenic belt to the west.

Holocene faulting, central Nevada

According to F. G. Poole, modified fault scarps in unconsolidated to poorly consolidated alluvium occur west of Alkali Flat in the northern part of Big Smoky Valley in northwestern Nye County, Nev. (loc. 5). The fault scarps, which have been traced for 4 km, lie approximately 2 km east of the Toiyabe Range opposite a bend in the range. The en echelon primary fault system trends N. 10–30° E. with scarp crests as high as 10 m. These primary faults are down on the east and parallel the range front. North-trending second-order faults along the west margin of the principal fault zone suggest left-slip movement of the primary faults, as well as vertical movement. The primary faults create favorable sites for springs and seeps where vegetation abounds. Some limonitic staining of the alluvium along the base of slope marks the trace of the primary faults. Degree of dissection, amount of rounding of the scarp crest, and slope of the scarp face suggest faulting less than 10,000 yr old.

Westward streamflow in Miocene of west-central Nevada

J. H. Stewart reported that the Miocene (11 m.y.–8 m.y.) Coal Valley Formation in the central part of the Walker Lake 2° quadrangle in Douglas, Lyon, and Mineral Counties, Nev. (loc. 6), as originally noted by M. W. Reynolds (USGS) and C. M. Gilbert (University of California) in 1973, was deposited in a basin much larger than any of the present-day valleys related to late Cenozoic basin-and-range structure, and the major basins and ranges in the quadrangle must be younger than the youngest part of the Coal Valley. Confirmation that the Coal Valley was deposited in a relatively large basin is based on 370 measurements of cross-strata orientations in fluvial sandstone layers within the formation. These current direction data indicate a relatively consistent pattern of westerly streamflow that is unrelated to present-day basins or ranges in an 80 by 30 km region extending across the north-central part of the Walker Lake 2° quadrangle. The westward current directions are toward the Sierra Nevada of California. Possible explanations of the Miocene drainage pattern are that (1) the Sierra Nevada range was topographically low 11 m.y.–8 m.y. ago, and the streams flowed westward to the Pacific Ocean, (2) the Sierra Nevada caused a deflection of the streams either to the north or south, or (3) the drainage was internal and did not flow to the Pacific Ocean.

Correlative Devonian eugeosynclinal rocks, California and Nevada

F. G. Poole reported that similar upper Lower and Middle Devonian eugeosynclinal rocks on Miller Mountain in Esmeralda and Mineral Counties of southwestern Nevada (loc. 7) and 300 km to the south in the central El Paso Mountains in Kern County of southeastern California (loc. 8) are characterized by thin to thick beds of calcareous quartz sandstone and sandy limestone. They are composed of well-rounded fine to very coarse grains of quartz, sparse plagioclase and potassium feldspar, and scattered angular grains, granules, and small pebbles of chert, argillite, and phosphorite, all set in a calcite matrix. Some beds are horizontally laminated, whereas others contain small-scale cross laminations, ripple laminations, and slump folds. At both localities, the Devonian unit is structurally interleaved with Ordovician eugeosynclinal rocks. The tectonically shuffled pseudohomoclinal assemblages of Devonian and Ordovician eugeosynclinal rocks on Miller Mountain and in the El Paso Mountains are probably parts of the Roberts Mountains allochthon emplaced in earliest Mississippian time. Rocks of the allochthon appear to be offset 200 to 300 km along an intervening northwest-trending left-lateral fault zone. Offset probably occurred in early Mesozoic time.

Controls of Pliocene and Pleistocene basaltic volcanism, southern Great Basin

At least three tectonic settings have been recognized by W. J. Carr for emplacement of Pliocene and Pleistocene basalts in the southern Great Basin of south-central Nevada and adjacent California (loc. 9): (1) small northeast-trending rift zones or relatively young basin-and-range tectonic depressions, (2) caldera ring-fracture zones, and (3) right-stepping offsets in northwest-trending right-lateral shear zones or intersections of northeast-trending faults with these zones. Combinations of some or all of the above settings may occur, or even be required, to bring basaltic magma to the surface. One of the settings may correspond to "leaky transform" faults (Weaver and Hill, 1978), which often yield basalts and which fit well into the overall Pliocene and Pleistocene stress field proposed for parts of the Great Basin (Carr, 1974; Thompson and Burke, 1973; Wright, 1976; Slemmons and others, 1979).

On the basis of present knowledge, the southern Great Basin may be zoned as to the risk of recurrence of basaltic volcanism in the following general way, from least to greatest probability: (1) areas that have experienced no Tertiary or Quaternary volcanism, (2) high-standing or positive structural blocks that were not volcanic source areas in the last 20 m.y. or were not volcanic source areas in the last 10 m.y., (3) grabens or rifts outside volcanic source areas, and (4) caldera ring-fracture zones or grabens within volcanic source areas. Special cases may exist with respect to these general risk zones; for example, resurgent domes of calderas may be less likely areas for recurrence of basaltic volcanism than areas in category 4 above. Also, in the southwestern Nevada volcanic field (Nevada Test Site region), where the volcanic rocks originating there are mainly 16 m.y.–7 m.y. old, the basin-and-range grabens have not significantly penetrated areas underlain by granitic basement rock. In other areas, such as central Nevada, where the volcanic rocks are about twice as old, basin-and-range faulting and large grabens have penetrated and broken through granitic rocks, both within and outside caldera areas.

Cretaceous thrust system, southern Nevada

Geologic mapping by R. G. Bohannon in the Muddy and North Muddy Mountains of Clark County, Nev. (loc. 10), indicates that the Muddy Mountains thrust of Cretaceous age exposed in the Buffington window in the western Muddy Mountains is continuous with the nearby east-west-trending Arrowhead fault. Bohannon interprets the Glendale thrust to the north as continuous with the Muddy Mountains thrust rather than as a structurally higher thrust. These reinterpretations of early work

by Longwell (1949) are significant because they suggest that the Muddy Mountains are in a thrust sheet above the Muddy Mountains thrust and that the North Muddy Mountains lie below the thrust. The lower plate, which includes the North Muddy Mountains, is complicated by a subsidiary fault, the Summit thrust, along which overturned Cambrian through Triassic strata have been thrust over relatively undeformed Jurassic Aztec Sandstone. The Muddy Mountains thrust sheet generally lies on relatively undeformed Aztec Sandstone, except where it overrode the upper plate of the Summit thrust in the southwest corner of the North Muddy Mountains.

These structural relations are similar to those described by Burchfiel and others (1974) for the Keystone thrust terrane 100 km to the southwest in the southern Spring Mountains. The Cretaceous Keystone thrust sheet, which occupies a structural position similar to the Muddy Mountains thrust sheet above relatively undeformed Aztec Sandstone, also locally lies on two intermediate or subsidiary thrusts, the Contact and the Red Spring.

The east-directed Cretaceous Keystone and Muddy Mountains thrusts probably were once continuous prior to offset along the Las Vegas Valley shear zone in late Miocene time (Longwell, 1974). The Contact, Summit, and Red Spring thrusts also may be remnants of a single large thrust that may have covered a wide area but was disrupted by high-angle faulting and erosion prior to being overridden by the Muddy Mountains–Keystone thrust system. Evidence suggests that these intermediate thrusts were not confined to a single stratigraphic level in their upper plates but instead climbed section eastward. Burchfiel and others (1974) suggested that the subsidiary Contact and Red Spring thrusts represent frontal parts of the main Keystone thrust which were deformed, detached from the trailing or pushing parts of the main thrust, and, subsequently, overridden by the Keystone thrust. A similar explanation may apply to the Muddy Mountains and Summit thrusts.

Metamorphic core complex, west-central Arizona

Geologic mapping by Ivo Lucchitta and N. H. Suneson in the Rawhide Mountains near the Bill Williams River in southern Mohave County, Ariz. (loc. 11) has added detailed information on the structural relations of upper- and lower-plate rocks of a metamorphic core complex previously recognized and mapped by Shackelford (1976, 1977) and studied by Davis and others (1979). The lower plate consists of lineated mylonitic quartz-feldspar gneiss. A complex allochthonous upper plate that contains interlayered fluvial, lacustrine, and volcanic rocks of Miocene age overlies the gneiss. The gneissic lower plate and nongneissic upper plate are separated by a detachment surface of regional extent (Whipple detachment fault) that dips gently northeastward and displays a penetrative cataclastic lineation also plunging gently northeastward. Northeast of the map area, upper-plate sedimentary rocks depositionally overlie Precambrian basement. This geometry is interpreted to indicate that displacement dies out northeastward because the package of detached rocks to the southwest is in depositional contact to the northeast. The relation suggests that arching along the metamorphic core complex in Miocene time resulted in southwestward movement of lower-plate rocks with respect to cover rocks. The detachment fault, which is the boundary between mobile lower-plate rocks and stationary upper-plate rocks, is at a lithologic break or preexisting structural discontinuity. Arching was accompanied by thrusting or gravity gliding off the uplifted area, as evidenced by displaced slabs within the metamorphic rocks and by megabreccia in the upper plate. These events were accompanied by listric faulting in the upper plate.

Easternmost metamorphic core complex, southern Arizona

Geologic mapping by C. H. Thormen in the Pinaleno Mountains of Graham County, Ariz. (loc. 12), has revealed a partially preserved record of a metamorphic core complex. This southeastern Arizona complex consists of a core of undeformed amphibolite facies rocks, Precambrian felsic gneisses and granitic plutons, and an Oligocene granitic pluton on its south flank (Swan, 1975). Along the base of the northern flank is a sheath of lineated mylonitic gneisses derived from Precambrian rocks in which mylonitization decreased rapidly downward. Another part of the metamorphic core complex framework includes two low-angle fault-bounded masses, referred to as the Greasewood Mountain and Underwood Canyon blocks. The Greasewood Mountain block, located at the southeast end of the range, comprises Tertiary volcanic rocks unconformably resting on Precambrian granite. Here, 23-m.y.-old quartz latite dikes in the footwall and hangings wall are cut by the fault. The Underwood Canyon block (Blacet and Miller, 1978; Bergquist, 1979), located on the northwest flank of the range near the Santa Teresa Mountains, consists of Tertiary sedimentary and volcanic rocks that are faulted over Precambrian rocks that are cut by 25-m.y.-old rhyolitic dikes. At both localities, rocks along the faults are brecciated but not mylonitized.

Present interpretation of the metamorphic core complex in the Pinaleno Mountains is that the mylonitic rocks represent a late Mesozoic décollement surface over which metamorphosed and (or) nonmetamorphosed Paleozoic and Mesozoic strata were thrust northeastward; these allochthonous rocks are not preserved

in the range but are preserved in many of the ranges containing metamorphic core complexes in Arizona, California, Nevada, and Utah. Differential uplift and erosion in early Tertiary time removed these rocks, and Eocene(?) and Miocene volcanic rocks accumulated on undeformed Precambrian rocks. Rapid uplift of the area since 23 m.y. ago caused gravity sliding of the Tertiary and Precambrian rocks off the elevated range; two such masses are preserved on the south flank of the range, but none has been found on the north side.

Dike trends and stress directions in western Arizona

According to Ivo Lucchitta and N. H. Suneson, orientation of igneous dikes of widely varying ages and composition in the Bill Williams River area in southern Mohave County, Ariz. (loc. 11), indicates the direction of least principal stress in Proterozoic Y time (1,200(?) m.y.) was north-northeast based on trends of diabase dikes; in "Laramide" time (70 m.y.–60 m.y.), it was N. 30–60°W., based on trends of aplite, pegmatite, and leucogranite dikes of presumed late Mesozoic and early Tertiary age; in middle to late Miocene time (13 m.y.–10 m.y.), it was N. 10–20° E., based on trends of rhyolite dikes; and in late Miocene time (7.5 m.y.–5.5 m.y.), it was east-west, based on trends of porphyritic olivine basalt dikes.

Cenozoic deformation, lower Colorado River area

Geologic studies by Ivo Lucchitta in western Mohave and western Yuma Counties, Ariz., and adjacent California and Nevada (loc. 13), have revealed that upper Miocene and lower Pliocene (6 m.y.–5 m.y.) rocks are distributed along the lower Colorado River as erosional remnants at various elevations above and below present sea level. The rocks were deposited near sea level in marine, estuarine, and lacustrine environments along and near the present course of the lower Colorado River from the mouth of the Grand Canyon to the Mexican border. These deposits include the marine and estuarine Bouse Formation and the lacustrine or marine Hualapai Limestone Member of the Muddy Creek Formation. Using the altitudes of these deposits, rate of uplift of the southwestern part of the Colorado Plateau with respect to sea level since 5 m.y. ago can be estimated. A profile joining the highest remnants of the deposits shows that northern reaches of the lower Colorado River region have risen at least 550 m through broad uniform upwarping at an average rate of 100 m/m.y. In addition to the 550-m upwarp, the adjacent Colorado Plateau has risen by movement along a bounding fault as much as 880 m at an average rate of 160 m/m.y. Before warping and faulting, the edge of the plateau was about 1,100 m above sea level. Near Yuma, Ariz., south of the region of uplift, the profile shows a south-sloping inflection and decrease in elevation to 1,000 m below sea level. This downwarping occurred at an average rate of 180 m/m.y. and probably was related to rifting along the San Andreas–Salton Sea fault system.

IGNEOUS ROCKS

Cretaceous volcanism, southwestern Nevada

Rubidium-strontium isochrons obtained by R. W. Kistler (USGS) and R. C. Speed (Northwestern University) for local siliceous volcanic rock units in the Excelsior and Pilot Mountains of Mineral County, Nev. (loc. 14), indicate ages, respectively, of 103 m.y. ± 5.7 m.y. and 142 m.y. ± 17 m.y. Both dated units occur in a complex sequence of terrigenous and volcanic rocks previously thought to be entirely early Mesozoic in age. The newly dated volcanic rocks of the Excelsior Mountains represent the first recognized volcanic center of Cretaceous age in the Great Basin and provide evidence that some thrusting and folding in the Excelsior Mountains region occurred in Cretaceous or later time. These dated volcanic rocks are generally comtemporaneous with recently discovered Cretaceous extrusive rocks in the central Sierra Nevada, thus suggesting that volcanism was widespread in Cretaceous time in eastern California and western Nevada.

GEOCHRONOLOGIC STUDIES

Persistent low level of Lake Bonneville during last 10,000 years

According to R. D. Miller, a radiocarbon date on shells from a humic layer in low-level fluvial and marsh deposits of Lake Bonneville in Box Elder, Davis, Salt Lake, and Utah Counties, Utah (loc. 15), supports the theory that the level of Lake Bonneville has not risen significantly above its level of about 10,000 to 11,000 yr ago. A date of 10,920 ± 150 yr on this humic layer, about 9 m above the present water level, and ostracode identification by R. M. Forester suggest that the lake had already dropped below the sample altitude and permitted fluvial and marsh deposits to accumulate. Material above the dated horizon was deposited in saline lake water when a shallow Lake Bonneville stood at the Gilbert shoreline, which is only 3 m above the dated beds and only 12 m above the present lake level. This upper material is probably equivalent to the Ridgeland Formation (Van Horn, 1979). The date agrees with those obtained earlier from Danger Cave near Wendover, Nev. (Broecker and Orr, 1958; Libby, 1955), and from the Hooper Drain near Ogden, Utah (Broecker and Kaufman, 1965; Rubin and Alexander, 1958). These two dates also support the theory of low-water level in Lake Bonneville since about 10,000 yr ago.

PACIFIC COAST REGION

OREGON

Debris flows and turbidites filling the basin of Crater Lake

A high-resolution geophysical survey was undertaken by C. H. Nelson and D. R. Thor in Crater Lake, Oreg., to study the volcanic history, heat flow characteristics, and geometry and type of sedimentation on the floor of this deep caldera lake. Since formation of the lake, about 7,000 yr ago, the basin has been receiving sediment from the caldera walls at an extremely high rate. Consequently, this closed basin provides an excellent opportunity to study turbidite facies of active density-current deposition in a small restricted basin setting.

Three depocenters were delineated—a northern, an eastern, and a southern. The eastern depocenter is the largest and contains an 80-m-thick section of sedimentary fill from the past several thousand years. Sediment type and geometry, as interpreted from seismic response, indicate the thickest sediment gravity flow deposits and coarsest sediment occur nearest the caldera walls, whereas bedding becomes thinner and sediment texture finer away from the walls, nearer the center of the basin. This geometry and texture distribution is interpreted to represent deposition by debris flows nearer the caldera walls and unchanneled turbidity-current deposition by sheet flows farther from the walls. High heat flow (D. L. Williams, pers. commun., 1979) in the southern depocenter is associated with igneous bodies that have intruded into the sedimentary fill from the floor and the wall(?) of the caldera. Faulting and surface scarps displace the sedimentary sequence indicating presently active volcanic faulting and geothermal activity of the lake floor.

WESTERN UNITED STATES

Quantitative pedology as a dating technique in the Western United States

D. E. Marchand and J. W. Harden have found that many soil properties can be used for dating Quaternary deposits and surfaces in the Western United States. Some of the more useful properties include bulk density, particle size, clay mineralogy, calcium phosphate content, dithionite-extractable iron and aluminum content, organic carbon content, and pH. Bulk chemical changes provide an especially valuable time index. Aluminum accumulates in B horizons and gives the best time plots. Si, Fe, Ca, and Mg are depleted relative to Ti with time and also yield excellent curves. Na, K, Mn, Ni, and Zr show clear but less systematic depletion with time. Depletion of zirconium with respect to titanium is particularly interesting because zirconium has commonly been assumed to be stable during weathering and is often used as an index element. Some soil properties (organic carbon, bulk density, total alumina) are especially useful for dating of young soils as they undergo a rapid initial change with time. Other properties (for example, dithionite-extractable iron, total iron, clay, calcium phosphate, total silicon) change more slowly and serve as better age indicators for older soil.

Horizon ratios, differential between horizons, and summations over the entire profile to an arbitrary depth generally yield the best plots against time. They also tend to adjust for differences in parent material and climatic-vegetation environment between chronosequences.

Rates of change in soil properties with time are nonlinear. A relatively rapid initial change is generally followed by a less rapid rate. Plots against linear time result in S-shaped curves that in many cases decrease in slope between 20,000 and 150,000 yr.

WASHINGTON

Lower to middle Eocene seamount chain, northwest Olympic Peninsula

Geologic mapping in the Cape Flattery area by P. D. Snavely, Jr., J. E. Pearl, and H. C. Wagner in the northwesternmost part of the Olympic Peninsula of Washington suggests that a chain of seamounts existed in early middle Eocene time along the present outcrop belt of the Crescent Formation and extended seaward off Vancouver Island along the so-called Prometheus High. This welt of pillow lava and breccia, with interbedded basaltic sedimentary rocks and mudflow breccias, appears to have separated two basins of deposition in which middle to middle upper Eocene deep-water sandstone and siltstone were deposited. The sedimentary rocks deposited in these two basins have markedly different lithofacies and compositions; northeast of the volcanic ridge, massive siltstone and thin and irregularly graded beds of sandstone and siltstone exist, whereas southwest of the ridge the sequence consists predominantly of medium-bedded turbidite sandstone with a few conglomerate channels. The sequence southwest of the ridge also contains thin-bedded siltstone and sandstone with interbedded lapilli tuff and mudflows consisting of a mixture of blocks of basalt and arkosic sandstone and siltstone. A study of foraminifers from both units indicates that the sedimentary rocks in both basins were deposited at bathyal depth. Based upon sedimentary structures and the distribution of lithofacies, it is theorized that the source of the sediments in the basin southwest of the seamount chain was from the west, whereas the sediments in the basin northeast of the welt were derived from the north or northeast (Vancouver Island).

Thrust faulting that occurred in middle upper Eocene time (Crescent thrust) juxtaposed lower Eocene pillow lavas (oceanic crust) and the middle to lower upper Eocene sedimentary rocks deposited in the basin southwest of the seamount chain. Upper Eocene sandstone and conglomerate overlapped the seamount ridge, as well as the Crescent thrust.

Unlike the tholeiitic basalts that form lower (lower Eocene) parts of the seamount chain, the youngest basalts extruded along the ridge are hornblende- or hypersthene-bearing alkalic basalts. In a number of places, as at Sekiu Mountain, silicified intrusive(?) basalt breccia forms large tabular masses in the upper part of the Crescent Formation.

Seismic zonation of geologic materials, Seattle area

Metropolitan Seattle, Wash., sits atop a flat-lying pile of interbedded Quaternary sand, gravel, and mudstone that is as much as 1,100 m thick in the downtown region but thins to 100 m or less some 5 km to the south of downtown, where the Quaternary sediments are underlain by steeply dipping east-west striking middle and lower Tertiary sedimentary and volcanic rocks. J. C. Yount and P. S. Mozley have investigated the subsurface nature and distribution of the major Quaternary units with the aim of developing a scheme for seismic zonation from the abundant geotechnical boring logs available from building sites and highway construction in the Seattle area.

Penetrometer data provide a convenient means to classify subsurface materials for purposes of seismic zonation. Much artificial fill, most sandy recent alluvium, and some well-sorted glacial sand units have particularly low resistance to penetration. In particular, sections of glacial advance outwash sand show low penetration resistance in the 10- to 20-m-thick zone immediately overlying impermeable mudstones, most likely due to water saturation of the sands along this contact.

D. R. Mullineaux, M. G. Bonilla, and Julias Schlocker (1967) reported that buildings damage during the April 1965 Seattle earthquake ($M = +6.5$) bore little relation to geologic units as mapped at the ground surface. Relatively severe damage occurred in areas underlain by artificial fill and alluvium, as might be expected. Less expected was the localized occurrence of severe damage on sections of compacted Pleistocene sediment in west Seattle but not on similar sections of compacted Pleistocene sediment in other parts of the city. The present study shows that west Seattle is underlain by advance outwash glacial sands which have low standard penetration near the contact with underlying Pleistocene mudstone units. Also, Tertiary bedrock underlies this contact by only 50 to 100 m beneath much of west Seattle. In other areas of Seattle, where similar low resistance sands lie above impermeable units, the depth to Tertiary bedrock is hundreds of meters to nearly a thousand meters. It is postulated that ground shaking was more severe during the 1965 earthquake where bedrock is close (<100 m) to sediments with low standard penetration than where thick compact Pleistocene sections occur between the bedrock surface and a potentially hazardous sediment section.

Diamictons of the Strait of Juan de Fuca

Sea-cliff exposures studied by D. R. Pevear at Blowers Bluff on Whidbey Island and at Point Williams along the southeast shore of the Strait of Juan de Fuca area of Washington contain pre-Vashon age diamictons whose upper surfaces are weathered. The diamictons vary laterally in texture but are in part fossiliferous glaciomarine pebbly clayey silts. In each, the upper 10 to 15 cm is dark brown (10YR 3/3) in contrast to the olive to olive gray (5Y 3/4–4/2) of the rest of the diamicton and to the olive marine silt that conformably overlies the dark brown zone. The weathered zone is interpreted as a paleosol, and laboratory data tend to support this interpretation.

Where the diamictons are sandy, the upper 60 cm is enriched in clay by a factor of 3. X-ray defraction shows striking changes from sharp peaks of mica, chlorite, and smectite in unaltered diamicton to broad peaks of chlorite and smectite in the paleosol. Considerable amounts of amorphous iron-oxide are present in the paleosol, and hypersthene is corroded and shows "cockscomb" terminations. In the fossiliferous glaciomarine diamicton, $CaCO_3$ is leached from the upper 40 cm and redeposited in the underlying 50 cm as joint fillings and concretions. The occurrence of this paleosol over a large area at a similar stratigraphic position suggests that it will be useful in resolving disrupted chronology of the middle Wisconsinan in the northern Puget lowland.

Landslide deposits, eastern Puget lowland

Reconnaissance mapping by J. P. Minard in the eastern Puget lowland between Seattle and the Skagit River showed landslide deposits to be abundant throughout that region in areas of moderate to steep slopes. Conditions leading to landsliding include high oversteepened slopes in unconsolidated surficial materials subject to stream erosion and wave action and concentrations of ground water in sediment susceptible to sapping, piping, and liquefaction above fine-grained relatively impervious layers. Many landslide-prone areas appear relatively stable at present but are subject to reactivation.

Coastal erosion and sediment transport, the Puget Sound region

Preliminary results from studies of coastal erosion by R. F. Keuler in the Puget Sound area of Washington indicate typical long term (>20 yr) recession rates of 3 to 12 cm/yr for bluffs in sheltered low wave energy areas, 7 to 20 cm/yr in zones of low to moderate wave energy, and 15 to 100 cm/yr in zones of moderate to high wave energy.

Bluff erosion provides nearly all the sediment available for longshore transport. The longshore transport system consists of many short (<15 km) littoral transport cells because of the dissected and embayed configuration of the coast. The boundaries of these cells and the directions of long-term net transport can be determined from longshore geomorphic and sedimentologic trends. Among the trends most useful for mapping are downdrift decrease in mean particle size, longshore change in sediment sorting, and downdrift increase in the degree of berm development and backshore width.

Preliminary uplift ages from fission-track studies

J. T. Whetten, R. A. Zimmerman, and C. W. Naeser collected apatite-zircon pairs from about 30 rock samples throughout the San Juan Islands and Cascade foothills in northwestern Washington for dating by the fission-track method. Practically all dates are discordant, which suggests that the samples were heated during burial to temperatures above the annealing temperature for apatite (~100°C). The apatite ages, thus, reflect the approximate time that the mineral was uplifted through the 100°C isotherm. This preliminary study suggests that uplift ages are relatively old in the southern and central San Juan Islands (>100 m.y.), somewhat younger in the northern San Juan Islands (<100 m.y., >50 m.y.), and youngest in the foothills (<50 m.y.).

Stratigraphy of the Naches Formation

Additional fission-track and potassium-argon dating of volcanic rocks by R. W. Tabor, V. A. Frizzell, Jr., and M. J. Hetherington in the Manastash Ridge area, central Washington, showed that the basal strata of the Naches Formation are about 43 m.y. old. This age agrees well with fission-track of ages 44 m.y., 45 m.y., and 44 m.y. obtained by J. A. Vance (University of Washington) from Naches tuffs in the same area. A tripartite section, from youngest to oldest, of the basalt of Frost Mountain, the Taneum Andesite, and the Manastash Formation included in the Naches Formation by earlier workers (Stout, 1964; Tabor and others, 1978), is older than the Naches Formation and appears to correlate with the Teanaway Basalt, Silver Pass Volcanics of Foster (1960), and the Swauk Formation. The basalt of Frost Mountain and basalts of the Teanaway Basalt have maximum whole rock potassium-argon ages of 47 m.y., 48 m.y., 47 m.y., and 47 m.y. Fission-track ages by zircon from welded dacite tuffs in the underlying Taneum Andesite and Foster's Silver Pass Volcanics are 52 m.y., 51 m.y., 53 m.y., 50 m.y., 51 m.y., and 49 m.y. The Naches Formation is not in depositional contact with the older rocks, which are separated by the southern extension of the Straight Creek fault and a breached anticline of pre-Tertiary metamorphic rock.

Tectonic evolution of the southeastern part of the Columbia Plateau

Eruption of the Columbia River Basalt Group centered on the dike swarm of the Grande Ronde Basalt of southeastern Washington and northeastern Oregon. V. E. Camp and P. R. Hooper have found that the Imnaha Basalt (N_0 magnetic polarity epoch) was extruded over virtually the whole southeastern part of the plateau, south and east of Lewiston, Idaho, about 17 m.y. B.P. It submerged the high relief of an east-oriented drainage system, with the most recent flows spreading west of La Grande, Oreg., and northeast into the Clearwater Embayment, Idaho. Grande Ronde Basalt (R_1, N_1, R_2, N_2 magnetic polarity epochs) followed without a break, spreading west and north to cover the Columbia Plateau in a vast plain. South of Hells Canyon, the Imnaha and Grande Ronde R_1 units thicken. In contrast, younger Grande Ronde units (N_1, R_2, and N_2) thin toward the southeast and east. The prebasalt basins in the southeastern corner of the plateau were filled by Imnaha and Grande Ronde R_1 basalt, but gradual uplift of the area by a combination of faulting and tilting had significant effect on the extrusion of all younger units. A large northeasterly dipping tectonic block was uplifted along the Limekiln fault after Grande Ronde R_2 time, forcing the younger Wanapum and Saddle Mountains Basalts to flow around the north of the block, as does the present Clearwater River. Uplift of the Blue Mountains is apparent as early as late Wanapum time with local north-trending faults developing in Oregon and Idaho. The Troy, Lewiston, and Stites Basins, together with the east end of the Blue Mountains uplift, existed throughout Saddle Mountains time. The shallow basins were filled by successive flows and interbedded lake sediments. Most faults associated with basins are subsequent to basalt extrusion.

Left lateral strike-slip riedel shears in the Yakima ridges

The Miocene Columbia River Basalt Group in the Columbia Plateau between lat 44° and 47° is deformed by seven relatively narrow (2–5 km) east-trending mobile zones (ridges) that are separated by 20-km-wide stable zones (valleys). Except for a 25-km-wide mobile zone along the Cle Elum–Wallula deformed belt (CLEW),

which obliquely crosses the plateau along the northwest-trending Olympic-Wallowa lineament, most of the plateau structures are along these uniformly spaced ridges. R. D. Bentley and S. M. Farooqui conclude that these ridges are zones of repeated thrust faulting and have monoclinal folds and commonly 10- to 200-m-wide steeply dipping zones of tectonic breccia. The ridges southwest of the CLEW trend N. 60–70° E. and have left-lateral en echelon folds crossing N. 80° E. across the ridges. The Tygh Ridge, Columbia Hills, Toppenish, and Yakima Ridge structures locally have left-lateral faults exposed along the ridges. The Columbia Hills, Simcoe–Horse Heaven Ridge, and Yakima Ridge structures have folded thrusts and demonstrable multiple phase deformational histories that began in Grande Ronde Basalt time (15 m.y.–16 m.y.). The ridges northeast of CLEW (Saddle Mountains and Frenchman Hills) have a similar geometry and multiphase tectonic history but have a N. 80° W. trend. The seven ridges may mark the position of fundamental riedel shears that first formed in early Miocene time by left-lateral strike-slip fractures in a north-south compressional stress system. These fundamental riedel fractures served as slip zones in later deformation, localizing most thrusting, folding, and subsequent minor left-lateral movement.

Holocene faulting, Toppenish Ridge

R. D. Bentley (USGS) and N. P. Campbell (Yakima Valley Community College) have mapped Holocene faults paralleling the Toppenish Ridge anticline for 32 km between 120°20′ and 120°45′ southwest of Toppenish, Wash. Approximately 95 surface ruptures with 0.5 to 4.0 m vertical displacement occur in 3 sets along the summit (S set), north slope (NS set), and north alluvial fan (NA set) of the ridge. The fault zone ranges in width from 0.5 to 2.2 km. As many as 12 surface ruptures occur in one highly faulted north-south profile. Most ruptures strike N. 85–90° E. and are en echelon to the N. 70–75° E.-trending Toppenish Ridge anticline. Most surface ruptures have south-facing scarps with the south side down. The ruptures vary in length from 0.1 to 9.0 km; most are less than 1 km long, and six extend for greater than 3 km. Most ruptures in the S and NS sets are high angle faults; five ruptures in the NA set are low angle. Ten en echelon grabens occur along the NA and NS sets. Sag ponds and disrupted drainage features are common along many of the surface ruptures. Landslides are closely associated with the ruptures. The S and NS sets cut Holocene(?) loess. The NA set cuts glaciofluvial slack water deposits possibly correlative with the "Touchet beds," which elsewhere contain Mount St. Helens tephra (S set ^{14}C date of 12,800 B.P.). Locally, post-"Touchet(?)" alluvial fans are cut by the NA set. NS faults cut bedrock units of Miocene to Pliocene age. The NA set is in the thrust zone of older Toppenish Ridge fault. Faults in the S and NS sets are interpreted as extension features formed in the older anticlinal hinge area. The pattern of the faults is consistent with a deep-seated left-lateral strike-slip fault paralleling Toppenish Ridge in a north-south (σ_1) compressional zone.

Miocene deformation and canyon cutting at Grayback Mountain

J. L. Anderson has found that flows of the Columbia River Basalt Group reveal a complex history of deposition and deformation near Grayback Mountain, along the Klickitat River adjacent to the Cascade Range in south-central Washington. Grayback Mountain is a structural high on the Simcoe–Horse Heaven anticlinal ridges, which trend N. 7° E. for 200 km from the Cascade Mountains to the Pasco Basin. The Klickitat River has eroded nearly 1 km into the asymmetric (steep to the north) anticlinal ridge, exposing the Grayback Mountain thrust fault and three intracanyon flows of the Frenchman Springs Member of the Wanapum Basalt. These flows, exposed north of the thrust, partly filled an ancient Klickitat River canyon carved into a structural high in the Grande Ronde Basalt; the ancient canyon was more than 400 m deep, extending through at least 200 m of reversely magnetized flows underlying normally magnetized flows. The structural high resulted from faulting that predated the thrust and major folding at Grayback Mountain. This initial episode of faulting occurred after Grande Ronde time (14.5 m.y.–16 m.y.) but before Wanapum time (13.5 m.y.–14.5 m.y.). The resulting high was probably related to uplift of the Cascade Mountains along a north-northeast trend and may be regionally significant, as it took place at a time when the chemistry of the Columbia River Basalt Group changed from relatively high SiO_2, FeO, and TiO_2 compositions (Wanapum Basalt). Subsequent deformations associated with the Simcoe–Horse Heaven anticlinal ridges resulted in thrusting of the Grande Ronde Basalt over the Frenchman Springs Member at Grayback Mountain.

Geometry and tectonic evolution of the Columbia Hills

The Columbia Hills anticline is a N. 70° E.-trending mobile zone 5 km wide and 240 km long crossing the Cascade Mountains and Columbia Plateau just north of the Columbia River. R. D. Bentley, Jack Powell, J. L. Anderson, and S. M. Farooqui have found that this zone consists of many N. 80° E. doubly plunging folds 1 to 5 km long that lie en echelon to the main structural trend. These folds plunge east and decrease in amplitude from 1 km near Lyle, Wash., to 0.1 km near Wallula Gap, Wash. This segmented fold pattern is distorted by later northwest-striking right-lateral faults and associated

folds with a N. 10° W. to N. 60° W. trend. Most of these younger structures have less than 100 m of structural relief and occur near, but not precisely at, the ends of the fold segments. The Wishram thrust fault occurs at the base of the steep asymmetric limb of the Columbia Hills anticline from Roosevelt westward to Wishram. West of Wishram, the anticline is asymmetrically steep to the north, with the Ortley fault along its north limb. The Ortley fault is an oblique slip (left-lateral) fold and fault zone that distorts the older Wishram thrust. Both faults may have nearly 2 km of structural shortening across their complex fault zones, which contain one or more slices of Grande Ronde Basalt juxtaposed against Ellensburg Formation. The Columbia Hills structures are consistent with a north-south compressional model in which deep seated left-lateral strike-slip faulting (N. 70° E.) localized the mobile zone. This zone has been subjected to extensive thrusting during Grande Ronde time (15 m.y.) and, subsequently, in Ellensburg time (later than about 10 m.y. in this area). The latest compressional phase had extensive right-lateral movement along the N. 30–60° W.-striking faults, as well as thrusting along the main N. 70° E. trend (3.5 m.y.–10 m.y.)

CALIFORNIA

Middle Wisconsinan Marine platform at Point Delgada

D. H. Sorg, R. J. McLaughlin, S. D. Morrison, and J. A. Wolfe have recently studied marine terrace deposits at Point Delgada, northern California. Point Delgada is near the northern termination of the San Andreas fault, adjacent to where it bends westward to join the Mendocino fracture zone. At this locality, a marine platform (2–3 m above sea level) cut upon bedrock of the Franciscan coastal belt complex is overlain by 0.5 to 2 m of wave-worked pea gravel that is, in turn, directly overlain by 10 m of moderately bedded fluvial gravel (poorly sorted angular clasts) and silt. Lenses of gray sandy silt at the base of the fluvial deposits contain abundant woody plant debris, including cones of spruce (*Picea breweriana*), indicative of a climate cooler than the present. Wood debris from this horizon yields a radiocarbon age of $34{,}380^{+730}_{-670}$ yr, and charcoal from a mudstone lens 5 m higher in the section yields a radiocarbon age of $29{,}030^{+610}_{-570}$ yr. Extrapolation of the sedimentation rate between these two horizons (about 1 m/1,000 yr) yields an approximate age of 24,000 yr for the uppermost fluvial deposits in the section. A flat surface cut into the top of these sediments may be as young as Holocene.

The 34,380-yr radiocarbon age for the base of the fluvial deposits establishes a minimum age, perhaps the approximate age of the underlying wave-cut platform. According to the sea-level curve of Bloom and others (1973), sea level was about 70 m below its present position 34,000 yr ago. If the tentative age of about 34,000 yr for the wave-cut platform is correct, the average tectonic uplift rate since middle Wisconsinan time has been about 2 m/1,000 yr in this region. This relatively high rate is consistent with uplift rates inferred elsewhere in California adjacent to large bends in the San Andreas fault.

Constraints placed upon location of the San Andreas fault by base and precious metal sulfide mineralization, Point Delgada, northern California

R. J. McLaughlin, D. H. Sorg, J. L. Morton, J. N. Batchelder, R. A. LeVeque, Chris Heropoulos, H. N. Ohlin, and M. B. Norman II have studied a previously unknown occurrence of base- and precious-metal sulfide mineralization along the San Andreas fault zone. At Point Delgada, in northern California, banded sulfides including argentiferous galena, sphalerite, pyrite, and chalcopyrite occur locally in veins along normal and left-lateral faults that dip steeply and strike N. 40° to 70° E. The sulfides are associated with a quartz-carbonate-adularia gangue, and the veins cut the upper part of an ophiolite and overlying Paleogene and Neogene rocks of the coastal belt of the Franciscan assemblage. Remobilization of the sulfides and mineralization of the northeast-striking faults probably are associated with middle Miocene basaltic volcanism.

Fluid inclusions in the vein quartz have low to moderate salinities and filling temperatures of 230° to 270°C. Based on the curves of Haas, depth of mineralization must have been greater than 600 m. Adularia in the vein assemblage has a potassium-argon age of 13.8 ± 0.4 m.y., which is also a minimum age for the northeast-striking fault set.

The mineralized northeast-striking faults intersect and are crossed with little or no offset by a steeply dipping northwest-striking fault that has been regarded by numerous workers as the northernmost onland extension of the San Andreas fault and is shown as such on most published geologic maps. However, the mineralization age and intersecting conjugate relation of the northeast-trending faults indicate that no significant offset has occurred along this purported San Andreas fault trace since late middle Miocene time. Because no evidence of a major active trace of the San Andreas fault is known immediately east of Point Delgada, the main San Andreas fault zone must lie offshore, west of Point Delgada.

Sedimentology of the Neogene Little Sulphur Creek basins

Mapping in Sonoma County, Calif., by T. H. Nilsen, R. J. McLaughlin, E. A. Griffin, and G. G. Zuffa showed the

Little Sulphur Creek basins developed in the Pliocene or later, as a response to right-lateral strike-slip faulting along the Maacama fault zone. These basins are filled primarily by coarse alluvial fan deposits but also contain fluvial, lacustrine, deltaic, and talus accumulations. Freshwater mollusks and ostracodes, as well as abundant plant material, have been recovered. Abundant synsedimentary slumps, faults, liquefaction features, and minor angular unconformities indicate penecontemporaneous tectonism and seismicity. Paleocurrent and maximum clast-size data indicate transport of coarse debris into the basins from the fault-bounded southwestern and northeastern margins, as well as longitudinal northwestward transport down the basin axes. Clast size in general decreases toward the basin centers and northwestward along the basin axes. The marginal facies consist primarily of megabreccia deposited as talus and landslide debris and conglomerate deposited by subaerial debris flows as small alluvial fans and cones. The longitudinal fill consists primarily of conglomerate and sandstone deposited by larger northwest-prograding alluvial fans in which debris-flow-dominated highly channelized inner-fan deposits grade northwestward into streamflow-dominated less channelized middle-fan deposits and nonchannelized outer-fan deposits. Fossiliferous lacustrine deposits in two basins consist of basin and plain-type turbidites that grade laterally into marginal distal alluvial fan deposits, fan deltas, and Gilberta-type sublacustrine deltas. Conglomerate clasts and sandstone petrography indicate derivation from surrounding Franciscan graywacke, ophiolite, and melange. The sandstone is typically subangular poorly sorted litharenite with phyllosilicate cement, where fluvial in origin, and carbonate cement, where lacustrine in origin. The pattern of sedimentation resembles that of much larger pull-apart basins such as the Ridge Basin in southern California along the San Andreas fault.

Upper Mesozoic rocks of the Wilbur Springs antiform

Northeast of Clear Lake in northern California, the Coast Range thrust is folded into the southeast-plunging Wilbur Springs antiform. R. J. McLaughlin, D. J. Thormahlen, J. W. Miller, and Christina Carlson foung that the upper plate of this thrust consists of highly disrupted Jurassic ophiolite, which locally is a mudstone-matrix ophiolite melange, overlain by Upper Jurassic (Tithonian) through Lower Cretaceous (Valanginian) conglomerate, sandstone, mudstone, and sedimentary serpentinite breccias of the Great Valley sequence that are folded around the nose of the Wilbur Springs antiform. The overlying Upper Cretaceous Great Valley strata to the east are apparently unaffected, possibly indicating that folding occurred before Late Cretaceous time.

Rocks of the Franciscan assemblage that consist of asymmetrically to isoclinally folded slate and minor phyllite, with rare included blocks of metachert and mafic metavolcanic rocks, are exposed in the core of the Wilbur Springs antiform. These rocks are weakly to highly metamorphosed texturally and contain trace amounts of lawsonite or pumpellyite. A Tithonian to Valanginian Age for the rocks of this Franciscan core unit is indicated by fossil collections from several localities. Axial-plane cleavage associated with the largely southeast-plunging isoclinal folds in the slate generally parallels the plunge of the Wilbur Springs antiform, suggesting that the folds formed in response to northeast-southwest compression that was similar in orientation to that which formed the Wilbur Springs antiform. Emplacement of the Franciscan core rocks beneath the Coast Range thrust postdated Valanginian time.

The southwest limb of the Wilbur Springs antiform is laterally sheared along a major N. 40° W.-trending fault zone, active as recently as Pliocene and Pleistocene time. This fault zone separates the slaty rocks of the antiform core from medium- to coarse-grained lawsonitic metagraywacke with prominent thick lenses of metachert and minor metatuffa on the southwest (probably equivalent to the Tithonian to Valanginian Yolla Bolly terrane).

Postmiddle Miocene accretion of Franciscan coastal belt rocks to northern California

R. J. McLaughlin, S. A. Kling, R. Z. Poore, K. A. McDougall, H. N. Ohlin,, and E. C. Beutner have found that deformed rocks in the King Range south of Cape Mendocino, Calif., overlie Upper Cretaceous Coniacian to Campanian ophiolitic basement whose upper part is well exposed along the coast at Point Delgada. These rocks of the Franciscan coastal belt are dominantly a broken formation of argillite and sandstone of arkosic to andesitic volcaniclastic composition that represent sedimentary facies of the inner to outer continental slope. Radiolarians, pollen, and planktic and benthic foraminifers indicate that the oldest rocks are of middle Miocene age—younger than any rocks yet reported from the Franciscan assemblage.

Partially coeval middle Miocene (Relizian) to Quaternary rocks, representing sedimentary facies of the inner shelf to outer continental slope, are present in the Humboldt Basin and adjacent isolated fault-bounded slivers north of the King Range. Wide zones of the penetrative shearing that probably delineate a middle Miocene or younger suture separate the deep-water Franciscan

rocks of the King Range from less severely deformed Neogene rocks of Humboldt Basin.

The King Range terrane appears to be a displaced fragment of oceanic basement that is overlain either structurally or depositionally by upper Paleogene(?) to Neogene sedimentary and igneous rocks of continental and oceanic derivation. This terrane was displaced an unknown distance and was accreted to California <15 m.y. ago, before or perhaps during northward passage of the Pacific–Farallon–North America plate junction.

Fault creep in Mendocino County, California

Seismic fault creep was documented by E. H. Pampeyan at two localities in Mendocino County, Calif., on fault breaks within the Maacama fault zone. Photogeologic studies and reconnaissance field mapping in the fault zone led to the discovery of two fault breaks showing evidence of current activity. Subsequent surveys by P. W. Harsh, E. H. Pampeyan, and J. M. Coakley showed offset cultural features; setting and monitoring of reference marks across the fault breaks verified the existence of creep and established a slip rate of 2 mm/yr.

Tectonism and plutonism, northwestern Sierra Nevada

Detailed geologic studies in the Feather River area of northern California by A. M. Hietanen-Makela suggest that the movement along major fault zones was underthrusting to the east of several coherent lithologic units. This underthrusting resulted in tectonic accretion to the continental American plate of island arcs, interarc and marginal basin floors, and slabs of oceanic crust and mantle. Subduction of the Pacific Ocean floor that later became a marginal basin floor and is now covered by the Calaveras Formation began along the Melones fault in Devonian time and continued to the Jurassic. The main late Paleozoic and early Mesozoic subduction was along the Big Bend fault zone where a wide zone of imbricated melange was formed (the Horseshoe Bend Formation); island-arc volcanism to the east (the Franklin Canyon Formation) was a result of this subduction. The two major sutures, the Melones and Big Bend fault zones join south of lat 38°30′ to form a major structural zone with melange bounded by the Melones and Bear Mountain faults. On a megascale, the regional structure between lat 38°30′ and 40°30′ is characterized by a similar imbricated and lensoid fault pattern, as typical of the Horseshoe Bend Formation. The width of this system of major sutures in the western Sierra Nevada is 7 km at lat 38°30′ and 40 km near lat 40° where its southerly trend turns to northwest towards the Klamath Mountains. Here the Rattlesnake Creek melange (Irwin, 1977) has the same tectonic position as the Horseshoe Bend Formation in the Feather River area. Both melanges are separated by a major suture from the Upper Jurassic rocks on the west and are in fault contact with a metavolcanic belt on the east. The ultramafic rocks shown on the geologic map of California (Jennings, 1977) on the western edge of the Sierra Nevada batholith between 36° and 37°, line up structurally with the southern continuation of this system of sutures and are probably remnants of trench-related ophiolite.

The late Paleozoic to Jurassic structures in the Feather River area are modified and cut by Upper Jurassic to Lower Cretaceous plutons. The plutonism between the Melones and Big Bend fault zones started in Late Jurassic (160 m.y. ago) at the time of volcanism on the west side of the Big Bend fault zone and continued into the Cretaceous. The Jurassic to Cretaceous magmas were formed by subduction along fault zones in the Coast Ranges and show a slight increase in potassium with time.

Tertiary hypabyssal intrusions, Sierra Nevada

Clyde Wahrhaftig reports that a series of laccolithlike and sill-like hypabyssal intrusions (mainly hornblende andesites) was intruded along the basal contact of the Tertiary sequence in the mountains south of Kennedy Creek in the northern part of the Tower Peak 15-min quadrangle in the Sierra Nevada, Calif. The intrusions lifted both the Miocene Merhten Formation and remnant patches of the Oligocene part of the Valley Springs Formation several hundred meters, locally. In places, the intrusion was along sheeting joints in the underlying Mesozoic granite at Sonora Pass, and a thin shell of granite weathered in early Tertiary time was lifted along with the overlying Tertiary rocks. These intrusions apparently account for the so-called normal fault offsets originally thought to exist along Kennedy Creek.

Uplift and tilt of the Sierra Nevada

Tilted stratigraphic planes and dated volcanic rocks have been used by N. K. Huber for new estimates of the amount and timing of uplift of the central Sierra Nevada, Calif. His analysis indicates that the San Joaquin River flowed from the Mono Basin area across the range until its channel at the present drainage divide was blocked by basalt erupted somewhat more than 3 m.y. ago. The site of Deadman Pass on the present drainage divide was uplifted approximately 3,400 m since deposition of the Eocene Ione Formation, about 2,150 m since eruption of a 10-m.y.-old trachyandesite in the Sierra Foothills, and 950 m since about 3 m.y. ago. The current rate of uplift at Deadman Pass is probably about 0.33 mm/yr and appears to be accelerating.

Volcanic greenschist in the subsurface of the southeastern San Joaquin Valley

Reexamination by D. C. Ross of more than 100 thin sections made in the 1940's from basement samples from oil wells in the southeastern San Joaquin Valley (largely from the Edison oil field) revealed a widespread, and until now largely ignored, greenschist terrane. Inexplicably, many of these rocks originally were described as containing orthopyroxene and clinopyroxene, which suggested that they were moderate- to high-grade metamorphic rocks. In reality, most of these rocks are "classic" volcanic greenschists composed chiefly of sodic plagioclase, chlorite, actinolite, and epidote; in part, these rocks preserve relict volcanic textures. These rocks may be related to the nearby surface exposures of the Pampa Schist of Dibblee and Chesterman (1953), but greenschist and low-grade amphibolitic rocks are not found at surface exposures at this latitude. This suggests, not surprisingly, lower metamorphic grade westward away from the main batholithic masses of the Sierra Nevada. More importantly, these greenschists may be a preserved part of the low-grade metamorphic belt of the Sierra Nevada foothills that is abruptly cut off by batholithic rocks about 200 km to the north. Possibly these greenschists are related also to ophiolitic remnants south of the foothills belt.

Source terrane for basement clasts of the Temblor Range

The source of granitic and metamorphic boulders in conglomerates of the Santa Margarita Formation of upper Miocene age in the Temblor Range of central California has long been a problem. The source terrane for these conglomerates, which butt against the eastern side of the San Andreas fault, presumably has been "beheaded" by lateral fault movement. The most recent model suggests that these conglomerates were derived from the basement terrane of the Gabilan Range. D. C. Ross has collected and studied a large number of clasts from these conglomerates, and these studies suggest some problems with the correlation model, particularly with regard to the metamorphic rocks. Dark metavolcanic clasts with readily visible volcanic textures, dark andalusite (chiastolite) hornfels, and a coarse trachytoid rock type are widespread in the Temblor Range conglomerates, but these rock types never have been reported from the Gabilan Range or from anywhere in the Salinian block. This suggests either that these rock types lie buried somewhere in the Salinian block or that the Salinian block is not a suitable source for the Temblor Range clasts. The former is possible, but the size of clasts (as much as 7 m) suggests an area of substantial relief, and the volume of sediment suggests the erosion of some 165 km^3 of bedrock—it is not easy to visualize the burial of such a positive area in this region since the late Miocene. The latter possibility suggests that source terrane has "sailed off" much greater distances than normally associated with San Andreas fault lateral movements. Neither alternative is particularly persuasive.

Southern Sierra Nevada uplift history

Working in the eastern San Joaquin Valley area of southern California, J. A. Bartow found that the scarcity of Tertiary deposits in the southern part of the Sierra Nevada has hindered analysis of the unlift history of the range, but nonmarine coarse clastics in the Tertiary strata at the southeastern margin of the San Joaquin Basin provide some evidence bearing on Sierran uplifts.

The Bealville Fanglomerate of Dibblee and Chesterman (1953) and correlative Tecuya Formation of late Eocene(?) to early Miocene age provide the earliest evidence of possible tectonic activity in the southern Sierra. These coarse alluvial fan deposits suggest a strong uplift of the area east or southeast of the south end of the present San Joaquin Valley.

The Miocene Bena Gravel also represents alluvial fans that prograded westward into the San Joaquin Basin and probably records an episode of strong uplift of the Sierran source area. A basal paralic facies of the Bena Gravel is as old as early Miocene, but the bulk of the alluvial fan facies is probably middle Miocene in age.

Both the Bealville Fanglomerate of Dibblee and Chesterman (1953) and the Bena Gravel are restricted to the area south of the Bakersfield arch; equivalent strata along the basin margin to the north are generally thinner and finer grained. This suggests that the Bakersfield arch, whatever its origin, formed an important tectonic boundary during early and middle Tertiary time.

A major regressional trend began at the end of the middle Miocene and continued into the Pleistocene with only relatively minor transgressional "kick-backs" in the late Miocene and early Pliocene. The resulting progradation of alluvial fan deposits into the basin appears to reflect accelerating uplift in the Sierras.

Upper Quaternary stratigraphy and structure of the Antelope Valley and vicinity, California

Studies by D. B. Burke in the Antelope Valley area of southern California of alluvial materials and the soils developed upon them indicate that deposition in the valleys and canyons of the area occurred largely during the major glaciofluvial episodes of the past 0.5 m.y. in conjunction with episodic and irregular rise of the San Gabriel and Techachapi Mountains and depression of structural basins beneath Antelope Valley on many active structures. Correlation based on geomorphic sequences of deposits and their soil catenas permits

relative dating of time of activity on faults and growing folds of the area, as well as comparison with alluvial sequences elsewhere in the Southwestern United States.

Deposits of the three oldest alluvial episodes occur as eroded remnants in canyons and on the mountain flanks and are apparently correlative with the Riverbank Formation of the San Joaquin Valley in central California. Substantial textural B profiles in their preserved depositional surfaces and red (5YR) soil colors indicate deposition prior to, and soil development during, the Sangamon interglacial interval. Deposits of the two next youngest intervals, with modest textural B soil profiles and brown (7.5YR) colors, occur as lower terraces upstream from and adjacent to young alluvial canyon fill and fans and are apparently correlative with the Modesto Formation of the early Wisconsinan glacial interval in the San Joaquin Valley. Young deposits in the canyon and valley bottoms of the area have little or no soil profile development and were deposited during and since the last Tioga glacial advance in the Wisconsinan interval.

Distribution and deformation of upper Quaternary deposits show that the north-central flank of the San Gabriel Mountains in the big bend of the San Andreas fault is being thrust and folded northward along a zone of structures over tectonic basins beneath the Antelope Valley. Deformation to the north and east of the valley in the west-central wedge of the Mojave Desert takes place on numerous small faults in right- and left-lateral conjugate systems. The southern flank of the Tehachapi Mountains to the northwest of the valley is rising as a southward-tilted block that is broken into rhomboid pieces by conjugate right- and left-lateral faults and northward-directed thrust faults.

Local warping over distances of several kilometers in the Antelope Valley during Holocene time is as much as 1 mm/yr. Uplift of the San Gabriel Mountains above the valley during the late Quaternary is as much as 3 mm/yr. Net late north-south shortening of the western Mojave wedge between the San Andreas and Garlock faults is probably about 0.01 microstrain per year.

Southern California borderland—environmental geology

A new tectonic model has developed by H. G. Greene, S. H. Clarke, Jr., and M. E. Field to explain the origin of structures in the Gulf of Santa Catalina in the southern California borderland. Interpretations of marine geophysical data and sea floor samples indicate that late Tertiary to Quaternary structural evolution of the Gulf of Santa Catalina is dominated by wrench-fault tectonics that formed the newly named "Catalina sliver." The "Catalina sliver" is a linear wedge of ductile sedimentary crust that has been elongated by differential rates of movement along its bounding fault zones, the Newport–Inglewood–Rose Canyon fault zone on the east and the Palos Verdes Hills–Coronado Banks fault zone on the west. Wrench-fault tectonics also produced compressional and dialational structures (horst and graben) within and adjacent to the "sliver." Because wrench-faulting is presently active, conjugate faults, as well as the primary fault zone, displace Quaternary sediments and locally offset the sea floor. La Jolla Canyon is a graben or tensional feature produced by wrench-fault tectonics, and Scripps Canyon appears to be a displaced head of La Jolla Canyon that resulted from right-slip along the Newport–Inglewood–Rose Canyon fault zone.

Mylonitic gneisses over a Cretaceous(?) pluton, Iron Mountains, southeastern California

Geologic mapping by D. M. Miller and K. A. Howard showed that a porphyritic granite pluton in the Iron Mountains, Calif., is deformed near its top where it grades into a mylonitic gneiss sheath, thicker than 1,300 m, with foliation dipping gently northwest and S. 80° W. lineation. Mylonitic gneisses of similar style and age(?) occur 80 km east in the Whipple Mountains, 15 to 65 km north in the Old Woman Mountains, and 10 km south in the Granite Mountains. The pluton in the Iron Mountains has a minimum potassium-argon age of 67 m.y. Its upper deformed part is interlayered with metasedimentary gneiss. The overlying mylonitic gneisses comprise three compositions similar to phases of the granite. Intrusive relations indicate that granite and metagranite units are successively older upward. Development of lineation increases upward. Crosscutting dikes in mylonitic gneisses contain the mylonitic fabric but generally are not folded. Mylonitic lineations developed in nearby mountains are oriented differently than those in the Iron Mountains, in contrast to the consistently oriented lineations observed in the Whipple Mountains and vicinity. Because the pluton is increasingly strained upward and compositionally similar to mylonitic gneisses above, much of the strain was probably related to pluton emplacement. A model in which crystallized hot borders of a pluton are flattened in sheath above a rising molten diapiric core is suggested.

Tectonic attenuation of Paleozoic rocks, southeastern California

In the Big and Little Maria and Riverside Mountains of southern California, being studied by W. B. Hamilton, the entire cratonic section of the Paleozoic is widely exposed and was metamorphosed and deformed both during and after the intrusion of Jurassic plutons. Because of the distinctiveness of the Paleozoic formations (Bolsa Quartzite, Bright Angel Shale, Muav Limestone, Martin (?) Limestone, Redwall Limestone, Supai Formation, Hermit Shale, Coconino Sandstone, and Kaibab Lime-

stone) and the continuity of their original stratigraphy, they can be recognized at all stages of metamorphism and deformation. The sandstones have been metamorphosed to quartzite; the limestones, to marble; and the shales, to schist. Ubiquitous isoclinal deformation was accomplished by transposition by discontinuous laminar flow, rather than by concertina compression. The metamorphosed Paleozoic section in most places is much attenuated tectonically. The entire section, with all formations easily recognizable and in stratigraphic order, has a total thickness of about 10 m and, hence, has been attenuated to less than 1 percent of its initial stratigraphic thickness for an outcrop length of several kilometers on the limb of one large isocline in the Big Maria Mountains. Individual formations, particularly the calcite marble, undergo still more attenuation locally while maintaining stratigraphic continuity. The Redwall Limestone, for example, had an initial thickness of about 100 m, is thinned to as little as 20 cm, yet maintains stratigraphic position and continuity and its typical metamorphic lithology and appearance.

Early large structures are characterized by range-sized upright isoclinal synclines, bounded on both sides by Jurassic granodioritic plutons (dated by L. T. Silver, California Institute of Technology), involving both Proterozoic basement rocks and lower Mesozoic clastic and volcanic rocks. These early folds apparently record drag by the rising plutons. Mountain-sized recumbent isoclines and gently dipping foliation are superimposed across all of the older rocks and their contacts. Vergence of major and minor structures is consistently northeastward in both limbs of each large syncline. This second deformation may record gravitationally driven eastward spreading of the midcrust in response to emplacement of large Cretaceous batholiths nearby to the west. The most extreme attenuation occurs where Cretaceous attenuation of perhaps 10:1 is superimposed on Jurassic attenuation of a similar amount.

Quaternary deformation in southern part of Elsinore fault zone

Mapping by V. R. Todd on the Elsinore fault zone, southern California, south of lat 33°7'30", indicates that the zone has been dominated by vertical tectonics since middle Pleistocene time. The eastern margin of the Santa Ana block consists of three northwest-striking fault-bounded segments, each up on the southwest. The fault zones, en echelon to the southeast, are the Chariot Canyon–Oriflamme Canyon zone, the Laguna Mountains escarpment zone, and a zone that includes frontal faults of the northern Jacumba Mountains. On the northeastern side of the Elsinore fault zone, Granite Mountain and the Vallecito Mountains were uplifted relative to the Chariot and Oriflamme Mountains and to the Mason, Vallecito, and Carrizo Valleys on the southwest and south, along a curving zone of dip-slip faults. The valleys form a graben bounded by normal and reverse faults that displace late Pleistocene and Holocene alluvial fans. Middle Cretaceous batholithic contacts cross the fault zone with no more than 2-km cumulative right-lateral offset.

Volcan Mountain is a horst bounded on the southwest by northwest-trending faults in Rodriguez and Banner Canyons and on the east by north-northwest faults that cross alluvial cones. In the northeastern wall of Banner Canyon, brecciated crystalline rocks overlie alluvial gravels with a flat contact. Northwest-striking faults are younger than the overridden alluvium. Dip-slip faulting has exposed three other areas of crushed crystalline rocks overlying Pleistocene and Holocene sediments along the Elsinore fault zone as far south as the frontal fault of the western Coyote Mountains. Their distribution along the fault zone suggests an origin as gravitational slide masses emplaced during an earlier period of block faulting.

Glacier snowlines and uplift of the San Bernardino Mountains

The snowline of the last glacial maximum (18,000 yr B.P.?) in the San Bernardino Mountains was determined by D. G. Herd and B. C. Cox to lie only 160 m below that of a readvance that, based on soil development and weathering criteria, appears to be the last Pleistocene ice advance (10,000–12,000 yr B.P.). The snowlines of the two ice advances are abnormally close in altitude. Several studies of equilibrium-line altitudes of former alpine glaciers in different hemispheres suggest that the snowlines of the two late Pleistocene glaciations should be separated by 300 to 450 m. The 140- to 290-m snowline compression could reflect an anomalously severe cooling of southern California between 10,000 to 12,000 yr ago (for which there is no climatic evidence). Alternatively, the close proximity of the two snowlines could represent uplift of the range (and a resulting apparent drop in snowline) between 10,000 and 18,000 yr B.P. The calculated rate of uplift (18–36 mm/yr) would be one of the fastest documented but would equal the 13 to 20 mm/yr uplift determined in the Western Transverse Ranges north of Los Angeles (Sarna-Wojcicki and others, 1979; Yerkes and others, written commun., 1980).

ALASKA

Significant new scientific and economic geologic information has been obtained from field and topical investigations conducted throughout Alaska during the past year. Discussions of the findings are grouped under seven subdivisions corresponding to six major

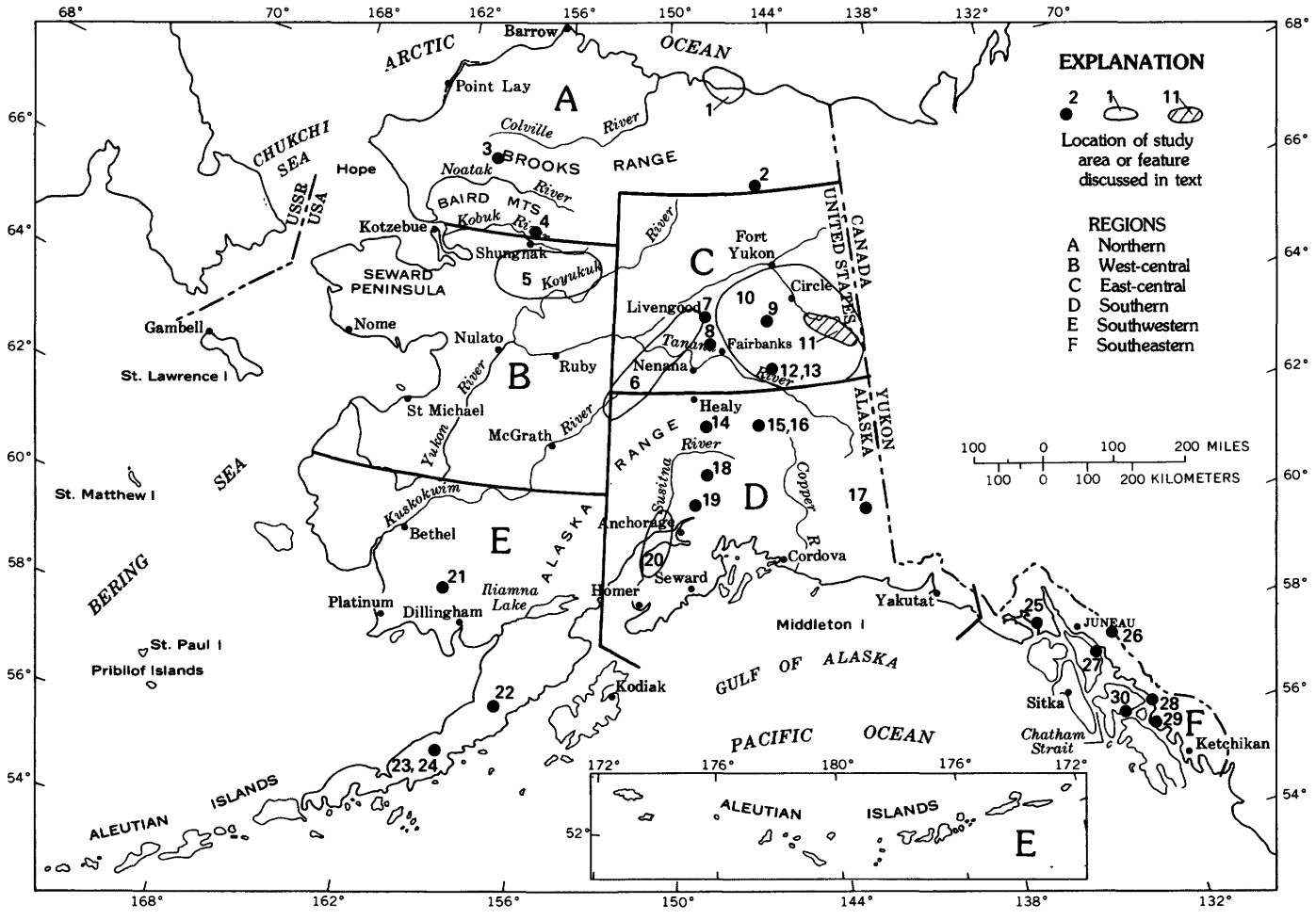

geographic regions and a general statewide category. Outlines of the regions and locations of the study areas are shown on the accompanying index map of Alaska.

STATEWIDE

Levels II, III, and IV mineral resource appraisals of Alaska

Because pending land decisions in Alaska, 90 percent of which currently are under Federal management, will affect the allocation, accessibility, and development of Alaska's vast lands and natural resources for generations, there is an urgent and growing demand by public and private interests for objective and timely information on Alaska's mineral endowment. To meet this demand, the USGS Alaska Mineral Resource Assessment Program (AMRAP), coordinated by H. C. Berg, has two coordinated objectives designed specifically to furnish information for decisions about Alaska's lands.

One objective, based on a 1:250,000-scale quadrangle format, is a systematic multidisciplinary assessment of Alaska's economic mineral potential for long-range national minerals policy planning and for Alaskan mineral exploration and development. Assuming increased levels of staffing and funding, the deadline for this goal is 1984. The other objective, based on a 1:1,000,000-scale map format, is a statewide mineral appraisal for short-range DOI and Congressional decisions on classification of Alaska's lands. This appraisal, informally termed "RAMRAP" (Regional AMRAP), was completed for most of Alaska in January 1978. A RAMRAP-type investigation of southeastern Alaska was begun in 1979; the tentative deadline for completing this investigation is 1982.

The AMRAP long-range program is being conducted mainly by geologists and their assistants in the Alaskan Geology Branch in collaboration with specialists from other branches and subactivities in the Geologic Division. In addition, geoscientists from the Alaska Division of Geological and Geophysical Surveys and several universities are collaborators.

Selected highlights of RAMRAP level II program

Level II studies (RAMRAP) were highlighted by the compilation, synthesis, and publication of basic

geological, geophysical, geochemical, and Earth satellite data and of regional (1:1,000,000-scale) resource assessments for all of mainland Alaska. In October 1978, these assessments were utilized extensively to update environmental impact statements for approximately 41 million ha of proposed National Interest Lands in Alaska. This update, urgently requested by the DOI, was completed within a 1-week deadline imposed by the Department, a deadline that would have been impossible to meet without the RAMRAP reports.

AMRAP levels III and IV program highlights

Field studies leading to multidisciplinary resource assessment have been completed to date in 22 1:250,000-scale ($1° \times 2°$ and $1° \times 3°$) quadrangles and are underway in 5 others. These quadrangles cover approximately 360,000 km^2. Mineral resource assessment folios have been published, or are in press or advanced preparation, for 22 quadrangles encompassing about 300,000 km^2. More than 100 other AMRAP-sponsored topical research reports on the geology, geochemistry, geophysics, and mineral resources of Alaska have been published, as well as a new tectonic (tectonostratigraphic) terrane map of southeastern Alaska.

AMRAP-sponsored level IV studies of ore genesis or of other mineral deposit research problems are underway or completed in 12 Alaskan mining districts.

Alaska fragments

Geologic and geophysical data collected by D. L. Jones, P. J. Coney, N. J. Silberling, C. S. Grommé, and J. W. Hillhouse show that much of Alaska constitutes a vast tectonic collage composed of separate fault-bounded geologic entities (terranes), each of which has its own unique stratigraphic sequence that differs in substantial ways from neighboring terranes. Paleomagnetic data show that early Mesozoic rocks in one terrane (Wrangellia) originated near the equator and, thus, have moved northward several thousand kilometers with respect to North America. More than 40 discrete terranes are now recognized. Those that are well studied appear to be rootless thrust sheets or nappes, and this structural style may characterize most of the terranes. The place of origin and the processes of movement and assembly of these allochthonous terranes remain fundamental geologic questions.

Paleotectonic setting of the Carboniferous of Alaska

The Carboniferous of Alaska represents preserved parts of several tectonic terranes, according to an analysis by J. T. Dutro, Jr., and D. L. Jones (1979). Northern Alaska may have been the leading edge of an Arctic plate that moved south nearly 1,000 km, starting in early Mesozoic time. Extreme western Alaska, including the Lisburne Peninsula, Cape York, and St. Lawrence Island, was part of an east Siberian region. East-central Alaska was the shelf edge and slope of the northwestern part of the North American platform. South-central Alaska was an arc or fore-arc trench at the northern edge of a paleo-Pacific plate. Southeastern Alaska consists of at least two fragments of the western edge of the North American plate that possibly moved independently northwestward in post-Triassic time. These fragments may once have occupied positions west of present-day Oregon, California, or Baja California. Scattered outcrops of deepwater radiolarian-bearing laminated cherts and argillites in central and western Alaska are possible remnants of an ancient north Pacific oceanic floor that have been preserved between plates that converged from all sides.

Geochemical definition of mineral provinces in the Alaska Range and Brooks Range

Results of geochemical research in Alaska have outlined a number of areas of regional extent in which various suites of metals in stream sediments and heavy mineral concentrates of stream sediments define belts and provinces of possible mineral occurrences of economic importance. Significant investigations include:

- Studies by G. C. Curtin and W. D. Crim using mainly heavy-mineral concentrate and stream sediment data suggest that a gold-, silver-, tin-, and tungsten-rich belt, which is present along the southeast flank of the Alaska Range in the Talkeetna and Talkeetna Mountains 1:250,000-scale quadrangles, central Alaska Range, cuts across the Alaska Range to the south and is present in the western part of the Lake Clark quadrangle. The belt is associated with a thick sequence of argillite, graywacke, and phyllite that has been intruded by a number of plutons ranging in composition from granite to peridotite in the Talkeetna and Talkeetna Mountains quadrangles. The similarity of geochemical expression and rock types in the Lake Clark quadrangle to those in the Talkeetna and Talkeetna Mountains quadrangles indicates the regional extent of this metalliferous belt.
- Interpretation of geochemical data and compilation of geochemical maps by J. B. Cathrall for the Survey Pass 1:250,000-scale quadrangle, central Brooks Range, show that mineralization includes a diverse suite of elements and that areas of mineral occurrences are substantial in size. The most important mineralized areas are (1) a zone rich in copper, lead, and zinc of stratiform volcanogenic origin with lesser amounts of silver, antimony, and molyb-

denum in the "schist belt" along the south-central flank of the Brooks Range, (2) tin-bearing granite bodies in the Arrigetch-Igikpak area, (3) polymetallic contact metamorphic mineralization around the Arrigetch-Igikpak plutons, and (4) copper, lead, and zinc sulfide mineralization in the northwest part of the quadrangle.

Alaskan mineral resources

Mineral resources are known in all major subdivisions of Alaska and have been described in reports issued during the last 80 years by the USGS, USBM, and various Alaska State and Territorial agencies. E. H. Cobb has summarized the published (and open-filed) references to mineral occurrences (other than organic fuels and construction materials) in fourteen 1:250,000-scale quadrangles in Alaska (Cobb, 1978, 1979a–g), thereby making readily available data from old out-of-print reports, as well as from results of current investigations.

NORTHERN

Permafrost distribution model

Detailed boring logs were compiled by D. M. Hopkins for the 20 offshore boreholes drilled in the Beaufort Sea lease area (index map, loc. 1). These logs and temperature readings from the boreholes have confirmed and expanded a paleovalley model for predicting the extent, depth, and character of offshore permafrost. The data show a wedge of Sangamonian marine silts and clays on the Continental Shelf that, in general, is thicker offshore and in the west and thins toward land and to the east. Little or no Sangamonian material is found in paleovalleys, however. The paleovalley of the Sagavanirktok River was carved between Midway and Return Islands, while that of the Shaviovik River was found in Mikkelson Bay. Temperature logs also show that offshore permafrost is found in all boreholes.

Significance of Middle Devonian clastic rocks of the eastern Brooks Range

Most of the Arctic quadrangle in northern Alaska (loc. 2) is underlain by a stratigraphic sequence typical of the central Brooks Range in which about 1,000 to 2,000 m of Middle and Upper Devonian rocks is present. However, the northernmost part is underlain by a sequence typical of the northeast Brooks Range in which Devonian rocks are generally absent or very thin beneath a Mississippian unconformity. The oldest rocks exposed in the southern part of the quadrangle are the pure carbonate rocks of the Skajit Limestone which, in this region, contains Late Silurian and Middle Devonian fossils and is about 600 m thick. The Skajit extends westward for about 600 km throughout the southern Brooks Range, and, because of its great lateral extent, it has been assumed that it once may have been continuous northward with the Middle(?) Devonian Nanook Limestone present locally beneath the Mississippian unconformity in the Sadlerochit Mountains about 50 km north of the Arctic quadrangle.

Recent mapping by W. P. Brosgé, H. N. Reiser, and J. T. Dutro, Jr., has shown that in the northernmost exposures of the central Brooks Range sequence in the Arctic quadrangle, about 40 km north of the exposed Skajit, the Middle Devonian is represented by at least 300 m of black shale interbedded with ferruginous argillaceous limestone, quartzite, and conglomerate and intruded by thin mafic sills. Thus, it seems unlikely that the Middle Devonian carbonate shelf was ever continuous across north-eastern Alaska. The newly discovered Middle Devonian rocks are probably transitional to the much thinner unit of Middle(?) Devonian shallow marine shale, sandstone, conglomerate, and limestone that occurs locally beneath the Mississippian unconformity in the northernmost Arctic quadrangle. The similarity of the Middle Devonian rocks in the northernmost part of the central Brooks Range sequence to those in the southernmost part of the northeast Brooks Range sequence suggests limited horizontal displacement on the thrust faults that separate the two sequences.

Gravity measurement of approximate tonnage of a Brooks Range barite deposit

Gravity measurements by D. F. Barnes have indicated the approximate size of a recently reported (Mayfield and others, 1979) barite deposit on the south flank of the Brooks Range. The deposit of high-grade barite forms a small hill that crops out about 3 km west of the junction of the Nimiuktuk River and Klim Creek (loc. 3). The dimensions of the hill (approximately $80 \times 50 \times 8$ m) suggest that the deposit contains less than 100,000 t of barite, but the gravity data indicate a greater extent of depth. East-west and north-south gravity traverses were centered on the hill and controlled by vertical angle stadia measurements. Both traverses indicate a local 2-mGal anomaly with a shape that suggests the deposit is centered below the south side of the hill and probably dips steeply to the southwest. The gradients are steep enough to indicate a local source. Use of Gauss's theorem and of circular approximations of the probability contours suggests that the total mass of the deposit may be almost 1 million t. Geochemical data suggest that barite is abundant in this part of Alaska, but geologic observations show that the sources may be either massive potential ore bodies or diffuse veinlets.

The sharpness of the gravity anomaly associated with the Nimiuktuk body suggests that gravity could be useful in locating and estimating the size of the massive ore bodies. The Nimiuktuk deposit is close to the NPR but lies within the Noatak land withdrawal.

Bornite deposit, Cosmos Hills, northwest arctic Alaska

The massive copper-zinc sulfide orebody at Bornite (loc. 4), in the Cosmos Hills of arctic Alaska, is estimated to have a value of $4 billion to $6 billion. The orebody in part is stratabound and is in carbonate rocks of Middle Devonian age. Examination of ore material in thin section by A. K. Armstrong shows the environments of deposition were cyclic shallow marine to supratidal. Associated with the carbonate rocks are thin beds of muscovite schist and possible metatuffs. Study of the core reveals that the orebeds are associated with intertidal to supratidal carbonate environments. Sedimentary structures are algal mats, interformational conglomerates, gypsum pseudomorphs, and birdseye structures. Petrographic studies of the cores indicate an original syngenetic deposition of the carbonate sediments and sulfide minerals in intertidal to supratidal environments under an arid climate. An orogenetic event occurred in Late Devonian time, exposing the carbonate rocks to vadose waters, removing gypsum-anhydrite by solution, and forming collapse breccias. The events, latest Devonian and Cretaceous time, are marked by regional stress and thermal metamorphism (350°C) of the rocks and by the development of tectonic breccias and remobilization of some of the sulfide ore bodies. In the Cretaceous, the carbonate rocks and enclosed orebodies were subjected to dislocation on a décollement.

Regional stratigraphy and depositional environment of the Kanayut Conglomerate

The Upper Devonian (Famennian) Kanayut Conglomerate is exposed in the Brooks Range for more than 600 km from east to west and 50 to 100 km from north to south. Regional studies during 1978 and 1979 by T. H. Nilsen have shown that the Kanayut is part of a single large delta complex 1,000 to 2,000 m thick. Throughout most of its east-west extent, the Kanayut consists of three fluvial members—a coarse middle member of conglomerate and sandstone that was deposited by braided streams and an upper member and a lower member composed mostly of fining upward cycles of sandstone and shale that were deposited by meandering streams. In the western half of the outcrop area, a fourth member, which consists of fluvial sediments interbedded with fossiliferous nearshore marine sandstone and shale, occurs beneath the three fluvial members. This partly marine member grades laterally and downward into the underlying Upper Devonian (Famennian and Frasnian) Hunt Fork Shale, which comprises the deeper marine parts of the delta. To the southwest and south, the upper and lower fluvial members become thin and locally pinch out.

Sedimentary features indicate that the Kanayut Conglomerate was derived from a chert-rich terrane to the east or northeast. The areal distribution of maximum size of conglomerate clasts indicates that the source area was to the north and east, and measurements of paleocurrents indicate that sediment transport was dominantly toward the southwest and west. Conglomerate and sandstone clasts are primarily of chert, with lesser amounts of quartz and quartzite.

The area in which the Kanayut occurs is limited on the northeast and east by large areas near the Canadian border in which the much thinner Mississippian Kekiktuk Conglomerate rests with angular unconformity on lower Paleozoic and Precambrian basement rocks. These basement rocks were probably part of the source area for the Kanayut. They were exposed to erosion in Late Devonian time, and those to the north include a thick unit of bedded chert. In addition, in some of its easternmost outcrops, the Kanayut rests directly on sheared conglomerate and reefs of the Upper Devonian (Frasnian) Beaucoup Formation, which ordinarily lies beneath the Hunt Fork Shale. This local pinch-out of the Hunt Fork suggests an unconformity beneath the Kanayut near its source.

However, the precise stratigraphic relations of the Kanayut to the younger Kekiktuk Conglomerate and to the older basement rocks along its eastern and northeastern margin are not clear. The area of positively identified Upper Devonian Kanayut is separated from the area in which the much thinner Mississippian Kekiktuk rests on basement by an outcrop zone 20 to 50 km wide. In this zone, the basement is overlain unconformably by a thick and variable conglomeratic sequence whose upper part is Mississippian, judging from plant fossils and lithic correlations, and whose lower part may be either Mississippian or Upper Devonian and, in some places, may be equivalent to a unit of Middle(?) Devonian clastic rocks that rests on basement beneath the Kekiktuk in a few places farther north. The belt of positively identified Kanayut has been thrust over this border zone to the north and probably has been thrust over it to the east. The thrust to the north probably does not have a large horizontal displacement because the base of the plate that contains the Kanayut is composed of Middle Devonian rocks similar to those that rest on the basement to the north.

WEST-CENTRAL

Ophiolites of western Alaska

Ophiolites in western Alaska crop out as narrow steeply dipping slabs rimming the Yukon-Koyukuk depression and as synclinal remnants of allochthonous sheets in the western Brooks Range and along the Rampart belt (loc. 5). All of these ophiolites appear to be genetically related and are thought by W. W. Patton, Jr., to represent fragments from the floor of the "Yukon-Koyukuk sea," a marginal ocean basin that extended over much of western Alaska during late Paleozoic and early Mesozoic time. Fossil and potassium-argon ages from the ophiolites indicate that the "Yukon-Koyukuk sea" had a long and complicated history beginning in Late Devonian or Mississippian time and ending in earliest Cretaceous time. Collapse of the sea and emplacement of the ophiolite and assemblages onto continental crust probably occurred in Middle Jurassic to earliest Cretaceous time along short-lived subduction zones near the present margins of the depression.

EAST-CENTRAL

Identification of Ordovician rocks in Lake Minchumina area

Graptolites discovered at and near Lake Minchumina (loc. 6) by Michael Churkin, Jr., J. H. Trexler, Jr., and R. M. Chapman provide a new age data for sedimentary and low-grade metasedimentary rocks that lie in a broad northeast-trending belt between the North Fork of the Kuskokwim and Kantishna Rivers. Graptolites from four collections have been studied by Claire Carter. Carter identified Middle Ordovician graptolites in two collections and probable Ordovician biserial graptolites in a third collection, all from thin shale beds in a section of siltstone-mudstone-argillite and shaly slaty phyllitic mudstone that crops out at the south end of Yutokh Hill on the south shore of Lake Minchumina. A Middle Ordovician(?) age was assigned to fragmentary graptolites found about 36 km northeast of Lake Minchumina in thin shaly mudstone beds interbedded with chert and cherty siltstone.

The rocks at the latter site are within a chert and slate unit that was partially mapped in 1974 and tentatively assigned an Ordovician age based on regional lithologic correlations (Chapman and others, 1975; USGS, 1975, p. 67). Subsequently, radiolarians from a chert in this unit were identified as of early Paleozoic (pre-Devonian) age by D. L. Jones (oral commun., 1978). New mapping by Chapman, W. E. Yeend, and Jones in 1979 has identified the chert and slate unit throughout a belt trending northeast from the Snohomish Hills (Mount McKinley D–6 quadrangle) to the Zitziana River (Kantishna River B–3 quadrangle). Radiolarian-bearing rocks were found and sampled at a number of sites within this belt. Lithologically similar chert units, along strike to the northeast, have been assigned a Cambrian or Ordovician age in the Dugan Hills and a Late Ordovician age in the Livengood area.

An argillaceous arenaceous sedimentary and low-grade metasedimentary rock sequence between Lake Minchumina and Bearpaw Mountain was mapped in 1979. These rocks lie on the southeast flank of the belt of chert and slate and are provisionally interpreted as underlying the chert and slate unit, although a contact was not seen. In addition to the Middle Ordovician graptolites, *Saffordophyllum* sp., a coral that ranges from Middle to Late Ordovician in age (Oliver and others, 1975), was found within this sequence on the north side of Yutokh Hill by F. R. Weber in 1959. A roughly similar unit of clastic rocks that underlies a unit of chert and siliceous shale in the Dugan Hills is inferred to be of pre-Ordovician and possible Proterozoic Z age (Péwé and others, 1966).

The 1979 mapping and fossil discoveries, pending further evaluation, support previously suggested regional correlations and Ordovician age of the chert and slate unit in the Kantishna River quadrangle. The Ordovician fossils found at Lake Minchumina rule out a pre-Ordovician age for at least most of the clastic rock sequence in the Lake Minchumina–Kantishna River area. These findings point out the need for detailed lithologic and paleontologic studies of similar rock units, mapped as Nilkoka Group, in the Dugan Hills 150 km northeast of Lake Minchumina.

Collision-deformed Paleozoic continental margin of Alaska—foundation for microplate accretion

Recognition of different types of multiple allochthonous terranes in Alaska has led to the hypothesis that much of the State is a mosiac of microplates that originally formed in widely separated parts of the Pacific basin. Michael Churkin, Jr., and Claire Carter are working to identify the backstop or docking mechanism for the accretionary terranes that collided with North America during the Mesozoic.

Noting the similarity of Paleozoic stratigraphy of Alaska to that of the more southerly parts of the Cordillera, Churkin and Carter theorized that a narrow belt of transitional rocks separating mainly carbonate rocks from siliceous strata represents a collision-deformed continental margin that served as the backstop for migrating terranes.

Work in the Livengood, Circle, and Lake Minchumina areas (loc. 7), in conjunction with field investigations by R. M. Chapman, H. L. Foster, and F. R. Weber, substantiates the placement of the Paleozoic continental

margin across the south-central part of Alaska. A new graptolite fauna was found in the Livengood Dome Chert, near the town of Livengood. The presence of another graptolite fauna found in the Lake Minchumina area confirms the extension and correlation of this siliceous shale and chert belt from the Livengood area to the Terra Cotta Mountains of the Alaska Range. This belt of graptolitic shale and chert represents a "shale-out" type of continental margin that developed along the outer margin of the North American carbonate platform in Alaska, as it did in more easterly and southerly parts of the Cordillera; for example, Selwyn basin of Yukon Territory and the central part of the basin-and-range area of Nevada and Idaho. Volcanic-rock-rich Ordovician sections of the Fossil Creek Volcanics and the quartz mica schist complexes of the Yukon-Tanana Upland, which both lie outboard of this continental margin, represent allochthonous terranes that collided and accreted themselves to this original continental backstop to migrating plates.

Geologic map of the Fairbanks gold belt

Large-scale mapping of the Fairbanks gold belt (loc. 8) was initiated in 1967 under the auspices of the USGS Heavy Metals Program. Intensive field mapping was conducted during the summers of 1967 and 1968, followed by detailed mapping at selected localities over the next few years. Geochemical and petrologic samples relating to the gold-bearing ore deposits have been analyzed on a continuing basis, collected during the more intensive fieldwork done from 1967 to 1969 and at times of opportunity resulting from new mine cuts. Further cuts were investigated, and more mapping was done from 1977 to 1978 by F. R. Weber.

Four geologic maps of the Fairbanks area on a 1:24,000 scale have been published. Fieldwork during the recent summers included continued detailed geology of the Ester dome mining area. Inch-to-the-mile maps of the whole area have been updated and will be published as open-file reports.

Geologic terranes of the Circle quadrangle

Geologic mapping in the Circle quadrangle (loc. 9) by H. L. Foster and F. R. Weber has led to the recognition of several distinct groups of rocks or terranes. The southern part of the quadrangle is composed of greenschist to amphibolite facies metamorphic rocks consisting of interlayered quartzite, pelite, marble, and amphibolite. A few small masses and isolated blocks of ultramafic rocks, mostly serpentinized, also are present. This metamorphic terrane is complexly folded and faulted. A dominantly quartzite terrane comprises the largest part of the quadrangle and ranges in metamorphic grade from low greenschist facies to low amphibolite facies. Marble and chloritic schists are locally interlayered. It may be in thrust relation with, or grade into, the metamorphic terrane to the south.

The quartzite appears to have been derived largely from a bimodal sandstone and is characterized by a matrix of medium- or small-sized quartz grains with rare to abundant large glassy, colorless, gray, or bluish-gray quartz grains appearing as "eyes." *Oldhamia*, a trace fossil, occurs probably in the upper part of the unit, suggesting a Proterozoic Z or Early Cambrian age for this part of the section.

Major faults, including the Tintina, separate the terranes to the north, which include the Crazy Mountains and the Little Crazy Mountains. At least two terranes are recognized here, both of which are traced eastward into the Circle quadrangle from the Livengood quadrangle. The older terrane consists mostly of volcanic rocks and slightly metamorphosed limestones. The younger terrane comprises chert conglomerate, sandstone, argillite (includes turbidite deposits), graywacke, and minor calcareous rocks. All of these rocks are somewhat metamorphosed but distinctly less so than the rocks of the southern part of the quadrangle.

Glacial advances in the Yukon-Tanana upland

The Yukon–Tanana upland (loc. 10) is one of the best areas in central Alaska in which to study Pleistocene history. The upland has been relatively stable since late Tertiary compared to the nearby tectonically active Alaska Range, so the glacial history should be less complex.

Original photogeologic work in the upland was summarized in a map published by Péwé and others (1967). Work by F. R. Weber suggests that there were at least three major glacial events instead of the two shown on the 1967 map. The oldest advance is considerably more extensive than those depicted on the original map. Each glaciation has a distinctive soil profile and other broadly similar physical characteristics. Two large glacial lake basins were recognized and examined. Samples were collected for carbon-14 age analysis. Work accomplished to date is preliminary, and the correlation of the upland glaciers with advances in other parts of Alaska is uncertain.

Application of aeromagnetic and gravity data to the geological interpretation of the Tintina fault and the Circle quadrangle

Using aeromagnetic data, J. W. Cady and H. L. Foster theorize that the northwest-trending right lateral Tintina fault has a more westerly direction in the Circle quadrangle (loc. 11) than previously thought. East of long 145°, the fault zone is marked by a 150-gamma

magnetic high with a width of 25 to 35 km and an estimated depth to source of about 5 km. Coincident with the magnetic high is a Bouguer gravity low of at least 30 mGal.

A physiographic break at the south side of the fault zone occurs north of the steep gradient bounding the south side of the magnetic high, suggesting that the fault plane dips to the south. One-hundred-twenty new gravity stations with spacings of 4 to 8 km were collected along four profiles across the fault. Modeling of these and previous data should determine whether the Tintina fault has a reverse component.

Southwest of the Tintina fault, elongate magnetic highs and lows with peak-to-trough amplitudes of 100 to 200 gammas trend about N. 60° E. The anomalies appear to reflect folds in a section containing nonmagnetic quartzite interlayered with magnetic chloritic quartz-mica schist. Some deep magnetic lows correlate with granitic plutons or felsic hypabyssal intrusive rocks and suggest the presence of granitic rock at depth. Tentatively, it is inferred that granitic rock occurs as comformable bodies in the cores of anticlines.

Northeast of the Tintina fault, most magnetic highs are in areas of nonmagnetic cover. The inferred sources of these highs are mafic volcanic rocks; however, exposed mafic volcanic rocks were found to be nonmagnetic, and the only magnetic rocks found at the surface belonged to a mafic intrusive body with an inferred area of about 75 km^2.

Metalliferous mineral resource potential of the Big Delta quadrangle

A study by W. D. Menzie and H. L. Foster of the mineral resource potential of the Big Delta quadrangle (loc. 12), based on the geology, geochemistry, geophysics, and past mining and prospecting history indicates that the quadrangle has a high probability for the occurrence of metalliferous mineral deposits (Menzie and Foster, 1978). Most of these areas are in the eastern part of the quadrangle. Three areas were delineated that are considered likely for the occurrence of porphyry copper deposits, although no porphyry copper deposits have yet been developed in the Yukon-Tanana Upland, probably because of estimated low grade and tonnage. Three areas were delineated as likely for the occurrence of volcanogenic sulfide and (or) lead-zinc deposits associated with metasedimentary rocks. Not enough information is available to establish the presence or absence of such deposits, but, in Canada, these types of deposits are known to occur in similar geologic settings. The quadrangle also has a potential for vein deposits; antimony and bismuth vein deposits are already known, and gold vein deposits have been mined.

Proterozoic cataclastic augen gneiss in the Big Delta quadrangle

New petrologic and isotopic data obtained by Cynthia Dusel-Bacon and J. N. Aleinikoff reveal that a large (700 km^2) body of augen gneiss in the Big Delta quadrangle (loc. 13) originally formed as a Proterozoic granitic pluton. The gneiss has a cataclastic texture with large (3- to 7-cm) perthitic microcline augen in a finely crystalline matrix of quartz, plagioclase, biotite, white mica, and potassium feldspar, with accessory zircon, sphene, apatite, and opaque minerals. Micaceous foliation is deflected around the augen, which commonly have myrmekitic margins. Although most porphyroclasts are eye-shaped, many larger crystals have survived deformation without losing their original idiomorphic habit. The augen gneiss has been metamorphosed to amphibolite facies and is surrounded by and includes other metamorphic rocks of similar grade.

A porphyritic granitic pluton protolith is suggested on the basis of the following field and textural evidence: (1) xenoliths within the augen gneiss, (2) large extent and uniform composition of the body, (3) concentricity of zones of inclusions within some idiomorphic augen, (4) recrystallization of monocrystalline porphyroclasts into polycrystalline aggregates with no indication that augen are porphyroblasts, and (5) euhedral shape of most accessory zircons.

Uranium-thorium-lead isotopic data from various splits of zircons from several augen gneiss samples form a linear array. A best-fit line through these data has upper and lower intercepts of 2,312 m.y. and 345 m.y., respectively. Dusel-Bacon and Alleinikoff interpret the upper intercept as the time the augen gneiss originally crystallized as a porphyritic granitic pluton and the lower intercept as a time of subsequent cataclasis and metamorphism.

Badlands on the north side of the Alaska Range

Badlands (vegetation-free areas of intricately dissected topography of a few hectares to 0.65 km^2 in extent) amount to 3 to 6 percent of the area of forest- and tundra-covered basins underlain by poorly consolidated Neogene continental sedimentary rocks on the north side of the central Alaska Range. Clyde Wahrhaftig reports the erosion process in badlands has an annual cycle, consisting of frost-riving of pebbles from conglomerate outcrops and of slabs from sandstone outcrops in winter, flushing of frost-rived debris from badland gullies into main stream by convective thundershower cloudbursts in early summer, and removal of the resulting alluvial fans by low-intensity long-duration cyclonic storms in late summer. Individual badlands go through cycles of birth (as landslide- and meander-scars

and headward gully-erosion nickpoints), development through picturesque topographic forms, and ultimate healing over by vegetation; cycles may span several hundred or a few thousand years. The rate of erosion of badlands, based on repeated photography and measurement of annual alluvial cones, is about 1m/30 yr, sufficient to account for all the erosion in the drainage basins in which they occur. The inception of these drainage basins can be dated as occurring in post-Kansan time. Thus, the bulk of the erosion at any time comes from a very small proportion of the drainage basin, whose locus constantly shifts.

SOUTHERN

Evidence for northwestward emplacement of Wrangellia terrane in the northern Talkeetna Mountains

Reconnaissance geologic mapping by Béla Csejtey, Jr., and D. R. St. Aubin along the Talkeetna thrust in the northern Talkeetna Mountains (loc. 14) provides strong evidence that the allochthonous terranes of southern Alaska were emplaced by northwestward thrusting in about middle Cretaceous time.

In the Talkeetna Mountains, the Talkeetna thrust delineates the leading edge of a large allochthonous block which has been correlated (Csejtey and others, 1978) with the Wrangellia terrane (Jones and others, 1977) of eastern Alaska. The thrust, trending northeast, brings the south upper Paleozoic and Upper Triassic dominantly volcanic rocks of Wrangellia against Lower Cretaceous argillites and graywackes. Although the Talkeetna thrust is poorly exposed, in the northern Talkeetnas several subsidiary southeastward-dipping imbricate thrusts were observed structurally above the Talkeetna thrust; that is, in rocks of the Wrangellia terrane. These imbricate subsidiary thrusts are exposed just south of the main Talkeetna thrust, at about 0.5 to 1-km surface intervals. They not only systematically brought older rocks of the Wrangellia section against younger ones, but some of the incompetent rocks in the upper plates clearly have been forced into northwestward overturned drag folds with amplitudes of from a few meters to 200 m. In front of the Talkeetna thrust, in a several-kilometer-wide zone, structurally underlying Cretaceous argillites also were thrown into large northwestward overturned tight folds.

Age brackets for this thrusting and for related deformation are provided by the age of the youngest involved rocks, the Lower Cretaceous argillites, and by the oldest undeformed rocks, granitic intrusive rocks of Late Cretaceous and Paleocene age.

Thus, observations in the northern Talkeetnas, in conjunction with other evidence from elsewhere in the Talkeetna Mountains (Csejtey and others, 1978; Csejtey, 1979), indicate that final emplacement of the numerous and widely disparate allochthonous terranes of southern Alaska took place by northwestward thrusting during a middle Cretaceous accretionary orogenic period that produced large and complex Alpine-type structures.

Accreted terranes in the southern Alaska Range

The Mount Hayes quadrangle in the eastern Alaska Range, south of the Denali fault (loc. 15), is a tectonic mosiac composed of three large tectono-stratigraphic terranes that accreted to North America during late Mesozoic or early Cenozoic time, according to W. J. Nokleberg. From north to south, these terranes are (1) the Maclaren terrane, a fragment of an Andean-type arc, consisting of the Barrovian-type Maclaren metamorphic belt and the regionally deformed and metamorphosed East Susitna batholith, (2) the Wrangellia terrane, a fragment of an island arc, consisting of upper Paleozoic andesite to dacite flows, tuffs, limestone, and argillite and unconformably overlying massive flows of the Triassic Nikolai Greenstone, and (3) the Tangellia terrane, a deeper water equivalent of the Wrangellia terrane, consisting of upper Paleozoic aquagene tuff, chert, minor andesite tuff and flows, and limestone and uncomformably overlying pillow lava and massive flows of the Triassic Nikolai Greenstone. The Tangellia terrane was intruded by gabbro dikes and sills that locally formed large mafic and ultramafic stratiform complexes. These, together with the Nikolai, represent rift-type magmatism. Each terrane generally has a unique geologic history and narrow time-stratigraphic sequence, a missing source of sediments or volcanic rocks, and bounding thrusts faults representing accretionary sutures. The Maclaren and Wrangellia terranes are juxtaposed along the Broxson Gulch thrust system, which forms an imbricate series of north-dipping thrust faults. Paralleling the Broxson Gulch thrust system a few kilometers south, is the north-dipping Eureka Creek thrust along which are juxtaposed the Wrangellia and Tangellia terranes

Gold placers in the Mount Hayes quadrangle

Studies by W. E. Yeend indicate that the source for the Holocene placer gold in the southern part of the Mount Hayes quadrangle appears to be Tertiary conglomerate that occurs in small isolated outcrops and as small fault slivers along the south flank of the Alaska Range (loc.16). Gold was panned from the Tertiary conglomerate at various localities between Slate Creek and Rainy Creek, a distance of 50 km. Because of the concentrating powers of the Pleistocene and Holocene streams, gold derived from Tertiary conglomerate now occurs in economic or near-economic grade.

Metallogenic and tectonic significance of isotopic data from the Nikolai Greenstone, McCarthy quadrangle

Preliminary studies of potassium-argon ages and stable isotope systematics from samples of the Nikolai Greenstone (loc. 17) and quartz-epidote veins that contain copper and copper sulfides in that unit have yielded data on the origin of the deposits and on the tectonic history of the Wrangellia terrane in south-central Alaska.

The Middle and (or) Upper Triassic Nikolai Greenstone, part of the allochthonous terrane of Wrangellia, is typically altered and locally metamorphosed to prehnite-pumpellyite facies, with chlorite and epidote as the most common secondary phases. Two types of concentrations of copper in the Nikolai are common—native-copper fillings of amygdules and rubble zones in some flows and veins and thin replacement zones in faults and fractures containing native copper and copper sulfates in quartz-epidote or calcite gangue. Oxygen isotope data from quartz and epidote from three copper-bearing veins yield calculated ore fluid temperatures of 250° to 300°C and ^{18}O of about +7, in agreement with a metamorphic-segregation origin of the deposits.

Upper Triassic sedimentary copper deposit in the western Clearwater Mountains

The Denali copper deposit in the western Clearwater Mountains of southern Alaska (loc. 18) was studied briefly by D. P. Cox, Béla Csejtey, Jr., and D. R. St. Aubin, and fossils were collected from thin supratidal limestone beds near the orebody. These were identified by D. L. Jones and N. J. Silberling as *Halobia* sp. of Late Triassic age. The Denali deposit is composed of very fine grained chalcopyrite and carbonaceous shale in thin varvelike layers (Seraphim, 1975) and appears to be an excellent example of a sedimentary copper deposit. The ore is deposited between mafic volcanic flow units believed to be part of the Nikolai Greenstone of Triassic age. The identification of nearby fossils as *Halobia* sp. confirms this relation. The Nikolai and other units in the Wrangellia terrane (Jones and others, 1977) are known to be potential hosts for copper ores throughout the eastern and central Alaska Range.

Seven potassium-argon ages of chloritized greenstone fall on an initial argon diagram with a zero intercept and a slope that yields an isochron age of 112 m.y. ± 11 m.y. The Cretaceous thermal-metamorphic episode responsible for this alteration and mineralization is younger than a major Jurassic orogeny, accompanied by granitic intrusion in the area, and appears unrelated to minor granitic intrusion in the middle to late Tertiary. M. L. Silberman, E. M. MacKevett, Jr., C. L. Connor, and Alan Matthews believe the Cretaceous event is related to accretion of Wrangellia to the North American continent. This age of accretion agrees with stratigraphic and structural evidence cited by MacKevett and others (1977) and Jones and others (1977).

Extensional volcanism in the Matanuska Valley region

Basement rocks under the northern part of the Matanuska Valley (loc. 19) consist largely of sandstone, siltstone, and shale of the Lower and Upper Cretaceous Matanuska Formation. Sedimentary units equivalent in age to the Arkose Ridge (Chickaloon) Formation and younger units overlie the Matanuska Formation. Volcanic, hypabyssal, and volcaniclastic rocks are interbedded with, intrude, and overlie the Tertiary sedimentary rocks. Intrusive rocks of this suite also cut the Matanuska and form a suite which ranges from basalt and diorite to rhyolite. Such variation, particularly with a considerable basaltic component, is characteristic of volcanic rocks emplaced and erupted in regions undergoing extension. Whole rock potassium-argon age determinations were made on several volcanic units by M. L. Silberman and Arthur Grantz. Preliminary results show a range from 40.9 m.y. ± 1.6 m.y. to 51.8 m.y. ± 1.5 m.y.

The data indicate that volcanic activity related to crustal extension started in this region at about the same time as the base of the Arkose Ridge Formation was deposited, about 53 m.y. to 50 m.y. ago. These ages by themselves would suggest an early Eocene age; however, plant fossils suggest a late Paleocene age. The onset of extensional tectonics in the Matanuska Valley also coincides with limits placed on the age of accretion of the Chugach terrane, to the south, of 52 m.y. for fissure vein mineralization at the Hope-Sunrise district.

Bootlegger Cove Clay–geographic and stratigraphic mollusk occurrences

A radiocarbon date of about 14,000 yr B.P. provided by Meyer Rubin on shells collected by H. R. Schmoll and A. D. Pasch from an outcrop of silty clay near the mouth of the Beluga River (loc. 20) indicates that the Bootlegger Cove Clay, previously known only at Anchorage and along Turnagain Arm, extends to the area on the west side of Cook Inlet as well. Given this known distribution, it is likely that the silty clay observed as much as 70 to 120 km up the Susitna Lowland along the Yentna and Susitna Rivers is also Bootlegger Cove Clay and that the ancestral Cook Inlet in which the Bootlegger Cove Clay was deposited extended across what is now northern Kenai Lowland between Chickaloon Bay and Kalifonsky Beach. The small number of shells collected at the latter place are insufficient for dating by present techniques.

A single shell recovered from a depth of 13 m below the known shell-bearing horizon in a test hole at Anchorage is also presently insufficient for dating purposes but indicates a wider stratigraphic range for the occurrence of mollusks within the Bootlegger Cove Clay than previously known. The age of the lower part of this formation, which relates directly to the late Pleistocene chronology of the Cook Inlet basin, is undetermined as yet, but material that may be suitable for dating purposes now is known to exist.

Relations to similar-appearing silty clay deposits at East Foreland and West Foreland, which are overlain by sand containing wood of an age beyond the range of the radiocarbon dating method, remain unclear, but it now seems more likely that this wood is transported older material, possibly Tertiary in age.

SOUTHWESTERN

Paleomagnetism of Permian basalts

The paleomagnetic properties of Permian volcanic rocks from Nuyakuk Lake (loc. 21) in the Dillingham D–8 and Goodnews D–1 quadrangles were investigated by S. M. Karl and J. M. Hoare to determine a paleomagnetic pole for comparison with the Permian paleomagnetic pole calculated for rocks formed within stable North America. The objective of the comparison was to determine whether the Nuyakuk Lake volcanic rocks originated in their present position.

Measurements were made using a cryogenic magnetometer on 124 cores cut from 35 oriented specimens that were collected from 9 sites across the width of the volcanic belt, which trends N. 45° W. and dips 15° to 25° SW. A paleomagnetic pole of 51.6° N. 101.6° E. was determined for tectonically uncorrected data, and one of 40° N. 131° E., for tectonically corrected data. The Permian pole calculated for stable North America (McElhinny, 1973) is 46° N. 117° E. No appreciable difference exists at the 95-percent confidence level between the two poles calculated for the basalts at Nuyakuk Lake and the Permian pole of stable North America. This suggests that the basalts at Nuyakuk Lake probably have not been displaced much since they formed.

Unfortunately, the data cannot be tested by a fold test or a reversal test (Hillhouse, 1977, p. 2585–2589) because the structure of the basalts is homoclinal and all specimens exhibit reversed magnetic polarity. However, the consistency of measurements from the different sites suggests that a true direction may have been determined and that the results are valid.

Holocene volcano on the Alaska Peninsula

A large volcano (1,345 m high) was discovered in the Ugashik quadrangle during field investigations in 1978 by R. L. Detterman and J. E. Case. The volcano at lat 57°01′08″ N., long 157°11′ W. (loc. 22), forms the southwest end of a chain of three volcanoes that trend N. 45° E. The three volcanoes are equidistant (18 km) and offset 25 km southeast from the main trend of volcanoes on the Alaska Peninsula. The composite cone is mainly hornblende andesite; block and ash flows extend 16 km down valley and are interlayered with short and steep lahars. At least some of the volcanic activity is Holocene in age.

Two Cenozoic igneous events on the Alaska Peninsula

Potassium-argon dating work and geologic mapping in the Chignik and Sutwik Island quadrangles (loc. 23) by F. H. Wilson, R. L. Detterman, J. E. Case, M. E. Yount, and others (Wilson and others, 1978; Detterman and others, 1979) have shown the existence of two major Cenozoic igneous episodes on the Alaska Peninsula. These events range in age from Eocene to late Oligocene and from early Miocene and late Miocene to Holocene. Both events include andesitic volcanism and shallow plutonism. Porphyry copper deposits are associated with each event. Dates on mineralized zones are Oligocene, Miocene, and Pleistocene, and undated zones probably span the entire range of the two igneous events. Compositions range from dacite to leuco-basalt (Streckeisen, 1979) for volcanic rocks and from tonalite to granodiorite (Streckeisen, 1973) for plutonic rocks.

Tertiary volcanic centers on the Alaska Peninsula

J. E. Case, R. L. Detterman, and F. H. Wilson report that Holocene volcanic centers in the Chignik and Sutwik Island quadrangles (loc. 24) on the Alaska Peninsula are characterized by ovoid clusters of magnetic highs and lows that coincide closely with volcanic edifices at Mount Veniaminof, Black Peak, and Aniakchak Crater. Similar clusters of anomalies occur over volcanoplutonic complexes at Kujulik Bay (10 m.y.–40 m.y.), Chiginagak Bay (5 m.y.–10 m.y.), Sutwik Island (30 m.y.–40 m.y.) and Nakchamik Island (5 m.y.–10 m.y.). These older complexes, presumably parts of older subduction-related magmatic arcs, are within 75 km of the Holocene volcanic centers, which suggests magmatic activity has occurred in nearly the same setting with respect to the present Aleutian Trench for the past 40 m.y.

SOUTHEASTERN

Newly recognized plutonic province displacement by the Chatham Strait fault

Recent studies of the granitic bodies in the southeastern part of Glacier Bay National Monument (loc. 25) by R. A. Sonnevil have defined a distinct group of plutons that are characterized by complex variations in composition, oscillatory-zoned plagioclase, interstitial

potassium feldspar, and abundant hornblende with local pyroxene cores and abundant sphene. Preliminary study of generally similar plutons nearby in northeastern Chichagof Island and farther away on Kuiu and Prince of Wales Island suggests that all of these bodies are part of the same petrologic province and that the Kuiu and Prince of Wales plutons have been displaced right laterally about 130 km on the Chatham Strait fault. The age of the intrusive event is not known yet; both Jurassic and Cretaceous potassium-argon ages and one Jurassic lead-alpha age have been reported for various bodies.

Mount Juneau orthogneiss pluton

The west margin of the Coast Mountains batholithic complex (loc. 26), along a distance of more than 225 km in northern and central southeastern Alaska, consists of a belt of generally well-foliated homogeneous sheetlike bodies of hornblende-quartz diorite or tonalite. Many are approximately concordant sills in country-rock schists and gneisses of mostly amphibolite-facies rank. Foliation within the bodies generally parallels contacts and foliation in country rocks, and the presence of pervasive crystalloblastic textures obscures most original magmatic features. Thus, a magmatic origin of many bodies is not readily discernible.

A magmatic intrusive origin, however, is particularly well documented by field relations for one of these bodies that extends southeastward from Mount Juneau to or beyond Taku Inlet. This body of orthogneiss was studied in detail by A. B. Ford and D. A. Brew to document its igneous origin and because this is the only body known that seems to show critical relations for linking early batholithic activity to the regional synkinematic metamorphism in the adjoining Barrovian schist belt.

The Mount Juneau orthogneiss pluton is strongly discordant to enclosing schists for a distance of about 5 km at its northwest end. Farther east, the body is nearly concordant to adjoining schist and gneiss of other origin. Gneissose foliation in its discordant western end is at high angle to the contact and parallels regional synkinematic foliation in the schists.

Textures within the body are typically metamorphic. Metamorphic minerals include garnet, biotite, green hornblende, sphene, quartz, and plagioclase. Relict grains of magmatic plagioclase are typically filled with numerous grains of epidote. The lack of a recognizable thermal aureole suggests that the body was emplaced during or prior to a period of elevated temperature in the schists. The body cuts isograds of staurolite, kyanite, and sillimanite in the schist belt and extends westward nearly to the garnet isograd. Crystallization of garnet, biotite, and hornblende and the albitization of plagioclase are related to a late stage of the regional metamorphism, to which the gneissose foliation is related. This apparently occurred during the decline from maximum-grade sillimanite-forming conditions in the schist belt and probably during garnet-grade activity.

Chemical analyses of 25 orthogneiss samples from along the 15-km length of the pluton show an average composition of quartz monzodiorite. Rock modal compositions are mostly quartz diorite. Chemical compositions show little variation along strike of the body.

Metallic mineral occurrences near the plutonic complex sill in the Coast Range

The mineral deposits in and around the plutonic complex sill in the Coast Range in the northern part of southeastern Alaska are concentrated in a zone about 20 km wide on the southwest side of the Coast Range sill (loc. 27) (Brew and others, 1976; Brew and Ford, 1978). This zone essentially coincides with the Juneau Gold Belt of Spencer (1907). Gold-silver stringer lodes and massive sulfide copper-zinc deposits are most important. H. C. Berg (1979a) has interpreted most of these deposits to be volcanogenic in origin. Regardless of the primary origin, reconstruction of the complex geologic history of this zone and the details of specific mineral deposits suggest that the present concentration of deposits is due to mobilization and redeposition of ore minerals in favorable structural and stratigraphic positions during a collision event probably in Late Cretaceous time that included significant deformation, metamorphism, and intrusion. The whole zone is probably favorable for the occurrence of metallic mineral deposits, and certain combinations of lithologies and structures are highly favorable. The zone, and not the original lithostratigraphic units, should be the main guide to mineral resource exploration in this part of southeastern Alaska.

Upper Triassic massive sulfide deposits near Wrangell

H. C. Berg reports layers and lenses of disseminated and massive pyrite, pyrrhotite, and metavolcanic and metasedimentary strata on Kupreanof Island, about 60 km northwest of the town of Wrangell, in southeastern Alaska (loc. 28). This mineral discovery is the first faunally dated occurrence of Upper Triassic massive volcanogenic sulfide deposits in the southeastern panhandle and one of the few such deposits to be dated by fossils anywhere in Alaska.

Preliminary field and laboratory studies of undated but similar mineral deposits elsewhere in southwestern Alaska suggest that several massive sulfide deposits and an active barite mine located in the Admiralty and Annette tectonostratigraphic terranes also are Late Triassic in age (Berg and others, 1978; Berg, 1979b).

The mineral deposits and their host rocks occur in a 300-km-long belt stretching the length of the panhandle from Ketchikan to Juneau. Berg believes that the belt comprises a major metallogenic province in southeastern Alaska composed of volcanogenic massive Zn-Pb-Ag (-Cu-Au) sulfide deposits in metamorphosed Upper Triassic strata. This newly recognized province appears to be restricted to the Admiralty and Annette terranes and is the first metallogenic province in southeastern Alaska to be recognized by integrating mineral deposit data, biostratigraphy, and regional stratotectonics. The discovery has important implications for regional mineral exploration and resource appraisal in southeastern Alaska, a geologically complex region about half the size of the State of California.

Structural analysis of plutonic and metamorphic rocks from an area east of Wrangell

Preliminary structural analysis of data from a 20- by 35-km area east of Wrangell (loc. 29) by S. J. Hunt has provided new information on the late Mesozoic and Cenozoic history of the region. The area is underlain by an igneous-metamorphic complex in which at least three types of plutonic bodies occur—the regionally mapped Mesozoic(?) plutonic complex sill in the Coast Range, several 80 m.y. to 85 m.y.(?) garnet-biotite granodiorite bodies, and a small 20-m.y.-old alkali granite. The metamorphic country rocks are basically fine-grained clastic rocks with abundant metavolcanic rocks and a few lenses of carbonate. The metamorphic grade ranges from greenschist to amphibolite facies, generally increasing eastward.

The results show a dominant N. 20° W.-trending regional foliation in the metamorphic rocks that is locally affected by the intrusion of granodiorite. A dominant foliation-normal joint set in the metamorphic rocks seems to confirm a northeast-trending compressional regime in effect during metamorphism. The structural data presently suggest that the granodiorite bodies, and possibly the linear plutonic complex sill in the Coast Range, are later postmetamorphic events. The data do not present any positive evidence that the Coast Range megalineament is a major structural discontinuity.

Tertiary granite stock, southwestern Kupreanof Island

A small (20 km^2) granite stock of possible economic interest intrudes the volcanic complex on southwestern Kupreanof Island (loc. 30). Preliminary data suggest that the country rocks are lower to middle Tertiary and range in composition from basalt to rhyodacite. The relations between the different volcanic flow units are not known but are apparently more complex than simple basalt and andesite flows to the west along Keku Strait.

The pluton itself is poorly exposed; the limited data available indicate it is a highly altered miarolitic biotite(?) granite or alkali granite. Regional considerations suggest it is 20 m.y. to 30 m.y. old.

No metallic mineral deposits are known to be associated with this stock, but somewhat similar bodies to the east have been explored for molybdenum and uranium-thorium resources and preliminary geochemical results from the stock and vicinity show unusually high eU values in both stream sediments and bedrock.

This stock and three others of the same general type, inferred to be the same age and within the volcanic-plutonic complex on Kuiu and Etolin Islands (Brew and others, 1976), all intrude complicated volcanic flow or dike-sill masses of about the same age. In contrast, the stocks of the same inferred age in the plutonic complex sill in the Coast Range to the east intrude older metamorphic and granitic rocks. It is tentatively suggested that these four granitic bodies, on Central Kuiuk, southwestern Kupreanof, southwestern Zarembo, and central Etolin Islands, mark eruptive centers within the Kuiu-Etolin volcanic-plutonic complex.

Plutonic complex tonalite sill in the Coast Range

The Coast plutonic complex sill is the name applied to a remarkably long and narrow belt of sheetlike plutons extending for over 620 km, from its intersection with the Chatham Strait fault north of Juneau south-southeastward to beyond Prince Rupert, British Columbia. The belt varies from 2 to 25 km in width, with the narrower segments consisting of a single pluton and the wider ones of as many as three plutons separated by 1- to 5-km-wide screens of migmatitic gneiss. The existence of the sill as an important regional feature was first noted by Brew and others (1976) and the relation of the sill to the parallel Coast Range megalineament is described in Brew and Ford (1978).

The plutons that make up the sill include tonalite, granodiorite, quartz diorite, and quartz monzodiorite, but some local patterns exist (that is, the pluton of Juneau in the Tracy Arm–Fords Terror quartz diorites). Hornblende is the dominant mafic mineral; biotite is present locally, as are garnet and sphene. Color indices are commonly in the range 15 to 35. The plutons are well foliated parallel to the foliation in the adjacent country rocks, but the actual contacts do not necessarily parallel the foliation. The relations and the presence of metamorphic features in the plutons suggest that the bodies were emplaced syn- to late-tectonically. The studies to date indicate that the belt of sills is locally interrupted in three different ways: (1) adjacent metamorphic rocks form persistent screens that cross the sill and

were not intruded, thus giving a rooflike aspect, (2) the sills fishtail out and are not exposed for some distance but reform again along strike, and (3) en echelon sills occur near others giving the effect of abrupt thickening of the belt.

GEOLOGIC MAPS

Geologic map of Colorado

A new color geologic map of Colorado was published in 1979. The map, compiled by O. L. Tweto, supersedes a map published in 1935 and reflects an enormous increase in the body of geologic knowlege concerning Colorado during the intervening 44 yr. The increase in knowledge results from a combination of detailed mapping, 1:250,000-scale mapping, paleontologic and stratigraphic studies, topical studies on particular types of rocks, geophysical and geochemical studies, and extensive radiometric dating of igneous rocks. In particular, the new map incorporates advances in subdivision and age classification of Precambrian rocks, upper Mesozoic and Tertiary volcanic and intrusive rocks, Tertiary sedimentary rocks, and Quaternary deposits. The map is plotted on a modern base that shows highways and 500-ft contours in color.

Maps of vertical movements during the past 10 million years, conterminous United States

A set of maps has been compiled by D. J. Gable and C. T. Hutton, Jr., from a synthesis of data on vertical movements of the Earth's crust in the conterminous United States during the last 10 m.y. These maps provide a basis for comparing relative tectonic stability of different regions of the country. The data are intended for use in evaluating the stability of regions in which sites are being considered for powerplants, waste repositories, dams, and other engineering facilities. Maps portray sources of data, neotectonics, and rates and magnitudes of vertical movements derived from a wide variety of geological and geophysical data. Gaps in the maps indicate those areas where additional investigations are needed to identify and quantify vertical movements.

Data presented on the map displaying magnitudes of vertical movements confirms that vertical movements have been greatest from the eastern edge of the Colorado Plateau to the Ventura–Sierra Nevada areas of California. Specific areas of greatest movement include the Rio Grande rift, western Colorado, Yellowstone–Snake River Plain area, Great Basin, and grabens of southwestern Arizona and California. Data presented on the map of rates of vertical movements demonstrates that rates of vertical movement are poorly understood, particularly east of the central Great Plains. In the Western United States, the highest rates of movement occur in the Ventura–Transverse Range area and Owens Valley and Death Valley areas, California.

Geologic map data file

A computerized map data file, which was developed by K. C. DeWitt, catalogs the availability of data shown on geologic and geophysical maps at scales ranging from 1:24,000 to 1:250,000 for the conterminous United States and Alaska. For published maps, the data file includes not only general geologic and geophysical information, but also information such as mining operations by commodity, occurrences of selected rocks and mineral types, and ages of youngest units cut by faults on a given map. The data file can be used to generate derivative maps, graphs, or charts summarizing the distribution or frequency of occurrence of selected geologic factors.

WATER-RESOURCE INVESTIGATIONS

The mission of the Water Resources Division is to provide, to interpret, and to apply the hydrologic information needed for the best use and management of the Nation's water resources (fig. 1). This is accomplished, in large part, through cooperative programs with other Federal and non-Federal agencies. The USGS also cooperates with the Department of State in providing scientific and technical assistance to international agencies.

The USGS conducts systematic investigations, surveys, and research on the occurrence, quality, quantity, distribution, use, movement, and value of the Nation's water resources. This work includes (1) investigations of floods and droughts and their magnitudes, frequencies, and relations to climate and physiographic factors, (2) evaluations of available water in river basins and ground-water provinces, including assessments of water requirements for industrial, domestic, and agricultural purposes, (3) determinations of the chemical, physical, and biological characteristics of surface and ground water and the relation of water quality and suspended-sediment load to various parts of the hydrologic cycle, and (4) studies of the interrelation of water supply with climate, topography, vegetation, soils, and urbanization.

One of the most important activities of the USGS is disseminating water data and the results of investigations and research by means of reports, maps, computerized information services, and other forms of public release.

The USGS (1) coordinates the activities of Federal agencies in the acquisition of water data on streams, lakes, reservoirs, estuaries, and ground water, (2) maintains a national network, (3) conducts special water-data acquisition activities, and (4) maintains a central catalog of water information for use by Federal agencies and other interested parties.

Supportive basic and problem-oriented research is conducted in hydraulics, hydrology, and related fields of science to improve the scientific bases for investigations and measurement techniques and to provide sufficient information about hydrologic systems so that quantitative predictions of their responses to stress can be made.

During fiscal year 1980, data on streamflow were collected at about 7,700 continuous-record discharge stations and at about 9,750 lake- and reservoir-level sites and partial-record streamflow stations. About 12,200 maps of flood-prone areas in all States and Puerto Rico have been completed to date, and about 825 pamphlets describing areas susceptible to flooding have been published in the past 5 yr. Studies of the quality of surface water were expanded; there were approximately 6,820 water-quality stations in the United States and in outlying areas where surface water was analyzed by the USGS. Parameters measured include selected major cations and anions, specific conductance of dissolved solids, and pH. Other parameters, measured as needed, include trace elements, phosphorus and nitrogen compounds, detergents, pesticides, radioactivity, phenols, BOD, and coliform bacteria. Streamflow and water-temperature records were collected at more than 4,050 water-quality stations. Sediment data were obtained at almost 1,280 locations.

Annually, about 500 USGS scientists report participation in areal water-resources studies and research on hydrologic principles, processes, and techniques. There are 1,414 active water-resource projects; 441 of the studies in progress are research projects. Of the current water-resource studies, 121 are related to urban-hydrology problems, 180 are related to energy, and 65 are related to water use.

In fiscal year 1980, 737 areal appraisal studies were carried out. Maximum and mean areas of the studies were about 1.5×10^6 and 0.064×10^6 km^2, respectively. Total areal appraisal funding was more than $58.5 million. Ground-water studies have been made or are currently in progress for all of the Nation. Long-term continuing measurements of ground-water levels were made in about 28,000 wells, and periodic measurements in connection with investigations of ground water were made in many thousands of other wells. Studies of saline-water aquifers, particularly as a medium for disposal of waste products, are becoming increasingly important, as are hydrologic principles and analytic and predictive methodologies for determining the flow of pollutants in ground-water systems. Land subsidence caused by ground-water depletion, the possibilities for induced ground-water recharge, and the practicality of subsurface disposal of wastes are under investigation. Ground-water supplies for energy development and the effects of coal-mining activities on both ground- and surface-water resources are being intensively studied.

The use of computers continued to increase in research studies of hydrologic systems, in expanding

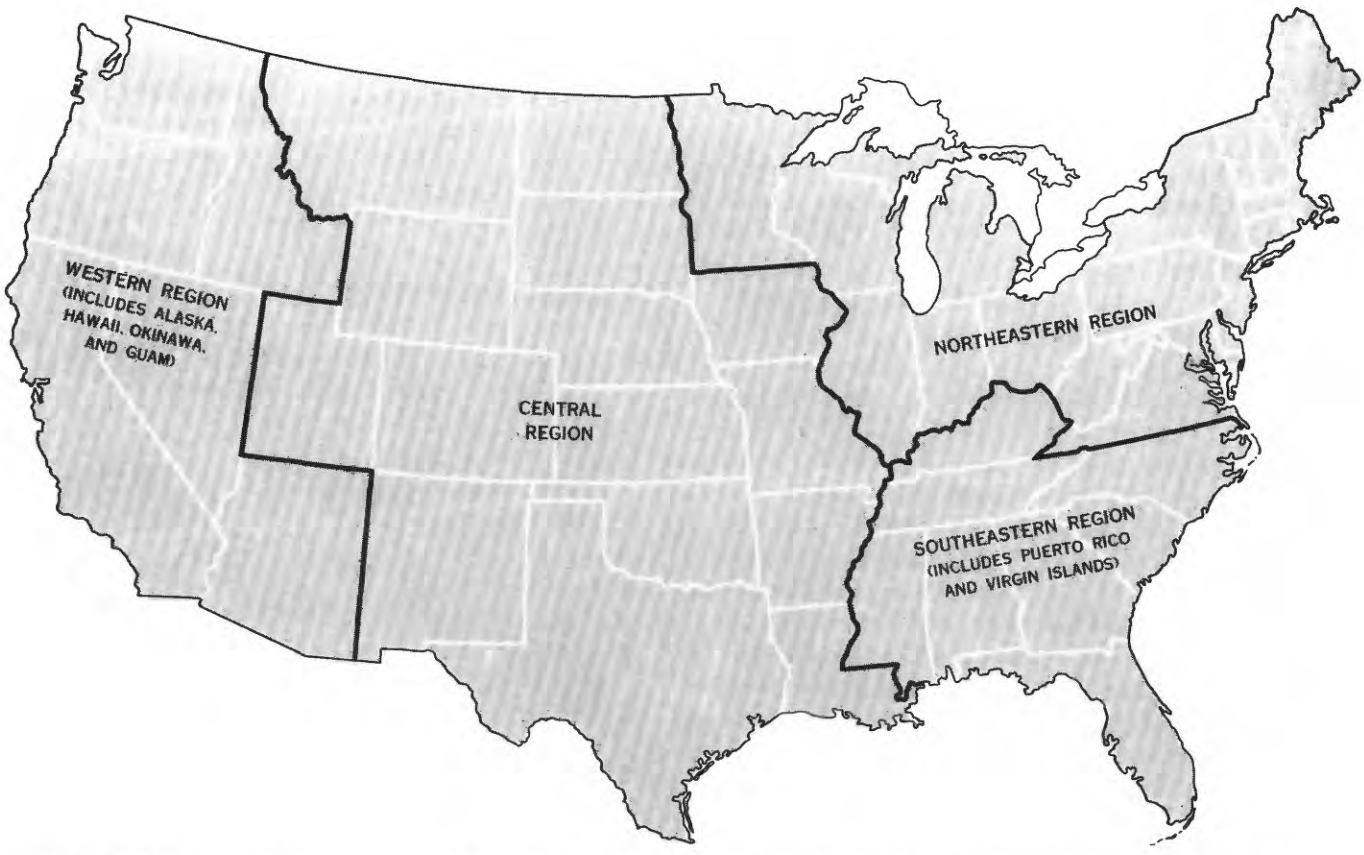

FIGURE 1. Index map of the conterminous United States showing areal subdivisions used in the discussion of water resources.

data-storage systems, and in quantifying many aspects of water-resource studies.

Records of about 320,000 station-years of streamflow acquired at about 17,600 regular streamflow stations are stored on magnetic tape, and data on about 580,000 wells and springs have been entered in a new automated system for storage and retrieval of ground-water data. Digital computer techniques are used to some extent in almost all of the research projects, and new techniques and programs are being developed continually.

NORTHEASTERN REGION

Hurricanes brought major flooding to Indiana, Maryland, and Ohio. Two major storms struck Indiana in July 1979. Hurricane Bob dumped 0.17 m of rain on central Indiana on July 13 and 14, causing serious flooding in Hendricks and Morgan Counties. From July 26 to 28, 1979, Hurricane Claudette released 0.3 m of rain in southern Indiana and 0.18 m in western Indiana just north of Terre Haute. Peak discharges of record were observed on several streams, and recurrence intervals ranged from 50 to 100 yr. The remnants of Hurricane David brought severe flooding to central Maryland on September 5 and 6. Peak discharges at several gaging stations exceeded 100-yr levels. Heavy rainfall, ranging from 0.11 to 0.18 m in 24 hr, from tropical disturbance Frederic resulted in flooding in central and northeastern Ohio. Some streams were reported to have had peak flows with recurrence intervals of more than 50 yr.

A 5-yr study of northern Atlantic coastal plain regional aquifers in a six-State region, from Long Island to North Carolina, has begun. The study is designed to delineate the flow system of the coastal plain aquifers and to evaluate potential aquifer response to regional ground-water development. Specific objectives include (1) defining the regional aquifer system, including geology, hydrology, and geochemistry, (2) defining the predevelopment flow system and the changes caused by development, (3) simulating the aquifer system by digital computer models, (4) using simulation models to determine the effects of stresses on the aquifer system and on streamflow, (5) evaluating plans for managing ground water, (6) determining the saltwater-freshwater interface and evaluating its movement, and (7) develop-

ing a management system for hydrologic data and designing a data-collection program for the future.

Studies directly related to land disposal of wastes and toxic spills include the coal-tar contamination of ground water in Saint Louis Park, Saint Paul, Minn., groundwater contamination by trichloroethylene at Wurtsmith Air Force base in Michigan, low-level radioactive waste burial in Sheffield, Ill., and PCB contamination of surface water and ground water along the Housatonic River in Massachusetts and Connecticut.

Evaluation of water quality was intensified in coal-producing States and in States where peat mining might be feasible. Streams were sampled synoptically during low and high flow throughout Illinois, Indiana, Maryland, Ohio, Pennsylvania, Virginia, and West Virginia. Samples of water and bottom material were analyzed to evaluate the water quality of both mined and unmined areas. Projects to study effectiveness of surface-mine reclamation and specific problems related to subsurface mining were begun. The disturbance of peat bogs by various mining techniques is being studied comprehensively, with emphasis on mobility of soluble and organically complexed metals and nutrients.

Urban hydrology projects were begun in Illinois, Maryland, Minnesota, New York, and Wisconsin to assess the impact of nonpoint loading of streams carrying suburban and urban runoff from some of the Nation's largest cities.

Eleven of the fourteen districts in the northeastern region were reviewed and advised on computer and word-processing hardware and software, as well as on computer staffing. This review has resulted in coordinated procurement of new computer and word-processing equipment that will allow increased productivity and communications between field units, the region, and main computers. The thrust of these computer efforts will continue to be toward "electronic offices" and the acquisition of many display terminals in all districts. These machines will enable the user community to become familiar with computers before minicomputers become generally available in the next few years.

CONNECTICUT

Ground-water resources in southwestern Connecticut

J. W. Bingham and Daniel Meade (Connecticut Department of Environmental Protection) investigated seven areas underlain by stratified drift in Fairfield County. Test drilling and seismic-refraction profiling were used to define aquifer geometry, saturated thickness, and grain-size characteristics. Maximum saturated thickness ranges from 15 to 37 m in the separate aquifers, and the estimated maximum transmissivity is about 1,100 m^2/d. Four of the stratified drift aquifers seem to be potential sources of future public water supply, but long-term yields will have to be further evaluated. Water quality in the aquifers and interconnected surface-water bodies also will have to be defined.

Aquifer characteristics and organohalides in ground water, Southbury and Woodbury

D. L. Mazzaferro completed the initial evaluation of hydrogeologic data on the stratified drift aquifer underlying the Pomperaug River valley in Southbury and Woodbury. Data indicate that the thickness of the aquifer exceeds 50 m in places and transmissivity is locally greater than 1,200 m^2/d. The most extensive deposits of saturated coarse sand and gravel underlie the central and southern parts of Woodbury and the northern part of Southbury.

A preliminary assessment of water quality in several observation wells tapping this aquifer indicates that organohalide contamination, first identified by the Connecticut Department of Health Services, is generally limited to the "Middle Quarter" area of Woodbury. Water sampled from a well 120 m from the public-supply well, where organohalide compounds were first discovered, had a maximum trichloroethane concentration of 260 Mg/L.

DELAWARE

Late Miocene aquifers

The two late Miocene aquifers tapped for municipal water supply in eastern Sussex County are separated by a thin leaky confining bed, according to A. L. Hodges, Jr. Pumping is seasonal, and, during periods of heavy pumping, water levels in wells tapping the two aquifers differ. When pumping decreases, however, water in the wells rises to essentially the same level. The unit response of the two aquifers to stress and its relief is an important factor in the model of ground-water flow now being designed.

ILLINOIS

Rating studies at Illinois River dam sites

Discharge of the Illinois River was measured below two Chanoine wicket dams near Peoria and LaGrange. According to D. M. Mades, these measurements confirm results of laboratory tests on the structures. At Peoria Dam, the discharge through the 76.2-mm-wide gap between adjacent wickets was determined to be 1.91 m^3/s for normal upper and lower pool depths of 4.69 and 1.34 m, respectively. At LaGrange Dam, flow over five lowered wickets, each 1.22 m wide, was 29 percent of

the total measured flow of 279 m^3/s. The remaining 71 percent (198 m^3/s) was estimated to be flow through 130 gaps between the remaining 130 raised wickets.

Potentiometric surface and chemical characteristics of shallow aquifers in McHenry County

Mapping of shallow aquifers in McHenry County reveals great differences in water levels caused by semiconfined conditions of multiple sand and gravel lenses within the drift, according to J. T. Krohelski. A potentiometric surface map that defines average water levels in wells may differ several meters from true levels, depending on the location and depth of the sand and gravel lens.

Most of the shallow ground water is a calcium bicarbonate type. Median values for selected constituents from 29 wells are nitrate nitrogen, 2.6 mg/L; ammonia nitrogen, 2.7 mg/L; and total organic carbon, 2.8 mg/L. The median pH was 7.8. Specific conductance, measured in 131 wells, ranged from 435 to 1,170 μmho/cm at 25°C and had a median value of 660. Specific conductance was higher where pumping was greater.

Testing deep wells in sandstone

Most deep wells tapping sandstone in northern Illinois penetrate multiple aquifers. According to M. G. Sherrill, many of these wells can be used to determine hydraulic and water-quality characteristics for individual aquifers by means of borehole logging and packer testing when the wells are shut down for servicing.

INDIANA

Nature and extent of the unconsolidated aquifers underlying the Indiana Dunes National Lakeshore

Preliminary results of test drilling at sites throughout the Indiana Dunes National Lakeshore, from Gary to Michigan City, indicated significant variation in the hydrogeology of the unconsolidated deposits, according to D. C. Gillies. These deposits range in thickness from 27 to 77 m and average 51 m. Bedrock is generally shale under the eastern half of the lakeshore and limestone under the western half. A layer composed of clay and silt immediately overlies the bedrock at most drilling sites. The aquifer units described by Meyer and Tucci (1978) have been tentatively identified in most of the lakeshore. Unit 1 seems to be areally more extensive than unit 3, however, because it was found at nearly every site. Unit 3 is apparently absent under the western one-fourth near Gary and at other isolated locations. Another aquifer unit has been tentatively identified in the bottom of a bedrock valley that trends north-south through the center. The potentiometric level in unit 3 is generally higher than in unit 1 where both units are present. The maximum difference in potentiometric level is at a site near Michigan City, where the level in unit 3 is about 9 m higher than the level in unit 1 and about 8 m above land surface.

Preliminary water-level data from a network of shallow piezometers that penetrate the shallow aquifer (unit 1) underlying the Great Marsh area illustrate the hydraulic relation between the water of the marsh and the shallow ground-water system. Ground water apparently discharges upward into the marsh and then downward in places to reenter the ground-water system. Upward ground-water flow may be caused by an absence of the confining layer (unit 2), allowing direct hydraulic connection between the confined aquifer (unit 3) and the shallow unconfined aquifer (unit 1). Downward flow seems to be concentrated along the northern downgradient edge of the marsh.

Southwestern Indiana lineament study

Areal photographs were used to map fracture traces and lineaments in three counties in southeastern Indiana where bedrock is overlain by thin drift. The bedrock consists of limestone, dolomite, and shale. Limestone and dolomite, principal aquifers in this area, have a low and highly variable transmissivity. Records of 425 wells were used to study the relation between well yields and their location with respect to lineaments and fracture traces. According to T. K. Greeman, preliminary data suggest that the yield of wells along lineaments, at their intersections, and at their intersections with fracture traces may be 1.5 times greater than other wells. Specific capacities of 275 wells range from 2,484 to 0.044 L/min/m of drawdown, with a median of 0.745 L/min/m of drawdown. Other factors that seem to favor higher yielding wells include location of the lowest local elevation and proximity of the wells to major drainageways.

Evaluation of ground water in Elkhart County

Three-dimensional flow model analysis and chemical sampling of the glacial-outwash aquifer underlying northwestern Elkhart County by T. E. Imbrigiotta and Angel Martin, Jr., suggest that proposed pumping at the city airport will not alter flow patterns enough to draw leachate from the nearby Himco Landfill. Transient model analysis indicates that pumping 0.4 m^3/s at the proposed airport site will produce steady-state conditions after approximately 600 d.

The plume issuing from the landfill was found, by using bromide as a leachate indicator, to be confined to depths less than 15 m, not laterally widespread, and extending less than 2 km downgradient. Volatile organic compounds were found in the industrial park vicinity but seemed to be highly localized. Thus, no plume could be defined from the present well network.

Results from initial model calibration

Initial calibration of the five ground-water flow models for Hamilton, Tipton, Madison, Delaware, and Randolph Counties has helped in understanding the flow system. Although outwash deposits in Hamilton County are significant sources of water, undeveloped outwash in counties upstream from Hamilton seem to contribute only a small component of total flow, according to W. W. Lapham and L. D. Arihood. The value of 160 m/d from specific capacity tests for hydraulic conductivity of sand and gravel proved to be a good estimate for computing aquifer transmissivity. Transmissivity has varied only by a factor of five and in most areas by less than five. Initial estimates of 2.32×10^{-3} m/d for vertical hydraulic conductivity of clay between confined aquifers had to be increased by one to three orders of magnitude. The original estimate of outwash recharge of 343 mm had to be reduced to 152 mm, whereas the till recharge ranged from 13 mm to 114 mm. Data were derived from about 2,000 private well logs, 100 observation wells, and 250 measured water levels per modeled area.

Water-level declines in Cambrian and Ordovician rocks in northwestern Indiana

R. J. Shedlock reported that measurements in two wells in extreme northwestern Indiana indicated that pumping from Cambrian and Ordovician rocks in the greater Chicago area has caused significant water-level declines. The water level in one well, finished in the Franconia, "Ironton," and "Galesville" Sandstones of Cambrian age, has declined about 75 m since 1933. The level in the second well, finished in Ordovician rocks, including the Trenton ("Galena") and Black River ("Platteville") Limestones and the St. Peter Sandstone, has declined 20 m since 1949.

MARYLAND

Aquifer studies in western Montgomery County

A recent appraisal of ground water in a 240-km² area of western Montgomery County indicated that lack of available ground water may limit additional population growth and industrial development. The area is underlain mainly by Triassic shale and sandstone and by lower Paleozoic phyllite and phyllitic schist. Yields of wells range from <1 to 25 L/s, and the yields of some of the best wells declined by as much as 35 percent during a dry period in 1978. This decline posed a problem for the town of Poolesville during the summer and fall of 1977 and 1978. Total ground water used in the report area in 1978 was estimated to be 1,987 m³/d, of which 931 m³/d was used by Poolesville.

MICHIGAN

Hydrologic analysis of Sands Plain

Sands Plain, 500 km² in area, is a potential site for sand and gravel mining, for water for public and mining supplies, and for disposal basins for tailings from iron-ore concentration. Development could alter the hydrologic system by changing infiltration, water levels, streamflow, and water quality. N. G. Grannemann reported that 38 wells were drilled through glacial deposits to bedrock to obtain lithologic and hydrologic data. Glacial deposits are as thick as 140 m, and water levels range from 1 to 50 m below land surface. In fiscal year 1979, 4 gaging, 19 partial record, 2 precipitation, and 3 continuous-record water-quality stations have been established. Models that simulate the relation between ground water and surface water will be used to predict the effects of development.

Flow model of Saginaw River

A one-dimensional unsteady flow model is being used by D. J. Holtschlag to simulate flow of the Saginaw River from Saginaw Bay to a point about 32 km upstream. A network of four gaging stations and two weather stations was established during 1979 to obtain stage and wind velocity. Channel and reservoir geometry were determined, and discharge was measured at selected locations.

High flow is being simulated by a preliminary flow model. Simulated flows compared favorably with both measured discharge and discharge estimates based on the currently used slope rating.

Study of ground water contaminated by trichloroethylene

Trichloroethylene (TCE) has contaminated a principal aquifer at Wurtsmith Air Force Base, Iosco County, north of Saginaw Bay. The extent of the contaminated area and the direction and rate of movement of ground water and TCE are being studied by J. R. Stark. Nearly 100 wells, 15 to 25 m deep, were installed to define aquifer characteristics and to collect water-quality samples and water-level information. The aquifer is composed primarily of sand and is underlain by relatively impermeable clay. Water levels in most wells are 4 to 8 m below land surface. Data from the wells are being compiled and analyzed to delineate the ground-water system. A model simulating ground-water flow also is being developed.

Model study of Michigan coal deposit

A three-dimensional model was used by J. R. Stark and M. G. McDonald to study ground-water constraints

to coal mining in a 51.8-km² area in Bay County. The principal coal bed is 1 m thick and about 45 m below land surface, typical of most coal deposits in Michigan.

Hydraulic conductivity and storage coefficient of seven lithologic units were evaluated by aquifer tests and a finite-difference flow model. A model simulating ground-water flow to a hypothetical mine was developed. Results of the study indicate that seepage probably will not be great enough to preclude mining. Also, pumping water to keep the mine dry will have little effect on heads in aquifers outside the mine during the first decade of mining.

MINNESOTA

Rainfall-runoff relations in the Coon Creek watershed, Anoka County

Based on the first year of data collection, A. D. Arntson reports that differences in rainfall-runoff characteristics between developed and undeveloped areas of the Coon Creek watershed are consistent with the basin response expected. Records from six storms indicated that 25 mm or more of rain was uniformly distributed over the 251-km² basin. Some storms did not produce a significant rise in stage, owing to low antecedent soil moisture and high infiltration capacity of the soils. The time from midpoint of rainfall to peak stage (response time) ranged from 2 to 30 h as determined at five automatic recorders. The shortest response times were from intense storms of 1 to 2 h duration in developed areas. The longest response times were from less intense storms of 12 to 19 h duration in undeveloped areas. The peak discharge and volume of runoff were greater for developed areas than for undeveloped areas, owing to more impervious area and less storage area.

Results of analyses of stream samples collected during storms generally show an increase in BOD, nutrients, and metals, and a reduction in DO compared with samples collected during base flow. Samples from streams draining developed areas showed higher concentrations of metals and total phosphorus and lower concentrations of nitrite, nitrate, chloride, and dissolved organic carbon, especially during storms, than samples from streams draining undeveloped areas.

Water quality of lakes in Eagan

M. A. Ayers, G. A. Payne, and M. R. Have reported that differences in the quality of water from 17 lakes in Eagan, in the Twin Cities area, were related to differences in urbanization during a study from 1972 to 1978. However, water-quality variations within each lake were affected more by climatic variations than by land-use changes.

Dissolved solids, alkalinity, and chloride concentrations varied most in lakes having urbanized watersheds, in lakes having outlets, and in lakes less than 2 m deep. The increase in chloride in certain lakes without outlets was caused in part by urbanization but was intensified by the drought of 1976–77.

Fifteen of the lakes are less than 3 m deep and frequently mix throughout their profiles during open water. These lakes are highly eutrophic, primarily because of high nutrient loading and recycling of nutrients. Three phosphorus-prediction models developed during the study are applicable to shallow (less than about 4 m) nonstratifying lakes and ponds.

Holland and Fish Lakes, 16 and 10 m deep, respectively, were the least eutrophic. These lakes limit continuous recycling of nutrients from bottom materials to surface waters through thermal stratification and entrapment of nutrients in the hypolimnion.

Potentiometric data from deep test well

A test well drilled to 170 m in Afton State Park in Washington County penetrated the Jordan Sandstone, St. Lawrence and Franconia Formations, and Ironton, Galesville, Eau Claire, and Mount Simon Sandstones, according to Jack Guswa and Jim Ruhl. Piezometers were installed in the St. Lawrence, Ironton-Galesville, and Mount Simon units; head measurements (altitude) made on January 23, 1980, were approximately 219, 222, and 217 m, respectively. The measurements indicate that water in the Ironton-Galesville aquifer may be moving both upward through the St. Lawrence Formation toward the nearby St. Croix River (altitude 206 m) and downward toward the Mount Simon Sandstone.

Baseline water quality established before highway construction

According to M. R. Have, chemical analysis showed that shallow Rogers Lake, in the Minneapolis–St. Paul area, is nutrient enriched. Sodium and chloride concentrations were relatively high compared with those of other lakes in the area. The lake is separated into two parts by a culvert; the upper part is smaller and shallower. The upper part tended to have higher concentrations of dissolved salts and nutrients. Blue-green algae predominated all year in both lakes, but the upper had generally higher cell counts. DO concentrations were generally lowest during ice cover, although DO was highest at one of the sites during this period. Generally, however, oxygen concentrations were highest during the growing season.

Ground-water appraisal of sand-plain areas in central Minnesota

According to G. F. Lindholm, glacial-outwash aquifers in Benton, Sherburne, Stearns, and Wright Counties

may yield from 125 to 190 L/s to wells. Transmissivity determined from aquifer tests was 12,000 m^2/d in buried outwash in Sherburne County and 9,000 m^2/d in surficial outwash in the Maine Prairie area of Stearns County. Water in surficial aquifers in heavily irrigated parts of Sherburne County contains greater than average concentrations of nitrate and chloride.

Numerical models of Sherburne County and the Maine Prairie area of Stearns County were used to simulate the response of the water table to various water-use and climatic conditions. The simulations indicated that water-level declines of 1.2 m can be attributed primarily to withdrawal by wells. Addition of several more pumping centers withdrawing at current average rates would probably cause little additional lowering of water levels if recharge rates remain average. If pumping is increased significantly and recharge is low, however, as during a drought, water-level declines of 3 to 5 m are possible.

Sensitivity analysis useful for planning data collection

R. T. Miller reported that sensitivity analysis was used successfully to schedule the drilling of 224 test holes and the locations of 33 observation wells. A preliminary two-dimensional flow model of the Pelican River sands aquifer in northwestern Minnesota was used for the analysis. Various boundary conditions were tested, such as no flow, constant head, and constant flux, and the effects on head and mass water balance were analyzed. The preliminary model was generally most sensitive to boundary conditions of no flow or constant flux and least sensitive to boundary conditions of constant head.

Results of the test drilling indicate that the aquifer consists of ice-contact deposits. Saturated thickness averages 17 m, and hydraulic conductivity is estimated to range from 10 to 120 m^2/d.

Hydrologic budget of Eagle Lake in central Minnesota

According to C. F. Myette (1980), 8.2×10^6 m^3 of water flowed through Eagle Lake in the 1978 water year. Analysis of the hydrologic budget indicated that inflow consisted of 45-percent surface water, 22-percent ground water, and 33-percent precipitation. Outflow was 73-percent surface water and 25-percent evaporation. About 2 percent of the budget was reflected by a net change in lake storage.

Appraisal of ground water in central Minnesota

Stage measurements of wells and streams indicate that water levels in surficial aquifers in Todd County remained above normal during most of 1979, according to C. F. Myette. Estimated recharge to the aquifer in 1979 was 270 mm. Annual streamflow was above the 25th percentile on the duration curve, which indicates high base flows. In late October, 33 flow stations were established on the Long Prairie River. Low-flow measurements at the stations showed that streamflow increased 28 L/s per river mile.

Analyses of samples from 28 wells and stream sites indicated that the water is of the calcium bicarbonate type. Concentrations of dissolved solids ranged from 190 to 395 mg/L; NO_2+NO_3, as N dissolved, ranged from 0 to 6.4 mg/L; pH ranged from 7.3 to 8.4; and specific conductance ranged from 330 to 650 μmhs. Samples from a well near Round Prairie showed trace amounts of atrazine, piometryne, and 2,4-D.

Water-quality monitoring in lakes in northeastern Minnesota

Water samples were collected by G. A. Payne (1979) at 14 sites in 4 lakes in Voyageurs National Park as part of a monitoring program. Measurements during August 1979 showed that Secchi-disk transparency improved 0.5 m in Sandpoint Lake and 0.8 m in Rainy Lake, compared with August 1978 measurements. Measurements of transparency in Kapetogama Lake and Black Bay were nearly the same as in 1978. Samples collected at the inlet and outlet of Sullivan Bay showed that water leaving the bay was of higher quality with respect to nutrients, algal productivity, and transparency than water entering the bay. Concentrations of As, Cd, Cr, Cu, Pb, and Hg in whole water samples were within limits recommended by EPA for public water supplies.

Effects of peat mining on hydrology in the Red Lake peat lands in north-central Minnesota

The lithology of drift and the depth to bedrock were determined from a deep test hole drilled in the Itasca Moraine near the subcontinental divide south of Black Duck. D. I. Siegel (1979a) reports that bedrock is about 50 m below land surface and is overlain by 18 m of basal sand and gravel that may extend under the Red Lake peatlands to the north. The sand and gravel is overlain by 30 m of till.

Effect of acid precipitation on water quality of the Filson Creek watershed in northeastern Minnesota

Concentrations of sulfate and H+ ion in Filson Creek increased during the snowmelt of 1979. D. I. Siegel (1979b) reports that sulfate increased from <1 to 4 mg/L in 1979, compared with an increase from <1 to 12 mg/L in 1977. The increase in 1979 was simultaneous with snowmelt, whereas that in 1977 was as long as 1.5 weeks after snowmelt. The delayed increase in 1977 is attributed to the soil-moisture deficit caused by the 1976 drought.

Hydrologic setting of Williams Lake in north-central Minnesota

In modeling the hydrologic system of Williams Lake, D. I. Siegel and T. C. Winter found that ground-water inflow to the lake is underestimated if calculated as a residual in the hydrologic budget equation. Results of the modeling suggest that ground-water interaction with the lake may be as much as 100 percent greater than indicated by the residual value commonly determined in budget analyses.

Ground-water appraisal in Big Stone County

Narrow sinuous sand and gravel deposits less than 3 m thick occur in much of northwestern Big Stone County. A steep-sided bedrock valley containing more than 30 m of fine quartz sand was identified; however, evidence of an extensive buried aquifer was lacking. Water in near-surface drift aquifers contains boron in concentrations toxic to most crops.

Appraisal of Cambrian and Ordovician aquifers in southeastern Minnesota

Five areally extensive aquifers of Cambrian and Ordovician ages are being studied in southeastern Minnesota as part of the Northern Midwest Regional Aquifer System Analysis, according to D. G. Woodward. Hydrogeologic maps have been constructed for each aquifer and for each confining unit to document geologic structure and thickness. Maps also have been constructed that show the potentiometric surface of each aquifer. Wells in the bedrock aquifers collectively supply 160 municipalities in the study area. M. A. Horn reports that ground-water withdrawal in the seven-county St. Paul–Minneapolis metropolitan area was about 300 million m^3 in 1976, with the Prairie du Chien–Jordan aquifer contributing about 80 percent and the Mount Simon–Hinckley aquifer about 10 percent. Since 1885, declines of the potentiometric surface of the Mount Simon–Hinckley and Prairie du Chien–Jordan aquifers in the metropolitan area exceed 70 m and 27 m, respectively.

NEW JERSEY

Drainage areas determined for New Jersey streams

Drainage area data have been determined by A. J. Velnich for more than 1,100 sites on New Jersey streams in the Delaware River and Delaware Bay basins. Included are data for all named streams at their mouths and gaged sites, as well as descriptive location, latitude, and longitude information.

NEW YORK

Preliminary hydrogeology of an artificial-recharge site

D. A. Aronson (1980) reported that recharge facilities at the Meadowbrook artificial-recharge site in central Nassau County have been completed. Water mains have been tested preparatory to transmittal of reclaimed waste water to the recharge site from the Cedar Creek tertiary treatment plant. Instruments to monitor flow through the unsaturated zone in manholes in two of seven recharge basins are being installed.

Preliminary results of chemical analyses of prerecharge water samples from 47 observation wells showed that water in the upper glacial aquifer and the upper parts of the Magothy aquifer contains significant concentrations of low-molecular-weight chlorinated hydrocarbons, organochlorine insecticides, and PCB's (Katz,1979). Bacteria are present in the ground water. Aerobic heterotrophs and nitrogen-transforming bacteria are generally present; however, the absence of fecal coliforms and fecal streptococci indicates that there is no fecal contamination.

Preliminary three-dimensional digital-model analyses were made to predict the water-table rise in Nassau County and parts of neighboring counties caused by recharge of as much as 0.18 m^3/s of reclaimed water to the ground-water reservoir. Results suggest that water-table mounds beneath recharge basins locally may exceed 6 m. Streamflow at East Meadow Brook may increase by more than 30 percent owing to artificial recharge.

Pumping test in southern Nassau County, Long Island

Results of a 2-d pumping test by J. B. Lindner and T. E. Reilly in southern Nassau County were analyzed by Stallman's curve-matching technique (Lohman, 1972) and modeled by using a finite-element model developed by T. E. Reilly for the transient response of a radially symmetric aquifer. Preliminary model results are in close agreement with the analytical solution and indicate a hydraulic conductivity of 4.9×10^{-4} m/s at this site in the upper glacial aquifer ($T\simeq1.2\times10^{-2}$ m^2s, a specific yield of 0.23 and an anisotropy of 7:1.

Surficial geology and well guides in Oswego County

According to T. S. Miller and E. H. Muller, all of Oswego County is underlain by drift. Low well yields are typical, but adequate water supplies for domestic and farm use can be obtained from lacustrine sand, till, and bedrock. Larger yields might be obtained from localized sand and gravel (kame) deposits.

Development of a Galerkin finite-element flow model for the transient response of a radially symmetric aquifer

A model program for evaluating radial flow of ground water was developed by T. E. Reilly. It is capable of simulating anisotropic, inhomogeneous, confined, or pseudounconfined aquifer conditions. Analytical solutions for simple radial-flow problems are available in the literature. More complex systems, however, require more complex analyses. The results of this model compared well with published analytical and model solutions. The program is being used at present to aid in the analyses of complex pumping tests on Long Island.

Utilization of a regional ground-water-flow model to evaluate boundary conditions for a subregional model

Proposed sewerage in Suffolk County, Long Island, will reduce recharge to the ground-water reservoir by 1.31 m^3/d, according to T. E. Reilly and H. T. Buxton. Treated effluent will flow directly to the ocean. Such reductions in recharge on Long Island have, in the past, lowered ground-water levels. As streamflow on Long Island is highly dependent upon baseflow seepage, fluctuations in local ground-water levels around streams can affect streamflow significantly.

To quantify the response of the hydrologic system to the proposed sewering, a three-dimensional finite-difference ground-water-flow model is being developed. The steady-state calibration has been completed. The model was found to simulate the long-term average hydrologic conditions in this complex multiaquifer system realistically, including interaction among streams, lakes, and the ground-water system.

A fine-grid subregional model simulating a large area around the sewer district was developed, but it represents only a part of the ground-water-flow system of Long Island. To simulate the entire hydrologic system realistically, long-term conditions will be simulated through the use of a large-scale regional model of the entire Long Island hydrologic system. Boundary conditions for the subregional model will then be calculated from the regional model.

Ground-water quality of a postglacial sand-dune environment

D. S. Snavely reported that water samples from 19 observation wells had chloride concentrations ranging from 150 to 200 mg/L. Concentrations were higher in wells close to major thoroughfares, which suggests that the chloride is derived from road salt. Additional samples will be analyzed this spring. The sand aquifer seems capable of yielding enough water for municipal supplies, but the water is of questionable quality for drinking.

Organic pollutants in ground water

R. A. Schroeder and D. S. Snavely reported that 50 municipal ground-water supplies in upstate New York were analyzed by computer-directed gas chromatography-mass spectrometry scans for the 114 EPA "Consent Decree" organic priority pollutants. Results indicate no pollution above the submicrogram-per-liter range at nearly all sites. Where pollution was found, it consisted mainly of such volatile compound types as organochlorines and substituted benzenes. Although sources of pollution were not sought, evidence suggests point discharges from isolated industries. Nonpoint pollution of ground water is unlikely in New York except in heavily populated areas.

Hudson River Estuary flows

D. A. Stedfast reports that on August 21, 1979, three discharge measurements were made simultaneously on the Hudson River Estuary, a 260-km reach extending from the Federal Dam at Troy to New York City Harbor. Measurements were continuous over 13 h (approximately one tidal cycle) at Albany, Kingston, and Poughkeepsie. Measurements at Albany were made with eight measurement cranes and meters. Measurements at Kingston were made from a moving boat approximately 2 km north of the Kingston-Rhinecliff Bridge. Vertical velocity measurements were made at the moving-boat site so that the surface velocities measured from the boat could be related to the mean velocities. Velocities were derived from a mean-velocity correlation developed from previous bridge measurements. Flow reversals were observed at all three sites. Sinusoidal discharge-time curves were observed at Poughkeepsie and Kingston, with the peak flows in each direction approximately equal to 6,200 and 4,800 m^3/s, respectively. The discharge-time curve for Albany was irregular, with the peak flow in each direction approximately equal to 570 m^3/s and with the flow reversal prevailing during only 2 of the 13 h measured. The unusual shape of the discharge-time curve at Albany probably was due to slightly varying inflows at the Federal Dam and the reflection of gravity waves off the dam. The flows at all three sites were compared with those calculated by a nonsteady-state flow model being developed for the estuary. The preliminary results of the model seem to indicate that flows in the estuary can be accurately simulated by the model, although further work is necessary to improve its calibration near Albany, owing to the complexity of flows in that area.

OHIO

Subsurface mines as a water source

Abandoned subsurface coal mines are a potential source of water for coal conversion or other industrial use in a region where ground water is meager. A study by J. O. Helgesen and T. M. Crouch of a 44-km^2 network of mines that contain water under pressure showed that 32 km^2 is hydraulically interconnected. Most water pumped from the mines would be derived either from intercepted discharge to streams or from increased leakage from overlying rocks. Practical sustained yield is estimated at 90 to 160 L/s, which could provide part of expected water demands for a typical coal-conversion facility. Much of the water has dissolved-solids concentrations of less than 2,000 mg/L and pH near 7.0. Iron and manganese concentrations are generally high, and some brackish water is present in remote parts of the mine system. Long-term changes in the quality of pumped water would probably not be substantial.

PENNSYLVANIA

Water-supply capability of carbonate rock, south-central Pennsylvania

A. E. Becher reports that the median calculated yield of wells in carbonate rocks of Franklin County is 1.9 L/s, the same as the yield of the Martinsburg Shale but much less than the 12 L/s for carbonate rocks farther north in the Cumberland Valley. Water-bearing zones in the carbonate rocks are shallow; almost 90 percent are less than 60 m below land surface. Wells in the Tomstown and Waynesboro Formations do not penetrate sufficient bedrock below the colluvium to adequately test their capacity. Data on water-bearing zones, thickness of overlying colluvium, and ground-water contributions to streamflow in Antietam Creek indicate a potential for large supplies of water at depths greater than 60 m below the colluvium. Water quality is generally good, although the water is very hard.

Premining water quality in the Stony Fork drainage basin, Fayette County

Streamflow data, including sediment, water quality, and biota, have been analyzed for the Stony Fork drainage basin by D. E. Stump, Jr. Data, collected before extensive surface mining, were used to define initial conditions. Daily sediment concentrations ranged from 590 to 2 mg/L. Specific conductance ranged from 170 to 50 μmho, with an annual average of 84 μmho; pH ranged from 7.4 to 5.5; and water temperature ranged from 0.5°C to 24°C and averaged 9.6°C. Biological sampling identified 20 fish species and a diversity index greater than 3.0 (indicating clean water).

RHODE ISLAND

Hydraulic properties of an anisotropic water-table aquifer in the Chipuxet River basin

Eighteen tests at ten locations of an anisotropic water-table aquifer in the Pawcatuck River basin in southern Rhode Island were analyzed by D. C. Dickerman and H. E. Johnston. The aquifer is composed of stratified drift consisting of complexly interbedded lenses of sand and gravel and subordinate amounts of interbedded silt and silty sand. The tests were made in the thick permeable parts of the stratified-drift aquifer, which is a major aquifer in the lower reaches of the Chipuxet River basin and adjacent parts of the Chickasheen Brook and White Horn Brook basins. The aquifer has an average saturated thickness of 24 m and a maximum saturated thickness of 60 m. The large-diameter (20–46 cm) pumping wells were 17 to 53 m deep and were pumped at 6.3 to 57 L/s for 4 to 124 h.

The analyses indicate that transmissivity of the more permeable parts of the aquifer ranges from 400 to 3,600 m^2/d and that average horizontal hydraulic conductivity ranges from 20 to 140 m/d. Test wells were not pumped long enough to obtain reasonable storage coefficients. Vertical hydraulic conductivity determined at seven sites ranged from 1.5 to 70 m/d; the median was 6.5 m/d. At these sites, the ratio of horizontal to vertical hydraulic conductivity ranged from 1.3:1 to 70:1; the median was 10:1. Transmissivities determined by the analyses were in agreement with those estimated from lithologic logs and specific capacity.

This investigation is the first of five planned for the principal ground-water reservoirs in the Pawcatuck River basin. It is part of a Rhode Island Water Resources Board program to locate, test, and acquire sites from which large quantities of ground water can be withdrawn in southern Rhode Island.

VIRGINIA

Hydrologic data collection, Great Dismal Swamp

B. J. Prugh reported that two synoptic discharge measurements at selected inflow-outflow sites to the Great Dismal Swamp indicate that outflow exceeds surface-water inflow by a factor of 10. The measurements were made during low-flow periods. Ground-water inflow is probably the source of the excess outflow.

According to J. F. Harsh and J. D. Larson, 12 observation wells were installed in the swamp in December 1978. Well arrays consisting of one shallow well having a screened interval below the water table and two deeper wells having screened intervals in the Pliocene Yorktown Formation were installed at two sites to pro-

vide information on water-level changes with depth. Preliminary analyses of the water-level data suggested that confined ground water at depth is under sufficient pressure to discharge into the swamp, where access is available.

Ground-water resources in James City County evaluated

Ground water in James City County is available to meet future water demands, provided pumping is distributed over the county, according to J. F. Harsh. Investigations revealed that four aquifers constitute a complex multilayer coastal plain system. The Cretaceous aquifer is the principal water-yielding unit. It furnishes nearly all ground water for industrial and municipal needs. The average rate of ground-water recharge from precipitation is estimated to be 3.3 m^3/s, compared with a total current pumping rate of 0.35 m^3/s. Movement of water in the Cretaceous aquifer is toward the cones of depression formed by two main pumping centers. All aquifers yield water that generally meets State standards for source waters used for drinking. Water in the principal aquifer is a sodium chloride bicarbonate type and has generally less than 1,000 mg/L dissolved solids. The dissolved-solids content and chloride content are greater in the deep aquifers. Saline water (more than 250 mg/L chloride content) is present in the deep aquifers, particularly near major pumping centers. Continued withdrawal at these centers is likely to promote the movement of saline water into freshwater aquifers.

Hydrogeology of the Culpeper Basin

Test drilling in the northeastern part of the Culpeper Basin provided significant new information on regional geology and geohydrolgy, according to Chester Zenone. Three holes, which ranged in depth from 215 to 330 m, were drilled in siltstone and sandstone of Triassic age in western Fairfax County. Two of the wells were pumped at 22 and 28 L/s. The potential of the rocks was initially suggested by the high yields (as great as 37 L/s) obtained from wells drilled at Dulles Airport 20 yr ago (Johnston, 1960), but most wells drilled since then have been shallow and generally yield less than 0.5 L/s. Observations and discharge measurements during drilling indicated that yield increased as water-filled fractures were penetrated. Aquifer test data at the site of one of the wells showed the strongly anisotropic permeability of these fractured-rock aquifers. A 48-h test was terminated after only 11 h of pumping because of excessive interference with nearby wells along the same bedrock fracture trace as the pumped well. Drawdown in observation wells offset from the trace, however, was virtually nonexistent.

Selection of the test-well sites along fracture-trace lineaments visible on aerial photographs or satellite (Landsat) images was based in part on an earlier analysis of yields of bedrock wells in Fairfax County, plotted against well locations with respect to such lineaments (Iwahashi and Heironimus, 1978; Johnston and Van Driel, 1979). Fracture-trace mapping seems to be a promising tool in locating successful water wells in the Culpeper Basin.

Chemical analyses of water from the Dulles Airport and the recently drilled test wells showed that water quality in the siltstone deteriorated rapidly (sulfate concentrations as great as 1,000 mg/L) with depth below 150 m.

WISCONSIN

Water resources of Forest County

According to E. L. Boyd, ground-water movement in Forest County is from northwest to southeast. The principal aquifer ranges in thickness from zero in the northern part of the county to 60 m in the south.

Ground water in Dodge County

R. W. Devaul and J. J. Schiller reported that water of generally good quality is available from four aquifers in Dodge County, in southeastern Wisconsin. Water from all aquifers is hard to very hard, and dissolved-solids concentration ranges from 280 to 2,340 mg/L. Yields of as much as 32 L/s are available from glacial deposits in about half the county. Sandstone and dolomite aquifers of Cambrian and Ordovician age are capable of yielding 32 L/s in most of the county and 63 L/s or more in some areas. Wells yielding as much as 32 L/s can be constructed in much of the Galena-Platteville aquifer in the eastern half of the county. Wells yielding as much as 6.3 L/s tap much of the Silurian dolomite.

Mole Lake hydrology

Dye dispersion in Rice Lake, on the Mole Lake Indian Reservation, was studied by R. A. Lidwin to determine the potential pattern of movement of pollutants entering the lake from Swamp Creek. Maps of macrophyte abundance and distribution in Rice Lake were prepared, as well as water-table and flow maps for the general study area. A generalized surficial glacial geology map was composited from mapping done by the Wisconsin Geological Survey.

Hydrogeology and ground-water quality in northeastern Waukesha County

The Silurian dolomite aquifer in Waukesha County is composed of several water-bearing strata separated by confining beds that are probably laterally continuous for several kilometers, according to J. J. Schiller. These strata are being defined by water-level data, drillers' reports, and chemical-quality data.

In urban areas, chloride concentrations in ground water may exceed 500 mg/L, even where drift cover is thicker than 15 m. Water from wells open only to lower strata is significantly lower in chloride concentration in urban areas. Relatively high concentrations of nitrate in water from several of these wells indicate probable septic-tank sources. Shallow wells where the drift is thin may be contaminated with coliform bacteria, but contamination is not a problem where the uppermost zone is cased out or the drift is thick.

Saint Croix River flood and water-quality data

To aid the National Park Service in developing support facilities on the Saint Croix River, a recreational stream in Wisconsin and Minnesota, E. E. Zuehls has determined flood elevations to be expected for various frequencies at five sites.

The Saint Croix River water is of generally excellent quality with regard to both chemical constituents and sediment concentrations. With this information, decisions can be made regarding placement of support facilities.

SOUTHEASTERN REGION

Hurricanes and floods struck the Southeastern States in 1979. Hurricane David, after moving up the east coast of Florida and Georgia in early September, moved inland at Savannah, Ga. Flooding was minor, but there was considerable wind damage. A few weeks later, Hurricane Frederic, which made landfall at Mobile, Ala., caused widespread flooding and wind damage. Frederick was one of the most intense hurricanes of record to strike the mainland. At Dauphin Island, at the mouth of Mobile Bay, winds of 230 km/h, accompanied by 215 mm of rain, were recorded. Considerable damage was caused by wind-driven tides from Moss Point, Miss., to Fort Walton Beach, Fla. The maximum tide at Mobile, Ala., the sixth highest of record since 1772, was estimated to have a recurrence interval of 25 to 30 yr.

The greatest flood of record on the Pearl River at Jackson, Miss., occurred from April 12 to 14, 1979. The peak discharge of about 2,900 m^3/s was more than twice the previously measured flood discharge. Frequency of the flood peak was estimated to be in excess of that expected every 100 yr. Flooding from the same storm system also was extensive on other rivers in east-central Mississippi and on rivers in north-central Alabama. Recordbreaking floods occurred on many streams in the upper reaches of the Tombigbee, Black Warrior, and Alabama Rivers, where recurrence intervals of peak discharges exceeded 100 yr at 16 gaging stations.

A series of major rainstorms in August and September 1979 caused extensive flooding in northwest Hillsboro County, Fla. The flooding was unusual in that it occurred in large closed depressions formed since Pleistocene time by the collapse of surficial sands and clays into solution cavities in the underlying carbonate rocks of the Floridan aquifer.

A number of sinkholes, which developed in the last few years in the Tampa, Fla., area, have been attributed to abrupt changes in ground-water levels caused by pumping from the Floridan aquifer. Collapse and subsidence apparently is caused by the withdrawal of support by declining ground-water levels of the surficial materials overlying and filling cavities in the carbonate aquifer.

The value of long-term data collection sites for evaluation of changes in the quality of water of rivers has been demonstrated in North Carolina. Evaluation of long-term records has shown a general decrease in some dissolved constituents evidently due to a reduction in point-source loads by industrial and municipal wastewater treatment facilities. Dissolved sulfates, however, have increased 50 to 125 percent since 1955. The increase is attributed to an increase in atmospheric sulfate that enters the rivers as rainfall runoff.

An investigation at Louisville, Ky., of chloroform in water from a well tapping an alluvial aquifer showed the apparent source of contamination to be a spill that had occurred 5 yr earlier. Test drilling showed that part of the chloroform was trapped in a silty zone in the alluvium above the water table and that the majority of the chloroform was concentrated at and just above the surface of the water table. The chloroform was not mixing with water in the aquifer but, even though heavier than water, was moving along the surface of the water table to the well.

ALABAMA

Hurricane Frederic

Tides and high seas generated by Hurricane Frederic flooded low-lying gulf coast areas from Moss Point, Miss., to Fort Walton Beach, Fla., on September 12 and 13, 1979. The most severe flooding was in the vicinity of Mobile Bay, Ala.

Frederic was one of the most intense hurricanes of record to enter the U.S. mainland. At Dauphin Island, Ala., where the hurricane made landfall, winds of 230 km/h accompanied by 215 mm of rain were recorded. R. H. Bingham and J. C. Scott reported maximum prevailing flood elevations were about 3.0 m at Dauphin Island, Ala., about 3.1 m at the U.S. Highway 98 Causeway across Mobile Bay, and about 4.4 m at Gulf Shore, Ala.

The maximum tide at Mobile, Ala., where storm tides have been documented since 1772, was 2.4 m, the sixth highest of record, and was estimated to have a recurrence interval at 25 to 30 yr.

Flood of April 1979

Heavy and intense rainfall from April 12 to 13, 1979, caused widespread flooding along many streams throughout north-central Alabama. Extensive flooding occurred along the middle and upper reaches of subbasins of the Mobile River basin; the Black Warrior, Tombigbee, and Noxubee Rivers, and the Alabama, Coosa, and Tallapoosa Rivers. Runoff from the storm resulted in recordbreaking floods on many streams. Recurrence intervals of peak discharges exceeded 100 yr at 16 streamflow gaging stations, according to H. H. Jeffcoat.

Baseline hydrology in coal areas

Intensive hydrologic monitoring in four relatively unmined basins in the Warrior coal field is providing information on baseline hydrology that is needed to determine the effect of surface mining of coal on water resources. Basins monitored are in the two dissimilar geologic environments that are found in the Warrior coal field. Preliminary results based on data collected during the first 2 yr (October 1976 through September 1978) of a planned 5-yr study indicated widely differing hydrologic characteristics.

Most of the Warrior coal field is underlain by relatively impermeable strata (indurated sandstone and shale interbedded with coal beds) of the Pottsville Formation of Pennsylvanian age. Along the southern and western boundary of the Warrior coal field, the Pottsville is overlain by permeable strata (unconsolidated sand and gravel) of the Coker Formation of Late Cretaceous age.

According to Celso Puente and J. G. Newton, well yields from the Pottsville generally range from 0 to 0.3 L/s, whereas well yields from the Coker generally range from 0.3 to 6.4 L/s. The pH of water in the Pottsville is in the near neutral range (6.0–7.8) and is moderately hard to very hard. Dissolved solids concentrations are generally less than 20 mg/L.

Streamflow distribution in both geologic environments reflects seasonal precipitation. Storm runoff is characterized by peak flows of short duration that rapidly recede to low-flow conditions. Streams draining basins underlain chiefly by the Pottsville frequently go dry, whereas those draining basins underlain chiefly by the Coker have well-sustained low flows.

Surface water in both geologic environments is generally soft and low in dissolved-solid concentrations (generally less than 80 mg/L). Stream pH is generally in the near-neutral range.

FLORIDA

Subsurface storage of liquid wastes

Liquid wastes are being injected into Florida's subsurface environment at greatly increasing volumes. As of 1976, seven systems were injecting liquid wastes at a combined average rate of 0.66 m^3/s, according to John Vecchioli, D. J. McKenzie, C. A. Pascale, and W. E. Wilson (1979). Other injection systems that are under study, testing, or construction or that have gone into operation since 1976 are expected to make more than a tenfold increase in the 1976 rate within the next decade.

Conditions are favorable in several parts of Florida for the injection of waste water into saltwater-filled aquifers, but the most favorable conditions occur in the southern part of the peninsula. There, a solution-riddled dolomite, known locally as the "Boulder Zone," constitutes a highly favorable stratum for injection of waste water at rates of several hundred liters per second per well. The favorability of conditions throughout the State has been assessed in a map report by J. A. Miller (1979).

Modifications to watershed model

Several input parameters have been eliminated in a version of the Georgia Tech Watershed Simulator, as modified by K. M. Hammett and J. F. Turner. Some of the eliminations result from deletion of algorithms; others result from merging conceptual algorithms. The elimination of these variables has simplified the response surface of the model and has made calibration easier. Mass balance and simulation accuracy are still being evaluated. However, there does not appear to be any loss in accuracy as a result of these modifications.

Use of "effective" impervious area in calibrating rainfall-runoff models for small urban basins

A hydraulically connected impervious area, as used with the USGS-distributed routing model, was computed for use with the USGS urban runoff model RRURBAN1. Roofs, driveways, parking lots, and paved streets not directly draining into a storm sewer or drainage ditch were not counted as effective impervious

areas. Using these criteria, the effective impervious area was reduced from 61 to 50 percent of the total area in a mixed commercial and high-density housing land-use basin and from 20 to 9 percent in a low-density housing land-use basin in the Tampa, Fla., area.

According to M. A. Lopez, the use of total impervious area with the urban run-off model RRURBAN1 resulted in simulated peak discharges 100 percent higher than observed peaks for storms with less than 6 mm of runoff. Simulated and observed peak discharges were not significantly different for storms with over 25 mm of runoff. Using the "effective" impervious area with the distributed routing model, however, resulted in simulated and observed peak discharges that were not significantly different regardless of the size of the storm.

Hydrogeology of the northern gulf coast area

Exploratory drilling and aquifer testing of the upper and lower units of the Floridan aquifer and the sand-and-gravel aquifers in southern Okaloosa and Walton Counties, Fla., were completed. L. R. Hayes (USGS) and Douglas Barr (Northwest Florida Water Management District) were able to define the eastern limits of the clay confining beds that are important to the hydrology of this northern gulf coast area. A lower Floridan test well drilled in Fort Walton Beach showed that saline aquifer to be under less artesian pressure than previously supposed. Completion of a two-dimensional digital model of the upper unit of the Floridan aquifer permitted estimates of water-level declines for the years 1990, 2000, and 2020. The results were consistent with the known hydrology and hydrologic history of the area.

Three-dimensional predictive model at Pensacola

Calibration of a three-dimensional model of the sand-and-gravel aquifer in the Pensacola area of Florida was completed. Further refinement of the model is planned by Henry Trapp who reports that his predictive model is sensitive to pumpage and aquifer transmissivity. A preliminary predictive run for the year 2020 was made using projected increases in pumping as estimated by the Corps of Engineers. The expanded cones of depression in the potentiometric surface and the reduction of streamflow portrayed by the model seemed reasonable in light of aquifer behavior under present conditions.

Water-budget analysis of Lake Jackson

Water-budget analysis by K. M. Hammett of Lake Jackson at Sebring, Fla., indicated that deficient precipitation was not the primary cause of a decline in lake stage from 1970 to 1973. Water-budget components for two 33-mo periods, 1954 to 1957 and 1970 to 1973, were compared. Rainfall deficiency was the same during both periods. The lake stage decline from 1970 to 1973 was, however, about three times greater than that of 1954 to 1957.

The analysis indicates that there was an impact on the ground-water system that resulted in a major change in the response of the lake during periods of deficient precipitation. From 1954 to 1957, inflow from the ground-water system kept lake levels relatively stable despite deficient precipitation. From 1970 to 1973, there was an almost continuous loss from the lake through outflow to the ground-water system. Two changes appear to have impacted about equally on Lake Jackson. The first was an increase in the water-table gradient on the south side of the lake as a result of channelization and deepening of drainage canals. The gradient change increased the potential for ground-water outflow through the shallow aquifer. The second change was a decline of about 7 m in the potentiometric surface of the Floridan aquifer underlying the Lake Jackson area. Previous studies have indicated probable downward leakage from lakes in the area. The decline in potentiometric surface probably increased the potential for downward leakage.

Sinkhole development as a result of hydrologic changes in the Tampa area

The area of municipal well fields on the Gulf Coastal Plain north of Tampa, Fla., is densely pitted with sinkholes and sinkhole lakes that have been developing since Sangamon time. Research by W. C. Sinclair indicates that the sinkholes are caused by the collapse of surficial sand and clay into solution cavities in the underlying carbonate rocks of the Floridan aquifer.

Recent occurrences of sinkholes have been related, in part, to abrupt changes in ground-water levels caused by pumpage. Collapse and subsidence is caused not by current solution of the limestone but by readjustment of the unconsolidated surficial material that overlies and fills existing cavities in the rock. The withdrawal of support from the surficial material by declining ground-water levels is the most common factor that triggers collapse.

Ground water pumped from the area in 1978 contained about 6,800 m^3 of limestone and dolomite (calcium, magnesium, and carbonate) in solution. Most solution takes place where acidic recharge water first reaches the limestone surface. However, the area of induced recharge is so extensive that the effect of induced limestone solution on sinkhole development is negligible.

The control of joint patterns in the bedrock on the location and occurrence of sinkholes is apparent from aerial photographs of the area. Wells located away from

such lineations may be less likely to induce sinkhole collapse than those located along a lineation.

Rains cause flooding in Pinellas, Hillsborough, and Pasco Counties

On May 8, 1979, a large weather disturbance became stationary over parts of south-central Florida. Rainfall of up to 450 mm was reported in Pinellas County, and of 280 to 360 mm was reported in northwestern Hillsborough and southeastern Pasco Counties. H. C. Rollins reported that many streams were out of their banks in Pinellas County and overflowed numerous road crossings. Flooding in Pasco and Hillsborough Counties was minor, with peaks on most streams near the mean annual flood level. The exceptions were Rocky Creek and Sweetwater Creek, which had frequencies of approximately 10 and 25 yr intervals, respectively.

Tropical storms caused extensive flooding in closed depressions in northwestern Hillsborough County, including north Tampa, in August and September 1979. Because of the lengthy period of heavy rainfall in August and September, many homes in the Forest Hills subdivision in north Tampa were flooded for an extended period, resulting in several millions of dollars worth of damage. Part of the subdivision is in a large depression that has no surface outlet. Curiosity Creek, which drains several lakes to the north, flows into the depression and was a significant source of flooding. According to W. R. Murphy, this same section had flooding in 1959 and 1960 that covered an even larger area. Several lakes in north Tampa reached record-high stages, including Lake Ellen near Sulphur Springs, which had a stage record beginning in 1946.

Position of saltwater-freshwater interface in southwest Florida

The position of the saltwater-freshwater transition zone in the Floridan aquifer along coastal southwest Florida is depicted by the 250 mg/L line of equal chloride concentration in the upper producing zone of the aquifer. The line was interpolated by K. W. Causseaux and J. D. Fretwell from chloride concentration data for wells open to the upper producing zone of the aquifer and plotted at a map scale of 1:250,000. The line generally lies inland of the Gulf of Mexico and Tampa Bay within 8 km of the coast from latitude 29° N. in Citrus County, southward to southern Hillsborough County. In Manatee and Sarasota Counties, the line generally lies within 3 km of the coast, except in southern Sarasota County where it turns eastward along the Charlotte-DeSoto County line. The position and movement of the 250 mg/L chloride line are important factors in the effective management of the groundwater resources of coastal areas. The present position of the line will be used as a basis for detecting future movement of the saltwater-freshwater interface.

North Tampa ground-water flow model

A two-dimensional finite-difference ground-water flow model has been calibrated by C. B. Hutchinson to depict steady-state water-level conditions in the Floridan aquifer over a 2,300-km area north of Tampa, Fla. The area contains two proposed and seven active municipal well fields that pump about 3 million m^3/d or about one-half the total daily pumpage from the Floridan aquifer for all uses. The model will be used to evaluate the impact of changing the distribution of pumpage among the existing well fields and to determine sites where additional well fields could be established with minimum impact on the aquifer.

Structure of shallow artesian aquifers

High-resolution continuous marine seismic-reflection profiling was used to define the structure of sedimentary material in Sarasota Bay, Charlotte Harbor, the lower reaches of the Peace and Myakka Rivers, and the Gulf Intercoastal Waterway between Sarasota Bay and Charlotte Harbor.

A uniboom that penetrated about 150 m of sedimentary rocks with good resolution was used as a sound source. According to R. M. Wolansky, the seismic profiles show that the Hawthorn Formation of Miocene age, which contains the secondary confined aquifer, is gently folded and of relatively uniform depth within the study area. The apparent folding is probably the result of depositional draping of Hawthorn sediments over the karstic surface of the underlying limestones of the Floridan aquifer. Limestone beds, which constitute the upper confined aquifer, in the Tamiami Formation of Pliocene age are not folded or areally consistent; these beds pinch out in southern Sarasota and Desoto Counties.

Hydrogeologic mapping, southwestern Florida

Hydrogeologic maps of southwestern Florida have been published or are nearing completion. The maps prepared by R. M. Wolansky show that (1) the thickness of the surficial aquifer ranges from less than 8 m in the western part of the area to 80 m in the eastern part, (2) the thickness of the confining beds overlying the Floridan aquifer range from less than 8 m in the northern part of the area to 220 m in the southern part, (3) the top of the Floridan aquifer is 30 m or more above the National Geodetic Vertical Datum (NGVD) of 1929 in the northern part of the area and 230 m below the datum in the southern part, (4) the bottom of the Floridan aquifer is 200 m below the NGVD of 1929 in the northern part of the area and 950 m below the datum in the southern part, (5) the thickness of the Floridan aquifer ranges from 150 m in the northern part of the area to 625 m in

the southern part, and (6) the top of the permeable dolomite, the most consistent water-bearing zone of the Floridan aquifer in southwestern Florida, is 30 m below the NGVD of 1929 in the northern part of the area and 500 m below the datum in the southern part.

Lake and aquifers relation verified

Fourteen navigable lakes in the Winter Haven chain of lakes in central Florida are interconnected by canals. The lakes occupy isolated basins created by subsidence of surficial sand into the cavernous limestone of the underlying Floridan aquifer. Although maintained at a common level by manmade controls, each lake is presumed to have its own unique hydrologic relation to the Floridan aquifer.

One canal was closed for 64 d, isolating Lake Roy from the remainder of the lakes. Following isolation, the stage of Lake Roy declined at a rate of 12 mm/d, 9 mm/d faster than the remainder of the lakes. The water lost averaged 40 L/s, according to W. C. Sinclair. Flow-net analysis indicated ground-water movement of about 28 L/s from Lake Roy through the surficial aquifer towards an area of lower altitude. The remainder of the water lost was presumed to have leaked to the underlying Floridan aquifer, whose potentiometric head was about 11 m lower than that of the lake.

Water quality of Caloosahatchee River

Land use in the Caloosahatchee River basin is predominantly agricultural in the upper third, native forest and swamp in the central third, and largely urban in the lower third. Drainage in the basin has been modified extensively. Streams in subbasins south of the river have been converted to canals in which water can flow either to or from the river. Streams in subbasins north of the river, however, are still predominantly natural. Early in the 1900's, the headwaters of the Caloosahatchee were connected by canal to Lake Okeechobee so that water from the lake now discharges to the river.

B. F. McPherson and H. R. LaRose reported that specific conductance in the headwaters of the river was in the range of 200 to 500 μmho in the early 1940's but usually was greater than 500 μmhos in the late 1970's, reflecting the increased mineralization of the water discharged from Lake Okeechobee. Specific conductance in the tributaries, both natural and canalized, generally decreases with distance from the river, but tributaries in the upper part of the basin have higher specific conductance than the river because brackish water used to irrigate citrus groves drains to them.

In the middle third of the basin, specific conductance in the river is lower than in the upper third due to dilution by inflow of low conductivity water from the relatively undisturbed land. Specific conductance increases in the lower third of the river because it receives drainage from urbanized areas and mixes with seawater moving up the river from the estuary.

Estuary quality affected by alterations in drainage in the Loxahatchee River basin

Canal-18, dug in 1958–59, has altered the salinity regime in the arm of the Loxahatchee River Estuary into which it drains. During much of the year, freshwater is impounded by manmade controls in Canal-18 and its basin. The estuary downstream of the controls in the canal is relatively saline. Another arm of the estuary, where drainage is more natural, shows a wide range in salinity from fresh to nearly that of seawater. Core samples of bottom sediment have indicated differences in the distribution and type of sediment deposited in the two arms of the estuary that also might be attributed to the influence of Canal-18.

Evaluation of cavity-riddled sandstone aquifer

Approximately 50 km of surface resistivity profiles were used to locate sites for 28 test holes drilled to delineate boundaries of a cavity-riddled zone in the unconfined sandstone aquifer in Palm Beach County. According to J. N. Fisher, the drilling confirms that the cavity zone extends north to south from Riviera Beach to Highland Beach, a distance of 43 km, with an average width of approximately 9 km. The eastern boundary of the zone is about 8 km from the Atlantic Ocean. The cavity zone dips to the southeast, lying at a depth of about 17 to 29 m below land surface in the northwest and 25 to 40 m in the southeast. Saltwater intrusion, the result of increased pumpage, is threatening the coastal well fields of most municipalities in Palm Beach County. The cavity zone, located further inland, is of importance, therefore, as a future supply of freshwater that is less susceptible to saltwater intrusion.

GEORGIA

Regional coastal plain sand aquifer study

Historical and present-day potentiometric surfaces of the Upper Cretaceous undifferentiated aquifer in east-central Georgia and the Upper Cretaceous Providence Sand aquifer in southwestern Georgia were mapped by R. E. Faye and J. S. Clarke. Declines in the potentiometric surface in excess of 30 m were noted in both aquifers, most significantly in the Albany area in southwestern Georgia and in the Twiggs County–Wilkinson County area in central Georgia.

Maps that show aquifer contributions to local streamflow indicate that Upper Cretaceous sediments in

areas of outcrop contribute as much as 450 mm/yr to stream runoff.

Interaquifer ground-water transfer through idle multiaquifer wells

Brine-trace studies made in eight wells in the Albany area by D. W. Hicks and R. E. Krause indicate that a significant amount of ground water is transferred from aquifers of higher artesian pressure to aquifers of lower pressure through idle multiaquifer wells. A concentrated sodium chloride solution was injected into the boreholes at specified depths, and its velocity and direction of movement were recorded by using special geophysical tracing sensors. Water was observed moving at velocities as great as 0.16 m/s from the underlying Providence and overlying Tallahatta aquifers, which have higher heads, through the boreholes into the Clayton aquifer. The potentiometric head in the Clayton has been lowered by extensive pumping of this aquifer in the Albany area.

To determine the total artificial recharge to the Clayton aquifer, rates of borehole velocity were assigned to each unmeasured multiaquifer well based on brine-trace data and well construction. From these velocities and pumpage-frequency data, an estimate of artificial recharge was calculated. In the Albany area, 26 multiaquifer wells act as conduits and transfer over 0.05 m^3/s of recharge to the Clayton aquifer.

Time-trend errors in low-flow analysis of streams

Accurate estimation of low-flow frequencies of streams has become a consideration of increasing importance because of the need for more accurate design flows to support water-quality modeling and to assist in low-flow management. Recent findings, from frequency analyses of selected streamflow stations in Georgia by T. R. Dyar and S. J. Alhadeff, show that low-flow characteristics of streams derived from 15 yr or less of record may differ as much as 60 percent from the values based on 35 to 40 yr of record. Two methods, the correlation and the ratio methods, are suggested means of reviewing and adjusting, if needed, short-term records to a longer hydrologic period.

Water levels and steady-state calibration of a two-dimensional flow model

Data from six test wells drilled in Decatur and Miller Counties indicate that in these areas the principal artesian aquifer is receiving recharge from the overlying residuum and is giving up water to the underlying Lisbon and Tallahatta Formations, according to L. R. Hayes. Water levels in the residuum are 5 to 10 m higher than water levels in the principal artesian aquifer, but water levels in the principal artesian aquifer are only 1 to 2 m higher than water levels in the Lisbon and Tallahatta Formations. This may indicate that the vertical hydraulic conductivity of the residuum is less than that of the Lisbon or Tallahatta.

The numerical model developed by P. C. Trescott, G. F. Pinder, and S. P. Larson (1976) is being used to simulate water-level changes in the principal artesian aquifer as a result of natural or manmade stresses. The model grid consists of 80 rows and 105 columns, with a node size of 1.6 km on a side. Calibration and sensitivity analysis of the model to steady-state conditions have shown that the model is most sensitive to input values of leakance of the confining bed and heads on the other side of the confining bed.

KENTUCKY

Chloroform concentration in alluvium at Louisville

One well at an industrial plant in southwestern Louisville has been pumping water containing about 2 to 35 mg/L of chloroform since July 1975. The well, screened in sandy Ohio River alluvium from 29 to 39 m below land surface, is about 37 m from a storage tank that in 1970 overflowed about 19 m^3 of chloroform on the land surface within a diked area.

Water sampling from temporary wells beside the tank showed no chloroform in the ground water at depths from about 23 m to bedrock at 35 m. However, water that was slightly below the water table, the top of the zone of saturation, at a depth of 17 m contained 25.3 mg/L of chloroform in August 1978. A second water sample in September 1978 from this well contained 16.9 m/L of chloroform. It was observed that chloroform concentrations in water from the industrial well varied with fluctuations in the water-table surface, increasing when water levels rose and decreasing when water levels declined.

It became apparent that most of the chloroform contaminant was above the water table in the unsaturated zone. Seven soil samples were taken from a test hole beside the storage tank at depths ranging from 7 to 16 m. The chloroform concentration ranged from 18.3 to 102 mg/kg, with greatest concentrations at 10.3 m, 48.5 mg/kg, and at 16 m, 102 mg/kg. The sample from 10.3 m was siltier than the other samples, which may explain the high concentrations; however, the sample from 16 m was in normal sandy alluvium but just above the water table and subject to concentration by water-table fluctuations.

Soil samples taken from the unsaturated zone at the same altitude, 127.5 m, as the 10.3-m sample in the area around the storage tank ranged from 0.8 to 43.8 mg/kg of chloroform. Samples from the same altitude, 121.7 m, as the 16-m sample ranged from 0 to 56.5 mg/kg of chloroform.

The chloroform contamination in both zones was oval shaped and centered below the storage tank. The dimensions were about 190 by 105 m at the 127.5 m altitude and 130 by 120 m at the 121.7 m altitude, with the long axis in a north-south direction or approximately 45° different from the northwest-sloping regional groundwater gradient.

R. W. Davis and E. W. Matthews (1980) concluded that the chloroform had been relatively stationary in the unsaturated zone until 1975 when the ground water rose to the base of the chloroform zone. Then, the chloroform moved along the surface of the water table, or slightly below, and entered the well by flowing down the permeable annular space surrounding the well casing to the screen.

MISSISSIPPI

Major flood on Pearl River at Jackson

The greatest flood of record on the Pearl River at Jackson occurred from April 12 to 14, 1979. The estimated peak discharge of 2,900 m^3/s at Jackson was more then twice any previously measured discharge, according to K. V. Wilson. The flood was considered to be in excess of the 100-yr recurrence interval.

Discharge measurements above the Ross Barnett Reservoir, which is upstream of Jackson, enabled reservoir managers to estimate inflow to the reservoir. They were able to regulate releases to take advantage of the meager flood-storage capacity of this water-supply reservoir. The flood crest in the reservoir came within 0.03 m of overtopping the blowout plug in the dam. Without the reservoir regulation, the estimated peak discharge at Jackson may have been 30 to 45 percent greater.

Large water-level declines in Eutaw-McShan aquifer

The potentiometric surface of the Eutaw-McShan aquifer in northeastern Mississippi forms a large north-south-trending trough that is centered on deep cones of depression at Tupelo and West Point. B. E. Wasson reported that long-term declines of the potentiometric lead in the trough have averaged about 0.6 m/yr over the past 30 yr. Within the past 10 yr, however, declines at Tupelo have averaged 2.7 m/yr and at West Point, 1.5 m/yr.

NORTH CAROLINA

Improvement in water quality of some rivers

Evaluation of data from several long-term stations in North Carolina by D. A. Harned and J. K. Crawford has shown a generalized pattern of recent improvement in water quality, probably because of improved industrial and municipal waste-water quality. Improvement caused by reduced point source load is particularly evident in the concentration of dissolved solids in the Rock and the French Broad Rivers (Daniel and others, 1979).

However, certain dissolved constituents, including sulfate and nitrate, do not follow this pattern of improvement. Dissolved-sulfate loads, in particular, show increases of 50 to 125 percent since 1955 at stations in the basins of the Neuse, Yadkin–Pee Dee, and Rocky Rivers (Harned, 1980). The long-term increases in sulfate and nitrate may be a result of an increase of these constituents in the atmosphere deposited on the land surface and in rivers. Current evidence, however, of long-term change in the pH of these rivers that could be attributed to acid rainfall is inconclusive.

SOUTH CAROLINA

Water-supply supplement from the Intercoastal Waterway

Ground water in the shallow water-table aquifer system in the Myrtle Beach area is of good quality, but the aquifer system does not appear to be of sufficient areal extent or sufficient yield to serve as a replacement or supplement to existing water supplies. However, the Intercoastal Waterway may supplement present water supplies, according to Allen Zack. The waterway is fresh (Johnson, 1977) along its length in the Myrtle Beach area, and flow is sufficient for limited water supplies. Prior to use, however, additional checks on the quality of the water to be used for public supply are necessary.

TENNESSEE

Ground water related to weathering products of facies of Fort Payne Formation

The occurrence of ground water in the Highland Rim area of Tennessee is related to the weathering products derived from the depositional facies of the Mississippian Fort Payne Formation. The Fort Payne Formation at Manchester, in the southeastern part of the Highland Rim, has been named the "Manchester aquifer" by Burchett and Hollyday (1974). The aquifer is composed of a few meters of chert rubble associated with coarse calcareous sands, which are composed predominantly of broken crinoid stems at the overburden-bedrock contact, and occasionally of several meters of solutioned limestone underlying the rubble zone. Test wells in the Manchester aquifer that penetrate 1.5 to 3 m of chert rubble have yielded water at rates of several tens of liters per second.

In the Fairview area, Ann Zurawske, C. R. Burchett, and A. K. Sparkes found that the overburden, which ranges in thickness from <1 m to as much as about 18 m, consists largely of clay or clay-sized particles, with relatively thin lenses of chert. In some wells, a zone of chert rubble that may yield some water is present in the lower part of the overburden. Most of the unweathered Fort Payne is dark-gray dolosiltstone or siltstone. Within the siltstone are zones of brown weathered material consisting of a porous fossiliferous silica residue, which is not always water bearing. It is not known whether the failure of the porous residue to yield water is due to clogging by clay-sized particles or by areal discontinuity of the zones. In some cases, however, the zones occur at the same stratigraphic horizon as the water-bearing zones in nearby producing zones.

Yields to test wells in Fairview are consistently less than yields at Manchester. Most wells produced between 0.3 and 3 L/s. Wells tapping a gypsum-bearing zone in the Fort Payne had larger yields but of highly mineralized water. Differences in yields between Fairview and Manchester can be explained by differences in the weathering products of facies within the Fort Payne. These differences have been summarized for central Tennessee by Milici and others (1979) and for the eastern Highland Rim by Moran (1977).

Strontium-90 transport through solution cavities in limestone

During 1946 through 1951, radioactive solid wastes at Oak Ridge National Laboratory (ORNL), Tenn., were disposed of by shallow trench burial in Burial Ground 3. This disposal site is underlain at shallow depth by the Chickamauga Limestone (Ordovician age) in which small solution cavities are known to occur. Studies headed by D. A. Webster (USGS) and A. M. Stueber (ORNL) have led to the tentative conclusion that ^{90}Sr leached from the buried waste is being transported by ground water through a linear network of solution openings in the Chickamauga. The network, trending northeast-southwest, is believed to occur near the contact of Unit G, a limestone unit, with Unit F, a calcareous siltstone and shale. Small concentrations of ^{90}Sr, ranging from <0.01 to 1.98 pCi/mL have been found in wells around the perimeter of the site; the largest concentrations are in wells to the northeast and to the southwest. About 350 m northeast of the burial ground, a tributary of Whiteoak Creek contains small but measurable concentrations of ^{90}Sr (<3 pCi/mL) starting immediately downstream from where it crosses the contact between Units E and F, and about 640 m southwest of the site. A tributary of Raccoon Creek also has been found to receive small concentrations of ^{90}Sr ranging from 0.09 to 0.18 pCi/mL near a point where it crosses these stratigraphic units.

CENTRAL REGION

Hydrologic studies and research activities related to energy development and associated environmental problems continued to be emphasized in the central region. Extensive programs in coal hydrology were undertaken in Arkansas, Iowa, Missouri, and Kansas, and data collection and analyses of the hydrology of lignite areas in Arkansas, Louisiana, and Texas were expanded. Investigations covering a broad spectrum of specific hydrologic problems related to the development of coal and oil shale were expanded in Colorado, Montana, North Dakota, Utah, and Wyoming. Hydrologic studies of small basins have been enlarged and intensified. The program for monitoring the water resources of major Federal coal-lease areas was augmented by the addition of many streamflow and surface-water-quality measuring sites and an expanded program of groundwater observation wells. Contractor services for monitoring the coal-lease areas continued to expand throughout the region.

Regional studies of six multi-State aquifer systems were continued under the national program for Regional Aquifer System Analyses. Studies include: (1) the Madison Limestone aquifer system of Mississippian age underlying parts of Montana, North Dakota, South Dakota, and Wyoming, (2) the northern Great Plains regional aquifer system including rocks of Cretaceous and younger age overlying the Madison aquifer, (3) the High Plains regional aquifer system consisting of the Ogallala Formation of late Tertiary age and younger deposits underlying parts of Colorado, Kansas, Nebraska, New Mexico, Oklahoma, South Dakota, Texas, and Wyoming, (4) that part of the Southwest alluvial basins regional aquifer system within Colorado and New Mexico, (5) that part of the northern Midwest regional aquifer system in Iowa, Missouri, and Nebraska, and (6) the central Midwest regional aquifer system in Arkansas, Kansas, Missouri, Oklahoma, and Texas. The Madison Limestone aquifer study was advanced by the completion of a report on the regional stratigraphy and a first draft on the regional geology. Water-level and water-quality maps for a multilayer digital model are well advanced, and model calibration is underway. The distribution of the permeability and porosity of the Madison Limestone has resulted largely from wrench-style deformational and depositional patterns in the Paleozoic rocks. In the northern Great Plains and the High Plains regional aquifer studies, emphasis was on areal investigations, advanced model development, and data compilations for water-use estimates. In the Southwest alluvial basins, northern Midwest, and central Midwest regional aquifer studies,

the emphasis was on data collection and analysis and on development of preliminary models.

Surface-water activities continued to be a principal part of the central-region program. Channel-geometry techniques were used for estimating the peak and mean-annual discharge at several proposed coal-mining areas in Montana, New Mexico, and Wyoming. Channel-geometry techniques also were used to study the relation of sediment to channel morphology in the Missouri River basin. Rainfall simulation on small plots was continued, and the data are being used to indicate infiltration rates for use in the precipitation-runoff model now under development. A daily flow model with a snowmelt routine is being calibrated for small basins in the Yampa River basin of Colorado. Studies of the Manning's roughness coefficient are being done for extensively vegetated flood plains in Louisiana and for steep channels in mountainous areas in Colorado. The purpose of both projects is to document and verify the roughness coefficient for those particular types of areas. Several techniques, including step backwater and fluorescent-dye methods, are being evaluated for estimating point depths and velocities in selected streams as part of an instream-flow project sponsored by the U.S. Fish and Wildlife Service.

Water quality continued to be emphasized in many studies conducted in the central region. Toxic organic chemicals were the focus of a study conducted in the downstream reaches of the Mississippi River. Relatively small concentrations of chloroform and other volatile organic compounds were detected in the water column, as were numerous semivolatile compounds such as atrazine and phthalates. Because of their relative insolubility in water, concentrations of organic compounds in bottom-sediment samples from the river were much larger than those in the water column. Several urban water-quality studies were initiated in the central region as part of the USGS–EPA National Urban Runoff Program (NURP). Studies are underway in Denver, Colo., Rapid City, S. Dak., and Salt Lake City, Utah. The study in Salt Lake City includes not only the water-quality aspects of urban runoff but also the impacts of the runoff on the receiving water bodies. Urban studies that are not part of NURP also are being conducted in Kansas and Texas. An "acid rain" study has been initiated in Colorado to obtain data on the chemical quality of precipitation and to study the potential effects of acid precipitation on lakes in the Rocky Mountain region. This study has been initiated because of the potential effects on precipitation of atmospheric emissions from oil shale processing plants and coal-burning electricity-generating powerplants in western Colorado and Utah. Water-quality modeling studies were conducted in the Yampa River basin in Colorado and in the L'Anguille River basin in Arkansas. The objective of these studies was to predict DO concentrations under various development and waste-treatment alternatives.

Hydrologic research in the central region included many studies related to energy development such as chemistry of water from surface coal mines, hydrologic impacts of surface mining on aquifers, quality of water studies, and changes in the organic quality of water with energy-related development. Other research investigations related to the chemical quality of water include development of modeling techniques for the prediction of solute transport in ground water, development and calibration of a sediment-transport model, and studies related to the movement of bed material. Research on the hydrology of geothermal systems is being conducted by onsite investigations and by the design and testing of downhole probes.

Research also is underway on the relation between ground water and lakes and wetlands, geochemistry and human health, causes and effects of land subsidence, geochemical kinetics under natural conditions, uranium mill tailings and transuranium materials in the environment, precipitation-runoff model development, groundwater flow modeling, and radionuclide migration in aquifers.

Geohydrology of Paleozoic rocks in the northern Great Plains

Potentiometric surface maps, based on drill-stem test data, were prepared by W. R. Miller for eight Paleozoic geologic units underlying the northern Great Plains of eastern Montana, western North and South Dakota, and northeastern Wyoming. These maps reflect the regional gradients within each unit and, when compared with paleo- and present-day structure, lithofacies, apparent water-restivity, and formation-temperature maps, they show the relation of the geologic framework to the hydrologic system. The potentiometric surface maps, in conjunction with the apparent water-resistivity maps, indicate that the flow of fresher water into the Williston Basin from the west may have displaced brines upgradient to the east.

Widely separated zones in the middle and upper parts of the Mission Canyon Limestone of the Madison Group of Mississippian age, the lower and upper units of the Madison Group and the Amsden and Tensleep Formations of Pennsylvanian age, penetrated by USGS test well 3 near Huntley, Mont., were perforated and tested; the well yield was 7.9 L/s. The three zones were isolated with inflatable packers; acid and propping agents then were injected under pressure to increase the well yield; the resulting discharge was 170 L/s.

KANSAS

Aquifer tests in the Wellington aquifer near Salina

The Wellington aquifer near Salina, Kans., consists of a fractured zone with cavities within the gypsiferous Permian Wellington Formation and contains brine with a chloride concentration of 150,000 mg/L. According to J. B. Gillespie, results of two aquifer tests indicated aquifer transmissivities of 90 and 68 m^2/d. The storage coefficient is estimated to be 0.005 at both sites.

Sandstone aquifers—potential source of water in southwestern Kansas

Sandstone aquifers in southwestern Kansas are potential sources of water in addition to that being obtained from unconsolidated aquifers, according to Jack Kume and J. M. Spinazola. The Ogallala Formation of late Tertiary age is the principal unconsolidated aquifer in the High Plains of western Kansas. This aquifer is being depleted, mostly by irrigation withdrawals, at a rate many times faster than it is being recharged. Water levels in wells have declined significantly, and, in some areas, the water reserves may last only a few more years. An alternative source of water is needed in these areas. Sandstone aquifers occur throughout southwestern Kansas in rocks of Jurassic and Cretaceous age. The Dakota Formation of Early Cretaceous age, which occurs throughout most of southwestern Kansas, is the principal source of freshwater in sandstone aquifers. Reported yields of as much as 8.8 m^3/min have been obtained from the Dakota. The water is used for irrigation, cooling in electricity-generating powerplants, and municipal, domestic, and stock supplies. The Jurassic aquifer, which occurs in the western one-half of southwestern Kansas, is the second most important source of freshwater from sandstone aquifers. The water is used for irrigation, domestic, and stock uses.

LOUISIANA

Digital model of the "2,000-foot" sand of the Baton Rouge area

L. J. Torak and C. D. Whiteman, Jr., have developed a two-dimensional finite-difference digital model of the "2,000-foot" sand, an aquifer of Miocene age that has been used extensively for industrial and public supplies in the Baton Rouge, La., area. Since 1914, withdrawals by wells have caused the potentiometric surface of the aquifer to decline as much as 128 m in the industrial district of Baton Rouge. The computer model, prepared in cooperation with the Capital Area Ground-Water Conservation Commission and the Louisiana Office of Public Works, will be used as a predictive tool to simulate future water-level declines.

For the immediate Baton Rouge area, data for aquifer and confining-layer thicknesses used as input to the model were obtained from the interpretation of electrical logs and from published reports. Outside the Baton Rouge area, where correlations with aquifers had not been made previously, L. J. Torak interpreted additional logs and used areal reports to provide thickness data for the entire model area, about 56,000 km^2. Initial values of transmissivity and storage coefficient used in the model, as well as historic water levels and pumping rates, were obtained from the files of the USGS.

Preliminary model results indicated that a significant source of recharge to the "2,000-foot" sand is leakage from confining layers. P. C. Trescott, G. F. Pinder, and S. P. Larson formulated modifications to the digital model that make possible the evaluation of the transient and steady-state components of leakage from a confining layer in contact with the "2,000-foot" sand. Simulations indicated that the confining layers and the aquifers above and below the "2,000-foot" sand contribute water to this aquifer when it is stressed by pumpage. Also, the transient-leakage effects were shown to be present at the end of the pumping period and to represent a loss of water from the system when the two-dimensional aquifer simulation is used.

Based on the concepts developed in these preliminary investigations, L. J. Torak has designed a three-dimensional finite-difference digital model to simulate an aquifer system comprised of the "1,500-", "2,000-", and "2,400-foot" sands and the confining layers separating these aquifers. The computer model used for this simulation was formulated by P. C. Trescott and modified by J. L. Tracy to account for transient-leakage effects that occur in confining layers when a stress is applied to the aquifers. Simulations using the three-dimensional model indicate acceptable leakage rates and aquifer sensitivity.

Sand-and-gravel aquifer overlies lignite deposits in Bienville Parish

Test drilling in an area about 6.5 km south-southwest of Ringgold, Bienville Parish, La., indicated that a sand-and-gravel aquifer occurs in the upland alluvial deposits of Pleistocene age at depths between 5 and 28 m below the land surface. The aquifer is located in an area with potentially minable lignite beds of Eocene age, according to J. L. Snider. Although the upland alluvial deposits generally are not considered an important source of water in this part of Louisiana, the deposits appear to be a significant local aquifer. Additional investigation will be necessary to determine the areal extent of the

aquifer. Dewatering this aquifer could be a problem for energy companies mining lignite, but the sand and gravel could have economic value.

MISSOURI

Ground water and water quality downstream from the proposed Prosperity Reservoir in Center Creek basin

A dye-tracer study was made on Grove Creek in the Center Creek basin to determine if Grove Creek will act as a ground-water drain after the completion of the Prosperity Dam. The study indicated that upper Grove Creek contributes water to Scotland Spring, the Cambrian and Ordovician dolomite aquifer (deep aquifer), and the Mississippian limestone aquifer (shallow aquifer).

Water-quality sampling indicated that fertilizer industry wastes discharged into Grove Creek are increasing the nutrient concentration in downstream reaches of Center Creek. If the dam is built, the nutrient concentration will increase in Center Creek because lower base flows will occur.

A seepage run, coordinated with water-quality sampling, indicated that ground water containing relatively large concentrations of zinc from the Oronogo-Duenweg mining belt seeps into Center Creek. The volume of water entering Center Creek ranges from 0.03 m^3/s during low baseflow to 0.05 m^3/s during high baseflow. This seepage is enough to increase the zinc concentration in Center Creek from 100 to 340 mg/L during low baseflows and from 150 to 210 mg/L during high baseflows. Construction and operation of Prosperity Reservoir will probably result in low-flow conditions being maintained throughout the year in Center Creek; thus, relatively large zinc concentrations in the downstream reaches of Center Creek would be expected.

MONTANA

Appraisal of aquifers in northern Cascade County

Geohydrologic data from about 110 wells were used by K. R. Wilke in an appraisal of aquifers in northern Cascade County. Aquifers occur within the Madison Group of Mississippian age, Swift and Morrison Formations of Jurassic age, Kootenai Formation of Cretaceous age, and the Colorado Group of Cretaceous age. These aquifers supply water for domestic and industrial uses throughout northern Cascade County. In addition to the bedrock aquifers, unconsolidated glacial deposits of Pleistocene age and unconsolidated alluvial deposits of Holocene age locally are important aquifers. Almost 25 percent of the wells were completed in the Madison Group. Depth to the Madison Group ranges from 60 to 150 m in and south of Great Falls on the crest of the Sweetgrass arch and from 210 to 300 m on the upland benches north and west of Great Falls.

Water samples were collected from 28 wells for laboratory chemical analyses. Average specific conductances of water from the aquifers in μmho/cm at 25°C are Madison Group, 1,640; Swift Formation, 1,140; Kootenai Formation, 1,960; Colorado Group, 4,270; glacial deposits, 1,490; and alluvium, 1,550.

Continued hydrologic studies of energy minerals rehabilitation inventory and analysis areas

M. E. McClymonds collected data in the Prairie Dog Creek area, 48 km southwest of Ashland in southeastern Montana where 47 test holes were drilled into coal-bed aquifers, overburden and interburden, and alluvial aquifers, and 27 aquifer tests were conducted. The coal-bed aquifers include the 12- to 18-m-thick Wall coal bed and the 5-m-thick Brewster-Arnold coal bed. Results of the aquifer test indicate that the coal-bed aquifers have an average transmissivity of about 1.2 m^2/d. Transmissivities ranged from 0.02 m^2/d in thin or deeply buried coal beds to 6 m^2/d in partly weathered shallow coalbeds. Transmissivities in the sandstones and silty layers found in overburden and interburden range widely depending on the percentage and coarseness of the sand. The alluvium is about 6 m thick from the upper reaches to near the mouth of the valley; near the mouth of the valley, the alluvium thickens to >15 m. Transmissivities in the alluvial aquifers generally range between 60 and 250 m^2/d. The largest transmissivity, 850 m^2/d, occurs near the mouth of the valley.

In 1979, M. R. Cannon began studies in the Cook Creek area, 5 km northeast of Ashland, and the Snider Creek area, 30 km north of Ashland. Eighteen test holes have been drilled in the two areas, and aquifer tests have been conducted for 11 of the holes. The Knoblock coal in the Cook Creek area has a thickness of 18 m and an average transmissivity of about 0.1 m^2/d. The Terret coal in the Snider Creek area is 3 to 5 m thick and is above the water table. The principal aquifer in the Snider Creek area is the alluvium, which has a transmissivity of about 60 m^2/d at a thickness of 12 m near the mouth of the valley.

Shallow alluvial aquifers evaluated in Helena Valley

Samples for water-quality analysis were collected from 52 test holes drilled in the Helena Valley, Lewis and Clark County, Mont., to determine the water quality in shallow alluvial aquifers underlying the valley. In addition, nitrate concentrations and specific-conductance values were determined in samples from 98 domestic

wells. Joe Moreland reported that the largest nitrate concentration was 52 mg/L as nitrogen in a sample from a test well near an abandoned landfill. In general, nitrate concentrations were less than 2.0 mg/L. Specific-conductance values ranged from about 200 to about 1,500 μmho/cm.

Robert Leonard conducted aquifer tests on five wells in the valley and found that the transmissivity of the shallow alluvial aquifers is about 900 m^2/d. The tests indicated that aquifers are overlain by leaky confining layers consisting of clay and silt. Analyses of drillers' and gamma-ray logs and shallow resistivity surveys indicate that the clay and silt layers are not continuous throughout the valley.

NEW MEXICO

Assessment of ground-water resources in Santa Fe County

The depth to the Espinaso Volcanics of Stearns (1943) of Tertiary age in the southern Santa Fe embayment was determined from drillers' logs and other geological data by W. A. Mourant, S. R. Sagstad, and Devon Rose. The Espinaso Volcanics, which consist of extrusive flows and water-laid tuffs and tuff-breccias, is overlain by interbedded sand, gravel, and clay in the Santa Fe Formation (or Group) of Tertiary and Quaternary age. A structure contour map showing the altitude of the top of the Espinaso Volcanics was prepared to provide an indication of the maximum thickness of the more permeable Santa Fe.

Assessment of ground-water resources on the Zuni Indian Reservation

The sandstones, siltstones, and carbonate rocks in the Glorieta–San Andres aquifer system of Permian age and sandstone units within the shales of the Chinle Formation of Triassic age provide much of the municipal and stock-water requirements for the Zuni Indian Reservation in west-central New Mexico, according to a study conducted by B. R. Orr. Permeability in these artesian aquifers is due primarily to interconnected fractures and solution channels within the fine-grained sandstones and siltstones and dense carbonates that constitute these geohydrologic units. Permeability tends to increase with proximity to regional structural folding. Some wells in these more fractured areas are capable of yielding as much as 10 L/s. However, potentiometric surfaces of these artesian aquifers are declining rapidly in response to pumping of wells. Additional supplies of water may be obtained from sandstones in the Zuni-Dakota system of Jurassic and Cretaceous age; the permeable eolian sand deposits in the Bidahochi Formation of Tertiary age, which mantle the western one-third of the reservation; and alluvial deposits of Quaternary age, which occur along existing stream channels.

Hydrologic properties of the Gallup Sandstone in McKinley County

The Gallup Sandstone aquifer of Late Cretaceous age is a principal source of potable water for Gallup and other communities in southwestern McKinley County. A 2.5-mo aquifer test was conducted in a municipal well field 11 km north of Gallup by J. S. McLean. A two-dimensional digital model of the Gallup Sandstone in the area was constructed using a storage coefficient of 0.10 in the outcrop areas. A modeled transmissivity of 28 m^2/d and storage coefficient of 10^{-4} resulted in good agreement between measured and simulated drawdowns.

NORTH DAKOTA

Buried-valley aquifers, McKenzie County

Data from test wells drilled in a north-trending valley that is now occupied by Red Wing and Cherry Creeks in north-central McKenzie County indicate that the valley is an abandoned north-trending channel of the Little Missouri River, according to M. G. Croft. Wisconsin Glaciation, probably during the Iowan Stage, blocked the northward flow of the Little Missouri River, formed lakes in front of the ice, and diverted the river from the valley now occupied by Red Wing and Cherry Creeks to its present course. Fluvial gravel, fine-grained lacustrine deposits, till, and colluvium underlie the valley bottom.

Test drilling and aquifer evaluation in Rattlesnake Butte area

Test drilling and preliminary aquifer evaluation have been completed in the Rattlesnake Butte area. Interpretation of stratigraphic data by W. F. Horak indicated that the hydrogeologic environment of the Sentinel Butte Member of the Fort Union Formation of Paleocene age is variable within the 259-km^2 study area. Lignite beds are significant sources of shallow ground water only in the eastern half of the study area. Locally occurring sand sections of variable thickness also are aquifers.

Surficial outwash aquifer in Logan County

R. L. Klausing reported that test drilling indicated the presence of a surficial outwash aquifer in northwestern Logan County, with an areal extent of about 52 km^2. The aquifer consists of sand and gravel deposits that have an average saturated thickness of about 5 m. The aquifer becomes thicker and occurs at deeper depths near Napoleon, N. Dak., where the aquifer is in

hydraulic connection with a northwest-trending buried valley.

OKLAHOMA

Geohydrology of the Arbuckle-Simpson aquifer in south-central Oklahoma

The Arbuckle-Simpson aquifer of Cambrian and Ordovician age in south-central Oklahoma is a relatively unused source of readily available freshwater. Although the total withdrawal of water from the aquifer is small at present, the aquifer represents a potential source of water for future municipal and industrial uses.

R. W. Fairchild, R. L. Hanson, and R. E. Davis determined that recharge to the aquifer amounts to more than 200 mm/yr. Discharge from the aquifer is mainly from springs, which contribute sufficient discharge to sustain flow in major perennial streams. As estimated from areal techniques, the average specific yield of the aquifer is 0.008, and the average transmissivity is 1,500 m^2/d. Based on an average saturated thickness of 1,070 m, the amount of water in storage is approximately 9,000 hm^3.

High Plains regional aquifer study

According to J. S. Havens, water-level declines of as much as 20 m have occurred in the Ogallala Formation of Tertiary age and associated deposits of Tertiary and Quaternary age in the High Plains of Oklahoma since the beginning of extensive water-level observations in the 1960's. Maps of water-table elevations for 1970, 1975, and 1978 show that water levels have declined most in areas of extensive irrigation pumpage.

The Oklahoma Water Resources Board (OWRB), under a contract issued by the USGS, is making extensive measurements of water levels in the High Plains aquifer outside the three Oklahoma Panhandle counties. Water levels in approximately 600 wells were measured by the OWRB from 1979 to 1980, and measurements of water temperature, pH, and specific conductance were made at most sites. Water-level data, drillers' logs of water wells from the files of the OWRB, and about 300 water-quality analyses from the files of the USGS have been entered into computer storage.

Mine ponds, a hydrologic asset in eastern Oklahoma

Ponds created by strip mining for coal in eastern Oklahoma occupy an estimated 1,600 ha. The average depth of the ponds is about 6 m; thus, the total amount of water stored in them is about 100 hm^3. Water from the ponds is used for watering stock, for irrigation, and by at least one community for municipal supply. The ponds also provide a habitat for stocked fish and a variety of other aquatic and semiaquatic life.

According to M. V. Marcher and R. L. Goemaat, profiles made in 34 mine ponds show that specific conductance generally increases with depth and that pH generally decreases. Values of specific conductance ranged from 93 to 4,440 μmho/cm at 25°C; about 55 percent of the 68 determinations were less than 1,000 μmho. Values of pH ranged from 6.4 to 8.9; about 20 percent of the 68 determinations were less than 7.0. Water samples from the ponds were analyzed by the Oklahoma Geological Survey to determine concentrations of chloride, iron, manganese, and sulfate. Chloride concentrations ranged from 2 to 27 mg/L and averaged 6 mg/L. Iron concentrations ranged from 10 to 8,100 μg/L; about 25 percent of the 68 determinations exceeded 500 μg/L. Manganese concentrations ranged from 10 to 13,600 μg/L; about 55 percent of the 68 determinations exceeded 500 μg/L. Sulfate concentrations ranged from 5 to 1,590 mg/L; about 30 percent of the 68 determinations exceeded 250 mg/L.

Model study of alluvial aquifer along the Beaver and the North Canadian Rivers

A two-dimensional finite-difference model was used by R. E. Davis and S. C. Christenson to predict the effects of future ground-water withdrawals in an alluvial aquifer with an area of 2,150 km^2 along the Beaver and the North Canadian Rivers in northwestern Oklahoma. In 1978, the aquifer had an average saturated thickness of about 9 m, and contained about 5,020 hm^3 of water. Results of model simulations indicate that, with 1978 stresses, aquifer storage will be 97 percent of the 1978 storage by 1993 and 94 percent of the 1978 storage by 2020. However, if the entire aquifer is stressed at an annual rate of 0.0043 hm^3/hm^2, aquifer storage will be 31 percent of the 1978 storage by 1993 and 24 percent of the 1978 storage by 2020.

Streamflow and water-quality characteristics of Coal Creek basin near Lehigh

As part of the EMRIA program, S. P. Blumer and Jonathon Scott have been studying the hydrology of Coal Creek basin (drainage area, 22 km^2) near Lehigh in Coal County, Okla. Due to basin size, geology, and annual rainfall distribution, streamflow occurs only in direct response to storm runoff; most storms occur during the spring. Chemical analyses of storm runoff indicated that total concentrations of iron, aluminum, and manganese, the predominant metals, ranged from 780 to 15,000 μg/L for iron, 250 to 12,000 μg/L for aluminum, and 70 to 1,500 μg/L for manganese. Specific conductance ranged from 75 to 250 μmho/cm at 25°C, pH ranged from 6.6 to 7.2, and dissolved-solids concentrations ranged from 55 to 160 mg/L.

Water from Gaines Creek and Gaines Creek arm of Lake Eufaula suitable for public supply

Gaines Creek and the Gaines Creek arm of Lake Eufaula, in eastern Oklahoma, are potential sources of municipal water supplies for the cities of McAlester and Wilburton. J. K. Kurklin reported that Gaines Creek had no flow during 35 percent of the monthly inspections made since May 1978; flows during other visits ranged from about 0.3 to 3.6 m^3/s. Specific-conductance measurements generally were less than 150 μmho/cm at 25° C, and pH values ranged from 5.5 to 8.0. DO values have been as small as 25 percent of saturation, and nitrogen values have been almost 10 mg/L. On two occasions, concentrations of fecal-coliform bacteria exceeded 2,000 colonies per 100 mL of water. In one-third of the phytoplankton analyses, blue-green algae constituted more than 50 percent of the total cells, indicating the possibility of occasional taste and odor problems. With few exceptions, constituent concentrations in water from Gaines Creek were within the limits established or recommended by Federal and State agencies for a public water supply. With adequate treatment, water from Gaines Creek should be suitable for public supply.

Chemical analyses of water samples collected quarterly at three cross sections on the Gaines Creek arm, made since May 1978, indicate that specific-conductance values generally were less than 250 μmho and pH values ranged from 6.0 to 8.0. DO usually decreased with depth during late summer. Occasionally, nitrogen concentrations exceeded 10 mg/L at each of the three cross sections. Lake phytoplankton commonly were dominated by blue-green algae. With adequate treatment, water from the Gaines Creek arm should be suitable for public supply.

SOUTH DAKOTA

Aquifer test of a glacial-outwash aquifer in central South Dakota

Glacial-outwash aquifers underlying about 80 km^2 of Jerauld and Aurora Counties were located by drilling 300 test holes and analyzing geohydrologic data from 800 wells. L. J. Hamilton conducted a controlled 3-d aquifer test of a 20-m-thick glacial-outwash aquifer in northeastern Jerauld County, S. Dak., using 19 observation wells located from 60 to 4,500 m from an irrigation well discharging 57 L/s. Water levels were drawn down 0.4 m at a distance of 1,000 m and 0.8 m at a distance of 100 m from the pumping well after 3 d of pumping. A preliminary analysis of the test data indicated that the aquifer has a transmissivity of 3,000 m^2/d and a coefficient of storage that increases from 0.0001 to 0.01 south of the pumped well where the aquifer is hydraulically connected with Sand Creek.

Tertiary bedrock outliers and preglacial channels of western origin in Yankton County

An analysis of test-drilling data from Yankton County, southeastern South Dakota, by E. F. Bugliosi indicates that two areas in the James Highland physiographic province are underlain by the Ogallala Formation of Tertiary age. The presence of this fine-grained poorly indurated deposit in the northeastern and southwestern parts of the county extends the limit of occurrence of a Tertiary bedrock unit in this area to the east by about 70 km.

The southwestern Ogallala outlier contains an incised channel deposit consisting of fluvial sand and gravel from a source area to the west. This channel deposit probably represents a tributary of the preglacial Niobrara River system, which drained to the east and south. The deposits are characterized by large concentrations of milky quartz and pink feldspar and by a lack of shale or chalk particles that are indigenous to the Yankton County area.

TEXAS

Effects of faults on the direction of flow in the Edwards aquifer

According to R. W. Maclay and T. A. Small, the carbonate rocks of the Edwards aquifer accumulated in three distinct depositional environments that differ significantly in characteristic carbonate facies and texture-related porosity and permeability (Maclay and Small, 1976). Highly permeable zones were developed by selective leaching of certain hydrostratigraphic units that contain evaporites or burrowed and dolomitized tidal deposits.

Many high-angle normal faults strike northeastward through the San Antonio, Tex., area. Fault displacements vary significantly along the strike, and vertical displacements locally are more than 200 m. This amount of displacement completely separates the Edwards aquifer and breaks the lateral continuity of permeable stratigraphic units. Therefore, faults exert a major control on the direction of ground-water movement within the San Antonio area.

The direction of ground-water flow in the outcrop area of the Edwards aquifer west of Medina Lake is southwest rather than south, as might be inferred from the flow lines on regional potentiometric maps. Ground water in the outcrop area in northwestern Bexar County does not flow directly into the confined aquifer downdip by crossing the Haby Crossing fault but probably moves toward stream channels where the Glen Rose Formation of Early Cretaceous age crops out. Ground water moves through a graben containing a full thickness of the Ed-

wards aquifer from the vicinity of Cibolo Creek toward Hueco Springs.

Jasper aquifer overlain by effective confining layer

The Jasper aquifer, which is one of several productive aquifers underlying the Texas coastal plain, is overlain by an effective confining layer, according to E. T. Baker, Jr., and Sergio Garza. This layer, which has been called the "Burkeville confining layer," consists mostly of clay, is 60 to 120 m thick, and separates the Jasper aquifer from the overlying Evangeline aquifer. Hydraulic pressures in the Jasper have been found to be significantly greater than pressures in the Evangeline. For example, in one area in southeastern Texas where a deep test hole was drilled, the static water level in the top of the Jasper was 32 m above land surface. This level was 20 m higher than the water level in the base of the Evangeline.

Source areas of salinity and trends of salt loads in streamflow in the upper Colorado River

Analyses of the quality and quantity of low flows in a 57-km reach of the Colorado River upstream from Colorado City, Tex., by Jack Rawson (1980) indicated that ground-water accretions throughout the reach are saline. Loads of dissolved constituents contributed by ground water are largest in three subreaches. Yields per kilometer of river channel from these subreaches during low-flow periods averaged more than 4.9 mg/d of dissolved solids, of which more than 1.6 mg were sodium and 2.6 mg were chloride.

The low-flow and salt-load trend studies indicated that part of the salinity resulted from the inflow of oil-field brine but that the major part is of natural origin. Neither the ban on open-pit disposal of oil-field brine nor the ban on pumping of saline ground water has significantly reduced the salinity of the upper Colorado River.

UTAH

Navajo Sandstone—a source of ground water for future energy-related development in the northern San Rafael Swell area

The Navajo Sandstone of Triassic(?) and Jurassic age is a major aquifer in southeastern Utah and is a potential source of water for energy-related development in that arid part of the State. J. W. Hood, assisted by D. J. Patterson, has extended a previous study near the Henry Mountains northward into the northern San Rafael Swell. Based on preliminary digital modeling of the sandstone-aquifer system, recharge to the sandstone is estimated to be about 3 hm^3/yr – less than in the area to the south. Direct recharge occurs in the swell where the sandstone crops out at relatively high altitudes, as indicated by localized areas of fresh ground water at these altitudes. The sandstone is nonhomogeneous and anisotropic. Laboratory tests of cores and outcrop samples indicated that the hydraulic conductivity ranges from less than 0.003 to about 0.3 m/d. Primary(?) cement is silica. Porosity is less than 10 percent where secondary(?) cement fills most pores and is as much as 26 percent where the sandstone is well leached by circulating water.

Despite the relatively small hydraulic conductivity and rate of recharge, the Navajo Sandstone is a major source of water and contains a large volume of freshwater to slightly saline water in storage. Small withdrawals for stock and domestic uses would have little effect on the hydrologic system. Large withdrawals are feasible if proper well spacing is maintained but would cause large drawdowns of water levels. Such development would cause some springs to cease flowing and ultimately could induce infiltration of some water from streams in the area.

Seepage and reservoir studies in the Price River basin

Seepage studies by K. M. Waddell and J. E. Dodge on two streams in the Book Cliffs area of the Price River basin indicated significant gains in flow near the contact of the Flagstaff Limestone of Tertiary age and the North Horn Formation of Tertiary and Cretaceous age. Springs along the two streams accounted for about 20 percent of the inflow, and diffuse seepage along the channels accounted for about 80 percent. Many springs also were observed along the Flagstaff–North Horn contact throughout the Book Cliffs area in the Price River basin.

Bathymetric and water-quality surveys were made in the Scofield Reservoir during September 1979. A preliminary comparison of cross sections prepared during this survey with a bathymetric map prepared in 1943 indicated that as much as 2.5 m of sediment had accumulated at a site about 1.6 km upstream from the dam. In the upstream end of the reservoir, changes in bottom elevations were minimal. In general, the gradient of the reservoir bottom in 1979 was much less than in 1943, with most of the sediment accumulation occurring toward the downstream end of the reservoir.

In situ measurements of specific conductance, water temperature, pH, and DO indicated that stratification and areal variations in the reservoir were minimal. Water in the reservoir was well mixed due to a recent turnover. Algae production was quite large. Limited inflow data from three streams indicated that most of the nutrients supporting algae production enter the reservoir from Pleasant Valley Creek, one of its minor tributaries.

WYOMING

Digital flow model of Bates Creek alluvial aquifer

K. C. Glover has developed a digital flow model of the Bates Creek alluvial aquifer. Results of a simulation with a large amount of surface-water irrigation and minimum ground-water pumpage indicated that leakage to Bates Creek would increase by 0.23 m^3/s after 10 yr. Results of a simulation with reduced surface-water irrigation and increased ground-water pumpage indicated that leakage to Bates Creek would decrease by 0.06 m^3/s after 10 yr. The simulations also indicated that changes in water levels throughout the aquifer generally would be less than 1.5 m after 10 yr.

Digital model of effects of ground-water withdrawals in Laramie County

Agricultural use of ground water in Laramie County, Wyo., began in about 1920. Since 1969, pumpage has increased substantially; in 1977, about 19,100 ha were irrigated by ground water in the study area, according to M. A. Crist. Water levels are declining as much as 1.2 m/yr in some areas.

A digital model of the hydrologic system in the post-Cretaceous rocks was developed for an area of about 6,000 km^2. The model accuracy was determined by comparing water-level changes measured in 37 observation wells in areas of irrigation pumping with water-level changes calculated by the model for 1971 to 1977. The calibrated model is capable of simulating hydrologic conditions in the post-Cretaceous rocks in Laramie County and may be used to predict the effects of applied stress to the system.

Regression model of effects of streamflow diversions on surface-water salinity

Potential effects of alternative development plans on surface-water salinity may be evaluated using a regression model that predicts changes in dissolved-solids concentrations downstream from proposed streamflow diversions. The model, developed by L. L. DeLong, was based on streamflow records and chemical analyses of water samples. The model takes into account seasonal effects by the inclusion of harmonic time functions.

Effects of two hypothetical water-development plans were simulated as examples, a diversion from the Big Sandy River, tributary to the Green River and an equivalent diversion from the Green River, upstream from the confluence of the Big Sandy River. During a 4-yr period, the average amount of dissolved solids removed by the first diversion would be more than 10 times greater than that removed by the second diversion. Dissolved-solids concentrations in the Green River near the town of Green River, which is downstream from the hypothetical diversions, would be affected most during winter. The first diversion would decrease the dissolved-solids concentration at this location by as much as 13 percent, whereas the second diversion would cause an increase of <1 percent.

Source-area sediment model of Big Sandy River basin

Using discrete samples of suspended-sediment loads and bedloads at five gaging stations in the Big Sandy River basin of Wyoming, J. E. Kircher developed a sediment-runoff model that identified principal source areas of sediment in the basin. The suspended-sediment data were obtained from several years of monthly samples collected at the gaged sites. The bedload data were obtained using a Helley-Smith bedload sampler for flows during summer months of 1978. The data were incorporated into a two-variable regression equation of sediment load versus water discharge; this equation was applied to long-term streamflow records to determine average loads from various tributaries.

The model showed that Pacific Creek, an intermittent tributary of Big Sandy River, supplies less than 7 percent of the runoff but more than 70 percent of the sediment load that eventually reaches the Green River. Principal source areas of runoff and sediment were similarly delineated for other parts of the basin.

Warm water in artesian aquifers in Carbon County

During exploratory drilling for coal in southwestern Carbon County, Wyo., several test holes penetrated artesian aquifers. E. A. Zimmerman measured flows of as much as 32 L/s from artesian aquifers as deep as 395 m. Water flowing from the 395-m test hole had a temperature of 23.3°C, which was considerably warmer than the typical temperature of about 9.0°C for shallow ground water in the area. A temperature log indicated that the water temperature at the bottom of the test hole was more than 30°C. The geothermal gradient of about 7.5°C/100 m may be attributed, in part, to the proximity of several faults because the faults may be conduits for deeply circulating ground water. The proximity of the faults also may account, in part, for the presence of anomalous concentrations of trace metals, particularly cadmium and lead, in water samples from some of the test holes.

Water study of energy-minerals area

A detailed multidisciplinary study of the drainage basin of Salt Wells Creek, an intermittent stream draining semiarid plains southeast of Rock Spring, Wyo., made from 1975 to 1978 by H. W. Lowham, L. L. DeLong, K. R. Collier, and E. A. Zimmerman was one of the first hydrologic studies to be made in the plains area

of southwestern Wyoming. These plains are rich in energy-mineral resources, and planned development of these resources will require an understanding of hydrologic processes in the desert environment.

Average annual flow of Salt Wells Creek is about 7.0 hm^3. Numerous small springs in the headwaters are sources of water supplies for wildlife and livestock.

Surface-water quality of the area is variable because the intermittent nature of streamflow affects water quality. A flushing of both dissolved solids and suspended sediments occurs during the early stages of periods of runoff. After this initial flushing of the basin and channel, concentrations of dissolved solids and suspended sediments are dependent upon the magnitude of discharge. Ground-water quality was found to be dependent upon the source aquifer, with dissolved-solids concentrations ranging from 300 to 2,000 mg/L. Calcium and magnesium were generally the dominant cations, and sulfate and bicarbonate, the dominant anions.

A serious erosion problem exists in the basin because of the deeply incised channels of the main stream and several of its tributaries. Erosion of the channels has occurred due to the cumulative effects of change in climate, change in base level downstream due to channelization, and changes in land use.

WESTERN REGION

The heavy snowfall and rainfall in calendar year 1978 that brought relief from the 1976 to 1977 drought in the Far Western States did not recur in 1979. Water levels in reservoirs at the end of the year were adequate in Arizona and California but below normal in Idaho, Nevada, Oregon, and Washington. Alaska had heavy rainfall in 1979, and rainfall in Hawaii was above normal. In general, runoff in 1979 was below normal in Idaho, western Oregon, and Washington. It was above normal in Arizona and the eastern part of Hawaii.

Damaging floods were experienced in southern California and at Hilo, Hawaii, in February 1979. In July, flash flooding in the desert of southern California caused $50 million in damage and one death. A M=6.7 earthquake occurred October 15 in the Imperial Valley and damaged canals and drains. There was severe flooding at Sitka and Petersburg, Alaska, in October. In November, the island of Hawaii had its second record flood of the year. Property and crop damage was estimated to be $5 million. Severe flooding, which caused two deaths, hit the Olympic Peninsula of Washington in December.

Major projects of the Water Resources Division in the western region in 1979 included the Truckee-Carson River Quality Assessment and three Regional Aquifer System Analyses. In the first year of the river-quality assessment, an interagency planning workshop was held; this resulted in a study workplan. Fieldwork included traveltime studies and synoptic water-quality studies to obtain model-calibration data. The Central Valley Aquifer Project in California, in its second year, involved test drilling, preliminary modeling, and water-quality sampling. The Snake River Aquifer Study began in 1979; most of the activity was in staffing and planning. In the Southwest Alluvial Basins Study, first-year activities included review and computerization of data and contracting for compilation and analyses of available gravity geophysical data, recharge data, and drillers' logs. Several models were begun in this study.

ARIZONA

Irrigation water available to Ak-Chin Indian Reservation

Sufficient ground water to provide 105 hm^3/yr, or about 2,600 hm^3 in a 25-yr period, is available for delivery to the Ak-Chin Indian Reservation from Federal land in the Vekol Valley, the Waterman Wash area, and the Bosque area, according to R. P. Wilson (1979). The three areas, which are being considered as a source of irrigation water for the Ak-Chin Indian Reservation, contain unconsolidated to partly consolidated "basin-fill" deposits. These deposits generally are saturated below a depth of 50 to 180 m, store large amounts of water in their pore spaces, and generally yield 30 to 160 L/s to wells. The deposits have a porosity of 8 to 20 percent and an estimated specific yield of 10 percent.

Vekol Valley contains 2,500 hm^3 of ground water in storage in the first 150 m of saturated basin fill in the southern part and 1,800 hm^3 in the northern part; the parts are separated by a buried ridge of consolidated rock. The Waterman Wash area contains 6,700 hm^3 of ground water in the first 150 m of saturated basin fill, of which 1,600 hm^3 is in the area being considered for development of the Ak-Chin water supply. The Bosque area contains 2,200 hm^3 of ground water in the first 150 m of saturated basin fill. Aquifer tests made at pilot wells and data from existing irrigation wells indicated probable well yields of 60 to 130 L/s in the Vekol Valley, 130 to 160 L/s in the Waterman Wash area, and 30 to 130 L/s in the Bosque area.

Arsenic concentrations in Verde Valley

S. J. Owen-Joyce found that some wells and springs in the Verde Valley of central Arizona yield water that contains arsenic concentrations greater than 50 μg/L, the maximum contaminant level (EPA, 1976) for arsenic in public water supplies. The wells and springs obtain their water from the Verde Formation of late Tertiary age, a

thick lacustrine sequence of interfingering lake facies and volcanic rocks. In 46 water samples from a random sampling of wells between Cornville and Camp Verde, the arsenic concentrations ranged from 2 to 240 μg/L; 19 of the samples contained arsenic concentrations greater than the maximum contaminant level of 50 μg/L. The spring that maintains the flow at Montezuma Well contained 100 μg/L of arsenic.

Rock samples from the Verde Formation contained 7 to 88 μg/g of arsenic. The highest concentrations were in the clay and argillaceous lime mud. Arsenic seems to be disseminated throughout the formation in the area near Camp Verde.

CALIFORNIA

Russian River response to waste-water discharge and drought

Results of work by M. A. Sylvester (USGS) and R. L. Church (California Regional Water Quality Control Board) show that the most important factors affecting water quality and quantity in the Russian River during the 1973 to 1978 low-flow seasons were treated waste-water discharges and a drought during 1976 and 1977. Cessation of low-flow discharges of treated waste water after 1975 resulted in marked decreases in fecal-coliform bacteria and nutrient concentrations. A diel study in August 1977 indicated that the aquatic community of the Russian River was dominated by heterotrophic organisms and that photosynthetic production of oxygen was not sufficient to offset respiration. These conditions were probably caused by deposits of oxygen-demanding material and nutrients from treated waste water discharged during the high flows and (or) discharged during low flows prior to the implementation of regulations prohibiting such discharges.

Ground water limited in north-central Santa Cruz County

M. J. Johnson identified the principal water-bearing units and evaluated their potential for ground-water development in a 115-km² area between the Zayante and San Andreas faults, in an area undergoing residential growth with increased water demand. An estimated water budget indicates adequate precipitation for recharge is available during years of normal rainfall, but steep topography and the fine-grained structure of the rocks limit recharge and subsequent storage. Of the many geologic units present in the study area, only the Purisima Formation of Pliocene age has the potential to sustain well yields greater than 380 L/min. Its location, however, is removed from and of limited use to the area's population. Most of the ground water demand comes from an area underlain by older Tertiary rocks with much lower well yields. Statistically, fewer than 10 percent of the area's wells yield over 60 L/min, while over 50 percent yield much less than 20 L/min, adequate for domestic use only in conjunction with large storage tanks.

Generally, the chemical quality of the ground water is suitable for most uses, although in some areas dissolved salts, iron, and manganese are in concentrations high enough to be objectionable. Septic-tank effluents pose a potential hazard in this area.

Classification of recharge in the Santa Cruz area

Ground-water recharge potential was classified by K. S. Muir and M. J. Johnson (1979) in parts of Santa Cruz County. Classification was based on three data elements that affect recharge—slope, soils, and geology. The three elements were mapped separately, and the numerical map of each element was based upon an arbitrary rating scheme. The three maps then were composited into a single numerical map. A final map was made from the composite map, using a classification system that ranked the numbers into areas of good, fair, and poor recharge potential. It was found that most of the Santa Cruz coastal area and the north-central part of the county have a poor recharge potential. Much of the Soquel-Aptos area was mapped as having a good to fair recharge potential.

Water quality assessment of Merced River

A study of the Merced River, conducted by S. K. Sorenson during the second year of a drought, showed the critical low-flow conditions in the river. No major impairment of water quality was found, but some degradation in quality due to high salts and nutrient data from primitive areas in Yosemite National Park showed nutrient concentrations above expected natural levels.

Ground-water recovery at Thousand Oaks

Ground-water levels at Thousand Oaks have returned to their predevelopment positions after years of recovery, according to J. J. French. The city plans to use ground water for irrigation at parks, golf courses, and other public land. Since its creation as a city in 1964, Thousand Oaks has been supplied entirely by imported water. During the early stages of urban development following World War II and until incorporation as a city, as many as 37 water companies were pumping ground water. Water levels had declined as much as 91 m, and, in many places in the 174-km² area, the chemical quality was poor. In French's study of the ground-water basin, he delineated areas of good water.

Appraisal data adequate for Owens Valley

A study of records of precipitation, streamflow, well logs, pumping and export amounts, and ground-water

levels by W. F. Hardt indicated that available data are generally adequate for appraising the hydrology of Owens Valley. Additional studies are needed to define the subsurface geology, the hydrologic relation between the deep and shallow aquifers, and the effects of a fluctuating shallow water table on the native vegetation. Owens Valley has been the subject of litigation since 1972 regarding the advisability of increasing ground-water pumping for export to Los Angeles. The USGS was asked to determine the adequacy of past hydrologic studies and reports for evaluation of specific hydrologic conditions and water imports, to identify data deficiencies, and to define the kinds of additional information required for development of a long-range water resources management plan.

IDAHO

Analyses of return flows to Snake River

C. A. Thomas reported that water budgets for the Snake River between the Heise and Shelley gaging stations in Idaho show that an average of 67 m^3/s of water is lost to ground-water recharge. Average annual ground-water recharge from 1932 to 1977 fluctuated in a narrow range, even though diversions for irrigation on adjacent lands, which add to aquifer recharge, increased significantly. The budgets suggest that the ground-water system absorbs recharge only up to a certain rate of application. Above this rate, the system rejects recharge, similar to the way in which soil rejects infiltrating rainfall after extended precipitation. The rejected water apparently returns to the river. Major ground-water discharge to the Snake River from the Snake Plain aquifer occurs in the Fort Hall bottoms near Pocatello and in the Thousand Springs reach between Milner and King Hill.

Assessment of ground-water quality in east-central Idaho

In a study of the relation of 1978–79 ground-water quality to the hydrogeologic and cultural environments of five river basins in east-central Idaho, D. J. Parliman reported that recharge to the aquifers is principally from precipitation in adjacent mountains and infiltration of surface water in valley lowlands. The most productive aquifers are flood-plain alluvium, glaciofluvial sediments, and jointed basalt. Water quality generally is acceptable for most uses, but highly mineralized water occurs in some places. For example, in Lemhi Valley, the dissolved solids and several constituents, including bicarbonate, sulfate, chloride, and iron, exceed standards for drinking water or tolerance thresholds for irrigation and livestock uses. The high concentrations are probably due to the influence of mineral-rich clay beds in the valley sediments.

Hydrologic conditions in Rockland Valley

In evaluating ground water–surface water relations in Rockland Valley, southeastern Idaho, R. P. Williams found that annual precipitation averages 508 mm and mean annual runoff is 38 mm, of which 23 percent is diverted for irrigation. Annual ground-water withdrawals and underflow were estimated to be 10.7 hm^3 and 74 hm^3, respectively. Direction of ground-water movement is northward, toward the Snake Plain aquifer. Runoff originating above an altitude of 1,830 m seldom reaches the valley floor as surface flow because of the permeable nature of the fractured carbonate rocks that compose the surrounding mountains. However, unique climatic conditions in January 1980, consisting of warm temperatures and rain on valley floor snowpacks, generated a 3-d-flow volume nearly equal to the mean annual runoff.

NEVADA

Ground water studied in Las Vegas area

J. R. Harrill studied ground-water conditions in the Las Vegas SE quadrangle (7.5-min) and found that water depths varied generally from 45 m in the southwest to 3 m in the northeast (Harrill and Katzer, 1980). Artificial recharge takes place on irrigated land (lawns, parks, and golf courses), and discharge, generally by transpiration, occurs along washes. Dissolved-solids concentrations in the ground water are as great as 1,500 mg/L. About 90 percent of the area is underlain by sedimentary valley-fill deposits, with high to low water-yielding capability. Consolidated rocks in the southeastern part of the quadrangle presumably yield only small quantities of water.

Geophysical investigations in Lemmon Valley

A geophysical survey of Lemmon Valley, near Reno, was used to determine the thickness of valley-fill deposits and the depth to freshwater beneath two playas. According to D. H. Schaefer and D. K. Maurer (1980), 235 gravity measurements were made in the study area, and residual anomalies were calculated. Depth to bedrock calculated from the residual anomalies was a maximum of 790 m in the western half of the valley and 300 m in the eastern part. Ten Schlumberger resistivity soundings were concentrated around the two playas. Depths to freshwater were variable, ranging from 13 to 150 m beneath Silver Lake playa on the west and from 37 to 170 m beneath the eastern playa.

OREGON

Chemical differences in Alvord Desert hot springs and cold springs

Cold springs and irrigation wells in the Alvord Desert of southeastern Oregon differ markedly in chemical character from nearby thermal springs, according to A. R. Leonard. Temperatures of the hot springs commonly are greater than 70°C, whereas those for other springs and for wells generally are less than 15°C. The hot springs have sodium bicarbonate or sodium chloride, or a combination of the two, as dominant ions and have silica concentrations of 120 to 200 mg/L. The colder water generally has calcium and magnesium bicarbonate as the dominant ions and less than 50 mg/L of silica. The dissolved-solids concentration of the hot springs (1,500–2,800 mg/L) generally is about 10 times that of the water from other sources, but concentrations of fluoride, arsenic, and boron differ far more. The fluoride concentration (6.5–16 mg/L) of the hot water is 50 times that of colder water. Arsenic concentrations in each type of water range over more than an order of magnitude, but, in the hot water, they are nearly 90 times as great (10–1,000 μg/L) as in water from cold springs and wells. Boron differences are greatest of all – hot springs have 350 times as much as colder water. The cold water is chemically suitable for drinking and for irrigation, but the hot springs have concentrations of fluoride, arsenic, and dissolved solids in amounts in excess of those recommended for drinking water. The hot springs also are unsuitable for irrigation because of the high percentage of sodium and the high boron concentration.

Estimating effective impervious area with rural and urban rainfall-runoff models

The use of impervious area that actually contributes to storm runoff (effective impervious area) yields more reliable storm-runoff estimates than the use of mapped impervious area, according to Antonius Laenen. Effective impervious area can be considerably different from mapped impervious area, depending on how drainage from the actual impervious areas is routed to the main channel. Any modification that reduces the speed at which rain runs off from impervious areas reduces the effect that the impervious area has on basin response. To fully catalog a basin of any size with respect to the actual contributing (effective) impervious area takes considerable time and manpower. A recent study in the Portland, Oreg., area showed that a good estimate of effective impervious area can be obtained by optimizing this parameter with the aid of a computerized rainfall-runoff model. Two separate field verifications showed this estimate to be within 15 percent of the actual effective impervious area. The study also showed that the computer-optimized effective impervious area ranged from 100 to 30 percent of the mapped impervious area.

Benthic oxygen demand in Portland Harbor

Total benthic demand in the Portland Harbor (Willamette River) is about 14 million g O_2/d. The demand was measured at 1.3 to 1.6 (g O_2/m^2)/d. Stuart McKenzie reported that about 50 percent of the oxygen is consumed by diffusion into the benthic material. The other 50 percent is consumed in the water column by material from the benthic deposits. Examples of the benthic material introduced into the water column include dissolved organic carbon, divalent manganese, ferrous iron, sulfide, and other reduced products of anaerobic digestion.

Digital simulation of a multilayer aquifer system near Portland

Data from five pumping tests have been used to calibrate a four-layer finite-difference model written by Douglas Posson. The model covers 181 km^2 and has more than 9,000 nodes. Initial estimates of system parameters (transmissivity, storage coefficient, and leakage factor) were derived from pumping-test and geologic data. During the transient analysis, storage coefficients and leakage factors were adjusted to minimize the deviation between observed and calculated response in various laterally and vertically spaced piezometers. According to David Morgan, good fits were obtained by using storage coefficients ranging from 0.0001 in the confined layers to 0.25 in the overlying unconfined layer. Leakage factors ranged from 8.0×10^{-11} in tight clay layers to 6.0×10^{-8} in areas where old channel sand of the Columbia River is believed to provide a good connection between the unconfined aquifer and the underlying sand and gravel. Transmissivity generally increases from east to west and is highest (5,000 m^2/d) in the gravel of the uppermost layer and lowest (200 m^2/d) in the silty sand and underlying layers. The model will eventually be used to predict the effects of large-scale extraction ($0.2–0.4\times10^6$m^3/d) for an emergency municipal water supply. The model has been used in its preliminary form to evaluate the impact of proposed well-field designs and pumping schedules on the ground-water system.

Improvement in ground-water conditions near The Dalles

A preliminary evaluation by S. J. Grady of ground-water levels in the vicinity of The Dalles, Oreg., suggests that water-level declines are moderating. In 1959, The Dalles was declared to be a critical ground-water area by the Oregon State Engineer because of rapidly declining water levels. Hydrographs of selected long-

term observation wells indicate that the rate of decline has decreased or that water levels have stabilized. One well indicates a reversal, with the water level rising about 1.8 m/yr since 1964. The principal aquifers are the Tertiary Columbia River Basalt Group and the overlying Dalles Formation. The improving conditions seem to be the result of regulated ground-water withdrawals and recharge from infiltration of Columbia River water used for irrigation.

WASHINGTON

Map of principal aquifers and general yields of wells

Four distinctive geologic units form the principal water-yielding materials in the State of Washington, according to Dee Molenaar. The aquifers include (1) Miocene basalt flows of the Columbia River Basalt Group, mostly in eastern Washington, (2) Miocene sedimentary deposits, including the Ellensburg Formation, the Pliocene Troutdale Formation of the Vancouver area, early Pleistocene terrace gravel along the western and southern lowlands of the Olympic Peninsula and northwestern Willapa region, and valley-fill sand and gravel in the Walla Walla River valley, (3) Pleistocene glacial drift in the Puget Sound region, Quincy and Pasco Basins, and most valleys of the northeastern region, and (4) Holocene alluvium in many valleys, including beach sand along the southern Washington coast. Pumping yields of wells tapping each of these aquifers range from a few liters per minute to 15,100 L/min from the basalt, 11,400 L/min from the sedimentary deposits, 37,900 L/min from the glacial drift, and 11,400 L/min from the alluvium.

Simulation of ground-water flow in basalt aquifers underlying the Columbia Plateau

The USGS three-dimensional ground-water flow model has been modified to handle 21,000 nodes for a four-layer model and to run on a CDC 7600 computer. The model is being used by D. B. Sapik to simulate late ground-water flow in basalt aquifers underlying a 44,000-km^2 area of the Columbia Plateau in southeastern Washington. A steady-state model is being calibrated.

Water budget estimated for Gig Harbor Peninsula

B. W. Drost concluded that average inflow to the hydrologic system of the Gig Harbor Peninsula (153 km^2) is 7,200 L/s. Outflow consists of evapotranspiration (2,500 L/s). In 1978, 68 of the 2,600 L/s of ground-water recharge was withdrawn by wells.

Ground-water levels affected by irrigation in Sequim Peninsula

Water diverted from the Dungeness River for irrigation on the Sequim Peninsula affects shallow (wells less than 15 m deep) ground-water levels, according to B. W. Drost. From November 1978 to March 1979, water levels declined an average of 0.5 m, with an average total irrigation rate of 910 L/s. From April to September 1979, levels rose 0.6 m with 3,300 L/s irrigation, and, from October to December 1979, the levels declined 0.3 m with 1,400 L/s irrigation.

Yakima River basin streamflow and irrigation diversions for 1977 drought year and 1960 to 1976

Surface-water diversion for irrigation in the Lower Yakima River basin in the 1977 drought year was about 10 percent below the mean for the 1960-76 period (2,340 hm^3 and 2,590 hm^3, respectively). Dee Molenaar determined that about 138,000 ha are under irrigation in the basin. Mean annual total discharge at selected sites in the 1977 water year was 61 percent of the 1960 to 1976 average, and the 1977 discharge of the Yakima River at Kiona, lowermost long-term gage in the basin, was 34 percent of the 1960-76 average.

Simulation of unregulated-streamflow record for the Yakima River at Union Gap

The Yakima Indian Tribe contends entitlement, by the treaty of 1865, to Yakima River water lost upstream of the reservation to five storage reservoirs and numerous diversion canals. During an initial investigation of project feasibility, D. E. LaFrance and C. H. Swift determined from preliminary computations of a streamflow simulation model that storage and diversion cause a reduction of roughly one-quarter of the unregulated flow from the 14,600-km^2 drainage basin. With project feasibility established, the investigation is continuing into a second phase that will improve the model and accurately determine the streamflow reductions.

SPECIAL WATER-RESOURCE PROGRAMS

DATA COORDINATION, ACQUISITION, AND STORAGE

OFFICE OF WATER DATA COORDINATION

With the assistance of water-oriented Federal and non-Federal organizations, continuing progress toward fulfillment of the mission assigned by the Office of Management and Budget Circular A-67 has been made. Cooperation by the participants and growing awareness of the need for coordination throughout the water com-

munity assures further progress toward a more effective National Water Data System.

The OWDC field coordination and planning cycle for fiscal year 1981 was completed. The procedure is now tied directly to the Master Water Data Index of NAWDEX, which serves as the base file of the "Catalog of Information on Water Data." In conjunction with the above, the report "Plans for Water Data Acquisition by Federal Agencies Through Fiscal Year 1981" was prepared and distributed. It consists of statements from more than 30 Federal agencies summarizing their water-data programs, including current and planned activities, as well as their anticipated future water-data needs. In September 1980, a special meeting of the Interagency Advisory Committee on Water Data (IACWD) was held to exchange information on plans and needs for water data acquisition.

The IACWD Subcommittee on Sedimentation, formerly a committee under the sponsorship of the WRC, continued to coordinate Federal agency activities on the collection, analysis, and exchange of sedimentation data. The subcommittee is responsible for producing an annual report entitled "Notes on Sedimentation Activities." Two reports, one for calendar year 1978 and one for calendar year 1979, were published during the year.

In cooperation with NAWDEX, the "Catalog of Information on Water Data" was updated through 1979, and an index to the catalog was prepared in 21 volumes, one volume for each of the 21 WRC regions. In addition to information on station activities, information on areal investigations and miscellaneous activities is now included in each of the volumes.

The directory of water-data acquisition activities in the coal-producing areas of the United States has been published. The directory, a special index to the "Catalog of Information on Water Data," was prepared to assist those involved in the development, management, and regulation of the Nation's coal resources by providing information on the availability of water data. The index is divided into five volumes covering the Eastern province, the Interior province, the northern Great Plains and Rocky Mountain provinces, the Gulf coast province, and the Pacific coast and Alaska provinces.

The "National Handbook of Recommended Methods for Water Data Acquisition" is nearing completion. Chapters on "surface water," "ground water," "snow and ice," and "hydrometeorological observations" were added to the handbook, while the Work Groups on Water Use Data and on Water Data Handling and Exchange produced first drafts of their chapters. When completed, the handbook will cover almost all phases of hydrology, as well as recommend metric units, conversion factors, precision of metric measurement, and metric conversion of equipment.

NATIONAL WATER DATA EXCHANGE

NAWDEX, a national confederation of water-oriented organizations cooperating to improve access to available water data, continued to expand during 1979. Voluntary membership in the program increased to over 160 organizations from the Federal, State, and local government, inter-State, academic, private, and foreign sectors.

Five additional Assistance Centers were added during the year. Fifty-nine centers were operating at the end of the year in 45 States and Puerto Rico. These centers responded to nearly 80,000 requests for data and information during the year.

Nearly 700 organizations have been registered in the computerized Water Data Sources Directory, which identifies organizations that are sources of water data, provide water-related data or information services, or are active in the field of water resources and produce reports and other information products of value to the hydrologic community. In addition, the directory data base was redesigned during the year to provide for the entry of information about water-related data available from registered organizations. This will allow the storage of information about water-use, land-use, meteorological, demographic, soil, and many other types of data that have significance to hydrologic studies.

Over 20,000 additional water-data sites were indexed in the computerized Master Water Data Index during 1979. By the end of the year, nearly 330,000 sites for 402 organizations had been indexed. In addition, work nearly was completed on a computerized interface with the water-data files of the Texas Natural Resources Information System, which will provide information on an additional 40,000 sites during 1980. This interface supplements those already completed for the WATSTORE system of the USGS and the STORET system of the EPA.

The second NAWDEX membership conference was held in May 1979 in New Orleans, La. This meeting continued to provide valuable input to the annual objectives of the program and resulted in several improvements in the operational activities of the program.

Two advisory subcommittees were established in February 1979 to monitor and advise the NAWDEX program, the Subcommittee on Water Data Exchange, working under the (non-Federal) Advisory Committee on Water Data for Public Use, and the Subcommittee on Water Data and Information Exchange, working under the (Federal) Interagency Advisory Committee on

Water Data. These subcommittees met in October and May 1979, respectively, and a joint meeting was held in October 1979 to initiate their activities of reviewing the annual program objectives of NAWDEX to provide advice on the needs and future requirements of the program, to serve as a forum to consider recommendations presented by member organizations, and to work toward improving communication throughout the water-data community.

NAWDEX is providing chairmanship of a Technical Working Group established in February 1979 for the development of recommended methods for the handling and exchange of water data. Work is underway on these methods, and a first draft is planned for completion in 1980. The methods will be published as Chapter 12 of the "National Handbook of Recommended Methods for Water-Data Acquisition."

WATER DATA STORAGE SYSTEM

The National Water Data Storage and Retrieval System (WATSTORE) is a large-scale computerized system developed to process and disseminate water-resource data collected by the USGS. The system consists of a central computer located in Reston, Va., and remote terminal facilities in every Water Resources Division district office. Direct access to the system also is maintained at 87 locations by other Federal, State, and local agencies. In the WATSTORE files, data are grouped and stored by common characteristics and data collection frequencies.

The Daily Values File contains values for water parameters that are either measured once daily or measured continuously and numerically reduced to one daily value. The file contains records for nearly 24,000 sites; of these, 8,000 are currently operating streamflow stations. Digital recorders in some areas transmit hydrologic data via satellite for entry to the file. Data in the Daily Values File are compatible with a variety of statistical programs for analyses on the basis of calendar years, water years, climatic years, or any other time period.

The Ground-water Site-Inventory File contains hydrologic, geologic, and well-inventory data for nearly 700,000 ground-water sites. To facilitate file management, the data base is divided into four files, each of which corresponds to one of four water-resource areas.

The Peak Flow File contains over 400,000 annual maximum-streamflow and gage-height values at surface-water sites. Peak flow records may also contain peak discharges that are above a base but are less than the maximum peak discharge for the year.

The Unit Values File contains data for parameters measured on a schedule more frequent than daily. Rainfall, stream discharge, and temperature data are examples of the types of data stored in the Unit Values File.

Representative WATSTORE products are computer-printed tables and graphs, digital plots, and data in machine-readable form. WATSTORE also interfaces with a proprietary statistical package to provide extensive analyses of data such as regression analyses, variance analyses, transformations, and correlations.

Minicomputers are being used in some States to maintain local files, to reproduce maps, plots, and other graphics, to model local hydrologic systems, and to process or preedit data before they are included in WATSTORE.

URBAN WATER PROGRAMS

The USGS is involved in a number of field studies intended to define the quality, quantity, and peak discharges of storm-water runoff from urbanized areas. The objective of these studies is to provide data to support generalized relation for estimating hydrologic changes resulting from urbanization.

USGS-EPA urban studies

The USGS has entered into an interagency agreement with the EPA to establish an urban storm-water data base. The intent of the data base is to characterize the quality of urban storm water and to assess the effectiveness of management controls. D. J. Lystrom (1979) described nationally consistent guidelines for these studies and a framework for data collection and analysis. Eight studies conducted by the USGS under this agreement have been initiated in the following cities: Baltimore, Md., Bellevue, Wash., Chicago, Ill., Denver, Colo., Long Island, N.Y., Milwaukee, Wis., Rochester, N.Y., and Salt Lake City, Utah.

Hydrologic modeling

W. H. Doyle, Jr., and J. E. Miller calibrated a distributed routing rainfall-runoff model to four urban watersheds near Miami, Fla. W. M. Alley and J. E. Veenhuis (1979) reported guidelines for determining basin characteristics for urban rainfall-runoff models. W. M. Alley and P. E. Smith developed a rainfall-runoff-quality model for urban areas. P. E. Smith and M. E. Jennings analyzed washoff and accumulation functions for Miami urban data and found that washoff coefficients varied significantly for various water-quality constituents.

Flood-frequency study

H. E. Allen, Jr., and R. M. Bejcek (1979) developed techniques for estimating the magnitude and frequency

of floods in the urban environment of northeastern Illinois. Multiple-regression analysis was used to define relations for estimating flood frequences ranging from 2 to 500 yr based on drainage area, channel slope, and percent imperviousness of drainage basins. Results of the study indicate that changes in land use associated with urbanization have increased flood-peak discharges by factors ranging up to 3.2.

A technique for estimating the magnitude and frequency of floods in the Houston, Tex., metropolitan area was developed by Fred Liscum and B. C. Massey (1980) using a multiple-regression flood-frequency analysis of flow data from unregulated streams in the area. A regression model, relating flood-peak discharge to concurrent rainfall and antecedent soil moisture conditions, was used to simulate 67-yr records of annual-peak discharges. Flood-frequency characteristics were determined for the simulated annual peaks and for the observed annual peaks at each of 22 gaging stations. Drainage area, bank-full channel conveyance, and percentage of urban development were used as independent variables; weighted flood-frequency discharges were used as dependent variables in the multiple regression analysis. Relations applicable to unregulated streams were developed for predicting floods with recurrence intervals of 2, 5, 10, 25, 50, 100, and 500 yr. Drainage basins ranged in area from 3.44 to 471 km^3. The percentage of urban development in these basins ranges from 37 to 98.9 percent. The relations indicate that, as a basin changes from a completely natural state to one of complete urbanization, the magnitude of a 2-yr peak discharge is increased by a factor of 4.2, the magnitude of a 50-yr peak is increased by a factor of 4.9, and the magnitude of a 100-yr peak is increased by a factor of 4.9.

Water-quality studies

Harold Mattraw and Robert Miller conducted a study of storm-water runoff from three small urban areas in Broward County, Fla., between 1974 and 1977. Thirty or more runoff-constituent loads were computed from chemical analyses of samples collected systematically from each of the homogeneous land-use areas. The areas sampled were single-family residential, highway, and a commercial shopping center. Total water-quality loads were computed for the collection period by totaling loads for individual storms. Loads for unsampled storms were estimated by using regression models and records of storm precipitation. Loadings in kilograms per hectare of hydraulically effective impervious areas were computed for the three land-use types. Total nitrogen, total phosphorus, and total residue loadings were highest in the residential area. COD and total lead loadings were highest in the commercial area. Loadings of atmospheric fallout were estimated from bulk precipitation samples collected at the highway and commercial sites. Atmospheric contributions to runoff loads were 49 percent or more for seven constituents at the two sites. Atmospheric loads exceeded the estimated storm-water runoff loads for total nitrogen, total phosphorus, and total zinc at the highway area. Total zinc from bulk precipitation exceeded runoff load at the commercial site.

Instruments were installed at two residential watersheds and one urban arterial watershed in Bellevue, Wash., to sample and measure dry and wet atmospheric fallout, precipitation, and watershed outflow. W. L. Haushild and J. C. Ebbert reported that laboratory determinations for samples of precipitation, dry atmospheric fallout, and basin outflow from a few storms indicate the following ranges in constituent concentrations. For residential basins, basin outflow concentrations ranged from 52 to 220 μg/L for total lead, 0.06 to 0.36 mg/L for nitrate, 0.51 to 1.8 mg/L for total organic nitrogen plus ammonia, and 0.10 to 0.19 mg/L for total phosphorus. For the urban-arterial basin, outflow concentrations ranged from 120 to 220 μg/L for total lead, 0.12 to 0.23 mg/L for nitrate, 0.62 to 0.87 mg/L for total organic nitrogen plus ammonia, and 0.08 to 0.15 mg/L for total phosphorus. Results, expressed in grams per hectare per day, for wetfall precipitation samples collected in one of the residential basins ranged from 2.5 to 18.5 for total lead, 27.9 to 107.5 for nitrate, 12.8 to 69.4 for total organic nitrogen plus ammonia, and 2.0 to 19.3 for total phosphorus. Correspondingly, dry fallout sample determinations, also expressed in grams per hectare per day, ranged from 0.5 to 2.5 for total lead, 1.2 to 4.7 for nitrate, 2.7 to 8.4 for total organic nitrogen plus ammonia, and 0.5 to 0.7 for total phosphorus.

Urban runoff data were collected from three watersheds in the Denver, Colo., metropolitan area from 1975 to 1977. S. R. Ellis and W. M. Alley (1979) stated that antecedent precipitation or the number of days since the last street sweeping had no apparent effect on rainfall-runoff quality. Snowmelt runoff loads of some water-quality constituents increased with the number of days that snow had been on the ground. The authors also indicated that urban storm runoff in the Denver area may be a significant contributor of total ammonia nitrogen, total nonfilterable residue, total copper, total iron, total lead, and total zinc to local receiving waters. During winter months, snowmelt runoff may be a significant contributor of sodium and chloride.

Transport of chemical constituents in urban storm water

A method for separating suspended sediments of specific particle size ranges from urban runoff water has been developed to aid in predicting the transport of

selected chemical constituents associated with sediments. The method incorporates particle-sizing techniques that are based on settling-velocity characteristics. Thus far, results of the technique are comparable to standard USGS particle size analyses. According to Joseph Rinella, the method has been used to separate suspended sediments of specific size ranges from more than 30 L of urban runoff water. After separation, the various size ranges of 62 to 16, 16 to 4, and <4 μm of suspended sediments have been analyzed for selected chemical constituents.

WATER USE

A data sheet was designed for tabulating 1980 water use, and studies of water use were made in project areas. The data will be included in the next report of the USGS 5-yr report series on water use (Murray and Reeves, 1977).

The National Water-Use Data Program, which began in 1978 with 15 States participating, had 47 States cooperating by mid-1980. Water-use plans have been completed for all the participating States, and each State has begun a program of data collection. The National Water-Use Data System has been developed and implemented and is now part of the USGS WATSTORE data system. A methods manual for the collection of irrigation water-use data has been developed by the Suwannee River Water Management District. Additional manuals are being prepared by State cooperators for the collection of water-use data for municipal, domestic, commercial, industrial, and public uses.

Irrigation and ground water in Newton and Jasper Counties, Indiana

M. P. Bergeron reported that water-level declines due to seasonal irrigation pumpage in confined and unconfined sand-and-gravel and limestone aquifers in Newton and Jasper Counties in northwestern Indiana have been substantial. Virtually all irrigation pumpage is from the limestone aquifer, which is overlain by 3 to 52 m of glacial drift. Irrigation pumpage varies from year to year because the use of irrigation is dependent on a set of unpredictable factors, including precipitation, evapotranspiration, and soil-moisture conditions. Heavy irrigation pumpage was documented during 1977, and pumpage was estimated to be 4.0×10^6 m^3, which was 62 percent of the total yearly pumpage. Because of the seasonal nature of withdrawals, the stress imposed by irrigation is better exemplified by examining daily irrigation use during the growing season. During the summer months of June through August 1977, irrigation pumpage was estimated to be 12.53 m^3/s. This pumpage was 94 percent of the total daily pumpage in the study area during that period. During 1977, widespread irrigation pumpage caused water-level declines of nearly 12 m in observation wells located near heavily irrigated areas. Hydrographs from the observation wells seem to indicate that water levels recover to prepumping levels during the nongrowing season.

Irrigation from deep wells in Audrain County, Missouri

Vibration timers were reported by L. F. Emmett and L. D. Hauth to have been installed on 17 deep irrigation wells that are open to the Cambrian and Ordovician aquifer in Audrain County, Mo. The timers recorded the number of hours the wells were pumped. Using this data and the reported well yields as determined by performance tests, Hauth estimated that 3.0 hm^3 of water was pumped for multiple irrigations in the period from July through September 1979. This is equal to the amount of water pumped from all the municipal wells in Audrain County for an entire year.

Ground-water use in the coastal-plain aquifer system of New Jersey

E. F. Vowinkel reported that a data base consisting of monthly pumpage totals from 1956 to 1978 for 1,311 major ground-water withdrawal sites was completed for wells located in the coastal-plain aquifer system of New Jersey. Aggregated yearly totals in mg/d, mg/yr, ft^3/s, or m^3/s can be retrieved by aquifer, county, or water-use category by tables and graphs. The Cretaceous Magothy and underlying Raritan Formations, including the Old Bridge Sand Member of the Magothy and Farrington Member of the Raritan, accounted for 67.5 percent, or 9.7 m^3/s, of the total major ground-water diversions within the coastal-plain aquifer system in 1978.

Camden, Gloucester, and Burlington Counties used the greatest amount of ground water, 6.0 m^3/s (41.8 percent of total), derived from the 11-county coastal plain in 1978. Public-supply ground-water withdrawals were 11.1 m^3/s, and industrial and irrigation demands were 2.6 m^3/s and 0.6 m^3/s in 1978, respectively.

REGIONAL AQUIFER-SYSTEM ANALYSIS PROGRAM

Three new regional aquifer studies were initiated during 1979. These included a study of unconsolidated aquifers of the northern Atlantic Coastal Plain, an investigation of sand aquifers of the Southeast coastal plain, and a study of the basalt aquifers of the Snake River Plain. Regional studies were continued for six other systems, including the Ogallala aquifer of the High Plains, the unconsolidated deposits of the California Central Valley, the aquifers of the northern Great Plains, the sandstone aquifers of the northern Midwest,

the carbonate aquifers of the Southeast, and the alluvial basins of the Southwest. Activities of these continuing studies are summarized below:

- In the High Plains study, several test areas were selected to define the relation between annual pumpage and irrigated crop acreage. Results indicated that pumpage can be estimated successfully by using irrigated acreage data and that irrigated acreage can be determined by using Landsat data. Procedures are being developed to estimate pumpage throughout the High Plains by using these methods.
- A three-dimensional model under development for the Central Valley project is being modified to incorporate land subsidence effects as well as groundwater flow.
- In the northern Great Plains study, a three-dimensional flow model incorporating the effects of fluid-density differences has been developed and is being used to determine predevelopment groundwater flow patterns.
- In the northern Midwest project, an automated data file has been established through which various kinds of hydrologic information are stored, processed, and utilized in ground-water flow simulations. A method of accounting for the effects of multiaquifer wells in three-dimensional simulations of the northern Midwest aquifer system has been developed.
- In the Southeastern carbonates study, a drill-stem test and water sampling operation were completed from an offshore rig approximately 80 km from the eastern coast of northern Flordia, through a contract with Tenneco, Inc. Results have confirmed theoretical projections of the position of the freshwater-saltwater interface at 80 km offshore.
- In the Southwest alluvial basins project, detailed studies and simulations of the flow system for representative basins are underway. These will help to determine the mechanisms controlling groundwater flow throughout the basins of the Southwest.

In the Atlantic Coastal Plain, Southeast coastal plain, and Snake River Plain projects, assembly of readily available data is in progress, and some new data-collection activities have been initiated.

MARINE GEOLOGY AND COASTAL HYDROLOGY

COASTAL AND MARINE GEOLOGY

CONTINENTAL MARGIN HAZARDS AND GEOLOGIC ENVIRONMENT OF THE SEAFLOOR

New techniques applied to studies of seafloor hazards and conditions

The difficulties and hazards of the seafloor environment have become both better known and yet more diversified as the petroleum industry and others have extended their exploration and operations. In response to the environmental stress and problems that must be overcome, an increasing number of costly precautions must be taken to assure safety of the operations and supporting installations. Among factors of particular concern are those associated with the stability of seafloor foundations to support the sophisticated structures needed to operate in adverse environments.

Because the foundation conditions of the seafloor are hidden and affected by the overlying water, the problems of observation and study are more challenging than those of land areas. The field of view through face mask or submarine porthole is limited to a few meters or less. Attempts to collect and transfer samples to the laboratory for conventional testing sometimes impair properties that are dependent on the overlying water pressure. The prospecting of submarine outcrops with ordinary pick and shovel is nearly impossible at depths exceeding a few meters. Obviously, alternative techniques must be used to "observe" the seafloor and determine the nature of the materials.

From the outset, USGS scientists, engineers, and technicians have devoted a large part of their efforts to the development and application of better seafloor mapping and sampling techniques. In 1979, working both separately and in collaboration with other researchers, the USGS began testing new instruments and techniques that are expected to attain widespread use in future studies of seafloor stability and siting of offshore installations. Of particular note are a Seafloor Earthquake Measurement System (SEMS), a Geotechnically Instrumented Seafloor Probe (GISP), and a digital acquisition system for collection of side-scan sonar data.

The original prototype of SEMS was developed jointly by the USGS, DOE, and five oil companies (Atlantic-Richfield, Chevron, Gulf, Mobil, and Shell) to measure the response of sediments to earthquakes. It consists of a probe containing a force-balance accelerometer and an attached pressure vessel housing a recorder and power supply. The probe has been installed in the Santa Barbara Channel off California where it was injected into the seafloor to a depth of 3.5 m. Additional prototypes have been prepared for deployment elsewhere within seismically active regions off the California and south Alaska coasts.

The GISP, developed cooperatively with the DOE, will be used to collect data on sediment properties such as pore-water pressures and their fluctations. These pressure systems are not well understood; the in situ measurements from this seafloor probe are expected to have significant value in studies of the submerged Mississippi Delta front and other regions of sediment instability and sliding.

The addition of the digital acquisition system for collection of side-scan sonar data permits scale-true surveys and mapping of seafloor features at various levels of detail. At a reconnaissance scale, the improved technique was used on the inaugural cruise developed under terms of a new 5-yr agreement between the USGS and the Natural Environment Research Council (NERC) of the United Kingdom. U.S. activities are supported jointly by the USGS and DOE. On the cruise aboard the U.K. Research Vessel *Starella*, Chief Scientists P. G. Teleki (USGS) and D. G. Roberts (Institute of Oceanographic Science, NERC) utilized a British wide-swath imaging sonar, together with gravity and single-channel seismic profiling equipment, to map portions of the Atlantic continental slope off Georges Bank, the slope off the Baltimore Canyon lease area, and the Blake Escarpment. In a preliminary assessment of the resulting true-scale sonar mosaic, Teleki was able to identify two broad areas of slumped sediments beneath relatively deep water—one near the Corsair Canyon (Georges Bank) at 2,000 m and the other seaward of the Baltimore and Wilmington Canyons at 1,500 to 2,500 m. He also noted several features along the continental slope of the Carolinas that he interprets to be the surface expression of salt-dome structures.

At a larger scale, a digitized side-scan sonar system has been applied to detailed mapping of the highly dynamic surfaces of the Mississippi Delta. This usage provides an especially clear example of how improved techniques contribute to the amounts and quality of knowledge that may be used to reduce the risk of loss or damage to offshore installations and to increase opera-

tional safety. The side-scan sonar data collected on a grid with line spacing of 240 m has been assembled to form a seafloor sonar mosaic that may be compared to an orthophotomap of land areas and on which instability features may be delineated and studied (Pryor and others, 1979).

Using the mosiacs, L. E. Garrison (USGS) and J. M. Coleman and D. B. Pryor (Coastal Studies Institute, Louisiana State University) have developed a broad morphologic classification of failure features that is being utilized in ongoing investigations of landslide movements. Thus far, the major classes of features are (1) collapse depressions, most of which are located in shallow water areas, have slope angles of only 0.1° to 0.2°, are nearly circular with diameters of less than 300 m, and are 1 to 3 m in depth, (2) bottleneck slides, which are found on slopes on 0.2° to 0.4° and have shapes that are more elongate than the foregoing with lengths of 150 to 600 m and narrow openings at their downslope end for debris discharge to the unfailed seafloor, and (3) elongate mudslides and debris flows, which extend across the delta front on slopes that average 0.5°, are commonly 8 to 10 km in length, and consist of a subsided bowl-shaped source area, a long transport chute, and a downslope depositional lobe. A comparison of historic bathymetric charts provides evidence of major changes in some large failure features, whereas repeated detailed surveys of small study areas during the past few years reveal less dramatic but equally important smaller scale changes.

The precise conditions responsible for sediment instability of low-angle delta-front slopes are difficult to determine. The transition from stability to instability, however, seems to involve the interaction of several variables. Of those that are known, the most important are (1) rapid sedimentation, which produces excess pore pressures and underconsolidated sediments, (2) biologic generation of methane, which may contribute additional pore gas and, thereby, raise pore pressures still further and reduce effective stress, and (3) wave loading, which imposes cyclic loads on shallower portions of the delta seafloor, thereby increasing pore pressures and destabilizing the affected areas.

Mass movement potential on the United States continental margins

The growing volume of seafloor data, collected chiefly by techniques that have become routine and conventional within the past few years, permits use of increasingly sophisticated methods of analysis to identify and assess geologic hazards that may affect offshore operations. The potential for mass movement is representative of a subject for which large amounts of data are available and amenable to a degree of quantification. This potential may be described as the result of some combination of external forces, such as earthquakes, storm waves, tides, or water circulation, acting on some combination of stability properties, including textures, shear resistance, and sedimentation rates. J. S. Booth (USGS) and D. A. Sangrey (Carnegie-Mellon University) have devised a nomograph to aid in defining combinations of the two sets of values. Using it in conjunction with consolidation theory and slope stability analyses, they have obtained results that aid in predicting the degree of sediment instability for selected sites along the U.S. continental margins (Booth and Sangrey, 1979). The Mississippi Delta, with its high rates of sedimentation, and the Copper River Delta off southern Alaska, with a high sedimentation rate and much seismic activity, were identified as having the highest levels of instability. The upper Continental Shelf of the Gulf of Mexico, which has generally high rates of sedimentation and is vulnerable to hurricane effects, and the southern California Borderlands, with locally high rates of sediment accumulation and many earthquake shocks, also are identified as areas of appreciable instability.

Potential geologic hazards on the inner Continental Shelf off southeastern Massachusetts

C. J. O'Hara and R. N. Oldale have distinguished a variety of potential hazards and constraints that could affect development within the coastal zone and on the inner Continental Shelf of southeastern Massachusetts. Through analyses of high-resolution seismic reflection profiles, side-scan sonar records, and vibracores obtained in eastern Rhode Island Sound and Vineyard Sound, O'Hara and Oldale were able to outline the distribution of seafloor outcrops of bedrock and coarse glacial debris (boulder till), buried channel deposits, faulted and gaseous sediments, and active sand-wave fields. Bedrock exposures and boulder pavements are common beneath eastern Rhode Island Sound, where they are associated with ridges and ledges that seem to be sites of active winnowing and erosion by waves and bottom currents, especially during major coastal storms. These areas are considered unsuited for the containment disposal of solid wastes and dredge spoils, and, where the boulder pavements overlie till, the boulders may preclude pipeline burial and may hamper mining of sand and gravel deposits. The buried channel deposits lie in the shallow subsurface, are texturally diverse, and consist of sand, gravel, mud, and, locally, freshwater or saltwater peat. Because they may be poorly compacted, the mud and peat of these deposits could be a cause of foundation settling. In two areas, acoustically turbid sediments were found to consist of organic gas-charged muds that may cause unstable foundation conditions.

The sand-wave fields and associated megaripples are generally restricted to Vineyard Sound, where the ocean waves and currents are most active. An area of silt and clay winnowing, it also is considered unsuited for contained disposal of fine-grained wastes and spoil but may be acceptable for clean-sand spoil. Folded and faulted sediments also were mapped but are confined to Pleistocene and older deposits and are mostly of glaciotectonic origin. O'Hara and Oldale failed to find any evidence for existing earthquake activity or other hazards that might be associated with these geologic structures.

Sediments and bedforms of western Massachusetts Bay

N. C. Lian was able to distinguish six mappable acoustic units on side-scan sonar records of the seafloor at depths of 10 to 35 m between Cape Ann and Duxbury in western Massachusetts Bay. Based on confirmatory data derived from subbottom profiles, cores, grab samples, and bottom photographs, the units are interpreted to be (1) bedrock, (2) boulder-rich till, (3) boulder-poor till, (4) coarse glacial outwash, (5) postglacial deposits of clay to medium sand, and (6) an undifferentiated complex of small areas of units 4 and 5. Bedrock outcrops generally occupy areas of rough bathymetry. Till typically surrounds the outcrops, predominates in the southern section and nearshore in the north, and is discontinuous in the central part of the area. Glacial units tend to grade laterally to fine sediments, which dominate the northern section but, in general, are confined to local depression and depths exceeding 45 m in the central and southern sections. Unit 6 dominates the central section. South of Marblehead, sand waves and ribbons at all depths of units 5 and 6 have orientations that suggest northwest or southeast directions of transport. The features and distribution of units are consistent with a history that began with deposition of glacial drift on bedrock, was followed by melt water reworking and deposition, and ended with marine working during the postglacial rise of sea level. Holocene sedimentation seems limited to continued reworking of the glacial deposits.

Acoustic stratigraphy of Nantucket Sound, Massachusetts

On the basis of a preliminary analysis of high-resolution seismic reflection records, C. J. O'Hara notes that unconsolidated coastal plain and continental shelf rocks of Late Cretaceous and probable Tertiary age lie seaward of an east-west-trending deeply eroded cuesta and cover most basement rocks beneath Nantucket Sound. The cuesta is attributed to fluvial erosion during late Tertiary or early Pleistocene time, with some modification by glacial ice during the Pleistocene. The coastal plain rocks occur much further north beneath Nantucket Sound than shown on the map of Weed and others (1974) and locally may extend beneath Cape Cod. Glacial drift deposits of inferred late Wisconsinan Age overlie the coastal plain rocks unconformably except in the north-central and northwesternmost parts of the Sound where they seem to overlie bedrock directly. Most drift deposits were probably derived from the Cape Cod Bay ice lobe, but, at places, some may be ascribed to the Buzzards Bay or Great South Channel ice lobes. The drift is thickest, in some places exceeding 75 m, where it fills preglacial valleys cut into the coastal plain sediments. The glacial deposits seem generally well stratified, as indicated by relatively flat-lying closely spaced internal reflections and are, therefore, thought to consist of outwash and preglacial lake sediments. Their upper surface is an unconformity that may be attributed either to streams during the postglacial interval of low sea level or, locally, to marine planation accompanying the subsequent rise of sea level to its present position. Holocene marine deposits, mostly in the form of linear sand ridges and tidal deltas, provide a surficial blanket as much as 12 m thick. These features may be considered potential sources of sand and gravel. Large sand-wave fields and megaripples commonly are associated with the ridges and indicate areas where tidal currents are most active. Acoustically turbid zones suggesting gassy organic sediments are present at many places, notably in the eastern part of Nantucket Sound.

Modern continental shelf sediment accumulation off southern New England

A site identified as one of continuing deposition on the Continental Shelf between Block Channel and Great South Channel to the south of Martha's Vineyard has attracted attention as a potential offshore sink for pollutants. The fine-grained sediments of the area, containing between 20 and 95 percent clay, formerly were thought to be relicts of deposition that took place as sea level rose about 8,000 yr ago. Analyses for ^{14}C and ^{210}Pb, however, provided data indicative of continuing accumulation (USGS, 1979a, p. 142). M. H. Bothner reports rates, determined by ^{14}C analyses of organic material within sediment cores, of 80 to 130 cm/1,000 yr near the center of the area and about 50 cm/1,000 yr near its eastern margin. Inventories of excess ^{210}Pb for undisturbed cores give profiles that suggest higher sedimentation rates. However, this may be a result of sediment mixing by organisms during deposition (USGS, 1979a, p. 142).

D. C. Twichell, Jr., C. E. McClennen, and Bradford Butman estimate a volume of 50 km^3 for the Holocene sediments overlying two buried shorelines that they could distinguish on high-resolution seismic reflection profiles through the areas of deposition and could date at 14,800 and 9,000 yr B.P. On the basis of eastward in-

creases in coarseness of the sediments and strength of the currents, they suggest that most of the Holocene sediment has come from Georges Bank and Nantucket Shoals. Any pollutants discharged in these areas of planned resource development could, therefore, be expected to move westward and into the area of apparently continuing deposition.

Suspended matter in continental shelf and slope waters of the Georges Bank area

The suspended matter in waters of Georges Bank originates primarily from biological production and from resuspension of bottom sediments. M. H. Bothner (USGS) and C. M. Parmenter and J. D. Milliman (Woods Hole Oceanographic Institution) observed highly variable concentrations on the central shoals during 10 cruises in an 18-mo period. These concentrations were independent of seasons but had compositions that showed a weak seasonal correlation. Major storms during any season have greatest effect on the central bank, raising concentrations from <mg/l to as much as 4 mg/l. Winter storms generate highest concentrations of noncombustible material throughout the water column, and summer storms apparently increase biological production by introducing additional nutrients to the photic zone. On the southeast flank of the bank, in water depths between 80 and 200 m, both total suspended matter and noncombustible material vary only slightly in comparison to the central shoals, and storm effects are far less noticeable.

Highest concentrations (>15 mg/l) of suspended matter in the entire area, observed in bottom waters south of Nantucket Island after winter storms, appear to have been derived mostly from resuspension of bottom sediment. Resuspended sediment is also common in near-bottom waters of the southwestern Gulf of Maine and near the intersection of the shelf-slope water mass front and the bottom.

Seasonal variations were observed in the distribution and species composition of phytoplankton. Coccoliths are predominant on the central bank during the winter but are concentrated on the eastern flank at deeper depths during the spring and summer.

Slope stability off the southeast Atlantic coast

Like those studying foundation conditions off New England, Peter Popenoe has placed emphasis on studies of seismic reflection records of the region southeast of Cape Hatteras, where slope stability may be a problem in petroleum exploration and development. Here planned tracts for lease sales are located on the continental slope and inner Blake Plateau where the water has depths of 500 to 2,000 m. A growth fault passes through many of the tracts. It strikes north-northeast, dips about 45° to the southeast, has at least 400 m of normal offset at depth, and can be traced for more than 185 km. The fault intersects the seafloor at an average water depth of about 700 m, but, because of low angle of dip, it can be distinguished beneath sediments of a large area to the east.

Seaward of the fault, the Blake Escarpment locally has steep slopes that are underlain in part by several discontinuous Upper Cretaceous(?) reefs. Erosion and slumping have exposed the reefs at some places. In many areas, low-angle rotation slump blocks are common below the reef, and, where the reefs are buried or poorly developed, the sediments of steep faces generally have slump features. The slopes of several profiles have steep scars that terminate the bedding and are as much as 75 m in height. Downslope from the scars, the profiles have chaotic bottom reflections that probably indicate slump deposits.

Surface turbidity and hydrographic variability on the South Texas Continental Shelf

Regional surface-water turbidity patterns and associated hydrography were monitored on the South Texas Continental Shelf during an 18-mo period (November 1975–May 1977) as part of an environmental study. On six monitoring cruises, quasi-synoptic surface measurements were made of water transmissivity, suspended-sediment concentrations, temperature, salinity, and drifter trajectories. On the basis of time-sequence patterns of these measurements, G. L. Shideler concludes that substantial spatial and temporal variability exists and that the temporal variations take place on both seasonal and annual time scales. Relatively turbid inner-shelf waters reflect the offshore and alongshore transport of sediment derived from coastal sources. Turbidity patterns along the inner shelf are characterized by a regional gradient of shoreward-increasing turbidity with superimposed local gradients established at major tidal inlets that serve as prominent sediment point sources and dispersal centers. Shideler attributes the turbidity variability along the inner shelf to interaction between amounts of coastal runoff, wind-driven currents, and flux from individual tidal inlets. Relatively nonturbid outer-shelf waters suggest the shelfward incursion of an open-ocean water mass regulated by deep-gulf circulation; the extent of incursion appears to vary spatially and temporally, resulting in outer-shelf turbidity variations. The overall shelf turbidity patterns reflect the degree of lateral interchange between the gulfward movement of turbid inner-shelf waters and the shelfward incursion of clear open-ocean waters.

California continental margin sediment dynamics

Off the west coast, earthquakes that can offset seafloor and associated processes such as slumping complicate studies of sediment movement. In an attempt to separate the effects of these processes from longer term ones, J. V. Gardner has located a relatively undissected segment of continental slope between two large submarine canyons to the west of the mouth of the Russian River off northern California. Reconnaissance geophysical mapping in this area revealed no evidence for active faulting and only minor slumping. The area, therefore, seems well suited for longtime-series measurements of sediment flux over the Continental Shelf and down the slope.

D. A. Cacchione, D. E. Drake, and H. A. Karl deployed a tripod-mounted instrument array, called GEOPROBE, to obtain long-term measurements of near-bottom currents and other sediment transport parameters. Preliminary results indicate a westward offshore movement of water and sediments. This previously unreported flow may have eluded earlier investigators because they made their measurements well above the bottom boundary layer. The offshore flow of bottom water and sediment suggests the possibility of a characteristic and persistent process throughout the "upwelling season" of April to October along the Pacific continental margin.

Cacchione, Drake, and Karl also found an offshore flow (1–3 cm/s) of near-bottom waters on the San Pedro Shelf off Los Angeles throughout a 40-d period of GEOPROBE measurements in April to May 1978. Here the flow may relate to upwelling of subsurface water in response to local winds.

To aid in the studies of sediment dynamics off California, S. L. Eittreim, J. W. Lee, and their associates at Menlo Park have constructed a deep-sea nephelometer after a design of R. L. Koehler and L. Armi (Woods Hole Oceanographic Institution). The USGS team successfully tested their instrument on the continental slope west of San Francisco. The package, which measures forward light scattering, proved sensitive to variations in water-column turbidity and permitted identification of a near-bottom nepheloid layer a few hundred meters in thickness and a midwater high-turbidity tongue at a depth of about 1 km.

Alaskan Continental Shelf sediment dynamics

On the basis of his study of sediment dynamics and shelf history, B. F. Molnia reports that a large late Pleistocene ice sheet covered the shelf of the northeast Gulf of Alaska until about 12,000 yr ago. Following deglaciation of the shelf, Holocene sedimentation, dominated by clayey silt from glaciers, began. Sand is a minor component of Holocene sediments and is restricted to a nearshore zone less than 15 km wide. Relict deposits of glacial sand and gravel, Tertiary bedrock outcrops, and neoglacial moraines are present at many places on the shelf but are being buried by the expanding Holocene silt wedge except where scour prevents fine-grained deposition. The sedimentation rates average 4.5 mm/yr and locally are as high as 28 mm/yr. The wedge has a volume of approximately 3,000 km^3, corresponding to an average thickness of about 400 m over the entire northeastern Gulf of Alaska.

The suspended loads of streams entering the northeastern Gulf of Alaska commonly exceed 1.5 g/L and may include sand-sized particles. Suspended sediment measurements and a limited discharge record for the Copper River, the largest stream entering the northeastern gulf, indicate that it may deliver about 0.1 km^3/yr of suspended sediment. In addition to the stream loads, outcrops of Tertiary rocks also serve as point sources for sediment.

Longshore currents transport sand westward and into coastal embayments such as Yakutat Bay and Icy Bay. Finer material is moved parallel to the shoreline and then across the shelf with an unknown percentage bypassing the shelf. Winds carry sediments as coarse as medium sand from bars, such as those of the Copper River, directly to the middle shelf. Eolian transport may be the only active mechanism, other than aperiodic ice rafting, to carry sand beyond the inner shelf.

In studies of sand transport and bedform movement in the lower Cook Inlet of Alaska, M. A. Hampton and A. H. Bouma have found that sand moves only during spring tides and during storms. Here the seafloor ripples, sand waves, sand ridges, dunes, and sand ribbons form intricate patterns that reflect complex water motions. A comparison of patterns of the small sand waves and sand ribbons that may be identified on 1978 and 1979 side-scan sonar records of the same areas provides the only method currently available of determining migration of the bedforms.

D. A. Cacchione and D. E. Drake have measured bottom velocity shear at trough and crest sites in a large sand-wave field of the lower Cook Inlet. They attribute the intensified stresses and higher rate of bottom-sediment transport found at crest positions to flow intensification (streamline convergence) and increased turbulence (higher Reynold's stresses). Tidal currents at both crest and trough positions are sufficient to cause sand ripples to reverse their orientations with ebb and flood cycles and to migrate slowly in the ebb direction (southward). Net migration of the 1- to 3-cm ripples is about 1 wavelength every 2 weeks.

In a synthesis of old and new GEOPROBE and cruise data for the outer Norton Sound, west Alaska,

Cacchione and Drake have found that, on the Yukon prodelta, the flux of under-ice sediment movement during winter is similar to that which takes place during fair weather in the summertime. Periods of greatest transport occur when late summmer–early autumn storms form large amplitude waves and wind-driven currents, which resuspend sediment of the prodelta surface. The regional flow then moves the sediment northward. This combined action is the chief cause for the low net accumulation of sediment on the prodelta.

Gas within sediments of the northern California to Oregon Outer Continental Shelf

S. H. Clarke, Jr., and M. E. Field report the discovery of modern sediments that contain anamolously high concentrations of gasoline-range hydrocarbons overlying the crest of a diapiric structure of the Eel River Basin off northern California. The hydrocarbons probably have had a thermogenic origin deep within the sedimentary section of the basin and have migrated through fractures of the diapiric ridges into the overlying unconsolidated sediments.

In both the Eel River and the Coos Bay Basins, Clarke and Field also have found acoustic anomalies. They attribute these to shallow accumulations of biogenic methane gas. In the Coos Bay Basin, seafloor cratering and gas seeps were found in the vicinity of the anomalies and the two are thought to be related. Future studies are needed to verify the compositions of the gases, to map distribution of the anomalies and associated phenomena, and to determine their effects on engineering properties of the sediments.

Seismic study of a subsea gas accumulation off southern California

G. W. Boucher used a cross-correlation technique to deconvolve digital seismic reflection data in a study of an acoustic anomaly produced by a near-surface accumulation of gas and an associated fault beneath the Santa Barbara Channel. The technique yields a zero-phase wavelet that, in turn, provides a minimum width for a given signal-band width and is unambiguous in phase. The result is maximized resolution permitting determination of the amplitude and sense, or sign, of each reflection. When applied, this method provided a clear delineation of the gas-bearing layers. Analyses of one layer, presumably a sand, provided two characteristic acoustic signatures, which reflected the presence or absence of gas. The technique also allowed precise correlation of sedimentary sections bounding the fault, yielding an unambiguous determination of its vertical offset.

Gas-charged sediments and associated features of the Alaskan Continental Shelf

Gas-charged surficial sediments and associated features have served as targets of USGS investigations at several sites on the Continental Shelf bordering the Gulf of Alaska and the seafloor of the Bering Sea. In studies near Yakutat, B. F. Molnia collected samples and data that may explain the mechanism by which the pockmarks and craters of the area are formed. The sediments in which these features occur consist of sand and silt, have water contents of as much as 140 percent of dry weight, and contain less than 2 percent organic material. Total conversion of the organic material to gas and subsequent degassing could not account for the size of the craters, the largest of which approach 300 m in diameter and 15 m in depth. Also, within this area, no evidence exists for leakages of gas from deeper sources. Molnia suggests a mechanism that combines degassing with a 20- to 40-percent decrease in water content as follows: the bacterial decomposition of organic matter to form methane that accumulates in the subsurface, as seen on seismic profiles, and that contributes added instability to the sediments, and the release of the overpressured gas by wave-loading, seismic shock, or other processes accompanied by dewatering to produce the craters.

M. A. Hampton and A. H. Bouma have identified three major areas and several smaller ones on the Kodiak Shelf where acoustic anomalies of seismic records suggest the presence of bubble-phase gas within the sediments. Study of seafloor gas seeps and gas-charged sediment cores from the area provided additional information, and chromatographic analyses of the gas indicate that it has a shallow microbial rather than deep-seated thermogenic origin. Hampton and Bouma found no signs of sediment failure, subsidence, or other processes indicative of gas-induced problems; however, study and testing of the areas are incomplete.

Within the dynamic environment of moderate tectonism, active erosion, and rapid deposition on the shallow floor of the northern Bering Sea, C. H. Nelson and D. R. Thor have found a number of potential geologic hazards, including several that involve gas or interaction with gas in the sediments. This gas is thermogenic and reaches seeps and near-surface sediments through pathways provided by faults (for example, south of Nome). In central Norton Sound, small surficial craters, 3 to 8 m in diameter and less than 1 m in depth, attest to periodic disruption of widely distributed gas-charged sediments by sudden venting of biogenic gas from the underlying peaty mud.

K. A. Kvenvolden and G. D. Redden have investigated the type and distribution of the gas that forms a com-

mon but minor constituent in most near-surface sediments of Norton Sound. At eight sites, the methane content increases markedly downward within the first 4 m of sediment, indicative of a gas-charged condition and possible hazardous instability. The isotopic compositions of the methane measured at four sites substantiate production of the gas by microbial processes within the near-surface sediments. At one other site with seepage from the seafloor, the near-surface sediment is charged CO_2, accompanied by minor concentrations of gas- and gasoline-range hydrocarbons. The molecular composition of the hydrocarbons and isotopic composition of the methane suggest derivation from deep thermal processes. The source of these hydrocarbons may be an immature petroleumlike condensate of lower temperature origin than normal petroleum.

Seafloor erosion and deposition, northern Bering Sea

In addition to hazards that involve faulting and gas within sediments, C. H. Nelson and D. R. Thor suggest that sediment liquifaction, ice gouging, scouring, storm-sediment transport, and sand-wave movement must be considered in developing the potential resources of the northern Bering Sea. Liquifaction by cyclic storm-wave loading of the upper 1 to 2 m of coarse silt and fine sand that form the floor of Norton Sound may be common and not only may trigger gas cratering but may enhance a variety of other erosional and depositional processes as well.

Ice gouges that scour the sediment to depths of 1 m are abundant on the Yukon prodelta and, although less common, are present elsewhere throughout the northern Bering Sea where water depths are less than 20 m. In the Yukon prodelta area and central Norton Sound where shoal areas constrict circulation and local topographic irregularities (such as ice gouges) cause turbulence, storm-induced currents have scoured depressions that are 50 to 150 m in diameter and less than a meter in depth. Muds of the Yukon Delta have abundant storm-sand layers, reflecting the significant effect on the bottom of storm-surge activity, particularly around the prodelta where the surge and waves of storms have generated bottom currents that transport and deposit sand as far as 75 km from land. West of Port Clarence, sand waves with heights of 0.5 to 5 m and wave lengths of 10 to 200 m apparently move only at times when storm-surge currents reinforce strong geostrophic currents that flow continuously to the north over the Bering Shelf.

Faults of the southern Bering Sea margin

Using records obtained with several seismic systems, J. V. Gardner and T. L. Vallier have distinguished and mapped faults of three types in the St. George Basin area of the southern Bering Sea. Major faults, which appear on both multi- and single-channel records, generally penetrate to depths ranging from several hundred meters to several kilometers beneath the seafloor and, in some cases, have displacements exceeding 60 m; most are found along or near the border of the St. George Basin and trend northwest to southeast, parallel to the long axis of the basin. Surface faults generally connect to major faults, affect the seafloor, and are most abundant along boundaries of the St. George Basin. Minor faults, most of which have displacements of 5 m or less, are scattered throughout the area but are most numerous in the middle of the basin; almost all approach to within 4 or 5 m of the seafloor. The ages of faulting have not been determined precisely, but both surface and minor faults offset upper Pleistocene sediments.

Quaternary sedimentary facies of the northeast Gulf of Alaska Continental Shelf

Using seismic and sedimentologic data, B. F. Molnia and P. R. Carlson distinguish and describe four major sedimentary units that crop out on the northeastern Gulf of Alaska Continental Shelf: (1) Holocene glaciomarine sedimentary unit, (2) Holocene end moraine unit, (3) Pleistocene and Neoglacial glacial sedimentary unit, and (4) Pleistocene and older lithified sedimentary unit. Each of the units is the product of one or more aspects of glaciation and may be subdivided further into facies that reflect depositional environments and are representative of parts of the Quaternary glacial and glaciomarine depositional histories of the northeastern Gulf of Alaska.

The Holocene glaciomarine sedimentary unit contains glacially eroded and transported sediment that has been deposited in the marine environment through glaciofluvial, eolian, and ice-transport mechanisms. Lithologies range from unimodal clayey silts to bimodal pebbly silts and clays with much ice-rafted material. The end moraine unit, which includes deposits marking farthest penetration of piedmont and valley glaciers onto the shelf, has lithologies ranging from massive boulder and cobble accumulations to fine silts and clays of basins within lobes of the moraines. The Pleistocene-Neoglacial unit is the most variable of the four units with a range from multimodal ablation and lodgment tills, through recessional lacustrine and outwash facies, to marine pebbly muds. Postdepositional winnowing has added to the textural and compositional variety of this unit. The lithified unit, representing glacial and glaciomarine events that predate Holocene time, has lithologies that correspond to those of the other three units. Stratigraphic and paleontologic data for the four units suggest little change in depositional environments since mid-Miocene time, with glaciation providing the

primary control in the shaping of the late Tertiary and Quaternary depositional framework.

Distribution of benthic foraminifers, Gulf of Alaska Continental Shelf

P. J. Quinterno, P. R. Carlson, and B. F. Molnia have examined and interpreted the occurrences of benthic foraminifers from grab samples and cores collected on the Continental Shelf and slope between Montague Island and Yakutat Bay in the Gulf of Alaska. Robust specimens of *Cassidulina californica, C. Limbata,* and *Cibicides lobatulus* dominate a fauna of coarse sediments from Tarr Bank, the Middleton Island platform, and along much of the outer shelf east of Kayak Island. This fauna may be relict because it occurs in areas that are devoid of the Holocene clayey silt that blankets much of the shelf. In several samples, it has associated glauconite, which suggests low rates of sedimentation.

Elphidium clavatum, typically an inner-shelf species, is abundant in a number of samples from the seafloor beneath unusually deep water. The species is dominant in sand layers and rare in the clayey silt layers that dominate a gravity core from a water depth of 295 m in the Bering Trough. In general, the Holocene sand is restricted to the inner shelf, as is *E. clavatum*; their occurrence in association with the clayey silt beds is considered evidence of downslope displacement, possibly by slumping. High abundances (>10 percent) of the shallow-water *Elphidium* in Kayak Trough and Hinchinbrook Sea Valley, areas of known slumps and slides, are apparently another example of the result of displacement from shallow depths. Three samples, which have abundant *Elphidium* and were collected seaward of the Holocene clayey silt in water depths of 163 to 265 m, may represent sediment deposited at shallower depths during a lower sea level stage of the Pleistocene.

Neogene sedimentation, southern Bering Sea

Samples of Neogene sedimentary rocks and sediments from the Alaska Peninsula and outer continental margin of the southern Bering Sea have little felsic material indicative of mainland sources but instead are dominated by volcanic components that probably were eroded from an emergent Aleutian Ridge. Based on this and other information concerning the rocks and their relations, T. L. Vallier, M. B. Underwood, J. V. Gardner, and J. A. Barron conclude that longshore currents, debris flows, and turbidity currents transported most sediments to depositional sites during times when sea level was low and the shore was near the outer margin of the shelf. They ascribe the fluctuations in sea level to a combination of worldwide glacioeustatic and regional tectonic effects. Large rivers, such as the Yukon and Kuskokwim, apparently had little direct influence on sedimentation along the continental slope and the Unmak Plateau in the southern Bering Sea. Instead, sediments from the rivers probably were delivered to the Aleutian Basin, to numerous basins that now underlie the Continental Shelf, and through the Bering Strait to the Arctic Ocean. Other than emergence of the Alaska Peninsula, depositional environments along the outer continental margin have not changed significantly since the middle Miocene time.

CONTINENTAL MARGIN GEOLOGIC FRAMEWORK AND RESOURCE STUDIES

The ocean-continent transition zone off the New Jersey coast

Continuing improvements in instrumentation and techniques for collecting and processing multichannel seismic reflection data are adding detail and clarity to an understanding of the Nation's continental margins. Additional samples, information from drill holes, and other geophysical methods are contributing to improved resource assessments. New knowledge of deep sedimentary and basement structures derived from an analysis of a recently acquired 48-channel seismic profile (USGS Line 25) provides an example. The profile extends 330 km southeastward from the New Jersey coast and crosses the widest and deepest part of the Baltimore Canyon Trough, as well as the ocean-continent transition zone.

Off the coast of New Jersey, the sedimentary wedge thickens from 5 km nearshore to 17 km just landward of the East Coast Magnetic Anomaly (ECMA), a geophysical feature that has become an established line of reference on the Atlantic continental margin. The ECMA lies 20 km landward of the shelf edge along the line of the seismic profile. A strong flat reflector that lies at a depth of 14 km and has a width of about 10 km accords with the ECMA. Over the next 40 km southeastward, the acoustic basement becomes obscure and appears to rise to a depth of 5 km beneath a Jurassic–Lower Cretaceous carbonate shelf-edge complex that extends 20 km seaward of the present shelf edge. Landward-dipping continental rise sediments exist to a depth of at least 13 km beyond the Jurassic shelf edge. The top of the oceanic basement becomes identifiable as a set of hyperbolic reflectors about 50 km seaward of the Jurassic shelf edge, where it lies at a depth of 11 km and dips gently landward. The prominent Middle Jurassic (J_3) horizon obscures it landward of this distance.

J. A. Grow, K. D. Klitgord, J. S. Schlee, and R. E. Mattick (1980) attribute features of the profile to

Jurassic and Early Cretaceous prograding of a carbonate reef complex to a distance of 40 km over oceanic crust. Differential subsidence and compaction of the basin west of the ECMA caused back tilting and arching of the shelf-edge deposits. The latter has created an anticline that is 20 km in width and has a 500-m closure beneath the upper continental slope. Other lines to the southwest indicate that the anticlinal arch extends southwestward at least 40 km. Similar "slope anticlines" have been reported off the coast of northwest Africa.

In another study of the region off the coast of New Jersey, Mattick has interpreted seismic data for the general vicinity of the Texaco natural gas discovery well in the Baltimore Canyon Trough. Here listric faults that may be products of diapirism (salt?) downslope offset beds beneath the shelf and, within the downthrown blocks, have rollover and lensing structures that could provide trapping reservoirs for oil and gas. He concludes that faulting associated with differential adjustments near continent-ocean boundaries is expectable and, therefore, may be common along the shelf edge and slope.

In a related study, Klitgord and Grow have mapped the extension onto the continental margin of fracture zones found within the Mesozoic magnetic anomalies of the deep seabed patterns to the east of the United States. At each of the intersections of the projected fracture zones and the ECMA, they found narrow zones of disturbed magnetics, suggesting an influence of the fracture zones and basement structure on formation and subsequent development of this narrow marginal zone and its resources. Klitgord and Grow were able to trace anomaly patterns of the northern Florida Paleozoic basement structures to the south offshore of northern Florida and, still further south, to follow seafloor fracture patterns across central and southern Florida to the Gulf of Mexico.

J. M. Robb has interpreted 600 km of high resolution seismic reflection profiles for a 10 km by 30 km area on the continental slope between Carteret and Lindenkohl Canyons, southeast of New Jersey, to determine the contribution of turbidite currents, mass movement, erosion, and other processes to development of the complex morphology and structures of the surficial Tertiary and Quaternary deposits. Here more than 300 m of Pleistocene sediments at the top of the continental slope thin seaward to less than 10 m beneath water depths of 1,000 m. Further downslope, the upper rise has thick masses of Pleistocene materials. The upper slope provides evidence for shallow slumping within the Pleistocene deposits, but more generally the mid- and upper-slope topography seems to reflect a complex of leveed depositional channels produced by Pleistocene turbidity currents. Cut-and-fill structures also can be distinguished in the profiles. At water depths greater than 1,000 m, a sequence of Miocene delta-front deposits crop out, and, at still greater depths, exposed Eocene to Miocene sediments are faulted and eroded.

R. E. Miller, D. M. Schultz, G. E. Claypool, and M. A. Smith have examined the organic components of samples from potential petroleum source rocks penetrated by the second stratigraphic test well (COST No. B–3) drilled near the outer edge of the shelf off New Jersey. Organic richness of the Tertiary, the Upper and Lower Cretaceous, and the Upper Jurassic, as determined by the weight percent of total organic carbon is 1.52, 0.83, 0.71, and 1.09, respectively. The Tertiary samples contain dominant marine algal hydrogen-rich kerogens, and the pre-Tertiary have predominant hydrogen-poor humic gas-prone kerogens. The ratios of hydrocarbon both to organic carbon and to total extractable organic matter increase with depth. A kerogen thermal alteration value of 2.0 and vitrinite reflectance value of R_o 0.48 percent at depths below 4,360 m apparently indicate conditions favorable to thermal maturation of the indigenous organic matter. An increase in C_1 to C_4 light hydrocarbon concentrations that correlates with a change toward a more mature character in the C_{15}^+ liquid-saturated paraffin-naphthene hydrocarbon gas chromatogram also suggests ongoing thermal maturation. A geologically significant concentration of 27.583 ppm methane with a gas wetness of 19 percent is present at a depth of 4,540 m. Gas recovered from this depth to the bottom of the well at 4,755 m may have migrated updip to present sites from a source in Jurassic sediments that lie seaward of the well site and are more deeply buried and thermally mature.

Continental slope stratigraphy of Texas and Louisiana

R. G. Martin, Jr., has identified many lobelike tongues of Middle and Upper Jurassic Louann Salt overlying strata as young as early Pleistocene on single- and multichannel seismic reflection profiles across the Sigsbee Escarpment at the foot of the continental slope off Texas and Louisiana. Along the escarpment, the salt tongues are thin enough to allow recording of seismic sound waves that have penetrated and been reflected from strata beneath the salt. Martin has succeeded in correlating these subsalt reflections with reflectors in adjacent continental rise and abyssal plain sequences that, in turn, can be identified with stratigraphic tops interpreted from drill holes in the abyssal plain. Subsalt reflections that approximate the tops of Miocene and Pliocene strata seem to be truncated by the nearly horizontal to northward-dipping interface at the base of the separate salt tongues. This angular relation between the base of the salt and continental rise layers can be

traced to distances of as much as 15 km into and beneath the continental slope. Pleistocene sediments both overlie and underlie the soft tongues along the escarpment.

The nature of the complex mechanism for emplacing the Jurassic Louann above the Tertiary and Quaternary strata is not entirely clear. Martin considers the salt tongues to be products of lateral flowage that probably took place as the Tertiary and Quaternary sediments were being deposited. Their leading edges may never have been more deeply buried than at present. The flowage can be compared to that of pressing bread dough (salt) with a rolling pin (prograding sediment load) and theoretically could have begun at any time between Late Jurassic and late Miocene time. Lacking sufficient seismic penetration to resolve fully the associated questions concerning amounts of flowage, shapes of the salt mass at depth, and relations to pre-upper Miocene strata, Martin proposes three likely models for the origin of the salt tongues: (1) they represent the leading edges of a Louann Salt mass that has been flowing laterally, as well as vertically, to form diapirs since the beginning of postsalt prograding sedimentation along the northern Gulf margin, (2) they constitute lobate overhangs and sills of deeply rooted salt ridges and massifs that have been introduced into the slope-rise sediments contemporaneously with deposition since late Miocene time, and (3) they are the overflow edges of a deep fault-bounded salt basin beneath the middle and lower continental slope and have been mobilized by rapid sediment loading since middle Tertiary time.

The Jurassic Louann tongues have an estimated subsurface areal extent of as much as 30,000 km^2 beneath the lower Texas-Louisiana slope. Impervious to hydrocarbon migration, the nearly horizontal to gently dipping contact between the salt and underlying turbidite-rich upper Tertiary and Quaternary sequence may provide a seal for petroleum reservoirs.

Tectonic framework of the Oregon continental margin

P. D. Snavely, Jr., H. C. Wagner, and D. L. Lander (1980) have integrated seismic reflection records with subsurface data from the offshore Standard-Union Nautilus deep-test well and with other onshore and marine data to construct a geologic cross section of the central Oregon continental margin and have interpreted the results in terms of plate interactions. The principal feature of the interpretation is a low-angle east-dipping megathrust along which the Pacific plate is underthrusting the North American plate, of which the Oregon continental margin constitutes a part of the leading edge. Zones of major upper plate crustal movement across the margin are uplift and compression along the continental slope and outer shelf expressed by broad folds and by an imbricate set of landward dipping thrust faults, subsidence of a nearshore marginal basin, and uplift of the Coast Range. Snavely, Wagner, and Lander attribute the zones and associated structures to molding by episodic periods of underthrusting, transcurrent faulting, and extension.

Rock units of the eastern Gulf of Alaska Outer Continental Shelf

Forty-two samples dredged from outcrops and suspected outcrops at depths of 3,150 to 200 m along the 250-km northwest-trending segment of the continental slope off Yakutat, Alaska (long 138° W. to 142°30′ W.), provide added control for interpreting the geology along the seaward margin of a Tertiary basin that underlies the adjacent shelf. Plafker, Winkler, and Claypool note striking differences among the lithologies and structures of the lower Tertiary sequence sampled on the continental slope, those of coeval rocks exposed onshore, and those of the succession of rocks penetrated in the unsuccessful exploratory wells drilled on the Yakataga segment of the OCS to the west. The samples of the Eocene and Oligocene units include abundant source rocks with organic components that reflect a thermal history of locally generated hydrocarbons. Most sandstones, obtained by dredging on the continental slope, have poor reservoir qualities, but friable sandstones from the Eocene to lower Oligocene rocks indicate probable local porosities to 31 percent and permeabilities to 36 mD. On seismic reflection profiles, layers that may be identified with these porous units appear to dip beneath a proposed lease-sale area where they provide favorable exploration targets if suitable structural or stratigraphic traps can be identified.

Crustal structure of the Aleutian Trench–Amlia fracture zone intersection

The Amlia fracture zone, a prominent seafloor feature that has distinctive ridge-and-trough relief and traverses the north Pacific Ocean in a north-south direction along long 173° W., intersects the east-west trending Aleutian Trench at lat 51° N. To determine the nature of this intersection and the behavior of the Pacific crust where it is being subducted beneath the Aleutian Ridge, D. W. Scholl and T. L. Vallier conducted a detailed seismic reflection survey over the trench. Of particular interest was the sedimentary wedge of chiefly Pleistocene turbidite beds that form the floor of the trench, suspected to contain evidence for any breakup of the underlying Pacific crust. The outcome was a series of profiles on which disruptions of lateral continuity in the turbidite beds are limited to minor folds and faults. Most of these minor structures could be ascribed to differential compaction over basement relief, although, in some areas, they may be linked to faulted or offset oceanic crust. In the vicinity of the trench-fault zone intersection, the maximum thickness

of the sedimentary fill increases from about 2.4 to 3.3 km, an amount that may be related to depositional infilling of the central trough of the fault zone.

Although evidence for significant crustal fracturing along the Amlia fault zone is lacking in the vicinity of the trench, farther north an offset in the linear trend of the Aleutian volcanoes and the presence of two large (70 by 40 km) summit basins may be indicative of rupturing along the fault zone beneath the Aleutian Ridge.

In another study that includes testing the concepts of subduction and plate convergence along the Aleutian Trench, R. E. von Huene and M. A. Fisher note the presence of local uplift amounting to 3,000 m or more, normal and reverse faulting, and transverse structures adjacent to the Kodiak Shelf. Most of these structures cannot be explained by simple steady-state compressional tectonisms. Instead, any explanation must include extensive decoupling across the presumed subduction zone. The identification of coherent sections of sedimentary rocks along the margin is not consistent with the subduction concept and complex imbricate faulting and casts doubts on the assumption that convergent margins are not attractive for petroleum exploration.

Geologic framework and hydrocarbon prospects of the eastern Bering Sea

Based on their synthesis of information, M. S. Marlow and A. K. Cooper conclude that the large sediment-filled basins beneath the eastern Bering Sea provide encouraging prospects for discovery of hydrocarbon deposits. At least 13 sediment-filled basins underlie the 800,000-km^2 shelf area south of St. Lawrence Island. The southeasternmost, Bristol Bay Basin, extends offshore from the Alaska Peninsula and has more than 3 km of sediment. The nearby St. George Basin to the northwest is a graben approximately 30 km long and 50 km wide that contains a sedimentary section about 10 km thick. The large (40,000 km^2) Navarin Basin province, which includes three subbasins, underlies the northwestern part of the shelf near Siberia and has sections as much as 15 km thick.

The slope bounding the Bering Sea shelf has a length of 700 km between Cape Navarin, Siberia, and the Aleutian Islands, descends from depths of 200 m to as much as 3,400 m, and is incised by several large submarine canyons. On single- and multichannel seismic reflection profiles across the slope, Marlow and Cooper have measured sedimentary sections above acoustic basements ranging from 0 to 10 km in thickness. The thickest sections, 7 to 10 km, underlie the base of the slope at its northern and southern ends. The maximum thickness of 10 km (5.9-s two-way traveltime) was measured on a profile across an uplifted section of rise deposits beneath an 800-m water depth near the mouth of Zemchug Canyon, midway along the slope.

Marlow and Cooper cite several aspects of these sediment wedges that make them favorable targets for future petroleum exploration along the Bering Sea margin: (1) large total thickness of Cenozoic sediment, (2) presence of subsurface structures, such as diapirs, faults, warps, onlaps, and pinchouts, and (3) likely presence of organic-rich source rocks and coarse-grained detrital deposits to serve as reservoirs.

In support of the foregoing synthesis, Cooper, J. R. Childs, Marlow, and their associates constructed an isopach map (Marlow and others, 1979) and a total sediment thickness map (Cooper and others, 1979b), using seismic reflection profiles and velocity data obtained with sonobuoys. Sonobuoy data also were used to examine the sedimentary and deeper crustal structure of the Umnak Plateau, which rises from the Aleutian Basin on the north side of the Aleutian Islands and to the west of the southern Bering Sea shelf. The determined velocities indicate that oceanic crust, rather than continental crust, underlies the plateau and that uplift of the oceanic material must have occurred during early to middle Tertiary time because structures of the later sediments are undisturbed and have continuity (Childs and others, 1979; Cooper and others, 1979a).

Petrology of rocks from the Pribilof Islands region, southern Bering Sea shelf

F. L. Wong and T. L. Vallier have examined 36 samples of Pleistocene alkali basalt from lava flows on St. George and St. Paul Islands and from two dredge hauls near St. George. The basalts from St. Paul Island are younger and have a broader range of chemical compositions than those from St. George Island and the dredge hauls. The samples have normal alkali-basalt petrographies, with two containing identifiable nepheline. The major-element chemistry reflects the alkali affinities with 44 to 50 percent SiO_2, 3 to 8 percent combined Na_2O-K_2O, and a trend for values plotted on an alkali-iron-magnesia diagram similar to that of other oceanic alkali-basalt suites. The basalts are both hypersthane- and nepheline-normative, with all samples from St. Paul Island in the nepheline group. Rubidium-strontium ratios range from 0.014 to 0.062, and thorium-uranium ratios, from 0.96 to 7.90. Olivine phenocrysts have 54 to 87 mole percent forsterite, and the clinopyroxenes of some samples are titanitum-rich, with as much as 3.4 percent TiO_2. The alkalic affinities of these basalts are consistent with the extensional tectonic setting of the Bering Sea margin and probably indicate the lack of a direct relation between Pribilof Island volcanism and Aleutian Arc tectonism.

T. L. Vallier, M. B. Underwood, J. V. Gardner, and D. L. Jones have examined specimens of Upper Jurassic (Kimmeridgian) sandstone and siltstone dredged from a probable drowned terrace near St. George Island and conclude that they come from a unit that may be correlated with the upper part of the Naknek Formation of the Alaska Peninsula and with rocks sampled by dredging on the continental slope. The discovery extends the known regional distribution of Upper Jurassic rocks and suggests that they underlie much of the southern Bering Sea continental margin.

DEEP SEA GEOLOGY AND RESOURCES

Hydrothermal activity and massive sulfides on the East Pacific Rise

Recent discoveries of hot-water vents and associated deposition of massive sulfides at the crests of the mid-ocean ridges have attracted widespread attention because they offer potentially rewarding opportunities to obtain added insights on the formation of mineral deposits. The USGS has contributed to the discoveries through efforts devoted to the development of techniques for gathering seafloor data and studies of seafloor mineralization and through participation on cruises to obtain information about the East Pacific Rise near lat 21° N., off central Mexico. Geologic and geophysical data obtained on a 1976 cruise of the USGS *R/V Samuel P. Lee* to the mouth of the Gulf of California were fundamental to planning of studies with the submersible ALVIN. These studies resulted in the April 1979 discovery and subsequent examination of the most spectacular vents that have yet been found (RISE Project Group, 1980).

W. R. Normark participated in the 1979 deep-tow surveys that extended earlier detailed mapping of the East Pacific Rise axis 10 km southward and served as the dive area for the ALVIN. The volcanic and tectonic zonation established in earlier deep-tow surveys to the northeast by Normark (1976) applies to this new map area as well. It was in this new area, however, that the 25 active hydrothermal vents and associated massive sulfide mounds were found over an 8-km segment of the fresh volcanic axial zone. Sulfide-bearing water emerges from the vents at temperatures of 3°C to more than 360°C and has built mounds and chimneys of massive sulfide that support colonies of a variety of bizarre organisms, some of which were previously unknown (RISE Project Group, 1980).

Using data from studies of samples from the mounds and chimneys, J. L. Bischoff (1980) concluded that subsurface temperatures of the sulfide-bearing water are probably about 420°C and that precipitation of metal sulfides begins within a few hundred meters of the seafloor as the waters expand and cool. He and others of the group formed to study the samples from both the Galapagos and 21° N. localities recognize two types of deposits: a polymetallic sulfide-rich association of pyrite-marcasite, sphalerite, chalcopyrite, and anhydrite and an iron-rich hydroxide material composed chiefly of goethite and limonite that is considered a seafloor "weathering" product of the sulfides (Hekinian and others, 1980). Bulk-chemicals analyses of the sulfides indicate 30 to 40 percent sulfur, 1 to 50 percent zinc, 0.3 to 2.0 percent copper, and less than 11 percent silicon dioxide. Silver values of 290 to 480 ppm also were measured.

Compositional relations of manganese nodules and associated sediments

In continuing studies of manganese nodules, D. Z. Piper has found that the copper-manganese and nickel-manganese ratios of nodules vary inversely to those of the fraction of associated sediment that is soluble in a weak reducing acid. Thus, nodules with relatively high copper-manganese and nickel-manganese ratios are associated with sediments that have low ratios. The REE, particularly cerium, are partitioned similarly. A possible interpretation of these relations entails enrichment of the nodules in nickel, copper, and REE, relative to manganese, and depletion in the fine-grained sediment fraction during postdepositional diagenesis.

Organic carbon of seafloor middle Cretaceous limestones

Middle Cretaceous limestones containing as much as 10 percent organic carbon were cored at two sites on southern Hess Rise and at one site in the Mid-Pacific Mountains, central North Pacific Ocean, during Leg 62 of the Deep Sea Drilling Project (Dean and others, 1979; Thiede and others, 1979). The carbonaceous limestone of the Mid-Pacific Mountains is associated with volcanic ash of early Aptian Age (ca. 110 m.y.–115 m.y. B.P.), a time when the site was south of the equator and shallower than at present (2,525 m). The beds of organic-rich limestone, implying deposition in an oxygen-deficient environment, are intercalated with normal pelagic limestones, overlie interbedded pelagic and clastic limestones containing locally derived shallow-water carbonate debris, and underlie cyclic interbeds of green, gray, and pink limestones. The organic-rich strata on southern Hess Rise are dark-olive laminated limestones with rare interbeds of altered volcanic ash of late Aptian to early Cenomanian Age (ca. 100 m.y. B.P.), a time when the site was passing under the equatorial high productivity zone and subsiding from shallow to intermediate water depths. The association of volcanogenic sediments with organic-rich strata on Hess Rise is not as striking as in the Mid-Pacific Mountains,

but the occurrences do suggest a coincidence of midplate volcanic activity and accumulation of organic matter at intermediate water depths in the tropical North Pacific during the middle Cretaceous.

Pyrolysis assay results indicate that lipid-rich kerogen from aquatic marine organisms composes most organic matter in the limestone on Hess Rise. Limestones from the Mid-Pacific Mountains contain considerably lower concentrations of organic carbon (maximum near 4 percent), making interpretation of pyrolysis results more tenuous. However, these limestones tend to have low ratios of pyrolytic hydrocarbons to organic carbon and low hydrogen indexes, suggesting that the organic matter may have a significant proportion of land-derived humic-rich material, probably from volcanic islands that must have existed when the site was shallower.

The organic-rich anoxic sediments of middle Cretaceous age on Hess Rise and in the Mid-Pacific Mountains are equivalent in age to organic-rich lithofacies elsewhere in the world oceans, particularly the Atlantic and Indian Oceans. However, strata of equivalent age in the Pacific Ocean deposited at greater depths are not organic rich. This shallower depth and proximity to the equator during the middle Cretaceous suggest that an expanded midwater oxygen minimum may have resulted in the preservation of organic matter in an anoxic or near-anoxic environment where it impinged on rises such as Hess Rise and the Mid-Pacific Mountains.

Submarine fans

In their continuing study of depositional features of submarine fans as mineral-resource habitats, W. R. Normark and G. R. Hess have examined the Laurentian fan south of Newfoundland, Canada. Here large leveed valleys with relief as great as 800 m dominate the upper fan. Internal levee structures generally consist of parallel-bedded sediments providing reflectors that extend continuously for tens of kilometers but are interrupted locally where slumping has disrupted the near-surface layers. The levees prograde across a low relief fan surface and appear similar to depositional lobes that extend from terminations of the valleys on the midfan.

In comparing the Laurentian with other modern submarine fans, Normark and Hess note that the depositional lobes have many distinct features. Channelized suprafan deposits cover tens of square kilometers on the smaller fans, and these in turn include small (1-km-wide) smooth lobes that emanate from individual distributary channels. Large fans, such as the Monterey fan off California, have extensive depositional lobes that may be intermediate in character between the suprafan features and the "lower fan" sand lobes that have been identified within ancient turbidite deposits.

COASTAL AND LIMNOLOGICAL STUDIES

Investigations and mapping of insular shelves

J. V. A. Trumbull reports that marine geologic mapping of the Puerto Rico shelf, conducted in cooperation with the Puerto Rico Department of Natural Resources, led to discovery during 1979 of the island's most promising offshore sand deposit. Seismic reflection records and sedimentologic data permitted delineation of a 7.5-km^2 area in which the deposit has an average thickness of about 5 m, is of excellent quality, and appears to be minable with minimum detrimental effects on the environment. This deposit represents a 10-yr supply for Puerto Rico's construction industry and is only one of many that are now being investigated.

Trumbull also reports that two 1979 hurricanes (David and Frederic) resulted in floods that carried river-derived sand, silt, and clay onto the insular shelf of Puerto Rico and deposited them as a blanket. Diving and sampling immediately after the storms confirmed the presence of presumably temporary deposits of mud with an extremely high water content in contact with well-sorted sand in depressions on the inner shelf and unusually close in on the outer shelf. In addition, fresh river sands had been deposited over older sands of other origins. Periodic observations of selected sites are underway to verify anticipated brief residence times for the flood deposits and probable retention of some of the sand on the shelf.

C. W. Holmes has collected and analyzed surface and core samples of sediments on the southern shelf of the U.S. Virgin Islands to determine the origin of the carbonate sands and to relate their origin to environmental processes. Results indicate that in situ biogenic processes of calcareous algae and mollusks have produced most of the sand and that zonation of the dominant sand producers has been related to an environmental settling like that of the present in which water depth has greatest influence. Carbon-14 dates and faunal analyses of cores as long as 5 m provide accumulation rates of slightly less that 1 mm/yr in areas of the thickest sands and indicate a climate similar to that of the last 5,000 yr. Changes in environmental conditions apparently were limited to an increase in water depths and concurrent shifts in patterns of water movement. Within sediments deposited about 1,500 yr ago, the disappearance of the subtidal barnacle *Balanus venustus* can probably be attributed to a rise in sea level, with loss of a previously protected lagoonal environment for the barnacles. In addition, a gradual increase in the amount of coralline algae is probably in response to greater circulation within formerly quiet waters on the lee side of offshore islands.

Coastal sedimentary processes off beaches

In one of a number of investigations that aim at gaining greater insight into the nature of the high energy environment of beaches, H. J. Knebel has acquired fathometer and side-scan sonar records in shallow waters off Nauset Beach, on the east coast of Cape Cod, Mass. The records reveal ubiquitous channels that have relief of 1 to 3 m, trend northeast, intersect the north-trending beach at an average angle of 56°, and have rippled bottoms that contrast with the smooth interchannel areas. The channels apparently are formed by rip currents that also have eroded the shoreface.

On the west coast, J. R. Dingler has devoted particular attention to the unusually stable profile of Monastery Beach to the south of Monterey Bay, Calif. The beach lies less than 200 m from the terminus of the Carmel Submarine Canyon, at a water depth of approximately 15 m. Surficial sediment on the beach and adjacent shelf is very coarse sand to fine gravels. The beach face is steep (approximately 10°), and the adjacent seafloor has large oscillation ripples.

Most Pacific coast beaches exposed to a wide range of wave climates have profiles that change through the year in response to storms and swell. In contrast, Monastery Beach has maintained the same swell profile for more than 2 yr. This may be attributed to large grain size of the sediment, which apparently controls the profile in two ways—the higher threshold of wave energy needed to initiate a switch in profile and the presence of the large offshore oscillation ripples that prevent nearshore sediment from being deposited on the beach during intervals of generally low energy swell conditions.

To measure and plot changing beach profiles elsewhere, A. H. Sallenger, Jr., has developed an instrumented sled that may be winched across the beach face and adjacent nearshore areas to distances of as much as 300 m from shore. The system was operated successfully during field tests at Monterey Bay at a time when breaking swell waves exceeded 6 m in height and bottom currents were greater than 3.5 m/s. During this event, a surf-zone profile 100 m across was eroded an average of 0.3 m.

Shallow shelf and beach heavy-mineral concentrations

R. L. Phillips has collected oriented cores at depths of 12 to 18 m from Estero Bay, Calif., to document the presence of summer and winter deposits and heavy-mineral concentrations in shallow shelf areas. The upper 20 cm of the cores is intensely bioturbated, reflecting a summer dominance of biological processes. The remainder of the cores contains numerous horizontal laminations that have high percentages of heavy minerals, resemble beach swash-zone heavy-mineral laminae, and apparently are produced by high-energy storm waves. Heavy-mineral contents increase seaward to 13.3 percent in the seawardmost core. Comparable concentrations are to be expected within other areas of the Continental Shelf subject to storm-wave reworking.

In studies of coastal deposits of Oregon and Washington adjacent to the mouth of the Columbia River, Gretchen Luepke finds that the weight percentage of heavy minerals is generally higher in dune samples than beach samples. The mean grain sizes of heavy minerals from the two environments do not appear to differ significantly, leading Luepke to suggest probable selective transport of the heavy-mineral grains from the beach to the dunes by wind.

Migration of Oregon coastal dunes

The large oblique dunes of the Oregon coast have generally been thought to have remained essentially stationary for a period of years as a consequence of offsetting effects of northwest summer winds and southwest winter winds. However, T. R. Alpha and R. E. Hunter report that aerial photographs taken in 1939, 1954, and 1975 provide evidence for northward movement of the dunes at an average rate of 4.5 m/yr. Evidently, the greater strength of the winter storm winds allows them to carry more sand than the summer winds, despite heavy rains accompanying the winter storms and very dry weather during the summers. Comparison of the photographs also gives evidence of a general eastward shift of the dune field and expansion to both the north and the south under the combined influence of summer and winter winds.

The Laguna Madre Flats, southern Texas

Lying within the driest part of the Gulf of Mexico coast, bisected by the Intracoastal Waterway, and having a nearly equidimensional area of approximately 500 km^2, the Laguna Madre Flats provide a distinctive hydrological, sedimentological, and geochemical tidal-flat environment. To obtain additional data about this environment, C. W. Holmes established 18 environmental monitoring sites along a 17-km east-west traverse across the flats. At each site, he and his associates sank wells to depths of 1.9 and 3.8 m, dug a shallow trench, obtained a 2- to 3-m sediment core, measured water depths within the wells and trench, and determined selected water properties. Among preliminary results, Holmes reports the identification of differing hydrologies within the subsurface water system on either side of the Intracoastal Waterway, the measurement of salinities ranging from 59,500 to 178,000 ppm, and evidence that some local geochemical processes remain similar to those that operated prior to construction

of the Intracoastal Waterway, despite changes in the hydrology of the system. Among the effects, construction of the waterway probably has caused some general modifications in the chemistry of the subsurface waters, such as the more reducing nature of the water on the landward side of the waterway.

Subsurface hypersaline brines

F. T. Manheim has examined interstitial water within samples from deep scientific boreholes drilled in the Georgia coastal zone and offshore on the Continental Shelf. These waters and, by interpretation of electric logs, those penetrated by oil industry wells have increasing total salt with depth. Deep hypersaline brine zones form limits for meteoric water penetration and, on land, have been suggested as potential waste storage sites. They are linked to buried evaporite deposits of Paleocene and Late Cretaceous(?) age.

Interdisciplinary study of the Potomac River Estuary

As a contribution to a broad interdisciplinary study of the Potomac River Estuary, H. J. Knebel has collected and examined high-resolution seismic profiles that depict marked differences in the sediments of the various reaches. Outcrops of hard substrata and sediment with interstitial gas characterize the upper and middle reaches of the estuary, whereas a relatively thick section of Holocene sediments obscures the configuration of the upper Pleistocene sequence, including ancestral channels of the Potomac River beneath the lower reaches.

E. A. Martin examined 17 undisturbed sediment cores from sites considered representative of the riverine, transitional, and estuarine zones of the Potomac River system between Washington, D.C., and the Chesapeake Bay to determine sedimentation rates and the stratigraphic distribution of selected trace elements. X-radiographs were made of each core to assess intensities of bioturbation, presence of shell fragment concentrations, major discontinuities in structure, and other factors that may be detrimental to the radiometric determination of sedimentation rates. Suitable cores were subsampled at 2-cm intervals for ^{210}Pb activity and for atomic absorption analyses of selected trace metals (Pb, Cd, Cu, Zn, Mn, and Fe). The ^{210}Pb sedimentation rates range from 0.16 to 4.6 cm/yr; highest rates were found in the riverine and transition zones and lowest where the Potomac River enters the Chesapeake Bay. Iron and manganese concentrations do not fluctuate significantly with depth. The concentrations of Pb, Zn, Cu, and Cd, however, increase upward in sediments deposited from about 1890 to present and are enriched from 2 to 10 times over the background levels provided by subsamples from lower in the cores. Because heavy industry does not exist along the Potomac, the increases can probably be ascribed to growth of the Washington, D.C., metropolitan area, with the presence of lead reflecting its use as an antiknock additive in automotive gasoline during the past 50 yr.

Correlation of trace elements between sediments and benthic fauna

G. W. Hill has found a positive correlation between trace-metal concentrations in benthic polychaetes (marine worms) and their host sediments on the seafloor off Port Aransas, Tex. The concentrations tend to be higher and the correlations better in deposit feeders (for example, *Nereis*) than in filter feeders (for example, *Dipatra*). Relative amounts of copper and lead are higher in *Nereis* and *Dipatra* than in the sediment. Zinc has a comparatively poor organism-sediment relationship in deposit feeders and apparently none in the filter feeders. Overall, the amounts of trace metals in the benthic polychaetes are several times those of the host sediments.

Lake sediments

Marine geological and geophysical techniques, including high-resolution seismic reflection profiling, were applied to USGS studies of three large well-known lakes during 1979—Lake George, eastern New York, Lake Ontario, northwestern New York, and Crater Lake, Oreg. At Lake George, H. J. Knebel obtained and examined profiles and sediment cores that show that unconsolidated sediments in the southern arm of the lake have a maximum thickness of 100 m and consist of sand and gravel, varved clay, and an organic mud. Three deep bedrock basins beneath the lake have controlled late Quaternary deposition. For eastern Lake Ontario, Knebel has used profiles and sedimentary data to outline the distribution of modern-lake, glacial-lake, and glacial-till deposits. The nature and distribution of these three types of deposits confirm a hypothesized low-water level within the lake following disintegration of the glacial ice dam within the St. Lawrence River.

At Crater Lake, C. H. Nelson and D. R. Thor undertook a geophysical survey to obtain added information on the volcanic lake's history, heat-flow characteristics, and sediments. Since formation of this lake about 7,000 yr ago, sediment from the caldera walls has entered the closed basin at a very high rate, thereby providing an opportunity to study turbidite facies of rapid density-current deposition in a restricted basin setting. Three centers of deposition exist—a northern, an eastern, and a southern. The eastern center is largest, containing an 80-m section of sedimentary fill. On the basis of their

seismic profiles, Nelson and Thor conclude that the coarsest sediment and thickest gravity flow deposits are closest to the caldera walls and that bedding becomes thinner and textures finer toward the center of the basin. They interpret this distribution to reflect deposition by debris flows near the caldera walls and unchanneled turbidity-current deposition from sheet flows farther from the walls. Faults within the sediments, including offset surfaces, are attributed to geothermal and other continuing volcanic activity.

Sacramento–San Joaquin Delta wetlands, San Francisco Bay, California

The topography and vegetation of the freshwater tidal wetlands reflect the preponderance of Sacramento River discharge across the combined Sacramento–San Joaquin Delta. Near distributaries of the Sacramento River, the wetlands have natural tree-covered levees that resemble upland riparian forests. In contrast, near distributaries of the San Joaquin, the wetlands lack natural levees and support an irregular patchwork of herbaceous and woody plants. Together, the wetlands contain three or four species of angiosperms that are regarded as rare and endangered and are not found within tidal wetlands west of Suisun Bay.

ESTUARINE AND COASTAL HYDROLOGY

ATLANTIC AND GULF COAST

Shallow stratigraphy of the Potomac River Estuary

H. J. Knebel and his coworkers have obtained fathometer, side-scan sonar, and seismic-reflection profiles during cross-channel and along-channel transects that were run from the Washington, D.C., metropolitan area downstream to Chesapeake Bay. The profiles outline the general environmental framework of the Potomac River Estuary. In the upper and middle reaches of the estuary, the profiles show outcrops of hard substrata along the channel margins, areas with unconsolidated sediments containing interstitial gas, and manmade dredged channels. In the lower estuary the records reveal the configuration of the pre-Holocene substrata, the thickness of the Holocene sedimentary fill, the buried channels of the ancestral Potomac River, and the change in texture from the marginal terraces (sand) to the main channel (mud). These data, when used in conjunction with previous sediment samples, will provide considerable insight into the sources, pathways, and sinks of sediments and pollutants that may be introduced into the river.

Variations in nutrient and sediment concentrations in the Potomac River Estuary

J. L. Glenn determined concentrations of sediments and selected nutrients in dissolved and sediment phases in water and suspended-sediment samples collected hourly over partial tidal cycles at verticals in cross sections near Alexandria and Quantico, Va. At Quantico, dissolved nutrients (total dissolved nitrogen; nitrite + nitrate nitrogen, NO_2+NO_3; total dissolved phosphorus, TDP; silica, SiO_2) varied only slightly and usually with no discernible pattern. NO_2+NO_3 and SiO_2 at all verticals, however, showed concentration maxima during early morning and late afternoon low water (low slack). Only NO_2+NO_3 varied within the cross section, being consistently lower at a right side vertical than at center and left side verticals. Dissolved nutrients at Alexandria varied more than at Quantico, but patterns of variations generally were unrelated to stage or current variations. Concentrations of dissolved nutrients at Alexandria were two to five times greater than concentrations at Quantico. Both TDP and SiO_2 were higher at a vertical on the left side of the channel than at a vertical on the right side.

Concentrations of sediments and nutrients associated with sediments (total sediment nitrogen, TSN; total sediment phosphorus, TSP) varied greatly at Quantico. Sediment concentration maxima at all verticals coincided with velocity maxima; ebb velocities, although comparable to flood velocities, consistently were accompanied by higher sediment concentrations. TSN and TSP trends were generally similar and were usually directly, for TSP, or inversely, for TSN, related to trends in sediment concentrations. Sediment concentrations at Alexandria varied in phase with current velocities but were higher for flood than for ebb currents. TSN and TSP fluctuated greatly in generally similar patterns that usually crudely followed patterns of variations in sediment concentration. Sediment concentrations at Alexandria and Quantico were similar, but nutrient concentrations in the sediment phase were generally lower at Alexandria than at Quantico.

Geochemistry of sediments and associated interstitial waters for the tidal Potomac River

D. L. Parkhurst and Edward Callender have begun a study of the interstitial water chemistry of Potomac sediments. The aim of the project is to determine the processes in the sediment that affect nutrient regeneration and exchange with the overlying river water. During two major cruises, core samples were collected from 30 locations in the tidal river and estuary. Each core was analyzed at 10 depth intervals for NH_4^+, PO_3^{-3}, Si, alkalinity, pH, Eh, Cl^-, SO_4^{-2}, S^{-2}, Fe, Mn, Ca^{+2}, Mg^{+2},

Na^+, and K^+. From these data it is possible to calculate regenerative fluxes by means of Fickian diffusion. These preliminary estimates of fluxes indicate that the bottom is a significant source of ammonia but only a minor contributor of phosphate.

The primary geochemical process in the sediments throughout the river and estuary is the breakdown of organic matter (OM). Near the mouth, there is considerable seasonal variation in the rate of decompostion of OM. Summer and fall nutrient profiles have much steeper gradients than winter profiles, indicating greater fluxes into the estuary at these times at the mixing zone. In the Maryland Point area, there is considerable benthic activity, which can greatly increase the regenerative flux of nutrients. Calculated fluxes probably grossly underestimate actual regeneration in this region. In the freshwater area near Mount Vernon, the absence of SO_4^{-2} and O_2 means that OM must break down anaerobically. Substantial amounts of methane probably are produced here.

The data indicate that several mineralogical processes are involved in the various reaches of the river. At the mouth, concentrations of iron are kept very low by the presence of sulfide. In freshwater and throughout the mixing zone, phosphate concentrations are low due to the high iron concentrations. Finally, there are indications that calcite may affect the carbonate concentrations in the freshwater zone.

Seasonal distributions of oxygen, carbon, nitrogen, and silicon in the Potomac River

Studies by D. H. Peterson and his coworkers have shown that high winter flows of the upper Potomac River are clearly a major source of oxygen, carbon, nitrogen, and silica (OCNSi) to the downstream tidal regime. Time variations in the upstream concentrations of these substances (for example, due to a storm event) are reflected in their downstream distributions, and estimates of the magnitudes of these river inputs (from OCNSi concentrations and river flows) appear large in comparison to estimates of other sources.

Dissolved nitrate and silica concentrations during winter in the river upstream of Washington, D.C., for example, are both on the order of 100 μg-at/L). This represents approximately 260t/d, using a typical winter flow of 500 m^3/s. Similarly, for an area of 3.8 by 10^6 m^2, approximately the downstream region from Chain Bridge to Maryland Point, this source is equivalent to 10 mg-at/m^2/d.

In contrast to the situation in winter, identifying major OCNSi sources and sinks in summer is complex. For example, summer river flow is on the order of 50 m^3/s. Furthermore, nitrate and silica concentrations are typically less than 25 μg-at/L. Making the same calculation as above for winter, the river supply is only 0.3 mg-at/m^2/d. To put this into perspective, using nitrogen as a measure of waste source, the Blue Plains sewage plant accounts for 3 mg-at/m^2/d, and summer phytoplankton-nitrogen assimilation averaged 24 h over the photic depth accounts for 5 mg-at/m^2/d. Preliminary estimates of benthic and atmospheric exchange rates (of OCNSi where appropriate) further indicate that these sources and sinks may exceed the magnitude of river sources during summer.

The typical condition of weak river flow during late summer, when water residence- or replacement-time of the tidal regime is very long (months), magnifies the importance of other sources and sinks. Preliminary results suggest there is another more subtle, but potentially important, phenomenon related to the weak summer river flows. During the dry late summer of 1977, dissolved silica concentrations were not maintained above concentrations that would be limiting for diatom growth. Diatoms were found to be relatively scarce, as is apparently typical. However, during the wet late summer of 1978, silica concentrations were considerably higher, and diatoms appeared to be more abundant. Such a covariation also is suggested by the seasonality in dissolved silica and, presumably, diatom abundance. This may be critical because diatoms are a primary food source.

Benthic fauna studies of the tidal Potomac River

R. L. Cory and P. V. Dresler are investigating seasonal and spatial variability of benthic fauna by determining species distribution and individual numbers of benthic fauna sampled from 59 stations located in 7 transects between Piney Point and Wilson Bridge and 10 stations in the Wicomico. The program is designed to enable assessments of estuary health by studying the benthic fauna assemblages related to changes in various environmental factors such as salinity, sediment type, and water quality.

The stations have been sampled during November 1977 and April, August, and November 1978. A total of six samples will complete the triennial data set for 2 yr. During November 1977, the average number of animals per square meter per transect varied from 350 per square meter near the mouth to 5,659 per square meter in the transition zone. Uneven distribution of the animals was observed at each transect area; in one, the total numbers per square meter ranged from 37 to 597.

Of over 50 species collected, an average of 20 species was identified from each transect area with a range of 18 to 25 species per transect. The greatest number of species was found at the middle of the transition zone. A definite transition in group numerical dominance can be seen as one progresses upriver. In the estuary, marine

annelid worms constituted 75 percent of the population, and mollusks, about 20 percent. In the transition zone, amphipod crustaceans made up about 25 percent of the population, with marine worms constituting about 50 percent. In the tidal river, oligochaetes and insect larva constituted 70 percent and crustaceans 25 percent. Representatives of all four groups were found in each of the transect areas.

Wetland studies of the Potomac River Estuary

As part of the interdisciplinary Potomac River Estuary study, V. P. Carter and coworkers documented the distribution and abundance of submersed aquatic vegetation in the Potomac River Estuary and tidal river during the 1978 and 1979 growing seasons. Systematic sampling revealed no vegetation in the fresh tidal river and its tributaries, 13 species of plants in the oligohaline and low mesohaline reaches of the estuary, and very low plant diversity and abundance in the higher salinity water of the lower estuary. This vegetation distribution differs considerably from the historic distribution in the tidal Potomac. It is theorized that heavy nutrient loading may be causing an imbalance in the traditional phytoplankton–submersed aquatic plant relation. As a result, plants overburdened with epiphytes have reduced photosynthetic efficiency and do not survive. However, because many other factors have been implicated in the decline of submersed aquatic vegetation throughout the Chesapeake Bay area, all water quality, sediment, and transport data collected by the Potomac River Estuary study are being analyzed for possible effects on plant distribution.

Appearance and water quality of turbidity plumes in Tampa Bay, Florida

Dredging to widen and deepen the main ship channel serving the Port of Tampa, Fla., began in early 1977, has continued on a relatively uninterrupted basis through 1979, and is expected to be completed within the next 2 or 3 yr. When it is finished, approximately 54 million m^3 of bay bottom sediments will have been removed from the channel and deposited in emergent and submergent areas within or adjacent to the bay.

Considerable concern has been expressed by various Federal, State, and local agencies, as well as by knowledgeable citizens, over the present and future environmentally damaging effects of the dredging project. The concern is amplified because of the magnitude of the project (largest of its type in the country), the size of one of the hydraulic dredges doing the work (largest in the world), and the importance of the Tampa Bay Estuary as a major nursery, breeding ground, and food source for many or most of the marine aquatic plants and animals inhabiting the central west coast area of peninsular Florida. One subject of particular concern is the appearance and water quality of turbidity plumes generated in Tampa Bay as a result of dredging operations.

A study undertaken by C. R. Goodwin has addressed the turbidity-plume issue by simultaneous water-quality sampling and aerial photography on a monthly basis to document the appearance and the quality of water directly affected by discharge of very fine sediment particles. Plume appearance was extremely variable, depending on factors such as type of material dredged, size and type of dredge plant, method of disposal, method of containment after disposal, and tidal conditions prior to and during the time of plume observation. Primary plume dimensions varied from <100 m to several kilometers primarily due to different tide conditions.

Plume intensity, measured by the concentration of sediment suspended in the water, varied from 8 mg/L near the water surface, in an area having a low percentage of fine material in the dredged sediment, to over 200,000 mg/L near the bay bottom, where dredged sediment was composed primarily of silt. Potential nutrient, metal, and pesticide contaminants associated with some of the dredged sediment tended to stay bound to the particles even after being dislodged and severely agitated by the dredging process.

Of 18 pesticides analyzed, only the pesticide 2, 4–D was detected at any time during the study. The mean concentration of 2, 4–D found within the plumes, however, was not statistically significantly different from the mean concentration found in the background (control) samples taken outside the plumes. Of 10 metals analyzed, only particulate iron showed a statistically significant general concentration elevation in the plumes. No statistically significant concentration elevation in the plumes was found for any nitrogen or phosphorus compound. In fact, phosphorus showed a consistent, though not significant, trend to a higher mean concentration in the background rather than in the plumes samples. This may indicate that sediment particles actively remove phosphorus from the waters of Tampa Bay.

Tampa Bay–Floridan aquifer interconnection study

A hydrologic investigation of the direction, quantity, and quality of interflow between Tampa Bay and the underlying Floridan aquifer will aid in the assessment of the impacts of nearby ground-water development, ship-channel widening and deepening, and other bay-area alterations. C. B. Hutchinson reported that leakage of freshwater to the bay averages about 5 million m^3/d. Preliminary runs of a ground-water flow model, constructed by M. C. Jindal for an area in the northern part of the bay where the deepened ship channel will remove confining beds and expose the top of the aquifer to salt

water, indicate that leakage to the bay will be increased by about 7,500 m^3/d.

PACIFIC COAST

Holocene sedimentation in the Tillamook embayment, Oregon

J. L. Glenn found that Holocene to modern sediment fill in the Tillamook embayment began to accumulate rapidly (2–5 m/1,000 yr) about 9,000 yr ago when locally derived sands and gravels were deposited in river valleys carved to depths at least 32 m below present sea level. Radiocarbon data suggest that the rate of sediment deposition roughly paralleled the rate of worldwide sea level rise; there is little evidence to indicate an increased sedimentation rate in historical time.

Stratigraphic and compositional data from 33 cores and from 24 km of acoustic subbottom survey samples were used to trace development of the sediment fill in the embayment and along the adjacent open ocean shoreline. Deposition of sands and gravels at 32-m depths in and upstream of the modern river deltas was followed abruptly by deposition of well-stratified mostly locally derived sandy silts and clays, which grade upward into modern flood basin and natural-levee deposits. Toward the marine end of the embayment, however, at depths of 32 m, only coarse sands with rare granules and pebbles are present, and heavy-mineral data indicate that the sediments are derived only in part from the local provenance. The granule and pebble sands pass upward into uniform medium to fine silty sands, which are overlain by modern intertidal and sand deposits or by coastal dune deposits; the bulk of the sand in the overlying deposits also came from outside the local provenance. On the open ocean shoreline just north of Tillamook Bay, the Holocene fill is represented by only 15 m of chiefly exogenous uniform sand.

Heavy minerals of Tillamook Bay surface sediments

Mineral studies by W. A. Niem have shown that three sources, river, shoreline, and marine, contribute sandy sediment to Tillamook Bay, an estuarine embayment on the northwestern flank of the Oregon Coast Range. An Eocene volcanic terrane east and northeast of the bay is drained by four large rivers (river source); clinopyroxene and igneous rock fragments dominate the nonopaque heavy-mineral suite from this source. Miocene sandstones of the Astoria Formation contribute sand carried by small streams flowing off the headland on the southwestern margin of the bay and from local shoreline erosion (shoreline source). In this recycled sediment, clinopyroxene constitutes more than half of the nonopaque part of the heavy-mineral assemblage, igneous rock fragments are less abundant, and numerous other mineral species are present in more than trace amounts. Longshore drift (marine source) carries sand with a more varied mineral content from drainage basins to the north and south of Tillamook Bay. Clinopyroxene and hypersthene are subequally abundant; igneous rock fragments are substantially reduced in abundance; garnet and hornblende are much more common.

Some mixing of heavy-mineral suites occurs in the tidal reaches of the rivers and in the central part of the bay. The dominance of sediment from river sources along the southeastern margin of the bay indicates that the sediment supply from river sources exceeds that from marine and shoreline sources in much of Tillamook Bay.

Long-term studies of benthic community structure in Puget Sound

A study by F. H. Nichols of the benthic community at a 200-m deep muddy station in the central basin of Puget Sound off Seattle, ongoing since 1963, has revealed considerable stability in species composition throughout the 17-yr period. However, there have been pronounced shifts in numerical dominance among several common species, primarily between the tellinid clam *Macoma carlottensis* and the polychaete *Pectinaria californiensis*. These dominance cycles, with periods greater than 2 yr, are reflected in cluster-analysis results. Elimination of the several dominant species from such an analysis, however, demonstrates the existence of a marked degree of similarity among all years. The consistency of the appearance of "rare" species in the samples apparently is the basis for the observed overall structural stability in this community.

Tidal wetland deposits of the Sacramento–San Joaquin Delta

B. F. Atwater found that the Sacramento–San Joaquin River Delta is unusual because its distributaries unite at a constricted outlet and discharge into a chain of estuarine bays and straits that transects coastal mountains. Stratigraphically, it is unusual because its Holocene deposits appear to lack delta-front and prodelta facies; the principal Holocene deposit is tidal wetland peat that directly overlies alluvium or eolian sand of late Pleistocene or early Holocene age. Stasis and transgression in the late Holocene delta were probably caused in part by diversion of suspended sediment from bays in the position of delta-front environments to an arm of San Francisco Bay that is situated in a coast-parallel tectonic valley and appended to the chain of "delta-front" bays. Pleistocene sediment underlying the delta consists mainly of alluvium, partly the glacial-age fan deposits of rivers draining the Sierra Nevada. Major high stands of the sea during Pleistocene time should

have produced intertidal peat at the site of the Delta. The scarcity or absence of Pleistocene peat implies glacial-age removal by running water, wind, and chemical decomposition.

A two-dimensional hydrodynamic model of San Francisco Bay

R. A. Walters and R. T. Cheng have developed a finite-element model that is used in the computation of tidal currents in San Francisco Bay. This numerical model is patterned after an existing algorithm and has been tested carefully in rectangular and curve-sided channels with constant and variable depth. One of the common uncertainties in this class of two-dimensional hydrodynamic models is the treatment of lateral-boundary conditions. In their model, special attention is paid specifically to addressing this problem. To maintain continuity within the domain of interest, "smooth" curve-sided elements must be used for all shoreline boundaries. The present model uses triangular isoparametric elements with quadratic basis functions for the two velocity components and a linear basis function for water-surface elevation. An implicit time integration is used, and the model is unconditionally stable. The resultant governing equations are nonlinear because of the advective and bottom-friction terms and are solved repeatedly at each timestep by the Newton-Raphson method. Model test runs have been made in the southern part of San Francisco Bay as well as in the bay west of Carquinez Strait. Because of the complex bathymetry, the hydrodynamic characteristics of the bay system are dictated by the generally shallow basins that contain deep relict river channels. Great care must be exercised to ensure that the conservation equations remain locally, as well as globally, accurate. Simulations have been made over several representative tidal cycles by using this finite element model, and the results compare favorably with existing data. In particular, the standing wave in the southern part of the bay and the progressive wave in the northern reach are well represented.

Microbial formation of ethylene and ethane in San Francisco Bay sediments

Intertidal sediments were found by R. S. Oremland and his coworkers to contain methane (1.7 ± 0.6 ml/L), ethylene (114 ± 12ml/L) and ethane (108 ± 34 ml/L). Incubation of homogenized sediment slurries at 22°C under H_2 results in the production of these gases. Methane and ethane formation were blocked by 2-bromoethanesulfonic acid (BES). Ethylene formation was unaffected by BES. Addition of ethylcoenzyme M to slurries stimulated production of ethylene and ethane; however, the amounts formed after a 3-week incubation period (ethylene $= 3.2 \pm 0.2$ nM per flask, ethane $= 22.5 \pm 1.5$ nM per flask) were not in stoichiometric balance with the quantity of ethylcoenzyme M added (160 μMol). Addition of HSCoM, CH_3CoM, or methionine to slurries did not stimulate production of ethane or ethylene. Incubation of slurries at 80°C inhibited the formation of methane and ethane and blocked H_2 uptake but stimulated ethylene production. Ethylene and ethane in sediments may arise from a common precursor molecule similar to ethylcoenzyme M. Ethane formation is mediated by methanogenic bacteria, whereas ethylene may arise from either biological activity and (or) chemical catalysis.

Anaerobic oxidation of acetylene by San Francisco Bay sediment slurries

C. W. Culbertson and R. S. Oremland have used acetylene blockage of N_2O reductase as a method for measuring denitrification. When sediment slurries from San Francisco Bay were incubated under N_2 plus 3 percent N_2O (shaken, at 22°C) a steady loss of N_2O occurred, which was accelerated by chlorate and slowed by nitrate ions. Autoclaving inhibited N_2O loss. Ten percent acetylene blocked N_2O loss for 5 d, at which time a total loss of N_2O and C_2H_2 accompanied by a rise in CO_2 was observed. CO_2 could account for only about 5 percent of the C_2H_2 loss. This activity could be transferred to flasks containing sterile mineral salts media and a $N_2 + N_2O + C_2H_2$ gas phase by injection of active slurries (4 percent volume transfer). No loss of N_2O or C_2H_2 occurred in flasks receiving filter-sterilized slurry. Addition of U/^{14}C-labeled C_2H_2 to slurry with $N_2 + N_2O + C_2H_2$ resulted in the disappearance of C_2H_2 (cold and hot), followed by loss of N_2O. Subsequently, production of $^{14}CO_2$ and a ^{14}C-labeled soluble intermediate present in the filtered acidified liquid phase occurred. $^{14}CO_2$ accounted for about 10 percent of the ^{14}C-C_2H_2 loss, with the rest in the soluble intermediate. This activity was inhibited by either autoclaving or chloramphenicol. In addition, a flask to which no N_2O was added also demonstrated total loss of C_2H_2 and production of $^{14}CO_2$ and ^{14}C-soluble intermediate. These results demonstrate that C_2H_2 can be oxidized under anaerobic conditions. As yet, it is uncertain which electron acceptor(s) is involved because sulfate-reduction also was stimulated by this process.

Hydrocarbon gases in surface sediments of San Francisco Bay

Although methane is known to be a common gaseous component of estuarine sediment, the occurrence of higher molecular-weight hydrocarbon gases has not been studied extensively. To understand the processes responsible for these gases in the estuarine environ-

ment, T. M. Vogel and his coworkers compared their distributions in anoxic surface sediments from a San Francisco Bay marsh and mudflat. Preliminary results showed that hydrocarbon gases are more abundant in the marsh than in the mudflat sediment. Microbial processes probably account for most of the methane, ethene, and propene in these sediments. The other hydrocarbon gases could result from microbial activity, low temperature chemical reactions, or pollution. Some initial experiments involving microbiological cultures and long-term monitoring of stored samples indicated that microbial processes are probably the source of the hydrocarbon gases observed.

Distribution and stable-isotope composition of carbon in San Francisco Bay

From their studies of the stable-isotope composition of bay waters and sediments, E. C. Spiker and L. E. Schemel have found that dissolved inorganic carbon (DIC) was supplied primarily to San Francisco Bay by ocean, delta, and municipal waste waters during the low delta-outflow period from March 1976 to March 1977. Delta-derived alkalinity was typically about half that of ocean water and increased slightly with time. The pCO_2 values were highest (2 to 3 times the atmospheric value of approximately 325 ppm) in the Sacramento River and southern boundary of the southern part of the bay and decreased to near-atmospheric values seaward of the Golden Gate. The $\delta^{13}C(\Sigma CO_2)$ was lowest in the Sacramento River (approximately -10 °/oo), increasing to marine values in the Gulf of the Farallones (approximately $+2$ °/oo). Golden Gate values were approximately 2 °/oo less than those seaward, indicating that at least 10 percent of the ΣCO_2 was biogenic and is apparently the product of respiration and the mineralization of organic matter in the bay. In the southern part of the bay, alkalinity and pCO_2 levels increased southward, whereas $\delta^{13}C(\Sigma CO_2)$ and salinity decreased. Municipal waste discharged into the southern part of the bay is the most probable source of the excess biogenic CO_2.

Distributions of particulate organic carbon (POC) in the northern part of the bay were influenced by in situ phytoplankton production and seaward dilution of riverine and estuarine POC. Apparent depletions of pCO_2 in the northern part of the bay coincide with chlorophyll *a*, POC, and $\delta^{13}C(\Sigma CO_2)$ increases. The $\delta^{13}C$(POC) values during March 1977 approached those predicted for in situ algal production, suggesting that about 80 to 90 percent of the POC was produced in the seaward part of the estuary. In situ algal production was an important source of POC in the river. However, in the high turbidity null zone, less than two-thirds of the POC appears to be derived from the river, the remaining one-third being produced in the estuary or associated with resuspended bottom sediment. Suspended POC in the southern part of the bay appears to be a mixture of resuspended bottom sediments, in situ-produced POC, and land-derived organic carbon. Based on $\delta^{13}C$ data, *Spartina* saltmarsh grass does not appear to be a significant source of detritus in the bay.

The ^{13}C of sediment total organic carbon (TOC) indicates that riverine carbon from the delta is diluted in the bay by estuarine and marine carbon. The suspended POC and sediment TOC $\delta^{13}C$-measurements approached marine values seaward of the Golden Gate.

Seasonal distributions of water properties in San Francisco Bay

T. J. Conomos and his coworkers have described the timing and general location of major processes modifying the distribution of conservative (temperature, salinity, alkalinity), as well as biologically reactive (oxygen, carbon, nutrients, pH), water properties. River-modulated physical effects on the distribution in near-surface midchannel water are characteristically defined by season (high versus low river inflow) and geographic region (northern versus southern reach of the estuarine system).

Delta outflow directly controls and often dominates the spatial and temporal distribution of most properties and biological processes in the northern reach. The outflow contributes suspended particles, DO, and silicate and generates an estuarine circulation cell and a turbidity maximum. The circulation pattern and associated features largely dictate spatial distributions. Seasonal changes, however, are caused by relative changes in outflow, which determine water-residence time and, thus, flushing rates, and light-limited biological activity, photosynthesis, nutrient uptake, and oxygen production. During the winter, mixing and advection control biological activity, whereas during summer, both biological activity and physical processes are important.

The relation between delta outflow and biological processes in the southern reach, however, is less direct. Biological activity has a relatively greater effect on the spatial and temporal distribution of these properties. Distribution of properties is dominated by the perennial inflow of detritus and nutrient-rich waste water at the southern boundary. These inputs are augmented during winter by discharges from local intermittent streams that may contribute large amounts of nitrogenous compounds. The substratum is the major source of particles and dissolved silicate. Greatest biological activity apparently takes place during spring rather than summer, as in the northern reach. This increased activity in the southern reach is caused in part by delta-outflow-induced stratification that tends to maintain algal cells in the photic zone.

Effects of river discharge on phytoplankton biomass and species composition in the northern San Francisco Bay Estuary

Extensive field studies by J. E. Cloern and his coworkers during the 1976 to 1977 drought have shown that reduced freshwater inflow had a significant impact on the biomass and species composition of phytoplankton in the northern San Francisco Bay Estuary. During years of normal hydrological conditions, there are spring and summer blooms of net-phytoplankton (neritic diatoms). Population growth of diatoms appears to be a consequence of two interacting factors, physical accumulation of dense suspended particles (including diatoms) by estuarine circulation and location of this suspended-particle maximum adjacent to shallow areas where light availability is sufficient to permit rapid cell division. During 1976 to 1977, river discharge was so low that gravitational circulation was weakened, and the suspended-particle maximum was located upstream, away from the productive shallow areas. Consequently, population growth of planktonic diatoms did not occur, and the phytoplankton community was dominated year round by relatively small numbers of microflagellates. The loss of diatom productivity during periods of low freshwater inflow may have important trophic-dynamic implications because the pathways and efficiencies of energy flow through flagellate-based food webs presumably differ from those in diatom-based food webs.

Simulation model of *Skeletonema costatum* population dynamics in northern San Francisco Bay

A pseudo-two-dimensional model has been developed by J. E. Cloern and R. T. Cheng to simulate population dynamics of one dominant phytoplankton species (*Skeletonema costatum*) in northern San Francisco Bay. The model is formulated around a conceptualization of this estuary as two distinct but coupled subsystems—a deep (10–20 m) central channel and lateral areas with shallow (<2 m) water and slow circulation. Algal growth rates are governed by solar irradiation, temperature, and salinity, while population losses are assumed to result from grazing by calanoid copepods. Consequences of estuarine gravitational circulation are approximated simply by reducing convective-dispersive transport in that section of the channel (null zone) where residual bottom currents are near zero, and lateral mixing is treated as a bulk-exchange process between the channel and the shoals.

Model output is consistent with the hypothesis that, because planktonic algae are light limited, shallow areas are the sites of active population growth. Seasonal variation in the location of the null zone (a response to variable river discharge) is responsible for maintaining the spring bloom of neritic diatoms in the seaward reaches of the estuary (San Pablo Bay) and the summer bloom upstream (Suisun Bay). Model output suggests that these spring and summer blooms result from the same general process—establishment of populations over the shoals, where growth rates are rapid, coupled with reduced particulate transport due to estuarine gravitational circulation. It also suggests, however, that the relative importance of physical and biological processes to phytoplankton dynamics is different in San Pablo and Suisun Bays. Finally, the model has helped determine those processes having sufficient importance to merit further refinement in the next generation of models, and it has given new direction to field studies.

Biological-chemical consequences of a major sewage spill in south San Francisco Bay

During September 1979, the sewage treatment facility of San Jose–Santa Clara, Calif., experienced a failure that resulted in the discharge of partly treated sewage into Coyote Creek, a tributary to south San Francisco Bay. Field studies by J. E. Cloern and his coworkers have shown several immediate consequences of the spill: (1) increased inputs of NH_4 and particulate organic carbon and nitrogen, (2) depressed concentrations of DO, (3) die-offs of invertebrates and the disappearance of fish, (4) radical shifts in the relative abundances of NH_4, NO_3, NO_2, and N_2O, presumably in response to nitrification and denitrification, (5) increased concentrations of CO_2, CH_4, and C_2H_4 in anaerobic waters, (6) elevated concentrations of enteric bacteria, and (7) changes in the biomass of phytoplankton. These changes were restricted to Coyote Creek and were short term. Other, longer term impacts on the biota of Coyote Creek may occur; documentation will require continued investigation.

Plant distributions in the tidal wetlands of the Sacramento–San Joaquin River Delta

Botanical studies by B. F. Atwater have shown that six remnants of tidal wetlands (marsh and swamp) in the Sacramento–San Joaquin Delta collectively support about 75 species of native plants. Two of the species were heretofore overlooked in the Central Valley, *Salix coulteri* Anderss and *Scutellaria galericulata* L. Geographic trends in the distribution of species in the delta's tidal wetlands reflect transition from the natural levees and alluvial flood basins of the Sacramento and San Joaquin Valleys to the brackish-water tidal marshes of Suisun Bay. For example, the number, stature, and areal abundance of arborescent species decrease toward Suisun Bay, mimicking a trend reported before the erection of artifical levees on the Sacramento River. Another botanical transition involves vertical zonation of *Scirpus acutus* Muhl. (common tule). This bulrush, the

principal native plant of the delta, inhabits both banks and interiors of remnant wetlands in the south-central part of the delta. Wetlands of the south-central delta possess neither natural levees, whose woody plants exclude *S. acutus* from banks of tidal sloughs in the northern delta that rise 10 to 20 cm above contiguous *S. acutus*-dominated wetlands, nor persistently saline soils, which exclude *S. acutus* from all except the lowest fringes of tidal marshes served by Suisun Bay and its sloughs. Thus, common tule is widespread in the south-central delta because of a combination of naturally unleveed wetland and generally fresh water that is unique to this part of the San Francisco Bay Estuary.

Population dynamics of dominant bivalves in San Francisco Bay

Population of *Gemma gemma* at three intertidal elevations in San Francisco Bay were studied by J. K. Thompson to describe population structure, stability, and production and to compare these to previous descriptions of *G. gemma* on the east coast. *G. gemma* is one of the most common animals found in the bay and, as one of the most productive animals reported in the literature, is a major constituent in the secondary production of the bay. A comparison of the population structure and biology of this bivalve in San Francisco Bay and some northeastern U.S. estuaries has shown that *G. gemma* are equally abundant on both coasts despite marked differences in reproductive behavior and community diversity. *G. gemma* populations in the upper intertidal areas are controlled by biologic factors in San Francisco Bay and by physical stresses of the environment on the east coast.

Long-term seasonal studies of *Macoma balthica* by F. H. Nichols and J. K. Thompson have shown that this bivalve is near the southern limit of its range. Growth in *M. balthica* from San Francisco Bay is highly seasonal despite a mild Mediterranean climate. Animals grow larger at a given age in San Francisco Bay than elsewhere in the world despite a similar growth-period length in all locations. A model developed from field measurements of growth aided in the estimation of slow growth-period rates and the distinction of recruitment periods and year classes.

Heavy-metal distributions in mollusks of San Francisco Bay

In his continuing heavy-metal studies of biota in San Francisco Bay, S. N. Luoma has reported concentrations of Ag, Cd, Cu, and Zn in clams (*Macoma balthica, Mya arenaria, Tapes japonica*), mussels (*Ischadium demissus*), and snails (*Nassarius obsoletus*) from mudflats. Compared to animals from harbors outside the bay, all species from stations within the southern part of the bay were substantially enriched in silver and copper. A point source of silver in the southernmost reach of the bay appeared to affect silver concentrations in animals throughout the southern part of the bay. Concentrations of copper in the sediments of the southern part of the bay were low compared to other urban-industrial estuaries. However, benthic organisms in San Francisco Bay appear to be highly susceptible to small increases in copper discharge, due to the effect of some physiocochemical characteristics of the bay on the bioavailability of copper.

Extraction of the biologically available fraction of sediment-bound trace metals was compared among 11 extraction techniques. A weak solution of hydrochloric acid extracted quantities of Ag, Cd, Co, and Pb from sediments that correlated more strongly with concentrations in estuarine-deposit feeders (clams and polychaetes) than did total sediment-bound concentrations. The fraction of copper extractable by the complexing agent DTPA correlated more closely with copper concentrations in clams than did other extractable fractions of copper. All sediment extractions were conducted within 24 h of sediment collection from the field. Experiments showed most methods of sediment storage (freezing, drying storage; wet at 25° or 4°C) affected the extractability of metals, especially by weak extractants such as DTPA, and (or) the physical characteristics of the sediments.

MANAGEMENT OF NATURAL RESOURCES ON FEDERAL AND INDIAN LANDS

The Conservation Division is responsible for carrying out the role of the USGS in classifying leasable mineral and potential water-resource development sites on Federal lands and managing the exploration and development of leasable minerals on Federal and Indian lands, including the Outer Continental Shelf. Primary functions are (1) classification and evaluation of Federal mineral lands for multiple use management and for leasing, (2) delineation and preservation of potential public-land reservoir and waterpower sites, (3) promotion of orderly exploratory development, conservation, and proper use of mineral resources on Federal lands under lease, (4) supervision of mineral operations to assure protection of the environment, the realization of a fair value from the sale of leases, and satisfactory royalties on mineral production, and (5) cooperation with other agencies in the management of Federal mineral and water resources.

CLASSIFICATION AND EVALUATION OF MINERAL LANDS

The organic act creating the USGS gave the Director the responsibility of classifying and evaluating the mineral resources of public-domain lands. There are about 101 million ha of land for which estimates of the magnitude of leasable mineral occurrences only partially have been made. Such appraisals are needed for multiple-use planning by Federal land managers and for leasing by the Bureau of Land Management. Estimates are based on existing data. When additional data are required, field studies and spot checks must be undertaken. Guidelines are prepared from time to time by the USGS to assure uniform executive action in the classification of leasable minerals on Federal lands.

CLASSIFIED LAND

With the passage of the Federal Land Policy and Management Act of 1976, numerous changes occurred in the classification program. For example, classification for retention of mineral rights is no longer appropriate. Also, fair market value is required for exchanges and conveyances of mineral rights. Classification to prevent improvident disposal of Federal mineral rights was a major responsibility under the former classification mission, but was not the only requirement. The Federal lands also were classified as to mineral character to delimit potential leasable mineral resources, conserve natural resources, provide data on Federal lands for multiple-use management, and inventory the resource potential for leasable minerals of Federal lands.

The following classification responsibilities still remain: (1) to identify competitive leasing areas for leasable minerals, (2) to inventory leasable mineral resources, (3) to furnish the Federal land-managing agencies with adequate leasable mineral data on Federal lands for land-use planning and multiple-use or best-use decisions, and (4) to furnish Congress and other Federal agencies leasable mineral data on the Federal lands being considered for withdrawal by Congressional or executive action.

As a result of USGS investigations, large areas of Federal land have been formally classified as mineral land. At the end of calendar year 1979, more than 17 million ha of land had been formally classified, and about 950 million ha had been designated prospectively valuable for a leasable mineral, as shown in the following table:

Lands classified

Commodity	During calendar year 1979		Total at end of calendar year 1979	
	Formerly classified (hectares)	Prospectively valuable (hectares)	Formerly classified (hectares)	Prospectively valuable (hectares)
Asphaltic minerals	0	0	0	7,262,766
Coal	78,219	0	17,468,881	142,040,102
Geothermal resources	0	4,662	0	41,866,764
Oil and gas	0	0	1,714	595,321,498
Oil shale	0	0	0	5,849,963
Phosphate	0	0	216,436	12,403,324
Potassium	0	0	0	35,676,410
Sodium	0	0	254,536	108,303,594

KNOWN GEOLOGIC STRUCTURES OF PRODUCING OIL AND GAS FIELDS

Under the provisions of the Mineral Leasing Act of 1920, as amended, the Secretary of the Interior is authorized to grant to any qualified applicant a noncompetitive lease to prospect for oil and gas unless the

Federal mineral estate is within a Known Geologic Structure (KGS) of a producing oil and gas field. Lands within a KGS must be competitively leased to the highest bidder. During calendar year 1979, 692,682 ha of onshore Federal land were classified as KGS lands, either as a new KGS or as additions to a previously established KGS. The total acreage in KGS's at the end of the year was over 8 million ha.

KNOWN GEOTHERMAL RESOURCE AREAS

The Geothermal Steam Act of 1970 provides for development by private industry of federally owned geothermal resources through competitive and noncompetitive leasing. During calendar year 1979, 11,351 ha were included in Known Geothermal Resource Areas (KGRA) and 2,851 ha were deleted, which brought the total to 1,266,410 ha.

The results of lease sales held in 1979 are summarized in the following table:

Geothermal lease sales for calendar year 1979

Sale date	State	Number of tracts offered	Hectares	Number of tracts leased	Hectares	Total accepted high bids
5/10/79	California	8	7,543	3	2,816	1,368,191
5/31/79	Montana	8	6,366	0	0	0
6/26/79	Nevada	29	26,125	11	9,833	657,469
9/18/79	New Mexico	12	7,042	4	2,858	240,631

KNOWN RECOVERABLE COAL RESOURCE AREAS

The Federal Coal Leasing Amendments Act of 1976 provides for the development by private industry of federally owned coal lands by private industry through competitive leasing and authorizes the Secretary of the Interior to designate Known Recoverable Coal Resource Areas (KRCRA). During calendar year 1979, 923,688 ha of coal land were included in KRCRA's, bringing the total to 8,684,530 ha. Drilling programs in support of coal land classification during 1979 totaled 117,969 m for 731 holes completed, at an average depth drilled of 161 m/hole.

COAL RESOURCE OCCURRENCE/COAL DEVELOPMENT POTENTIAL REPORTS

During calendar year 1979, 200 Coal Resource Occurrence/Coal Development Potential (CRO/CDP) reports were placed in open file by the end of calendar year 1980.

During calendar year 1978, mapping of 234 additional quadrangles was contracted for in the States of Colorado, North Dakota, New Mexico, Utah, and Wyoming. During calendar year 1979, 14 quadrangle reports were contracted for in Oklahoma.

KNOWN LEASING AREAS FOR POTASSIUM, PHOSPHATE, AND SODIUM

During calendar year 1979, known phosphate leasing areas were increased by 9,540 ha, for a total of 53,338 ha. The known sodium leasing areas totaled 326,934 ha classified for competitive leasing. The known potassium leasing acreage totaled 145,430 ha.

WATERPOWER CLASSIFICATION—PRESERVATION OF RESOURCE SITES

Suitable sites for water-resource development are valuable natural resources. The waterpower classification program is conducted to identify, evaluate, and protect from disposal and injurious uses those Federal lands located in sites having significant potential for future development. USGS engineers review maps, aerial photographs, and streamflow records to determine potential dam and reservoir sites. Topographic, engineering, and geologic studies are made of the identified sites to determine whether the potential value warrants formal classification of the affected Federal lands. These resource studies provide the land-administering agencies and others with information that is basic to management decisions and effective land-use planning. Previous classifications are reviewed as additional data become available and as funds permit. If the sites are no longer considered suitable for development, revocation of the classification of the affected Federal lands is recommended. If the lands are not reserved for other purposes, they are returned to the unencumbered public domain for possible disposition or other use. During calendar year 1979, about 800 ha of previously classified lands in four Western States were released, and reviews of classifications were conducted in river basins in Arizona, Idaho, and New Mexico.

To assure consideration of potential reservoir and waterpower sites in the preparation of land-use plans, information concerning such sites was furnished to the Bureau of Land Management and the U.S. Forest Service for several planning units in the Western States and Alaska.

MANAGEMENT OF MINERAL LEASES ON FEDERAL AND INDIAN LANDS

Supervision of competitive and noncompetitive leases for the development and recovery of leasable minerals in deposits on Federal and Indian lands is a function of the USGS, delegated by the Secretary of the Interior. It includes geologic and engineering examination of applied-for lands to determine whether a lease or a permit is appropriately applicable, approval of operating plans, inspection of operations to insure compliance with regulations and approved methods, and verification of production and the collection of royalties (see table 1).

Before recommending approval of a lease or a permit, USGS engineers and geologists consider its possible effects on the environment. Of major concern are the esthetic value of scenic and historic sites, the preservation of fish and wildlife and their breeding areas, and the prevention of land erosion, flooding, air pollution, and the release of toxic chemicals and dangerous materials. Consideration also is given to the amount and kind of mining land reclamation that will be required.

TABLE 1.—*Mineral production, value, and royalty for calendar year 1979*

[New accounting procedures include production data, production values, and royalties for both gasoline and LPG (liquid petroleum gas) under the heading "Gas liquids"; the heading "Other" designates all minerals except petroleum products and includes coal, potassium, sodium minerals, and so forth.]

Lands	Oil (tonnes)	Natural Gas (cubic meters)	Gas liquids (liters)	Other* (tonnes)	Value (dollars)	Royalty (dollars)
Public	20,057,265	29,248,487,427	1,347,826,536	67,045,493	$ 4,392,806,732	$ 435,523,662
Acquired	816,616	663,141,375	37,732,275	644,033	388,561,737	27,174,567
Indian	3,270,290	3,351,700,462	69,687,281	29,654,898	779,499,667	88,868,466
Military	39,366	376,925,663	33,087,618	–	14,452,491	2,374,887
OCS	39,118,567	132,338,769,216	18,620,353	–	9,273,278,309	1,515,347,950
Total	63,302,104	165,979,024,143	1,469,713,357	97,344,424	$14,848,598,936	$2,069,289,532

Onshore oil and gas lease sales

During calendar year 1979, there were 13 competitive sales of oil and gas leases on Federal lands at which a total of 20,463 ha was sold for $10,141,033. An exceptionally high per acre bid of $13,501 was received for a small tract in Oklahoma in January. The KGS lands that received the highest totals of accepted bids were offered at the New Mexico sale in September ($2,971,530) and the Colorado sale in April ($2,173,266). The average price per acre received from oil and gas lease sales on Federal lands during calendar year 1979 was $184, compared to $135 the previous year.

The results of lease sales held in 1979 are summarized in the following table:

Onshore oil and gas lease sales during calendar year 1979

Sale date	State	Number of tracts offered	Hectares	Number of tracts leased	Hectares	Total accepted high bids
1/17/79	Wyoming	19	1,486	19	1,486	$ 280,641
1/30/79	Oklahoma	22	572	22	521	329,827
3/14/79	California	12	536	12	2,596	88,384
3/14/79	Colorado	6	1,135	6	1,135	152,654
3/20/79	New Mexico and Texas	46	2,633	46	2,083	798,052
4/11/79	Colorado	35	4,342	28	3.402	2,173,266
4/17/79	Oklahoma	17	814	15	774	403,748
4/18/79	Kansas	1	65	1	65	4,160
6/20/79	Wyoming	22	2,030	22	2,030	995,765
7/10/79	Oklahoma and New Mexico	29	1,349	28	1,319	957,430
9/12/79	Wyoming	26	1,082	26	1,082	269,994
9/18/79	Oklahoma	21	1,072	21	1,026	715,582
9/18/79	New Mexico	34	2,943	33	2,927	2,971,530

MANAGEMENT OF OIL AND GAS LEASES ON THE OUTER CONTINENTAL SHELF

The Outer Continental Shelf (OCS) Lands Act of 1953 authorizes the Secretary of the Interior to issue oil and gas leases on a competitive basis in the submerged lands of the OCS. The functions of the USGS, delegated by the Secretary of the Interior, include (1) participation in tract selection and evaluation to insure orderly resource development, protection of the marine environment, and receipt of a fair market value, (2) review and approval or disapproval of proposed exploration plans and development and production plans, (3) inspection of operations to insure compliance with regulations and approved methods, and (4) verification of the amount and value of production and the assessment and collection of rentals and royalties.

The Outer Continental Shelf Lands Act Amendments of 1978 provided the Secretary of the Interior with policy guidance for administration of the leasing provisions of the amended Act and provided an additional enforcement tool in the form of civil penalties. The USGS administers the civil penalties that are assessable for any failure to comply with any provision of the Act, any term of a lease, license, or permit issued under the Act, or any regulation or order under the Act. USGS review and approval of proposed exploration plans and development and production plans also must assure compliance with the new statutory requirement to use the best available and safest technologies on all new drilling and production activities.

Outer Continental Shelf lease sales for oil and gas

Six OCS oil and gas lease sales were held in calendar year 1979. Sales were held for leases in the mid- and North Atlantic in February and December, respectively, southern California in June, central and western Gulf of Mexico in July and November, and the Beaufort Sea in December. A summary of the results of these individual lease sales is presented in table 2. For the entire Federal OCS, 666 tracts totaling 1,380,923 ha were offered for lease. High bids of $4.590 billion were accepted on 327 tracts totaling 680,562 ha. Litigation involving the Beaufort Sea sale has delayed the acceptance of high bids totaling $491.7 million on 25 tracts.

TABLE 2.—*OCS oil and gas lease sales for calendar year 1979*

Sale number	Area and date	Number of tracts offered	Hectares	Number of tracts leased	Hectares	Total bonus accepted
49	Mid-Atlantic 2/28/79					
	Total	109	251,136	39	89,856	$ 40,001,631
	Sliding-scale	58	133,632	23	52,992	20,558,061
	Cash bonus	51	117,504	16	36,864	19,443,570
48	Southern California 6/29/79					
	Total	148	320,864	54	116,658	$ 572,825,418
	Sliding-scale	74	166,768	28	41,312	71,422,415
	Cash bonus	74	154,096	26	75,346	501,403,003
58	Central and western Gulf of Mexico 7/31/79					
	Total	123	233,718	81	158,309	$1,247,489,022
	Sliding-scale	52	107,468	32	68,276	433,426,038
	Cash bonus	71	126,250	49	90,570	814,062,984
58A	Central and western Gulf of Mexico 11/27/79					
	Total	124	238,204	90	170,587	$1,913,337,938
	Sliding-scale	51	104,592	33	66,583	763,373,800
	Cash bonus	73	133,612	57	104,004	1,149,964,138
42	North Atlantic 12/18/79					
	Total	116	267,264	63	145,152	$ 816,516,546
	Sliding-scale	55	126,720	35	80,640	604,862,346
	Cash bonus	61	140,544	28	64,512	211,654,200
BE	State and Federal Beaufort 12/11/79[1]					
	Total	46	69,737	(2)	(2)	(2)
	Sliding-scale	46	69,737	—	—	—
	Cash bonus	—	—	—	—	—

[1] Federally managed tracts only
[2] Awarding of leases delayed due to litigation

COOPERATION WITH OTHER FEDERAL AGENCIES

The USGS acts as a consultant to other Federal agencies in land-disposal cases. In response to their requests, the USGS determines the mineral character and water-resource development potential of specific tracts of Federal land under their supervision that are proposed for sale, exchange, or other disposal. About 550 such reports were made during calendar year 1979.

GEOLOGIC AND HYDROLOGIC PRINCIPLES, PROCESSES, AND TECHNIQUES

GEOPHYSICS

ROCK MAGNETISM

Tectonic rotation of the Seven Devils Group, Oregon and Idaho

The Seven Devils Group in Hells Canyon, Oregon and Idaho, is remarkably similar to the Upper Triassic rock assemblages of Vancouver Island and the McCarthy quadrangle, Alaska, in terms of paleontology, age, and lithostratigraphy. These assemblages are part of a geologic terrane called Wrangellia. Paleomagnetic results from the Nikolai Greenstone indicate that the northern part of Wrangellia originated far south of its present position relative to North America. J. W. Hillhouse and C. S. Gromme sampled basalt flows and volcaniclastic rocks of the Seven Devils Group for paleomagnetism to determine whether the Seven Devils Group originated at the same low latitude as the Nikolai Greenstone. Three components of remanent magnetization were detected: (1) a steep northeasterly component that postdates folding, (2) an easterly component with low negative inclination, and (3) a northwesterly component with low positive inclinations. Presumably, the latter two components, corresponding to paleolatitude $\pm 18°$, are original Triassic magnetizations of normal and reversed polarity. The steep northeasterly component is identical to the magnetization found in nearby Jurassic and Cretaceous plutons. Apparently, hydrothermal circulation accompanying these intrusions chemically reset the magnetization of large parts of the Seven Devils Group. More than one-half of the samples, especially the basalt flows, are completely remagnetized; 45 percent of the samples reveal low inclinations characteristic of northern Wrangellia. Magnetic inclinations of the Jurassic and Cretaceous plutons and the associated secondary overprint are consistent with the apparent polar wander path of central North America, indicating that, by Early Cretaceous times, the Seven Devils Group was bonded to the continental margin. However, anomalous declinations determined from the plutons and the secondary magnetization of the Seven Devils Group indicate a clockwise rotation of 50° of the region.

Northward movement of the Chugach terrane, Alaska

The Chugach terrane of southern and southeastern Alaska is composed of upper Mesozoic flysch and mafic volcanic rocks and extends from Kodiak Island on the west to Baranof Island on the southeast. This tectonostratigraphic terrane is arcuate in shape and is bounded by major faults on all sides. In the Fairweather Range at approximately the latitude of Glacier Bay, the Chugach terrane is intruded by three or four large plutons of layered gabbro. Recent radiometric dating of one of these, gabbro at La Perouse, indicates that it is Oligocene in age. Paleomagnetic data have been obtained by C. S. Gromme from two of the gabbros, gabbros at La Perouse and Astrolabe. The paleomagnetic pole derived from these data is anomalous, falling in the region of the west-central Pacific at 25° N., 160° E. The paleomagnetic declination is 90° west of what would be expected for Oligocene time, and the paleolatitude computed from the inclination is 27° south of the present latitude of these rocks. Therefore, since Oligocene time, the part of the Chugach terrane intruded by, and including, these gabbros has moved northward a distance of 3,000 km and has rotated approximately 90° counterclockwise. The minimum rate of northward movement was 12 cm/yr, which is at the upper limit of crustal plate velocities observed at the present time. Almost identical anomalies in declination and paleolatitude have already been reported by Gromme and J. W. Hillhouse for the Upper Cretaceous ophiolite of the Resurrection Peninsula, which is within the western part of the Chugach terrane. Considered together, the data may be interpreted to mean that the entire Chugach terrane moved northward as a unit and was not significantly distorted in shape when it collided with, or was accreted to, Alaska. However, the arcuate shape of the Chugach terrane and the structural trends within it, which follow the so-called Alaska orocline, seem to contradict this conclusion. An alternative interpretation is that all of the Chugach terrane moved northward at the same time, but that gross deformation accompanied collision and, hence, the similarity of the paleomagnetic declination anomalies is fortuitous.

Paleomagnetic correlation of volcanic rocks

Many of the lava flows on the island of Hawaii have recently been dated by the carbon-14 method. D. E. Champion and R. T. Holcomb used the paleomagnetic directions evidenced in these rocks to reconstruct the history of geomagnetic secular variation at Hawaii. A well-documented history now exists for the past 1,000 yr, and a partially documented record exists for the past 6,000 yr.

Almost 90 percent of the surface of Kilauea Volcano on Hawaii is mantled by lava flows less than 1,000 yr old. Many of these lava flows have been dated and mapped by matching their paleomagnetic directions to the reconstructed secular variation curves. The result is a much more detailed history of the recent volcanism of Kilauea than was previously available. Champion has applied the same technique to correlation of lavas penetrated by drill holes at the Radioactive Waste Management Complex of the Idaho National Engineering Laboratory. The paleomagnetic correlations are corroborated by the petrographic characteristics of the lavas, and the resulting knowledge of the volcanic stratigraphy has enabled an evaluation of the volcanic hazard at that waste isolation site.

Maghemitization of oceanic crust

Both theoretical considerations and available experimental results indicate that the magnetic effects of low-temperature oxidation of ocean-floor basalts (maghemitization) are strongly dependent on the grain size of the originally unoxidized titanomagnetite and that these changes are quite different for single domain and multidomain grains. However, the behavior of pseudosingle domain titanomagnetite, which is the main carrier of remanence in the submarine extrusive rocks that are the main source of marine magnetic anomalies, cannot be predicted easily. E. A. Mankinen (USGS) and Michel Prevot and Alain Lecaille (University of Paris) have combined electron microprobe analyses, Curie temperature measurements, and cell-edge determinations to determine the oxidation degree of titanomagnetites from pillow basalts recovered from the rift valley of the Mid-Atlantic Ridge. The magnetic properties of these rocks then were compared to the older and more highly oxidized Deep-Sea Drilling Project Leg 37 pillow basalts to investigate the behavior of pseudosingle domain grains. The intermediate magnetic behavior of these rocks during maghemitization was characterized by the absence of large changes in coercivity and susceptibility. However, a chemical remanent magnetization seems to be acquired, making the interpretation of paleomagnetic directions from highly maghemitized rocks, which constitute most of the ocean floor, more difficult. For pillow basalts less than 0.7 m.y. old, little direction change can occur, but, for older rocks, successive antiparallel chemical remanent magnetizations acquired during different periods of geomagnetic polarity could drastically modify the original direction, provided the net chemical remanent magnetization has a polarity different from the primary remanence. This process may be responsible for the scattered and anomalously low magnetic inclinations in basalts from Deep-Sea Drilling Project Leg 37, site 332, which were erupted just prior to a geomagnetic polarity reversal.

Random crustal magnetization and its effect on marine magnetic anomalies

The Deep-Sea Drilling Project has penetrated several hundred meters into layer 2A, the uppermost basaltic part of the oceanic basement. The magnetic properties of these cores show that this part of the magnetic layer is extremely complex, containing units with both polarities, with intermediate directions, and with large differences in intensities. Because these volcanic units may extend for hundreds of meters with little change in magnetic properties (Hall and Ryall, 1977), the average magnetization of the crust may have substantial lateral variation. R. J. Blakely has shown that these occurrences are compatible with linear short-wavelength anomalies frequently caused by paleomagnetic field behavior. Statistical models were developed for the lateral variation of the average magnetization of layer 2A—a Poisson series for reversals of the Earth's field and a stairstep random series for discrete magnetic units. The power-density spectra of these statistical models, derived by ensemble averaging, indicated that lateral inhomogeneities must average out over distances of less than a few hundred meters in the order observed short-wavelength anomalies appear. Specifically, individual magnetic units of the type seen at Deep-Sea Drilling Project Site 332 cannot extend for distances greater than a few hundred meters.

GEOMAGNETISM

New magnetic observatory near Fresno, California

A site for a new magnetic observatory, to replace the one at Castle Rock, Calif., was established by J. D. Wood, R. A. Martin, and D. P. Klein at the U.S. Forest Service's San Joaquin Experimental Range, approximately 40 km north of Fresno, Calif. Induction studies made in the region around the site and local magnetic surveys indicated that this is an excellent site from a technical standpoint. Access is good, and there should be no interference from industrial development in the foreseeable future. Long-term use of this site is provided

for through a memorandum of understanding between the USGS and the Pacific Southwest Forest and Range Experimental Program, U.S. Forest Service.

Five instrument shelters were constructed to house magnetometer electronics, recorders, and transmission equipment; the pier and equipment for absolute observations; and sensors for fluxgate and proton magnetometers. The shelter for the fluxgate sensor was well insulated and put below ground level to minimize temperature fluctuations. One of the principal difficulties in building these shelters was in obtaining nonmagnetic concrete and nonmagnetic fixtures. The necessary power and telephone lines have been run to the site, and installation of equipment is in progress.

Operation of the International Magnetospheric Study Network

According to R. W. Kuberry, the special network of magnetometer stations for the International Magnetospheric Study became fully operational during 1979, and data are being made available to the principal investigators and to the World Data Center A on a routine basis. Under National Science Foundation funding, the USGS supplied the instrumentation for all 27 stations, 4 of which are directly operated by the USGS. Logistical problems forced the closing of two stations in the auroral zone. Overall, data recovery at the stations has been very good. For example, a detailed analysis of the 5-mo interval of July through November 1978 indicated a recovery rate of 93 percent from the 23 stations that were in service at that time. From 1977 to 1980, there have been no failures caused by the microprocessor chip. Most operational problems have been due to radio, power supply, and magnetometer malfunctions. Damage from lightning has been a major problem at some installations.

New geomagnetic observatory instrumentation

R. W. Kuberry designed an improved automated system for the USGS geomagnetic observatories. The new system uses a dedicated minicomputer to poll the stations by means of a telephone autodial system. Synchronous Meteorological Satellite/Geostationary Operational Environmental Satellite data-collection-platform radio sets are provided for those stations outside the conterminous United States. A microprocessor-based controller provides for onsite recording to backup the telemetry system. An improved uninterruptable power system has been designed to eliminate lightning-generated power transients.

Determination of *K*-indices by computer

Normally, *K*-indices, which are the most used measure of magnetic activity, are hand scaled from magnetograms produced by standard photographic recording magnetograph systems. L. R. Wilson has written computer programs to determine *K*-indices, using digital fluxgate magnetometer data from two observatories. Preliminary tests comparing computer and hand-scaled *K*-indices show 95-percent agreement within ± 1 unit, which is comparable to differences in individual hand scalings. Thus, computer-derived *K*-indices can be determined for automated observatories not having normal magnetograms available.

Magnetic declination measurements in Vermont

Under a new program planned and carried out by R. G. Green, detailed magnetic declination (compass variation) coverage of the State of Vermont is now available for a large number of Vermont's cities, towns, and villages and for most of the airports and landing fields. These data are the primary input to the original compilation of an isogonic chart of Vermont. At least one significant anomaly, within which the declination ranged from 12° W. to 21° W., has been found.

New magnetic declination map of the United States

A new map of the magnetic declination in the United States for 1980, prepared by E. B. Fabiano and N. W. Peddie, is scheduled for publication in July 1980. The map was derived from polynomial analysis incorporating 20,000 surface and aeromagnetic measurements in the conterminous United States, with selected grid values synthesized from a new spherical harmonic model developed by Peddie and Fabiano for Alaska, Hawaii, and the border regions of the conterminous 48 States.

To obtain current secular change estimates, survey measurements made at 54 U.S. repeat stations from 1978 to 1979 and regional magnetic observatory data were used for data reduction and derivation of isoporic curves. The root mean square fit to main field data is of the order of 0.4°; the root mean square differences between the secular model and recent station measurements is 0.5 min/yr.

Long wavelength magnetic anomalies

Studies by J. C. Cain of the magnetic anomaly structure between global wave numbers of 4 to 18 indicate that, although the source of observed field clearly changes from the core to crustal regions as the wave number increases, there is no unique way to distinguish between waves originating in the core and those originating in the crust. Some of the very large scale features appear to have the stationary characteristic associated with crustal magnetization, although com-

putations of possible amplitude based on allowable magnetic contrast and depth to the Curie point give values that are much too small for waves originating in the crust.

Rectangular harmonic analysis of magnetic fields

Spherical harmonic analysis of the Earth's magnetic field is limited in the resolution that can be obtained because the fundamental wavelength is the circumference of the Earth. Resolution of wavelengths as short as 100 km requires a spherical harmonic analysis to degree and order 400 involving 160,800 coefficients. This is impractical even with modern computers. L. R. Alldredge has shown that this limitation can be overcome by using rectangular harmonic analysis in successively smaller areas until the desired resolution is obtained. Rectangular harmonic analysis and spherical harmonic analysis are complementary. Both are needed in the complete analysis of the Earth's magnetic field.

Observation of induced electric currents in the Alaska oil pipeline

Currents in the 128,000-km-long Alaska oil pipeline, induced from the ionospheric auroral electrojet, were determined at three sites, near Fairbanks, Paxson, and Valdez, Alaska, from magnetic field measurements using a gradient configuration of two fluxgate magnetometers. The observed pipeline current magnitudes, which reached 50 A during times of mild geomagnetic activity, displayed a linear relation with differences in electric earth potential measured between electrodes 300 m apart. Using the induction relation between the electric and magnetic fields and the typical spectral composition of the geomagnetic field at high latitudes, W. H. Campbell obtained a spectral plot of the currents that shows a maximum in the 4.5- to 10-min range. Near Fairbanks, the pipeline current amplitudes, I (amperes), could be represented, approximately, by $I = 0.65\ B_x T^{-0.5}$, where B_x (nT) is the north-south geomagnetic field variation amplitude and T^x (min) is its apparent period. There is much less pipeline current at the sites south of Fairbanks. A previously established relation between the local electric field and the planetary geomagnetic activity index, Ap, permitted a prediction of the pipeline current surge amplitudes in the Fairbanks region to be approximately $I = 5.0$.

PETROPHYSICS

Digital classification of Landsat data for identification of hydrothermal alteration

R. G. Schmidt developed a digital classification scheme to be used with Landsat data to prepare maps of altered areas for mineral evaluation studies of an area in the Sonoran Desert, southern Arizona. The classification system is a rectilinear subdivision of five spaces where the input is either the various ratios of Landsat bands or the total reflected energy. The slices or boundaries are defined on the basis of data collected from selected areas of known hydrothermal alteration in the vicinity of the Northern Silver Bell orebody, from unaltered rocks of similar spectral response to those of hydrothermally altered rocks collected from widely scattered sites, and from felsic and mafic rock categories from locations in the Quijotoa Mountains quadrangle. Five areas have been identified as probably being made up of hydrothermally altered rock. Final evaluation of the technique will be based on the results of field checking in these areas.

Electrical and magnetic borehole studies useful for defining nuclear waste repositories in volcanic rocks

Four holes were drilled and cored at Yucca Mountain, Nev., to define the location of near-surface electrical conductors detected with surface electrical measurements. Borehole geophysical studies conducted by J. J. Daniels included (1) resistivity, magnetic susceptibility, induced polarization, neutron, gamma ray, acoustic velocity, and density well logging measurements recorded on digital tape, (2) hole-to-surface DC-resistivity measurements made by placing a current source in each of the four holes and measuring the resulting total electric field on the surface, and (3) hole-to-hole DC-resistivity measurements made between all pair-combinations of the four drill holes.

Daniels' well-logging measurements indicate that conventional nuclear well logs will not be adequate to define the complex facies changes within a partially altered volcanic sequence. However, borehole electrical (resistivity and induced polarization) and magnetic susceptibility measurements show distinct anomalies resulting from variations in rock type and rock alteration. Measuring hole-to-surface DC-resistivity helps to define the near-surface lateral geologic changes, whereas hole-to-hole DC-resistivity helps to define lateral geologic changes that are located at depth between the drill holes.

Spectral signatures in the 0.4- to 1.1-μm range

On the basis of laboratory reflection spectra recorded from an extended suite of rocks, G. R. Hunt has made the following generalizations to assist in remote sensing activities:

- For unaltered rocks, (1) felsic rocks display the highest overall featureless reflectance, (2) intermediate rocks have lower featureless reflectance, (3) mafic rocks have the lowest reflectance, with a band near 1.0 μm due to Fe^{2+}, (4) ultramafic rocks are more

reflective than mafic rocks and display a very intense 1.0 μm band due to Fe^{2+}, and (5) sedimentary and metamorphic rocks, when transparent, display characteristic bands due to crystal field transitions, such as those due to Mn^{2+} in marbles and due to Cr^{3+} in quartzites.

- Altered rock spectra are dominated by features due to ferric oxides, oxyhydroxides, and sulphate. The color of altered rocks is largely a function of Fe^{3+} concentration. Absorption due to change transfer in Fe^{3+}-O dominates the short wavelengths, and crystal field bands due to Fe^{3+} occur near 0.65 and 0.9 μm. Hematitic and geothitic rocks can be distinguished on the basis of the exact location of the 0.9-μm feature. A sharp feature near 0.435 μm indicates the presence of jarosite.
- Sulfides display a sharp absorption edge whose position is characteristic of the metal ion present.

Physical property statistics and geologic noise

G. R. Olhoeft performed a statistical analysis of the physical properties data base of the USGS Petrophysics Laboratory. Using the statistical variability of dry bulk density as an indicator of the statistics of other physical properties (because most are related to density in a variety of ways), a statistical measure of the amount of irreducible scatter or geologic noise may be deduced for field measurements of geophysical parameters in various media. Statistics were determined for 16 different rock types, with most falling near a geologic noise of 9 percent. This geologic noise was found to vary from <1 percent in locally homogeneous regions, such as a salt dome or a granite quarry, to 3 percent in all granites, 9 percent in all gabbros, 16 percent in all sandstones, to 24 percent in all basalts. Thus, an anomaly that is detectable in granite may be hidden by geologic noise in sandstone or basalt. This has serious implications for the detectability of small mineral deposits and for the certification of the absence of faults or other anomalies in the waste isolation problem.

In addition, the statistical distributions for most rocks are not symmetrical distributions. Thus, the mode and mean are not the same. A least-square fit to a formula for seismic velocity versus density used in field data interpretation could cause serious error because least-square regression finds the mean, when finding the mode would be more appropriate.

Electrical properties of geothermal materials

G. R. Olhoeft (USGS) and H. Ucok (University of Southern California) completed a series of experiments on the electrical properties of brine and of brine-saturated sandstones, basalt, and granite as a function of brine concentration (to saturation), temperature (to 375°C), and frequency under 30 MPa hydrostatic pressure. The brine-saturated-rock studies confirmed that surface conduction along altered pore walls could be more important than volume conduction through the pore water. Thus, the traditional Archie's Law interpretation of electrical resistivity in terms of simple porosity and pore-water resistivity is invalid in rocks with strong water-rock interactions. Of the three types of rock studied, the sandstone had the least water-rock interaction unless significant clays were already present in the sample. The basalt reacted strongly, producing zeolites lining the pore walls. The granite dissolved and porosity increased from 0.7 to 1.4 percent, after 2 h at a temperature >200°C in 5 wt-percent NaCl brine, and to 2.4 percent porosity, with after an additional 2 h in the brine.

Resistivity sounding investigation in the Syncline Ridge area, Nevada

The results of a resistivity sounding survey made in the general vicinity of Syncline Ridge and its northern extensions indicate from apparent lithologic discontinuities that the region has undergone long-term tectonic upheaval. The survey, conducted by L. A. Anderson, has shown that the argillaceous argillite of the Eleana Formation, considered suitable for emplacement of radioactive waste materials, has appreciable thickness in the northern sector of the area but that its horizontal extent is probably insufficient to meet the minimum requirements set forth for waste isolation sites. Because of the lack of structural integrity of the Eleana and the limited volume of rock that can be identified as primarily argillaceous argillite, no suitable site can be identified as having the necessary attributes for nuclear waste containment.

Borehole geophysical technique to determine geologic inhomogeneities in nuclear waste storage sites

J. J. Daniels developed and tested a technique to measure the areal surface distribution of the total electric field vector (magnitude and direction) caused by a current source located in a drill hole. These measurements can be useful for locating buried geologic features, with anomalous resistivities, away from a drill hole. When these measurements are recorded in conjunction with resistivity well logs and hole-to-hole resistivity measurements, a comprehensive interpretation can be made of both the vertical and horizontal resistivity distributions that are associated with anomalous geologic features.

Daniels developed and tested a computer-assisted interpretation procedure for geophysical well logs. Product and ratio values of well logs can be used to interpret a rock type that exhibits more than one characteristic physical property. The use of product and ratio well logs

enables the interpreter to utilize all the available well log data that identify the characteristic physical properties of individual lithologies. The interpretation of product and ratio well logs can be facilitated by the use of a digital computer.

Near-infrared spectroscopy determination of degree of serpentinization in ultramafic rocks

Visible and near-infrared (0.35–2.5 μm) bidirectional reflection spectra were recorded by G. R. Hunt and R. C. Evarts for a suite of particulate samples from mineralogically well-characterized serpentinized ultramafic rocks. The spectra typically exhibit well-defined bands due to electronic and vibrational processes in the individual mineral constituents. The contrast of near-infrared spectral features of primary magnesian silicate minerals and secondary hydrous-serpentine-group minerals can be used to indicate the degree of serpentinization of the rock, provided <1 percent of finely divided magnetite is present. Magnetite, apparent in rocks with >50 percent serpentine, reduces the overall reflection and the contrast of spectral features. Near-infrared spectrometry is potentially a rapid and reliable technique for detecting the highly serpentinized rocks that constitute target areas for asbestos exploration.

Nonlinear complex resistivity logging

G. R. Olhoeft and J. H. Scott have successfully tested the first nonlinear complex resistivity logging system in the GP-1 Sulfur Gulch borehole near Delta, Colo. The initial field tests confirmed that nonlinear responses expected from theory and measured in the laboratory were observable in the field. Interpretation of the data showed the usefulness of the technique in delineating and discriminating oxidation-reduction-reacting material lithologies (oxides, sulfides, and so forth) from cation-exchange-reacting lithologies (clays and zeolites). Relative amounts of sulfide, carbonaceous matter, and clays were determined readily by the nonlinear complex resistivity technique, and relative changes in cation-exchange capacity were logged. The various types of nonlinear response cited by Olhoeft (1979) were confirmed to be present in situ. Thus, nonlinear complex resistivity logging can be used to measure geochemical parameters such as ground-water Eh and pH, to discriminate sulfides versus clays, to map relative changes in cation-exchange capacity, and to determine the oxidation state of minerals. Careful application of the technique and computer analysis also can determine whether the current oxidation state of the minerals in situ is in equilibrium with the existing ground water.

Tectonic features in southeastern Missouri from remote-sensing and geophysical data

"Linear-feature" maps produced from computer-enhanced Landsat images of southeastern Missouri by D. H. Knepper, Jr., reveal unusual patterns of linear-feature concentration. Of greatest interest is a pattern of linear-feature concentration that suggests the presence of a circular feature 50 km in diameter in the central St. Francois Mountains. The feature does not appear on published geologic maps, but some mapped structures apparently coincide with its perimeter, which follows closely the drainage divide around the Black River drainage basin.

The circular feature is more evident in geophysical maps, but it was originally detected through the interpretation of remote-sensing data. The Rolla 2° quadrangle gravity map shows that the feature consists of an outer ring of low gravity anomalies surrounding a prominent central gravity high. An aeromagnetic anomaly map shows a corresponding outer ring of magnetically low relief and low intensity terrain surrounding terrain of high magnetic relief and intensity. The source of the geophysical anomalies is in the Precambrian basement; it may be the deeply eroded roots of a caldera associated with the eruption of Proterozoic Z ash-flow tuffs.

The reevaluation of the gravity and magnetic data also revealed numerous northeast- and northwest-trending geophysical lineaments in southeastern Missouri. The lineaments are discontinuities in the Precambrian basement, probably shear zones, that juxtapose basement rocks of different geophysical characteristics and appear to have influenced geologic processes in the region. Mafic to ultramafic rocks of Precambrian to late Paleozoic age in the region all lie along lineaments, as do the Decaturville, Hazelgreen, and Crooked Creek cryptovolcanic features. Some of the lineaments also are expressed in the topography of the basement surface and in structure-contour maps of lower Paleozoic strata. Northwest-trending lineaments extend southeastward from the Ozark region to link with northwest-trending magnetic lineaments by Hildenbrand and others (1979) on the northwest side of the northeast-trending Proterozoic Z(?) rift zone (Reelfoot graben) in the upper Mississippi embayment. Spatial relations of mafic and ultramafic rocks to lineaments in southeastern Missouri suggest that the lineaments may have provided suitable pathways along which igneous material generated along the rift zone may have migrated and been emplaced outside the borders of the rift. This may explain the ultramafic affinities found in geochemical analyses of the lead deposits in southeastern Missouri.

APPLIED GEOPHYSICS

Computer programs for resistivity soundings over three vertical layers

A. A. R. Zohdy and R. J. Bisdorf have written three computer programs for the Hewlett Packard 9845–T desk top computer. These programs compute and plot theoretical apparent resistivity sounding curves obtained over three vertical layers using either the pole-dipole (also known as half-Schlumberger, Lögn, or Bristow) array in which the current electrode is fixed and the potential electrodes are moved, the dipole-pole array in which the potential electrodes are fixed and the current electrode is moved, or the symmetric Schlumberger array. All three programs are for arrays oriented at right angles to the strike of the vertical layers, and all programs are based on the Gauss–La Guerre method of numerical integration. Each program is suitable for the computation and plotting of a single specific sounding curve or for a set of master curves. Extensive graphical diagrams, prompting statements, and error messages are displayed on the 9845–T CRT to simplify the use of the programs.

New technique for electromagnetic modeling and inversion

A new technique (Anderson, 1979) for the rapid evaluation of related Hankel transform integrals was developed. This method, using digital linear filter theory, is extremely rapid in comparison with conventional numerical quadratures. Accuracy of the digital filters is good to approximately 10^{-5} relative errors when tested with known (analytical) Hankel transform pairs. Application of this method to many practical forward and inverse electromagnetic solutions results in significant savings in computer time. For example, inversion of loop-loop electromagnetic frequency soundings using related-convolution methods is about 50 to 80 percent faster than using direct-convolution methods.

Inversion of self-potential data

D. V. Fitterman developed a procedure for inverting self-potential data produced by a vertical contact. The method was used successfully on data collected at the Cerro Prieto geothermal field by R. F. Corwin (University of California at Berkeley) (Fitterman and Corwin, 1979). Estimated model parameters agree well with what is known about the production zone. The inversion technique, however, has some shortcomings. Several of the model parameters are correlated highly; therefore, only products or ratios of changes of these parameters can be determined. The addition of geologic information is helpful in constraining the models. The exact source mechanism of the Cerro Prieto anomaly still is not clear; prime candidates are streaming potentials and thermoelectric effects. More laboratory measurements at in situ conditions are needed before a definitive statemen about the source mechanism can be made.

Improved methods of seismic refraction interpretation

H. D. Ackerman has written an interactive computer program for interpretation of seismic refraction data in terms of both depth to refraction horizons and lateral velocity changes. This program is being used on a routine basis in the interpretation of refraction data. Correlation of seismic results with drill hole data is very satisfactory.

Model study of experimental electromagnetic method

M. C. Olm carried out model studies of a method to reduce the effects of a conductive overburden on electromagnetic measurements. In this technique, the quadrature responses are normalized by frequency and then differenced for various pairs of frequencies. Results using this technique were highly effective over a limited range of frequencies and conductivities for a model orebody beneath an inhomogeneous overburden.

Electromagnetic response of cultural features

Several airborne INPUT electromagnetic and ground slingram and VLF-EM lines were made over a pipeline near Denver and over a pipeline in northern Wisconsin. According to J. C. Wynn, a relatively large INPUT anomaly was observed over the pipeline in Wisconsin, whereas no INPUT anomaly was observed over the pipeline near Denver. Conversely, the ground slingram and VLF anomalies were smaller for the Wisconsin pipeline than for the Denver pipeline. The differing results probably are due to the large difference in earth resistivity, which is about 20 ohm-m at the Denver site and >100 ohm-m at the Wisconsin site, and to large differences in the induction numbers for the INPUT and slingram systems.

Borehole measurements to differentiate sulfides and clays

J. H. Scott and J. J. Daniels tested a nonlinear complex resistivity borehole measurement probe that has four platinum electrodes arranged in the Wenner configuration. Results indicated that the probe can detect and distinguish between anomalies produced by clays and metallic sulfides, both of which are associated with uranium mineralization and often form halos around uranium deposits. The presence of clays and sulfides is indicated by a phase shift of the received sinusoidal waveform, and differentiation between the two is accomplished by analysis of harmonic distortion of the waveform.

Resistivity study of the San Augustine aquifers, New Mexico

A. A. R. Zohdy and R. J. Bisdorf made 63 intermediate (AB/2=3 km) and deep (AB/2=10 km) Schlumberger resistivity soundings over an area of approximately 700 km² in the San Augustine plain, N. Mex., to study the lateral and depth distribution of aquifers with potable water and to delineate areas with poor quality waters. The sounding data were interpreted automatically, and 10 computer-generated geoelectric cross sections were prepared. In the northeastern part of the plain, the geoelectric sections are characterized by the presence of about 50 m of 35 to 100 ohm-m material (near-surface aquifer of silt, sand, and gravel) that is underlain by material having a relatively low resistivity of about 10 ohm-m (clays?) to a depth of about 300 m. Volcanic(?) rocks having a resistivity of 100 to 200 ohm-m, which may form a deep aquifer with water of good quality, underlie the section to a depth of at least 1 km. In the middle part of the plain, the near-surface aquifer extends to a depth of 100 to 400 m and is underlain by clays(?) having a resistivity of 10 to 15 ohm-m to depths of about 1,000 m. In the southwestern portion of the plain, the aquifer is primarily characterized by very low resistivities (1–5 ohm-m), except near the margins of the plain, indicating the predominance of saltwater in the aquifer.

Airborne geophysical survey for uranium

A combined helicopter-borne magnetic, electromagnetic, and radiometric survey was made of the Schwartzwalder mine area near Golden, Colo. B. D. Smith and V. J. Flanigan found that total count, uranium, thorium, and potassium anomalies occur only where there has been surface contamination from existing mining operations. However, electromagnetic and magnetic data can be used to indicate areas where there are regional faults. Further, the electromagnetic anomalies probably indicate the portions of the fault zones that are most permeable because of locally intensive fracturing and alteration. At the Schwartzwalder mine, the most permeable zones are most favorable for uranium mineralization. The airborne geophysical data correlate well with available ground geophysical data where the two types of surveys are coincident. The ground geophysical data resolve details of the geology better than the airborne data. However, the airborne survey demonstrates that such combined surveys may be used effectively to define favorable geologic settings for uranium mineralization where standard radiometric methods are not definitive.

Mineral resource assessment using aerial geophysical data

Interpretation of radiometric and magnetic data collected in an aerial survey of the Sierra Ancha Wilderness Area and vicinity, Gila County, Ariz., by J. S. Duvall and J. A. Pitkin accurately locates the majority of known uranium deposits and asbestos-iron mineralization sites. The characteristics of known deposits were used to establish criteria to construct a map that indicates where uranium or asbestos-iron mineralization may occur. Many of the known and possible mineralized sites lie within or near the wilderness area.

The radiometric data also show that some areas of diabase have significantly different values from those of most of the diabase within the survey area. The diabase in these areas may have a different chemical-physical origin than most of the mapped diabase. An area characterized by low magnetic intensity, low gravity values, and high geochemical values for a number of elements suggests the existence of a buried pluton that could be mineralized. The location of this suspected pluton lies to the west of the Sierra Ancha Wilderness Area.

Aerial gamma-ray spectrometric and magnetic data were obtained to aid in analysis of the mineral resource potential of the proposed Salmo-Priest Wilderness and of Pend Oreille County, Wash., and Boundary County, Idaho. Interpretation of the geophysical data shows that concentrations of radioactive and magnetic minerals can be explained by normal lithologies and mapped structures.

Mineral geophysical surveys in Wisconsin and Michigan

The results of a regional INPUT electromagnetic (EM) airborne geophysical survey of part of the Iron River 2° quadrangle have been used by B. D. Smith to help reinterpret the regional geology of the survey area. EM anomalies within the area suggest a moderate potential for the occurrence of structurally controlled uranium mineralization. Stratigraphic units within a metavolcanic sequence can be differentiated and assessed separately for the potential occurrence of massive sulfide deposits. Consequently, regional airborne EM surveys can be used very effectively to (1) aid geologic mapping, (2) assist in the development of making genetic-models for particular types of mineral deposits, and (3) assist in estimating potential mineral resources.

Detailed airborne geophysical surveys on selected Indian lands in Wisconsin have defined anomalies that may indicate the presence of massive sulfide mineralization. Ground EM, magnetic, and gravity methods have been used to define drilling targets. A comparison of ground EM techniques indicates that all the techniques can detect the airborne anomalies. However, the work to date suggests that conventional geophysical methods should not be used solely as anomaly finding techniques but should be interpreted as completely as

possible to indirectly detect favorable areas for potentially economic mineralization.

Geophysical studies of earth fissures

Precise geophysical surveys across ground failure zones related to ground-water withdrawal at nine sites in the Picacho Basin in south-central Arizona indicate that earth fissures in alluvium near exposed bedrock are associated spatially with local gravity and magnetic anomalies ranging from local highs to convex-upward changes in slope. R. C. Jachens and T. L. Holzer have interpreted the gravity anomalies, which range from 0.1 to 1 mGal with half-widths of 50 to 300 m, to be caused by convex-upward irregularities in the bedrock surface underlying the alluvial aquifer. Most irregularities are inferred to be at depths <250 m. Bedrock irregularities were not detected beneath failures that are >2 km from bedrock outcrop. The association of earth fissures with zones of variable aquifer thickness suggests that differential compaction is occurring near these fissures. Estimates, based on the finite element method, of horizontal strains generated by localized differential compaction suggest that this mechanism is the dominant source of horizontal tension causing earth fissures in Picacho Basin. Analysis indicates that tensile strains at fissures at the time of formation ranged from 0.1 to 0.4 percent.

Prediction of the location of earth fissures near exposed bedrock in the Picacho Basin and in adjacent basins with similar geologic settings appears feasible by delineation of convex-upward bedrock irregularities. Failures far from exposed bedrock, however, may not be as readily predicted on this basis. If the rheological properties and thicknesses of subsurface materials are known, the amount of water-level decline required to induce sufficient differential compaction and to cause failure at potential earth fissures can be predicted.

Geomagnetic variation studies

Geomagnetic transfer functions for data collected in the eastern Snake River Plain, Idaho, indicate a reversal in direction across the plain. D. V. Fitterman reports that this change in the direction of the induction arrows probably is due to a conductivity anomaly associated with the eastern Snake River Plain. A secondary feature, rotation of the arrows toward the southwest, may be due to current flowing from the Basin and Range province across the plain.

A new technique for analyzing short segments of data was used to obtain these results. In this procedure, consecutive data segments are analyzed to obtain high-frequency information and then are lowpass filtered and decimated. The decimated data then are analyzed to obtain information at lower frequencies.

Geophysical studies of the Rio Grande Rift

Compilations of regional geophysical data by L. E. Cordell show the Rio Grande Rift to encompass uplifts of the Southern Rocky Mountains and their southern extension, as well as axial fault blocks. Gravity gradients delineate major faults, which show a gridded or en echelon pattern over distances on the order of tens of kilometers. Aeromagnetic data show these faults to be alined with basement structural grain; by inference, the Neogene-age rift faults zigzag along preexisting basement cracks.

Gravity-magnetic surveys in southeast Missouri

L. E. Cordell has shown that gravity and aeromagnetic data from the southeast Missouri lead district delineate felsic plutons associated with ash flow tuff and related rocks of the St. Francois Mountains and delineate a large mafic pluton near Salem, Mo. The geophysical data do not support concepts of a "Taum Sauk caldera" and "fundamentally gridded" basement fabric previously proposed. New aeromagnetic data west of the known lead district show contrasting magnetic patterns over volcanic versus plutonic terranes similar to patterns observed in the St. Francois Mountains.

Study of diabase dikes

Previous research on diabase dikes in eastern North America has subdivided the diabase magma types into three main groups: (1) high-titanium quartz-normative, (2) low-titanium quartz-normative, and (3) olivine-normative. A study of recent USGS regional aeromagnetic data from the North Carolina Piedmont by Isidore Zietz (USGS) has provided a basis for reexamination of the predominately olivine-normative types by R. C. Ragland and R. D. Hatcher, Jr. (Florida State University).

Based upon dike orientations and geographic distributions, four domains are recognized from southwest to northeast: I, dominated by northwest-southeast-trending dikes; II, north-south dikes; III, northwest-southeast dikes; and IV, a composite domain exhibiting several dike sets. Major and trace element data were compared for dikes within these domains. Tentative conclusions are (1) diabase magmas from domain I were more primitive (less evolved) than those from domain II, (2) based upon an inadequate sample, diabases from domain IV may be more similar to I than to II, (3) domain III is chemically enigmatic, and (4) apparently two and possibly three olivine-normative magma types existed in the Piedmont.

Presently, no information is available concerning the relative ages of these magma types. However, these data suggest that the Mesozoic history of rifting in

eastern North America is much more complex than can be explained by existing tectonic models, such as that of May (1971) or deBoer and Snider (1979).

Present-day convergent margin tectonics is defined by an arcuate distribution of volcanic-plutonic rocks. The curvature of these arcs has been used to estimate convergence rates and angles of subduction. Recognition of such arcuate distribution of igneous rocks belonging to a single orogeny in the geologic past provides important constraints on paleotectonics.

Along the Eastern United States (Maryland to Georgia), the distribution of Hercynian (330 m.y.–260 m.y.) plutons defines an acceptable arc pattern. Although extensive erosion has removed all evidence of volcanic rocks, the plutons define a radius of curvature with an angle of 5.6° (Tovish and Schubert, 1978) and, by analogy with recent arcs, a spreading rate of less than 5 cm/yr. Although the geochemical and geophysical evidence is complicated by a late Hercynian continent-continent collision, the intergrity of the arcuate pattern suggests that only minor readjustment of the arc has occurred. This model suggests that the allocthonous nature of portions of the central Appalachians (Blue Ridge province and inner Piedmont), as documented by recent COCORP (Consortium for Continental Reflection Profiling) data, may not extend beyond the present-day fall line or even the King's Mountain Belt.

Evidence for fossilized rifts and reactivation of basement faults

A quantitative study of aeromagnetic data by J. D. Phillips for central and western New York has revealed basement structures that are interpreted to be fossilized Precambrian rift zones. The best defined of these rests lies along the north-northeast trending Clarendon-Linden fault zone in western New York. Another parallel rift zone is seen 100 km to the east of the Clarendon-Linden structure. Aeromagnetic anomalies over the rift zones display some degree of axial symmetry. Depth estimates made from the aeromagnetic data show depression of the magnetic basement within the rift zones and also help locate the border faults of the rifts. A limited amount of deep-well data suggests that the relief on the crystalline basement over the rift zones is much less than the relief on the magnetic basement. This would be the case if the former rift fill material had been altered metasediments without becoming strongly magnetic. In addition to the rifts, the magnetic depth estimates reveal other apparent basement structures such as faults, ridges, and domes.

Seismic activity along the Clarendon-Linden fault zone indicates that basement faults can be reactivated under the present-day east-west compressive stress regime. A strong correlation exists between magnetic basement structures and surface lineaments in south-central New York. Thus, much of the surface topography and drainage pattern in this area may be controlled by post-Alleghanian reactivation of basement faults.

GEOCHEMISTRY, MINERALOGY, AND PETROLOGY

EXPERIMENTAL AND THEORETICAL GEOCHEMISTRY

Correct use of the rule of tangents and its petrologic applications

In ternary systems, the rule of tangents is the commonly used method of determining the relative proportions of two solid phases at any instant during equilibrium crystallization from a liquid. However, if one or both of the solid phases are solid solutions, the rule of tangents does not apply. A graphical method was developed by B. R. Lipin for determining the proportions and compositions of solid solutions crystallizing at any instant in a ternary system.

Pyroxene-tridymite relations in the system MgO-FeO-SiO_2 were examined using this geometrical analysis, and a criterion was set up for determining whether, and at what point during equilibrium crystallization, resorption will take place in any ternary system, without resorting to successive approximation using many three-phase triangles. An important petrologic principle is illustrated by the pyroxene-tridymite-phase relations—the proportions of two crystallizing solid phases can vary considerably along a straight boundary curve. The solid phases vary their proportions in response to their own compositional changes during crystallization. This phenomenon can explain the occurrences of some mineral-graded layers in stratiform intrusions.

Relations between lattice dynamics and thermodynamic properties of minerals

A simple approximation to the lattice vibrational spectra of minerals has been developed in a series of papers by S. W. Kieffer (1979a, b, c) and applied to problems in prediction of heat capacities as a function of pressure and temperature, in phase equilibria, and in oxygen isotope fractionation. In this model, the primitive unit cell, containing s atoms, is chosen as the fundamental vibrating unit of the crystal; it has $3s$ degrees of freedom, three of which are acoustic modes. Anisotropy of these modes is included by using anisotropic shear velocities for the two shear branches; dispersion is included by using a sinusoidal dispersion relation between frequency and wave vector for all three acoustic branches. Optic modes, which have $3s$–3 degrees of

freedom, are represented by a uniform continuum, except for "intramolecular" stretching modes (such as SiO or O-H stretching modes) that can be enumerated and identified as isolated from the optic continuum. Parameters for the model are obtained from elastic and spectroscopic data. The model is independent of any calorimetric data. The average deviation of predicted 298 K entropies from well-determined calorimetric values is ~2 percent. The model is only a simple approximation to real lattice vibrational spectra but appears to work well for a large number of minerals (more than 30 examined to date) and is useful in correlating structural, compositional, elastic, spectroscopic, and thermodynamic properties for the purposes of extrapolation and prediction of these properties.

Reevaluation of the thermodynamic properties of minerals in the system CaO-Al_2O_3-SiO_2-H_2O

J. L. Haas, Jr., G. R. Robinson, Jr., and B. S. Hemingway (1979) completed a revision of the data for heat capacity, entropy, enthalpy of formation, and free energy of formation for gibbsite, diaspore, boehmite, kaolinite, dickite, halloysite, pyrophyllite, kyanite, sillimanite, andalusite, wollastonite, cyclowollastonite (pseudowollastonite), rankinite, calcium-olivine, larnite, bredigite, anorthite, gehlenite, grossular, calcium-aluminum clinopyroxene, margarite, zoisite, and prehnite. The revision includes major changes in the data for anorthite, gehlenite, grossular, calcium-aluminum and rankinite (Robie and others, 1978).

Novel heating-freezing fluid inclusion stage

A gas-flow heating-freezing stage has been developed by R. W. Werre, Jr., R. J. Bodnar, P. M. Bethke, and P. B. Barton, Jr., that allows rapid accurate fluid-inclusion measurements from −150° to >700°C. Heating and cooling are accomplished by forcing externally heated or chilled gas over the sample. The INVAR alloy sample may be observed using a X 32 (without hemispheres) universal stage objective having a 6-mm working distance; a chamber accommodating plates up to 5 mm thick is available for use with a X 10 objective having a 14-mm working distance. Triple silica-glass windows are placed above and below the sample with dead air enclosed by the outer pairs. Gas first passes between the innermost pairs above and below the sample chamber, into the sample chamber, and finally out through exit ports in the walls of the chamber. This circulation pattern provides nearly instantaneous thermal response while minimizing thermal gradients within the chamber. Gradients over approximately 75 percent of the viewing area are ~1°C at 150°C, ~3°C at 350°C, and ~5°C at 550°C. The temperature distribution is repeatable, allowing corrections to be made, reducing the temperature uncertainty to approximately ±1°C at 500°C. The large sample chamber greatly simplifies sample preparation and documentation and minimizes setup time. This and the rapid response time allow many fluid inclusions to be examined in a relatively short time when compared with other stages in current use, with no loss in precision or accuracy. The external temperature control and simple design minimize "down time" due to equipment failure.

Decomposition mechanism and kinetics in clinopyroxenes

Identification of the mechanism and determination of the kinetics of exsolution processes in clinopyroxenes provide a useful geologic parameter for determining the subsolidus thermal history of rocks. G. L. Nord, Jr. (USGS), and R. H. McCallister (Purdue University) examined both natural and synthetic clinopyroxenes by X-ray diffraction and by transmission electron microscopy to calibrate the exsolution kinetics.

Twelve subcalcic diopsides ($Fe/(Mg+Fe)=0.12$–0.14) from eight kimberlite pipes in Lesotho and South Africa were examined for evidence of exsolution. Five samples having $Ca/(Ca+Mg)\geq 0.33$ show no evidence of exsolution, whereas of seven samples having $Ca/(Ca+Mg)<0.33$, six have exsolved $pigeonite_{ss}$, and one shows no phase separation. The exsolved pigeonite is always coherent on (001) with the host $diopside_{ss}$, and the interlamellar spacing ranges from 13.4 to 31.4 nm. Compositional estimates of both the host and exsolved phases were made using measured β*s on *h0l* X-ray precession photographs. Host compositions of three exsolved kimberlitic diopsides with $Ca/(Ca+Mg)_{bulk}=0.32$ plotted on the coherent solvus give quench temperatures from 1,040° to 1,245°C, which reflect differences in the P–T path followed by the kimberlite.

To follow the development and calibrate the kinetics of exsolution in the kimberlite clinopyroxenes, synthetic clinopyroxenes ($Ca_{0.25}Mg_{0.31}Fe_{0.44}Si_2O_6$) were crystallized from a gel with excess SiO_2 at 1,200°C, 20 kbar for 24 h. The quenched-in microstructure consisted of poorly defined ~10 nm-wide lamellae oriented near (001) and (100), which caused minor streaking in *h0l* electron-diffraction patterns; no evidence for two lattices was observed.

Portions of the $Wo_{25}En_{31}Fs_{44}$ clinopyroxene product were wrapped in platinum foil with iron filings to maintain reducing f_{O_2} conditions; sealed in evacuated silica tubes; heated isothermally at 1,000°, 900°, and 800°C for 0.3, 3, 39, 359, 1,600, and 3,887 h; quenched; sectioned; ion-thinned; and examined in a 200-kV transmission-electron microscope. Only one set of lamellae, now perfectly periodic and parallel to (001), was observed; it gave rise to sharp satellite reflections. Wavelengths (λ) were measured from images and were

calculated from satellite spacings in both *h0l* and *0kl* diffraction patterns. Amplitudes (composition differences) were determined from the value of β for each phase. λ remained constant during decomposition—~2.50 nm at 1,000°C, ~14.5 nm at 900°C, and ~8.5 nm at 800° C, whereas amplitude increased with time. After completion of decomposition (~1,000 h in the 1,000°C run), λ began to increase, and the amplitude remained constant.

The results of this set of experiments prove that the spinodal decomposition mechanism operates in iron-bearing clinopyroxene. That is during isothermal decomposition, λ is constant with increasing time, whereas composition differences increase with increasing time. When the lamellar compositions are on the coherent solvus, decomposition ceases and coarsening begins; the amplitude remains constant, and λ increases with time. Because there is no nucleation barrier to spinodal decomposition, the kinetics of decomposition are controlled only by the activation energy for diffusion and the diffusion rates. These parameters can be determined by careful experimentation, and a general kinetic theory for decomposition in pyroxene, therefore, can be developed.

Combined energy dispersive and wavelength dispersive analysis

L. B. Wiggins has combined wavelength dispersive (WD) and energy dispersive (ED) electron microprobe analysis techniques on the ARL microprobe in Reston, Va., so that they operate simultaneously to produce a single electron microprobe chemical analysis. The combined operating mode for analyses of rock-forming minerals and ores is faster (2 to 3 min versus 5 min) than WD mode alone and reduces mechanical wear on the spectrometers. The ED mode also offers easier and more rapid element standardization than does the WD mode. Precision of analyses obtained under combined mode is comparable to WD mode alone if data for elements with low atomic number (for example, sodium or magnesium) and minor or trace elements are collected by the WD portion of the system.

Thermodynamic properties of minerals

R. A. Robie and B. S. Hemingway have measured the heat capacities of tephroite (Mn_2SiO_4), forsterite (Mg_2SiO_4), fayalite (Fe_2SiO_4), cobalt olivine (Co_2SiO_4), and chalcopyrite ($CuFeS_2$) by cryogenic adiabatic calorimetry between 5 and 380 K to obtain their standard entropies at 298.15 K (25.0°C). The entropies derived from the measurements are tephroite, 155.9±0.4; forsterite, 94.11±0.10; fayalite, 151.0±0.4; cobalt olivine, 146.6±0.2; and chalcopyrite, 124.9±0.1 J/(mol·K).

Liebenbergite (Ni_2SiO_4), tephroite, fayalite, and cobalt olivine exhibit paramagnetic to antiferromagnetic transitions at 29.1, 47.38, 64.88, and 49.76 K, respectively, which are expressed by sharp λ-type maxima in their heat capacities at these temperatures.

Robie and Hemingway also completed evaluation of their earlier measurements on the heat capacities of paragonite ($NaAl_2[AlSi_3O_{10}](OH)_2$) and phlogopite ($KMg_3[AlSi_3O_{10}](OH)_2$) and developed a new approach to correct for impurities in solid solution in the samples. The resultant values of entropy difference, $S°_{298}$-$S°_0$, are 277.1±0.6 and 315.9±0.9 J/(mol·K), respectively.

Melting relations in the system Fe-S-O

The outer core of the Earth must contain appreciable amounts of a light element(s) because its density is 8 to 10 percent lighter than that of iron at the same pressure and temperature. Models for the origin of the Earth's core by segregation of iron melts enriched in oxygen (Ringwood, 1977) or sulphur (Murthy and Hall, 1970) have been proposed to account for the anomalous density. To evaluate these alternatives and to better understand the processes of planetary core segregation, R. F. Wendlandt and J. S. Huebner determined the melting relations of portions of the system Fe-S-O at 30 kbar. The solubility of oxygen in the ternary eutectic melt (Fe+FeO+FeS+L) decreased with increasing pressure from 7.5 wt percent at 1 atm (Naldrett, 1969) to less than 1 wt percent at 30 kbars. Therefore, iron melt segregations in the upper mantle, presumably occurring at an early stage of the Earth's postaccretional evolution, did not contain appreciable oxygen. These results suggest that the presence of sulphur in the core is more likely than that of oxygen.

MINERALOGIC STUDIES IN CRYSTAL CHEMISTRY

Copper-rich sulfides—low chalcocite and djurleite

H. T. Evans, Jr., and J. A. Konnert have continued a program on the crystal chemistry of the copper-rich sulfides with studies of covellite (Geological Survey Research 1976, p. 166, 1976), betekhtinite, stromeyerite, low chalcocite, and djurleite. The most notable achievement was the successful structure analysis by Evans of low chalcocite and djurleite, which are principal ore minerals of copper. The crystal structure of low chalcocite, Cu_2S (from Bristol, Conn.), was solved some time ago and that of djurleite, $Cu_{1.94}S$ (from Ozark mine, Sweetwater, Mo.), quite recently; both structure models have been brought to a high degree of refinement. The number of atoms found in the structure analyses confirms the simple stoichiometry of low

chalcocite (Cu:S = 24:12 = 2:1) and the lower copper content of djurleite (62:32 = 1.938:1). This composition for djurleite is at the lower end of the range of homogeneity, 1.934 to 1.965, determined by electrochemical means by R. W. Potter II (1977). Presumably, an additional site for a copper atom exists in the structure that would yield a ratio corresponding to the upper end (63:32 = 1.969:1), but it could not be found in this crystal. Both structures are monoclinic and very complex. Low chalcocite contains 12 different sulfur atoms and 24 copper atoms; djurleite contains 32 sulfur atoms and 62 copper atoms, all in different sites. Both structures contain sulfur atoms in hexagonal close packing, with about one-third of the copper atoms located in alternating sulfur triangles in the close-packed layers, and the remainder located in sloping triangular sites between the layers. In djurleite, one copper atom is in linear twofold coordination. These structures provide a rich source of data for studying the copper-sulfur bond—over 300 links averaging about 0.232 nm but ranging from 0.216 to 0.263 nm. Copper-copper interactions are also significant, with 390 approaches less than 0.3 nm, averaging about 0.275 nm but some as short as 0.245 nm. Data from these structures and from comparison with other structures indicate that the coordination of copper with sulfur trends, with increasing Cu:S, from tetrahedral (for example, chalcopyrite) to triangular (chalcocite, djurleite) to linear (djurleite). The valence-bond interpretation of bond lengths that is useful in explaining oxide structures does not work in interpreting sulfides. More work is needed to improve understanding of the chemical bonding in sulfide structures.

Alkali-iron sulfides from Coyote Peak, Humboldt County, California

An unusual suite of alkali-iron sulfides was reported previously by R. C. Erd and G. K. Czamanske (Geological Survey Research 1978, p. 178, 1978). The crystal structures of three of these sulfides have been solved in a cooperative program by J. R. Clark, H. T. Evans, Jr., and J. A. Konnert. Clark (USGS) and G. E. Brown (Stanford University) found the structure of rasvumite, KFe_2S_3, to be isostructural with synthetic $BaFe_2S_3$. This precise structure determination corrects the erroneous composition reported for this mineral in the original Russian description. The orthorhombic structure consists of FeS_4 tetrahedra highly condensed by edge sharing to form infinite double chains interconnected by K^+ ions.

The structure of monoclinic erdite, $NaFeSD_2 \cdot 2H_2O$, was solved by Konnert and Evans and found to be very similar to the structure of the synthetic phases $KFeS_2$, $RbFeS_2$, $CsFeS_2$, and $TlFeS_2$. The crystals are soft, fibrous, and built of FeS_4 tetrahedra linked by sharing opposite edges into single chains. The presence of interchain water molecules was established clearly in the structure analysis, complementing the uncertain (indirect) determination in the microprobe analysis. This water is lost readily when erdite is heated in a vacuum and then regained when erdite is exposed to air.

The structure of tetragonal bartonite, $K_6(S,Cl)Fe_{21}S_{26}$, has been solved by J. R. Clark and found to be related closely to cubic djerfisherite, $K_6ClFe_{24}S_{26}$, and pentlandite, $(Fe,Ni)_9S_8$. All contain the compact Fe_8S_{14} cluster consisting of eight highly condensed edge-shared tetrahedra. In bartonite and djerfisherite, one-fourth of the clusters in the pentlandite cubic unit cell are replaced by $K_6(S,Cl)$ units; the two differ mainly in the stacking sequence of the Fe_8S_{14} clusters. Microprobe study of bartonite (Czamanske) indicates a considerable deficiency in iron, which may be independently determined by crystal structure refinement. This study is being continued.

Tachyhydrite

The extremely hydrophilic mineral tachyhydrite, $2MgCl_2 \cdot CaCl_2 \cdot 12H_2O$, is an important constituent of many salt beds. The crystal structure of a synthetic tachyhydrite has been solved and refined to a high degree of accuracy, including direct determination of hydrogen positions, by J. R. Clark. The rhombohedral structure consists of $Mg(H_2O)_6$ octahedra and $CaCl_6$ octahedra loosely linked together by hydrogen bonds. Its chemistry, thus, is best expressed by the formula $[Mg(H_2O)_6]_2[CaCl_6]$. The structure is closely related to that of $[Ni(H_2O)_6][SnCl_6]$ and many other synthetic double chloride hydrates, but tachyhydrite is the first accurate structure determination in the group. A report on the structure and crystral chemistry has been prepared by Clark and H. T. Evans.

VOLCANIC ROCKS AND PROCESSES

HAWAIIAN VOLCANO STUDIES

Activity at Kilauea Volcano in 1979

After a 26-mo period of quiescence, Kilauea Volcano erupted briefly on November 16–17, 1979, on its upper east rift zone. Activity commenced at 0805 on November 16, with copious emission of steam from cracks east of Pauahi Crater. Lava first welled up at 0818, 230 m east of the steaming area, from a 100-m-long fissure along which a curtain of fire fountaining 5 to 10 m high quickly developed. Three min later, a fissure opened in the northwest lobe of Pauahi Crater, with the formation of low fountains at a vent on

the northeast wall. The initial eastern curtain of fire, after migrating eastward during the course of an hour, ceased erupting at 0915, but the activity in Pauahi Crater persisted. At 1130, two more vents opened in Pauahi Crater, followed shortly by a fourth; at about the same time, fountaining ceased at the first vent on the northeast wall. During the next 1½ h, five more vents opened progressively west of the crater, but before 1600 they began to wane and within the next hour ceased. Lava emission at three remaining vents in Pauahi Crater was relatively constant until 0100 on November 17, but then they, too, gradually waned and finally ceased at 0630. The entire eruptive episode lasted less than 22 h, and the volume of erupted lava was small (500,000–700,000 km^3). The lava was initially olivine-poor, fairly viscous, and probably of low temperature compared to that produced during the vigorous 1969 to 1971 Mauna Ulu eruption.

During the 26-mo interval between the 1979 Pauahi eruption and the preceding 1977 Kalalau eruption, the Kilauea summit area, with minor fluctuations, had been inflating nearly continuously; at the onset of the 1979 eruption, 95 percent of the deflation that accompanied the 1977 eruption had been regained. At 2100, on November 15, 1979, a seismic swarm was recorded near Pauahi Crater, and, 30 min later, abrupt deflation was recorded by the summit tiltmeters. Simultaneously, two borehole tiltmeters detected inflation in the upper east rift zone. During the short eruption, deflation of the summit decayed exponentially, and the total tilt amounted to only 8.04 μrad, about 6 percent of the deflation that accompanied the 1977 eruption. Reinflation of the summit commenced at 0400 on November 17, and, by December 4, about 94 percent of the deflation had been regained. Long-term records of borehole tiltmeters on the upper rift zone did not show significant tilt changes signaling that an eruption was imminent. Thus, magma from the summit area probably was intruded below Pauahi just before the eruption, possibly during the prominent seismic swarm that preceded the eruption by 30 min. However, preliminary petrography suggests that the erupted lava probably had resided below Pauahi for some time and that the migrating summit magma probably replaced it without being extruded itself.

Seismic activity during the year prior to the November 1979 eruption was sustained at moderately high levels, 200 to 400 microearthquakes per day at the summit and 100 to 200 per day on the east rift. Good correlation between tilt rate and seismicity suggests that the short-period summit earthquakes were related to keystone-type faulting produced by extension during inflation. Seismicity on the east rift increased to 200 to 300 microearthquakes per day in March 1979. In May, July, August, and September, sharp earthquake swarms occurred; those in May and August were accompanied by small summit deflations and rapid downrift propagation of earthquakes, suggesting downrift migration of magma from the summit reservoir. During the 2-mo period before the 1979 eruption, earthquakes in the upper rift zone fluctuated up to 800 events per day, and there was a notable increase in summit inflation. The main preeruption swarm that began at 2100 on November 15 near Pauahi Crater peaked in intensity at about 2400 on November 15 and gradually declined through the eruption. Weak harmonic tremor began in the upper rift zone with the onset of the seismic swarm and continued for 3 h; shallow tremor increased sharply in the vicinity of Pauahi at 0700 on November 16, about 1 h before the lava outbreak.

Field, petrographic, seismologic, and deformation studies confirmed that the erupted lava came from a shallow magma source in the rift zone, that it had re sided there for some time prior to eruption, and that it was replaced by magma migrating from the summit. The localization of seismicity near the eruption site 30 min before the onset of deflation of the summit, together with the lack of propagation of seismicity downrift from the summit, suggests that the eruption was initiated by structural events near the eruption site, possibly caused by strain accumulated during the preceding 26-mo period of summit inflation. The vents exhibited a right-stepping pattern suggesting the action of a left-lateral shear couple. The simultaneous onset of deflation at the summit and of inflation at the eruption site indicates that changes in pressure in the rift were transmitted immediately to the magma at the summit. This suggests that a fairly unobstructed conduit system extended between the rift and summit and that deflation of the summit probably was produced by passive draining of the summit chamber. The fairly rapid return of the summit almost to its previous state of inflation indicates that the volcano remained in a potentially eruptive condition at the end of 1979.

Mauna Loa Volcano quiescent in 1979

Continuing deformation, seismic, and gas monitoring surveys on Mauna Loa Volcano during 1979 indicated that inflation of the volcano diminished, that the earthquake count was low, and that, although the 1975 fumaroles remained very hot, the sulfur content was low.

Mauna Loa rift zones

Flow-by-flow mapping by P. W. Lipman of the 65-km-long southwest rift zone and adjacent flanks of Mauna Loa Volcano, together with about 50 new ^{14}C dates by

Meyer Rubin and E. C. Spiker on charcoal from beneath these flows, permitted estimates of rates of lava accumulation and volcanic growth over the past 10,000 yr.

The sequence of historic eruption along the southwest rift zone, beginning in 1868, shows a general pattern of uprift migration and increasing eruptive frequency and volume, culminating in the major eruption of 1950. No event comparable to 1950, in terms of volume or vent length, is evident for at least the previous 1,000 yr. Rates of lava accumulation during the historic period were several times greater than average rates for the preceding several thousand years along the southwest rift zone and adjacent flanks. Rates of lava accumulations along the zone have been subequal to those of active Kilauea Volcano during the historic period but were much longer in prehistoric time (Kilauea data by R. T. Holcomb). Thus, about 90 percent of the surface of Kilauea, but only about 30 percent of the surface of the southwest side of Mauna Loa, has been covered by lava during the last 1,000 yr.

Rates of surface covering and volcanic growth have been markedly asymmetrical along Mauna Loa's rift zone. Accumulation rates on the northwestern (Kona) side of the rift zone have been about 1.5 times greater than those on the southeastern (Kau) side. The difference apparently reflects a westward lateral shift of the rift zone of Mauna Loa away from Kilauea Volcano, which may have acted as a barrier to symmetrical growth of the rift zone.

Similar studies on the northeast rift zone of Mauna Loa by J. P. Lockwood have resulted in the discovery of two exceptionally large prehistoric lava flows, to a great extent covered by younger flows, in the dense tropical rain forest above Hilo. One flow, named the "Kuloloa flow," is a tube-fed pahoehoe originating from vents at an elevation of 2,650 m. It consists of four principal flow lobes, two of which extend over 40 km to within a few kilometers of Hilo. It has an original areal extent of over 65 km^2 and a volume of at least 250×10^6 m^3. Four ^{14}C dates by Rubin and Spiker average 1,375 yr B.P. The other flow, named the "Panaewa Picrite," consists of viscous pahoehoe and aa, issued from a vent at an elevation of 1,555 m, and is at least 30 km long. It has an original areal extent of over 60 km^2, a volume in excess of 500×10^6 m^3, and is nearly 4 km wide where it enters the Hilo quadrangle. A single ^{14}C date indicates an age of 2,890 yr B.P. for this flow.

Loihi Seamount—active submarine volcano

Loihi Seamount is an elongate submarine volcano on the south submarine slope of Kilauea Volcano. The summit of Loihi is at a depth of 945 m and is separated from the Kilauea slope by a saddle at a depth of 1,830 m. It appears unrelated to the southwest rift of Kilauea. Persistent swarms of earthquake epicenters recorded on the Island of Hawaii occur in the Loihi area.

During 1978, the USGS *R/V Samuel P. Lee* took bottom photographs and recovered a large dredge haul (300 kg) near the summit of the seamount. The photographs showed fresh-looking coherent pillowed lava flows, pillow joint-block talus, and pockets of sand and gravel. The dredge recovered apparently young pillow fragments with a glassy surface crust. All samples were covered by a thin iron-rich red-brown coating possibly formed by submarine hot spring activity. Despite the presence of interior pipe vesicles 2 to 4 mm in diameter and up to 3 cm long in many of the samples, the outer glassy rind of the pillows was remarkably poor in vesicles, averaging 1.0 volume-percent.

The seismicity at Loihi Seamount south of the summit of Kilauea confirms geologic interpretation of the seamount as an active submarine volcano. Earthquakes at Loihi occur mostly in intense swarms of a few months duration; their magnitude-frequency distribution has a high slope, or b value, of about 1.5. Both swarm nature and high b value are common characteristics of earthquakes directly associated with volcanism. A few earthquakes occur near the seamount summit at depths of 5 to 10 km below the sea floor. Unlike Kilauea, no vertical earthquake distribution occurs below the observed Loihi seismic source, and very shallow earthquakes, like those associated with the caldera and rift zones on Kilauea, appear to be absent.

Origin of Hawaiian tholeiitic basalt

T. L. Wright, H. R. Shaw, R. I. Tilling (USGS) and R. S. Fiske (Smithsonian Institution) have proposed a quantitative model for the tholeiitic stage of Hawaiian volcanism based on age-distance data for the Hawaiian volcanic chain and based on specific parameters for Kilauea Volcano. These data include an average inter-volcano distance of 55 km, a locus-line offset of 50 km, a volcano propagation rate of 2.7×10^{-4} km/yr, and a magma supply rate of 0.11 km^3/yr. They also include the assumptions that (1) magma is produced by 30 percent melting of a peridotite source, (2) asthenosphere flow beneath the Hawaiian chain is equal and opposite to the volcano propagation rate, (3) the base of the lithosphere is at 40 km, (4) the minimum thickness of the melting zone in the asthenosphere is about 27 km, and (5) tholeiitic magma is produced by shear melting potentially over the entire source volume and migrates upward at the same rate as its generation, so that little or no magma is stored in the asthenosphere. The melt is assumed to rise through the lithosphere to a shallow (2–6 km) reservoir complex along upward converging paths that define an inverted funnel of 10^4-km^3 volume. Mechanical properties of the lithosphere require that the

melt fraction within this funnel be 10^{-5} to 10^{-4}, which fixes lithosphere residence times at 1 to 10 yr.

The recent eruptive history of Kilauea is marked by the appearance at intervals of several months to years of chemically distinct batches of tholeiitic magma, the compositions of which correspond to partial melts modified only by loss of some olivine. Preservation of these compositions is explained by successive partial melting events occurring in separate parts of the source volume and by rapid transport of the melt within isolated converging fracture systems. In shallow storage, mixing of batches is retarded by lack of permeability with the reservoir complex and by greater bulk density of successive batches due to greater suspended olivine. Only single batches are involved in summit eruptions. During and between rift-zone eruptions, lateral intrusion may lead to magma crystallization and fractionation as well as mixing of batches, resulting in eruption of fractionated and hybrid magmas.

The model implies a close connection between melting, eruption, and refilling of shallow reservoirs. The lack of xenoliths in tholeiitic lavas is explained by discontinuous pulsating magma transport through narrow fractures rather than by steady-state flow through large conduits. The lithospheric funnel through which magmas are transported is deformed gradually and carried away from the active zone of melting by counterflow between lithosphere and asthenosphere and is consistent with southeastward displacement of deeper (35 ± 5 km) earthquakes beneath Kilauea. Disconnection from the source area eventually leads to termination of tholeiitic volcanism at one center and initiation of a new tholeiitic shield-building episode to the southeast along the volcanic locus line.

ICELANDIC STUDIES

Surtsey Volcano drill hole

During July and August 1979, a 180-m-deep hole was drilled through Surtsey Volcano, a young island volcano that formed off the south coast of Iceland from 1963 to 1967. The drilling was funded as a cooperative scientific effort by the Geothermal Program of the USGS and the Icelandic Museum of Natural History to explore the structure, alteration, and hydrothermal regime of the substructure of the volcano. The petrology of the core and cutting is being studied jointly by J. G. Moore (USGS) and S. P. Jacobsson (Icelandic Museum).

The main geologic events recorded in the vicinity of the drill site on the east rim of the eastern tephra cone were (1) construction of the eastern tephra cone beginning about November 7, 1963, on the sea floor, breaking the sea surface on November 15, and ending January 31, 1964 (this tephra was 15.5 to 15.7 years old at the time of drilling), (2) intrusion of feeder dikes and extrusion of lava in the vicinity of the eastern cone from August 19, 1966, to June 5, 1967, or 12.0 to 13.0 yr before drilling, and (3) development of a hydrothermal system centered on the eastern cone indicated by the steady rise of near-surface temperature and by palagonitization and induration of the tephra beginning in 1969. Excellent core recovery (4.7-cm diameter) was obtained to a depth of 157 m, below which loose tephra permitted only intermittent recovery of core, as well as cuttings. The hole bottomed 122 m below sea level in loose fresh glassy ash clearly belonging to the Surtsey eruption. Preeruption bathymetric maps indicate water depth in the area was 120 to 130 m. Hence, except for the possibility of local subsidence, the hole bottom was 10 m above the preeruption volcanic-derived sediments that carpet the ocean floor in this region.

The hole was almost entirely in glassy basalt tephra and its alteration products. A 2-m-thick lava flow occurred near the top, and a subvertical dike complex cuts the tephra between 72- and 85-m depth. No pillow lava was present. Water level was first encountered very close to sea level at 57- to 58-m depth. Water within the hole was hot, and the top of the water column was boiling on several occasions after drilling had ceased for a few days. Maximum temperature within the hole about 1 mo after drilling was 139°C at 100-m depth, below which the temperature fell to 47°C at 190-m depth.

The basalt tephra, originally very similar throughout the hole, showed no marked differences between that deposited above and below sea level. It was composed primarily of vesicular sideromelane glass fragments (averaging about 40 percent vesicles) ranging in size from 1 cm to fine dust. Bulk specific gravity of the tephra ranged from 1.4 to 2.1. Olivine and plagioclase phenocrysts and microphenocrysts were common. Small basalt bombs averaging 10 cm in size, with a porous vesicular core, were widely distributed. In addition, xenoliths of sediments, some containing shell fragments, were present.

The alteration of this tephra is related to the water level in the hole and to present downhole temperatures. Above water level, the glass was fresh or slightly palagonitized, and olivine was unaltered. Below water level, near the bottom of the hole where the temperature was below about 75°C, the degree of alteration of glass and olivine were similar. However, above about 105°C, the glass was extensively altered to smectitic clay, and olivine was largely altered to clay minerals. Samples at 88-, 114-, and 136-m depth contained no residual glass. In addition, zeolite minerals dominated by analcime were distributed widely through the hole both above and below sea level, except in a zone above the water table from 30- to 58-m depth.

Hydrogen gas monitor at Krafla Volcano

Motoaki Sato, K. A. McGee, and T. J. Casadevall have installed two hydrogen gas monitors at Krafla Volcano, which has resumed activity recently in central Iceland and which is the site of a 60-MW geothermal powerplant. One monitoring station was established near a major steam vent at the center of the Krafla caldera and another at a fuming fissure at the southern flank of the caldera. On early November 11, 1978, the volcano began deflating, and, within 30 min thereafter, the hydrogen monitoring record, received at the powerplant by radio telemetry, showed about a 50-percent decrease in hydrogen emission. The sudden decrease coincided with the start of seismic swarms that migrated northward from the center of the volcano. Icelandic scientists interpreted these events as the result of magma injection into subterranean fissures extending northward from the central vent.

COLUMBIA RIVER PLATEAU STUDIES

Eastern extent of Picture Gorge Basalt

The Picture Gorge Basalt of the Columbia River Basalt Group contains the most magnesian flows in the Columbia River Basalt Group and has the lowest $^{87}Sr/^{86}Sr$; some petrologists consider it akin to ocean ridge tholeiite. The Picture Gorge is known chiefly from the John Day Basin of north-central Oregon. Flows in extreme northeast Oregon, originally considered as equivalent to the Picture Gorge, have been shown to be older and neither as magnesian nor as low in $^{87}Sr/^{86}Sr$; these flows are assigned to the Imnaha Basalt. A broad area separates the known Picture Gorge and Imnaha Basalts. In 1977, P. R. Hooper (Washington State University) and R. D. Bentley (Central Washington University) found plagioclase-porphyritic flows similar to both the Picture Gorge and the Imnaha in the upper Grande Ronde River area, about halfway between known occurrences of the two formations. Mapping of this area by D. A. Swanson in 1979 shows that these porphyritic flows conformably underlie flows of the R_2 magnetostratigraphic unit of the Grande Ronde Basalt and, hence, are most likely too young to be Imnaha Basalt. The porphyritic flows are, therefore, correlated with the Picture Gorge Basalt. Such a correlation extends the eastern known limit of the Picture Gorge about 60 km and raises the possibility of vents in the upper Grande Ronde River area.

Diatremes in the Grande Ronde graben

The Grande Ronde graben is a major extensional structure, as much as 20 km wide, with marginal vertical displacements up to 1,200 m or more. Trending N. 10° W. from Indian Rock, four diatremes occur at approximately 1.5-km intervals. The diatremes, discovered by W. H. Taubeneck (Oregon State University), are the first reported in the Columbia River Basalt Group. Gray Rock, a fifth diatreme, 2.4 km to the west of the trend of the four diatremes, is associated with a solitary basalt dike that trends about N. 10° W. for at least 8 km. All diatremes cut the upper part of the Grande Ronde Basalt (magnetostratigraphic unit N_2) or are within 35 m of the basalt N_2 flow. Therefore, the diatremes transect a minimum of 630 to 780 m of Grande Ronde Basalt. Most Grande Ronde Basalt along the east escarpment of the graben is capped by diktytaxitic olivine basalt and overlying platy andesite without hornblende. Remnants of these two units cap the west escarpment south of the diatremes. Xenoliths of both units in the diatremes prove that these rocks originally extended north of the diatremes. Hornblende andesite is best exposed 15 km northeast of the graben, where 230 m of this unit overlie the diktytaxitic olivine basalt. Well-rounded xenoliths of hornblende andesite up to 2 m in diameter are common, especially in the first diatreme north of Indian Rock. The andesite xenoliths are at least 265 m below their original stratigraphic level and verify widespread former distribution of rocks now occurring in only two areas, the nearer 8 km away. One probably pre-Tertiary xenolith is known, but few of the millions of xenoliths have been examined carefully.

EVOLUTION OF SILICIC MAGMA CHAMBERS

Quenched mafic magma in rhyolite, Coso Range, California

High-silica rhyolite domes and flows were emplaced in seven episodes between 0.04 m.y. to 1.0 m.y. ago in the Coso volcanic field of eastern California. Concurrently, basalt was erupted adjacent to the rhyolite. Studies by Jenny Metz and C. R. Bacon show that less than 2 cm (but as large as 20 cm) sparse (< 1 percent) vesicular (about 20 percent porosity) spheroidal xenoliths of basaltic andesite contain phenocrysts of plagioclase $\pm$ olivine $\pm$ clinopyroxene in a groundmass of plagioclase $\pm$ clinopyroxene $\pm$ magnetite $\pm$ olivine $\pm$ hornblende $\pm$ biotite $\pm$ ilmenite. Some xenoliths contain partly digested xenocrystic olivine and plagioclase as well as dioritic and scoriaceous basaltic inclusions. SiO_2 contents are rhyolite, 77 percent; xenoliths, 55 to 58 percent; and basalt, 48 to 54 percent. Crenulated or diffuse boundaries between andesite and glassy rhyolite, between andesite and andesitic xenocrysts within rhyolite glass, and between rhyolite glass and quartz xenocrysts in andesite record limited mixing of two magmas. Dendritic groundmass ilmenite, skeletal and plumose plagioclase and plagioclase with acicular projections,

and compositionally zoned margins of xenoliths indicate rapid quenching of xenoliths. Trains of 0.1- to 0.5-mm-diameter vesicles within larger xenoliths parallel and adjacent to their margins indicate that xenoliths are intact "pillows" and suggest that they were liquid at the time of inclusion. The presence of basaltic xenocrysts, of feldspar phenocryst compositions, and of major-element compositions suggests that the xenoliths are differentiates of basaltic magma, rather than mixtures of rhyolite and coeval basalt. Groundmass hornblende and biotite in some xenoliths imply crystallization at elevated f_{H_2O}. Geophysical studies have suggested that basaltic magma was the heat source for generation and maintenance of the Coso rhyolitic system; the xenoliths may represent blobs of a slightly differentiated portion of this magma that were incorporated in overlying rhyolitic magma.

Large caldron complex in central Idaho

Reconnaissance mapping in the northeastern part of the Challis 1°×2° quadrangle by R. F. Hardyman and E. B. Ekren has led to the recognition of a multiple caldron complex approximately 48 km in diameter centered at about lat 44°42′ N. and long 114°32′ W. The southern, eastern, and northern boundaries of the complex are fairly well defined, but the western boundary is obscured by complexities related to Tertiary intrusive masses. The caldron complex formed principally as a result of eruption of two widespread ash-flow sheets, the rhyodacite tuff of Ellis Creek and the younger red rhyolite tuff of Challis (McIntyre and Hobbs, 1978). The red rhyolite tuff, also known as the "rhyolite of Yankee Fork," was dated by Armstrong (1975) at 43.8 m.y. ± 1.3 m.y.

Ash-flow tuffs and genetically related lavas within the caldron complex probably total more than 4,500 m aggregate thickness. All the intracomplex rocks older than the red tuff of Challis are hydrothermally altered to some degree, locally intensely. The rocks are extensively faulted, and most fault planes observed thus far display oblique-slip slickensides.

Deep erosion of the strata along the northeastern boundary, both within and outside the complex, has exposed a welded tuff feeder vent. This vent, which forms Van Horn Peak – a prominent landmark sculptured by erosion into a nearly perfect cone – is nearly circular and about 1 km in diameter. The vent intrudes an intracaldron facies of the tuff of Ellis Creek on its eastern flank and a considerable variety of intracaldron tuff, debris flows, and lacustrine strata on its western flank. Thick ash-flow tuffs of the same lithology as that in the vent crop out within the caldron complex but thus far have not been recognized outside the complex.

Deep drill hole in buried caldera, Snake River Plain, Idaho

At the Idaho National Engineering Laboratory (INEL), the deepest hole yet drilled on the eastern Snake River Plain, penetrated 658 m of fresh basaltic lavas and sediments and then a 1,830-m sequence of rhyolitic tuffs and tuffaceous sediments. This thick rhyolitic sequence, which contains several welded tuff units each thicker than 150 m, together with limited field evidence from the surrounding area, suggests to L. A. McBroome, D. J. Doherty, and M. A. Kuntz that the hole penetrated a buried Pliocene caldera. In the mountains directly north of the drill site, spoon-shaped faults down-thrown toward the plain and probable ash-flow tuffs may be related to caldera collapse. The location of middle to upper Pleistocene rhyolite domes, as well as many basaltic vents in the area, suggests control by buried caldera ring faults.

The maximum temperature recorded at 3,081 m in the drill hole was 150°C, but fluid pressures were relatively low, probably because of reduced permeability caused by hydrothermal alteration of the rocks. Zeolite minerals were observed in cuttings and core from below 488 m. Although INEL–1 proved to be nonproductive for geothermal use, a Butte City municipal water well, located nearer the inferred caldera ring-fracture zone, has a thermal gradient of 200°C/km, suggesting that the structure may yet have geothermal potential.

Isotopic modification of magma, Yellowstone caldera, Wyoming

Collapse related to eruption of the 1,000-km³ Lava Creek Tuff 600,000 yr ago created the 70 by 45 km Yellowstone caldera. In less than a few thousand years after collapse, more than 50 km³ of lava erupted in the caldera to form the Upper Basin Member of the Plateau Rhyolite. The Upper Basin magma was chemically and thermally continuous with the high-temperature part of the chemically zoned Lava Creek magma. However, studies by E. W. Hildreth, R. L. Christiansen, and J. R. O'Neil show that the Upper Basin magma had higher oxygen fugacity and higher $^{87/86}Sr$ and $^{206/204}Pb$ than the Lava Creek magma. $\Delta^{18}O$ of quartz phenocrysts from the Upper Basin lava is +0.8 to +1.5, compared to +6.0 to +6.6 for Lava Creek. The Upper Basin phenocryst assemblage is a partially resorbed equivalent of the Lava Creek suite; xenocrysts are rare, and refractory zircon is absent. Although it is possible that the Pb- and Sr-isotope ratios were modified by assimilation of collapsed roof rocks, the extreme lowering of oxygen-isotope ratios by 5 per mil in hundreds of cubic kilometers of magma requires either rapid postcollapse interaction of the magma with a mass of low ^{18}O water far in excess of saturation solubility or some other mechanism, possibly accelerating kinetic fractionation.

CASCADE VOLCANISM

The climatic eruption of Mount Mazama, Oregon

Detailed geologic mapping of the walls of Crater Lake caldera by C. R. Bacon has provided evidence for a new interpretation of events immediately prior to and during the climatic 6,600-yr-old eruption of Mount Mazama. Many deposits previously thought to have been of glacial origin are now recognized to be products of pyroclastic flows. The late history of the volcano according to Bacon probably consisted of the following events: (1) eruption of silicic air-fall tephra and of the rhyodacite flow at Llao Rock from a vent on the northwest flank of the volcano, (2) eruption of the rhyodacite flow at Cleetwood Cove approximately 6,600 yr B.P. from a vent on the north flank of the volcano, (3) eruption of a large volume of silicic tephra, probably from a vent near the summit of Mount Mazama immediately after emplacement of the Cleetwood Cove flow, (4) eruption and emplacement in radial valleys of small-volume nonwelded ash flows including the relatively widespread welded tuff at Wineglass, (5) inception of caldera collapse and simultaneous openings of vents below the summit with emplacement of voluminous main stage ash flows and a lithic-rich pyroclastic flow near the present caldera rim, followed by pyroclastic flows rich in mafic scoria, (6) accumulation of final pumice, ash, and crystal fall deposits during waning stages of climatic eruption, (7) completion of caldera collapse, and (8) postcaldera eruption of Wizard Island volcano and other extrusive features on the lake bottom. Events 2 through 7 probably took place during a period of a very few years.

Hydrothermal alteration at Mount Baker, Washington

Hydrothermal clay minerals are locally abundant at Sherman Crater and at Dorr Fumarole Field on Mount Baker. Studies by D. G. Frank show that the silt- and clay-sized fraction of volcanic debris currently undergoing alteration around active fumaroles at Sherman Crater is dominated largely by alunite and a silica phase (opal or cristobalite) but contains some kaolinite and montmorillonite. This mineralogy is consistent with the chemistry of surface solutions, represented by the crater-lake water, which favors formation of alunite over kaolinite. In contrast, vent-filling debris ejected from fumaroles in 1975 contains more than 20 percent clay-sized material, which is dominantly kaolinite and smectite, and the next older (probably 19th century) eruptive deposit on the crater rim contains as much as 27 percent clay-sized material, consisting mainly of kaolinite, smectite, pyrophyllite, and mixed-layer illite-smectite, produced by alteration prior to ejection. Significant amounts of kaolinite and alunite also are incorporated in five large Holocene mudflows that originated on the upper cone of Mount Baker. Kaolinite in these deposits occurs in increasingly greater amounts in progressively younger units, suggesting that, during Holocene time, either erosion has cut progressively deeper into more thoroughly kaolinized parts of Sherman Crater or that kaolinitic alteration has increasingly affected shallower zones at Sherman Crater. Resolution of these alternatives has important bearing on whether the present hydrothermal activity on the mountain is a short-term transient phenomenon or is part of a long-term process that has been continuous and possibly intensifying during Holocene time.

VOLCANIC ROCKS IN EASTERN UNITED STATES

Pre-Cretaceous subsurface volcanic rocks in Georgia

David Gottfried completed a geochemical study of two separate suites of pre-Cretaceous igneous rocks beneath the coastal plain of Georgia. Major and trace-element data were obtained on samples of diabase and felsic volcanic rocks to clarify the nature of the subsurface rocks and the tectonic history of the region. Four samples of diabase from central and southern Georgia have geochemical features (REE, Th, and U) similar to those found in the subsurface basalts near Charleston, S.C. (Gottfried and others, 1977). The results support previous inferences that the diabases are Triassic and Jurassic in age and occur in a major early Mesozoic subsurface basin.

Subsurface felsic volcanic rocks occur as lava flows, welded tuffs, and ash deposits in eastern Georgia. These felsic rocks are dacitic to rhyolitic in composition and are believed to be of Paleozoic age. Geochemical data on 13 samples indicate that the felsic rocks are mainly of the calc-alkaline magma type. Trace-element data (REE, Th, U, Hf, and Ta) suggest a formerly active orogenic continental margin tectonic setting. The preponderance of felsic volcanoes in the region implies a relatively thick continental crust at the time of their eruption.

Proterozoic Y zoned ash-flow sheet, Mount Rogers, Virginia

The rhyolite of Wilburn Ridge, the youngest volcanic unit of the 810-m.y.-old Mount Rogers Formation in southwestern Virginia, is a chemically and mineralogically zoned ash-flow sheet of peralkaline affinity, according to D. W. Rankin. The zonation is inferred to represent, in inverted succession, the compositional gradients originally formed in a differentiated source magma chamber. The main phenocrysts in the tuff are quartz and perthite, which make up about 30 percent of the

rock. Microprobe analyses by S. W. Novak of heated feldspar phenocrysts show that their compositions range from Or_{46} to Or_{67} and are not systematically related to present bulk-rock compositions. A thin basal zone about 20 m thick having less than 10 percent quartz and feldspar phenocrysts typically contains groundmass acmite, $(Na_{0.99}Ca_{0.03})$ $(Fe^{+3}_{0.92}$ $Al_{0.04}Mg_{0.01})Si_{2.01}O_6$, and riebeckite, $(Na_{0.08}K_{0.03})$ $(Ca_{0.04}Na_{1.96})$ $(Zn_{0.13}Ti_{0.22}Mn_{0.27}Mg_{0.55}Fe^{+2}_{2.42}Fe^{+3}_{1.28}Al_{0.12}(Si_{8.02})$ $O_{22}(OH)_2$. Acmite is restricted to this basal zone, but reibeckite persists to higher levels although in decreasing amounts. In the top one-third of the tuff sheet, minor biotite, $(K_{1.03})$ $(Zn_{0.03}Mg_{1.68}Mn_{0.05}Fe_{0.94}Ti_{0.04}Al_{0.23})$ $(Al_{0.99}Si_{3.01})$ $(F_{0.81}OH_{1.19})$, is the only groundmass mineral. Accessory minerals include zircon, fluorite, magnetite, and ilmenite. These mineralogic changes are accompanied by changes in bulk-rock chemistry. TiO_2 decreases from 0.25 to 0.14, whereas fluorine increases from 0.08 to 0.19 wt percent toward the base of the sheet. Other changes toward the base of the sheet include increases in molecular Na + K/Al, Fe/Fe + Mg, and differentiation index. Semiquantitative spectrographic analyses indicate that Ba, La, Ce, and Nd are depleted toward the base of the tuff sheet, whereas Nb, Sn, Be, Dy, and Gd are enriched. The composition of the groundmass riebeckite also reflects the chemical zonation showing an increase in Al_2O_3 (from 0.61 to 1.03 wt percent) and in MnO (from 0.73 to 2.60 wt percent) toward the base of the sheet. TiO_2 also increases in amphiboles (from 0.64 to 1.83 wt percent) toward the base of the sheet, but this opposes the trend of bulk-rock compositions. These chemical and mineralogical changes toward the base of the sheet presumably correspond to changes toward the top of the source magma chamber.

PLUTONIC ROCKS AND MAGMATIC PROCESSES

Episodic plutonism in the Coast batholith of southeastern Alaska

More than 150 K-Ar, U-Pb, and Rb-Sr ages have been determined by J. G. Smith, T. W. Stern, and J. G. Arth from the Coast Mountains of southeastern Alaska between lat 54°54′ and 56°15′ N. These ages indicate at least three episodes of metamorphism and five episodes of igneous intrusion during the Mesozoic and Cenozoic. Mesozoic metasedimentary and metavolcanic rocks were intruded during the Triassic or Jurassic by the Texas Creek Granodiorite ~205 m.y. ago. Jurassic tonalite and granodiorite intruded a migmatite and gneiss complex (central gneiss complex of Canadian workers) on Portland Peninsula, and metasedimentary and metavolcanic rocks on southern Revillagigedo Island ~140 m.y. ago. During Cretaceous time, ~90 m.y. ago, garnet-bearing granodiorite and tonalite were intruded on northern Revillagigedo Island. A suite of Eocene granite and granodiorite batholiths intruded the eastern Portland Peninsula 52 m.y. to 42 m.y. ago. Widely scattered epizonal granite and granite porphyry plutons were intruded during the Oligocene and Miocene from 31 m.y. to 19 m.y. ago.

A Paleocene and Eocene thermal disturbance centered on the Portland Peninsula reset all K-Ar ages over an area of 7,000 km², producing apparent hornblende ages of 58 m.y. to 46 m.y. and apparent biotite ages of 48 m.y. to 42 m.y. A $^{40}K/^{40}Ar$ isochron plot for hornblende indicates complete resetting of ages. Westward from the area of maximum thermal disturbance K-Ar ages approach U-Pb ages, although complete agreement is not reached even at distances of 40 km. Initial results from the Coast Mountains near Skagway suggest that the pattern of regional thermal disturbance and widespread resetting of K-Ar ages exists there.

Multiple intrusion of the La Perouse layered gabbro, Alaska

R. A. Lonay (USGS) and G. R. Himmelberg (University of Missouri) have made electron probe analyses of olivine in 33 samples from the La Perouse layered gabbroic intrusion, Fairweather Range, Alaska. Although the intrusion has an exposed thickness of approximately 10,000 m, the olivine compositions range only from Fo_{50} to Fo_{73}, with 80 percent of those samples analyzed having compositions between Fo_{60} and Fo_{70}. The olivine compositions show no relationship with stratigraphic height in the intrusion. Coexisting orthopyroxene and clinopyroxene, currently being analyzed, show a similar limited fractionation trend. These data tentatively suggest that the La Perouse intrusion crystallized from frequent injections of magma batches rather than from a single large volume of magma.

New data on magnetite and ilmenite from the granitoid rocks in White Pine County, Nevada

D. E. Lee and R. E. Van Loenen (1979), as part of a detailed study of granitoid rocks in White Pine County, Nev., have noted characteristics of the metallic opaque minerals that are of potential petrologic significance. Magnetite in these rocks contains only very minor amounts of titanium. In the most mafic parts of the granitic exposures, where magnetite is most abundant, it contains less TiO_2 (about 0.4 percent) than the rock itself (about 0.7 percent). The magnetite is found to have a very similar chemical composition throughout the range of granitic rock types (quartz monzonite with 75.5 percent SiO_2). The ilmenite in these same rocks is noteworthy because of its relative high content of MnO (up to 16.9 percent).

Experimental studies of these magnetites and ilmenites suggest lower crystallization temperatures

(>600°C) and a lower fugacity of oxygen (less than 10^{-18} atm f_{O_2}) than was found for coexisting biotites in a previous study by Lee and Van Loenen (1970). They observed that the biotite in the most mafic granitic rocks crystallized at 780°C with an oxygen fugacity of about 10^{-13} atm f_{O_2} and that biotite in the more felsic rocks crystallized at about 735°C with an oxygen fugacity of about 10^{-15} atm f_{O_2}.

Vladi Marmo (1959), in a study of magnetite from granodiorite in central Sierra Leone, noted "a lower TiO_2 content of magnetite would thus indicate that the primary material was sedimentary." The TiO_2-poor magnetites from White Pine County, Nev., which were recovered from hybrid granitoid rocks that have assimilated sedimentary host rocks, appear to corroborate Marmo's findings.

Petrology and geochemistry of the Oliverian domes of New England

Continuing study of the Oliverian domes by G. W. Leo, including both the plutonic core gneisses and the mantling volcanic rocks, has revealed the following:

- Oliverian gneiss intrudes the overlying Ammonoosuc Volcanics (Middle Ordovician) in most of the domes with contact zones as much as hundreds of meters thick that show evidence of potassium metasomatism of Ammonoosuc Volcanics and (or) loss of potassium from the Oliverian gneiss.
- The stratified core gneiss of the Mascoma dome is chemically and texturally similar to the felsic phase of Ammonoosuc Volcanics and should not be referred to as Oliverian.
- Most of the core gneisses are calc-alkaline with granite or granodiorite composition (SiO_2 ~62–78 percent, K_2O ~3–6 percent), but gneisses in several of the southern domes are trondhjemitic (SiO_2 ~72–78 percent, K_2O <1.4 percent). The latter gneisses, whose major- and trace-element compositions are generally similar to those of felsic Ammonoosuc, may be comagmatic with the Ammonoosuc Volcanics and mantle derived. The calc-alkaline core gneisses, by contrast, probably were generated in the upper crust.
- Ammonoosuc Volcanics consist of mafic and felsic phases with only minor amounts of intermediate compositions and local nonvolcanic lithologies. The mafic phase is mostly hornblende-plagioclase amphibolite having a tholeiitic composition (CaO = 7.7–12.2 percent, K_2O = 0.9 percent, Rb = 8 ppm) and REE patterns that are generally similar to abyssal and island-arc tholeiites. Rocks containing calcium-poor amphiboles (anthophyllite-gedrite and (or) cummingtonite) constitute a widespread mafic subtype. Such rocks have lower CaO contents (2–5.5 percent) and show a somewhat greater iron enrichment than the hornblende-plagioclase amphibolites. The felsic phase is typically slightly peraluminous, highly siliceous (SiO_2 ~70–79 percent), and very low in potassium and rubidium; REE patterns are relatively flat and show distinct negative europium anomalies. Felsic Ammonoosuc rocks appear to be mostly volcaniclastic.
- Hypabyssal rocks with well-preserved volcanic texture and rhyolitic composition are closely associated with some small near-surface plutons, notably the Sugar Hill pluton, near Littleton, N.H. The hypabyssal rocks contain abundant potassium-feldspar and, thus, are unlike the felsic Ammonoosuc, but the hypabyssal rocks probably represent post-Ammonoosuc volcanism that was associated with the small near-surface plutons.
- The new chemical, petrologic, and field data are compatible, assuming certain conditions, with a current plate tectonic model, which suggests that the Oliverian domes represent the roots of an Ordovician island arc beneath an east-dipping subduction zone. The Ammonoosuc tholeiites resemble modern oceanic tholeiites of mantle derivation in young island arcs. The associated felsic, highly siliceous but potassium-poor, dominantly clastic deposits, however, seem to require a partly epiclastic source such as might be found in a relatively shallow and restricted basin. The existence of such a restricted basin in Middle Ordovician time is inferred from the presence of sulfidic and graphitic schists that overlie the Ammonoosuc Volcanics. The calc-alkaline granitic plutons that intrude the Ammonoosuc Volcanics cannot be reconciled with an oceanic-arc environment; their source must be continental crust (Avalonian basement?) that underwent partial melting not long after the eruption of Ammonoosuc Volcanics. The general lack of volcanic rocks of intermediate compositions suggests that little mixing or assimilation of the calc-alkaline and potassium-poor magmas took place even though both magmas were closely associated in space and time.

Hoffman Park stock, Colorado, and its relation to the Mount Antero Granite

J. M. Hammarstrom and Priestley Toulmin III report that the results of microprobe analyses of essential and accessory minerals from the granite stock associated with the Hoffman Park (Mount Aetna) molybdenite prospect, near Monarch, Colo. (Steininger and Arehart, 1976), indicate that the rock is distinct from, though closely related to, the Mount Antero Granite (Toulmin, 1976). Biotite in the Hoffman Park stock is richer in iron

and lower in magnesium and aluminum than that of the Mount Antero Granite, but the two are similar in their high contents of titanium, manganese, and fluorine. Sphene is less abundant and poorer in aluminum in the stock than in the Mount Antero Granite; iron plus aluminum replace up to 30 percent of the titanium in Mount Antero sphenes, but only about 10 percent in sphenes from the stock and the associated quartz monzonitic units. Sphenes in granites of both the Hoffman Park and Mount Antero and in the associated quartz monzonites are rich in REE (up to 3.5 percent). These relations confirm the consanguinity of these rock units and indicate that the Hoffman Park stock is in some respects intermediate between the calc-alkaline intrusive and extrusive rocks of the Mount Aetna center and the Mount Antero Granite, perhaps reflecting shallower emplacement or an intermediate stage of differentiation. The new results are consistent with the suggestion (Toulmin, 1976) that the Hoffman Park stock represents the late silicic stage of magmatism in the Mount Aetna volcanic center.

Inclusions in upper Cenozoic volcanic rocks of the central Sierra Nevada, California

Suites of inclusions have been collected by F. C. Dodge, P. K. Brooks, and J. P. Lockwood from rhyodacite at Jackson Butte, from trachyandesite at Big Creek and Red Mountain, and from alkali olivine basalt at Oak Creek and Waucoba. Peridotite and pyroxenite inclusions occur at all sites. Felsic xenoliths of low-grade metamorphic rocks are abundant at Jackson Butte and scarce at Big Creek and Waucoba. Garnet-bearing inclusions, present only at Big Creek, include abundant pyroxene-rich high-grade metamorphic rocks, scarce amphibolite and peridotite, and rare sillimanite gneiss.

Textures in the peridotite inclusions from Oak Creek and Waucoba range from coarse-grained poikilitic with a pyrometamorphic overprint to porphyroclastic. At Big Creek, the peridotite inclusions range from very coarse grained allotriomorphic-granular to tabular equigranular. The garnet peridotite inclusions at Big Creek are also commonly allotriomorphic-granular but with incipient porphyroclastic features. The garnet pyroxenite inclusions at Big Creek commonly are granofels composed of either colorless to pale-pink garnet and colorless to pale-green pyroxene (5 to 10 percent have pyroxene with exsolved lamellar garnet microlites) or pink garnet and dark-green pyroxene.

$^{87}Sr/^{86}Sr$ determined by R. W. Kistler and the textures of the peridotite inclusions at Big Creek suggest that they could be either autoliths or xenoliths, whereas the peridotite inclusions at Oak Creek and Waucoba are exclusively autoliths. Suggested protoliths for some of the inclusions at Big Creek are upper crustal country rock for the felsic low-grade metamorphic xenoliths and the granitic inclusions, intermediate to lower crustal mafic igneous rock for the amphibolites, and the lower crustal or upper mantle materials for the garnet pyroxenites and peridotites.

METAMORPHIC ROCKS AND PROCESSES

Amphibolite facies mineral assemblages and the fractionation of CaO, U, and Th, Colorado

Precambrian amphibolite facies metamorphic rocks from the Front Range, Colo., were sampled by George Phair for uranium and thorium (255 samples), for rock forming oxides (119 samples), and for semiquantitative modal analysis (99 samples). Metasedimentary rocks made up about 85 percent of the metamorphic rocks analysed. Metasedimentary rocks rich in potassium-bearing minerals such as microcline, biotite, and (or) muscovite (originally shale) and those rocks rich in calcic minerals such as plagioclase, hornblende, pyroxene, and (or) epidote (originally graywacke) fall in widely separate fields when plotted on CaO-K_2O and CaO-K_2O-Al_2O_3 variation diagrams. Quartz-feldspar rocks (originally sandstone) plot separately in an area of low K_2O, low Al_2O_3, and low to intermediate CaO. The metasedimentary rocks can be subdivided into six diagnostic mineral assemblages in order of increasing average CaO content:

Assemblage	CaO (wt-percent)	U (ppm)	Th (ppm)
biotite + quartz microcline	0.08	6.2	14.9
biotite + quartz + sillimanite	0.41	4.1	15.2
quartz + plagioclase	0.95	3.0	9.3
biotite + quartz + sillimanite + plagioclase	1.50	2.9	9.8
biotite + quartz + plagioclase	2.48	2.8	6.7
hornblend + biotite + quartz + plagioclase	6.79	2.5	4.5

The trends of increasing uranium and thorium with diminishing CaO are remarkably similar to those in the calc-alkalic igneous rocks that are the ultimate sources of the metasedimentary rocks.

GEOCHEMISTRY OF WATER AND SEDIMENTS

The primary objectives of geochemical studies in hydrogeology are to understand the hydrochemical processes that control the chemical character of water and the mineralogic changes in sediments and rocks, to increase understanding of the physics of flow systems by application of geochemical principles, to understand the rates of chemical reactions and the rates of transport of physical and chemical masses within the geohydrologic

system, and to understand the concomitant chemical changes between water and sediments.

Ground-water geochemical models

Determination of the gypsum mass-removal rate in a highly conductive ground-water system near Carlsbad, N. Mex., was made by H. C. Claassen, who calculated the difference in water chemistry between recharging water and water downgradient. Effective surface area of gypsum in contact with a unit volume of ground water was determined from mass-removal rate and estimates of aquifer residence time, reaction rate constants for gypsum dissolution, and values for the maximum amount of gypsum that could be dissolved by the ground water. The computed surface area indicates that the flow regime consists principally of open fractures or conduits, a conclusion corroborated by drill-hole data. Furthermore, the rate of increase of individual conduit openings was calculated to be about a few centimeters per year.

The above study shows that, in certain cases, characterization of the hydraulic regime can be made using kinetically derived water-quality data. Changes in this regime over a period of time also can be predicted. These data are necessary for realistic predictions of transport of ground-water pollutants.

Mass transport modeling of many ground-water systems requires definition of chemical weathering rates of a silicate aquifer. The weathering of glassy silicates is partly a function of mobility and interdiffusion of components through the silica-aluminium-oxygen framework. Experiments by A. F. White and Claassen showed that volcanic glasses weathered at 25°C for periods of up to 3 mo have parabolic increases in aqueous sodium, potassium, calcium, and magnesium, with time, suggesting diffusion control. Successive leachings of reacted glass surfaces by dilute hydrofluoric acid reveal S-shaped concentration-distance profiles, in which the depth of cation depletion increases with time and decreases with increasing pH and aqueous concentration. The profiles are reproduced successfully by a numerical solution to the diffusion equation, employing a concentration-dependent diffusion coefficient. Calculations indicate outward cation diffusion is significantly slower than inward diffusion of water during hydration. Mass balance calculations show that formation of this cation-depleted surface layer coupled with secondary surface retreat quantitatively explains aqueous cation mass transfer.

Organic compounds on kaolinite

Polyacrylamide (propenoic acid amide) is a synthetic linear organic polymer that is adsorbed strongly on surfaces of mineral particles in water. It is used as a coagulating or settling agent to help remove suspended solids from solutions. Experiments by S. G. Marshall and J. D. Hem showed that adsorbed amounts sufficient to enhance settling of kaolinite suspensions (about 9 mg/g of clay) did not measurably affect the cation exchange capacity or the selectivity for exchange of potassium or calcium for sodium at the clay mineral surface.

This finding is rather unexpected, and it is uncertain whether it can be extended to systems and conditions other than the one studied. However, the experiment shows that a thin coating, approximating a monomolecular layer of organic material, can substantially alter the physical behavior of a sediment particle without greatly influencing its chemisorption properties.

Lithium as a tracer

Scientists need a harmless very low background tracer that can be placed in streams to study the rate at which sorbable solutes are removed by stream sediments. Work by V. C. Kennedy, G. W. Zellweger, and R. J. Avanzino indicated that lithium has potential for such use. Studies in which lithium and chlorine, as a conservative reference, were injected into a small natural cobble-bed stream (Little Lost Man Creek in Redwood National Park) and into an artificial plastic channel, which had large amounts of periphyton but little or no inorganic sediment, indicated that very little lithium was sorbed by the periphyton in the artificial channel. A considerable fraction of the lithium was lost in the stream reach containing sediments coated with periphyton. This suggests that lithium is removed selectively by sediments as compared to periphyton on a streambed. The dissolved solids in Little Lost Man Creek are low, as indicated by a conductivity of 60 μ mho at 25°C; lithium may not be as good a tracer of sorbents at higher concentrations of competing cations.

Rates of formation of manganese oxides

Laboratory studies by J. D. Hem of oxidation rates of divalent manganese in aerated water between 0° and 40°C, from pH 9.0 to 7.0, showed that Mn_3O_4 (hausmannite) is produced at the higher temperatures, but a more highly oxidized form MnOOH (beta manganite) accompanies it at temperatures near and below 25°C. Near 0°C, the product is entirely beta manganite. The rate of formation of hausmannite is much more strongly temperature dependent than the rate of formation of beta manganite, and this appears to explain the behavior observed near 0°C. Beta manganite is less stable thermodynamically than hausmannite, but both oxides may disproportionate to form still more stable varieties approximating the composition MnO_2. In natural open

systems, the flux of reactants (Mn^{2+}, O_2 aq, and H^+ or OH^-) toward precipitation sites can support a feedback cycle that involves both oxidation and disproportionation and builds up a deposit of MnO_2 as the final product.

STATISTICAL GEOCHEMISTRY AND PETROLOGY

Batholithic rocks of southern California

A. T. Miesch (USGS) and A. K. Baird (Pomona College, Claremont, Calif.) have completed a joint investigation of chemical variation in the batholithic rocks of southern California. Application of an extended form of *Q*-mode factor analysis (Miesch, 1976) to chemical data on 8 major oxides in 497 composite samples (Baird and others, 1979) led to the development of a petrologic mixing model for the origin of these rocks. The compositional structure in the batholithic rocks as a group was found to be similar to that of the Sierra Nevada batholith (Miesch and Reed, 1979) and indicates that the mixing model requires four end members. Two of the end members were assumed to represent a two-component range of mineral assemblages that separated from the magma either by crystal fractionation or by removal of refractory material on partial melting. The assemblages consist of varying proportions of plagioclase, hornblende, magnetite, and ilmenite. The remaining two end members for the model were assumed to represent the extremes in a two-component range of source materials that varied between a gabbro similar to those that occur in the southwestern part of the region and a quartzofeldspathic material that may represent continental materials incorporated into the magmatic system. The precise compositions of the end members were determined by factor analysis methods. The model allows examination of its individual components, specifically the regional variation in the compositions of the source materials and the mineral assemblages that were separated from the source materials to form the batholithic rocks. Maps of the chemical variation in the source materials show sharp discontinuities along a north-south line in the vicinity of the San Jacinto fault zone, about 35 km southwest of the San Andreas fault zone. Chemical variation across the San Andreas is continuous. The discontinuity coincides approximately with other previously noted discontinuities in the mineralogic, petrologic, isotopic, and structural properties of the batholithic rocks and is interpreted to mark the southwestern limit of major contributions of continental materials.

R-mode and *Q*-mode factor analysis

Both *R*-mode and *Q*-mode factor analyses have been used extensively in geochemistry and petrology. The distinction between the two types was formerly made on the basis of the size of the matrix that was factored by extraction of the eigenvectors. With the *R*-mode method, the factored matrix is $m \times m$ in size, where m is the number of variables. With the *Q*-mode method, however, it was necessary to factor the generally much larger $n \times n$ matrix, where n is the number of observations or samples. Some workers have followed the practice of performing both types of analyses on the same set of data, the *R*-mode to study relations among the variables and the *Q*-mode to study relations among the samples. This distinction between *R*-mode and *Q*-mode, however, has not been valid since Klovan and Imbrie (1971) showed geologists how the same *Q*-mode results could be obtained by factoring a matrix $m \times m$ in size. A. T. Miesch reports that the only differences between *R*- and *Q*-mode methods are the manner in which the data are scaled prior to the other computations and whether one chooses to scale the factor loadings or the factor scores by the square root of the eigenvalues. He also suggests that one analysis, either *R*-mode or *Q*-mode, can be used to study both the relations among the variables and the relations among the samples.

Identification of geochemical anomalies

Two important statistical tests described by G. L. Tietjen and R. H. Moore (1972) have been overlooked as means of identifying anomalies in geochemical exploration. One of the tests determines whether the k largest values or the k smallest values are significantly different from the remaining $n-k$ observed values. The other test determines whether the k values farthest from the mean, either above or below, are significantly different. The first test requires computation of the L_k statistic, and the second requires computation of E_k. These statistics then are compared with tabulated critical values and are significant if found to be smaller than the critical values. Because the tables of critical values are applicable only where k is 10 or less and n is no larger than 50, A. T. Miesch has prepared a computer program, TMTABLES, to derive the critical values for any k or n. Another program, ORDAT, identifies the values in the data set that are farthest from the mean, and another, TMTEST, computes the L_k and E_k statistics.

ISOTOPE AND NUCLEAR CHEMISTRY

ISOTOPE TRACER STUDIES

Strontium isotopes along the Uinta trend

A series of volcano-plutonic complexes trend west-southwest across northern Utah from Park City to Gold Hill. They lie along the so-called "Uinta Trend," which has been intermittently active as a tectonic zone since Proterozoic Z time. Most of the volcano-plutonic rocks in

this zone are middle Tertiary, but several Laramide plutons occur along the trend, and there are Jurassic plutons toward the western end. Initial strontium isotope ratios of igneous rocks along the trend were determined by C. E. Hedge and W. J. Moore and exhibit a progressive increase from east to west. In the area of Park City, Utah, initial $^{87}Sr/^{86}Sr$ ratios are low (0.7075–0.7068). At the other extreme, along the Utah-Nevada border, they are higher and more variable (0.7095–0.7068). The data seem to require the involvement of middle-to-upper crustal types of materials in magma genesis along the Utah-Nevada border, whereas a deep source is indicated for the rocks at the east of the trend.

Lead isotopes in ores and rocks of southwest New Mexico

Data were obtained by M. H. Delevaux and J. S. Stacey from about 50 Laramide and Tertiary ore and rock samples in southwest New Mexico. A secondary isochron for galena samples between Silver City and Socorro, a distance of about 250 km, indicates a basement age of 1,480 m.y. ± 60 m.y. (95-percent confidence limits). A zircon age on a Proterozoic Y granite in the Gold Hill district near Silver City is about 1,445 m.y.

All Laramide and Tertiary intrusions in this region of New Mexico seem to be derived from 1,450 m.y.- to 1,600-m.y. Proterozoic Y lower crust. The middle Tertiary deposits exhibit linear relations characteristic of high temperature "near-source" and low temperature "far-from-source" types. Galena lead from porphyry copper deposits is similar to the feldspar lead of the unmineralized Laramide stocks; that from pyrites and other secondary minerals is slightly more radiogenic. Lead in these porphyry copper deposits is similar to that of large producers in other Rocky Mountain States, with $^{206}Pb/^{204}Pb$ values in the range of 17.8 to 18.4.

Lead and neodymium isotopes in Hawaiian volcanic rocks

Lead and neodymium data obtained by Mitsunobu Tatsumoto for Hawaiian volcanic rocks clearly indicate that each of the five volcanoes on Hawaii has a distinct isotopic character and that the Mauna Loa and Mauna Kea trends are isotopically distinct from one another. The neodymium and lead isotopic composition of basalt from the Loihi Seamount suggests that this seamount belongs to the Mauna Loa series. The neodymium and lead isotopic data show that Hawaiian volcanic rocks did not originate from a randomly heterogeneous mantle. Mixing is indicated by the regular increase in radiogenicity of lead and neodymium toward the southern (younger) volcanoes observed in both the Mauna Loa and Mauna Kea loci, by the preservation of isotopic identities for each volcano as well as for the Mauna Loa and Mauna Kea trends, and by the positive correlation of lead and neodymium isotopes coupled with an anticorrelation of neodymium isotopes with Sm:Nd. Furthermore, these relations suggest that the mixing probably did not occur in the mantle but more likely occurred via contamination of mantle-derived magmas. The 0.94-b.y. ± 0.42-b.y. trend suggested by the $^{207}Pb/^{204}Pb$–$^{206}Pb/^{204}Pb$ relations, therefore, is not a valid age.

Samarium-neodymium study regarding evolution of the Earth's mantle

A Sm-Nd age of 2.980 b.y. ± 0.046 b.y. and an initial $^{143}Nd/^{144}Nd$ of 0.50914 ± 0.00004 was obtained by Mitsunobu Tatsumoto from a group of Precambrian rhyolites and carbonatites from the Vinjamun province of southern India. The initial ratio suggests that the rocks were derived from a source that was slightly depleted in light REE relative to chondrites ($\varepsilon_I^{Nd} = +6$). The collinearity of the rhyolites and carbonatites suggests that both were derived from the same or similar sources and that the silica-rich and carbonate-rich liquids may be immiscible.

Neodymium isotopes provide important information about the source region of the alkalic ultrabasic kimberlites, the only rock type known to be derived from 200 km in the mantle. The initial $^{143}Nd/^{144}Nd$ of kimberlites ranging in age from 90 m.y. to 1,300 m.y. from South Africa, India, and the United States are identical to the ratio in the basaltic achondrite Juvinas (Basu and Tatsumoto, 1979) that represents the bulk chondritic earth in rare earth elements. This correlation indicates the existence of primeval mantle beneath these continents. Further, carbonatite and melilite basalt from the Cape Verde Islands in the Atlantic Ocean show identical chondritic signature in their $^{143}Nd/^{144}Nd$, indicating the presence of a primeval layer in the suboceanic mantle.

The neodymium isotopic study of ultramafic xenoliths in both kimberlites and alkali basalts shows that kimberlites are derived from a different (deeper) source than the included xenoliths. The $^{143}Nd/^{144}Nd$ of minerals in a garnet lherzolite xenolith from the Bulfontein kimberlites pipe are all lower than in the host kimberlite (Basu and Tatsumoto, 1979). On the other hand, the neodymium isotopic composition of a garnet lherzolite xenolith from Salt Lake Crater, Oahu, is identical to those of basalts from southeastern Oahu. Thus, the various rock types on southeastern Oahu may have been derived from a single source.

STABLE ISOTOPES

Light-stable isotopes and fluid inclusion study of the Thompson Creek and Little Boulder Creek deposits, Idaho

A light-stable isotope and fluid inclusion investigation is being conducted by W. E. Hall and J. W. Batchelder on the Little Boulder Creek and Thompson Creek molybdenum deposits, Custer County, Idaho. Homogenization and freezing temperature measurements of fluid inclusions indicate depositional temperatures of 371° to 377° ± 3°C and salinities of approximately 5 to 10 equivalent wt-percent NaCl. The $\delta^{18}O$ values for quartz range from ± 10.7 to + 11.2 per mil with calculated $\delta^{18}O$ H_2O value ranging from + 4.7 to + 5.3 per mil. The δD values of fluid inclusion water from quartz range from − 121 to − 83 per mil. Sulfide minerals have $\delta^{34}S$ values ranging from + 9.6 to + 11.4 per mil. These preliminary data indicate that the ore fluids of both deposits probably were composed of both meteoric and magmatic waters. The Thompson Creek ore fluids had as much as 35 percent magmatic water. Sulfur in both deposits probably was derived from the surrounding Paleozoic sedimentary rocks.

ADVANCES IN GEOCHRONOMETRY

Samarium-neodymium age of the Stillwater Complex, Montana

A samarium-neodymium systematics study has been made on five whole-rock samples of the Stillwater Complex ranging from anorthosite to pyroxenite and mineral separates of two norites, by Mitsunobu Tatsumoto (USGS) and Denis Coffrant (Colorado School of Mines). The whole-rock samples show a variation in $^{147}Sm/^{144}Nd$ from 0.15 to 0.22 and yield an isochron that defines an age of 2,896 m.y. ± 0.034 m.y. (95 percent confidence level) and an initial $^{143}Nd/^{144}Nd$ of 0.508799 ± 0.000044. The initial $^{143}Nd/^{144}Nd$ is distinctly smaller than that of the basaltic achondrite Juvinas at the emplacement age ($\varepsilon_{Nd} = -2.4 \pm 0.4$) and indicates that the ultrabasic magma was either melted from an older upper mantle region having lower Sm:Nd or, more plausibly, contaminated with much older crustal rocks.

One internal isochron for a norite yielded an age of 2,742 m.y. and an initial $^{143}Nd/^{144}Nd$ of 0.508987 ± 0.000020, whereas Sm-Nd data of another norite yielded an imprecise isochron of 2,793 m.y. ± 126 m.y. and an initial $^{143}Nd/^{144}Nd$ of 0.508931 ± 0.000126. DePaulo and Wasserburg (1979) obtained an internal isochron Sm-Nd age from a norite of 2,701 m.y. ± 8 m.y. and a whole-rock Sm-Nd age for six rocks of the complex of 2,653 m.y. ± 73 m.y. These whole-rock data points all lie within experimental uncertainty on the mineral isochron. They interpreted the internal Sm-Nd age to correspond to the emplacement of the complex. The internal isochron ages of Tatsumoto and Coffrant are marginally in agreement with that obtained by DePaulo and Wasserburg, although the whole-rock isochron is distinctly older.

These data are interpreted to mean that the whole-rock age corresponds to the age of emplacement of the complex and that the internal isochron ages are partially reset by later metamorphic events. The higher initial $^{143}Nd/^{144}Nd$ of the norites are compatible with the above interpretations. The imprecise age of a norite probably is due to the later disturbance of the Sm-Nd system. Nunes and Tilton (1971) obtained an age of 2,708 m.y. (adjusted for new uranium decay constants) by a uranium-lead systematics study of zircons separated from a noritic diabase from the complex basalt zone. They interpreted the age to be the emplacement age of the complex. However, because the zircon age is obtained for a basal zone sample from the Nye Basin that contains abundant granitic dikes, the age probably corresponds to the later event of siliceous igneous intrusion (Page, 1977). Even if the zircons are in primary phase crystallized from basaltic magma, the discordant uranium-lead data can be interpreted for a higher primary age when an episodic loss of about 1,600 m.y. to 2,000 m.y. age is used, as indicated by the uranium-lead data of apatites of Nunes and Tilton (1971).

Radiocarbon dating of pre-Holocene carbonate deposits

S. W. Robinson has measured contamination of carbonate samples by younger carbon, using radiocarbon analysis of samples believed to be too old to contain any original radiocarbon. Buried mollusk shell and tufa samples were found to contain 0.4 to 0.8 percent of modern radiocarbon concentration, while samples exposed to the atmosphere and surficial weathering contained about 3 percent. These results were used to fix the parameters of a simple model of the contamination process that indicates that radiocarbon dates on buried carbonate deposits are not seriously in error for the last 25,000 yr.

Dating Arctic Quaternary raised marine deposits by uranium series and amino acid ratios

A complex of raised marine sediments and glacial deposits (sections showing two to four tills) crop out in wave-cut cliffs at many localities along the coast of eastern Baffin Island, Canada. Mollusk shells from these marine deposits are dated by both the uranium-series methods (B. J. Szabo, personal commun., 1980) and the amino acid ratios (Miller and others, 1977). Samples were collected from sites at three areas – Kivitu foreland

between Narpaing and Quajon Fiords, Clyde foreland between Clyde Inlet and Eglinton Fiord, and Broughton Island.

Because of its location, climatic shifts have a major effect on Baffin Island. Major ice buildup, initiated during glacial periods, causes glacioisostatic depression of the coastline. During the advancing phase of glaciation, marine sediment is deposited at some localities along the coastline and then is overridden by glacial till; during the retreating phase, marine deposits are laid down over the till at most localities, then both marine and glacial deposits are uplifted isostatically above sea level.

The proposed scheme of Quaternary history of eastern Baffin Island, based on uranium-series dates and amino acid dates that generally are in agreement, is shown below:

Broughton Island	Kivitu foreland	Clyde foreland	Age (yrs)	Marine stage
Marine Sand	Quajon interstade	Upper Kogalu	65,000	3
Harbour Till	Kivitu Till	Ayr Till, Lower Kogalu		4
Broughton interstade	Marine unit-3	Upper Kuvinkilk	130,000	5
Platform Till	Narpaing Till	Clyde Till Lower Kuvinilk		6
	Marine unit-2	Cape Christian interglacial	200,000	7
	Kangeeak Till	Sledgepointer Till		8
	Marine unit-1		≥ 350,000	9

Lead isotopes, southwest New Mexico

Data obtained by M. H. Delevaux and J. S. Stacey from about 50 ore and rock samples in southwest New Mexico yield a remarkably uniform picture. A galena secondary isochron for samples from Silver City to Socorro, a distance of about 250 km indicates a basement age of 1,480 m.y. ± 60 m.y. (95-percent confidence limits). A zircon age on a Precambrian granite in the Gold Hill district near Silver City (analyses of three different-sized fractions) yields an age of about 1,445 m.y.

Whole-rock, feldspar, and galena lead data indicate that there was little or no involvement of older crustal material in the formation of the crust in this area 1,450 m.y. to 1,600 m.y. ago. This is quite different from the situation in Colorado and Utah where older Proterozoic and Archean components are indicated by lead isotope data.

All Laramide and Tertiary intrusions in this region of New Mexico seem to be derived from the 1,450-m.y. to 1,600-m.y. Proterozoic Y lower crust. The middle Tertiary deposits exhibit linear relations characteristic of high temperature "near-source" and low temperature "far-from-source" types. Galena lead from porphyry copper deposits is similar to the feldspar lead of the unmineralized Laramide stocks; that from pyrites and other secondary minerals is slightly more radiogenic. Lead in these porphyry copper deposits is similar to that of large producers in other Rocky Mountain States, $^{206}Pb/^{204}Pb$ values being in the range of 17.8 to 18.4.

Lead isotopes indicate tectonic division in Saudi Arabia

J. S. Stacey has found that isochron model ages indicate mineralization activity occurred in the Saudi Arabian Shield between 700 m.y. and 400 m.y. ago. Intensity of mineralization activity appears to have peaked in three periods between 750 m.y. and 650 m.y., 600 m.y. and 550 m.y., and 500 m.y. and 450 m.y. ago.

Low $^{207}Pb/^{204}Pb$ for all the deposits in the southern part of the shield indicate that the Saudi Arabian Craton was formed in an oceanic crustal environment in the late Precambrian. Involvement of significantly older upper crustal material in the formation of the ore deposits in this southern part of the shield is precluded by their low $^{207}Pb/^{204}Pb$ and $^{208}Pb/^{204}Pb$ characteristics. Lead samples from the Al Amar fault region to the east exhibit slightly higher $^{207}Pb/^{204}Pb$ and distinctly higher $^{208}Pb/^{204}Pb$ characteristics that distinguish them from those in deposits to the west. This is the first isotopic evidence to support current ideas that the Al Amar fault region is of tectonic significance. These different characteristics are interpreted to indicate the presence of Proterozoic X lower crustal basement rocks in the Al Amar region from which mineral deposits were formed 650 m.y. to 450 m.y. ago.

Two galena analyses, one from South Yemen and one from Oman, indicate the existence of upper crustal continental rocks possibly of Proterozoic X age in the south and east of the Arabian Peninsula. These are the first isotopic data indicating older continental rocks in the region. Models for the tectonic evolution of this part of the Earth's crust will have to be given consideration.

Proterozoic material in the Yukon-Tanana Upland, central Alaska

Geochronologic studies (Nd-Sn and U-Th-Pb) by J. N. Aleinikoff and Kiyoto Futa on a large body of augen gneiss in the vicinity of the Taylor Mountain batholith show that the gneiss comprises material that was separated from the mantle approximately 2,000 m.y. ago. U-Th-Pb systems in zircons were largely reset 350 m.y. ago, probably by sillimanite facies metamorphism. The existence of such a large Precambrian body is particularly significant because previous Alaskan studies indicated only minor occurrences of Precambrian material.

Zircon fission-track ages of a Pleistocene ash, California and Nevada

The informally named "Maidu" ash is a widespread mid-Pleistocene marker bed that has been recognized at

numerous localities in northern California and western Nevada (Sarna-Wojcicki and others, 1977). The ash has been identified on the basis of its glass chemistry and petrography. Fission-track and K-Ar ages of this ash from several localities, however, are scattered, ranging from 0.4 m.y. to 2.1 m.y. A recent modal study by C. E. Meyer, M. J. Woodward, and A. M. Sarna-Wojcicki of zircon fission-track ages on several hundred crystals indicates that the principal mode for the dominant clear euhedral glass-coated crystals is about 0.46 m.y., which is in good agreement with the K-Ar ages of this ash that have the lowest analytical errors (0.45 m.y.–0.50 m.y.). A subordinate mode for pink euhedral glass-coated crystals is 0.59 m.y. This population of crystals has a distinctly higher uranium concentration than the clear zircons. The pink zircons may be partly annealed xenocrysts derived from older volcanic units in the source area during eruption of the "Maidu" ash. Ages on euhedral, anhedral, and rounded zircon crystals of clear, pink, yellow, and hyacinth color range from about 0.3 m.y. to about 2.0 m.y., while one crystal gave a high age of 98 m.y., indicating presence of detrital as well as xenocrystic contamination. These findings underscore the importance of examining a large number of crystals in fission-track age analyses to eliminate the problem of xenocrystic and detrital contamination.

Klinker dating

D. A. Coates and C. W. Naeser collaborated on a study of klinker developed by the natural burning of the Wyodak coal bed. In the eastern Powder River Basin, Campbell County, Wyo., there are a number of klinker beds that form resistant ridges. Zircons separated from sediments baked during the burning of the coal can be dated with the fission-track method. It is assumed that, as the water table drops because of headward erosion by the stream, the coal starts burning. A series of 11 samples of baked sandstone and shale was collected along the top of a mesa north of east-flowing Little Thunder Creek. The length of the mesa is about 13 km east-west, and the top of the frontal face is about 200 m above the creek. The fission-track ages of the zircons get younger to the west. The oldest burn was about 700,000 yr ago on the easternmost exposure of klinker. The westernmost sample has an age of less than 80,000 yr (no tracks were observed in the zircon from this locality). Thus, there has been about 200 m of down cutting and about 13 km of headward cutting by Little Thunder Creek in the last 700,000 yr.

Two generations of Archean gneiss in the Big Horn Mountains

The Rb-Sr and U-Pb methods were used by J. G. Arth, T. W. Stern, and Fred Barker to study gneisses in the Lake Helen 7½-min quadrangle of the Big Horn Mountains, Wyo. Two episodes of magmatism, deformation, and metamorphism occurred during the Archean. Trondhjemitic to tonalitic orthogneisses and amphibolite of the first episode (E-1) are cut by a trondhjemite pluton and a calc-alkaline intrusive series of the second episode (E-2). The E-2 series includes hornblende-biotite quartz diorite, biotite tonalite, biotite granodiorite, and biotite granite.

The Rb-Sr whole-rock isochron on E-1 gneisses indicates an age of 3,007 m.y. ± 34 m.y. (1 sigma) and an initial $^{87}Sr/^{86}Sr$ of 0.7001 ± 0.0001. U-Pb determinations on zircon from E-1 gneisses yield a concordia intercept age of 2,947 m.y. ± 50 m.y. The low initial strontium ratio suggests that the gneisses had no significant crustal history prior to metamorphism and that the magmas from which they formed had originated from a mafic source.

A Rb-Sr whole-rock isochron for E-2 gneisses gives an age of 2,801 m.y. ± 31 m.y. The initial $^{87}Sr/^{86}Sr$ is 0.7015 ± 0.0002 and precludes the existence of the rocks for more than 150 m.y. prior to metamorphism. The E-2 magmas may have originated from melting of E-1 gneisses or from a more mafic source.

Paleozoic events in the Piedmont near Fredericksburg, Virginia

Several suites of plutonic rocks have been revealed by geologic mapping by Louis Pavlides in the polydeformed and metamorphosed (amphibolite-grade) Piedmont near Fredericksburg, Va. Two of these suites were dated by U-Pb (zircons) and Rb-Sr (whole-rock) methods by T. W. Stern, J. G. Arth, K. G. Muth and M. F. Newell. The oldest suite is the Falls Run Granite Gneiss (formerly called the Berea pluton), a coarse-grained, strongly foliated, and highly metamorphosed rock that ranges in composition from adamellite to monzonite. The chief mass of Falls Run Granite Gneiss is intrusive into the Holly Corner Gneiss of Early Cambrian(?) age. Both these gneisses are allochthonous remnants of the inverted limb of a recumbent fold; subsequent deformation formed a type II interference fold. U-Pb and Rb-Sr studies indicate that the Falls Run is 410 m.y. old and has an initial $^{87}Sr/^{86}Sr$ of 0.707.

Younger granitoid plutons, dikes, and sills are assigned to the Falmouth Intrusive Suite and are widespread in the area. These plutons are abundant in the eastern part of the area but are rare west of the Quantico Formation. Rocks of the Falmouth consist of strongly to weakly foliated biotite adamellite and granodiorite having a Rb:Sr less than 0.2 (group a) and muscovite-biotite adamellite and granite having a Rb:Sr greater than 0.4 (group b). Concordant zircon ages and two whole-rock isochrons indicate that both groups are 300 m.y. to 330 m.y. old. The initial $^{87}Sr/^{86}Sr$ of group a

is 0.704, which suggests a lower crust or mantle source, whereas that of group b is 0.709 and suggests crustal involvement in the magma generation. Recently reported ages from North and South Carolina are similar to those of the Falmouth. Thus, an extensive belt of 300-m.y.- to 330 m.y.-old plutons is present in the eastern Piedmont.

Rejuvenation of an ancient craton

The epizonal granite of Section 28 in the Minnesota River valley was found by B. R. Doe to have a Pb-Pb age of 1.84 b.y. $\pm$ 0.05 b.y. on the basis of data obtained on HF-leached and unleached feldspars and HCL-leached and unleached whole rocks. The mesozonal late-Tectonic Archean Sacred Heart Granite of Lund (1956) in the Minnesota River valley was found to have a Pb-Pb age of 2.605 b.y. $\pm$ 0.006 b.y. on the basis of data obtained on HF-leached and unleached feldspars and HCL-leached and unleached whole rocks.

As was predicted on the basis of Mesozoic and Cenozoic analogs for these kinds of granites in this type of tectonic environment, the initial leads in the granites indicate that they were derived from source material having values of $^{238}U/^{204}Pb < 9$ normalized to the present day. This feature is common in Mesozoic and Cenozoic igneous rocks penetrating Precambrian terrains but rarely observed in pre-Mesozoic igneous rocks. Lund's Sacred Heart Granite is the oldest igneous rock known to show this effect and is the first representative of a mesazonal granite. The uranium depletion event appears to have been a granulite-facies metamorphism, but the age of that metamorphism cannot be determined from the available data. The model-lead-age information, however, suggests that it occurred prior to 2.78 b.y. ago. The source materials for both granites also underwent an earlier stage of extensive but unknown duration during which $^{238}U/^{204}Pb < 9$. In Phanerozoic rocks, such values are characteristic of ensialic tectonic environments. Similar development of ensialic environments apparently was occurring in ancient time.

Irradiation of samples for $^{40}Ar/^{39}Ar$ dating using the Geological Survey TRIGA Reactor

G. B. Dalrymple, M. A. Lanphere, and G. P. Kraker, Jr. (USGS), working with Calvin Alexander (University of Minnesota), have determined the characteristics of the Geological Survey TRIGA Reactor (GSTR) as a source of fast neutrons for the $^{40}Ar/^{39}Ar$ technique of K-Ar dating using data from more than 45 irradiations in the central thimble (core) facility. The GSTR has a flux over the entire energy spectrum of 1.1×10^{17} n/cm^2 /MWh and a fast-thermal ratio on the centerline of the central thimble of 1.17 for fast neutron energies >0.6 MeV. This results in an ^{39}Ar production of about 7×10^{-13} mol/gr-percent K_2O and a cross section for the reaction $^{39}K(n,p)/^{39}Ar$ of $(69 \pm 4) \times 10^{-31}$ m^2 for epithermal neutrons (>0.6 MeV). Most $^{40}Ar/^{39}Ar$ dating applications require about 10 to 40 h of irradiation in the GSTR at the maximum continuous power level of 1 MW.

The peak neutron flux in the central thimble is 4 cm above the physical centerline, and the flux gradient in the centermost 20 cm varies from a small fraction of a percent to a maximum of about 3.5 percent per centimeter. The effect of this gradient can be effectively canceled by suitable sample encapsulation and the use of a sample holder designed for the purpose. The horizontal flux gradient is barely detectable statistically and is less than 0.5 percent over the width of the central thimble tube. Shelf-shielding in a solid rock core of diabase 2.40 cm in diameter by 2.54 cm in height was found to be approximately 3 percent from the outside to the center, but shelf-shielding is probably negligible for the 0.6- to 0.8-cm diameter of a typical dating sample.

Corrections for interfering argon isotopes produced by neutron reactions with calcium are relatively reproducible with values of $2.64 \pm 0.017 \times 10^{-4}$ for $(^{36}Ar/^{37}Ar)_{Ca}$ and $6.73 \pm 0.037 \times 10^{-4}$ for $(^{39}Ar/^{37}Ar)_{Ca}$. The measured values whose cause is unknown is not unique to the GSTR but has been reported for other reactors used in $^{40}Ar/^{39}Ar$ dating. The corrections for interfering argon isotopes can be minimized by choosing the appropriate sample size and irradiation parameters for the age and K:Ca of the sample using optimization curves for the GSTR.

An investigation of more than 100 possible neutron reactions in common rocks and minerals showed that only 26 need be considered for purposes of radiological safety. The activity produced by these reactions upon irradiation of samples can be conveniently and accurately predicted by either a computer program or graphs specifically devised for the GSTR.

GEOTHERMAL SYSTEMS

Geoelectrical study of the Rio Grande Rift

Simultaneous observations by J. N. Towle of geomagnetic field variations across the Rio Grande Rift at approximately lat 35° N. during the spring of 1977 extended Schmucker's earlier observation of a geomagnetic variation reversal across the southern portion of the rift, in the vicinity of Las Cruces, to the central portion of the rift near Belen. Several instances of current channeling (that is, earth current flow in the rift due to geomagnetic induction elsewhere) were recorded, allowing a straightforward interpretation of electric current density and the electrical conductivity structure in the central portion of the rift.

The close spacing of observations in this study allowed a more detailed interpretation by Towle of the geoelec-

trical structure of the Rio Grande Rift than has been possible. The interpretation indicates a general upwelling of the mantle, or aesthenolith, beneath the rift with an extent of almost 200 km. There is also a considerably smaller intrusion of conductive material to a depth of 15 km, indicative of partial melting in the upper crust beneath the rift. The geoelectrical interpretation agrees very well with other geophysical evidence, including a detailed heat-flow study of the rift.

Aeromagnetic anomalies on Kilauea's east rift zone, Hawaii

C. J. Zablocki compiled low-level (~60-m ground clearance) aeromagnetic data from Kilauea's east rift zone. The compilation revealed a linear dipolar anomaly about 2 km in width that continues unbroken from near the summit to 25 km downrift. The anomaly coincides with the surface expression of the present-day rift zone and is produced by a shallow (0.2- to 0.6-km depth) dike complex. Another anomaly, related to a deeper and broader feature, exists about 2 km to the north and parallels the shallower one. It extends from near the upper east rift zone to at least the east end of the island. This feature may be related to a previously suggested paleorift. These results reinforce the concept of a transform fault in Kilauea's lower east rift zone (Zablocki, 1977).

Extreme self-potential anomalies found on Mount Hood, Oregon

Self-potential surveys by D. B. Hoover near and above the timberline on Mount Hood, Oreg., revealed self-potential anomalies of 3 to 4 V. These potentials are about one order of magnitude larger than those normally observed and are as large as any reported. The anomalies of interest are not related to the topographic gradient; that is, the equipotentials do not follow the topographic contours but often run normal to the topographic contours. A satisfactory explanation for these large potentials is not available.

The Mount Hood data, however, does show a correlation with elevation that is attributed to a streaming potential due to ground-water flow down the mountain. This is in addition to the above-mentioned anomalies. The observed elevation coefficient at Mount Hood is 2.0 V/300 m.

Zonation of clay and zeolite minerals, Raft River geothermal boreholes, Idaho

Samples from Raft River geothermal boreholes 2, 4, and 5 were analyzed by H. R. Covington (USGS) and P. T. Kolesar (Utah State University) for clay and zeolite mineralogy using X-ray fluorescence techniques. Drill cuttings from the geothermal boreholes were sampled at 30-m intervals. Three mounts were made for each sample – a randomly oriented powder mount, a 115-μ-oriented mount, and a 2-μ-oriented mount. The three mounts were then X-rayed, after which the two oriented mounts were glycolated and X-rayed again.

The analysis showed a sequence of zonation for both the zeolites and clay minerals in the geothermal boreholes. In general, the clays progress downward from montmorillonite, to mixed-layer clays, to illite. The zeolites show a downward progression from clinoptilolite, to analcite, to wairakite, to laumontite. The depths at which given minerals occur vary from borehole to borehole as do some of the minor minerals.

The results of this study, when all boreholes have been completed, may yield information as to the temperature and chemistry of the environment in which the clay and zeolite minerals formed, as well as a better characterization of the geothermal reservoir through time and space.

Geothermal resource of the eastern Snake River Plain

A 3-year coordinated program by the USGS, DOE, and the Idaho Department of Water Resources to assess the geothermal resources of southern Idaho has been completed. Field work consisted of geologic mapping, geophysical and geochemical surveys, hydrologic studies, and drilling. The program culminated in the drilling of the first deep hole on the eastern Snake River Plain, a 3-km-deep test well by DOE at the Idaho National Engineering Laboratory. The well penetrated 2.5 km of primarily volcanic rock and was bottomed in a dense rhyodacite. The bottom hole temperature was about 150°C, and the well produced very little water.

With the exception of the very large Bruneau–Grand View system and possible extensions, no evidence of large hydrothermal convection systems with reservoir temperatures over 90°C has been found on the Snake River Plain. In the central part of the eastern Snake River Plain, measured thermal gradients are less than 50°C/km, and the crust is thicker and the Curie isothermal surface deeper than in adjoining areas. Little evidence of active faulting is apparent. These factors suggest that the central part of the eastern Snake River Plain is not favorable for the development of higher temperature geothermal systems within 3 km of the surface. However, the margins of the plain appear more promising. Here thermal gradients are higher, and active faults are present.

Interrelations among epithermal ore deposits and geothermal systems depositing mercury, gold, and silver

Geothermal systems associated with active deposition of mercury, such as at Sulphur Bank, Calif., and Ngawha, New Zealand, and of gold and silver, such as at Broadlands, New Zealand, and Steamboat Springs, Nev., provide data for a tentative general model of interrelations. D. E. White and Chris Heropoulous found that new data on the "epithermal" suite of elements (As, Sb, Hg, Au, Ag, and Ti) supplement previous studies of these and related systems (White, 1967; Weissberg and others, 1979; and Nolan, 1933). Group associations presently recognized and tentatively explained include:

1. Mercury deposits, commonly with no other recovered metal, but small quantities of the other "epithermal" metals may be present. Suggested critical factors in transport and deposition are (1) source regions of fluids and Hg >200°C, (2) a through-going (rather than local) vapor phase, normally coexisting with liquid, (3) instability of HgS at high temperatures, especially in the presence of a vapor phase (Krauskopf, 1951; Dickson, 1964) (HgS may slowly decompose to Hg and S, requiring a vapor phase for major transport), (4) enough CO_2 (or other gases) to form a separate vapor phase at great depths where pressures are too high for boiling of pure water, and (5) efficient deposition of mercury from the vapor may require outlet temperatures below 100°C for Hg to condense and react with sulfur (high-temperature discharge of vapor may result in dispersal rather than concentration of mercury).
2. Au-Ag deposits relatively high in Au, As, Sb, Hg, and Tl (as well as B and Ge?) but low in base metals and only moderately high in Ag. These deposits may form in the near-surface parts (upper few hundred meters?) of high-temperature hot-spring systems. Metal-sulfide complexes may be more important in high-level transport than chloride complexes. The gold-silver group includes the recently recognized Carlin-type disseminated gold as well as the gold-dominated epithermal vein deposits (Nolan, 1933).
3. Ag-Au deposits relatively high in Ag and base metals but probably lower in Hg, Tl, As, and Sb than group 2 (but commonly with Ag sulfosalts of these metals). Metal-chloride complexes are probably critical in transport, with the complexes breaking down and most of the silver and base metals depositing as temperature and, possibly, salinity decrease.

Zoning of the "epithermal" suite of metals with depth is convincingly shown at Steamboat Springs, Nev. (pub. and unpub. data). A similar pattern of zoning is evident at Broadlands, New Zealand, but deep exploration has revealed an intermediate relatively barren zone overlying the base-metal-silver zone. Base-metal-silver concentrations are generally at depths greater than 600 m, where temperatures generally exceed 200°C. Sphalerite is the most common base-metal sulfide, but galena and chalcopyrite are locally dominant; arsenopyrite and a silver telluride occur as inclusions in sphalerite.

The ideas expressed above are highly speculative, but they suggest the possibility that group 3 deposits may normally underlie group 2 deposits, with a relatively barren intervening zone that has discouraged deep exploration. T. B. Nolan (1933) notes that group 2 deposits generally have not been highly productive, which may have discouraged deep exploratoion. The barren zone may be related to changes in the dominant mechanisms of metal transport, with chloride complexes dominant at depth and bisulfide complexes dominant near the surface.

Magma chamber in The Geysers–Clear Lake area

B. C. Hearn, Jr., J. M. Donnelly, and F. E. Goff examined evidence for a magma chamber, believed to be the deep heat source for The Geysers steam field and the hot water system inferred from spring geochemistry, beneath the Clear Lake Volcanics in The Geysers–Clear Lake area, northern California (Hearn and others, 1981). The shape and depth extent of the magma chamber are not well defined. As modeled from the negative gravity anomaly, the chamber is a 14-km-diameter sphere centered at a 14-km depth below a point 2.5 km south-southwest of Mount Hannah on the southwest edge of the Clear Lake volcanic field (Isherwood, 1976). As modeled by teleseismic P-wave delay data, the chamber is partly coincident with the gravity model, is slightly elongated northeast and southwest, and extends to at least 30 km in depth (Iyer and others, 1979).

Significant volumes of fractionated silicic volcanic rocks are present in The Geysers–Clear Lake region in two age groups, 10 km^3 from 0.8 m.y. to 1.1 m.y. and 40 to 50 km^3 from 0.3 m.y. to 0.6 m.y. These silicic lavas imply that silicic magma was present at shallow levels in the crust during those periods. However, no volcanic rocks younger than 0.3 m.y. are present above the magma chamber that is inferred, on the basis of geophysical evidence, to exist now. The youngest group of volcanic rocks, 0.01 m.y. to 0.1 m.y., are largely mafic and lie north-northeast of the postulated magma chamber.

The only rhyolite in the youngest group, that of the rhyolite of Borax Lake, is more fractionated than earlier rhyolites and, thus, could have been laterally erupted from the evolving main chamber. Alternatively, because the rhyolite of Borax Lake lies within a north-south line of vents for mafic rocks that show strontium isotopic characteristics (Futa and others, 1981) of deep origin, the rhyolite may have been erupted from a small magma chamber above a new focus of deep heating. Future geophysical studies could provide better resolution of the extent of one or more magma chambers and their related geothermal systems.

Properties of multiphase fluids and their influence on geothermal phenomena

Physical properties of multiphase fluids may be drastically different from those of the component end members; for example, a two-phase mixture of H_2O liquid + vapor or H_2O liquid + dissolved gases has very dif-

ferent compressibilities and sound speeds from either the liquid or vapor components. The unusual physical properties of the multiphase fluids dramatically influence the observed properties of geothermal systems such as flow velocity. S. W. Kieffer (1977a) calculated the sound speed of water-air and water-steam mixtures and devised a new thermodynamic representation (entropy versus density) that graphically illustrates many of the physical properties of mixtures relevant to fluid dynamics problems (Kieffer and Delaney, 1979). Analysis of CO_2 and H_2O fluids ascending isentropically from crustal and mantle reservoirs using these graphs demonstrates qualitative as well as quantitative differences in the thermodynamic behavior of the fluids. Whereas CO_2 is likely to ascend from mantle reservoirs in the vapor-phase, H_2O may undergo different phase changes depending upon its initial entropy. These concepts have been applied to problems in terrestrial and Ionian volcanism as well as to geothermal phenomena (Kieffer, 1977b; Kieffer, 1979d,e; and Smith and others, 1979).

Revised Na/K geothermometer

R. O. Fournier reevaluated the Na/K geothermometer using data from wells drilled in geothermal systems in a wide variety of geologic environments and spanning a large temperature (t) range. A new equation recommended for geothermometry is:

$$t°C = \frac{1{,}217}{\log (Na:K) + 1.483} - 273.15,$$

where sodium and potassium concentrations are in parts per million. Most waters from reservoirs with temperatures above 100°C have Na:K between those expected for solution equilibrium with low-albite plus microcline and those with high-albite plus sanidine. The Na/K geothermometer generally works well for waters from reservoirs with temperatures greater than 150° to 200°C but is likely to give anomalously high estimated temperatures when applied to waters from environments where temperatures are less than 100°C.

Source of steam at Larderello geothermal system, Italy

A. H. Truesdell (USGS), in collaboration with Franco D'Amore (International Institute for Geothermal Research, Pisa, Italy), interpreted detailed data on the evolution of the chemistry of Larderello steam to indicate that three sources contribute progressively to the steam produced.

Initially, almost all steam comes from vaporization of a condensate layer just above the two-fluid-phase vapor-dominated reservoir. This steam has a high flow rate because it originates close to the well bottom and is low in temperature and gas and high in boron and ammonia.

After 10 to 15 yr, flows decrease to less than 10 percent of their initial values as steam originating from greater distances in the vapor-dominated reservoir feeds the well. With a lower water to rock ratio and substantial amounts of original vapor, this steam is high in temperature and gas content and low in boron and ammonia.

Steam flow in the Larderello and The Geysers geothermal systems

A. H. Truesdell (USGS), in collaboration with Franco D'Amore (International Institute for Geothermal Research, Pisa, Italy), found that steam compositions from Larderello and The Geysers show similar patterns with concentric zonation of decreasing ^{18}O, boron, and (at Larderello) chloride contents and increasing gas and ammonia contents from the center of a producing area toward the edges. This was interpreted to indicate that the preexploitation steam flow in these systems was laterally from boiling (or inflow) zones of limited size toward the edges of the systems. Conductive heat loss to the surface resulted in partial condensation of the steam. The condensate leached silica and other materials from the reservoir rock to produce the cavernous porosity observed in these systems and flowed downward to a deep water table and back to the boiling zone. This process can be modeled as a Raleigh condensation that obeys the equation:

$$\frac{C}{C_o} = \left(\frac{M}{M_o}\right)^{A-1},$$

where C is the concentration of a steam component at any point in space or time, C_o is the original concentration before condensation occurred (at the center), M and M_o are the equivalent steam masses, and A is the distribution of the component between liquid and vapor ($A = {}^{c}liq./{}^{c}vapor$). The magnitudes of the observed changes (-3 ‰ in $\delta^{18}O$, $+5x$ in CO_2, and $+3x$ in NH_3 at Larderello; -5 ‰ in $\delta^{18}O$, and $+18x$ in CO_2 at The Geysers) suggest that steam is 80 percent condensed at Larderello and 95 percent condensed at The Geysers at the limit of productive drilling.

After 15 to 25 yr, chloride appears in the steam, and the gas contents decrease as vaporization of deep brine becomes the major steam source.

Three new gas geothermometers

Three new gas geothermometers for vapor-dominated and hot water systems were developed by A. H. Truesdell (USGS), in collaboration with Franco D'Amore (International Institute for Geothermal Research, Pisa, Italy). The methods used are based on the observed control of oxygen, carbon, and sulfur fugacity by mineral-water reactions. The geothermometers can be used on well discharges (requiring concentrations in the total fluid of CO_2 and CH_4, H_2, or H_2S)

or from gas ratios of hot spring discharges. Used on vapor systems, they indicate the reservoir temperature away from the well bottoms. When combined with flowing steam temperatures at the well bottom, calculated using equations derived by Manuel Nathenson, the geothermometer temperatures indicate the original ratio of liquid water to rock and, therefore, the yield of steam from a rock volume. These are the only geothermometers that can be used on steam systems, and they also work, with modifications, in hot water fields.

Production-induced changes in the aquifer of Cerro Prieto geothermal area, Mexico

A. H. Truesdell, N. L. Nehring, and C. J. Janik found that the Cerro Prieto geothermal reservoir appears to behave very differently from the Wairakei reservoir. Cerro Prieto brines originally were nearly steam saturated, and pressure drawdown, which occurred soon after the start of power production, caused widespread boiling. After 2 yr, the drawdown was so great (water levels in shut-in wells dropped as much as 200 m) that a breakthrough of cooler waters occurred. This caused partial recovery of aquifer pressures and decreased the amount of boiling. The breakthrough occurred as three fronts—pressure, chemical, and thermal. The pressure front was nearly instantaneous and was observed in the 1975 recovery of water levels; the chemical front required the passage of water to the wells and was observed in the decrease in chloride in fluids from wells of the south-central part of the field from 1974 to 1976; the thermal front has yet to be observed but should arrive in the early 1980's. These complex reservoir processes are indicated by the changes in chloride, enthalpy, Na:K, and silica in the well fluids and supported by limited physical data on the temperature and pressure in the reservoir.

Origin of Cerro Prieto, Mexico, brines

A. H. Truesdell, N. L. Nehring, and C. J. Janik developed a model for the origin of the water and dissolved salts of the Cerro Prieto brine based on Cl:Br, salinities, and deuterium concentrations that are not affected by high temperature interaction with ordinary rocks. The deuterium concentration of the geothermal brine ($\delta D = -93$–96 ‰) is similar to that of Colorado River water ($\delta D = -100$–110 ‰) and very different from other local waters (rain, -60 ‰; seawater ~ 0 ‰). However, the salinity is half that of seawater, and the Cl:Br is nearly identical; other water sources have different Cl:Br or differ greatly in salinity or both. It is suggested that seawater, evaporated ~ 5 times in coastal lagoons, infiltrated the deltaic sediments, and was diluted ~ 10 times with Colorado River water to produce the brine that was then altered by rock reactions (without change in δD, Cl:Br, or salinity) to its present composition.

Reservoir processes at Steamboat Springs

Chemical and isotopic analyses of hot spring and shallow well waters at Steamboat Springs, Nev., were used by N. L. Nehring to model the boiling, cooling, and mixing processes and to determine the compositional changes occurring as water ascends from the deep reservoir. Two distinct paths of water flow from the reservoir to the surface were shown by an enthalpy-chloride diagram. The dominant path is flow up fissures and faults to the surface or out into uncemented near-surface alluvium. After boiling and losing steam, this water feeds the springs and the shallow wells north of the main hot spring area. A lesser amount of water flows from the reservoir to the intermediate depth (80–330 m) wells. This water flows slowly through the rock and is cooled conductively. Mixing is observed near the edges of the thermal area. The calculations show that the reservoir water has about 700 mg/kg chloride and $\delta D = -119.5$ ‰. The indicated recharge area is at about 2100-m elevation in the Carson Range immediately west of the springs.

Thermal properties of rocks

Thermal properties of all common rocks—igneous, metamorphic, and sedimentary—can be calculated knowing the mineral composition or mode, the texture, including porosity and layering, and the pressure and temperature conditions. E. C. Robertson plotted basic data on thermal conductivities and specific heats of rocks on graphs from all available laboratory measurements, showing the effects of mode, porosity, pore fluid content, and temperature. Tabulated data for minerals and rocks were listed for diffusivity, thermal inertia, conductivity, thermal expansion, specific heat, and the effects of pressure, radiation, and anisotropy on conductivity. Combinations of the graphs and tables can be used to estimate within 10 percent the important thermal properties for all except very uncommon rocks under almost every condition to be expected in the Earth's crust and upper mantle. This information is needed to evaluate rock repositories for radioactive waste management and to solve geothermal problems for energy.

Internal friction experiments in granite

Louis Peselnick and Hsi-Ping Liu designed and constructed an apparatus for measuring the internal friction from Q^{-1} of rocks directly from stress-strain

hysteresis loops at seismic m_b-wave periods and small strain amplitudes. Stress-strain loops for the Young's modulus mode were obtained for Westerly Granite for strains of 10^{-6} and 10^{5} at room pressure and temperature and at 0.2 Hz, respectively. A value of Q of 87 ± 7 was determined under these conditions. The shapes of hysteresis loops contain information relating to the anelastic properties of the rock. Previous investigations showing "cusped-shaped" loops led to the conclusion that such cusps result from nonlinear behavior between stress and strain in the rock. In contrast with such results and conclusions, Peselnick and Liu found noncusped hysteresis loops for strain amplitudes of 10^{-5}. Additionally, they made theoretical calculations that demonstrated that hysteresis loop shapes for an anelastic linear solid satisfying $Q^{-1} = \text{constant}$ with frequency are sensitive to the cycling stress-wave form. Observations of cusped or asymmetrical hysteresis loops are compatible with linear behavior and do not necessarily imply a nonlinear attenuation mechanism.

Heat flow in relation to hydrothermal activity in the southern Black Rock Desert, Nevada

As part of an investigation of the Gerlach NE KGRA, J. H. Sass, M. L. Zoback, and S. P. Galanis, Jr., made 13 heat-flow measurements in playa sediments of the southern Black Rock Desert, northwestern Nevada (Sass and others, 1979; Sass and Zoback, 1979). These data, together with additional previously unpublished heat-flow values, reveal a complex pattern of heat flow with values ranging from 1.0 to 5.0 HFU (40–100 MWm^{-2}) beyond the hot springs area. The mean background heat flow for the southern Black Rock Desert is 1.8 ± 0.15 HFU (75 ± 6 MWm^{-2}).

The complexity of the pattern of heat flow is believed to arise from hydrothermal circulation supporting the numerous hot springs throughout the region. The occurrence of the lowest observed heat flow in the deepest part of the basin strongly suggests that fluid movement within the basin represents part of the recharge for the hydrothermal system. Hence, the heat-flow data do not support a "thermal blanketing" model to explain the geothermal activity (Keller and others, 1978). The nature of the modern activity is believed to be related to deep circulation of meteoric water. Such deep circulation and subsequent upwelling along range-front faults is typical of geothermal systems throughout the Basin and Range province. Microearthquake activity indicates active fracturing to the required depths (4–7 km) circulation.

A thermal balance for the system incorporating both anomalous conductive heat loss and convective heat loss from the spring systems indicates a total energy loss (above background of about 8.0 Mcal/s or 34 MW within an estimated 1,000-km^2 region). Consideration of this additional heat loss yields a mean regional heat flow of 2.5+ HFU (100+ MWm^{-2}) and warrants inclusion of this region in the Battle Mountain heat-flow high.

Near-surface heat flow in Saline Valley, California

C. W. Mase, S. P. Galanis, Jr., and R. J. Munroe found that, with the exception of values from one borehole drilled at Palm Springs and three boreholes drilled around Saline Valley dry lake, eight new heat-flow values in Saline Valley, Calif., are within or somewhat below the range expected for this region of the Basin and Range heat-flow province (Mase and others, 1979). The lack of recent volcanism in the area and the apparently normal basin-and-range heat flow suggest that geothermal systems within the valley are stable stationary phases supported by high regional heat flow and forced convection.

Temperature survey in Raft River geothermal system

Relogging by T. C. Urban of 24 shallow temperature-monitoring wells in November 1978 and July 1979 drilled in the Raft River geothermal system indicated that most of the holes had returned to near their predrilling undisturbed temperatures. The few anomalous holes may be reflecting either shallow disturbances in the immediate vicinity of the holes or some perturbation induced by the geothermal system.

Average elevation map of the conterminous United States

T. C. Urban produced an average elevation map of the conterminous United States (1:2,500,000) to aid in examining geological and geophysical data on a more regional basis. The averaging scheme used initially is one James Gilluly used for the southwestern part of the country. In this scheme, the average elevations of nine 15-min quadrangles were added together, with the central quadrangle weighted double, and the result divided by 10. Thus, a moving average is generated for every 15-min quadrangle on the map, and the resulting averaged elevations are then contoured. At present, the maps are in the final stage of drafting. Future efforts will encompass alternate averaging schemes, comparisons to geological and geophysical data, and an analysis of geothermal anomalies and their relations to trends in elevation.

Chapter completed in "Geothermal Source Book"

W. H. Diment completed a chapter for the DOE-sponsored "Geothermal Source Book." The chapter was entitled "Geology and Geophysics of Geothermal Areas" and covered many aspects of what is known about geothermal systems and techniques.

Temperature distribution caused by flow up a fault

Manuel Nathenson, T. C. Urban, and W. H. Diment (1979) obtained an approximate analytical solution for the temperature distribution caused by the flow of water up a fault. Temperature versus depth profiles calculated at several distances from the fault show that near the fault there is large curvature, but, at a distance of one fault depth away, there is little perturbation of the background linear temperature profile. Comparison with a temperature versus depth profile obtained in well RRGE–1 at Raft River, Idaho, shows that the well is located close to the fault, and the flow up the fault is 6 L/s for each kilometer of fault length.

Earthquake-induced thermal changes at Yellowstone National Park, Wyoming

The strongest correlation yet observed between Yellowstone seismic activity and changes in thermal features occurred in the Mud Volcano thermal area in late 1978 and early 1979. A. M. Pitt noted that, from January 1973 to May 1978, earthquake activity within 5 km of the Mud Volcano area was limited to occasional events up to $M = 2.4$. On May 25, earthquakes with local magnitudes between 2.5 and 3 began occurring beneath the thermal area at depths of 2 to 4 km. Increased seismic activity continued until the middle of November, with intense swarms (100 events per hour) occurring on October 23 and November 7. The largest event, $M = 3.1$, occurred on November 14. Heat flow out of the Mud Volcano thermal area began increasing in December 1978. Old thermal features became more active, new features appeared, and trees were killed along a 2-km-long northeast-trending zone. Increased heat flow continued through September 1979. This spatial and temporal association of earthquakes and increased heat flow at Mud Volcano suggests that the seismic activity could have expanded fracture systems, permitting increased fluid flow from depths of several kilometers.

Seismic velocity structure at Coso geothermal area

Teleseismic P-wave arrivals were recorded by a dense array of seismograph stations located in the Coso geothermal area, California. The resulting pattern of relative residuals reveals an area showing approximately 0.2-s excess traveltime that migrates with changing source azimuth, suggesting that the area is the "delay shadow" produced by a deep low-velocity body. Inversion of the relative residual data by P. A. Reasenberg for a three-dimensional velocity structure determined the lateral variations in velocity to a depth of 22.5 km beneath the array. An intense low-velocity body, which coincides with the surface expressions of late Pleistocene rhyolitic volcanism, high heat flow, and hydrothermal activity, was resolved at depths between 5 and 20 km. The low-velocity body has a maximum velocity contrast of over 8 percent between 10 and 17.5 km. The shallowest part of this body is centered below the region of highest heat flow; at depth, it is elongate in approximately the north-south direction. The hypothesis that this low-velocity body is caused by the presence of partial melt in the middle crust is consistent with the local seismic, geologic, and thermal data.

Upper crustal structure beneath the Coso Range, California

C. S. Weaver studied the structure of the upper crust beneath the Coso Range, Calif. These studies indicate that the region is highly uniform, with no seismic evidence of a magma chamber in the upper 10 km. The most important seismic velocity is 6.0 km/s, identified in a layer extending from 2.5 km down to 10 km. Seismic wave travel paths through this region have very small traveltime residuals (± 0.05 s), contraindicating the presence of a low-velocity zone that would be anticipated if a magma body were present. Consistent with this structural information, the depth of the seismogenic zone is nearly constant across the entire Coso Range. The lack of a shallowing of earthquake hypocenters beneath the Pleistocene rhyolite field is interpreted as evidence that no widespread volume of the near-surface crust is near liquidus temperatures.

Upper crustal structure of the Mount Hood region, Oregon

W. M. Kohler, J. H. Healy, and S. S. Wegener performed a seismic refraction experiment to study the crustal structure and to investigate the geothermal potential of the region around Mount Hood, Oreg. One hundred portable seismic recorders were used to make recordings at 200 locations from 10 explosions at 6 shot points, all within an area of about 4,000 km^2 centered around Mount Hood. A time-term analysis of the data indicates a refractor velocity of 6.1 ± 0.2 km/s and time terms varying from 0.2 to 1.2 s. Maps of reduced traveltimes and time terms reveal previously unrecognized structures. A major feature in the time-term map is a northeast-trending anomaly. The data indicate that crustal rocks in the Mount Hood region are mildly anisotropic. The degree of apparent anisotropy is about 2 percent, with the maximum velocity in a north-south direction.

In addition to the experiment described above, a 275-km-long reversed profile was made between Mount Hood and Crater Lake along the crest of the Cascade Range. This profile is expected to provide information about the deep crustal structure under the Cascades.

P-wave delays at two geothermal areas

Mahadeva Iyer (USGS) and Russell Robinson (New Zealand Department of Scientific and Industrial Research) analyzed P-wave residual data from the Roosevelt Hot Springs geothermal area, Utah, and found a low-velocity body in the crust and mantle under the region characterized by recent volcanism and high heat flow (Robinson and Iyer, 1979). The body has a diameter of 10 km and extends from 5-km depths into the uppermost mantle. The compressional wave velocity inside the body is 5 to 7 percent less than in the surrounding rock. One possible interpretation of the composition of the body is that it is magmatic with about 2 to 3 percent partial melt. If this is true, it implies that the body is the heat source responsible for the geothermal phenomena in the area and that the thermal energy available is much more than would be expected from deep hydrothermal circulation models.

Analysis of P-wave delay results by J. R. Evans and Iyer (1979) from two long northwesterly profiles across the eastern Snake River Plain indicates the presence of anomalously low compressional-wave velocities in the upper mantle. Geochronologically, the oldest volcanism in this section of the Snake River Plain is 2 m.y. to 6 m.y. The observed low velocity in the upper mantle probably is a continuation of the large crust-mantle magma body found under the Yellowstone caldera, considered to be the latest expression of the northeasterly progression of volcanism along the Snake River Plain. Detailed interpretation of P-wave delay data from the Snake River Plain, together with the available Yellowstone results, is expected to give valuable insight into the evolution of the Snake River Plain–Yellowstone volcanic system.

Pressurized fractures in hot rock

A small group of minette dikes and plugs crops out in flat-lying siltstones and shales near Ship Rock, N. Mex. D. D. Pollard and P. T. Delaney mapped the northeast dike, which has an outcrop length of 2,900 m, an average thickness of 7.2 m, and is composed of 35 discrete segments arranged en echelon. Orientation of segments ranges systematically between 52° N. and N. 66° E. Prominent joints strike parallel to the segments and occur within several tens of meters of the dike. Regional joints are not parallel to the dike. Small offsets and wedge-shaped bodies of crumpled host rock within segments mark sites of coalescence of smaller segments during dike growth. Bulges in the dike wall indicate where wall rocks were brecciated and eroded during flow of magma. Breccias make up about 9 percent of the total 7,176-m^2 area of the dike, are concentrated in its southwestern half, and are commonly associated with bulges. Three plugs that are subcircular, less than 30 m in diameter, and laterally associated with a dike contain abundant breccias. Field evidence indicates that the plugs grew from the dikes by brecciation of wall rocks and that the bulges in the wall of the northeast dike represent an initial stage of this process.

Pollard and Delaney concluded that dike propagation is the dominant mechanism for creating conduits for magma ascent. At a given driving pressure, dikes dilate to accept greater volumes of magma than plugs, and less work is done on host rocks for a given dilation. The form of the northeast dike is best matched by treating it as 10 cracks dilating in an elastic solid rather than as 35. This is attributed to coalescence of nearby segments below the present outcrop and to inelastic deformation at segment ends. Using a driving pressure of 2 MN/m^2 (20 bars), Pollard and Delaney estimated a shear modulus of about 10^3 MN/m^2 for host rocks, in agreement with laboratory tests on soft shales. A propagation criterion based upon stress intensity at segment ends indicates a fracture toughness of host rocks of about 100 $MN/m^{3/2}$, two orders of magnitude greater than values reported from laboratory tests. The segmentation of the dike probably is due to local rotation of the direction of least principle compressive stress with depth.

From theoretical models of magma and heat flow in elliptical conduits, Pollard and Delaney concluded that magma flows far more rapidly and at less relative heat loss in plugs than dikes. Although dikes are the preferred form for emplacement, plugs are the preferred form for flow of magma. For the northeast dike, flow rate is very sensitive to conduit geometry, but rate of heat loss to wall rock is not. As emplacement of the northeast dike progressed, local flow rate increased where wall rocks were eroded, reaching a maximum of about 45 times the mean initial rate. Maximum rate of heat loss to wall rocks was less than 1.6 times the mean initial rate. The inferred progression from continuous flow along a dike to flow from a plug agrees well with observations of modern eruptions that begin from fissures and later localize to discrete vents. The driving pressure gradient for magma flow was probably on the order of 25 N/m^3 (0.25 bar/km), or 10 percent of the body weight of the magma, and less than 1 percent of the heat convected up from the source region was lost to wall rocks.

Mapping on the Colorado Plateau indicates that magma may solidify along parts of a basic dike while it continues to flow elsewhere. Hawaiian eruptions reveal that extrusion begins from a dike and progresses to discrete vents. Commonly, this channelization of flow occurs in less than 24 h. Apparently, parts of dikes become inactive because magma freezes and not because driving pressure for flow decreases. Analysis of heat transport indicates that rate of heat conduction into wall

rock is initially a minute fraction of rate of convection along a dike. Although most of the flow is nearly adiabatic, larger temperature gradients exist within a thin boundary layer along the contact, where the flow is strongly nonadiabatic. Because the viscosity of magmas increases by over one order of magnitude for temperature drops that are only 5 to 10 percent of the temperature contrast between the magma and wall rock, modest heat loss within this layer is sufficient to effectively freeze the magma. Processes of unsteady heat conduction in host rock and unsteady heat conduction and convection in flowing magma are coupled at a moving contact that corresponds to a growing glassy rind within the dike. For properties, thicknesses, and driving pressures typical of basaltic magmatism, volumetric flow rates of magma can be expected to drop to less than 10 percent of their initial values in less than 24 h as a solidifying front propagates into the dike. Magma continues flowing at substantial rates in parts of dikes that thicken due to erosion of wall rock.

Using Kilauea Volcano as the principal source of data, equations were derived from continuum mechanics to describe certain physical aspects of the eruptions of Hawaiian volcanoes. Conceptual models based on dikes extending from a mantle source to a summit reservoir are untenable. Previous work has shown that cracks filled with less dense fluid rise gravitationally in more dense solids while maintaining finite heights by closure at the lower tip. Using density distributions determined by experiments and seismic velocity structures under Kilauea, as well as fracture toughness values from field studies of dikes, the height of ascending cracks was found to be greater than previously estimated. This results from using fracture toughness values (30–110 $MN/m^{3/2}$) for magma-filled cracks about two orders of magnitude greater than typical laboratory values. As an ascending dike of limited height reaches the reservoir, added bouyancy causes pressurization and inflation. Two necessary and sufficient conditions were delineated to distinguish the summit eruptions from intrusive events that may be accompanied by lateral flow of magma into rift zones. First, the volcanic edifice must store enough elastic strain energy during inflation to balance the increase in potential energy of magma ascending to the surface. Second, the reservoir must not rupture until sufficient strain energy is stored. For a depth of 3 km, a pressure increase of more than 10 MN/m^2 is required for a summit eruption; a circular reservoir must have a radius of about 5 km to supply the necessary volume at this pressure. If the reservoir ruptures at lower pressure, dike intrusion, possibly followed by lateral propagation into rift zones, may ensue, but no summit eruption will occur. During rift intrusions, dikes of limited height (1 km) may extend greater distances (100 km) along the rift zones and may pierce the surface of fissure eruptions. Previous work has shown that adjacent volcanoes and gravitational loading of the rift may control this extraordinary dike form. Pollard and Delaney believe that the contrasting densities of magma and host rock drive dikes downward, whereas vesiculation of magma and mechanical interaction with the Earth's surface drives dikes upward.

Complex stratigraphy at Medicine Lake Volcano

Detailed mapping by J. M. Donnelly-Nolan of 90 km^2 on the northwestern flank of Medicine Lake Volcano, northeastern California, revealed a complex volcanic stratigraphy. An andesite ignimbrite, previously interpreted to precede the building of the volcano, actually erupted midway in the volcano's history. The maximum thickness of the ignimbrite is about 7 m, one order of magnitude less than previously published estimates. Significant volumes of silicic lavas, along with more mafic lavas, were erupted prior to the andesite ignimbrite; a similar complex sequence followed. The volcano is not a basaltic shield, as thought by some previous workers. The presence of significant amounts of early rhyolite and dacite, the complex chemical evolution indicated by the eruptive products, and several rhyolite flows erupted within the last 1,200 yr suggest that the volcano may have significant geothermal potential.

Field tests of real-time magnetotelluric systems

Analysis by W. D. Stanley of data from over 100 magnetotelluric soundings in the Cascade Range revealed that there is a major electrical contact in the deep crust that may be observed from Mount Shasta to south of Mount Hood. This contact occurs approximately at the boundary between the western and High Cascades and appears to coincide with gravity, magnetic, and thermal anomalies. The western Cascades on the west side of the contact appear to be more resistive to depths of about 10 km and considerably more electrically complex than the High Cascades to the east of this contact. Most of the soundings east of this contact, which includes most of central and east-central Oregon and California north of Mount Shasta, are remarkably similar. This implies that the crust is electrically simple and that the layering observed consists of a resistive surface layer of volcanic flows, a more conductive layer of altered volcanics, a resistive basement complex, and, finally, a deep conductive zone at depths of 10 to 20 km similar to that observed on the Snake River Plain and at many other areas in the Basin and Range province. Modeling has not been completed; therefore, detailed information is not available, but a general picture as described has emerged.

SEDIMENTOLOGY

Sedimentology, the study of sediments and sedimentary rock, encompasses investigations of principles and processes of sedimentation and includes development of new techniques and methods of study. The USGS sedimentology studies are directed toward the solution of water-resource problems and the determination of the genesis of sediment and application of this knowledge to sedimentary rocks to gain a more precise interpretation of their depositional environments. Many USGS studies involving sedimentology have applications to other topics such as marine, economic, and engineering geology and to regional stratigraphic and structural studies; these are presented elsewhere in this volume under their appropriate headings.

Studies of fluvial sedimentation are directed toward the solution of water-resource problems involving water-sediment mixtures. Sediment is being considered more and more as a pollutant. Inorganic and organic sediment, transported by streams to sites where deposition takes place, carries major quantities of sorbed toxic metals, pesticides, herbicides, and other organic constituents that accelerate the eutrophication of lakes and reservoirs. A knowledge of erosion processes, the movement of sediment in rivers and streams, and the deposition of sediment in stream channels and reservoirs is of great economic importance to the Nation.

VARIABILITY OF SEDIMENT YIELDS

Sediment-yield estimates for central Powder River Basin, Montana and Wyoming

L. M. Shown and L. Y. Shiao found that the peak discharge resulting from a 2-yr, 24-h rainfall event (Q_p) explained 61 percent of the variation in annual sediment yield (SY) from small grassland watersheds in the central Powder River Basin of Montana and Wyoming. The equation is $\text{Log } (SY+100)=1.8008 \text{ log } (Q_p+100)-1.39926$.

The 20 watersheds used represent significant variation in soil types, vegetative cover, and topographic relief. SY values for these basins, 0.41 to 4.58 km² in area, ranged from 9.5 to 1,381 m³/km². The discharges were computed with the runoff-curve-number method of the U.S. Soil Conservation Service (Kent, 1973), which accounts for infiltration, amount of cover, and slope steepness, in addition to the amount of rainfall from a storm of given frequency and duration. The concept of the equation was adapted from the 1974 modification of Flaxman's equation (1972), and both equations include adjustments for the amount of annual runoff that results from snowmelt. The above equation, with a modest standard error of estimate of 24 percent, requires less data and gives much better estimates of SY in the central Powder River Basin than Flaxman's equation, which was developed from data for semiarid basins throughout the Western United States.

Sediment yields in northeastern Indiana

In an evaluation of suspended-sediment data for 58 stream sites in Indiana, L. J. Mansue found that the quantity of suspended sediment transported in the glaciated part of Indiana is primarily dependent upon the nature of the unconsolidated deposits in the vicinity of the sampling sites. Also, the sediment yield decreases with increasing drainage area.

The lowest computed suspended-sediment yield ranges from 2 to 7 t/km²/yr in the northeastern part of Indiana. The highest sediment yields range from 105 to 245 t/km²/yr. These values are attributed to headward erosion into glacial ground moraine.

Storm sediment yield measured in Nederlo Creek basin, Wisconsin

P. A. Kammerer, Jr., and W. G. Batten reported that sediment deposition resulting from an intense 12-h storm was measured in a small reservoir to determine the sediment yield for the event.

About 18 cm of rainfall fell on Nederlo Creek basin, Wisconsin, in a 12-h period, June 30 to July 1, 1978. The sediment deposition was measured in a normally dry floodwater-retarding reservoir that was constructed in 1975 to control runoff from a 6.0-km² drainage area in the basin. The drainage basin is characterized by rugged topography with 90- to 120-m relief between ridgetop divides and the valley bottom. Total design storage capacity of the reservoir was 0.263 hm³, including 0.082 hm³ allocated to sediment-deposition storage. Measurements of the deposited sediment made after the storm showed that 0.005 hm³ was trapped in the reservoir. This represents a sediment yield of 840 m³/km² for the 12-h period. About 5 percent of the design sediment-deposition storage was filled as a result of this single 12-h storm event.

STREAM MORPHOLOGY

Channel morphology and sedimentation in Pheasant Branch near Middleton, Wisconsin

W. R. Krug reported that streamflow, sediment, and channel cross section data have been collected on Pheasant Branch at Middleton, Wis., to calibrate and verify rainfall-runoff-sediment models for the basin. The models will be used to predict changes that will result from urbanization of the basin.

At some sites within the city of Middleton, the channel thalweg of Pheasant Branch has lowered 1 to 1.2 m.

Downstream from the city, average channel width increased from about 11 to 15 m, and the average channel cross section area increased about 86 percent. Six erosion-control structures previously installed by the city in the urban reach appear to have had some benefit in controlling head cutting in the channel.

Aggradation of Powder River valley during 1978 flood

The effects of the flood of May 1978, the largest since 1923 on the Powder River, have been documented in a 90-km reach in southeastern Montana by R. H. Meade, J. A. Moody, and H. A. Martinson. Channel changes in the reach included two avulsive cutoffs and a significant amount of lateral bank erosion (65 m of bank erosion was measured at one monumented cross section). An average thickness of 0.10 to 0.15 m of new overbank sediment was deposited on a 500-m width of the flood plain. The amount of sediment carried into the upper end of the 90-km reach during the flood was 10 percent greater than the amount carried out of the lower end. The amount of sediment newly deposited on the flood plain was nearly twice the amount eroded from the channel. Although the net effect of the flood on the channel was erosion, the overall net effect on this reach of the valley was aggradation.

SEDIMENT TRANSPORT

Total sediment load, Snake and Clearwater Rivers near Lewiston, Idaho

Since March 1972, the USGS, in cooperation with the U.S. Army Corps of Engineers, Walla Walla District, has been investigating suspended- and bedload-sediment transport in the Snake and Clearwater Rivers in the vicinity of Lewiston, Idaho.

M. L. Jones reported that the total sediment load transported in these two rivers during the 1979 runoff period was 607,000 t. This compares to the highest recorded annual load of 6,200,000 t in 1974 and the lowest of 56,500 t in 1977.

Curves of accumulative sediment transport as a function of time for suspended sediment in the Snake River show that more suspended sediment was transported in a single day (0.27 percent of time) of 1974 than was transported in all of 1973 or 1977.

Comparison curves of bedload and bed-material particle-size distributions show that material transported as bedload during the study period contained many more silt- and sand-sized particles than occurred in the steambed, indicating that numerous sandbar deposits along both rivers contributed a large amount of material to the bedload. Bedload material transported during 1979 contained fewer large particles than in any other year of the study, except possibly during the 1977 drought period.

Suspended-sediment discharge in northeastern Wyoming streams

Quantity of suspended sediment discharged by streams in northeastern Wyoming is as much a function of streamflow rate as it is a function of total quantity of flow, according to observations made by B. H. Ringen. As an example, the Little Powder River below Dry Creek, near Weston, Wyo., discharged 164 m^3/s of water in 1974 and 149 m^3/s in 1975. The suspended-sediment discharge in 1974 was 63,430 t with a weighted mean concentration of 4,420 mg/L. The suspended-sediment discharge in 1975 was 29,100 t, with a weighted mean concentration of only 2,230 mg/L. In 1974, the bulk of both discharges was the result of a single runoff event of short duration, and, in 1975, both discharges were the result of sustained medium flows lasting longer periods of time.

Bedload movement in East Fork River, Wyoming

In the East Fork River of western Wyoming, movement of fluorescent particles and changes in bed elevation during the 1979 snowmelt runoff event showed that bed sediment moved downriver in fairly discrete slugs. The bed material (median diameters, 1.0–1.5 mm) was stored during low-water seasons in areas of the channel whose centers were about 500 m (25–30 channel widths) apart. Preliminary analyses of the data by R. H. Meade, W. W. Emmett, and R. M. Myrick suggest that the mean distance between centers of storage corresponds to the mean annual distance of bedload transport. Because bedload material moves in separate slugs rather than in a continuous blanket, the relations between water discharge and bedload transport are not uniform but vary markedly from one part of the river to another.

The nature of bedload-material transport, New River, Tennessee

Several bedload-transport measurements were made on the New River in Tennessee in an effort to characterize the nature of the material moving along the bed of a stream draining a heavily mined basin. According to W. P. Carey (1979), these measurements, made over a range of discharges from 59 to 340 m^3/s, indicated that large quantities of bed material ranging in size from fine sands (0.125–0.25 mm) to very coarse gravel (32–64 mm) are mobilized during runoff events. Coal consistently accounted for all the material moving in the coarsest two or three size categories and for 70 to 90 percent by weight of the entire sample. The mean particle size of the bedload material ranged from 0.4 to 9.8

mm across the channel during a single measurement and from 2 to 10 mm among the different measurements. Both the large volume of material moving and the wide range of particle sizes in motion are attributed to the large amount of coal available for transport.

Laboratory study of bodload-transport processes

Observations made by J. P. Beverage, D. W. Hubbell, J. V. Skinner, and H. H. Stevens, Jr., in connection with the testing and calibration of bedload samplers, verified that accurate mean bedload discharges can be determined only by collecting numerous samples at each measurement point. Measurements of bedload transport made in a 2.75-m-wide by 1.22-m-deep laboratory flume showed that, when moderately uniform (6.5- and 2.1-mm diameter) bed materials were formed into dunes, the transport rate varied over the dune-bed form. The transport rate was zero, or near zero, in the troughs and approximately four times the long-term mean rate at the crests. This transport pattern produced a cyclic temporal record of bedload discharge at a point in which the cycles were positively skewed and had amplitudes roughly four times the mean rate and periods the same as bed-elevation periods.

INSTRUMENTATION

New large volume depth-integrating sampler

J. V. Skinner and J. P. Beverage reported that the Federal Inter-Agency Sedimentation Project has completed the design of a new depth-integrating suspended-sediment sampler. The new D–77 sampler holds a 3-L plastic sample container having a Mason-jar thread and a screw-on bottle cap. The unique feature of this sampler is the molded plastic nose cone that also has a standard Mason-jar thread. The nose cone, plastic intake nozzle, and container are autoclavable for use in bacteriological investigations in rivers. Laboratory tests have verified that costly calibration of individual units will not be necessary.

GLACIOLOGY

Sliding speed of Black Rapids Glacier, Alaska

Investigations of the instability of Black Rapids Glacier by L. R. Mayo and D. C. Trabant showed an increase in the sliding speed of the ice over the underlying rock. The glacier, a 40-km-long surge-type glacier in the Alaska Range, last surged in 1937. The glacier is gradually steepening and may become unstable and surge again.

Since 1974, changes in the sliding speed of Black Rapids have been measured indirectly throughout the length of the glacier. At 8 km from the head of the glacier, the winter surface speed averages 45.1 ± 1.0 m/yr with no apparent progressive change, but the summer speeds vary between 49.3 and 68.9 m/yr. Displacement at the ice surface is caused by basal sliding and ice deformation. The steady winter speed observed from 1974 to 1979 is probably caused entirely by strain deformation. Assuming that the same strain rate occurs in the summer, it follows that the summer increase in speed represents sliding motion. This probably is caused by water lubrication at the glacier bed. From 1974 through 1978, the basal sliding was small, ranging from 10.0 to 17.6 m/yr, and represented only 5 to 9 percent of the annual motion. In the summer of 1979, the sliding increased to 38.0 m/yr. The sliding speed approached the average deformation speed (45.1 m/yr) and was 17 percent of the annual motion.

Black Rapids Glacier, when it surges, may attain a sliding speed of approximately 10,000 m/yr. Whether the observed increase in sliding is a precursor to surging is not known because very few observations have ever been made of a surge-type glacier during the onset of instability.

Glacier surges monitored by satellite

R. M. Krimmel has collected Landsat imagery of most of Asia's glaciers as part of the "Satellite Image Atlas of Glaciers" project. Thirty-meter resolution RBV images of many of the glacier areas are available. These images can be used to predict and monitor glacier surges. Of particular interest is an area of surging glaciers in the Pamir Mountains, USSR. A July 12, 1973, Landsat image of the Bivachnii Glacier showed that this glacier had a medial moraine pattern suggestive of a regular surge cycle, and a surge was predicted in the next few years. A September 28, 1977, Landsat image showed that the glacier had surged and progressed through the predicted cycle, but, by September 29, 1979, the surge had far exceeded previous surge magnitudes. This surge behavior demonstrates that, even though a glacier may exhibit regular surges for several successive cycles, the pattern can be upset by unknown factors.

CLIMATE

Climate is of direct interest to earth scientists for a number of reasons. It affects sediment production, transport, and deposition; controls the distribution of plants and animals and, therefore, is a factor in interpreting the fossil record; and is responsible for the frequency and intensity of atmospheric events that initiate

geologic processes that are imprinted on the geologic record. One responsibility of earth scientists studying sedimentary deposits, therefore, is to infer from the geologic record the nature of the prevailing climate to assure the correct interpretation of the other elements of the record. Conversely, this also allows them to establish a basis for estimating how future climates, if predicted to change, would produce local changes in certain Earth surface processes, possibly create hazards, and alter natural balances that affect our land and water resources. A second major use of geologic data that reflect climate is to establish the record of past natural climate changes—their magnitude, timing, and sequence. These, in turn, become a basis for testing computer models of global climate to determine whether they can account for the events that the geologic record shows have happened.

February 1977 windstorm in Great Plains

In February 1977, strong winds of the first winter storm reached the drought-stricken High Plains and produced the largest duststorm yet observed by geostationary weather satellites. Two dust plumes, one originating near the Colorado-Kansas border and the other near the Texas–New Mexico border, were first observed on GOES–1 satellite images taken February 23. By February 24, dust totally obscured about 400,000 km^2 of the ground surface of the south-central United States in the satellite pictures. By February 26, the visible dust pall had moved to a position over the mid-Atlantic Ocean, suggesting that atmospheric transport of dust eastward from the Great Plains to the Atlantic Ocean may be of sedimentologic significance.

Wind erosion and deposition caused by the February 1977 storm were investigated in the Texas–New Mexico border area by J. F. McCaulty, C. S. Breed, and M. J. Grolier, using aerial and ground reconnaissance. They found that plowed fields were eroded locally to depths greater than 1 m with the production of myriads of small yardangs and that fine sand winnowed from vulnerable soils was deposited in lobate sheets up to 1 m deep and several kilometers long. The eolian sand, silt, and clay soils were unusually vulnerable to the wind because they were dry from a long period of drought, as well as because of certain land-use practices that had resulted from a combination of economic conditions and governmental policies.

December 1977 windstorm in San Joaquin Valley

During December 1977, a severe windstorm in the southern San Joaquin Valley of California removed more than 25 million t of soil from grazing lands bordering the valley and comparable amounts from agricultural lands of the valley floor. A sediment plume was transported at least 650 km northward to the end of the Sacramento Valley, causing a dramatic increase in incidence of valley fever. Measurements by H. G. Wilshire and J. K. Nakata show that the wind removed as much as 60 cm of soil from natural surfaces and 35 cm of weathered granite from outcrops. Weathered granitic rocks exhumed from soil mantles were eroded to comparable depths. Rocks as large as 9.5 cm across were mobilized by the wind, and others 2.5 cm in diameter were windborne to heights of at least 1.6 m. Eolian material deposited during the storm included well-developed residual gravel pavements on gently sloping alluvial fan surfaces; coarse to fine gravel, granule, and sand ripples and dunes on lee sides of fences, vineyards, and orchards; and laminated sand sheets in alfalfa fields, in drainage depressions, and on the lee sides of hills. Besides the exceptionally intense wind velocities, the principal factors contributing to the severity of the storm's impact were drought, overgrazing, and a general lack of windbreaks in the agricultural land.

Satellite relay meteorological stations to study wind erosion

Because of the severe damage that can result from windstorms like those in the San Joaquin Valley and Great Plains areas, several studies of the mechanisms by which wind erodes and transports natural materials have been initiated recently. A study by J. F. McCauley, C. S. Breed, M. J. Grolier, D. J. MacKinnon, and A. W. Ward, Jr., is establishing a network of automated satellite relay meteorologic stations. The first of these was deployed in 1979. This machine is presently monitoring wind speed and direction, air and soil temperature, humidity, barometric pressure, and precipitation, all of which affect the capability of the wind to erode, transport, and deposit materials in the high cold desert of the Navajo Reservation in northeast Arizona. Data from this area will be compared with those from a second station now ready for deployment in the low hot desert near Yuma, Ariz.

Ancient eolian deposits in western Great Plains

Nearly one-third of Colorado east of the 105th meridian is mantled by eolian deposits—loess, sheet sand, and dune fields—that are the results of windstorms over periods of geologic time. This area, unlike that near and within the ranges of the Southern Rocky Mountains, is characterized more by aggradational than degradational eolian landforms, according to studies by R. F. Madole. Eolian sand buries stream terraces and valley floors over broad areas, particularly southeast of the South Platte River and along the northwest sides of the

Arikaree River and the North Fork of the Republican River.

The prevailing northwesterly winds of eastern Colorado appear to be similar in direction to those that formed fields of parabolic dunes here during at least two different times in the past. Two ages of dunes are recognized on the basis of topographic expression and soil development. The younger dunes, of late Pleistocene(?) and Holocene age, are distinct topographically and have weakly developed soil profiles. The older dunes, definitely of pre-Holocene age, are less distinct topographically and have more strongly developed soil profiles.

Records of past climates in Elk Lake sediments

Elk Lake, located close to the present forest-prairie border in northwestern Minnesota, drains into the west basin of Lake Itasca, which is the source of the Mississippi River. Because of the high organic productivity of Elk Lake, oxygen is depleted by early summer, and varve laminations are preserved in the sediments of the deepest part of the lake (29.5 m). The combination of the proximity of Elk Lake to the climatically sensitive forest-prairie border and the varved sedimentary record appears to make the lake an ideal site for obtaining a high-resolution paleoclimatic record of the Holocene. Consequently, a continuously laminated 22-m core was collected from Elk Lake in December 1978 by W. E. Dean, Jr., and J. P. Bradbury (USGS) and H. E. Wright, Jr. (University of Minnesota). It contains 11,072 varves that encompass the entire late Pleistocene and Holocene history of the lake, which apparently formed by melting of buried ice blocks after withdrawal of late Pleistocene ice sheets. The remarkable correspondence between the varve-count data and a radiocarbon date from the base of a nearby bog ($11{,}000 \pm 90$ yr ago, Y-1418) suggests that study of the sediments from Elk Lake will provide essentially annual resolution of changes between forest and prairie conditions in this part of northwestern Minnesota during the late Pleistocene and Holocene. The varve laminations have been counted and measured, and they provide the time calibration for other analyses. Analyses of pollen, diatoms, physical properties, mineralogy, geochemistry, and paleomagnetics presently are being conducted on samples collected at equal-time intervals. This varve-calibrated sampling will enable calculation of all influxes of sediment and other properties on an absolute basis.

To better interpret the annual sedimentary cycle in Elk Lake and how it changed with time in response to climatic change, self-monitoring sediment traps, designed and built by R. Y. Anderson (University of New Mexico), have been placed in the lake. They are equipped with a mechanism to mark the collected sediment column with a thin layer of teflon powder every 15 d. Preliminary results from the varve analyses and the sediment trap data for the first 6 mo of 1979 reveal clear chemical and biological characteristics associated with winter stagnation, spring overturn, and early summer algal productivity. Under a cooperative agreement with the University of Minnesota Limnological Research Center and Biology Department, water samples were collected and profiles of temperature and oxygen were made every 2 weeks to provide the limnological baselines for the sediment trap data.

Records of past climates in Clear Lake sediments

Radiocarbon dates of peat beds and carbonaceous lake sediments in a core from the southeast-trending Highland Arm of Clear Lake, Calif., permitted J. D. Sims to estimate ages for ash beds and seismotectonic and palaeoclimatic events for approximately the last 40,000 yr. Chronological control for the upper part of a longer core, from the main basin of the lake, is based upon correlations of its ash beds and pollen curved with their radiometrically dated counterparts. Analyses by D. P. Adam of pollen from two cores show repeated abrupt alternations between high pollen abundance of oak (*Quercus*) and pine (*Pinus*). These changes are interpreted to be caused by fluctuations in the distribution of oak in the hills surrounding Clear Lake in response to changes in climate. The shape of the oak-pollen curve strongly resembles the shapes of curves of oxygen-18 content in deep-sea foraminifera from dated marine sections, and, by inference, this dates the oldest sediment recovered in the Clear Lake cores as approximately 130,000 yr old.

Records of past climates in lake sediments from Yellowstone Park area

The Quaternary geology of the Yellowstone Park area has been studied for several years by G. M. Richmond (USGS) who identified several potentially informative sections for paleoclimate study, sampled them (locally with others), and arranged for their analysis and dating. Pollen analyses by R. G. Baker (University of Iowa) of sections of pre-Pinedale lake silts have revealed evidence of a younger cold interstadial, a warm interstadial, and an earlier interglacial. The two interstadials have been dated, respectively, at about 68,000 yr B.P. and >70,000, by the Groningen Radiocarbon Laboratory. Pollen analyses of another section by J. P. Bradbury (USGS) have revealed evidence of a still younger cold interstadial, the lower beds of which have been dated at about 54,000 yr, also by the Groningen Laboratory. Analyses of several other sections by Professor William Mullenders (University of Louvain La

Neuve, Belgium) have revealed still other interstadials that, together with the above, form a sequence extending from the Holocene to about 180,000 yr ago. Some of the older sections analyzed by Mullenders contain an unusual proportion of deciduous trees not now present in the park but no pollen of extinct deciduous species common to the local Tertiary rocks. This suggests that a deciduous element may have existed in the park at times and that the climate of those times was more humid than at present. A few analyses of beds 590,000 and 2 m.y. old suggest that the climates of those times were, respectively, similar to that of today and somewhat warmer.

Three-million-year record of climate in Searles Lake sediments

A 3-m.y. record of climates as they affected sedimentation in a closed basin lake is provided by a 930-m core recovered in 1968 by the Kerr-McGee Chemical Corporation from an area near the center of Searles Lake, Calif. It was made available for study by USGS scientists in 1976. The upper 68 m of lake sediments, well known from previous studies and described elsewhere, represent the last 130,000 yr. New studies of the deeper lake sediments by G. I. Smith (USGS), V. J. Barczak and G. F. Moulton (Kerr-McGee Chemical Corp.), and J. C. Liddicoat (Lamont-Doherty Geological Observatory) have allowed quantitative documentation of the evaporite mineralogy, based on analyses of the acid-soluble components and X-ray diffraction data, and reconstruction of the history of chemical sedimentation and the probable climatic regimes that controlled it. Ages of the stratigraphic units are based on carbon-14 and paleomagnetic data. Apparent sedimentation rates average 46 yr/cm, an order of magnitude more rapid than most deep-sea sediments.

The 625 m of older lacustrine sediments are subdivided into units that have the following compositions and ages, and they are inferred to indicate the following regional climates:

Age (m.y.)	Sediment composition	Inferred climate
0.13–0.33	Salines (deposited in a shallow lake) and greenish-yellow marls (deposited in a moderately deep lake).	Intermediate between wet and dry, cool, fluctuating.
0.33–.065	Salines (dry lake)	Dry, warm, occasionally wet.
0.65–1.02	Greenish marls (deep lake), some salines	Wet mostly, some brief dry periods.
1.02–1.40	Greenish marls	Wet, cold(?).
1.40–1.94	Interbedded salines and greenish marls	Wet most of time, interrupted by 17 brief(?) dry periods.
1.94–2.57	Reddish calcareous silt (playa lake deposits).	Dry, warm(?), occasionally wet.
2.57–3.17	Green calcareous silt (deep lake)	Wet.

Sedimentary materials underlying these lacustrine deposits consist of 220 m of reddish-brown alluvial gravels which rest on 15+ m of quartz monzonite bedrock.

The amount of water entering the lake appears to have gradually decreased with time (partly a result of uplift of the Sierra Nevada, which created an enlarging rain shadow), but climatically induced variations in runoff caused fluctuations in inflow that exceeded the more gradual change. Correlation of the deep-lake deposits in Searles Valley with older glacial tills in the Sierra Nevada suggests that at least one of the older glacial stages started about 1.40 m.y. ago, waned about 1.02 m.y. ago, but did not cease until 0.65 m.y. ago. One or more still earlier stages might correlate with the wet period that extended from 2.57 m.y. to 3.17 m.y. ago. However, with the exception of the beginning of lacustrine deposition (3.17 m.y. ago) and selected events during the "last" glaciation (0.01 to 0.13 m.y. ago), climatic reconstructions based on this core are conspicuously different from the marine isotopic record of global glaciation.

End of "Little Ice Age" in Glacier National Park

From an analysis of tree-ring cores taken from the forest trimline areas in front of the Agassiz and Jackson Glaciers in Glacier National Park, Mont., P. E. Carrara found that an advance during the mid-1800's resulted in the maximum ice extent of the post-Pleistocene Epoch. Retreat from this "Little Ice Age" maximum began during the 1860's and has continued to the present day. Many glaciers of 100 yr ago have been reduced to stagnant ice bodies or have disappeared entirely. One of the most drastic reductions in ice volume has been that of the Agassiz Glacier. During the mid-1800's, this glacier was 3.5 km in length, approximately 2.5 km^2 in area, and at least 200 m in thickness. Today, it has been reduced to a small (0.25 km^2) stagnant ice mass that is probably less than 10 m thick throughout. Presently, its total volume is probably less than 5 percent of its "Little Ice Age" maximum.

End of Pinedale Glaciation, north-central Colorado

Previously, it was thought that Pinedale-age glaciers in north-central Colorado might have persisted into Holocene time, possibly to as recently as 6,500 yr ago. For many years, the only radiocarbon age (6,179 ± 240 years, W–145) upon which to base an estimate of the end of Pinedale Glaciation in the area came from postglacial sediments at the locality for which the "Long Draw glacial substage" was named in La Poudre Pass. However, the stratigraphy and new radiocarbon ages

obtained by R. F. Madole at three sites near Buffalo Pass in the Park Range and at two sites on La Poudre Pass in the Front Range suggest that (1) the age assigned to the upper boundary of Pinedale Glaciation in north-central Colorado should be revised to at least 10,000 yr B.P. and possibly to 11,000 yr B.P., (2) in the southern part of the Park Range, where the area along the divide is lower and broader and glaciers descended from an ice cap rather than cirques, Pinedale deglaciation was complete prior to 11,000 yr ago, and (3) at Long Draw, the stade is at least 10,000 yr old.

Late Pinedale Glaciation in the Northern Rocky Mountains

R. F. Madole has mapped glacial deposits that document the existence of several small 1.5- to 6.5-km-long valley glaciers in the Elkhead Mountains of northwestern Colorado during late Pleistocene time. They occur on summits whose altitudes lie between 3,200 and 3,300 m. The largest concentration is in the western part of the Elkhead Mountains. Most of the deposits are believed to correlate with the Pinedale Glaciation. The long-term average of equilibrium-line altitudes indicated by the deposits is estimated to have been about 2,925 m. This is similar to that estimated for the west flank of the adjoining Park Range but is about 245 m lower than that estimated for the Front Range farther east. It appears that during time of late Pleistocene glaciation, as now, the Elkhead Mountains and adjoining Park Range received more precipitation at a given altitude than did the Front Range.

Relation between late Pleistocene snowfields and "landslides"

When glaciers existed on the higher peaks of the Elkhead Mountains, snowfields undoubtedly also were extensive. Large, perhaps nearly continuous, snowfields probably were prevalent in the zone between 3,000 and 3,200 m, which includes most of the peaks of the Elkhead Mountains, and a partial cover of snowfields may have extended down to an altitude of 2,600 m or lower. The treeline was probably depressed 300 to 500 m. Heavy precipitation during late Pleistocene time, the snowfields, and their melt water are believed to have been factors partly responsible for the extensive landslide deposits that occur throughout the Elkhead Mountains, most of which appear to be of pre-Holocene age. However, much of what resembles, and has been mapped as, landslide deposits is believed by R. F. Madole to be the product of nivation—erosion of rock and soil around the fluctuating margins of snowbanks by frost action, chemical weathering, melt-water transport, and flowage by solifluction. The poorly consolidated Tertiary formations, Wasatch (Eocene) and Browns Park (Miocene), which are widespread in the Elkhead Mountains, would have been particularly susceptible to nivation.

A 100,000-year cave record of atmospheric temperatures

Calcite precipitates formed in caves (speleothems) in the western Sierra Nevada, Calif., have been found by J. C. Tinsley III, J. R. O'Neil, and B. J. Szabo and appear to be in isotopic equilibrium with the water that is depositing them. Temperatures calculated from oxygen isotopic ratios measured from recently deposited calcite and from the ground water precipitating the calcite agree with thermometer readings obtained in the cave near the sample site. Cave temperatures are normally very near mean annual temperatures for the area, and the isotopic paleoclimate record of air temperatures preserved in the cave's calcite deposits is considered indicative of changes in those mean values as global glaciations waxed and waned. Uranium-series age determinations on these western Sierran speleothems indicate that an isotopic paleotemperature record in excess of 100,000 yr was preserved.

Climatic influence on alluvial deposition, northwest Colorado

Alluvial deposits in the White River basin of northwestern Colorado have been studied by J. W. Whitney, particularly in the oil shale-rich areas between Meeker and Rangely. The flood plain of the White River appears to be underlain by fill that was graded to the last Pleistocene stand of ice in the upper reaches of the drainage basin, and its flood plain can be traced to moraines in the South Fork of the White River that exhibit typical soil development of Pinedale-age till. The older first terrace above the flood plain yields an "infinite" carbon-14 age on bog material and is probably associated with upstream deposits of Bull Lake-age till. Above the first terrace lie two closely related terraces that exhibit strongly developed soil profiles analogous to "pre-Wisconsin-age soils" commonly described in the Rocky Mountains. These two fill levels may be the same as and closely related to deposits associated with Illinoian Glaciation. The highest persistent terrace in the basin contains deposits of "Pearlette type 0" ash, and the valley, therefore, was undergoing aggradation during a period that included 600,000 yr ago.

The late Wisconsin-age gravel fill of the White River has acted as a stable base level for its tributary streams for the duration of the Holocene. Drilling in the deposits of the lower tributary valleys indicates that the White River fill acted as a dam, creating shallow lakes that deposited fine clayey silt during early Holocene time. Valley aggradation seems to have been interrupted only briefly by small periods of arroyo cutting until about 1,100 to 1,150 yr B.P. At that time, the character of

sedimentation changed from basin-wide aggradation of sandy silt deposits to an environment characterized by the prograding of coarse alluvial deposits from valley walls and smaller streams over the finer grained deposits of the main White River tributaries. Pollen analysis suggests that there was not a significant botanical change at this time. This indicates that there was little change in total precipitation and yearly temperature averages but it is possible that the precipitation changed to a regime characterized by a greater number of summer convective thunderstorms, resulting in greater localized runoff. This environment, with small changes toward greater aridity occurring in the 13th century, has persisted to the present day. Teeth and bones of modern-day cattle are common in many of the entrenched fills of the tributaries of the White River, suggesting a close relation between land use by man and historical arroyo cutting in this drainage basin.

Holocene sea-level change—a possible record of global climatic change

A glacioeustatic record of sea-level changes during the Holocene would represent the integrated effect of global climates on volumes of land ice (mainly continental and alpine glaciers) over the past 10,000 yr. There is, however, no generally accepted sea-level-change curve for the Holocene, mainly because of the fragmentary character of the evidence and the difficulty of distinguishing between climatic and tectonic (or other) effects on local sequences that are diagnostic of changing levels. Many researchers, though, accept the interpretation of a progressive rise in sea level concurrent with rapid late Pleistocene melting of continental ice that started sometime prior to 10,000 yr ago and reached present level about 5,000 to 6,000 yr ago or later, with that level persisting or oscillating a few meters since then. Data compiled by T. N. V. Karlstrom show that some researchers also find a systematic pattern of secondary oscillations reflecting one or more components of an inferred series of harmonically related cycles with periodicities of about 1,100, 500, and 275 yr. The 550-yr component evident in coastal data from Cook Inlet, Alaska, is reported also from South American and Northern European coastal evidence, from high resolution deep-sea-core "temperature" records, from varve-dated retreat rates of the Baltic ice sheet, and from earlier analyses of sea-level changes. The 275-yr cyclical component is less well documented because higher resolution records are required. It appears to be represented in closely dated Danish bog records, in the Cook Inlet tidal bog records, in the historical record of hydrologic changes in the Nile River Delta, and in multiple hydrologic indices from the southwest.

Synthesis of published biologic and geologic paleoclimatic information from western North America supports the conclusion that high resolution records from Alaska to Mexico demonstrate synchronous regionwide climatic changes at frequency levels of a few hundred to thousands of years. These climatic trends appear to Karlstrom to be in phase with the inferred glacioeustatic record and with the intervals of warmer/drier climate generally coinciding with intervals of higher sea level. The highest resolution paleoclimatic and meteorological data appear to indicate that these longer term climatic trends have been essentially synchronous over large parts of the globe, whereas the decadal-to-century trends became increasingly nonsynchronous from region to region as the wavelengths of climate-variation intervals decreased.

GROUND-WATER HYDROLOGY

Major research emphasis in ground-water hydrology by the USGS has been directed to a broad range of subjects that reflect the continued expansion of ground-water development and the need to better understand ground-water systems through the application and development of various hydrologic methods.

During the past year, research on and application of digital modeling continued, with an increase in the sophistication of hydrologic problems being treated by these methods. A digital model to simulate transport of chloride ions was developed for the Spokane aquifer, and a digital-model analysis was used to propose ways to reduce severe ground-water decline in west-central Kansas. A new procedure appears to be capable of yielding much better estimates of hydrogeologic parameters for steady-state ground-water-flow models than standard regression.

Recharge studies continued to receive attention during the year. An analysis of artificial-recharge tests in east-central Nebraska indicated that long-term recharge to a Pleistocene sand and gravel aquifer was possible through a recharge well before sediment in the water caused plugging. A method was developed to estimate the extent of areas contributing recharge to stratified drift aquifers. Effects of streambed infiltration on water produced from the Ohio River were evaluated through gas analyses of ground-water samples. Results provided by a preliminary two-dimensional ground-water-flow model were used to evaluate recharge to the water table from four lagoons in a surface mine area. The movement of imported water recharged into an alluvial fan was successfully traced with stable isotopes of oxygen and hydrogen.

Other efforts in fiscal year 1980 included the compilation of data on hydrologic parameters and an analysis of the equation of motion for transient flow of water in a water-table aquifer as it relates to changes in water level

and transmissivity. Completed contamination studies, geophysical investigations, stratigraphic assessments of aquifers, reconnaissance hydrogeologic mapping, and ground-water system studies provided a better understanding of the hydrology in various States.

AQUIFER-MODEL STUDIES

Solute transport in the Spokane aquifer

J. J. Vaccaro and E. L. Bolke developed and used a digital model to simulate transport of the chloride ion in the Spokane aquifer of Washington. The transport model calculates a solute-flux budget from all sources—rivers, treatment plants, boundary inflows, septic tanks, and other contributing land uses. Specifically, the model was used to estimate the impact of chloride from septic-tank seepage and from infiltration of irrigation water on the water quality of the Spokane aquifer.

Digital-model simulation of the Spokane aquifer

E. L. Bolke and J. J. Vaccaro developed a digital-computer model for the Spokane aquifer in Spokane Valley, Wash. The model was used to show the effects of increased pumpage on ground-water levels and streamflow. Model results indicated that doubling the 1977 pumping rates lowered water levels in the Spokane aquifer less than 1 m during a 1-yr simulation period and decreased discharge of the Spokane River at Spokane about 4.2 m^3/s during the summer and about 1.4 m^3/s during the rest of the year. Leakage from the aquifer to the Little Spokane River was decreased by less than 0.3 m^3/s by doubling the ground-water pumpage.

Ground-water model, west-central Kansas

A digital computer model study of a small area in west-central Kansas by L. E. Dunlap and Jack Kume (USGS) and J. G. Thomas (Kansas State University) examined several alternative management schemes that could be implemented by the Ground-Water Management District. Results showed that, if farmers reduced ground-water withdrawal by 50 percent by partial irrigation of grain sorghum, a 60-percent reduction in the projected rate of water-level decline could be expected. Other tests indicated that reducing the quantity of water pumped in a small controlled area of pumpage would reduce the rate of water-level decline in the small area, but declines near the edge of the control area would be greater than those near the center as a result of heavy pumpage from wells outside the area boundary.

MISCELLANEOUS STUDIES

Interaquifer flow through well bores

According to M. F. Hult, flow through well bores open to more than one aquifer is a major factor in the distribution of contaminants in the St. Louis Park area, Minnesota. In addition to vertically transporting contaminants from shallow to deep bedrock aquifers, the flow creates cones of depression and impression in the potentiometric surfaces of the connected aquifers. These cones change the rate and direction of horizontal flow within the aquifers.

Seismic-refraction exploration, northwestern Pennsylvania

J. T. Gallaher reported that six seismic-refraction lines, totaling 8.5 km in length, which were run in eastern and western Erie County, Pa., by F. P. Haeni and J. T. Gallaher, crossed deeply buried valleys to determine thickness of glacial fill and width and direction of preglacial channels. Results showed a maximum thickness of about 120 m of drift in French Creek valley near Corry, Pa. In the Albion, Pa., area, the deepest part of the buried channel is less than 3 m above the present level of Lake Erie, about 11 km to the north. Subsequent drilling in the area of the Albion seismic line indicated an accuracy well within the anticipated 10 percent of error.

Quality of water in the Wilcox aquifer

Reconnaissance studies in the Mississippi alluvial plain in northeastern Arkansas by M. E. Broom have defined a substantial recharge area for the Wilcox aquifer. In this region, eastward-dipping Tertiary units that crop out at higher elevations on Crowleys Ridge are truncated and blanketed by thick alluvial deposits. The Wilcox aquifer, which is the deepest Tertiary aquifer, yields significantly less mineralized water than any of the overlying aquifers and, thus, is the preferred ground-water source for nearly all municipal and industrial water supplies in a 7,800-km^2 area east of Crowleys Ridge.

Previous hydrologic mapping (Hosman and others, 1968, pl. 3) showed no outcrop area for the Wilcox aquifer in the alluvial plain in northeastern Arkansas but, instead, showed the Wilcox truncated by alluvial deposits west of Crowleys Ridge. A redefinement of the truncated and outcrop areas of Tertiary units now provides a substantial outcrop and recharge area for the Wilcox aquifer in its downdip areas.

Model insensitive to variations in transmissivity

According to R. E. Krause, varying transmissivity by 50 to 100 percent in modeling the Southeast limestone

aquifer system has negligible effects on simulated drawdowns in most of the area. The three-dimensional finite-difference model developed by P. C. Trescott (1975) and S. P. Larson (Trescott and Larson, 1976) is being used by R. E. Krause to simulate the steady-state ground-water-flow system in the principal artesian-Floridan aquifer in the eastern half of the coastal plain of Georgia, southern South Carolina, and northeastern Florida. Doubling transmissivity in preliminary calibration runs has no appreciable effect on the drawdown in the downdip area of interest, even though transmissivity ranges from 2,000 to 23,000 m^2/d. However, near the outcrop area (a constant head source), drawdowns are 2 to 6 m greater when the transmissivity is doubled. Transmissivity ranges from 35 to 9,000 m^2/d in this area.

Mathematical simulation of hydrogeologic systems

R. L. Cooley developed a new procedure that appears capable of yielding better estimates of hydrogeologic parameters for steady-state ground-water-flow models than standard regression. Ridge regression, which biases parameters toward zero, and a new variant of ridge regression, which incorporates biased prior estimates of parameters, were developed and tested. Results showed that both techniques are capable of improving, often markedly, the parameter estimates but that the variant usually gives much better results, while demanding no more prior information than the estimates and limited measurements commonly available.

RECHARGE STUDIES

Artificial recharge of ground water

W. F. Lichtler (USGS) and D. I. Stannard and Edwin Kouma (Nebraska Water Resources Center, University of Nebraska) reported that more than 6,434.5 m^3 of water that was withdrawn from a well recharged by the nearby Platte River was recharged to a Pleistocene sand and gravel aquifer through a well in the Big Blue River basin in east-central Nebraska, where water levels are declining.

The water was recharged at an average rate of 46 L/s for 6 mo from 1977 to 1978 and 8 mo from 1978 to 1979. During both tests, the water level in the recharge well continued to rise slowly after the water level in observation wells as close as 4.83 km had virtually stabilized, indicating slow plugging was occurring. In the first test, recharge could have continued for several years before renovation of the well was required, but, in the second test, the rate of plugging increased dramatically when casing failure in the withdrawal well allowed large quantities of sediment to enter the recharge well. Before the casing failure, the sediment content of the recharge water had been about 0.04 mg/L. Analyses of data indicated that entrained air, bacteria, or chemical reactions were not significant causes of plugging.

Estimating recharge areas for stratified drift aquifers, Connecticut

As part of Connecticut's 208 program, Elinor Handman developed a method for estimating the extent of areas contributing recharge to stratified-drift aquifers. The method is applicable where the stratified-drift aquifer underlies a valley within a basin that has relatively fixed and coincident surface- and ground-water drainage divides. Recharge to stratified drift aquifers is derived from (1) precipitation on the area overlying the aquifer that percolates to the saturated zone, (2) precipitation on adjacent till and bedrock uplands that percolates to the saturated zone and flows downgradient into the stratified drift, and (3) recharge from surface-water bodies that are hydraulically connected to the stratified drift. These recharge areas can be defined from topographic and geologic maps.

Carbon dioxide and methane outgassing from ground-water samples

Ken Stevens found that gas analyses made on ground-water samples from the Ohio River alluvium indicate that concentrations of carbon dioxide are as much as 10 times the atmospheric levels. Significant outgassing occurs when the pressure drops below 41.4 kPa, and methane occurs in the dissolved gases in water from the aquifer.

Ground water produced by induced infiltration from the Ohio River probably contains less than half the concentration of carbon dioxide and lower concentrations of methane than the aquifer water contains.

Mine-spoil hydrology

According to G. L. Patterson, results from a preliminary two-dimensional ground-water-flow model indicated that three lagoons constructed entirely above compacted mine spoil do not contribute recharge to the water table, whereas one lagoon built partially into uncompacted mine spoil supplies recharge on the order of 1.8×10^{-9} m/s to the water table.

Slug test results also indicated that hydraulic conductivity ranges from 2.1×10^{-7} m/s to 2.7×10^{-6} m/s in the surface-mine spoil underlying the four large sludge-storage lagoons in Fulton County, Ill. Gamma-density logs showed a distinct increase in density where mine spoil was compacted during lagoon construction. The water-table elevation and the elevation of the bottom of

the more dense material are essentially equal, indicating the compacted material acts as a semiconfining layer partially controlling water-table elevation.

Stable-isotope technique used to trace ground-water movement

K. S. Muir and Tyler Coplen reported that the stable-isotope technique can be used to trace ground-water movement. The study by the USGS in cooperation with the Santa Clara Valley Water District was an attempt to trace the movement of imported water recharged into the Penitencia Creek alluvial fan, using the stable isotopes of oxygen and hydrogen. In 1965, California began supplying annually about 123 hm^3 of water to the Santa Clara Valley; about half of this amount is used for recharge.

The results of the study indicate that the stable-isotope technique can be used to calculate the relative amounts of local ground water and imported recharged water of a different isotopic composition. Therefore, it is possible to trace the movement of the imported water through the aquifer.

Aquifer evaluations, North Dakota

W. F. Horak has found from hydrogeologic studies that the Harmon lignite bed of the Tongue River Member of the Fort Union Formation is the most reliable shallow aquifer in the Wibaux-Beach deposit area of western North Dakota. The lower sand section of the Tongue River that varies in thickness and occurrence is also a productive aquifer. Potentiometric data for both aquifers indicate a northward flow gradient with downward vertical leakage.

Dissolved-solids content of the water ranges from about 400 to 3,000 mg/L. The shallowest ground water is generally a calcium-magnesium sulfate type and commonly contains dissolved iron concentrations in excess of 1.0 mg/L. Ground water sampled from wells deeper than about 46 m is generally a sodium-bicarbonate type with little iron content.

Potentiometric-head relations, lower Paleozoic rocks, Kansas

A. J. Gogel analyzed potentiometric head relations in lower Paleozoic rocks that are both aquifers and hydrocarbon reservoirs in Kansas. The Arbuckle Group of Cambrian and Ordovician age, the Simpson Group and Viola Limestone of Ordovician age, Mississippian rocks, and the Lansing and Kansas City Groups of Pennsylvanian age range in thickness from 60 m in northeastern Kansas to more than 1,400 m in southwestern Kansas. Head values derived from drill-stem tests indicate that the range in potentiometric heads among the aquifers is limited to about 125 m and that the relative distribution of heads may vary from one area to another. However, the head distribution in the Lansing and Kansas City aquifer average about 60 m higher in elevation than the underlying units.

Thinning of aquifer by solution

G. E. Welder reported that the Roswell ground-water basin is a large dual-aquifer system that formed in a complex geohydrologic framework characterized by lithologic changes, solution of evaporites, and collapse features. Maps of the San Andres Limestone of Permian age in the northwestern part of the Roswell basin indicate that as a result of solution, this artesian water-bearing unit is locally 120 to 180 m thinner than in other localities.

Perturbation solutions of water-table aquifer equations

A recent analysis by E. A. Prych (1980) indicated that linearizing the equation-of-motion for transient flow of water in a water-table aquifer can account partially for the changes in aquifer transmissivity caused by changes in water level. This new linearized equation can be solved numerically to yield solutions that are more accurate and that require very little additional computation than an equation that is linearized by an older method and cannot take into account the changes in transmissivity.

Porosity, permeability, distribution coefficients, and dispersivity

R. G. Wolff recently completed a chapter on porosity, permeability, distribution coefficients, and dispersivity for a DOE-sponsored book on "Physical Properties of Rocks". The chapter presents a wide range of published data for these parameters. Because of the increasing usage of predictive models, the representativeness of the input data is most significant. This compilation and basic interpretation represents the beginning for a basic appraisal of available data.

SURFACE-WATER HYDROLOGY

The objectives of research in surface-water hydrology are to develop improved techniques for estimating the magnitude and variability of streamflow in time and space, both under natural and man-modified conditions, to understand the flow process in stream channels and estuaries, and to define the rate of movement and the dissipation of pollutants in stream.

Precipitation-runoff modeling

A precipitation-runoff modeling system designed to assess the effects of land-use and climate changes on the hydrology of small drainage basins was completed by

G. H. Leavesley, R. W. Lichty, B. M. Troutman, and L. G. Saindon. The system is modular in design. The model system simulates mean daily flows from rainfall and snowmelt and simulates storm-flow hydrographs for individual rainfall events. Sediment-modeling capabilities are currently being added. Parameter optimization and sensitivity analysis options are available for fitting and evaluating the sensitivity of model parameters. Calibration of the modeling system was begun on 20 basins in the coal development areas of the Rocky Mountain and Southeastern regions of the United States.

Lichty investigated the utility of rainfall simulator data to quantify the infiltration characteristics of a basin for model application. An analysis was made of rainfall simulator data on two distinctly different soil types in a 4.1-km^2 basin in central Wyoming. The simulator data gave reasonably good initial estimates of the hydraulic conductivity and effective capillary-drive model parameters.

Troutman investigated the effect of precipitation-runoff model input errors on runoff prediction. Spatial variability of precipitation resulted in consistently biased runoff predictions and biased parameter estimates. Precipitation spatial variability also caused inflation of the error of prediction when measurements from too few or noncentrally located gages were used. These prediction and estimation problems were examined using both a stochastic areal-rainfall model and rain-gage network data from Dallas, Tex.

Saindon completed development of a hydrologic modeling data-base management system to interface the USGS precipitation-runoff modeling system with the USGS WATSTORE computer system.

Flow modeling

H. E. Jobson (1980) developed and verified an unconditionally stable and practical water-quality transport model for use in upland streams and rivers. Basing the model on the Lagrangian reference frame rather than the Eulerian reference frame greatly reduced the numerical problems associated with solving the advective terms of the convective-diffusion equation. The model contains almost no numerical dispersion, is conceptually simple, and is relatively easy to code. Model results closely simulated dye concentrations measured in the Chattahoochee River near Atlanta, Ga., under highly unsteady flow conditions.

Chintu Lai identified eight areas of discipline that are essential in effectively simulating unsteady open-channel flows by computer. Although the scope and the technology involved in present-day modeling preclude proficiency in every aspect of these areas, a general knowledge of the various aspects should help those who deal with computer modeling and particularly those who coordinate or oversee the entire process of unsteady flow simulation.

Lai determined that the extrapolation procedure may be used to raise the numerical accuracy of flow computation with little additional computational effort. This conclusion is based on a series of experiments conducted for a Sacramento River reach, together with Lai's previous investigations.

D. R. Basco studied the "filter-scheme" method, a new numerical technique for the solution of partial differential equations; it is fundamentally different from finite-difference and finite-element methods. The method utilizes the basic concept that the output of any physical (linearized) system at some time can be calculated if the amplitude response function is known for the system. The primary advantage of the method is its ability to selectively filter out undesirable wave numbers, thus producing very accurate outputs. A series of numerical experiments has confirmed this method to be extremely accurate but also has shown it to be rather time-consuming (computer time). The applicability of this approach depends on how well the method can handle nonlinear terms and how much the computer time can be reduced through future research. Because of its accuracy, the method may be utilized as a standard for measuring the accuracy of other numerical methods and schemes.

Analyses of numerous low-flow traveltimes of small streams in Wisconsin by L. B. House indicated that average reach velocity for extreme low-flow events such as the 7-d, 10-yr discharge ($Q_{7,\ 10}$) can be reliably extrapolated from known velocities at average annual low flow. Traveltime data, previously gathered by using dye-tracing methods, show that a straight-line extrapolation of the measured discharge versus average reach velocity data down to the $Q_{7,\ 10}$ discharge has little room for error. This is because the average reach velocity at normal low flows does not drop much lower with decreasing discharge.

W. R. Krug and House developed a digital streamflow and reservoir operation model that they used to generate 62 yr of streamflow record at each of the gaging stations on the Wisconsin River under present reservoir operating conditions. Comparison with historic records indicates a slight reduction in 100-yr flood discharge due to the reservoirs. Krug developed a similar model to evaluate the effects of changes in the water-level management of Lake Winnebago.

Hydrologic studies

G. D. Tasker proposed a weighting technique to improve parameter estimates in a regression of recurrence interval- (T-) year peak flows on basin characteristics.

Weights are used to account for differences in reliability of the T-year peaks estimated at gaging stations and are derived from a combination of theory and residual analysis. A simulation is used to compare weighted least-squares and ordinary least-squares regression. Results indicate that weighted least squares can improve estimates of regression parameters.

H. W. Lowham related mean width, depth, cross-sectional area, and velocity of streamflow to several indices of channel-forming flow including bankful discharge, the 2-yr peak flow, and the geometric mean of the annual peak-flow array. Data were obtained from 51 gaged sites in Wyoming. He also made dye-tracer measurements on six streams in the study area; with a few exceptions, the measured velocities compared favorably with those computed from the generalized "at-a-station" relations. Relations of this type are useful for predicting channel changes in response to developments that alter the streamflow regimen.

H. C. Riggs (1979) proposed two indices to characterize hydrologic droughts quantitatively: the recurrence of 30-d annual low flow and the draft that could have been maintained, given a fixed amount of storage, during a multiyear drought. The latter measure, which shows the relative effect of the drought on streamflow available for use, is computed from the annual mean flows of record. Applications of the method to long-term streamflow records indicate that the maximum multiyear drought index for a stream depends on the flow variability.

Channel hydraulics

S. A. Druse defined stage-discharge relations at three ephemeral streamflow stations by using the standard step-backwater method. These relations were checked within 15 percent at the more critical high ends by subsequent discharge measurement.

G. J. Arcement verified a method for determining the roughness coefficients in densely vegetated flood plains. The "vegetative density" at a cross section is the relative amount of space occupied by trees and bushes; it is related to the Manning's "n" for the cross section. The method was tested and verified at 14 densely vegetated sites in Louisiana, Alabama, and Mississippi where "n" values were known.

PALEONTOLOGY

Research by USGS paleontologists involves biostratigraphic, paleoecologic, taxonomic, and phylogenetic studies of a wide variety of plant and animal groups. The results of this research are applied to specific geologic problems related to the USGS program of geologic mapping, resource investigation, and provision of a biostratigraphic framework for synthesis of the geologic history of North America and the surrounding oceans. Some of the significant results of paleontologic research attained during the past year, many of them as yet unpublished, are summarized in this section by major geologic age and area. Many additional paleontologic studies are carried out by USGS paleontologists in cooperation with USGS colleagues. The results of these investigations ordinarily are reported under other sections in this volume.

MESOZOIC AND CENOZOIC STUDIES

First recognition of the molluscan *Exogyra cancellata* subzone, South Carolina

The Burche Ferry area on the Peedee River, S.C., has been visited and discussed by numerous authors since early in the century. The locality has assumed special importance because the belemnite guards recovered here were the basis for the original isotopic temperature analyses performed by Urey and Lowenstam. All previous authors have assigned the lower beds of the section to the Black Creek Formation and the upper part to the Peedee Formation. The presence of *Exogyra costata* Say, associated with *Belemnitella americana* in the Peedee beds, and absence of fossils in the beds assigned to the Black Creek Formation led all workers to assume that beds assignable to the *Exogyra cancellata* zone were missing in South Carolina, although they are well represented to the north. This locality was visited by N. F. Sohl and J. P. Owens in October 1978, at an especially low water stage. At this time, 1.3 m of section not previously reported were seen. The lower meter consisted of dark-gray sparingly micaceous calcareous bioturbated clayey fine- to medium-grained sand. Phosphatic grains, pebbles, and bone material are common, along with both whole and worn calcitic shelled fossils. The upper contact of the unit is burrowed with sand from the overlying unit, piping downward. Among other fossils, *Anomia tellenoides* Morton and *Flemingaostrea subspatulata* (Forbes) (early form) occur in abundance. This association is typical of the molluscan assemblage common to the *Exogyra cancellata* subzone that is traceable from New Jersey to Mexico. The identification of this interval in South Carolina contravenes the necessity for assuming a nondepositional history for the early Maestrichtian between the Peedee River area and the Cape Fear River area of North Carolina.

Upper Cretaceous geology of the Tombigbee River, Alabama and Mississippi

By far the most spectacular and stratigraphically complete exposures of Upper Cretaceous strata within the Gulf Coastal Plain area are outcrops in long bluffs and low banks along the Tombigbee River and its tributaries in western Alabama and eastern Mississippi. Understanding the stratigraphic distribution of these sediments, their paleontology and biostratigraphy, petrology and sedimentary structures, and depositional history are of utmost importance in investigations by the USGS of tectonic history of the Mississippi embayment area. Their study also is critical to the USGS efforts to relate Upper Cretaceous strata of the eastern gulf coast with those of the southern Atlantic Coastal Plain area. Unfortunately, the great majority of these exposures are being lost because of inundation during construction of the Tennessee–Tombigbee Waterway Project by the U.S. Army Corps of Engineers.

In March 1979, C. C. Smith (USGS), C. W. Copeland, Jr. (Alabama Geological Survey), and E. A. Mancini (University of Alabama) initiated a project to study the geology of the Tombigbee River, with the initial phase of the project focused on river and tributary exposures in most imminent danger of inundation. During fiscal year 1979, study of the geology of 121.3 km of the Tombigbee River, located between Pickensville, Ala., to just north of Aberdeen, Miss., was completed. Over 100 outcrop exposures were measured, photographed, and described in detail, with over 400 microfossil samples collected for future micropaleontologic investigations. Many oriented samples were collected for paleomagnetic studies, and numerous bulk samples were taken for sedimentologic and petrographic investigation, as well as for extraction of both smaller vertebrate and invertebrate megafossils. Preliminary analyses of the field data indicate that the Tombigbee Sand Member of the Eutaw Formation varies considerably in thickness, from as little as 50 cm thick at Pickensville, Ala., to about 300 m thick in the vicinity of Columbus, Miss., and over 600 m in thickness near Aberdeen, Miss. The reason(s) for this previously undocumented thickening of the Tombigbee is currently under investigation.

Dinoflagellates and increased biostratigraphic resolution

Preliminary range studies by L. E. Edwards using undescribed, as well as published, species of dinoflagellates indicate that delineation of a fine biostratigraphic subdivision of the Paleocene using dinoflagellates is possible. Outcrop and shallow core material in Georgia and Alabama include a range of depositional environments in which dinoflagellates are found. Calcareous nannofossils (L. M. Bybell, unpub. data) provide age data on marine dinoflagellate assemblages to which marginal marine dinoflagellate floras may be compared. The improved biostratigraphic resolution in marginal marine deposits is especially encouraging. Additional diversity studies are beginning to provide paleoecological information.

Coccolith correlation for Ardath Shale, San Diego County, California

The Ardath Shale of the La Jolla Group from the seacliffs below Salk Institute and nearby in San Diego contains lower middle Eocene coccoliths of the *Rhabdosphaera inflata* subzone, including guide species *Discoaster sublodoensis* Bramlette and Sullivan and *Rhabdosphaera inflata* Bramlette and Sullivan. J. D. Bukry reports that preliminary study of coccoliths from a mollusk-bearing exposure of the Santiago Formation, sampled by Thomas Demeré (San Diego Museum of Natural History), in the seacliff at Leucadia shows a possibly correlative shallower water assemblage. Shallow-water indicator taxa in common between the San Diego and Leucadia sites include *Braarudosphaera bigelowii* (Gran and Braarud), *B. discula* Bramlette and Riedel, *Micrantholithus basquensis* Martini, *M. flos* Deflandre, *M. parisiensis* Bouché, and *Pemma rotundum* Klumpp. These pentaliths, and the placoliths in common, indicate that the Leucadia assemblage could be simply a shallow-water biofacies of the Ardath assemblage. If substantiated, this would alter the extant mollusk-based correlation that equates the Santiago Formation at Leucadia to the upper upper Eocene Mission Valley Formation of San Diego. The great dissimilarities between lower middle and upper upper Eocene shallow-water coccolith assemblages are not evident at Leucadia, and the presence of *Helicosphaera lophota* Bramlette and Sullivan and *Sphenolithus spiniger* Bukry suggest a level no higher than middle Eocene.

Late Miocene Pacific correlation by *Dictyocha neonautica* Bukry

The elongate silicoflagellate *Dictyocha neonautica* Bukry is associated with the upper Miocene *Amaurolithus primus* subzone of coccoliths (Bukry, 1971) in the North Pacific at DSDP Sites 77, 157, 158, and 310. J. D. Bukry reports that this substantial widespread occurrence of a naviculopsoid silicoflagellate population some 10 m.y. following the extinction of genus *Naviculopsis* (Frenguelli, 1940) in early Miocene is exceptional. It follows closely the appearance of genus *Amaurolithus* (Gartner and Bukry, 1975) and apparently also occurs just above the level of a significant change in carbon isotope ratios (Loutit and Kennett, 1979; Gerta Keller, written commun., 1979), that is being studied by the Cenozoic Paleo-Oceangraphy Project group. *D. neonautica* may provide a useful siliceous biostratigraphic guide, in addition to calcareous *Amaurolithus*,

to assist in locating the level of carbon change for further interpretation. The widespread and brief occurrence of the unusual *D. neonautica* morphology supports a general perturbation in oceanic near-surface conditions.

Three periods of intense high-latitude cooling in the middle to late Miocene

Study of the upper Cenozoic diatom biostratigraphy and paleoceangraphy of DSDP Leg 63, off southern California and Baja California, by J. B. Barron has revealed the presence of three periods of widespread hiatus (sedimentary gap) development in the eastern North Pacific. These periods at 12 m.y. to 1 m.y. B.P., 10 m.y. to 9 m.y. B.P., and 7.2 m.y. to 6.2 m.y. B.P. apparently correspond to times when bottom currents removed sediment by erosion or chemical corrosion in response to pronounced high-latitude cooling and Antarctic ice growth.

Extent of northern hemisphere Pliocene glaciation

Results of studies by R. Z. Poore on material from DSDP samples in the North Atlantic (Legs 37, 48, and 49) confirm that the first ice-rafting in the North Atlantic was about 3.0 m.y. B.P. and that, during the Pliocene, icebergs penetrated as far south as lat 45° (DSDP Hole 410) but not as far south as lat 37° (DSDP Holes 333 and 335). The estimated age of 3.0 m.y. B.P. for the onset of Northern Hemisphere low-elevation glaciation derived from the North Atlantic is supported by a 3.2-m.y.-B.P. estimate suggested by paleomagnetically controlled isotopic data from the Equatorial Pacific. Isotopic studies and North Atlantic planktonic foraminiferal assemblages show that a long period of stable global ice volume and warm sea-surface temperatures in the northwestern Atlantic preceded the initiation of Northern Hemisphere glaciation.

Quaternary climates, eustacy, and tectonism, southeastern United States

Based on the work of T. M. Cronin, T. A. Ager, B. W. Blackwelder, and B. J. Szabo, the Quaternary record of the southeastern Atlantic Coastal Plain is shown to consist of successive marine transgressive-regressive cycles related primarily to glacioeustatic sea-level fluctuations but complicated by subtle crustal movements. Each marine transgression yields pollen and ostracode assemblages signifying predominantly interglacial continental and nearshore oceanic climates. Evidence for glacial environments such as those during the Wisconsinan interval is lacking in the onshore marine record, and these data indicate that coastal plain marine episodes represent only warm interglacial intervals and, hence, corresponding high stands of sea level. Uranium series disequilibrium dating of corals (performed by B. J. Szabo, USGS) from some of these units in Virginia and North and South Carolina has produced age clusters of approximately 450,000 to 500,000 yr B.P., 188,000 yr B.P., 120,000 yr B.P., 94,000 yr B.P., and 72,000 yr B.P. Relative sea-level positions in parts of the coastal plain for all but the 120,000-yr-B.P. transgression would not be expected from current models of global sea level during these intervals, based on deep-sea isotope data; therefore, either these models need revision or crustal uplift has altered the original position of some of these deposits or both.

Temperature aspects of late Quaternary marine molluscan faunas

The temperature aspects studied by G. L. Kennedy of dated Pleistocene and Holocene molluscan faunas along the west coast of the United States primarily reflect relative sea levels and not upwelling, as previously thought. Faunas dated by radiocarbon at 1,000 to 7,000 yr old from emergent terraces (up to 20 m) near Seattle, Wash., and Cape Mendocino, Point Conception, and Ventura, Calif., are similar to the faunas living at those latitudes today. Faunas dated by amino-acid racemization at 40,000 to 85,000 yr old from emergent terraces on the California, Oregon, and Washington coasts are relatively cool-water faunas, which are consistent with lower sea levels and cooler conditions during the last major glacial epoch. Faunas dated at 125,000 yr old by amino-acid racemization and uranium-series techniques have temperature aspects warmer than faunas living at equivalent latitudes today. The relatively warm aspect of these faunas is consistent with the slightly higher sea level and warmer conditions during the early part of the last major interglacial period.

Tectonic uplift rates near Gaviota, California

K. R. Lajoie reports that amino-acid age estimates of about 250,000 yr on a 38-m marine terrace and about 85,000 yr on a 27-m marine terrace near Gaviota in Santa Barbara County, Calif., yield uplift rates of 0.15 to 0.32 m/1,000 yr. However, an average carbon-14 date of 7,500 yr on a marine deposit (16.5 m) between these two terrace localities indicates the rate of uplift has accelerated to about 2.2 m/100 yr in Holocene time. Geodetic data obtained in 1901 and 1919 indicate the uplift rate has risen to 10 mm/yr (10 m/1,000 yr) for short periods of time. Gaviota lies near the western terminus of the Palmdale Bulge. The acceleration of uplift during Holocene time may be the initial phase of uplift associated with the bulge in this area. Faults that offset Holocene deposits 5,000 to 8,000 yr old near Point

Conception (proposed LNG terminal) may be associated with this recent pulse of tectonic activity.

PALEOZOIC STUDIES

Correlation of the Middle Pennsylvanian Series

The lowest marine fauna in the type Middle Pennsylvanian Series of the proposed Pennsylvanian System stratotype occurs in the Eagle Limestone of I. C. White (1891) in the lower part of the Kanawha Formation of central West Virginai. T. W. Henry and MacKenzie Gordon, Jr., have identified several taxa of brachiopods and the goniatite cephalopod *Gastrioceras occidentale* (Miller and Girley) from the White Eagle; this suggests that his Eagle is no older than the Dye Shale Member of the Bloyd Shale of the type Morrowan Provincial Series. Brachiopods diagnostic of the *Linoproductus nodosus* Assemblage zone of Henry and Sutherland (1977), including the name-bearer, occur in the Kanawha Formation as high as the roof shale of the Cedar Grove coal bed. Thus, additional invertebrate biostratigraphic information tends to corroborate earlier correlations of the lower and middle parts of the Kanawha Formation with the upper part of the type Morrowan Provincial Series.

The Winifrede Limestone of Hennen (1914) in the upper part of the Kanawha Formation contains a megafauna that appears to correlate with the Atokan Provincial Series of the midcontinent and the Kanawha Black Flint of White (1891) in the Kanawha Formation; the youngest marine bed in the Kanawha is either Atokan or early Des Moinesian in age.

Correlation of the Dunkard Group

Discovery of *Callipteris conferta* (Sternberg) Brongniart and *Sphenuphyllum thoni* by W. H. Gillespie and H. W. Pfefferkorn (University of Pennsylvania) in the lower and middle parts of the Dunkard Group in the Pennsylvanian System stratotype study area of central West Virginia allows correlation of these strata with the Autunian Stage of western Europe and supports earlier observations that the Dunkard is, in part, Permian in age.

Foraminiferal faunas at the Mississippian-Pennsylvanian boundary, south-central Idaho

B. A. L. Skipp reports that calcareous foraminiferal faunas in the southern White Knob Mountains, Idaho, indicate that the Mississippian-Pennsylvanian boundary lies within the lowermost beds of the Bloom Member of the Snaky Canyon Formation above the Bluebird Mountain Formation (Skipp and others, 1979). The Bluebird Mountain Formation of latest Mississippian age is a thin (7.6–23.7) sandstone sequence within a regional Carboniferous carbonate bank buildup that contains no recognized hiatus at the Mississippian-Pennsylvanian boundary. The top of the Mississippian is picked at the highest occurrence of *Eosigmoilina rugosa* Brazhnikhova, whose range is confined to Upper Mississippian strata throughout North America. In the White Knob Mountains, *Eosigmoilina rugosa* is present through 110 m of strata, including the top of the Surrett Canyon Formation, the Bluebird Mountain Formation, and the basal 10 m of the Bloom Member of the Snaky Canyon Formation. Above the level of the eosigmoilinids, about 90 m of limestone contain a posteosigmoilinid fauna without typical Pennsylvanian millerellids (for example, *Millerella marblensis* group), which appear in overlying beds. The fauna, instead, is characterized by very small discoidal-planispiral Eostaffellidae with few volutions (1–2½), few chambers per volution, a relatively large proloculus (almost one-third of the total diameter), chomata, involute coiling habit, and nonkeeled periphery and by primitive globivalvulinids, along with other longer ranging faunas (Skipp and Brenckle, 1979). The distinctive eostaffellid and globivalvulinid forms are considered to be of probable earliest Pennsylvanian age, and they range upward into the zone of *Millerella*.

Extension of age terrestrial vertebrates

A collection of Pennsylvanian plants from red beds of the Cutler Formation in El Cobre Canyon, north-central New Mexico, has important bearing on the antiquity of terrestrial tetrapod vertebrates. The plants were associated with a pelycosaur-dominated fauna and were collected by M. A. Fracasso (Yale University). S. H. Mamay examined the plants and recognized two taxa characteristic of Missourian and Virgilian rocks. Previously, the Wolfcampian of north-central Texas has been regarded as the source of the oldest known tetrapods, but the New Mexico collections extend the age of the tetrapods from the Permian into the Pennsylvanian.

Evolution of the corals

It has been suggested that the Mesozoic-Cenozoic coral order Scleractinia originated or evolved either by direct descent from the Paleozoic order Rugosa or by the development of a skeleton in members of the anemone groups that probably existed throughout Phanerozoic time. Recent analysis of this problem by W. A. Oliver, Jr., developed the following points:

1. Rugosan septal insertion is serial; Scleractinian insertion is cyclic; no intermediate stages have been demonstrated. Apparent intermediates are Scleractinia having bilateral cyclic insertion or teratological Rugosa.

2. There is convincing evidence that the skeletons of many Rugosa were calcitic, and none are known to be or to have been aragonitic. In contrast, the skeletons of all living Scleractinia are aragonitic, and there is evidence that fossil Scleractinia were aragonitic also. The mineralogic difference almost certainly is due to intrinsic biologic factors.
3. No Early Triassic corals are known. If the Rugosa-Scleractinia were one evolving group of animals, it is very unlikely that two major changes (1 and 2 above) would have taken place at the same time and during the only age in the history of the corals in which corals are not known to occur. Probably, the Rugosa became extinct at or near the end of the Paleozoic, as did many other groups of animals. This vacated a niche that had been successfully occupied for 250 m. y. (As soon as any existing group of sea anemones "experimented" with secreting a skeleton, the way was open for the niche to be occupied by a new group of corals, the Scleractinia.)

PLANT ECOLOGY

Damage to flood-plain forests along the Potomac River

Flow characteristics during great floods appear to determine many differences in the composition, age, and form of flood-plain forests. A study by T. M. Yanosky indicated that damage to flood-plain vegetation following the 1972 Hurricane Agnes flood varied locally along the Potomac River near Washington, D.C. Destruction appeared to be related to velocity of flood flow, which, in turn, was related to flood magnitude and channel shape. Trees exposed to maximum flood force were damaged or uprooted in greater numbers than trees sheltered by channel shape. Trees in sheltered areas predate the catastrophic 1942 flood, whereas trees along heavily damaged reaches became established after 1942. In addition, species varied in ability to withstand damage from the Hurricane Agnes flood. Least likely to recover were species growing on infrequently flooded surfaces, which may explain, in part, their absence at lower flood-plain elevations.

Flood rings in trees along the Potomac River

Cross sections of 36 green ash trees (*Fraxinus pennsylvanica* Marsh.), collected by T. M. Yanosky along the Potomac River flood plain near Washington, D.C., ranged in age from 8 to 60 yr. The 1972 growth ring of most samples showed distinct abnormal layers of cells along the entire circumference of the latewood; vessels formed later in the 1972 growth ring were often strikingly larger than those formed earlier in the 1972 latewood. Defoliation and subsequent resumption of growth following the catastrophic Hurricane Agnes flood are believed to be the cause of this phenomenon. In addition, evidence was found for smaller floods that occurred between May 1, 1940, and June 30, 1979. Of 19 yr in which flooding occurred, evidence for at least 10 of these events was found in samples.

Dendroclimatic investigations of hickory and oak

According to J. F. Hill, annual ring widths of pignut hickory, *Carya glabra* (Mill.) Sweet, and post oak, *Quercus stellata* Wang., growing in thin soil on a rocky Maryland site along the Potomac River showed a considerable correlation with growing-season precipitation. Hickory-ring widths showed especially large year-to-year variation and correlation with precipitation. Post oak ring-width patterns were comparable to those of red oak, *Q. rubra* L., and white oak, *Q. alba* L., growing at the same site. When episodes of uniform minimal yearly growth were deleted from the hickory data, the result was a greater correlation with precipitation. Hickories growing with their stem bases directly on exposed rock showed stronger correlations with precipitation than did trees rooted in soil.

Spacing of bands of longitudinally oriented parenchyma cells in the hickory wood was shown to be directly correlated with growth rate and with growing season precipitation. This finding is significant for X-ray densitometric analysis of wood.

Potomac Estuary Study

As part of the Interdisciplinary Potomac Estuary Study of the Wetland Studies Project, V. P. Carter and P. T. Gammon documented the distribution and abundance of submersed aquatic vegetation in the Potomac River Estuary and tidal river during the 1978 and 1979 growing seasons. A systematic sampling program revealed no vegetation in the fresh tidal river and its tributaries, 13 species of plants in the oligohaline (low salt) and low mesohaline (medium salt) reaches of the estuary, and very low plant diversity and abundance in the higher salinity water of the lower estuary. This vegetation distribution differs considerably from the historic distribution in the tidal Potomac. Heavy nutrient loading may be causing an imbalance in the traditional phytoplankton–submersed aquatic plant relation; as a result, plants overburdened with epiphytes have reduced photosynthetic efficiency and do not survive. However, because many other factors have been implicated in the decline of submersed aquatic vegetation throughout the Chesapeake Bay area, all water-quality, sediment, and transport data collected by the Potomac Estuary Study are being analyzed for possible effects on plant distribution.

Evidence of modern slope movement in the Appalachian Mountains

Periodic movement of some central Appalachian block fields was found by C. R. Hupp and R. S. Sigafoos through tree-ring analysis. The block fields spread downslope during intense rainfall; this movement correlates with dates of flooding on a nearby stream. Further, this study indicates that Appalachian block fields are an active part of Holocene climate rather than a relict of the Pleistocene. A hydrostatic mechanism of movement is postulated.

Tree-species distribution and ages have been related to hydrology and geology on the slopes of Buzzard Rock, a part of Massanutten Mountain, Va. Avalanching contributes large quantities of debris to the bedload of Passage Creek. Natural establishment and destruction of trees on the block field modify slope stabililty and instability. In a related study, C. R. Hupp extended the flood record of Passage Creek by at least 50 yr, using techniques described by Sigafoos (1964). Flood frequency and magnitude appear to be prime factors in flood-plain vegetation pattern, age, and growth rates.

Trees of the Apalachicola River flood plain

As part of the Apalachicola River Quality Assessment, Helen Leitman and Ann Redmond identified tree species along eight transects totaling 20 km in the 51,000-ha flood plain of the Apalachicola River, Fla. Forty-six species of trees were recognized by prism sampling. Dominant tree species in the flood-plain areas of lowest elevation are water tupelo (*Nyssa aquatica*), ogeechee tupelo (*N. ogeche*), and bald cypress (*Taxodium distichum*). Medium and high areas are covered by a wide variety of bottomland hardwood species. Tree identifications, diameters, relative height, and ground elevation data are assembled into a computerized data-storage system.

CHEMICAL, PHYSICAL, AND BIOLOGICAL PROPERTIES OF WATER

CHEMICAL AND BIOLOGICAL QUALITY OF SURFACE WATER

Low heavy-metal concentration in the Red River, Louisiana

An analysis of historical data by C. R. Demas showed that, since 1974, the concentration of selected heavy metals in the water of the Red River in Louisiana has been relatively low. The Red River near Shreveport, at Boyce, at Alexandria, and at Moncla was sampled either quarterly or monthly each year for A, Be, Cd, Cr, Cu, Pb, Hg, Ni, Se, and Zn. Of the 10 metals determined, only cadmium exceeded EPA-recommended "alert-limits." The cadmium values that exceeded the alert limit value of 10 μg/L were 14 μg/L at Alexandria (once in 1974) and 12 μg/L at Boyce (once in 1978). An annual mean concentration exceeded the alert limit in 1974 when the total cadmium annual mean at Alexandria was 11 μg/L. Since that time, none of the selected constitutents has exceeded alert limits.

Water quality of major tributaries, Chesapeake Bay

Monitoring of the chemical quality of three major tributaries to Chesapeake Bay began in April 1979. The monitoring stations are located on the Susquehanna River at Conowingo, Md., the Potomac River at Washington, D.C., and the James River at Cartersville, Va. These three rivers drain 67 percent of the drainage area surrounding the Chesapeake Bay.

D. J. Lang reports that a multiple-regression analysis was used to correlate chemical parameters with discharge, specific conductance, temperature, and suspended sediment that are collected on a continuous or daily basis. Several correlations have been found: (1) major ions correlate well with discharge and specific conductance, (2) total phosphorus correlates well with discharge and suspended sediment, and (3) aluminum, iron, and manganese (both suspended and dissolved) correlate well with suspended sediment and specific conductances. Of the 32 pesticides being determined, atrazine, prometryne, 2,4,D, and 2,4,5,T were detected most frequently, with their maximum concentrations occurring during the late summer.

Sediment transport on the lower Susquehanna River is extremely complex because of three hydroelectric dams downstream from Harrisburg, Pa. At the present time, the correlation of suspended sediment with discharge at Conowingo is extremely poor at low and medium flows. The correlation improves with increasing discharge.

Water monitoring of coal-mining areas, Virginia

P. M. Frye and P. W. Hufschmidt reported that, in the coal-mining areas of southwestern Virginia, dissolved sulfate and manganese concentrations appear to be reliable indicators of mine drainage. Three synoptic sampling trips have been completed to date, and analyses of the samples collected show that the dissolved manganese concentrations of many streams have exceeded the drinking-water standard of 200 μg/L.

An extremely dense network of 115 monitoring stations is being used to monitor approximately 6,000 km^2 in the most rugged terrain of Appalachia. Research at this time indicates that the station density needs to be increased to detect specific sources of stream pollution.

Statistical analyses of surface-water quality, Nebraska

Descriptive statistics for 29 chemical and biological constituents were prepared for 109 stream sites in Nebraska by R. A. Engberg. Also prepared for each site were regression equations relating specific conductance to each of 12 chemical constituents and a regression equation relating specific conductance to stream discharge.

The descriptive statistics, presented by river basins, show that the quality of surface water in Nebraska is highly variable. Of the 13 river basins in Nebraska, water leaving the Niobrara River basin had the lowest mean specific conductance (266 μmho/cm at the Niobrara River near Verdel), and water leaving the South Platte River basin had the highest mean specific conductance (1,890 μmho/cm at the South Platte River at Roscoe). Ground-water seepage from a wide range of geologic formations, overland runoff, and irrigation return flow account for the variability. Statewide, the principal cations in streamflow are calcium and sodium, and the principal anions are bicarbonate and sulfate.

Based on regression equations, dissolved solids, hardness, calcium, magnesium, and bicarbonate, with some exceptions, correlate well with specific conductance for all stream sites.

Aquatic macroinvertebrates, Wyoming

The numerically dominant benthic macroinvertebrates in samples collected throughout Wyoming were *Trichoptera, Ephemeroptera, Diptera,* and *Coleoptera,* in that order. D. A. Peterson found the greatest density of organisms and most diverse communities in streams draining the east slope of the Bighorn Mountains.

Samples from perennial and intermittent streams in the energy-mineral development areas of the Powder River Basin contained mostly *Diptera, Trichoptera, Hemiptera,* and *Gastropoda.* In these streams, *Chironomidae* were the most common dipterans, although *Simuliidae* dominated certain sites. *Hydropsychidae* were the most common trichopterans. *Ephemeroptera* present were mainly those with operculate gills on the second abdominal segment, the *Tricorythidae* and *Caeniidae. Plecoptera* were absent from samples collected in the central part of the Powder River Basin in Wyoming.

Inverted-microscope method for the identification and enumeration of periphytic diatoms

According to D. B. Radtke, the inverted-microscope method offers an improved technique that permits the enumeration of periphytic or phytoplanktonic diatoms with the use of high-resolution objectives and high-power magnification after diatom frustules have been cleaned by oxidative digestion. Other advantages are: (1) the method is reliable and reproducible because of better overall counting efficiency and the reduction of the coefficient of variation, (2) quality-control procedures can be applied more easily to the method and analysis, (3) the slower oxidation procedure results in less breakage of the frustules and, therefore, increases counting efficiency, and (4) a greater number of organisms are enumerated from the sample population, which is advantageous when using the data for indices or other statistical applications in data analysis.

Limnology of West Point Reservoir, Georgia and Alabama

According to D. B. Radtke and G. R. Buel, water-quality data from West Point Reservoir on the Chattahoochee River at the Georgia-Alabama State line show severe hypolimnetic oxygen deficiency occurring in the reservoir once thermal stratification is established in the spring. This environment was favorable for the release of iron, manganese, ammonia, phosphorus, hydrogen sulfide, and other constituents from the sediments. During this period, the water released from West Point Reservoir has consistently failed to meet water-quality management objectives for iron, manganese, and DO concentrations. Hydrogen sulfide odor also was evident in the area immediately downstream from the dam during periods of stratification.

The lentic section of the reservoir showed the greatest biological activity in terms of plankton standing crop, adenosine triphosphate (ATP), and chlorophyll production. PCB and chlordane concentrations in the bottom sediments were also relatively high in this section of the reservoir and at the reservoir dam pool. At these locations, PCB and chlordane were detected in concentrations of up to 740 and 210 μg/kg, respectively.

Young bullhead-catfish and largemouth-bass tissue samples analyzed for chlorinated hydrocarbons and heavy metals showed significant amounts of chlordane and PCB in both whole fish and fillet samples. Concentrations of PCB and chlordane in fish tissue ranged from 19 to 388 μg/kg and from 6.0 to 280 μg/kg.

CHEMICAL AND BIOLOGICAL QUALITY OF GROUND WATER

Concentrations of heavy metals in ground water, Wisconsin

Analyses of ground-water samples taken by C. A. Harr from the four principal aquifers in Wisconsin indicated very low concentrations of heavy metals. Concentrations of heavy metals were below the detection limit of 1 μg/L in the following percentages of wells sampled: As, 62; Cd, 63; Co, 76; Cu, 54; Pb, 16; Ni, 40;

Se, 92; and Ag, 97. Chromium and zinc concentrations were below the detection limit of 10 μg/L in water from 84 and 11 percent, respectively, of the wells sampled, and mercury concentrations were less than the detection limit of 0.5 μg/L in water from 97 percent of the wells sampled.

The highest concentrations of the heavy metals were much lower than the limiting concentrations for various beneficial uses, except for concentrations of 2,400 μg/L of copper in water from one well, 62 and 80 μg/L of lead in water from two wells, and 6,600 and 7,600 μg/L of zinc in water from two wells.

Water-quality monitoring for radioisotopes, California

According to C. D. Farrar, treated industrial waste water containing low levels of radioisotopes produced at the General Electric Vallecitos Nuclear Center in Alameda County, Calif., is discharged into a tributary to Vallecitos Creek. Water-quality analyses show that effluent containing radioisotopes enters the surface- and ground-water systems that provide water for public supply, recreation, and wildlife. Ground-water movement is from the northeast toward the southwest. The velocity of ground-water movement is approximately 0.3 to 0.6 m/d in deposits locally known as the Livermore Gravel and 0.6 to 1.5 m/d in the alluvium. Both the Livermore Gravel and the alluvium supply water to domestic wells in Vallecitos Valley. The areal extent of ground-water contamination is not known. A network consisting of six ground-water sampling sites and four surface-water sampling sites is proposed to monitor water quality in Vallecitos Valley.

Median concentrations of chemical constituents in aquifers, southwestern Louisiana

According to D. J. Nyman, a statistical summary of the quality of water from wells in southwestern Louisiana showed that median concentrations of dissolved solids, hardness, iron, and chloride decrease with aquifer depth, whereas median values of pH increase with depth. The three major aquifers are the upper sand unit of the Chicot (shallowest), the Evangeline, and the Jasper (deepest). Median aquifer concentrations are given in the following tabulation (number in parentheses is number of samples):

	Chicot		Evangeline		Jasper	
Dissolved solids (mg/L)	520	(115)	325	(232)	255	(24)
Hardness (mg/L)	195	(118)	20	(233)	10	(24)
Iron (μg/L)	930	(115)	200	(185)	50	(22)
Chloride (mg/L)	86	(118)	13	(233)	7	(24)
pH (units)	7.5	(118)	7.8	(233)	8.3	(24)

Compared to Chicot water, the water in deeper aquifers is better suited for domestic or public-supply uses. However, the Jasper contains freshwater in only the extreme northern part of southwestern Louisiana, and the Evangeline contains freshwater in only the northern half, whereas the Chicot contains freshwater in most of southwestern Louisiana.

Summary of ground-water quality data, Wisconsin

Ground-water-quality data stored in the USGS computer system (WATSTORE) was summarized by P. A. Kammerer, Jr. The summary includes water-quality data for 2,443 wells that are open to one of the State's three major aquifers (sand and gravel, Silurian dolomite, and sandstone). Concentration data for dissolved solids, hardness, alkalinity, calcium, magnesium, sodium, potassium, chloride, sulfate, fluoride, iron, manganese, and nitrate were summarized by aquifer and by county, and locations of wells where data are available are shown for each aquifer. Calcium, magnesium, and alkalinity are the major dissolved constituents present in Wisconsin's ground water. Hardness and iron concentrations are objectionably high in much of the State's ground water. Trace constituent concentrations (selected heavy metals, arsenic, boron, and organic carbon) impair water quality in only a few isolated wells.

Methane-producing bacteria in deep aquifer

G. G. Ehrlich and E. M. Godsy isolated methane-producing bacteria from undisturbed areas of the Floridan aquifer at three locations. The three locations were near Pensicola, St. Petersburg, and West Palm Beach, Fla. Pure cultures of *Methanobacterium bryantii*, a rod-shaped methane-producing bacteria, were obtained by enrichment culture techniques. The final step involved growing mixed cultures of methane-producing bacteria and other bacteria in special broths containing antibiotics. Growth of nonmethane-producing bacteria was inhibited, and methane producers proliferated freely, leading to eventual isolation of pure cultures of *M. bryantii*.

M. bryantii was not found in parts of the aquifer affected by subsurface injection of industrial wastes. Presence of toxic agents such as oxygen in the injected waste solutions probably accounted for the absence of methane-producing bacteria in areas where native ground water had been displaced by waste water.

SURFACE-WATER-QUALITY MODELS AND PROCESSES

Deterministic models of surface-water systems

D. P. Bauer, M. E. Jennings, and J. E. Miller developed a one-dimensional steady-state water-quality model for general use in USGS studies. This model was applied to the Chattahoochee River in Georgia for four sets of steady-state flow conditions and one unsteady-flow condition. Water-quality conditions analyzed included DO, BOD, coliforms, and nitrogen. A nitrification routine for use in one-dimensional stream analyses was developed also and included in the model.

Benthic sediments and the dissolved-oxygen deficit in L'Anguille River basin, Arkansas

As part of a water-quality assessment of the L'Anguille River basin in northeastern Arkansas, C. T. Bryant, J. E. Terry, and E. E. Morris calibrated a one-dimensional steady-state stream-water-quality model. The calibration data set was collected under steady medium-flow conditions. The model was used to simulate and to predict concentrations of DO, carbonaceous BOD, nitrogen compounds, total- and fecal-coliform bacteria, orthophosphate-phosphorus, and suspended sediment. Terms in the model included utilization of oxygen by carbonaceous and nitrogenous substances and sediment deposits (sediment-oxygen demand), the uptake of phosphate by streambed materials, and the die-off of total- and fecal-coliform bacteria.

Calibration of the model revealed that the benthic oxygen demands had a much greater impact on the DO profile than did either the carbonaceous or nitrogenous demands. More than 70 percent of the DO deficit created in every modeled reach of the river was caused by the benthic demands.

Transport and degradation of acetone in streams

R. E. Rathbun, D. Y. Tai, D. W. Stephens, and D. J. Shultz injected acetone continuously into a small river model at the Gulf Coast Hydroscience Center near Bay St. Louis, Miss., to study the degradation rate. This river model, which is rich in organic detritus, is about 230 m long, is about 1 m wide, and is fed by an artesian well with a discharge of about 1.2 L/s. Although laboratory experiments had suggested that acetone would be readily degraded by bacteria in the river after a short acclimation period, very little degradation of the acetone was observed. Only small changes in the acetone concentrations occurred over a 24-h period, apparently as a result of temperature effects on the volatilization coefficient.

Volatilization of ketones from water

R. E. Rathbun and D. Y. Tai measured the volatilization coefficients of acetone, methyl ethyl ketone, 2-pentanone, 3-pentanone, methyl isobutyl ketone, 2-heptanone, and 2-octanone in the laboratory over a range of mixing conditions in a water bath. The least volatile, least soluble 2-octanone had the largest volatilization coefficient for a specific mixing condition; the most volatile, most soluble acetone had the smallest volatilization coefficient. The volatilization coefficients of 2-octanone had the greatest dependence on mixing conditions in the water; the acetone coefficients had the smallest dependence.

Volatilization of priority pollutants from streams

R. E. Rathbun and D. Y. Tai measured the volatilization coefficients of benzene, chloroform, methylene chloride, and toluene, concurrently with the measurement of the oxygen absorption coefficient, in the laboratory over a range of turbulence conditions. The organic solute volatilization coefficients were equal to 0.655 of the oxygen absorption coefficient. Application of this constant to the modified tracer technique for the measurement of stream reaeration coefficients permits the determination of the volatilization coefficients of these solutes for any stream or river without direct introduction of these substances into the natural waters.

Nutrient yield of the Apalachicola River

An investigation by H. C. Mattraw, Jr., and J. F. Elder revealed numerous sources and sinks of the nutrients carbon, nitrogen, and phosphorus in the Apalachicola River basin in northwestern Florida. A variety of techniques are being used in the Apalachicola River Quality Assessment to determine nutrient input to the system from atmospheric fallout, ground water, upstream watersheds, and the flood plain. The dense vegetation on the 51,000-ha forested wetland flood plain of the Apalachicola River produces more than 40,000 kg/ha of organic material annually, thus providing a rich sourch of nutrients. Retention or loss of these nutrients in the flood plain is being evaluated and compared to the river yield to Apalachicola Bay, a highly productive estuary.

Carbon to nitrogen to phosphorus concentration ratios in the lower reaches of the river were characteristically 140:15:1. During low-flow periods, there appeared to be an increase in phosphorus concentrations from the headwaters to the lower river. Analyses of nutrient fractions indicated that most of the phosphorus was associated with the suspended sediment and that most of the nitrogen was dissolved. Within the dissolved nitrogen fraction, organic nitrogen and nitrate concentrations were about equal.

GROUND-WATER-QUALITY MODELS AND PROCESSES

Solute transport in porous media

Water-saturated laboratory soil columns were used by R. V. James and Jacob Rubin (1979) to test the applicability of solute-transport models based on the assumption of local chemical equilibrium. Two kinds of coarse-textured solid materials were employed to study the effects of calcium self-exchange on calcium transport. When the flow rate of solute-carrying water was 1.5 cm/d, the model based on the local equilibrium assumption predicted the experimental results very well. Such predictions were inadequate in the case of systems in which the water flow rate was 1.5 m/d.

A classification scheme for solute transport affecting chemical reactions, devised by Jacob Rubin, demonstrates why and how the nature of these reactions determines the basic mathematical structure and the numerical methods required by computer-based models predicting transport of ground-water solutes. According to this scheme, the first criterion to be considered for a given system is whether the reaction is fast enough to allow the local chemical equilibrium assumption to be employed. The second criterion involves determining whether a surface reaction (adsorption, ion exchange) or one of the reactions of classical chemistry (like precipitation oxidation) is involved. An additional determining factor is whether the reaction is homogeneous or heterogeneous.

AREAWIDE CHEMICAL LOADING

Effects of agriculture on stream quality, southwestern Georgia

Water-quality data from two basins in southwestern Georgia were reported by D. B. Radtke to show consistently low concentrations of chemical constituents and suspended sediment. The concentrations remain relatively constant even during periods of storm runoff. These low concentrations probably result because the highly permeable soil reduces overland runoff and subsequent upland erosion. This reduction in upland erosion limits not only the supply of silt and clay available to receiving streams but also the supply of chemical constituents that attach themselves to the silt- and clay-sized material. Current agricultural practices in the two study basins, with the possible exception of the use of some pesticides, are having no significant effect on water quality in terms of standards for public water-supply sources.

Phosphorus loading of lake water related to land uses

R. J. Gilliom (1980) has developed methods for estimating loadings and concentrations of phosphorus for lakes in the Puget Sound region using data that are already available. Phosphorus is the primary cause of lake eutrophication in this region. Using models that relate lake phosphorus concentrations to phosphorus-loading rates and hydraulic characteristics of the lake, the phosphorus-loading rate needed to create the observed lake phosphorus concentration is estimated. Nonpoint phosphorus loading from forest-land runoff, bulk precipitation, residential area runoff, septic tank systems, and agricultural area runoff was calculated in this manner. Loading by bulk precipitation was estimated to be 20 kg/km^2/yr. The empirically estimated yield of phosphorus from forest land ranged from 2 to 25 kg/km^2/yr and was found to be logarithmically related to annual runoff. The regression equation expressing this relation explained 73 percent of the sample variance and was used to estimate forest-land phosphorus yield for individual lakes. Estimated phosporus yield from residential areas averaged 7 ± 2 kg/km^2/yr greater than forest-land phosphorus yield. Estimated phosphorus loading from nearshore septic tank systems was significantly correlated with the number of nearshore homes around lakes in 1940, providing a limited capability to estimate present-day loading from this potential source. Agricultural source phosphorus loading can be estimated as the difference between the total loading of phosphorus to a lake (as calculated from the measured lake-water concentration) and the estimated loading from all other sources. The above phosphorus-loading relations were applied to a group of 29 lakes located in an area north of Seattle, and the results indicate a wide range of background (predevelopment) phosphorus levels and degrees and causes of human-related phosphorus enrichment.

RELATION BETWEEN SURFACE WATER AND GROUND WATER

Water flow in the unsaturated zone

Using laboratory columns of several different soil materials, C. D. Ripple and Jacob Rubin studied infiltration of water into soils at controlled predetermined rates. All tested rates were lower than the saturated hydraulic conductivity of the material studied. Rain infiltration, as well as infiltration through porous plates, was investigated. In experiments with stepwise-increasing water input rates, ponding was produced at rates that were nonponding during infiltration trials with constant rates. These results could not be explained by changes in soil structure or by restriction of air flow by column walls. The results are of theoretical significance because they are not predicted by the currently accepted theory of water flow in unsaturated

soils. They also are of practical importance for predicting runoff occurrence during rainfall.

Influence of water-table mounds on seepage through lakebeds

T. C. Winter reported that one of the principal factors affecting outseepage from lakes and wetlands is the presence of water-table mounds on the side of the water body toward the major ground-water discharge area. A finite-element model that handles variably saturated conditions was used to analyze the detailed patterns of growth and dissipation of water-table mounds under an unsaturated zone of varying thickness. Preliminary results have shown that water-table mounds tend to grow initially immediately adjacent to the surface-water body and then to fill in gradually under the land-surface high. In geologic material of high hydraulic conductivity, it may take days or weeks to raise the water table directly beneath a land-surface high, and, in material of low hydraulic conductivity, the water table might seldom, if ever, be highest beneath the land-surface high. This dynamic lateral movement of water-table mounds has significant implications on siting of observation wells in studies of the interaction of lakes and ground water.

Hydrology of prairie wetlands

Continuing controversy over the role of prairie wetlands in the hydrologic system has prompted renewed study of these surface-water features. Preliminary numerical analysis by T. C. Winter and M. R. Carr of vertical sections through a large segment of the Missouri Coteau in North Dakota suggests that ground-water flow systems of various magnitudes (local, intermediate, and regional) occur within the glacial drift. The interactions of small lakes and wetlands that occur high topographically are sensitive to anisotropy (the ratio of horizontal to vertical permeability) of the deposits. If anisotropy is less than about 500, outseepage is unlikely from small wetlands that are sinks for local flow systems. If anisotropy is as high as 1,000, considerable outseepage from them is likely. The large saline lakes that occur low topographically are sinks for local and intermediate flow systems regardless of anisotropy of the deposits. The numerical analysis also indicates that, in areas where the thickness of drift is less than about 60 m, local flow systems extend to the base of the drift and there is no regional flow passing at depth beneath them. Even in areas of thicker drift, deep regional flow occurs only if anisotropy is near 1,000.

Streamflow augmentation with ground water

The feasibility of pumping ground water from the upper glacial aquifer and into a dry stream channel to induce or augment streamflow on Long Island, N.Y., was investigated by K. R. Prince. The rate of infiltration was found to be governed by many factors. Temperature effects and streambed clogging by algae were observed during augmentation conducted in December 1979. Changes of only 2°C were calculated to change infiltration rates by as much as 13 percent. However, the effects of the algae could not be quantified nor could the effect of summer temperature on the growth of algae be assessed. Soil moisture in the unsaturated zone directly beneath the streambed, as measured with a neutron logger, increased from 20 percent (a highly drained state) before augmentation to 40 percent (nearly saturated) after 10 d of stream augmentation. As the soil moisture increased, infiltration into the streambed increased by as much as 37 percent, as evidenced by a shortening of the stream length by 230 m out of a total length of about 625 m. The average infiltration rate after the stream length stabilized was 2.26×10^{-2} L/s/m^2. The recharge mound beneath the stream rose as much as 1.2 m above preaugmentation levels and extended laterally from the stream channel only a few tens of meters. The mound never rose high enough to intersect the streambed. Three rates of augmentation were used to define the relation between stream length and rate of augmentation, 0.014, 0.028, and 0.045m^3/s. The length of wetted channel was directly proportional to the rate of augmentation. Extrapolation indicates that streamflow will be induced for a distance of about 14,000 m down the stream channel for each 1 m^3/s of flow introduced at the source of augmentation.

Planning for conjunctive water-supply systems

Inclusion of separate economic supply and demand curves for surface- and ground-water sources in a dynamic programing formulation by M. E. Moss extends the scope of optimal water-supply planning techniques. Dynamic programing is used to maximize net benefits derived from investments in a conjunctive ground- and surface-water supply system for a hypothetical expanding community. Results provide an optimal pattern of investments over time for a water-supply reservoir and for water-supply wells under a set of assumed economic supply and demand curves.

EVAPORATION AND TRANSPIRATION

Evaporation from water surfaces and the combined evaporation and transpiration from vegetated land surfaces play a major role in hydrology by returning about 70 percent of the incident precipitation in the conterminous United States to the atmosphere. Moreover, evapotranspiration from a given area may be substantially altered by changes in land use, such as irrigation development, reforestation, drainage of wetlands, clear-

ing of phreatophytes, and urbanization. Consequently, knowledge of evapotranspiration under various land-use and climatic conditions is needed for planning purposes.

Water use by saltcedar and by replacement vegetation in the flood plain of the Pecos River, New Mexico

Saltcedar (*Tamarix chinensis*) has been eradicated by the Water and Power Resources Service from 7,600 ha of land in the flood plain of the Pecos River between Acme and Artesia, N. Mex. Saltcedar was controlled by mowing from 1967 to 1974 and by rootplowing, a much more effective method, from 1974 to present (1980). Initially, R. W. Mower, J. W. Hood, R. L. Cushman, R. L. Borton, and S. E. Galloway (1964) estimated that such phreatophyte clearing would result in an annual saving of about 3.5 million m^3 of water from evapotranspiration. However, base-flow studies by G. E. Welder (unpub. data, 1979) indicated that detectable rates of salvage have not been produced. Consequently, E. P. Weeks and G. E. Welder have been conducting measurements of water use by saltcedar and by the replacement vegetation *Kochea scoparia*, a common weed, to determine whether the initial estimates of water use for the two vegetation categories were in error. Preliminary measurements by eddy-correlation and energy-budget methods in July 1979 indicated that the *Kochea* was using about 3 mm of water per day over a 7-d period at that time. Measurements of saltcedar were made for 1 d before the experiment was rained out. Water use by the saltcedar on that day was also about 3 mm, but the day was atypically cloudy and, thus, not representative of July weather in southeastern New Mexico.

Another set of measurements was made by the eddy-correlation method in October 1979. These measurements indicate that the *Kochea* and *Tamarix* were using about 0.5 and 2.0 mm of water a day, respectively, at that time. These measurements suggest that some water should be salvaged by clearing the saltcedar. However, too few measurements are available as yet to determine the magnitude of such salvage.

LIMNOLOGY AND POTAMOLOGY

Although the term "limnology" originally applied only to the study of lakes, in its current usage it also refers to the study of streams and rivers. Limnology is the study of sources and nature of freshwater, its motion and changing condition, and, perhaps most significantly, the life it supports. The term "potamology" is more restrictive, applying only to river investigations.

Functional and structural responses of a stream community to copper

Changes in community function and structure of periphyton in a pristine stream during continuous low-level exposure to copper were determined by H. V. Leland. The study site, Convict Creek, is located at an elevation of 2,300 m on the eastern escarpment of the Sierra Nevada in California. Total copper concentrations maintained in stream water of the four study sections (each 350–490 m long) for 4 mo were approximately < 0.5 (control), 2, 8, and 20 μg Cu/L. Inhibition of photosynthetic carbon fixation and sulfate assimilation was observed within the first 48 h at 8 and 20 μg Cu/L but not at 2 μg Cu/L. Additional effects observed during long-term continuous exposure to the two higher copper concentrations were reductions in standing crop (chlorophyll *a* and ash-free dry weight), rate of colonization, rate of nitrogen fixation, rate of microbial decomposition of leaf litter, and algal species diversity. Abundances of the following species were reduced significantly by the presence of 8 and 20 μg Cu/L: *Chrysophyta*—*Achanthes minutissima, Cymbella microcephala, C. minuta, Synedra acus, S. rumpens,* and unidentified species of *Gomphonema, Navicula,* and *Synedra*; *Chlorophyta*—unidentified species of *Cladophora, Spirogyra, Mougeotia, Zygnema,* and *Ulothrix*; and *Cyanophyta*—unidentified species of *Calothrix.* An inhibitory effect of copper on community function at 2 μg Cu/L during long-term continuous exposure was evidenced by reduced rates of photosynthetic carbon fixation and sulfate assimilation relative to the control and by a lower rate of colonization of artificial substrates. Numbers of species of *Protozoa* and (or) *Rotifera* were found to be more reproducible measures of effect of copper on the community than was the presence or the absence of any one species. Species eliminated by the presence of 8 and 20 μg Cu/L were as follows: *Ciliophora*—*Aspidisca costata, Paramecium bursaria,* and unidentified species of *Amphileptus, Pleuronema, Stentor,* and *Sylonychia*; *Rotifera*—*Colurella adriatica, Dicranophorus epicharis, D. forcipatus, Euchlanis dilata, Lepadella ovalis, Lecane lunaris,* and unidentified species of *Colurella* and *Trichocerca.*

Artificial substrate sampler with increased habitat complexity

Artificial substrate samplers in common use for benthic invertebrates are selective for organisms that inhabit hard or eroding substrates; burrowers or other forms associated with fine sediment are poorly represented. In a study of benthic invertebrate distribution in streams of the East Fork Salmon River, Idaho, a new type of artificial substrate sampler was devised to provide a more complex habitat in an effort to collect more nearly representative samples of the naturally occurring fauna. The new sampler consists of a rock-filled polyethylene bag perforated with 6.4-mm-diameter holes on 5-cm centers. The relatively small percentage

of open space provided by the holes permits slow flushing but also results in accumulation of sediment within the rock-filled bag. Thus, the habitat is suitable for inhabitants of both hard and soft substrates, according to L. J. Tilley, S. S. Hahn, and K. V. Slack. Following 41 d of exposure in streams ranging from order 2 to order 7, the plastic-bag samplers collected substantially larger and more diverse benthic samples than the Hester-Dendy multiple-plate samplers at the same sites. The 7-site mean number of organisms, exclusive of the dipteran family *Chironomidae*, was 471 for the plastic bag samples compared to a mean of 57 for the multiple-plate samples. The plastic-bag samplers also collected nearly twice as many taxa, a mean of 24 species compared to 13 species for multiple-plate samplers. The samples from the multiple-plate devices exceeded those of the plastic bags for only one group, the insect order *Ephemeroptera*. Three times as many mayflies, but only one more species, occurred in multiple-plate samples as in plastic-bag samples. All other groups were more abundant in the bag samples. In addition to their sampling effectiveness for benthic invertebrates, the plastic-bag samplers are inexpensive, simple to use, and require no elaborate anchoring, and sections of the polyethylene bags can be used for samples of the periphyton community.

Chrysomonad cysts as paleoenvironmental indicators

Studies of sediment cores from California lakes have revealed a rich stratigraphic record of chrysomonad cysts in some localities. These siliceous cysts are the resting stages of chrysophyte algae and range in size between about 2.5 and 20 μm. They only rarely have been used as paleoenvironmental indicators, in part because their small size has made them difficult to observe. These observational difficulties now have been largely overcome by D. P. Adam, using scanning electron microscopy and differential phase contrast microscopy. Results to date indicate that the study of chrysomonad cysts can be developed into an important new tool for paleoecology. To evaluate fossil lake core material, about 300 modern chrysomonad samples were collected from a variety of environments. Most samples contained cysts, of which there are at least hundreds of distinct forms, some of them quite striking in appearance. The cysts appear to be most common in fluctuating freshwater environments of low pH (acid conditions), which suggests that they may be useful in monitoring acid rain. Mountain lakes in California contain numerous cysts in their sediments, but lakes at low elevations, including Clear Lake, have few, if any, cysts; this is true also of Lake Atitlan in Guatemala. Blooms of cyst-producing algae have been observed also beneath winter ice in Scandinavian lakes. These observations indicate that additional study of fossil chrysomonad samples may yield valuable information on paleoclimates.

Evaluation of empirical water-quality prediction models in reservoirs

Limnological investigations of two Colorado reservoirs were conducted by J. W. LaBaugh to test the applicability to reservoirs of several published empirical models derived from lake data. Total phosphorus budgets of the two reservoirs were different, reflecting contrasting land uses in the watersheds. Model predictions of total phosphorus concentrations based on budget data did not produce results consistent with actual concentrations observed. During the summer period of thermal stratification, the two reservoirs had significantly different concentrations of total phosphorus and chlorophyll *a* in the euphotic zone and significantly different Secchi-disk transparencies. For the reservoir with significantly higher total phosphorus and chlorophyll *a* concentrations, 60 percent of the variability in chlorophyll *a* could be attributed to total phosphorus. No significant relation between total phosphorus and chlorophyll *a* concentrations was observed in the other reservoir. However, one of the several empirical models tested did show good predictability of euphotic zone chlorophyll *a* concentration from total phosphorus data.

Phosphorus and nitrogen as limiting nutrients in two Arctic lakes

Laboratory bioassays were used by G. A. McCoy to examine nutrient limitation of algal growth in two Arctic lakes. Trace element and vitamin additions to lake water in the laboratory cultures did not stimulate cell growth. Phosphorus was found to limit algal growth early in the open water season (June and July). Later in the summer, less response to phosphorus addition to the cultures was observed, but simultaneous additions of phosphorus and nitrogen stimulated growth equal to that achieved under the same culture conditions in early summer. It is hypothesized that phosphorus is a limiting nutrient in these lakes in early summer and that the lakes tend toward colimitation by nitrogen and phosphorus in late summer. This hypothesis is being tested by directed fertilization experiments.

Limnology of reservoirs, eastern Montana

Limnological data were collected for 12 reservoirs in Phillips County, Mont., by R. F. Ferreira and R. L. Clements to provide information for their management as multiple-use reservoirs. In August, surface areas ranged from 0.5 to 70 ha, and depths, from 0.5 to 5.5 m. The reservoirs were weakly thermally stratified, and variations in DO, pH, and specific conductance with

depth were small. Shallow reservoirs were more turbid than deep reservoirs. Ice cover on larger reservoirs was about 1 m in February, whereas the shallow reservoirs froze solid. Specific conductance of surface waters varied from 193 to 7,100 μmho/cm in August. Values of pH were generally above 7.0 and increased in some reservoirs to greater than 9.0 in late summer. Concentrations of major constituents increased under ice cover. All of the reservoirs had high concentrations of nutrients, dense growths of aquatic plants alongshore, and algal blooms in spring and late summer.

NEW HYDROLOGIC INSTRUMENTS AND TECHNIQUES

Several new hydrologic instruments have been developed by the Hydrologic Instrumentation Facility of the USGS. As reported by F. C. Koopman, prototype battery-operated water-quality monitors for the in situ measurement and recording of water temperature and specific conductance were provided for installation and evaluation at 50 field sites throughout the country. Prototype models of pH and DO probes have been completed, and they are being integrated into the network of several hundred monitors that will be deployed.

The USGS also deployed over 1,000 "sentry" units, which are, literally, small sealed instruments (equal in size to a matchbox) that are capable of monitoring the accumulated operating times of water well pumps. Each sentry unit features a piezometric crystal that is activated by vibration. Activation generates a low-voltage current sufficient to transfer, electrochemically, silver in solution onto an internal electrode. The electrochemical process can be reversed, when desired, by a readout device that gives a measure of the accumulated time over which the sentry unit sensed vibration. In field use, the unit is fastened magnetically to the housing of a well pump, and, whenever the pump operates, vibration is induced. Cumulative hours of pump operation are readily translatable into volume of ground water pumped. The sentry units have proven to be a simple and inexpensive way of amassing the large volume of data needed to meet goals of the National Water-Use Data Program and numerous ground-water studies.

Prototype equipment for field evaluation has been developed for interfacing electromagnetic point velocity meters with integrators and recorders at 25 stream sites where variable backwater conditions occur. This equipment monitors water velocity for a time period and frequency that are selectable, temporarily stores such monitor data over a selectable time interval, and eventually averages and records the stored data in the desired format.

M. C. Goldberg reported on a study of the sources of fluctuations in Raman intensities in a conventional Raman spectrometer and of a method to compensate for such fluctuations. A photon-counting system was employed, and the Raman signal counts were large enough that $\sqrt{N}$ (square root of the number of counts) noise was neither significant nor so large as to produce pulse pile-up errors. Large-scale signal-intensity fluctuations were found to be correlated with ambient temperature changes of several degrees Celsius. The fluctuations decreased to a level of 0.5 percent by employing the following source-compensation method: a fraction of the Raman signal passing the entrance slit of the spectrometer was split off to a reference photomultiplier tube whose output was ratioed to that of the signal channel, and the signal counts were normalized to this ratio, thus, compensating for intensity fluctuation; the remaining 0.5-percent fluctuation considerably exceeds purely random noise and is closely correlated with ambient temperature changes.

P. A. Kammerer, Jr., and G. J. Allord reported on a computer-plotting procedure that was developed to store and to manipulate hydrogeologic data during the early phases of a ground-water-quality appraisal of Wisconsin's aquifers. Characteristics of the aquifers made it expedient to compile available geologic and well construction data on cross-sectional profiles to aid in data extrapolation and identification of regional inter- and intra-aquifer relations between hydrogeology and water quality. The plotting system produced cross-sectional profiles along preselected lines that traverse the State. Surface topographic data and cultural features were digitized from topographic quadrangle maps and were entered in automatic data processing files that were used to generate cross-sectional profiles at a choice of scales. The system provides for storing and plotting well construction and hydrogeologic data for wells on and near the cross section.

SEA-ICE STUDIES

Aircraft remote sensing of satellite Arctic program

The first set of a new series of aircraft remote-sensing missions was flown in October and November 1978 and in September and October 1979 with the NASA Convair 990 *Galileo II* flying laboratory and the NASA C–130 aircraft over the Arctic regions. These flights were part of the Polar Ice Program for the Seasat 1 and Nimbus 7 satellites, which were launched previously, and as a part of the Norwegian Sea Ice Experiment (W. J. Campbell, 1979). The aircraft carried active and passive microwave instruments simulating those on board the satellites, as

well as photographic equipment, and the flights were coordinated with satellite passes whenever possible. Data were collected on sea ice in the Bering, Beaufort, East Greenland, Barents, and Norwegian Seas and Baffin Bay, on ice sheets in Greenland, and on the polar ocean front in the Norwegian and Barents Seas. Flights were coordinated also with surface-truth experiments in the Barents and Norwegian Seas (Norway), Pond Inlet and Beaufort Sea (Canada), and other data buoys in the Bering Sea (United States). The remote-sensing flights were highly successful, and the data will aid in the verification, interpretation, and application of active and passive microwave data collected by both satellites in the Arctic.

Ocean topography by radar altimetry for iceberg towing

The towing speeds of large tabular icebergs to be used as a water resource will be approximately 1 kn above ambient ocean currents. Recent research has shown that the oceans are primarily made up of many meandering eddies rather than large steady-state streams like the Kuroshia and the Gulf Stream. W. J. Campbell (USGS), R. E. Cheney and J. G. Marsh (NASA), and N. M. Mognard (University of Washington, Seattle) (1980) have shown how satellite radar altimetry can be used to locate, measure, and track these midocean eddies. Because icebergs rotate at speeds as great as 2 kn, the only apparent approach to successful iceberg towing is by preferential eddy jumping along proposed towing routes.

Passive microwave imagery time-lapse film of Arctic sea-ice variations

W. J. Campbell (USGS), R. O. Ramseier (Department of Environment, Canada), and Per Gloersen and H. J. Zwally (NASA–Goddard Space Flight Center) (1980) have produced four films of Arctic sea-ice variations from time-lapse passive microwave imagery. The films consist of a series of color-enhanced brightness temperature images from the electronic scanning microwave radiometer on board Nimbus 5, taken every 3 d from September 1973 to December 1974, showing the seasonal variation of sea-ice morphology and concentration in various Arctic areas of Alaska, Canada, Norway, and Greenland. Repetitive viewing of the films revealed many aspects of short- and long-term changes in ice structure and motion that were not noticeable when analyzing individual images. Analyses of the films by the above individuals and Charles Elachi (Jet Propulsion Laboratory, Pasadena, Calif.) showed that interannual variability of the Arctic ice-cover structure and extent is more pronounced than understood previously from nonsynoptic data (Campbell and others, 1980). Along the ice edge, complex wave forms appear and migrate, reaching speeds of 100 km in a week in areas of high meteorological activity. One of the most important results was the discovery that large areas of low ice concentration occur within the Arctic pack throughout the year. Previously, the main pack near the pole was believed to be essentially 100 percent, but areas with concentrations as low as 50 percent were disclosed in the films.

Polar ice remote-sensing satellite program

W. J. Campbell is a member of the Experiment Teams for the Synthetic Aperature Radar on Seasat 1 and the Scanning Multichannel Microwave Radiometers on both Seasat 1 and Nimbus 7 and has planned the polar experiments for validation of these instruments. Since their launch, the satellites have collected much passive microwave data for sea ice, ice sheets, and snow fields in the Arctic and Antarctic. Campbell participated in surface-truth programs to aid in interpretation of the satellite data, including missions on oceanographic vessels, on coordinated aircraft remote-sensing flights, and with ground-based teams. The extensive NASA 990 remote-sensing-aircraft experiments were planned also as a part of this effort. Although Seasat 1 failed 3 mo after launch, valuable sea-ice and ice-sheet data were collected and reported on by P. G. Teleki and W. J. Campbell (USGS), R. O. Ramseier (Department of Environment, Canada), and Duncan Ross (NOAA, Goddard Space Flight Center) (1979), and the data from Nimbus 7 appears to be equally useful. The fall surface-truth experiments were highly successful, and these satellite programs should provide much information on sea ice and ice sheets.

Sea-ice dynamics observed by radar imagery

Side-looking radar images of Arctic sea ice were obtained as part of the Arctic Ice Dynamics Joint Experiment (Ling and others, 1978). Repetitive coverages of a test site in the Arctic were used to measure sea-ice drift, employing single images and blocks of overlapping radar image strips; the images were used in conjunction with data from the aircraft inertial navigation and altimeter. Also, independently measured accurate positions of a number of ground control points were available. From the work of W. J. Campbell (USGS), Franz Leberl (Technical University of Graz, Austria), and M. L. Bryan, Charles Elachi, and Thomas Farr (Jet Propulsion Laboratory, Pasadena, Calif.) (1979), tests of the method were carried out with repeated coverages of a land area on the Alaska coast (Prudhoe). Absolute accuracies achieved were essentially limited by the accuracy of the initial navigation data. Errors of drift measurements were found to be definition of identical features in sequential images. The drift of adjacent ice

features with respect to one another could be determined with errors of less than +0.2 km.

Sea-ice model

A sea-ice model has been developed by C. H. Ling, L. A. Rasmussen, and W. J. Campbell (1980). It is a quasi-steady-state model that uses both the equation of continuity and the equation of momentum. The model is compared to concentration data of the Antarctic that were acquired by the Nimbus 5 satellite using an electronically scanning microwave radiometer (ESMR). The computer results of the model match the ESMR data reasonably well. This model is now in the process of being combined with another sea-ice model, the Parkinson model, which uses the momentum equation and an energy equation. The Parkinson model does not have internal ice-stress terms in the momentum equation, which is generally considered most important; Ling's model does not have a specific energy equation. Therefore, the combined model should have the merits of both models and should give better results than either one used singly. Efforts are being made to work out the computer program for the combined model.

ANALYTICAL METHODS

ANALYTICAL CHEMISTRY

OPTICAL SPECTROSCOPY

Determination of nanogram amounts of bismuth in silicate rocks

J. S. Kane (1979) reported bismuth concentrations as low as 10 ng g^{-1} in 100-mg samples of geologic materials determined by atomic absorption spectrometry with electrothermal atomization. After HF-$HClO_4$ acid decomposition of the sample, bismuth is extracted as the iodide into methyl isobutyl ketone and is then stripped with ethylenediamine tetraacetic acid into the aqueous phase. Aliquots of this solution are pipetted into the graphite furnace and dried, charred, and atomized in an automated sequence. Atomic absorbance at the bismuth 223.1-nm line provides a measure of the amount of bismuth present. Results from four replicate determinations of bismuth in 14 USGS standard rocks indicate that, for bismuth concentrations above 150 ng g^{-1}, the relative standard deviation is 15 to 25 percent and the accuracy of analysis is within 10 to 12 percent of accepted concentrations. The method has been applied to rock samples containing bismuth in the concentration range of 14 to 1,030 ng g^{-1}.

Germanium concentrations in USGS rock standards as determined by electrothermal atomization atomic absorption spectrometry

Germanium in 13 USGS standard silicate rocks was determined by electrothermal atomization atomic absorption spectrometry using a procedure that permits the determination of 0.2 ppm of germanium in 50 mg of sample. The mean germanium concentration (in parts per million) found by M. M. Schnepfe (1979) is, for the new USGS standards, BHVO-1, 1.60; SDC, 1.51; STM-1, 1.32; QLO-1, 1.28; and RGM-1, 1.24 and, for the older USGS standards, W-1, 1.53; BCR-1, 1.39; G-1, 1.19; GSP-1, 1.16; AGV-1, 1.06; G-2, 0.96; PCC-1, 0.80; and DTS-1, 0.72.

X-RAY SPECTROSCOPY

Point-source discharge of phosphorus into the Potomac River

An intensive sampling was conducted by P. P. Hearn and L. F. Ruppert in the Potomac River near the Blue Plains, Md., treatment-plant outfall to study the flow pattern and behavior of dissolved and particulate phosphorus species associated with the treatment-plant effluent. Phosphorus in the effluent is present primarily as dissolved orthophosphate (80 percent of total). The flux of effluent into the main stem of the river was shown to be delayed by its movement through a secondary channel, which is separated from the main stem by a shoal area. This area serves as a natural holding lagoon where dissolved phosphorus is removed from the water column by adsorption and complexation by both suspended and bottom sediments. Suspended sediments were shown to remove up to 1.5 mg/g phosphorus (dry weight). The level of uptake of phosphorus by bottom sediments has not been satisfactorily measured, but bulk analyses indicate levels of phosphorus up to two times the background value for sediments in the general area. Initial estimates of phosphorus loss indicate approximately a 25-percent depletion in the immediate study area. Further analysis will provide a more accurate estimate of phosphorus flux into the river for budget calculations and also will yield information that can be applied in gaging the impact of other treatment plants in the river.

RADIOCHEMISTRY

Siderophile elements in the Earth's upper mantle

A suite of 19 garnet and spinel lherzolites of probable mantle origin was collected as part of the Basaltic Volcanism Study Project and analyzed for siderophile and volatile elements. The results reported by J. W. Morgan and G. A. Wandless are particularly interesting for the five highly siderophile elements, Os, Re, Ir, Pd,

and Au (Morgan and Wandless, 1979). In these rocks, the abundances of 3 platinum metals (Os, Ir, Pd) are very uniform regardless of locality (Europe, North and Central America, Australia, Hawaii), and their relative proportions are very close to chondritic proportions. The cosmochemically refractory elements osmium and iridium are highly correlated and retain their cosmic ratio. Palladium is more volatile (about as volatile as nickel), but the palladium-iridium ratio in ultramafic rocks nearly approximates the chlorine chondrite value. If the data for highly siderophile elements are normalized to iridium and chlorine chondrite abundances, palladium, iridium, and osmium show little fractionation, but gold and rhenium show depletion in some samples from initially cosmic proportions relative to platinum metals. Even in the most depleted samples, however, the rhenium-gold ratio remains close to the cosmic value. Apparently, the highly siderophile elements were added as a chondritic component after separation of the Earth's core. The high abundances of rhenium and gold in crustal material are believed to be the result of crust-mantle partitioning and not due to some peculiarity of mantle-core fractionation.

TRACE ELEMENTS IN PLANETARY MATERIALS BY ACTIVATION ANALYSIS

Chemical composition of Mars

The bulk composition of Mars has been derived (Morgan and Anders, 1979) by combining new petrological and geophysical considerations with a previous study of Martian volatile elements (Anders and Owen, 1977). These have been incorporated by J. W. Morgan into a modified version of the cosmochemical model of Ganapathy and Anders (1974).

The mantle of Mars is an iron-rich [Mg/(Mg+Fe)= 0.77] garnet wehrlite similar to the estimate of T. R. McGetchin and J. R. Smyth (1978) but richer in calcium and aluminum. It is nearly identical to the bulk Moon composition of J. W. Morgan, Jan Hertogen, and Edward Anders (1978). The core makes up 0.19 of the mass of the planet and contains 3.5 percent sulfur—a much lower estimate than other models. The volatile elements show a nearly Moon-like distribution, but, even so, there is sufficient water for at least a 9-m layer, and there may be up to 11 times more. Comparison of calculated bulk compositions for five differentiated planets (Earth, Venus, Mars, Moon, and the eucrite parent body) suggests that, for these at least, volatile depletion correlates more with size than with radial distance from the Sun.

ANALYSIS OF WATER

Ion chromatography

An ion-chromatographic technique for the determination of seven major anions in rain and in surface water was evaluated by M. J. Fishman and G. S. Pyen (1979). Analysis of a single sample involving simultaneous determination of bromide, chloride, fluoride, nitrate, nitrite, orthophosphate, and sulfate requires approximately 20 min. Minimum detection limits range from 0.01 mg/L for fluoride to 0.20 mg/L for chloride and sulfate. The relative standard deviations of the determinations were found to be less than 9 percent for all anions except nitrite in Standard Reference Water Samples. To determine the accuracy of the results, several samples were spiked with known amounts of each constituent and reanalyzed; recoveries ranged from 95 to 104 percent. Chloride, nitrate, nitrite, orthophosphate, and sulfate concentrations in several samples also were determined independently by automated colorimetric procedures, and fluoride concentrations were determined by an automated ion-selective electrode method. The results obtained were in generally acceptable agreement with results obtained by ion chromatography.

Automated colorimetric determination of bromide ions

G. S. Pyen, M. J. Fishman, and A. G. Hedley adapted the rapid, sensitive, and accurate indirect method for determination of bromide in natural waters (Fishman and Skougstad, 1963) to a completely automated system. The method is based on the catalytic effect of bromide on oxidation of iodine to iodate by potassium permanganate in sulfuric acid solution. Twenty samples per hour can be analyzed to levels as low as 0.01 mg/L bromide. Analysis of samples containing known added amounts of bromide gave values ranging from 94 to 110 percent of the concentration calculated to be present. Bromide in several samples was determined independently by a similar manual method; the observed correlation coefficient was 0.98.

Adenosine triphosphate in aquatic samples

D. W. Stephens evaluated several procedures for extracting adenosine triphosphate (ATP) from a variety of aquatic samples and determined that a cold sulfuric-oxalic acid procedure was best suited to water samples, sediments, and periphyton from substrates. However, due to cation and fulvic acid interferences, a spike with a known quantity of ATP is necessary to estimate losses when extracting sediments. Variations in colonization densities for periphyton require that several replicates

be extracted to characterize accurately a periphyton community. An extraction method was developed for periphyton that involves three replicate extractions of four 4-mm-diameter subsamples of a periphyton strip. The observed error (95-percent confidence interval) was ±10 percent at 200 ng/cm², with a coefficient of variation of 15 percent.

Organic compounds in bed sediment

A synoptic survey was undertaken by W. E. Pereira and T. R. Steinheimer of an area impacted by heavy industrial activity to determine the occurrence and environmental significance of organic compounds adsorbed on bed sediment. Extraction was effected on a Soxhlet apparatus using a freeze-dried sample. The organic extract was fractionated using silica gel microcolumn adsorption chromatography. Separation and identification of the organic compounds was accomplished by capillary gas-chromatography–mass-spectrometry techniques. More than 50 different compounds were tentatively identified, including saturated hydrocarbons, olefins, aromatic hydrocarbons, alkylated polycyclic aromatic hydrocarbons, and oxygenated compounds, such as aldehydes and ketones.

Pesticide partition between sediment and water

M. C. Goldberg evaluated two calculation methods for determining partition of pesticide materials between suspended sediment and water in environmental systems. The equations relate suspended-sediment surface area, pesticide concentration on the sediment, and pesticide concentration in the water. The first, a linear equation, proved sufficiently accurate to calculate 45 of 49 data points to within one order of magnitude of the observed values. The second, a 7th degree polynominal, was tested on the same data set and resulted in calculation of 46 of 49 values to within one order of magnitude. Comparisons as to relative accuracy within the order of magnitude agreement revealed that the linear equation was capable of reproducing the observed values to within 10 percent for 39 percent of the data set tested and that the 7th degree polynominal was capable of achieving this accuracy for 52 percent of the same data set. The correlation of surface area with pesticide partitioning demonstrates the use of a readily measurable parameter (sediment surface area) to permit calculation of a nonmeasurable parameter (pesticide concentration in water). Thus, it becomes possible to calculate the approximate concentration of a pesticide in water at levels of concentration below the measurable limits of present-day analytical techniques.

Methylation of humic and fulvic acids

R. L. Wershaw and D. J. Pinckney developed an improved two-step procedure for the methylation of acidic and phenolic groups in humic and fulvic acids. In the first step, the sample is dissolved in dimethyl formamide (DMF), and acid groups are methylated with diazomethane. The second step involves reaction with methyl iodide and sodium hydride in DMF and extraction into methylene chloride. Examination of the infrared spectra of samples methylated by this procedure showed no residual hydroxyl groups remaining after the second step. This is an improvement over previously used procedures because methylation of all hydroxyl groups is assured.

GEOLOGY AND HYDROLOGY APPLIED TO HAZARD ASSESSMENT AND ENVIRONMENT

EARTHQUAKE STUDIES

SEISMICITY

Operations and special investigations

NEIS continues to serve as a focus for seismological information from an international group of cooperating seismic observatories. NEIS provides three principal services to a wide variety of users in the scientific, governmental, private, and public sectors, according to E. P. Arnold. These services are determination of earthquake parameters, primarily hypocenters, which are used as a data base for a substantial part of all research in seismology; performance of a clearinghouse function for general information about earthquake phenomena; and provision of early information on location, magnitude, and relevance of all large and damaging earthquakes to disaster relief agencies, scientists, and the public. Data-gathering projects include U.S. Seismic Network, Seismic Observatories, Northeast Seismic Network, United States Earthquakes, Seismic Research Observatories, ARPA Seismic Data Analysis, and Glen Canyon Dam.

C. W. Stover reports that 116 earthquakes in 20 States were investigated during fiscal year 1979, using questionnaires and field studies to collect felt and (or) damage data. The data will be published in book and map form, describing the effects to the community, and as a quarterly circular "Earthquakes in the United States," showing the geographical extent of the effects. The circular also will contain hypocenters, magnitudes, and intensities.

The largest earthquake ($M_s = 7.2$) to occur in the United States during fiscal year 1979 was the February 28 event in southeastern Alaska at lat 60°38.57′ N., long 141°35.04′ W. It occurred in the same area as M = 8.3 and M = 8.6 earthquakes in 1899 and just north of a M = 7.9 earthquake in 1958. No major damage resulted from the 1979 earthquake, which had a maximum intensity VII (Modified Mercalli Intensity Scale), at Icy Bay.

Work by J. W. Dewey and W. J. Spence shows that the aftershock sequences of the great Peru earthquakes of 1966 ($M_s = 7.75$–8), 1970 ($M_s = 7.8$), and 1974 ($M_s = 7.8$) all occurred in two or more spatial clusters. The aftershock clusters that were spatially removed from the 1970 and 1974 main shocks were characterized by focal mechanisms that were distinct from the corresponding main shock focal mechanisms. One explanation for this disparity is that the events in the subsidiary clusters were triggered by the respective main shocks and did not represent a complex form of the main shock rupture.

A synthesis of published information about the tectonics of western Peru and northern Chile indicates that horizontal compressive east-west stress exists in the Nazca plate and across the Peru-Chile trench into the South American plate. This condition may reflect a present-day coupling between the Nazca and South American plates.

Preliminary analysis by F. G. Fischer and J. R. Pelton has disclosed hypocentral trends in the Garm Source Mechanism Studies. Approximately 150 local earthquakes recorded on Develocorder film in Garm, U.S.S.R., since 1975 were picked and then located using a BASIC version of the location program HYPOINVERSE run on an HP 9845 computer in Garm. This data set provided basic information on the nature of seismicity within the USGS Peter I Range array and established a basis for spectral and source-mechanism studies. Preliminary analysis of the seismicity pattern for the well-located events of the data set indicated that (1) shallow events (0–10 km) are scattered within a northeast-trending zone roughly corresponding to the crest of the Peter I Range, (2) deeper events (10–30 km) are confined to an area located just south and southeast of the crest of the Peter I Range, and (3) a clear gradation from shallow to deep events exists in the northwest-southeast cross section.

J. W. Dewey has redetermined hypocenters of eastern United States earthquakes. One hundred and forty-seven hypocenters of seismic events that occurred in the Eastern United States and adjacent Canada have been redetermined. Forty-four percent of these shocks have 90-percent confidence ellipses on their epicentral coordinates that are less than 10 km in length, and 76 percent of the shocks have 90-percent confidence ellipses on their epicentral coordinates that are less than 20 km in length. Data from 23 seismic events whose locations are known independently of the traveltime data indicate, however, that there is some location error not accounted for by the confidence ellipses. Only 70 percent of the nominally 90-percent confidence ellipses cover the

independently known epicenters of the 23 events. For some regions, there is about a 5-km location bias apparently caused by lateral variations of velocity that are not accounted for in the location procedure.

The use of subsidiary phases and regional velocity models significantly improves accuracy of computed focal depths of earthquakes. Most computed hypocenters lie in the uppermost 10 km of the Earth's crust. Excluding earthquakes from the province of Quebec, of the 71 earthquakes whose focal depths are estimated to be accurate to 20 km at a 90-percent level of confidence, 89 percent occurred in the upper 10 km of the Earth's crust. Of the 12 Quebec earthquakes whose focal depths are estimated to be accurate to 20 km at a 90-percent level of confidence, however, 50 percent occurred in the depth range of 10 to 20 km.

The Albuquerque Seismological Laboratory (ASL) continued to provide technical and logistical support for the Worldwide Standardized Seismograph Network (WWSSN). The WWSSN was started in 1961, and ultimately 116 stations of identical instrumentation were installed, of which 106 are still operational. The data are photographically recorded, forwarded periodically to the USGS for quality control, and then sent to the Environmental Data and Information Service (NOAA) in Boulder, Colo., for film reduction. Copies of the records are made available to researchers at a moderate cost. In addition, the ASL provides technical advice and assistance to the USGS and to cooperating observatories, as well as providing engineering support, equipment replacement, calibration, repair services, and operational supplies.

The Albuquerque Seismological Observatory, run by ASL, is a continuing project that provides data to scientists from the following instrumental systems: (1) WWSSN, (2) SRO, (3) Wood-Anderson System, (4) Lo-Gain LP system, (5) New Mexico Tech LP system, and (6) New Mexico statewide system.

ASL Systems Engineering supports seismic instrumentation at the ASL, the Branch of Global Seismology, and other USGS branches. The objective of the program is to develop the best seismic instrumentation possible using the latest electronic industry components with the lowest system cost. The use of low-cost microprocessors in new seismic systems provides flexible functional systems at approximately 60 to 90 percent of the cost of conventional electronic systems.

According to H. M. Butler, 12 seismic research observatories (SRO), abbreviated seismic research observatories (ASRO), and 3 high-gain long-period (HGLP) systems are operational. An in-depth analysis of the SRO data system by J. R. Peterson resulted in the development of new techniques for evaluating seismograph systems and provided a more accurate and comprehensive understanding of the potentials and limitations of the SRO network.

Equipment for the Digital World-Wide Standardized Seismograph Network (DWWSSN) has been purchased, and some systems assembled. The first of these systems will be installed soon. The Global Digital Network will provide improved geographical coverage, using highly sensitive short- and long-period seismic sensors with analog and digital magnetic tape recordings.

The Digital Network Data Processing System provides digital seismic data from a global network on magnetic tape in a convenient format ready for computer analysis. The tape is edited, corrected where possible, and forwarded to the user with complete calibration data.

Seismic network studies

Seismic observatories are located at Newport, Wash., Cayey, Puerto Rico, Agana, Guam, and Adak, Alaska. H. S. Whitcomb coordinates the operations of these observatories. They provide data that are used to describe the occurrence of earthquakes and their effects on lives and property, to monitor and record vibrations in the Earth caused by earthquakes and large manmade disturbances, and to update regional and world charts and maps. The observatories at Guam and Newport provide input on a 24-h basis to the Tsunami Warning Service operated by NOAA in Honolulu.

J. W. Taggart reports that a seismic station at the South Pole was operated throughout fiscal year 1979 by two part-time observers from the Topographic Division of the USGS. The observers serviced and maintained the seismic station and measured phase arrival times, periods, and amplitudes of recorded earthquakes. These data were reported on a timely basis by radiotelegraph to NEIS in Golden, Colo.

According to M. A. Carlson, data from Glen Canyon Dam have been compiled and interpreted, and local earthquakes have been located in the vicinity of the dam and reservoir. The data are used to determine whether changes in water level in the reservoir produce detectable influences on seismicity. Thus far, seismicity patterns have not been established because of limited data gathered to date.

W. J. Spence reports that the Denver Water Department, through a high-quality microearthquake monitoring network, has located two zones of microearthquake activity at midcrustal depth beneath the region of the proposed Strontia Springs reservoir.

According to L. H. Jaksha, results of a detailed study of an earthquake sequence near the Albuquerque volcanoes suggest that this still-active zone is located about 3 km west of the fissure through which the volcanoes erupted. About 300 earthquakes have been

observed. They range in magnitude from negative values to about 2.5 (Mc). The average focal depth is 9.5 km. According to fault plane solutions, the events occur along a high-angle normal fault downthrown to the west. The fault strikes N. 5° E., in good agreement with the fissure of the volcanoes. These earthquakes appear to be structurally related to the volcanoes, but the details of the relation are unclear.

Seismic data bases

W. H. K. Lee has maintained and updated a bibliographic data base and retrieval system for current earthquake literature. Bimonthly indexes of current earthquake literature were distributed. A modern seismic data processing system for visual seismograms was built using surplus components primarily. The system is capable of processing seismograms in any existing format at a rate several times faster than that of previous techniques.

SEISMOLOGY

Central California

A. G. Lindh, using an adaptation of the crustal model of Eaton, O'Neill, and Murdock (1970), relocated earthquakes from 1969 to 1976 within 30 km north and south of the epicenter of the 1966 Parkfield, Calif., earthquake. South of the epicenter, but within the zone that broke in 1966 (also within the zone in which the creep rate decreased to the south from 3 cm/yr to <1 cm/yr), Lindh reported that the pattern of earthquakes was dominated by small clusters of activity outlining the 1966 rupture, similar to the aftershock pattern of that earthquake. The b slope of $-0.8\ (\pm 0.15)$ for these earthquakes compared very favorably with a value of -0.85 for 1966 aftershocks along the same stretch. Lindh found that, north of the 1966 epicenter where the plate motion is dominated by aseismic slip of 2 to 3 cm/yr, there is a shallow diffuse pattern of seismicity dominated by small events ($b = -1.25 \pm 0.15$). Thus, high $-b$ values at Parkfield seem to be associated with regions dominated by aseismic slip, and low $-b$ values with regions dominated by periodic large earthquakes and seismic slip. Near the 1966 epicenter, at the boundary between these regions, two events of approximately $M = 4.5$ occurred in 1975 near the bottom edge of the seismic zone (10–15 km). Lindh concluded that this may be the hypocentral region of the next Parkfield earthquake.

J. P. Eaton has studied Pn velocities (velocities of seismic waves in the uppermost mantle) beneath the central California network by using a modified time-term method applied to about 20 moderate ($M = 4+$) local and regional earthquakes. He found a velocity contrast of approximately 0.15 km/s across a line that cuts the net longitudinally (the San Andreas fault south of Hollister and the Calaveras, Hayward, Healdsburg, and Maacama faults north of Hollister). The Pn velocity averages about 8.10 km/s west of this line and 7.95 km/s east of this line. Pn time terms increase systematically by about 1 s across the Coast Ranges from the coastline to the western edge of the Great Valley.

W. H. Bakun reported that the correlation between the seismicity and discontinuities or bends in the mapped fault trace is the basis for an extension and refinement of the "stuck" and "creeping" patch model of the San Andreas fault in central California (Bakun and McEvilly, 1979). Patch boundaries extend from the free surface down through the seismogenic zone. Creeping patches lie beneath smooth continuous segments of the fault trace. Stuck patches lie beneath discontinuities or bends in the fault trace. Bakun related the geometrical arrangement of the segments to controlling the location and sequence of earthquakes.

High-precision hypocenter solutions for earthquakes occurring in the Dry Lake, Calif., region have conclusively demonstrated that the seismogenic expression of the San Andreas fault is coincident with the mapped zone of recent movement, according to W. L. Ellsworth and B. L. Moths. They reported that the fault zone is characterized by both a relatively low compressional wave velocity and a strong attenuation of compressional and shear waves. However, it is not yet clear whether these properties are genetically related to the fault itself or to thick sedimentary sequences that abut the fault zone in this region. Shear velocities within the uppermost 2 km of the section were found to be anomalously low, locally reaching only 40 percent of the compressional velocity. More normal values of Poisson's ratio were suggested below about 2 km depth.

C. G. Bufe and W. H. Bakun (USGS) and T. V. McEvilly (University of California, Berkeley) examined historic seismic activity in relation to the 1979 Coyote Lake, Calif., earthquake sequence. They reported that four earthquakes (1911, 1949, 1955, and 1979) with $M_L > 5$ have occurred on the southern half of the Calaveras fault system since 1910. S (secondary) and P (primary) time intervals at Mount Hamilton and Berkeley were sufficient to locate aftershocks of the 1911 shock if the epicenters were constrained to the trace of the Calaveras fault. Published S-P time intervals imply a 20-km-long aftershock zone for the 1911 shock from near Mount Hamilton southeast to the epicenter of the August 6, 1979, $M_L = 5.9$ Coyote Lake main shock. The similar lengths of the 1911 and 1979 aftershock zones and the similarity of the felt reports

suggested that the 1911 and 1979 shocks were comparable events on abutting sections of the Calaveras fault. The $M_L = 5.2$ shock of 1949 was located on the southeastern part of the 1979 Coyote Lake aftershock zone. The 1955 $M_L = 5.5$ shock occurred about 10 km northwest of Mount Hamilton. Activity on the Calaveras fault in the 12 mo preceding the 1979 Coyote Lake earthquake was concentrated southeast of the 1955 shock, near the inferred northwest end of the 1911 aftershock zone.

Coast Ranges

C. G. Bufe, S. M. Marks, W. P. Irwin, and D. H. Warren studied the seismicity of the Coast Ranges north of San Francisco, Calif., from 1969 to 1978. During these years, seismographic coverage of this area (lat 38°–40° N.) increased from 2 relatively low-gain stations to more than 50 high-gain telemetered stations. Seismicity has been episodic, with peaks of activity in late 1969, late 1973, and late 1977 to early 1978. P-wave first motions indicate regional tectonic stress oriented with maximum compression N. 20° E. and minimum compression N. 70° W. Two broad linear zones of microearthquakes traverse the region. A western zone trends N. 28° W., following the Hayward–Rodgers Creek–Maacama–Talmage fault system in an en echelon pattern interrupted for 50 km between Richmond and Petaluma by an aseismic gap. An eastern zone trends N. 20° W. along the Concord–Green Valley fault system and continues for at least 40 km northwest of Lake Berryessa. Both zones are offset or deflected near lat 38°05′ N. and 30°35′ N. Between the linear zones, the pattern of earthquakes is diffuse, with microearthquakes most concentrated in the developed portion of The Geysers steam field and the young Clear Lake Volcanics but nearly absent in the older Sonoma Volcanics. Focal depths range from exclusively shallow (0–5 km) in The Geysers–Clear Lake geothermal area to unusually deep (15–22 km) near Antioch. The western Coast Ranges, including the historically active San Andreas fault, which trends N. 38° W. along the coast north of San Francisco, are relatively aseismic at present.

Southern California

One of the major goals of the USGS in southern California is to characterize background seismicity patterns so that variations might be recognized when they occur. C. E. Johnson has described the difficulty of this task by contrasting two earthquake sequences occurring 3 mo apart and separated by about 40 km. The first was the Homestead Valley sequence beginning on March 15, 1979, with a maximum $M_L = 5.2$, followed by more than 3,000 locatable aftershocks during the following 2 mo with a b value of 1.12. The second sequence, Big Bear, began on June 29,1979, comprising 30 events over a 2-d period with a peak $M_L = 4.9$ and an overall b value of 0.34. Johnson found the differences between these two sequences that were so close in space and time to be of particular interest. The principal difference between these two sequences in terms of tectonic setting appears to be related to depth. For the Homestead Valley sequence, nearly all events are shallower than about 3 km, while, for the Big Bear sequence, all are deeper than about 9 km. This difference would not have been apparent were it not for the presence of a dense portion of the Southern California Seismic Network in the immediate vicinity.

One of the most valuable results to emerge from studies in the Imperial Valley was a deterministic model capable of explaining both short- and long-term aspects of Imperial Valley seismicity (Johnson, 1979). Following the theoretical work of Rice and Simons (1976), Johnson related the progressive onset of earthquake clusters along the trend of several main faults to the propagation of episodic creep at depth. The clusters illuminated a planar hypocentral distribution developing from a point of initiation on a main fault. The most likely interpretation for individual clusters is that they are associated with either the formation or rejuvenation of a single fracture. If this interpretation is correct, it is a likely explanation for the maintenance of porosity in the presence of highly indurating geothermal brines and should prove critical in understanding the dynamics of geothermal systems in the Imperial Valley, as well as other tectonic environments.

Field work on a detailed seismological study of the Imperial Valley was completed by W. D. Mooney. Analysis of the data revealed a complex velocity structure in the thick sedimentary blanket overlying basement rocks. A velocity gradient in the sediments and a velocity contrast between the sediments and basement give rise to high amplitude multiples in the recorded seismograms. The velocity structure that has been determined and the identification of the multiples allow for more precise determinations of earthquake locations and more accurate predictions of ground-motion hazards.

Hawaii

Research by E. T. Endo showed that a recently discovered zone of cracks on the southeast slope of Mauna Loa confirmed right-lateral strike-slip faulting suggested by seismic data. The zone lies at 1610-m elevation and is approximately 8 km northwest of a topographically prominent but inactive step fault that strikes N. 43° E. Mapping done at a scale of 1:900 clearly showed a system of east-west tension fissures connected by north-south popups. Crack topography and

the lack of shear failure along tension fissures suggested initial Mode I displacements and then Mode II displacements. The largest measured displacement is 80 cm. The mapped cracks formed a zone of en echelon tension fissures. The offset to the left was consistent with right-lateral shear suggested by focal mechanism studies of a 1974 M=5.5 earthquake that was located less than 2 km north of the mapped crack zone. The cracks are located in the aftershock region of the earthquake that was nearly equidistant between the two active volcanoes Mauna Loa and Kilauea. Inferred maximum (compression) axes for the mainshock and aftershocks have azimuths that are parallel to a line joining the 1974 inflation centers of the two volcanoes.

Induced seismicity

Impoundment of Monticello Reservoir, S.C., in December 1977 resulted in the triggering of numerous shallow earthquakes. To study the mechanical processes responsible for the events, measurements of the state of in situ stress, pore pressure and permeability, and the distribution of natural fractures and joints were made in two 1-km-deep wells drilled into clusters of activity. Analysis of these data by Mark Zoback showed that the small increase in subsurface pore pressure due to reservoir impoundment (approximately 5 bars) was sufficient to trigger near-surface earthquakes. The earthquakes apparently occur in finite zones where relatively high horizontal stresses cause thrust-type motion on well-oriented fracture and joint planes. Because the vertical lithostatic stress increases more rapidly than the horizontal stresses, these events are apparently limited to depths less than several hundred meters. This is in good agreement with seismic data that indicated that nearly all events occur at depths <0.5 km.

Data analysis

G. L. Choy has been studying body-wave analysis of rupture characteristics of earthquakes. He found that the stability and high quality of the SRO digital data preserved the high-frequency spectral-phase information that is necessary for the accurate measurement of pulse characteristics. Using body-wave data from the small number of available SRO recordings, Choy was able to detect some variation of wave forms around the focal sphere for three deep earthquakes. This enabled him to constrain the rupture geometry and to obtain some source parameters for the earthquakes. He used this approach, in a preliminary analysis of body waves generated by a shallow-focus earthquake, to determine that the St. Elias, Alaska, earthquake consisted of three subevents.

J. B. Fletcher has been using spectral- and time-domain analysis to study near-field recordings of earthquakes. Analysis of about 30 high-dynamic-range digital recordings of earthquakes at Oroville, Calif., according to the Brune source model, suggested that stress drops increase with depth and magnitude. The ratio of the P-to S-wave corner frequency (about 1.7) is in agreement with a set of dynamic source models but not with the more popular kinematic models.

According to Fletcher, preliminary analysis of seismograms from South Carolina suggested that, for even very small events ($M_L \approx 0$), a degree of directivity is apparent in the corner frequencies (ranging from about 10–40 Hz for a single event). The direction of propagation is away from the reservoir. The depths of events are extremely shallow, most at less than 2 km.

S. W. Steward and M. E. O'Neill have devised a practical and fairly simple method to determine the frequency-amplitude response characteristics of the seismograph systems that are used in the central California short-period seismic telemetry network. Each system consists of the following main components: (1) the seismometer, (2) the field amplifier and signal modulator, (3) the demodulator located at the central recording site, and (4) the recording device. Response curves for each of these components are determined individually, either from theoretical considerations or from laboratory calibration. Each response curve can be represented by an appropriate number of poles in the complex frequency plane. The magnification response for the complete seismograph system is then found by complex multiplication, in the frequency domain, of the representation by poles of the frequency response of the individual system components. Peak magnification of the seismograph system typically is slightly greater than 1 million.

During fiscal year 1979, continued refinements have been made by W. H. K. Lee in inversion of P-wave arrival times recorded by microearthquake networks and in seismic ray tracing of heterogeneous medium. In particular, the seismic ray-tracing problem has been solved using both initial- and boundary-value approaches.

In addition, a draft of an invited review paper on principles and application of microearthquake networks was completed by Lee. This paper has 9 chapters and treats the subject thoroughly, reviewing over 1,500 published articles.

The initial processing design of the minicomputer system was revised extensively by P. R. Stevenson, and routine processing of central California earthquakes has begun. One of the key elements, the SELECT program, which selects the stations to be digitized, was completely rewritten. The History File/Dub Control File/SELECT portion of the system is operational. A dub verification

program was written that compares dub library files with dub requests and detects discrepancies. A seismic trace plotting program was written to plot data on the Varian plotter. Seismic trace files from the earthquake processing system provide the input data. Two Eclipse minicomputers were connected by installing an Inter-Processor Bus. This allows greater flexibility in the two Central Processing Units accessing the 92 Mb disk. All dubbing is done on a third Eclipse.

EARTHQUAKE PRECURSORS

Seismicity

D. H. Harlow, in his study of the seismicity of Central America has reported a seismic gap near Nicaragua. Analysis of data from a high-gain seismograph network that has been operating in Nicaragua since April 1975 revealed a 5,750-km^2 area of low seismic activity at shallow depth on the subduction zone near western Nicaragua. No large earthquake has originated from the vicinity of the quiet zone since 1898 ($M_L = 7.9$), and teleseismic data indicate that the quiet zone has existed for at least 28 yr. The frequency of small- and moderate-sized earthquakes along the edges of the quiescent area has been increasing during the last 4 yr. Because these results are similar to observed patterns of seismic activity that are precursory to large earthquakes, the potential for a large earthquake in the quiet area appears high. The magnitude of an earthquake rupturing the entire quiescent area is estimated to be 7.8 ± 0.3. It is not yet possible, however, to predict the exact time of such an earthquake.

The Hawaiian seismic studies project gathers, analyzes, distributes, and archives high-quality earthquake data from Kilauea crater and the island of Hawaii. The data are essential for monitoring the crater and for collecting a data base for particular studies, such as determining precursors to the 1975 Kalapana earthquake. F. W. Klein reports that several precursors have been found: (1) a delay in teleseismic P waves, (2) a decrease in seismicity, (3) a rotation of stress orientation derived from earthquake focal mechanisms, and (4) a change from geodetic strain accumulation to strain release.

Using teleseismic data, J. W. Dewey, E. R. Engdahl, and W. J. Spence (USGS) and Selema Billington (Cooperative Institute for Research in Environmental Sciences) tested the characteristics of seismicity prior to two large earthquakes, the Peruvian earthquake of October 3, 1974 ($M_S = 7.8$), and the Adak, Alaska, earthquake of November 4, 1977 ($M_S = 6.7$), against characteristics of prior seismicity recognized in other studies. They have come to the following conclusions:

- The Peru and Adak data provide additional support for the widely accepted seismic gap hypothesis.
- Both the Peru and the Adak data show increased seismicity near the main-shock source region during an extended period before the main shock. In both cases, there were at least several distinct sources of prior seismicity in the vicinity of the main-shock rupture surface, suggesting that critical stresses were being approached throughout an area of at least a few tens of kilometers in extent.
- In neither case was there evidence for a short-term increase of seismicity throughout a broad region larger than the source dimensions of the subsequent main shock.
- In neither case was there a dramatic increase in short-term seismic activity from the immediate vicinity of the source region of the main shock.
- Relocation of teleseismically recorded earthquakes relative to a "calibration event" recorded by a local network of seismographs was important to each study to demonstrate that the source region of each shock had not ruptured in earthquakes over a period of time necessary to accumulate sufficient elastic strain for a sizeable earthquake and to demonstrate that prior seismicity occurred very near, but just outside, the aftershock zone of the main shock.

Theoretical mechanics of earthquake precursors

Theoretical analysis of two-dimensional models of interacting faults by W. D. Stuart and G. M. Mavko suggested that fault slip depends on both the regional stress and the slip history on nearby fault segments. In one model, the fault stress was assumed to obey a pressure dependent "friction" law. When slip softening was used to simulate larger earthquakes, an increase in regional stress induced fault-slip changes that were partially consistent with observed creep records. In a second model, fault slip was imposed as a boundary condition, with slip assumed to be a function of the number (not moment) of small nearby earthquakes. Some past earthquakes were successfully anticipated by earlier computed stress changes, and observed geodetic line length changes were partially consistent with computed changes.

Crustal strain

Geodetic tilt measurements were analyzed by J. C. Savage, W. H. Prescott, and, Michael Lisowski. Changes in tilt were measured by annual or semiannual spirit level surveys of small-aperture (40–400 m) bench mark arrays located at borehole tiltmeter sites along the

San Andreas fault in California. Because there are six or more bench marks in most arrays, the tilt is overdetermined, and realistic estimates of uncertainties can be made. The large arrays (aperture 300 m) afford a precision (two standard deviations) of about 3 μrad in measuring tilt, and the measured tilt remains constant to within ± 5 μrad over periods of up to 5 yr. The small arrays (aperture < 100m) afford a precision of about 6 μrad in measuring tilt, but the measured tilt exhibits a high variability significant even at that level of precision. The lower precision of the small arrays is primarily a consequence of minor bench mark instabilities and local short-wavelength elevation disturbances (rms variability of perhaps of 0.25 mm), but the high variability of tilt measured by the small arrays appears to be a product of local intermediate-wavelength (50–300 m) elevation disturbances rather than true tectonic tilting. These results imply that tectonic tilt at the surface can be measured only by very long baseline measurement.

Line length changes measured across the Hollister multiwavelength distance measuring (MWDM) network were analyzed by A. F. McGarr to determine lower bounds on average fault slip across the Calaveras fault and to estimate average strain changes within the network. Four episodes of deformation that are convincingly identifiable in the MWDM data for the year following September 1975 can be modeled as right-lateral slip on the Calaveras fault and can be correlated with data from creepmeters within the network. Lower bounds on the moment for each episode of slip were calculated, and the results indicate that aseismic slip is the dominant mechanism of strain release in the Hollister area. The combined moment of 1.2×10^{24} dyne-cm for the four episodes far exceeds the moments of earthquakes during the same time period. Creepmeter data taken in conjunction with the lower bound of the moment indicate that the aseismic slip extends well below the seismogenic zone.

Creep measurements

W. D. Stuart studied precursory creep retardation in central California. Creep rate at the SHR 1 instrument, which spans the Calaveras fault near the south end of the aftershock zone, was nearly zero for 3 yr before the Coyote Lake, Calif., earthquake (August 1979, M = 5.9). Before 1976, the average creep rate was about 11 mm/yr. During the year before the earthquake, the creep rate showed a slight increase, as did the nearby seismicity. The creep retardation appears to be another example of the precursory retardation noticed earlier by R. O. Burford.

Tilt observations

C. E. Mortensen reported that a tilt anomaly has been observed preceding a pair of earthquakes ($M_L = 4.2$, origin time 0014 G.m.t., and $M_L = 3.9$, origin time 0018 G.m.t., both on August 29, 1980, on the Calaveras fault near San Jose, Calif. (Iwatsubo and Mortensen, 1979). These earthquakes occurred at hypocentral depths of 5.5 and 6.0 km, respectively, and are located 6.0 and 4.5 km northwest of the Mount Hamilton, Calif., tiltmeter site (MTH). The anomaly is similar in shape and time scale to signals observed on other tiltmeters at the times of recorded surface creep events (Mortensen and others, 1977). The anomalous behavior began approximately 63 h before the earthquake pair and consisted of gradual down-to-the-east tilting followed by rapid down-to-the-north-northeast tilting at a rate of 0.5 μrad/h. This was succeeded by 1 h of rapid down-to-the-east tilting amounting to 1.5 μrad. The maximum peak tilt of 8.6 μrad down-to-the-northeast was followed by gradually decelerating tilting down-to-the-southwest constituting partial recovery. An anomaly of nearly identical form, but smaller in amplitude and duration, preceded a $M_L = 2.5$ aftershock on September 5, 1978. Other creep-eventlike signals have occurred preceding local earthquakes near the MTH tiltmeter site; however, other nearby earthquakes as large as $M_L = 4.7$ have occurred without accompanying creep-eventlike signals. A similar, but much smaller (0.74 μrad), creep-eventlike signal preceded a $M_L = 3.5$ earthquake with an epicenter 2.3 km east of the Black Mountain, Calif., tiltmeter site. However, short-term tilt anomalies such as these are not generally observed to precede local earthquakes within the central California tiltmeter network.

Gravity measurements

A high-precision gravity network covering areas of known or suspected uplift in southern California, established during fall 1976, was remeasured concurrently with the Southern California Releveling Program by R. C. Jachens and C. W. Roberts during spring 1978. Relative gravity, with respect to a primary reference station located near Riverside, Calif., was measured at each station either directly or through 1 of 13 secondary reference stations. Riverside was selected for the primary reference station because it was outside the area of the 1959 to 1974 uplift. Computed standard errors associated with the measured changes in relative gravity between the two surveys averaged about 9 μGal. Assuming that gravity at the primary reference station was invariant, most of the measured gravity changes were small and probably reflected random

errors in the measurement process. The average change over the entire network was +2.5 μGal, and the magnitudes were distributed almost normally with a standard deviation of 12 μGal. Based on 30-min averages of the data, about 75 percent of the area showed changes smaller than 10 μGal. The spatial distribution of the 1976 to 1978 apparent gravity changes showed no correlation with the form of the 1959 to 1974 southern California uplift, as illustrated by the following comparisons:

Uplift, 1959–74	Gravity change, 1976–78
>30 cm	+2.4 μGal
15–30 cm	+6.6 μGal
<15 cm	+2.1 μGal

The gravity results imply elevation changes of at most, only a few centimeters and suggest that the collapse of the uplift that began in 1974 did not continue during the interval between the gravity surveys. Limited repeat leveling data covering roughly the same period as the gravity data also revealed changes of only a few centimeters.

Magnetic studies

Magnetic field changes of about 10 gamma have been observed by M. J. Johnston near the San Jacinto–San Andreas faults. These changes appear to have been associated with the partial collapse of the southern California uplift between 1974 and 1976. Since this time, the magnetic field change has decreased by about 5 gamma. Leveling data obtained during this time indicated an increase in elevation in that area.

Another facet of Johnston's work included gathering paleomagnetic data in New Zealand. These data indicated an absence of deformation in the Fiordland area at a distance greater than 15 km from the Alpine fault. The implication of this study is that shear deformation is concentrated in a narrow zone near the fault.

According to Johnston, the records from a magnetometer located less than 15 km from the hypocenter of the August 6, 1979, Coyote Lake, Calif., earthquake indicated that no observable magnetic field precursors occurred. Simple tectonomagnetic models show that this instrument, although within one source dimension of the earthquake, was installed at a point of near-minimum expected change.

Radon variations

According to Chi-Yu King, radon content of subsurface soil gas recorded in central California showed some broad-scale episodic increases of about a factor of two above long-term average levels during a period of several weeks to several months along a long but limited fault segment (approximately 100 km). These episodes occurred in different seasons and did not appear to be systematically related to changes in meteorological conditions. However, they coincided reasonably well in time and space with larger local earthquakes of magnitudes that range from 4.0 to 4.3. A radon episode of longer duration and larger spatial extent was recorded prior to a M=5.7 earthquake that occurred on August 6, 1979, near Coyote Lake, Calif. However, no significant changes were recorded at some stations that were close to the earthquake epicenter.

TECTONOPHYSICS

Paleogeodetics

Analysis of geodetic measurements and integration of Quaternary geologic data by W. R. Thatcher indicated an intimate relationship between current movements and geologic structure on the northwest margin of the southern California uplift. The 1952 earthquake slippage on the White Wolf fault and the 20th century uplift rate are closely matched by the movement history of the past approximately 1 m.y., during which deformation has been much more intense than that seen in earlier times. Results suggested the two recent geodetically measured uplifts are part of a continuing process of Transverse Range mountain building, peripheral basin subsidence, and active reverse dip-slip faulting. Comparison of the 1952 fault slippage with offsets of Quaternary marker beds indicated a recurrence interval of 200 to 400 yr for 1952-type events.

Mechanics of discontinuous faults

Geometric discontinuities in the trace of individual faults are found at many length scales and are observed in different tectonic settings and rock types. Furthermore, discontinuities appear to control the distribution of slip along faults following earthquakes and, in some cases, the distribution of seismicity along fault systems. D. D. Pollard and Paul Segall derived a two-dimensional solution for any number of nonintersecting cracks (discontinuous fault segments) arbitrarily located in a homogeneous elastic material. Crack surfaces were assumed to stick or slip according to a linear friction law. For faults comprising many segments, the ratio of slip to total fault length significantly underestimated the stress change on the fault, whereas the ratio of slip to segment length slightly overestimated the stress change. Two parallel en echelon cracks subjected to uniform remote shear stress exhibited opposite behavior for right- and left-stepping discontinuities. For right-lateral shear and left-stepping cracks with overlapping ends, normal tractions acting across the overlapped crack ends increased and inhibited sliding, whereas for

right-stepping cracks, normal tractions decreased and facilitated sliding. The mean compressive stress between right-stepping cracks decreased and promoted secondary fractures that tended to link the cracks and allowed slip to be transferred through the discontinuity. For left-stepping cracks, secondary fracturing was more restricted spatially and tended not to link the cracks until greater shear was applied. Opposite behavior resulted if the sense of shear was left lateral. Predicted distributions of surface displacements and deformation compared favorably with observations near a left step in the Coyote Creek fault and a right step in the Imperial-Brawley fault system, both in southern California. For right-lateral shear, right steps are sites of enhanced seismicity, whereas left steps store elastic strain energy and are potential sites of large earthquakes. Imperial Valley seismicity, as well as aftershocks of the 1966 Parkfield, Calif., earthquake, clusters near right steps in faults. Discontinuities in geometry may play an important role in rupture triggering and stopping and as a source of the fault heterogeneity required by source mechanism studies.

Rock friction

An apparatus was designed and constructed for measuring internal friction (Q^{-1}) of rocks directly from stress-strain hysteresis loops at seismic body-wave periods and small strain amplitudes (approximately 10^{-6}). Stress-strain loops were obtained for Westerly Granite at 0.2 Hz and for strains from 10^{-6} to 10^{-5}. A Q of 80 was determined. The shape of hysteresis loops contains information relating to the anelastic properties of the rock. B. McKavanagh and F. D. Stacey (1974) concluded from their measurement in samples of granite that the observed cusped loops represent an intrinsic nonlinear effect in the attenuation mechanisms down to 10^{-6} strain. In contrast to their result, H. P. Liu and Louis Peselnick obtained hysteresis loops with no cusps at strain from 10^{-6} to 10^{-5}.

Theoretical calculations have been carried out by Liu to show that mechanical hysteresis loop shapes for a linear anelastic solid satisfying $Q^{-1} \approx$ constant over a wide frequency range are sensitive to the cycling stress-wave form. Cusped or asymmetrical hysteresis loops are compatible with linear anelastic behavior and do not necessarily imply a nonlinear attenuation mechanism. Detailed observation of the stress time function, the hysteresis loop shapes, and an experimental determination of the creep function may provide a direct and stringent test of the linearity of rock attenuation.

J. H. Dieterich (1979) proposed a velocity-dependent friction law that explains his experimental data for velocity-controlled rock friction tests. This law, however, is not formulated in a differential or integral form. Consequently, problems may arise when this law is applied to cases where the slip velocity varies continuously with time. A differential equation reformulation of the friction law was achieved for which the law proposed by Dieterich is a special solution. Liu has found that there exists a dynamic friction coefficient μ_0 greater than the static friction μ_s, at which stable sliding is possible. When the ratio of the applied traction to the normal stress exceeds μ_0, unstable accelerating slide results. When the ratio of the applied traction to the normal stress is less than μ_0 but greater than μ_s, the result is a stable transient sliding.

Deviatoric stresses

Whether the magnitudes of deviatoric stresses in the Earth's crust and uppermost mantle are on the order of a kilobar (or somewhat greater) or 100 bars (or somewhat less) remains a major unanswered question in the geophysical community. A study done by M. K. McNutt did not provide a definitive answer to this question but did furnish further insight into the problem. For stable interiors of lithospheric plates, the upper 30 to 40 km of the Earth supports deviatoric stress in excess of a kilobar, regardless of the rheological model assumed. Near plate margins, data can be, and have been, interpreted in terms of both high- and low-stress models. The diversity in stress estimates may result from a lack of knowledge in deducing stress from various data types. It is more likely, however, that much of the difference is real, reflecting the diversity in the geologic processes shaping the Earth. For fault zones such as the San Andreas, the key to resolving the stress question lies in determining the role of water under lithospheric conditions. McNutt concluded, therefore, that the Earth's crust and uppermost mantle can support kilobars of deviatoric stress, but whether it actually does support high stress at plate boundaries may depend on the mechanical, chemical, and thermodynamic properties of water.

Rheology of rocks and minerals

S. H. Kirby summarized his studies of the rheology of rocks and minerals as follows:

- A review of the experimental strength of rocks at low to intermediate temperatures indicated that the principal factor controlling rock strength is the magnitude of the least principal stress compared to the applied stress. This discovery allows bounds to be placed on the depth of the brittle-ductile transition in the Earth (Kirby, 1980).
- In examining the rheology of water-weakened quartz, it was found that quartz exhibits a strong

anisotropy in impurity diffusion rates and that this property is apparently responsible for the strong contrasts in the rheology of single-crystal synthetic quartz with compression direction.

- While studying the plasticity of rock-forming minerals, the slip systems for $MgAl_2O_4$ spinel at temperatures below 1,000°C were determined (Kirby and Veyssiere, 1979).

Heat flow

A. H. Lachenbruch and J. H. Sass studied heat flow and stress in the San Andreas fault zone. One-hundred heat-flow measurements near the San Andreas fault indicated that, north of Cape Mendocino, heat flow is low (1.0 HFU) and that it rose over a distance of about 200 km southward, to an average of about 2.0 HFU, characteristic of the remaining 550 km of the California Coast Ranges (Lachenbruch and Sass, 1979). Heat flow was significantly lower (1.6 HFU) farther south along the 150-km fault segment that bounds the Mojave block (Lachenbruch and others, 1978). No evidence for a local heat-flow anomaly due to fault friction existed at any latitude. Thermal springs near the fault are inadequate to remove significant frictional heat; their combined discharge (excluding The Geysers and Salton Sea geothermal areas) could be supplied by approximately 5 bars of fault friction. Their study confirmed earlier results; the average (dissipative) frictional resistance in the seismogenic layer of the fault was probably less than 100 bars. The most plausible explanation, consistent with experiments on rock friction, is that average fluid pressure is superhydrostatic during fault slip. Such pressures could be a transient effect of fluid expansion caused by heating during large earthquakes or a steady-state condition of the fault. In the first case, the frictional strength and tectonic stress could be large ($\geq$1 kbar), but the seismic efficiency and apparent stress would be large also. If, as is often reported, the seismic stress drop and apparent stress are substantially less than 100 bars, then the local tectonic stress and fault strength are small (~100 bars), and steady-state superhydrostatic fluid pressure probably exists. Growth of the broad Coast Range anomaly southward from Cape Mendocino could be a transient effect of northward migration of the Triple Junction. If so, most of the resistance to plate motion may not be on the fault, but on horizontal surfaces that partially decouple the brittle seismogenic layer from more ductile lower crust in a broader interplate shear zone.

Circulation of ground water along the San Andreas fault

Mesozoic granitoid rocks adjacent to the San Andreas fault in central California have retained their radiogenic argon for the last 70 m.y. but have, generally, the highest ^{18}O and H_2O^+ contents and the lowest D contents of all granitoid rocks in California, according to J. R. O'Neil and T. C. Hanks. The geographical coincidence of the D, ^{18}O, and H_2O^+ patterns to the present trace of the San Andreas fault leave little doubt that some kind of ground-water circulation system has operated in the vicinity of the fault in central California. This water-rock interaction probably took place at temperatures less than 200°C, although its depth, extent, and timing are not resolved.

Whether it be in favor of low (less than 100 bars) frictional stresses or high (more than 1 kbar) the resolution of the stress paradox for the San Andreas fault is likely to involve water in one way or another. The geochemical evidence presented here for extensive circulation of ground water in the upper crust of tectonically active areas, specifically along the San Andreas fault, and the relatively high permeabilities for most rocks of the upper crust, recently compiled by W. F. Brace, would seem to rule out nearly lithostatic fluid pressures as an ambient condition of the upper crust. In addition, ground-water circulation, at least in principle, is an efficient mechanism for diffusing the heat-flow anomaly that arises in heat-transport calculations that are based on thermal conduction alone.

EARTHQUAKE HAZARD STUDIES

TECTONIC FRAMEWORK AND FAULT INVESTIGATIONS

Size estimates for future earthquakes

The sizes of earthquakes that an active fault can produce often are estimated from the empirical relations between fault-rupture length and earthquake magnitude, but, where faults and fault zones consist of parallel or en echelon segments, determining which segments constitute a particular fault can be difficult. Analysis of historic surface faulting by M. G. Bonilla (1979) shows that adjacent fault segments with stepover distances (the perpendicular distances between en echelon or parallel segments) of as much as 6.5 km have participated in single faulting events. For estimates of potential rupture length and earthquake size, fault segments with stepover distances of at least this amount can be considered a single fault.

Rates of tectonic deformation in Alaska

Land emergence in southeastern Alaska causes shoals to become shallower, islands to become peninsulas, and clamming areas to disappear as tide levels fail to cover them; locally, youthful marine deposits have been identified as much as 150 m above present sea level. During 1959 and 1960, the U.S. Coast and Geodetic Survey, by

comparing sea-level measurements with tidal bench mark elevations (Hicks and Shofnos, 1965), measured uplift, calculated rates of emergence, and showed that uplift was greatest in the area encompassing Cross Sound, Glacier Bay, and regions east to Lynn Canal. Uplift rates as high as 4 cm/yr were determined at Bartlett Cove in Glacier Bay. Some of this land emergence probably is related to isostatic rebound following deglaciation and some to vertical movement during faulting, especially along the Fairweather fault. To learn more about the cause of emergence, Travis Hudson, Kirk Dixon, and George Plafker remeasured selected tidal bench mark elevations in 1979.

Comparison of the 1979 data with those of 1959 and 1960 shows that the principal area of rapid emergence—the peninsula region between Glacier Bay, Icy Strait, and Lynn Canal—has risen as much as 50 cm or more since 1960. The area of uplift roughly corresponds to that determined by the 1959 to 1960 survey (Hicks and Shofnos, 1965), but the pattern of uplift since 1960 may be slightly different. Differential uplift may have taken place across Lynn Canal–Chatham Strait, and one locality of very rapid uplift (150 cm since 1960) seems indicated at Composite Island in Glacier Bay. The new data indicate that rapid land emergence continues in northern southeastern Alaska, that uplift since 1960 is large enough to be easily measured by reconnaissance techniques, and that the pattern of uplift is roughly similar to that for the period prior to 1959.

The tilt of the water surface of a large lake can be monitored to a precision of ± 4 mm, and, at Illiamna Lake, the largest in Alaska, three simultaneous measurements of lake level were made in 1966 and referenced to bedrock bench marks. S. H. Wood has reproduced these measurements to within 4 mm over 50-km separations of three recording stations in a triangular array. His results show that regional tilt in this part of the Alaskan Peninsula has been <0.08 μrad over the past 13 yr.

Saint Elias, Alaska, earthquake of 1979 and related seismic gap

The Saint Elias, Alaska, earthquake ($M_S = 7.7$) of February 28, 1979, ruptured only a fracture of the seismic gap along the complex Pacific–North American plate boundary between Yakutat Bay and Prince William Sound. To evaluate the potential for a future earthquake in the remainder of the gap, J. C. Lahr and C. D. Stephens have formulated from geologic and seismic data a kinematic model of neotectonic deformation in southern Alaska. In this model, the part of the North American plate next to the Gulf of Alaska is divided into subblocks, which are partly coupled to the Pacific plate. Based on the model, the gap-filling rupture or ruptures most likely would follow the north-dipping thrust faults of the Pamplona Zone between Icy Bay and the Aleutian megathrust. If the accumulated strain of 4 m postulated for this region were released in one earthquake involving the remainder of the gap, that earthquake could be as large as $M = 8$.

Evidence of young faulting in the northern Sacramento Valley, California

Geologic mapping of the Cenozoic volcanic and alluvial deposits of the northern Sacramento Valley by E. J. Helley, J. A. Barker, and D. S. Harwood has revealed a large-scale east-west fault zone. Named the Battle Creek–Cottonwood Creek fault zone for the two major drainages that have developed consequent to the faulting, the fault zone extends 80 km west-southwesterly from near Mount Lassen to its termination against the Coast Range thrust at the western edge of the Sacramento Valley. In its eastern part, the fault zone exhibits about 200 m of topographic expression; young volcanic rocks that both overlie the fault and are cut by it provide a basis for determining the age of faulting. On the west side of the valley, the fault displaces a series of terrace deposits. Fault movement is up to the north on the eastern side of the valley and up to the south on the western side. Large meanders along the Sacramento River at this latitude are structurally controlled by a series of plunging folds that are probably related to the faulting.

Trench exposures of young faults in southern California

Three trenches along fault scarps of the Cucamonga fault zone on the Day Canyon fan north of Fontana, Calif., exposed bouldery alluvium, according to D. M. Morton. In two of these trenches, fault features were moderately to well defined; in the third, only slight evidence of faulting was visible. The trench with the most clearly defined fault features exhibits evidence of multiple episodes of ground rupture, showing that ground rupture recurs in essentially the same position in bouldery alluvium along the Cucamonga fault. The dip of the fault in the trenches was about 40°, similar to the dip of the Cucamonga fault in bedrock and in basement-alluvium fault contacts. Lack of well-defined fault features in the third trench reemphasizes the difficulty of detecting faults in crudely bedded bouldery alluvium.

R. V. Sharp's trenching of the Coyote Creek fault in Lower Borrego Valley has been completed. Revised ages of marker lakebeds at the site, together with data on vertical displacement from an earlier trench study, permit the recurrence time for $M = 6+$ earthquakes to be estimated. In this region, the recurrence time for such earthquakes is within the range of 20 to 100 yr.

Sharp also reports that faults cut late Holocene lake sediments at several places within 5 km of Bombay Beach on the northeast shore of the Salton Sea. The

discontinuous faults lie along the southeastward projection of the closest nearby surface expression of the San Andreas fault, but they trend more northerly, and they approximately parallel an active seismic belt that traverses central Imperial Valley. Trench exposures along a linear surface feature near the north limits of the town of Bombay Beach revealed a complex shear zone about 7 m wide; the shear zone cuts highly deformed sediments that Sharp estimates to be of middle Pleistocene age. The trench data confirm that the linear surface feature is a fault, show that the town of Bombay Beach is built astride this fault, and suggest that this fault may extend northward into other faults with known late Holocene displacement. The possibility of continuity with known Holocene faulting implies that the newly found fault should be regarded as potentially active.

Fault relations near the Salton trough, southern California

Three strike-slip displacements of strata with known approximate ages have been measured at two locations on the San Jacinto fault zone. Northeast of Anza, minimum horizontal offset of between 5.7 and 8.6 km in no more than 0.73 m.y. indicates an average slip rate of at least 8 to 12 mm/yr since late Pleistocene time. More recent rates of displacement were determined from trench exposures of stratigraphic offsets on the Coyote Creek fault in the western Imperial Valley. A horizontal slip of 1.7 m, calculated from the data of Clark and others (1972) for the youngest sediment of Lake Cahuilla since its deposition 283 to 478 yr B.P., corresponds to a slip rate of between 3 and 5 mm/yr. Right-lateral offset of 10.9 measured on a buried stream channel older than 5,000 but younger than 6,800 yr yields an average slip rate of 1 to 2 mm/yr from ±400 to ±6,000 yr B.P. R. V. Sharp interprets these results as evidence that the San Jacinto fault zone was relatively aseismic from about 4000 B.C. to about A.D. 1600. He views such fluctuations in slip rate as normal for major strike-slip faults and suggests that the San Jacinto and adjacent segments of the San Andreas fault zones may alternate as the major structural feature separating the Pacific and American plates. Although it is now relatively inactive, the segment of the San Andreas fault in the northern Salton trough may have accommodated most of the plate motion within the last 400 yr.

Near-field leveling results across the Brawley and Imperial faults prior to the October 15, 1979, Imperial Valley earthquake also are reported by Sharp. Between October 1977 and January 1979, repeated leveling on 200-m-long lines across the Brawley fault showed a steplike displacement of 8 mm at Harris Road on the fault rupture associated with the January to February 1975 earthquake swarm. Although the time of displacement is unknown, it was up on the east, the same as other known Holocene displacements. The most recent releveling, in April 1979, indicated no additional vertical movement on the Brawley fault.

Leveling data for the Imperial fault at Harris Road between January and October 1977 show no displacement at the fault trace but an eastward tilt of about 48 μrad. During the next 15-mo interval, which included the late events of an October 1977 earthquake swarm, the west side of the fault rose about 5 cm relative to the datum at the east end of the line. About 60 percent of the level change appears to be vertical displacement at the known fault trace; the rest may be either a steep tilt or displacement at another suspected fault between 90 and 105 m east of the known trace. No new movement was detected in the badly cracked pavement at the known fault trace nor at the location of the suspected fault. During the interval of measurement between January and April 1979, downward tilting to the east resumed without displacement at either the known or suspected fault trace. The tilt rate during this period was about 18 μrad/mo across the survey line. Releveling in July 1979 showed no significant tilting between the ends of the line, but a 10-m-wide collapse of 1.2 cm formed just west of the fault trace.

Recent movement on the Potrero Canyon fault, Pacific Palisades area, Los Angeles

Geologic studies of the Pacific Palisades area by J. T. McGill provided new information concerning the late Quaternary history of the Potrero Canyon fault, an element of the east-trending Santa Monica fault zone, which forms part of the south boundary of the Transverse Ranges and extends through the central Los Angeles area. The Potrero Canyon fault is a north-dipping reverse fault, like other major faults in the zone, and is the probable eastward continuation of the Malibu coast fault.

The Potrero Canyon fault displaces the upper Pleistocene main (Pacific Palisades) marine terrace platform and overlying surficial deposits. At the mouth of Potrero Canyon, where the wave-cut platform is underlain by Pliocene siltstone, vertical separation of the platform is about 29 m on a vertical branch fault plus 5 m on the main fault, and total vertical shift (including fault drag adjacent to the main fault) of the platform is about 47 m. Strands of the vertical fault have been traced upward to within about 4 m of the ground surface at the top of the alluvial cover and, in 1932, reportedly were traceable to that surface. The main fault cannot be traced upward more than about 10 m in the lower part of the thick alluvial section. The age of the marine terrace deposits is estimated to be about 125,000 yr B.P. and is probably correlative with the highest eustatic late

Quaternary sea level (Bloom and others, 1974). The alluvial cover presumably was deposited during the succeeding eustactic fall of sea level, which may have lasted until about 116,000 yr B.P. (Bloom and others, 1974).

Physiographic evidence of deformation along the Potrero Canyon fault is present to the east on the upper surface of the main coastal terrace remnants or mesas between Potrero Canyon and Santa Monica Canyon. A well-defined but gentle scarp is alined for a distance of 1.2 km with the inferred trace of the vertical fault, which trends about N. 75° E. The scarp height decreases eastward from about 8 to 3 m or less and the width decreases from about 100 to 30 m. The natural slope of the scarp is about 5° to the south, whereas the general slope of the terrace surface in the vicinity is about 2° to the south.

Movement on the Potrero Canyon fault contributed significantly to uplift of the main coastal terrace. Much warping of the marine platform and most postplatform fault movement occurred during alluviation. As much as 8 m of the 34-m total vertical separation may have occurred after the alluvial cover was deposited, and possibly 2 m of that occurred after formation of the highest stream terrace but apparently before formation of lower stream terraces. If, as appears likely, 26 m of vertical separation took place between about 125,000 and 116,000 yr ago, the average rate of displacement during that period was about 3 mm/yr.

Geodetic and geologic studies related to the southern California uplift

Preliminary analysis of the 1978 general releveling of southern California by R. O. Castle indicates that, between 1974 and 1978, the southern California uplift sustained pervasive collapse characterized by a tilt to the north. Moreover, southeast of the uplift, a northward-migrating collapse within the Salton trough apparently accompanied the uplift through at least a part of its evolution. Between 1977 and 1978, the collapse showed a major reversal of tilt that was associated with locally accelerating tectonic subsidence (as much as 0.35 m between 1974 and 1978 in the area between El Centro and Ocotillo).

The northwest Santa Barbara Channel area lies near the southwest margin of the southern California uplift, generally in the same domain of north-south compressive deformation as the rest of the western Transverse Ranges. The area, currently being studied by R. F. Yerkes, is characterized by a unique bathymetric feature, the Arguello–North Channel slope, a south-facing submarine escarpment that extends more than 115 km from off Point Arguello to near Santa Barbara. Within and east of the Santa Barbara Channel, the structure is dominated by through-going east-trending reverse faults for which numerous fault-plane solutions indicate reverse to reverse-left-oblique slip. West of the Santa Barbara Channel, recognized faults are northwest-trending landward-dipping reverse, for which sparse but widespread evidence suggests nearly pure left slip. One of the reverse faults has been traced almost continuously for more than 140 km from west of Point Conception to beyond Ventura on the basis of mapped structure, seismic profiles, and its sea-floor expression as the Arguello–North Channel slope. That feature is interpreted to be a fault-line scarp dating from before 16,000 yr B.P. when its crest had been planed to a horizontal surface during a low stand of the sea level at −100 m. The crest since has been arched about 46 m in the Point Conception–Gaviota area, where it is cut by the South Santa Ynez fault. West of Point Conception, the North Channel reverse fault appears to merge with or override a series of imbricate reverse or thrust faults; northwest of Point Arguello, the escarpment trends toward the offshore Lompoc fault, an east-dipping reverse fault exposed at the sea floor. The 1927 (M = 7.3) earthquake was probably located either on the Lompoc fault or on a similar reverse fault 10 km to the south that offsets the sea floor. The western Santa Barbara Channel earthquake of December 21, 1812 (M = 7–7.5), was probably on a fault along the Arguello–North Channel slope.

The Point Conception–Gaviota area and its offshore bench are underlain by shallow landward-dipping reverse faults that deform the bedrock surface and its thin cover. Yerkes has found that, as a unit, this area is being uplifted at long-term (16,000 yr B.P. to present) average rates of 3 to 4 mm/yr, with historic (1904–14) pulses that exceed 20 mm/yr. Although these rates are comparable to the highest such rates (4–10 mm/yr) recorded on the west coast of the conterminous United States, they may represent a small part of the total deformation in the area, which appears to be characterized by east-trending slip vectors with low plunges.

Holocene displacement along the Hilton Creek fault, eastern Sierra Nevada, California

The Hilton Creek fault is one of the main normal faults by which the eastern front of the Sierra Nevada steps westward from Owens Valley into the Mammoth embayment. It has the largest Holocene displacement (25 m, normal) yet measured along the eastern front of the Sierra Nevada, and it extends 25 km north-northwesterly from near Rock Creek Lake to the Long Valley caldera. M. M. Clark reports that, within the Sierra Nevada, this fault chiefly follows the base of a steep 1,000-m-high bedrock scarp, along which rates of displacement are difficult to determine. Where the fault

crosses the mouths of three glaciated valleys, however, it vertically displaces deposits of the Tioga Glaciation (latest Pleistocene). Near Rock Creek, the glacial deposits are offset by 1 to 2 m. About 3 km northwest, at Hilton Creek Lakes, they are offset by 1 to 7 m. About 7 km further northwest, Tioga lateral moraines of McGee Creek are displaced by 25 m, and Tioga and post-Tioga outwash of McGee Creek are displaced by 17 m. The increase of vertical displacement from Rock Creek Lake to McGee Creek is accompanied by an increase in overall height of the mountain front above the fault.

An eastward and downward projection of the Hilton Creek fault, assuming a dip of 45° to 60° to the northeast, passes through the focal region of the October 4, 1978, earthquake northeast of Bishop ($M_L = 5.8$; focal depth, roughly 13 km). No surface ruptures were found, however, along the Hilton Creek fault after the earthquake.

Lake Bonneville soils, stratigraphy, and shorelines

Surface and buried soils are used widely to date the latest movement on faults. Preliminary investigations by R. R. Shroba of buried and surface soils of the Lake Bonneville Group near Salt Lake City, Utah, indicate that buried soils in a similar stratigraphic position differ from site to site and lack the diagnostic morphological features reported by previous workers. This is especially true in the case of the Promontory Soil, which formed during the interval between the last two pluvials. Stratigraphic studies by R. B. Morrison and recent investigations by W. E. Scott suggest that this soil is formed in deposits inferred to be about 150,000 yr old and overlain by deposits about 15,000 to 20,000 yr old.

Typically, the Promontory Soil consists of a B and Bt horizon formed in a thin layer of colluviated eolian silt overlying a K or a Cca horizon formed in pebbly alluvial or lacustrine gravel. Argillic B horizons tend to be thickest and best developed in areas of higher precipitation along the Wasatch Front where they are about 90 cm thick, to show evidence of clay movement including moderately thick clay films and a several percent increase in clay, and to have a redder hue (commonly 7.5 *YR*) and a stronger chroma (4–6) than the original parent material. Calcic horizons tend to be thickest and best developed in areas of lower precipitation away from the Wasatch Front. These soils are characterized by Stage III K horizons about 150 cm thick overlying Stage I Cca horizons greater than 65 cm thick.

Shroba attributes much of the lateral variability of the Promontory Soil to environmental factors, as well as to local differences in the amount of erosion and deposition; at some localities, it is multistory and is composed of two or three soil profiles that are individually less developed than a single story profile. In addition, the type Promontory Soil tends to be better developed than stratigraphically equivalent soils at other localities. Contrary to the views of previous workers, the type Dimple Dell Soil is difficult to distinguish from these soils.

Deposits of the Lake Bonneville Group can provide valuable data for assessing fault activity along the Wasatch Front if their age and their fault offset or lack of offset can be determined. Results of recent work by W. E. Scott indicate that the age of certain deposits as interpreted by previous workers may be in error by as much as an order of magnitude.

As used by previous workers, the Bonneville Formation contains the deposits of the last lake cycle (12,000–20,000 yr old), and the Alpine Formation contains deposits of the next-to-the-last lake cycle (35,000–75,000 yr old, or, more likely, about 150,000 yr old). Both formations have been mapped at altitudes near the Bonneville shoreline, which was the highest level reached during the last lake cycle. Scott, however, interprets the contact between these formations near the level of the Bonneville shoreline as a facies change or a minor disconformity and suggests that some sediment previously assigned to the Alpine Formation was deposited during the last lake cycle about 15,000 to 20,000 yr ago. If this interpretation is correct, tectonic slip rates calculated on the basis of earlier age estimates may be an order of magnitude too low.

At altitudes more than about 65 m below the level of the Bonneville shoreline, the contact between deposits of the two lake cycles is shown at numerous localities. Typically this contact is an unconformity characterized by a buried soil or buried soil complex, disconformity, and subaerial deposits. In most places, the older sediments are deeply buried and little exposed. At the two highest of these exposures, about 65 m below the level of the Bonneville shoreline, the older deposits consist of shore facies, and they display stratigraphic relations that suggest these deposits mark the highest level attained during the next-to-the-last lake cycle. These older lacustrine and related deposits are potentially useful fault data, but they are both faulted and well exposed in only a few places.

One such older deposit is located north of the mouth of Big Cottonwood Canyon, where large gravel operations expose deposits of the next-to-the-last lake cycle that are cut by a fault zone about 0.5 km wide and consist of at least five breaks. Scott reports that deposits of the last lake cycle here are offset about 8 m, which indicates an average slip rate of about 0.5 mm/yr. The older sediments are displaced at least 16 m, which indicates a minimum slip rate of 0.1 mm/yr.

At four widely separated localities in western Utah, R. C. Bucknam measured profiles across wave-cut scarps cut at the high stand of Lake Bonneville. The

data were treated in the same manner as the fault scarp profiles described by Bucknam and Anderson (1979). Data from the shoreline profiles define a line ($\Theta = 3.84 + 21.0$ log H) nearly parallel to those from similar data from fault scarps. Although the shoreline scarps transect a variety of alluvial fan environments from apex to toe, the standard deviation of observations about the regression line is only 1.6°. This suggests that, whatever variations in grain size and sorting may exist in unconsolidated alluvial fan deposits, they have no apparent effect on the relations between scarp slope angle and log scarp height.

Rate and periodicity of movement, Hurricane fault, southwestern Utah

An understanding of the seismotectonics of the Hurricane fault is important to the evaluation of seismic hazards in relatively small, but growing, population centers such as Cedar City and Saint George. Long-term vertical displacement rates on the northern Hurricane fault calculated from vertical offsets of dated basalts range from 0.31 to 0.47 mm/yr. These rates are comparable to a rate of 0.4 mm/yr determined by C. W. Naeser (written commun., 1979) for the Bountiful-Odgen segment of the Wasatch fault. Despite the similarity in long-term displacement rates, continuous youthful-looking scarps in alluvium, such as those along the Wasatch fault, are not found along the northern Hurricane fault. Geomorphic evidence for Holocene displacement on the Hurricane fault has not been found, whereas geomorphic and geologic evidence for multiple Holocene movements on the Wasatch fault is mounting rapidly (Schwartz and others, 1979; Swan and others, 1979). To explain these observations, R. E. Anderson suggests that stress has been stored on the northern Hurricane fault at a rate consistent with the long-term average and that the return period for stress release in the form of large magnitude earthquakes is long—similar in length to the Holocene Epoch. The Hurricane fault appears to be capable of generating large-magnitude earthquakes, as judged from geologic evidence at the mouth of Shurtz Creek about 8 km south-southwest of Cedar City. At that locality, a fault scarp 20 m high and in very coarse bouldery alluvium has a slope angle of 29°; from its profile, Anderson estimates it is probably earliest Holocene or slightly older.

Historic surface faulting at Hansel Valley, Utah

Elevation changes in the epicentral area of the 1934 Hansel Valley, Utah, earthquake have been derived from first-order leveling data from surveys made in 1911, 1934, and 1953 by the U.S. Coast and Geodetic Survey. According to R. C. Bucknam, the data define a zone about 15 km wide that subsided as much as 40 cm between 1911 and 1934. The subsidence is superimposed on a broad uplift of about 20 cm relative to bench marks east of the Wasatch Front as shown by surveys made in 1911 and 1953. Postearthquake surveys show that significant (about 8 cm) up-to-the-west tilt occurred across a 35-km interval in the epicentral area between 1934 and 1953.

The zone of surface faulting associated with the 1934 earthquake trends northerly, and most of the observed displacements on the surface faults were down to the east, with a maximum observed displacement of 50 cm. Many of the major surface fractures produced by the earthquake are still visible on aerial photographs. A map of the fractures based on field and aerial photograph studies shows that the zone of subsidence indicated by the leveling data lies between about 5 and 10 km west of the zone of surface faulting. The breadth of the zone of subsidence and its location on the relatively upthrown side of the surface fractures suggest to Bucknam that the observed fractures may be secondary features, such as shallow antithetic faults adjacent to a buried west-dipping fault.

Geologic and geophysical investigations near New Madrid, Missouri, in the Mississippi embayment

The most striking surficial structure in the northern Mississippi embayment is the Lake County uplift, an enlongate composite feature that is associated with faulting and modern seismicity. New evidence gained from geomorphic studies and seismic reflection profiles indicates that this structure upwarps the surface of the Mississippi Valley as much as 10 m in parts of northwestern Tennessee, southeastern Missouri, and southwestern Kentucky. The Lake County uplift can be subdivided into three smaller topographic features, namely, the Tiptonville dome, Ridgely Ridge, and the southern part of Sikeston Ridge.

Tiptonville dome, an asymmetrical monoclinal ridge bounded on its eastern flank by Reelfoot scarp, formed chiefly between 200 and 2,000 yr ago, but the northwest and southeast parts of the dome were uplifted again during the 1811 to 1812 New Madrid earthquakes. A convex Mississippi River low-water profile, measured from 1954 to 1975, is interpreted by D. P. Russ as evidence of continuing uplift along the northwestern and western edge of the dome.

Ridgely Ridge is a northeasterly-trending symmetrical bulge, which appears to be older than the Tiptonville dome, but geomorphic evidence suggests to Russ that it is younger than 6,000 yr B.P. The southern end of Sikeston Ridge and adjacent areas of the

Mississippi Valley have undergone broad shallow upwarping, probably during late Wisconsinan or early Holocene time.

Approximately 75 percent of the microearthquakes recorded from July 1974 through June 1978 in the general region between Ridgely, Tenn., and New Madrid, Mo., has occurred in the Lake County uplift area. Intense seismic activity is occurring along the northwestern part of the Tiptonville dome near the 1812 uplift and in the vicinity of Ridgely Ridge. No historic movement of Ridgely Ridge is documented, and the relations of seismicity to subsurface structure under the ridge is unknown.

R. M. Hamilton reports that seismic reflection profiles in the New Madrid region show excellent continuous reflections from contacts between rock units of Eocene and Paleocene age, Paleocene and Late Cretaceous age, and Late Cretaceous and Paleozoic age. Locally continuous reflections are seen high in the Eocene section. Hamilton recognizes a major fault zone in northeastern Arkansas that coincides with the main northeast-striking seismic zone. The fault zone is 9 km wide and vertically displaces Paleozoic rocks a cumulative total of about 1,000 m. The top of the Paleozoic rocks and younger horizons have a cumulative vertical displacement of about 50 m across the fault zone.

The profiles also show a northeast-striking horst and graben system near Ridgley, Tenn. The system is subparallel to patterns of overlying surface deformation, suggesting that structural elements in the system have been active during the late Holocene. The main graben is bounded on the southeast by a fault with about 80 m of postmiddle Eocene vertical displacement. The intrusion of igneous rock beneath the graben has domed overlying Mesozoic and Tertiary rocks. The graben, when projected to the northeast, passes under Reelfoot Lake.

T. G. Hildenbrand's continuing analysis of aeromagnetic data from the upper Mississippi embayment region indicates that the northeast-trending graben cuts the Precambrian surface, has structural relief of 1.6 to 2.6 km, and is probably associated with a pre-Late Cambrian boundary or suture separating contrasting basement rock types. He suggests that tensional stresses caused the crust to fail by brittle fracture and shear and that subsequent crustal thinning and partial melting of the crust led to plutonism and possibly to volcanism with mafic or ultramafic plutons intruded along both rift-border and rift-axial faults. From the interpreted ages of some of these intrusions, Hildenbrand concludes that a major igneous event took place after middle Mesozoic time and hundreds of millions of years after the structural graben formed. The magnetic data suggest that the graben or rift zone terminates northward in western Kentucky and southern Illinois, a region characterized by intense Paleozoic igneous activity and faulting, but continues southwest, beyond the surveyed area, into south-central Arkansas.

D. P. Russ has derived a tectonic model for the Lake County uplift from fault plane solutions determined by Herrmann (1979) and Herrmann and Canas (1978) and from subsurface faults identified in recent reflection profiles. The fault-plane solutions indicate that the major compressive stress in the New Madrid region is horizontal and trends approximately east-west and that northeast-trending faults have right-lateral strike-slip motion on them. The Lake County uplift lies between two northeast-trending zones of seismicity that are interpreted as fault zones. The uplift therefore, may be explained by the opposing horizontal motion on the two fault zones being translated into a vertical strain.

Seismic reflection evidence, seismicity, and geologic structure at Charleston, South Carolina

H. D. Ackerman, J. C. Behrendt, and R. M. Hamilton report that profiles in the Charleston region show several excellent reflectors that can be correlated over most of the region. The strongest reflector is associated with the top of a 257-m-thick basalt of Jurassic age, which was encountered at a depth of about 750 m in coreholes near Clubhouse Crossroads. Offsets of about 50 m in the surface of the basalt reflector appear on three profiles and define a northeast-trending fault zone, which passes through the cluster of seismicity near Summerville, S.C. This cluster of seismicity is near the area of maximum intensity for the 1886 earthquake. Additional reflection data from below the top of the basalt will help researchers interpret the nature of the Triassic-Jurassic basin that underlies the seismic region.

Surface displacement associated with the Tabas, Iran, earthquake of September 16, 1978

R. V. Sharp's aerial and ground reconnaissance in the Tabas, Iran, area between October 9 and 18, 1978, revealed two broadly arcuate and discontinuous zones of thrust faulting west of and dipping toward the Shotori Range. The ruptures extended about 55 km northwestward and northward from near the village of Paykuh to near the village of Deshtak, about 3 km south of Tabas. Although the preliminary instrumental epicenter lay within the Shotori Range between Paykuh and Dehuk, no evidence of new movement was found along any faults that cut the range. The western and outer arc of surface faulting followed a previously unrecognized fault that forms the western boundary of an eroded badlands of highly deformed upper Cenozoic sediments. The longest fault rupture in this discontinuous zone of surface faulting extended about 28 km southeast from the village of Fahalanje. The fault trace

typically consisted of a zone of multiple subparallel but interlacing thrust breaks along the base of a preexisting west-facing fault scarp. The zone of thrusting varied in width, number of fault breaks, and complexity; widths as great as 20 m were common. Parallel zones of antithetic normal faults and other faults of unknown nature extended several kilometers within the upper plate east of the fault trace. The inner arc of surface faulting, 8 to 12 km closer to the Shotori Range, also was an eastward-dipping thrust fault but was less continuous than the western breaks. This zone appeared steeper than the western break and probably had more displacement; the vertical components of displacement probably ranged from 1 to 2 m near the southern end of the fault where it approached to within 3 km of the Shotori Range.

GROUND-FAILURE INVESTIGATIONS

Landslides in historic earthquakes

D. K. Keefer has analyzed data from 20 historic earthquakes to determine types, distribution, and geologic settings of earthquake-induced landslides. He finds the most frequently reported types of earthquake-induced landslides are (1) rock falls and slides of rock fragments from steep slopes, (2) shallow debris slides from steep slopes, (3) liquefaction-induced lateral spreads from bluffs, riverbanks, deltas, lakeshores, seacoasts, and artificial fills, (4) soil slumps and block slides from moderate to steep slopes, and (5) rock slumps and block slides from moderate to steep slopes. Relatively few dormant slumps and block slides are reactivated by earthquakes.

Large earthquake-induced rock and soil avalanches and subaqueous landslides are less frequent, but they are particularly hazardous to human life and property. Many subaqueous landslides attack the distal margins of deltas where some port facilities are sited. Rock avalanches originate on steep high slopes in weak rocks; soil avalanches originate on weakly cemented materials, including loess and volcanic pumice, that form steep stable slopes under nonseismic conditions.

The size of the region affected by earthquake-induced landslides depends on the earthquake's magnitude, its focal depth, and its ground-motion characteristics and on topographic and geologic conditions. For many earthquakes, landslides abound where shaking is no more intense than M = VII; some landslides accompany even lower intensities.

Experimental mapping of seismic-induced landslide susceptibility

To depict regional zones of seismic landslide susceptibility in the San Francisco Bay area, E. L. Harp, G. F. Wieczorek, and R. C. Wilson have prepared an experimental seismic slope stability map for the La Honda 7½-min quadrangle, San Mateo County, Calif. A dynamic numerical analysis was used to develop criteria for evaluating seismic slope stability. The analysis considered lithology, material strength, slope, and strong-motion records from several earthquakes. Failure criteria were derived by (1) grouping lithologic units into three catagories of shear strength, (2) grouping slopes into six categories, and (3) combining categories of lithology and slope and calculating, for each combination, the displacement of a potential landslide mass by integrating that part of a strong-motion record that exceeded the acceleration necessary to cause static slope failure.

From these calculations, generalized criteria were established for each combination of slope and lithology, which were then incorporated with geologic and slope maps to construct a seismic slope stability map of the La Honda quadrangle. Approximately 50 percent of the area has a high susceptibility to failure, 10 percent is unlikely to fail, and the remaining 40 percent has intermediate susceptibility to failure depending on season ground-water conditions.

Dynamic analysis of slope failure from August 6, 1979, Coyote Lake, California, earthquake

The August 6, 1979, Coyote Lake earthquake (M = 5.9) on the Calaveras fault in southern Santa Clara County, Calif., reactivated a preexisting landslide on the northeast shore of Lake Anderson. The landslide fissure, studied by R. C. Wilson, extended more than 20 m obliquely across an asphalt roadway and onto the dirt shoulders on both sides. The horizontal opening was 12 to 18 mm, with 5 to 10 mm of vertical displacement (down to the south). The fissure appears to follow the scarp of an older slump landslide in weathered shales of the Cretaceous Berryessa Formation of Crittenden (1951). The measured displacements show that the landslide mass was displaced approximately 20 mm during the earthquake.

Because of its proximity to strong-motion instruments, which recorded this earthquake, the slope failure provides a valuable check of the validity of current methods of analyzing seismic slope stability. Using field measurements, standard slope stability measurements, and estimates of the strength of the shale, Wilson estimates the critical acceleration (threshold of seismic-induced movement) of the Lake Anderson landslide to be 15 to 25 percent g (acceleration of gravity). Using the N. 50° E. component of the accelerogram from Gilroy Station No. 6, 10 km southeast of the landslide, and these critical displacements, the dynamic analysis predicted displacements of 10 to 25

mm. This is in excellent agreement with the 20-mm displacement measured in the field. This result is significant because strong-motion records and well-documented slope failures rarely coincide, making physical validation of analytical techniques difficult.

SEISMICITY INVESTIGATIONS

Charleston, South Carolina

Relocated earthquakes in the Summerville–Middleton Place area of South Carolina roughly delineate two subparallel northwest-trending seismic zones with a possible northeast-trending zone between them. B. S. Rhea used a refined crustal model and retimed phase arrivals in the computer program HYPOELLIPSE to locate the hypocenters. Her analysis of the best-located earthquakes, as defined by error ellipsoids with longest dimension less than 2.5 km, yielded single-event and composite focal mechanisms whose nodal planes are consistent with the vertical profiles of the hypocenters. The two northwest-trending zones and the northeast-trending zone have near-vertical nodal planes and indicate reverse faulting. These zones of seismicity are associated with local gravity and magnetic anomalies from which other workers have inferred basement structures. Rhea associates the northeast-trending zone with a graben-and-horst feature in the basement.

Central basin platform, Texas and New Mexico

Most of the seismicity during the past year was in the vicinity of the War-Wink gas field, where earthquake swarms of several hundred events were recorded in August 1978 and from January to February 1979. From August 1978 through June 1979, A. M. Rogers located a total of 737 earthquakes; all were M = 3.0 or less.

Seismic attenuation studies

A. F. Espinosa (USGS) and E. F. Chiburis and Robert Cicerone (Weston Observatory, Boston College) have evaluated the attenuation of Lg waves in the northeastern United States. Data used in the investigation came chiefly from seismograms of the Northeastern U.S. Seismic Network, which is partly subsidized by the USGS and other government agencies. A total of 20 earthquakes and 55 quarry blasts recorded at distances of about 20 to 350 km was used to derive a preliminary attenuation relation for Lg waves in the New England region.

A. F. Espinosa has derived a magnitude scaling from the strong-motion data of the San Fernando earthquake of February 9, 1971. He compared the results with other strong-motion recordings obtained from 62 earthquakes in the Western United States. The M_L values from this investigation agree well with those evaluated by Kanamori and Jennings (California Institute of Technology). The empirical scaling law applies to significant earthquakes in the Western United States from 1933 through 1971; their local magnitudes range from about 4 to 7.2, and they were recorded at epicentral distances of about 5 to 300 km. The proposed method for evaluating the local magnitude extends the procedure of local-magnitude determination for moderate and large earthquakes at near- and intermediate-epicentral distances from strong-motion recordings.

Saint Elias, Alaska, earthquake of February 1979

C. D. Stephens and J. C. Lahr determined that epicenters of the 221 aftershocks that occurred within 15 d of the Saint Elias, Alaska, earthquake of February 1979 define a zone about 65 by 80 km southeast of the epicenter of the main shock. The distribution of the epicenters is nonuniform; most of the aftershocks are clustered about 50 km to the southeast of the main shock. The depths of most of the aftershocks are poorly controlled, but those that are best located are shallower than about 35 km. Together with a focal mechanism for the main shock, these data suggest a low-angle thrust as the primary rupture mechanism for the main shock.

Stephens and Lahr also studied the statistical properties of the aftershock data set, which is complete for events M = 3.3 or larger, starting 1 d after the main shock. Two of the three largest aftershocks, all with magnitudes between 5.0 and 5.2 m_b, occurred within this time. The b value of the frequency-magnitude relation is close to 1.0. The p value, which describes the rate of decay of seismicity, is 1.1, which is within the range of values normally observed. Focal mechanisms, determined for most of the larger aftershocks, exhibit nearly horizontal compression axes, but the orientations of the axes change from north-south near the epicenter of the main shock to northwest-southeast in the cluster to the southeast.

Thessalonica, Greece, earthquake of June 1978

C. J. Langer reports results from a 10-station portable seismograph network that was deployed to study aftershocks of the $m_b = 6.4$ Thessalonica, Greece, earthquake of June 20, 1978. Monitoring, which commenced 13 d after the mainshock and continued for 20 d, located the hypocenters of 116 aftershocks in the magnitude range 2.5 to 4.5. Epicenters defined an area some 30 km (east-west) by 18 km (north-south); focal depths were between 4 and 12 km. Composite focal mechanism solutions for selected aftershocks indicate reactivation of mapped

normal faults and possible splay faulting (strike-slip) off the western end of the surface ruptures.

The epicenters for four foreshocks M=4.8 or larger and the mainshock were relocated using the method of joint epicenter determination. Collectively, those five epicenters form an arcuate pattern that is 5 km north of the observed surface rupturing.

GROUND-MOTION INVESTIGATIONS

Variables affecting the nature of strong ground motion

Several investigators, using both field data and mathematical analyses of theoretical models, have provided new insight into the variable character of ground motion caused by earthquakes. Observations of strong ground motion for seismic events ranging in magnitude from −1 to almost 7 indicate to A. F. McGarr that peak acceleration and peak velocity are definitively related to the seismic source parameters of stress drop and source radius. Moreover, peak accelerations also vary with processes that are very small scale compared to the source dimension, and peak acceleration appears to be proportional to the frequency band width of the recording system. From underground observations of faulting, McGarr concludes that the small-scale features influencing peak accelerations may be associated with the en echelon pattern of fractures that comprise fault zones; such patterns may give rise to localized regions of high stress drop.

By numerically simulating earthquakes and by analyzing strong ground-motion records, Ralph Archuleta has shown that the pattern of strong ground-motion amplitudes varies greatly near the fault where the earthquake originates. This variation can be caused by the distribution of stress drop on the rupture surface, the location of the hypocenter, the rupture velocity, or the medium itself. Each earthquake has different combinations of these variables, and factors that are important for one earthquake may not be important for another; thus, each earthquake must be analyzed separately.

According to R. K. McGuire, acceleration values from seismic hazard calculations in the San Francisco Bay area have statistical uncertainties on the order of 0.2 to 0.4 g. The smallest uncertainties are found about 50 km from the major faults; larger values, which occur close to faults and at distances of 100 km or more, are due to uncertainties in depth of energy release, seismicity, and mean acceleration.

Probabilistic hazard and risk assessment

S. T. Algermissen reports that computer programs for estimating the probability of different levels of ground motion can now accommodate variability in attenuation, maximum earthquake magnitude, and fault length. Efficient and economical, these programs are well adapted for use in hazard mapping. Geologic data on the recurrence rate of large (M=7–7.5) earthquakes on the Wasatch fault have been incorporated in a probabilistic model for estimation of ground acceleration. If the Wasatch fault is considered to be a separate seismic source zone, ground accelerations are about three times those previously estimated in the vicinity of the fault.

Using interim peak velocity attenuation functions, D. M. Perkins, S. C. Harmsen, and S. T. Harding have prepared hazard maps based on probabilistic peak velocity. These functions were devised using a method similar to that of P. B. Schnabel and H. B. Seed (1973) for acceleration attenuation. For larger earthquakes, the velocity attenuations differ from acceleration attenuations in that they show greater separation between attenuation waves and a slower decay with distance. Because of these differences, the maps expressing earthquake hazard in terms of velocity show a greater dependence on maximum magnitude assumed for the source zones (because maximum magnitudes can seldom be determined from historical data, more geological and geophysical work will be needed to estimate maximum magnitudes) and a greater smoothing in the detail depicted. Thus, velocity maps are less affected by details of source zone boundaries, but velocity hazards extend further from the source of large-magnitude earthquakes.

Local amplification effects, Mississippi Valley and Wasatch fault, Utah

S. T. Algermissen's reevaluation of Modified Mercalli intensity data for damaging earthquakes in the Mississippi Valley shows pronounced local ground amplification effects associated with the valleys of major rivers. These amplification anomalies resemble those mapped for the 1886 Charleston, S.C., earthquake. For the Mississippi Valley, Algermissen has derived intensity attenuation relations of the form $I-I_0=A+B \log (r)+C(r)$, where I_0 is maximum intensity, I is intensity, and r is distance.

W. W. Hays' preliminary analysis of the broadband nuclear explosion ground-motion data recorded at 27 sites in Salt Lake City and at 11 sites in Provo has shown that various types of consolidated and unconsolidated surficial material respond to ground shaking in a distinct and similar manner. In both urban areas, the ground response at sites underlain by thick deposits of water-saturated fine-grained sands and clays is as much as a factor of 10 greater than that for sites underlain by rock or thin deposits of semisaturated gravels and sands. From these ground-response values, Hays concludes that, during an earthquake along the Wasatch

fault zone, parts of each urban area would be susceptible to enhanced levels of ground shaking and to significant potential damage. Ground-motion measurements from moderate earthquakes in the region are needed to confirm these indications.

STOCHASTIC MODELING OF FAULTING

The number-size distribution of earthquakes requires that irregularities exist on a fault at all length scales. To formulate a stochastic description of the faulting process, D. J. Andrews assumes self-similar irregularity, a random irregularity that remains statistically similar upon a change of length scale. Self-similar geometric irregularity of a fault surface is represented in Andrews' model by stress and friction functions that fluctuate self-similarly on a plane. If the set of rupture areas of all earthquakes on the brittle portion of a fault plane is assumed to be self similar, then the number of ruptures with area greater than A is proportional to 1/A. If stress drop is independent of earthquake size, then the number of earthquakes with moment greater than M_0 is proportional to $M_0^{-2/3}$. The size of an earthquake is determined by spatial fluctuation of the initial stress and sliding friction functions. The spectrum of the stress function is related both to the average stress drop as a function of earthquake size and to the number-moment distribution. A model of the slip-and-stress change functions of an earthquake is constructed in the Fourier transform domain. Although stress function becomes smoother in an earthquake at the length scale of the rupture, it becomes rougher at shorter length scales to prepare the fault for future smaller earthquakes. Seismicity is a cascade of stored elastic energy from longer to shorter wavelengths.

ENGINEERING GEOLOGY

Research in rock mechanics

A statistical summary of worldwide subsidence experience in shale and crystalline rocks, including an annotated bibliography of the most significant references on mining-induced subsidence in these rocks, was prepared by F. T. Lee (USGS) and J. F. Abel, Jr. (Colorado School of Mines). No measurements were reported of subsidence in competent "massive" shale and crystalline rocks. Consequently, predictions about such types of rocks, based on information gained from less competent rocks, will be subject to unknown and possibly large errors. Subsidence apparently is controlled by a complex combination of mining and geologic factors. For example, as the percentage of shale in the rock mass increases, the angle of draw (the inclination from vertical of a line connecting the edge of the underground excavation and the edge of the area of subsidence) decreases, thereby decreasing the maximum size of the potential subsidence area. In fractured crystalline rocks, the angle of draw and the resulting surface deformation are controlled not by properties of the rock substance, as in shale, but by preexisting joints and faults. Control of subsidence by backfilling subsurface openings is highly successful. In one case, the predicted subsidence opening was nearly 20 times larger than that measured using backfill application.

Lee also directed studies that determined in situ stresses in "Mount Waldo Granite" and Passagassawakeag Gneiss near Bucksport, Maine (Lee and others, 1979) to assist in assessing the suitability of crystalline rocks of coastal New England as sites for oil storage chambers. Three techniques were used in the investigation: stress-relief overcoring of surface-placed strain gages, overcoring of the USBM borehole deformation gage, and measurement of stress by hydrofracture. Stress-relief measurements from the surface-strain gage show considerable scatter and are susceptible to near-surface variations in temperature, moisture, fracturing, and mineralogy. At greater depths (down to 26 m), the orientation and magnitude of in situ stresses are controlled by sheeting fractures and tectonic joints. Stress magnitudes were found to be three times as high at a mountain location in massive rock as in an adjacent valley underlain by more closely sheeted weaker rock.

The sheeting process apparently expended energy derived from residual stresses (the predominant component of the in situ stress field), resulting in rock-stress magnitudes that are controlled by the volume of unfractured rock in which the measurement was made. The chemical effects of water may facilitate the release of stresses and fracturing. Stress orientations below sheeting and alteration boundaries in granite and gneiss are more consistent with the tectonic framework of the area (right-lateral strike-slip faulting) than are stresses at shallower depths. The inference that the least principal stress is normal to sheeting surfaces was supported by hydrofracture measurements.

Geotechnically, near-surface storage of oil appears feasible in fractured destressed granitic rock if fluid levels are kept below well-developed open sheeting fractures. Perched water levels in some mountainside quarries lose little water annually, other than that lost through evaporation. Pressure-flow tests in strongly foliated gneiss are approximately the same as in sheeted granite.

Research in computer modeling for engineering geology

An analytic model for the prediction of surface displacements resulting from subsidence in karst terrain has been developed by W. Z. Savage. The model

assumes that the subsiding region is an infinitely long layer resting on a rigid base, deformed under its own weight into an opening at its lower edge. Because of the form of the analytical solution used, this model is best applied to predict surface displacements resulting from subsidence in a karst terrain where a thick and relatively soft soil layer overlies a solution cavity in much stiffer limestone or dolomite. Of particular interest is the prediction by this model of the formation of a ridge at the edge of the subsidence trough, a phenomenon often observed in the field.

LANDSLIDES

Costs of landslide damage

Studies of the costs of landslide-caused damage have been evaluated at several locations in the United States to provide a better basis for estimating the total annual cost of landslide damage in the United States. In 1979, F. A. Taylor surveyed costs of damage in Hamilton County and Cincinnati, Ohio, from 1973 to 1978. Annual costs of landslide damage for the 6 yr were nearly $31 million or about $5.80 per person per year. This estimate supports other previously published estimates that the annual costs of landslide damage in the United States exceed $1 billion per year.

Japanese landslide experts visit

Seventeen landslide experts from governmental agencies, universities, and private companies in Japan participated in a tour of major landslide areas along the Pacific coast, arranged in part by E. E. Brabb. They visited several landslide areas near Los Angeles (including areas that failed during the 1971 San Fernando earthquake) and near San Francisco, the Columbia River, and British Columbia. A hand-assembled guidebook of the trip is available for reference in the Menlo Park library of the USGS.

Studies of the recent landslide near Manti, Utah

Field studies of a large landslide in Manti Canyon, Utah, were completed by R. W. Fleming, R. L. Schuster, and R. B. Johnson. The landslide was triggered by a rockslide and debris flow above an inactive landslide. The rockslide and debris flow piled debris on the upper part of the inactive landslide. Renewed movement of the inactive landslide started at the top and progressed downslope. Ultimately, the slide was nearly 3 km long and 1 km wide. Different parts of the slide moved at different rates over the 6-yr record of measurements.

Disruption of the forest cover by landslide movement was studied by S. S. Agard to document the technique of tree-ring analysis where the history of movement is known. Trees that survived the slide movement were tilted, uprooted, split, abraded, or buried to varying degrees. Preliminary analysis of tree cores and sections collected from the landslide indicates that the external disturbances in turn caused datable internal growth responses:

- Trees tilted more than 20° from vertical generally displayed pronounced reaction wood and eccentric growth.
- Many trees tilted more than 45° to 50° did not show reaction wood but instead showed severe growth suppression.
- Some trees tilted up to 20° from vertical showed no apparent growth changes, while others displayed reaction wood, eccentric growth, or suppressed growth.
- Trees that were split, abraded, uprooted, or partially buried by debris generally showed suppressed growth.

Preliminary tree-ring analysis indicates that most trees growing on the slide at the time of reactivation accurately record the event to within a growing season of the date of disturbance. Trees disturbed in 1974 showed a datable response in 1974 or 1975; trees disturbed in 1975 showed a datable response in 1975 or 1976. Preliminary tree-ring analysis also suggests that at least one major mass-movement event occurred before 1974 in the upper two-thirds of the slide. Trees growing at the head of the slide have been inundated by debris flows repeatedly during the last 200 yr. Growth responses of most of these trees indicate that a major debris flow inundated the area in 1968. Many trees sampled from the upper two-thirds of the slide (below the head) displayed growth changes that suggest that slide movement was partially reactivated in 1968. The precipitation records for adjacent Ephraim Canyon reveal above average spring snowfall during 1968 (January–April, 130 percent of average; April, 210 percent of average).

Tree-ring studies of recent landslides in San Miguel County, Colorado

Analysis of tree rings from samples collected by S. S. Agard on the Ames landslide in the South Fork River valley, eastern San Miguel County, Colo., indicated that movement occurred both before and after the "recorded" event of 1929 to 1930 and that the movement history was related to precipitation patterns. Major movement began in the upper and central portions of the slide as early as 1926 or 1927, possibly in response to above-average spring precipitation and seepage from beaver ponds at the head of the slide (as suggested by earlier workers). Movement increased between 1926 and 1930, propagated downslope, disrupted a railroad track at the toe, and was reported by local newspapers.

Movement decreased markedly during the early 1930's, when drought conditions prevailed (total precipitation for 1930–37 was only 50–60 percent of normal). Slide movement increased abruptly in 1941 and continued into the early 1950's. This corresponded to an abrupt increase in precipitation in 1941 (175 percent of normal), followed by continuous above-average precipitation until 1950. Since then, the slide has been relatively stable except for soil creep and small-scale movements in local areas.

Catastrophic rockfall avalanches

R. D. Brown, Jr., studied the physical and geological characteristics of large ($\geq 0.5 \times 10^6$ m^3) high velocity (≥ 100 km/h^{-1}) rockslides. These avalanches, the deposits of which are widespread in certain areas around the world, have tremendous destructive potential at the site of the slide and may generate a complex sequence of destructive events. Past events included damming of streams by slide debris, upstream flooding as the level of water behind the debris dam rose, sliding of saturated valley walls into a slide-blocked lake, and sudden failure of the debris dam followed by catastrophic flooding downstream. Most of these slides resulted from natural causes; a few were triggered by quarrying, underground mining, or impoundment of reservoirs.

Field evidence and theory helped define potential sites of such slides and provided a basis for maps outlining regions that are susceptible to catastrophic rockslides. Among the important geologic characteristics found in these regions were high relief, together with other evidence of recent tectonic activity (historic seismicity or volcanism, faulting, or deglaciation in late Pleistocene or Holocene time), rocks with at least average bearing and shear strengths, and one or more structural discontinuities (joints, bedding, or shear zones) that are so oriented that they are potential failure surfaces.

Other geologic influences clearly were important locally but more difficult to evaluate without carefully designed site investigations; examples included the level of ground shaking caused by nearby earthquakes, the effects of pore pressure where ground water occupied potential failure zones, and the role of stream erosion as it affected potentially unstable slopes.

Landslide studies in the Appalachians

W. E. Davies and his associates are studying areas of landslide deposits and areas susceptible to landsliding in the Appalachians from Pennsylvania to Alabama. Studies in 1979 led to some preliminary conclusions about the effects of precipitation and type of material on landslide styles and abundance. They found that the effect of precipitation in activating landslides varied according to the amount of coarse-grained material in the deposits. When clay and silt formed over 80 percent of the material, there was little direct response to heavy precipitation (22.5 cm or more in 24 h). Some small shallow debris flows occurred during the period of precipitation, but there was generally a lag of 1 to 2 yr before persistent slow large-scale movement was initiated (Pomeroy, 1979).

Where coarser grained material, primarily sand, formed about 25 percent or more of the deposit along with silt and clay (for example, in the soils weathered from the Breathitt Formation in Kentucky), large-scale landslides were activated during periods of heavy precipitation. Where void space was large, as in the case of stony sandy soils, extremely rapidly moving debris avalanches were activated during periods of heavy precipitation.

Gliding or sledging of relatively small flat blocks of rock was noted to be a significant form of mass wastage in areas of thick massive sandstones in ledges of cliffs. Blocks up to 10 m in diameter detached from outcrops and moved laterally onto material susceptible to sliding. The blocks moved downslope by gravity, and evidence indicated they sledged along the slope with no evidence of rolling or tumbling. Although the initiation of movement of the rocks varied and was not related to a single geologic event, the boulders accumulated and created the appearance of a large rockfall.

REACTOR HAZARDS

The USGS Reactor Hazards Research Program comprises 45 projects in selected subjects. Most of the effort is in regional tectonics, methods of age dating, and earthquake ground motion. These research projects generally are discussed in other more appropriate chapters of this report dealing with regional investigation; therefore, only a few of the many projects of this program will be discussed here.

Charleston, South Carolina

For several years, the USGS has been studying the Charleston, S.C., area to develop a better understanding of the seismicity of the region and to determine, if possible, the source mechanism of the severe earthquakes such as that of August 31, 1886. Two parts of the investigations are geology and geophysics.

Geology

Near Charleston, S.C., sedimentary lithoclasts of crystalline rocks found in lower Mesozoic conglomeratic red beds from USGS Clubhouse Crossroads No. 3 well (Dorchester County) are the only materials available for

direct geologic study of the basement rocks. No deep well has penetrated the pre-Mesozoic basement in the Charleston area. Various sedimentary characteristics of the host red beds indicate that the lithoclasts have not been transported far from their source.

According to G. S. Gohn, four categories of crystalline rocks have been recognized; in order of increasing abundance, these are mylonite, basalt, microbreccia, and granodiorite. The granodiorite lithoclasts are phaneritic plutonic rocks that range in apparent composition from quartz diorite to granite with the largest lithoclasts typically in the granodiorite compositional range. These lithoclasts show evidence of moderate deformation including ductilely produced microstructures in quartz and feldspar, orientation of secondary minerals, and poorly defined compositional layering. The alinement of chlorite and epidote in the dynamically produced texture and saussuritization of plagioclase indicate that dynathermal metamorphism took place under greenschist-grade conditions.

Mylonite lithoclasts have been ductilely deformed to a greater degree than the granodiorite lithoclasts. In the mylonite, fluxion structure (mylonitic foliation) is defined by thin sinuous bands of fine-grained epidote between similar bands of fine-grained quartz, altered feldspar, and segmented stringers of quartz. Small porphyroclasts of quartz and feldspar also occur but are sparse. Brittle deformation of granodiorite is recorded by microbreccia lithoclasts that consist of a highly fractured protolith of quartz, saussuritized plagioclase, perthite, and secondary minerals and veins of epidote and (or) quartz zeolite(?).

The presence of a cataclastic texture in some of the granodiorite (microbreccia) lithoclasts and the mineralogic resemblance of the mylonite lithoclasts of the granodiorite suggest that this plutonic rock has experienced periods of both ductile and brittle deformation under greenschist and subgreenschist(?) conditions, respectively. The restriction of the deformation textures and epidote mineralization to lithoclasts in the deposit indicates that the recorded deformations could not be younger than the enclosing red beds (lower Mesozoic).

Basalt lithoclasts in the red beds are weathered and deuterically(?) altered but do not show any evidence of shearing. Relict textures in these clasts are diabasic, and the present mineralogy is saussuritized and sericitized plagioclase, chlorite, epidote, and opaque minerals. Based on the texture and mineralogy, these lithoclasts are tentatively interpreted to represent otherwise unsampled basalt flows, sills, or dikes that occur downsection from the lower Mesozoic basalt flows encountered above the red-bed section in Clubhouse Crossroads No. 3 well.

Geophysics

Several important results stand out from geophysical work in the Charleston area during fiscal year 1979. (1) Definitions were refined for depths and velocities of pre-Cretaceous basement, as well as for the shape and extent of the Summerville basement ridge, a feature of the deeper crystalline basement that may represent a horst block dating from early Mesozoic continental breakup, according to H. D. Ackermann. This work became possible using a flexible new analytic procedure for treating refraction seismic data that has been collected over the past 3 yr. The work gives a general overview of velocities and structures to be expected in the Charleston area and provides a framework for planning the detailed contract reflection seismic work that is being done there. (2) Indications were given by deep magnetotelluric (MT) soundings that extreme electrical anisotropies may be present and measurable from the surface in the immediate vicinities of active seismic zones, as defined by modern epicenters. Of 22 MT soundings in the Charleston area, only 3 showed the effect—at Middleton Place, at Adams Run, and in the seismic gap between Summerville and Bowman. This is the first geophysical evidence for a fault at midcrustal depths in the Charleston area. (3) Poor correlations have been demonstrated, on paleomagnetic grounds, between basalt flow sequences seen in coreholes 1 and 2, according to J. D. Phillips. The evidence argues for a fault between the two coreholes, supporting earlier interpretations by Gohn and COCORP (Consortium for Continental Reflection Profiling).

Quaternary dating and neotectonics

Dating studies by K. L. Pierce of alluvial fans near Arco, Idaho, reveal that caliche rinds on stones from the soil profile can be dated using uranium-thorium isochron methods and that the thickness of such rinds can be used as a simple numerical dating technique. A range-front fault at the base of the Lost River Range offsets a sequence of alluvial fans, with no offset on the youngest fans. This fault is northwest of the Reactor Testing Station at the Idaho National Engineering Laboratory. John Rosholt has determined uranium-thorium isochron ages using a new technique that involves soluble and insoluble phases from several layers of each caliche rind from stones collected from three ages of faulted fans. Out of eight ages determined, seven are both stratigraphically consistent and compatible with available independent age control; these ages date three fans with increasing fault offset as 35,000, 110,000, and 160,000 yr old. Measurements of the average rind thickness on these fans show an average rate of caliche rind accumulation of 0.6 mm/10,000 yr. The accuracy of this rate as a local dating technique is estimated to be

±40 percent or better. These datings studies show late Quaternary offset on the Arco fault at an average rate of 1 m/10,000 yr.

Faults, southeast Texas

Hundreds of faults have offset Pleistocene and Holocene sediments and the land surface developed on them in the Houston metropolitan area. Known and mapped scarps at the land surface are typically 0.5 to 1.5 m high, and many are growing higher at average rates of 0.5 to 2.0 cm/yr. Damage to property by creep along the more than 200 km of active faults so far identified is both widespread and costly.

Electric logs and high-resolution seismic profiles across several of these faults reveal that they are growth faults and have, thus, been active to some degree throughout much of late Pleistocene and Holocene time. The influence of faulting on the geomorphic development of the region locally is apparent where both abandoned Pleistocene channels and modern-day streams follow the base of fault scarps or meander within narrow topographically expressed grabens. Scarps of some faults are clearly visible on detailed (1-ft contour interval) topographic maps surveyed from 1915 to 1916. The 1915 topography, however, appears to differ substantially from the present landscape. Most faults whose present scarps are high enough to have been reflected on the old maps are not in evidence. Neither is there much visual sign of these scarps on 1930 photographs, although they stand out clearly on photographs of comparable scale and tonal contrast taken in the 1970's. This evidence of rapid and recent growth of scarp heights, together with the observed high rate of present fault movements, suggests that large-scale fluid withdrawal in the Houston metropolitan area may have accelerated or reinitiated movement on preexisting faults. Cause and effect have never been demonstrated, however, and the degree to which fluid withdrawal may amplify natural fault movements, if indeed it does at all, remains in doubt.

Cenozoic stratigraphy and structure of the northern part of the Virginia coastal plain

W. L. Newell reports that continued reconnaissance mapping of nearshore marine sediments underlying the uplands of northern tidewater Virginia has defined an upper Pliocene (post-Yorktown Formation) transgressive-regressive sequence of marine, estuarine, and fluvial deposits. The distribution of the deposits and facies relations record the beginnings of the Rappahannock River Estuary. The middle to late Pliocene proto-estuary was cut into the preexisting regressive facies of the lower Pliocene Yorktown Formation. Elsewhere in tidewater Virginia, these deposits appear to be correlative with the "Bacons Castle Formation" of the lower James River area.

Other data from maps and outcrops of Miocene and younger sediments suggest a complex pattern of subsurface faults and folds that correlate with major geophysical anomalies in the crystalline rocks below the coastal plain. A regional comparison of surficial deposits associated with the Sangamon estuarine system suggests that warping or minor faulting may have occurred along the zone of subsurface structures as recently as late Pleistocene.

This work is part of a larger ongoing study demonstrating the deformation (warping and faulting) of coastal plain deposits on the east coast. Tectonism in this area was formerly discounted. Although the effects of deformation are subtle, they are of importance in designing criteria of sensitive manmade structures.

Late Mesozoic and Cenozoic stratigraphic and structural framework near Hopewell, Virginia

J. B. Dischinger, Jr., reports that detailed mapping and power augering have defined a north-south striking and eastward-dipping zone of reverse faults extending at least 12 km near the confluence of the Appomattox River with the James River at the city of Hopewell, Va. The local coastal plain stratigraphic section includes Cretaceous, Tertiary, and Quaternary sediments. The regional occurrence of linear topographic features, geophysically determined subsurface lineaments, and Cretaceous outcrops at anomalously high elevations along both rivers indicates that local sediment deposition and geomorphology have been tectonically controlled. The reverse faults parallel the topographic and subsurface lineaments.

A trench dug across the fault zone exposed sediments of the Lower Cretaceous Potomac Group faulted over the Paleocene Aquia Formation. Undeformed upper Quaternary terrace sediments truncate the fault. At other localities along the Dutch Gap fault zone, Lower Cretaceous sediments are faulted against units as young as Pliocene. Minimum vertical displacement on the Cretaceous-Paleocene horizon is 20 m.

Structural similarities are evident between the Dutch Gap fault zone and several recently studied fault zones in Virginia and Georgia. This study adds significantly to an increased understanding of Cenozoic faults, their style of deformation, age, rate of deformation, and regional tectonic framework.

Northeastern United States seismicity and tectonics

Diamond core drilling has been completed at three localities along the Mesozoic border fault (Ramapo fault) in New York and New Jersey. Analysis of recovered fault-zone materials shows that the fault dips southeast

at 70° at Stoney Point, N.Y., 60° at Ladentown, N.Y., and 45° to 50° at Bernardsville, N.J. Zones of unconsolidated gouge, which are 0.5 to 1 m thick and rich in chlorite and calcite, mark the actual fault at depths as great as 150 m. Because the fault material is not healed, shear strength of the gouge zone is interpreted to be quite low.

Structural analysis of fault materials in cores shows that the rocks of the hanging-wall block commonly exhibit a monogenetic conjugate-fracture system consistent with right-oblique normal slip, although multiple slickensides indicative of left-lateral displacement also are common. Rocks of the foot-wall block (Precambrian gneiss or Paleozoic rocks) contain polygenetic fault fabrics and abundant evidence of multiple faulting. These results indicate that the dip of the Ramapo fault satisfies some earthquake hypocenters located in the Newark basin. The nonhealed gouge zones characteristic of the Ramapo fault may be indications of recent near-surface activity.

Many zones of recent seismicity lie off the Ramapo fault within the Reading Prong and are not, at present, known to be related to proven Mesozoic faults. However, they may be associated with phyllonitic ductile shear zones of probable Ordovician age. The distribution of ductile fault zones and brittle faults within the area of current seismicity has been determined in the area north of the Mesozoic Newark basin.

Brittle tectonics

The study of brittle tectonics in the southeastern United States has shown that the effects of Cenozoic tectonism are quite widespread but generally subdued by older geologic features. Paleozoic ductile fault zones in the southeastern Piedmont have had numerous periods of later brittle movement, but this movement probably occurred prior to the late Mesozoic. Late Mesozoic and Cenozoic faults and folds have formed independently of preexisting Paleozoic structures in response to a general east-west compression. In areas where water impoundment currently is producing seismic activity, stress release along subhorizontal joints may be the mechanism. A direct relation between recent seismicity and mapped geologic faults is still undefined because of the preliminary stages of investigation.

Foothills fault system, Sierra Nevada, California

The Foothills fault system extends from lat 37°30′ N. to 40° N. and is divided into two main zones, the western (Bear Mountains) and the eastern (Melones). The Bear Mountains fault zone has been mapped only as far north as lat 38°30′ N.; its northward continuation has been a matter of speculation and is significant if the fault zone marks the presence of a subduction zone. Results of this mapping extend the Bear Mountains fault zone due north along State Highway 49 on a line through Auburn and Nevada City, Calif., and suggest that the fault continues northward to link up with the Big Bend fault.

Evidence for extending the Bear Mountains fault zone north of Auburn stems primarily from comparing the range of characteristics of all faults in this northern area with those of the fault zone to the south. Similarities are that (1) a melange zone lies along and east of the fault zones, (2) the fault zones mark the westernmost serpentinite bodes of any size, (3) rocks to the west have a mappable stratigraphic sequence that abuts with angular disconformity into the fault zones, and (4) the "coincidence" of parallelism of the Bear Mountains and Melones fault zones in the south continues throughout their extent.

Tephra hazards from Cascade volcanoes

Stratigraphic studies east of Crater Lake, Oreg., show that the Mazama airfall tephra can be subdivided on the basis of texture and that some layers within the deposit traced laterally for tens of kilometers. Several of the layers are coarse and thick and form downwind lobes in southeasterly and northeasterly directions. At distances of 30 to 40 km downwind, six layers consist mostly of lapilli and are at least 40 cm thick.

Certain widespread, thin, and fine layers within the sequence indicate that eruption of the Mazama tephra was not continuous. Such thin layers mark at least two events of unknown duration when tephra eruption apparently ceased entirely. These pauses indicate that the hazard from an eruption like that of Mount Mazama would be somewhat less than the hazard from an event of the same magnitude that was continuous.

Deep electromagnetic soundings

Geomagnetic variation measurements in the Northeastern United States have been interpreted using differential geomagnetic sounding techniques to establish the presence of a regional geoelectrical current flow pattern that appears to coincide with the boundary of high-grade metamorphism and seismicity in central New England. The geoelectrical currents are concentrated in aseismic regions to the west and north of the Cape Ann–White Mountains seismic region. Earlier studies have identified a conductive region beneath Nova Scotia, which is also aseismic. Although no causal relation between the geoelectrical structure and seismic activity has yet been established, these observations may outline the northern extension of a major tectonic boundary suggested by the New York–Alabama lineament. Geomagnetic variations studies have identified a possi-

ble Proterozoic fracture zone of similar extent in the central North American basement.

ENVIRONMENTAL ASPECTS OF ENERGY

Effects of geology on highway construction, southeast Montana

The current construction of Interstate Highway 90 in southeast Montana south of Crow Agency is in Bearpaw Shale in the northern part and rises stratigraphically into the lower lower part of the Hell Creek Formation in the southern part toward Lodge Grass. S. P. Kanizay reports that extension of the highway southward to the Wyoming border will probably continue to take advantage of the geomorphic "bench" formed by the Bearpaw, except near the border, where the Hell Creek and Fort Union Formations will be crossed as the route aims at a connection with the Wyoming section, probably to take place in the Lebo Shale Member of the Fort Union Formation. The physical and engineering properties vary widely from geologic unit to geologic unit, requiring especially rigorous engineering design of the highway. Geologic problems encountered include expanding and shrinking clays, unstable slopes, and variable excavatability and erodibility. Also, the Lebo contains deposits of subbituminous coal that pose unique engineering problems.

Mining activities and seismicity, Powder River Basin

C. H. Miller and F. W. Osterwald have found, in their field seismic monitoring activities, that earth tremors are caused by blasting at large open pit coal surface mines, as well as by naturally produced earthquakes in the Powder River Basin of Wyoming and Montana. The basin is classified as a place of little or no risk of damage to life or property from naturally produced earthquakes, although the closer seismic surveillance in the last few years indicates slightly more seismic activity than previously thought.

Thousands of tonnes of explosives are detonated each year in coal mining activities in the basin, and the total energy that presently is expended by blasting each year greatly exceeds that expended by documented earthquakes during any year in the past. The maximum weight of explosive charge and the minimum amount of delay between blasts are regulated, however, so that no damage results to nearby structures and the residents are not disturbed.

Small earth tremors that originate near coal mines after blasting have been detected during three periods of operation of a mobile microseismic recording system near large mines in the basin. Most of these tremors occur within 30 min after blasts. The tremors are very small and are imperceptible to persons outside the mine area. These aftershocks probably are caused by redistribution of natural stresses as a result of loosening large amounts of coal and rocks by blasting.

One possible little exploited scientific benefit from the surface-mine blasting is the acquisition of seismograms from blasting for crustal or exploration studies. Normal-sized coal mine blasts have produced usable seismograms at magnifications of 200,000 and at epicentral distances of about 250 km but not at 600 km. Both compressional and shear waves are discernible on certain seismograms taken at optimum epicentral distances.

Toxic effects of trace elements examined in the northern Great Plains

Nutritional problems in livestock, particularly in cattle, that may be related to the geochemical environment of northwestern South Dakota and southwestern North Dakota appear to be much more widespread than originally thought. Preliminary sampling of forage plants and soils from several ranches in the area by J. A. Erdman and R. R. Tidball has yielded results that suggest a general copper deficiency aggravated by high levels of molybdenum in the forage. Moreover, the occurrence of rhenium in two samples of alfalfa is apparently the first time this metal has been found, or at least reported, in agricultural plants. Despite the statement by Venugopal and Luckey (1978) that there are no reports of rhenium in plant tissue, rhenium was reported for the first time in plants associated with claims from uranium mining districts (Myers and Hamilton, 1961).

A subsequent detailed biogeochemical study by L. R. Stone in the Flint Butte area at Ludlow, S. D., has provided strong evidence that the incidence of molybdenosis (a molybdenum-induced copper-deficiency disease) is linked directly to the local geology. Results from a sampling grid with 500-m centers at Flint Butte show low copper-to-molybdenum ratios and high levels of molybdenum, arsenic, and uranium in sweetclover and western wheatgrass collected from those sites located on the Tongue River Member of the Paleocene part of the Fort Union Formation. Samples from the underlying Ludlow Member showed more normal concentrations. The Tongue River Member is well known, at least in this area, for the several seams of uraniferous lignite. The pH of soil from the Tongue River Member was consistently high, allowing molybdenum to be more readily absorbed by the plants. Significant positive correlations of molybdenum and arsenic with uranium in the plant tissue are consistent with these associations reported in rocks of the Fort Union Formation (Pipiringos, 1966). These results provide fairly clear evidence that molybdenum-related problems in livestock, either frank or subclinical, should be expected in other localities in the region where a similar geologic setting occurs.

Origin of the Bald Range, southeast Wyoming

Surficial geologic mapping in the Evanston 30′×1° quadrangle, Wyoming, has required a reinvestigation of the Bald Range, a 65-km² area of barren hills in the southeast corner of the quadrangle. Bounded on the north by Henrys Fork and by its north-flowing tributaries Beaver Creek and Burnt Fork Creek on the west and east, respectively, the Bald Range is a complete anomaly in its area.

A. B. Gibbons and W. R. Hansen report that comparison with areas in either direction along the east-west trend of the north flank of the Uinta Mountains indicates that the site of the Bald Range should be occupied by uniformly drab-colored badlands of the Tertiary Bridger Formation separating flood plains and terraces surfaced by quartzite gravel from the Uintas. The Bald Range, in fact, is underlain by mudstone, sandstone, and coarse conglomerate of the partly red Wasatch Formation present in demonstrable outcrop no nearer than some kilometers to the south and by angular blocks of Paleozoic limestone and probably Mesozoic fine sandstone that are as much as 2 m across. Surface drainage is sharp where developed, but considerable areas are poorly drained, and many small areas consist of closed depressions. The Wasatch material is in great part steeply dipping with a tendency to east-west strikes. Individual beds, including beds of soft mudstone, can be traced for as much as 30 m but apparently not much farther.

The anomalous aspect of the Bald Range was noticed by Bradley (1936), who characterized it as a complex of moraines. Retention of physical integrity over large masses of fragile material does not seem consistent with ice transport, however. The almost total lack of material from the quartzite core of the Uinta Range, the only part of the region high enough to generate glaciers, also argues against a glacial origin for the deposit.

It is tentatively believed that the Bald Range is a landslide or landslides, whose age and precise mechanism of movement are uncertain. Relations at the north end of the range suggest that the floor of such a landslide would have to be about 30 m above modern drainage. This would be consistent with landsliding during the Pleistocene on a slope of less than 5°

Landslide-susceptible units, Kaiparowits Plateau

As a result of recent aerial and ground studies of landslides in the Kaiparowits coal basin area of southwest Utah, V. S. Williams has substantiated the earlier belief that the Tropic Shale of Late Cretaceous age and the uppermost part of the Wasatch Formation and overlying poorly consolidated volcanic sediments are the two principal units subject to landsliding. The Tropic Shale underlies and crops out beneath the coal-bearing Straight Cliffs Formation on the Kaiparowits Plateau. Numerous landslides occur on the east and south sides of the plateau.

The age of the most recent major slide movement in Coyote Gulch, just east of the Kaiparowits Plateau, has been bracketed by carbon-14 and archeological dating. One sample of charcoal (W–4336) and one sample of twigs and bark chips (W–4334) from two separate sites near the base of an alluvial fill graded to the slide toe give dates of 1,370±110 and 1,680±70 yr B.P., respectively.

Pottery shards at the surface of the same fill directly above the charcoal sample have been dated by Dr. Adrienne Anderson (Regional Archeologist, National Park Service) as between 600 and 1,250 yr old and probably between 625 and 1,000 yr old.

Williams and K. A. Sargent, thus, conclude that major slide movement produced at least 20 m of aggradation 10 km below the slide toe between 1,750 and 600 yr ago. Some of the aggradation may have occurred rapidly. Lake sediments on Dry Fork of Coyote Gulch just above its junction with Coyote Gulch indicate damming by rapid deposition of landslide alluvium in Coyote Gulch. The wide distribution of landslide-derived alluvium combined with this new evidence of recent and rapid deposition support the theory that burial by such alluvium may be a significant hazard in several areas.

The uppermost part of the Wasatch Formation and Tertiary volcanic sediments occur on the flanks of the Aquarius Plateau and underlie a dense caprock of Tertiary lavas and ash-flow tuff. Here, also, the sediments have failed, resulting in numerous landslide blocks. A map (Miscellaneous Investigations Series I-1033) prepared by H. K. Fuller, Williams, R. B. Colton, and J. E. Holligan, showing areas of landslides and potential landsliding in the Kaiparowits coal-basin area, should be most useful to road construction and townsite planners and coal-area developers.

Sargent and Williams anticipate that, when coal is developed on the northern part of the Kaiparowits Plateau, considerable impact will fall on the small town of Escalante. A detailed geologic map of the Escalante 7½-min quadrangle is being prepared to provide information on geologic materials and processes at the townsite.

The town presently occupies two quartzite gravel terraces of the Escalante River about 20 and 30 m above the stream bed. The area covered by the town probably constitutes the finest gravel deposit in the quadrangle, but other similar deposits exist nearby to the west. Future expansion of the town probably will extend onto a lower fine-textured terrace and onto slopes of sheetwash alluvium over the Carmel and Entrada Formations.

North of Escalante, movement of a debris flow during Holocene time has blocked and diverted Pine Creek, a major tributary of the Escalante River. The creek has cut a new channel below the toe of the slide, but renewed movement of the slide could result in blockage of drainage, causing flooding. Six levels of terraces extending up to 130 m above Pine Creek probably indicate a complex history of uplift and downcutting punctuated by episodic pulses of landsliding that released large quantities of coarse volcanic boulder alluvium into the stream.

The 1:24,000-scale Escalante map and the 1:125,000-scale maps of geology, hydrology, and derivative subjects of the Kaiparowits Plateau Miscellaneous Investigations Series (I-1033) are expected to be of importance in land-capability assessments as mining, pipeline routing, and development occur in that remote area.

Computer-assisted reclamation potential mapping, Gillette, Wyoming

In the Gillette 30′×1° quadrangle, Wyoming, the highest estimated reclamation potential within the area of strippable coal is on upland divides between major eastward-flowing streams, such as the Belle Fourche River, Caballo Creek, and Donkey Creek. Factors that contribute to this finding include presence of alluvial valley floors in the stream valleys, highest quality scenery in the valleys, better soil in valleys, and the existence of the best cropland and range in the valleys. Other factors that influence estimates of reclamation potential are the choice of factors and weighting assigned to them by the investigator. D. W. Moore, in consultation with J. N. Van Driel, recently finished refinements of a computer program that allows weighting and combination of various factors and graphic portrayal of the various values in map form.

HYDROLOGIC ASPECTS OF ENERGY

When considering the options in the Nation's energy future, many items other than the absolute availability of energy resources must be factored into the development equation. Water is one such factor. Water is required in the generation of electricity, in the conversion of coal and oil shale to liquid and gaseous fuels, in mining operations, in slurry pipelines, in support of the population expansion necessary to mine the resources and refine the fuels, and in a wide range of other needs. In addition, some mining and industrial operations can affect the availability of water for other purposes and the quality of the water remaining.

The USGS program of water resources studies covers topics such as potential local hydrologic impacts, areal hydrologic assessments, development of laboratory analytical techniques for determining water-quality parameters, and computer modeling techniques for predicting future hydrologic conditions under various development scenarios.

Organic solute transport by waste waters produced by in situ oil shale retorting

H. A. Stuber (1979) reported that a method for assaying aromatic amines in oil shale retort waters was developed. The aromatic fraction was isolated first by selective absorption on and desorption from XAD-8 resin. This fraction was next liquid-chromatographed on a reverse phase C-8 silica column. The best peak resolution was obtained with a 5-μm particle-sized packing and inclusion of a NaH_2PO_4 (pH 7) buffer in the mobile phase.

An automated analysis method for the thiocyanate ion, used as a tracer solute for retort water, was developed by J. A. Leenheer (1979). The method is based upon the use of the Technicon autoanalyzer and measurement of the colored ferric thiocyanate complex. Colored organic interferants were removed by adsorption on XAD-8 resin contained in an inline column. Twenty samples per hour were analyzed for thiocyanate with a limit of detection of 10 μg/L.

In a soil column study of retort water-soil interactions, Leenheer and Stuber found that ion exchange of calcium and magnesium in the soil for ammonium in the retort water caused a calcium carbonate precipitate that nearly plugged the soil column. Distilled water leaching of the soil following its reaction with retort water extracted large amounts of humic and fulvic acids and caused additional plugging because of the dispersion of ammonium saturated soil colloids. A distilled water leachate study of a soil sampled at the DOE Rock Springs, Wyo., experimental in situ oil shale retorting site found high concentrations of sodium, calcium, and magnesium chlorides, sulfates, bicarbonates, and nitrates. The presence of high nitrate concentrations (as much as 9,700 mg/L) in the initial soil leachate fraction was a major finding of the study.

Methodology for hydrologic assessment of potential surface-mine sites

R. F. Hadley, D. G. Frickel, L. M. Shown, and R. F. Miller evaluated methodology for assessment of the effects of surface mining and reclamation on the hydrologic system for three potential mine sites in southeastern Montana, south-central Wyoming, and northwestern New Mexico.

Assumed postmining topography was the result of "lifting off the overburden, removing the coal," to a maximum depth of 61 m, and "placing bulked overburden back where it was before mining." Any changes in elevation were a function of the thickness of the coal relative

to the thickness of overburden that had been "bulked" 20 or 25 percent. Premining and postmining runoff volumes were estimated with the Soil Conservation Service (SCS) method and by basin-characteristic regression models. The SCS method was favored for the Wyoming and New Mexico sites because it is more applicable to small basins and it addresses important effects of soils and vegetation on runoff at these sites. Estimates of premining and postmining soil loss from different landforms were made with the Universal Soil Loss Equation. Estimates of sediment yields from small basins were made by applying a sediment delivery ratio to the weighted mean soil loss and by measurements of sediment deposition in stock ponds. Postmining estimates of streamflow and sediment yield were made with the assumption that reclamation would be complete when the soils, vegetation, and stream channels had stabilized to premining conditions. Postmining estimates of peak discharges, streamflow volumes, and sediment yields were less than premining estimates because of assumed decreases in gradients of steep slopes and the use of deep alluvium and (or) pulverized sandy bedrock for soil on areas where soils were formerly shallow or otherwise unfavorable for vegetation habitats.

Future lignite mining and impacts on important Claiborne aquifers, south-central Arkansas

Lignite beds ranging in thickness from a few centimeters to 5 m or more are interbedded in the Sparta Sand and the Cockfield Formation of the Claiborne Group of Tertiary age. J. E. Terry and A. H. Ludwig (Terry and others, 1979) report that surface mining this lignite may have a significant impact on the Claiborne aquifers, which are extensively tapped by municipal, industrial, and domestic wells. The area in which these aquifers crop out (or subcrop beneath alluvial or terrace material) covers most of 16 counties in south-central Arkansas.

Preliminary estimates of saturated thicknesses of the two Claiborne aquifers in the outcrop area range from 0 to 180 m for the Sparta Sand and from 0 to 120 m for the Cockfield Formation. In much of the area, the top of the saturated zone is at a depth of 15 m or less below land surface. Thus, for mine cuts of 45 to 60 m, potential dewatering problems can be expected to occur. Groundwater modeling, to define more clearly existing hydrologic relations and to predict the possible impacts of surface mining, is now in progress.

Effects of strip mining on runoff, Illinois

Peak discharges for streams draining strip-mined land are reduced up to 90 percent compared to those of streams draining unmined land, according to T. P. Brabets. Regional flood-frequency equations were used to compute the 2-yr flood for streams draining unmined land. These values ranged from 0.78 to 2.13 $m^3/s/km^2$. On nearby basins having part of their basin strip mined, 2-yr flood peaks ranged from 0.063 to 0.39 $m^3/s/km^2$.

Wide variations in water quality in final cut impoundments, Illinois

Water-quality measurements in 2 of 15 final cut lakes in Illinois showed marked stratification in water chemistry. The two lakes had low pH values ranging from 2.9 to 5.7 in the surface layer, with significantly higher pH values ranging from 6.0 to 6.5 in the bottom layers of both lakes, according to D. B. Peart. One of the two lakes showed marked stratification in dissolved solids. Variation in specific conductance of 5,150 μmho at one site and 4,000 μmho at another was observed in a 0.5-m vertical span. Two very high total iron values also were recorded in the same lake, 5,500 and 1,400 μg/L.

Coal-mining effects on surface-water quality of Levisa Fork basin, Kentucky and Virginia

J. E. Dysart reports that changes in the character of the surface-water quality in the Levisa Fork basin from Big Rock, Va., to Paintsville, Ky., are attributed to coal-mining activity, regulation of streamflow by reservoirs in the area, and increases in overland runoff.

Increases in pH, concentrations of dissolved constituents, and sediment yield appear to be associated with increases in coal production in the watersheds of the 22 tributary streams investigated in the study area. In mined watersheds, 13 of 17 stations had low flow pH values exceeding 7.9. In the unmined Dicks Fork basin, the pH was as low as 6.2 for each of 533 d of continuous record, but a pH as high as 8.0 occurred on only 9 d. Calcium and sulfate were the dominant ionic constituents in the surface water of the Levisa Fork, and they decreased downstream apparently because of deposition in the four reservoirs in the study area. For example, the mean concentration of calcium was 45 mg/L at the upstream Big Rock, Va., site and decreased to 25 mg/L downstream at Paintsville, Ky. Similarly, sulfate decreased from a mean 164 to 80 mg/L, and dissolved solids (residue on evaporation) decreased from a mean of 337 to 188 mg/L. In the unmined Dicks Fork basin, the mean values for calcium, sulfate, and dissolved solids were 5.8, 18, and 53 mg/L, respectively. Sediment yield from this unmined basin was 88 t/km^2. Sediment yields from mined basins ranged from 256 to 630 t/km^2.

Coal mining impacts surface-water quality, western Maryland

Coal mining has had a significant impact upon the hydrology of western Maryland. The North Branch of the Potomac River basin has a long history of both deep and surface mining. During low flow in 1979, the pH of

this stream was recorded as low as 3.9, and conductivities as high as 780 μmho/cm. Concentrations of total iron and manganese were observed in excess of 3,200 and 850 μg/L, respectively, and dissolved sulfate exceeded 320 mg/L. Samples with similar chemical-quality characteristics were obtained from Georges Creek, whose watershed also is mined intensively for coal.

The Savage River watershed is adjacent to Georges Creek basin and is composed largely of protected forest lands. The Savage River is characterized by waters with a pH of 7.9, conductivities less than 83 μmho/cm, and total iron and manganese of less than 210 and 90 μg/L, respectively; dissolved sulfate was 18 mg/L.

Hydrology of coal areas, northwestern New Mexico

H. R. Hejl, Jr., has developed regression equations to predict ephemeral streamflow characteristics in the San Juan Basin in northwestern New Mexico. Preliminary results indicate that the standard error of estimate for predicting annual runoff using drainage area as the independent variable was 142 percent, with 8 of 13 gaged sites used in the analysis having only 1 water year of data. The coefficient of regression, when relating drainage area to annual runoff, was significant at the 1-percent level. Preliminary results also indicate that it is feasible to predict streamflow characteristics using hydrologic soil group classifications based on runoff potential. The standard error of estimate for predicting peak discharges with recurrence intervals of 2, 5, 10, 25, 50, and 100 yr using active-channel width as the independent variable averaged about 50 percent, and the regression coefficient was significant at the 1-percent level. Using drainage area to predict peak discharges resulted in a standard error of estimate that averaged about 60 percent and a regression coefficient significant at the 10-percent level. The standard error of estimate averaged about 45 percent when active-channel width and drainage area were related to peak discharges in multiple regression analyses.

Premining ground-water hydrology in potential surface-mine areas, east-central Ohio

J. O. Helgesen and E. J. Weiss report that premining ground-water systems in five small watersheds are being studied as part of an investigation of the effects of surface mining on water resources. Stratified sedimentary rocks underlie the watersheds, and each site contains two major perched saturated zones within the top 75 m. These zones generally constitute local flow systems; recharge is mostly from local precipitation, and discharge is mostly as downward leakage, springflow, and stream base flow. System analysis is being facilitated by the development and calibration of quasi-three-dimensional digital flow models. Shallow ground water is commonly of the calcium bicarbonate type, whereas deeper water is of diverse types and generally more mineralized.

Relation of acid discharge to daylighting operation, central Pennsylvania

L. A. Reed and R. A. Hainly have found that daylighting operations in the Anna S mine have increased the amount of acid being discharged to Babb Creek. About 15 percent of the abandoned deep mines have been removed by daylighting, and acid discharge has increased about 100 percent. Water discharge from the mines remains about the same (0.04 m^3/s), but the acidity (as $CaCO_3$) has increased from 350 to 700 mg/L. However, the area is still unstabilized, and the acid discharges may be reduced significantly when the area is regraded and reseeded.

Investigation of hydrologic effects of coal mining, southern West Virginia

Preliminary findings of J. W. Borchers, T. A. Ehlke, S. C. Downs, and M. V. Mathes indicate several marked differences in the hydrologic environment of three small deep- and surface-mined stream basins as compared to two unmined control basins. Initial results indicate that deep- and surface-mined basins may exhibit different streamflow, ground-water flow, and ground- and surface-water quality characteristics than unmined basins. Stream flood peaks appear reduced in magnitude in the mined basins, with runoff to streams delayed somewhat. Preliminary flow duration analyses show that actively mined basins have a higher discharge per square kilometer of drainage area at 90 percent flow duration (that is, during low flow periods) than unmined basins. Streams in mined basins contain considerably higher concentrations of dissolved solids and are of different water type than streams in unmined basins. An interesting phenomenon, consistently alkaline mine drainage waters, was observed in areas of active mining. It is believed that limestone dusting of mine interior walls, floors, and ceilings (which is required by safety laws and reduces the explosiveness of coal dust) acts to neutralize mine drainage waters that would otherwise be quite acidic. Water wells above active deep mines may have lower yields and lower specific capacities than wells in unmined areas. A significant amount of ground water may be diverted from valley aquifers by deep mines that underlie valleys. Suspended sediment concentrations and loads are higher in streams where the land surface has been disturbed whether by surface mining or other activities. Silt and clay fractions of the suspended sediment load are higher than the sand fractions in areas where the land surface has been disturbed. Number and diversity of benthic invertebrate species is greater in unmined basins than in mined basins.

GEOLOGY AND HYDROLOGY RELATED TO NATIONAL SECURITY

The USGS, through interagency agreements with the DOE and the DOD, investigates the geologic, geophysical, and hydrologic environment of each site within the NTS where underground nuclear explosions are conducted. In addition, the USGS compiles geologic and hydrologic information pertaining to underground nuclear explosions conducted within the U.S.S.R. Geologic and hydrologic data are needed to assess the safety, engineering feasibility, and environmental effects of nuclear explosions. The USGS researches specialized techniques needed to acquire geophysical and hydrologic data at nuclear explosion sites; some of the results of this research are summarized below.

Containment of all underground nuclear tests (no release of radioactivity into the atmosphere) is a national commitment. Containment requires an expert appraisal of the geologic, geophysical, and hydrologic environment for each test. The USGS, through the Special Projects Branch, is providing this expertise.

Geologic and geophysical investigations at the NTS in support of the Los Alamos Scientific Laboratory, the Lawrence Livermore Laboratory (LLL), the Sandia Laboratories, and the Defense Nuclear Agency have continued to develop a clearer understanding of Quaternary alluvium, Tertiary volcanic rocks, and Paleozoic carbonate and clastic rocks and their structural setup in the Great Basin. Interdisciplinary communication within the USGS is the key to this clearer understanding. As new drill-hole data become available, isopach maps of the alluvium and total Cenozoic fill under Yucca Flat have been updated and refined by A. T. Fernald and D. L. Healey. P. P. Orkild and E. C. Jenkins provided maps, cross sections, and lithologic logs of the Pahute Mesa area to LLL. A report presenting a map of the tuff aquitard in Yucca Flat, NTS, was published. Another report was published by G. E. Brethauer on physical-properties data from Pahute Mesa using the GRASP storage and retrieval system.

Research is being conducted by D. C. Muller on a continuing basis to improve the geophysical logging investigations. Logging tools and measurement techniques are being upgraded continually to improve the quality of the data. Experiments are designed to test new tools and new techniques to increase the number of measured physical parameters needed to characterize the emplacement media for nuclear detonations. Correlation techniques are being developed to provide estimates of mineralogic content and rock parameters such as grain density and water content from geophysical logs. Interpolation procedures are used to estimate physical properties of environments lying between drill holes in known areas, and extrapolation procedures are used in less well-known areas.

An extensive program was undertaken by W. L. Ellis, R. D. Carroll, J. D. Kibler, and J. E. Magner to document explosion-induced relative displacements across faults in the vicinity of an underground nuclear detonation. The problem of induced fault motion is of critical concern in underground siting of command centers and missile systems. A total of 27 fault documentation stations was established within a tunnel system associated with an underground nuclear test. The purpose of the program was to determine which faults are most susceptible to induced motion and what magnitude of displacements may occur. Results of the program to date indicate that one fault, located relatively near the site of detonation, underwent a final induced displacement of 3.1 m. Displacements of less than 0.2 m were noted at greater distances from the detonation site. Examination of fault geometries with respect to the detonation location and the sense of induced fault motion indicate that the displacements are driven by ground motion from the explosion and are not the result of tectonic stress release. As yet, there appears to be no quantitative rationale for determining which faults are most likely to move. Data and experience from this program are providing important empirical information that may be useful in developing and verifying predictive capabilities for induced fault motion.

Five subsidence sinks overlying underground nuclear explosion sites at Yucca Flat, NTS, were equipped with instruments to evaluate these sinks as potential recharge sites. Preliminary indications are that, during most precipitation events, most of the water accumulating in the sink bottoms originates from precipitation on the surface area of the individual sink rather than inflow from the surrounding drainage area.

A treaty between the United States and the U.S.S.R. governing conduct of underground nuclear explosions for peaceful purposes has been concluded but not yet ratified. This treaty provides that, under certain conditions, the country conducting a peaceful nuclear explosion (PNE) will allow teams from the other country to be present at the site to verify certain aspects of the project. One of the teams will have as its objective the verification of the geology of the project site and the close-in geology at the explosion point. Development and training of verification teams have been assigned to the DOE.

A Comprehensive Test Ban Treaty currently being negotiated between the United States and the U.S.S.R. would ban all underground nuclear explosions. This treaty provides that onsite inspections (OSI) would be allowed in case of suspected treaty violation. Details of

OSI plans are classified because the treaty is presently under negotiation, but the USGS is providing input to verification-technology planning and operations. The Special Projects Branch of the USGS is represented on working groups that provide earth science expertise to the DOE Verification Technology Planning Committee in regard to PNE's and OSI's.

Cooperative work with the DOD and other U.S. Government agencies on areas of underground nuclear explosions in the U.S.S.R. was continued by W. J. Dempsey, S. M. Bonham, Salilh Faizi, and Jack Rachlin. The study of Soviet deep seismic sounding data has provided information on the structure and physical properties of the crust and upper mantle in relation to the propagation of seismic waves, especially in areas of nuclear explosions and monitoring stations.

RELATION OF RADIOACTIVE WASTES TO THE GEOLOGIC AND HYDROLOGIC ENVIRONMENTS

Research on radioactive-waste repositories in geologic formations and the assessment of environmental effects of existing repositories continued in 1979. The search for repositories is concerned with the disposal of high-level and transuranic wastes. High-level wastes include fission products that initially have a high level of beta and gamma radiation and a high rate of heat generation; they also include transuranic elements with a long toxic life. Transuranic waste contains long-lived alpha emitters at concentrations greater than 10 nCi/g and generates little or no heat. Studies of existing repositories involve low-level wastes that consist, in part, of miscellaneous solid materials that have become contaminated through use and of products of reactors and fuel reprocessing plants.

The USGS continued its research program to complement and augment the DOE program for geologic disposal of high-level radioactive waste. In general, the USGS program is designed to provide concepts, methods, data, and analytical results that can be used by Federal agencies having operational and regulatory responsibilities for radioactive waste disposal. A primary objective of the program is to identify regions whose geologic and hydrologic characteristics embody relatively independent multiple natural barriers to the movement of waste nuclides. In addition to studies of areas whose geologic and hydrologic characteristics would appear to make them suitable for locating radioactive waste repositories, the program includes generally applicable research in geology, hydrology, geophysics, and geochemistry.

The DOE financed the investigations of low-level radioactive waste disposal at Oak Ridge National Laboratory, Tenn., regional studies to identify potential geologic repositories for high-level wastes, investigations of the Waste Isolation Pilot Plant site in New Mexico and the Idaho National Engineering Laboratory site, and some geophysical research.

Relation of repository size to its period of assured safety

E-an Zen (1979) examined repository size as a factor in design and concluded that, if all else were equal, it would appear desirable to have many small repositories rather than a few large units. Zen argues that, in a ground-water breach of a radioactive waste repository resulting in leaching of the nuclides, the net quantity of nuclides available for short-term transportation into the biosphere is the major concern, not the fraction leached as such. This quantity depends on many factors, but, if leaching is rapid and retentivity low, large migrations might occur. He demonstrated mathematically that, if the basic objective is to keep the total escaped amount of any particular radioactive isotope below some specified value, the time needed to attain a specific level of safety varies exponentially as the amount of waste originally emplaced in the repository.

Repository size, however, is only one of many factors in risk assessment; if the probability of a breach is size independent, the proliferation of repositories increases the chance of a breach somewhere. Construction of many small units also involves other technological and institutional problems. A compromise consideration is construction of a few large repositories, each consisting of water-tight compartments resistant to interaction after a breach (or separate repositories at the same over-all site). The nature and quality of backfill may become critical factors.

Contribution to National Bureau of Standards handbook on rock salt properties and minerals

The National Center for the Thermodynamic Data of Minerals (Data Center) at the USGS cooperated with the Office of Standard Reference Data at the National Bureau of Standards, Department of Commerce, in preparing a handbook on the properties of rock salt and its component minerals. The Data Center reviewed and summarized the data for the geology, geochemistry, and geophysics of salt deposits. Other chapters prepared by other Data Centers in the National Standard Reference Data System included those on physical properties, thermodynamic properties, and transport properties of rock salt and its component minerals. The primary application of the evaluated data is to the design of safe nuclear waste repositories in rock salt.

STUDIES OF LOW-LEVEL RADIOACTIVE WASTE DISPOSAL SITES

Radionuclide transport, in glacial drift, Sheffield, Illinois

The glacial deposits underlying the disposal site at Sheffield, Ill., include a continuous pebbly sand unit whose high hydraulic conductivity (about 0.9 m/d) relative to adjacent till and silt deposits makes it the predominant pathway for shallow ground-water flow and for any migration of radionuclides that may reach the water table. According to J. B. Foster and J. R. Erickson, the unit extends across the middle of the site and beyond the site boundaries to the northeast, west, and southwest. The pebbly sand is unsaturated in the east-central part of the site and saturated in the northern part.

Continuous soil cores were collected during construction of an 88-m horizontal tunnel beneath four burial trenches. The soil moisture extracted from the cores contained tritium in concentrations generally less than 10 Ci/L except for a section beneath trench 11 where concentrations reached 100 Ci/L, and beneath trench 1 where concentrations were as high as 44 Ci/L. No gamma-ray emitting waste radionuclides were detected in the soil. Any radionuclides other than tritium that may be contained in the trench leachate are apparently being adsorbed by the soil beneath the trench floors.

Tritium migration in glacial drift, Palos Forest Preserve, Illinois

A burial site for radioactive wastes is located at Palos Forest Preserve, Ill., on the former grounds of the Argonne National Laboratory, about 50 km southwest of Chicago. In analyzing data on tritium (^3H) concentrations in ground water and glacial drift at this site, J. C. Olimpio found that flow through alternating layers of clay, silt, and sand has carried tritium at least 30 m vertically and 400 m horizontally in less than 35 yr. Average tritium concentrations in ground water farthest from the site are 0.01 to 1 percent of the concentrations directly beneath the site.

Hydrologic studies of the unsaturated zone, Beatty, Nevada

The hydrology of the unsaturated zone at the burial site near Beatty, Nev., northwest of Las Vegas, is being studied by W. D. Nichols. Matric potentials measured by means of soil thermocouple psychrometers at depths of 3, 4, 5, 6, 7, and 10 m during the past year have ranged from about −20 bars to −80 bars. Seasonal soil temperatures ranged from 9.3°C at 3 m to 3.4°C at 10 m. Monthly profiles of soil-moisture content, based on neutron moisture meter measurements, strongly suggest small amounts of downward moisture movement, usually amounting to volumetric moisture-content changes of not more than 0.5 percent. Analyses of similar stoney soil in southern Nevada suggest an unsaturated hydraulic conductivity in the range from 1×10^{-5} to 1×10^{-4} cm/d for the matric potential and volumetric water content measured at the study site.

Relation of vertical and horizontal hydraulic conductivity of till, West Valley, New York

Vertical and horizontal hydraulic conductivities of the clay-rich till containing burial trenches at West Valley, N.Y., were studied to determine the degree of anisotropy. Initial computer simulation of pressure heads in a cross section perpendicular to the north trenches, when water levels in the trenches were high in February 1976, suggested that the horizontal hydraulic conductivities of the till might be 100 times greater than the vertical (Prudic and Randall, 1977, p. 9). Laboratory measurements on cores, presented by Fickies and others (1979), showed horizontal conductivities to be 40 times greater than the vertical (although only half of the overburden pressure was applied in the horizontal direction, which may have affected the observed difference). These results are inconsistent with or could not be substantiated by field and laboratory investigations and computer analysis. Field observations of the migration of water from the trenches indicated that the movement was greater vertically than horizontally (Prudic and Randall, 1977, p. 15). Results of laboratory tests where no confining pressures were applied to the samples indicated that the average values for vertical hydraulic conductivity were two times greater than the horizontal. Preliminary analysis by R. G. LaFleur of several vertically oriented thin sections of the till did not show any preferred horizontal orientation of the clay grains. Computer-simulated pressure heads for February 1978, after water was pumped from the nearly full trenches, did not match the observed ground-water levels using the anisotropic relation suggested by the pressure-head simulation for February 1976. These results indicate that the till can be treated as an isotropic medium for the purposes of the current model study.

Strontium-90 transport in limestone solution cavities at Oak Ridge National Laboratory, Tennessee

From 1946 through 1951, radioactive solid wastes at Oak Ridge National Laboratory (ORNL) were disposed of by shallow trench burial in Burial Ground 3. This disposal site is underlain at shallow depth by the Chickamauga Limestone (Ordovician), which is known to contain small solution cavities. Studies by D. A. Webster (USGS) and A. M. Stueber (ORNL) (1980) suggest that ^{90}Sr leached from the buried waste is being transported by ground water through a network of linear solution openings in the Chickamauga. The net-

work, trending northeast-southwest, is believed to occur near the contact of unit G, a limestone, with unit F, a calcareous siltstone and shale. Small concentrations of ^{90}Sr (<0.01–1.98 pCi/ml) were found in wells around the perimeter of the site, with the largest concentrations in wells to the northeast and to the southwest. About 350 m to the northeast of the burial ground, a tributary of Whiteoak Creek contained small but measurable concentrations of ^{90}Sr (<3 pCi/ml) starting immediately downstream from its crossing of the contact between units F and G. About 640 m southwest of the site, a tributary of Raccoon Creek contained small concentrations of ^{90}Sr (0.09–0.18 pCi/ml) near a point where it crosses these stratigraphic units.

REGIONAL STUDIES

Hydraulic characteristics of caprock on Salt Valley anticline, Grand County, Utah

Three exploratory test wells were drilled by the DOE in Salt Valley, Utah, as part of a study to evaluate the suitability of bedded salt in the Paradox Basin as a host rock for radioactive wastes. M. S. Whitfield reported that caprock, salt, and interbeds of the Paradox Member of the Hermosa Formation were penetrated and that the depth to the caprock-salt interface ranged from 163 to 191 m. Approximately the upper 100 m of caprock was unsaturated. Within the saturated part of the caprock, hydraulic heads generally decreased with depth and to the southwest, and ion concentrations in the water generally increased with depth.

The hydraulic conductivity of the caprock, as determined from pumping tests, may be on the order of 5×10^{-3} m/d; as a result, ground-water flow rates in the caprock are probably very low. A carbon-14 specific activity for caprock water yielded an uncorrected age of >36,000 yr. The hydraulic conductivity of the salt and interbeds is probably $<1\times10^{-4}$ m/d.

Hydrologic conditions near salt domes in north-central Louisiana

A group of salt domes in the gulf coast region is under study by the DOE to determine if conditions are suitable for developing a high-level waste repository. In support of this study, the USGS is studying the hydrology in the vicinity of Rayburns dome in Bienville Parish and Vacherie dome in Webster and Bienville Parishes.

Hydrologic data near the two domes were collected through 1979 and published by G. N. Ryals and R. L. Hosman (1980). The principal aquifer in northwest Louisiana is the Wilcox Group. Ryals found that water levels in four small-capacity wells in the Wilcox aquifer on the flanks of Rayburns salt dome are about 52 m above the National Geodetic Vertical Datum of 1929 (NGVD). Several kilometers from Rayburns dome and up the regional hydraulic gradient, water levels are about 46 m above the NGVD. The higher water levels at Rayburns dome suggest that the Wilcox is being recharged locally. On the edge of Vacherie dome, the water level in a well screened in the Wilcox is significantly higher than in nearby wells around the dome. Recharge probably is occurring at the Vacherie dome, but the data are inconclusive. The Wilcox could be receiving recharge at both domes through sand beds that have been uplifted to or near the land surface during dome growth.

NEVADA TEST SITE AND VICINITY

Geologic, hydrologic, and geophysical investigations were conducted at the NTS and contiguous areas in Nevada, south of lat 39°N. in an effort to locate and define areas suitable for developing high-level repositories and to identify suitable host rocks for the waste.

These investigations included (1) field reconnaissance of potentially suitable areas for locating repositories, (2) geologic mapping and mineral-resource appraisals of granitic masses, (3) hydrologic studies of selected areas, (4) test drilling to characterize selected areas, and (5) an inventory and study of geophysical methods to determine the spatial characteristics of potential repository sites.

Extensive geophysical studies consisting of gravity, magnetic, seismic, galvanic electrical, and electromagnetic methods, combined with geological investigations, provided sufficient evidence for the termination of exploration effort at two locations at the NTS. The potential waste emplacement medium at both locations was an inferred intrusive body. The DOE rejected both locations on the basis of USGS investigations that revealed structural complexity and faulting, inferred a lack of competent unaltered rock within repository depth limits, and indicated a potential for mineralization with the possibility of future human intrusion by mining.

Paleohydrology of the southern Great Basin

Knowledge of the magnitude of water-table rise and of the resultant shortening of ground-water flow path during Pleistocene pluvial climates is mandatory for an evaluation of the NTS or other arid-zone sites as repositories for high-level or transuranic-element radioactive wastes. I. J. Winograd and Gene Doty reported that the distribution of calcitic veins filling fractures in alluvium and of tufa deposits between the Ash Meadows, Nev., spring discharge area and the NTS

indicates that the potentiometric level in the regional Paleozoic carbonate-rock aquifer may have been a maximum of 48 m higher during the Pleistocene pluvial periods and that the flow path may have been 14 km shorter. Use of the underflow equation (relating discharge to transmissivity, aquifer width, and hydraulic gradient) and assumptions regarding pluvial recharge independently suggest that a rise in the potentiometric level in the carbonate-rock aquifer of more than 61 m beneath Frenchman Flat was implausible during Wisconsin(?) time, particularly if the ground-water base level then was approximately at the same altitude as that at the modern spring lineament at Ash Meadows. Future rises of over 30 m beneath Frenchman Flat appear unlikely.

Neither the cited rise in the potentiometric level in the regional carbonate-rock aquifer nor the shortened flow path precludes utilization of the NTS as a repository for high-level or transuranic-element radioactive wastes. Deep-water tables and long ground-water flow paths characterized the region during the Pleistocene Epoch and presumably will characterize it during future pluvials.

Characterization of buried intrusive using induced polarization profiles

Induced polarization (IP) profiles were made by D. B. Hoover at a proposed repository site at Wahmonie Flat to characterize a buried intrusive and to determine whether it might be a suitable host medium in a waste repository. The IP data indicated a large body of rock containing highly polarizable material at a depth of about 300 m, which is probably the intrusive mass of interest. The large IP values suggested a sulfide content of about 2 percent. Because there is an abandoned silver mine in the area, the site appeared to be an attractive target for mineral exploration and possible intrusion of any repository that might be developed. Therefore, the DOE decided to discontinue exploration of the site.

Sensitivity analysis of ground-water flow model

R. K. Waddell and D. I. Leap reported that sensitivity analyses of a regional ground-water flow model of the NTS and vicinity were performed in 1979 using various statistical techniques. Results of the cooperative study with DOE indicate that simulated hydraulic gradients in the vicinity of a hypothetical nuclear waste repository in the southwestern part of the NTS are most sensitive to values assigned for hydraulic conductivity of rocks in the repository area and in the Eleana Range (northern part of NTS), the amount of recharge on Pahute Mesa (northwestern part of NTS), and the correlation structure describing the relation between input and output functions corresponding to recharge and discharge.

Use of plant fossils to interpret Pleistocene and Holocene climates and hydrologic conditions

A significant concern in developing a waste repository is the prediction of future climatic conditions with attendant changes in hydrologic regime that can affect the transport of radioactive wastes to the biosphere. W. G. Spaulding reported that the identification and radiocarbon dating of vegetative matter found in ancient packrat middens allow a deduction of ancient climates and resulting precipitation and an estimation of ground-water recharge. Initial results indicated that middens at and near the NTS, at elevations ranging from about 1,190 to 1,830 m, can yield paleoclimatic data as old as 40,000 yr B.P. Similar climatic conditions in the future can be expected to produce similar hydrologic conditions.

WASTE ISOLATION PILOT PLANT SITE, SOUTHEASTERN NEW MEXICO

Trend analysis of formation elevations

Trend analysis methods were used by G. E. Brethauer and R. P. Snyder to map known or suspected structural anomalies in the vicinity of the waste isolation pilot plant site. Computer-generated structure contour maps were prepared of three horizons. By adjusting standard contouring variables such as radius of search and minimum number of points used for interpolation, maps were obtained that compared very favorably with those contoured by hand. Trend surfaces then were generated mathematically for each horizon. A cubic equation produced the best-fit surface for the upper two horizons, and a quartic equation produced the best-fit surface for the lowermost horizon. Finally, computer-generated residual contour maps were prepared by subtracting the trend surfaces from the observed structure contour maps. The resultant maps showed all the structural anomalies that were known or suspected, as well as several unsuspected anomalies.

IDAHO NATIONAL ENGINEERING LABORATORY

Geohydrologic conditions interpreted from deep well in eastern Snake River Plain, Idaho

Information on the geohydrology of the deeper parts (below 450 m) of the Snake River Plain has been meager because wells had not penetrated beyond this depth. A 3,159-m well (INEL–1) was drilled in 1979 by the DOE to obtain information on the possibility of liquid radioactive wastes moving downward in the Snake River Plain aquifer. The rocks penetrated by the well are principally volcanic–basalt with interbedded sediments, rhyolite (nonwelded and welded ash-flow tuffs), and rhyodacite(?) (ash flow). Below 488 m, the permeability

of the rocks decreases because of filling of fractures by secondary minerals. J. T. Barraclough (1980) subdivided the rocks into three aquifers: the upper near-surface Snake River Plain aquifer (highly permeable basalt), the lower Snake River Plain aquifer (less permeable basalts and sedimentary strata), and rhyolites beneath the Snake River Plain aquifer (markedly less permeable). Separating the aquifers are aquitards composed of amygdaloidal basalt, altered clay-rich strata, and altered tuffaceous sedimentary strata. With depth, the artesian head increases, and the water becomes more mineralized. The deeper water is a soft sodium-bicarbonate type. The bottom-hole temperature is 137°C. Liquid radioactive wastes are not expected to migrate downward to the lower Snake River Plain aquifer.

Volcanic hazards

The USGS, in cooperation with the DOE, has been evaluating the recurrence intervals of volcanic activity at the INEL on the eastern Snake River Plain. Two studies recently completed have determined the ages and recurrence interval of basalt lava flows that cover a proposed breeder reactor site and a radioactive waste burial storage facility. These studies involved field mapping by M. A. Kuntz, H. R. Covington, and B. H. Lefebvre, potassium-argon age determinations by G. B. Dalrymple, carbon-14 age determinations by E. C. Spiker and Meyer Rubin, and paleomagnetic work by D. E. Champion.

The study for the radioactive waste burial facility shows that it lies in a shallow topographic depression and has been covered by lava flows emitted from vents located from 5 to 30 km away. Potassium-argon and paleomagnetic studies show that the burial site has been inundated by lava flows at least 10 times within the last 500,000 yr. The 19 flows and flow units are arranged in 7 groups, each group consisting of 1 to 5 flows and flow units that were erupted from a single vent. The average eruption rate is, thus, approximately one eruption event per 70,000 yr, but the eruptions have been episodic rather than periodic.

The Craters of the Moon lava field covers an area of approximately 600 km^2 in the eastern Snake River Plain and includes flows that come within 20 km of the site. Stratigraphic, radiocarbon, and paleomagnetic data show that the field was formed in at least five major bursts of volcanic activity from vents located along the Great Rift. These bursts occurred 14,000 to 12,000, approximately 11,000, 7,000 to 6,500, approximately 4,000, and approximately 2,000 yr B.P.

Geologic mapping suggests that the lengths and orientations of volcanic rift zones, the areal density and types of volcanic vents, and subtle topographic features in lava flows of the eastern Snake River Plain are partly controlled by buried segments of caldera ring fractures, and others appear to terminate at caldera margins. Areas of sparse or no vents appear to overlie buried calderas. Basaltic cinder cones, low topographic ridges, and rhyolite domes may coincide with ring fractures, whereas arcuate depressions may reflect collapsed "moat" zones.

GEOPHYSICS

Attenuation of seismic waves in granite gneiss

Thermal stresses produced by the heat from radioactive wastes in a repository would fracture surrounding rocks, increasing their permeability and water content. Another result is the attenuation of seismic waves. Experimental measurements of attenuation in samples of granite gneiss from Idaho Springs, Idaho, were made at room temperature by J. D. Sherman. Preliminary results indicated low attenuation in the rock, suggesting that periodic measurements with appropriate seismic velocity measuring instruments could be used to measure the extent of microfracturing developing around a repository.

In situ analysis of water content in salt deposits

Experiments are being conducted by F. E. Senftle to test the feasibility of measuring with a borehole sonde the water content in salt deposits using neutron activation and high-resolution gamma-ray spectrometry. Although salt has been assumed to be essentially dry, water does occur in cracks and vacuoles and tends to move toward a source of heat because the solubility of salt in water increases with temperature.

Neutron capture gamma-ray spectra were made in the laboratory in 90-kg samples of dry NaCl and in brines, using a ^{252}Cf fission neutron source, to study the peak intensities, interferences, and other characteristics of the NaCl spectrum. Spectra were taken using various neutron source-to-detector distances, shields, and so forth. Concurrently, rock salt was ordered from four different mines, each of which had a different average water content. To make artificial boreholes, five large steel casks, 1.2 m in diameter and 1.5 m in height, were constructed with a 10.2-cm pipe along the axis. Each cask was filled with about 2,270 kg of salt and hermetically sealed. Thus, each cask could simulate a borehole in a salt deposit having a different water content.

The average mine analysis of the salt in the three completed casks was 0.007, 0.04, and 0.25 percent water. Preliminary spectra were taken in the casks using both water-filled and dry boreholes, but these have not been

completely analyzed. It was apparent from these data that the hydrogen capture peak by itself is not a sensitive measure of water content in the range being considered. However, hydrogen is an effective moderator of fast neutrons, and preliminary results indicated that the intensities of gamma rays resulting from fast-neutron inelastic scattering from sodium and chloride in the formation and iron in the sonde may be sensitive to hydrogen when the water content is up to several percent. The capture lines from chlorine are essentially independent of water in this range, whereas the inelastic scattering and annihilation peak intensities vary significantly with water content.

GEOCHEMISTRY

Boiling properties of bittern brines

Natural rock salt typically contains up to 0.5 wt percent water as fluid inclusions of bittern brines. These brines range from 20 to 40 wt percent total dissolved solids and can be described by the system Na, K, Mg, Ca/Cl, SO_4–H_2O. Under temperature gradients such as those imposed during heater tests of rock to evaluate its potential for use as a host medium in a radioactive waste repository, these brines dissolve additional solids and migrate toward the heat source. Upon arrival at the heater site, the brine is decompressed and boiling begins. Water is lost from the brine in two ways, by separation of steam and by precipitation of hydrous phases (for example, tachyhydrite $CaMg_2Cl_6 \cdot 12H_2O$ and carnallite $KMgCl_3 \cdot 6H_2O$). Boiling ceases when sufficient water is lost to raise the boiling temperature to the ambient temperature of the heater area. Studies of the boiling properties of bittern brines by R. W. Potter III and D. B. Stewart have allowed the formulation of a simple equation that relates the amount of steam collected in a heater test to the actual amount of brine present prior to boiling.

Chemical behavior of plutonium in waters from low-level waste-disposal trenches

Filtration studies and radiochemical analyses of trench waters from the Maxey Flats, Ky., low-level radioactive waste disposal site, by J. M. Cleveland, Jr., indicate that most of the plutonium in these waters is probably not colloidal but is in true solution. This finding is somewhat unexpected because of the extreme insolubility of plutonium at near-neutral pH values and its tendency to form colloidal species. The presence of organic solutes in these waters suggests that the plutonium has been solubilized by formation of very stable organic complexes. If substantiated, this behavior could have significant effects on the mobility of plutonium in ground water.

Literature review of geochemical and geologic controls on the mobility of uranium mill tailings and contained radionuclides

Edward Landa (1979) made a critical review of the literature on uranium mill tailings, emphasizing the geochemical and geologic controls on the long-term containment of radionuclides. Landa concluded that, because of the 77,000-yr half-life of ^{230}Th, the parent of ^{226}Ra, the environmental effects associated with radionuclides contained in these tailings must be considered within the framework of geologic and geochemical processes operating over geologic time. The magnitude of erosion of cover materials and tailings and the extent of geochemical mobilization of the contained radionuclides to the atmosphere and hydrosphere should be considered in the evaluation of the potential long-term consequences of all proposed uranium mill tailings management plans.

FLOODS

The three major categories of USGS flood studies are measurement of stage and discharge, definition of the relation between the magnitude of floods and their frequency of occurrence, and delineation of the extent of inundation of flood plains by specific floods or by floods having specific recurrence intervals.

OUTSTANDING FLOODS

Wyoming floods of May 16 to 20, 1978

G. S. Craig, Jr. (Parrett, 1978), reported that north-central, northeastern, and south-central Wyoming experienced damaging floods from fairly heavy rains from May 16 to 18, 1978. Rainfall measuring 76 to 127 mm fell over a wide area of already saturated ground. Because of the prolonged and widespread storms, the larger drainage areas generally produced the more significant flows.

Floods in excess of 100-yr recurrence intervals occurred on the Tongue River at the Montana State line, on the South Fork Powder River near the Powder River, on the Cheyenne River near Riverview, and on the Belle Fourche River below Moorcroft. Floods in excess of 50-yr recurrence intervals occurred on Fifteen Mile Creek near Worland, on Goose Creek below Sheridan, and on the Medicine Bow River above Seminoe Reservoir near Hanna, Wyo.

No loss of life was reported. Estimated damage to buildings, highway structures, and agricultural land was about $16.3 million, of which $2.5 million was to private facilities and $1.5 million was to public facilities. President Carter declared 12 Wyoming counties eligible for Federal flood disaster funds.

Floods in central Texas, August 1978

E. E. Schroeder, B. C. Massey, and K. M. Waddell (1979) reported that catastrophic floods, which resulted in millions of dollars in property damage and the loss of 33 lives, occurred in central Texas from August 1 to 4, 1978, as a result of intense rainfall produced by the remnants of Tropical Storm Amelia. Rainfall in excess of 760 mm was reported unofficially at several locations, while the highest 24-h amount recorded by the National Weather Service was 738 mm, at Albany in Shackelford County.

Major flooding occurred on the Medina River and its tributaries above Medina Lake and on the Guadalupe River and its tributaries above Canyon Lake. Minor to severe flooding occurred on the tributaries of the Nueces River, on the Clear Fork Brazos River and its tributaries, and on the Llano and Pedernales Rivers, which are tributaries of the Colorado River.

Peak discharges at several streamflow stations exceeded the historic peaks, and the flood magnitude and frequency data for the Guadalupe River above Canyon Lake, for the Medina River near Pipe Creek, and for the Clear Fork Brazos River indicate that the August 1978 flood had a recurrence interval in excess of 100 yr. The highest unit discharge observed during this flood was 71.70 m^3/s from a 36.5-km^2 drainage area of Spring Creek, which is a tributary of the Pedernales River.

Floods of March and April 1979, Mississippi and Alabama

K. V. Wilson and J. R. Harkins reported that a series of storms in March and April produced record-breaking floods in the central parts of Alabama and Mississippi. Streams throughout the area were high in early March because of storms centered over the Chunky River basin in east-central Mississippi and Satilpa Creek basin in west-central Alabama. The March 4 flood on the Chunky River near Chunky, Miss. (drainage area, 953 km^2), was the greatest flood since records began in 1938. This flood, which had a recurrence interval of about 100 yr, was not exceeded by the April flood.

Stages on many streams were still high when torrential rains that fell within 48 h or less from April 11 to 13, 1979, caused severe flooding from Mississippi across Alabama to Georgia. The band was approximately 115 km wide, extending from about 70 km north to 40 km south of Birmingham. The heaviest rains fell in the central area of the Tombigbee River basin in Pickens County, Ala., which borders Mississippi. There were two areas of extremely heavy rainfall, one in Chilton County and the other in northern Shelby County. Most of the area had rainfall in excess of 180 mm, and much of the area had rainfall greater than 250 mm.

Flood flows on the Coosa and Tallapoosa Rivers combined to cause flooding along the entire length of the Alabama River. Recurrence intervals approached or exceeded 100-yr recurrence intervals on main stems and tributaries in the Tombigbee, Pascagoula, Pearl, and Big Black River basins. Along the Tombigbee River, the flood was the greatest of record at Gainesville and Demopolis, Ala., since 1892 and 1874, respectively.

At all gaged sites on Pearl River, from Burnside downstream to Jackson, Miss., the flood was the greatest since 1874 and exceeded the stage of the record flood of April 1902 by 1.77 m at Jackson. Recurrence intervals of peak discharges on most streams in the northern and eastern parts of the basin far exceeded 100- yr recurrence intervals. A near-peak discharge of 4,050 m^3/s was measured in Ross Barnett Reservoir at Mississippi State Highway 43, about 16 km upstream from the Ross Barnett Reservoir Dam. The peak discharge attenuated to 3,620 m^3/s at U.S. Highway 80 in Jackson. Flooding on the Pearl River forced the evacuation of at least 15,000 people in Jackson.

Hurricane Frederic tidal floods of September 12 to 13, 1979, along the gulf coast, Mississippi, Alabama, and Florida

The approximate areas flooded by Hurricane Frederic tides of September 12 to 13, 1979, along coastal areas of Alabama, Florida, and Mississippi extended from about 13 km west of Fort Walton Beach, Fla., westward along the gulf coast through Alabama to Moss Point, Miss., a distance of about 185 km.

J. C. Scott, L. R. Bohman, and M. A. Franklin reported that Hurricane Frederic was one of the most intense hurricanes of record to enter the United States mainland. A NWS–NOAA research aircraft reported a flight-level wind of 256 km/h (138 knots) a short time prior to landfall. A wind velocity gage maintained by the NWS near Dauphin Island, Ala., recorded a maximum wind speed of about 233 km/h (126 kn). The maximum recorded precipitation along the coast during the passage of the hurricane was about 220 mm, at Dauphin Island, Ala.

Flooding and water-related damages were most severe at Dauphin Island and Gulf Shores, Ala. However, significant flooding and damage occurred as far east as Pensacola Beach, Fla., and as far west as Moss Point, Miss. Maximum prevailing flood elevations were about 2.96 m above the National Geodetic Vertical Datum of 1929 at Dauphin Island, Ala., about 3.14 m at the U.S. Highway 98 Causeway across Mobile Bay, Ala., and about 4.36 m at Gulf Shores, Ala.

American Red Cross casualty figures list 10 known deaths in Alabama, 1 in Florida, and 2 in Mississippi. The total number of storm-related injuries and illnesses for the three States is 4,711. Estimates indicate that the total damage caused by Hurricane Frederic probably will exceed $2 billion. In comparison, the total damage for Hurricane Camille (1969) was $1.3 billion.

FLOOD-FREQUENCY STUDIES

Flood-frequency analyses in Idaho

A study of skews (the degree of curvature of log-Pearson type III flood-frequency curves) at gaging stations on Idaho streams shows that two distinct kinds of flood events exist, each with different statistical characteristics.

L. C. Kjelstrom found that it is preferable to analyze rainstorm and snowmelt floods separately, rather than to analyze the annual maximum discharges, which include both kinds of floods. Generalized skew coefficients for rainstorm floods ranged from +0.2 to +0.5, but skews from snowmelt floods had little range; most were very close to −0.3.

In addition, a regression analysis of basin characteristics and floods of various recurrence intervals produced a set of equations for estimating floods at ungaged sites in Idaho. These equations, which are based on station data with an adjusted average skew, have standard errors ranging from 42 to 90 percent for the 50-yr flood.

New flood-frequency equations developed for streams in Indiana

R. L. Gold reported that new flood estimating equations have been developed for streams in the State of Indiana for the 2- and the 10-yr recurrence-interval floods. These equations update previously published relations by the inclusion of data collected on small streams as part of the analysis. The data were analyzed with a regression model that determined that the most significant basin characteristics were drainage area and precipitation. The form of the resulting equations is $Q = bA^xP_i^y$, where Q = flood discharge, b = constant, A = drainage area, P_i = precipitation index, x and y are regression coefficients. These equations are valid for all size drainage areas, whereas previously published equations were valid only for drainage areas larger than 39 km^2.

Depth-frequency relation for mapping flood-prone areas in South Dakota

A simple method has been developed by L. D. Becker for estimating the depths of flow associated with floods having a 1-percent likelihood of annual exceedance (100-yr flood) at ungaged sites on selected drainage basins in South Dakota. This method of determining flood depth has proven especially useful in the delineation of flood-prone areas in rural areas of the State.

Drainage basin size was related by linear regression analysis to known flood depth determined at 45 gaging stations. Drainage basin size ranged from 12 to 3,990 km^2, and flood depth ranged from 0.8 to 5.2 m. The estimating equation developed is $D = aA^b$, where flood depth, D, represents the difference between the water-surface elevations of the 2- and 100-yr floods at the gaged or ungaged site. Area, A, is the contributing drainage area above the site, and the regression constant and coefficient are represented by a and b, respectively. This approach could provide general depth-frequency relations for various recurrence intervals applicable throughout South Dakota.

Flood-flow characteristics of streams in the Wasatch Plateau coal field in Utah

M. J. Graham and J. E. Tooley developed a method for estimating peak discharges and volumes of runoff on a number of ungaged streams as part of a comprehensive hydrologic investigation of the central Wasatch Plateau in Utah. These estimates are needed to determine potential flood hazards during development of the area's large coal reserves.

Twenty-four gaging stations with records of 10 or more yr and which drain areas hydrologically similar to those in the study area were chosen by the authors for multiple regression analysis. The peak discharges and volumes for selected return periods determined at each of these stations were related to respective basin characteristics. The basin characteristics used were drainage area, channel slope, mean basin elevation, and 2-yr, 24-h rainfall intensity. For recurrence intervals less than 25 yr, the significant independent variables were channel length, mean annual precipitation, and 2-yr, 24-h rainfall intensity. For recurrence intervals greater than 25 yr, drainage area and mean annual precipitation were significant. The standard error of estimate for the relations averaged about 40 percent. These relations provided a means of predicting peak discharges and volumes at ungaged sites of the Wasatch Plateau coal field.

This method is superior to others for estimating peak discharges and volumes for several reasons. First, sufficient data required for calibration of watershed models could not be obtained during the short duration (2 yr) of this project. Second, the authors feel that existing watershed models would not adequately describe the flood characteristics in the study area even if sufficient data were available. Third, channel geometry relations cannot be used because the stream channels are cut into sandstone and do not have normal channel features.

Magnitude and frequency of floods on ephemeral streams in eastern Washington

W. L. Haushild (1979) developed equations from regression analyses to estimate the magnitude of floods for various occurrence intervals at ungaged sites on ephemeral streams that drain small relatively undeveloped basins in the semiarid part of eastern

Washington. The regression analyses used the logarithms of the longitude indexes of gaged sites (station longitude, 117°00′), forest cover, and drainage areas of the upstream basins as independent variables and used the logarithms of the discharges for selected exceedance probabilities at 51 to 53 gaged sites as dependent variables. These equations may be used to estimate floodflows with probabilities of 50, 20, 10, 4, 2, and 1 percent of being exceeded in any year in natural flow ephemeral streams that drain relatively undeveloped basins with areas and forest covers less than about 105 km² and 30 percent, respectively. The standard errors of estimate for the equations ranged from 55 to 100 percent. Equations that used longitude index as a substitute for a precipitation index more accurately estimated floods than equations that used mean annual precipitation, which, in turn, were better than the equations that used the 24-h precipitation with an exceedance probability of 50 percent. The superior results obtained by using the longitude index suggest that the index is more representative of the effects of the study area's physiography (shielding by Cascade Range and orographic uplift provided by hills along the eastern border of Washington) than is either of the relatively poorly defined precipitation variables.

Soil permeability—a significant parameter in flood-frequency relations on streams in Wisconsin

D. H. Conger found that soil permeability is a significant parameter in flood-frequency relations on streams in Wisconsin. This parameter was significant in flood-frequency equations in four out of the five areas comprising the State of Wisconsin. The soil permeability was obtained from a State soil permeability map. This parameter replaces soil index, which is difficult to determine.

FLOOD MAPPING

Flood-hazard studies in Kansas

S. V. Bond used step-backwater, synthetic hydrograph, and photointerpretation techniques to delineate flood boundaries of the 100-yr and the 500-yr floods in the unincorporated areas of Riley and Lyon Counties, Kans. Also, flood profiles for the 10-yr and the 50-yr floods were determined. Flood hazard areas were identified in the communities of Manhattan, Riley, Ogden, and Americus and in other developing areas of Riley and Lyon Counties. Information obtained from these studies will provide a technical basis for flood-plain-management decisions. The data will enable governing bodies to carry out the comprehensive flood-plain-management programs required by the Federal flood insurance program.

Risk analysis in bridge design

V. R. Schneider and K. V. Wilson investigated total highway-stream-crossing costs including the approach fills on flood plains and all necessary waterway openings that could be designed and constructed for the least total expected cost to the public. The total expected cost included the capital investment in the highway, expected replacement and repair costs as a result of flood damages, expected user costs from traffic interruption and detour, and expected backwater drainages during the service life of the highway. Techniques for making engineering and economic studies of the least-cost design are presented along with suggestions for managing the time and work required for such studies. A unique design flood is defined for each bridge as the flood whose upstream stage is equal to the lowest elevation of the approach fill or bridge deck. Two examples were prepared to illustrate the application of the method to a rural site (low backwater damage) and an urban site (high potential traffic interruption and backwater damage).

Flood hazards in Elko County, Nevada

R. R. Squires and C. V. Schroer defined the extent and severity of flood hazards in the cities of Elko, Carlin, and Wells and in selected unincorporated areas in Elko County, northeastern Nevada. The study meets the objectives of the National Flood Insurance Act of 1968 and the Flood Disaster Protection Act of 1973. The flood-hazard information is used in the administration of the regular program of flood insurance by the Federal Insurance Administration and by local and regional planners.

Inundation maps of urban areas

Maps showing areas inundated by major floods, flood profiles, discharge frequency relations, and stage-frequency relations were published during the current year as Hydrologic Investigations Atlases for Kreole–Grand Bay SW, Miss., Grand Bay, Chickasaw, Mobile, Hollingers Island–Theodore, Coden–Bellefontaine, Heron Bay–Little Dauphin Island–Fort Morgan–Fort Morgan NW, the Basin–Bay Minnette North–Creola NE, Ala. (Bohman and Scott, 1980a-h); Hurricane, Bridgehead, Daphne–Point Clear, Magnolia Springs, Bon Secour Bay, Pine Beach–St. Andrews Bay–Fort Morgan, Gulf Shores, Orange Beach, and Lillian, Ala. (Scott and Bohman, 1980a-i); Perdido Bay, Fla. (Scott and Franklin, 1980); West Pensacola, Oriole Beach–Garcon Point–Holley–South of Holley–Navarre, Fla. (Franklin and Bohman, 1980a-b); Gulf Breeze–Fort Barrancas, Fla. (Franklin and Scott, 1980).

Maps of flood-prone areas

Areas inundated by the 100-yr flood are outlined on topographic maps as part of the National Program for Managing Flood Losses. Nearly 13,000 such maps have been completed for all States, the District of Columbia, and Puerto Rico. The objectives of this activity are to inform rapidly cities and towns of the general extent of their potential flood problems and to identify areas of potential flooding downstream from dams or reservoirs where structural failure could result in extensive loss of life and catastrophic flood damages. Flood-hazard maps are used extensively to meet local planning needs and the objectives of the National Flood Insurance Act of 1968, the National Disaster Protection Act of 1973, and Executive Order 11988.

EFFECTS OF POLLUTANTS ON WATER QUALITY

SURFACE-WATER POLLUTION

PCB's in Hudson River

R. A. Schroeder reports that the concentration of PCB's was monitored at five sites on the riverine Hudson, at five sites on the estuarine Hudson, at one site at the mouth of the Mohawk River, and at the Waterford Municipal Water Plant, which draws its supply from the riverine Hudson. Results obtained since 1977 continue to show that the Hudson's waters are contaminated by PCB's, with most of the loading coming from the upper river near a historic point source. Statistically significant changes in contamination levels have not been noted during 3 yr of record. Average PCB concentrations at Waterford upstream from the confluence with the Mohawk River are 0.4 μg/L. Within the upper 150 km of the estuary, average concentration decreases from 0.24 μg/L at the head to 0.15 μg/L downstream. The lower concentrations in the estuary are due to dilution by uncontaminated Mohawk River water, which empties into the Hudson River just above the estuary, and tributary waters that empty into the Hudson estuary. Treatment at the Waterford Plant is effective in removing PCB's to below public drinking-water standards of 0.1 μg/L.

Movement of percolating waste-water effluents in Yellowstone National Park, Wyoming

Chloride and sulfate concentrations and specific conductance of water in observation wells, waste-water effluents, and selected streams were used to study the effects on nearby lakes and streams of waste-water effluents that percolate from sewage lagoons at four sites in Yellowstone National Park. According to E. R. Cox, chloride, sulfate, and specific conductance are much higher in the effluent than in nearby ground water, and contours of chloride and sulfate concentrations and specific conductance show the direction and extent of the movement of percolating effluents.

Impact of urban storm runoff on stream quality near Atlanta, Georgia

J. B. McConnell assessed the impact of stormwater runoff from point and nonpoint sources on the water quality of receiving streams in the Atlanta area. Emphasis was placed on the collection of water-quality data in the summer and autumn to determine the impact of streams from runoff produced by thunderstorms.

Stormwater runoff significantly increased the concentration of suspended sediment BOD, total organic carbon, total ammonia nitrogen, total phosphorus, fecal coliform bacteria, and trace metals over that observed during dry-weather flow in most receiving streams in the Atlanta metropolitan area. Stormwater runoff increased the mean concentration of most constituents two- to fivefold.

In most tributaries to the Chattahoochee River, the DO concentrations increased to near saturation during periods of stormwater runoff due to high turbulence. In the Chattahoochee River near Fairburn during a period of low flow in July, the DO concentration reached a low of 1.5 mg/L (a decrease of 4 mg/L) as a result of runoff from a thunderstorm. Low flow during the summer and autumn occurs about 21 percent of the time because of flow regulation of the river.

GROUND-WATER POLLUTION

Effect of drainage wells on water quality in the Orlando metropolitan area, Florida

G. R. Schiner and E. R. German extended the work of J. O. Kimrey (1978) and reported that about 400 drainage wells concentrated in a 1,036-km^2 area of metropolitan Orlando emplace more than 189,000 m^3/d of predominantly urban runoff, by gravity injection, directly into a highly transmissive producing zone in the Floridan aquifer with little apparent effect of the water quality of nearby public-supply wells. All the drainage wells discharge directly into a freshwater zone generally laterally upgradient of the flow pattern and often within 400 m of public-supply wells finished in the same zone. The disposal zone is often less than 122 m above a deeper zone also used for public supply. Analysis of variance for selected constituents indicates that the quality of water from drainage wells differs significantly from the public-supply wells for turbidity, color, specific conductance, iron, nitrogen, phosphorus, arsenic, cad-

mium, chromium, coliform, atrazene, and mercury. Generally, except for iron and coliform, waters pumped from drainage wells are within the recommended limits for drinking water. Since about 1956, when disposal of raw waste waters into drainage wells was discontinued, no cases of pollution of public-supply wells have been attributable to drainage-well injections.

Organic pollutants in ground water in New York

R. A. Schroeder and D. S. Snavely reported that water samples from about 50 locations in upstate New York were analyzed by computer-directed gas chromatography–mass spectrometry scans for the 114 EPA "Consent Decree" Organic Priority Pollutants in municipal ground-water supplies. Generally, concentrations of constituents were less than 1 μg/L. Volatile compounds such as organochlorines and substituted benzenes were occasionally found in concentrations >1 μg/L. Although sources of contamination were not investigated, evidence suggests point discharges from isolated industrial activity. Nonpoint contamination of ground water is unlikely to occur in New York except in heavily populated areas such as Long Island.

Nitrate concentrations in ground water, Suffolk County, New York

Ground-water-quality data have been collected since housing construction began in the "Twelve Pines" area of south-central Suffolk County, N.Y. The study, done in cooperation with Suffolk County Department of Environmental Control, evaluated the effects of various sources of nitrogen on the shallow ground-water system. J. B. Lindner, B. G. Katz, and W. J. Flipse reported that, during the study period, the data indicate that the regional nitrate concentration (the median of the median values reported at observation wells) increased at a rate of 0.26 mg/L/yr. The largest potential source of nitrogen is that leached from lawn and garden fertilizers; other potential sources are animal wastes and nitrogen in precipitation and irrigation water. There is no significant amount of seepage from the sewers installed at the time of housing construction; therefore, nitrogen loading from this source is considered negligible.

Sewage effluent disposal by spray irrigation

Long-term effects of sprayed sewage effluent on ground water have been studied by L. J. Slack and, recently, by M. C. Yurewicz. Secondarily treated sewage effluent has been applied at varying rates on sandy soil since 1966 at the Thomas P. Smith Waste Water Renovation Plant southwest of Tallahassee, Fla.

In December 1977, the spray irrigation field was expanded to the east. Water from a well open to the upper Floridan aquifer was degraded as a result. In the fall of 1976, spray irrigation in the west portion of the spray field was discontinued because of construction of holding ponds and pipelines. With the suspension of spraying, the quality of water from several wells in that area has improved.

Landfill impacts on the ground-water system in Franklin County, Ohio

According to J. T. deRoche and A. C. Razem, pumping of water from glacial outwash and underlying limestone aquifers adjacent to several landfills in southern Franklin County, Ohio, has modified the local ground-water flow pattern. The cone of depression intercepts flow from three of the five landfills.

Native ground water is a calcium-bicarbonate type with high concentrations of dissolved iron and sulfate. Water sampled from wells downgradient from disposal sites is a calcium-bicarbonate-chloride type, with higher dissolved solids and chloride than the native water. Chemical quality changes have been observed in water downgradient from four of the five sites. Because of insufficient data, the ground-water quality from the remaining site cannot be evaluated.

Contamination of ground water by coal tar, St. Louis Park, Minnesota

M. F. Hult and M. E. Schoenberg report that operation of a coal-tar distillation and wood-preserving plant in St. Louis Park, Minn., between 1917 and 1972 resulted in contamination of ground water to depths of at least 250 m. Carcinogenic coal-tar compounds, including Benzo(a)pyrene have been identified in fluid and core samples from contaminated aquifers.

Coal-tar derivatives have entered the ground-water system three different ways: infiltration of spills and drippings on the site through the unsaturated zone to the water table, ground-water recharge from water-table ponds that received surface runoff and process water from the plants, and a spill into a multiaquifer well originally drilled to a depth of about 280 m. Contaminated water in shallow bedrock aquifers is moving into deeper aquifers through (1) confining beds, (2) drift-filled bedrock valleys where the confining beds have been removed by erosion, and (3) multiaquifer wells.

The first municipal well completed in the Prairie du Chien–Jordan, the area's major aquifer, was drilled in 1932 and abandoned in 1933 because the water tasted of coal tar. Use of five additional municipal wells in the Prairie du Chien–Jordan aquifer was discontinued in 1978 and 1979 when carcinogenic coal-tar compounds were detected in the water.

Dissolved contaminants can move relatively rapidly through the Prairie du Chien–Jordan aquifer because the upper part of the aquifer is a solution-channel carbonate rock with high transmissivity and dispersivity and low effective porosity. The local direction of groundwater flow in the aquifer is controlled primarily by pumpage from municipal and industrial wells and by the injection of water into the Prairie du Chien Group through multiaquifer wells. The long history of contamination, continually changing pumping patterns, effects of multiaquifer wells, and probable high velocities of contaminant transport combine to produce a complex distribution of contaminants. It is unlikely that a single distinct contaminant plume exists in the Prairie du Chien–Jordan aquifer.

The effects of solid-waste leachate on shallow aquifer water quality

D. J. McKenzie conducted a ground-water-quality investigation at two Dade County, Fla., solid-waste landfills to characterize the landfill leachate and assess some of the effects of the leachate on the water quality of the shallow Biscayne aquifer.

The leachate consisted of large concentrations of organic decomposition products, principally ammonia, organic nitrogen, and carbon dioxide. Chloride, alkalinity, and chemical oxygen demand were useful indicators of leachate and appeared to be effective leachate tracers.

The concentration of leachate constituents varied considerably with location and depth of monitor wells, age of solid-waste materials, and seasonal rainfall. A highly concentrated leachate was generated in the area filled with new waste materials, but the leachate that was monitored in the wells on the downgradient edge of the landfill was found to be very much diluted.

Migration of contaminated ground water near toxic waste sites

H. R. Anderson (State University of New York Research Center, Oswego) identified six locations where toxic materials are stored or have been incorporated in landfills. Test drilling conducted by the USGS identified a thin layer of fine sandy silt underlying the original Pollution Abatement Services site that may allow contaminated ground water to flow approximately 0.8 km north into Lake Ontario. As much as 9 m of saturated sand and gravel overlying a buried drumlin underlies the Volney landfill site and may allow contaminated ground water to flow into Bell Creek, which flows along the east edge of the landfill site and eventually to Lake Ontario. The remaining four sites are near streams and may have potential for contaminating both ground water and surface streams.

Hydrological assessment of ponding-treated landfill leachate in Pinellas County, Florida

Leachate from open landfill trenches is being treated and disposed of in shallow oxidation ponds in Pinellas County. The landfill, on a flat coastal area having a high water table, is about 3 km west of Old Tampa Bay. The pond area, according to Mario Fernandez, Jr., is underlain by two principal types of sediment, a surficial layer of fine to very fine sand and shell about 4 m thick and a marl or calcareous layer at least 4 m thick. Nineteen clusters of surficial aquifer wells, totaling 77 wells, were installed within and around the pond to determine the hydrologic properties of the pond and to monitor water-quality changes. Preliminary data indicate the existence of contamination of ground water only up to 0.3 m below the bottom of the pond. Ground water outside the pond remains uncontaminated.

ENVIRONMENTAL GEOCHEMISTRY

Element content of fourwing saltbush under natural conditions and when grown on mine-reclaimed land at the San Juan coal mine, northwest New Mexico

L. P. Gough and R. C. Severson (1980) report that concentrations of Al, As, B, Co, Cu, F, Fe, Mn, Na, Pb, and U in the stems and leaves of fourwing saltbush growing in August 1977 on mine-reclaimed land at the San Juan coal mine were high compared to their concentrations in reference samples of native plants collected at the same time from the San Juan Basin. The geometric mean concentration of sodium was 72 ppm (dry weight basis) in saltbush from the basin, whereas samples from the mine were usually >10,000 ppm. Concentrations of the other elements were from two to five times higher in plants from mine-reclaimed land than from native land. The mine samples were from an area that was regraded, topsoiled, and reseeded with alkali sacaton and fourwing saltbush in 1974. Some irrigation was used initially to revegetate the site.

In the San Juan Basin and mine topsoils, little difference was noted between the total content of these 11 elements and the extractable content of B, Co, Cu, Fe, Na, and Pb. However, generally higher concentrations of total and extractable elements were found in mine spoil than in basin C-horizon soils. The basin soil and plant samples were collected at random points throughout the western and southern portions of the basin, an area underlain with coal-bearing rocks of the Kirtland Shale and Fruitland Formation and the undifferentiated Mesaverde Group of Cretaceous age.

Seasonal differences in the element content of Wyoming big sagebrush

With an increase in the surface mining of minerals and subsequent land reclamation, alterations can be expected in the element content of plants revegetating these areas. Such changes can be better interpreted, however, if the magnitude of local seasonal concentration differences, intrinsic to the plant is known. Therefore, knowledge of baseline concentrations for both biologically "active" and "inactive" elements in native plants of the northern Great Plains is important.

Only a few studies of the element content of big sagebrush in the Western United States have been made. These reports, in general, are concerned with the forage quality of big sagebrush and, therefore, give concentrations for only a few of the major elements. In this study, L. P. Gough and J. A. Erdman (1980) present the concentration of 30 elements in the dry material of *Artemisia tridentata* ssp. *wyomingensis* (Wyoming big sagebrush, a common and ecologically important shrub in the northern Great Plains) collected from a small locality in the eastern plains of Wyoming. To quantify the intrinsic seasonal variability in the concentration of these elements in sagebrush, they sampled young and old tissue in September, January, April, and July. This information elucidates the differences in the concentration of different elements with season and with tissue type, demonstrates the need for caution when comparing sample data with established element concentration baselines, and stresses the importance of collecting the proper tissue type in biogeochemical prospecting studies using big sagebrush.

These data were analyzed using a two-way analysis-of-variance design that allowed for the partitioning of the total variance in element concentration between the two tissue types and among the four seasons. From these results, four groups of elements were constructed based upon similar seasonal patterns for both young and old tissue. The trends of one group, consisting of the major essential elements Ca, Mg, P, K, and S, directly reflect phenological events that alter the proportion of leaf-to-stem tissue in the samples. These trends are dominated by strong positive relations among themselves and with ash yield and by high values in July or July and September. In general, the element composition of younger tissue fluctuates more, has higher concentrations, and shows greater differences between seasons than older material.

Soil chemical quality and choosing material for topsoiling mine-reclaimed land

Reconnaissance sampling of soils by R. C. Severson (1978a,b,c), from an area likely to be impacted by energy development in the San Juan Basin of New Mexico, shows that certain areas possess undesirable chemical characteristics if these soils are used as topsoil in mine-land reclamation. Grouping of these soils, based on taxonomic criteria, is not effective in distinguishing chemical character. Spoil material has many undesirable chemical properties for unrestricted plant growth; however, topsoiling of mine-reclaimed areas has reduced these problems. Chemical properties of the Doak and Sheppard soil series appear favorable for their use as topsoil in mine-land reclamation.

Soil preparation and analysis of soil extracts for trace metals

A laboratory study by R. C. Severson, J. M. McNeal, and J. J. Dickson (1979) has shown that varying methods of sample preparation, such as disaggregating versus sieving or grinding, may have significant effects on concentrations of trace metals measured in soil extracts, depending on the element and its form in different soil horizons. Nickel exhibited little difference between methods; however, iron, manganese, and zinc were increased 200 to 400 percent by grinding or sieving, when compared to disaggregating the soil sample. Copper and lead concentrations were increased by sieving, but not by grinding, over that of disaggregated soil. If extraction methods are used in formulating regulatory guidelines for trace metals in soils, rocks, or mine spoil, sample preparation methods should be standardized.

Acid-rain influences on Adirondack lake basins

In a study of the effects of acid precipitation on the transport of heavy metals, D. E. Troutman and N. E. Peters obtained input-output ratios of total loads of iron, manganese, lead, and zinc over a 20-mo period from October 1977 to May 1979 at three Adirondack Mountain lake watersheds. The watersheds are within 25 km of each other, are geologically similar, and receive equal quantities of acidic atmospheric deposition; each differs, however, in degree of acid neutralization. Water in Woods Lake ranged in pH from 4.0 to 5.0, in Sagamore Lake from 5.0 to 6.7, and in Panther Lake from 5.2 to 7.2, during the study.

Transport of manganese and zinc was greatest from the Woods Lake watershed, a poorly buffered predominantly acidic system, and was lowest in the Panther Lake Watershed, a relatively neutralized system. Ratios of manganese entering to that leaving the watershed were Woods, 0.27; Sagamore, 0.33; and Panther, 0.77; the corresponding ratios for zinc were 0.73, 0.75, and 1.7, respectively. These ratios suggest increased dissolution of maganese and zinc under the more acid conditions. Ratios of lead entering to that leaving were 1.0 or higher in all three watersheds (Woods, 7.1; Sagamore, 3.2; and Panther, 3.5), indicating a net retention of lead in all three watersheds, with possibly higher

accumulation in the Woods watershed. Ratios of iron entering to that leaving in the three watersheds (Woods, 0.81; Sagamore, 0.56; and Panther, 0.99) suggest a lack of correlation between acidity and iron transport in the basin studied.

Anomalously high concentrations of molybdenum in pond waters, northwestern South Dakota

To determine if the occurrence of molybdenosis in cattle in northwestern South Dakota could be related to anomalously high concentrations of molybdenum in surface-water drinking supplies, a reconnaissance surface water sampling program was conducted in the area during August 1979. G. L. Feder and L. T. Stone report that anomalously high molybdenum values were found in surface waters in the area. Water in an abandoned uranium mining pit at Twin Buttes contained 910 μg/L molybdenum, while waters from farm ponds unaffected by runoff from the uranium mining operation contained up to 200 μg/L molybdenum. This high value indicates that surface-water supplies in undisturbed areas of northwestern South Dakota may still have high enough concentrations of molybdenum to be of concern to farmers. Erdman, Ebens, and others (1978) have shown that cattle forage in this area may contribute to molybdenosis.

LAND SUBSIDENCE

Threat to land development by coal mine subsidence and fire, Sheridan, Wyoming, area

Studies of recent surface subsidence and underground fires in the abandoned New Monarch coal mine near Sheridan, Wyo., indicate that subsidence and fire potential should be considered carefully before lands above abandoned mines are developed for residential or industrial use. Alternative treatments of abandoned mines are to stabilize the mine workings and protect them from outbreak of fire by backfilling with incombustible material or to design surface structures to withstand deformations caused by subsidence and take steps to prevent ignition of the coal.

Subsidence depressions, pits, and cracks locally are present above abandoned coal mines in the area where the overburden is less than about 10 to 15 times the thickness of coal mined (Dunrud and Osterwald, 1980). The cracks, pits, and poorly sealed mine portals or shafts enable air and water to reach unmined coal in the abandoned mines and can cause spontaneous ignition. Once ignition occurs, the fire can sustain combustion and spread by ventilating through the cracks, pits, and poorly sealed mine portals or shafts.

Before the occurrence of subsidence pits and fire in the New Monarch mine area from 1977 to 1978, the area appeared to be prime land for residential development. The area now is a hazard to people and animals. Smoke and steam issue from subsidence pits and create serious air-pollution problems, and more pits continue to develop above the mine openings as the underground fire spreads. The heat and steam from the fire apparently softens the overburden rocks (composed mainly of claystones, shales, and lenticular sandstones) and promotes rapid collapse.

Six seismometers and four tiltmeters were installed in the New Monarch area to determine the extent of the fire and to obtain information on rates and processes of subsidence and burn rates of the fire. The fire, although not as large and polluting as the fire in the nearby Acme coal mine, is of particular concern because it is near a major interstate highway system and a high-voltage powerline that services much of the surrounding area.

Analysis of the seismic and tiltmeter data shows that some of the fire barriers and seals constructed in 1953 when the mine was abandoned have been destroyed by mine explosions and that the fire appears to be spreading southward and eastward toward Interstate 90, which is about 1 km away. As many as 2,500 tremors, caused by underground caving, surface collapse, and small underground explosions, were recorded during a 24-h period in the fire area. Tiltmeter records generally show that the surface above the fire is tilting and lowering episodically as the fire softens and burns the coal pillars below.

Studies by C. R. Dunrud and F. W. Osterwald (1978, 1980) indicate that the fire may best be controlled by strip mining the coal around the fire and selectively mining out coal in the mine area where feasible, thus cutting off the supply of coal. Another possibility is to construct a trench around the fire and fill it with incombustible material. However, this method would not recover much coal, would leave other parts of the mine susceptible to future burning, and would allow the isolated fire to burn and cause more subsidence hazards and pollution problems until the supply of coal is burned up.

Preconsolidation stress of aquifers in subsiding areas

The relation between land subsidence and water-level decline indicates that many aquifer systems in Arizona, California, and Texas appear to have been naturally overconsolidated before man-induced water-level declines began. In general, the relation is bilinear and shows a significant increase in the ratio of subsidence to unit water-level decline when water-level declines cause the vertical effective stress to exceed the original or natural preconsolidation stress. The amount by which

the preconsolidation stress of these aquifer systems exceeded the original overburden stresses is estimated to range from approximately 0.16 to 0.62 MPa.

Faulting caused by ground-water level decline, San Joaquin Valley, California

Approximately 230 mm of modern aseismic vertical offset of the land surface across the Pond–Poso Creek fault in the San Joaquin Valley, Calif., probably is related to ground-water withdrawal for crop irrigation. Several facts support this hypothesis. Modern faulting, averaging approximately 15 mm/yr, postdates the beginning of water-level declines and associated subsidence, and movement detected by precise leveling surveys from February 1977 to March 1979 was seasonal, occurring during periods of water-level decline. Furthermore, fault offset was greater in the year with the lower seasonal low water level. The modern movement probably is caused by localized differential compaction induced by differential water-level declines across the preexisting fault.

Differential subsidence across earth fissures in Arizona, California, and Nevada

Long linear tension cracks associated with declining ground-water levels at sites in subsiding areas in south-central Arizona, Fremont Valley, Calif., and Las Vegas Valley, Nev., occur at points of maximum convex-upward curvature in subsidence profiles oriented perpendicular to the cracks. Profiles are based on repeated precise vertical control surveys of lines of closely spaced bench marks. Association of these fissures with zones of localized differential subsidence supports a previously proposed mechanism that linear earth fissures are caused by horizontal tensile strains induced by localized differential compaction. At three of the sites, horizontal tensile strains across the fissures at the point of maximum convex-upward curvature, ranging from approximately 100 to 700 μ strains (0.01 to 0.07 percent) per year, were indicated based on measurements either with a tape or electronic distance meter.

Recognition that earth fissures at these sites are associated with zones of localized differential subsidence indicates a method, based on precise vertical control surveys of closely spaced bench marks, by which potential locations of linear earth fissures can be predicted in areas with declining ground-water levels. Results indicate that predictions sometimes can be made after only 1 yr of monitoring.

Geomechanical model describing subsidence induced by salt-solution mining in the Detroit area

A geomechanical model describing subsidence and sinkhole formation resulting from salt-solution mining in the Detroit area has been constructed, based on a yearlong field and laboratory study by J. R. Ege (USGS) and Daniel Stump (University of Illinois) in cooperation with BASF Wyandotte Corporation at a field site on Grosse Ile Island. Voids are created in the salt beds at depths between 300 and 400 m by dissolution of salt and removal of brine through borings. As the span of the void reaches a critical width, the cavity roofs and overlying rocks deflect downward into the openings creating shallow subsidence depressions at the surface. Normally, ground movement ceases when upward stoping and rock fragments falling from overlying beds fill the void; however, there have been three cases of recent unexpected development of sinkholes in the Detroit area. Examination of drill cores and outcrops and laboratory testing of rock samples from the sinkhole site revealed that the Sylvania Sandstone, a rock unit and aquifer found locally at depths of approximately 75 to 105 m, has unique mechanical properties. The Sylvania, upon application of stress, will disintegrate and flow as a slurry when wet.

Based on subsidence model studies, it is proposed that large-span voids created by salt dissolution cause sufficient deflection of the overburden rock, which induces disintegration of the Sylvania sandstone. The resulting sand slurry flows both into fractures and voids of the underlying dolomitic rocks and down-ruptured brine borings into the salt-dissolved voids, leaving cavities in the overlying sandstone. Continued flow enlarges the sandstone cavity until the span exceeds the rock strength and roof collapse ensues, causing rapid upward stoping through the remaining 75 m of overburden to the surface and formation of a sinkhole.

Subsidence in areas of the Texas gulf coast region

Releveling of the Houston-Galveston region by the National Geodetic Survey was completed in 1978. Results of the survey, analyzed by R. K. Gabrysch and K. W. Ratzlaff, showed that the maximum subsidence of the land surface from 1943 to 1978 was about 2.73 m, of which about 0.38 m occurred from 1973 to 1978. The data indicate that maximum subsidence from 1906 to 1978 may have been as much as 3 m.

Previously reported changes in the patterns of ground-water withdrawals and land-surface subsidence were maintained during 1979. Borehole extensometer records indicate no subsidence for 1979 in the area where, historically, maximum subsidence had occurred. In the western part of Harris County, where ground-water pumpage has increased, 4.0 cm of aquifer compaction was measured by an extensometer in 1979 as compared to 3.9 cm in 1978 and 3.5 cm in 1977. The average annual rate of subsidence from 1975 to 1978 was 3.2 cm.

In the rest of the Texas gulf coast region, total subsidence has generally been less than 15 cm. Notable

exceptions are the Jackson County area, where as much as 0.6 m of subsidence has resulted from ground-water withdrawals; the Saxet oil field near Corpus Christi, where 1.6 m of subsidence has resulted from production of oil and gas; and the Spindletop oil field area near Beaumont, where about 1.5 m of subsidence has resulted from oil and gas production and an additional 3 m of subsidence has resulted from sulphur production.

First subsidence-monitoring well instrumented in Virginia

H. T. Hopkins reports that the first subsidence-monitoring well in Virginia has been instrumented and placed in operation at Franklin, in southeastern Virginia. B. L. Wallace conferred in the design and installation of the borehole extensometer equipment.

The monitoring well is in the center of a major drawdown cone where water levels have declined about 67 m since large-scale pumpage began prior to 1940. Although subsidence in the area has been a subject of discussion for many years, this is the first attempt at measuring compaction of the aquifer system and relating it to ground-water withdrawal and land-surface subsidence. Repeated leveling by the National Geodetic Survey has shown that land surface in the area is subsiding at an average annual rate of about 5 mm/yr, but these measurements do not distinguish among the various processes that may result in vertical movement of the land surface.

Land subsidence along the New Jersey coast

William Kam reports that preliminary evaluation of first-order leveling data, for 1930 and 1964, indicates that land subsidence has apparently occurred along the coast of New Jersey between Sea Girt and Seaside Park. The maximum elevation difference noted is about 0.19 m at Mantoloking. The cause of this apparent subsidence may be the effect of ground-water withdrawals from the Englishtown aquifer. The decline in head is in excess of 84 m over a period of 70 yr.

HAZARDS INFORMATION AND WARNINGS

Erosion and overwash hazard on Fenwick Island, Maryland

Coastal processes and urban development along Fenwick Island (Ocean City), Md., were analyzed by Robert Dolan, Harry Lins, and John Stewart (1980) to determine the hazard potentials that exist on the island. Fenwick Island was selected because it is representative of many developed barrier islands on the Atlantic and gulf coasts and provides a generally applicable example. Two of the most important considerations in barrier island planning and management are the hazards associated with erosion and those associated with storm surge (overwash). With the current long-term trend in sea level rise and the frequent impact of storm waves and surges, barrier islands are, in general, continually moving toward the mainland. In the case of Fenwick Island, this movement has averaged about 0.5 m/yr over the past 40 yr. Current evidence indicates that the natural processes that have been forcing barrier islands landward for many decades will continue in the near future. Based on the rates of erosion and the widths of storm surge (or overwash) penetration on Fenwick Island over the past 4 decades, 30-yr projections of the shoreline location and storm surge penetration lines were made. Assuming no human intervention to preserve the beach and no catastrophic natural events, these projections indicate that many of the present beach front structures will be seaward of the predicted mean-high water line in 30 yr. This condition could be especially critical for the numerous structures along the beach front of the northern reaches of Fenwick Island where the erosion problem is most severe. Perhaps of greater significance is the projected 30-yr storm surge or overwash penetration zone, which encompasses roughly 35 percent of the currently developed land area. Significantly, the rates of erosion and the width of storm surge penetration along Fenwick Island are relatively low compared to many other stretches of Atlantic and gulf coast shorelines. Because of the high-density urban development of Fenwick Island, however, it has a higher potential for damage due to natural coastal processes. This indicates that the amount and type of development on barrier islands are factors to be carefully considered in the determination of hazard potential.

Earthquake "gap," Yakataga, Alaska

A "seismic gap" in southern Alaska, where an earthquake registering 8 or more on the Richter scale is likely within the next several decades, was targeted for special study. The center of the Yakataga seismic gap lies along the Gulf of Alaska about 240 km southeast of Valdez. A great earthquake could produce potentially damaging ground motion over an area as large as 77,700 km^2. The USGS study of the region has been intensified to develop a more complete understanding of the potential for large earthquakes and to observe the processes leading up to them. Both Alaskan and Canadian officials were notified of the reasons and nature of the special study.

Faults, Houston area, Texas

Eight faults in the Houston, Tex., area have been mapped (Verbeek and others, 1979). Seven of the faults are known to be active and capable of causing future

damage; past movement on these faults has caused considerable damage to roads and structures. This research is part of a joint USGS–NASA study that has identified more than 150 faults in the Houston area. A notice of potential hazard was sent to State and local officials, who will be kept informed of further research results of the joint USGS–NASA study.

Recent eruptive history of Mount Hood, Oregon, and potential hazards from future eruptions

Each of three major eruptive periods at Mount Hood (which occurred about 12,000–15,000, 1,500–1,800, and 200–300 yr ago, respectively) produced dacite domes, pyroclastic flows, and mudflows but virtually no pumice. Mount Hood is located approximately 80 km east of Portland, Oreg. Most of the fine lithic ash that mantles the slopes of the volcano and the adjacent mountains fell from ash clouds that accompanied the pyroclastic flows. The widely scattered pumice lapilli that are present at the ground surface on the south, east, and north sides of Mount Hood may have erupted during the most recent volcanic activity.

The recent geological history of Mount Hood suggests that the most likely eruptive event in the future will be pyroclastic flows with the formation of another dome, probably within the present south-facing crater. The principal hazards that could accompany the pyroclastic flows include mudflows moving from the upper slopes of the volcano down to the valleys and ash clouds that can deposit as much as 1 m of fine ash close to the flow source and as much as 20 cm at 11 km downwind from the source. Other hazards include laterally directed explosive blasts that could propel rock fragments outward from the side of a dome at high speed and toxic volcanic gases. The scarcity of pumiceous ash erupted during the last 15,000 yr suggests that explosive pumice eruptions are not a major hazard at Mount Hood; thus, there seems to be little danger that any future eruptions would affect significantly the Portland metropolitan area.

ASTROGEOLOGY

PLANETARY STUDIES

GALILEAN SATELLITES

GENERAL GEOLOGY

Volcanoes on Io

On March 5, 1979, the NASA spacecraft Voyager I flew past Jupiter and its satellites, acquiring high resolution views of Io, Ganymede, and Callisto – Jovian moons that are as large as the planets of the inner solar system. On July 9, 1979, Voyager II acquired images of Europa, the fourth large Galilean satellite of Jupiter, imaged hemispheres of Ganymede and Callisto that Voyager I had not seen, and studied Io continuously for more than 10 h in a "volcano watch." The primary scientific finding from the geologic analysis, which has been supported predominantly by the USGS, has been the discovery of active volcanism of Io of an intensity much greater than that on the Earth. Eight active volcanoes jetting material 100 to 300 km above the surface were discovered by Voyager I. Preliminary models reported by L. A. Soderblom suggest that magmatic intrusions into sulfur or sulfur intrusions into liquid sulfur dioxide zones could produce phreatic eruptions on Io of the magnitude observed. These hypotheses are strengthened by discovery of a tenuous sulfur dioxide atmosphere on Io by the infrared experiment aboard Voyager.

Ganymede, Callisto, and Europa

The lack of significant early topographic relief on Europa, Ganymede, and Callisto is consistent with the theory that a large fraction, perhaps 10 to 50 percent, of their interiors is composed of water. Europa's bright pastel surface is covered by a network of linear stripes, some of which are several thousand kilometers long and 100 km wide. L. A. Soderblom speculates that the stripes may have been produced when the planet's icy crust froze and expanded. Ganymede has undergone intense lateral tectonism; pieces of crust have been sheared and moved past one another, perhaps much like plates move about on the Earth. Callisto is one of the most primitive bodies in the solar system, displaying impact craters side by side. Systems of giant concentric bright rings on the surfaces of Callisto and Ganymede suggest that at some point their crusts were so soft and mobile that large impacts, which would normally produce basin-scale features like those on the Moon, Mars, and Mercury, simply disrupted the crust and formed concentric fractures along which material erupted from their interiors. Since that time, the crusts of Ganymede and Callisto have strengthened through loss of heat and have become rigid enough to support substantial topographic relief, up to 1 km on Ganymede.

CARTOGRAPHY

R. M. Batson reports publication of preliminary maps of the Galilean satellites of Jupiter at a scale of 1:25,000,000 from Voyager I and II image data. These maps show shaded relief and surface markings on Io, Europa, Ganymede, and Callisto in black and white. A map of surface markings on Io in natural color was prepared using an airbrush. A map showing radar reflectivity on Venus based on Earth-based radar images and on Venus Pioneer spacecraft data also has been prepared by airbrush.

PIONEER VENUS RADAR

Radar and image data obtained during the mission of Pioneer Venus have been reduced and merged with the base map produced from Earth-based radar telescopic facilities at Arecibo, P.R., and Goldstone, Calif. Harold Masursky reports that a planetwide contour map of the area between lat 75° N. and 63° S. shows the Venusian surface to be composed predominantly of a vast lowland plains area. Three highland areas rise above the lowland plains; the largest of these, Ishtar Terra or "the great northern plateau," is 1,550 km wide and 1,000 km long. The northern plateau rises as much as 10 km above the surrounding lowlands. Maxwell Montes rise as much as 4.5 km above the plateau surface; another mountainous area flanks the northwestern edge of the plateau. Other mountainous areas have been delineated by the Pioneer Venus altimetry data, as well as depressions, ridges, basins, and circular features – possibly craters.

MARTIAN GEOLOGIC INVESTIGATIONS FROM VIKING DATA

RESULTS FROM THE SURFACE LANDERS

Physical properties at the Viking landing sites

After the Viking Primary Mission, the surface samplers and cameras continued to operate during the Extended Mission until early May 1978. Major Extend-

ed Mission accomplishments reported by H. J. Moore include (1) excavation of deep trenches, (2) acquisition of more samples (chiefly for the X-ray fluorescence experiment), (3) construction of conical piles of materials in the sample fields, (4) backhoe touchdown experiments, (5) acquisition of contiguous pictures of the surface beneath No. 2 terminal descent engines using mirrors, (6) pushing and pulling rocks, and (7) other experiments for the physical properties investigation. Both pictures and surface sampler data acquired chiefly during the Extended Mission indicate that the surface materials in the sample fields of the Viking Landers may be grouped into four categories (in order of increasing strength): drift material, crusty to cloddy material, blocky material, and rocks. The response of the surface materials to engine exhaust erosion, data from other experiments, rock populations at the sites, and theory indicate that the surface should be relatively stable and resistant to wind erosion. However, erosion of the surface may occur when wind speeds are sufficiently high and when local conditions are favorable.

Mars surface materials

Laboratory simulations and model calculations by Priestley Toulmin, H. J. Rose, Jr., and J. G. Hammarstrom (USGS) in collaboration with A. K. Baird (Pomona College, Claremont, California) and Klaus Biemann (Massachusetts Institute of Technology, Cambridge, Massachusetts) indicate that (1) the principal source of H_2O evolved by the Martian surface samples during heating in the Viking gas chromatograph–Mars spectrometer is more likely to be a clay mineral of the smectite type than a hydrous iron oxide such as goethite and (2) particle-size effects may be very important in the interpretation of data from the Viking X-ray fluorescence spectrometer. Very fine grained mixtures (as the Martian samples are thought to be) may have significantly different spectral signatures than more coarsely granular material of the same bulk composition.

GLOBAL AND BROAD-SCALE RESULTS

The new geologic map of Mars

Geologic mapping using Viking moderate and high-resolution images has revealed many geologic units not shown on previous large- or small-scale maps of Mars. D. H. Scott reports that volcanic flows in the northern plains and around the large volcanoes of the Tharsis region have been reclassified and subdivided on the 1:15,000,000-scale map. The effects of water as an erosive agent are more widespread than previous mapping indicated. Alluvial flood-plain deposits in the Memnonia quadrangle are about the same age as volcanic flows of intermediate age in the Tharsis region. Sheet flooding on Lunae Planum appears to have originated from numerous local sources of collapsed and chaotic terrain.

Thermal properties of Mars

Martian global dust storms are triggered after dust injected into the atmosphere from local storms reaches a critical level. Reporting further results from the Viking infrared thermal mapper, H. H. Kieffer finds that Mars has two residual polar caps composed of different materials, the northern cap of water and the southern cap of carbon dioxide. The unexpectedly low brightness temperatures of the Martian polar caps in winter may be due to intrinsic optical properties of solid carbon dioxide. Finally, Kieffer reports that large areas of Martian terrain may differ specifically from those sampled by the two Viking Landers.

Surficial geology of the Martian equatorial region

Comparisons of a global multispectral map made from Viking Orbiter images with a thermal-inertia map derived from the Viking infrared-thermal mapper indicated that the materials in the equatorial region of Mars fall into four classes. L. A. Soderblom reports that dark materials in the southern equatorial belt contain the least oxidized and coarsest unit, which occurs as young lava plains devoid of dendritic channel networks, and very oxidized materials with lower thermal inertia (indicating they are finer), which occur as ancient highland units, crater rims, and intercrater plains riddled with dendritic networks. A third material, also of higher thermal inertia, is intermediate in albedo and also highly oxidized. Preliminary interpretation is that this is the duricrust unit seen at the Viking landing sites. Fine materials, which are oxidized and brighter than coarse materials, have been cemented into clods, increasing their thermal inertia. The fourth material, very bright, oxidized, and fine grained, occupies the extensive bright regions of the north equatorial region and is mobile on an annual cycle.

MARTIAN CHANNELS

History of the Chryse hydrographic basin

Clearly defined displacements in the relative positions of crater density curves generated from high resolution Viking photographs appear to confirm the hypothesis that channeling on Mars was episodic and occurred over a long period of Martian history, according to Harold Masursky. Geologic analysis of Viking mosaics showing the northern boundary of the basin seems to further strengthen the intermittent channeling hypothesis. No

water-cut shorelines or deposits that might have collected in a body of standing water are recognized; discharge from individual channel-forming floods is thought to have spread widely in the northern lowland area and then evaporated or sunk into the substrata.

Origin of large Martian channels

M. H. Carr proposed the following model for the formation of large Martian channels. Many large Martian channels arise full scale from discrete areas of chaotic terrain. Estimates of peak discharges based on channel dimensions range from 10^6 to 10^8 m^3/s. The large channels may have been eroded by water released rapidly, under great pressure, from deeply buried aquifers. Early in the planet's history, the old cratered terrain was probably highly permeable to depths of several kilometers as a result of its volcanic origin and intense brecciation meteorite impact. Extensive dissection of the old cratered terrain by fine channels suggests that fluvial action was widespread at that time and that warmer climatic conditions prevailed. Much of the water that cut the fine channels was probably removed from surface circulation and entered the ground-water system. Subsequent global cooling trapped the ground water under a thick permafrost layer and formed a system of confined aquifers. Thickening of the permafrost and warping of the surface created high pore pressures within the aquifers, particularly in low areas. Episodic breakout of water from the aquifers could have been triggered either by impact or by power pressure reaching the lithostatic pressure. The rate of outflow would have depended on the aquifer thickness and permeability, its depth of burial, and the diameter of the region over which water had access to the surface. Plausible values give discharges that range from 10^5 to 10^7 m^3/s. Outflow from the aquifer probably caused undermining of the adjacent areas and collapse of the surface to form chaos. Flow ceased when the aquifer was depleted or when the hydraulic gradient lowered around the chaos, and, thus, the flow was so reduced that the flow could freeze. The process could be repeated if the aquifer were recharged.

GLACIAL AND POLAR FEATURES OF MARS

Inventory of polar ice

Recently produced topographic contour maps from single stereophotogrammetric models in the north and south polar regions of Mars have allowed estimates to be made of the thickness and volume of each residual polar cap. Harold Masursky reports that both ice caps are about 2.2 km thick. Based on this figure, the north polar cap contains more than 2 million km^3 of water ice and particulate material, dust, or clay particles; volume of the carbon dioxide ice and dust or clay particles in the south polar cap is 400,000 km^3. Additional volumes of ice are contained as interstitial cementing material in the extensive dune and layered deposits that occur beneath and to the south of the permanent ice.

Martian outflow channels sculpted by glaciers

According to a study by B. K. Lucchitta, channel morphologies are well explained by a glacial origin, based on the following morphologic analogs with Earth. (1) Martian outflow channels widen, constrict, anastomose, and become locally incised. (2) Martian channels acquire a U-shaped profile where they constrict. (3) Hanging valleys occur where distributaries and tributaries merge with main channels. (4) Long even terraces (scour marks) occur on valley walls, and islands occur in channels. (5) Longitudinal ridges and grooves are conspicuous on Martian valley floors. (6) Channel islands on Mars are dimensionally similar to flood islands in the Channeled Scablands of Washington (Baker, 1978). (7) The width of Martian outflow channels varies widely. The grooved terrain of Kasei Vallis reaches 160 km but is generally less, and deeply incised troughs are a few kilometers to 20 km wide. (8) Steep scarps on channel sides and islands on Mars are as much as 2,000 m high.

EOLIAN LANDFORMS OF MARS

Restricted global distribution of Martian "sand"

Large accumulations of dune "sand" on Mars are restricted to the north circumpolar erg and to isolated crater-floor dune fields scattered throughout the planet. C. S. Breed and J. F. McCauley report that dune distribution differs greatly from that on Earth, where sand seas are widespread in the mid- to low-latitude deserts. Most of the Martian dune accumulations closely resemble the "sand-trapping" massive barchanoid forms typical of many desert basins on Earth. Belts of through-going longitudinal dunes, such as those that typically transport sand across the desert plains of western Egypt and central Australia, seem to be absent from Mars. The supply of "sand"-sized particles suitable for saltation on Mars may have been sparse always. The concentration of dune "sand" probably has resulted from a long history of wind transport of a limited supply of "sand" into areas where topographic barriers favor accumulation and retard further migration.

Pitted rocks on Mars—probable ventifacts

J. F. McCauley, M. J. Grolier, and C. S. Breed report that fluted and pitted quartzite and basalt rocks observed during a 1978 expedition in the Western Desert

of Egypt bear a striking resemblance to the pitted and fluted rocks seen by the Viking Landers. These rocks have generally been interpreted as vesicular basalts only slightly modified by wind erosion. Wind tunnel studies of the air flow over and around nonstreamlined hand specimens from the Western Desert show that windward abrasion coupled with negative flow, secondary flow, and vorticity in a unidirectional wind can explain the complex arrays of pits and flutes (McCauley and others, 1979). The field and laboratory observations suggest that the pitted rocks at the Viking Lander sites are also ventifacts and, thus, the Martian surface may be far more wind eroded than previously thought.

MARTIAN VOLCANISM

Aureole deposits of Olympus Mons

The large shield volcano Olympus Mons is surrounded by an asymmetrical aureole of grooved terrain that extends almost 1,000 km northwest from the center but only 600 km southeast. The 8.4×10^5 km^2 aureole is composed of a series of curvilinear ridges and troughs 10 to 100 km long and 1 to 5 km wide. The ridges rise about 0.5 to 1.5 km above the surface, and their crests, for the most part, form an accordant surface. The ridges are generally parallel to their outer boundaries and form an anastomosing pattern that varies in length and width over different parts of the aureole. Detailed mapping by E. C. Morris has shown the aureole to consist of several roughly circular overlapping sheets of material of great areal extent that are superimposed upon one another. Lobate scarps form the terminal edges of the deposits and, at some places, the aureole material appears to have been deflected during its emplacement around barriers, such as old crater rims, indicating a viscous flow. The ridges that make up the surfaces of the deposits are interpreted to be pressure ridges formed normally to the direction of flow and parallel to the margins of the deposits. Morris believes that the deposits are ash flows from huge pyroclastic eruptions that occurred at various times prior to the construction of Olympus Mons. There were at least four and possibly six eruptions, the oldest and largest extruded over 2.5×10^6 km^3 of pyroclastic material.

Olympus Mons and lesser volcanic features

In addition to the conspicuous shield volcanoes on Mars, other provinces have been discovered that indicate volcanism on a smaller scale. C. A. Hodges has identified specific landforms that appear to be analogous to and of the same order of magnitude as such terrestrial features as low shields (Greeley, 1977), pit craters, rhyolite domes, cinder cones, pseudocraters, table mountains, tuff cones and rings, and volcanic erosional remnants. Hodges and H. J. Moore speculate that Olympus Mons and its associated aureole deposits may have had subglacial beginnings; the 3 to 6 km scarp encircling the base of the volcano, thus, would be comparable to the scarps of table mountain pedestals that are composed of nonresistant pillow lavas and palagonitized tuff breccias (Van Bemmelen and Rutten, 1955). The prominent gravity high that extends from the shield northwest, coincident with the maximum accumulation of aureole deposits, is explained by the presence of magmatic source rocks beneath these materials, interpreted as subglacial eruptives that did not surface above the ice to form protective subaerial lava cap rocks.

IMPACT CRATERS

Large Australian impact crater established

Goat Paddock, a 5-km-diameter depression in the Kimberley District, Western Australia, was determined to be an impact crater by D. J. Milton (USGS), J. E. Harms (Broken Hill Pty., Ltd.) and J. A. Ferguson (Bureau of Mineral Resources, Australia). Tertiary lake sediments 210 m deep cover the floor, but drill holes penetrate to shatter-coned and comminuted sandstone bedrock. The upper walls, about 120 m high, are cut by valleys that expose cross sections of the walls and rim, perhaps the best such exposures anywhere in the world. Features outside the rim crest include ejecta flaps, thrust slices, and rim anticlines. Inside the rim crest, upturned strata are truncated by the crater wall, which has a slope of 35° to 50° or more.

Cratering mechanics at the Flynn Creek impact crater

A deep drilling program (21 holes) has been completed by D. J. Roddy at the Flynn Creek impact crater in north-central Tennessee. Preliminary analysis of the drill core indicates that the region of total brecciation and extensive excavation formed during cratering had the approximate shape of a broad flat-floored cavity with a deep central zone of intensely disrupted and uplifted strata. This configuration is presently interpreted as the approximate shape of the maximum transient cavity (Roddy, 1979).

Impact cratering mechanics at Meteor Crater

A series of detailed computer calculations has been completed for modeling the formational processes of the largest well-preserved terrestrial meteorite impact crater, Meteor Crater, Ariz. Results of the first calculations indicate that the impact energy was about 10 Mt, a factor of two more than estimated from earlier work,

and suggest a lower impact velocity (about 20 km/s) than previously expected. A set of initial impact conditions and material properties was furnished by D. J. Roddy (1978). The computer-code simulations, conducted in conjunction with K. N. Kreyenhagen and S. H. Schuster (California Research and Technology), involved adaptations of the highly advanced formulations now in use for explosion cratering research.

LUNAR INVESTIGATIONS

IMPACT BASINS

Lunar basin ages

D. E. Wilhelms has determined the relative ages of 22 of the 32 definite lunar ringed impact basins 250 km wide and larger by comparing size-frequency distributions of superposed primary impact craters. Pre-Nectarian, Nectarian, and Imbrian basins emerged as three distinct groups. Consideration of differential burial, the primary-secondary crater distinction, superposition relations, and other geologic variables helped resolve the relative ages of basins with similar size-frequency curves.

Lunar basin structure

D. E. Wilhelms has remapped basin rings and deposits on both lunar hemispheres and noted irregularities that have not been considered fully in previous attempts to explain ring origin. Regular interior ring structure is interrupted in some sectors of large basins by irregular or chaotic zones that apparently resulted from differential interior uplift. Diverse morphologies and bifurcations of outer rings may have been caused by differential exterior deformation or by differential excavation in sectors preconditioned by spalling or other deformation. Well-exposed basins have asymmetrical ejecta blankets and secondary-impact distributions that apparently resulted from oblique impacts. The general process of ringed-basin formation seems to be one of irregularities imposed by oblique impacts, layering in the target material, or other geologic variables upon a more regular pattern dictated by impact magnitude.

LUNAR SAMPLE INVESTIGATIONS

Cooling history of a lunar fragmental melt

Fragment-laden lunar basalt 77115 is thought to be a sample of the impact-generated melt sheets produced about 3.8 b.y. ago, at the termination of the cataclysmic stage when planetesimals collided with the Moon. J. S. Huebner, R. F. Sanford, and C. R. Thornber used microprobe analysis, experimental petrology of a synthetic analog of the sample, and diffusion and heat-flow modeling to limit the possible interpretations of the thermal history of basalt sample 77115. The results indicate that the melt sheet was never completely molten, that it cooled rapidly (>10°C/h but<500°C/h) while most of the crystals were precipitating, then cooled at less than 7°C/h near the solidus. Compositional zoning in lunar olivine xenocrysts indicates that iron-magnesium diffusion occurred but that the diffusion process did not go to completion. Thus, the sample must have been annealed for approximately 90 to 625 d at 1,050° to 950°C. The rapid initial cooling, followed by lengthy annealing at elevated temperatures, implies that the temperature of 77115 approached that of a hot, presumably adjacent, material. Although the results do not rule out a number of short thermal events rather than a single event, the sample could have continued to cool slowly because the heterogeneities in the olivine would have disappeared. A possible cause for a final stage of rapid cooling, which would terminate diffusion in the olivine, is the excavation and exposure at the surface of the crystallized, but still warm, melt sheet by slumping at a crater rim or by a subsequent meteorite impact.

Consortium studies of Serenitatis ejecta

Clasts extracted from Apollo 17 breccia 73255 are providing data on the Serenitatis Basin event and on the lithology and chemistry of the early lunar crust. O. B. James and her associates have made detailed petrologic studies of two clasts of noritic rocks (James and McGee, 1979). These clasts are relatively coarse-grained granular rocks in which the predominant minerals are plagioclase and orthopyroxene. Both clasts had very similar histories. Their parent rocks were igneous highland rocks, probably formed by crystallization of internally generated melts rather than impact melts. The parent rock of one of the clasts was clearly a cumulate, and both probably crystallized below the lunar surface. Both parent rocks had appreciable subsolidus re-equilibration after they crystallized. Both were later shocked, granulated, and injected with iron-sulfur-rich vapor, and fragments from them were incorporated in the 73255 fragment-laden melt. Histories of the two rocks differ only in detail; one crystallized more slowly and was more strongly shocked but less strongly granulated than the other. Despite this similarity in history, the parent rocks of the two clasts appear to have been derived from distinct magma types. One was characterized by plagioclase and orthopyroxene as the major constituents and by a relatively high content of potassium, niobium, and zirconium. The other contained augite, as well as plagioclase and orthopyroxene, as the

major constituent and had a relatively low content of potassium, niobium, and zirconium. It is unlikely that these two magma types were related by crystal fractionation processes.

URANIUM-THORIUM-LEAD SYSTEMATICS OF CHONDRITIC METEORITES

The 4.53 b.y. to 4.54 b.y. Pb-Pb internal isochron ages obtained for the Richardton and Barwell meteorites by Mitsunobu Tatsumoto provide evidence that the equilibrated ordinary chondrites (petrographic grades 5–6) may be younger than achondrites (~4.55 b.y.). The ages obtained may not correspond to the formation ages of the meteorite parent bodies but, rather, may reflect metamorphism. The Pb-Pb internal isochron ages are older than the 4.504 ± 0.015-b.y. Rb-Sr "age of condensation" (Minster and Allegre, 1978) determined from a whole-rock isochron of both ordinary and enstatite chondrites. This discrepancy could be accounted for by a ~1-percent error in the ^{87}Rb half-life. Alternatively, the age differences could be real, reflecting different closure ages (temperatures) for the U-Pb and Rb-Sr systems. However, if this were true, the Rb-Sr ages would be older than the U-Pb ages because Pb is much more volatile than Rb or Sr. Uranium-lead relations suggest that both Barwell and Richardton have experienced a recent (<100 m.y.) thermal or shock event that caused partial reequilibration of the U-Pb system. Apparent recent disturbances are commonly found in U-Pb studies of meteorites, but the ages of the recent events cannot be determined precisely enough to establish whether the young ages correspond to the event that created the meteoroid or to its entry into the Earth's atmosphere.

REMOTE SENSING AND ADVANCED TECHNIQUES

EARTH RESOURCES OBSERVATION SYSTEMS OFFICE

The Earth Resources Observation Systems (EROS) Office supports and coordinates research in applications of remote sensing technology and conducts demonstrations of these applications within bureaus and offices of the DOI. The EROS Data Center (EDC) in Sioux Falls, S. Dak., is the principal archive for and distributor of data collected by USGS and NASA research aircraft and by Landsat, Skylab, Apollo, and Gemini spacecraft. The center's other major functions are assistance and training in the use of remotely sensed data and development and demonstration of remote sensing technology.

Scientists and other members of the Data Analysis Laboratory staff at the EDC cooperate with Federal and State user agencies in projects that demonstrate the applications of remote sensing techniques to resource management problems. The cost effectiveness and usefulness of the techniques are assessed and documented, and the user agencies gain experience in carrying out procedures. Research in the applications of remotely sensed data also is conducted by scientists in the EROS Office headquarters in Reston, Va., and at a field office in Flagstaff, Ariz.

CARTOGRAPHIC APPLICATIONS

Composite mapping

D. D. Greenlee (Technicolor Graphic Services, Inc., Sioux Falls, S. Dak.) used composite mapping techniques to create six water-depth information images of the 57,500-ha Shark Slough in the Everglades National Park, Fla. A temporal overlay was created by registering the images from six Landsat subscenes to a 100-m Universal Transverse Mercator grid. The inundation levels and water volumes in Shark Slough then were determined for each season of the year.

Improved Landsat image maps of glaciers

Research continued on ways to improve the information content of Landsat images used to map glacier-covered areas. Richard S. Williams selected for study the largest temperate ice cap in Iceland, Vatnajökull, which has approximately 100 outlet glaciers and numerous surging glaciers. Two experimental 1:500,000-scale fall and winter Landsat image maps of Vatnajökull, Iceland (U.S. Geological Survey, 1976, 1977), were prepared in cooperation with the Iceland Geodetic Survey and the National Research Council of Iceland. At the relatively high solar elevation angle (25°) of the fall scene, the interior part of the ice cap is completely white except for the shadow cast by the southern edge of the Grimsvötn caldera in the west-central part of Vatnajökull. At the low solar elevation angle (7°) of the winter scene, on the other hand, considerable morphologic detail on the ice cap surface can be discerned on the image map.

Although morphologic, geologic, and hydrologic details of the fall Landsat image of Vatnajökull were recorded by the MSS bands 4, 5, 6, and 7, they were not imaged photographically by the electron beam recorder. To recapture this information, computer enhancement techniques developed by the Jet Propulsion Laboratory (JPL) were applied to the computer-compatible tapes containing the image data. The resulting computer-enhanced fall image of Vatnajökull then contained the subtle morphologic detail seen before only on low solar angle (winter) images of the ice cap (Williams and others, 1977).

At the EDC, additional enhancement techniques were applied to the fall Vatnajökull image. The research at both the JPL and EDC established that computer enhancement can markedly improve Landsat image maps of glaciers.

Landsat image maps of Cape Cod

Recent observations indicate that Monomoy Island, Cape Cod, Mass., was breached several times in the historical past, but the breaches were usually repaired by littoral drift within a few days or weeks. From February 6 to 7, 1978, one of the most severe storms of the 20th century assaulted the New England coast, and a breach occurred as predicted by Oldale and others (1971). After the storm, R. S. Williams, Jr., analyzed Landsat 2 and 3 MSS and RBV images to determine if the progression of the breach could be observed. A January 6, 1978, Landsat MSS image (21080–14135) showed Monomoy Island intact; a February 11, 1978, MSS image (21116–14151) showed a breach in Monomoy Island at Hammonds Bend, although the 80-m resolution of the image limited its usefulness to a qualitative carto-

graphic and geologic assessment. On March 9, 1978, however, a Landsat 3 RBV image (30004-14435-B) was recorded, which clearly showed that the breach was approximately 500 m wide at near-high tide. Two Landsat 3 RBV images acquired on April 15, 1978 (30041-14433-D), at near-low tide, and on August 19, 1978 (30167-14444-D), at near-high tide, with an estimated 25- to 35-m spatial resolution (A. P. Colvocoresses, 1978), were more useful. They permitted delineation of the breach and the subsequent changes caused by continuing erosion and deposition of beach, dune, and shoal sediments in and around the breach area. Significant planimetric detail in the shoals surrounding Monomoy Island was also visible in the 0.505- to 0.75- μm spectral region of the Landsat 3 RBV image. This confirms that Landsat 3 RBV images can be used to monitor dynamic geological phenomena such as coastal change (Williams, 1979a).

Preliminary research suggests that Landsat 3 RBV images, either singly or in mosaics, can be enlarged to a 1:100,000 scale without objectionable image degradation and with a planimetric accuracy superior to that of Landsat MSS images (Williams, 1979b). These images and mosiacs also can be used as an orthoimage base map for geologic maps.

GEOLOGIC APPLICATIONS

Analogous geomorphic processes in Iceland and on Mars

R. S. Williams, Jr., compared the orbital spacecraft images of Iceland and Mars to study the interaction of volcanic, glacial, tectonic, and eolian geomorphic processes. The images showed that landforms resulting from all of these processes probably are present in both places. However, on Landsat images of Iceland, the approximately 100-m ground resolution cannot be used to discriminate all of the diverse types of landforms. A similar lack of detail is present on orbital images ($\geq$100-m resolution) of Mars. On Landsat images of Iceland, both subaerial and subglacial (table mountain) shield volcano landforms are well represented. On orbital images of Mars, shield volcano landforms are also prominent. Glacial features on Landsat images of Iceland include concentric and sinuous recessional moraines at the margins of icecaps. Within the ablation zones of some icecaps, successive light and dark bands are present because of the deposition of glaciovolcanic eolian materials (mostly tephra, but some loess). On Viking Orbiter images of Mars, along the margins of the relict north polar cap, light and dark bands also may represent eolian materials deposited during recurring periods of ice accumulation. In Iceland, local icecaps form where the volcanic landform is higher than the regional firn limit. On Mars, localized icecaps also may have existed outside polar areas during different climatic conditions in the past. On the northwest flank of the large shield volcano, Arsia Mons, in the Tharsis Montes area, concentric and isolated sinuous ridges very similar in appearance to recessional moraines occur, implying that a local icecap may have existed in the past. If the extrapolar icecap hypothesis is correct, then some of the volcanic areas on Mars may have been the source of catastrophic outburst floods (similar to Icelandic jökulhlaups) resulting from subglacial volcanic activity. This geomorphic process may have caused the fluvial erosion of the Martian surface.

Fraunhofer line discriminator

According to R. D. Watson and Arnold Theisen, a luminescence image acquired by the Fraunhofer line discriminator (FLD) of the Alpine Mill and surrounding area in the Pinenut Mountains, Nev., revealed luminescence patterns that correlated well with the distribution of outcrops observed in aerial photographs. The outcrops were identified in the field as limestone. Certain areas shown in the image also had a very high luminescence.

Data from geochemical maps of the area supplied by the AMAX Co. and data from the images were used to produce correlation diagrams of mineralization versus luminescence, particularly of the areas of anomalously high luminescence. One mineral, fluorite, was found to have a correlation between concentration and luminescence of 0.88 at the 99-percent confidence level and is suspected to be the major contributor to the anomalous values shown in the image. The luminescence image also was used as a guide for sampling surface materials for geochemical analysis.

International cooperation in fuels and minerals exploration

D. G. Orr and G. B. Bailey (USGS) and P. D. Anderson (Technicolor Graphic Services, Inc., Sioux Falls, S. Dak.) participated in a cooperative scientific exchange between the USGS and the People's Republic of China Scientific Research Institute for Petroleum Exploration and Development. Geologic interpretations based on analyses of standard and enhanced Landsat data acquired over the major portion of the Tsaidam Basin of China were used to produce a geological structure map with an accuracy of 75 to 80 percent. This map compared very favorably with a geologic map compiled from ground sources during the past 20 yr. The detail of the two maps also is very comparable. The analytic and interpretive work for the Landsat-data derived map was accomplished in only 2 man-weeks. This accomplishment has great significance for petroleum exploration in this and other remote parts of the world.

Lineaments of the conterminous United States

W. D. Carter conducted an analysis of lineaments in selected areas of the conterminous United States by examining Landsat images and image mosaics at scales ranging from 1:250,000 to 1:20,000. Carter found that a variety of scales is useful in lineament mapping. Extremely small-scale data provide general information for mapping large areas, whereas large-scale data are useful for the field mapping of smaller areas. Color-composite images of the State of Maine at a scale of 1:250,000 were analyzed and compiled into a single map that was subsequently reduced to a 1:500,000 scale to fit the Geologic Map of Maine published by the Maine Geological Survey. Field studies of the principal northeast-trending straight courses of the Penobscot and Kennebec Rivers indicate that the rivers are, in part, controlled by formational contacts that are also fault zones of probable strike-slip origin. A horizontal displacement of as much as 12 km may have taken place near Skowhegan, Maine. When combined with data from an oil and gas map, a basement map, and a gravity map of the United States, the small-scale lineament maps show major basins in the Precambrian surface of North America that could be ancient impact craters modified by geologic processes.

Satellite altimetry applications to land subsidence

Population growth in Arizona has increased demands on ground-water resources so that withdrawal of ground water now exceeds recharge by 2,700 hm^3/yr. According to W. D. Carter, this has resulted in land subsidence and earth cracks that are most prevalent between southern Phoenix and Casa Grande. In this area, leveling indicated subsidence of as much as 4 m, and the subsidence is continuing at a rate of approximately 0.1 m/yr. More recently, subsidence has been observed in the area immediately north of Tucson, Ariz.

Geodynamics Experimental Ocean Satellite (GEOS) 3 and Seasat 1, carrying radar altimeters designed primarily to measure ocean wave heights, passed over areas of land subsidence in Arizona. A preliminary analysis of two GEOS 3 passes suggests that the satellite can measure subsidence to an accuracy of about 0.1 m.

HYDROLOGIC APPLICATIONS

Enhancement of water turbidity patterns on Landsat images

Continuing research by G. K. Moore has shown that a nearly maximum enhancement of obscure water turbidity patterns can be obtained by using an albedo image calculated from Landsat digital data. Albedo is the sum of radiances in Landsat bands 4, 5, 6, and 7 and can be calculated using a relatively simple algorithm. Tests on small water bodies in surface mining regions of the Eastern United States have shown that estimates of the flood hazard and degree of eutrophication can be made quickly and inexpensively using this method. Equal or better results might be obtained with broad band RBV data, but MSS band 7 data are needed to distinguish land from water. The albedo algorithm also should prove useful for making estimates of water depth in clear lakes in playas.

Evaluation of hydrologic data relay

GOES was used to relay hydrologic data from seven network stations in central Florida from 1976 to 1979. W. M. Woodham reported that the relay system was about as reliable as conventional methods of data collection. Benefits of the system include cost and manpower reduction, improved data accuracy, real-time data transmission, and a capability for computer storage and analysis of data. Manpower needs were reduced about 15 to 18 percent at single-parameter sites, such as those used for measuring stream stage, rainfall amount, and ground-water levels. Savings of about 50 percent may be possible for multiple-parameter sites, the data from which now require complex manual computations.

Flood plain inundation in the Apalachicola River basin

J. R. Lucas and D. J. Stetz (Technicolor Graphic Services, Inc., Sioux Falls, S. Dak.), in cooperation with the USGS in Tallahassee, Fla., developed a procedure using Landsat data to delineate the area of inundation within the forested wetlands along the Apalachicola River in Florida. Landsat data for different times of the year were analyzed to determine the optimal land cover conditions for determining the extent of flooding. Inundated lands were best displayed on winter images from November through March. Well-developed vegetation canopies masked inundated areas during other months of the year.

Landsat scenes that corresponded to critical periods of the highest and lowest river flows were selected for analysis. Conventional photointerpretation techniques and digital image processing were used to delineate the areal extent of floods within the watershed boundaries of the Apalachicola River basin on a February 1977 Landsat scene (a period of peak flow). The area of inundation mapped by photointerpretation techniques was measured using a leaf-area meter. The areal extent of the flood also was determined using an unsupervised maximum likelihood classification of geometrically corrected Landsat data. Vegetative communities and other resources were classified into inundated and noninun-

dated groups. However, more Landsat scenes must be analyzed before a statistical relation between river state and area of inundation can be established.

Improvement in streamflow estimates

According to G. J. Allord, estimates of low flows and floodflows in several streams in southwestern Wisconsin were improved when data on land cover in the basins were included in the regression equations. These equations commonly are used to estimate streamflow statistics at ungaged sites. Landsat digital data were used to classify and measure the areas of different land cover types in the basins. The results of these measurements were then tested for significance. Standard errors of estimate of flood frequencies having 10-, 50-, and 100-yr recurrence intervals were reduced by 14 percent. The error of estimate for the least of the annual 7-d low flows having 2- and 10-yr recurrence intervals was lowered by 9 percent.

Integration of Landsat data and hydrologic data for water management of the Everglades National Park, Florida

D. J. Stetz, J. R. Lucas, and D. G. Gehring (Technicolor Graphic Services, Inc., Sioux Falls, S. Dak.) undertook a cooperative demonstration project with the National Park Service (NPS) in which satellite remote sensing techniques were merged with hydrologic data to meet NPS resource information requirements in Everglades National Park. Geometrically corrected Landsat subscenes of the 57,400-ha Shark Slough acquired on six dates were analyzed on an interactive multispectral image analysis system to determine the areal extent of contracting and expanding water margins. Results of the cooperative project included (1) maps, derived from Landsat data, of the spatial distribution of water in the slough on each of the six dates, (2) digitally produced images showing the distribution of water levels within the slough on each date, (3) the distribution of water depths within the inundated areas of the slough on each date, and (4) calculations of total water volume stored within the slough on each date based on Landsat-derived inundation information merged with water-level data. This project provided Everglades National Park personnel with information on the areal extent, depth, and quantity of water within Shark Slough that will help them more effectively manage the ecologically critical water budget of the park.

Inventorying and monitoring ground-water resources

J. R. Lucas and D. J. Stetz (Technicolor Graphic Services, Inc., Sioux Falls, S. Dak.) are conducting an investigation to assess the usefulness of Landsat data for targeting potential sites of shallow ground water in glaciated terrains of the upper Midwestern United States. Patterns delineated on selected springtime Landsat images and a springtime Landsat mosaic were found to be related to continental glaciation. Glacial features characterized by high sand and gravel content are considered potential sites for ground-water exploration because the deposits are highly permeable. Pattern analyses were undertaken on Landsat images of Iowa, Kansas, Wisconsin, Minnesota, Illinois, and Missouri and on a high-altitude aircraft mosaic of north-central Iowa.

Irrigation water use in the Columbia River Basin

G. E. Johnson, W. H. Anderson, and T. R. Loveland (Technicolor Graphic Services, Inc., Sioux Falls, S. Dak.), in cooperation with the U.S. Army Corps of Engineers, used Landsat images to monitor historical irrigation developments and to analyze potential sites for future irrigation development in selected pilot areas in the Columbia River Basin. Digital Landsat data stored in a geographic information system were composited with digital terrain and digitized soil data. The technique also was used to evaluate distance and elevation from a source of irrigation water as inputs into a model of potential irrigation development.

In cooperation with the Kansas Geological Survey, Lucas and Stetz examined Landsat images of northeastern Kansas for evidence of buried alluvial valleys. On numerous images, narrow bands of distinct tones could be seen extending over large distances in northeastern Kansas. Some of these patterns were found to correspond to, or continue from, known buried valleys, while others bore no relation to the valleys. The patterns possibly are related to lateral differences in surficial materials or soil moisture or to other characteristics of the buried-valley fills that contrast with the surrounding deposits.

Large-scale marine eddies

A Landsat MSS band 4 (0.5–0.6 μm) image (2514–12021), acquired on June 19, 1976, just south of the Vestmann Islands, Iceland, showed some near-surface large-scale marine current patterns. The scene imaged cuts across the insular slope along the southwest coast of Iceland where water depths range from 100 to $<$2,000 m. According to R. S. Williams, Jr., at least eight well-defined eddies are visible on the image, and at least three well-developed double eddies (one turning clockwise; the other, counterclockwise) are shown in the near-surface waters. Individual eddies associated with the double eddies are 20 to 30 km in diameter, and individual stream currents leading to the double eddies extend for 50 to 70 km.

The coastal shelf area to the north of the image is rich in phytoplankton and zooplankton, which support a large fish population. The image also showed light-toned water that spectrally resembles sediment-laden water. However, the distance of the light-toned water from the Icelandic coast suggests that the light tone is the result of some other condition, possibly a high concentration of phytoplankton. This research suggests that Landsat MSS band 4 images may represent an important new source of data on the marine environment.

Oil well blowout in the Gulf of Mexico

Morris Deutsch closely monitored the blowout from Mexico's Pemex oil well Ixtoc 1 in the Gulf of Mexico. The monitoring was done in collaboration with the U.S. Coast Guard and NASA. Landsat data were used to detect and delineate oil floating westward from the well in the Bay of Campeche to the coastline between Vera Cruz and Tampico, then northward into Texas waters between Brownsville and Galveston. A mosaic of four Landsat images, prepared by the USGS, was used as a guide for July flights of the Coast Guard C–130 Airborne Oil Surveillance System aircraft to oil-contaminated areas and to aid the Scientific Support Coordinator of NASA and the On-Scene Coordinator of the Coast Guard in predicting when oil from the runaway well would reach U.S. Waters.

Satellite image atlas of glaciers

According to R. S. Williams, Jr., 55 glaciologists and scientists from 30 U.S., foreign, and international organizations are involved now in producing a satellite image atlas of glaciers. The atlas will cover 12 geographic areas and will include 8 topical chapters. The best available Landsat images of Antarctica, Greenland, Iceland, New Zealand, and Asia were identified and forwarded to the chapter authors. Landsat 3 RBV images, which have a resolution about three times better than the Landsat MSS and Landsat 1 and 2 RBV images, were used to map glaciological phenomena. When used in mapping glacier termini in Iceland, Landsat 3 RBV images were found to provide better tonal discrimination of features on outwash plains than MSS images or MSS color composites. It was determined also that Landsat 3 RBV images of glaciers could be enlarged to a scale of 1:100,000 and still retain acceptable image detail and planimetric accuracy (Williams and Ferrigno, 1979).

TECHNIQUES IN PROCESSING LANDSAT IMAGE DATA

Application of principle components analysis and canonical analysis

S. K. Jenson and F. K. Waltz (Technicolor Graphic Services, Inc., Sioux Falls, S. Dak.) presented mathematical definitions of principal components analysis and canonical analysis, described the effects the procedures have on image data acquired by aircraft and satellites, and suggested circumstances under which the techniques can be most effectively applied to analysis of aircraft and satellite data.

Principal components analysis and canonical analysis aid in dimensionality reduction, overall image enhancement, and enhancement before classification. Both analysis methods use linear combinations of image data while preserving the variance of the original axes; new axes are created, however, in which the relations in the data are rearranged. Both of these techniques are based on the assumption that the variance of image data may be used as a measure of the information content of the image.

Principal components analysis of X original x-variables determines a linear transformation that condenses essentially all of the variance in the original data into Y new y-variables so that the y-variables are uncorrelated (orthogonal) even though the x-variables remain correlated. Generally, the greater the correlations among the x-variables, the smaller Y will be relative to X. This is the case in most MSS images because a high degree of correlation usually exists between the data of two channels.

Canonical analysis produces a data transformation that is based on the spectral characteristics of categories, or classes, defined from the data, by maximizing the between-category covariance matrix and minimizing the within-category covariance matrix. The first new axis represents uncorrelated data and accounts for the greatest amount of variance, whereas succeeding axes contain successively smaller amounts of variance. Therefore, this transformation enhances differences between categories.

These two techniques are effective tools for analyzing MSS data of four spectral dimensions or for analyzing multitemporal images of eight or more bands produced from two or more four-band images of different dates registered to each other. Also, when additional data sets are added to data from the original four bands, principal components and canonical analysis can be used to combine all of the data types, and useful displays can be created by color compositing the transformed variables.

Data sets produced by arithmetic functions, such as ratioing, are usually highly correlated with the original four-band image data, as well as with each other. Multitemporal data also are characterized by high correlations. This redundancy is removed by both techniques when the correlated values from the original axes are transformed to uncorrelated values of the new axes. Fewer axes are needed then to represent all the variance.

Digital processing of Fraunhofer line discriminator data sets

Using digital enlargement and smoothing techniques, P. S. Chavez produced high-quality images of small data arrays, such as those obtained by FLD measurements. Two significant advantages of these techniques are the ease and speed of data reduction and the easy recognition of patterns in the image. Features such as the distribution of oil seeps in the Santa Barbara Channel, Calif., and luminescence contrasts related to mineralization anomalies in the Pinenut Mountains, Nev., could be seen. The image format is such that geometric corrections can be applied readily. The resulting image is enhanced easily through either color density slicing or continuous color coding.

Some effects of nearest neighbor, bilinear interpolation, and cubic convolution resampling on Landsat data

C. A. Nelson (Technicolor Graphic Services, Inc., Sioux Falls, S. Dak.) and Jeanne Etheridge (Purdue University) undertook a study of the effects of three resampling methods—nearest neighbor, bilinear interpolation, and cubic convolution. The transformation of Landsat MSS data from its coordinate system to a map projection coordinate system makes the data more usable, but little is known about how the brightness values for pixels are modified during this transformation.

Problems in mapping shallow seas and small islands by the Defense Mapping Agency, Hydrographics Office, led to the study of data from Bimini Island and part of the Great Bahama Bank. The study was conducted as follows: (1) data from a subset of the scene were destriped, (2) the destriped data and three sets of destriped resampled data were independently classified and displayed as nine spectral classes using the analysis software, and (3) the destriped, resampled, and classified data sets were studied and compared. Significant results were:

- The cubic convolution resampling method produced brightness values outside the ranges of both the original and destriped data. This anomaly suggests overshooting (high values of the data increased and low values decreased along the boundary between high and low values).
- The ranges and standard deviations of the data in all channels were smaller in bilinear resampling than in cubic convolution and nearest neighbor resampling.
- The nearest neighbor resampled data most accurately preserved the uncorrected shapes of small islands and the data values for the water surrounding these islands.
- Peaks and valleys in the data along a line traversing an island were smoothed by bilinear methods but were exaggerated by cubic convolution resampling; in some cases, additional peaks were introduced.
- There was no significant difference in the maximum likelihood classifications of data resampled by the three methods.

LAND RESOURCE APPLICATIONS

Arid land monitoring using Landsat images

C. J. Robinove calculated the albedo of an arid area in western Utah from the reflectances in each of the four bands recorded by the Landsat multispectral scanner. Albedo maps of an area at different times were differenced to obtain an albedo change map. Areas of increase or decrease in albedo were mapped and field-checked to determine the cause of change. Annual changes in albedo from 1972 to 1976 were found to be caused by increases or decreases in vegetation density, changes in soil moisture, and erosion. The principal determinant of albedo change was winter and spring precipitation; the effect of grazing was not significant.

Classification of wildland vegetation in Arizona using Landsat MSS data and digital terrain data

Wayne G. Rohde (USGS) and Elizabeth Hertz and W. A. Miller (Technicolor Graphic Services, Inc., Sioux Falls, S. Dak.) reported that Landsat MSS data, acquired in August 1977, were used to classify approximately 1,000,900 ha in northwestern Arizona into nine land cover types using an interactive image analysis system at the EDC. A simple random cluster sample was used to estimate that 54 percent (standard error = 5 percent) of the Landsat pixels were classified correctly. An accuracy estimate and sampling error also were calculated for each land cover type.

Digital terrain data were acquired for the project area and registered to the Landsat data. These terrain data then were used to calculate the elevation, slope, and aspect of each Landsat picture element, and large-scale aerial photographs were used to determine the vegetation cover type of selected picture elements. The vegetation cover data and elevation data were combined to determine the elevation range of each cover type. The elevation range of each cover type and of each

computer-derived vegetation class then were used to derive elevation decision rules for revising the Landsat classification results. The accuracy of the classification of vegetation in the project area was estimated to be 73 percent (standard error = 5 percent). The use of digital elevation data also improved the accuracy of the classification of each land cover type.

The digital terrain data also were combined with the Landsat classification results to produce output products for specific resource management applications. Examples of such applications are the location of potential pinyon-juniper chaining areas, mule deer winter ranges, and sagebrush treatment areas. BLM personnel defined the vegetation cover type, elevation range, slope, and aspect of each of these examples. The combined Landsat cover-type classes and terrain data were processed to tabulate those picture elements that met the criteria defined for each application. The results then were tallied as area summaries and displayed on map overlays.

Detection of water-stressed plants by remote measurement of fluorescence

R. D. Watson (USGS) and J. D. McFarlane (EPA) conducted an experiment at the University of Arizona Citrus Experiment Farm in Tempe, Ariz., to detect water-stressed plants by remote measurement of fluorescence. Thirteen mature lemon trees were selected for study. The withholding of irrigation water from all trees for 3 weeks induced water stress that was clearly indicated by both stomatal resistance and water potential measurements. An FLD, mounted on a platform 12 m above the ground, was used to measure the luminescence of the trees. Measurements showed no difference in the mean luminescence of irrigated and nonirrigated trees in the prenoon hours. However, differences in the fluorescence were evident in the afternoon, and the luminescence of the unwatered trees was 25 percent greater than that of the watered trees. Correlation between stomatal resistance (an indicator of stress) and luminescence was found to be 0.8 at the 95 percent confidence level.

Forest classification in western Washington

G. R. Johnson (Technicolor Graphic Services, Inc., Sioux Falls, S. Dak.) and E. W. Barthmaier, T. W. D. Gregg, and R. E. Aulds (Washington Department of Natural Resources) investigated the usefulness of the digital analysis of Landsat data for classifying forest stands in western Washington. Landsat data were geometrically alined with forest stand data from two 94-km^2 study areas. The results of the digital clustering of Landsat data were compared with the forest stand data to determine what forest resource groups should be used for classification. Landsat data were classified into the resource groups and the classification accuracy determined.

In the Clearwater study area, the primary concerns were to determine the separability of old-growth and second-growth sawtimber and to determine the classification of established plantations and previously clear-cut areas into discrete age and stocking classes. Landsat classifications (composed of clear-cut, established plantations, and older forest classes) agreed with forest stand classifications in 87 percent of the independent samples of resource plots. The Landsat classifications of the more detailed discrete age and stocking classes agreed with forest stand classifications in 56 percent of the plots. Most misclassifications at this, the more detailed level, occurred between classes composed of similar vegetation cover types, such as recently planted clear cuts and young established plantations.

Studies in the Capitol Forest area illustrated the extent to which Landsat data could be used to separate second-growth stands into young plantations, poletimber, and sawtimber size classes. Because the spectral clusters typically included Landsat data representing several timber size classes, the resource classes based on these data generally did not correspond to a single size class. However, the proportion of each timber size class in each Landsat resource class could be quantified from the forest stand data, and each Landsat class assigned to the most frequently occurring size class.

Mapping wildland vegetation in Arizona using visually interpreted Landsat images

Kris Bonner (Technicolor Graphic Services, Inc., Sioux Falls, S. Dak.) reported that broad vegetation cover types in northwestern Arizona were manually (visually) interpreted on single-data standard and enhanced Landsat false-color composite images at a scale of 1:250,000. The maps produced from the standard and enhanced images were 83 percent correct and 88 percent correct, respectively. An existing BLM vegetation map of a large area within the study site was estimated to be 68 percent correct. While there was no significant difference between the overall accuracies of the maps produced from the standard and enhanced Landsat images, there was a significant difference between both of these maps and the BLM vegetation map. The cost of producing the vegetation maps using visual interpretation of Landsat data was less than 1.2 cents per hectare.

Use of large-scale photographs to document changes in rangeland vegetation

Large-scale color and color-infrared 70-mm aerial photographs were acquired over a range site in northeastern California in July 1978. D. M. Carneggie compared the photographs with similar large-scale aerial photographs acquired in July 1967 and 1969. Measurements of foliar cover and plant numbers indicate that two dominant shrub species in the plant community (Bitterbrush, *Purshia tridentata,* and Big sagebrush, *Artemisiatridentata*) doubled in number between 1969 and 1978. Moreover, the total foliar cover of these two shrubs also doubled. Ground sampling during the summer of 1978 verified the accuracy of these estimates.

Vegetation mapping in the Pictured Rocks National Lakeshore, Michigan

The Pictured Rocks National Lakeshore (PRNL) Demonstration Project, initiated in August 1977, was designed to determine the usefulness of large-scale (1:63,000) digitally processed Landsat images for vegetation cover mapping. W. H. Anderson (Technicolor Graphic Services, Inc., Sioux Falls, S. Dak.) reported that a draft vegetation cover map derived from Landsat images was completed in October 1978. Color-infrared aerial photographs (1:24,000-scale stereographic coverage) were purchased in January 1979 for use in a field verification effort designed to check and revise the draft vegetation map.

The vegetation cover map was completed and used extensively during fiscal year 1979 to prepare a general management plan (GMP) for the PRNL. One of the most significant uses of the map was to select a route for a translakeshore highway. Proposed alinements were based on incomplete information about vegetation units. By using the cover map, the location of bogs and other critical wetlands were accurately determined, allowing a route to be selected that would have minimum impact on these sensitive areas. As a result of better vegetation information, the former "best choice" alinement was demonstrated to be environmentally unsound and costly.

Several additional aspects of the GMP benefited from improved vegetation information. For example, a proposed campground was considerably reduced in size when the vegetation map showed that an adjacent bog was much larger than previously thought.

The use of Landsat-derived vegetation information is continuing at the PRNL and already has been proven timely and valuable in the park management planning process.

APPLICATIONS TO GEOLOGIC STUDIES

Improvement of airborne glacier sounding

Airborne radio echo soundings of temperate glaciers are affected by long complex echoes that mix returns from distinct features and by oblique echoes (caused in part by antenna nondirectionality) that place reflectors in erroneous apparent positions. R. D. Watts has successfully compressed the long echoes into short distinct ones and has used "wave migration" methods to move reflections to the true reflector positions. This process facilitates interpretation and bottom-elevation map production, but it does not account for lateral variations of geometry to the sides of the flight line.

Lineament studies, San Juan Basin, New Mexico

Numerous linear features were mapped for the open-file report "Landsat linear feature data set of the Gallup-Grants uranium district," and statistical methods were employed to measure preferred orientations and length characteristics of the linear features. From these analyses, three significant trends were identified (34°–40°, 60°–80°, 298°–312°). Preliminary analysis of the trends by R. S. Zech and limited field verification indicate two of the trends may be related to regional fracture patterns and sedimentary depositional trends.

Subsidence structures in the Cascade Range

Preliminary visual analysis of linear features mapped from computer-enhanced Landsat images of the Cascade Range in southern Washington and northern Oregon by D. H. Knepper, Jr., indicates that numerous new faults or fault zones and extensions of previously mapped faults have been found. Most of the features appear to be subsidence structures associated with large volcanoes, such as Mount Hood, or with a large complex north-trending graben block that contains the Cascade volcanoes.

Structural and heat flow implications of infrared anomalies at Mount Hood, Oregon, 1972 to 1977

Aerial infrared line-scan surveys performed in April 1973 and September 1977 display surface thermal features over an area of approximately 9,700 m^2 at Mount Hood. From the distribution of the thermal anomalies below the summit of Mount Hood, J. D. Friedman theorizes that structural control is by a fracture system and a brecciated zone peripheral to a

hornblende-dacite plug dome (Crater Rock) and by a concentric fracture system associated with the development of the present crater. The extent and estimated temperatures of the hot areas permit a preliminary estimate of a heat discharge of 4 to 10 MW, exclusive of subsurface heat loss to circulating ground water. This figure includes a heat loss of 2 to 4 MW via conduction, diffusion, evaporation, and radiation to the atmosphere and a somewhat less certain loss of 3 to 6 MW via fumarolic mass transfer of vapor and advective heat loss from runoff and ice melt. The estimated heat loss of 2 to 4 MW is based on two-point models for differential radiant exitus and differential flux via conduction, diffusion, evaporation, and radiation from heat balance of the ground surface and on a shallow temperature probe traverse across the Devil's Kitchen fumarole field. Alternate methods for estimating volcanogenic geothermal flux that assume a quasi-steady-state heat flow yield values in the 5 to 11 MW range. The estimated heat loss equivalent to cooling of the dacite plug dome is insufficient to account for the heat flux at the fumarole field.

Mapping of altered and unaltered rock types in the East Tintic Mountains, Utah

Six channels of multispectral middle-infrared (8–14 μm) aircraft scanner data were acquired over the East Tintic mining district, Utah, an area of moderate vegetation and high relief consisting mainly of Tertiary silicic igneous rocks and Paleozoic quartzite and carbonate rocks that have been locally hydrothermally altered. These digital image data were computer processed to create a color-composite image based on principal component transformation. L. C. Rowan (USGS) and A. B. Kahle (Jet Propulsion Laboratory) note that the color differences are related to the spectral differences in the surface material and allow discrimination of several rock types, depending primarily on their silica content. When combined with a visible and near-infrared color-composite image from a previous flight, along with limited field checking, it is possible to distinguish between silicate (quartzite, quartz latite–quartz monzonite, latite-monzonite) and nonsilicate (limestone, dolomite) rocks and among some of the silicate rocks, including quartzite, quartz latite–quartz monzonite, and latite-monzonite. When combined with visible and near-infrared multispectral images that include spectral bands near 1.6 and 2.2 μm, silicified and argillerized rocks can be separated; these image data also are needed to distinguish between vegetation and carbonate rocks because they appear similar in the thermal-infrared images.

Regional geologic analysis from thermal-satellite data

Before the launch of the Heat Capacity Mapping Mission (HCMM) satellite in 1978, the primary sources of thermal information were either aircraft data, which were very restricted in geographic coverage and of limited availability and accessibility to the scientific community, or meteorological satellite data, which were acquired at too low a spatial and thermal resolution or at inappropriate times for most regional geologic studies.

Thermal-infrared data provide geologic information that can complement multispectral data obtained from Landsat. Thermal inertia, a property derived from the surface-temperature response of materials to the diurnal heating flux, is dependent on the density, the water content, and the composition of geologic materials. In addition, thermal inertia is sensitive to the thermal properties of geologic materials that are masked from reflectance analysis by surface coatings and thin covers.

The thermal inertia of geologic materials correlates in a roughly linear fashion with bulk density. Quartz content also is important, and carbonate rocks exhibit diagnostic differences (that is, dolomites generally have thermal inertias roughly twice those of limestones). Most igneous rocks, however, have very similar thermal inertias. The moisture content of soils has a very significant effect on thermal inertia (an 8 percent increase in moisture of sandy soil results in a 6 percent density increase and a 75 percent thermal-inertia increase). Thus, thermal property measurements can be used to discriminate certain lithologic types, to map alteration associated with silicification or dolomitization, to differentiate soils with varying moisture contents and porosities, and to discriminate geologic units that are obscured by the presence of surface cover, such as thin soil or desert varnish.

As with Landsat data, optimal usage of thermal data requires specialized digital computer processing, necessitating the introduction of a thermal model and, thus, implying the need for regional meteorologic information and the production of registered day-night thermal image pairs.

Based on preliminary analysis of HCMM thermal-satellite data of the Powder River Basin, Wyo., Kenneth Watson indicates the presence of an anomalous thermal zone that may represent a demarcation between two distinctly different geologic environments. The zone, although thermally distinct, is expressed only in part as a very subtle topographic feature but may correspond to a boundary between two structurally distinct regions as detected by lineament analysis of Landsat data.

Identification of geologic discontinuities near potential radioactive waste disposal sites in the Paradox Basin, Utah

Lineaments of the Paradox Basin were mapped by J. D. Friedman at a scale of 1:400,000 from high-quality Landsat images that were planimetrically rectified and processed using USGS digital computer patterns and texture of the topographic surface. Statistical analyses and comparison of rosette diagrams reveal significant correspondence between dominant azimuthal strike frequencies of the lineaments and strike frequencies of geologically mapped faults and fold axes, axes of gravity- and magnetic-field anomalies, and zones of steepened gradient of the two potential fields. The analyses suggest that deep-seated structures are reflected through or have penetrated the overlying sequence of younger rocks, perhaps during late Phanerozoic reactiviation of Precambrian basement structures. Structural control of major segments of the Colorado, Gunnison, and Dolores Rivers also is implied. The statistically dominant strike frequency for all lineaments mapped is N. 40° to 50° E.; this coincides with second-order gravity-field and third-order magnetic-field trends (represented before in geological mapping only by fourth-order fault trends, the Roberts-rift trend of Hite, and the postulated Colorado lineament zone). The numerically dominant strike frequency of major lineaments (those>20 km in length) is N. 40° to 60° W. This trend coincides with the first-order strike frequencies of geologically mapped faults and fold axes and gravity- and magnetic-field trends and is parallel to the axes of the major salt anticlines and to an inferred boundary fault zone of the Uncompahgre uplift. These azimuthal trends are interpreted as representing the dominant tectonic plan, as well as the directions of anisotropy of the fracture pattern within the region. Tectonic trends strongly represented by the lineament sets parallel the Uncompahgre and Wasatch trends of late Mesozoic and Cenozoic age.

Remote sensing and geological and geophysical studies in the Allegheny Plateau of New York and Pennsylvania

J. D. Phillips has analyzed recently acquired aeromagnetic surveys by computer modeling and defined fault block systems characterized by vertical movements within the basement. The Precambrian faults are parallel and subjacent to lineaments previously identified. Most notable is the northeast-trending Cortland-Ithaca lineament, which correlates well with the projection of the Rome trough northeastward from Pennsylvania, a fault system that served as a depositional hinge line in Ordovician time. Although this system acted as a rapidly subsiding zone in Pennsylvania, its expression in New York is minimized, indicating reduced downdropping to the northeast. Subsurface control is insufficient to determine whether the system is throughgoing or if the changes are gradual or abrupt. The strong northerly lineament pattern is not a prominent and is interpreted as a contrast in crystalline rock lithologies. Faulting, particularly strike-slip movement, may have caused these rock contrasts.

M. H. Podwysocki and J. D. Phillips compiled a subsurface horizon map at or near the basement-Paleozoic contact. Time to this horizon increases abruptly along an east-west line crossing the Seneca Lake lineament. This change of about 50 ms, equivalent to a 70-m down displacement to the east, is consistent with a basin hinge line that controlled salt deposition. Time-to-basement continues to increase to the east, suggestive of basement-sloping downward. Another marked change, interpreted as a down-to-the-east fault, is suggested in proximity to the north-trending Van Etten–Towanda lineament. Approximately 25 km to the east, time-to-basement decreases about 0.4 s and remains relatively flat for 50 km eastward. Although there is a large data gap between the two areas, the marked depth change may coincide with the east edge, or hinge line, of the thick Salina salt block. Its east edge marks the easternmost extent of the north-south-trending lineament concentration.

Based on purchased seismic-reflection surveys, J. D. Phillips has constructed time-contour maps for a series of horizons in the vicinity of Van Etten, N.Y. Some basement structure is evident. Subsalt structure within the Paleozoic rocks shows north-south block faulting, downdropped east along the Van Etten–Towanda lineament. Silurian salt units are strongly deformed by thrust faulting. Horizons within the salt could not be traced laterally for any distance. Horizons above the salt show the effect of thrust faulting. The crest of the regional Van Etten anticline, one of the east-trending Alleghenian folds, is downdropped, similar to the Sabinsville anticline at Woodhull, N.Y. The Van Etten–Candor lineament corresponds to one of the east-west-trending thrust faults.

H. A. Pohn has found that the pencil siltstones, highly acicularly cleaved areas of siltstones, probably are related to thrust and tear faulting or stratigraphic units within and above the Silurian salts of the Salina Formation and possibly to basement block faulting. The direction change coincides with some of the previously

mapped lineaments. Most notable is the occurrence of six pencil siltstone localities along the Van Etten–Towanda lineament.

Mineral assessment by remote-sensing techniques in the Richfield 1°×2° quadrangle, Utah

M. H. Podwysocki mapped lineaments from small-scale meteorological satellite images that show a strong northeast trend that appears to control hydrothermal alteration patterns in the western portion of the Richfield 1°×2° quadrangle. An east-west pattern of lineaments is not as common and is not obvious on small-scale images, but is apparent on Landsat images. The most obvious east-west lineament zone corresponds to the Pioche mineral trend of Nevada. Another prominent east-west trend is associated with the White Mountain area of the southern Shauntie Hills.

Limonitic materials were mapped by a digital classification procedure for 85 percent of the quadrangle using Landsat MSS ratio data. A supervised Euclidian distance classifier was applied to data consisting of Landsat MSS ratios 4:5, 4:6, 5:6, and 6:7.

The 6:7 ratio provided no unique ratio information and was eliminated from the classification. Using the other ratios, limonitic and nonlimonitic rocks were readily differentiated. Based on the ratio values, limonitic rocks were subdivided into three categories—strongly limonitic, weakly limonitic, and limonite with thin vegetation cover. Most known hydrothermally altered rocks were in the strongly limonitic category and were fringed commonly by a weakly limonitic area. However, numerous unaltered rocks, such as pink tuff and purple quartzite, also were categorized as strongly limonitic. This confirms prior efforts by others that show that hydrothermal limonite signatures are not unique.

A large oval feature, defined by the Sevier and Clear Creek drainages and the Cricket Mountains, has been mapped from a Landsat image. It measures approximately 100 km in diameter in an east-west direction. Young (Pliocene and Pleistocene) basalt occupies its center, and rocks along the flank appear to dip radially off the feature. Gravity data show a 40-mGal closure oval. Present interpretation by T. A. Steven suggests the feature is a mantle diapir, possibly associated with the relaxation of compressional forces and the formation of basin-and-range structures.

Small-scale terrain features of the Rolla 2°quadrangle, Missouri, and their geological relation

A morphometric analysis of remote sensing data covering the Rolla 2° quadrangle, Missouri, undertaken by D. W. O'Leary, reveals that a number of successive geologic events affected the Ozark landscape. Four terrains have developed in the quadrangle. The most distinct of these is essentially an exhumed Precambrian terrain. It is bordered on the east and northwest by two different terrains developed on the surfaces of Ordovician and Cambrian rocks during post-Paleozoic time. These two terrains are being eroded by dissected terrain of high relief, possibly no older than Oligocene age, controlled by subsidence of the Mississippi embayment.

Lineaments are well expressed in the areas of high relief, which suggests that the structures that give rise to lineaments also facilitate erosional etching, hence high relief. However, the high relief area along the Current River also shows evidence of post-Eocene differential uplift, in contrast to the high relief terrain of the Saint Francois Mountains.

Long north-south-trending lineaments are present in the massif terrain; these may reflect the oldest episodes of brittle extensional fracturing in the area. Northwest-oriented and N. 60° E.-oriented lineaments are found throughout the quadrangle; these probably reflect extensional breakage and differential uplift during and after deposition of Paleozoic units. N. 40° E.-oriented lineaments are well developed in dissected terrain south of the regional drainage divide in the quadrangle; these relatively young features seem to reflect tectonic influences of the Mississippi embayment. If lineament-related fractures have controlled zinc-lead ore fluid migration in this area, they are most likely among the groups trending north to south, north to west, and N. 60° E.

APPLICATIONS TO HYDROLOGIC STUDIES

Research on the applications of remote sensing continued in three areas—wetlands mapping, relation of land cover to streamflows, and enhancement of water turbidity patterns. Testing of the GOES satellite data relay system also continued, and tests have shown that large savings in cost and manpower are possible in central Florida.

Ecological research in wetlands

The remote-sensing procedures that were used to map vegetation in the Great Dismal Swamp (Carter and Gammon, 1976) have now been documented and published (Gammon and Carter, 1979). A stringent accuracy

evaluation of Landsat digital classification results is continuing, in cooperation with personnel at the USGS EROS Data Center.

USGS orthophotoquadrangles (1:24,000 scale) and 35 mm color infrared photographs of the Chowan River Swamp in North Carolina were used to develop a method for mapping wetland vegetation (Mead and Gammon, 1979). This method is designed for use by resource managers; it does not require sophisticated equipment or knowledge of advanced remote sensing techniques.

LAND USE AND ENVIRONMENTAL IMPACT

MULTIDISCIPLINARY STUDIES IN SUPPORT OF LAND-USE PLANNING AND DECISIONMAKING

Many of the scientific and economic results reported elsewhere in this volume have application to natural-resource planning and management. The Earth Sciences Assistance Office of the Office of Earth Sciences Applications sponsors a series of projects designed not only to support and encourage the application of those results but also to stimulate the development and application of earth-sciences information for resource-use decisionmaking on a broader scale nationwide.

SAN FRANCISCO BAY REGIONAL STUDIES

The San Francisco Bay Region Environment and Resources Planning Study (SFBRS), jointly supported by the USGS and HUD, Office of Policy Development and Research, was formally concluded. During fiscal year 1979, a series of final interpretive earth-science reports describing inventories of uses and interviews with users and documenting the impacts of the study were published.

Seismic safety and land-use planning

A USGS–HUD report, "Seismic Safety and Land-Use Planning–Selected Examples from the San Francisco Bay Region, California" (Blair and Spangle, 1979), was published. The report discusses the earth-science data needed for effective land-use planning and the method that can be used by local and regional governments to reduce earthquake hazards to acceptable levels. In California, seismic safety planning is mandated by law, and, although legal procedures differ in other States, basic earth-science planning strategies are applicable wherever earthquake hazards exist. Several examples of seismic safety planning by cities and counties are included. This report is a companion volume to "Studies for Seismic Zonation of the San Francisco Bay Region" (Borcherdt, 1975).

Flatland deposits and land-use planning

A USGS–HUD report, "Flatland Deposits–Their Geology and Engineering Properties and Their Importance to Comprehensive Planning–Selected Examples from the San Francisco Bay Region, California" (Helley and others, 1979), was published. The report describes the flatland deposits of the region and their significance in land-use planning. The geologic units mapped include the bay mud and marsh deposits and alluvial-fan, channel, flood-basin, levee, dune, and beach deposits. The depositional processes and ages of these units form the basis for predicting potential geologic hazards and describing the natural resources of the units. The first section of the report identifies and evaluates the different types of deposits underlying the area, and the second section shows how planners and decisionmakers can use this information to assess potential or alternative uses of the land.

Slope stability and land-use planning

A USGS–HUD report, "Relative Slope Stability and Land-Use Planning–Selected Examples from the San Francisco Bay Region, California" (Nilsen and others, 1979), was published. The report describes a method for evaluating slope stability based on a knowledge of the geology, slope, and number of landslide deposits in the bay area. As development of hillsides in some areas has increased, the cost of repairing damage from landslides and slope failure also has increased. These losses can be reduced greatly by using geologic information to identify slopes that are potentially unstable and then applying this information in planning the use of the hillside areas. Maps prepared at a scale of 1:125,000 and based on six categories representing a range from stable to unstable land illustrate how the method has been applied in the bay area.

Quantitative land-capability analysis

A USGS–HUD report on "Quantitative Land-Capability Analysis–Selected Examples from the San Francisco Bay Region, California" (Laird and others, 1979), was published. The report describes a method of evaluating land-use proposals by estimating the costs of development as they relate to geologic and hydrologic characteristics. These costs can be estimated by determining the need for future mitigative measures, the probability of future damage, or the loss of resource development potential. Because cost can be expressed in dollars, it provides a common basis for evaluating and

comparing different land uses and different geologic and hydrologic constraints and resources. The method is new and is being tested, but it appears to be flexible and applicable to other regions where geologic and hydrologic characteristics are important in land-use decisionmaking. The Santa Clara Valley south of the San Francisco Bay was used to demonstrate the method.

Evaluation and examples of the use of earth-science information

A critical evaluation of regional agency use of more than 100 earth-science products prepared as part of the SFBRS study was completed by W. J. Kockelman (1979). The uses of products were inventoried in nine regional agencies, and interviews were conducted with more than 50 users, including regional officials, employees, and consultants. The inventories and interviews were designed to document applications of the products, to evaluate the extent and usefulness of the applications, and to identify ways of applying earth-science information more effectively. Kockelman concluded that the regional agencies in the bay area are familiar with, have made frequent use of, and will continue to use SFBRS products for a wide range of regional planning and decisionmaking activities. Fifteen selected applications of SFBRS products to various regional planning and decisionmaking activities are discussed and illustrated (Kockelman, 1979, p. 53–111). The activities include producing earthquake intensity and damage maps by computer, developing coastal erosion guidelines for blufftop development, evaluating alternate transportation corridors, applying mineral resource information to water-quality management, planning for coastal zone resource conservation and open-space preservation, determining legal boundaries and areas of jurisdiction for regulating development, and preparing environmental impact reports.

Examples of how decisionmakers have applied earth-science information to reduce geologic hazards, protect natural resources, and avoid possible property damage were reported by Kockelman (1980). The examples show how (1) development in fault-rupture areas is regulated, (2) potential waste-disposal sites are identified, (3) aquatic and wildlife habitats are protected, (4) site investigations are required in hazardous areas, (5) supplemental building standards can be applied to unstable baylands, and (6) hazards information is made available to real estate buyers. In addition, six examples of how cities and counties have applied the seismic zonation method developed under the SFBRS (Borcherdt, 1975) were reported by Kockelman and E. E. Brabb (1979).

MULTIDISCIPLINARY STUDIES IN OTHER AREAS

Subsurface exploration in northeast Culpeper Basin

Exploratory water well test-drilling in the northeastern part of the Culpeper Basin provided new and significant information on the regional geology and ground-water hydrology. Four deep holes drilled in Triassic siltstone and sandstone were geophysically logged, pump tested, and sampled for chemical analysis. Preliminary evaluation of the drilling indicates that three of the four test wells are capable of high potential yields (18–30 L/s). The existence of the high-yielding water wells at Dulles Airport suggests that this geohydrologic setting may be similar over broad areas of the basin. Each drilling encountered effective water-bearing fractures, joints, and bedding-plane partings in siltstone and sandstone at depth, and high yields may be possible from deep drilling at sites carefully located along fracture-trace lineaments. Some high-yielding wells located on prominent alinements may interfere with shallow domestic wells if drilled into the same interconnected fracture system. Water quality in the siltstone aquifer progressively deteriorates with depth, with mineralized water below 167 m showing increased total dissolved solids, hardness, and sulfate. However, it is possible that high-yielding wells with good-quality water may be drilled in fractured shallow siltstone above that depth or in sandstone aquifers to depths of as much as 300 m. Finally, wells located in siltstone near diabase intrusive bodies may encounter metamorphosed siltstone at depth with low yields of ground water despite evidence of abundant fractures.

Exploratory trenching of suspected faults by B. D. Leavy (1979) along the northeast margin of the Culpeper Basin at several sites in Fairfax, Loudoun, and Prince William Counties, Va., exposed segments of a high-angle border-fault system. Several steep normal faults, joints, sedimentary slump structures, and channel-fill structures were exposed within the Triassic rocks. Subsequent augering on the down-thrown blocks showed minimum vertical displacement of 17 to 27 m along the border fault. The sedimentary slump features and some of the faults within the Triassic section appeared syndepositional, but well-developed shear zones along the basin-Piedmont contact areas and at least one fault in the Triassic rocks indicate that movement occurred after deposition and lithification of these sediments. Before recent Geologic Division studies, the eastern margin of the basin was presumed to be largely unfaulted.

Geologic input to sensitive lands maps

Reconnaissance geologic mapping by J. P. Minard in the eastern part of the Puget Sound lowland, northwestern Washington, provided valuable input to the "Sensitive Areas Map Folio" of King County, especially with regard to potential landslide hazards. The folio is an integral part of the county's sensitive lands zoning ordinance, adopted in July 1979. The folio is maintained by King County to display the distribution of sensitive areas characterized by landslide hazards, wetlands, coal mine (mined-land) hazards, seismic hazards, fish-bearing waters, or flood hazards. The map folio provides a valuable resource that county officials and the public can use to identify, plan, and manage sensitive areas more effectively.

Earth-sciences information for recreational planning

A multidisciplinary team led by D. P. Dethier (1979) completed reconnaissance mapping of geologic settings, potential hazards, and lake characteristics in the Alpine Lakes Wilderness Area, in the Cascade Range of west-central Washington State. The mapping information was furnished to the U.S. Forest Service (USFS) to be used in developing a recreational use plan for the wilderness area. The information provided a scientific basis for deciding which areas and lakes could support heavier recreational use (for example, those that are environmentally stable and relatively free of hazards). The field work was done by personnel of the USGS, The USFS, and the Washington Department of Game.

Landfill site planning and computer mapping

A computer composite mapping technique is being used to produce a map showing physical conditions related to sanitary landfill siting. The map is based on information from four source maps that show areas (1) with sufficient on-site loosely consolidated low-permeability material, (2) with adequate thickness of low permeability overburden to provide a buffer zone at or around the base of the landfill, (3) without adjacent streams or large bodies of water, and (4) without exposed bedrock or underlying fractured bedrock.

The computer composite mapping technique makes it possible to combine these source maps to derive information that is difficult or impossible to produce in any other way. This composite landfill map will provide valuable information to planners and public officials responsible for finding safe and usable landfill sites in a rapidly urbanizing county.

LAND-USE AND LAND-COVER MAPS AND DATA AND OTHER GEOGRAPHIC STUDIES

Land-use and land-cover maps and the associated maps showing hydrologic units, census county subdivisions, political units, and Federal land ownership were completed for 3,567,000 km² of the United States. These maps are based on the land-use and land-cover classification system published in Professional Paper 964 (Anderson and others, 1976). The standard 1:250,000-scale and, for selected areas, the new 1:100,000-scale planimetric maps were used as bases for compilation. Twelve States were mapped under joint funding agreements between the specific State or groups of States and the USGS. Of a possible 480 map sets covering the 48 conterminous States and Hawaii, 269 sets of land-use and land-cover and associated maps were completed (see figure 2). Reproducibles of the maps are placed on open file, and many of the data sets are available on computer-compatible tapes. Printed two-color land-use and land-cover maps for 33 quadrangles of the United States were published in the newly established Geological Survey L series. Although the associated maps will not be formally published, they are available on open file. In addition, several selected maps are being published in a multicolor format that illustrates land-use and land-cover patterns.

DEVELOPMENT OF AUTOMATED TECHNIQUES FOR LAND-USE MAPPING

Automated technology aids in the production of (1) land-use and land-cover maps and data, (2) visual displays for interactive viewing of spatial relationships, and (3) other thematic maps for future editions of the "National Atlas of the United States." Land-use and land-cover maps of Pittsburgh, Pa., Kansas City, Mo.-Kans., Atlanta, Ga., Washington, D.C., Seattle-Tacoma, Wash., Three Mile Island and vicinity, Pennsylvania, and Alaska's National Petroleum Reserve area illustrate different aspects of the development of automated thematic mapping techniques. These experimental maps are similar in main theme, scale, adaptability to a geographic information system, and method of reproduction (four-color offset lithography). The preparation of each map, however, posed a unique challenge.

The map of Kansas City, Mo.-Kans., shows Level I land-use and land-cover categories by color-coded

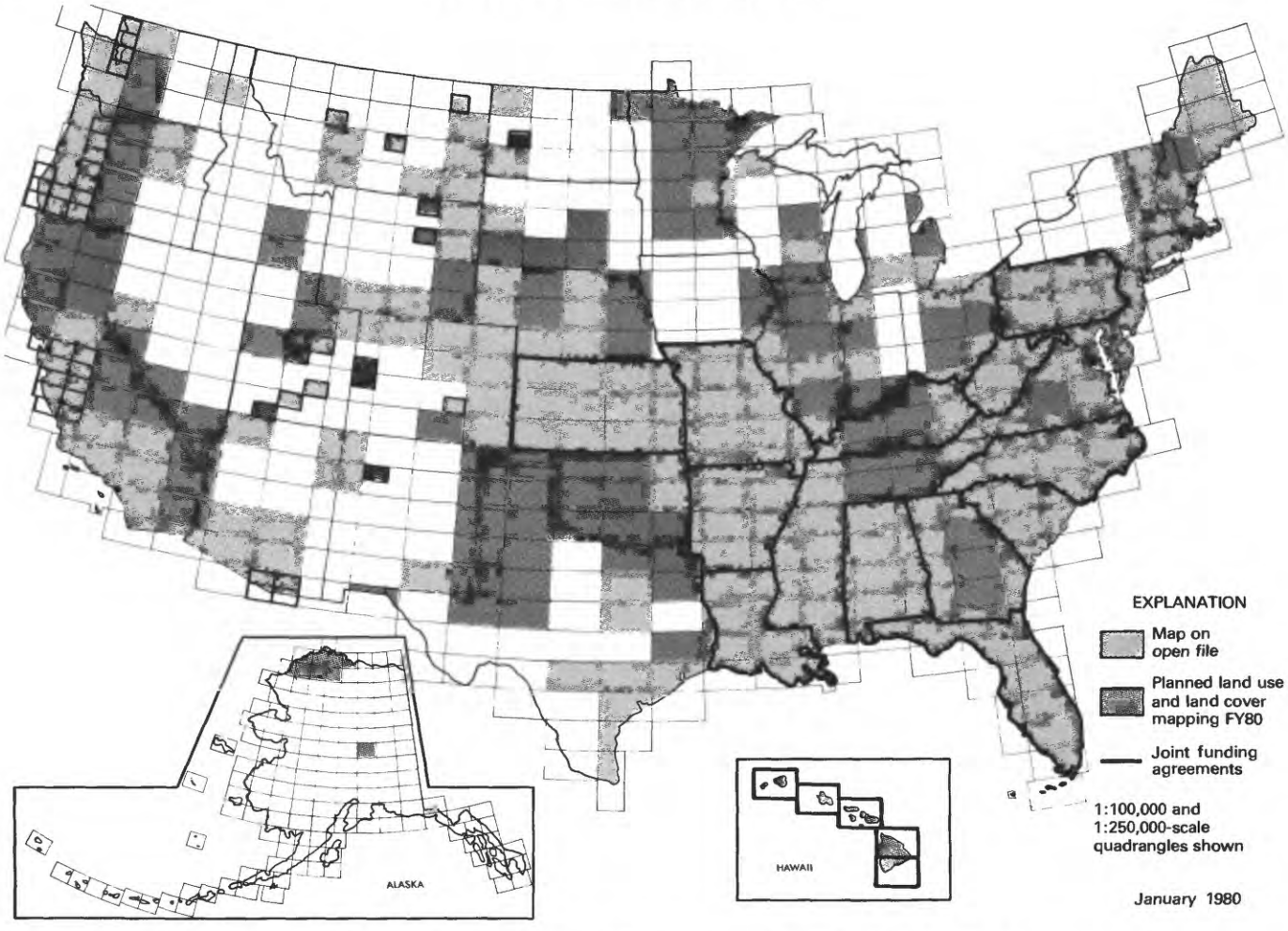

FIGURE 2.—Land-use and land-cover and associated maps on open file as of January 1, 1980.

polygons (USGS, 1978). The digitized Level I polygons were scribed by computer directly onto negatives from which the printing plates were made. Level II polygon outlines also appear, but they are not distinguished by separate colors. Some supporting operations such as the labeling of category codes still required extensive manual preparation.

Color separations for the Pittsburgh, Pa., land-use and land-cover map (Wray, 1980) were prepared by traditional manual scribing and peeling of open-window negatives. This map differs from previous land-use and land-cover maps by having a color scheme depicting Level I categories for forest land, water, and agriculture, while showing Level II categories in more detail. The Pittsburgh map also contains a table showing the changes in land uses from 1969 to 1973 in Allegheny County and a computer-compiled gazetteer of place names and their locations on the map.

A pair of land cover maps for Washington, D.C. (Gaydos and Wray, 1978a,b), was prepared with computer-aided analysis of Landsat multispectral data. The data also were used to provide a statistical analysis of land cover by map grid cell. A small-format laser plotter then was used to prepare screen separations for the printing plates. In contrast to the Washington, D.C., and the Kansas City maps, a scribed map of the greater Atlanta, Ga., metropolitan area was digitized first by a laser scanner. Color separations then were prepared by a technician using an interactive console to manipulate the data in the computer. The results were transferred to a large-format laser plotter that was used to prepare screen color separation films. The printing plates were made from the films. A detailed area measurement of each land-cover category was produced as a byproduct of the digitized data base.

Digital land-cover maps of the Seattle and Tacoma, Wash., 1:100,000-scale topographic quadrangles are examples of further improvement beyond the Washington, D.C., and Atlanta, Ga., maps. Using the digital classification prepared and described earlier (Gaydos

and Newland, 1978), the Seattle-Tacoma digital land-cover data were transferred directly from tape to screened color-separation films for plate-making. The screens also were prepared and angled on the laser plotter.

After the accident that occurred in March 1979 at the Three Mile Island nuclear powerplant in Pennsylvania, the USGS prepared an experimental land-use and land-cover map of the plant vicinity with census tracts. The map was prepared in a few hours with a computer-driven plotter. Data for the map were derived from the digitized land-use data base for the State of Pennsylvania, which was completed in 1978 under a cost-sharing agreement between the USGS and the Pennsylvania Department of Environmental Resources. The data were combined from digitized parts of two quadrangles to center on the nuclear powerplant at Three Mile Island. The map is a tool that planners, government leaders, and utility company managers can use in decisionmaking. Similar mapping elsewhere could aid in the selection of plant and powerline sites, in the planning of waste-water treatment facilities, and in the assessment of damages from natural or manmade disasters.

MAPPING LAND COVER IN NORTHERN ALASKA WITH LANDSAT DIGITAL DATA

Reproducing the digital land-cover classification for the National Petroleum Reserve–Alaska (NPRA) posed a challenge. Spectral classes for each of the Landsat scenes were determined by computer and then correlated with land-cover categories by comparison with aerial photographs and field data. Land-cover data for 1-ha cells from 10 different Landsat scenes in the NPRA area needed to be transferred from the separate scenes and fitted to a base map for printing at a scale of 1:1,000,000. After several trials, researchers found that a combination of automated and photo-mechanical techniques would provide theme separations for the land-cover classes. Before the map was printed, however, a technique was developed to do the mosaicking by computer. Sectional maps of the NPRA now can be printed from the same data base and fitted to the USGS $1° \times 3°$ topographic quadrangle at 1:250,000 scale. Area measurements of land cover by land survey townships also can be included. A smoothing technique, designed by USGS geographer Randall Ennis, was applied to the NPRA maps. The technique minimizes the "salt-and-pepper" look common to maps in digital format.

LAND-USE PATTERN ANALYSIS

An experiment was performed to interface digitized data from land-use and land-cover maps in the State of Florida with census data for the same areas using a computer. Densities of population and housing were measured from the resultant data comparisons. In another experiment, aerial photographs and maps covering the past 40 yr were compared with recent land-use and land-cover maps of Carroll County, Ga. The comparison revealed a dramatic reversion of cropland to forest land in almost one-third of the county. Preliminary findings from computer experiments with Landsat multispectral scanner data or Seasat radar data show that these data might be useful for improving the discrimination of glacial ice from perennial snow fields and of wetland forest from dry land forest. Seasonality of the data plays an important part in such land-cover pattern discrimination.

ASSESSMENT OF ACCURACY OF LAND-USE AND LAND-COVER MAPS PRODUCED FROM LANDSAT DIGITAL IMAGERY

Preliminary studies were completed to develop techniques and tools for assessing the accuracy of land-use and land-cover maps prepared from Landsat digital data. The sample size necessary to validate accuracy of a given classification category was investigated and an algorithm was developed for the sample selection of an adequate number of sample points to ascertain accuracy of the maps. This algorithm then was merged with the Geographic Information Retrieval and Analysis System for use with digitized land-use and land-cover data.

UPDATING LAND-USE AND LAND-COVER MAPS

V. A. Milazzo (1980) reviewed and evaluated various considerations in accomplishing map update within the framework of the present USGS land-use and land-cover mapping program. Based on this research, recommendations for updating land-use and land-cover maps in accordance with the goals of the USGS land-use and land-cover mapping program were offered. The recommendations are listed below:

- Initiate periodic inspection of land-use and land-cover maps using available remotely sensed source materials to identify changes.
- Continue to use small-scale high-altitude photographs as the principal remotely sensed source material for updating land-use and land-cover maps.

- Use the 1:250,000-scale base maps for updating land-use and land-cover maps of those areas where 1:100,000-scale bases are not available or for those regions where it is desirable to continue the presentation of map data at 1:250,000 scale. Use the 1:100,000-scale base maps for updating all other maps.
- Update the complete map sheet for existing 1:250,000- and 1:100,000-scale land-use and land-cover maps that are to be updated at their respective scales. For existing 1:250,000-scale maps that are to be converted to the 1:100,000-scale bases, update should be by whole 1:100,000-scale map sheets covering either the full 1:250,000-scale map area or selected quadrants.
- Use the original map-to-new source material method as the principal land-use and land-cover change detection technique. Supplement this method by using the original remotely sensed compilation source material where needed and when available.
- Update maps using the updated-original approach in which only the outdated portions of the original map are replaced with new data. Present data in a complete land-use and land-cover map format. Provide updated statistics on land use and land cover. Provide a separate overlay showing only the polygons of change as an optional associated map supplement. Conduct recompilations only when necessary.

NATIONAL WETLAND CLASSIFICATION SYSTEM

The USGS cooperated with the U.S. Fish and Wildlife Service to develop a new national wetland classification system for the ongoing Fish and Wildlife Service National Wetlands Inventory (Cowardin and others, 1979). The system allows for countywide comparison of inventory data by ecological system, by physiographic region, by wetland class and subclass, and by drainage basin or hydrologic unit.

LAND-USE CLIMATOLOGY

Climate is controlled significantly by complex energy exchanges. These exchanges result from a basic process—incoming solar radiation warms the terrestrial surface, which in turn warms the atmosphere above. When these energy exchanges and their resultant interactions are altered by land uses, the climatic environment also may be altered. Such energy exchange interactions have been analyzed by R. W. Pease, C. B. Jenner, and J. E. Lewis (1980). The authors studied these interactions by viewing the spatial distributions of surface features and then analyzing the energy exchange processes involved. Two tools used for the analysis were remotely sensed data, which were used to interpret surface-energy exchange processes, and a numerical simulation model of the complex of energy transfers. A satellite-borne multispectral scanner was used as an imaging radiometer that was made feasible by devising a gray-window model that corrects measurements made in space for the effects of the atmosphere in the optical path. The simulation model is a combination of mathematical models of energy transfer processes at or near the surface. These two analytical approaches were integrated and applied to the Washington-Baltimore area to coincide with an August 1973 Skylab 3 overpass. This application provided data for constructing maps of the energy characteristics of the Earth's surface.

Urbanization changes the radiative, thermal, hydrologic, and aerodynamic properties of the Earth's surface; therefore, a knowledge of such properties is essential to urban climate analysis. Surface, or aerodynamic, roughness for urban areas is not well documented because of practical constraints in measuring wind profiles in urban areas. Using an empirical method and an analysis of surface roughness calculated for 324 sample areas in Baltimore, Md., F. W. Nicholas and J. E. Lewis, Jr., (1980) found a strong statistical relation between surface roughness and urban and built-up land uses. Generally, surface roughness values measured in urban areas are high due to the concentration of tall buildings and other structures. The research further indicated that statistically significant differences exist in estimated surface roughness values when different land-use classification systems are used as surrogates. A Level III extension of the USGS land-use classification system provided the most accurate measurement of surface roughness values. An evaluation of the physical association between the surface roughness and the surface climate indicates that changes in roughness induce important changes in the climate.

Geographic data in the form of terrain information are a primary input to climate simulation models. Five urban terrain parameters—silhouette ratio, substrate diffusivity, obstruction height, surface relative humidity fraction, and albedo—were examined in a study by G. M. Greene (1980). He tested the sensitivity of model-predicted surface temperatures to simulated changes in the five parameters to determine influences of these parameters on the urban thermal regime of Baltimore, Md. The results indicate that changes in the individual urban terrain parameters of approximately 30 percent have relatively little effect on surface temperatures. However, when two or more of these parameters are grouped together, collective changes of approximately 30 percent have a more significant effect on surface temperature. The urban climate model in this analysis is

not of value as a predictive tool but rather as a method for examining relations between the input components.

ENVIRONMENTAL IMPACT STUDIES

The Environmental Impact Analysis (EIA) program provides an integrated USGS response to the National Environmental Policy Act requirements for the preparation and review of environmental impact statements (EIS's). The program (1) supplies direction, coordination, and expertise in the preparation of EIS's for which the USGS has lead or joint-lead responsibility, (2) furnishes technical information and expertise to support the preparation of EIS's to which the USGS is a contributor, (3) provides technical analysis, review, and comment on EIS's prepared by the USGS and other agencies, and (4) stimulates, promotes, and conducts environmental research related to EIS's and the anticipated needs of the program.

During fiscal year 1979, EIA administered the USGS lead or joint-lead responsibility with State or other Federal agencies for 12 EIS's, all of which were energy related (10 concerned coal, 1 petroleum, and 1 power transmission lines). The EIS's completed during the year involved development of the Caballo, Pronghorn, and Coal Creek coal mines in Wyoming; the Peabody Big Sky and Spring Creek coal mines in Montana; and regional impacts of coal development in southern and central Utah.

The USGS participated in the preparation of 21 additional EIS's under the lead of other Federal agencies—the BLM, the BIA, the U.S. Forest Service (USFS), the EPA, and the TVA. Seventeen of these statements were energy related; three dealt with critical minerals, and one dealt with a land dispute. The USGS also provided technical information to the USFS for five EIS's on geothermal energy resources and to the BLM for 12 EIS's on oil and gas leasing on the OCS.

Environmental impacts emphasized in the draft environmental statements prepared in fiscal year 1979 under USGS lead included the following:

- Disruption of aquifers.
- Reduction of air quality as the result of the introduction of dust from mining operations and as a result of a temporarily devegetated ground surface.
- Degradation of livestock and wildlife grazing, recreational hunting, and open-space qualities until reclamation is completed.
- Disruption of the existing land surface, vegetation, and soils.
- Reduction in the future productivity of the disturbed ground.
- Modification of socioeconomic patterns, including permanent increases in population, traffic, roads, powerlines, and buildings and increases in the need for public services and recreational facilities.
- Increases in tax and royalty income to the affected States and (or) counties.

Preliminary assessments are modified after Federal, State, and public review and comment on the draft statements, and the modifications are incorporated into the final statements.

Oilspill risk analyses (OSTA's) were conducted to determine the relative environmental hazards of developing oil in different regions of the U.S. OCS. These studies used a large mathematical model to analyze the probability of spill occurrences, likely movement of spilled oil, and locations of resources vulnerable to spilled oil. The combined results yield estimates of the overall oilspill risks associated with development of proposed lease areas. The OSTA's were conducted for the OCS lease areas of the northern Gulf of Alaska, central and northern California, and Kodiak Island, Alaska.

EIA program staff members reviewed and commented on more than 1,800 statements and related documents to support in-house environmental studies and to assist other agencies in areas of USGS jurisdiction and expertise. During fiscal year 1979, the EIA program supported research on the effects of various energy related activities on the physical and social human environment.

Offsite movement of radioactive materials

Preliminary results of a sampling of the La Bajada uranium mine and surrounding area in Santa Fe County, N. Mex., by P. F. Narten, E. L. Meyer, J. W. Allingham, and E. R. Landa did not indicate significant movement of uranium from the deposit to the surrounding environment. This mine, where urano-organic matter is associated with massive sulfide deposits, has not been worked for 13 yr but contains a strongly radioactive surface mine dump and ore stockpile remnants within 100 m of the Santa Fe River. Both radioactive surveys and the analyses of waters from the river, mine pits, irrigation ponds, and the associated sediments, aquatic plants, terrestrial plants, and the soils in which they are rooted indicated that high levels of uranium were restricted to the immediate mine area and that the uranium dissipates rapidly in all media within a 10- to 20-m radius of the mine. Levels of radium-226 in solution in the Santa Fe River were not found to be elevated downstream from the mine.

Mode of deformation of Rosebud coal

The mode of deformation at a subbituminous B coal from the Rosebud seam, Northern Powder River Basin,

Mont., was determined in triaxial compression by J. M. White at confining pressures up to 102.0 MPa. At confining pressures up to 6.8 MPa, the coal exhibited brittle behavior and failed by extension fracture. At confining pressures of 10.2 to 61.2 MPa, the coal exhibited behavior transitional between brittle and ductile and failed by shear fracture. Ductile behavior occurred at confining pressures of 68.0 to 102.0 MPa and appeared to result from extensive microfracturing and cataclasis.

Shear zones in some deformed specimens in the area resembled natural faults. Factors such as creep processes, varying mechanical properties of adjacent rocks, elevated temperatures, and scale effects prevented any direct correlation of the shears observed in the specimens and faults identified in the field. Scale effects particularly complicate the behavior of large masses of coal. Deeply buried coal, however, may deform in a ductile manner under some natural conditions.

Reclamation potentials for western coal mines

P. F. Narten, S. F. Lintner, J. W. Allingham, and H. C. McWreath III (USGS) and Lee Foster and D. M. Larsen (U.S. Forest Service) examined the vegetation on spoil surfaces at 22 western coal mines (in North Dakota, Montana, Wyoming, Colorado, Utah, New Mexico, and Arizona) to determine the status of and potentials for reclamation. Reclamation was evaluated based on general requirements of the Office of Surface Mining (OSM) that productive, diversified, and primarily native plant populations be reestablished on coal mine spoils.

No long-term revegetated surfaces were identified that could meet the OSM general requirements. The investigators concluded that 25 to 50 yr may be needed to define firmly the revegetation potentials for some western strip-mined lands. Strict application, however, of existing reclamation technologies that have been developed for individual mine sites should achieve the OSM goals in most places, although lower plant productivity may be expected. Availability of diverse kinds of planting materials may be a short-term problem. Postmining land-use management is a major factor in the success of reclamation efforts, especially in the drier areas.

Socioeconomic impact assessment for East Gillette and North Antelope mines

R. R. Reynolds, Jr., assessed the impacts of coal production on Campbell County, Wyo., and the service-base community of Gillette, Wyo. His assessment includes a description of the environment, evaluation of impacts of the proposed mining actvity on the social and economic environment, specification of unavoidable adverse effects, and specification of irreversible social and economic effects. In contrast to previous EIS-related socioeconomic studies, a social disorganization perspective of the energy-impacted base community was not assumed. Instead, a social change theoretical perspective was applied to the analysis of various data sets. Both positive and negative impacts on the well-being of various segments of the population at different points in time were revealed.

The project studies also revealed that some prevalent conceptions about the negative social effects in "boom" communities do not necessarily apply. For example, an examination of social data on Wyoming revealed no significant relation between rapid growth in Campbell and similar counties and the rates of divorce and certain types of crime or the amount of welfare dependency. Potential measures for mitigating the negative consequences of development also were recommended. For example, negatively affected segments of the population such as elderly people or dislocated ranchers were discussed as candidates for certain special assistance programs.

Oilspill risk analysis

K. J. Lanfear, Anastase Nakassis, W. B. Samuels, and C. T. Schoen (1979) conducted an oilspill risk analysis to determine the relative environmental hazards of developing oil in different regions of the northern Gulf of Alaska (Proposed Sale 55) OCS lease area. The study analyzed the probability of spill occurrences, likely movement of spilled oil, and locations of resources vulnerable to spilled oil. The combined results yield estimates of the overall oilspill risks associated with development of the proposed lease area. The analysis included estimates of oil degradation rates and slick dispersion paths and indicated the possibilities of mitigating effects by cleanup efforts. The leasing and development of the tracts proposed for Sale 55 will result in an expected 0.28 spills with a most likely number (mode) of 0.00 spills. The estimated probability that land will be contacted by one or more spills that have weathered at sea less than 30 d is 0.84; however, this probability varies greatly for specific target locations at different times.

Analysis of digitized maps of synthetic fuel resources

Using software recently developed by the EIA program, Research and Training Branch, information from maps of different scales and projections was digitized and combined in a matrix storage scheme. Natural resource and environmental data related to synthetic fuels development in the United States was stored in this manner. A digitized map of county boundaries was compared with this data to prepare a county-by-county

summary for input into the Domestic Information Display System. A unique feature of this project is the development of software that performs logical tests to identify regions of the United States with combinations of resources and environmental characteristics important to synthetic fuels production.

Physical effects of off-road vehicles

In research conducted by H. G. Wilshire and J. K. Nakata, the streets of the Wahmonie, Nev., ghost town, abandoned 51 yr ago, showed substantial effects of soil compaction and reduced permeability. Recovery trends indicated a recovery time of about a century. The vegetation in the disturbed areas consisted of short-lived perennials, whereas that in surrounding undisturbed areas was mostly long-lived perennials.

Preliminary observations in the tank maneuver areas indicated that single passes of General Patton's tanks were still visible because of lower concentrations of annual vegetation and less dense concentrations of lag gravel in the tracks. Lichen and algae appeared to have recovered even in areas intensely disturbed by General Patton's tank troup exercises of the 1940's. Lichen may not have recovered in areas disturbed in the 1960's by the Desert Strike tank maneuvers.

RESOURCE AND LAND INVESTIGATIONS

ENVIRONMENTAL STATISTICS AND INDICATORS

As part of a project undertaken by the USGS and the Council on Environmental Quality (CEQ), a report, "Environmental Statistics 1978," containing approximately 200 tables of data showing trends in the environment was published (CEQ, 1979). The project goal is to make more accurate statistical information and better analysis techniques available to environmental decisionmakers. The data in the report were collected on environmental factors such as air and water pollution, population growth and distribution, transportation, solid wastes, cropland, wildlife, and energy. The tables represent only a small portion of the environmental data being gathered by the Federal Government.

The report was released by CEQ Chairman Charles Warren during the ministerial meeting of the Environment Committee of the Organization for Economic Cooperation and Development held in Paris. This report will provide the U.S. input for a greater exchange of environmental data among nations. "Environmental Statistics 1978" is the basis for a companion volume, "Environmental Conditions and Trends," a graphic and textual description of the state of the environment, to be released in 1980.

WESTERN COAL PLANNING ASSISTANCE PROJECT

The USGS entered into a cooperative agreement with the Missouri River Basin Commission (MRBC) to undertake a project to assist State and local governments in resolving problems associated with coal and energy development. The project focuses on the major coal areas of Montana, North Dakota, and Wyoming and consists of two major tasks in Phase I: (1) a detailed assessment of planning problems and information needs associated with coal mining and related activities in these three States and (2) the development of a planning reference system to assist planners and decisionmakers in identifying, analyzing, and evaluating impacts associated with coal mining and related activities.

Through personal interviews, questionnaires, and workshop panel discussions, more than 250 planners and decisionmakers participated in a survey to identify high-priority planning problems and information needs associated with coal development and related impacts. Survey results were used in the final design of other project activities conducted during Phase I. The Phase I Final Report (MRBC and USGS, 1979a) summarizes the identified problems and needs and contains conclusions and recommendations that evolved during that phase of the project.

A four-volume planning reference system that provides basic information on analyzing and planning for impacts associated with coal and energy development was published. Each volume addresses a separate need, and together they provide a complimentary reference system:

- The "Fact Book for Western Coal/Energy Development" (MRBC and USGS, 1979b) gives the reader a wide range of coal-related facts. The document discusses existing coal fields and mines, coal-related facilities, transportation, legislation, and primary and secondary impacts of coal production.
- "A Guide to Methods for Impact Assessment of Western Coal/Energy Development" (MRBC and USGS, 1979c) surveys various methodologies for predicting environmental, social, and fiscal impacts. A definitive method for estimating population changes caused by increased employment is presented.
- "Forecasts for Western Coal/Energy Development" (MRBC and USGS, 1979d) provides a detailed explanation of coal and energy forecasts and forecast methodologies. The forecasts are compared on the basis of their utility to State and local planners.
- The "Source Book for Western Coal/Energy Development" (MRBC and USGS, 1979e) lists important sources of information, technical assistance, and

funding for solving specific coal- and energy-related problems associated with production facilities, transportation, legislation, and primary and secondary impacts of development.

Workshops were designed and held in Miles City, Mont., Sheridan, Wyo., and Bismarck, N. Dak., to explain the four-volume planning reference system. Each workshop lasted approximately 1.5 days and emphasized participation by local planners and decisionmakers. A Workshop Report was prepared to provide a summary of the presentations at each workshop.

Phase II of the project focuses on updating and revising the Phase I products, expanding information on the transportation of coal and coal products and the possible impacts on energy and transportation-centered communities, and developing and conducting experiential workshops that use the Phase I products in conjunction with natural resource, social, and economic information for case studies.

CONFLICT MANAGEMENT RESEARCH

The objectives of the conflict management research project are the identification, application, and refinement of new approaches to the settlement of environmental disputes in which the Federal Government is a major participant. The CEQ and USGS have attempted to expand the tools that can be used within the procedures established in the National Environmental Policy Act (NEPA). By contract with the American Arbitration Association (AAA), the USGS and CEQ are developing methods to anticipate, analyze, manage, and resolve multiparty disputes that delay Federal decisions or lead to NEPA litigation. The project's research team identified 40 environmental disputes and assessed their potential for resolution through conflict management techniques.

The Heritage Conservation and Recreation Service requested that the research team assist them in minimizing and managing potential conflicts over the conversion of an abandoned railroad right-of-way to a recreation facility in Columbia, Mo. The research team initiated a project to minimize the conflicts. Although some landowners remained hostile to the conversion, the team, together with city officials, was successful in reducing the general opposition. This allowed the city officials to focus their time and attention on the resolution of the specific concerns of a few landowners and to progress with the conversion program. The research team functioned as a neutral third party by providing assistance to both city officials and landowners.

The research team designed and presented two workshops on conflict mediation techniques for National Park Service (NPS) park planners, superintendents, and regional office staff members. The purpose of the workshops was twofold: to develop sufficient background material on NPS disputes so that mediation techniques could be tailored to resolve conflicts confronting the NPS and to introduce NPS personnel to the techniques of mediation and negotiation and give them practice in using these techniques. A workshop handbook addressing the concerns of NPS and the use of conflict management techniques was prepared and distributed at the workshops. Participants felt that the mediation and negotiation techniques could be useful in resolving their operational problems.

BLM requested that the research team investigate conflict management approaches to the resolution of disputes associated with BLM's California Desert planning responsibilities. This project was carried out in cooperation with the Southwest Border Regional Commission. The first phase of the project focused on a proposed competitive motorcycle event in the Cadiz Valley, Calif. The research team, serving as a neutral third party, met with both environmental and motorcycle advocates and attempted to develop a compromise acceptable to both groups. Although substantial progress was made, the parties could not come to an agreement and BLM did not permit the race. Following this initial effort, BLM asked the research team to perform a conflict assessment of their California Desert Plan. The research team interviewed approximately 40 individuals representing mining, grazing, off-road vehicle, native American, and conservationist interests. Based on its assessment, the team made recommendations to improve the California Desert Plan public review process. Details of these project activities are contained in two interim reports (McGlennon and Marcus, 1980a,b) released by the AAA.

OUTER CONTINENTAL SHELF OIL AND GAS INFORMATION PROGRAM

The Outer Continental Shelf Information Program (OCSIP) produces documents that are designed to assist State and local officials in planning for nearshore and onshore impacts of potential OCS oil and gas development and production. As stated in the Geological Survey Regulations 30 CFR Part 252 and mandates of the OCS Lands Act Amendments of 1978 (92 Stat. 629), the OCSIP shall prepare (1) regional indexes of reports and documents used by the Federal Government in making decisions for leasing, exploration, development, and production of OCS oil and gas and (2) regional summary reports covering OCS activities and onshore impacts.

During 1979, seven regional meetings were held to identify State and local needs and issues involved with the initial development and production of the summary

reports and indexes. Four initial indexes and four updates covering the Atlantic, Gulf, Pacific, and Alaska regions (USGS, 1979b,c,d, and e) and six summary reports covering the mid-Atlantic (USGS, 1979f), South Atlantic, Pacific, Gulf, and Alaska regions (USGS, 1980a, b, c, and d) have been published. The indexes are updated annually. The summary reports are completely revised only if significant events occur, but updates as to the status of the data in the reports are published every 6 mo.

In response to the needs and requests of participants at regional meetings, a directory to Federal, State, and local OCS-related activities and contacts (USGS, 1979g) was published. In the directory, Federal, State, and local agencies involved with OCS oil and gas activities are identified.

INTERNATIONAL COOPERATION IN THE EARTH SCIENCES

In 1979, the USGS celebrated its 100th year of existence and its 39th year of international scientific and technical cooperation with other governments. Much of this cooperation has been concerned with technical assistance to developing countries. Although technical assistance is still an important part of its international effort, in the last few years, the USGS has developed a wide-ranging program of scientific cooperation and exchange, not only with the developing countries but also with many of the industrially developed nations. The USGS presently has 33 active agreements under which it cooperates with 23 countries, and 21 agreements are being negotiated, 13 of which are with countries with which the USGS does not now cooperate. USGS international activities are of six types: international resource assessment, resource data systems analysis, scientific cooperation and research, technical assistance to developing countries, training, and scientist exchange and representation. The boundaries between categories are not always clear, but within these categories the current programs are concerned in one way or another with assessment of international energy, mineral, and water resources; with disaster prediction and hazard mitigation; with protection of the environment; or with institutional development. Many projects are undertaken as an extension of the domestic program.

In fiscal year 1979, the Policy Assessment Staff of the U.S. Department of State and the USGS began a joint study to assess the international role of the USGS as related to U.S. foreign policy objectives. This study, along with similar studies to be made with other technical agencies, is intended to identify current or potential programs that are important in the conduct of U.S. foreign policy, to assess the need for long-range plans for programs that affect foreign policy, and to develop a mechanism to relate these programs to foreign policy objectives. Preliminary results of the study show that many of the international activities of the USGS are significant in relation to U.S. international interests and that there is a growing interrelation between the domestic and international programs of the USGS. The international programs contribute to a favorable atmosphere for cooperative research and scientific exchange and provide opportunities for study of geologic phenomena that are important for domestic program objectives.

INTERNATIONAL RESOURCES ASSESSMENT PROGRAM

Energy assessment

The USGS is involved in several areas of activity in international natural resources assessment. Among these is a program to assess worldwide availability of energy resources, undertaken on behalf of the DOE. Such programs help other countries find and develop additional energy resources to improve the worldwide balance of energy supply and demand.

Under authority of Title V of the Nuclear Non-Proliferation Act of 1978, and on behalf of the DOE, which is managing the activities under this Act, the USGS has undertaken a program of assessment of energy resources and development options for selected developing countries. The USGS investigates and assesses the resources for fossil fuels (oil, gas, coal, oil shale, and tar sands), nuclear raw materials, geothermal energy, water resources, and energy-related minerals that are indigenous to a particular country. The USBM also has participated in studies of mining methods and possibilities for extraction of raw materials. Phase I studies consist of compilation and evaluation of the available published information on a country's energy resources. In Phase II, specialists work with counterpart scientists in collecting additional information, in field examination, and in preparing an assessment of the resource potential. Utilizing this assessment, the DOE, on the basis of a supply-demand analysis of all potential energy sources, advises on energy options open to the country, thereby providing a basis for policy decisions on energy production and development.

In 1979, Phase I studies were completed for Argentina, South Korea, Portugal, and Nigeria; Phase II studies were completed in Egypt and Peru (USGS, 1979h,i). M. J. Bergin coordinates the USGS work with the DOE.

In a separate but related program, the Foreign Energy Supply Assessment Program, which is restricted to assessment of petroleum resources, the DOE and USGS completed a study of Nigeria (DOE–USGS, 1979).

Program of the Committee for Coordination of Joint Prospecting for Mineral Resources in Asian Offshore Areas

The Committee for Coordination of Joint Prospecting for Mineral Resources in Asian Offshore Areas, referred to briefly as the Coordinating Committee for Offshore Prospecting (CCOP), is an intergovernmental body established in 1965 under the sponsorship of what is now the United Nations Economic and Social Commission for Asia and the Pacific (ESCAP). Initially, its purpose was to promote geophysical surveys of the marine shelf areas of the ESCAP region, eastern and southwestern Asia. The objectives of CCOP have broadened considerably since 1965. They now include landward geology and geophysics of areas bordering the sea and the use of remote-sensing techniques in the search for and investigation of mineral and hydrocarbon potential, ranging from the near onshore areas through the littoral and the shelf to the deep ocean. Research in related geoscientific problems and training of Asian geoscientists are also a part of this effort. The 12 countries of the CCOP region (Thailand, Malaysia, Indonesia, Papua New Guinea, the People's Republic of China, Vietnam, Kampuchea, the Philippines, Korea, Japan, Singapore, and the Trust Territories) are assisted by the United States and other industrialized countries, a joint endeavour of 21 countries.

The USGS has been represented in the Technical Advisory Group of CCOP since its inception. J. A. Reinemund and W. A. Fischer have been among the USGS representatives in that group. F. H. Wang, marine geologist, has been Senior Technical Advisor from 1972 into 1979, and numerous others have served temporary duty assignments in advisory or training capacities.

Coordinated by CCOP, large-scale pioneering geological and geophysical surveys, principally for petroleum, have been carried out over vast shelf areas of the region with encouraging results. The recently established substantial offshore hydrocarbon production being continually developed in waters off Indonesia, Malaysia, the People's Republic of China, the Philippines, and Thailand constitutes an increasing element in their national economies and contributes significantly to the energy needs of the world.

A natural complement to CCOP's programs was its participation in the International Decade for Ocean Exploration (IDOE), a program of the Intergovernmental Oceanographic Commission in which the National Science Foundation (NSF) has a major role. NSF, through IDOE, brought together many scientists and academic institutions to undertake a large-scale program on Studies of East Asia Tectonics and Resources (SEATAR). The objectives of this program are to intensify and extend geological and geophysical surveys into the oceanic regions and to the unexplored shelf and coastal areas. Multidisciplinary research along several key transects across oceanic trenches and adjoining island areas and marginal basins and shelf areas is being emphasized.

In preparation for the SEATAR program, F. H. Wang assisted the CCOP and the IDOE office in preparing and convening the second workshop on the IDOE program for SEATAR held in Bandung, Indonesia, October 1978, CCOP–IOC (Inter-governmental Oceanographic Commission, sponsored by UNESCO). The workshop assessed the scientific achievements and economic implications of the program during the previous 5 yr and formulated recommendations for further research during the next decade.

At the request of the Commission for the Geological Map of the World (CGMW) and in response to a recommendation adopted by CCOP during a recent session, a multilateral program was started to compile geological maps of the sea floor and continental margin of eastern Asia at a scale of 1:5,000,000. F. H. Wang is currently the coordinator and principal investigator representing the USGS. In cooperation with the Circum-Pacific Map Project, the CGMW maps will be compiled by geoscientists in several Asian countries that possess pertinent offshore data. The maps will constitute a portion of the third edition of the Geological Map of South and East Asia to be published by CGMW.

The successful CCOP concept generated the Committee for Coordination of Joint Prospecting for Mineral Resources in South Pacific Areas (CCOP/SOPAC) for South Pacific offshore areas in 1972. The need for assistance for the new Southwest Pacific island nations became obvious at the time of their independence. Definition and development of their indigenous natural resources are necessary for their economic stability, and the need for programs similar to those of the original CCOP was recognized. M. J. Terman is the USGS representative most active in this regard, serving as consultant on several occasions, a capacity that compliments his work on the Circum-Pacific Map Project.

F. H. Wang assisted R. P. Sheldon and W. C. Burnett in organizing the Workshop on Marine Phosphorite, held in Honolulu, February 1979, sponsored by the East-West Resource Systems Institute in cooperation with the USGS, CCOP, CCOP/SOPAC, and the Circum-Pacific Council for Energy and Mineral Resources. The report of the workshop includes critical analyses of various models, of the known and unknown factors related to the formation of submarine phosphorites, and of proposed new approaches to investigate unsolved problems. The report will serve as a valuable source book for scientists and organizations pursuing research in this field.

Resource Attache program

D. F. Davidson is the USGS coordinator for the Resource Attache program, a cooperative venture of the USGS, the USBM, and the U.S. Department of State. The program was set up to help meet the need for information on mineral resources and reserves in deposits in other countries. Resource Attaches are now assigned to 10 countries, and Mineral Reporting Officers are assigned to 9 countries. These officers gather reports, publications, and other materials that are forwarded to the USGS for review and appropriate use by commodity specialists.

RESOURCE DATA SYSTEMS

The USGS has been involved in a number of international mineral-resource data-analysis activities as part of an attempt to begin a global assessment of sources and supplies of nonrenewable energy resources and critical mineral resources. In these activities, which include the International Geological Correlation program, the Resource Attache program, and the Circum-Pacific program, the USGS cooperates with a number of international organizations through the Department of State and coordinates its efforts with the USBM and other U.S. agencies. A. L. Clark coordinates USGS activities, which consist, in part, of helping foreign governments and international organizations evaluate their particular data systems requirements and devising data systems to fill these needs. Several countries requested this assistance in 1979.

Coordinating Committee for Offshore Prospecting data systems program

At the request of ESCAP, the USGS detailed A. L. Clark and J. L. Cook to CCOP to provide assistance to its member countries through a contract between ESCAP and the International Union of Geological Sciences (IUGS), under which the services of the Committee on Storage, Retrieval, and Automatic Processing of Geologic Data (COGEODATA) are provided. COGEODATA is a committee of the IUGS, and Clark has charge of a major part of the COGEODATA program.

Clark and Cook guided development of petroleum data storage and retrieval programs for the member countries and identified major problems that can be resolved by implementing a sequential development program to meet the need for data storage and retrieval, beginning with systematic data acquisition and archiving and proceeding to an integrated system for storage, retrieval, and analysis of petroleum data. A transition from manual handling of data to the development of main frame and minimicro computer processes is necessary. Clark, Cook, and Richard Sinding-Larsen (Norwegian Geological Institute) also completed preliminary analyses of the data storage and retrieval system needs during visits to Indonesia, Korea, Malaysia, Thailand, the Philippines, Papua New Guinea, and Japan. They found that the Japanese National Oil Company (JNOC) is well advanced in computer storage, retrieval, and analysis of petroleum data. They suggested that JNOC compile an international well data base and a national-international oil and gas pool data base that might be used by other CCOP member countries. CCOP and IUGS sponsored the visits.

Energy data

The USGS is cooperating with the International Energy Agency in developing an international coal data system that will play an important part in a world coal reserve and coal resource assessment program. G. H. Wood, Jr., is Chairman of the Executive Committee for World Coal Resources and Data Bank Service. The USGS also is actively supporting development of the International Atomic Energy Agency. W. I. Finch and T. W. Offield are chairmen of international working groups associated with that agency. Worldwide uranium resource information is being computerized in standard format for use in international resource appraisal.

Marine data

F. H. Wang assisted the Marine Data Experts Group of NOAA during its mission to the People's Republic of China to develop bilateral programs on marine data exchange.

TECHNICAL ASSISTANCE AND PARTICIPANT TRAINING

TECHNICAL ASSISTANCE TO DEVELOPING COUNTRIES

Currently, the USGS is involved in technical assistance programs with 20 developing countries. These programs are carried out as authorized under the Foreign Assistance Act, sponsored in part by AID, U.S. Department of State, and other Federal agencies, in part by international organizations, and in part under reimbursable agreements with other countries. A fully reimbursable program in Saudi Arabia involves almost 40 man-years of work per year and has been operating continuously for 17 yr. (See summary by country for additional data.) Other continuing assistance projects are active in Egypt, Indonesia, Jordan, and Tunisia. Agreements with Bangladesh, Chile, Malaysia, and Yemen are currently being negotiated.

Under the auspices of AID, a new program in Indonesia became operational in 1979 with the arrival in Bandung of W. W. Olive as USGS Chief of Party. The project is assisting Indonesian agencies to increase their capabilities for research in energy and mineral resources, environmental geology, and geologic hazards associated with volcanism, earthquakes, and landslides.

A program in Egypt includes investigations of mineral resources; design, construction, and implementation of a photographic-cartographic laboratory; and training in cartography and publication methods, geologic data management, remote sensing, and laboratory techniques. Roger Shaff is assigned full time in Cairo, and J. E. Gair and S. J. Gawarecki completed short tours of duty during 1979.

In Jordan, G. E. Andreasen prepared specifications for airborne geophysical surveys for the Jordanian National Resources Authority and helped evaluate the results.

The USGS assisted the United Nations under the provisions of P.L. 85–795 by transferring M. J. Cruikshank, Conservation Division, to serve as Exploration Geologist in Burma in a mineral development program.

TRAINING AND SCIENTIST EXCHANGE

Some aspect of counterpart training is associated with almost all USGS international assistance programs. Training and transfer of technology are accomplished through seminars, training courses, and workshops presented by the USGS in the United States or in foreign countries; by on-the-job training in the host agency as part of the cooperative program; or by experience gained in the field, offices, and laboratories with the staff of the USGS. Since the assistance programs began in the 1940's, more than 2,000 participants from 110 countries have completed study assignments in the United States, either provided by or coordinated by the USGS. During this report period, USGS scientists have undertaken 300 formal assignments in 60 countries (see table 3), and 217 earth scientists and engineers from 56 countries have completed academic, observational, or intern training in the United States. Since 1940, more than 2,860 technical and administrative documents authored by or closely supervised by USGS personnel have been issued. During fiscal year 1979, 53 administrative documents were prepared, and 58 maps and (or) reports were released (see table 4).

TABLE 3.—*Technical assistance to other countries provided by the USGS during FY 1979*

Country	USGS personnel assigned to other countries			Scientists from other countries in United States	
	Number	Type	Type of activity[1]	Number	Field of training
Latin America					
Argentina	2	Geologists	A, B	--	
Brazil	1	Graphic arts specialist	B	5	Hydrology.
	2	Cartographers	B	1	Data processing.
	3	Geologists	A, D	1	Applied geophysics.
				1	Geophysics.
Chile	1	Geologist	A	1	Marine geology.
	1	Geophysicist	D	3	Remote sensing.
Colombia	1	Geologist	A	1	Digital image processing.
	1	Physical scientist	A	2	Hydrology.
Costa Rica	1	Geophysicist	D	2	Hydrology.
				1	Geomagnetics.
El Salvador	1	Electronics technician	A	1	Hydrology.
	1	Geophysicist	A	--	
Mexico	5	Hydrologists	D	4	Remote sensing.
	1	Geophysicist	A	--	
	1	Hydraulic engineer	C	--	
	2	Hydraulic technicians	C	--	
	2	Geologists	A, D	--	
	1	Physical scientist	D	--	
Peru	1	Mining engineer	B	--	
	1	Hydrologist	B	--	
	5	Geologists	A, B, D	--	
	1	Geophysicist	D	--	
	1	Structural engineer	D	--	
	1	Physical scientist	D	--	
Venezuela	1	Geophysicist	D	1	Uranium geophysics.
	1	Physical scientist	D	--	

See footnote at end of table.

TABLE 3.—*Technical assistance to other countries provided by the USGS during FY 1979*—Continued

Country	USGS personnel assigned to other countries			Scientists from other countries in United States	
	Number	Type	Type of activity[1]	Number	Field of training
Africa					
Algeria	1	Remote sensing specialist	D	2	Remote sensing.
Bangui				2	Seismology.
Botswana	1	Geophysicist	B	2	Hydrology.
	1	Geologist	B	--	
	2	Hyrologists	B	--	
Cameroon				1	Remote sensing.
Congo				4	Remote sensing.
Egypt	1	Cartographer	A	1	Geologic mapping.
	11	Geologists	A, B	1	Cartography.
	1	Physical scientist	B	3	Remote sensing.
Ethiopia				1	Hydrology.
Ghana				1	Remote sensing.
Kenya	1	Hydrologist	D	--	
	1	Research coordinator	D	--	
	1	Photographer	D	--	
	1	Cartographer	D	--	
Libya	1	Cartographer	A	1	Chemistry.
Malawi				2	Remote sensing.
Mali	1	Geographer	A	--	
Nigeria	1	Cartographer	D	1	Remote sensing.
				1	Geologic interpretation.
Somalia	1	Hydrologist	C	--	
Sudan				1	Remote sensing.
				1	Administration.
Swaziland				2	Remote sensing.
				1	Hydrology.
Tunisia	1	Geologist	D	8	Remote sensing.
	4	Remote sensing specialists	A, B	--	
	2	Photographic technologists	A, B	--	
Near East and South Asia					
Afghanistan				1	Uranium exploration.
Bangladesh	1	Geologist	A	4	Hydrology.
CENTO/Turkey	2	Geologists	D	--	
India	2	Geophysicists	D	4	Remote sensing.
	2	Geologists	D	1	Isotope geology.
				2	Hydraulics.
				2	Hydrology.
Iran				1	Digital image processing.
Iraq				1	Hydrology.
Jordan	1	Cartographer	A	--	
	1	Hydrologist	D	--	
	5	Geophysicists	A	--	
Korea				1	Computer processing.
Kuwait				1	Management.
				1	Hydrologic technology.
Morocco	1	Remote sensing specialist	D	--	
Pakistan	3	Geologists	B, D	4	Hydrology.
				1	Exploration geology.
				1	Uranium exploration.
				1	Ground water.
Saudi Arabia	34	Geologists	A, B	8	Publication.
	14	Geophysicists	A, B	7	Remote sensing.
	1	Physicist	A, B	1	Fission track.
	1	Administrative officer	A, B	1	Air photo interpretation.
	1	Electronics technician	A	2	Analytical chemistry.
	1	Computer technician	A	3	Administration.
	1	Remote sensing specialist	A	8	English.
	1	Computer specialist	A	2	Business administration.
	1	General services specialist	A	2	Rock preparation technique.
	1	Field operations officer	A	1	Health physics.
	1	General supply specialist	A	1	Spectroscopy.
	1	General supply assistant	A	1	Computer science.
	1	General services officer	A	1	Computer technology.
	5	Cartographers	A, B	1	Seismology.
	1	Physical scientist administrator	A, B	3	Hydrology.
	3	Computer specialists	A	--	

See footnote at end of table.

TABLE 3.– *Technical assistance to other countries provided by the USGS during FY 1979*– Continued

Country	USGS personnel assigned to other countries			Scientists from other countries in United States	
	Number	Type	Type of activity[1]	Number	Field of training
Near East and South Asia—Continued					
Saudi Arabia—Continued	2	Mathematicians	A	--	
	1	Physical scientist	A, B	--	
	1	Computer system administrator	A	--	
	1	Photographer	A	--	
	1	Technical publications editor	A	--	
	1	Procurement and supply specialist.	A	--	
	1	Electronics technician	A	--	
	1	Chemist	A	--	
	1	Cartographer technician	A	--	
	1	Hydrologist	A	--	
Sri Lanka				1	Remote sensing.
Syria				4	Remote sensing.
				1	Exploration geophysics.
Turkey	2	Hydrologists	C	4	Remote sensing.
	2	Geologists	B, D	1	Geophysics.
	1	Physical scientist	B	1	Ground water.
	1	Chemist	A	--	
Yemen	1	Hydrologist	A	2	Remote sensing.
	2	Geologists	B	1	Management.
Far East and Pacific					
Australia	1	Geologist	B	3	Remote sensing.
Burma	1	Mining engineer	A	1	Geochemical exploration.
China, People's Republic of	8	Geologists	A, B, D	2	Remote sensing.
Fiji	1	Electronics technician	C	--	
	1	Geologist	D	--	
Indonesia	18	Geologists	A, B	3	Administrative.
	1	Geophysicist	A, B	1	Volcanology.
	2	Physical scientists	A, B	2	Remote sensing.
	1	Senior scientist	A, B	1	Land use.
Japan	1	Physical scientist	A	6	Remote sensing.
	1	Senior scientist	A	1	Isotope geology.
	2	Geologists	A, D	1	Geophysics.
				1	Natural zeolites.
				1	Geochronology.
				1	Isotope studies.
				1	Water quality.
				1	Sediment transport.
Korea	2	Geologists	A, D	--	
	1	Physical scientist	A	--	
Malaysia	2	Physical scientists	A	--	
	5	Geologists	A, B	--	
New Guinea	1	Physical scientist	A	--	
	2	Geologists	A, D		
New Zealand	1	Geologist	A	1	Engineering geology.
				1	Digital image processing.
Philippines	9	Geologists	A, B	1	Computer mapping.
	1	Physical scientist	A	1	Remote sensing.
				1	Digital image processing.
Thailand	6	Geologists	A, B, D	1	Phosphate deposits exploration.
	1	Senior scientist	A	1	Remote sensing.
	2	Physical scientists	A, D	--	
Europe					
Austria	1	Visual information officer	D	--	
	2	Hydrologists	D	--	
	4	Geologists	D	--	
Cyprus	1	Geologist	D	--	
Czechoslovakia	1	Hydrologist	D	1	Engineering geology.
England	1	Geologist	D	--	
France	2	Hydrologists	D	1	Paleomagnetism.
	5	Geologists	A, D	--	
	6	Geophysicists	A, D	--	

See footnote at end of table.

TABLE 3.—*Technical assistance to other countries provided by the USGS during FY 1979*—Continued

Country	USGS personnel assigned to other countries			Scientists from other countries in United States	
	Number	Type	Type of activity[1]	Number	Field of training
Europe—Continued					
Germany	1	Geologist	D	1	Seismic research.
				1	Organic geochemistry.
				1	Geothermal energy.
Greece	1	Geologist	D	1	Seismotectonics.
Hungary	1	Hydrologist	A, B	--	
	1	Geophysicist	A, B	--	
	1	Geologist	A, B	--	
Iceland				1	Remote sensing.
Italy	1	Geologist	B	3	Remote sensing.
	1	Geophysicist	A	2	Seismology.
	1	Hydrologist	D	2	Geochemistry.
Netherlands				2	Remote sensing.
Norway	1	Physical scientist	A	--	
	1	Geologist	A	--	
Poland	1	Geologist	D	4	Remote sensing.
Portugal	2	Hydrologists	D	--	
Romania	1	Civil engineer	A	--	
	2	Geophysicists	A	--	
	1	Physicist	A	--	
Spain	1	Geologist	D	--	
Switzerland	1	Visual information officer	D	2	Remote sensing.
	1	Geologist	A	1	Seismic research.
				1	Seismology.
				1	Geothermal.
United Kingdom				1	Astrogeology.
				1	Paleobotany.
				1	Stratigraphy.
				1	Petrochemistry.
U.S.S.R.	2	Hydrologists	D	--	
Yugoslavia	1	Geologist	A	1	Remote sensing.
Other					
Canada	1	Geologist	D	1	Remote sensing.
				1	Isotope geology.
				1	Paleontology.
Diego Garcia (Chagos Islands)	1	Hydrologist	C	--	
Haiti				2	Remote sensing.
Iceland	1	Geologist	D	--	
Trinidad and Tobago	2	Geologists	D	1	Administration.
				2	Photolithography.
				1	Water resource management.

[1]A, broad program of assistance in developing or strengthening earth science institutions and cadres; B, broad program of geologic mapping and appraisal of resources; C, special studies of geologic or hydrologic phenomena or resources; D, short-range advisory help on geologic or hydrologic problems and resources.

Workshops in the applications of remote-sensing techniques to various disciplines are presented each year at the EROS Data Center, Sioux Falls, S. Dak. During 1979, 37 students from 21 countries participated in these workshops. Advanced training in the application of remote sensing to land-use planning, environmental applications, geology, and digital image processing are presented at the Astrogeology Center, Flagstaff, Ariz. During 1979, 18 foreign scientists from approximately 12 countries attended these courses.

A biennial course, "Hydrologic techniques for international participants," is given at the National Training Center in Denver. The course was given for 8 weeks in April and May 1979, for 14 students from Africa, Brazil, Costa Rica, and the Near East. Fundamental techniques applied to ground water, surface water, and water quality were covered.

A 4-week work-study course on processing and printing of side-look airborne radar imagery and design of a cartographic-photographic laboratory was given in Brazil. Another short-term project provided guidelines for an oil and gas exploration program for the State of Sao Paulo. The USGS also assisted the East Africa Region Remote Sensing Center, Nairobi, Kenya, in presenting two short courses on remote sensing applied to earth-resources investigations.

The USGS has compiled and issued the proceedings of the last CENTO Workshop on Applications of Remote Sensing Data and Methods. The Workshop was held in Istanbul, Turkey, in October 1976, for members of the

TABLE 4.—*Technical and administrative documents issued during the period October 1978 through October 1979 as a result of USGS technical and scientific cooperation programs*

Country or region	Reports or maps prepared			
	Project and administrative	Approved for publication by counterpart agencies or USGS	Published	
			In technical journals	By USGS
Afghanistan	1	1	--	1
Argentina	1	--	--	--
Bolivia	1	1	--	1
Botswana	2	--	--	--
Brazil	--	1	1	3
China	1	--	--	--
Colombia	1	1	--	1
Costa Rica	--	1	--	--
Egypt	3	3	2	3
Greece	1	1	--	1
Indonesia	3	--	--	1
Iran	--	2	--	--
Jordan	--	1	--	1
Korea	1	2	--	1
Liberia	--	2	--	2
Mexico	--	--	1	--
Morocco	1	--	--	--
Pacific region	2	3	1	2
Pakistan	--	2	--	1
Peru	1	1	--	--
Portugal	3	--	--	--
Philippines	--	--	--	1
Saudi Arabia	24	27	3	24
Turkey	1	1	--	2
Yemen	3	1	--	1
General	3	4	3	1
Total	53	55	11	47

CENTO countries (Pakistan, Iran, Turkey); 22 of the 24 papers presented at the workshop and published in the proceedings cover applications to regional country environmental conditions. A limited number of copies are available from the Geological Survey of Pakistan, the Minerals Exploration and Research Institute of Turkey, and from the Office of International Geology (USGS).

Manual for a field course in mineral deposit appraisal

As a result of the success of the summer-long field training programs in mineral deposit appraisal conducted in the CENTO countries from 1966 to 1978, E. H. Bailey (USGS) and coinstructors J. W. Barnes (Swansea University, Wales) and M. P. Nackowski (University of Utah) were requested to prepare a manual that might be used as guidance for others involved in similar work. To expedite preparation, the British Ministry of Overseas Development funded Barnes to travel to Bailey's office in Menlo Park where, in August and early September, much of the manual was written. Nackowski also was able to participate in preparation of the manual at Menlo Park, for a shorter period of time.

The manual includes information on organizational planning required before the program, logistics and equipment needed during the program, and instruction in the many skills and techniques needed to evaluate a mineral deposit. This includes advice on how to do regional and local geologic mapping, underground mapping, geochemical prospecting, sampling, reserve calculation, analysis of mining and recovery methods and costs, and, ultimately, deposit evaluation. The manual is directed particularly to geologists in the underdeveloped nations to aid in the appraisal of resources and the training of economic geologists.

J. N. Jordan, U.S. member of the Commission on Geophysics (OAS), was coorganizer of a training course held in the Canal Zone, July 1979, for seismograph station operators in Latin America. Dr. Alberto Giesecke (Director, Geophysical Institute of Peru) and Professor Bert Shelton (Geology Department, University of Panama) were other organizers of the course, which was sponsored by the PAIGH, OAS, Inter-American Geodetic Survey, University of Panama, and the Regional Center for Seismology for South America. Twenty-six participants came from Ecuador, the Dominican Republic, Costa Rica, El Salvador, Guatemala, Peru, Honduras, and Venezuela, and the instructors came from the Universities of Mexico, Peru, and South Africa and the USGS. D. H. Harlow and C. F. Knudson provided instruction in seismic data systems and strong motion instruments, respectively. This was a timely scheduled course and workshop in that new national networks are under way in Guatemala and El Salvador, and networks are being planned for Mexico and Panama. The Nicaragua network has been operating successfully for several years.

SCIENTIFIC COOPERATION AND RESEARCH

All activities in the category of scientific cooperation and research are undertaken primarily as an extension of the domestic program. This category includes a wide variety of topical research, sponsored by or coordinated by international and regional organizations or under bilateral agreements with 19 countries.

Hazards programs

The Earthquake Hazards Reduction Act of 1977 (P.L. 95-124) authorizes and provides funds for the USGS to carry out earthquake research in foreign countries. Under the Act, the Office of Earthquake Studies (OES) has developed cooperative agreements for earthquake research with the U.S.S.R. and sponsors earthquake

research in Mexico, Australia, Iceland, Venezuela, and the People's Republic of China. The cooperative program with the U.S.S.R. is carried out under the U.S.–U.S.S.R. Joint Committee on Cooperation in the Field of Environmental Protection. This agreement is led by the EPA; the OES works with that agency in the conduct of the program.

The OES also maintains a network of about 120 seismographs at various cooperating institutions throughout the world. The equipment at these stations has been given to the cooperating institutions with the understanding that the local institution will operate the station and the USGS will provide supplies, spare parts, and maintenance visits. Data from these stations are sent to the USGS for interpretation. The stations also provide a mechanism for detection of nuclear explosions.

As part of a cooperative program with the Office of Foreign Disaster Assistance (OFDA) in the Department of State, the USGS provided two consultants, R. W. Fleming and Mahadeva Iyer, both of whom participated in the South Asia Disaster Preparedness Seminar in New Delhi, India, from January 23 to February 1, 1979. The seminar was attended by representatives of seven countries in the region. Fleming presented a seminar paper on "Landslides–Causes and Precursors," discussed specific problems with the other participants, and provided USGS literature on the subject to each delegation. Iyer contributed a paper on "Regional Seismicity" and its relation to earthquake and landslide disaster investigation. The seminar was aimed at administrators, who formed the majority of the audience. Through discussions with the speakers and other scientists present, specific information was gained on climatic influences on landsliding, and ideas were generated for research that would be helpful in a program for reduction of hazards due to ground failure in the United States.

Special Foreign Currency Program

The Special Foreign Currency Program (SFCP) provides, under Public Law 480, for the funding of scientific research in foreign countries from U.S.-owned special foreign currencies deposited in qualifying countries. The USGS has SFCP projects in Poland and Yugoslavia, under joint-funding agreements. The agreements with both Poland and Yugoslavia expire at the end of 1980, and discussions are underway with both countries to extend the agreements and develop new projects.

A research project was recently completed in Poland on base metals in carbonate rocks, the results of which appeared in a major publication in English and Polish in late 1979 (Karkowski and others, 1979; Zartman and others, 1979). Two continuing projects, on the geology of coal basins and on coal geochemistry, were scheduled for completion at the end of calendar year 1979, and three new projects (on native sulfur, copper in black shales, and fission track dating) were begun in 1979.

In Yugoslavia, projects nearing completion under the current agreement include research on rare metals in granitoid massifs, applications of geophysics to defining permeability in karstic terrain, problems of urbanization in earthquake prone regions, and deep seismic sounding to determine crustal structure.

International Geological Correlation Program

The International Geological Correlation Program (IGCP) is a program of geological correlation, broadly defined, involving nearly all aspects of geology, and concerned with problems of international scope. The program is sponsored jointly by the International Union of Geological Sciences (IUGS) and UNESCO.

IGCP was established in 1967 under the auspices of the IUGS to improve the worldwide dating and correlation of geologic events. Its reorganization and cosponsorship by UNESCO in 1973 gave it a broader mandate, with new emphasis on the geology of mineral and energy resources and on the geologic aspects of environmental protection. Nevertheless, the program still has a strong orientation toward stratigraphic correlation.

IGCP now consists of 51 projects in four research areas: (1) time and stratigraphy, (2) major geologic events in time and space, (3) distribution of mineral and energy resources in time and space, and (4) quantitative methods in geologic correlation. More than 1,500 earth scientists, representing 71 member countries, are participating in the program. The United States has been a member country of IGCP since 1967, and nearly 400 U.S. earth scientists participate in 24 IGCP projects, of which 9 have U.S. leadership internationally.

IGCP has made progress in stimulating research worldwide on important problems in geology. While its primary emphasis remains on basic research and, particularly, research on stratigraphic correlation, it has established other projects, such as those on computer standards in resource analysis, on remote sensing and mineral exploration, and on sulfide mineral deposits, that have direct application to economic questions and the needs of developing countries. This aspect of IGCP is especially important to UNESCO.

Perhaps the most significant accomplishment of the program to date is its stimulation of international communication and cooperation in research. It has brought together scientists from different countries to work on problems of mutual interest, to examine together the field evidence relating to these problems, and to share the results of their research.

The USGS is a major contributor to IGCP, providing international leaders for 4 projects and the chairman of 12 domestic working groups. Many other USGS scientists have participated in IGCP-sponsored research activities. Some of the recent U.S. contributions to those projects that involve USGS personnel are described below.

Project 23: Genesis of kaolins. The 10th Kaolin Symposium was held in Budapest, Hungary, in September 1979 and was followed by field trips in Hungary and Czechoslovakia. The trip in Hungary, led by Drs. Viczián and Mátyás (Hungarian Geological Institute), visited several kaolin districts in the northeastern part of the country. The trip in Czechoslovakia, led by Professor Ivan Kraus (Comenius University), visited halloysite, kaolin, bentonite, and magnesite deposits. Approximately 60 geologists participated in the symposium and field trips.

Members of the Kaolin Working Group from the United States who attended and took part in the symposium and field trip were S. H. Patterson (USGS), W. D. Keller (University of Missouri), H. H. Murray (Indiana University), and S. W. Bailey (University of Wisconsin). The U.S. working group is compiling a manuscript summarizing information on the age and genesis of North American kaolin deposits, as a contribution to the planned two-volume terminal report of Project 23, and is planning a 1981 symposium and field excursion in the United States for a successor kaolin project.

Project 24: Correlation of glaciations in the Northern Hemisphere. G. M. Richmond is chairman for the U.S. working group that continued preparation of a series of stratigraphic columns for Quaternary deposits of North America. Members met on several occasions to discuss progress and results of regional compilations of data that include "solid" criteria, such as radiometric dates and identifiable ash beds.

Project 27: The Caledonide orogen. The U.S. working group for Project 27, chaired by R. B. Neuman, served as hosts for two Appalachian field excursions separated by a 4-d symposium for the International Working Group, August 29 to September 15. The first excursion had 94 participants, including 61 scientists from 10 foreign countries. The various lithotectonic terranes that compose the orogen of the northern Appalachians in Maine, the Connecticut Valley, and westward to Albany, N.Y., were inspected.

The symposium, held from September 6 to 9 at Blacksburg, Va., attracted nearly 200 attendees, including project representatives of 13 countries. A day of workshops was followed by 3 d of symposia on a variety of subjects and regions of project interest, after which 87 attendees participated in a field trip across the lithotectonic belts of the southern Appalachians from the Cumberland Plateau in Tennessee to the edge of the Carolina coastal plain.

Project 39: Ophiolites. An International Ophiolite Symposium was held in Nicosia, Cyprus, from April 1 to 8, 1979, cosponsored by the Government of the Republic of Cyprus, the International Association of Volcanology and Chemistry of the Earth's Interior, IGCP Project 39, and the Hellenic Mining Co., Ltd. R. G. Coleman is the chairman of the U.S. working group. Thirty-five scientists from the United States participated in the symposium, which included 14 field trips to various parts of the Troodos Ophiolite Complex and the Paphos area of Cyprus. All aspects of ophiolites were covered by papers presented at the symposium including petrology, structure, associated sediments, and economic geology.

Immediately after the Cyprus Symposium, the subgroup of the Metallogenetic Maps of the Ophiolite Belts of the World held a field meeting from April 9 to 15 in Yugoslavia. The field meeting was led by Professor S. Karamata who guided the group through the geology and ore deposits of Yugoslav ophiolites. B. R. Lipin presented preliminary maps of ore deposits in ophiolites of the Western United States. These maps were prepared by J. P. Albers, J. A. Peterson, and N. J. Page.

Project 60: Correlation of Caledonian stratabound sulphides. The International Working Group for IGCP Project 60 held its 1979 meeting in Trondheim, Norway, following a premeeting field trip to sulfide mines of northern Norway and Sweden. Visits were made to the Bleikvassli, Mofjellet, Joma, and Lokken mines, Norway, and to the Laisvall and Stekenjokk mines, Sweden. The 3-d symposium was attended by about 60 people, of whom 40 also went on the premeeting excursion. Members of the working group from the USGS are J. E. Gair (chairman), and J. F. Slack.

The meeting featured a display of the project's special 1:1,000,000-scale map compilation of stratabound sulfide deposits for the entire Caledonide-Appalachian orogen from Alabama to northern Scandinavia. Maps and tables of mineral deposits now have been prepared by the working group of each country and are either now available to the public or will be within a few months.

Project 98: Computer application in resource studies. IGCP Project 98, "Standards for Computer Application in Resource Studies," headed by A. L. Clark, has met a worldwide need for standardization of resource assessment techniques by integrating several disciplines in earth sciences and computer sciences. Eighty-five percent of the participants of project conferences and working groups are from countries other than the United States, and slightly more than 50 percent are from developing countries. Although the groups are highly

diverse with respect to individual national needs and objectives, a common understanding of standards has been achieved.

Project 98 has cooperated with other IGCP projects (Projects 143 and 156) and with several international organizations including the U.N. Development Programme, U.N. Centre for Natural Resources, Energy, and Transport, U.N. Institute for Training and Reserve, IUGS, COGEODATA, World Band, International Tin Council, CCOP, Association of Geoscientists for International Development, Regional Conference on Geology and Mineral Resources of Southeast Asia, and the International Atomic Energy Agency. Through these international bodies, the project has advanced the concept of resource assessment by conducting seminars and conferences and by distributing literature.

The results of the project's major conferences were published and made available to all participants and interested parties within 10 mo of each meeting. Case studies and projects initiated by project participants resulted in a well-defined knowledge base of the resource endowments of specific regions. This work has been accompanied by advanced training and project development in several countries including Mexico, Colombia, Turkey, Israel, Thailand, Kenya, Swaziland, Bulgaria, Cyprus, Finland, and Indonesia. Twenty-two of 80 project attendees participated in various aspects of Project 98 training and continued education.

Project 98 has achieved its objectives within the guidelines of the IGCP and the time frame specified, has stimulated a growing interest in resource assessment methods in less developed countries (LDC's), has provided a focal point for LDC scientists to initiate resource assessment programs, and has described, in detail, the scope of resource assessment techniques.

Project 115: Siliceous deposits of the Pacific region. The Penrose Conference on Siliceous Deposits was sponsored jointly by IGCP Project 115, the Geological Society of America, and the University of British Columbia. Conducted over a 3-d period at the University of Vancouver, the Conference consisted of morning and evening "overview" lecture sessions on various aspects of siliceous deposits, with intervening "round table" colloquia. The conference was followed by a 2-d field excursion to examine the controversial cherts and limestone of the Cache Creek Formation in south central British Columbia. J. R. Hein (chairman, U. S. working group for "Siliceous Deposits in the Pacific Region") attended a meeting at San Jose, Costa Rica, and took part in a field excursion conducted by the project's Central and South American members during late August and early September 1979. Several members of the U.S. working group presented the results of their research on various aspects of chert and other siliceous deposits at a meeting of the Geological Society of America in San Diego, Calif., in November. A 1,500-entry bibliography of Russian, Japanese, American, and other literature of siliceous deposits of the Pacific region was completed and currently is being prepared for publication.

Project 143: Remote sensing and mineral exploration. Project 143 led by W. D. Carter (chairman) participated in a variety of domestic and foreign meetings, some of which were sponsored and conducted in part by the U.S. group. Among activities of special note were a 2-d workshop held as part of the 23rd Committee on Space Research meeting in Bangalor, India, and a 5-d workshop staged by the project in La Paz, Bolivia. Results of research on methods of image enhancement, on criteria for spectral interpretation, and on new applications provided subjects for a large number of articles that were written by members of the working group and published during late 1978 and 1979.

Project 156: Phosphate of the Proterozoic-Cambrian. The U.S. working group for Project 156 staged an 8-d field workshop and seminar, from August 9 to 18, prior to an East-West Resource System Institute workshop and conference that dealt with fertilizers, held in Honolulu, Hawaii, from August 20 to 31. The field workshop and seminar featured evening discussions preceding daytime visits to late Paleozoic phosphorite deposits in Wyoming and Idaho and, during the last 3 d, early Paleozoic sections in Logan Canyon and the House Range of Utah. Both seminars and field inspections emphasized the investigation of sedimentary environments of phosphate deposition and possible analogues of the "Phosphoria Model," which has been used successfully in the search for new phosphate sources. Organized by R. P. Sheldon (chairman), the excursion attracted 48 participants representing 20 countries, most of which lie within the Indo-Pacific region.

Arranged on short notice following cancellation of a planned Project 156 meeting in India, the international flavor of the field workshop and seminar was achieved because only modest additional support was needed for the participants who were already scheduled to attend the East-West Center's Fertilizer Raw Material Resources Workshop and Fertilizer Flows Conference in Honolulu. A broad representation of national working groups provided an opportunity to discuss possible expansion in the scope of Project 156 to include consideration of upper Paleozoic to contemporary phosphate deposits and environments that may help explain the nature and distribution of Proterozoic and Cambrian phosphorites.

Project 161: Sulfide deposits in mafic and ultramafic rocks. The U.S. working group held its first formal meeting during August 1979, following a joint excursion and conference with members of the Project 92 working

group, to the Stillwater Complex, Mont., a feature of interest to members of both projects. The meeting, led by representatives of the Anaconda Company, Johns-Mansville Corporation, and the USGS, included daytime visits to deposits in the complex, followed by evening sessions at which the participants outlined the nature of their research. In accord with plans agreed on at the project organizational meeting, which was held in Canada during October 1978 and attended by 3 members of the U.S. working group, responsibility for compilation of data on U.S. sulfide deposits was delegated among individuals of the group. Before the Montana meeting, the U.S. working group chairman, G. K. Czmanski, with input from the project's international leader and others, prepared a handbook and data collection form for use internationally by those participating in the project.

North American Commission on Stratigraphic Nomenclature

Revision of the American Code of Stratigraphic Nomenclature is underway by representatives of numerous U.S. (N. F. Sohl, E. E. Brabb, and D. S. Fullerton, USGS), Canadian, and Mexican institutions under the auspices of the North American Commission on Stratigraphic Nomenclature. Objectives are to respond to the needs of rapidly developing new specialties, such as magnetostratigraphy, seismic stratigraphy, and the more widespread current recognition of lithotectonic units, while rectifying deficiencies in meeting the needs of longer established specialties (that is, nomenclature applied to metamorphic and plutonic terrains). Innovative approaches are being sought for promulgating new concepts, principles, and practices of classification that, subsequently, may be adopted by the IUGS Commission on Stratigraphy. Liaison is being established with appropriate bodies of the IGCP and the IUGS commission.

Time-stratigraphic charts for the Precambrian rocks of the United States and Mexico have been compiled by the IUGS Working Group on the Precambrian and are scheduled for publication as a single issue of *Economic Geology* in late 1980. A proposal for a time-scale for the Precambrian, based in part of the data presented in the charts, has been presented to the IUGS Subcommission on Precambrian Stratigraphy and to the North American Commission on Stratigraphic Nomenclature.

Circum-Pacific Map Project

The Circum-Pacific Map Project is an activity of the nonprofit Circum-Pacific Council for Energy and Mineral Resources, a cooperative international venture. Under the leadership of J. A. Reinemund (general chairman), the USGS coordinates the map project, which is compiling a series of thematic maps (geologic, tectonic, plate tectonic, geodynamic, energy, and mineral resources). These maps are intended to develop a better understanding of the energy and mineral resource potential in the Pacific region. The project is organized into five panels of regional area scientists responsible for the four quadrants of the Pacific basin and for the Antarctic region. The USGS is taking an active role in compiling the northeast quadrant maps and, to a lesser extent, the southeast and northwest quadrant maps. W. O. Addicott has taken over the direction of these USGS activities from P. W. Richards.

The fourth annual meeting for review of project progress was held in Menlo Park, Calif., in May 1979. Reinemund chaired the meeting with the assistance of Richards. Emphasis was placed on the relation of tectonics to mineral deposits. The results of the meeting are discussed by Richards (1979) in an open-file report.

USGS work on elements of the plate tectonic map of the northeast quadrant involves compilation of new or previously unpublished data on plate boundaries, plate motions, fracture zones, seismic epicenters, volcanoes, and magnetic lineations. This map, scheduled to be published in 1981, is serving as a standard for the four additional maps in this series. A fundamental premise of this international effort is that basic geologic and geophysical data form the framework for each resource map.

Other cooperative programs

Under a cooperative agreement with Colombia, the USGS is providing scientific and technical guidances in the development and operation of a computerized geological resource data base.

The USGS has an agreement with the Bureau de Recherches Géologiques et Minières of France for cooperation and scientific exchange in geophysics applied to regional geology, mineral resources, and engineering geology. The USGS also has an agreement with the Institut Francais du Petrole for cooperation in research in marine geology, but no activity took place in fiscal year 1979.

Under the science and technology agreement between the United States and Hungary, the USGS and the Central Office of Geology, Hungarian People's Republic, held discussions in fiscal year 1979 that will conclude in a bilateral agreement for scientific cooperation and exchange for calendar year 1980–81.

The USGS and the Consejo de Recursos Minerales of Mexico continued, under an extension of a joint project partially funded by the National Science Foundation, a research project on mineral exploration in the Sonoran environment.

The USGS and the National Environment Research Council of the United Kingdom have concluded a 5-yr agreement for cooperation in the geological, geophysical, and oceangraphic sciences, under which the USGS and the Institute of Oceanographic Sciences carried out, in fiscal year 1979, a joint survey of the continental slope between Georges Bank and the Bahamas, to map the sea-floor morphology and to identify areas of seafloor instability.

INTERNATIONAL COMMISSIONS AND REPRESENTATION

Representation, which includes participation in international symposia, unions, congresses, and commissions, is an important facet of USGS activities and promotes cooperation and development of new concepts in the earth-science community. USGS members serve on standing committees and councils and frequently represent the United States as delegates at international forums or meetings. H. W. Menard is a member of the World Energy Conference (U.S. National Committee). He is also an ex-officio member of the U.S. National Committee on Geology, the U.S. adhering body to the IUGS, and he or his designate head the U.S. delegation to the quadrennial meeting of the IUGS council. J. A. Reinemund is treasurer of the IUGS. Mackenzie Gordon, Jr., H. L. James, R. M. Kosanke, W. R. Oliver, Jr., R. J. Ross, Jr., and P. K. Sims are members of the USGS Commission on Stratigraphy; A. L. Clark and D. F. Davidson serve on the IUGS Committee on Geological Data. V. E. McKelvey is an international advisor for the Law of the Sea. Linn Hoover is the secretary of the IGCP and vice president for the Geological Map of the World. P. W. Guild is the president of the Subcommission for the Metallogenic Map of the World. USGS members chair the International Union of Geodesy and Geophysics (IUGG) Commission on Earthquake Prediction and the Commission on Strong Motion Seismology and are members of the IUGG working groups on the World Volcanic Map and on Radiogenic Isotopes. D. L. Peck is a member of the U.S. National Committee for the IUGG. The U.S. National Committees for the International Association of Geochemistry and Cosmochemistry, the International Union for Quaternary Research, the International Association of Hydrogeology, and the International Association for the History of Geology have USGS geologists as members. The USGS is represented on the Special Committees for Antarctic Research and for Oceanic Research, and R. B. Southard is the U.S. member of a work group on Geodesy and Cartography of the Scientific Committee on Antarctic Research (sponsored by the International Council of Scientific Unions). He also is the U.S. member of the Commission on Cartography of the Pan-American Institute of Geography and History (PAIGH). P. F. Bermel is chairman of the Committee on Topographic Maps and Aerophotography, and Alfredo Terrazas is chairman of the working group on a Glossary of Cartographic Nomenclature of PAIGH. C. W. Beetschen is a representive on the National Committee for the International Cartographic Association. Roy R. Mullen is a member of Working Group IV-1 of the International Society of Photogrammetry, and A. P. Colvocoresses is the chairman of Working Group IV-4.

INTERNATIONAL HYDROLOGICAL PROGRAM AND RELATED ACTIVITIES

The International Hydrological Program (IHP) is an outgrowth of the International Hydrological Decade. The program is sponsored by UNESCO. One hundred and thirty nations are members of the IHP. The major functions of the IHP are (1) the promotion of a scientific program, including studies of the hydrological cycle, assessment of water resources, and evaluation of the influence of man's activities on water regimes, (2) the promotion of education and training in hydrology, (3) the enhancement of exchange of information, (4) the support of technical assistance programs, and (5) the promotion of regional cooperation.

International guidance and supervision of the program is carried out by the Intergovernmental Council, a group consisting of 30 member countries, half of which are elected every 2 yr from the IHP membership by the General Conference of UNESCO. The United States was not a member of the IHP Council from 1977 to 1979 but was reelected to membership from 1979 to 1981. The IHP Bureau is the executive body of the council and is composed of one representative from each of the five IHP regions. A new bureau is elected for each phase of the IHP by the council members. Philip Cohen (Chief Hydrologist, USGS) was elected to represent region one, which includes Western Europe, Canada, and the United States, from 1979 to 1981. The bureau is charged with preparing for sessions of the council, supervising the implementation of the resolutions, monitoring the status of the IHP activities, and, from 1979 to 1981, preparing the work plan for Phase III of the IHP. Phase II is a 2-yr phase rather than the traditional 4-yr, so that the IHP program can be brought into phase with the UNESCO budgetary cycle.

United States participation in the IHP is guided by the U.S. National Committee on Scientific Hydrology (USNC/SH). The USNC/SH is chaired by Chief

Hydrologist Cohen. The membership includes representatives of eight other Federal agencies and six nongovernmental organizations. Associate Chief Hydrologist R. H. Langford is the alternate chairman. Della Laura is the Executive Secretary of the USNC/SH. The USGS Office of International Hydrology serves as secretariat of the USNC/SH.

The major functions of the USNC/SH are (1) to formulate the U.S. program of participation in the IHP, (2) to serve as a channel of communication for U.S. international hydrological activities, (3) to promote international hydrological activities, (4) to help the Department of State prepare U.S. positions on hydrology, and (5) to coordinate U.S. activities related to requests concerning hydrology from other countries and international organizations, insofar as possible.

Much of the work of the IHP is done through individual rapporteurs and working groups. The rapporteurs generally work alone to prepare short reports summarizing the state of knowledge on specific topics. Working groups are composed of four to eight members representing different countries and generally are concerned with broader topics than rapporteurs. There are 13 rapporteurs and 17 working groups in Phase II of the IHP. The United States furnished four rapporteurs and eight members of working groups; of these, two rapporteurs and four working group members were from the USGS.

The USNC/SH held its sixth annual meeting in Sioux Falls, S. Dak., from June 6 to 8, 1979. The committee met jointly with the Canadian Associate Committee on Hydrology, which represents Canada for the IHP. The two committees proposed the selection of a joint project to be undertaken on some problem of mutual interest on a river flowing in both countries. The committees also discussed the proposals for Phase II of the IHP that were to be considered at the November 1979 meeting of the Intergovernmental Council.

During calendar year 1979, USGS hydrologists participated in several IHP-related activities. R. H. Brown represented the United States at the UNESCO planning group session for the preparation of the scientific and educational work plan for the second phase (1981–83) of the IHP, in Paris, France, from March 5 to 9, 1979.

The third session of the Intergovernmental Council of the IHP was held in Paris, France, from November 9 to 16, 1979. The United States was represented by Cohen (head of the delegation), Langford, and Laura (USGS); R. A. Clark (NOAA/NWS); and J. M. Wiggert (Universities Council on Water Resources (UCOWR). The extensive agenda included selection of the new bureau, review of Phase I projects, ratification of Phase II projects and budget, review of the results of major conferences, and acceptance of reports on the activities of other international organizations working in the field of hydrology. The new bureau consists of representatives from Ghana (chairman), the People's Republic of China, Bulgaria, Cuba, and the United States. The bureau's official work began January 1980.

D. A. Stephenson (USNC/SH–Geological Society of America) represented the United States at the second session of the IHP "Committee on Man's Influence on the Hydrological Cycle" from November 8 to 9, 1979. Wiggert (USNC/SH-UCOWR) represented the United States at the second session of the IHP "Committee on Training and Education and on Technical Assistance for Developing Countries" from November 8 to 9, 1979.

Thomas Maddock, Jr., continued his work as a member of the IHP working group on the "Investigation of the Water Regime of River Basins Affected by Irrigation." He attended a meeting from August 24 to September 7, 1979, in Leningrad, U.S.S.R., where the draft report was reviewed. J. F. Poland served as chairman of the IHP working group on "Land Subsidence Due to Ground-Water Exploitation" in Paris, France, in February and was codirector of an IHP "Workshop on Land Subsidence" held in Mexico City, Mexico, from September 15 to 29, 1979. J. D. Bredehoeft, chairman of the IHP working group on "Use of Ground Water Models for Management Purposes," attended the working group's final meeting in Paris, from November 17 to 25, 1979, where the report was finalized. L. N. Plummer participated in a seminar on "Radiocarbon Dating of Ground Water" in Heidelberg, Federal Republic of Germany, November 1979. The meeting was sponsored by the German National Committee for the IHP. H. F. Matthai attended the International Symposium on "Hydrologic Aspects of Droughts," held in New Delhi, India, which was sponsored by the Indian National Committee for the IHP, International Association of Hydrological Sciences (IAHS), and UNESCO, from December 2 to 7, 1979.

R. L. Nace continued work on the book "The Physical Basis of Hydrology." The first three chapters have been completed and have been transmitted to UNESCO. He also edited the English translation of "World Water Resources and Their Future" by M. I. L'vovich of the U.S.S.R., which is being published by the American Geophysical Union as a contribution to the IHP.

L. R. Mayo attended the IHP working group on the "Hydrology of Northern Research Basins" in Quebec City, Canada, from June 11 to 15, 1979.

G. H. Davis, chairman of the working group on the study of the "Hydrological Problems Arising from Development of Energy Resources," continued work on a worldwide casebook, an outgrowth of the recently published preliminary report by Davis and corapporteur A. L. Velikanov (U.S.S.R.) under the title "Hydrological

Problems Arising from the Development of Energy."

In addition to its primary responsibility to UNESCO's IHP, the USNC/SH is also involved in the hydrologic activities of several other international organizations.

ACTIVITIES RELATED TO OTHER INTERNATIONAL ORGANIZATIONS

J. S. Cragwall, Jr. (Associate Director, USGS), is Hydrologic Advisor to the Permanent Representative of the United States to the WMO. He attended the Eighth WMO Congress in Geneva, Switzerland, in May 1979. C. R. Wagner participated at Fredericton, New Brunswick, in writing the final report of the WMO's project on the application of World Weather Watch for the Saint John River Basin. H. H. Barnes, Jr., participated in the second session of the working group of WMO's Regional Association IV (Northern and Central America) in Mexico City, Mexico, January 1979, and served on the working group for revisions to the "Guide and Technical Regulations" in Geneva, Switzerland, from October 21 to 26, 1979. M. E. Moss continued work for the WMO working group on "Network Region and Areal Assessment of Hydrological Elements." V. R. Schneider continued work for the WMO working group on "Improvement and Standardization of Instruments and Methods of Observation for Hydrological Purposes."

The International Standardization Organization (ISO) is another agency with which the USGS cooperates regularly. Among its aims are the standardization of hydrologic equipment and data collection methods to assure that data from equipment made in different countries are mutually acceptable and compatible. J. K. Culbertson, H. H. Barnes, A. F. Pendleton, E. D. Cobb, C. E. Kindsvater, and D. E. Click participated at meetings of ISO Technical Committee 113 on "Surface Water Hydraulics" held in Ottawa, Canada, from May 28 to June 8, 1979. During calendar year 1979, S. M. Lang has been involved in the development of several draft standards for data representations as U.S. delegate to the ISO Technical Committee 97 on data standards.

Activities of the International Atomic Energy Agency (IAEA) related to hydrology were significant in 1979. G. D. DeBuchananne attended a seminar of the IAEA working group on "Low Level Waste Disposal" in Prague, Czechoslovakia, in July; a meeting convened by the Organization for Economic Cooperation and Development, Nuclear Energy Agency, on "Geologic Disposal of Radioactive Waste" in Paris from October 12 to 18, 1979; and an advisory group meeting of the IAEA concerning "Low-level Radioactive Waste Disposal" in Vienna in December. J. B. Robertson participated in a session of the advisory group of the IAEA in Vienna from November 10 to 19, 1979, on "Application of Isotope Techniques in Mining and Waste Disposal Hydrology."

In other international activities concerned with radioactive waste disposal, P. R. Stevens participated in a program on "Radioactive Waste Management" sponsored by the Atomic Energy Canada Limited at Niagara Falls, Ontario, Canada, in April 1979. In July 1979, J. M. Cleveland and J. B. Robertson attended the "International Symposium on the Underground Disposal of Radioactive Wastes," held at Otaniemi, Finland. They also visited waste disposal sites in Germany, Sweden, and England.

William Back participated in a working group of the "Karst Commission of the International Association of Hydrogeologists," in Ireland, from May 23 to 27, 1979, to prepare a book on case histories in karst hydrogeology. G. H. Davis attended the "Third International Water Resource Association Congress" in Mexico City, Mexico, from April 23 to 29, 1979. Edward Callender consulted in April on estuarine hydrology at the Institute of Oceanographic Sciences, in Wormly, England, and the Water Research Centre in London. R. F. Miller presented papers on water harvesting and spreading at a seminar on "Rainfed Agriculture" sponsored by the FAO Near East Regional Office in Amman, Jordan, from April 25 to May 6, 1979.

W. M. Alley attended seminars in urban hydrology sponsored by the EPA, the University of Montreal, and the Urban Hydrology section of the American Society of Civil Engineers, in Montreal, Canada, from May 22 to 25, 1979. G. E. Williams attended a conference of the Canadian Water Resources Association in Ottawa, Canada, from May 29 to June 1, 1979. M. W. Skougstad presented a lecture at the Fifth Australian Symposium on Analytical Chemistry in Perth, Western Australia, in August. C. F. Nordin attended the Eighteenth Congress of the International Association for Hydraulic Research in Cagliari, Italy, from September 8 to 16, 1979.

B. L. Massey and F. S. Riley attended the Geothermal Energy Symposium in Mexicali, Mexico, from October 16 to 23, 1979. M. F. Meier and H. C. Riggs attended the Seventeenth General Assembly of the International Union of Geology and Geophysics in Canberra, Australia, from December 2 to 21, 1979, and participated in the associated symposia and workshops. J. K. Culbertson presented the keynote address at the binational U.S.–Pakistan symposium on "Mechanics of Alluvial Channels," Lahore, Pakistan, from June 21 to 30, 1979. R. H. Meade presented a paper entitled "Man's Influence on the Discharge of Fresh Water, Dissolved Materials, and Sediments by Rivers to the Atlantic Coastal Zone of the U.S.A." at the workshop on "River Inputs to Ocean Systems," in Rome, Italy, from March 19 to 31, 1979.

Other nongovernmental international organizations that the USGS cooperated with include the International Association of Hydrological Sciences, the International Water Resources Association, the International Association of Hydrogeologists, and the Association of Geoscientists for International Development.

INTERNATIONAL COMMISSIONS

The USGS participates in the work of the International Joint Commission (IJC) composed of U.S. and Canadian representatives. J. S. Cragwall, Jr., attended meetings of the International Souris–Red Rivers Engineering Board in Winnipeg, Manitoba, Canada, January 1979, and in Regina, Saskatchewan, Canada, from September 17 to 21, 1979. R. C. Averett participated in the Poplar River Water Quality Board meeting in Ottawa, Ontario, Canada, from May 7 to 11, 1979. He also attended public hearings reviewing the work of the International Poplar River Water Quality Board in Regina, Saskatchewan, from October 15 to 18, 1979.

D. R. Albin, J. T. Armbruster, J. A. Buker, J. A. Bettendorf, J. E. Biesecker, F. T. Schaefer, and L. A. Martens, attended the Tenth Meeting of the Atlantic Hydrology Group, which coordinates the work on the International Gaging Stations functioning under the IJC, in Quebec City, Quebec, Canada, from February 8 to 9, 1979.

REPRESENTATIVE ACTIVITIES IN SELECTED COUNTRIES

ARGENTINA

M. J. Bergin, in a Phase I study for the DOE of published data on the energy resources of Argentina, found that the country has significant energy resources, but its consumption exceeds production; thus, it is an energy-importer. Energy is now produced from hydroelectric power, oil and gas, coal, and oil shale. Production of energy from radioactive materials, geothermal sources, tidal action, and renewable sources is being investigated as part of Phase II investigations. Argentina's future energy plans include substitution of plentiful natural gas for oil where feasible and substitution of coal for oil in generating electricity. Geologic studies indicate that greatest potentials for increasing energy supply lie in development of hydroelectric power and exploration for new sources of coal and offshore oil and gas.

Relocation of aftershocks

J. N. Jordan and S. T. Algermissen redetermined the positions of loci of aftershocks of the November 23, 1977, San Juan, Argentina, earthquake. The positions show an average shift of about 25 km to the southwest. The relocations correlate rather well with the field seismic effects but do not relate to specific faults as currently mapped. These studies, even though widely separated geographically, show that caution must be used in seismic risk and in "site-specific" studies.

BOTSWANA

By invitation of the Minister, W. C. Overstreet and G. E. Andreasen visited the Geological Survey Department (GSD) of the Ministry of Mineral Resources and Water Affairs to advise on Botswana's requirements for mineral resource exploration programs. They found that, although the GSD has been aware of the impact of mining, as well as of grazing, on the fragile environmental balance of the Kalahari, its efforts to measure and interpret the many interacting natural factors of the Kalahari have been less successful than its other geological programs. Because of the rapidity with which the mining sector is opening major deposits, the GSD must increase its studies of the geologic, hydrologic, seismic, and climatic conditions of the Kalahari.

Under the auspices of AID, E. A. Moulder and L. A. Wood visited Botswana from March 24 to April 12, 1979, to review the organizational structure and status of water-resource activities. They assembled information on the occurrence and availability of water in Botswana and developed preliminary project proposals for (1) a deep-drilling project, (2) an improved surface-water data project, (3) the design of a data storage and retrieval system, and (4) a village water supplies project. They also suggested possible modifications of current hydologic activities to increase effectiveness by reducing investigation and development costs or by increasing hydologic understanding.

BRAZIL

Two USGS professional paper chapters were recently published on geologic structure in Goias and Minas Gerais. A. A. Drake, Jr., and B. A. Morgan III (1980) discuss the plate tectonics of the Brazilian Shield in the Quadrilatero Ferrifero, and Drake (1980) describes a window in Goias.

BRITISH INDIAN OCEAN TERRITORY

D. A. Davis was detailed to the U.S. Navy in November 1978 on Diego Garcia, chief island of the

Chagos Archipelago, to consult with local authorities on the enhancement of potable water supplies.

CANADA

W. S. Keys and F. L. Paillet continued a cooperative effort with the Canadian Government to study fractures in igneous rock at the Whiteshell Nuclear Reactor Establishment in Manitoba. The purpose of this study is to evaluate igneous plutons as possible sites for the storage of high level radioactive waste. Fractures that are probably capable of transmitting significant quantities of water have been found at depths as great as 750 m using an acoustic televiewer. Hydraulic test data are being compared to digitized acoustic wave forms to characterize the fractures using borehole geophysics.

CARIBBEAN AREA

Crustal setting of mafic and ultramafic belts and associated ore deposits

J. E. Case, in a study supported in part by the National Science Foundation, reports that major mineral deposits are associated with mafic and ultramafic (MUM) belts that crop out around the Caribbean region. Some rocks in these belts represent ophiolites associated with spreading centers, but other rocks probably represent mafic volcanism associated with primitive magmatic arcs that were associated with subduction zones. Analyses of gravity data and limited seismic refraction data indicate that, in Caribbean basins, the oceanic crust is somewhat thicker than normal (≥20 km, in comparison to 8–15 km) and that, in many areas around the Caribbean that are associated with large positive gravity anomalies, the crust is of high density and substantially thicker than normal (20–30 km) indicating a multiple oceanic crust.

Most of the MUM belts coincide with active or inactive plate boundaries. Most belts are areally associated with Mesozoic metamorphic rocks; blueschists in these metamorphosed rocks in Guatemala, Cuba, Jamaica, Hispaniola, Venezuela, and Colombia indicate subduction episodes. The final emplacement age (by tectonic detachment) of most belts was late Mesozoic and early Cenozoic.

Ore deposits of the belts include nickel-iron-cobalt laterites, podiform chromite, copper (massive sulfides), magnesite, talc, asbestos, manganese, platinum, gold(?), and possibly mercury. Many younger porphyry copper deposits of Puerto Rico, Panama, and western Colombia appear to have formed mainly on a foundation of multiple oceanic crust near major convergence zones, some of which were bidirectional.

MUM belts of Guatemala and Honduras (nickel-cobalt-iron; copper-massive sulfides) are situated in and near a suture-transform zone between two blocks of continental crust (20–45 km thick); they are sites of lead-zinc-silver deposits, with local slivers of oceanic crust (El Tambor Formation). MUM belts of Cuba (nickel-chromium), Hispaniola (nickel), and Jamaica occur near convergence zones where the crust is multiple oceanic (20–25 km thick). A MUM belt in Puerto Rico (nickel), part of which contains strata of Late Jurassic and Early Cretaceous age, occurs in a complex convergence zone; porphyry copper deposits are at a multiple oceanic crust site (30 km thick). The crust is thought to be multiple oceanic (25–30 km thick) beneath the Lesser Antilles, but the only exposed MUM is at La Desirade (native copper). MUM belts of the Netherlands Venezuelan Antilles and Venezuelan margin are at sites of multiple oceanic (25–30 km thick) or transitional crust. MUM belts (nickel) of the Venezuelan Coastal Ranges appear to occur on continental crust (30–35 km thick), locally in convergence zones, but they probably have been displaced southward from a province of oceanic crust. One of the MUM belts in central Colombia (nickel-chromium) lies along a zone of complex late Mesozoic convergence between oceanic crust to the west and continental crust (40–45 km thick) to the east. Belts in western Colombia (platinum-gold?), Panama (manganese-gold?), and Costa Rica (manganese) are mainly at sites of multiple oceanic crust (20–30 km thick) and possibly primitive magmatic arcs (pre-middle Eocene).

EGYPT

The USGS is cooperating with the Geological Survey of Egypt (GSE) in a program funded by AID. As part of the program, S. J. Gawarecki spent 6 weeks in Egypt in March and April 1979 assisting photogeologists from the GSE in the interpretation of Landsat imagery to the 1:500,000-scale mapping program and to introduce some new techniques in Landsat image interpretation. Two weeks of field work in the Eastern Desert included checking interpretation and noting relations, where possible, of ore deposits to features defined on Landsat images.

Under the same program, J. E. Gair and counterparts made a geologic reconnaissance of a number of metallic mineral deposits and associated nonmetallic deposits in the Eastern Desert. The mineral areas visited were stratabound, disseminated, and massive sulfides at Um Gheig, Hamata, Gebel Khashir, Gebel Darhib (Dirhid), and Um Samiuki; gold-quartz veins at Atud, Barramiya, and Um Garrayat; disseminated copper-nickel sulfides in lenslike or layered mafic to ultramafic intrusive(?) rock at Abu Swayel and Gebel Geneina El Gharbiya; and chromite in serpentinite at Wadi Arais.

The sulfide deposits and geologic conditions observed in the Eastern Desert indicate that the most likely places to find additional significant amounts of sulfide mineralization are in belts of rhyolitic-andesitic or rhyolitic-andesitic-basaltic volcanic rocks. Within the volcanic belts, felsitic zones that have been brecciated and (or) that show talcose or siliceous alteration are the most favorable places for sulfides. If these favorable signs exist at a particular locality, the presence of gossan, which indicates sulfide mineralization at the land surface also would be favorable, but the absence of gossan should not by itself be considered a negative sign. Sulfide minerals are likely to be distributed in lenses and might exist in a zone having other favorable signs, but the lenses may not reach the surface and, thus, may not produce a gossan cap.

EL SALVADOR

Site tests for seismic stations of a centrally recording radiotelemetric network in El Salvador were made by J. N. Jordan and E. S. Medina as part of a joint program of earthquake hazards reduction sponsored by AID. Network design, strong-motion and portable instrument specifications, spare parts, and test equipment were described in sessions with personnel of the Centro de Investigaciones Geotecnicas of the Ministry of Public Works. El Salvador is the most populous and industrialized country in the region, and its high seismicity permits informative studies relevant to the U.S. Earthquake Hazards Reduction Program.

J. N. Jordan and Peter Hubiak were involved in redetermining earthquake epicenters in and around El Salvador from 1964 to 1974 using the Joint Hypocenter Determination program of J. W. Dewey. Dewey's program shows a more internally consistent grouping of the three source-type seismic classes: (1) shallow offshore shocks (thought to be tensional), (2) down-slab shocks concentrated at depths of 100 to 150 km under the volcanic region, and (3) very shallow shocks in the central valley generally bordered by volcanoes. The new epicenter positions are, on the average, about 25 km to the southwest of the previous positions.

GERMAN FEDERAL REPUBLIC

USGS–BGR cooperation

Cooperation between the USGS and the Bundesanstalt fur Geowissenschaften und Rohstaffe (BGR), formalized under a 3-yr Memorandum of Agreement that became effective July 16, 1975, was continued under a 5-yr Extension Agreement. Activities carried out under the agreement in fiscal year 1979 included cooperation in research on methods of exploration for ore deposits.

Under a contract funded by the USGS, Helmuth Wedow participated with BGR geologists (funded by BGR) in a research project on target area characterization applied to exploration for base-metal deposits in the Appalachian Basin. The study involves both resource modeling and data-base development and management. An empirical model for stratiform base-metal and barite deposits in clastic sedimentary environments, developed by Duncan Large and Wolfgang Klau in BGR, was reduced cooperatively to about 50 attributes applicable to the Appalachian region. In the first application, model attributes were reviewed for the Appalachian Basin to develop Devonian target areas with high exploration potential. For regional analysis, 7½-min quadrangles were used as information cells. In fiscal year 1979, about 20 attribute maps were completed for computer input.

As part of the project activities, BGR geologists also visited mineral deposits in the Western United States under the guidance of several USGS geologists.

Cooperation in research on applications of geophysics to exploration for chromite was initiated by a visit in May 1979 of geophysicist J. C. Wynn to a BGR field project in northern Greece and a visit to BGR in Hanover, Germany. During the visit, plans were made for BGR geophysicists to visit chromite areas in the United States. In addition, several short exchange visits were made for discussions and exchange of information on digital-image processing for mineral exploration, airborne geochemical methods of mineral exploration, and radioactive waste disposal.

HUNGARY

Hydrology exchange

S. M. Lang participated in a scientific exchange visit to Budapest under the auspices of the Department of State in support of the 1977 U.S.–Hungarian Cultural Educational Agreement. He visited with a number of individuals in the principal units under the direction of the National Water Authority from December 14 to 22, 1978. The principal discussion topic was the collection and handling of hydrologic data and included organizational structures, operational programs, and study techniques for water-resource assessment and management. Technical subjects for potential future scientific exchange were identified by both parties.

INDONESIA

W. R. Hansen, environmental specialist, reviewed projects being undertaken by the Directorate of Environmental Geology; he also visited field projects in Java and Kalimantan and classified the areas according to types of hazards that may be covered by adverse geologic conditions.

R. D. Krushensky visited volcanoes in central Java that are being monitored by the Directorate of Volcanology and reviewed the equipment and methods being used to measure volcanic activity and predict eruptions. He also recommended to the Directorate the types of assistance and training that might increase its present capability to lessen the destructive results of volcanic activity.

ITALY

During October 1978, Allen Moench visited the Pisa area to obtain data for transient-pressure analysis of wells in the Larderello vapor-dominated geothermal system. He worked with scientists and engineers of the Italian energy agency ENEL. The data were used to verify a two-phase finite-difference numerical model of a geothermal steam reservoir. Results were published in the Proceedings of the Fifth Workshop on Geothermal Reservoir Engineering, Stanford University, Stanford, Calif., December 12 to 14, 1979.

JORDAN

G. E. Andreasen has been overseeing geophysical surveying for the Government of Jordan on behalf of AID. He assisted in establishing contract specifications and in evaluating bidders' responses. Presently, he is monitoring the airborne surveys and will review the contract company's interpretations of the data.

KOREA, REPUBLIC OF

Only hydroelectric power and coal are utilized presently as sources of energy from minerals indigenous to the Republic of Korea, according to a review by M. J. Bergin as Phase I of an energy-resource assessment program sponsored by the DOE. Small reserves of thorium have been reported, and the discovery of uranium was reported in 1977. Petroleum, natural gas, and geothermal energy sources may exist in South Korea, but their potential for development is low. About 55 percent of the energy used in the Republic is produced from petroleum, most of which is imported as crude and is refined in-country. Domestically produced coal supplies about 32 percent of the energy used, hydroelectric power about 4 percent, and other sources (firewood, charcoal, and dung) about 9 percent. South Korea's latest energy program stresses construction of additional hydroelectric power installations, increased production of coal, initiation of energy production by atomic reactors, onshore and offshore exploration for petroleum and natural gas, generation of energy by tidal power, and energy savings through conservation.

MEXICO

Geothermal

The cooperative program continued between the DOE and the Mexican Commission Federal de Electricidad for research, development, and demonstration of applications of geothermal energy in the Cerro Prieto geothermal field in the Mexicali Valley, the southern extension of the Imperial Valley in California. In March 1979, B. L. Massey, R. G. Pugh, and R. L. Ireland resurveyed the horizontal-control network established earlier to monitor ground movement in the area. This is one of the subtasks of the larger investigative program. Massey and other U.S. and Mexican scientists participated in a DOE-sponsored symposium in Mexicali in October 1979 to review progress on the total program, to plan future activities, and to inspect field installations and conditions. J. W. Ball collected samples of geothermal effluent for specialized chemical analysis in the Cerro Prieto geothermal area in Mexicali, Mexico, from January 22 to 26, 1979.

Water quality

J. F. Ficke was detailed to the Pan American Health Organization during part of February and March 1979 to assist units of the Mexican Government in evaluating the existing water-quality monitoring system and laboratory facilities necessary for implementing a project on Global Water Quality Monitoring. That project is being sponsored by WHO, UNESCO, and WMO of the United Nations family agencies.

Flood-control projects

At the invitation of the Mexican Ministry of Agriculture and Water Resources, C. F. Nordin (USGS) and E. R. Pemberton (Water and Power Resources Service) visited sites of two flood-control project areas in January 1980 to assess their sediment problems. Following aerial and ground reconnaissance of tributary reaches of the Rio Grijalva basin in the State of Tabasco and the Rio San Pedro in the State of Nayarit, recommendations were made to local and Federal officials in regard to study approaches and data needs.

MOROCCO

A Memorandum of Understanding has been signed with Morocco in which the Geological Service of Morocco and the USGS have agreed to procedures for cooperation for the exchange of technical knowledge and the increase of technical capabilities of both parties for a period of 5 yr. The activities are expected to include

exchange of information and joint studies of geological phenomena of interest to both parties. The activities may include, among other subjects, remote sensing applied to geologic mapping and mineral resources; geophysics, mineral resource analyses and data systems, and sedimentary basin studies; paleogeography; and continental shelf studies.

NIGERIA

As part of the Energy Resources Assessment program sponsored by the DOE, R. W. Fary, Jr., reviewed the data available for Nigeria. Nigeria produces petroleum and coal commercially. A small percentage of the natural gas that is produced along with petroleum is sold (448 million m^3 in 1976), but 97 percent was flared. Hydroelectric power generation commenced with construction of the Kainji Dam, completed in 1968, under the Niger Dams Authority.

The prospects of finding economically producible nuclear fuel minerals or conditions favorable for development of geothermal power sources appear to be poor.

Nigeria also was selected as the first country to be studied in the DOE's Foreign Energy Assessment Program, with which the USGS is associated. Resource appraisal methods, developed by B. M. Miller to estimate the undiscovered oil and natural gas resources of Nigeria, were employed to assess field size distributions and the projected finding rates for future developments in Nigeria's petroleum exploration and production programs.

A report prepared jointly by the DOE and the USGS (1979) includes a section "Geology and Resource Analysis," by Miller. Geological data and resource appraisals for the report were prepared by K. H. Carlson, R. W. Allen, and L. A. Sears. O. W. Girard, Jr., wrote Appendix B, "Petroleum geology of the Niger Delta."

OMAN

R. G. Coleman is studying the Semail ophiolite, which is an integral part of the alpine mountain chain that makes up the northern boundary of the Arabian-African plate. The Semail ophiolite represents a part of the Tethyan ocean crust that formed at a spreading center of Early Cretaceous age (Aptian). During the Cretaceous spreading in the Tethyan Sea, Gondwana Land continued to break up, and the Arabian-African plate drifted northward about 10°; this, combined with the opposite rotation of Eurasia and Africa, began the closing of the Tethyan Sea during the Late Cretaceous. In the earliest stages of closure, downwarping of the Arabian continental margin, combined with the compressional forces of closure from Eurasia, initiated obduction of the Tethyan oceanic crust along preexisting transform faults. Amphibolites developed at the base of the detached hot oceanic crust as it was thrust southward over oceanic volcanic and sedimentary rocks. Plate configurations, combined with palinspastic reconstructions, show that subduction and attendant large-scale island-arc volcanism did not commence until after the Tethyan Sea began to close and after the Semail ophiolite was emplaced southward across the Arabian continental margin. The Semail ophiolite nappe now rests upon a melange consisting mainly of pelagic sediments, volcanic material, and detached fragments of the basal amphibolites, which, in turn, rest on autochthonous shelf carbonates of the Arabian platform. Laterites and conglomerates associated with reworked laterites on the eroded upper surface of the ophiolite indicate a period of emergence prior to the deposition of shallow-water Maestrichtian carbonate beds. Following emplacement (Eocene) of the Semail ophiolite, the Tethyan oceanic crust began northerly subduction, and active arc volcanism started just north of the present Jaz Murian depression in Iran.

As part of the comprehensive study of the Semail ophiolite, M. A. Lanphere measured potassium-argon ages of rocks and minerals from the sheet of metamorphic rocks beneath the ophiolite. Hornblendes from amphibolites within 3 m of the contact with the peridotite member of the ophiolite, and phyllites farther from the peridotite contact, have weighted mean K^{40}/Ar^{39} ages of 90.0 m.y. ± 3.0 m.y. and 79.5 m.y. ± 3.0 m.y., respectively. The amphibolites represent the first tectonic slice welded to the base of the Semail ophiolite after it was detached from the Tethyan oceanic crust. Formation of the amphibolites occurred no more than 5 m.y. to 8 m.y. after crystallization of plagiogranite in the ophiolite. The phyllites represent another tectonic slice of ocean floor sediments welded to the ophiolite as it was transported farther from the Tethyan spreading axis. The potassium-argon ages suggest, assuming a half-spreading rate of 2 to 5 cm/yr, that detachment of the Semail ophiolite and formation of amphibolite facies rocks occurred no more than 100 to 400 km from the spreading center. Using the same spreading rate, one can calculate a minimum half-width of 300 to 750 km for the Tethyan Sea during the Late Cretaceous. A maximum half-width of 540 to 1,400 km can be inferred from isotopic and stratigraphic data.

N. J. Page, Joseph Haffty, and colleagues have determined platinum-group metal (PGM) distributions, contents, and ratios in chromitites from two sections, 250 km apart, through the basal ultramafic member of the Semail ophiolite. Chromitite occurs either as lenses in dunite within foliated harzburgite of mantle origin or as layers at the base of the overlying cumulate sequence.

Both sections show similar abundances of the PGM's. Average contents are listed below with the assumed stratigraphic position as measured down from the base of the cumulate rocks:

Section	Pd	Pt	Rh	Ir	Ru
Rajmi-Rayy:					
>4 km	<4.0	18.0	10.0	<36.0	<120.0
4 to 0.5 km	15.2	18.0	4.2	79.2	136.0
0.5 to 0 km	3.6	11.6	3.3	36.0	108.5
Ibra:					
>7.2 km	5.0	tr	6.0	30.0	<100.0
7.2 to km	5.0	12.0	13.8	35.3	160.0
Base of cumulates	11.5	21.0	tr	<30.0	<100.0

Tentative conclusions are that (1) the middle parts of the sections contain the greatest amounts of total PGM's and are slightly enriched in iridium and ruthenium, (2) all PGM contents are lower than average values for stratiform intrusions, (3) for both sections, coexisting silicate and chromite abundances and chromite compositions do not correlate with the PGM contents and ratios, suggesting that the PGM's occur in discrete sulfide phases rather than in lattice sites in major oxides and silicates, (4) the Pd:PGM, on the average, increases upward for both sections, and (5) the upper parts of sections appear to show some cryptic variation in PGM concentrations.

PEOPLE'S REPUBLIC OF CHINA

A favorable climate for negotiation of agreements for scientific cooperation with the People's Republic of China (PRC) has developed from an early visit by a U.S. delegation including H. W. Menard and led by Frank Press, Director, Office of Science and Technology Policy and Science Advisor to the President, in June 1978. After normalization of relations between the two countries signified by the signing of a Science and Technological Cooperation Agreement by President Carter and Vice Premier Deng on January 31, 1979, C. D. Masters, M. J. Terman, and R. L. Wesson delivered four agency-to-agency Protocols to PRC counterparts in Beijing in June. These covered geoscience and tectonics, geoscience and resources, resources research, and earthquake research.

Two Protocols ultimately were signed by H. W. Menard and the Chinese; these concern scientific and technical cooperation in earth sciences and earthquake studies and are to remain in force for 5 yr. They set the legal basis for future USGS–PRC cooperative work. Several exchange visits have taken place, and the Chinese have sent more than 50 scientists to the United States to discuss future cooperative programs.

N. C. Matalas and C. F. Nordin, Jr., were members of a 10-man U.S. River Engineering Delegation that visited the PRC from September 25 through October 13, 1978. The invitation was extended by the PRC Society of Hydraulic Engineers for the exchange of information concerning water resources development, particularly in flood control, sedimentation, regional planning, and management of large river systems. Research and academic facilities were visited, as well as several major project sites along the middle reach of the Yellow River.

PHILIPPINES

A USGS energy resource study of the Philippines (Phase I) was made by G. A. Younse as part of a program of compilation for energy-resource studies. The Philippine Archipelago is adjacent to oil-producing areas and has had limited production of its own (4,000 barrels a day in April 1970). Production was expected to reach 40,000 barrels a day by the end of 1979. Thick sedimentary sequences of Tertiary age have been shown to be producible and to contain significant potential source and reservoir rocks. In the past, most drilling has been aimed at large anticlinal structures, but reefs and stratigraphic traps now are considered the most important targets. Reefs of early Miocene age, already proven productive elsewhere, and reefs of late Pliocene age are regarded as the formations having the greatest potential, both onshore and offshore.

Exploration has been hindered by inadequate capital and lack of experience with advanced methods. Many failures were the result of drilling with little or no supporting geophysical data. Conditions such as rapid facies changes, intricate tectonic patterns, unconformities, and structures migrating with depth can be sorted out best by more sophisticated techniques. Increased commitment of risk capital, more extensive acquisition and processing of geophysical data (notably seismic) prior to drilling, and a better understanding of depositional environments are key factors in developing the oil potential of the Philippines. Those areas previously drilled for structural traps warrant a reevaluation of the geology relative to possible presence of stratigraphic traps, notably in carbonate rocks.

POLAND

The USGS and the Geological Institute of Poland are cooperating under the Special Foreign Currency Program (SFCP) in several related projects. J. H. Medlin is project officer for research on the geochemistry of coals in Poland and the United States. A. J. Bodenlos has begun a study of the geology of native sulfur deposits in evaporite beds in Poland and the United States. D. A. Lindsay is studying copper mineralization in the black shales of Poland and the United States.

Under the direction of K. J. Englund, a comparative study of the characteristics of coal basins in Poland and the United States is being made. Comparison of procedures for coal investigation and correlation has disclosed the presence of a widespread tonstein bed in the upper part of the Westphalian B stage of the Polish coal basins. The presence of a lithically similar and extensive tonstein bed in a coal bed at the equivalent stratigraphic position in the Appalachian Basin indicates a period of worldwide volcanic activity and presents a potential tool for worldwide correlation of coal beds.

Also under the SFCP, in cooperation with the Research Centre for Geological Sciences, Polish Academy of Sciences, C. W. Naeser has begun a fission-track geochronologic study of apatite and sphene in metamorphic rocks surrounding the Karkonosze granite, Poland.

Helmuth Wedow reported that a project with the Geological Institute of Poland on base metals in carbonate rocks of Upper Silesia was concluded with publication of a symposium volume in Polish and English in 1979. Results of project studies indicate that the lower Muschelkalk strata were deposited in a tidal-flat environment and are marked by anomalous concentrations of as much as 0.2 percent zinc and lead. Diagenesis of Muschelkalk carbonate strata further concentrated the metals in the primary sediments to form the first generation of disseminated fine-grained bedded sulfides. Later epigenetic ores were concentrated in paleokarst terrains; the primary control seems to be the transition facies between primary limestone and early diagenetic dolomites.

From these studies by Polish and American geologists, it has been generally, although not unanimously, concluded that the zinc-lead karst ore concentrations are not directly related geochemically to other sulfide mineralization in older rocks in the basement. Instead, they were formed by four main periods of influx of highly saline paleobrines in a sequence that extends from Triassic through Quaternary time. One influx in Liassic time during the initial formation of the Alpine geosyncline was the most influential. These infiltration stages probably correspond to several stages of brecciation and karst development.

PORTUGAL

A review of energy resource information of Portugal (Phase I) was made by M. J. Bergin on behalf of the DOE. The country lacks sufficient supplies of organic fuels to meet demands and, therefore, must import large quantities of petroleum and coal. Electricity is produced by hydro- and thermal-power stations. No resources of oil, gas, condensate, or natural asphalt or bitumen are known in Portugal. Coal production has decreased from about 400,000 kg from five mine areas in 1964 to about 200,000 kg from only one mine in 1974. Uranium is mined, and ore is stockpiled at the rate of about 160 kg/d. Development of geothermal energy sources in the Azores is planned.

S. S. Papadopulos and J. D. Bredehoeft were detailed to UNESCO during parts of April, May, and June 1979, to (1) assess the effects of ground-water development in the Setubal Peninsula using analytical techniques, (2) provide training for project personnel through informal seminars and technical discussions, and (3) provide guidance on the data requirements and techniques for mathematical modeling of the aquifer systems. UNESCO is assisting the Hydrogeology Division of the Portuguese General Direction of Hydraulic Resources and Developments (DGRAH) in a 2-yr UNDP project "Study of the Ground-Water Resources of the Setubal Peninsula." Nine DGRAH engineers and geologists contributed to the conduct of the study and participated in training seminars.

SAUDI ARABIA

Granites of the Arabian Shield

A study of the Arabian Shield granites is being made by D. B. Stoeser and J. E. Elliott. The granites of the Arabian Shield appear to have evolved in only one cycle. Compositions range from island-arc-type tonalites and trondhjemite to calc-alkaline granodiorite and monzogranite. These rocks were emplaced approximately 950 m.y. to 600 m.y. ago, all the monzogranites being younger than about 670 m.y.

The shield appears to have been involved in a continental collision during the period 540 m.y. to 600 m.y.; the event was accompanied by the emplacement of peralkaline granites throughout much of the Arabian-Nubian Shield, which is possibly the largest field of such granites in the world.

No economic mineral deposits are known presently to be associated with the Arabian granites. Much of the shield, however, is prospective for tungsten, tin, and molybdenum. The peralkaline suite is enriched in excluded elements and associated deposits of REE's. Niobium, tantalum, uranium, and thorium are potential exploration targets.

Geophysical exploration

Interpretation by M. E. Gettings of electromagnetic, self-potential, mise a la masse, induced potential, magnetic, and gamma-ray spectrometric surveys at the Mahd adh Dhahab ancient gold mine (lat 23°30′ N., long 40°30′ E.) has indicated five exploration targets. Drilling of geological and geophysical targets by a private firm holding an exploration license on the area has

confirmed the presence of a gold-silver orebody of significant economic proportions. Full exploration of the geophysical targets has not been completed. Paleomagnetic studies and apparent resistivity and self-potential logs of boreholes strongly suggest fault repetition of the stratigraphic units that are the host for the orebody. The geophysical studies constitute the framework for continued exploration outward from the known orebody, the limits of which are undetermined as yet.

Mineral potential in the Arabian Shield

J. E. Elliott has developed criteria for evaluating different areas of the shield for the presence of mineral deposits associated with the younger granites: (1) the distribution of mineral anomalies, (2) the distribution and abundance of younger granites, including both calc-alkaline and alkaline to peralkaline types, (3) the presence of favorable host rocks and (or) structures, and (4) the level of emplacement of the younger granites represented by the present level of erosion. The shield was arbitrarily divided into five areas: northwest, northeast, west-central, east-central, and southern. On the basis of the criteria outlined above, the northeastern and east-central shield areas are considered to have the highest potential for mineral deposits associated with the young granites; the west-central and southern shield areas are considered to have the lowest potential. Although the potential for mineral deposits is not as high in the northwestern shield as elsewhere, further exploration in that area is warranted.

Jabal Ishmas–Wadi Tathlith gold belt

Potential gold resources in the Jabal Ishmas–Wadi Tathlith gold belt are of three types: gold-bearing quartz veins, placer deposits, and gold-bearing bedded syngenetic deposits. The gold-bearing quartz veins have limited potential; only three of the deposits are considered worthy of intensive exploration.

Although only hydrothermal gold-quartz vein deposits are known in the gold belt, an unevaluated potential for gold exists in other types of environments. Massive sulfide deposits, volcanic ironstones, quartzitic clastic rocks, and porphyritic subvolcanic intrusives and flows of felsic composition are all present within the belt, and all are favorable exploration targets for gold deposits, according to R. G. Worl.

Base-metal deposits in the southern Arabian Shield

Results of geologic mapping by C. W. Smith and A. M. Helaby within the Rabathan anomalous zone indicate that the rocks are of volcanic origin, principally tuffs. Most are gray-green fine-grained chlorite schist that grades into buff-colored siliceous dolomitic rock containing carbonaceous material; previous investigations determined that the carbonaceous material was derived from algal mats growing on a shallow sea floor. The rocks are tightly folded, and both layering and schistosity strike north along the trend of Wadi Bidah.

Siliceous limonitic beds associated with gray chert are scattered along the anomalous zone within the gradational contact zone of gray-green tuffs and buff-colored siliceous dolomitic rocks. They range in length from a few meters to 200 m and, in places, resemble banded iron formation. They are cut everywhere by a network of white quartz stringers and, in places, are highly manganiferous. These beds, which are as much as 20 m thick, contain pockets of hematitic boxwork pseudomorphs after pyrite.

Brian Waters completed mapping of the Belajemal area where gossans are interbedded with felsic volcanic tuffs. The gossans crop out within an area approximately 1 km^2 where the layered sections form a broad syncline with a shallow plunge to the north. There are two distinct gossans; the so-called lower gossan is interbedded at the contact zone of two types of felsic tuffs that are distinguishable by grain size and weathering characteristics. This gossan is limited in area and is considered economically unimportant. The upper, or main, gossan with felsic tuff weathers cream to brown and displays green-gray banding locally. This unit is overlain by a quartz crystal tuff, weathers gray to white, and contains blue-gray quartz crystals.

The gossans are extensively folded, on a scale of tens of meters, along semihorizontal or north-plunging axes. They are 2 to 3 m thick and can be traced approximately 800 m in a northerly direction.

Sabkhahs on the east coast

Sabkhahs are common features on and near the east coast of Saudi Arabia. C. L. Smith has found that near-surface brines associated with the sabkhahs have high concentrations of major elements including magnesium and that several of the brines are saturated with sodium chloride. Authigenic gypsum and anhydrite nodules are common in the sediments of the coastal sabkhahs.

Three known salt deposits within 50 km of the east coast of Saudi Arabia range from 3 to 7 m in thickness and extend over several square kilometers. These deposits are either at or within 4 m of the surface and indicate that further exploration for salt in this region is warranted.

Institutional development

Four USGS technical staff members now advise the Publications Department of the Saudi Arabian

Directorate General. Under their guidance, the staff of 44 counterpart professional and technical employees is continuing to increase its capability to produce high-quality geoscientific reports. During fiscal year 1979, eight geologic reports were published.

Water resources advisory services

Four USGS hydrologists continued to work with the Water Resources Development Department of the Saudi Arabian Ministry of Agriculture and Water. They and other personnel from the U.S. Departments of Interior and Agriculture provide a variety of advisory services within the Agriculture and Water Project, one of the activities under the aegis of the U.S.–Saudi Arabian Joint Commission on Economic Cooperation. Significant progress was made in the computerization of groundwater, surface-water, water-quality, and climatological data for the kingdom. This included coding, punching, loading, and editing and the preparation of software programs necessary for data management, retrieval, display, and operational use. Exemplifying the latter was the collection and preparation of data for digital modeling of the Minjur aquifer. W. J. Shampine and others (1979) evaluated an accumulation of data on isotope concentrations in the ground water of Saudi Arabia. A crest-stage gage network was designed to sample the magnitude of the brief peak-discharge events in the several climatic zones. Installation of gages to implement the network began during 1979. Ministry officials were advised on the hydrologic aspects of a number of water development projects.

THAILAND

G. A. Younse compiled available information of petroleum resources in Thailand as part of an effort to assemble background information on energy raw materials. As of December 1978, oil production in Thailand amounted to 200 barrels a day from the nearly depleted Boh Ton Kham and Mae Soon oil fields. Estimates of original oil reserves were 350,000 and 1,000,000 barrels for the Boh Ton Kham and Mae Soon oil fields, respectively. The estimate of proved oil reserves in Thailand as of January 1979 is 200,000 barrels. The main problem in the production of oil, most of which comes from the Mae Soon oil field, is obstruction of flow systems resulting from the high wax content of the crude oil, which solidifies at normal temperatures of 30°C and, thus, must be heated to flow.

No gas has been produced in Thailand; however, production will be realized as a consequence of recent gas discoveries in the Gulf of Thailand. Estimates of gas reserves in the Gulf range from 8 trillion ft^3 to 4.4 trillion ft^3.

Oil shale and lignite deposits are fairly large in northern Thailand. Deposits of oil shale at Li have been estimated to be 15 million t, from which 2 million t with an average oil content of 15 gal/ton of shale could yield about 700,000 barrels of crude oil. Lignite deposits at Mae Sot show possible yields of 25 to 70 gal of oil per ton of lignite, and total oil recoverable by retorting of the lignite is estimated to be between 3 billion and 2.8 billion barrels.

TUNISIA

As part of a program sponsored by AID, J. O. Morgan, assisted by U.S. experts in several remote-sensing disciplines installed photographic reproduction and image interpretation laboratories at the Division of Soils, Ministry of Agriculture, Tunis, and trained counterparts in use of the facilities. The U.S. team also presented a seminar-workshop for 80 Tunisians that covered preparation and use of digitally enhanced and multitemporal Landsat image maps.

TURKEY

Data processing techniques and hydraulic laboratory operations

C. O. Morgan and A. I. Johnson visited the facilities of the Turkish State Hydraulic Works (DSI) in January 1979 on detail to the UNDP project aimed at strengthening the technical competence of DSI in the area of ground water. Morgan advised on automatic data processing techniques, and Johnson evaluated hydraulic laboratory operations. Both men instructed DSI staff representatives. At the request of the United Nations, Morgan returned to the DSI establishment in December to review progress on the implementation of his earlier recommendations.

VENEZUELA

In a review of available information on Venezuela (Phase I of a DOE-sponsored program), R. W. Fary and others summarized Venezuela's energy position as follows.

Venezuela's estimated proven reserves of oil, at 18.2 billion barrels, place it 11th among the countries of the world and should provide for almost 22 yr more of production at current rates. It was fifth in petroleum production in 1977, producing an estimated average 2.28 million barrels per day. Its natural gas reserves (estimated proven for 1978) of 41 trillion ft^3 place it ninth in rank in that category. Prospects for discovery of new oil and gas reserves are best in offshore areas from the Gulf of Venezuela to the mouth of the Orinoco

River. In addition, the Orinoco heavy oil belt is believed to contain 1.05 to 3.0 trillion barrels of petroleum. Coal reserves of the Guasare belt alone are estimated at 290 million tons. Other coal-producing areas are present in Tachira, Aragua, Miranda, and Anzoategui States.

Hydrologic conditions are favorable for the development of hydropower in selected areas, especially on the Caroni and the Orinoco Rivers. Hydroelectric generating facilities provided 46 percent of the country's electrical power capability in 1976, and plans were to increase that percentage to 75 by 1980. Uranium minerals are known to occur both in igneous and in sedimentary rocks in several regions of Venezuela; an exploration program in the Andean State of Tachira is planned. Thermal springs are present in the mountain belt from Tachira, in the west, to Sucre, in the northeast. To date, there has been no evidence of high-temperature sources necessary for steam plant operation, but known springs might be suitable for space heating, air conditioning, and agricultural applications.

YEMEN

Surface-water data collection activities

B. N. Aldridge was detailed to the AID mission in the Yemen Arab Republic during October and November 1979 to review the surface-water data-collection activities, principally, of the newly formed Department of Hydrology (DOH). The few existing installations and the data obtained at them were examined, and a reconnaissance for new gage sites was made, partly as a training exercise for the DOH personnel. Some training was given also in field and office procedures for the measurement and computation of streamflow data. Recommendations were developed for improvements in program planning, operational practices, training, manpower management, equipment procurement, and gaging-station construction.

YUGOSLAVIA

Several USGS geologists have been engaged as USGS Project officers in Special Foreign Currency Program (SFCP) projects in Yugoslavia. M. F. Kane reports that the Geophysical (Institute for Geological and Geophysical Research, Belgrade), under a project of deep seismic sounding to determine crustal structure, has completed one-way coverage of a fifth seismic line across Yugoslavia, from Tetovo, on the Albanian border, to Delsevo, on the Bulgarian border. Analysis of data from four completed deep-sounding seismic profiles across Yugoslavia, incorporated with gravity data, has led to the proposal of a model of dynamic isostasy for the Dinaride region.

A geochemical program undertaken by Henry Bell III shows that tin and beryllium are enriched in two-mica granite at Cer, northwest Serbia, and, to a lesser extent at other granitoid massifs in Yugoslavia. The two-mica granite probably resulted from post-magmatic alkali-metasomatism which is greisenization, acting on granodioritic and quartz monzonitic rocks. Other associated rare metals are bismuth, lithium, and niobium.

Scott Keyes reports that the Institute for Geological and Geophysical Research, Belgrade, has been mapping karst terrane by geophysical methods to predict possible collapse and disastrous flooding. Seismic detection of bombs exploded at timed intervals in underground streams has proved effective in mapping underground streams. Repeated measurement of electrical resistivity along an established network of stations promises to yield useful results in defining permeability and in detecting changes in permeability with time and with fluctuations in water level in adjacent reservoirs. From the data, it may be possible to predict collapse and disastrous flooding.

Ernest Dobrovolny cooperated with Yugoslavian geologists of the Geological Research Institute of Sarajevo in developing a methodology for evaluating geologic hazards and environmental problems that result from urbanization and economic growth in an earthquake-prone area and in producing a useful innovative series of maps to show the data.

ANTARCTIC PROGRAMS

The USGS headed only one field party during the 1979 to 1980 austral summer, but several USGS geologists participated in non-USGS projects. The single USGS project was that of D. P. Elston and S. L. Bressler, who conducted sampling and paleomagnetic investigations of glacial deposits in the Dry Valleys. L. M. Force and K. S. Kellogg (USGS) were engaged in sedimentologic and paleomagnetic studies of lower Paleozoic rocks of the Ohio Range, as part of a New Zealand field party led by M. A. Bradshaw (Canterbury Museum, Christchurch). E. L. Yochelson and John Pojeta, Jr. (USGS), collected and studied fossils from Paleozoic rocks in the Ellsworth Mountains as a part of a major project in that range under the general direction of G. F. Webers (Macalester College, Minnesota).

Stateside work consisted of petrologic and geochemical investigations and compilation of geophysical data from samples and data collected from the Dufek intrusion during the 1978 to 1979 field season. Data compilation, petrology, and paleontology of

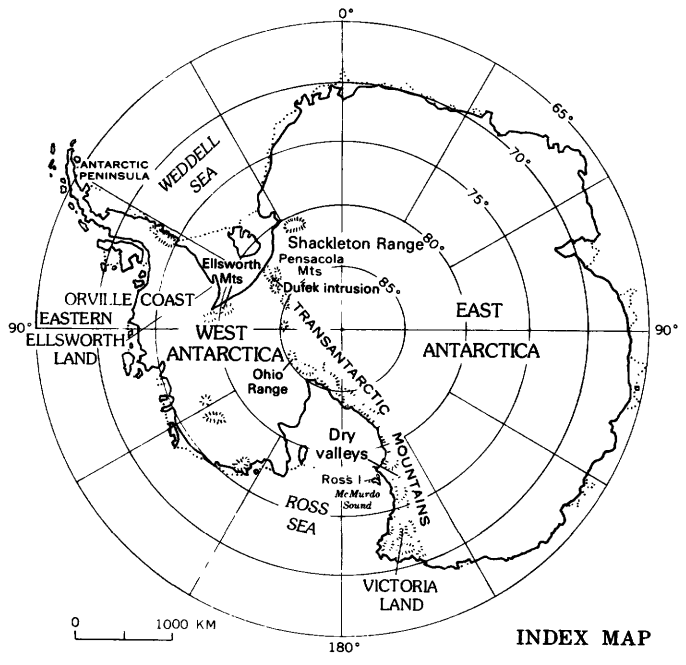

samples and data from the 1977 to 1978 Orville Coast field party continued. Paleomagnetic studies on rock cores obtained in the Dry Valleys also were done.

Multiple emplacement of magma of the Dufek intrusion

Geologic mapping by A. B. Ford, R. L. Reynolds, Carl Huie, and S. J. Boyer during the 1978 to 1979 austral summer showed that many conspicuous layers of plagioclase cumulates of the stratiform gabbroic Dufek intrusion have much greater lateral extent than known previously from the first reconnaissance study in 1965 to 1966. Individual plagioclase cumulate layers in the Forrestal Range were traced during this 1:50,000-scale mapping for distances of about 30 km. A widespread gabbroic cumulate layer, containing a great abundance of noncumulus anorthosite and leucogabbro inclusions in chaotic array, lies with an angular discordance of about 10° on gently tilted cumulates of the middle part of the Forrestal Range cumulate section. The inclusion-rich layer appears analogous to a megabreccia in a sedimentary sequence and is interpreted to record a comparatively catastrophic event in a late stage of solidification in the magma chamber. Blocks of anorthosite and leucogabbro were apparently torn from the roof or walls of the chamber during late-stage subsidence that appears to be associated with magma withdrawal from depths during intrusion at a high level in the body (Ford and others, 1979).

Plagioclase variation in the Dufek intrusion

Plagioclase is a dominant cumulus phase throughout the exposed stratigraphic sections of the Dufek intrusion, except in thin layers of pyroxenite cumulate in the Dufek Massif and of iron-titanium oxide cumulate in the Forrestal Range. In most rocks, plagioclase is also a postcumulus phase, as small irregular interstitial fillings or, more commonly, as rims around cumulus grains. Plagioclase from 30 samples previously analyzed for pyroxenes and iron-titanium oxides were analyzed by electron microprobe in this study. Most plagioclase is compositionally zoned, with cores generally containing 1 to 2.5 percent more anorthite than rims. Some of the zoning probably is related to cumulus growth but most is probably postcumulus around original primocrysts. Anorthite content of plagioclase shows a general decrease with stratigraphic height, from about An_{80} near the base to about An_{55} at the top of the cumulate sequence and in overlying granophyre (Abel and others, 1979). The fractionation trend is similar to that in other layered intrusions of this type. The plagioclase compositional trend shows a major reversal at the level in the Forrestal Range where field evidence is found, suggesting emplacement of a new batch of magma.

Minor-metal variation related to differentiation in the Dufek intrusion

The cumulates and capping granophyre of the Dufek intrusion form a differentiation sequence showing strong iron enrichment. Results of analysis for platinum, palladium, and rhodium by Joseph Haffty, W. D. Goss, and A. W. Haubert (written commun., 1980); for copper, vanadium, cobalt, chromium and nickel by R. E. Mays (written commun.,1980); and for total sulfur by B. P. Fabbi and L. F. Espos (written commun., 1980) are interpreted in terms of variation with differentiation (Ford and others, written commun., 1980). Elements showing statistically significant (+) correlations with stratigraphic height and, thus, differentiation include titanium, vanadium, and copper. Elements whose average abundance is much greater in late-stage versus early-stage cumulates also show enrichment with differentiation, including platinum, palladium, cobalt, and sulfur. Nickel and chromium show strong depletion with differentiation in the cumulate sequence. Ni:Co has strong (−) correlation with height and appears to be a good parameter of differentiation. The abundance of platinum-group elements shows strong correlation with vanadium and TiO_2. As in the Stillwater Complex of Montana, vanadium appears to have the greatest potential as a geochemical tracer for platinum-group elements in the Dufek intrusion.

Origin of magma variation in the Jurassic Ferrar tholeiite province

Geochemical variations in tholeiite of the Jurassic Ferrar magmatic province in Antarctica led A. B. Ford and R. W. Kistler to suggest that the province contains two petrologically distinct subdivisions: a Transantarctic Mountains subprovince showing anomalously high initial $^{87}Sr/^{86}Sr$ and a Weddell Sea subprovince showing normal strontium isotopic ratios. Major and minor element characteristics of the two subprovinces are highly distinctive. Study of Ferrar-like dikes and sills in the Pensacola Mountains by Ford and Kistler indicates a close affinity with the Ferrar of the Transantarctic Mountains type. Whereas the Ferrar of the Transantarctic Mountains is closely comparable to Jurassic Tasmanian tholeiite, the Ferrar of the Weddell Sea is much more like the South African Karroo tholeiites. Both Ferrar subprovinces are related to initial rifting in late Early Jurassic time in Gondwanaland. The Weddell Sea Ferrar, and probably the Karroo, was associated with rifting that was later completed in Middle Jurassic time with the generation of new ocean crust and separation of Antarctica from southern Africa. Ferrar magmatism in the Transantarctic Mountains was associated with a failed arm of this rift system.

Glacial geology of the Dufek Massif and Forrestal Range

During field studies in the 1978 to 1979 austral summer, S. J. Boyer found the Dufek Massif and Forrestal Range to contain a glacial geologic record apparently correlative with events in the Ross Sea (McMurdo Sound) area of Antarctica. Older events in the area probably correlate with Taylor III–Taylor V events near McMurdo Sound, and later events probably correlate with the Alpine I and Taylor I stages near McMurdo Sound (Boyer, 1979). Evidence in the Dufek Massif and Forrestal Range points to (1) very old subpolar- or temperate-type valley gaciation, (2) a former ice-sheet level as much as 400 m higher than exists today, (3) multiple advance and retreat of local alpine ice since the last major ice-sheet retreat, and (4) a complex glacial, glaciofluvial, and lacustrine history locally in Davis Valley. Remains of a former ice-marginal drainage system occur up to 200 m above present ice levels and suggest that early-stage ice sheets (>4 m.y.(?) ago) may have been wet based, as in the carving of early glacial valleys near McMurdo Sound.

Geophysical information on the size of the Dufek intrusion

The combination of the aeromagnetic method with radar ice sounding measurements allows the direct comparison of magnetic anomalies with bedrock topography over the largely ice-covered Dufek stratiform mafic intrusion of Jurassic age. Data collected in 1978 by J. C. Behrendt along 4,200 km of traverse lines indicate that the intrusion extends 200 km north of its previously known extent, to about lat 80°30′ S., long 45° W. Thus, the minimum area underlain by the intrusion is 50,000 km^2, of which only 3 percent is exposed. The intrusion, therefore, is comparable in size to the Bushveld Complex. Magnetic anomalies directly over outcrops range in amplitude from 50 to 3,600 nT. Measured magnetizations (Beck and others, 1968) range from 0.0006 to 0.1 emu/cm^3. Magnetic models based on the subice topography required normal and reversed magnetizations that were computed to range from 10^{-4} to 10^{-2} emu/cm^3. Previous workers (Ford, 1970) showed that the magnetization, mafic index, and density in the body decrease downward; thus, erosion selectively removed layers, allowing stratigraphic sampling down the section by the aeromagnetic and radar profiles. Because of the sheetlike character of the intrusion, magnetization reversals produced by upward and downward moving isotherms during cooling and field reversal would be expected to produce horizontal layered reversal sequences. These would not cause magnetic anomalies except at the edges (which were identified in only one area). The observed magnetic anomalies probably are due to erosion, which would result in juxtaposition of rocks of different magnetizations (Behrendt and others, 1979a,b).

Magnetic correlation of upper Cenozoic DVDP cores

Magnetic polarity and susceptibility zonation by D. P. Elston from four drill cores from Taylor Valley, Antarctica, have been combined with paleontologic, geochemical, and sedimentologic data to derive a synthesis of the late Tertiary geologic history of the Dry Valley region. Temporal and stratigraphic correlations imply deposition of diamictite in deep-water (600 m) fjords beginning about 7 m.y. ago. An unconformity is recognized at approximately the Miocene-Pliocene boundary (about 5 m.y.) that reflects the onset of volcanism, the introduction of sediment derived from the McMurdo Volcanics, and uplift to create comparatively shallow marine conditions. Additional late Pliocene to early Pleistocene uplift resulted in erosion and deposition associated with alpine glaciation.

HYDROLOGIC STUDIES

Under an agreement with the National Science Foundation, Office of Polar Programs, S. M. Hodge journeyed to the Pensacola region of Antarctica late in 1978 as part of a USGS team investigating the Dufek

Pluton. Hodge was responsible for gravity and ice-sounding studies.

ARCTIC REGIONS

W. J. Campbell and J. A. Weyenberg participated in a NASA-sponsored overflight of polar regions in Alaska, Greenland, and Norway in November 1978, in support of continuing polar studies of Seasat A and Nimbus G remote-sensing target areas.

TOPOGRAPHIC SURVEYS AND MAPPING

FIELD SURVEYS

DOPPLER TRANSLOCATION POSITIONING

Since 1975, the USGS has been operating small easily transportable satellite Doppler receivers to establish geodetic control. These receivers measure the Doppler shift on signals transmitted by satellites of the Navy Navigation Satellite System. The position and height of the station is computed from the signal measurement and the satellite ephemeris. Two types of ephemeris data are available: the ephemeris broadcast continuously by each satellite and the more accurate ephemerides that are available for a limited number of satellites a few months later. The broadcast ephemeris is used for real-time navigation applications and translocation positioning. The precise ephemeris is used for single-point positioning where greater accuracy is required and time is not a critical factor.

Translocation positioning involves the use of two Doppler receivers. One receiver collects data at a geodetic control station while the other collects data from the same satellite pass at a new station. Using only the common data at both stations, the position of the new station is computed relative to the control station. Final positions are obtained by applying the relative position to the base station position. The primary advantage of translocation positioning is the tendency to cancel systemic errors such as those caused by errors in the ephemeris data. The observation data are gathered rapidly, and the results are computed quickly without waiting for the delayed precise ephemeris.

Translocation positioning was tested from the USGS National Center, Reston, Va. Five stations in various directions and at ranges of up to 10 km were positioned using the translocation technique and by conventional second-order surveying methods. The position differences obtained by the two methods were less than 1 m for solutions that involved Doppler data from eight satellite passes.

The six satellite Doppler receivers of the USGS have been used for establishing control for mapping in Antarctica, Alaska, Texas, Missouri, and Saudi Arabia. On one special assignment, two receivers were used to establish control along the Appalachian Trail in Vermont in support of a National Park Service project.

INERTIAL SURVEYING

As part of a continuing program to evaluate the application of inertial surveying systems in the National Mapping Program, the SPAN MARK inertial surveying system was used in the Trenton, N.J., area to test existing maps and to establish horizontal and vertical control for future mapping. During a 1-mo period, 1,540 km of double-run survey lines were established with the system mounted in a four-wheel-drive van. Two lines were profiled to determine whether the data will be of use in the USGS mapping program. The standard error of 50 vertical test points was 0.12 m. The maximum error was 0.41 m. Of the 50 test points, 49 meet the accuracy requirements for the production of 10-ft-contour-interval maps. The maximum horizontal error from five test points was 0.85 m, well within map control requirements.

AERIAL PROFILING OF TERRAIN SYSTEM

The USGS has been studying the concept of measuring accurate terrain profiles from low-flying aircraft using a laser altimeter and inertial guidance technology the Aerial Profiling of Terrain (APT) project. The desired accuracy of 15 cm vertically and 61 cm horizontally can be achieved for extended missions if positional updates are provided at 3-min time intervals. The project has progressed from a developmental phase beginning in 1974, through completion of system design, to the midpoint of fabrication of a prototype system.

The APT airborne instruments include a laser profiler, a TV camera, an inertial measuring unit (IMU), a laser tracker, an onboard computer, and a magnetic tape recorder. The airborne computer interacts continuously with the sensors by directing their actions and performing the necessary computations for initial alinement and calibration, for navigation to survey site, and for execution of profile surveys. The laser tracker provides update data by measuring distances and directions to ground reflectors. In addition, the computer feeds data to the onboard magnetic tape recorder to be used later for final computation.

The fabrication of APT components is proceeding on schedule. The major hardware components IMU, profiler tracker, TV imaging system, and computer and peripherals are under construction or have been

purchased. Development of the mathematical processing system and APT software is proceeding as expected. A computer program that simulates the APT error growth during a hypothetical flight mission has been under continual development, and recent results verify that the desired survey accuracies will be met.

Paralleling the fabrication effort is the effort to obtain an aircraft suitably modified to carry the APT system. A Twin Otter has been selected for the project and will be made available from existing DOI resources in June 1981 when the extensive aircraft modifications will begin.

The APT program will continue until the operational prototype is completed and flight-tested. Further activities will be based on the results of actual field tests of the prototype. Costs to date have been approximately $7 million. The fabrication and assembly phase began in October 1978 and is scheduled for completion in 1981.

PHOTOGRAMMETRY

HORIZONTAL MAP ACCURACY TESTING

National Map Accuracy Standards require that 90 percent of the map features tested at scales of 1:20,000 or smaller be accurate within 1/50 inch (0.05 cm) of the correct map position. This map testing has traditionally been performed by field surveying techniques on a small sample basis.

In the past, several photogrammetric methods have been used to test quality control of map compilation. One method has been the measurement, during aerotriangulation, of extra points over and above those needed for map compilation. These extra points subsequently are used solely for accuracy testing of the completed map manuscripts. Another method has used separately flown photographs that are aerotriangulated to provide control for checking the map manuscript.

These various testing procedures have demonstrated the feasibility of using photogrammetric methods to test the accuracy of the horizontal map positions. However, all methods either employed the original photographs, camera systems, and aerotriangulation adjustment or required the acquisition of additional specially flown photographs at additional cost.

With the recent advent of the High-Altitude Aerial Photography (HAP) program, the entire nation will be photographed on a cyclical basis, generally every 3 yr. The photographs will be quadrangle-centered – that is, alternate photographs will be centered on standard 1:24,000-scale quadrangles. Thus, each quadrangle will have photographs for map accuracy testing that are independent of those used for map compilation.

To assess the feasibility of HAP for this testing, the National Mapping Division compared HAP test points in three quadrangles in North Carolina to a test by field-survey techniques of the area. In this particular project, the planimetric features of the maps also had been derived from the HAP; therefore, although a good correlation with the field-derived test points was obtained, a truly independent test was not achieved. A second study is in progress using the "cyclic" HAP for the Middleburg and Arcola quadrangles, Va., for which the original manuscripts were prepared using low-altitude photographs.

Since aerotriangulation and testing using available photographs are far less costly than the maintenance of field parties, it is anticipated that the results of the second study will demonstrate an economical method of horizontal map accuracy testing to insure the production of high-quality map products.

RESOLUTION TARGETS

An array of resolution targets has been painted on the roof of the USGS National Center, Reston, Va. The target array consists of standard bar targets and a Siemens star target.

The bar targets, based on a design used by the National Bureau of Standards, consist of alternating black and gray bars arranged in two groups perpendicular to each other. Each group is 20 by 100 ft (6.1 by 30.5 m) and contains six sets of bars. Each set contains six individual bars, three black and three gray of equal width. The individual bar widths of each set are, in descending order, 6.0 ft (1.8 m), 4.0 ft (1.2 m), 2.5 ft (0.75 m), 1.5 ft (0.45 m), 1.0 ft (0.03 m), and 0.75 ft (0.23 m).

The Siemens star consists of alternating black and gray wedges every 5 degrees of arc. The target diameter is 140 ft (42.7 m) yielding a maximum wedge width of 6 ft (1.8 m). The design contrast ratio for both the bar and star targets was 2.5:1; measured ratios are 2.3:1 for the star and 2.1:1 for the bar. This relatively low contrast was chosen to simulate that typically found in aerial photography.

These permanent targets provide the USGS and other agencies with the capabilities of testing the resolution of camera systems, evaluating image motion compensation devices, and measuring the effects of other aircraft actions.

SATELLITE APPLICATIONS

MAPSAT

Eight years of experiments and investigations of data from Earth-orbiting satellites have culminated in a proposal for an operational satellite system for Earth resources investigations. This system, known as Mapsat, utilizes many Landsat parameters (including multispectral imaging) but features improved resolution, geometry, and stereocoverage and emphasizes simplicity and cost-effectiveness. The proposed sensor is composed of several thousand detectors in a linear array that makes possible a one-dimensional flow of data that can be processed by a relatively simple computer program. Topographic maps at scales as large as 1:50,000 are envisioned as products of the sytem. A contract for a feasibility study has been let to investigate further the conceptual design of Mapsat.

MAP PROJECTIONS FOR SATELLITE APPLICATIONS

An investigation of map projections resulted in a summary of the most appropriate projections for various satellite applications. The Space Oblique Mercator, which is basically conformal, shows the curving satellite groundtrack true to scale. A new satellite projection whose formulas have not yet been derived is the Space Oblique Conformal Conic. It may be adaptable to side-looking radar scanning on satellites such as Seasat.

Other projections that have been summarized are the Cylindrical Satellite-Tracking projection, the Conic Satellite-Tracking projection with two conformal parallels, and the Conic Satellite-Tracking projection with one standard parallel. There are accurate programable alternatives to the traditional projections that have been used for satellite mapping and tracking to date, but each is highly specialized in its optimum applications.

LANDSAT

RBV experiments

Landsat 3 RBV imagery has been used in two specific remote sensing applications: (1) in the production of an image-base-controlled map and (2) as an intermediate-scale map revision tool.

First, the USGS experimented with the production of a precisely controlled Landsat 3 RBV map of the Cape Cod area, Massachusetts, at 1:100,000 scale. During previous experiments with Landsat 3 RBV imagery, control points had been identified on 1:24,000-scale paper maps and visually transferred to the much smaller 1:500,000-scale RBV image for measurement. The reliability of visually transferring a map point to a much smaller scale image raised questions about the degree of accuracy lost. A substantially more accurate positioning of control points on the RBV image was accomplished by direct transfer of points from conventional ground-controlled photographs to the RBV imagery, using a Wild PUG-2 point marking device, effectively eliminating the optical transfer errors from the intermediate maps.

The 4 RBV images constituting the mapped area had a selection of 53 control points transferred from the photographs. These image points then were measured on a precise monocomparator for geometric analysis. A direct similarity transformation fitted the image points to ground coordinates for subsequent creation of a control base. The adjustment obtained in the transformation yielded a rms error of 33.9 m for the control fit of all four images.

To determine the feasibility of using RBV imagery as a map revision tool, images of specific mapped areas were examined to determine what map information could be seen. Selected RBV imagery was acquired for the Marion, Ohio, and Vidalia, Ga., quadrangles. In both instances, current conventional photography either was missing or did not cover the mapped area. The selected scenes were enlarged without rectification to 1:100,000 scale and registered to the maps for the correction of cartographic detail. Current map revision policies guided the revision. At this scale, results indicate that the RBV imagery could be used to update specific features such as highways, streams, and woodland.

Advantages in using RBV imagery for map revision include (1) coverage cycle of 18 d, (2) currency of images, (3) enlargement without rectification, and (4) total 1:100,000-scale map sheet coverage from a single enlarged RBV scene.

Water-depth determination

In the past 3 yr, a large percentage of the world's shallow seas has been imaged by Landsat. The multispectral scanners were operated in the high-gain mode to optimize low-level responses such as those that underwater features produce. Previous studies of remote water-depth determination were analyzed. It was determined that an empirical approach utilizing Landsat data coupled with limited boat or aircraft surveys offers a feasible method of remote bathymetry.

HEAT CAPACITY MAPPING MISSION

The Heat Capacity Mapping Mission (HCMM) satellite records the radiation from Earth in the 10.5 to 12.5 m thermal band using an instantaneous field of view of 600 by 600 m. A test of HCMM data was conducted on Lake Anna, Va., to determine whether a satellite can provide meaningful temperature data of such a water body. After thermometer records were used to calibrate the satellite data, the satellite data corresponded to the on-site records with rms error of about 1°C. Other sites of known surface-water temperature must be tested before conclusions can be reached about the areal and temporal frequency of calibration needed to effectively map surface-water temperature using HCMM data.

SEASAT

A study to analyze the performance of the Seasat radar altimeter in overland tracking was completed under a contract jointly funded and monitored by the National Geodetic Survey and the USGS. Although the Seasat altimeter originally was designed for open-ocean tracking with little consideration given to overland data acquisition, the altimeter acquired meaningful data over smooth terrain and large ice sheets. This was cause for further investigation.

Five areas were chosen for analysis: the San Joaquin Valley, Houston-Galveston, Phoenix-Tucson, and large ice sheets in Greenland and Antarctica. In each area, the altimeter acquired topographic profiles agreeing within a few meters with large-scale topographic maps or Doppler satellite positioning (geoceiver) elevations. Comparison with GEOS 3 profile intersections, however, indicated that improvement approaching 10-cm precision could be obtained by additional analysis of the recorded radar waveform data.

Another contract has been awarded to study the waveform retracking that may provide geodetic-quality terrain profiles. Initial results indicate that a radar altimeter optimized for overland tracking from a near-polar-orbiting satellite could provide terrain profiles of mapping quality over most nonmountainous areas of the world at relatively low cost.

SATELLITE IMAGE MAP

A recent 1:500,000-scale map of the Berry Islands, Bahamas, is the first to combine space imagery with bathymetric data and, thus, introduces a new concept in the mapping of the Earth's shallow seas. The map involves NASA's Landsat 2 satellite, image enhancement performed by the USGS, and bathymetric geodetic grid, marginal data, and printing by the DMA.

DIGITAL CARTOGRAPHY

Stereomodel compilation-digitization is developing from a research activity to an efficient method for producing photogrammetric manuscript and selected color separates. The USGS currently is involved in production-evaluation activities for photogrammetric digital compilation and the required special map-finishing operations.

The prospects of automating part of the map compilation process look very promising. However, total automation probably will require the development of new mapping specifications. Present cartographic symbols and specifications have been designed with the abilities and limitations of the human draftsman in mind. Computer-driven plotters offer new possibilities, but they are subject to constraints different from those of the draftsman. These new possibilities and limitations must be examined; they may require new specifications geared to the capability of automated drafting and the needs of the map users.

INTERACTIVE COMPILATION AND EDITING

The USGS has been evaluating the compilation and revision potential of using a stereoplotter online with an interactive editing system. Two objectives were pursued: (1) to develop procedures for an interactive (online) digital map compilation and editing system and (2) to evaluate the potential of the interactive system for new map compilation and for photorevision of existing digital files. Using a Kern PG–2 stereoplotter interfaced to the M&S digital data editing system (DDES), one quadrangle map was compiled for comparison of online versus offline methods, and one quadrangle map in digital form was photorevised.

Online digitization-compilation of the Van Metre 2 NW 7½-min quadrangle, S. Dak., was conducted in a manner similar to that used on a standard graphic digitizing-interactive editing work station. Use of the interactive editing system allowed the operator to digitize directly from the stereoplotter and immediately view and edit the data using the graphic screens. After processing, the data were plotted for proofing. Online compilation resulted in a 31-percent reduction in time needed to compile and edit a quadrangle, as compared to offline compilation methods for the same quadrangle.

Online digitization-revision of the Rosati 7½-min quadrangle, Mo., was accomplished by the operator

digitizing new data and tagging obsolete data for deletion from the existing files. After processing, the three types of files—the original files without modifications, the modified files containing deletions, and the files containing new revision data—were plotted for proofing. Revision of this quadrangle map by digital methods proved to be technically feasible, as well as cost effective, when compared to manual photorevision methods.

OFFLINE COMPILATION

Digitized analog stereomodel data and automatic plotting techniques have been used to produce map color separates. The project area consisted of the Princes Ranch 7½×15-min quadrangle, S. Dak. Mapping was planned at a scale of 1:25,000 with a 5-m contour interval. The Van Metre 2 NE and Van Metre 2 NW 7½-min quadrangles were compiled and digitized at 1:24,000 scale, and the digital files were merged to produce the color separates for the Princes Ranch quadrangle.

The data were collected from the stereomodel and recorded on magnetic tape in a format that was compatible for input to the DDES. The data were tagged with sufficient attribute information to allow subsequent processing as color separates. Two methods of entering attribute codes were used and evaluated in this study, manual keyboard entry and voice entry.

Several computer programs were developed to process the data sets and combine features according to attribute codes. Plotting programs were developed for generating the photogrammetric manuscript used as a proof for determining shaping and registration problems that required subsequent interactive editing. Particular attention was directed to the symbol generation necessary for final-quality color separates.

Two color composites were plotted using different production methods. (1) One composite was generated using only digital techniques for all plotting, including the lettering. Spot elevation, contour label, map title block, and General Land Office type were automatically plotted using the Hersey fonts and the text-placing capabilities of the DDES. This was an experimental digital version of the Princes Ranch quadrangle. (2) The other composite was generated using a combination of digital and manual methods. The contour plate required manual rescribing, and the lettering was manually placed. This composite is of reproduction quality, and the respective color separates will be used for publication of the Princes Ranch map.

As a byproduct of digital stereocompilation, accurate digital elevation model files (commensurate with the contour interval) and digital line graph files are available for data base entry.

The primary advantages of digital mapping are to provide the map user with either more or different kinds of information (digital or graphic) than can be shown on a standard topographic map; to provide usable substitute maps with a minimum of touchup for certain areas that cannot be mapped on a timely basis by conventional mapping methods, such as Three Mile Island; and, in some projects, to shorten the map cycle for new mapping projects.

SPECIAL MAP DIGITIZING

Mining area subsidence research

The Waltonville 7½-min quadrangle, Ill., map was chosen for digitizing public landlines, transportation, boundaries, and hypsography categories in support of mining studies. Data collection was performed on an Altek digitizer table and was processed on the IBM 370 at the USGS National Center in Reston. This information is being used by the Department of Mining, Petroleum and Geological Engineering, University of Missouri, as an interactive digital data base for developing algorithms in mined areas to predict probable areas of subsidence and the relative ground movement expected.

VOICE TERMINAL

The USGS is developing a voice input-output terminal that has particular significance in the mapmaking process. The ability to make data entries while occupied with a hand-and-eye-busy task is one of the major advantages of the terminal. The digitizer operator using a voice terminal is not required to divert his attention from the source material to use the digital data recording system. He needs only to speak the appropriate words or phrases from a predefined and pretrained vocabulary to accomplish the required input operation. The terminal confirms his input by repeating the word or phrase through a voice synthesizer. It also can prompt the operator through the voice synthesizer for required inputs.

The terminal hardware configuration was assembled using an LSI-11 microcomputer system specially programed to provide the necessary data buffering, control functions, and interfaces. A Threshold 600 Voice Entry Terminal implemented the voice input function, and a commercial voice synthesizer was used to implement the voice output. The synthesizer was modified for adaptation to the LSI-11 interface.

The operating system to control the terminal was written on the DEC Modular Instrumentation Computer (MINC-11), which was used as a development system

for the LSI–11 microcomputer in DEC's macro 11 assembly language.

COORDINATE TRANSFORMATION SYSTEM

The USGS continued an investigation into the feasibility of using a multiple microcomputer data processor to transform sets of digital cartographic data from one coordinate system to another. Currently, the time-consuming transformation programs are run on mainframe computers at high expense. Overall system design and computer hardware selection and acquisition were completed on a dedicated Coordinate Transformation System (CTS) utilizing a high-speed direct-memory-access interconnection scheme between sequentially selected microcomputers and a front-end processor (FEP) minicomputer. Assembly and debugging are in progress.

The CTS utilizes commercially available direct-memory-access (DMA) interprocessor links and specially designed DMA data bus electronic switches. The switches provide program-controlled connection of the FEP to 3 (16 maximum) microcomputers using time-division multiplexing. Performance evaluation of a prototype will follow debugging.

System speed has been improved by a factor of 2.5 by replacing the original microcomputers with higher performance units. They are more cost effective than either user-developed microcoded floating-point arithmetic instructions or custom-designed high-speed arithmetric hardware.

COMPUTER-ASSISTED MAP SYMBOL PLACEMENT

The placement of letters and symbols on topographic and thematic maps represents a significant activity in the map-finishing operation. In a continuing effort to reduce these labor requirements, an Altek AC–90–SM angle digitizer and a Kongsberg flatbed plotter are being used to meet immediate letter and symbol placement needs. The digitizer, in a single step, can assign the x and y coordinates of a symbol with 0.007-cm accuracy, its identification, and its correct orientation within 0.5-degree precision at least five times faster than by manual methods.

The flatbed plotter has a custom photohead symbol disk with 70 of the most frequently used USGS map symbols. Operational speed is in excess of 50 times the rate of manual symbol placement methods.

GESTALT PHOTO MAPPER II SOFTWARE DEVELOPMENTS

The USGS has increased its capability to produce orthophotos and digital elevation data by acquiring two Gestalt Photo Mapper II (GPM2) systems. A new operating system will increase the efficiency of the GPM2's through improved online procedures and the elimination or reduction of time required for some offline procedures. The primary technical objectives of the development are:

1. To provide USGS the capability for maintaining the operating software of the GPM system.
2. To design and build the operating software with the following photogrammetric capabilities:
   - Rigorous algorithms for establishing interior orientation.
   - Online or offline determination of exterior orientation.
   - Application of corrections for radial lens distortion, atmospheric refraction, film deformation, and Earth curvature.
   - Online mosaicking and scanning in a unified reference system of 1, 2, or n models.
   - Algorithms to prevent redundant scanning of any portion of adjoining models. These algorithms have been designed to eliminate wasted efforts in overscanning and expensive resampling of elevation data when combining several models into a single digital elevation model.
3. To design the GPM central system to be independent from the operational requirement of individual tasks.

PUBLICATIONS TECHNOLOGY

COLOR PROOFING

Color proofs of new topographic quadrangle maps, until recently produced by sequential manual wipe-on light-sensitive colors, are now made by color photography. An Ektacolor proofing system uses filter combinations in a remotely controlled filter wheel to expose color-separate films on Ektacolor 78 paper. Processing is done in Ektaprint II developer and a bleach fix solution, with a water rinse and line drying. This method provides sharper lines and more vivid colors than the wipe-on method, is less tedious to the photographer, saves man-hours, and produces topographic quadrangle films as intermediate products.

SCREENLESS PRINTING

Orthophotoquads are monocolor photographic image maps produced by the USGS in standard quadrangle format without topographic detail. They are prepared quickly and for about one-twentieth the cost of a standard line map or an orthophotomap with line, symbol, and lettering enhancement. Most have not been lithographed but are available as diazo or photographic prints.

Orthophotoquads contain extensive image detail at National Map Accuracy Standards. However, the standard halftone lithographic process degrades the image into a grid structure of dots.

The screenless lithographic method structures the image as random dots equivalent to the very fine chemical grain structure of a commercially presensitized anodized aluminum lithographic plate. In addition to the improved resolution of image detail, the monocolor screenless orthophotoquad gives the impression that the image is printed with two ink colors rather than one. The combination of an apparent two-color (duotone) process and the fine random-dot structure results in a significantly more usable product.

Platemaking

The advantage of the screenless plate process as compared to the screenless film process used for orthophotomap production is in the reduction in photographic steps. The pressplates are used as if they were photographic film. They can be tone-corrected by flash exposure to extend image shadow range and bump exposure with a highlight-film mask to improve highlight detail. The main exposure of the orthophotoimage controls the midtones.

No special orthophotograph image requirements are made for the screenless plate process because the same densities for good halftone process reproductions are used. The plate, however, is a positive working plate so that the continuous-tone film positive made for platemaking needs to be reversed as a mirror image for emulsion-to-emulsion plate exposure.

Monocolor printing

A screenless printing research project produced the Greenwood, Miss., orthophotoquad as a simulated duotone. The screenless plate for the imagery was exposed from an unscreened continuous-tone positive made from the same standard source materials that had been used to print the monocolor halftone version.

A single mixture of ink, five parts PMS–363 green and four parts process black, was used for the image plate. Without the halftone dot structure, the impression of the image is that of a duotone. Two distinct colors are evident at the two extremes of the tonal image – near black at high-density tones and almost pure green at the low-density tones. This was demonstrated clearly by visual comparison of two step wedges printed in the map margin, one screened and the other unscreened. The reason for the unusual duotone impression is that, in the middle and quarter tones, the halftone dot leaves exposed much of the paper that contains toners that make the color appear "dirtier" than the screenless lithography.

The names and grid information were printed in process black, a pure black in contrast to the imagery, and the grid was registered with the imagery on the press rather than by the pin system.

The screenless method introduces a new design for lithographed orthophotoquads that previously had been printed in a single ink (black) for imagery, names, and grid. As a result of this success, a block of 16 contiguous quadrangles in the Boston area has been printed by screenless lithography.

Color proofing

The primary obstruction to using screenless printing has been the lack of a predictable means of proofing the continuous-tone reproducible imagery before printing. Conventional halftone proofing methods are not acceptable because they are designed for high-contrast imagery.

The USGS has used color photographic printing paper as a proof for four-color imagery printed by screenless lithography. Continuous-tone negatives for each color are exposed with complementary-color filters in contact with the photographic color process paper. Press inks were specifically ordered to match the dyes in the photographic color paper. A four-color Landsat image map of the Grand Canyon was proofed successfully by this method, establishing it as a reliable quality-control procedure.

EXPERIMENTAL SATELLITE-IMAGE MAP OF THE GRAND CANYON

The printing of satellite imagery of the Grand Canyon area applied screenless lithography to Landsat imagery. Objectives were to develop screenless printing quality control and a proofing technique to fit modern production practices and to print Landsat imagery without screening to eliminate the halftone dot that can cause a disturbing moire pattern with the pixels. Printing a color image exploited the economies and the improved color and tone-reproduction capabilities of screenless lithography.

The Grand Canyon area had been imaged by Landsat MSS in May 1975 and digitally mosaicked by NASA from four subscenes. A unique USGS computer technology had been used on the digital data of this scene to generate a blue component, which the MSS does not record, from the bands that are recorded. The blue band of digital data was derived by algorithms written to predict or calculate from the responses of the other four bands. Different algorithms were used for each of three

classes of Earth materials – water, vegetation, and soils and bedrock. The ratio of the infrared band to the red band determined which algorithm to use for each pixel of the image. Other corrections applied to the digital data, before reconstitution in color film separates, consisted of removing effects of atmospheric haze and noise patterns and applying a technique of image-edge sharpening. The color-banded data were output as film separates for blue, green, and red at 1:1,600,000 scale.

The color separates were brought to 1:250,000-scale film positives on the Wild E–4 rectifier-enlarger based on a least-squares adjustment to points scaled from existing maps. A 20,000-m UTM grid was computed and fitted to the image with a rms error of 300 m in relation to the well-defined features.

The film positives were used to expose the positive-working screenless printing plates for process-color printing using cyan, magenta, and yellow inks. No black plate was necessary for the image area because of the large quantity of ink laid down on the paper in screenless lithography; black ink was used for the UTM grid and type overlays. A continuous-tone type C color print was made of the composited color separates, which served as a proof copy. A close litho reproduction of the proof was obtained by matching the printing inks to the dyes used to make the color print.

The printed features were conveyed from inks that in the screenless process were transferred to the paper in equivalence to about a 600-line-per-inch screen. They were in colors that simulated nature: green for vegetation, white for snow, bluish-gray for lava, and an abundant variety of browns, mustards, and tans representing soil and bedrock.

The screenless printing technique, coupled with the special digital image processing, made this satellite image map of great interest to geologists.

COMPUTER RESOURCES AND TECHNOLOGY

During 1979, the Computer Center Division (CCD) received many requests from USGS scientists for additional data communications facilities. Data storage requirements continued to increase. Many of the USGS scientists increased their use of distributed systems, batch systems, interactive systems, digital graphic analyzers, and word processing equipment.

To provide improved service to the USGS divisions and offices, the CCD expanded and upgraded its computational facilities. The following paragraphs outline the major actions taken to provide computing service to the USGS scientists. Four areas are discussed – Data Communications, Batch Computing, Interactive Computing, and ADP Training.

DATA COMMUNICATIONS

Trends within the USGS's computer-using community provided impetus to the growth of data communications. With the growing acceptance of distributed processing and word processing, users requested increased data communications capabilities. Scientists continually intermixed data processing with their scientific research. Much of their research required computerized data to be transferred to and from geographically dispersed locations. These trends are expected to continue.

The CCD added more data communications equipment to its computing facilities. New modems and multiplexers were installed. Upgrading of the communications processors at Reston, Va., was completed. These actions provided some of the capabilities to support the growing data communications requirements of the USGS scientific community.

The capabilities of TYMNET, a Value-Added Network (VAN) service used by the USGS, required upgrading during 1979. This upgrade included an increase in the capacity and support of the 300 to 1,200 bits-per-second (bps) communications lines at Menlo Park, Calif., Denver, Colo., and Reston, Va. Access to the IBM computer systems (RE–1 and RE–2) via TYMNET was provided to USGS computer users as part of this upgrade.

Plans to procure the services of an additional network, the Advanced Research Projects Agency (ARPA) Network, were completed. Orders were issued for the necessary components to interface the ARPA Network with the USGS host computers. Delivery and installation of the components are scheduled for completion by the end of 1981.

ARPANET is a resource sharing, host-to-host data communications network that links a wide variety of digital computers for communication purposes. This communications network will link together the five large USGS computer systems (MULTICS, RE–1 and RE–2 at Reston, MULTICS at Denver, and MULTICS at Menlo Park) for file transfer capabilities.

Substantial improvements in the USGS communications network were made. For example, the three installed Memorex 1270 Terminal Control Units (TCU'S) connected to RE–1 and RE–2 were replaced by a single 3690 COMTEN Intelligent Front-End Processor (FEP). This COMTEN FEP has the capability of handling up to 400 port connections, which represents a 400 percent increase in capacity over that provided by the Memorex 1270 TCU's. With this increased port capacity, the remote computing community of the USGS should enjoy ample port connections. The addition of the COMTEN FEP provides the capability to dynamically reconfigure modems, ports, and other communications devices when network components or lines malfunction.

Codex Statistical Multiplexers were procured and delivered to Reston, Va., Denver, Colo., and Metairie, La. Codex Statistical Multiplexers provide for simultaneous support of multiple communications in the transmission speed ranges from 300 to 9,600 bps over single communications leased (private) lines. As a result, the USGS scientific community and other DOI agencies are provided with state-of-the-art communications capabilities and improved service. The USGS scientific community and these DOI agencies will benefit from the line cost reductions achieved by installing these computer communications components.

BATCH COMPUTING

Efforts continued on the project to replace the IBM 370/155's (RE–1 and RE–2). Both RE–1 and RE–2 are operating at overload capacity. Attempts to secure a Delegation of Procurement Authority (DPA) from the General Services Administration for IBM compatible systems were delayed. These delays have caused the procurement cycle to take additional time. However, these previous efforts paved the way for an approval of the USGS plans by the General Services Administration

and the DOI. The plans include replacing the aging central processing units (cpu's) of RE-1 and RE-2 with IBM-compatible processing systems.

A DPA from the General Services Administration was included with this approval. The project for replacing the cpu's of RE-1 and RE-2 is moving forward. The installation of IBM-compatible systems will provide the needed increases in computing capacity to handle the continual growth of batch processing. When a new system is installed at the USGS in Reston, Va., the computing workload from RE-1 and RE-2 and a portion of the computing workload from RE-3 will be moved to the new computer system.

The USGS computer workload continued to be dominated by batch processing. Overall, the batch workload increased by more than 30 percent. Much of this batch workload was entered via remote batch terminals such as the Data 100 Keybatch Station and the Data Point 5500 Remote Job Entry Terminal. Many of these remote batch terminals are located at remote locations such as Lawrence, Kans., and Albuquerque, N. Mex.

To provide for overload processing, the CCD extended the Telecommunications Services Program. American Management Systems received a new contract for the RE-3 computer resource. This resource continued to be used to process the USGS batch overload requirements.

The CCD upgraded its disk storage capacity. The upgrade provided ITEL 7330-11 dual density disks as replacements for the ITEL single density (100 megabyte) disks that are connected to the IBM 370/155's. This upgrade brought the total storage capacity of ITEL 7330-11 (200 megabyte) disks on the RE-1 and RE-2 computer resources to 12.2 billion bytes on 61 disk drives. All of the ITEL disks have the capability that allows them to be interfaced to and used with any IBM-compatible cpu.

INTERACTIVE COMPUTING

Most hardware components to supplement the USGS's interactive computing systems were procured and installed in 1977 and 1978. During 1979, the USGS scientific community took advantage of these computing facilities and increased its usage of the interactive computing resources by approximately 30 percent. This level of increase is expected to continue for the next several years.

Some of the increases in interactive computing were the result of interactive graphics usage. Software and hardware enhancements were developed and installed on the USGS Reston computer facilities to support limited investigations in color graphics. Color graphics capabilities are valuable to USGS scientists who require an additional dimension to highlight or emphasize certain areas of pictorial data for reports. To support the requirements for color graphics, a 6500 Xerox Color Graphics Printer was procured and installed at the Reston Computer Center. The 6500 Xerox Color Graphics Printer operates as a peripheral device when it is attached to a graphics terminal.

ADP TRAINING

In 1979, the CCD sponsored 79 d of ADP-related training. It provided 161 additional days of training involving CCD personnel to support the software and computers maintained by the CCD. This large demand for ADP training typifies the continual demand for computer services supplied through the CCD to its users.

U.S. GEOLOGICAL SURVEY PUBLICATIONS

PUBLICATIONS PROGRAM

Books and maps

Results of research and investigations conducted by the USGS are made available to the public through professional papers, bulletins, water-supply papers, circulars, miscellaneous reports, and several map and atlas series, most of which are published by the USGS. Books are printed by the Government Printing Office, and maps are printed by the USGS. Both books and maps are sold by the USGS.

All books, maps other than topographic quadrangle maps, and related USGS publications are listed in the catalogs "Publications of the Geological Survey, 1879–1961" and "Publications of the Geological Survey, 1962–1970," available at nominal cost, and in yearly supplements, available free on request, that keep the catalogs up to date.

New publications, including topographic quadrangle maps, are announced monthly in "New Publications of the Geological Survey." A free subscription to this list can be obtained on application to the *U.S. Geological Survey, 329 National Center, Reston, VA 22092.*

State list of publications on hydrology and geology

"Geologic and Water-Supply Reports and Maps, [State]," a series of booklets, provides a ready reference to these publications on a State basis. The booklets also list libraries in the subject State where USGS reports and maps can be consulted; these booklets are available free on request to the USGS.

Surface-water, quality-of-water, and ground-water-level records

Surface-water records through water year 1970 were published in a series of water-supply papers titled "Surface-Water Supply of the United States"; through water year 1960, each volume covered a single year, but the period from 1961 to 1970 was covered by two 5-yr volumes (1961–65 and 1966–70).

Quality-of-water records through water year 1970 were published in an annual series of water-supply papers titled "Quality of Surface Waters of the United States."

Both surface-water and quality-of-water records for water years 1971 to 1974 were published in a series of annual reports titled "Water Resources Data for [State]." Some of these reports contained both types of data in the same volume, but others were separated into two parts, "Part 1: Surface-Water Records" and "Part 2: Water-Quality Records." Limited numbers of these reports were printed, as they were intended for local distribution only. Since the data in these reports will not be republished in the water-supply paper series, reports are sold by the National Technical Information Service.

Records of ground-water levels in selected observation wells through calendar year 1974 were published in the series of water-supply papers titled "Ground-Water Levels in the United States." Through 1955, each volume covered a single year, but, during the period from 1956 to 1974, most volumes covered 5 yr.

Starting with water year 1975, records for surface water, quality of water, and levels of ground-water-observation wells are all published under one cover in a series of annual reports issued on a State-boundary basis. Reports for water year 1975 and subsequent water years appear in a series of reports entitled "Water-Resources Data for [State]"; these reports are sold by the *National Technical Information Service, U.S. Department of Commerce, Springfield, VA 22161.*

State hydrologic unit maps

State hydrologic unit maps, which are overprints of the 1:500,000-scale State base maps, show culture in black, hydrography in blue, hydrologic subdivision boundaries and codes in red, and political (FIPS county) codes in green. The Alaska State map is at 1:2,500,000 scale, and the Puerto Rico map is at 1:240,000 scale. All river basins having drainage areas greater than 700 mi^2 (except for Alaska) are delineated on the maps. The hydrologic boundaries depict (1) water-resources regions, (2) water-resources subregions, (3) National Water-Data Network accounting units, and (4) cataloging units of the USGS "Catalog of Information on Water Data." These maps are available for every State and Puerto Rico.

State water-resources investigations folders

A series of folders entitled "Water-Resources Investigations in [State]" is a project of the Water Resources Division to inform the public about its current

programs in the 50 States and Puerto Rico, the U.S. Virgin Islands, Guam, and American Samoa. As the programs change, the folders are revised. The folders are free on request as follows: for areas east of the Mississippi River, including Minnesota, Puerto Rico, and the Virgin Islands—*Branch of Distribution, U.S. Geological Survey, 1200 South Eads Street, Arlington, VA 22202,* and for areas west of the Mississippi, including Alaska, Hawaii, Louisiana, Guam, and American Samoa—*Branch of Distribution, U.S. Geological Survey, Box 25286, Federal Center, Denver, CO 80225.*

Open-file reports

Open-file reports, which consist of manuscript reports, maps, and other preliminary material, are made available for public consultation and use. Reports and maps released only in the open files are listed monthly in "New Publications of the Geological Survey," which also lists places of availability for consultation. Most open-file reports are placed in one or more of the three USGS libraries: Room 4A100, National Center, 12201 Sunrise Valley Drive, Reston, VA 22092; 1526 Cole Boulevard at West Colfax Avenue, Golden, Colo. (mailing address: Stop 914, Box 25046, Federal Center, Denver, CO 80225); and 345 Middlefield Road, Menlo Park, CA 94025. Other depositories may include one or more of the USGS offices listed on p. 365 and interested State agencies. Some open-file reports are superseded later by formally printed publications.

Microfiche and (or) paper copies of most open-file reports can be purchased from the *Open-File Services Section, Branch of Distribution, U.S. Geological Survey, Box 25425, Federal Center, Denver, CO 80225.*

Earthquake publications

The "Earthquake Information Bulletin" is published bimonthly by the USGS to provide information on earthquakes and seismological activities of interest to both general and specialized readers. Each issue also lists a worldwide summary of felt earthquakes and a State seismic history.

The USGS National Earthquake Information Service locates most earthquakes above magnitude 5.0 on a worldwide basis. A chronological summary of location and magnitude data for each located earthquake is published in the monthly listing "Preliminary Determination of Epicenters." The "Earthquake Data Report," a bimonthly publication, provides a chronological summary of location and magnitude data for each located earthquake and contains station arrival times, individual distances, azimuths, and traveltime residuals. "Earthquakes in the United States" is published quarterly as a USGS circular. The circulars supplement the information given in the monthly listing "Preliminary Determination of Epicenters" to the extent of providing detailed felt and intensity data as well as isoseismal maps for U.S. earthquakes.

"United States Earthquakes [year]" is published jointly by the USGS and the NOAA. This annual sourcebook on earthquakes occurring in the United States gives location, magnitude, and intensity data. Other information such as strong-motion data fluctuations in well-water levels, tsunami data, and a list of principal earthquakes of the world also is given.

PUBLICATIONS ISSUED

During fiscal year 1980, the USGS published 6,356 maps comprising some 14,975,712 copies:

Kind of map printed	*Number*
Topographic	5,233
Geologic and hydrologic	891
Maps for inclusions in book reports	18
Miscellaneous (including maps for other agencies)	214
Total	6,356

In addition, six issues of the "Earthquake Information Bulletin," 176 technical book reports, and 338 leaflets and maps of flood-prone areas were published.

At the beginning of fiscal year 1980, more than 103.8 million copies of maps and 1.9 million copies of book reports were on hand in the USGS distribution centers. During the year, 9,806,694 copies of maps, including 469,798 index maps, were distributed. Approximately 6.9 million maps were sold, and $5,913,758 was deposited to Miscellaneous Receipts in the U.S. Treasury.

The USGS also distributed 368,555 copies of technical book reports, without charge and for official use, and 1,319,115 copies of booklets, free of charge, chiefly to the general public; 360,000 copies of the monthly publications announcements and 500,000 copies of a sheet showing topographic map symbols were sent out.

The following table compares USGS map and book distribution (including map indexes and booklets, but excluding map-symbol sheets and monthly announcements) during fiscal years 1979 and 1980:

Number of maps and books distributed

Publication	Fiscal year 1979	Fiscal year 1980	Change (percent)
Maps	9,800,625	9,806,694	0.001
Books	351,901	436,817	24.1
Popular publications	1,375,943	1,319,115	−4.1
Total	11,528,469	11,562,626	0.3

HOW TO OBTAIN PUBLICATIONS

OVER THE COUNTER

Book reports

Book reports (professional papers, bulletins, water-supply papers, "Topographic Instructions," "Techniques of Water-Resources Investigations," and some miscellaneous reports) can be purchased from the *Branch of Distribution, U.S. Geological Survey, 604 South Pickett Street, Alexandria, VA 22304*, and from the USGS Public Inquiries Offices listed below under "Maps and Charts" (authorized agents of the Superintendent of Documents).

Some book publications that can no longer be obtained from the Superintendent of Documents are available for purchase from authorized agents of the Superintendent of Documents.

Maps and charts

Maps and charts can be purchased at the following USGS offices:

Branch of Distribution:

1200 South Eads St.,
Arlington, Va.

Building 41, Federal Center,
Denver, Colo.

Alaska Distribution Section:

Federal Bldg.,
101 Twelfth Ave.,
Fairbanks, Alaska

National Cartographic Information Center:

1400 Independence Rd.,
Rolla, Mo.

Public Inquiries Offices:

Rm. 108, Skyline Bldg.,
508 2d Ave.,
Anchorage, Alaska

Rm. 7638, Federal Bldg.,
300 North Los Angeles St.,
Los Angeles, Calif.

Rm. 122, Bldg. 3,
345 Middlefield Rd.,
Menlo Park, Calif.

Rm. 504, Customhouse,
555 Battery St.,
San Francisco, Calif.

Rm. 169, Federal Bldg.,
1961 Stout St.,
Denver, Colo.

Rm. 1028, General Services Bldg.,
19th and F Sts., NW.,
Washington, D.C.

Rm. 1C45, Federal Bldg.,
1100 Commerce St.,
Dallas, Tex.

Rm. 8105, Federal Bldg.,
125 South State St.,
Salt Lake City, Utah

Rm. 1C402, National Center,
12201 Sunrise Valley Dr.,
Reston, Va.

Rm. 678, U.S. Courthouse,
West 920 Riverside Ave.,
Spokane, Wash.

USGS maps are also sold by some 1,750 commercial dealers throughout the United States. Prices charged are generally higher than those charged by USGS offices.

Indexes showing topographic maps published for each State, Puerto Rico, the U.S. Virgin Islands, Guam, American Samoa, and Antarctica are available free on request. Publication of revised indexes to topographic mapping is announced in the monthly "New Publications of the Geological Survey." Each index also lists special and U.S. maps, as well as USGS offices and commercial dealers from which maps can be purchased.

Maps, charts, folios, and atlases that are out of print can no longer be obtained from any official source. They may be consulted at many libraries, and some can be purchased from second-hand book dealers.

BY MAIL

Book reports

Technical book reports and some miscellaneous reports can be ordered from the *Branch of Distribution,*

U.S. Geological Survey, 604 South Pickett Street, Alexandria, VA 22304. Prepayment is required and should be made by check or money order in U.S. funds payable to the U.S. Geological Survey. Postage stamps are not accepted; please do not send cash. On orders of 100 copies or more of the same report sent to the same address, a 25-percent discount is allowed. Circulars, publications of general interest (such as leaflets, pamphlets, and booklets), and some miscellaneous reports can be obtained free from the Branch of Distribution.

Maps and charts

Maps and charts, including folios and hydrologic atlases, are sold by the USGS. Address orders for maps of areas east of the Mississippi River, including Minnesota, Puerto Rico, and the U.S. Virgin Islands, to *Branch of Distribution, U.S. Geological Survey, 1200 South Eads Street, Arlington VA 22202,* and for maps of areas west of the Mississippi River, including Alaska, Hawaii, Louisiana, Guam, and American Samoa, to *Branch of Distribution, U.S. Geological Survey, Box 25286, Federal Center, Denver, CO 80225.* Residents of Alaska also may order maps of their State from the *Alaska Distribution Section, U.S. Geological Survey, Federal Building-Box 12, 101 Twelfth Avenue, Fairbanks, AK 99701.*

Prepayment is required. Remittances should be by check or money order in U.S. funds payable to the U.S. Geological Survey. On an order amounting to $300 or more at the list price, a 30-percent discount is allowed. Prices are quoted in lists of publications and in indexes to topographic mapping for individual States. Prices include the cost of surface transportation.

Earthquake Information Bulletin

Subscriptions to the "Earthquake Information Bulletin" and the "Preliminary Determination of Epicenters" are by application to the *Superintendent of Documents, Government Printing Office, Washington, DC 20402.* Payment is by check payable to the Superintendent of Documents or by charge to your deposit account number. Single issues can be purchased from the *Branch of Distribution, U.S. Geological Survey, 604 South Pickett Street, Alexandria, VA 22304.*

National Technical Information Service

Some USGS reports, including computer programs, data and information supplemental to map or book publications, and data files, are released through the National Technical Information Service (NTIS). These reports, available either in paper copies or microfiche or sometimes on magnetic tapes, can be purchased only from the *National Technical Information Service, U.S. Department of Commerce, Springfield, VA 22161.* USGS reports that are released through NTIS, together with their NTIS order numbers and prices, are announced in the monthly "New Publications of the Geological Survey."

REFERENCES CITED

Abel, K. D., Himmelberg, G. R., and Ford, A. B., 1979, Petrologic studies of the Dufek intrusion—Plagioclase variation: Antarctic Jour. United States, v. 14, no. 5, p. 19–21.

Ahlbrandt, T. S., Huffman, A. C., Jr., Fox, J. E., and Pasternack, Ira, 1979, Depositional framework and reservoir-quality studies of selected Nanushuk Group outcrops, North Slope, Alaska, *in* Ahlbrandt, T. S., ed., Preliminary geologic, petrologic, and paleontologic results of the study of Nanushuk Group rocks, North Slope, Alaska: U.S. Geol. Survey Circ. 794, 163 p.

Alden, W. C., 1953, Physiography and glacial geology of western Montana and adjacent areas: U.S. Geol. Survey Prof. Paper 231, 200 p.

Allen, H. E., Jr., and Bejcek, R. M., 1979, Effects of urbanization on the magnitude and frequency of floods in northeastern Illinois: U.S. Geol. Survey Water-Resources Inv. 79–36, 48 p.

Alley, W. M., and Veenhuis, J. E., 1979, Determination of basin characteristics for an urban distributed routing rainfall-runoff model, *in* Stormwater Management Model (SWMM) User's Group Meeting, May 24–25, 1979, Proceedings: U.S. Environmental Protection Agency Rept. EPA–600/9–70–026, p. 1–27.

Allmendinger, R. W., Oriel, S. S., and Platt, L. B., 1979, Younger-over-older thrust plates in southeastern Idaho, pt. 2 *of* Preliminary dynamic analysis: Geol. Soc. America, Abs. with Programs, v. 11, no. 6, 265 p.

American Geological Institute, 1972, Glossary of Geology, *with a* Forward by Ian Campbell, Gary, Margaret, McAfee, Robert, Jr., and Wolf, C. L., eds.: American Geol. Inst., Washington, D.C. 805 p.

Anders, E., and Owen, T., 1977, Mars and Earth: Origin and abundance of volatiles: Science 198, p. 453–465.

Anderson, A. L., 1939, Geology and ore deposits of the Atlanta district, Elmore County, Idaho: Idaho Bureau Mines and Geol. Pamph., 49 p.

———1947, Geology and ore deposits of the Boise Basin, Idaho: U.S. Geol. Survey Bull. 944–C, p. 141–144.

Anderson, J. R., Hardy, E. E., Roach, J. T., and Witmer, R. E., 1976, A land use and land cover classification system for use with remote sensor data: U.S. Geol. Survey Prof. Paper 964, 28 p.

Anderson, W. L., 1979, Numerical integration of related Hankel transforms of orders 0 and 1 by adaptive digital filtering: Geophysics, v. 44, no. 7, p. 1287–1305.

Armstrong, R. L., 1975, The geochronometry of Idaho: Isochron/West, no. 14, p. 50.

Aronson, D. A., 1980, The Meadowbrook artificial recharge project in Nassau County, Long Island, New York: Long Island Water Resources Bull. 14, 23 p.

Bachman, G. O., Baltz, E. H., and Griggs, R. L., 1957, Reconnaissance of geology and uranium occurrences of the upper Alamosa Creek Valley, Catron County, New Mexico: U.S. Geol. Survey Trace Elements Inv. Rept. 521, 39 p.

Baird, A. K., Baird, K. W., and Welday, E. E., 1979, Batholithic rocks of the northern Peninsular and Transverse Ranges, southern California, *in* Abbott, P. L., and Todd, V. R., eds., Mesozoic crystalline rocks: Dept. Geol. Sci., San Diego State Univ., p. 111–132.

Baker, V. R., 1978, A preliminary assessment of the fluid erosional processes that shaped the martian outflow channels: Proc. Lunar and Planet. Sci. Conf., 9th, p. 3205–3223.

Bakun, W. H., and McEvilly, T. V., 1979, Earthquakes near Parkfield: Comparing the 1934 and 1966 sequences: Science, v. 205, no. 4413, p. 1375–1377.

Barraclough, J. T., 1980, Geohydrology of the Eastern Snake River Plain, Idaho, as shown by a two-mile-deep well [abs.]: EOS, Am. Geophs. Union Trans., v. 61, no. 6, p. 70.

Barrett, J. K., Pearl, R. H., and Pennington, A. J., 1976, Map showing thermal springs, wells, and heat-flow contours in Colorado: Colorado Geol. Survey Inf. Ser. 4, scale 1:1,000,000.

Barrett, L. P., 1952, Iron formation sampling, Marquette Range, Michigan: U.S. Atomic Energy Comm. RMO 886, 13 p.

Basu, A. R., and Tatsumoto, Mitsonobu, 1979, Samarium-neodymium systematics in kimberlites and in the minerals of garnet lherzolite inclusions: Science, v. 205, p. 398–401.

Bayley, R. W., 1968 (1969), Geologic map of the Bradley Peak quadrangle, Carbon County, Wyoming: U.S. Geol. Survey Geol. Quad. Map GQ–773, scale 1:24,000.

Beck, M. E., Jr., Ford, A. B., and Boyd, W. W., Jr., 1968, Paleomagnetism of a stratiform intrusion in the Pensacola Mountains, Antarctica: Nature, v. 217, no. 5128, p. 534–535.

Behrendt, J. C., Drewry, David, Jankowski, Edward, and England, A. W., 1979a, Aeromagnetic and radar ice sounding data indicates substantially greater area for Dufek intrusion in Antarctica: EOS, Am. Geophys. Union Trans., v. 60, 18, p. 245.

———1979b, Aeromagnetic and radar ice sounding survey of the Dufek intrusion, Antarctica: Geol. Soc. America, Abs. with Programs, v. 11, 7, p. 386.

Berg, H. C., 1979a, The significance of geotectonics in the metallogenesis and resource appraisal of southeastern Alaska—a progress report [abs.]: Alaska Geol. Soc. Symposium on "Alaska's mineral and energy resources, economics, and land status: Anchorage," April 1979, Program and Abs., p. 42–43.

———1979b, Significance of geotectonics in the metallogenesis and resource appraisal of southeastern Alaska, a progress report, *in* Johnson, K. M., and Williams, J. R., eds., The United States Geol. Survey in Alaska: Accomplishments during 1978: U.S. Geol. Survey Cir. 804–B, p. B116.

Berg, H. C., Jones, D. L., and Coney, P. J., 1978, Map showing pre-Cenozoic tectonostratigraphic terranes of southeastern Alaska and adjacent areas: U.S. Geol. Survey Open-File Rept. 78–1985, 2 sheets, scale 1:1,000,000.

Bergin, M. J., 1957, Maybell-Lay area, Moffat County, Colorado, *in* Geologic investigations of radioactive deposits, semiannual progress report, December 1, 1956, to May 31, 1957: U.S. Geol. Survey TEI–690, p. 280–291.

Bergquist, J. R., 1979, Reconnaissance geologic map of the Blue Jay Peak quadrangle, Graham County, Arizona: U.S. Geol. Survey Misc. Field Studies Map MF–1083, scale 1:24,000.

Beyer, L. A., 1979, Borehole gravity study of the density and porosity of selected Frontier, Tensleep, and Madison reservoirs in the Bighorn Basin, Wyoming [abs.]: Am. Assoc. Petroleum Geologists Bull., v. 63, no. 5, p. 822.

Beyer, L. A., and Isaacs, C. M., 1979, Porosity of Miocene siliceous shale in California [abs.]: Soc. of Petroleum Engineers (AIME) Annual California Regional Meeting, 49th, Program, April 18–20, 1979, Ventura, Calif.

Billings, M. P., 1956, The geology of New Hampshire, Part II, Bedrock geology: Concord, N.H., New Hampshire State Planning and Development Comm., 203 p.

Bird, K. J., and Andrews, Jack, 1979, Subsurface studies of the Nanushuk Group, North Slope, Alaska, *in* Ahlbrandt, T. S., ed., Preliminary geologic, petrologic, and paleontologic results of the study of Nanushuk Group rocks, North Slope, Alaska: U.S. Geol. Survey Circ. 794, p. 32–41.

Bischoff, J. L., 1980, Geothermal system at 21° N., East Pacific Rise: Physical limits on geothermal fluid and role of adiabatic expansion: Science, vol. 207, p. 1465–1469.

Blacet, P. M., and Miller, S. T., 1978, Reconnaissance geologic map of the Jackson Mountain quadrangle, Graham County, Arizona: U.S. Geol. Survey Misc. Field Studies Map MF–939, scale 1:62,500.

Blair, M. L., and Spangle, W. E., 1979, Seismic safety and land-use planning—selected examples from California: U.S. Geol. Survey Prof. Paper 941–B, 82 p.

Bloom, A. L., Broecker, W. S., Chappel, J. M. A., Mathews, R. K., and Mesolella, K. J., 1974, Quaternary sea level fluctuations on a tectonic coast—new $^{230}Th/^{234}U$ dates from the Huon Peninsula, New Guinea: Quaternary Research, v. 4, no. 2, p. 185–205.

Boer, de, Jelle, and Snider, F. G., 1979, Magnetic and chemical variations of Mesozoic diabase dikes from eastern North America: Evidence for a hotspot in the Carolinas?: Geol. Soc. America Bull., Pt. 1, v. 90, p. 185–198.

Bohman, L. R., and Scott, J. C., 1980a, Hurricane Frederic tidal floods of September 12–13, 1979, along the gulf coast, Kreole–Grand Bay SW quadrangles, Mississippi: U.S. Geol. Survey Hydrol. Inv. Atlas HA–621.

———1980b, Hurricane Frederic tidal floods of September 12–13, 1979, along the gulf coast, Grand Bay quadrangle, Alabama: U.S. Geol. Survey Hydrol. Inv. Atlas HA–622.

———1980c, Hurricane Frederic tidal floods of September 12–13, 1979, along the gulf coast, Chickasaw quadrangle, Alabama: U.S. Geol. Survey Hydrol. Inv. Atlas HA–623.

———1980d, Hurricane Frederic tidal floods of September 12–13, 1979, along the gulf coast, Mobile quadrangle, Alabama: U.S. Geol. Survey Hydrol. Inv. Atlas HA–624.

———1980e, Hurricane Frederic tidal floods of September 12–13, 1979, along the gulf coast, Hollingers Island–Theodore quadrangles, Alabama: U.S. Geol. Survey Hydrol. Inv. Atlas HA–625.

———1980f, Hurricane Frederic tidal floods of September 12–13, 1979, along the gulf coast, Coden–Bellefontaine quadrangles, Alabama: U.S. Geol. Survey Hydrol. Inv. Atlas HA–626.

———1980g, Hurricane Frederic tidal floods of September 12–13, 1979, along the gulf coast, Heron Bay–Little Dauphin Island–Fort Morgan–Fort Morgan NW quadrangles, Alabama: U.S. Geol. Survey Hydrol. Inv. Atlas HA–627.

———1980h, Hurricane Frederic tidal floods of September 12–13, 1979, along the gulf coast, The Basin–Bay Minette North–Creola NE quadrangles, Alabama: U.S. Geol. Survey Hydrol. Inv. Atlas HA–628.

Bonilla, M. G., 1979, Historic surface faulting—map patterns, relation to subsurface faulting, and relation to preexisting faults, *in* Conference IX, 1–5 April, 1979, Analysis of actual fault zones in bedrock: U.S. Geol. Survey Open-File, Rept. 79–1239, p. 36–65.

Booth, J. S., and Sangrey, D. A., 1979, Mass movement potential of recent sediments on the United States continental margins: Geol. Soc. America 1979 Ann. Meeting, Abs. with Programs, vol. 11, no. 7, p. 391.

Borcherdt, R. D., ed., 1975, Studies for seismic zonation of the San Francisco Bay region: U.S. Geol. Survey Prof. Paper 941–A, 102 p.

Bourland, W. G., and Glover, Lynn, III, 1976, Tectogenesis and metamorphism of the Piedmont from Columbia to Westview, Virginia, along the James River: Blacksburg, Va., prepared for U.S. Nuclear Regulatory Commission, 111 p.

Boyer, S. J., 1979, Glacial geologic observations in the Dufek Massif and Forrestal Range: Antarctic Jour. United States, v. 14, no. 5, p. 46–48.

Bradley, W. H., 1936, Geomorphology of the north flank of the Uinta Mountains: U.S. Geol. Survey Prof. Paper 185–I, p. 163–199.

Brew, D. A., and Ford, A. B., 1978, Megalineament in southeastern Alaska marks southwest edge of Coast Range batholithic complex: Canadian Jour. Earth Sci., v. 15, no. 11, p. 1763–1772.

Brew, D. A., Ford, A. B., Grybeck, D. J., Johnson, B. R., and Nutt, C. J., 1976, Key foliated quartz diorite sill along southwest side of Coast Range Complex, northern southeastern Alaska, *in* Cobb, E. H., ed., U.S. Geol. Survey in Alaska: Accomplishments during 1975: U.S. Geol. Survey Circ. 733, p. 60.

Broecker, W. S., and Kaufman, Aaron, 1965, Radiocarbon chronology of Lake Lahontan and Lake Bonneville II, Great Basin: Geol. Soc. America Bull., v. 76, p. 537–566.

Broecker, W. S., and Orr, P. C., 1958, Radiocarbon chronology of Lake Lahontan and Lake Bonneville: Geol. Soc. America Bull., v. 69, p. 1009–1032.

Brown, C. E., 1973, Northeast-trending faults in Grenville series, New York: U.S. Geol. Survey Prof. Paper 850, p. 35–36.

Browne, P. R. L., and Ellis, A. J., 1970, The Ohaki-Broadlands hydrothermal area, New Zealand: Mineralogy and related geochemistry: Am. Jour. Sci., v. 269, p. 97–131.

Bucknam, R. C., and Anderson, R. E., 1979, Estimation of fault-scarp ages from a scarp-height—slope-angle relationship: Geology, v. 7, p. 11–14.

Buie, B. F., Hetrick, J. H., Patterson, S. H., and Neeley, C. L., 1979, Geology and industrial mineral resources of the Macon-Gordon kaolin district: U.S. Geol. Survey Open-File Rept. 79–526, 36 p.

Bukry, J. D., 1971, Cenozoic calcareous nannofossils from the Pacific Ocean: San Diego Soc. Nat. Hist. Trans., v. 16, p. 303–327.

Burchett, C. R., and Hollyday, E. F., 1974, Tennessee's newest aquifer: Geol. Soc. America, Abs. with Programs, v. 6, no. 4, p. 338.

Burchfiel, B. C., Fleck, R. J., Secor, D. T., Vincelette, R. R., and Davis, G. A., 1974, Geology of the Spring Mountains, Nevada: Geol. Soc. America Bull., v. 85, no. 7, p. 1013–1022.

Campbell, W. J., 1979, Sea-ice studies, *in* Geological Survey Research 1979: U.S. Geol. Survey Prof. Paper 1150, p. 230–231.

Campbell, W. J., Cheney, R. E., Marsh, J. G., and Nognard, N. M., 1980, Ocean eddy structure by satellite radar altimetry required for iceberg towing: Cold Regions Sci. and Tech., no. 1 (1980), p. 211–221.

Campbell, W. J., Gloersen, Per, Zwally, H. J., Ramseier, R. O., and Elachi, Charles, 1980, Simultaneous passive and active microwave observations of near-shore Beaufort Sea ice: Annual Offshore Technology Conference, 9th, Houston, Texas, May 2–5, 1977, Proceedings, p. 287–294.

Campbell, W. J., Ramseier, R. O., Zwally, H. J., and Gloersen, Per, 1980, Arctic sea ice variations from time-lapse microwave imagery: Boundary Layer Meteorology, v. 18, p. 99–106.

Carey, W. P., 1979, Sediment characteristic of the New River, Tennessee, *in* Proceedings Symposium on Surface Mining Hydrology, Sedimentology and Reclamation: Univ. Kentucky Bull. 119, p. 197–202.

Carr, W. J., 1974, Summary of tectonic and structural evidence for stress orientation at the Nevada Test Site: U.S. Geol. Survey Open-File Rept. 74-176, 53 p.

Carter, Virginia, and Gammon, P. T., 1976, Great Dismal Swamp vegetative cover map: U.S. Geol. Survey Open-File Rept. 76-615, 1 figure.

Cecil, C. B., Renton, J. J., Stanton, R. W., and Dulong, F. T., 1979, Some geologic factors controlling mineral matter in coal, *in* Donaldson, A. C., Presley, M. W., and Renton, J. J., eds., Carboniferous coal short course and guidebook: West Virginia Univ. Geol. and Geog. Dept., p. 227-238.

Cecil, C. B., Renton, J. J., Stanton, R. W., and Finkelman, R. B., 1979, Mineral matter in coals of the central Appalachian Basin [abs.]: Internat. Cong. Carboniferous Stratigraphy and Geology, 9th., Abs., p. 32.

Chao, E. C. T., Minkin, J. A., and Thompson, C. L., 1979, Application of automatic image analysis to coal petrography: Internat. Cong. Carboniferous Stratigraphy and Geology, 9th, Abs., p. 34.

Chapin, C. E., Osburn, G. R., Hook, S. C., Massingill, G. L., and Frost, S. J., 1979, Coal, uranium, oil, and gas potential of the Riley-Puertocito area, Socorro County, New Mexico: New Mexico Bur. Mines and Mineral Resources, Technical Report, March 1979, 33 p.

Chapman, R. M., Yeend, W. E., and Patton, W. W., Jr., 1975, Preliminary reconnaissance geologic map of the western half of Kantishna River quadrangle, Alaska: U.S. Geol. Survey Open-File Rept. 75-351, scale 1:250,000.

Chappel, B. W., and White, A. J. R., 1974, two contrasting granite types: Pacific Geology, v. 8, p. 173-174.

Chieu, H. Y., and Collins, W. D., 1978, A spectroradiometer for airborne remote sensing: Photogramm. Eng. and Remote Sensing, v. 44, no. 4, p. 507-517.

Childs, J. R., Cooper, A. K., and Parker, A. W., 1979, Sonobuoy studies of Umnak Plateau, Bering Sea: EOS, Am. Geophys. Union Trans., v. 60, no. 18, p. 390.

Clark, M. M., Grantz, Arthur, and Rubin, Meyer, 1972, Holocene activity of the Coyote Creek fault as recorded in sediments of Lake Cahuilla, *in* The Borrego Mountain earthquake of April 9, 1968: U.S. Geol. Survey Prof. Paper 787, p. 112-130.

Coats, R. R., Consul, Jerry, and Neil, S. T., 1979, Massive zunyite rock from western Elko County, Nevada: U.S. Geol. Survey Open-file Rept. 79-764, 7 p.

Cobb, E. H., 1978, Summary of references to mineral occurrences (other than mineral fuels and construction materials) in the Healy quadrangle, Alaska: U.S. Geol. Survey Open-File Rept. 78-1062, 112 p.

———1979a, Summary of references to mineral occurrences (other than mineral fuels and construction materials) in the Mount Hayes quadrangle, Alaska: U.S. Geol. Survey Open-File Rept. 79-238, 140 p.

———1979b, Summary of references to mineral occurrences (other than mineral fuels and construction materials) in the Afognak, Karluk, Kodiak, and Trinity Islands quadrangles, Alaska: U.S. Geol. Survey Open-File Rept. 79-860, 47 p.

———1979c, Summary of references to mineral occurrences (other than mineral fuels and construction materials) in the Cordova quadrangle, Alaska: U.S. Geol. Survey Open-File Rept. 79-973, 74 p.

———1979d, Summary of references to mineral occurrences (other than mineral fuels and construction materials) in the Anchorage quadrangle, Alaska: U.S. Geol. Survey Open-File Rept. 79-1095. 183 p.

———1979e, Summary of references to mineral occurrences (other than mineral fuels and construction materials) in the Valdez quadrangle, Alaska: U.S. Geol. Survey Open-File Rept. 79-1241, 166 p.

———1979f, Summary of references to mineral occurrences (other than mineral fuels and construction materials) in the Bering Glacier, Icy Bay, Middleton Island, and Yakutat quadrangles, Alaska: U.S. Geol. Survey Open-File Rept. 79-1246, 40 p.

———1979g, Summary of references to mineral occurrences (other than mineral fuels and construction materials) in the Gulkana quadrangle, Alaska: U.S. Geol. Survey Open-File Rept. 79-1247. 36 p.

Collins, H. R., 1979, Devonian bentonites in eastern Ohio: Am. Assoc. Petroleum Geologists Bull., v. 63, no. 4, p. 655-660.

Colvocoresses, A. P., 1978, Landsat 3 return beam vidicon (RBV) imagery: U.S. Geol. Survey Open-File Rept. 78-507 (EC-62-Landsat), 3 p.

Cook, H. E., 1979, Small-scale submarine slides on intercanyon continental slope areas, Paleozoic, Nevada [abs.]: Geol. Soc. America, v. 11, p. 405.

Cooper, A. K., Childs, J. R., Scholl, D. W., Marlow, M. S., and Gardner, J. V., 1979a, Evolution of Umnak Plateau, Bering Sea: EOS, Am. Geophys. Union Trans., v. 60, no. 18, p. 390.

Cooper, A. K., Marlow, M. S., Parker, A. W., and Childs, J. R., 1979b (1980), Structure-contour map on acoustic basement in the Bering Sea: U.S. Geol. Survey Misc. Field Studies Map MF-1165, scale 1:2,500,000.

Council on Environmental Quality, 1979, Environmental Statistics 1978: Council on Environmental Quality, 264 p.

Cowardin, L. M., Carter, Virginia, Golet, F. C., and LaRoe, E. T., 1979, Classification of wetlands and deep-water habitats of the United States: U.S. Fish and Wildlife Service Rept. FWS/OBS-79/31, 103 p.

Crittenden, M. D., Jr., 1951, Geology of the San Jose-Mount Hamilton area, California: California Dept. Nat. Resources, Div. Mines Bull. 157, 74 p.

Csejtey, Bela, Jr., 1979, Regional significance of tectonics of the Talkeetna Mountains, south-central Alaska, *in* Johnson, K. M., and Williams, J. R., eds., The U.S. Geological Survey in Alaska: Accomplishments during 1978: U.S. Geol. Survey Circ. 804-B, p. B90.

Csejtey, Bela, Jr., Nelson, W. H., Jones, D. L., Silberling, N. J., Dean, R. M., Morris, M. S., Lanphere, M. A., Smith, J. G., and Silberman, M. L., 1978, Reconnaissance geologic map and geochronology, Talkeetna Mountains quadrangle, north part of Anchorage quadrangle, and southwest corner of Healy quadrangle, Alaska: U.S. Geol. Survey Open-File Rept. 78-558-A, 60 p.

Daniel, C. C., III, Wilder, H. B., and Weiner, M. S., 1979, Water quality of the French Broad River, North Carolina-an analysis of data collected at Marshall, 1958-77: U.S. Geol. Survey Water Resources Inv. 79-87, 53 p.

Davis, G. A., Anderson, J. L., Frost, E. G., and Shackelford, T. J., 1979, Regional Miocene detachment faulting and early Tertiary(?) mylonitization, Whipple-Buckskin-Rawhide Mountains, southeastern California and western Arizona: San Diego State Univ. guidebook of geological excursions in the southern California area, Geol. Soc. America Ann. Meeting, papers and field trip roadlogs, p. 75-108.

Davis, R. W., and Matthews, E. W., 1980, Chloroform contamination in part of the alluvial aquifer, southwest Louisville, Kentucky: U.S. Geol. Survey Open-File Rept. 80-219, 34 p.

Dean, W. E., Thiede, Jörn, and Claypool, G. E., 1979, Origin of organic-rich limestones of mid-Cretaceous age, Mid-Pacific Mountains and southern Hess Rise, central Pacific Ocean [abs.]: Geol. Soc. America, Abs. with Programs, v. 11, no. 7, p. 411.

Deiss, C. F., 1939, Cambrian stratigraphy and trilobites of northwestern Montana: Geol. Soc. America, Spec. Paper 18, 135 p.

DePaulo, D. J., and Wasserburg, G. J., 1979, Sm-Nd age of the Stillwater complex and the mantle evolution curve for neodymium: Geochim. et Cosmochimic. Acta 43, p. 999–1008.

Dethier, D. P., Heller, P. L., and Safioles, S. A., 1979, Reconnaissance data on lakes in the Alpine Lakes Wilderness Area: U.S. Geol. Survey Open-File Rept. 79–1465, 199 p.

Detterman, R. L., Miller, T. P., Yount, M. E., and Wilson, F. H., 1979, Generalized geologic map of Chignik and Sutwik Island quadrangles, Alaska: U.S. Geol. Survey Misc. Field Study Map MF–1053–A, scale 1:250,000.

De Voto, R. H., 1978, Uranium geology and exploration: Colorado School of Mines, Golden, Colorado, 396 p.

Dibblee, T. W. J., and Chesterman, C. W., 1953, Geology of the Breckenridge Mountain quadrangle, California: California Dept. Nat. Resources, Div. Mines Bull. 168, 56 p.

Dickson, F. W., 1964, Solubility of cinnabar in Na_2S solutions at 50–250° and 1–1,800 bars with geologic applications: Econ. Geology, v. 59, p. 625–635.

Diem, K. L., and Kennington, G. S., 1979, Rhyolite radionuclide uptake by selected plant species and pocket gophers in Yellowstone National Park: Conference on Scientific Research in the National Parks, 1st, Proceedings, p. 301–305.

Dieterich, J. H., 1979, Modeling of rock friction, pt. 1, experimental results and constitutive equations: Jour. Geophys. Research, v. 84, p. 2161–2168.

Dolan, Robert, Lins, Harry, and Stewart, John, 1980, Geographical analysis of Fenwick Island, Maryland, a middle Atlantic coast barrier island: U.S. Geol. Survey Prof. Paper 1177–A, 24 p.

Donovan, T. J., Forgey, R. L., and Roberts, A. A., 1979, Aeromagnetic detection of diagenetic magnetite over oil fields: Am. Assoc. of Petroleum Geologists Bull., v. 63, no. 2, p. 245–248.

Dover, J. H., 1969, Bedrock geology of the Pioneer Mountains, Blaine and Custer Counties, central Idaho: Idaho Bur. Mines and Geology Pamph. 142, 61 p.

Dover, J. H., Hall, W. E., Hobbs, S. W., Tschanz, C. M., Batchelder, J. N., and Simons, F. S., 1976, Geologic map of the Pioneer Mountains region, Blaine and Custer Counties, Idaho: U.S. Geol. Survey Open-File Rept. 76–75, scale 1:62,000.

Drake, A. A., Jr., 1980, The Serra De Caldas window, Goias: U.S. Geol. Survey Prof. Paper 1119–A, p. A1–A11.

Drake, A. A., Jr., and Morgan, B. A., III, 1980, Precambrian plate tectonics in the Brazilian Shield—evidence from the Pre-Minas rocks of the Quadrilatero Ferrifero, Minas Gerais: U.S. Geol. Survey Prof. Paper 1119–B, p. B1–B19.

Dunrud, C. R., and Osterwald, F. W., 1978, Effects of coal mine subsidence in the western Powder River Basin, Wyoming: U.S. Geol. Survey Open-File Rept. 78–473, p. 59–67.

———1980, Effects of coal mine subsidence in the Sheridan, Wyoming area: U.S. Geol. Survey Prof. Paper 1164, 49 p.

Durham, D. L., 1979, Preliminary map of uranium occurrences in the Temblor Range, Kern and San Luis Obispo Counties, California: U.S. Geol. Survey Misc. Field Studies Map MF–1047, scale 1:24,000.

Dutro, J. T., Jr., and Jones, D. L., 1979, Paleotectonic setting of the Carboniferous in Alaska [abs.]: Internat. Cong. Carboniferous Stratigraphy and Geology, 9th, Urbana, Illinois, 1979, Abs., p. 58–59.

Eaton, J. P., O'Neill, N. E., and Murdock, J. H., 1970, Aftershocks of the 1966 Parkfield-Cholame, California, earthquake: A detailed study: Seismol. Soc. America Bull., v. 60, p. 1151–1197.

Ellis, S. R., and Alley, W. M., 1979, Quantity and quality of urban runoff from three localities in the Denver metropolitan area, Colorado: U.S. Geol. Survey Water-Resources Inv. 79–64, 60 p.

Emmons, W. H., and Calkins, F. C., 1913, Geology and ore deposits of the Philipsburg quadrangle, Montana: U.S. Geol. Survey Prof. Paper 78, 271 p.

Englund, K. J., 1971, Displacement of the Pocahontas Formation by the Russell Fork fault, southwest Virginia: U.S. Geol. Survey Prof. Paper 750–B, p. B13–B16.

Epstein, A. G., Epstein, J. B., and Harris, L. D., 1977, Conodont color alteration—an index to organic metamorphism: U.S. Geol. Survey Prof. Paper 995, 27 p.

Erdman, J. A., Ebens, R. J., and Case, A. A., 1978, Molybdenosis: A potential problem in ruminants grazing on coal mine spoils: Jour. Range Management, v. 31, no. 1, p. 34–36.

Evans, J. R., and Iyer, H. M., 1979, Deep structure under Yellowstone and the eastern Snake River Plain from teleseismic P-wave delays [abs.]: Am. Geophys. Union Trans., v. 60, p. 942.

Fickies, R. H., Fakundiny, R. H., and Mosley, E. T., 1979, Geotechnical analysis of soil samples from test trench at Western New York Nuclear Services Center, West Valley, New York: Washington, D.C., U.S. Nuclear Regulatory Commission Rept. NUREG/CR–0644, 21 p.

Fishman, M. J., and Pyen, G. S., 1979, Determination of selected anions in water by ion-chromatography: U.S. Geol. Survey Water-Resources Inv. 79–101, 30 p.

Fishman, M. J., and Skougstad, M. W., 1963, Indirect spectrophotometric determination of traces of bromide in water: Anal. Chemistry, v. 35, p. 146.

Fitterman, D. V., and Corwin, R. F., 1979, Inversion of self-potential data from Cerro Prieto geothermal field, Mexico [abs.]: Geophysics, v. 45, no. 4, p. 588.

Flaxman, E. M., 1972, Predicting sediment yield in the Western United States: American Society of Civil Engineers, Journal of Hydraulics Div., Proceedings, v. 98, no. HY12, p. 2073–2085.

Fleck, R. J., Anderson, J. J., and Rowley, P. D., 1975, Chronology of mid-Tertiary volcanism in High Plateaus region of Utah, *in* Anderson, J. J., Rowley, P. D., Fleck, R. J., and Nairn, A. E. M., Cenozoic geology of southwestern High Plateaus of Utah: Geol. Soc. America Spec. Paper 160, p. 53–62.

Ford, A. B., 1970, Development of the layered series and capping granophyre of the Dufek intrusion of Antarctica, *in* Bushveld igneous complex and other layered intrusions—a symposium: Geol. Soc. South Africa Spec. Pub. 1, p. 492–510.

Ford, A. B., Reynolds, R. L., Huie, Carl, and Boyer, S. J., 1979, Geological field investigation of the Dufek intrusion: Antarctic Jour. United States, v. 14, no. 5, p. 9–11.

Foster, R. J., 1960, Tertiary geology of a portion of the central Cascade Mountains, Washington: Geol. Soc. America Bull., v. 71, p. 99–126.

Franklin, M. A., and Bohman, L. R., 1980, Hurricane Frederic tidal floods of September 12–13, 1979, along the gulf coast, West Pensacola quadrangle, Florida: U.S. Geol. Survey Hydrol. Inv. Atlas HA–639.

———1980, Hurricane Frederic tidal floods of September 12–13, 1979, along the gulf coast, Oriole Beach–Garcon Point–Holley–South of Holley–Navarre quadrangles, Florida: U.S. Geol. Survey Hydrol. Inv. Atlas HA–641.

Franklin, M. A., and Scott, J. C., 1980, Hurricane Frederic tidal floods of September 12–13, 1979, along the gulf coast, Gulf Breeze–Fort Barrancas quadrangles, Florida: U.S. Geol. Survey Hydrol. Inv. Atlas HA–640.

Frenguelli, Joaquin, 1940, Consideraciones sobre los silicoflagelados fosiles: Museo La Plata Revista, Paleontologia, v. 2, no. 7, p. 37–112.

Futa, K., Hedge, C. E., Hearn, B. C., Jr., and Donnelly, J. M., 1981, Strontium isotopes in the Clear Lake Volcanics, Clear Lake Area, California: U.S. Geol. Survey Prof. Paper 1141, ch. 4, p. 61–66.

Galpin, S. L., 1915, A preliminary report on the feldspar and mica deposits of Georgia: Georgia Geol. Survey Bull. 30, 190 p.

Gammon, P. T., and Carter, Virginia, 1979, Vegetation mapping with seasonal color infrared photographs: Photogramm. Eng. and Remote Sensing, v. 45, no. 1, p. 87–97.

Ganapathy, Ramachandran, and Anders, Edward, 1974, Bulk compositions of the Moon and Earth, estimated from meteorites: Lunar Sci. Conference, 5th, Proceedings, p. 1181–1206.

Gartner, Stefan, and Bukry, J. D., 1975, Morphology and phylogeny of the coccolithophycean family Ceratolithaceae: U.S. Geol. Survey Jour. Research, v. 3, p. 451–465.

Gaydos, Leonard, and Newland, W. L., 1978, Inventory of land use and land cover of the Puget Sound region using Landsat digital data: U.S. Geol. Survey Jour. Research, v. 6, no. 6, p. 807–814.

Gaydos, Leonard, and Wray, J. R., 1978a, Land cover map from Landsat, 1973, with place names, Washington urban area, D.C., Md., and Va.: U.S. Geol. Survey Misc. Inv. Map I–858–E, scale 1:100,000.

———1978b, Land cover from Landsat, 1973, with census tracts, Washington urban area, D.C., Md., and Va.: U.S. Geol. Survey Misc. Inv. Map I–858–F, scale 1:100,000.

Gilliom, R. J., 1980, Estimation of background loadings and concentrations of phosphorus for lakes in the Puget Sound region, Washington: U.S. Geol. Survey Open-File Rept. 80–328, 37 p.

Goldhaber, M. B., and Reynolds, R. L., 1979, Origin of marcasite and its implications regarding the genesis of roll-front uranium deposits: U.S. Geol. Survey Open-File Rept. 79–1696, 38 p.

Gottfried, David, Annell, C. S., and Schwarz, L. J., 1977, Geochemistry of subsurface basalt from the deep corehole (Clubhouse Crossroads Corehole 1) near Charleston, South Carolina–magma type and tectonic implications, *in* Rankin, D. W., ed., Studies related to the Charleston, South Carolina, earthquake of 1886–a preliminary report: U.S. Geol. Survey Prof. Paper 1028, p. 91–113.

Gough, L. P., and Erdman, J. A., 1980, Seasonal differences in the element content of Wyoming big sagebrush: Jour. Range Manage., v. 33, 24 p.

Gough, L. P., and Severson, R. C., 1980, Element content of *Atriplex canescens* under natural conditions in northwest New Mexico, and when grown on mine-reclaimed land at natural conditions in northwest New Mexico, and when grown on mine-reclaimed land at the San Juan Coal Mine [abs.]: Am. Assoc. Adv. Sci. National Meeting, 146th, San Francisco, California, Jan. 3–8, 1980, Abs., p. 119–120.

Greeley, Ronald, 1977, Basaltic "plains" volcanism, *in* Greeley, Ronald, and King, J. S., eds., Volcanism of the eastern Snake River Plain, Idaho: NASA Rept. CR–154621, p. 25, 44.

Green, M. W., 1975, Paleodepositional units in Upper Jurassic rocks in the Gallup-Laguna uranium area, New Mexico: U.S. Geol. Survey Open-File Rept. 75–610, 13 p.

Greene, G. M., 1980, Testing an urban climate simulator: U.S. Geol. Survey Prof. Paper 1099–E, 17 p.

Griggs, R. L., 1954, A reconnaissance for uranium in New Mexico, 1953: U.S. Geol. Survey Circ. 354, 9 p.

Grow, J. A., Klitgord, Kim, Schlee, J. S., and Mattick, R. E., 1980, The ocean-continent transition zone off southern New Jersey [abs.]: Geophysics, v. 45, no. 4, p. 575.

Haas, J. L., Jr., Robinson, G. R., Jr., and Hemingway, B. S., 1979, Thermodynamic data for CaO-Al_2O_3-SiO_2-H_2O system [abs.]: EOS Am. Geophys. Union. Trans., v. 60, p. 968.

Hall, J. M., and Ryall, P. J. C., 1977, Paleomagnetism of basement rocks, Leg 37: Deep Sea Drilling Project, Initial Reports, v. 37, p. 425–445.

Hall, W. E., Batchelder, J. N., and Douglass, R. C., 1974, Stratigraphic section of the Wood River Formation, Blaine County, Idaho: U.S. Geol. Survey Jour. Research, v. 2, no. 1, p. 89–95.

Hanson, A. M., 1952, Cambrian stratigraphy in southwestern Montana: Montana Bur. Mines and Geology Mem. 33, 46 p.

Harned, D. A., 1980, Water quality of the Neuse River, North Carolina–variability, pollution loads, and long-term trends: U.S. Geol. Survey Water Resources Inv. 80–36, 88 p.

Harrill, J. R., and Katzer, Terry, 1980, General ground-water map 3AF: Reno, Nevada, Bur. Mines and Geology Envir. Ser., Las Vegas SE quadrangle, scale 1:24,000.

Hatcher, P. G., Rowan, R., and Mattingly, G. A., 1980, ^{1}H and ^{13}C NMR of marine humic acids: Org. Geochem. v. 2, p. 77–85.

Hatcher, P. G., VanderHart, D. L., and Earl, N. L., 1980, Use of solid-state ^{13}C NMR in structural studies of humic acids and humin from Holocene sediments: Org. Geochem., v. 2, p. 87–92.

Hatcher, R. D., 1978, Tectonics of the western Piedmont and Blue Ridge, southern Appalachians, review and speculation: Am. Jour. Sci., v. 278, p. 276–304.

Haushild, W. L., 1979, Estimation of floods of various frequencies for the small ephemeral streams in eastern Washington: U.S. Geol. Survey Open-File Rept. 79–80, 22 p.

Hearn, B. C., Jr., 1979, Preliminary map of diatremes and alkalic ultramafic intrusion in the Missouri River Breaks and vicinity, north-central Montana: U.S. Geol. Survey Open-File Rept. 79–1128, 1 over-size sheet.

Hearn, B. C., Jr., Donnelly, J. M., and Goff, F. E., 1981, The Clear Lake Volcanics, California: Tectonic setting and magma sources: U.S. Geol. Survey Prof. Paper 1141, ch. 2, p. 25–45.

Hekinian, R., Fevrier, M., Bischoff, J. L., Picot, P., and Shanks, W. C., 1980, Sulfide deposits from the East Pacific Rise near 21° N.: Science, v. 207, p. 1433–1444.

Helley, E. J., Lajoie, K. R., Spangle, W. E., and Blair, J. L., 1979, Flatlands deposits of the San Francisco Bay region, California–their geology and engineering properties and their importance to comprehensive planning; selected examples from the San Francisco Bay region, California: U.S. Geol. Survey Prof. Paper 943, 88 p.

Henderson, R. G., and Allingham, J. W., 1964, The magnetization of an inhomogenous laccolith calculated on a digital computer, *in* Computers in the mineral industries, pt. 2: Stanford Univ. Pubs. Geol. Sci., v. 9, no. 2, p. 481–497.

Hennen, R. V., 1914, Kanawha County: West Virginia Geol. Survey, p. 26–28.

Henry, T. W., and Sutherland, P. K., 1977, Guidebook for field trips for Second North American Paleontological Convention, Lawrence, Kansas, *in* Sutherland, P. K., and Manger, W. L., eds., Upper Chesterian-Morrowan stratigraphy and the Mississippian-Pennsylvanian boundary in northeastern Oklahoma and northwestern Arkansas: North American Paleontology Convention, 2d, Lawrence, Kansas, 1977, Guidebook 18, Oklahoma Geol. Survey, p. 107–115.

Herrmann, R. B., 1979, Surface wave focal mechanisms for eastern North American earthquakes with tectonic implications: Jour. of Geophys. Research, v. 84, no. 137, p. 3543–3552.

Herrmann, R. B., and Canas, J. A., 1978, Focal mechanism studies in the New Madrid seismic zone: Seismol. Soc. America Bull., v. 68, no. 4, p. 1095–1102.

Hicks, S. D., and Shofnos, William., 1965, The determination of land emergence from sea level observations in southeastern Alaska: Jour. Geophys. Research, v. 70, no. 14, p. 3315–3320.

Higgins, M. W., 1976, Age, origin, regional relations and nomenclature of the Glenarm Series, central Appalachian Piedmont: A reinterpretation: Reply: Geol. Soc. America Bull., v. 87, p. 1523–1528.

Higgins, M. W., Sinha, A. K., Zartman, R. E., and Kirk, W. S., 1977, Problems with interpretation of zircon "ages" from the central Appalachian Piedmont: A possible case of inherited radiogenic lead: Geol. Soc. America Bull., v. 88, p. 125–132.

Hildenbrand, T. G., Kane, M. F., and Hendricks, J. D., 1979, Structural control of upper Mississippi embayment seismicity inferred from analysis of aeromagnetic and gravity data: Geol. Soc. America, Abs. with Programs, v. 11, no. 2, p. 149.

Hillhouse, J. W., 1977, Paelomagnetism of the Triassic Nikolai Greenstone, McCarthy quadrangle, Alaska: Canadian Jour. Earth Sci., v. 14, no. 11, p. 2578–2592.

Holdaway, M. J., 1972, Thermal stability of Al-Fe epidote as a function of f_{O_2} and Fe content: Contr. to Mineralogy and Petrology, v. 37, p. 307–340.

Hosman, R. L., Long, A. T., Lambert, T. W., and others, 1968, Tertiary aquifers in the Mississippi embayment: U.S. Geol. Survey Prof. Paper 448–D, 29 p.

Irwin, W. P., 1977, Review of Paleozoic rocks of the Klamath Mountains, *in* Paleozoic paleography of the Western United States, Pacific Coast Symposium 1: Soc. Econ. Paleontologists and Mineralogists, p. 441–454.

Isaacs, C. M., 1979, Lateral diagenesis in Monterey Shale, Santa Barbara coast, California [abs.]: Am. Assoc. Petroleum Geologists Bull., v. 63, no. 3, p. 473.

Isherwood, W. F., 1976, Gravity and magnetic studies of The Geysers–Clear Lake geothermal region, California: United Nations Symposium on the Development and Use of Geothermal Resources, 2d, San Francisco, 1975, Proceedings, v. 2, p. 1065–1073.

Iwahashi, Toru, and Heironimus, T. L., 1978, map showing Landsat imagery alinements in Fairfax County, Virginia: U.S. Geol. Survey Open-File Rept. 78–525, scale 1:48,000.

Iwatsubo, E. Y., and Mortensen, C. E., 1979, Short-term tilt anomalies preceding three local earthquakes near San Jose, California: EOS, Am. Geophys. Union Trans. v. 60, no. 18, p. 319.

Iyer, H. M., Oppenheimer, D. H., and Hitchcock, Tim, 1979, Abnormal P-wave delays in The Geysers–Clear Lake geothermal area, California: Science, v. 204, p. 495–497.

James, O. B., and McGee, J. J., 1979, Consortium breccia 73225: Genesis and history of two coarse-grained "norite" clasts: Lunar and Planet. Sci. Conference, 10th, Proceedings, p. 713–744.

James, R. V., and Rubin, Jacob, 1979, Applicability of the local equilibrium assumption to transport through soils of solutes affected by ion exchange, *in* Jenne, E. A., ed., Chemical modeling in aqueous systems: Am. Chem. Soc. Symposium Ser., p. 225–235.

Jennings, C. W., 1977, Geologic map of California: California Div. Mines and Geology, scale 1:750,000.

Jobson, H. E., 1980, A practical Lagrangian transport model: U.S. Geol. Survey Open-File Rept. 80–206, 31 p.

Johnson, C. E., 1979, II. Seismotectonics of the Imperial Valley of Southern California: California Inst. Tech. Ph. D. thesis, 334 p.

Johnson, F. A., 1977, A reconnaissance of the hydrology of the Intracoastal Waterway from Bucksport to Little River Inlet, South Carolina: South Carolina Water Resources Comm. Rept., no. 7, 33 p.

Johnston, P. M., 1960, Ground-water supplies in shale and sandstone in Fairfax, Loudoun, and Prince William Counties, Virginia: U.S. Geol. Survey Circ. 424, 7 p.

Johnston, R. H., and Van Driel, J. N., 1979, Evaluation of potential yield of water wells in bedrock aquifers of Fairfax County, Virginia: U.S. Geol. Survey Open-File Rept. 79–525, scale 1:48,000.

Jones, D. L., Silberling, N. J., and Hillhouse, J. W., 1977, Wrangellia–a displaced terrane in northwestern North America: Canadian Jour. Earth Sci., v. 14, p. 2565–2577.

Kane, J. S., 1979, Determination of nanogram amounts of bismuth in rocks by atomic absorption spectrometry with electrothermal atomization: Anal. Chim. Acta, v. 106, p. 325–331.

Karkowski, Lukasy, Kozlowski, Andrezej, and Roedder, Edwin, 1979, Gas-liquid inclusions in minerals of ores of zinc and lead ores from the Silesia-Crakow region [Poland], *in* Research on the genesis of zinc-lead deposits of Upper Silesia, Poland: Prace Instytutu Geologicznego, v. 95, p. 87–94.

Katz, B. G., 1979, Background organic-chemical quality of a sole-source aquifer intended for artificial recharge on Long Island, New York [abs.]: Am. Geophys. Union Trans., v. 60, no. 46, p. 826.

Kauffman, M. E., 1965, Cambrian stratigraphy in the Drummond-Garnet Range area: Billings Geol. Soc. Guidebook 16, p. 79–88.

Kay, C. A., 1964, Outline of Pleistocene geology of Martha's Vineyard, Massachusetts: U.S. Geol. Survey Prof. Paper 501–C, p. C134–C139.

Keller, G. V., Grose, L. T., and Crewdson, R. A., 1978, Speculations on nature of geothermal energy in Basin and Range province of western United States: Colorado School of Mines Quart., v. 73, no. 4, p. 71–76.

Kent, K. M., 1973, A method for estimating volume and rate of runoff in small watersheds: U.S. Dept. Agriculture, Soil Conserv. Serv. Tech. Paper 149, 19 p. and Appendix.

Kieffer, S. W., 1977a, Sound speed in liquid-gas mixtures: Water-air and water-steam: Jour. Geophys. Research, v. 82, p. 2895–2904.

———1977b, Fluid dynamics during eruption of water-steam and magma-gas systems: Geysers, maars, and diatremes: International Kimberlite Conference, 2d, Santa Fe, New Mexico, Abs.

———1979a, Thermodynamics and lattice vibrations of minerals: 1. Mineral heat capacities and their relationships to simple lattice vibrational models: Reviews of Geophysics, v. 17, p. 1–19.

———1979b, Thermodynamics and lattice vibrations of minerals: 2. Vibrational characteristics of silicates: Reviews of Geophysics, v. 17, p. 20–34.

———1979c, Thermodynamics and lattice vibrations of minerals: 3. Lattice dynamics and an approximation for minerals with application to simple substances and framework silicates: Reviews of Geophysics, v. 17, p. 35–59.

———1979d, The sound speed of multiphase mixtures: a parameter of importance in dynamic volcanism: Hawaii Symposium on Intraplate Volcanism and Submarine Volcanism, sponsored by LAVCEI, Hilo, Hawaii, Abs. volume, p. 167.

———1979e, The Ngauruhoe "Flashing Arc" eruptions of 1974 and 1975: A multiphase fluid flow model: EOS, Am. Geophys. Union Trans., v. 60, p. 413.

Kieffer, S. W., and Delaney, J. M., 1979, Isentropic decompression of fluids from crustal and mantle pressures: Jour. Geophys. Research, v. 84, no. B4, p. 1611–1620.

Kiilsgaard, T. H., Freeman, V. L., and Coffman, J. S., 1970, Mineral Resources of the Sawtooth Primitive Area, Idaho: U.S. Geol. Survey Bull. 1319–D, p. D1–D147.

Kimrey, J. O. 1978, Preliminary appraisal of the geohydrologic aspects of drainage wells, Orlando area, central Florida: U.S. Geol. Survey Water-Resources Inv. 78–37, 24 p.

Kirby, S. H., 1980, Tectonic stresses in the lithosphere: Constraints provided by the experimental deformation of rocks: Jour. of Geophys. Research, v. 85, p. 6353–6363.

Kirby, S. H., and Veyssiere, Patrick, 1979, Plastic deformation of MgO (Al_2O_3), spinal at $0.28T_m$: Preliminary results: Philosophical Mag., v. A41, p. 129–136.

Kleinkopf, M. D., and Mudge, Melville, 1972, Aeromagnetic, Bouguer gravity, and generalized geologic studies of the Great Falls–Mission Range area, northwestern Montana: U.S. Geol. Survey Prof. Paper 726–A, 19 p.

Klovan, J. E., and Imbrie, John, An algorithm and FORTRAN IV program for large-scale *Q*-mode factor analysis and calculation of factor scores: Jour. Internat. Assoc. Math. Geology, v. 3, no. 1, p. 61–77.

Knepper, D. H., Jr., 1978, Analysis of linear features, Rio Grande Rift zone, central New Mexico, *in* Conference Proceedings, 1978, International Symposium on the Rio Grande Rift, Santa Fe, New Mexico [abs.]: Los Alamos Scientific Laboratory Report LA–7487–C, Los Alamos, New Mexico, p. 48–49.

Kockelman, W. J., 1979, Use of U.S. Geological Survey earth-science products by selected regional agencies in the San Francisco Bay region, California: U.S. Geol. Survey Open-File Rept. 79–221, 173 p.

———1980, Examples of the use of earth-science information by decisionmakers in the San Francisco Bay region, California: U.S. Geol. Survey Open-File Rept. 80–124, 88 p.

Kockelman, W. J., and Brabb, E. E., 1979, Examples of seismic zonation in the San Francisco Bay region, *in* Brabb, E. E., ed., 1979, Progress on seismic zonation in the San Francisco Bay region: U.S. Geol. Survey Circ. 807, p. 73–84.

Krauskopf, K. B., 1951, Physical chemistry of quicksilver transportation in vein fluids: Econ. Geology, v. 46, p. 498–523.

Kunosz, I. A., 1976, Lithium resources—prospects for the future, *in* Vine, J. D., ed., Lithium resources and requirements by the year 2000: U.S. Geol. Survey Prof. Paper 1005, p. 26–30.

Lachenbruch, A. H., and Sass, J. H., 1979, Heat flow and stress in the San Andreas fault zone [abs.]: EOS, Am. Geophys. Union Trans., v. 60, no. 46, p. 955.

Lachenbruch, A. H., Sass, J. H., and Galanis, S. P., Jr., 1978, New heat-flow results from southern California [abs.]: EOS, Am. Geophys. Union Trans., v. 59, no. 12, p. 1051.

Laird, R. T., Perkins, J. B. Bainbridge, D. A. Baker, J. B., Boyd, R. T., Huntsman, Daniel, Staub, P. E., and Zucker, M. B., 1979, Quantitative land capability analysis—selected examples from the San Francisco Bay region, California: U.S. Geol. Survey Prof. Paper 945, 115 p.

Landa, E., 1979, Isolation of uranium mill tailings and their component radionuclides from the biosphere—some earth science perspectives: U.S. Geol. Survey Circ. 814, 32 p.

Lanfear, K. J., Nakassis, Anastase, Samuels, W. B., and Schoen, C. T., 1979, An oilspill risk analysis for the northern Gulf of Alaska (proposed sale 55) Outer Continental Shelf lease area: U.S. Geol. Survey Open-File Rept. 79–1284, 79 p.

Law, B. E., Spencer, C. W., and Bostick, N. H., 1980, Evaluation of organic matter, subsurface temperature, and pressure with regard to gas generation in low-permeability Upper Cretaceous and lower Tertiary strata in the Pacific Creek area, Sublette and Sweetwater Counties, Wyoming: Mountain Geologist, v. 17, no. 2, p. 23–35.

Leavy, B. D., 1979, Tectonic and sedimentary structures along the eastern margin of the Culpeper Basin, Virginia [abs.]: SE section, Geol. Soc. Am.

Leberl, Franz, Bryan, M. L., Elachi, Charles, Farr, Thomas, and Campbell, W. J., 1979, Mapping of sea ice and measurement of its drift using aircraft synthetic aperture radar images: Jour. Geophys. Research, v. 84, no. C4, p. 1827–1835.

Lee, D. E., and Van Loenen, R. E., 1970, Biotites from hybrid granitoid rocks of the southern Snake Range, Nevada, *in* Geological Survey Research 1970: U.S. Geol. Survey Prof. Paper 700–D, p. D196–D206.

———1979, Accessory opaque oxides from hybrid granitoid rocks of the southern Snake Range, Nevada: U.S. Geol. Survey Open-File Rept. 79–1608, 14 p.

Lee, F. T., Miller, D. R., and Nichols, T. C., Jr., 1979, The relation of stresses in granite and gneiss near Mount Waldo, Maine, to structure, topography, and rockbursts: U.S. Symposium on Rock Mechanics, 20th, Austin, Texas, p. 663–674.

Leenheer, J. A., 1979, Assessment of various solutes as tracers to determine ground-water migration of retort water produced by in situ oil shale processing [abs.]: 1979 Am. Soc. Testing Materials Symposium on Waste waters from Synthetic Fuel Production, Pittsburgh, Pennsylvania, June 1979.

Lesure, F. G., Force, E. R., Windolf, J. F., and Hill, J. J., 1977, Mineral resources of the Joyce Kilmer–Slickrock Wilderness, North Carolina–Tennessee: U.S. Geol. Survey Bull. 1416, 89 p.

Libby, W. F., 1955, Radiocarbon dating: Chicago University Press, 125 p.

Ling, C. H., Rasmussen, L. A., and Campbell, W. J., 1978, Flight path curvature distortion in side-looking airborne radar imagery: Photogramm. Eng. and Remote Sensing, v. 44, no. 10, p. 1255–1260.

———1980, A continuum sea ice model for a global climate model; sea ice processes and models: AIDJEX Symposium, University of Washington Press, Sept. 6–9, 1977, Proceedings, p. 187–196.

Liou, J. G., 1973, Synthesis and stability relations of epidote, $Ca_2Al_2FeSi_3O_{12}(OH)$: Jour. Petrology, v. 14, p. 381–413.

Liscum, Fred, and Massey, B. C., 1980, Technique for estimating the magnitude and frequency of floods in the Houston, Texas, metropolitan area: U.S. Geol. Survey Water-Resources Inv. 80–17, 42 p.

Lohman, S. W., 1972, Ground water hydraulics: U.S. Geol. Survey Prof. Paper 708, p. 34–38.

Longwell, C. R., 1949, Structure of the northern Muddy Mountain area, Nevada: Geol. Soc. America Bull., v. 60, no. 5, p. 923–967.

———1974, Measure and date of movement on Las Vegas Valley shear zone, Clark County, Nevada: Geol. Soc. America Bull., v. 85, no. 6, p. 985–990.

Loutit, T. S., and Kennett, J. P., 1979, Application of carbon isotope stratigraphy to late Miocene shallow marine sediments, New Zealand: Science, v. 204, no. 4398, p. 1196–1199.

Love, J. D., Antweiler, J. C., and Williams, F. E., 1975, Mineral resources of the Teton Corridor, Teton County, Wyoming: U.S. Geol. Survey Bull. 1397-A, 51 p.

Ludwig, K. R., Naesser, C. W., and Nash, J. T., 1978, Uranium-lead ages of uranium ores from the Midnite mine, Washington [abs.]: Geol. Assoc. Canada, Abs. with Programs, v. 3, p. 448.

Lund, E. H., 1956, Igneous and metamorphic rocks of the Minnesota River Valley: Geol. Soc. America Bull., v. 67, no. 11, p. 1475–1490.

Lyons, J. B., and Livingston, D. E., 1977, Rb-Sr age of the New Hampshire plutonic series: Geol. Soc. America Bull., v. 88, p. 1808–1812.

Lyons, P. C., and Chase, H. B., Jr., 1979, Compilation of proximate and ultimate analyses of coal, impure coal, and carbonaceous mudrock (Pennsylvanian) from Massachusetts and Rhode Island: U.S. Geol. Survey Open-File rept. 79-1242, 11 p., 3 sheets.

Lystrom, D. J., 1979, U.S. Geological Survey-U.S. Environmental Protection Agency urban studies program: Regional Conference on Urban Storm Water Management, Water Resources Research Institute, Univ. of North Carolina, Raleigh, North Carolina, April 10–11, 1979, Proceedings, p. 170–179.

McCauley, J. F., Breed, C. S., Grolier, M. J., Whitney, M. I., Ward, A. W., and Greeley, Ronald, 1979, Wind tunnel simulation studies of airflow patterns around pitted and fluted ventifacts from the Western Desert of Egypt [abs.]: U.S. National Aeronautics and Space Administration Rept. TM 80339, p. 288–289.

McElhinny, M. W., 1973, Paleomagnetism and plate tectonics: Cambridge University Press, Cambridge, 358 p.

McGetchin, T. R., and Smyth, J. R., 1978, The mantle of Mars: Some possible geological implications of its high density: Icarus 34, p. 512–536.

McGlennon, J. A. S., and Marcus, P. A., 1980a, Conflict management of ORV events in the California Desert: A case study: Am. Arbitration Assoc., February 1980, Interim Report, 26 p.

———1980b, Recommendation in the preparation of the final plan for the California Desert: Am. Arbitration Assoc., March 1980, 31 p.

McIntyre, D. H., and Hobbs, S. W., 1978, Geologic map of the Challis quadrangle, Custer County, Idaho, U.S. Geol. Survey Open-File Rept. 78-1059, scale 1:62,500.

McKavanagh, B., and Stacey, F. D., 1974, Mechanical hysteresis in rocks at low strain amplitudes and seismic frequencies: Physics of the Earth and Planetary Interiors, v. 8, p. 246–250.

MacKevett, E. M., Jr., Albert, N. R. D., Barnes, D. F., Case, J. E., Robinson, Keith, and Singer, D. A., 1977, The Alaska Mineral Resources Assessment Program: Background information to accompany folio of geologic and mineral resource maps of the McCarthy quadrangle, Alaska: U.S. Geol. Survey Circ. 739, 23 p.

Maclay, R. W., and Small, T. A., 1976, Progress report on geology of the Edwards aquifer, San Antonio area, Texas, and preliminary interpretation of borehole geophysical and laboratory data on carbonate rocks: U.S. Geol. Survey Open-File Rept. 76–627, 65 p.

Marlow, M. S., Cooper, A. K., Parker, A. W., and Childs, J. R., 1979, (1980), Isopach map of strata above acoustic basement in the Bering Sea: U.S. Geol. Survey Misc. Field Studies Map MF-1164, scale 1:2,500,000.

Marmo, Vladi, 1959, On the TiO_2 content of magnetites as a petrogenic hint: Am. Jour. Sci., v. 257, no. 2, p. 144–149.

Mase, C. W., Galanis, S. P., Jr., and Munroe, R. J., 1979, Near-surface heat flow in Saline Valley, California: U.S. Geol. Survey Open-File Rept. 79-1136, scale 1:125,000.

May, P. R., 1971, Pattern of Triassic-Jurassic diabase dikes around the North Atlantic in the context of predrift position of the continents: Geol. Soc. America Bull., v. 82, p. 1285–1292.

Mayfield, C. F., Curtis, S. M., Ellersieck, I. F., and Tailleur, I. L., 1979, Reconnaissance geology of the Ginny Creek zinc-lead-silver and Nimiuktuk barite deposits, northwestern Brooks Range, Alaska: U.S. Geol. Survey Open-File Rept. 79-1092, 20 p., 2 plates.

Mead, R. A., and Gammon, P. T., 1979, A practical and easily implemented method for mapping wetlands using small format aerial photography, *in* Biennial color aerial photography workshop, 7th, California, 1979, Proceedings: Am. Soc. of Photogramm., p. 53–62.

Meissner, C. R., Jr., and Miller, R. L., 1979, Geologic map of the Honaker quadrangle, Russell, Tazewell, and Buchanan Counties, Virginia: U.S. Geol. Survey Geol. Open-File Rept. 79-528, 34 p., 4 pl., scale 1:24,000.

Menzie, W. D., and Foster, H. L., 1978, Metalliferous and selected nonmetalliferous mineral resource potential in the Big Delta quadrangle, Alaska: U.S. Geol. Survey Open-File Rept. 78-529-D, 62 p., 1 pl., scale 1:250,000.

Meyer, C. E., and Hemley, J. J., 1967, Wall rock alteration, *in* Barnes, H. L., ed., Geochemistry of hydrothermal ore deposits: New York, N.Y., Holt, Rinehart, and Winston, 670 p.

Meyer, William, and Tucci, Patrick, 1978, Effects of seepage from fly-ash setting ponds and construction dewatering on groundwater levels in the Cowles Unit, Indiana Dunes National Lakeshore, Indiana: U.S. Geol. Survey Water-Resources Inv. 78-138, 95 p.

Miesch, A. T., 1976, *Q*-mode factor analysis of geochemical and petrologic data matrices with constant row-sums: U.S. Geol. Survey Prof. Paper 574-G, 47 p.

Miesch, A. T., and Reed, B. L., 1979, Compositional structures in two batholiths of circumpacific North America: U.S. Geol. Survey Prof. Paper 574-H, 31 p.

Milazzo, V. A., 1980, Alternative considerations in updating USGS land use and land cover maps: U.S. Geological Survey Circ. 826, 19 p.

Milici, R. C., Briggs, Garrett, Knox, L. M., Sitterly, P. D., and Statler, A. T., 1979, The Mississippian and Pennsylvanian (carboniferous) Systems in the United States–Tennessee: U.S. Geol. Survey Prof. Paper 1110-G, 38 p.

Miller, G. H., Andrews, J. T., and Short, S. K., 1977, The last interglacial-glacial cycle, Clyde foreland, Baffin Island, N.W.T.: Stratigraphy, biostratigraphy, and chronology: Canadian Jour. Earth Sciences, v. 14, p. 2824–2857.

Miller, J. A., 1979, Potential subsurface zones for liquid-waste storage in Florida: Florida Bur. Geol. Map Series 94, 1 sheet, scale 1:1,800,000.

Minster, J. F., and Allegre, C. J., 1978, ^{87}Rb-^{87} Sr dating of L and LL chondrites: Effect of shock and brecciation: Meteoritics 13, p. 563–564.

Miser, H. D., 1922, Deposits of manganese ore in the Batesville district, Arkansas: U.S. Geol. Survey Bull. 734, 273 p.

Missouri River Basin Commission and U.S. Geological Survey, 1979a, Western Coal Planning Association Project–phase I Final Report: February 1979, 58 p.

———1979b, Western Coal Planning Association Project–fact Book for Western Coal/Energy Development: January 1979, 526 p.

———1979c, Western Coal Planning Assistance Project–a Guide to Methods for Impact, Assessment of Western coal/energy development: January 1979, 292 p.

———1979d, Western Coal Planning Association Project–forecasts for Western Coal/Energy Development: January 1979, 135 p.

———1979e, Western Coal Planning Association project—source book for western coal/energy development: January 1979, 236 p.

Mixon, R. B., and Newell, W. L., 1977, Stafford fault system: Structures documenting Cretaceous and Tertiary deformation along the Fall Line in northeastern Virginia: Geology, v. 5, p. 437–440.

Moran, M. S., 1977, The Fort Payne Formation and differential aquifer development along the eastern Highland Rim, central Tennessee: Vanderbilt University, Master's thesis (unpub.), 125 p.

Morey, G. B., and Sims, P. K., 1976, Boundary between two Precambrian W terranes in Minnesota and its geologic significance: Geol. oc. America Bull., v. 87, p. 141–152.

Morgan, J. W., and Anders, Edward, 1979, Chemical composition of Mars: Geochim. et Cosmochim. Acta, v. 43, p. 1601–1610.

Morgan, J. W., Hertogen, Jan, and Anders, Edward, 1978, The Moon: Composition determined by nebular processes: The Moon and Planets, v. 18, p. 465–478.

Morgan, J. W., and Wandless, G. A., 1979, Terrestrial upper mantle: Siderophile and volatile trace-element abundances: Lunar and Planetary Science X, pt. 2, p. 855–857.

Mortensen, C. E., Lee, R. C., and Burford, R. O., 1977, Observations of creep-related tilt, strain, and water-level changes on the central San Andreas fault: Bull. Seismol. Soc. Amer., v. 67, no. 3, p. 641–649.

Mower, R. W., Hood, J. W., Cushman, R. L., Barton, R. L., and Galloway, S. E., 1964, An appraisal of potential ground-water salvage along the Pecos River between Acme and Artesia, New Mexico: U.S. Geol. Survey Water-Supply Paper 1659, 98 p.

Muffler, L. J., 1966, Stratigraphy of the Keku Islets and neighboring parts of Kuiu and Kupreanof Islands, southeastern Alaska: U.S. Geol. Survey Bull. 1241-C, 52 p.

Muir, K. S., and Johnson, M. J., 1979, Classification of ground-water recharge potential in three parts of Santa Cruz County, California: U.S. Geol. Survey Open-File Rept. 79–1065, 1 over-sized sheet.

Mullineaux, D. R., Bonilla, M. G., and Schlocker, Julius, 1967, Relation of building damage to geology in Seattle, Washington, during the April 1965 earthquake: U.S. Geol. Survey Prof. Paper 575-D, p. D183–D191.

Murray, C. R., and Reeves, E. B., 1977, Estimated use of water in the United States in 1975: U.S. Geol. Survey Circ. 765, 39 p.

Murthy, V. R., and Hall, H. T., 1970, The chemical composition of the Earth's core: Possibility of sulfur in the core: Physics of the Earth and Planetary Interiors v. 2, p. 276–282.

Myers, A. T., and Hamilton, J. C., 1961, Rhenium in plant samples from the Colorado Plateau, *in* Geological Survey Research 1961: U.S. Geol. Survey Prof. Paper 424-B, p. B286–B288.

Myers, P. E., 1969, The geology of the Harpster quadrangle and vicinity, Idaho: Dissertation Abstracts, section B, v. 30, no. 1, p. 261.

Myette, C. F., 1980, Hydrologic budget for Eagle Lake near Willmar, Minnesota: U.S. Geol. Survey Open-File Rept. 80–163, 13 p.

Naldrett, A. J., 1969, A portion of the system Fe-S-O between 900 and 1,080°C and its application to sulfide ore magmas: Jour. Petrology, v. 10, p. 171–201.

Naney, M. T., 1977, Phase equilibria and crystallization in iron- and magnesium-bearing granitic systems: Stanford University, Ph.D. thesis (unpub.), 229 p.

Nash, J. T., 1979, Geology, petrology, and chemistry of Leadville Dolomite: Host for uranium at the Pitch mine, Saguache County, Colorado: U.S. Geol. Survey Open-File Rept. 79–1566, 51 p.

Nash, J. T., and Ludwig, K. R., 1979, Limitations on genesis of uranium ores, Midnite mine, Washington, based on lead-uranium ages: U.S. Geol. Survey Open-File Rept. 79–1178, 7 p.

Nathenson, Manuel, Urban, T. C., and Diment, W. H., 1979, Approximate solution for the temperature distribution caused by flow up a fault and its application to temperatures measured in a drillhole at Raft River geothermal area, Cassia County, Idaho: Geothermal Resources Council, Trans., v. 3 p. 477–480.

Neuschel, S. K., 1970, Correlations of aeromagnetics and aeroradioactivity with lithology in the Spotsylvania area, Virginia: Geol. Soc. America Bull., v. 71, p. 3575–3582.

Nicholas, F. W., and Lewis, J. E., Jr., 1980, Relationships between aerodynamic roughness and land use and land cover in Baltimore, Maryland: U.S. Geol. Survey Prof. Paper 1099-C, 36 p.

Nilsen, T. H., 1977, Paleography of Mississippian turbidites in south-central Idaho, *in* Stewart, J. H., Stevens, C. H., and Fritsche, A. E., eds., Paleozoic paleogeography of the Western United States: Soc. Econ. Paleontologists and Mineralogists, Pacific Section, Pacific Coast Paleogeography Symposium, 1st, p. 275–299.

Nilsen, T. H., Wright, R. H., Vlasic, T. C., and Spangle, W. E., 1979, Relative slope stability and land-use planning—selected examples from the San Francisco Bay Region, California: U.S. Geol. Survey Prof. Paper 944, 96 p.

Nolan, T. B., 1933, Epithermal precious-metal deposits, *in* Ore deposits of the Western States, Lindgren Volume: Am. Inst. of Mining and Metall. Eng., p. 623–640.

Normark, W. R., 1976, Delineation of the main extrusion zone of the East Pacific Rise at lat 21° N.: Geology, vol. 4, p. 681–685.

Norton, G. H., 1956, Evidence of unconformity in rocks of Carboniferous age in central Montana, *in* Billings Geological Society, Guidebook, Annual Field Conference, 7th, August 1956, p. 52–66.

Nunes, P. D., and Tilton, G. R., 1971, Uranium-lead ages of minerals from the Stillwater igneous complex and associated rocks, Montana, Geol. Soc. America Bull. 82, p. 2231–2250.

Oldale, R. N., Friedman, J. D., and Williams, R. S., Jr., 1971, Changes in coastal morphology of Monomoy Island, Cape Cod, Massachusetts, *in* Geological Survey Research 1971: U.S. Geol. Survey Prof. Paper 750-B, p. B101–107.

Olhoeft, G. R., 1979, Nonlinear electrical properties, *in* Neel, Louis, ed., Nonlinear behavior of molecules, atoms, and ions in electric, magnetic, or electromagnetic fields: Amsterdam, Elsevier Scientific Publishing Co., p. 395–410.

Oliver, W. A., Jr., Merriam, C. W., and Churkin, Michael, Jr., 1975, Ordovician, Silurian, and Devonian corals of Alaska: U.S. Geol. Survey Prof. Paper 823-B, p. 24.

Oriel, S. S., and Platt, L. B., 1979, Younger-over-older thrust plates in southeastern Idaho: Geol. Soc. America, Abs. with Programs, v. 11, no. 6, p. 298.

Page, N. J, 1977, Stillwater complex, Montana: Rock succession, metamorphism, and structure of the complex and adjacent rocks: U.S. Geol. Survey Prof. Paper 999, 79 p.

Parrett, Charles, Carlson, D. D., Craig, G. S., Jr., and Hull, J. A., 1978, Data for floods of May 1978 in northeastern Wyoming and southeastern Montana: U.S. Geol. Survey Open-File Rept. 78–985, 16 p.

Patchen, D. G., 1977, Subsurface stratigraphy and gas production of the Devonian shales in West Virginia: U.S. Department of Commerce National Technical Information Service Rept. MERC/CR-77/5, 35 p.

Patchen, D. G., Schwarz, K. A., DeBrosse, T. A., Bendler, E. P., Hermann, J. B., Diotrouwski, R. T., Cozart, C. L., and Kelly, W. W., Jr., 1979, Oil and gas developments in Maryland, Ohio, Pennsylvania, Virginia, and West Virginia in 1978: Am. Assoc. Petroleum Geologists Bull., v. 63, no. 8, p. 1244–1277.

Patton, W. W., Jr., and Matzko, J. J., 1959, Phosphate deposits in northern Alaska: U.S. Geol. Survey Prof. Paper 302-A, 17 p.

Pavich, M. J., and Markewich, H. W., 1979, Soil stratigraphy of fluvial terraces along the Potomac and Rappahannock Rivers, Virginia, [abs.]: Geol. Soc. America, v. 11, no. 4, p. 207.

Pavlides, Louis, 1973, Stratigraphic relationships and metamorphism in the Fredericksburg area, Va., *in* Geological Survey Research 1973: U.S. Geol. Survey Prof. Paper 850, p. 37–38.

———1976, Guidebook for field trips 1 and 4: Piedmont geology of the Fredericksburg, Va., area and vicinity: Geological Society of America, Northeast-Southeast Meeting, Arlington, Virginia, 44 p.

———1980, Revised nomenclature and stratigraphic relationships of the Fredericksburg Complex and the Quantico Formation of the Virginia Piedmont: U.S. Geol. Survey Prof. Paper 1146, 29 p.

Payne, G. A., 1979, Water-quality reconnaissance of lakes in Voyageurs National Park, Minnesota: U.S. Geol. Survey Open-File Rept. 79–556, 40 p.

Pease, R. W., Jenner, C. B., and Lewis, J. E., 1980, The impact of land use on climate: An analysis of the Washington-Baltimore area that couples remote sensing with numerical simulation: U.S. Geol. Survey Prof. Paper 1099–A, 39 p.

Peterman, Z. E., and Hildreth, R. A., 1978, Reconnaissance geology and geochronology of the Precambrian of the Granite Mountains, Wyoming: U.S. Geol. Survey Prof. Paper 2055, 22 p.

Péwé, T. L., Burbank, Lawrence, and Mayo, L. R., 1967, Multiple glaciation of the Yukon-Tanana Upland, Alaska: U.S. Geol. Survey Misc. Geol. Inv. Map I–507, scale 1:500,000.

Péwé, T. L., Wahrhaftig, Clyde, and Weber, F. R., 1966, Geologic map of the Fairbanks quadrangle, Alaska: U.S. Geol. Survey Misc. Geol. Inv. Map I–455, scale 1:250,000.

Pickering, S. M., Jr., 1976, Geologic map of Georgia: Georgia Geol. Survey, scale 1:500,000.

Pipiringos, G. N., 1966, Origin of elements associated with uranium in the Cave Hills area, Harding County, South Dakota: U.S. Geol. Survey Prof. Paper 476–B, p. B1–B75.

Pomeroy, J. S., 1979, Storm-induced landslides in the Johnstown area, Pennsylvania, July 19–20, 1977: Geol. Soc. America, Abs. with Programs, v. 11, no. 2, p. 49.

Potter, R. W., II, 1977, An electrochemical investigation of the system copper-sulfur: Econ. Geol. v. 72, p. 1524–1542.

Prudic, E. D., and Randall, A. D., 1977, Ground-water hydrology and subsurface migration of radioisotopes at a low-level solid radioactive-water disposal site, West Valley, New York: U.S. Geol. Survey Open-File Rept. 77–566, 28 p.

Prych, E. A., 1980, Perturbation solutions of water-table aquifers: Jour. Hydraulics Div., Am. Soc. Civil Engineers, v. 106, no. HY 4, p. 603–608.

Pryor, D. B., Coleman, J. M., and Garrison, L. E., 1979, Digitally acquired undistorted side-scan images of submarine landslides, Mississippi River Delta: Geology, vol. 7, no. 9, p. 423–425.

Ramspott, L. D., and Scholten, Robert, 1964, Early Paleozoic batholith in the Beaverhead Range, Idaho-Montana: Geol. Soc. America, Special Paper 82, p. 159–160.

Rankin, D. W., 1975, The continental margin of eastern North America in the southern Appalachians: The opening and closing of the proto-Atlantic Ocean: Am. Jour. Sci., v. 275a, p. 298–336.

Ratté, J. C., and Zartman, R. E., 1970, Bear Mountain gneiss dome, Black Hills, South Dakota: Age and structures: Geol. Soc. America, Abs. with Programs, v. 2, no. 5, p. 345.

Rawson, Jack, 1980, Source areas of salinity and trends of salt loads in streamflow in the upper Colorado River, Texas: U.S., Geol. Survey Open-File Rept. 80–224, 65 p.

Reid, R. R., 1963, Reconnaissance geology of the Sawtooth Range: Idaho Bur. Mines and Geol. pamph., 129 p.

Reid, R. R., Bittner, Enid, Greenwood, W. R., Ludington, Steve, Lund, Karen, Motzer, W. E., and Toth, Margo, 1979, Geologic section and road log across the Idaho batholith: Idaho Bur. Mines Geol. Circ. 34, 20 p.

Rice, J. R., and Simons, D. A., 1976, The stabilization of spreading shear faults by couple deformation–diffusion effects in fluid infiltrated porous materials: Jour. of Geophys., v. 81, p. 5322–5334.

Richards, P. W., 1979, Status of the Circum-Pacific Map Project: U.S. Geol. Survey Open-File Rept. 79–1561, 41 p.

Riggs, H. C., 1979, Characterizing streamflow droughts: International Symposium on Hydrological Aspects of Droughts, New Delhi, India, Dec. 3–7, Proceedings, 1979, 7 p.

Riley, G. H., 1970, Isotopic discrepancies in zoned pegmatites, Black Hills, South Dakota: Geochim. et Cosmochim. Acta, v. 34, p. 713–725.

Ringwood, A. E., 1977, Composition of the core and implications for origin of the Earth: Geochem. Jour., v. 11, p. 111–135.

RISE Project Group, 1980, East Pacific Rise: Hot springs and geophysical experiments: Science, vol. 207, p. 1421–1433.

Roberts, A. E., 1979, Analytical and stratigraphic data on the upper phosphatic mudstone member of the Santa Margarita Formation at Newsome Canyon, southern Cuyama Valley, California: U.S. Geol. Survey Open-File Rept. 79–1466, 64 p.

Robie, R. A., Hemingway, B. S., and Fisher, J. R., 1978, Thermodynamic properties of minerals and related substances at 298.15 K and 1 bar (10^5 pascals) pressure and at higher temperatures: U.S. Geol. Survey Bull. 1452, 456 p.

Robinson, Russell, and Iyer, H. M., 1979, Evidence from teleseismic P-wave observations for a low-velocity body under the Roosevelt Hot Springs geothermal area, Utah: Geotherm. Resources Council, Trans., v. 3, p. 585.

Roddy, D. J., 1978, Pre-impact geologic conditions, physical properties, energy calculations, meteorite and initial crater dimensions, and orientations of joints, faults, and walls at Meteor Crater, Arizona: Lunar Planet. Sci. Conf., 9th, Proceedings, p. 3891–3930.

———1979, Structural deformation at the Flynn Creek impact crater, Tennessee: A preliminary report on deep drilling: Lunar Planet. Sci. Conf., 10th, Proceedings, p. 2519–2534.

Roehler, H. W., and Stricker, G. D., 1979, Stratigraphy and sedimentation of the Torok, Kukpowruk, and Corwin Formations of Cretaceous age in the Kokolik-Utukok River region, National Petroleum Reserve in Alaska: U.S. Geol. Survey Open-File Rept. 79–995, 80 p.

Rosholt, J. N., Zartman, R. E., and Nkomo, I. T., 1973, Lead isotope systematics and uranium depletion in the Granite Mountains, Wyoming: Geol. Soc. America Bull., v. 84, p. 989–1001.

Rubin, Meyer, and Alexander, Corrinne, 1958, U.S. Geological Survey radiocarbon dates IV: Science, v. 127, p. 1476–1487.

Ruppel, E. T., 1978, Medicine Lodge thrust system, east-central Idaho and southwest Montana; U.S. Geol. Survey Prof. Paper 1031, 23 p.

Ryals, G. N., and Hosman, R. L., 1980, Selected hydrologic data from the vicinity of Rayburns and Vacherie salt domes, northern Louisiana salt-dome basin: U.S. Geol. Survey Open-File Rept. 80–217, 36 p.

Sandberg, C. A., 1975, McGowan Creek Formation, new name for Lower Mississippian flysch sequence in east-central Idaho: U.S. Geol. Survey Bull. 1405–E, 11 p.

Sandberg, C. A., and Gutschick, R. C., 1979, Guide to conodont biostratigraphy of Upper Devonian and Mississippian rocks along the Wasatch Front and Cordilleran Hingeline, Utah, *in* Sandberg, C. A., and Clark, D. L., eds., Conodont biostratigraphy of the Great Basin and Rocky Mountains: Brigham Young University Geol. Studies, v. 26, pt. 3, p. 107–134.

Sandberg, C. A., and Poole, F. G., 1977, Conodont biostratigraphy and depositional complexes of Upper Devonian cratonic-platform and continental-shelf rocks in the Western United States, *in* Murphy, M. A., Berry, W. B. N., and Sandberg, C. A., eds., Western North America, Devonian: Univ. California, Riverside, Campus Museum Contrib. 4, p. 144–182.

Sarna-Wojcicki, A. M., Hall, N. T., Bowman, H. R., Naeser, C. W., and Russell, P. C., 1977, Correlation and age of a widespread Pleistocene ash bed in northern California and western Nevada [abs.]: Geol. Soc. America, National Meeting, Nov. 1977, Seattle, Wash., Abs. with Program, p. 1155.

Sarna-Wojcicki, A. M., Lajoie, K. R., Robinson, S. W., and Yerkes, R. F., 1979, Recurrent Holocene displacement on the Javon Canyon fault, rates of faulting, and regional uplift, Western Transverse Ranges, California [abs.]: Geol. Soc. America, Abs. with Programs, v. 11, no. 3, p. 125.

Sass, J. H., and Zoback, M. L., 1979, Heat flow in relation to hydrothermal activity in the southern Black Rock Desert, Nevada [abs.]: EOS, Am. Geophys. Union Trans., v. 60, p. 946.

Sass, J. H., Zoback, M. L., and Galanis, S. P., Jr., 1979, Heat flow in relation to hydrothermal activity in the southern Black Rock Desert: U.S. Geol. Survey Open-File Rept. 79–1467.

Sauck, W. A., and Sumner, J. S., 1970, Residual aeromagnetic map of Arizona: Univ. Arizona, Tucson, Arizona, scale 1:1,000,000.

Sawatzky, D. L., 1967, Tectonic style along the Elkhorn thrust, eastern South Park and western Front Range, Colorado: Colo. School Mines, Ph. D. dissertation (unpub.), 206 p.

Scarborough, Robert, and Wilt, J. C., 1979, A study of uranium favorability of Cenozoic sedimentary rocks, Basin and Range province, Arizona: U.S. Geol. Survey Open-File Rept. 79–1429, 101 p.

Schnabel, P. B., and Seed, H. B., 1973, Accelerations in rock for earthquakes in the Western United States: Seismol. Soc. America Bull., v. 63, p. 501–516.

Schaefer, D. H., and Maurer, D. K., 1980, Geophysical reconnaissance of Lemmon Valley, Washoe County, Nevada: U.S. Geol. Survey, Open-File Rept. 80–1123, 35 p.

Schnepfe, M. M., 1979, Germanium contents of USGS standard rocks by flameless atomic absorption: Geostandards Newsletter, v. 3, no. 1, p. 93–96.

Scholten, Robert, 1957, Paleozoic evolution of the geosynclinal margin north of the Snake River Plain, Idaho-Montana: Geol. Soc. America Bull., v. 68, no. 2, p. 151-170.

Schroeder, E. E., Massey, B. C., and Waddell, K. M., 1979, Floods in central Texas, August 1978: U.S. Geol. Survey Open-File Rept. 79–682, 29 p.

Schwartz, D. P., Swan, F. H., III, Knuepfer, P. L., Hanson, K. L., and Cluff, L. S., 1979, Surface deformation along the Wasatch fault, Utah: Geol. Soc. America, Abs. with Programs, v. 11, no. 3, p. 127.

Scott, J. C., and Bohman, L. R., 1980a, Hurricane Frederic tidal floods of September 12–13, 1979, along the gulf coast, Hurricane quadrangle, Alabama: U.S. Geol. Survey Hydrol. Inv. Atlas HA–629.

———1980b, Hurricane Frederic tidal floods of September 12–13, 1979, along the gulf coast, Bridgehead quadrangle, Alabama: U.S. Geol. Survey Hydrol. Inv. Atlas HA–630.

———1980c, Hurricane Frederic tidal floods of September 12–13, 1979, along the gulf coast, Daphne–Point Clear quadrangles, Alabama: U.S. Geol. Survey Hydrol. Inv. Atlas HA–631.

———1980d, Hurricane Frederic tidal floods of September 12–13, 1979, along the gulf coast, Magnolia Springs quadrangle, Alabama: U.S. Geol. Survey Hydrol. Inv. Atlas HA–632.

———1980e, Hurricane Frederic tidal floods of September 12–13, 1979, along the gulf coast, Bon Secour Bay quadrangle, Alabama: U.S. Geol. Survey Hydrol. Inv. Atlas HA–633.

———1980f, Hurricane Frederic tidal floods of September 12–13, 1979, along the gulf coast, Pine Beach–St. Andrews Bay–Fort Morgan quadrangles, Alabama: U.S. Geol. Survey Hydrol. Inv. Atlas HA–634.

———1980g, Hurricane Frederic tidal floods of September 12–13, 1979, along the gulf coast, Gulf Shores quadrangle, Alabama: U.S. Geol. Survey Hydrol. Inv. Atlas HA–635.

———1980h, Hurricane Frederic tidal floods of September 12–13, 1979, along the gulf coast, Orange Beach quadrangle, Alabama: U.S. Geol. Survey Hydrol. Inv. Atlas HA–636.

———1980i, Hurricane Frederic tidal floods of September 12–13, 1979, along the gulf coast, Lillian quadrangle, Alabama: U.S. Geol. Survey Hydrol. Inv. Atlas HA–637.

Scott, J. C., and Franklin, M. A., 1980, Hurricane Frederic tidal floods of September 12–13, 1979, along the gulf coast, Perdido Bay quadrangle, Florida: U.S. Geol. Survey Hydrol. Inv. Atlas HA–638.

Seay, W. M., 1979, Southern Appalachian tectonic study: Division of Water Management Report DWM–26, Tennessee Valley Authority, Geol. Services Branch, 66 p., 14 pl.

Seeland, D. A., 1976, Relationships between early Tertiary sedimentation patterns and uranium mineralization in the Powder River Basin, Wyoming, *in* Geology and energy resources of the Powder River: Wyoming Geol. Assoc. Guidebook, Annual Field Conference, 28th, 1976, p. 53–64.

Seiders, V. M., 1978, U-Pb zircon dates from the central Appalachian Piedmont: A possible case of inherited radiogenic lead: Discussion: Geol. Soc. American Bull., v. 89, p. 1115–1116.

Seiders, V. M., Mixon, R. B., Stern, T. W., Newell, M. F., and Thomas, C. B., Jr., 1975, Age of plutonism and tectonism and a new minimum age limit on the Glenard Series in the northeast Virginia Piedmont near Occoquan: Am. Jour. Sci., v. 275, p. 481–511.

Senftle, F. E., Tanner, A. B., Philbin, P. W., Boynton, G. R., and Schram, C. W., 1978, In situ analysis of coal using a ^{252}Cf-Ge(Li) borehole sonde: Mining Eng. (AIME) 30, p. 666–674.

Seraphim, R. H., 1975, Denali—a nonmetamorphosed stratiform sulfide deposit: Econ. Geol., v. 70, p. 949–959.

Severson, R. C., 1978a, Spatial variation in total element content in soils in northwest New Mexico and differences in soil composition at the great group taxonomic level, *in* U.S. Geological Survey, Geochemical survey of the western energy regions, fifth annual progress report, July 1978: U.S. Geol. Survey Open-File Rept. 78–1105, p. 2–34.

———1978b, Variation in element content of the Doak, Shiprock, and Sheppard soil association in New Mexico, *in* U.S. Geological Survey, Geochemical survey of the western energy regions, fifth annual progress report, July 1978: U.S. Geol. Survey Open-File Rept. 78–1105, p. 35–46.

———1978c, Spatial variation in total element content of mine-soils at the San Juan Mine in northwest New Mexico, *in* U.S. Geological Survey, Geochemical survey of the western energy regions, fifth annual progress report, July 1978: U.S. Geological Survey Open-File Report 78–1105, p. 47–56.

Severson, R. C., McNeal, J. M., and Dickson, J. J., 1979, Effects of soil preparation on DTPA extractable elements in soils of the northern Great Plains: Soil Science, v. 128, no. 2, p. 70–79.

Shackelford, T. J., 1976, Structural geology of the Rawhide Mountains, Mohave County, Arizona: Univ. Southern California, Ph.D. thesis, 176 p.

———1977, Late Tertiary tectonic denudation of a Mesozoic(?) gneiss complex, Rawhide Mountains, Arizona [abs.]: Geol. Soc. America, Abs. with Programs, v. 9, no. 7, p. 1169.

Shampine, W. J., Dincer, T., and Noory, M., 1979, An evaluation of isotope concentrations in the ground water of Saudi Arabia, *in* Isotope Hydrology, 1978: International Atomic Energy Agency-Unesco International Symposium on Isotope Hydrology, Neurerberg, F.R.G., June 19-23, 1978, Proceedings, v. II, p. 443-463.

Shapiro, L. H., 1971, Structural geology of the Fanny Peak lineament, Black Hills, Wyoming-South Dakota, *in* Symposium on Wyoming tectonics and their economic significance: Wyoming Geol. Assoc. Guidebook, Field Conference, 23rd, 1971, p. 61-64.

Shinn, E. A., Halley, R. B., Hudson, J. H., and Lidz, B. H., 1977, Limestone compaction, an enigma: Geology, v. 5, p. 21-24.

Siegel, D. I., 1979a, Potential hydrologic effects of peat mining in the Red Lake peatlands, north-central Minnesota—a project plan: U.S. Geol. Survey Open-File Rept. 79-1591, 9 p.

———1979b, Sulfate contributions from snowmelt to Filson Creek watershed, northeastern Minnesota [abs.]: EOS, Am. Geophy. Union Trans., v. 60, no. 18, p. 259.

Sigafoos, R. S., 1964, Botanical evidence of floods and flood-plain deposition; U.S. Geol. Survey Prof. Paper 485-A, 35 p.

Skehan, J. W., S.J., and Murray, D. P., 1978, The coal-bearing Narragansett Basin of Massachusetts and Rhode Island, v. 1, Geology: Weston Observatory, Boston College, Report on National Science Foundation Grant No. AER76-02147, variously paged.

Skipp, B. A. L., and Brenckle, P. L., 1979, Foraminiferal faunas at the Mississippian-Pennsylvanian boundary in south-central Idaho, Nevada, and Arkansas [abs.]: Internat. Carboniferous Cong., 9th, Urbana, Ill., Abs. of papers, p. 202.

Skipp, B. A. L., and Hait, M. H., Jr., 1977, Allochthons along the northeast margin of the Snake River Plain, Idaho: Wyoming Geol. Assoc. Guidebook, Annual Field Conference, 29th, p. 499-515.

Skipp, B. A. L., Hoggan, R. D., Schleicher, D. L., and Douglass, R. C., 1979, Upper Paleozoic Carbonate Bank in East-central Idaho—Snaky Canyon, Bluebird Mountain, and Arco Hills Formations, and their Paleotectonic significance: U.S. Geol. Survey Bull. 1486, 78 p.

Skipp, B. A. L., Prostka, H. J., and Schleicher, D. L., 1979, Preliminary geologic map of the Edie Ranch quadrangle, Clark County, Idaho, and Beaverhead County, Montana: U.S. Geol. Survey Open-File Rept. 79-845, scale 1:62,500.

Slack, J. F., Force, E. R., Behum, P. T., and Williams, B. B., 1979, Mineral resources of the Citico Creek Wilderness Study Area, Monroe County, Tennessee: U.S. Geol. Survey Open-File Rept. 79-231, 33 p.

Slemmons, D. B., van Wormer, D., Bell, E. J., and Silberman, M. L., 1979, Recent crustal movements in the Sierra Nevada-Walker Lane region of California-Nevada, pt. 1 *of* Rate and style of deformation: Tectonophysics, v. 52, p. 561-570.

Sloss, L. L., 1954, Lemhi arch, a mid-Paleozoic positive element in south-central Idaho: Geol. Soc. America Bull., v. 65, no. 4, p. 365-368.

Smith, B. A., Shoemaker, E. M., Kieffer, S. W., and Cook, A. F., 1979, The role of SO_2 in volcanism in Io: Nature, v. 280, p. 738.

Snavely, P. D., Jr., Wagner, H. C., and Lander, D. L., 1980, Interpretation of the Cenozoic geologic history, central Oregon continental margin: Summary: Geol. Soc. America Bull., v. 91, no. 3, p. 143-146.

Spencer, A. C., 1907, The Juneau Gold Belt, Alaska: U.S. Geol. Survey Bull. 287, 161 p.

Stearns, C. E., 1943, The Galisteo Formation of north-central New Mexico: Jour. Geol., v. 51, no. 5, p. 301-319.

Stearns, D. W., 1978, Faulting and forced folding in the Rocky Mountains foreland, *in* Matthews, Vincent, III, ed., Laramide folding associated with basement block faulting in the western United States: Geol. Soc. America Mem. 151, p. 197-214.

Steininger, R. C., and Arehart, G. B., 1976, Geology of the Mt. Aetna molybdenum prospect, Chaffee County, Colorado, Geol. Soc. America, Abs. with Programs, v. 8, no. 5, p. 635.

Stephenson, L. W., and Crider, A. F., 1916, Geology and ground waters of northeastern Arkansas: U.S. Geol. Survey Water-Supply Paper 399, 315 p.

Stout, M. L., 1964, Geology of a part of the southern-central Cascade Mountains, Washington: Geol. Soc. America Bull., v. 25, p. 317-334.

Streckeisen, Albert, 1973, Plutonic rocks, classification and nomenclature recommended by the IUGS Subcommission on the Systematics of Igneous Rocks: Geotimes, v. 18, no. 10, p. 26-30.

———1979, Classification and nomenclature of volcanic rocks, lamprophyres, carbonates, and melilitic rocks: Recommendations and suggestions of the IUGS Subcommission on the Systematics of Igneous Rocks: Geology, v. 7, p. 331-335.

Stuber, H. A., 1979, Selective concentration of aromatic amines using a resin adsorbent applied to liquid chromatographic analysis of oil shale retort waters [abs.]: Northwest Regional Meeting Am. Chem. Soc., 34th, Richland, Washington, June 1979.

Stuckless, J. S., and Nkomo, I. T., 1978, Uranium-lead isotope systematics in uraniferous alkali-rich granites from the Granite Mountains, Wyoming: Implications for uranium source rocks: Econ. Geol., v. 73, p. 427-441.

———1980, Preliminary investigations of U-Th-Pb systematics in uranium-bearing minerals from two granitic rocks from the Granite Mountains, Wyoming: Econ. Geol., v. 75, no. 2, p. 289-295.

Stueber, A. M., Webster, D. A., Munro, I. L., Farrow, N. D., and Scott, T. G., 1980, An investigation of radionuclides release from Solid Waste Disposal Area 3, Oak Ridge National Laboratory: U.S. Department of Energy, Oak Ridge National Laboratory, ORNL/TM 3 27.

Swan, F. H., III, Schwartz, D. P., Hanson, K. L., Knuepfer, P. L., and Cluff, L. S., 1979, Recurrence of surface faulting and large magnitude earthquakes along the Wasatch fault zone, Utah: Geol. Soc. America, Abs. with Programs, v. 11, no. 3, p. 131.

Swan, M. M., 1975, The Texas lineament-tectonic expression of a Precambrian orogeny [abs.]: Geol. Soc. America, Abs. with Programs, v. 7, no. 7, p. 1288.

Tabor, R. W., Frizzell, V. A., Jr., Gaum, W. C., and Marcus, V. L., 1978, Revision of Naches Formation, *in* Geological Survey Research 1978: U.S. Geol. Survey Prof. Paper 1100, p. 78-79.

Tanner, A. B., Moxham, R. M., and Senftle, F. E., 1977, Assay for uranium and determination of disequilibrium by means of in situ high-resolution gamma-ray spectrometry: U.S. Geol. Survey Open-File Rept. 77-571, 22 p.

Teleki, P. G., Campbell, W. J., Ramseier, R. O., and Ross, Duncan, 1979, The offshore environment: A perspective from Seasat SAR data: Annual Offshore Technology Conference, 11th, Houston, Texas, April 20-May 3, 1979, Proccedings, p. 215-224.

Terry, J. E., Bryant, C. T., Ludwig, A. H., and Reed, J. E., 1979, Water-resources appraisal of the south Arkansas lignite area: U.S. Geol. Survey Open-File Rept. 79-924, 162 p.

Thiede, Jörn, T. L. Vallier, E. Vincent, R. R. Schmidt, A. Schaaf, C. A. Sancetta, P. Cepek, A. Boesma, N. Fujii, W. O. Sayre, K. E. Windom, K. E. Seifert, D. K. Rea, V. I. Koporulin, W. E. Dean, C. G. Adelseck, 1979, Middle Cretaceous oxygen-deficient paleoenvironments in Mid-Pacific Mountains and on Hess Rise, central North Pacific Ocean [abs.]: Am. Assoc. Petroleum Geologists Bull., v. 63, no. 3, p. 538–539.

Thompson, G. A., and Burke, D. B., 1973, Rate and direction of spreading in Dixie Valley, Basin and Range province, Nevada: Geol. Soc. America Bull., v. 84, p. 627–632.

Tietjen, G. L., and Moore, R. H., 1972, Some Grubbs-type statistics for the detection of several outliers: Technometrics, v. 14, no. 3, p. 583–597.

Toulmin, Priestley, III, 1976, Oligocene volcanism near Mt. Aetna, southern Sawatch Range, Colorado, Geol. Soc. America, Abs. with Programs, v. 8, no. 5, p. 640–641.

Tovish, Aaron, and Schubert, Gerald, 1978, Island arc curvature, velocity of convergence and angle of subduction: Geophys. Research Letters, v. 5, no. 5, p. 329–332.

Trescott, P. C., 1975, Documentation of finite difference model for simulation of three-dimensional ground-water flow: U.S. Geol. Survey Open-File Rept. 75–438, 32 p.

Trescott, P. C., and Larson, S. P., 1976, Documentation of finite-difference model for simulation of three-dimensional ground-water flow: U.S. Geol. Survey Open-File Rept. 76–591, 21 p.

Trescott, P. C., Pinder, G. F., and Larson, S. P., 1976, Finite-difference model for aquifer simulations in two dimensions with results of numerical experiments: U.S. Geol. Survey Tech. of Water-Resources Inv. v. 7, chap. C1, 116 p.

Tschanz, C. M., Kiilsgaurd, T. H., and Seeland, D. A., 1974, Mineral resources of the eastern part of the Sawtooth National Recreation Area, Custer and Blaine Counties, Idaho: U.S. Geol. Survey Open-File Rept. 74–1100, p. 683.

Tweto, Ogden, 1979, The Rio Grande rift system in Colorado, *in* Riecker, R. E., ed., Rio Grande rift: Tectonics and magnetism: Am. Geophys. Union, Wash., D.C., p. 33–56.

U.S. Department of Energy and U.S. Geological Survey, 1979, Report on the petroleum resources of the Federal Republic of Nigeria: National Technical Information Service, Foreign Energy Assessment Prog. Ser., DOE/IA-0008, UC-92 and 92a, 131 p.

U.S. Environmental Protection Agency, 1976, National interim primary drinking water regulations: Federal Register, v. 41, no. 25, p. 5281.

U.S. Geological Survey, 1975, Geological Survey Research 1975: U.S. Geol. Survey Prof. Paper 975, p. 67.

———1976, Vatnajökull, Iceland (Fall Scene): U.S. Geol. Survey Landsat Image Format Ser., N6359WO1723, Experimental Printing, scale 1:500,000.

———1977, Vatnajökull, Iceland (winter scene): U.S. Geological Survey Landsat Image Format Series, N6359WP1723, Experimental Printing, scale 1:500,000.

———1978, Land use and land cover, Kansas City; Missouri, Kansas, 1973: U.S. Geol. Survey Misc. Inv. Map I–1117, scale 1:250,000.

———1979a, Geological Survey Research 1979: U.S. Geol. Survey Prof. Paper 1150, p. 142.

———1979b, Outer Continental Shelf oil and gas information program: Atlantic index (January 1975—April 1979): U.S. Geol. Survey, May 1979, 68 p.

———1979c, Outer Continental Shelf oil and gas information program: Gulf of Mexico index (January 1977–June 1979): U.S. Geol. Survey Open-File Rept. 79–1347, 76 p.

———1979d, Outer Continental Shelf oil and gas information program: Pacific index (January 1975–May 1979): U.S. Geol. Survey Open-File Rept. 79–1327, 75 p.

———1979e, Outer Continental Shelf oil and gas information program: Alaska index (December 1974–June 1979): U.S. Geol. Survey Open-File rept. 79–1345, 91 p.

———1979f, Outer Continental Shelf oil and gas activities in the mid-Atlantic and their onshore impacts: A summary report, November 1979: U.S. Geol. Survey Open-File Rept. 80–17, 63 p.

———1979g, Outer Continental Shelf oil and gas information program: Directory to Federal, State, and local OCS-related activities and contacts: U.S. Geol. Survey Open-File Rept. 79–1481, 192 p.

———1979h, Energy resources of Egypt, Vol. 1, Annex 1, *in* Joint Egypt/U.S. report on Egypt/United States cooperative energy assessment (report prepared for the U.S. Department of Energy): National Technical Information Service Rept. DOE/IA-002/02, Dist. Category UC–2, 13, 184 p.

———1979i, Energy resources of Peru, Vol. 1, Annex 1, *in* Joint Peru/U.S. report on Peru/United States cooperative energy assessment (report prepared for U.S. Department of Energy): National Technical Information Service Rept. DOE/IA 0009–2, 155 p.

———1980a, Outer Continental Shelf oil and gas activities in the South Atlantic and their onshore impacts: A summary report: U.S. Geol. Survey Open-File Rept. 80–626, 62 p.

———1980b, Outer Continental Shelf oil and gas activities in the Pacific (southern California) and their onshore impacts: A summary report: U.S. Geol. Survey Open-File Rept. 80–645, 134 p.

———1980c, Outer Continental Shelf oil and gas activities in the Gulf of Mexico and their onshore impacts: A summary report: U.S. Geol. Survey Open-File Rept. 80–864, 116 p.

———1980d, Outer Continental Shelf oil and gas activities in the Gulf of Alaska: A summary report: U.S. Geol. Survey Open-File Rept. 80–1028, 78 p.

Van Alstine, R. E., 1976, Continental rifts and lineaments associated with major fluorspar districts: Econ. Geol., v. 71, no. 6, p. 977–987.

Van Bemmelen, R. W., and Rutten, M. G., 1955, Tablemountains of northern Iceland: Leiden, E. J. Brill, 219 p.

Van Horn, Richard, 1979, The Holocene Ridgeland Formation and associated Decker Soil (new names), near Great Salt Lake, Utah: U.S. Geol. Survey Bull. 1457–C, 11 p.

Vecchioli, John, McKenzie, D. J., Pascale, C. A., and Wilson, W. E., 1979, Active waste-injection systems in Florida, 1976: U.S. Geol. Survey Open-File Rept. 79–1296, 33 p.

Venugopal, B., and Luckey, T. D., 1978, Metal toxicity in mammals, pt. 2, Chemical toxicity of metals and metalloids: New York, Plenum Press, 409 p.

Verbeek, E. R., Ratzlaff, K. W., and Clanton, U. S., 1979, Faults in parts of north-central and western Houston metropolitan area, Texas: U.S. Geol. Survey Misc. Field Studies Map MF–1136, scale 1:24,000.

Wallace, A. R., 1979, Alteration and vein mineralization, Ladwig uranium mine, Jefferson County, Colorado: U.S. Geol. Survey Open-File Rept. 79–1615, 34 p.

Watson, T. L., and Powell, S. L., 1911, Fossil evidence of the ages of the Virginia Piedmont States: Am. Jour. Sci., 4th Ser., v. 31, p. 33–44.

Weaver, C. S., and Hill, D. P., 1978, Earthquake swarms and local crustal spreading along major strike-slip faults in California: Pure and Applied Geophysics, v. 17, p. 51–64.

Weed, E. G. A., Minard, J. P., Perry, W. J., Jr., Rhodehamel, E. C., and Robbins, E. I., 1974, Generalized pre-Pleistocene geologic map of the northern United States Atlantic continental margin: U.S. Geol. Survey Misc. Inv. Map I–861, scale 1:1,000,000.

Weed, W. H., 1901, Geology of the Shonkin Sag and Palisade Butte laccoliths in the Highwood Mountains of Montana: Am. Jour. Sci., 4th Ser., v. 12, p. 1–17.

Weissberg, B. G., Browne, P. R. L., and Seward, T. M., 1979, Ore metals in active geothermal systems, *in* Barnes, H. L., ed., Geochemistry of hydrothermal ore deposits, 2d ed.: New York, Holt, Rinehart, and Winston, 798 p.

Wells, J. D., 1974, Geologic map of the Alberton quadrangle, Missoula, Sanders, and Mineral Counties, Montana: U.S. Geol. Survey Geol. Quad. Map GQ-1157, scale 1:62,500.

West, R. E., and Sumner, J. S., 1973, Bouger gravity anomaly map of Arizona: Univ. Arizona, Tucson, Arizona, scale 1:1,000,000.

White, D. E., 1967, Mercury and base-metal deposits with associated thermal and mineral waters, *in* Barnes, H. L., ed., Geochemistry of hydrothermal ore deposits: New York, Holt, Rinehart, and Winston, p. 575–631.

White, I. C., 1891, Stratigraphy of the bituminous coal field of Pennsylvania, Ohio, and West Virginia: U.S. Geol. Survey Bull. 65, 212 p., 11 pl.

Willard, M. E., 1959, Tertiary stratigraphy of northern Catron County, New Mexico, *in* Guidebook of west-central New Mexico: New Mexico Geol. Soc. Guidebook, Field Conference, 10th, p. 92–99.

Williams, P. L., and Hackman, R. J., 1971, Geology, structure, and uranium deposits of the Salina quadrangle, Utah, U.S. Geol. Survey Misc. Inv. Ser. I-591, scale 1:250,000.

Williams, R. S., Jr., 1979a, Delineation of recent changes in the coastline of Monomoy Island, Cape Cod, Massachusetts with Landsat 3 images (MSS and RBV): Am. Soc. Photogramm., Ann. Meeting, 45th, Wash., D.C., 1979, Proceedings, v. 1, p. 190–291.

———1979b, Regional geological mapping using Landsat 3 return beam vidicon images: Examples from Iceland and Cape Cod, Massachusetts [abs.]: Geol. Soc. America, Ann. Meeting, Boulder, Colorado, 1979, Proceedings, v. 11, no. 7, p. 541.

Williams, R. S., Jr., and Ferrigno, J. G., 1979, Satellite image atlas of glaciers [abs.]: William T. Pecora Symposium, Satellite Hydrology, 5th, Sioux Falls, South Dakota, 1979, Abs., p. 5–3.

Williams, R. S., Jr., Mecklenburg, T. N., Abrams, M. J., and Guomundsson, Bragi, 1977, Conventional versus computer-enhanced Landsat image maps of Vatnajökull, Iceland [abs.]: Geol. Soc. America, Ann. Meeting, Boulder, Colorado, v. 9, no. 7, Abs. with Programs, p. 1228–1229.

Wilson, F. H., Detterman, R. L., and Silberman, M. L., 1978, New ages of intrusive rocks and altered zones on the Alaska Peninsula, *in* Johnson, K. M., ed., The United States Geological Survey in Alaska -accomplishments during 1977: U.S. Geol. Survey Circ. 772-B, p. B63–B65.

Wilson, M. T., and Thomas, H. E., 1964, Hydrology and hydrogeology of Navajo Lake, Kane County, Utah: U.S. Geol. Survey Prof. Paper 417-C, 26 p.

Wilson, R. P., 1979, Availability of ground water on Federal land near the Ak-Chin Indian Reservation, Arizona—a reconnaissance study: U.S. Geol. Survey Open-File Rept. 79-1165, 36 p.

Wood, G. H., Jr., Trexler, J. P., and Kehn, T. M., 1969, Geology of the west-central part of the Southern anthracite field and adjoining areas, Pennsylvania: U.S. Geol. Survey Prof. Paper 602, 150 p.

Woodward, L. A., 1967, Stratigraphy and correlation of late Precambrian rocks of Pilot Range, Elko County, Nevada, and Box Elder County, Utah: Am. Assoc. Petroleum Geologists Bull., v. 51, p. 235–243.

Wray, J. R., 1980, Land use and land cover in the greater Pittsburgh region, Pennsylvania, 1973: U.S. Geol. Survey Misc. Inv. Ser. I-1248, scale 1:125,000.

Wright, L. A., 1976, Late Cenozoic fault patterns and stress fields of the Great Basin and westward displacement of the Sierra Nevada block: Geology, v. 4, p. 489–494.

Yellich, J. A., Kramer, R. T., and Kendall, R. G., 1978, Copper Mountain, Wyoming, uranium deposits rediscovered: Annual Field Conference, 13th Wyoming Geological Association, Guidebook, p. 311–327.

Zablocki, C. J., 1977, Self-potential studies in East Puna, *in* Geoelectric studies on the east rift, Kilauea Volcano, Hawaii Island: Hawaii Inst. Geophys., Univ. of Hawaii Tech. Rept. HIG-77-15, p. 175–195.

Zartman, R. E., 1979, U-Pb zircon dates from the central Appalachian Piedmont: A possible case of inherited radiogenic lead: Reply: Geol. Soc. America Bull., v. 89, p. 1115–1117.

Zartman, R. E., Pawlowska, Jadwiga, and Rubinowski, Zbigniew, 1979, Lead isotopic composition of ore deposits from the Silesia–Crakow Mining District, *in* Research on the genesis of zinc-lead deposits of Upper Silesia, Poland: Prace Instytutu Geologicznego, v. 95, p. 133–149.

Zartman, R. E., and Stern, T. W., 1967, Isotopic age and geologic relationships of the Little Elk Granite, northern Black Hills, South Dakota, *in* Geological Survey Research 1967: U.S. Geol. Survey Prof. Paper 575-D, p. D157–D163.

Zen, E-an, 1979, Possible size factor in repository design for radioactive wastes: Geol. Soc. America, Abs. with Programs, v. 11, no. 7, p. 546.

Zen, E-an, Taylor, M. E., and Wilson, L. A., 1979, Middle Cambrian *Albertella* from Pioneer Mountains, southwest Montana, and its stratigraphic implications: Geol. Soc. America, Abs. with Programs, v. 11, no. 6, p. 306.

Zietz, Isidor, and B. C. Hearn, Jr., M. W. Higgins, G. D. Robinson, and D. A. Swanson, 1971, Interpretation of an aeromagnetic strip across the northwestern United States: Geol. Soc. America Bull., v. 82, no. 12, p. 3,347–3,372.

Zubovic, Peter, Hatch, J. R., and Medlin, J. H., 1979, Assessment of chemical composition of coal resources: Conference on World Coal Prospects, Katowice, Poland, 1980, Proceedings, 24 p.

INVESTIGATIONS IN PROGRESS IN THE GEOLOGICAL SURVEY

Investigations in progress during fiscal year 1980 are listed below together with the names and headquarters of the individuals in charge of each. Headquarters at main centers are indicated by NC for the National Center in Reston, Va., D for Denver, Colo., and M for Menlo Park, Calif. The lowercase letter after the name of the project leader shows the Division technical responsibility: c, Conservation Division; l, Land Information and Analysis; w, Water Resources Division; no letter, Geologic Division.

The projects are classified by principal topic. Most geologic-mapping projects involve special studies of stratigraphy, petrology, geologic structure, or mineral deposits but are listed only under "Geologic mapping" unless a special topic or commodity is the primary justification for the project. A reader interested in investigations of volcanology, for example, should look under the heading "Geologic Mapping" for projects in areas of volcanic rocks, as well as under the heading "Volcanology." Likewise, most water-resource investigations involve special studies of several aspects of hydrology and geology but are listed only under "Water Resources" unless a special topic—such as floods or sedimentation—is the primary justification for the project.

Areal geologic mapping is subdivided into mapping at scales smaller than 1:62,500 (for example, 1:250,000) and mapping at scales of 1:62,500 or larger (for example, 1:24,000).

Abstracts. *See* Bibliographies and abstracts.
Aluminum:
Resources of the United States (S. H. Patterson, NC)
Analytical chemistry:
Activation analysis (J. J. Rowe, NC)
Analytical methods:
Textural automatic image analyzer research (M. B. Sawyer, D)
Water chemistry (M. J. Fishman, w, D)
Analytical services and research (J. I. Dinnin, NC; Claude Huffman, Jr., D; C. O. Ingamells, M)
Mineral deposits, characteristic analysis (J. M. Botbol, NC)
Organic geochemistry and infrared analysis (I. A. Berger, NC)
Organic polyelectrolytes in water (R. L. Wershaw, w, D)
Plant laboratory (T. F. Harms, D)
Radioactivation and radiochemistry (H. T. Millard, D)
Rock chemical analysis:
General (D. R. Norton, D)
Rapid (Leonard Shapiro, NC)
Services (L. B. Riley, D)
Trace analysis methods, research (F. N. Ward, D)
Ultratrace analysis (H. T. Millard, D)
X-ray spectrometer for Viking lander (Priestley Toulmin III, NC)
See also Spectroscopy.
Arctic engineering geology (Reuben Kachadoorian, M)
Artificial recharge:
Artificial recharge methods (W. F. Lichtler, w, Lincoln, Nebr.)
Artificial recharge research (E. P. Weeks, w, Lubbock, Tex.)
Beaver-Badger Creeks recharge (A. W. Burns, w, D)
Chemical reactions, mineral surfaces (J. D. Hem, w, M)
Columbia River basalt recharge (M. R. Karlinger, w, Tacoma, Wash.)
Deepwell waste injection (R. W. Hull, w, Tallahassee, Fla.)
Fort Allen recharge (J. R. Diaz, w, Fort Buchanan, P.R.)
Fresh water storage, saline aquifers (J. N. Fischer, w, Miami, Fla.)
Heat storage (D. R. Cline, w, Tacoma, Wash.)
Injection wells, Santa Rosa County (R. W. Hull, w, Tallahassee, Fla.)
Lee County freshwater injection (F. A. Watkins, w, Fort Myers, Fla.)

Artificial recharge—Continued
Nassau County recharge (T. M. Robison, w, Syosset, N.Y.)
Recharge feasibility factors (J. Rubin, w, M)
Salina hydrology (R. M. Waller, w, Ithaca, N.Y.)
Salt-Gila recharge (P. B. Rohne, w, Phoenix, Ariz.)
Subsurface storage, waste heat (J. D. Bredehoeft, w, NC)
Supplemental recharge by storm basins (D. A. Aronson, w, Syosset, N.Y.)
Automated cartography:
Datamap (Cooperative Mapping Program) (D. Peuquet, l, NC)
Raster Mode Geoprocessing (D. Peuquet, l, NC)
Barite:
Geology, geochemistry, and resources of barite (D. A. Brobst, NC)
Base metals. *See* base-metal names.
Bibliographies and abstracts:
Luna bibliography (J. H. Freeberg, M)
Borates:
California (N):
Furnace Creek area (J. F. McAllister)
Searles Lake area (G. I. Smith)
Chromite. *See* Ferro-alloy metals.
Clays:
Georgia, Kaolin investigations (S. H. Patterson, NC)
Climate:
Tree ring analysis (S. Agard, D)
Climatic changes:
California, Quaternary (D. P. Adam, M)
Coal:
Appalachia, Safe mine waste disposal (W. E. Davies, NC)
Geochemistry of United States coal (V. E. Swanson, D)
Geotechnical research in western energy lands (F. W. Osterwald, D)
National Coal Resources Data System (M. D. Carter, NC)
Natural combustion and metamorphism of overlying rocks (J. R. Herring, D)
Regional geotechnical studies, Powder River Basin (S. P. Kanizay, D)
States:
Alaska:
Bering River coal field (C, Anchorage)

Coal—Continued

States:

Alaska:—Continued
- Nenana (Clyde Wahrhaftig, M)
- Regional engineering geology of Cook Inlet coal lands (H. R. Schmoll and L. A. Yehle, D)
- Shallow geophysical logging for coal-National Petroleum Reserve in Alaska (J. E. Callahan, c, Anchorage)

Arizona, Collection of coal samples for analysis (R. T. Moore, Tucson; V. E. Swanson, D)

Colorado (c, D, except as otherwise noted):
- Citadel Plateau (G. A. Izett)
- Collection of coal samples and coal resource data in Colorado and entry of data into the USGS National Coal Resources Data System (D. K. Murray; M. D. Carter, NC)
- Disappointment Valley, eastern (D. E. Ward, D)
- Douglas Creek Arch area (B. E. Barnum)
- Geology and energy resources of the Book Cliffs coal field (R. S. Garrigues)
- Geology and energy resources of the Danforth Hills area (J. R. Smith)
- Geology and energy resources of the Grand Hogback and adjacent areas (D. H. Madden)
- Geology and energy resources of the Grand Mesa coal field (S. L. Covington)
- Geology and energy resources of the Paonia and Crested Butte coal fields (D. L. Gaskill)
- Geology and energy resources of the Rawlins coal field, Wyoming-Colorado (C. S. V. Barclay)
- Geology and energy resources of the Trinidad coal field (G. W. Rice)
- Geology and energy resources of the Yampa coal field (M. E. Brownfield)
- North Park area (D. J. Madden)
- Smizer Gulch and Rough Gulch quadrangles (W. J. Hail, D)

Idaho, Collection of coal samples in Idaho (C. R. Knowles, Moscow; V. E. Swanson, D)

Illinois, Preparation of Illinois coal resource and chemical data for entry into the USGS National Coal Resources Data System (H. J. Gluskoter, Urbana; M. D. Carter, NC)

Kentucky (D):
- Adams quadrangle (D. E. Ward)
- Blaine quadrangle (C. L. Pillmore)
- Louisa quadrangle (R. M. Flores)
- Richardson quadrangle (P. T. Hayes)
- Sitka quadrangle (P. T. Hayes)

Missouri, coal data collection and transfer to the National Coal Resources Data System (C. E. Robertson, Rolla; M. D. Carter, NC)

Montana:
- Birney coal area (V. D. Niermeier, c, Casper, Wyo.)
- Collection of coal samples in Montana (R. E. Matson, Butte; V. E. Swanson, D)
- Geology and energy resources of the Williston Basin, North Dakota, South Dakota, and Montana (J. S. Hines, c, Billings)

Nevada, Collection of coal samples in Nevada (J. A. Schilling, Reno; V. E. Swanson, D)

New Mexico:
- Collection of coal samples in New Mexico (F. E. Kottlowski, Socorro; V. E. Swanson, D)
- Gallup East quadrangle (E. D. Patterson, c, Roswell)
- Manuelito quadrangle (J. E. Fassett, c, Farmington)
- Twin Butte quadrangle (M. L. Millgate, c, Farmington)

Coal—Continued

States—Continued

New Mexico:—Continued
- Western Raton field (C. L. Pillmore, D)

North Dakota (c, Billings, Mont., except as otherwise noted):
- Adams, Bowman, and Slope Counties—lignite resources (R. C. Lewis)
- Clark Butte 15-minute quadrangle (G. D. Mowat)
- West-central North Dakota lignite resources (E. A. Rehbein)
- Williston area lignite resources (J. M. Spencer)

Oklahoma (c, Tulsa, except as otherwise noted):
- Blocker quadrangle (E. H. Hare, Jr.)
- Collection of coal samples in Oklahoma (S. A. Friedman, Norman; V. E. Swanson, D)
- Hackett quadrangle (E. H. Hare, Jr.)
- Panama quadrangle (E. H. Hare, Jr.)
- Spiro quadrangle (E. H. Hare, Jr.)

Pennsylvania (NC, except as otherwise noted):
- Collection of coal samples for analysis (W. E. Edmunds, Pennsylvania State Geological Survey, Harrisburg; M. J. Bergin)
- Northern anthracite field (M. J. Bergin)
- Southern anthracite field (G. H. Wood, Jr.)

Utah (c, D, except as otherwise noted):
- Basin Canyon quadrangle (Fred Peterson)
- Blackburn Canyon quadrangle (Fred Peterson)
- Engineering geologic studies, east-central Utah (E. E. McGregor, D)
- Geology and coal resources of Wasatch Plateau coal field (L. F. Blanchard)
- Geology and energy resources of the Henry Mountains coal basin (W. E. Bowers)
- Geology and energy resources of the Emery coal field (L. F. Blanchard)

Virginia and West Virginia, Central Appalachian Basin (K. J. Englund, NC)

Washington, Collection of coal samples for analysis (V. E. Livingston, Jr., Olympia; V. E. Swanson, D)

West Virginia:
- Formatting coal data for National Coal Resources Data System (M. C. Behling, Morgantown; M. D. Carter, NC)
- Louisa quadrangle (C. W. Connor, D)

Wyoming (c, D, except as otherwise noted):
- Coal mine deformation studies, Powder River Basin (C. R. Dunrud, D)
- Engineering geologic mapping, Sheriden-Buffalo area, Wyoming (E. N. Hinrichs, D)
- Engineering geologic studies, Kemmerer 1:100,000 sheet (D. D. Dickey, D)
- Geology and coal resources of the Rock Springs Uplift (D. H. Madden)
- Geology and energy resources of the Powder River Basin (L. H. Jefferis, c, Casper)
- Geology and energy resources of the Rawlins coal field, Wyoming-Colorado (C. V. S. Barclay)
- Hilight coal area (L. H. Jeffries, c, Casper)
- Weston SW quadrangle (R. A. Katock c, Casper)

Construction and terrain problems:

Areal slope stability analysis, San Francisco Bay region (S. D. Ellen, M)

Damsite investigations (F. N. Houser, D)

Electronics instrumentation research for engineering geology (J. B. Bennetti, D)

Construction and terrain problems—Continued
- Engineering geologic map of United States (D. H. Radbruch-Hall, M)
- Fissuring-subsidence research (T. L. Holzer, M)
- Geophysical studies for engineering geology (C. H. Miller, D)
- Geotechnical measurements and services (H. W. Olsen, D)
- Geotechnical research in western energy lands (F. W. Osterwald, D)
- Landslide overview map of the conterminous U.S. (D. H. Radbruch-Hall, M)
- Reactor hazards research (W. H. Hays, D)
- Reactor site investigations (R. H. Morris, D)
- Regional geotechnical studies, Powder River Basin (S. P. Kanizay, D)
- Research in rock mechanics (F. T. Lee, D)
- Safe mine waste disposal, Appalachia (W. E. Davies, NC)
- Sino-Soviet terrain (L. D. Bonham, I, NC)
- Solution subsidence and collapse (J. R. Ege, D)
- Special intelligence (L. D. Bonham, I, NC)
- Tephra hazards from Cascade Range volcanoes (D. R. Mullineaux, D)
- Volcanic hazards (D. R. Crandell, D)
- *States:*
- Alaska, Regional engineering geology of Cook Inlet coal lands (H. R. Schmoll and L. A. Yehle, D)
- California (M, except as otherwise noted):
  - Geology and slope stability, western Santa Monica Mountains (R. H. Campbell)
  - Pacific Palisades landslide area, Los Angeles (J. T. McGill, D)
- Colorado, Coal mine deformation studies, Somerset mining district (C. R. Dunrud, D)
- Hawaii, Seismic hazards of the island of Hawaii with special emphasis on the Hilo 7½-min. quad. (J. Buchanan-Banks, Hawaii)
- Nevada:
  - Seismic engineering program (K. W. King, Las Vegas)
  - Surface effects of nuclear explosions (R. P. Snyder, D)
- Utah, Engineering geologic studies, east-central Utah (E. E. McGregor, D)
- Wyoming:
  - Coal mine deformation studies, Powder River Basin (C. R. Dunrud, D)
  - Engineering geologic mapping, Sheridan-Buffalo area (E. N. Hinrichs, D)
  - Engineering geologic studies, Kemmerer 1:100,000 sheet (D. D. Dickey, D)
- *See also* Urban geology; Land use and environmental impact; Urban hydrology.

Copper:
- United States and world resources (D. P. Cox, NC)
- *States:*
- Alaska, Southwest Brooks Range (I. L. Tailleur, M)
- Arizona, Ray porphyry copper (H. M. Cornwall, M)
- Colorado, Precambrian sulfide deposits (D. M. Sheridan, D)
- Maine-New Hampshire, Porphyry with molybdenum (R. G. Schmidt, NC)
- Michigan (NC):
  - Greenland and Rockland quadrangles (J. W. Whitlow)
  - Michigan copper district (W. S. White)
- Virginia, Massive sulfides (J. E. Gair, NC)

Crustal studies. *See* Earthquake studies; Geophysics, regional.

Drought studies:
- Drought in Colorado (T. R. Dosch, w, D)
- Northwest Iowa (M. R. Bukart, w, Iowa City)
- Tree rings and drought (R. L. Phipps, w, NC)

Earthquake studies:
- Active fault analysis (R. E. Wallace, M)
- Comparative elevation studies (R. O. Castle, M)
- Computer fault modeling (J. H. Dieterich, M)
- Computer operations and maintenance (T. C. Jackson, M)
- Crustal inhomogeneity in seismically active areas (S. W. Stewart, M)
- Crustal strain (J. C. Savage, M)
- Crustal studies (ARPA) (Isidore Zietz, NC)
- Dynamic soil behavior (A. T. F. Chen, M)
- Earth structure studies (J. H. Healy, M)
- Earthquake field studies (W. J. Spence, C. J. Langer, J. N. Jordan, M)
- Earthquake-induced landslides (E. L. Harp, M)
- Earthquake-induced sedimentary structures (J. D. Sims, M)
- Earthquake recurrence and history (R. D. Nason, M)
- Eastern United States (R. K. McGuire, D)
- Experimental liquefaction potential mapping (T. L. Youd, M)
- Fault-zone tectonics (J. C. Savage, M)
- Fluid injection, laboratory investigations (J. D. Byerlee, Louis Peselnick, M)
- Geologic parameters of seismic source areas (F. A. McKeown, D)
- Ground failure related to the 1811–12 New Madrid earthquakes (S. F. Obermeier, NC)
- Ground failures caused by historic earthquakes (D. K. Keefer, M)
- Ground-motion modeling and prediction (W. B. Joyner, M)
- Ground-motion studies (R. D. Borcherdt, R. P. Maley, M)
- Interaction of ground motion and ground failure (R. C. Wilson, M)
- Microearthquake data analysis (W. H. K. Lee, M)
- National Earthquake Information Service (A. C. Tarr, D)
- National Strong-Motion Instrumentation Network (R. B. Matthiesen, M)
- New seismic instrumentation for geothermal surveys (P. A. Reasenberg, M)
- Nicaragua, Central America, technical assistance in establishing center for earthquake hazard reduction (P. L. Ward, M)
- Plate-tectonic studies (E. D. Jackson, M)
- Precursory phenomena (P. L. Ward, M)
- Prediction, animal behavior studies (P. A. Reasenberg, M)
- Prediction monitoring and evaluation (R. N. Hunter, D)
- Recurrence intervals along Quaternary faults (K. L. Pierce, D)
- Reduction of noise in precursor signals (J. A. Steppe, M)
- Reservoir-induced seismicity, statistical approach, (D. E. Stuart-Alexander, M)
- Seismic-risk studies (S. T. Algermissen, D)
- Seismic-source studies (W. R. Thatcher, M)
- Seismic studies for earthquake prediction (C. G. Bufe, M)
- Seismicity and Earth structure (J. N. Taggart, D)
- Seismological research observatories (J. R. Peterson, Albuquerque, N. Mex.)
- Spectral and time domain analysis of near field recordings of earthquakes (J. B. Fletcher, M)
- Stress studies (C. B. Raleigh, M)
- Surface faulting studies (M. G. Bonilla, M)
- Synthetic strong-motion seismograms (W. B. Joyner, M)
- Tectonic studies (W. B. Hamilton, D)

Earthquake studies—Continued
- Teleseismic search for earthquake precursors (J. W. Dewey, D)
- Theoretical seismology (A. F. Espinosa, D)
- Worldwide Network of Standard Seismographs (J. R. Peterson, Albuquerque, N. Mex.)
- *States and territories:*
- Alaska:
  - Earthquake hazards, southern part (George Plafker, M)
  - Microearthquake studies (R. A. Page, M)
  - Turnagain Arm sediments (A. T. Ovenshine, M)
- California (M, except as otherwise noted):
  - Basement rock studies along San Andreas fault (D. C. Ross)
  - Continental Shelf fault studies (S. C. Wolf)
  - Depth of bedrock in the San Francisco Bay region (R. M. Hazlewood)
  - Earthquake hazards:
    - San Francisco Bay region (E. E. Brabb)
    - Southern part (D. M. Morton, Los Angeles)
  - Foothills fault system (D. E. Stuart-Alexander, M)
  - Geodetic strain (W. H. Prescott)
  - Geophysical studies, San Andreas fault (J. H. Healy)
  - Measurement of seismic velocities for seismic zonation (J. F. Gibbs, R. D. Borcherdt, T. E. Fumal)
  - Microearthquake studies:
    - Central part (J. H. Pfluke)
    - New Melones (J. C. Roller)
    - Southern part (D. P. Hill)
  - Tectonics:
    - Central and northern part (W. P. Irwin)
    - Central San Andreas fault (D. B. Burke, T. W. Dibblee, Jr.)
    - Salton Trough tectonics (R. V. Sharp)
    - Southern part (M. M. Clark)
  - Theory of wave propagation in anelastic media (R. D. Borcherdt)
- Colorado, Rangely (C. B. Raleigh, M)
- Hawaii, Seismic hazards of the island of Hawaii with special emphasis on the Hilo 7½-min. quad. (J. Buchanan-Banks, Hawaii)
- Idaho, active faults, Snake River Plain (S. S. Oriel, M. H. Hoit, W. E. Scott, D)
- Massachusetts, Fault definition, northeastern Massachusetts (A. F. Shride, D)
- Missouri:
  - Ground failure related to the New Madrid earthquake (S. F. Obermeier, NC)
  - New Madrid fault-zone geophysics (M. F. Kane, D)
- Montana, Yellowstone National Park, microearthquake studies (A. M. Pitt, M)
- Nevada, Tectonics, west-central (E. B. Ekren, D)
- New Mexico, Seismotectonic analysis, Rio Grande rift (E. H. Baltz, Jr., D)
- Puerto Rico, Preliminary assessment of liquefaction potential in and near San Juan (T. L. Youd, M)
- South Carolina, microearthquake studies (A. C. Tarr, D)
- Utah, Wasatch Front surficial geology (R. D. Miller, D)
- Washington (M):
  - Earthquake hazards, Puget Sound region (H. D. Gower, P. D. Snavely, Jr.)
  - Hanford microearthquake studies (J. H. Pfluke)

Ecology:
- Estuarine plankton dynamics (J. E. Cloern, w, M)

Engineering geologic studies. *See* Construction and terrain problems; Urban geology.

Environmental assessment:
- Analysis of digitized maps of synthetic fuel resources (K. J. Lanfear, l, NC)
- Analysis of synthetic fuel development (C. T. Schoen, L. A. Yost IV, l, NC)
- Colstrip #3 and #4 power transmission line, (C. Albrecht, l, D)
- Comparative study of change and disorganization in energy development communities of the Great Plains (R. R. Reynolds, Jr., l, NC)
- Guidelines for preparation of EIS's (J. R. Burns, l, NC)
- Kerr-McGee East Gillette mine (W. G. Weist, Jr., l, D)
- Mobil Oil Company Rojo Caballos coal mining (L. G. Marcus, l, NC)
- Mode of deformation of Rosebud coal, Colstrip, Montana—Room temperature, 102.0, MPa (J. M. White, c, Billings)
- National Petroleum Reserve Alaska, environmental analysis (W. J. Schneider, w, M)
- Northern Powder River Basin regional coal (Glenn Malmberg, w, Billings)
- Off-site movement of radioactive materials, La Bajada mine, New Mexico (P. F. Narten, E. L. Meyer, l, NC)
- Oilspill trajectory analysis (K. J. Lanfear, l, NC)
- Peabody Big Sky mine (Glenn Malmberg, w, Billings)
- Physical effects of off-road vehicles (H. G. Wilshire and J. K. Nakata, M)
- Powder River Basin, uranium (E. S. Santos, D)
- Reclamation potentials for western coal mines (P. F. Narten, l, NC)
- Review of environmental impact statements (L. D. Bonham, l, NC)
- South Florida environment (B. F. McPherson, w, Miami)
- Spring Creek mine (Glenn Malmberg, w, Billings)
- Supplemental socioeconomic assessment of the East Gillette mine and a socioeconomic assessment of the North Antelope mine (R. Reynolds, Jr., l, NC)
- Tracking of environmental laws and regulations (H. C. McWreath, l, NC)
- Volatile elements from natural coal burning (J. R. Herring, D)

Environmental geology:
- Quaternary dating applications—overview map (K. L. Pierce, D)
- *States:*
- Alaska:
  - Peterburg quadrangle (D. A. Brew, M)
  - Regional engineering geology of Cook Inlet coal lands (H. R. Schmoll and L. A. Yehle, D)
- Montana:
  - Environmental study of the Big Fork-Avon area (I. J. Witkind, D)
  - Land resources, Helena region (R. G. Schmidt, NC; G. D. Robinson, M)
- Utah:
  - Cedar City 2° quadrangle (K. A. Sargent, D)
  - Central Utah energy lands (I. J. Witkind, D)
  - Kaiparowits Plateau coal basin (K. A. Sargent, D)
- Wyoming, Hams Fork coal basin (A. B. Gibbons, D)
- *See also* Construction and terrain problems; Land use and environmental impact; Urban geology.

Evapotranspiration:
- Evaporation, Colorado lakes (N. E. Spahr, w, D)
- Evapotranspiration data analyses (T. E. A. van Hylckama, w, Lubbock, Tex.)
- Evapotranspiration theory (O. E. Leppanen, w, Bay St. Louis, Miss.)
- Mechanics of evaporation (G. E. Koberg, w, D)
- Pecos evapotranspiration studies (E. P. Weeks, w, D)
- Vegetation ecohydrology (R. M. Turner, w, Tucson, Ariz.)

Extraterrestrial studies:
- Lunar analog studies, explosion craters (D. J. Roddy, Flagstaff, Ariz.)
- Lunar data synthesis:
  - Imbrium and Serenitatis Basins (J. F. McCauley, Flagstaff, Ariz.)
  - Sample petrology and stratigraphy (H. G. Wilshire, M)
  - Synoptic lunar geology (D. E. Wilhelms, M)
- Lunar microwave (G. R. Olhoeft, Denver)
- Lunar sample investigations:
  - Chemical and X-ray fluorescence analysis (H. J. Rose, Jr., NC)
  - Lunar igneous-textured rocks (O. B. James, NC)
  - Major lunar breccia types (E. C. T. Chao, NC)
  - Mineralogical analyses (R. B. Finkelman, NC)
  - Oxygen fugacities and crystallization sequence (Motoaki Sato, NC)
  - Petrologic studies (Edwin Roedder, NC)
  - Pyroxenes (J. S. Huebner, NC)
- Planetary analog studies, mass movements (E. C. Morris, Flagstaff, Ariz.)
- Planetary investigations:
  - Geologic mapping of Mars (D. H. Scott, J. F. McCauley, Flagstaff, Ariz.)
  - Geologic synthesis of Mars (Harold Masursky, Flagstaff, Ariz.)
  - Image-processing studies (L. A. Soderblom, Flagstaff, Ariz.)
  - Mariner Jupiter-Saturn (L. A. Soderblom, Flagstaff, Ariz.)
  - Mariner Venus-Mercury TV (N. J. Trask, NC)
  - Mars mineralogy and chemistry, Viking lander (Priestley Toulmin III, H. J. Rose, Jr., NC)
  - Mars topographic synthesis (S. S. C. Wu, Flagstaff, Ariz.)
  - Planetary cartography (R. M. Batson, Flagstaff, Ariz.)
  - Radar applications (G. G. Schaber, Flagstaff, Ariz.)
  - Viking mission:
    - Lander (E. C. Morris, Flagstaff, Ariz.)
    - Orbiter TV (M. H. Carr, M)
    - Physical properties of Mars (H. J. Moore, M)
    - Site analysis (Harold Masursky, Flagstaff, Ariz.)

Ferro-alloy metals:
- Chromium:
  - Geochemistry (B. A. Morgan III, NC)
  - Resource studies (T. P. Thayer, NC)
- Molybdenum-rhenium resource studies (R. U. King, D)
- *States:*
- North Carolina, Tungsten in Hamme district (J. E. Gair, NC)
- Oregon, John Day area (T. P. Thayer, NC)
- Pennsylvania, State Line district (B. A. Morgan III, NC)

Flood-hazard mapping:
- Alabama (C. O. Ming, w, Montgomery)
- Arkansas (R. C. Gilstrap, w, Little Rock)
- California (J. R. Crippen, w, M)
- Colorado (T. R. Dosch, w, D)
- Connecticut (M. A. Cervione, Jr., w, Hartford)
- Idaho (W. A. Harenberg, w, Boise)
- Indiana (J. B. Swing, w, Indianapolis)
- Iowa (O. G. Lara, w, Iowa City)
- Kansas (D. B. Richards, w, Lawrence)
- Kentucky (C. H. Hannum, w, Louisville)
- Louisiana (A. S. Lowe, w, Baton Rouge)
- Maine (R. A. Morrill, w, Augusta)
- Massachusetts (S. W. Wandle, Jr., w, Boston)
- Michigan (R. L. Knutilla, w, Lansing)

Flood-hazard mapping—Continued
- Minnesota (G. H. Carlson, w, St. Paul)
- Missouri (L. D. Hauth, w, Rolla)
- North Carolina (R. W. Coble, w, Raleigh)
- North Dakota (O. A. Crosby, w, Bismarck)
- Ohio (D. K. Roth, w, Columbus)
- Oregon (D. D. Harris, w, Portland)
- Pennsylvania (Andrew Voytik, w, Harrisburg)
- Puerto Rico (E. D. Cobb, w, San Juan)
- South Carolina (W. T. Utter, w, Columbia)
- South Dakota (H. L. Dixson, w, Huron)
- Texas (J. D. Bohn, w, Austin)
- United States (G. W. Edelen, w, NC)
- Virginia (B. J. Prugh, w, Richmond)
- Washington (J. H. Bartells, w, Tacoma)
- West Virginia (G. S. Runner, w, Charleston)
- Wisconsin (C. L. Lawrence, w, Madison)

Flood-insurance studies:
- Arizona (P. L. Stiehr, w, Tucson)
- Connecticut (M. A. Cervione, Jr., w, Hartford)
- Florida (S. D. Leach, w, Tallahassee)
- Idaho (W. A. Harenberg, w, Boise)
- Illinois (G. W. Curtis, w, Champaign)
- Indiana (R. L. Miller, w, Indianapolis)
- Kansas (K. D. Medina, w, Lawrence)
- Kentucky (C. H. Hannum, w, Louisville)
- Louisiana (G. J. Wiche, w, Baton Rouge)
- Maine (R. M. Morrill, w, Augusta)
- Minnesota (G. H. Carlson, w, St. Paul)
- Missouri (L. D. Hauth, w, Rolla)
- Montana (R. J. Omang, w, Helena)
- Nebraska (G. B. Engel, w, Lincoln)
- Nevada (C. V. Schroer, w, Carson City)
- New Jersey (R. D. Schopp, w, Trenton)
- New York (R. T. Mycyk, w, Albany)
- Ohio (D. K. Roth, w, Columbus)
- Oklahoma (T. L. Huntzinger, w, Oklahoma City)
- Oregon (D. D. Harris, w, Portland)
- Pennsylvania (Andrew Voytik, w, Harrisburg)
- Puerto Rico (J. R. Harkins, w, San Juan)
- Tennessee (W. J. Randolph, w, Nashville)
- Texas (J. D. Bohn, w, Austin)
- United States (E. J. Kennedy, w, NC)
- Virginia (E. H. Mohler, w, Fairfax)
- Washington (C. H. Swift, w, Tacoma)
- Wisconsin (C. L. Lawrence, w, Madison)

Flood investigations:
- Countermeasures, scour and erosion (J. C. Bruce, w, M)
- Dating infrequent floods (R. A. Sigafoos, w, NC)
- Documentation of extreme floods (H. H. Barnes, Jr., w, NC)
- Flow frequency analysis (W. O. Thomas, w, NC)
- Hydraulics laboratory studies (V. R. Schneider, w, Bay St. Louis, Miss.)
- Model bridge-site report (H. H. Barnes, w, NC)
- Nationwide flood-frequency (A. G. Scott, w, NC)
- *States and territories:*
- Alabama, Floods, bridge-site studies (C. O. Ming, w, Montgomery)
- Arkansas (T. E. Lamb, w, Little Rock)
- Arizona, 1977–78 flood report (B. N. Aldridge, w, Tucson)
- California:
  - Flood hydrology, Butte basin (J. C. Blodgett, w, Sacramento)
  - Floods-small drainage areas (A. O. Waananen, w, M)
  - Park and monument flood risk (J. R. Crippen, w, M)

Flood investigations—Continued
States and territories—Continued
Colorado (w, D):
Floods, Elbert County (T. R. Dosch)
Foothill floods (R. C. Christensen)
Connecticut, Small stream flood characteristics (L. A. Weiss, w, Hartford)
Florida (w, Tampa):
Bridge site studies (W. C. Bridges, w, Tallahassee)
Regional flood-frequency study (M. A. Seijo)
Georgia:
Atlanta flood charactersitics (E. J. Inman, w, Doraville)
Flood and bridge site studies (McGlone Price, w, Doraville)
Urban flood-frequency (E. J. Inman, w, Doraville)
Hawaii, Special flood-data collection (R. H. Nakahara, w, Honolulu)
Idaho (W. A. Harenburg, w, Boise)
Illinois, Urban floods in northeastern Illinois (H. E. Allen, Jr., w, Dekalb)
Indiana, Flood frequency (R. L. Gold, w, Indianapolis)
Iowa (w, Iowa City):
Flood data for selected bridge sites (O. G. Lara)
Flood profiles, of Iowa streams (O. G. Lara)
Kentucky:
Small-area flood hydrology (C. E. Schoppenhorst, w, Louisville)
Hydraulics of bridge sites (C. H. Hannum, w, Louisville)
Louisiana, Roughness coefficients (G. J. Arcement, w, Baton Rouge)
Maryland, Floods—small drainage areas (D. H. Carpenter, w, Towson)
Minnesota:
Flood-plain studies (G. H. Carlson, w, St. Paul)
1979 flood—Red River (D. W. Ericson, w, Grand Rapids)
Mississippi, Multiple-bridge hydraulics (B. E. Colson, w, Jackson)
Nevada (w, Carson City):
Environmental study (P. A. Glancy)
Flood investigations (Otto Moosburner)
New Jersey:
Flood peaks and flood plains (R. O. Schopp, w, Trenton)
Somerset County (J. B. Campbell, w, Trenton)
New Mexico, Flood analysis (R. P. Thomas, w, Santa Fe)
New York, Flood investigations (Bernard Dunn, w, Albany)
Oklahoma:
Small watersheds (T. J. Huntzinger, Jr., w, Oklahoma City)
Urban flood analysis in Oklahoma City (T. L. Huntzinger, w, Oklahoma City)
Pennsylvania, Bridge waterways analysis (J. O. Shearman, w, Harrisburg)
Puerto Rico:
Eloise floods (K. G. Johnson, w, San Juan)
St. Croix flood of October 7–8, 1977 (K. G. Johnson, w, San Juan)
South Carolina, Hydraulic site reports (B. H. Whetstone) w, Columbia)
Tennessee (W. J. Randolph, w, Nashville)
Virginia:
Hydrology, Wytheville fish hatchery (J. R. Hendrick, w, Marion)
Statewide (B. J. Prugh, w, Richmond)
Washington, Flood profiles (J. E. Cummans, w, Tacoma)
Wisconsin (w, Madison):
Flood-control effects on Trout Creek (D. A. Wentz)
Flood documentation in Wisconsin (P. E. Hughes)
St. Croix scenic river waste study (C. L. Laurence)
Wyoming, Flood investigations (G. S. Craig, w, Cheyenne)

Fluorspar:
Cenozoic lacustrine deposits of the United States (R. A. Sheppard, D)
Colorado, Bonanza and Poncha Springs quadrangles (R. E. Van Alstine, NC)
Illinois-Kentucky district, regional structure and ore controls (D. M. Pinckney, D)
Foreign nations, geologic investigations:
Brazil, mineral, resources and geologic training (S. A. Stanin, Rio de Janeiro)
Poland:
Characteristics of coal basins (K. J. Englund, NC)
Geochemistry of coal and computerization of coal data (V. E. Swanson, D)
Saudi Arabia, crystalline shield, geologic and mineral reconnaissance (F. S. Simons, Jiddah)
Spain, marine mineral resources (P. D. Snavely, Jr., M)
Thailand, remote-sensing program (J. O. Morgan, Bangkok)
Foreign nations, hydrologic investigations. *See* Water resources; Foreign countries.
Fuels, organic. *See* Coal; Oil shale; Petroleum and natural gas.
Gas, natural. *See* Petroleum and natural gas.
Geochemical distribution of the elements:
Basin and Range granites (D. E. Lee, D)
Botanical exploration and research (H. L. Cannon, D)
Coding and retrieval of geologic data (T. G. Lovering, D)
Data of geochemistry (Michael Fleischer, NC)
Data systems (R. V. Mendes, D)
Element availability:
Soils (R. C. Severson, D)
Vegetation (L. P. Gough, D)
Geochemistry of belt rocks (J. J. Connor, D)
Light stable isotopes (J. R. O'Neil, M)
Phosphoria Formation, organic carbon and trace element distribution (E. K. Maughan, D)
Sedimentary rocks, chemical composition (T. P. Hill, D)
Selenium, tellurium, and thallium, geochemical exploration (H. W. Lakin, D)
Statistical geochemistry and petrology (A. T. Miesch, D)
Tippecanoe sequence, Western Craton (L. G. Schultz, D)
Trace elements in oil shale (W. E. Dean, Jr., D)
Urban geochemistry (H. A. Tourtelot, D)
Western coal regions:
Geochemical survey of rocks (R. J. Ebens, D)
Geochemical survey of soils (R. R. Tidball, D)
Geochemical survey of vegetation (J. A. Erdman, D)
Geochemical survey of waters (G. L. Feder, D)
Western energy region, Geochemistry of clinker (J. R. Herring, D)
States:
California, Sierra Nevada batholith, geochemical study (F. C. W. Dodge, M)
Colorado, Mt. Princeton igneous complex (Priestley Toulmin III, NC)
Pennsylvania, Greater Pittsburgh region, environmental geochemistry (R. P. Biggs, Carnegie)
Geochemical prospecting methods:
Application and evaluation of methods of chemical analysis to diverse geochemical environments (J. G. Viets, D)
Application of silver-gold geochemistry to exploration (H. W. Laking, D)
Botanical exploration and research (H. L. Cannon, D)
Development of effective on-site methods of chemical analysis for geochemical exploration (W. L. Campbell, D)
Elements in organic-rich material (F. N. Ward, D)

Geochemical prospecting methods—Continued
Gamma-ray spectrometry (J. A. Pitkin, D)
Geochemical characterization of metallogenic provinces and mineralized areas (G. J. Neuerburg, D)
Geochemical exploration:
Glaciated areas (H. V. Alminas, D)
Research in arctic, alpine, and subalpine regions (J. H. McCarthy, D)
Techniques:
Alpine and subalpine environments (G. C. Curtin, D)
Arid environments (M. A. Chaffee, D)
Gold composition analysis in mineral exploration (J. C. Antweiler, D)
Instrumentation development (R. C. Bigelow, D)
Jasperoid, relations to ore deposits (T. G. Lovering, D)
Lateritic areas, southern Appalachian Mountains (W. R. Griffitts, D)
Mercury, geochemistry (A. P. Pierce, D)
Mineral exploration methods (G. B. Gott, D)
Mineralogical techniques in geochemical exploration (Theodore Botinelly, D)
New mineral storage and identification program (George Van Trump, Jr., D)
Ore-deposit controls (A. V. Heyl, Jr., D)
Pattern recognition and clustering methods for the graphical analysis of geochemical data (J. B. Fife, D)
Research in methods of spectrographic analysis for geochemical exploration (E. L. Mosier, D)
Sulfides, accessory in igneous rocks (G. J. Neuerberg, D)
Surface and ground water in geochemical exploration (G. A. Nowlan, D)
Volatile elements and compounds in geochemical exploration (M. E. Hinkle, D)
Volatile elements released by natural coal burning and baking of overlying rocks (J. R. Herring, D)
States:
Alaska, Geochemical exploration techniques (G. C. Curtin, D)
New Mexico, Basin and Range part, geochemical reconnaissance (W. R. Griffitts, D)
Geochemistry, experimental:
Coal combustion and rock metamorphism (J. R. Herring, D)
Combustion metamorphism (J. R. Herring, D)
Environment of ore deposition (P. B. Barton, Jr., NC)
Experimental mineralogy (R. O. Fournier, M)
Fluid inclusions in minerals (Edwin Roedder, NC)
Fluid zonation in metal deposits (J. T. Nash, M)
Geochemistry of clinker (J. R. Herring, D)
Geologic thermometry (J. S. Huebner, NC)
Hydrothermal alteration (J. J. Hemley, NC)
Impact metamorphism (E. C. T. Chao, NC)
Kinetics of igneous processes (H. R. Shaw, NC)
Late-stage megmatic processes (G. T. Faust, NC)
Mineral equilibria, low temperature (E-an Zen, NC)
Neutron activation (F. E. Senftle, NC)
Oil shale:
Colorado, Utah, and Wyoming (W. E. Dean, Jr., D)
Organic geochemistry (R. E. Miller, D)
Organic geochemistry (J. G. Palacas, D)
Organometallic complexes, geochemistry (Peter Zubovic, NC)
Solution-mineral equilibria (C. L. Christ, M)
Stable isotopes and ore genesis (R. O. Rye, D)
Statistical geochemistry (A. T. Miesch, D)
Geochemistry, water:
Chemical constituents of ground water (William Back, w, NC)
Chemical reactions at mineral surfaces (J. D. Hem, w, M)
Chemistry of hydrosolic metals (J. D. Hem, w, M)
Geochemistry, water—Continued
Computer modeling of rock-water interactions (J. L. Haas, Jr., NC)
Elements, distribution in fluvial and brackish environments (V. C. Kennedy, w, M)
Factors determining solute transfer in the unsaturated zone (Jacob Rubin, w, M)
Gases, complexes in water (D. W. Fischer, w, NC)
Geochemistry of geothermal systems (Ivan Barnes, w, M)
Geochemistry of San Francisco Bay waters and sediments (D. H. Peterson, w, M)
Geologic perspectives—global carbon dioxide (E. T. Sundquist, w, NC)
Geothermal trace-element reactions (E. A. Jenne, w, M)
Hydrologic studies of paleoclimate (B. B. Hanshaw, w, NC)
Interaction of minerals and water in saline environments (B. F. Jones, w, NC)
Interface hydrochemistry and paleoclimatology (I. J. Winograd, w, NC)
Mineralogic controls of the chemistry of ground water (B. B. Hanshaw, w, NC)
Organic geochemistry (R. L. Malcolm, w, D)
Redox reactions (D. C. Thorstenson, w, NC)
Trace-element partitioning (E. A. Jenne, w, M)
Uranium mill tailings (E. R. Landa, w, NC)
Water-clinker interactions (J. R. Herring, D)
See also Quality of water.
Geochemistry and petrology, field studies:
Basalt, genesis (T. L. Wright, NC)
Basin and Range granites (D. E. Lee, D)
Epithermal deposits (R. G. Worl, D)
Geochemical studies in southeastern States (Henry Bell III, NC)
Geochemistry of clinker (J. R. Herring, D)
Geochemistry of diagenesis (K. J. Murata, M)
Geochemistry of marine sediments (W. E. Dean, D)
Geochemistry of Tippecanoe Sequence, Western Craton (L. G. Schultz, D)
Inclusions in basaltic rocks (E. D. Jackson, M)
Layered Dufek intrusion, Antarctica (A. B. Ford, M)
Layered intrusives (N. J. Page, M)
Mercury, geochemistry and occurrence (A. P. Pierce, D)
Nobium and tantalum, distribution in igneous rocks (David Gottfried, NC)
Organic petrology of sedimentary rocks (N. H. Bostick, D)
Petrogenesis and metallogeny—western U.S. volcanic belts and ore deposits (C. M. Conway, M)
Rare-earth elements, resources and geochemistry (J. W. Adams, D)
Regional geochemistry (W. E. Dean, Jr., D)
Regional metamorphic studies (H. L. James, M)
Residual minor elements in igneous rocks and veins (George Phair, NC)
Solution transport of heavy metals (G. K. Czamanske, M)
Submarine volcanic rocks, properties (J. G. Moore, M)
Thermal waters, origin and characteristics (D. E. White, M)
Trace elements in oil shale (W. E. Dean, Jr., D)
Trondhjemites, major and minor elements, isotopes (Fred Barker, D)
Ultramafic rocks, petrology of alpine types (R. G. Coleman, M)
Uranium, radon and helium—gaseous emanation detection (G. M. Reimer, D)
Western coal regions:
Geochemical survey of rocks (R. J. Ebens, D)
Geochemical survey of soils (R. R. Tidball, D)

Geochemistry and petrology, field studies—Continued
- Western coal regions-Continued
  - Geochemical survey of vegetation (J. A. Erdman, D)
  - Geochemistry of clinker (J. R. Herring, D)
- Western energy regions:
  - Element availability—plants (L. P. Gough, D)
  - Element availability—rocks (J. M. McNeal, D)
  - Element availability—soils (R. C. Severson, D)
  - Geochemistry of clinker (J. R. Herring, D)
- *States:*
- Alaska (M):
  - La Perouse layered intrusion (R. A. Loney)
  - Metasedimentary and metaigneous rocks, southwestern Brooks Range (I. L. Tailleur)
  - Petersburg quadrangle (D. A. Brew)
- Arizona (M):
  - Ray program:
    - Mineral Mountain (T. G. Theodore)
    - Silicate mineralogy, geochemistry (N. G. Banks)
  - Stocks (S. C. Creasey)
- California:
  - Geochemistry of sediments, San Francisco Bay (D. S. McCulloch, M)
  - Granitic rocks of Yosemite National Park (D. L. Peck, NC)
  - Kings Canyon National Park (J. G. Moore, M)
  - Long Valley Caldera-Mono Craters volcanic rocks (R. A. Bailey, NC)
  - Sierra Nevada xenoliths (J. P. Lockwood, M)
- Colorado:
  - Geochemistry of clinker (J. R. Herring, D)
  - Petrology of Mt. Princeton igneous complex (Priestley Toulmin III, NC)
  - Tertiary-Laramide intrusives (E. J. Young, D)
- Hawaii, Ankaramites (M. H. Beeson, M)
- Idaho, Wood River district (W. E. Hall, M)
- Idaho-Montana-Wyoming, Petrology of the Yellowstone Plateau volcanic field (R. L. Christiansen, M)
- Montana:
  - Diatremes, Missouri River Breaks (B. C. Hearn, Jr., NC)
  - Geochemistry of clinker (J. R. Herring, D)
  - Geochronology, north-central Montana (B. C. Hearn, Jr., NC; R. F. Marvin, R. E. Zartman, D)
  - Wolf Creek area, petrology (R. G. Schmidt, NC)
- Nevada, Igneous rocks and related ore deposits (M. L. Silberman, M)
- New Mexico, Geochemistry of clinker (J. R. Herring, D)
- Pennsylvania, Geochemistry of Pittsburgh urban area (H. A. Tourtelot, D)
- South Dakota, Keystone pegmatite area (J. J. Norton, Rapid City)
- Wyoming, Geochemistry of clinker (J. R. Herring, D)

Geochronological investigations:
- Carbon-14 method (Meyer Rubin, NC)
- Geochronology and rock magnetism (G. B. Dalrymple, M)
- Geochronology of uranium ores and their host rocks (K. R. Ludig, D)
- Igneous rocks and deformational periods (R. W. Kistler, M)
- Lead-uranium, lead-thorium, and lead-alpha methods (T. W. Stern, NC)
- Magnetic chronology, Colorado Plateau and environs (D. P. Elston, E. M. Shoemaker, Flagstaff, Ariz.)
- Quaternary dating techniques, numerical and relative-age (K. L. Pierce, D)
- Radioactive-disequilibriun studies (J. N. Rosholt, D)
- San Francisco volcanic field (P. E. Damon, University of Arizona)

Geochronological investigations—Continued
- *States:*
- Alaska, K-Ar dates, southwest Brooks Range (I. L. Tailleur, M; R. B. Forbes, D. L. Turner, Fairbanks)
- Colorado, Geochronology of Denver area (C. E. Hedge, D)
- *See also* Isotope and nuclear studies.

Geologic mapping:
- Map scale smaller than 1:62,500:
  - Antarctica, Dufek Massif and Forrestal Range, Pensacola Mountains (A. B. Ford, M)
  - Belt basin study (J. E. Harrison, D)
  - Columbia River basalt (D. A. Swanson, M)
  - Engineering geology map of the U.S. (D. H. Radbruch-Hall, M)
  - *States:*
  - Alaska (M):
    - Ambler River and Baird Mountains quadrangles (I. L. Tailleur)
    - Charley River quadrangle (E. E. Brabb)
    - Craig quadrangle (G. D. Eberlein, Michael Churkin, Jr.)
    - Delong Mountains quadrangle (I. L. Tailleur)
    - Geologic map (H. M. Beikman)
    - Glacier Bay National Monument (D. A. Brew)
    - Hughes-Shungnak area (W. W. Patton, Jr.)
    - Iliamna quadrangle (R. L. Detterman)
    - Juneau and Taku River quadrangles (D. A. Brew)
    - Metamorphic facies map (D. A. Brew)
    - Natural landmarks investigation (R. L. Detterman)
    - Petersburg quadrangle (D. A. Brew)
    - St. Lawrence Island (W. W. Patton, Jr.)
  - Arizona (Flagstaff):
    - North-central part (D. P. Elston)
    - Phoenix 2° quadrangle (T. N. V. Karlstrom)
    - Shivwits Plateau (Ivo Lucchitta)
  - Arkansas (B. R. Haley, Little Rock)
  - California, Tectonic studies, Great Valley area (J. A. Bartow, D. E. Marchand)
  - Colorado (D):
    - Colorado Plateau geologic map (D. D. Haynes)
    - Denver 2° quadrangle (B. H. Bryant)
    - Geologic map (O. L. Tweto)
    - Greeley 2° quadrangle, western half (W. A. Braddock)
    - Leadville 2° quadrangle (O. L. Tweto)
    - Pueblo 2° quadrangle (G. R. Scott)
    - Sterling 2° quadrangle (G. R. Scott)
  - Idaho (D):
    - Challis Volcanics (D. H. McIntyre)
    - Dubois 2° quadrangle (M. H. Hait and B. A. Skipp)
    - Idaho Falls 2° quadrangle (M. A. Kuntz)
    - Preston 2° quadrangle (S. S. Oriel)
    - Snake River Plain, central part, volcanic petrology (H. E. Malde)
    - Snake River Plain region, eastern part (S. S. Oriel)
  - Missouri, Rolla 2° quadrangle, mineral-resource appraisal (W. P. Pratt, D)
  - Montana, White Sulphur Springs 2° quadrangle (M. W. Reynolds, D)
  - Nevada:
    - Elko County:
      - Central (K. B. Ketner, D)
      - Countywide (R. A. Hope, M)
      - Western (R. R. Coats, M)
    - Geologic map (J. H. Stewart, M)
    - Lincoln County, Tertiary rocks (G. L. Dixon, D)

Geologic mapping—Continued:
Map scale smaller than 1:62,500—Continued
States—Continued
New Jersey, Pennsylvania, New York, Newark 2° quadrangle (A. A. Drake, Jr., NC)
New Mexico (D):
North Church Rock area (A. R. Kirk)
Sanostee (A. C. Huffman, Jr.)
Santa Fe 2° quadrangle, western half (E. H. Baltz, Jr.)
Socorro 2° quadrangle, (G. O. Bachman)
North Carolina, Charlotte 2° sheet (Richard Goldsmith, NC)
South Carolina, Charlotte 2° sheet (Richard Goldsmith, NC)
South Carolina, Georgia, North Carolina, Greenville 2° quadrangle (A. E. Nelson, NC)
Utah (M):
Delta 2° quadrangle (H. T. Morris)
Richfield 2° quadrangle (T. A. Steven, P. D. Rowley)
Tooele 2° quadrangle (W. J. Moore)
Wasatch Front surficial geology (R. D. Miller, D)
Wasatch-Uinta tectonics, Salt Lake City and Ogden 2° quadrangles (B. H. Bryant, D)
Washington, Wenatchee 2° sheet (R. W. Tabor, R. B. Waitt, Jr., V. A. Frizzell, Jr., M)
Wyoming:
Geologic map (J. D. Love, Laramie)
Preston 2° quadrangle (S. S. Oriel, D)
Wasatch-Uinta tectonics, Ogden 2° quadrangle (B. H. Bryant, D)
Teton Wilderness (J. D. Love, Laramie)
Map scale 1:62,500 and larger:
States and territories:
Alaska:
Anatuvuk Pass (G. B. Shearer, c, Anchorage)
Bering River coal field (R. B. Sanders, c, Anchorage)
Geology and mineral resources of the Ketchikan quadrangle (H. C. Berg, M)
Nelchina area, Mesozoic investigations (Arthur Grantz, M)
Nenana coal investigations (Clyde Wahrhaftig, M)
Nome area (C. L. Hummel, M)
Regional engineering geology of Cook Inlet coal lands (H. R. Schmoll and L. A. Yehle, D)
West Chichagof-Yakobi Islands (B. R. Johnson, M)
Arizona:
Bagdad, vicinity of Old Dick and Bruce mines (C. M. Conway, M)
Cummings Mesas quadrangle (Fred Peterson, D)
Hackberry Mountain area (D. P. Elston, Flagstaff)
Mazatzal Wilderness (C. M. Conway and C. T. Wrucke, M)
Mt. Wrightson quadrangle (H. D. Drewes, D)
Ray district, porphyry copper (H. R. Cornwall, M)
Sedona area (D. P. Elston, Flagstaff)
Western Arizona, tectonic studies (Ivo Lucchitta, Flagstaff)
California (M, except as otherwise noted):
Coast Range, ultramafic rocks (E. H. Bailey)
Condrey Mountain and Hornbrook quadrangles (P. E. Hotz)
King Range-Chemise area (R. J. McLaughlin)

Geologic mapping—Continued
Map scale 1:62,500 and larger—Continued
States and territories—Continued
California (M, except as otherwise noted)—Continued
Long Valley caldera (R. A. Bailey, NC)
Merced Peak quadrangle (D. L. Peck, NC)
Northern Coast Ranges (K. F. Fox, Jr.)
Pacific Palisades landslide area, Los Angeles (J. T. McGill, D)
Palo Alto, San Mateo, and Montara Mountain quadrangles (E. H. Pampeyan)
Peninsular Ranges (V. R. Todd, La Jolla)
Regional fault studies (E. J. Helley, D. G. Herd, B. F. Atwater)
Ryan quadrangle (J. F. McAllister)
Santa Lucia Range (V. M. Seiders)
Searles Lake area (G. I. Smith)
Sierra Nevada batholith (P. C. Bateman)
The Geysers-Clear Lake area (R. J. McLaughlin)
Western Santa Monica Mountains (R. H. Campbell)
Colorado (D, except as otherwise noted):
Barcus Creek quadrangle (W. J. Hail)
Barcus Creek SE quadrangle (W. J. Hail)
Bonanza quadrangle (R. E. Van Alstine, NC)
Central City area (R. B. Taylor)
Citadel Plateau (G. A. Izett)
Coal mine deformation studies, Somerset mining district (C. R. Dunrud)
Cochetopa area (J. C. Olson)
Denver metropolitan area (R. M. Lindvall)
Desert Gulch quadrangle (R. C. Johnson)
Disappointment Valley, geology and coal resources (D. E. Ward)
Middle Dry Fork quadrangle (R. C. Johnson)
Northern Park Range (G. L. Snyder)
Poncha Springs quadrangle (R. E. Van Alstine, NC)
Rocky Mountain National Park (W. A. Braddock)
Rustic quadrangle (K. L. Shaver)
Ward and Gold Hill quadrangles (D. J. Gable)
Connecticut, Cooperative mapping program (M. H. Pease, Jr., Boston, Mass.)
Georgia, Macon-Gordon district (S. H. Patterson, NC)
Idaho (D, except as otherwise noted):
Bayhorse area (S. W. Hobbs)
Black Pine Mountains (J. F. Smith, Jr.)
Boulder Mountains (C. M. Tschanz)
Goat Mountain quadrangle (M. H. Staatz)
Grouse quadrangle (B. A. Skipp)
Hawley Mountain quadrangle (W. J. Mapel)
Malad SE quadrangle (S. S. Oriel)
Montour quadrangle (H. E. Malde)
Patterson quadrangle (E. T. Ruppel)
Strevell quadrangle (J. F. Smith)
Upper and Lower Red Rock Lake quadrangles (I. J. Witkind)
Wood River district (W. E. Hall, M)
Yellow Pine quadrangle (B. F. Leonard)
Kentucky, cooperative mapping program (E. R. Cressman, Lexington)
Maine:
Blue Hill quadrangle (D. B. Stewart, NC)
Castine quadrangle (D. B. Stewart, NC)
Orland quadrangle (D. R. Wones, NC)
Rumford quadrangle (R. H. Moench, D)
The Forks quadrangle (F. C. Canney, D)

Geologic mapping—Continued
Map scale 1:62,500 and larger—Continued
States and territories—Continued
Maryland (NC):
Delmarva Peninsula (J. P. Owens)
Northern Coastal Plain (J. P. Minard)
Western Maryland Piedmont (M. W. Higgins)
Massachusetts:
Boston and vicinity (C. A. Kaye, Boston)
Cooperative mapping program (J. O. Peper, NC)
Michigan, Gogebic Range, western part (R. G. Schmidt, NC)
Minnesota, Vermilion greenstone belt (P. K. Sims, D)
Montana:
Cooke City quadrangle (J. E. Elliott, D)
Craig quadrangle (R. G. Schmidt, NC)
Crazy Mountains Basin (B. A. Skipp, D)
Elk Park quadrangle (H. W. Smedes, D)
Lemhi Pass quadrangle (M. H. Staatz, D)
Melrose quadrangle (H. W. Smedes and G. D. Fraser, D)
Northern Pioneer Range, geologic environment (E-an Zen, NC)
Wolf Creek area, petrology (R. G. Schmidt, NC)
Nebraska, McCook 2° quadrangle (G. E. Prichard, D)
Nevada:
Austin quadrangle (E. H. McKee, M)
Bellevue Peak quadrangle (T. B. Nolan, NC)
Carlin region (J. F. Smith, Jr., D)
Jordan Meadow and Disaster Peak quadrangles (R. C. Greene, M)
Kobeh Valley (T. B. Nolan, NC)
Midas-Jarbridge area (R. R. Coats, M)
Round Mountain and Manhattan quadrangles (D. R. Shawe, D)
New Mexico:
Acoma area (C. H. Maxwell, D)
Alma quadrangle (J. C. Rattë, D)
Bull Basin quadrangle (J. C. Rattë, D)
Church Rock-Smith Lake (C. T. Pierson, D)
Cretaceous stratigraphy, San Juan Basin (E. R. Landis, D)
Dillon Mountain quadrangle (J. C. Rattë, D)
Glenwood quadrangle (J. C. Rattë, D)
Hillsboro quadrangle (D. C. Hedlund, D)
Holt Mountain quadrangle (J. C. Rattë, D)
Iron Mountain (A. V. Heyl, Jr., D)
Laguna Peak (J. L. Ridgley, D)
Manzano Mountains (D. A. Myers, D)
Mongollon quadrangle (J. C. Rattë, D)
O-Block Canyon quadrangle (J. C. Rattë, D)
Pinos Altos Range (T. L. Finnell, D)
Raton coal basin, western part (C. L. Pillmore, D)
Reserve quadrangle (J. C. Rattë, D)
Saliz Pass quadrangle (J. C. Rattë, D)
Valles Mountains, petrology (R. L. Smith, NC)
New York, Geologic correlations and mineral resources in Precambrian rocks of St. Lawrence lowlands (C. E. Brown, NC)
North Carolina, central Piedmont (A. A. Stromquist, D)
Pennsylvania (NC):
Northern anthracite field (M. J. Bergin)
Southern anthracite field (G. H. Wood, Jr.)
Wind Gap and adjacent quadrangles (J. B. Epstein)
Puerto Rico (R. D. Krushensky, NC)

Geologic mapping—Continued
Map scale 1:62,500 and larger—Continued
States and territories—Continued
South Dakota:
Black Hills Precambrian (J. A. Redden, Hill City)
Keystone pegmatite area (J. J. Norton, Rapid City)
Medicine Mountain quadrangle (J. C. Rattë, D)
Texas:
Agency Draw NE quadrangle (G. N. Pipiringos, D)
Bates Knolls quadrangle (G. N. Pipiringos, D)
Tilden-Loma Alta area (K. A. Dickinson, D)
Utah (c, D, unless otherwise noted):
Basin Canyon quadrangle (Fred Peterson)
Blackburn Canyon quadrangle (Fred Peterson)
Confusion Range (R. K. Hose, M)
Matlin Mountains (V. R. Todd, M)
Ogden 4 NW quadrangle (R. J. Hite)
Salt Lake City and vicinity (Richard VanHorn, D)
Sheeprock Mountains, West Tintic district (H. T. Morris, M)
Sunset Flat quadrangle (Fred Peterson)
Wah Wah Summit quadrangle (L. F. Hintze, Salt Lake City)
Wasatch Front surficial geology (R. D. Miller, D)
Willard Peak area (M. D. Crittenden, Jr., M)
Virginia (NC):
Culpeper Basin (K. Y. Lee)
Delmarva Peninsula (J. P. Owens)
Northern Blue Ridge (G. H. Espenshade)
Rapidan-Rappahannock (Louis Pavlides)
Washington:
Chewelah No. 4 quadrangle (F. K. Miller, M)
Glacier Park area (F. W. Cater, Jr., D)
Northern Okanogan Highlands (C. D. Rinehart, M)
Olympic Peninsula, eastern part (W. M. Cady, D)
Stevens County (R. G. Yates, M)
Togo Mountain quadrangle (R. C. Pearson, D)
Wisconsin, Black River Falls and Hatfield quadrangles (Harry Klemic, NC)
Wyoming (c, D, unless otherwise noted):
Albany and Keystone quadrangles (M. E. McCallum, D)
Alkali Butte quadrangle (M. W. Reynolds, D)
Badwater Creek (R. E. Thaden, D)
Devils Tooth quadrangle (W. G. Pierce, M)
Eagle Peak quadrangle (H. W. Smedes and H. J. Prostka, D)
Fortin Draw quadrangle (B. E. Law)
Gillette East quadrangle (B. E. Law)
Grand Teton National Park (J. D. Love, Laramie)
Gros Ventre Range (F. S. Simons)
Moyer Springs quadrangle (B. E. Law)
Oriva quadrangle (B. E. Law)
Two Ocean Pass quadrangle (H. W. Smedes, D)
Wapiti quadrangle (W. G. Pierce, M)

Geologic-related hazards:
Hazards warning, preparedness, and technical assistance (J. C. Stephens, I, NC)

Geomagnetism:
External geomagnetic-field variations (W. H. Campbell, D)
Geomagnetic-data analysis (C. O. Stearns, D)
Geomagnetic observatories (J. D. Wood, D)
Geomagnetic secular variation (L. R. Alldredge, D)
Magnetic-field analysis and U.S. charts (E. B. Fabiano, D)
World magnetic charts and analysis (E. B. Fabiano, D)

Geomorphology:
- Morphology, provenance, and movement of desert sand (E. D. McKee, D)
- Quaternary landforms and deposits interpreted from Landsat 1 imagery, Midwest and Great Plains (R. B. Morrison, D)
- *States:*
- Arizona, Post-1890 A.D. erosion features interpreted from Landsat 1 imagery (R. B. Morrison, D)
- Colorado, Hydraulics of stream channels (E. D. Andrews, w, D)
- Florida, Geohydrology of sinkholes (W. C. Sinclair, w, Tampa)
- Idaho, Surficial geology of eastern Snake River Plain (W. E. Scott, M. D. Hait, Jr., D)
- New Mexico, Chaco Canyon National Monument (H. E. Malde, D)
- Utah, Quaternary geology (W. E. Scott, D)
- Wyoming (D):
  - Wind River Mountains, Quaternary geology (G. M. Richmond)
  - Yellowstone National Park, glacial and postglacial geology (G. M. Richmond)
- *See also* Sedimentology; Geochronological investigations.

Geophysics, regional:
- Airborne and satellite research:
  - Aeromagnetic studies (M. F. Kane, D)
  - Electromagnetic research (F. C. Frischknecht, D)
  - Gamma-ray research (J. S. Duval, D)
  - Regional studies (Isidore Zietz, NC)
- Antarctic, Pensacola Mountains, geophysical studies (J. C. Behrendt, Woods Hole, Mass.)
- Basin and Range geophysical studies (W. E. Davis, M)
- Crust and upper mantle:
  - Aeromagnetic interpretation of metamorphic rocks (Isidore Zietz, NC)
  - Aeromagnetic studies of the United States (Isidore Zietz, NC)
  - Analysis of traveltime data (J. C. Roller, M)
  - Seismicity and Earth structure (J. N. Taggart, D)
  - Seismologic studies (J. P. Eaton, M)
- Engineering geophysics (H. D. Ackermann, D)
- Florida Continental Shelf, gravity studies (H. L. Krivoy, NC)
- Gravity surveys:
  - Dona Ana, Otero, Lincoln, Sierra, and Socorro Counties, New Mexico (D. L. Healey, D)
  - Maryland cooperative (D. L. Daniels, NC)
- Ground-water geophysics (W. D. Stanley, D)
- Magnetic chronology, Colorado Plateau and environs (D. P. Elston, E. M. Shoemaker, Flagstaff, Ariz.)
- Mobile magnetometer profiles, Eastern United States (M. F. Kane, D)
- New England, magnetic properties of rocks (Andrew Griscom, M)
- Program and systems development (G. I. Evenden, W. L. Anderson, D)
- Ramier Mesa (J. R. Ege)
- Rocky Mountains, northern (D. L. Peterson, M. D. Kleinkopf, D)
- Southeastern States geophysical studies (Peter Popenoe, NC)
- Southwestern States geophysical studies (D. L. Peterson, NC)
- Thermal modeling investigations (Kenneth Watson, D)
- Ultramafic rocks, geophysical studies, intrusions (G. A. Thompson, M)
- United States, aeromagnetic surveys (E. R. King, NC)

Geophysics, regional—Continued
- *States and territories:*
- Alaska, Ambler River and Baird Mountains quadrangles, gravity studies (D. F. Barnes, M)
- California, Sierra Nevada, geophysical studies (H. W. Oliver, M)
- Idaho, Snake River Plain (D. L. Peterson, D)
- Massachusetts, Geophysical studies (M. F. Kane, NC)
- Minnesota (NC):
  - Keweenawan rocks, magnetic studies (K. G. Books)
  - Southern part, aeromagnetic survey (E. R. King)
- Nevada, Engineering geophysics, Nevada Test Site (R. D. Carroll, D)
- New Mexico, Rio Grande graben (L. E. Cordell, D)
- Pennsylvania, Magnetic properties of rocks (Andrew Griscom, M)
- Puerto Rico, Seismicity of Puerto Rico (A. C. Tarr, D)

Geophysics, theoretical and experimental:
- Borehole electrical techniques in uranium exploration (J. J. Daniels, D)
- Borehole geophysical research in uranium exploration (J. H. Scott, D)
- Earthquakes, local seismic studies (J. P. Eaton, M)
- Elastic and inelastic properties of Earth materials (Louis Peselnick, M)
- Electrical properties of rocks (R. D. Carroll, D)
- Electrical resistivity studies (A. A. R. Zohdy, D)
- ERDA/DOE geothermal petrophysics (G. R. Olhoeft, D)
- Experimental rock mechanics (C. B. Raleigh, M)
- Gamma-ray spectrometry in uranium (J. S. Duval, D)
- Gamma-ray spectrometry for uranium exploration in crystalline terranes (J. A. Pitkin, D)
- Geophysical data, interpretation using electronic computers (R. G. Henderson, NC)
- Geophysical studies for engineering geology (C. H. Miller, D)
- Geophysical studies relating to uranium deposits in crystalline terranes (D. L. Campbell, D)
- Ground-motion studies (J. H. Healy, M)
- Infrared and ultraviolet radiation studies (R. M. Moxham, NC)
- Magnetic and luminescent properties (F. E. Senftle, NC)
- Magnetic Properties Laboratory (M. E. Beck, Jr., Bellingham, Wash.)
- Microwave studies (A. W. England, D)
- Mineral Research Petrophysics (G. R. Olhoeft, D)
- NASA, electrical properties for the detection and mapping of waters on Mars (G. R. Olhoeft, D)
- NASA, laboratory microwave-, radar-, and thermal-emission-studies of basalt soil in vacuum (G.R. Olhoeft, D)
- Paleomagnetism, Precambrian and Tertiary chronology (D. P. Elston, Flagstaff, Ariz.)
- Petrophysics-geothermal (G. R. Olhoeft, D)
- Remanent magnetization of rocks (C. S. Gromné, M)
- Resistivity interpretation (A. A. R. Zohdy, D)
- Rock behavior at high temperature and pressure (E. C. Robertson, NC)
- Seismicity patterns in time and space (C. G. Bufe, M)
- Stress studies (C. B. Raleigh, M)
- Theory of gamma rays for geological applications (J. S. Duval, D)
- Thermal modeling investigations (Kenneth Watson, D)
- Thermodynamic properties of rocks (R. A. Robie, NC)
- Ultramafic intrusions, geophysical studies (G. A. Thompson, M)
- Uranium geophysics in frontier areas (J. W. Cady, D)
- Uranium petrophysics (G. R. Olhoeft, D)
- Volcano geophysics (E. T. Endo, M)

Geophysics, theoretical and experimental—Continued
States:
California, Mass properties of oil-field rocks (L. A. Beyer, M)
Nevada (D):
Nevada Test Site:
Interpretation of geophysical logs (R. D. Carroll)
Seismic velocity measuring techniques (R. D. Carroll)
Vermont, in-situ stress in a granite quarry (G. E. Brethauer, D)

Geotechnical investigations:
Computer modeling research for engineering geology (W. Z. Savage, D)
Dynamic soil behavior (A. T. F. Chen, M)
Earthquake-induced landslides (E. L. Harp, M)
Electronics instrumentation research for engineering geology (J. B. Bennetti, Jr., D)
Experimental liquefaction potential mapping (T. L. Youd, M)
Fissuring-subsidence research (T. L. Holzer, M)
Geomechanics of radioactive waste storage (H. S. Swolfs, D)
Geotechnical measurements and services (H. W. Olsen, D)
Ground failure related to the New Madrid earthquake (S. F. Obermeier, NC)
In-situ stress in shales (T. C. Nichols, Jr., D)
Interaction of ground motion and ground failure (R. C. Wilson, M)
Marine geotechnique (H. W. Olsen, D)
In-situ stress (T. C. Nichols, Jr., D)
Miscellaneous landslide investigations (R. W. Fleming, D)
Open-pit slope stability (W. K. Smith, D)
Research in rock mechanics (F. T. Lee, D)
Solution subsidence and collapse (J. R. Ege, D)
States:
Alaska, Regional engineering geology of Cook Inlet coal lands, Alaska (H. R. Schmoll and L. A. Yehle, D)
Colorado, Coal mine deformation at Somerset (C. R. Dunrud, D)
Montana-Wyoming, Regional geotechnical studies, Powder River Basin (S. P. Kanizay, D)
Virginia, Reston (S. F. Obermeir, NC)
Wyoming, Coal mine deformation studies, Powder River Basin (C. R. Dunrud, D)

Geothermal investigations:
Broad-band electrical surveys (Mark Landisman, University of Texas)
Colorado Plateau, potential field methods (R. R. Wahl, D)
Convection and thermoelastic effects in narrow vertical fracture spaces:
Analytical techniques (Gunnar Bodvarsson, Oregon State University)
Numerical techniques (R. P. Lowell, Georgia Institute of Technology)
Development of first-motion holography for exploration (Keiiti Aki, Massachusetts Institute of Technology)
Electrical and electromagnetic methods in geothermal areas (D. B. Jackson, D)
Evaluation of intermediate-period seismic waves as an exploration tool (D. M. Boore, Stanford University)
Evaluation of noble gas studies in exploration (Emanuel Mazor, Weizmann Institute of Science, Rehovot, Israel)
Exploration and characterization from seismic activity (E. A. Page, ENSCO, Inc.)
Geochemical exploration (M. E. Hinkle, D)
Geochemical indicators (A. H. Truesdell, M)
Geochemistry of geopressured systems (Y. K. Kharaka, w, M)
Geophysical characterization of young silicic volcanic centers, eastern Sierran Front (W. F. Isherwood, D)
Geothermal, Coachella Valley (J. H. Robison, w, M)

Geothermal investigations—Continued
Geothermal coordination (F. H. Olmsted, w, M)
Geothermal geophysics (D. R. Mabey, D)
Geothermal hydrologic reconnaissance (F. H. Olmsted, w, M)
Geothermal investigations (H. W. Young, w, Boise, Idaho)
Geothermal petrophysics (G. R. Olhoeft, D)
Geothermal reservoirs (Manuel Nathenson, M)
Geothermal resource assessment (L. J. P. Muffler, M)
Geothermal studies (A. H. Lachenbruch, M)
Gravity variations as a monitor of water levels (J. M. Goodkind, University of California, San Diego)
Heat flow (J. H. Sass, A. H. Lachenbruch, M)
Isotopic and chemical studies of geothermal gases (Harmon Craig, University of California, San Diego)
Low-frequency electromagnetic prospecting system (J. Clarke and H. F. Morrison, University of California, Berkeley)
Mercury geochemistry as a tool for geothermal exploration (P. R. Buseck, Arizona State University)
Oxygen isotopes (J. R. O'Neil, M)
Physics of geothermal systems (W. H. Diment, M)
Radioactivity series isotopic disequilibrium (J. K. Osmond and J. B. Cowart, Florida State University)
Regional geoelectromagnetic traverse (J. F. Hermance, Brown University)
Regional volcanology (R. L. Smith, NC)
Remote sensing (Kenneth Watson, D)
Rock-water interactions (R. O. Fournier, M)
Seismic exploration (P. L. Ward, M)
Signal processing methods for magnetotellurics (W. C. Hernandez, ENSCO, Inc.)
Statistical characteristics of geothermal resources, Basin and Range province (W. F. Isherwood, D)
Thermal waters (D. E. White, M)
Western United States—geothermal waters (R. H. Mariner, w, M)
States:
Alaska, Geothermal reconnaissance (T. D. Miller, M)
Arizona:
Geothermal water: Salt River Valley (R. P. Ross, w, Flagstaff), Verde Valley (P. P. Ross, w, Flagstaff)
San Francisco volcanic field (E. W. Wolfe, Flagstaff)
California:
Coso area, passive seismology (P. A. Reasenberg, M)
Geology of Long Valley-Mono basin (R. A. Bailey, NC)
Long Valley, Active seismology (D. P. Hill, M)
Medicine Lake Volcano (J. R. Donnelly-Nolan, M)
Mercury in soils of geothermal areas (R. W. Klusman, Colorado School of Mines)
Microearthquake monitoring:
Imperial Valley (D. P. Hill, M)
The Geysers-Clear Lake (C. G. Bufe, M)
Mt. Lassen thermal areas (L. J. P. Muffler, M)
The Geysers area, seismic noise (H. M. Iyer, M)
The Geysers-Clear Lake (B. C. Hearn, Jr., NC)
The Geysers-Clear Lake area, pre-Tertiary geology (R. J. McLaughlin, M)
Colorado:
Colorado geothermal (R. E. Moran, w, D)
Geochemical and hydrological parameters of geothermal systems (R. H. Pearl, Colorado Geological Survey)
Geothermal resources (G. L. Galyardt, c, D)
Relationship between geothermal resources and ground water (J. C. Romero, Colorado Geological Survey)
Georgia, Heat flow and radioactive heat generation studies in Southeastern United States (D. L. Smith, University of Florida)

Geothermal investigations—Continued

States—Continued

Hawaii, Kilauea Volcano, potential field methods for subsurface magma mapping (C. J. Zablocki, D)

Idaho:

Raft River surface and subsurface geology (H. R. Covington, D)

Snake River Plain surface and subsurface geology (M. A. Kuntz, D)

Sugar City area (H. J. Prostka, D)

Montana:

Geothermal investigations in Montana (R. B. Leonard, w, Helena)

Geothermal reconnaissance in southwestern Montana (R. A. Chadwick, Montana State University)

Nevada:

Geothermal reconnaissance (R. K. Hose, M)

Black Rock desert geothermal (A. H. Welch, w, Carson City)

New Mexico, Evaluation of geothermal potential of the Basin and Range province (G. P. Landis, University of New Mexico)

Oregon:

Geophysical investigation of the Cascade Range (R. W. Couch, Oregon State University)

Geophysical investigations of the Vale-Owyhee geothermal region (R. W. Couch, Oregon State University)

Geothermal reconnaissance (N. S. MacLeod, M)

Hydrologic reconnaissance of geothermal areas (E. A. Sammel, w, M)

Hydrothermal alteration, Cascades (M. H. Beeson, M)

Utah:

Geothermal reconnaissance in Utah (F. E. Rush, w, Salt Lake City)

Geothermal resources (G. L. Galyardt, c, D)

Petrology and geochronology of late Tertiary and Quaternary volcanic rocks (W. P. Nash, University of Utah)

Regional heat flow and geochemical studies (S. H. Ward, University of Utah)

West Virginia, Eastern Warm Springs (W. A. Hobba, Jr., w, Morgantown)

Wyoming, Yellowstone thermal areas, geology (M. H. Beeson, M)

Glaciology:

Changes in glacier volumes (M. F. Meier, w, Tacoma, Wash.)

Electromagnetic methods for measuring snow (M. F. Meier, w, Tacoma, Wash.)

Glacier response to climate (S. M. Hodge, w, Tacoma, Wash.)

Ice Age modelling (D. P. Adam, M)

Knik Glacier (L. R. Mayo, w, Fairbanks, Alaska)

Photo collection (A. S. Post, w, Tacoma, Wash.)

Reconstruction of streamflow (S. M. Hodge, w, Tacoma, Wash.)

Water, ice, and energy balance of mountain glaciers and ice physics (M. F. Meier, w, Tacoma, Wash.)

Gold:

Composition related to exploration (J. C. Antweiler, D)

Great Lakes region (D. A. Seeland, D)

States:

Alaska, Seward Peninsula, nearshore (D. M. Hopkins, M)

California, Klamath Mountains (P. E. Hotz, M)

Montana (D):

Cooke City quadrangle (J. E. Elliott)

Ore deposits, southwestern part (K. L. Wier)

Gold—Continued

States—Continued

Nevada (M, except as otherwise noted):

Aurora and Bodie districts, Nevada-California (F. J. Kleinhampl)

Carlin mine (A. S. Radtke)

Comstock district (D. H. Whitebread)

Dun Glen quadrangle (D. H. Whitebread)

Goldfield district (R. P. Ashley)

Round Mountain and Manhattan districts (D. R. Shawe, D)

New Mexico, Placer deposits (Kenneth Segerstrom, D)

North Carolina, Gold Hill area (A. A. Stromquist, D)

Oregon-Washington, Nearshore area (P. D. Snavely, Jr., M)

South Dakota, Keystone area (W. H. Raymond, D)

Wyoming, Northwestern part, conglomerates (J. C. Antweiler, *See also* Heavy metals.

Ground water-surface water relations:

Bank storage reconnaissance (W. D. Simons, w, M)

States:

Florida, Hydrologic base, Dade County (L. J. Swayze, w, Miami)

Idaho (w, Boise), hydrology:

Island Park-Henrys Lake (R. L. Whitehead)

Weiser Basin (H. W. Young)

New Mexico, Pecos River, miscellaneous (G. E. Welder, w, Roswell)

Wisconsin, Hydrology, Cedar Lake (R. S. McLeod, w, Madison)

Heavy metals:

Appalachian region:

Mineral resources, Connecticut-Massachusetts (J. P. D'Agostino, NC)

South-central (A. A. Stromquist, D)

Hydrogeochemistry and biogeochemistry (T. T. Chao, D)

Mineral paragenesis (J. T. Nash, M)

Regional variation in heavy-metals content of Colorado Plateau stratified rocks (R. C. Cadigan, D)

Rocky Mountain region, fossil beach placers (R. S. Houston, Laramie, Wyo.)

Solution transport (G. K. Czamanske, M)

Southeastern States, geochemical studies (Henry Bell III, NC)

States:

Alaska (M):

Gulf of Alaska, nearshore placers (Erk Reimnitz)

Hogatza trend (T. P. Miller)

Southeastern part (D. A. Brew)

Southern Alaska Range (B. L. Reed)

Southwestern part (J. M. Hoare)

Yukon-Tanana Upland (H. L. Foster)

Idaho, Washington Peak quadrangle (D. A. Seeland, D)

Nevada:

Aurora and Bodie districts, Nevada-California (F. J. Kleinhampl, M)

Basin and Range (D. R. Shawe, D)

Hydrologic data collection and processing:

Data file for well records (R. S. McLeod, w, Madison, Wis.)

Hydrologic probability models (W. H. Kirby, w, NC)

New Mexico data bank (D. R. Posson, w, Albuquerque, N. Mex.)

Store-retrieve hydrologic data (G. W. Hawkins, w, Mineola, N.Y.)

See also Hydrologic instrumentation.

Hydrologic instrumentation:

Chipps Island acoustic flowmeter (S. H. Hoffard, w, M)

Drilling techniques (Eugene Shuter, w, D)

Ground-water Site Inventory Data Base (L. J. Topinka, w, Tacoma, Wash.)

Hydrologic instrumentation—Continued
- Instrumentation and environmental studies (G. E. Ghering, w, D)
- Instrumentation coordination (R. W. Paulson, w, NC)
- Instrumentation research, water (F. C. Koopman, w, Bay St. Louis, Miss.)
- Interagency sedimentation project (J. V. Skinner, w, Minneapolis, Minn.)
- Kriging analysis: precipitation data (M. R. Karlinger, w, Tacoma, Wash.)
- Laser spectroscopy (M. C. Goldberg, w, D)
- Satellite data relay project (W. G. Slope, w, NC)
- Suspended solids sensors (J. V. Skinner, w, Minneapolis, Minn.)
- Techniques of flood-plain mapping (R. H. Brown, w, Bay St. Louis, Miss.)
- Telemetry evaluation program (W. M. Woodham, w, Tampa, Fla.)
- *See also* Hydrologic data collection and processing.

Hydrology, ground water:
- Analysis of ground water systems (S. S. Papadopulos, w, NC)
- Appalachian Basin, waste storage (P. M. Brown, w, Raleigh, N. C.)
- Aquifer systems:
  - Field research (B. E. Lofgren, w, Sacramento, Calif.)
  - Theoretical aspects (D. C. Helin, w, Sacramento, Calif.)
- Borehole geophysics (W. S. Keys, w, D)
- Central midwest regional aquifer system analyses (D. G. Jorgensen, w, Lawrence, Kan.)
- Climax heater experiment (R. K. Waddell, w, D)
- Consultation and research (C. V. Theis, w, Albuquerque, N. Mex.)
- Digital modeling, ground-water flow (S. P. Larson, w, NC)
- Energy transport in ground water (A. F. Moench, w, M)
- Fate of organisms in ground water (G. G. Ehrlich, w, M)
- Fissuring-substance research (T. L. Holzer, M)
- Fractured hydrogeologic systems (C. R. Faust, w, NC)
- Geopressured-geothermal resources (R. H. Wallace, w, Bay St. Louis, Miss.)
- Ground-water geophysics research (A. A. R. Zohdy, w, D)
- Ground-water staff functions (S. W. Lohman, w, D)
- Ground-water tracer studies (R. J. Sun, w, NC)
- Hydro characteristics of anhydrite (William Thordarson, w, D)
- Hydrologic analysis of petrofabrics (R. T. Getzen, w, M)
- Hydrologic laboratory (F. S. Riley, w, D)
- Hydrology of the Madison aquifer (E. M. Cushing, w, D)
- Hydrology of Wilcox Formation with reference to liquid waste emplacement in the Gulf Coastal Plain (R. H. Wallace, Jr., w, Bay St. Louis, Miss.)
- Impact of mining on aquifers (N. J. King, w, D)
- In-situ stress measurements (J. D. Bredehoeft, w, NC)
- Liaison, U.S. Geological Survey-Bureau of Land Management (F. W. Giessner, w, D)
- Limestone hydraulic permeability (V. T. Stringfield, w, NC)
- Modeling of geothermal systems (M. L. Sorey, w, M)
- Northern Great Plains aquifer study (G. A. Dinwiddle, w, D)
- Northern midwest regional aquifer study (W. L. Steinhilber, w, Madison, Wis.)
- Paradox basin hydrology (F. F. Rush, w, D)
- Planning, northern coastal plain (H. Meisler, w, Trenton, N.J.)
- Role of confining clays (R. G. Wolff, w, NC)
- Southeast limestone aquifer study (R. H. Johnston, w, Atlanta, Ga.)
- Transport phenomena in porous media (J. W. Mercer, w, NC)
- Tropical carbonate aquifers (William Back, w, NC)

Hydrology, ground water—Continued
States and territories:
- Alabama:
  - Cretaceous aquifer simulation (R. A. Gardner, w, Montgomery)
  - Environmental hydrogeology highways (J. C. Scott, w, Montgomery)
- Alaska (w, Anchorage):
  - Data summary, Cook Inlet (D. R. Scully)
  - Eagle River Valley ground water (L. L. Dearborn)
  - Hydrologic data (L. L. Dearborn)
  - Kenai Borough project (G. L. Nelson)
- Arizona:
  - Ground water to Colorado River (S. A. Leake, w, Yuma)
  - Southern Apache County (T. W. Anderson, w, Flagstaff)
  - Special site studies (R. D. MacNish, w, Tucson)
  - Water supply, Lake Mead area (R. L. Laney, w, Phoenix)
- Arkansas:
  - Ground water, lower Mississippi region (J. E. Terry, Jr., w, Little Rock)
  - Hydrology of Claiborne and Wilcox (M. E. Broom, w, Little Rock)
- California:
  - Central Valley aquifers (G. L. Bertoldi, w, Sacramento)
  - City of Merced ground water appraisal (C. L. Londquist w, Sacramento)
  - Data Antelope-Valley East Kern (C. E. Lamb, w, Laguna Niguel)
  - Geohydrology, Mojave River basin (Anthony Buono, w, Laguna Niguel)
  - Ground water:
    - Indian Wells Valley (D. J. Downing, w, Laguna Niguel)
    - Santa Barbara (J. A. Singer, w, Santa Barbara)
    - Thousand Oaks (J. J. French, w, Laguna Niguel)
  - Ground water model—Modesto (C. J. Londquist, w. Saccramento)
  - Ground water, Pescadero (K. S. Muir, w, M)
  - Ground water, U.S. Marine Corps Twentynine Palms (W. R. Moyle, w, Laguna Niguel)
  - Ground water, seaside area (K. S. Muir, w, M)
  - Imperial Valley geothermal model (R. E. Miller)
  - Owens River basin study (W. F. Hardt, w, Laguna Niguel)
  - Palmdale Bulge earthquake prediction (J. R. Moyle, w, Laguna Niguel)
  - Redding basin ground water appraisal (M. J. Pierce, w, Sacramento)
  - Seawater intrusion, Soquel-Aptos (K. S. Muir, w, M)
  - Sole-source aquifer studies (G. L. Faulkner, w, M)
  - Water resources, Indian Reservations (J. R. Freckleton, w, Laguna Niguel)
  - Water resources, Vandenberg AFB (C. E. Lamb)
- Colorado (w, D):
  - Arkansas River basin (J. L. Huges, w, Pueblo)
  - Aquifer testing (F. A. Welder)
  - Ground water, Denver Basin (S. G. Robson)
  - Ground water investigations, Rio Blanco County (F. A. Welder, w, Meeker)
  - Ground water studies in coal areas (J. J. D'Lugosz)
  - High Plains aquifer study (R. G. Borman)
  - Intensive monitoring northwest Colorado (R. S. Parker)
  - Roan-Parachute ground-water model (R. D. Pratt)
  - Routt County ground water (T. R. Ford, w, Meeker)
  - West Slope aquifers (D. J. Ackerman, w, Grand Junction)

Hydrology, ground water—Continued

States and territories—Continued

Connecticut (w, Hartford):
- Farmington ground-water potential (D. L. Mazzeferro)
- Recharge areas for stratified drift (E. H. Handman)

Florida:
- Aquifer characteristics in southwest Florida (R. M. Wolansky, w, Tampa)
- Aquifer mapping, south Florida (W. J. Haire, w, Miami)
- Dade City ground water (C. H. Tibbals, w, Orlando)
- Englewood Water District (H. R. Sutcliffe, w, Sarasota)
- Fernandina saltwater intrusion investigation (D. P. Brown, w, Jacksonville)
- Floridan aquifer—Withlacoochee (P. W. Bush, w, Orlando)
- Freshwater resources, Big Pine Key (C. E. Hanson, w, Miami)
- Ground water, Ft. Lauderdale (W. J. Haire, w, Miami)
- Ground water—Kissimmee River basin (R. G. Belles, Jr., w, Orlando)
- Hydrology, Cocoa well-field (W. D. Wood, w, Orlando)
- Injecting monitoring, Tampa Bay area (J. J. Hickey, w, Tampa)
- New well fields, Dade County (Howard Klein, w, Miami)
- Northwest Volusia (A. T. Rutledge, w, Orlando)
- Potentiometric maps in Southwest Florida Water Management District (D. K. Yobbi, w, Tampa)
- St. Johns County, shallow aquifer study (Henry Trapp, w, Jacksonville)
- Shallow aquifer, Palm Beach County (A. L. Knight, w, Miami)
- South Florida limestone aquifer study (F. W. Meyer, w, Miami)
- Storage of storm waters (J. J. Hickey, w, Tampa)
- Subsurface disposal—Pinellas (J. J. Hickey, w, Tampa)
- Technical assistance, Hillsborough County (J. D. Fretwell, w, Tampa)
- Technical support, Pinellas County (L. R. E. Mills, w, Tampa)
- Technical support, Southwest Florida Water Management District (W. C. Sinclair, w, Tampa)
- Upper east coast (G. W. Hill, w, Jupiter)
- Water for desalting Florida Keys (W. L. Miller, w, Miami)
- Water resources, Everglades (B. G. Waller, w, Miami)
- Water resources, Lake Worth (D. V. Maddy, w, Miami)
- Water supply, southwest Brevard County, (Michael Planert, w, Orlando)
- Water-table aquifer study, DuVal County (B. J. Franks, w, Jacksonville)
- Well fields, west central Florida (D. M. Johnson, w, Tampa)
- Winter Haven lakes study (W. C. Sinclair, w, Tampa)

Georgia:
- Ground water, Atlanta region (C. W. Cressler, w, Doraville)
- Southeast limestone aquifer study (R. E. Krause, w, Doraville)

Hawaii (w, Honolulu):
- Exploratory drilling (R. L. Soroos)
- Dike-impounded water, Oahu (K. J. Takasaki)
- Honolulu basal aquifer (R. H. Dale)
- Kipahulu water resources (R. L. Soroos)
- Water resources of southeast Oahu (K. J. Takasaki)

Idaho:
- Banbury hot springs (R. E. Lewis, w, Boise)
- Geohydrologic data, Mud Lake aquifer (R. F. Norvitch, w, Boise)

Hydrology, ground water—Continued

States and territories—Continued

Idaho—Continued
- Snake River Plain regional aquifer system analyses (G. F. Lindholm, w, Boise)
- Water resources of the Camas Prairie (H. W. Young, w, Boise)
- Water resources, Rockland Valley (H. W. Young, w, Boise)

Illinois:
- Regional aquifer study in Illinois (M. G. Sherrill, w, Champaign)
- Shallow ground water, McHenry County (J. T. Krohelski, w, DeKalb)

Indiana (w, Indianapolis):
- Decatur County (T. K. Greenman)
- Elkhart ground water study (T. E. Imbrigiotta)
- Ground water, Upper West Fork of the River basin (W. W. Lapham)
- Indiana dunes ground-water study (D. C. Gillies)
- Jennings County fracture trace (William Meyer)
- Johnson-Morgan ground-water study (D. C. Gillies)
- Newton Jasper, ground water (R. J. Shedlock)
- Regional aquifer study in Indiana (R. J. Shedlock)
- Southeast Indiana lineaments (T. K. Greeman)
- Vincennes ground-water study (R. J. Shedlock)

Iowa (w, Iowa City):
- Carbonate terrane hydrology (Phase 1) (K. D. Wahl)
- North-central Iowa (J. W. Cagle)
- Pennsylvanian aquifers, coal region (J. C. Cagle)
- Regional aquifer study in Iowa (M. R. Burkart)

Kansas:
- Aquifer test evaluation (R. D. Burnett, w, Lawrence)
- Geohydrologic maps, southwestern Kansas (E. D. Gutentag, w, Garden City)
- Geohydrology for planning in western Kansas (Jack Hume, w, Garden City)
- Hydrologic data base, Ground Water Management District 3 (H. F. Grubb, w, Garden City)
- Liquid waste, Arbuckle Group (A. J. Gogel, w, Lawrence)
- Models North and South Fork Solomon (J. B. Gillespie, w, Lawrence)
- Sandstone aquifer, southwest Kansas (Jack Hume, w, Garden City)
- Wellington aquifer parameters (J. B. Gillespie, w, Lawrence)

Kentucky, Mississippi Plateau potentiometric map (T. W. Lambert, w, Louisville)

Louisiana (w, Baton Rouge):
- Red River waterway study (J. E. Rogers, w, Alexandria)
- Southwestern Louisiana (D. J. Nyman)

Maine (w, Augusta):
- Androscoggin, ground water (G. C. Prescott, Jr.)
- Ground water, Upper Androscoggin River basin (G. C. Prescott)
- Maine sand and gravel aquifers (G. C. Prescott)
- Water resources, Acadia National Park (B. P. Hansen, w, Boston)

Maryland (w, Towson):
- Environmental geohydrologic studies (E. G. Otton)
- Garrett County, well inventory (L. J. Nutter)
- Ground water resources—urbanization, Harford County (L. J. Nutter)
- Hydrology of water-table aquifer (L. L. Bachman)
- Maryland Aquifer Studies III (F. K. Mack)

Hydrology, ground water—Continued

States and territories—Continued

Maryland (w, Towson)—Continued
- Sole-source aquifer study (C. A. Richardson)
- Special studies—ground water (C. A. Richardson)
- Western Montgomery County ground water study (E. G. Otton)

Massachusetts (w, Boston):
- Cape Cod sole-source aquifer (B. J. Ryan)
- Coal hydrology, Massachusetts and Rhode Island (M. H. Frimpter)
- Estimating maximum ground water levels (M. H. Frimpter)
- Ground water, Cape Cod (D. R. LeBlanc)
- Monitoring Cape Cod's ground water (B. J. Ryan)
- Northeastern Massachusetts river basins (R. A. Brackley)
- Water resources, Blackstone River basin (E. H. Walker)

Michigan:
- Ground water in Shelby Township (M. G. McDonald, w, Lansing)
- Ground water of coal deposits, Bay County, Michigan (J. R. Stark, w, Lansing)
- Hydrology of Sands plain area (N. G. Grannemann, w, Lansing)
- Water resources Marquette iron range (N. G. Grannemann, w, Lansing)

Minnesota (w, St. Paul):
- Ground-water appraisal, Pelican River sand plain (R. T. Miller)
- Ground water:
  - Big Stone County (W. G. Soukup, w, Grand Rapids)
  - Four-county area (G. F. Lindholm, w, Grand Rapids)
  - Southwestern Minnesota (D. G. Adolphson)
  - Todd, Cass, Morrison Counties (C. F. Myette)
- Hydrology of Red Lake peatlands (D. I. Siegel)
- Lake Williams—water balance (D. I. Siegel)
- Pelican River sand plain (D. G. Adolphson)
- Reconnaissance of sand-plain aquifers (H. W. Anderson)
- Regional aquifer study in Minnesota (D. G. Woodward)
- Twin Cities tunnel-system hydrology (E. L. Madsen)
- Water resources, Buffalo River (R. J. Wolf)

Mississippi (w, Jackson):
- Hydrology-Tennessee-Tombigbee (A. G. Lamonds)
- Potentiometric mapping (B. E. Wasson)
- Water, developing areas (B. E. Wasson)

Missouri (w, Rolla):
- Prosperity ground water (W. R. Berkas)
- Regional aquifer system in Missouri (L. F. Emmett)
- Water in southeastern Missouri lowlands (R. R. Luckey)

Montana:
- Energy Minerals Rehabilitation Inventory and Analysis site studies (N. E. McClymonds, w, Helena)
- Geohydrologic maps, Fort Union area (J. D. Stoner, w, Billings)
- Geohydrologic maps, Madison aquifer (R. D. Feltis, w, Billings)
- Geohydrology, Cascade County (K. R. Wilke, w, Helena)
- Hydrology of Paleozoic rocks (W. R. Miller, w, Billings)
- Mining effects, shallow water (S. E. Slagle, w, Billings)
- Northern Great Plains aquifer study (W. R. Hotchkins w, Helena)
- Water monitoring—coal, Montana (K. R. Wilke, w, Helena)

Hydrology, ground water—Continued

States and territories—Continued

Nebraska:
- Butler County (M. H. Ginsberg, w, Lincoln)
- Hydrology, Platte-Loup area NE (J. M. Pechenpaugh w, Lincoln)
- Platte-Republican watershed (J. W. Goeke, w, North Platte)

Nevada (w, Carson City):
- Beatty disposal site investigation (W. D. Nichols)
- Consolidated-rock water supply (T. L. Katzer)
- Fernley area water resorces (F. E. Arteaga)
- Ground-water levels, Topaz Lake (J. O. Nowlin)
- Lemmon Valley geophysics (D. H. Schaefer)
- Pumping effects on Devil's Hole (H. L. McQueen)
- Storage depletion, Pahrump Valley (J. R. Harrill)
- Water resources, Walker Indian Reservation (D. H. Schaefer)

New Hampshire, Ground water in Lamprey River basin (J. E. Cotton, w, Concord)

New Jersey (w, Trenton):
- Digital model, Potomac-Raritan-Magothy aquifer system (J. E. Luzier)
- Geohydrology, east-central New Jersey (G. M. Farlekas)
- Pumpage inventory (William Kam)

New Mexico (w, Albuquerque, except as otherwise noted):
- Capulin ground water (D. L. Hart)
- Northwest New Mexico ground waters (P. F. Frenzel)
- Elephant Butte Irrigation District well-field evaluation (C. A. Wilson, w, Las Cruces)
- Lower Rio Grande valley (C. A. Wilson)
- Northern High Plains (E. G. Lappala)
- Roswell Basin, quantitative (G. E. Welder, w, Roswell)
- Sandia-Manzano Mountains (D. W. Wlikins)
- San Agustin plains ground water (C. A. Wilson, w, Las Cruces)
- Urban areas reconnaissance (W. E. Hale)
- Water resources:
  - Acoma Pueblo (F. B. Lyford)
  - Laguna Reservation (F. P. Lyford)
  - Mimbres Basin (J. S. McLean)
  - Santa Fe (W. A. Mourant)
- Water supply, Tijeras Canyon (J. D. Hudson)
- Zuni (B. R. Ott)

New York:
- Buried-channel aquifers, Albany (R. M. Waller, w, Albany)
- Geohydrology, North Brookhaven, Long Island (E. J. Koszalka, w, Syosset)
- Ground water, Oswego County (T. S. Miller, w, Albany)
- Hydrogeology of Suffolk County, (H. M. Jensen, w, Syosset)
- Subsurface storage of chilled water (Julian Soren, w, Syosset)

North Carolina, Ground-water network review (M. D. Winner, w, Raleigh)

North Dakota (w, Bismarck, except as otherwise noted):
- Ground water:
  - Bottineau-Rolette, (P. G. Randich)
  - Logan County (R. L. Klausing)
  - McHenry and Sheridan Counties (P. G. Randich)
  - McIntosh County (R. L. Klausing)
  - McKenzie County (M. G. Croft)
- Ground-water availability, Fort Union coal (M. G. Croft)
- Hydrology of Madison Group (R. D. Butler)
- Mining and reclamation, Mercer County (M. E. Crawley)
- Northern Great Plains aquifer study (R. D. Butler)

Hydrology, ground water—Continued
States and territories—Continued
Ohio (w, Columbus):
Dayton digital model (S. E. Norris)
Ground water in Geauga County (V. E. Nichols)
Mine-site investigations (S. E. Norris)
Piketon investigation (S. E. Norris)
Oklahoma, Arbuckle aquifer (R. W. Fairchild, w, Oklahoma City)
Oregon (w, Portland):
Bend-Redmond ground water (J. B. Gonthier)
Dalles-Monmouth ground-water study (J. B. Gonthier)
Ground water, Clackamas County (A. R. Leonard)
Ground water, Hood basin (S. J. Grady)
John Day fossil beds (F. J. Frank)
Myrtle Creek ground-water study (F. J. Frank)
Reedsport water supply (F. J. Frank)
Special studies (D. D. Harris)
Pennsylvania (w, Harrisburg, except as otherwise noted):
Ground water, central Columbia County (O. B. Lloyd, Jr.)
Hydrogeology:
Erie County (J. T. Gallaher w, Meadville)
Great Valley (A. E. Becher)
Hydrology of Gettysburg Formation (C. R. Wood)
Philadelphia ground water (C. R. Wood, w, Malvern)
Susquehanna ground water (J. R. Ritter)
Water levels and quality monitoring (W. C. Roth)
Puerto Rico:
Ground water, Canovanas-Rio Grande area (A. E. Torres-Gonzalez, w, Ft. Buchanan)
Ground-water reconnaissance, Central Lajas Valley, (H. J. McCoy, w, San Juan)
Manati water resources (Fernando Gomez-Gomez, w, Ft. Buchanan)
Water for North Coast rice (J. R. Diaz, w, San Juan)
Water-resources appraisal of St. Croix, Virgin Islands (H. J. McCoy, w, San Juan)
Water resources of Rio Guanajibo basin (Eloy Colon, w, Ft. Buchanan)
Water resources, Rio Cibuco area (A. E. Torres-Gonzalez, w, Ft. Buchanan)
Rhode Island, ground water in Pawcatuck River basin (H. E. Johnston, w, Providence)
South Carolina (w, Columbia, except as otherwise noted):
Assessment of ground-water resources (A. L. Zack)
Ground water resources in northeast South Carolina (G. K. Speiran, w, Columbia)
Ground water resources of Sumter and Florence (B. C. Spigner)
Study of geohydrologic problems (A. L. Zack)
Water resources evaluation—Horry, Georgetown (A. L. Zack)
South Dakota:
High Plains aquifer study (H. L. Case, w, Rapid City)
Hydrology of the Madison Group (L. W. Howells, w, Huron)
Northern Great Plains aquifer study (H. L. Case, w, Rapid City)
Water resources, Walworth County (E. P. LeRoux, w, Huron)
Tennessee (w, Nashville):
Hydrology of hard rock aquifers (E. F. Hollyday)
Memphis aquifer studies (W. S. Parks, w, Memphis)
Texas:
Salinity control, Brazos and Red Rivers (S. Garza, w, Austin)
Salt dome hydrology (phase I) (J. E. Carr, w, Houston)
Trinity River alluvium (S. Garza, w, Austin)
Utah (w, Salt Lake City):
Ground water in Sevier Desert (R. W. Mower)
Hydrology, Tooele Valley area (A.G. Razem)

Hydrology, ground water—Continued
States and territories—Continued
Utah (w, Salt Lake City)—Continued
Morgan Valley (J. S. Gates)
Navajo Sandstone, Southwestern Utah (R. M. Cordova)
Reconnaissance, Fish Springs Flat (E. L. Bolke)
Vermont, Ground water in Rutland area (R. E. Willey, w, Montpelier)
Virginia:
Coastal plain studies (H. T. Hopkins, w, Richmond)
Culpeper Basin study (Chester Zenone, w, Fairfax)
Fairfax County urban-area study (Chester Zenone, w, Fairfax)
Ground water resources, Blue Ridge Parkway (H. T. Hopkins, w, Richmond)
Hydrology of James City County (J. F. Harsh, w, Richmond)
Washington (w, Tacoma, except as otherwise noted):
Clallam County water resources (B. W. Drost)
Gig Harbor water resources (B. W. Drost)
Hydrologic basin analysis (K. L. Walters)
Kitsap Peninsula study (A. J. Hansen, Jr.)
Lower Yakima summary (Dee Molenaar)
Muckleshoot ground water (Dee Molenaar)
Nisqually ground water (W. E. Lum)
Shoalwater water resources (W. E. Lum)
Spokane ground-water quality (E. L. Bolke)
Water data for coal mining (F. A. Packard)
Water, Yakima Reservation (J. A. Skrivan)
West Virginia (w, Charleston):
Ecology and underground coal mining (J. W. Borchers)
Elk River basin study (G. T. Tarver)
Remotely sensed ground water (W. A. Hobba, w, Morgantown)
Water resources of Tug Fork basin (J. S. Bader)
Wisconsin (w, Madison):
Ground water, Dodge County (R. W. Devaul)
Ground-water quality (P. A. Kammerer, Jr.)
Regional aquifer study in Wisconsin (P. J. Emmons)
Iron River hatchery study (S. M. Hindall)
Washington-Ozaukee Counties (H. L. Young)
Water resources of Forest County (E. L. Boyd)
Wyoming (w, Cheyenne):
Bighorn Basin aquifers (M. E. Cooley)
Hanna basin water resources (P. B. Freudenthal)
High Plains aquifer study (C. F. Avery)
Madison limestone (C. R. Joy)
Model of Bates Hole (K. C. Glover)
Northern Great Plains aquifer study (D. T. Hoxie)
Tertiary aquifers, Laramie County (M. A. Crist)
Wheatland Flats model (M. A. Crist)

Hydrology, surface water:
Channels, sediment loads, and streamflows (G. P. Williams, w, D)
Circulation, San Francisco Bay (T. T. Conomos, w, M)
Hydrology defined by rainfall simulation (G. C. Lusby, w, D)
Isotope fractionation (T. B. Coplen, w, NC)
Numerical simulation (R. A. Baltzer, w, NC)
Platte River hydrology (C. F. Nordin, w, D)
Runoff simulation (R. W. Lichty, w, NC)
Water-quality-model development and implementation (R. A. Baltzer, w, NC)
States and territories:
Alabama (w, Tuscaloosa):
Environmental study, Birmingham (R. H. Bingham)
Flow characteristics of streams (C. O. Ming, w, Montgomery)
Mobile River study (J. E. Bowie, w, Montgomery)

Hydrology, surface water—Continued

States and territories—Continued

Alabama (w, Tuscaloosa)—Continued
- Small-stream studies (D. A. Olin)

Alaska, Kenai morphology (K. M. Scott, w, Anchorage)

Arizona, Flood hydrology of Arizona (B. N. Aldridge, w, Tucson)

Arkansas (w, Little Rock):
- Arkansas basin flows (G. G. Ducret)
- Duration and frequency of streams (T. E. Lamb)

California (w, Sacramento, except as otherwise noted):
- California lakes and reservoirs (W. L. Bradford, w, M)
- Tidal River discharge computation (R. N. Oltmann)

Colorado (w, D):
- Arkansas River Compact (J. F. Blakey)
- Instream flow evaluation (D. P. Bauer)
- Inventory of water resources on Ft. Carson (P. J. Emmons)
- Mannings "N" value study (R. D. Jarrett)
- Peak discharge small watershed (D. R. Minges)

Connecticut, Water quality of Lake Waramang (K. P. Kulp, w, Hartford)

Delaware, Delaware River master activity (F. T. Schaefer, w, Milford, Pa.)

Florida:
- Freshwater inflow to estuaries (R. F. Giovanelli, w, Tampa)
- Hillsborough River basin water supply (J. F. Turner, w, Tampa)
- Hydrology Area B, Sarasota County (H. R. Sutcliffe, w, Sarasota)
- Hydrology of lakes (G. H. Hughes, w, Tallahassee)
- Jumper Creek investigation (Warren Anderson, w, Orlando)
- Low flows in northwestern Florida (R. P. Rumenik, w, Tallahassee)
- St, Johns River deepening study (R. B. Stone, w, Jacksonville)
- Small stream flood frequencies (W. C. Bridges, w, Tallahassee)
- Volusia wetlands delineation (P. W. Bush, w, Orlando)

Georgia (w, Doraville):
- Seasonal low flow (T. R. Dyar)
- Storage requirements for Georgia streams (R. F. Carter)
- Time-of-travel, Georgia streams (J. L. Pearman)

Idaho:
- Bedload in North Fork Teton River (R. P. Williams, w, Boise)
- Skew mapping (L. C. Kjelstrom, w, Boise)

Illinois:
- Dam ratings (D. M. Mades, w, DeKalb)
- Illinois River miles (R. W. Healy, w, Champaign)
- T and K studies on Illinois streams (R. F. Fuentes, w, Champaign)

Indiana:
- Mapping of Big Long Lake (R. R. Contreras, w, Indianapolis)
- River mileage (G. E. Nell, w, Indianapolis)
- Streamflow characteristics (D. W. Blevins, w, Indianapolis)

Kansas (w, Lawrence):
- Channel geometry, coal areas (E. E. Hedman)
- Channel geometry, Kansas River (W. R. Osterkamp)
- Channel geometry, regulated streams (E. E. Lawrence)
- Flood investigations (H. R. Hejl, Jr.)
- Sediment-active geometry (W. R. Osterkamp)
- Soldier Creek (W. J. Carswell)

Hydrology, surface water—Continued

States and territories—Continued

Kansas (w, Lawrence)—Continued
- Streamflow characteristics (P. R. Jordan)
- Water yield, Kansas (W. J. Carswell)

Louisiana, Characteristics of streams (M. J. Forbes, Jr., w, Baton Rouge)

Maine (w, Augusta):
- Drainage areas (R. A. Fontaine)
- Flow and water quality character, Maine streams (G. W. Parker)
- Hydrology of selected Maine rivers (D. J. Cowing)
- Water resources (G. C. Prescott)

Maryland:
- Flow characteristics of Maryland streams (D. H. Carpenter, w, Towson)
- Low-flow studies in Maryland (R. W. James, w, Towson)

Michigan, Flow model of Saginaw River (D. J. Holtschlag, w, Lansing)

Minnesota, Small streams program (K. T. Gunard, w, St. Paul)

Mississippi:
- Documentation of bridge backwater (B. E. Colson, w, Jackson)
- Drainage areas, Mississippi streams (J. W. Hudson, w, Jackson)

Montana (w, Helena, unless otherwise noted):
- Bridge-site investigations (R. J. Omang)
- Limnology of lakes in eastern Montana (R. F. Ferreira)
- Peak flow, small drainage areas (R. J. Omang)
- Watershed model (L. E. Cary, w, Billings)

Nevada, Lake Mead recreation area flood hazards (Otto Moosburner, w, Carson City)

New Jersey:
- Base flow studies (R. D. Schopp, w, Trenton)
- Drainage areas of streams (A. J. Velnich, w, Trenton)

New Mexico:
- Channel adjustment, Cochiti Dam (J. D. Dewey, w, Albuquerque)
- Precipitation-runoff modeling (H. R. Hejl, w, Albuquerque)
- Runoff from channel geometry (J. P. Borland, w, Santa Fe)

New York (w, Albany):
- Acid lakes (N. E. Peters)
- Low-flow study (B. B. Eissler)
- Pine bush hydrology (D. S. Snavely)
- Reaeration studies (S. D. Schiano)
- Stream gazetteer (L. A. Wagner)

North Carolina (w, Raleigh):
- Channelization effects, Chicod Creek (C. E. Simmons)
- Data site information for 208 study (C. E. Simmons)

Ohio (w, Columbus):
- Floods versus channel geometry (E. E. Webber)
- Hydraulics of bridge sites (R. I. Mayo)
- Low-flow frequency analyses (D. P. Johnson)
- Low flow of Ohio streams (R. I. Mayo)
- Rural hydrology (E. E. Webber)
- Rush Creek water quality (C. G. Angelo)
- Time-of-travel studies of Ohio streams (A. O. Westfall)

Oklahoma, Coal field hydrology (A. W. Smart, w, Oklahoma City)

Oregon, Oregon lakes and reservoirs (D. D. Harris, w, Portland)

Pennsylvania (w, Harrisburg):
- Flow routing, Susquehanna River (D. L. Bingham)
- Low-flow regionalization (H. N. Flippo)
- Mean discharge (H. N. Flippo)
- Time of travel, Lehigh River (C. D. Kaufman)

Hydrology, surface water—Continued
States and territories—Continued
Puerto Rico, Islandwide 208 assistance study (A. E. Torres , w, San Juan)
South Carolina (w, Columbia):
Data reports, flood forecasting (C. S. Bennett)
Low-flow characteristics (W. M. Bloxham)
Non-point discharges, Reedy River (D. I. Cahal)
South Dakota (w, Huron):
Flood-frequency study (L. D. Becker)
Small-stream flood frequency (L. D. Becker)
Tennessee (w, Nashville, except as otherwise noted):
Miscellaneous data services (V. J. May)
Tennessee bridge scour (W. J. Randolph)
Texas, Small watersheds (B. O. Massey, w, Austin)
Utah, mined lands rehabilitation (G. W. Sandberg, w, Cedar City)
Virginia, Historic streamflow record—Occoquan (B. J. Prugh, w, Richmond)
Washington (w, Tacoma):
Duwamish toxicant study (E. A. Prych)
Low flow of Washington streams (E. H. McGavok)
Makah Project (K. L. Walters)
Newaukum basin study (E. R. Prych)
Tulalip water resources (B. W. Drost)
Unregulated flow at Union Gap (J. J. Vaccaro)
Water resources of the Hoh Indian Reservation (W. E. Lum)
West Virginia, small drainage areas (G. S. Runner, w, Charleston)
Wisconsin (w, Madison):
Bridge Creek hydrology (B. K. Holmstrom)
Drainage areas (E. W. Henrich)
Flood-frequency study (D. H. Conger)
Hydrology of Lake Owen (D. A. Wentz)
Low-flow stream geometry (L. B. House)
Low-flow study (B. K. Holmstrom)
Nonpoint source pollution (S. J. Field)
Pheasant Branch study (W. R. Krug)
Streamflow estimates in lake basins (R. P. Novitzki)
Water-quality control (B. K. Holstrom)
See also Evapotranspiration; Flood investigations; Marine hydrology; Plant ecology; Urbanization, hydrologic effects.

Industrial minerals. *See specific minerals.*

Iron:
Resource studies, United States (Harry Klemic, NC)
States:
Michigan, Gogebic County, western part (G. G. Schmidt, NC)
Wisconsin, Black River Falls (Harry Klemic)

Isotope and nuclear studies:
Instrument development (F. J. Jurceka, D)
Isotope fractionation (T. B. Coplen II, w, NC)
Isotope ratios in rocks and minerals (Irving Friedman, D)
Isotopic hydrology (F. J. Pearson, w, NC)
Lead isotopes and ore deposits (R. E. Zartman, D)
Mass spectrometry and isotopic measurements (J. S. Stacey, D)
Nuclear irradiation (G. M. Bunker, D)
Radioisotope dilution (L. P. Greenland, NC)
Reactor facility (G. P. Kraker, Jr., w, D)
Stable isotopes and ore genesis (R. O. Rye, D)
Upper mantle studies (Mitsunobu Tatsumoto, D)
See also Geochronological investigations; Geochemistry, water; Radioactive-waste disposal.

Land resources analysis:
Idaho, eastern Snake River Plain region (S. S. Oriel, D)

Land Subsidence
Coastal plain land subsidence (H. T. Hopkins, w, Richmond, Va.)
Fissuring-subsidence research (T. L. Holzer, M)
Geothermal subsidence, Mexicali (B. E. Lofgren, w, Sacramento, Calif.)
Geothermal subsidence research (B. E. Lofgren, w, Sacramento, Calif.)
Land subsidence studies in California (R. L. Ireland, w, Sacramento, Calif.)
States:
Arizona:
Land subsidence-earth fissures (R. L. Laney, w, Phoenix)
Subsidence fissures, Tucson Basin (H. H. Schumann, w, Tuscon)
New Jersey, Land subsidence (William Kam, w, Trenton)
New Mexico, land subsidence in the Known Potash Leasing Area (M. L. Millgate, c, Roswell)
Texas, coastal subsidence studies (R. K. Gabrysch, w, Houston)

Land use and environmental impact:
Accuracy assessment of land use and land cover maps produced from Landsat digital data (G. H. Rosenfield, l, NC)
Development of automated techniques for land use mapping (J. R. Wray, l, NC)
Geographic Information Systems software development (W. B. Mitchell, l, NC)
Geographic Information Systems operation and development (W. B. Mitchell, l, NC)
Hazard prediction and warning, socioeconomic and land use planning implications (R. H. Alexander, l, Boulder, Colo.)
Land use and land cover:
Land use pattern analysis (C. W. Spurlock, l, Gainesville, Fla.)
Mapping and data compilation (G. L. Loelkes, l, NC)
Mapping in Alaska based on Landsat digital data (Leonard Gaydos, l, Moffett Calif.)
Maps and data and other geographic studies (J. R. Anderson, l, NC)
Land use and land cover map update (V. A. Milazzo, l, NC)
Land use impact on solar-terrestrial energy systems (R. W. Pease, l, NC)
Multidisciplinary studies:
Earth-science information for decisionmakers (R. D. Brown, Jr., M)
Use of earth-science information by planners and decisionmakers (W. J. Kockelman, l M)
States:
Virginia, Culpeper Basin earth-sciences applications study (A. J. Froelich, NC)
Washington, Puget Sound region, earth sciences applications study, (B. R. Foxworthy, w, Seattle)
See also Construction and terrain problems; Urban geology; Urban hydrology.

Landslide studies:
Earthquake-induced landslides (E. L. Harp, M)
Ground failures caused by historic earthquakes (D. K. Keefer, M)
Landslide overview map of the conterminous U.S. (D. H. Radbruch-Hall, M)
Miscellaneous landslide investigations (R. W. Fleming, D)
Safe mine waste disposal, Appalachia (W. E. Davies, NC)
Tree ring analysis (S. Agard, D)
States:
California, Pacific Palisades landslide area, Los Angeles (J. T. McGill, D)
Missouri, Ground failure related to the New Madrid earthquake (S. F. Obermeier, NC)

Lead, zinc, and silver:
- Lead resources of United States (C. S. Bromfield, D)
- Zinc resources of the United States (Helmuth Wedow, Jr., Knoxville, Tenn.)
- *States:*
- Alaska, southwest Brooks Range (I. L. Tailleur, M)
- Colorado (D):
  - Precambrian sulfide deposits (D. M. Sheridan)
  - San Juan Mountains:
    - Eastern, reconnaissance (W. N. Sharp)
    - Northwestern (F. S. Fisher)
- Illinois-Kentucky district, regional structure and ore controls (D. M. Pinckney, D)
- Nevada (M):
  - Comstock district (D. H. Whitebread)
  - Silver Peak Range (R. P. Ashley)
- Utah, Park City district (C. S. Bromfield, D)

Limnology:
- Interrelations of aquatic ecology and water quality (K. V. Slack, w, M)
- Oxygen cycle in streams (R. E. Rathbun, w, Bay St. Louis, Miss.)
- Relation of ground water to lakes (T. C. Winter, w, D)
- Water quality of impoundments (J. L. Barker, w, Harrisburg, Pa.)
- *States and territories:*
- Colorado, lake reconnaissance (D. A. Wentz, w, D)
- Maine, Limnological study of lakes (D. J. Cowing, w, Boston, Mass.)
- Massachusetts, Hager Pond nutrient study (W. D. Silvey; w, Boston)
- Montana, limnology of Valley County lakes (R. F. Ferreira, w, Helena)
- Ohio, limnology of selected lakes (C. G. Angelo w, Columbus)
- Puerto Rico, Quality of Water, Lago Carraizo (Ferdinand Quinones-Marquez, w, San Juan)
- Wisconsin, hydrology of lakes (R. W. Devaul, w, Madison)
- *See also* Quality of water.

Lithium:
- Cenozic deposit history (J. R. Davis, D)
- Exploration for and resource appraisal of nonpegmatite deposits (J. D. Vine, D)
- Geochemistry of lithium clays (R. K. Glanzman, D)
- Regional distribution (E. F. Brenner-Tourtelot, D)

Lunar geology. *See* Extraterrestrial studies.

Manganese. *See* Ferro-alloy metals.

Marine geology:
- Atlantic Continental Shelf:
  - Environmental impact of petroleum exploration and production (H. J. Knebel, Woods Hole, Mass.)
  - Geophysics studies (J. C. Behrendt, Woods Hole, Mass.)
  - Magnetic chronology (E. M. Shoemaker, D. P. Elston, Flagstaff, Ariz.)
  - New England coastal zone (R. N. Oldale, Woods Hole, Mass.)
  - Organic geochemistry of Atlantic Continental Shelf and nearshore environments (R. E. Miller, NC)
  - Site surveys (W. P. Dillon, Woods Hole, Mass.)
  - Stratigraphy (J. C. Hathaway, Woods Hole, Mass.)
  - Stratigraphy and structure (J. S. Schlee, Woods Hole Mass.)
- Caribbean and Gulf of Mexico:
  - Coastal environments (H. L. Berryhill, Corpus Christi, Tex.)
  - Estuaries (C. W. Holmes, Corpus Christi, Tex.)
  - Mississippi delta studies (L. E. Garrison, Corpus Christi, Tex.)
  - Natural resources and tectonic features (R. G. Martin, Jr., Corpus Christi, Tex.)

Marine geology—Continued
- Carribbean and Gulf of Mexico—Continued
  - Oil migration and diagenesis of sediments (C. W. Holmes, Corpus Christi, Tex.)
  - Tectonics, Caribbean (J. E. Case, Corpus Christi, Tex.)
  - Tectonics, Gulf (L. E. Garrison, Corpus Christi, Tex.)
- Geotechnical investigations (D. A. Sangrey, D)
- Marine mineral resources, worldwide (F. H. Wang, M)
- Pacific and Arctic geochemistry of sediments (W. E. Dean, D)
- Pacific coast sedimentology (H. E. Clifton, M)
- Pacific Ocean, biostratigraphy, deep ocean (J. D. Bukry, La Jolla, Calif.)
- Pacific reef studies (J. I. Tracey, Jr., NC)
- Small Boat Surveys (Harley J. Knebel, Woods Hole, Mass.)
- Spanish continental margin (Almeria Province) (P. D. Snavely, Jr., H. G. Greene, H. F. Clifton, W. P. Dillon, J. M. Robb, M)
- Volcanic geology, Mariana and Caroline Islands (Gilbert Corwin, NC)
- World offshore oil and gas (T. H. McCulloh, Seattle, Wash.)
- *States and territories:*
- Alaska (M, except as otherwise noted):
  - Arctic coastal marine processes (Erik Reimnitz)
  - Beaufort-Chuckchi Sea Continental Shelf (Arthur Grantz)
  - Beaufort Sea environment studies (P. W. Barnes)
  - Bering Sea:
    - General study (D. W. Scholl)
    - Northern:
      - Environmental geologic studies (C. H. Nelson)
      - Sea floor (C. H. Nelson)
  - Coastal environments (A. T. Ovenshine)
  - Continental Shelf resources (D. M. Hopkins)
  - Cook Inlet (L. B. Magoon III)
  - Gulf of Alaska (B. F. Molnia)
  - Seward Peninsula, nearshore (D. M. Hopkins)
  - Tectonic history (R. E. von Huene, NC)
- California (M):
  - Borderlands:
    - Geologic framework (A. E. Roberts)
    - Southern part (G. W. Moore)
  - Continental Margin, central part (E. A. Silver)
  - La Jolla marine geology laboratory (G. W. Moore)
  - Monterey Bay (H. G. Greene)
  - San Francisco Bay:
    - General study (D. S. McCulloch)
    - Geochemistry of sediments (D. H. Peterson)
- Oregon, land-sea transect, Newport (P. D. Snavely, Jr., M)
- Oregon-California, black sands (H. C. Clifton, M)
- Oregon-Washington, nearshore (P. D. Snavely, Jr., M)
- Puerto Rico, coooperative program (J. V. A. Trumbull, Santurce)
- Texas, barrier islands (R. E. Hunter, Corpus Christi)

Marine geotechnique:
- Marine geotechnical investigations (H. W. Olsen, D)

Marine hydrology:
- Hydrologic-oceanographic studies (F. A. Kohout, w, Woods Hole, Mass.)
- *States and territories:*
- Maryland, estuarine ecology (R. L. Cory, w, Edgewater)
- Puerto Rico, San Juan lagoons (S. R. Ellis, w, San Juan)
- *See also* Hydrology, surface water; Quality of water; Geochemistry, water; Marine geology.

Mercury:
- Geochemistry (A. P. Pierce, D)
- Mercury deposits and resources (E. H. Bailey, M)

Mercury—Continued
State:
California, Coast Range ultramafic rocks (E. H. Bailey, M)
Metamorphism:
Combustion, high temperature minerals (J. R. Herring, D)
Meteorites. *See* Extraterrestrial studies.
Mine drainage and hydrology
Chemical models—coal hydrology (D. C. Thorstenson, w, NC)
Water monitoring-coal mining, Northeastern region (F. T. Schaefer, w, NC)
Water monitoring—coal mining, Southeastern region (C. A. Pascale, w, Atlanta, Ga.)
States:
Alabama, Water monitoring—coal mining (J. R. Harkins, w, University)
Georgia, Water monitoring—coal mining (W. H. Norris, w, Doraville)
Illinois (w, Champaign):
Mine reclamation hydrology (E. A. Magner)
Water monitoring-coal mining (E. E. Zuehls)
Indiana (w, Indianapolis):
Effects of strip mining and reclamation (J. C. Peters)
Hydrology of coal mine area (J. S. Zogorski)
Uranium, remote sensing for uranium exploration (G. L. Raines, D)
Water monitoring—coal mining (S. E. Ragone)
Kansas, Coal hydrology of east-central Kansas (C. D. Albert, w, Lawrence)
Kentucky (w, Louisville):
Downstream effects of coal mining (J. E. Dysart)
Water from coal mines (D. S. Mull)
Water monitoring—coal mining (Ferninand Quinones)
Maryland:
Hydrologic effects of coal mining (M. T. Duigon, w, Towson)
Water monitoring—coal mining (W. W. Staubitz, w, Towson)
New Mexico, San Juan coal monitoring (J. D. Dewey, w, Albuquerque)
Ohio:
Mine reclamation, Lake Hope Basin (T. M. Crouch, w, Columbus)
Water monitoring—coal mining (R. O. Hawkson, w, Columbus)
Pennsylvania (w, Harrisburg):
Coal hydrology of Big Sandy Creek (D. L. Bingham)
Daylighting—hydrology of Babb Creek (L. A. Reed)
Mine-site application for Office of Surface Mining (W. J. Herb)
Water monitoring—coal mining (J. R. Ritter)
Western Middle anthracite hydrology (D. J. Growitz)
Tennessee:
Landsat basin characteristics (E. F. Hollyday, w, Nashville)
Water monitoring, coal mining (V. J. May, w, Nashville)
Utah (w, Salt Lake City):
Ferron sandstone, Castle Valley (G. C. Lines)
Huntington coal hydrology (T. W. Danielson)
Price River basin (K. M. Waddell)
Water monitoring—coal mining (K. M. Waddell)
Virginia:
Reconnaissance of coal areas (S. M. Rogers, w, Richmond)
Water monitoring—coal mining (P. M. Frye, w, Richmond)
West Virginia (w, Charleston):
Deep-mine collapse hydrology (W. H. Hobba)
Quantitative mine-water studies (G. G. Wyrick)
Water monitoring—coal mining (D. H. Appel)
Wyoming, water monitoring coal mining (S. A. Druse, w, Cheyenne)
Mineral and fuel resources—compilations and topical studies:
Application massive sulfides, Virginia deposits (J. E. Gair, NC)
Arctic mineral-resource investigations (R. M. Chapman, M)
Basin and Range, geologic studies (F. G. Poole, D)
Colorado Plateau (R. P. Fischer, D)
Information bank, computerized (J. A. Calkins, NC)
Mineral-resource surveys:
Mineral resource estimation (W. D. Menzie, M)
Mineral resources of Precambrian rocks in St. Lawrence County, New York (C. E. Brown, NC)
Minerals for energy production (L. F. Rooney, NC)
Primitive, Wilderness, and RARE II Areas:
Beaver Creek, Kentucky (K. J. Englund, NC)
Beaver Creek Wilderness and Troublesome RARE II, Kentucky (K. J. Englund, NC)
Big Sandy-W. Elliotts Creek RARE II, Alabama (S. H. Patterson, NC)
Bob Marshall Wilderness Area, Montana (R. L. Earhart, D)
Caney Creek Wilderness, Arkansas (G. E. Erickson, NC)
Cheat Mountain RARE II, West Virginia (K. J. Englund, NC)
Cohutta Wilderness, Georgia-Tennessee (J. E. Gair, NC)
Cornplanter RARE II, Pennsylvania (F. G. Lesure, NC)
Devils Fork RARE II, Virginia (K. J. Englund, NC)
Dolly Ann RARE II, Virginia (F. G. Lesure, NC)
Elkhorn Wilderness Study Area, Montana (W. R. Greenwood, D)
Ellicott Rock Wilderness, South Carolina-North Carolina-Georgia (R. W. Luce, NC)
Florida RARE II (S. H. Patterson, NC)
Gates of the Mountains Wilderness Area, Montana (M. W. Reynolds, D)
Gee Creek Wilderness, Tennessee (J. E. Epstein, NC)
Glacier Bay National Monument Wilderness Area, Alaska (D. A. Brew, M)
Illinois RARE II (J. S. Klasner, Macomb, Ill.)
James River Face Wilderness Area, Virginia (C. E. Brown, NC)
John Muir Wilderness, California (N. K. Huber, M)
King Range—Chemise Mountains, California (R. J. McLaughlin, M)
Linville Gorge Wilderness, North Carolina (J. P. D'Agostino, NC)
Little Frog RARE II, Tennessee (E. R. Force, NC)
Madison—Gallatin study area, Montana (F. S. Simons, D)
Mazatzal Wilderness, Arizona (C. T. Wrucke and C. M. Conway, M)
Mount Hood and Zigzag Wilderness Areas, Oregon (T. E. C. Keith M)
North Georgia RARE II (A. E. Nelson, NC)
Otter Creek Wilderness, West Virginia (K. J. Englund, NC)
Pecos Wilderness, New Mexico (R. H. Moench, D)
Pennsylvania RARE II (S. P. Schweinfurth, NC)
Rawah Wilderness Area and nearby study areas, Colorado (R. C. Pearson, D)
Sandy Creek RARE II, Mississippi (E. G. A. Weed, NC)
Selway-Bitterroot Wilderness, Idaho and Montana (W. R. Greenwood, D)
Shinbone-Adams Creek RARE II, Alabama (G. E. Tolbert, NC)

Mineral and fuel resources—compilations and topical studies—Continued
Mineral-resource surveys—Continued
Primitive, Wilderness, and RARE II Areas—Continued
Shining Rock Wilderness, North Carolina (F. G. Lesure, NC)
Sipsey River, Alabama (S. P. Schweinfurth, NC)
Sipsey River Wilderness and RARE II Additions, Alabama (S. P. Schweinfurth, NC)
Snow Mountain Wilderness Area, California (D. Grimes, D)
Snowy Range Wilderness Study Area, Wyoming (R. S. Houston, D)
Southern Massanutten RARE II, Virginia (F. G. Lesure, NC)
Superstition Wilderness, Arizona (D. W. Peterson, D)
Washakie Wilderness, Wyoming (J. C. Antwiler, D)
West Chichagof-Yakobi Wilderness Study Area, Alaska (B. R. Johnson, M)
Nonmetallic deposits, mineralogy (B. M. Madsen, M)
Oil and gas resources:
Central and northern California Continental Shelf (C. W. Spencer, D)
Outer Continental Shelf (R. B. Powers, E. W. Scott, D)
Permian Basin (G. L. Dolton, S. E. Frezon, Keith Robinson, A. B. Coury, K. L. Varnes, D)
Petroleum potential of southern California borderland appraised (C. W. Spencer, D)
Resource analysis, economics of mineral resources (J. H. DeYoung, Jr., NC)
Wilderness Program:
Geochemical services (D. J. Grimes, D)
Geophysical services (M. F. Kane, D)
States:
Alaska (M):
AMRAP Program (J. E. Case)
Mineral resources (E. H. Cobb)
Petersburg quadrangle (D. A. Brew)
Southwestern Brooks Range (I. L. Tailleur)
Colorado:
Precambrian sulfide deposits (D. M. Sheridan, D)
Summitville district, alteration study (R. E. Van Loenen, D)
Missouri, Rolla 2° quadrangle, mineral-resource appraisal (W. P. Pratt, D)
Nevada, igneous rocks and related ore deposits (M. L. Silberman, M)
United States:
Central States, mineral-deposit controls (A. V. Heyl, Jr., D)
Iron-resources studies (Harry Klemic, NC)
Lightweight-aggregate resources (A. L. Bush, D)
Metallogenic maps (P. W. Guild, NC)
Northeastern States, peat resources (C. C. Cameron, NC)
Southeastern States, mineral-resource surveys (R. A. Laurence, Knoxville, Tenn.)
Wisconsin, northern, mineral-resource survey (C. E. Dutton, Madison)
See also specific minerals or fuels.

Mineralogy and crystallography, experimental:
Crystal chemistry (Malcolm Ross, NC)
Crystal structure, sulfides (H. T. Evans, Jr., NC)
Electrochemistry of minerals (Motoaki Sato, NC)
Mineralogic services and research (R. C. Erd, M)
Mineralogical crystal chemistry (J. R. Clark, M)
Mineralogy of heavy metals (F. A. Hildebrand, D)
Planetary mineralogical studies (Priestley Toulmin III, NC)
Research on ore minerals (B. F. Leonard, D)
See also Geochemistry, experimental.

Minor elements:
Geochemistry (George Phair, NC)
Niobium:
Colorado, Wet Mountains (R. L. Parker, D)
Niobium and tantalum, distribution in igneous rocks (David Gottfried, NC)
Phosphoria Formation, stratigraphy and resources (R. A. Gulbrandsen, M)
Nonpegmatic lithium resources (J. D. Vine, D)
Rare-earth elements, resources and geochemistry (J. W. Adams, D)
Trace-analysis methods, research (F. N. Ward, D)

Model studies, geologic and geophysical:
Computer modeling:
Research for engineering geology (W. Z. Savage, D)
Rock-water interactions (J. L. Haas, Jr., NC)
Tectonic deformation (J. H. Dieterich, M)
Ice Ages (D. P. Adam, M)

Model studies, hydrologic:
Alluvial fan deposition (W. E. Price, w, NC)
Atchafalaya River basin model (M. E. Jennings, w, Bay St. Louis, Miss.)
Ground-water hydrology, strip-mining areas (J. O. Helgesen, w, Columbus, Ohio)
High Plains aquifer study (J. B. Weeks, w, D)
Hydrodynamics of a tidal estuary (R. T. Cheng, w, M)
Miocene aquifer study (E. T. Baker, Jr., w, Austin, Tex.)
Modeling organic solute transport (J. B. Robertson, w, M)
Nevada Test Site hydrologic model (D. I. Leap, w, D)
Numerical simulation (V. C. Lai, w, NC)
Operation models, surface-water systems (M. E. Jennings, w, Bay St. Louis, Miss.)
Physical modeling (V. R. Schneider, w, Bay St. Louis, Miss.)
Rainfall-runoff modeling (G. H. Leavesley, w, D)
Regional Studies Coordination (G. D. Bennett, w, NC)
Simulation of hydrogeologic systems (R. L. Cooley, w, D)
Streamflow models (P. R., Jordan, w, Lawrence, Kans.)
Surface-water-quality modeling (S. M. Zand, w, M)
Systems Analysis Laboratory (I. C. James, w, NC)
Transient flow (C. E. Mongan, w, Cambridge, Mass.)
Transport in fluid flow (Akio Ogata, w, M)
Water-quality modeling (D. B. Grove, w, D)
Watershed modeling (J. F. Turner, w, Tampa, Fla.)
States:
Arizona:
Coconino aquifer—Apache County, Arizona (P. P. Ross, w, Phoenix)
Southwest alluvial basins (T. W. Anderson, w, Tucson)
Arkansas (w, Little Rock):
Bartholomew Stream Flow Subsystem (M. E. Broom)
Illinois River model (C. T. Bryant)
California:
Develop ground-water models, Salinas Valley (M. J. Johnson, w, M)
Digital model of Carmel Valley (M. J. Johnson, w, M)
Ground water, Model Fresno County (H. T. Mitten, w, Sacramento)
Impact of Marble Cone Fire (K. W. Lee, w, M)
Sacramento Valley ground water (S. K. Sorenson, w, Sacramento)
Water supply forecast evaluation (K. L. Wahl, w, M)
Colorado:
Geochemical investigation (R. L. Tobin, w, D)
Rocky Mountain Arsenal DIMP contamination (S. G. Robson, w, D)
Water management—High Plains (R. G. Borman, w, D)

Model studies, hydrologic—Continued
States—Continued
Delaware:
Coastal aquifers study (A. L. Hodges, Jr., w, Dover)
Delaware Potomac aquifer study (P. P. Leahy, w, Dover)
Florida:
Ground water, Ft. Lauderdale (Ellis Donsky, w, Miami)
Hydrologic effects, west-central Florida (D. M. Johnson, w, Tampa)
Southeast limestone, east-central Florida (C. H. Tibbals, w, Orlando)
Southeast limestone, west-central Florida (P. D. Ryder, w, Tampa)
Water resources, Ft. Walton Beach area (L. R. Hayes w, Tallahassee)
Watershed modeling (K. M. Hammet, w, Tampa)
Georgia (w, Doraville):
Cretaceous-Tertiary Aquifer (L. D. Pollard)
Ground water models (W. C. Meeks)
Principal artesian aquifer (L. R. Hayes)
Idaho, Rathdrum Prairie aquifer (H. R. Seitz, w, Boise)
Indiana (w, Indianapolis):
Dissolved Oxygen Modeling and Assimilation Studies (S. E. Ragone)
Logansport ground-water study (D. C. Gillies)
Kansas, Ground water-surface water, north-central Kansas (L. E. Stullken, w, Garden City)
Maryland (w, Towson):
Aquia-Piney Point-Nanjemoy aquifers (F. H. Chapelle)
Ground water from Maryland coastal plain (W. B. Fleck)
Small basin modelling (R. E. Wiley)
Massachusetts, De-icing chemicals, ground water (L. R. Frost, w, Boston)
Minnesota, Evaluation of quality-of-water, data for management (M. S. McBride, w, St. Paul)
Mississippi:
Ground water model—Yazoo River navigation (J. M. Kernodle, w, Jackson)
Modeling of Tupelo ground-water system (J. M. Kernodle w, Jackson)
Nebraska, High Plains aquifer study (R. A. Pettijohn, w, Lincoln)
Nevada (w, Carson City):
Eagle Valley ground-water model (F. E. Artega)
Jones-Galena Creek water resources (T. L. Katzer)
Las Vegas Valley ground-water models (J. R. Harrill)
Sediment Transport Model E. FK. Carson R. (T. L. Katzer)
New Jersey (w, Trenton):
Englishtown Formation (W. D. Nichols)
Simulation of multilayer aquifer (A. W. Harbaugh)
New York:
Chemical weathering model (N. E. Peters, w, Albany)
Flow routing—Upper Susquehanna (T. J. Zembrzuski, w, Albany)
Ground water in western Long Island (Julian Soren, w, Syosset)
Ground water models, Long Island (T. E. Reilly, w, Syosset)
Hudson River estuary flow model (W. N. Embree, w, Albany)

Model studies, hydrologic—Continued
States—Continued
New York—Continued
Impact and mitigation of sewering (G. E. Kimmel, w, Syosset)
Tioughnioga River ground water (O. J. Cosner, w, Albany)
Ohio, Franklin County digital model (A. C. Razem, w, Columbus)
Oklahoma (w, Oklahoma City):
North Canadian hydrology (R. E. Davis)
Coal Creek basin, (S. P. Blumer)
Great Salt Plains study (J. E. Reed)
High Plains aquifer study (J. S. Havens)
Oregon, Portland Well Field Model (J. E. Luzier, w, Portland)
Pennsylvania (w, Harrisburg):
Delaware River streamflow model (J. O. Shearman)
Flow routing, Chemung (J. T. Armbruster)
Flow simulation, Juniata River (J. T. Armbruster)
Laurel Run Dam failure (J. R. Armbruster)
Schuylkill River, quality (G. L. Pederson)
West Branch Brandywine Creek stormwater model (R. A. Sloto, w, Malvern)
South Dakota:
Digital model, James River basin (L. K. Kuiper, w, Huron)
Water resources of Big Sioux Valley (N. C. Koch, w, Huron)
Tennessee, Memphis ground-water model (J. V. Brahana, w, Nashville)
Texas, High Plains Aquifer Study (I. D. Yost, w, Austin)
Utah, Hydrology of Beryl-Enterprise area (R. W. Mower, w, Salt Lake City)
Washington (w, Tacoma):
Columbia River basalt model (D. B. Sapik)
Spokane drainfield study (E. L. Bolke)
Wisconsin (w, Madison):
Lake Winnebago digital model (W. R. Krug)
Land-use changes, southwest Wisconsin, (W. R. Krug)
Nonpoint pollution in Fox basin (P. E. Hughes)
Wisconsin River model (W. R. Krug)
Wyoming, Digital model, La Grange area (W. B. Borchert, w, Cheyenne)
Molybdenum. *See* Ferro-alloy metals.
Moon studies. *See* Extraterrestrial studies.
Nickle. *See* Ferro-alloy metals.
Nuclear explosions, geology:
Engineering geophysics, Nevada Test Site (R. D. Carroll, D)
Environmental effects (P. P. Orkild, D)
Geologic investigations:
Nevada Test Site:
Nevada Test Site (P. P. Orkild, D)
Northern Yucca Flat and Pahute Mesa (W. D. Quinlivan, D)
Pahute Mesa and central and southern Yucca Flat (G. L. Dixon, D)
Nuclear explosions, hydrology:
Nuclear explosive underground engineering, hydrology (J. E. Weir, w, D)
Yucca Flat hydrology (G. C. Doty, w, Mercury, Nev.)
States:
Alaska, Hydrology of Amchitka Island Test Site (D. D. Gonzalez, w, D)
Nevada, Nevada Test Site, hydrology (W. W. Dudley, Jr., w, D)

Oil shale:
- East-central Uinta Basin (G. N. Pipiringos, D)
- Organic geochemistry (R. E. Miller, D)
- Petrology (J. R. Dyni, D)
- Regional geochemistry (W. E. Dean, Jr., D)
- Stratigraphic studies, eastern Uinta Basin (W. B. Cashion, Jr., D)
- Trace elements (W. E. Dean, Jr., D)
- *States:*
- Colorado (D):
  - Central Roan Cliffs area (W. J. Hall)
  - Lower Yellow Creek area (W. J. Hall)
  - Piceance Creek basin:
    - East-central (R. B. O'Sullivan)
    - Experimental mining (R. P. Snyder)
    - General (J. R. Donnell)
    - Northwestern (G. N. Pipiringos)
    - Stratigraphy of the Green River Formation (R. C. Johnson, D)
- Colorado-Utah-Wyoming, geochemistry (W. E. Dean, Jr., D)
- Colorado-Wyoming, Eocene rocks (H. W. Roehler, D)
- Nevada, Investigations of oil shale of Tertiary age (B. Solomon, c, M)
- Utah, South ½ Nutters Hole quadrangle (W. B. Cashion, Jr., D)

Paleobotany, systematic:
- Diatom studies (G. W. Andrews, NC)
- Floras:
  - Cenozoic:
    - Pacific Northwest (J. A. Wolfe, M)
    - Western United States and Alaska (J. A. Wolfe, M)
  - Devonian (J. M. Schopf, Columbus, Ohio)
  - Paleozoic (S. H. Mamay, NC)
- Fossil wood and general paleobotany (R. A. Scott, D)
- Modern seeds, California (J. A. Wolfe, D. P. Adam, M)
- Plant microfossils:
  - Mesozoic (R. H. Tschudy, D)
  - Paleozoic (R. M. Kosanke, D)

Paleoecology:
- Faunas, Late Pleistocene, Pacific coast (W. O. Addicott, M)
- Fish, Quaternary, California (R. Casteel, D. P. Adam)
- Foraminifera, ecology (M. R. Todd, NC)
- Ostracodes, Recent, North Atlantic (J. E. Hazel, NC)
- Paleoenvironmental studies, Miocene, Atlantic Coastal Plains (T. G. Gibson, NC)
- Pollen, Quaternary, California (D. P. Adam, M)
- *Tempskya*, Southwestern United States (C. B. Read, Albuquerque, N. Mex.)
- Vertebrate faunas, Ryukyu Islands, biogeography (F. C. Whitmore, Jr., NC)

Paleontology, invertebrate, systematic:
- Brachiopods:
  - Carboniferous (Mackenzie Gordon, Jr., NC)
  - Ordovician (R. B. Neuman, NC; R. J. Ross, Jr., D)
  - Upper Paleozoic (J. T. Dutro, Jr., NC)
- Bryozoans, Ordovician (O. L. Karklins, NC)
- Cephalopods:
  - Cretaceous (D. L. Jones, M)
  - Jurassic (R. W. Imlay, NC)
  - Upper Cretaceous (W. A. Cobban, D)
  - Upper Paleozoic (Mackenzie Gordon, Jr., NC)
- Chitinozoans, Lower Paleozoic (J. M. Schopf, Columbus, Ohio)
- Conodonts, Devonian and Mississippian (C. A. Sandberg, D)
- Corals, rugose:
  - Mississippian (W. J. Sando, NC)
  - Silurian-Devonian (W. A. Oliver, Jr., NC)

Paleontology, invertebrate, systematic—Continued
- Foraminifera:
  - Fusuline and orbitoline (R. C. Douglass, NC)
  - Cenozoic (M. R. Todd, NC)
  - Cenozoic, California and Alaska (P. J. Smith, M)
  - Mississippian (B. A. Skipp, D)
  - Recent, Atlantic shelf (T. G. Gibson, NC)
- Gastropods:
  - Mesozoic (N. F. Sohl, NC)
  - Miocene-Pliocene, Atlantic coast (T. G. Gibson, NC)
  - Paleozoic (E. L. Yochelson, NC)
- Graptolites, Ordovician-Silurian (R. J. Ross, Jr., D)
- Mollusks, Cenozoic, Pacific coast (W. A. Addicott, M)
- Ostracodes:
  - Lower Paleozoic (J. M. Berdan, NC)
  - Upper Cretaceous and Tertiary (J. E. Hazel, NC)
  - Upper Paleozoic (I. G. Sohn, NC)
- Pelecypods:
  - Inoceramids (D. L. Jones, M)
  - Jurassic (R. W. Imlay, NC)
  - Paleozoic (John Pojeta, Jr., NC)
  - Triassic (N. J. Silberling, M)
- Trilobites, Ordovician (R. J. Ross, Jr., D)

Paleontology, stratigraphic:
- Cenozoic:
  - Diatoms, Great Plains, nonmarine (G. W. Andrews, NC)
  - Foraminifera, smaller, Pacific Ocean and islands (M. R. Todd, NC)
  - Mollusks:
    - Atlantic coast, Miocene (T. G. Gibson, NC)
    - Pacific coast, Miocene (W. O. Addicott, M)
  - Pollen and spores, Kentucky (R. H. Tschudy, D)
  - Vertebrates:
    - Atlantic coast (F. C. Whitmore, Jr., NC)
    - Pacific coast (C. A. Repenning, M)
    - Panama Canal Zone (F. C. Whitmore, Jr., NC)
    - Pleistocene (G. E. Lewis, D)
- Mesozoic:
  - Pacific coast and Alaska (D. L. Jones, M)
  - Cretaceous:
    - Alaska (D. L. Jones, M)
    - Foraminifera:
      - Alaska (H. R. Bergquist, NC)
      - Atlantic and Gulf Coastal Plains (H. R. Bergquist, NC)
      - Pacific coast (R. L. Pierce, M)
    - Gulf coast and Caribbean (N. F. Sohl, NC)
    - Molluscan faunas, Caribbean (N. F. Sohl, NC)
    - Western Interior United States (W. A. Cobban, D)
  - Jurassic, North America (R. W. Imlay, NC)
  - Triassic, marine faunas and stratigraphy (N. J. Silberling, M)
- Paleozoic:
  - Devonian and Mississippian conodonts, Western United States (C. A. Sandberg, D)
  - Fusuline Foraminifera, Nevada (R. C. Douglass, NC)
  - Mississippian:
    - Stratigraphy and brachiopods, northern Rocky Mountains and Alaska (J. T. Dutro, Jr., NC)
    - Stratigraphy and corals, northern Rocky Mountains (W. J. Sando, NC)
  - Mississippian biostratigraphy, Alaska (A. K. Armstrong, M)
  - Onesquethaw Stage (Devonian), stratigraphy and rugose corals (W. A. Oliver, NC)

Paleontology, stratigraphic—Continued
Paleozoic—Continued
Ordovician:
Bryozoans, Kentucky (O. L. Karklins, NC)
Stratigraphy and brachiopods, Eastern United States (R. B. Neuman, NC), Western United States (R. J. Roxx, Jr., D)
Paleobotany and coal studies, Antarctica (J. M. Schopf, Columbus, Ohio)
Palynology of cores from Naval Petroleum Reserve No. 4 (R. A. Scott, D)
Pennsylvanian:
Fusulinidae:
Alaska (R. C. Douglass, NC)
North-central Texas (D. A. Myers, D)
Spores and pollen, Kentucky (R. M. Kosanke, D)
Permian, floras, Southwestern United States (S. H. Mamay, NC)
Silurian-Devonian:
Corals, Northeastern United States (W. A. Oliver, Jr., NC)
Upper Silurian-Lower Devonian, Eastern United States (J. M. Berdan, NC)
Subsurface rocks, Florida (J. M. Berdan, NC)
Upper Paleozoic, Western States (Mackenzie Gordon, Jr., NC)
Paleontology, vertebrate, systematic:
Artiodactyls, primitive (F. C. Whitmore, Jr., NC)
Pinnipedia (C. A. Repenning, M)
Pleistocene fauna, Big Bone Lick, Kentucky (F. C. Whitmore, Jr., NC)
Tritylodonts, American (G. E. Lewis, D)
Paleotectonic maps. *See* Regional studies and compilations.
Petroleum and natural gas:
Automatic data-processing system for field and reservoir estimates (K. A. Yenne, c, Los Angeles, Calif.)
Borehole gravimetry, application to oil exploration (J. W. Schmoker, D)
Catagenesis of organic matter and generation of petroleum (N. H. Bostick, D)
Devonian black shale, Appalachian Basin:
Borehole gravity study (J. W. Schmoker, D)
Clay mineralogy (J. W. Hosterman, NC)
Conodont maturation (A. G. Harris, NC)
Data storage and retrieval system
Geochemical study (G. E. Claypool, D)
Stratigraphy (J. B. Roen, NC)
Structural studies (L. D. Harris, NC)
Uranium and trace-element study (J. S. Leventhal, D)
Gulf of Mexico, oil and gas resources of the Gulf of Mexico (B. M. Miller, D)
Methods of recovery (F. W. Stead, D)
Oil and gas map, North America (W. W. Mallory, D)
Oil and gas resource appraisal methodology and procedures (B. M. Miller, D)
Organic geochemistry (J. G. Palacas, D)
Origin and distribution of natural gases (D. D. Rice, D)
Origin, migration, and accumulation of petroleum (L. C. Price, D)
Petroleum prospecting with helium detector (A. A. Roberts, D)
Rocky Mountain States, seismic detection of stratigraphic traps (R. T. Ryder, D)
Tight gas sands (D. D. Rice, D)
Western Interior Cretaceous studies (C. W. Spencer, D)
Petroleum and natural gas—Continued
Western United States:
Devonian and Mississippian (C. A. Sandberg, D)
Devonian and Mississippian flysch source-rock studies (F. G. Poole, D)
Properties of reservoir rocks (R. F. Mast, D)
Source rocks of Permian age (E. K. Maughan, D)
States:
Alaska (M):
Cook Inlet (L. B. Magoon III)
Northeastern Arctic Slope Federal-State field project (I. F. Palmer, c, Anchorage)
North Slope, petroleum geology (R. D. Carter)
NPRA (National Petroleum Reserve Alaska) Oil and Gas Source Rock Study (L. B. Magoon III, M)
Arkansas, Sandstone reservoirs (B. R. Haley, Little Rock)
California:
Carpenteria and Hondo-Santa Ynez field reserves, OCS (D. G. Griggs, c, Los Angeles)
Eastern Los Angeles basin (T. H. McCulloh, Seattle, Wash.)
Salinas Valley (D. L. Durham, M)
Southern San Joaquin Valley, subsurface geology (J. C. Maher, M)
Colorado:
Citadel Plateau (G. A. Izett, D)
Grand Junction 2° quadrangle (W. B. Cashion, Jr., D)
Piceance Creek basin—low permeability gas sands (R. C. Johnson, D)
New Mexico, San Juan Basin (E. R. Landis, D)
Utah, Grand Junction 2° quadrangle (W. B. Cashion, Jr., D)
Wyoming, Stratigraphy, lower Upper Cretaceous formations (E. A. Merewether, D)
Wyoming-Montana-North Dakota-South Dakota, Williston Basin (C. A. Sandberg, D)
Petrology. *See* Geochemistry and petrology, field studies.
Phosphate:
Phosphoria Formation, stratigraphy and resources (R. A. Gulbrandsen, M)
States:
Idaho, Lower Valley quadrangle (P. Oberlindacher, c, M)
Montana, Melrose phosphate field (G. D. Fraser, c, D)
Nevada:
Loray quadrangle (S. T. Miller, c, M)
Montello Canyon quadrangle (S. T. Miller, c, M)
United States, southeastern phosphate resources (J. B. Cathcart, D)
Utah, Ogden 4 NW quadrangle (R. J. Hite, c, D)
Wyoming:
Pickle Pass quadrangle (M. L. Schroeder, c, D)
Pine Creek quadrangle (M. L. Schroeder, c, D)
Placers:
Placers of Alaska (Warren Yeend, M)
Plant ecology:
Element availability:
Hydrology and Pinyon-Juniper (J. J. Owen, w, D)
Soils (R. C. Severson, D)
Vegetation (L. P. Gough, D)
Periodic plant-growth phenomena and hydrology (R. L. Phipps, w, NC)
Vegetation and hydrology (R. S. Sigafoos, w, NC)
Western coal regions, geochemical survey of vegetation (J. A. Erdman, D)
See also Evapotranspiration; Geochronological investigations; Limnology.

Platinum:
Mineralogy and occurrence (G. A. Desborough, D)
States:
Montana, Stillwater complex (N. J. Page, M)
Wyoming, Medicine Bow Mountains (M. E. McCallum, Fort Collins, Colo.)

Potash:
Colorado and Utah, Paradox Basin (O. B. Raup, D)
New Mexico, Carlsbad, potash and other saline deposits (C. L. Jones, M)

Primitive areas. *See under Mineral and fuel resources*—compilations and topical studies, mineral-resource surveys.

Public and industrial water supplies. *See* Quality of water; Water resources.

Quality of water:
Atlanta Central Lab atomic absorption (F. E. King, w, Doraville, Ga.)
Atlanta Central Lab automated methods (A. J. Horowitz, w, Doraville, Ga.)
Atlanta Central Lab—biological analyses (R. G. Lipscomb, w, Doraville, Ga.)
Atlanta Central Lab—manual methods (E. R. Anthony, w, Doraville, Ga.)
Atlanta Central Lab—organic analyses (L. E. Lowe, w, Doraville, Ga.)
Atlanta Central Lab—special methods (D. K. Leifeste, w, Doraville, Ga.)
Bedload samplers (D. W. Hubbell, w, D)
Benchmark network (R. R. Pickering, w, NC)
Biological information assessment (B. W. Lium, w, Doraville, Ga.)
Central Laboratories (W. A. Beetem, w, NC)
Chemistry of New Zealand waters (I. K. Barnes, w, M)
Data evaluation support (R. E. Gust, w, D)
Denver Central Lab—atomic absorption (D. B. Manigold, w, D)
Denver Central Lab—automated methods (V. C. Marti, w, D)
Denver Central Lab—biological analyses (S. A. Duncan, w, D)
Denver Central Lab—logistical support (R. E. Gust, w, D)
Denver Central Lab—manual methods (S. A. Duncan, w, D)
Denver Central Lab—organic analyses (D. B. Manigold, w, D)
Denver Central Lab—physical properties (R. L. McAvoy, w, D)
Denver Central Lab—radiochemical analyses (S. A. Duncan, w, D)
Denver Central Lab—special methods (R. L. McAvoy, w, D)
Denver Central Laboratory (R. L. McAvoy, w, D)
Development of biological methods (B. W. Lium, w, Atlanta, Ga.)
Development of water methods (B. A. Malo, w, D)
Digital model-waste transport (J. B. Robertson, w, Idaho Falls, Idaho)
Geochemical kinetics studies (H. C. Claassen, w, D)
Geochemical kinetics, volcanic rocks (H. C. Claassen, w, D)
Geochemistry, oil field waters, Alaska (Y. K. Kharaka, w, M)
Geochemistry, Western coal region (G. L. Feder, w, D)
Hydraulic fracturing waste disposal (R. J. Sun, w, NC)
Hydrologic interpretations (E. J. Pluhowski, w, NC)
Hydrology of central Nevada (G. A. Dinwiddie, w, D)
Improvement of QW data system (D. A. Goolsby, w, NC)
Instrumentation, petrochemical (W. A. Beetem, w, NC)
Laboratory evaluation (V. J. Janzer, w, D)
Methods coordination (M. W. Skougstad, w, D)

Quality of Water—Continued
Methods development (W. A. Beetem, w, NC)
Methods development support (D. E. Erdman, w, Doraville, Ga.)
Methods for organics (W. E. Pereira, w, D)
Methods for pesticides (T. R. Steinheimer, w, D)
Methods for trace metals (H. E. Taylor, w, D)
Modeling mineral-water reactions (L. N. Plummer, w, NC)
National river quality (J. F. Ficke, w, NC)
National water quality laboratories—quality assurance report (D. Boyle, w, D)
Nevada Test Site geochemistry (A. F. White, w, D)
Nevada Test Site tracer studies (D. I. Leap, w, D)
Nevada Test Site waste sites (G. C. Doty, w, Mercury, Nev.)
Nuclear hydrology services (W. W. Dudley, w, D)
Organic deep waste storage (R. L. Malcolm, w, D)
Organic polyelectrolytes (R. L. Wershaw, w, D)
Organic substances in streams (R. E. Rathbun, w, Bay St. Louis, Miss.)
Organics in oil-shade residues (J. A. Leenheer, w, D)
Organics in water (D. F. Goerlitz, w, M)
Pesticide monitoring network (R. J. Pickering, w, NC)
Poplar River waste quality (R. C. Averett, w, D)
Potomac Estuary studies (J. P. Bennett, w, NC)
Precipitation quality network (R. J. Pickering, w, NC)
Quality assurance (W. A. Beetem, w, NC)
Quality assurance (L. J. Schroder, w, D)
Quality assurance procedures (L. C. Friedman, w, D)
Radioanalytical methods (L. L. Thatcher, w, D)
Radiochemical techniques of water resources investigations (V. J. Janzer, w, D)
Radiohydrology of explosion sites (H. C. Claassen, w, D)
Radionuclide migration at Nevada Test Site (H. C. Claassen, w, D)
Radionuclides on sediments (D. D. Gonzalez, w, D)
Standard reference water sample program (M. J. Fishman, w, D)
Techniques of water resources investigations manuals (M. J. Fishman, w, D)
Temperature modeling in natural streams (A. P. Jackman, w, M)
Thermal modeling (H. E. Jobson, w, Bay St. Louis, Miss.)
Thermal pollution (G. E. Harbeck, Jr., w, D)
Toxic substances in aquatic ecosystems (H. V. Leland, w, M)
Trace-element availability in sediments (S. N. Luoma, w, M)
Transition metal hydrogeochemistry (Edward Callender, w, NC)
Transport in ground water (L. F. Konikow, w, D)
Transuranium research (J. M. Cleveland, w, D)
Turbulent diffusion and thermal loading (Nobuhiro Yotsukura, w, NC)
Waste management off Nevada Test site (J. E. Weir, w, D)
Water quality analysis—other federal agencies (J. P. Monis, w, D)
Water quality and health (G. L. Feder, w, D)
Water-quality-data evaluation (W. H. Doyle, Jr., w, D)
States and territories:
Alabama, Water resources in oil fields (W. J. Powell, w, Tuscaloosa)
Alaska, Arctic lakes (G. A. McCoy, w, Anchorage)
Arizona:
Ground-water, Little Colorado basin (S. G. Brown, w, Tucson)
Papago-arsenic in drinking water (L. J. Mann, w, Tucson)
Arkansas (w, Little Rock):
L'anguille assessment (C. T. Bryant)
Soil Conservation Service watershed studies (T. E. Lamb)
Waste-assimilation capacity (C. T. Bryant)
California:
Colorado River salinity (D. T. Hartley, w, Laguna Niguel)
Ground-Water Quality Inventory (G. L. Faulkner, w, M)

Quality of water—Continued

States and territories—Continued

California—Continued

Ground-water quality, Santa Ana (L. A. Eccles, w, Laguna Niguel)

New River water quality (J. G. Setmire, w, Laguna Niguel)

Quality of water, California streams (W. L. Bradford, w, M)

San Francisco Bay urban study (R. D. Brown, M)

Santa Barbara ground water (Peter Martin, w, Laguna Niguel)

Thermograph network evaluation (J. T. Limerinos, w, M)

Water quality studies design-National Park Service (W. L. Bradford, w, M)

Water resources Upper Coachella (Anthony Buono, w, Laguna Niguel)

Colorado (w, D, except as otherwise noted):

Aquatic biology of Piceance Creek (K. J. Covay, w, Meeker)

Colorado landfills (J. T. Turk)

Colorado River salinity (K. E. Goddard, w, Grand Junction)

Effects of feedlots on ground water (R. G. Borman)

Effects of sludge basins on ground water (S. G. Robson)

Hayden powerplant study (R. L. Tobin, w, Meeker)

In-situ uranium mining (J. W. Warner)

Lowry landfill ground-water quality (N. G. Gaggiani)

Northwestern Colorado, water quality (T. R. Ford, w, Meeker)

Quality of water characteristics of Colorado streams (M. W. Gaydos)

Quality of water in underground coal mines (R. E. Moran)

Sediment chemistry (J. T. Turk)

Upper Colorado energy impacts (T. D. Steele)

Water quality, Jefferson County (D. C. Hall)

Yampa Valley ground-water reconnaissance (W. E. Hofstra)

Connecticut:

Changes in ground-water quality (E. H. Handman, w, Hartford)

PCB in the Housatonic River (K. P. Kulp, w, Hartford)

Florida:

Apalachicola River quality (H. C. Mattraw, w, Tallahassee)

Aquifer pollution, Lake County (G. F. Taylor, w, Orlando)

Bay-aquifer interconnection (C. B. Hutchinson, w, Tampa)

Drainage wells, Orlando area (C. H. Tibbals, w, Orlando)

Environmental studies, Statewide (G. A. Irwin, w, Tallahassee)

Ground-water quality, Dade County (D. J. McKenzie w, Miami)

Lakes Faith, Hope, and Charity (A. G. Lamonds, Jr., w, Orlando)

Radionuclides in ground water (Horace Sutcliffe, Jr., w, Sarasota)

Salt water interface, southwest Florida (K. W. Causseaux, w, Tampa)

Salt water intrusion, Cape Coral (D. J. Fitzpatrick, w, Fort Myers)

Subsurface waste storage (G. L. Faulkner, w, Tallahassee)

Water quality, Broward County (W. J. Haire, w, Miami)

Georgia (w, Doraville):

Coal region, north Georgia (J. B. McConnell)

Ground water irrigation, southwest Georgia (R. G. Grantham)

Quality of water, West Point reservoir (D. B. Radtke)

Stream quality, southwest Georgia, agriculture area (J. B. McConnell)

Quality of water—Continued

States and territories—Continued

Hawaii, monitoring of critical ground-water areas (K. J. Takasaki, w, Honolulu)

Idaho (w, Boise):

East Idaho ground-water quality (H. R. Seitz)

Ground-water-quality assessment (H. R. Seitz)

Ground water—quality of water monitoring (R. L. Whitehead)

Idaho phosphate radiation study (W. H. Low)

Illinois (w, Champaign):

Radwaste study, Palos Forest Preserve (J. C. Olimpio)

Sludge irrigation hydrology (R. F. Fuentes)

Sludge storage in strip-mine land (G. L. Patterson)

Strip mine hydrology (T. P. Brabets)

Indiana (w, Indianapolis):

Cypress Creek watershed (L. L. Bobo)

Landfill monitoring, Marion County (J. R. Marie)

Surface-water quality study (M. A. Hardy)

Watershed water quality (S. E. Ragone)

Iowa (w, Iowa City):

Indian-Twin Ponies water quality (L. J. Slack)

Water quality, Iowa coal region (M. G. Detroy)

Kansas (w, Lawrence):

Enhanced oil recovery, Kansas (D. G. Jorgensen)

Ground-water-quality network evaluations (A. M. Diaz)

Quality of water in mined areas in southeast (A. M. Diaz)

Saline discharge, Smoky Hill River (J. B. Gillespie)

Solute transport in *Equus* beds (J. B. Gillespie)

Urban storm water quality (A. M. Diaz)

Kentucky (w, Louisville):

Chloroform in alluvial aquifer (R. W. Davis)

Louisville alluvial aquifer test (K. E. Stevens)

Mine-site investigation (R. W. Davis)

Louisiana (w, Baton Rouge):

Pollution capacity of streams (R. F. Martien)

Quality of lower Mississippi River (C. R. Demas)

Maine:

Limnological study of Maine lakes (L. R. Frost, w, Augusta)

Maine lakes (W. J. Nichols, w, Augusta)

Public inquiries (R. C. Wagner, w, Augusta)

Massachusetts (w, Boston):

Ground-water contamination (D. F. Delaney)

Highway de-icing chemicals in ground water (S. J. Pollock)

Impact of Otis Air Force Base waste disposal (D. R. LeBlanc)

Lake Cochituate nutrients (F. B. Gay)

Water quality management (M. H. Frimpter)

Michigan, Ground water modeling, Wurtsmith Air Force Base (M. G. McDonale, w, Lansing)

Minnesota (w, St. Paul):

Coal-tar derivatives in ground-water (M. F. Hult)

Ground-water quality network (M. F. Hult)

Karst well hydraulics (M. F. Hult)

Voyageurs National Park (G. A. Payne)

Water quality of highway runoff (M. R. Have)

Mississippi, Tennessee-Tombigbee Divide quality-of-water monitoring (C. H. Tate, w, Jackson)

Missouri (w, Rolla):

Coal hydrology (J. H. Barks)

Prosperity water quality (J. H. Barks)

Urban runoff in Springfield (John Skeleton)

Montana:

Geohydrology of Helena Valley (A. J. Boettcher, w, Helena)

Thermal study—Madison River (A. J. Boettcher, w, Helena)

Quality of water—Continued
States and territories—Continued
Nebraska, Analysis surface-water quality data (R. A. Engberg, w, Lincoln)
Nevada (w, Carson City):
Ground-water contamination by explosives wastes (A. S. Van Denburgh)
Ground-water-quality monitoring network (J. O. Nowlin)
Lahontan Reservoir water quality (T. L. Katzer)
Pond seepage, Weed Heights (R. J. LaCamera)
Truckee-Carson assessment (J. O. Nowlin)
New Hampshire, Effects of waste disposal—Peace Air Force Base (Edward Bradley, w, Augusta)
New Jersey, Fishkills, Cape May County (G. R. Kish, w, Trenton)
New Mexico:
Malaga Bend evaluation (J. L. Kunkler, w, Santa Fe)
Quality-of-water monitor in Chaco River basin (Kim Ong, w, Albuquerque)
San Juan River valley (F. P. Lyford, w, Albuquerque)
New York (w, Albany):
Biology of landfill leaching (T. A. Ehlke)
Ground-water pollution, Olean (A. D. Randall)
Landfills in Oswego County (R. M. Waller)
Organic compounds in ground water (J. T. Turk)
PCB transport in the Upper Hudson (R. A. Schroeder)
Recharge and nitrates, Cornell Farm (A. D. Randall)
Sediment nutrient dynamics (J. T. Turk)
Switzer Creek nonpoint pollution (D. A. Sherwood, w, Ithaca)
Westchester County waste management (R. J. Archer)
North Carolina (w, Raleigh):
Chemical quality atmospheric deposition (R. C. Heath)
Effects of channelizing Black River (C. E. Simmons)
Water-quality of major North Carolina rivers (D. A. Harned)
North Dakota, Mining effects, Gascoyne area (M. G. Croft, w, Bismarck)
Ohio (w, Columbus):
Brine investigation (S. E. Norris)
Landfill impacts on ground water system (A. C. Razem)
Miscellaneous water resources studies (R. V. Swisshelm,)
Quality of water monitor network (A. A. Gordon)
Rattlesnake Creek water quality (K. F. Evans)
Oklahoma (w, Oklahoma City):
Blue Creek quality (J. K. Kurklin)
Coal hydrology eastern Oklahoma (M. V. Marcher)
Gaines Creek quality (J. K. Kurklin)
PCB's in the Arkansas River (J. D. Stoner)
Salt-water infiltration (J. J. D'Lugosz)
Surface water suitability (J. D. Stoner)
Zinc mine water quality (J. D. Stoner)
Oregon (w, Portland):
Portland, Harbor study (S. W. McKenzie)
Stream quality in Oregon (T. L. Miller)
Water in western Douglas County (D. A. Curtiss)
Willamette River basin low flow (S. W. McKenzie)
Pennsylvania (w, Harrisburg, unless otherwise noted):
Anthracite mine discharge (D. J. Growitz)
Coal hydrology, Greene County (D. R. Williams, w, Pittsburgh)
Ground-water quality in Pennsylvania (H. E. Koester)
Little Blue Run Lake—fly ash (D. R. Williams, w, Pittsburgh)
Nonpoint sources, Pequea Creek basin (J. R. Ward)

Quality of water—Continued
States and territories—Continued
Pennsylvania—Continued
Pennsylvania Gazetteer of Streams, Part II (L. C. Shaw)
Stream conditions—Chester County (J. J. Murphy, w, Malvern)
Water quality—Blue Marsh Lake (J. L. Barker)
Water quality in Tioga River basin (J. R. Ward)
Puerto Rico (w, San Juan):
Effects of oil spillage on ground water (A. E. Torres)
Freshening, Cano Tiburones area (J. R. Diaz, w, Ft. Buchanan)
Surface impoundents, (J. R. Diaz)
Well monitoring (J. R. Gonzalez, w, Ft. Buchanan)
Rhode Island, Quality of Rhode Island streams (H. E. Johnston, w, Boston, Mass.)
South Carolina (w, Columbia):
Fluoride in ground water, coastal plain (J. M. Rhett)
Ground water data definition at radwaste site (J. M. Cahill)
Savannah River plant (D. I. Cahal)
Tennessee, Burial-ground studies at Oak Ridge National Laboratory (D. A. Webster, w, Knoxville)
Texas, Colorado River salinity (Jack Rawson, w, Austin)
Utah (w, Salt Lake City):
Reconnaissance of Utah coal fields (K. M. Waddell)
Surface-water quality, Dirty Devil River basin (J. C. Mundorff)
Water quality, San Rafael River basin (J. C. Mundorff)
Weber River basin water quality (K. R. Thompson)
Vermont, Ground-water quality (R. E. Willey, w, Montpelier)
Virginia:
Coastal plain salt water (J. D. Larson, w, Richmond)
Dredge spoil disposal (J. F. Harsh, w, Richmond)
Washington (w, Tacoma):
Columbia basin demonstration project (P. R. Boucher)
Ground-water-quality network (J. C. Ebbert)
Hydrology of Pine Lake (N. P. Dion)
Quimault ground-water quality (Dee Molenaar)
Salt-water intrusion (N. P. Dion)
Spokane ground water quality (E. L. Bolke)
Sulphur Creek program (P. R. Boucher)
West Virginia, effects of deep mining (J. W. Borchers, w, Charleston)
Wisconsin (w, Madison):
Chemical loading to Lake Michigan (C. C. Harr)
Ground-water quality, Waukesha County (J. J. Schiller)
Nederlo Creek biota (P. A. Kammerer, Jr.)
Stream reaeration (L. B. House)
Wyoming (w, Cheyenne):
Herbicides North Platte (J. R. Schuetz)
North Platte reservoirs (S. J. Rucker IV)
Nutrient release, Lake DeSmet (D. J. Wangsness)
See also Geochemistry; Hydrologic instrumentation; Hydrology, surface water; Limnology; Marine hydrology; Sedimentology; Water resources.

Quicksilver. *See* Mercury.

Radioactive materials, transport in water. *See* Geochemistry, water.

Radioactive waste disposal:
Favorable radioactive waste disposal areas (W. E. Hale, w, Albuquerque, N. Mex.)
Geomechanics of radioactive waste storage (H. S. Swolfs, D)
Hydrology of nuclear landfill (D. E. Prudic, w, Albany, N.Y.)
Hydrology of salt domes (G. N. Ryals, w, Baton Rouge, La.)
Implications of long-term climate changes (D. P. Adam)
In-situ stress in shales (T. C. Nichols, Jr., D)

Radioactive-waste disposal—Continued
- National Overview Atlas (J. P. Ohl, D)
- Nevada waste coordination (W. W. Dudley, w, D)
- Pierre Shale (G. W. Shurr, D)
- Radioactive byproducts in salt (J. W. Mercer, w, Albuquerque, N. Mex.)
- Radioactive-waste burial (George Debuchananne, w, NC)
- Radioactive-waste-burial study (J. M. Cahill, w, Columbia, S. C.)
- Radiohydrology technical coordination (George Debuchananne, w, NC)
- Sheffield site investigation (J. B. Foster, w, Champaign, Ill.)
- Waste-disposal sites (L. A. Wood, w, NC)
- Waste emplacement crystalline rocks inconterminous United States (H. W. Smedes, D)
- *States:*
- Idaho, Hydrology of subsurface waste disposal (J. T. Barraclough, w, Idaho Falls)
- Kentucky, Maxey Flats investigation (H. H. Zehner, w, Louisville)
- New Mexico (D):
  - Eddy and Lea counties, exploratory drilling (C. L. Jones)
  - Southeastern, waste emplacement (C. L. Jones)
- Utah (D):
  - Paradox Basin (L. M. Gard)
  - Salt Valley anticline (L. M. Gard)
- *See also* Geochemistry, water.

Rare-earth metals. *See* Minor elements.

Regional studies and compilations, large areas of the United States:
- Appalachians-Caledonides synthesis analysis (R. B. Neuman, Washington, D.C.)
- Basement rock map (R. W. Bayley, M)
- Characterization of crystalline rock terrane (H. W. Smedes and D. J. Gable, D)
- Paleotectonic map folios:
  - Devonian System (E. G. Sable, D)
  - Mississippian System (L. C. Craig, D)
  - Pennsylvanian System (E. D. McKee, D)
- Physiography of Southeastern United States (J. T. Hack, NC)
- Volcanic rocks of the Appalachians (D. W. Rankin, NC)

Remote sensing:
- Cartographic applications:
  - Composite mapping and topographic analysis (D. D. Greenlee, Technicolor Graphics Services, Inc., Sioux Falls, S. Dak.)
- *State:*
- Massachusetts, Landsat image maps of Cape Cod (R. S. Williams, Jr., l, NC)
- Geologic applications:
  - Airborne and satellite research:
    - Aeromagnetic studies (M. F. Kane, D)
    - Development of an automatic analog earthquake processor (J. P. Eaton, M)
    - Electromagnetic research (F. C. Frischknecht, D)
    - Fraunhofer line discriminator studies (R. D. Watson, l, Flagstaff, Ariz.)
    - Gamma-ray research (J. S. Duyal, D)
    - Geochemical plant stress (F. C. Canney, D)
    - Heat Capacity Mapping Mission: Thermal-inertia mapping (Kenneth Watson, D)
    - Geothermal resources (Kenneth Watson, D)
    - Geologic investigations with integrated geophysical and remotely sensed data (D. G. Orr, l, Sioux Falls, S. Dak.)
    - Infrared surveillance of volcanoes (J. D. Freidman, D)
    - Interpretation studies (R. H. Henderson, NC)
    - National aeromagnetic survey (J. R. Henderson, D)

Remote sensing—Continued
- Geologic applications—Continued
  - Airborne and satellite research—Continued
    - Remote sensing of dynamic geological phenomena and geologic hazards (R. S. Williams, Jr., l, NC)
    - Remote-sensing geophysics (Kenneth Watson, D)
    - Satellite magnetometry (R. D. Regan, NC)
    - Surficial and thematic mapping (T. N. V. Karlstrom, Flagstaff, Ariz.)
    - Urban geologic studies (T. W. Offield, D)
    - Volcanic gas monitoring (Motoaki Sato, NC)
  - Landsat experiments:
    - Evaluation of Great Plains area (R. B. Morrison, D)
    - Iron-absorption band for the discrimination of iron-rich zones (L. C. Rowan, NC)
    - Landsat applications program (D. R. Hood, Technicolor Graphic Services, Inc., Sioux Falls, S. Dak.)
    - Lineaments of the conterminous United States (W. D. Carter, l, NC)
    - Morphology, provenance, and movement of desert and seas in Africa, Asia, and Australia (E. D. McKee, D)
    - Optimum Landsat spectral bands (G. L. Raines, D)
    - Petroleum geology investigations in the People's Republic of China (G. B. Bailey, l, Sioux Falls, S. Dak.)
    - Prototype volcano surveillance network (J. P. Eaton, M)
    - Remote sensing for energy resources and mineral exploration (W. D. Carter, l, NC)
    - Study of multispectral imagery, northwestern Saudi Arabia (A. J. Bodenlos, NC)
    - Suspended particulate matter in nearshore surface waters, northeast Pacific Ocean and the Hawaiian Islands (P. R. Carlson, M)
    - Synthetic stereo in Landsat imagery (Gordon Swann, Flagstaff, Ariz.)
    - Targeting mineral exploration effort (G. B. Bailey, l, Sioux Falls, S. Dak.)
    - Thermal surveillance of active volcanoes (J. D. Friedman, NC)
  - Skylab/EREP studies:
    - Evaluation of Great Plains area (R. B. Morrison, D)
    - Marine coastal processes on the Puerto Rico-Virgin Islands Platform (J. V. A. Trumball, Santurce, P.R.)
    - Remote-sensing geophysics (Kenneth Watson, D)
    - Skylab/visual observations:
      - Desert sand seas (E. D. McKee, D; C. S. Breed, Flagstaff, Ariz.)
      - Volcanologic features (J. D. Friedman, D)
    - Time-lapse satellite data for monitoring dynamic hydrologic phenomena (Morris Deutsch, S. Serebreny, l, C)
    - Uranium, remote sensing for uranium exploration (G. L. Raines, D)
- *States:*
- Alaska (M):
  - Beaufort Sea, inner shelf and coastal sedimentation environment (Erk Reimnitz)
  - Remote sensing of permafrost and geologic hazards (O. J. Ferrians, Jr.)

Remote sensing—Continued
States—Continued
Arizona:
Arizona Regional Ecological Test Site:
North-central (D. P. Elston, Flagstaff)
Post-1890 A. D. episode erosion (R. B. Morrison, D)
Basin and Range-Colorado Plateau boundary investigation (D. P. Elston, Ivo Lucchitta, Flagstaff)
Remote sensing of porphyry copper alteration zones (R. G. Schmidt, NC)
Satellite altimetry evaluation (W. D. Carter, l, NC)
Colorado, Effects of atmosphere on multispectral mapping rock types by computer, Cripple Creek-Canon City (H. W. Smedes, D)
Colorado-Wyoming, Analysis of Cortez-Uinta mineralized areas from Landsat digital data (L. C. Rowan, NC)
Texas, Monitoring changing geologic features, Texas gulf coast (R. B. Hunter, Corpus Christi)
Hydrologic applications:
Aircraft and spacecraft observations of Arctic sea ice (W. J. Campbell, w, Tacoma, Wash.)
Area estimation of flood-plain inundation in the Apalachi cola River basin using Landsat images (James Lucas, Technicolor Graphic Services, Inc., l, Sioux Falls, S. Dak.)
COMSAT General pilot project (W. G. Shope, w, NC)
Hydrologic remote sensing (G. K. Moore, w, Sioux Falls, S. Dak.)
Ice dynamics (W. J. Campbell, w. Tacoma, Wash.)
Columbia River basin irrigated lands study (G. E. Johnson, Technicolor Graphic Services, Inc., l, Sioux Falls, S. Dak.)
Polar-ice remote sensing (W. J. Campbell, w, Tacoma, Wash.)
Remote sensing, quality of water (M. C. Goldberg, w, D)
Satellite image atlas of glaciers (R. S. Williams, Jr., l, NC)
Sierra Cooperative Pilot Project:
Satellite monitoring of cloud-top temperatures (O. H. Foehner, Bureau of Reclamation, Denver, Colo.)
Targeting, inventorying, and monitoring groundwater resources (J. R. Lucas, Technicolor Graphic Services, Inc., Sioux Falls, S. Dak.)
Testing of satellite uplinked remote surface weather stations in the Sierra Nevada (Donald Rottner, Bureau of Reclamation, Denver, Colo.)
Wetlands research (V. P. Carter, w, NC)
States:
Alaska, Meteor burst telemetry (R. D. Lamke, w, Anchorage)
Arizona, snow-cover mapping (H. H. Schumann, w, Phoenix)
Connecticut, Connecticut River estuary (F. H. Ruggles, Jr., w, Hartford)
Florida:
Integration of Landsat data and hydrologic data for water management of the Everglades National Park (D. T. Lauer, James Lucas, Technicolor Graphic Services, Inc., l, Sioux Falls, S. Dak.)
Southern, Landsat (A. L. Higer, w, Miami)
Kansas, Mined land hydrology, southeast Kansas (A. M. Diaz, w, Lawrence)
Pennsylvania, GOES, Juniata basin (C. D. Kauffman, w, Harrisburg)
Land-resource applications:
Colorado River natural resources and land use data inventory (H. D. Newkirk, Bureau of Reclamation, Denver, Colo.)
Development of automatic techniques for land use mapping from remote-sensor data (J. R. Wray, l, NC)

Remote sensing—Continued
Land-resource applications—Continued
Drought and desertification indicators from Landsat imagery (C. J. Robinove, l, NC)
Forest fire fuels mapping (G. R. Johnson, Mark Shasby, Technicolor Graphic Services, Inc., l, Sioux Falls, S. Dak.)
Land resource analysis using airborne scanner data (R. L. Hansen, Bureau of Reclamation, D)
Reclamation land use analysis (R. L. Hansen, Bureau of Reclamation, D)
States:
Alaska, Resource assessment in Wrangell—St. Elias National Monument (David Carneggie, l, Anchorage)
Arizona, Wildland vegetation inventory (W. G. Rohde, Technicolor Graphic Services, Inc., Sioux Falls, S. Dak.)
California, Large-scale photographs for range-trend analysis (D. M. Carneggie, l, Sioux Falls, S. Dak.)
Michigan, Vegetation mapping in the Pictured Rocks National Lakeshore (William Anderson, Technicolor Graphic Services, Inc., l, Sioux Falls, S. Dak.)
Washington, Department of Natural Resources forest classification (G. R. Johnson, Technicolor Graphic Services, Inc., l, Sioux Falls, S. Dak.)
Techniques in processing Landsat image data:
Data Analysis Laboratory activity (F. A. Waltz, Technicolor Graphic Services, Inc., Sioux Falls, S. Dak.)
Reservoirs. *See* Evapotranspiration; Sedimentology.
Resource and land investigations:
Coastal Zone Management Act coordination (R. Schoen, l, NC)
Conflict management research (E. T. Smith, l, NC)
Identification of critical New England water resources criteria to evaluate and compare alternative power plant sites (P. A. Marcus, l, NC)
Inventory of computer software for spatial data handling (O. Kays, l, NC)
National Environmental Indicators report (E. T. Smith, l, NC)
Natural resource data management system for water and related land resources planning (W. J. Ulman, l, NC)
Outer Continental Shelf Oil and Gas Information Program (D. A. Nystrom, l, NC)
Planning methodology for urban water conservation programs (K. A. Fitzpatrick-Lins, l, NC)
Western Coal Planning Assistance Project (W. J. Ulman, l, NC)
States:
Illinois Coal Basin Planning Assistance Project (W. W. Doyel, l, NC)
Washington, Colville Indian Reservation, case study on land use planning (E. T. Smith, l, NC)
Rhenium. *See* Minor elements; Ferro-alloy metals.
Saline minerals:
Mineralogy (B. M. Madsen, M)
States:
Colorado and Utah, Paradox Basin (O. B. Raup, D)
New Mexico, Carlsbad potash and other saline deposits (C. L. Jones, M)
Wyoming, Sweetwater County, Green River Formation (W. C. Culbertson, D)
Saltwater intrusion. *See* Marine hydrology; Quality of water.
Sedimentology:
Arctic fluvial processes, landforms (K. M. Scott, w, Laguna Niguel, Calif.)

Sedimentology—Continued
Bedload-transport research (W. W. Emmett, w, D)
Channel morphology (L. B. Leopold, w, Berkeley, Calif.)
Coon Creek morphology (S. W. Trimble, w, Los Angeles, Calif.)
Estuarine intertidal environments (J. L. Glenn, w, D)
Forest geomorphology, Pacific coast (R. J. Janda, w, M)
Measurement of sediment-laden flows (A. G. Scott, w, NC)
Petrology Laboratory (L. G. Schultz, D)
Sediment-hillside morphology (G. P. William, w, D)
Sediment movement in rivers (R. H. Meade, Jr., w, D)
Sediment transport phenomena (D. W. Hubbell, w, D)
States:
Alabama:
Hydrology of Warrior coal field (Celso Puento, w, Tuscaloosa)
Water problems in coal-mine areas (Celso Puente, w, Tuscaloosa)
Alaska:
Coastal environments (A. T. Ovenshine, M)
Hydrology and quality of water of Keta River basin (G. O. Balding, w, Juneau)
Tanana River sediment study (R. L. Burrows, Fairbanks)
Arizona, Sediment—Paria River, Lees Ferry (W. B. Garrett, w, Tucson)
California:
Los Padres reservoir study (L. F. Trujillo)
Santa Clara River sediment (C. E. McConaughy, w, Laguna Niguel)
Colorado, Suspended-sediment pumping samplers (W. F. Curtis, w, D)
Hawaii:
Haiku-Kamooalii-Halawa water quality (S. S. Chinn, w, Honolulu)
Peak flow-sediment discharge relations (B. L. Jones, w, Honolulu)
Plan of study—Waikele basin (J. J. Yee, w, Honolulu)
Idaho, Snake and Clearwater Rivers, sediment (H. R. Spitz, w, Boise)
Illinois:
Sediments, North Ditch (A. W. Noehre, w, DeKalb)
Urban construction stream quality (H. E. Allen, w, DeKalb)
Indiana, Analysis of sediment data base (L. J. Mansue, w, Indianapolis)
Iowa, Sedimentation study—Lake Panorama (O. G. Lara, w, Iowa City)
Kansas, Fluvial sediment in Kansas (C. D. Albert, w, Lawrence)
Kentucky, Sediment characteristics, Kentucky streams (R. F. Flint, w, Louisville)
Maryland, Trap efficiency—Rock Creek (W. J. Herb, w, Towson)
Minnesota:
Quality of water, Coteau Des Prairies (C. J. Smith, w, St. Paul)
Red clay sediment and quality-of-water evaluation (E. G. Giacomini, w, St. Paul)
North Carolina, Sediment study (C. E. Simmons, w, Raleigh)
North Dakota (w, Bismarck):
Park River water-quality assessment (D. J. Ackerman)
Water monitoring—coal mining (N. D. Haffield)
Ohio (w, Columbus):
Highway 315 sediment study (D. R. Helsel)
Sediment movement, strip-mined areas (C. G. Angelo)
Sediment yields (P. W. Anttila)
Surface mine sediment transport (D. R. Helsel)
Oregon, water quality, Bull Run watershed (M. V. Shulters, w, Portland)

Sedimentology—Continued
States—Continued
Pennsylvania (w, Harrisburg):
Highway erosion-control measures (L. A. Reed)
Predicting sediment flow (L. A. Reed)
Sediment control in mining areas (K. L. Wetzel)
Tennessee:
Hydrologic study, coal mining study, New River (W. P. Carey, w, Nashville)
Water quality of Big South Fork National River and Recreation area (B. J. Frederick, w, Knoxville)
Washington (w, Tacoma):
May Creek sediment study (W. L. Haushild)
Sediment data for irrigated agriculture (P. R. Boucher)
West Virginia:
Coal River sediment (S. C. Downs, w, Charleston)
Sediment yield of Taylor Run (S. M. Ward, w, Morgantown)
Water resources of Gauley River basin (G. S. Runner, w, Charleston)
Wisconsin, White River reservoir study (S. M. Hindall, w, Madison)
See also Geochemistry, water; Geochronological investigations; Hydraulics, surface flow; Hydrologic data collection and processing; Stratigraphy and sedimentation; Urbanization, hydrologic effects.
Selenium. *See* Minor elements.
Silver. *See* Heavy metals; Lead, zinc, and silver.
Soil moisture:
Infiltration and drainage (Jacob Rubin, w, M)
Snow hydrology (W. W. Embree, w, Albany, N.Y.)
See also Evapotranspiration.
Spectroscopy:
Mobile spectrographic laboratory (D. J. Grimes, D)
Spectrographic analytical services and research (A. W. Helz, NC; A. T. Meyers, D; Harry Bastron, M)
X-ray spectroscopy (H. J. Rose, Jr., NC; Harry Bastron, M)
Stratigraphy and sedimentation:
Antler flysch, Western United States (F. G. Poole, D)
Middle and late Tertiary history, Northern Rocky Mountains and Great Plains (N. M. Denson, D)
Pennsylvania System stratotype section (G. H. Wood, Jr., NC)
Permian, Western United States (E. K. Maughan, D)
Phosphoria Formation, stratigraphy and resources (R. A. Gulbrandsen, M)
Rocky Mountains and Great Basin, Devonian and Mississippian conodont biostratigraphy (C. A. Sandberg, D)
Sedimentary structures, model studies (E. D. McKee, D)
Tight gas sands (D. D. Rice, D)
States:
Alabama-Florida, Stratigraphy (J. A. Miller, w, Tallahassee, Fla.)
Alaska, Cretaceous (D. L. Jones, M)
Arizona:
Hermit and Supai Formations (E. D. McKee, D)
Magnetic chronology, Colorado Plateau and environs (D. P. Elston, E. M. Shoemaker, Flagstaff)
Arizona-New Mexico, Paleomagnetic correlation, Colorado Plateau (D. J. Strobell, Flagstaff, Ariz.)
California, Southern San Joaquin Valley, subsurface geology (J. C. Maher, M)
Louisiana, Continental Shelf (H. L. Berryhill, Jr., Corpus Christi, Tex.)
Montana, Ruby Range, Paleozoic rocks (E. T. Ruppel, D)
Montana-North Dakota-South Dakota-Wyoming, Williston Basin (C. A. Sandberg, D)

Stratigraphy and sedimentation—Continued
States—Continued
Nebraska, Central Nebraska Basin (G. E. Prichard, D)
Nevada, Indian Trail Formation, abandonment of name (G. L. Dixon, D)
New Mexico, western and adjacent areas, Cretaceous stratigraphy (E. R. Landis, D)
Oregon-California black sands (M):
Geologic investigations (H. E. Clifton)
Hydrologic investigations (P. D. Snavely, Jr.)
Utah, Promontory Point (R. B. Morrison, D)
Wyoming, Lamont-Baroil area (M. W. Reynolds, D)
See also Paleontology, stratigraphic; *specific areas under* Geologic mapping.
Structural geology and tectonics:
Central Appalachian tectonics (A. A. Drake, Jr., NC)
Contemporary coastal deformation (R. O. Castle, M)
Rock behavior at high temperature and pressure (E. C. Robertson, NC)
Structural studies, Basin and Range (F. G. Poole, D)
States:
Arizona, southeastern tectonics (Harold Drewes, D)
California-Nevada, transcurrent fault analysis, western Great Basin (R. E. Anderson, D)
Nevada, central, east-trending lineaments (G. L. Dixon, D)
See also specific areas under Geologic mapping.
Talc:
New York, Pope Mills and Richville quadrangles (C. E. Brown, NC)
Tantalum. *See* Minor elements.
Thorium:
Analytical support (C. M. Bunker, D)
Investigations of thorium in igneous rocks (M. H. Staatz, D)
States:
Colorado (D):
Cochetopa area (J. C. Olson)
Wet Mountains, thorium resources appraisal (T. J. Armbrustmacher)
Wyoming, Bear Lodge Mountains (M. H. Staatz, D)
Tungsten. *See* Ferro-alloy metals.
Uranium:
Exploration techniques:
Geochemical techniques (R. A. Cadigan, D)
Geochemical techniques of halo uranium (J. K. Otton, D)
Morrison Formation (L. C. Craig, D)
Uranium in streams as an exploration technique (K. J. Wenrich-Verbeek, D)
Genesis of tabular uranium deposits on the Colorado Plateau (R. A. Brooks, D)
Geophysics:
Borehole electrical techniques in uranium exploration (J. J. Daniels, D)
Borehole geophysical research in uranium exploration (J. H. Scott, D)
Gamma-ray spectrometry in uranium (J. S. Duval, D)
Gamma-ray spectroscopy for uranium exploration in crystalline terranes (J. A. Pitkin, D)
Geophysical studies relating to uranium deposits in crystalline terranes (D. L. Campbell, D)
Hydrogenochemistry of uranium deposits (C. G. Bowles, D)
Ore-forming processes (H. C. Granger, D)
Paleomagnetism applied to uranium exploration (R. L. Reynolds, D)
Petrophysics (G. R. Olhoeft, D)
Precambrian sedimentary and metasedimentary rocks (F. A. Hills, D)

Uranium—Continued
Radium and other isotopic disintegration products in springs and subsurface water (R. A. Cadigan, J. K. Felmlee, D)
Remote sensing for uranium exploration (G. L. Raines, D)
Resources of radioactive minerals (A. P. Butler, Jr., D)
Resources of United States and world (W. I. Finch, D)
Southern High Plains (W. I. Finch, D)
United States:
Eastern:
Appalachian Basin Paleozoic rocks (A. F. Jacob, D)
Basin analysis as related to uranium potential in Triassic sedimentary rocks (C. E. Turner, D)
Uranium vein deposits (R. I. Grauch, D)
Southwestern, basin analysis related to uranium potential in Permian rocks (J. A. Campbell, D)
Western:
Relation of diagenesis and uranium deposits (M. B. Goldhaber, D)
Vein and disseminated deposits of uranium (J. T. Nash, D)
Uranium daughter products in modern decaying plant remains, in soils, and in stream sediments (K. J. Wenrich-Verbeek, D)
Uranium geophysics in frontier areas (J. W. Cady, D)
Volcanic source rocks (R. A. Zielinski, D)
States:
Arizona-Colorado-New Mexico-Utah, Colorado Plateau (D):
Basin analysis of uranium-bearing Jurassic rocks (Fred Peterson)
Tabular deposits (R. A. Brooks)
Arizona-Nevada-Utah, Uranium potential of Basin and Range province (J. E. Peterson, D)
Colorado (D):
Cochetopa Creek uranium-thorium area (J. C. Olson)
Colorado Plateau (Summary) Report (R. P. Fischer)
Marshall Pass uranium (J. C. Olson)
Schwartzwalder mine (E. J. Young)
Uranium-bearing Triassic rocks (R. D. Lupe)
Colorado-New Mexico-Texas-Utah-Wyoming, Organic chemistry of uranium (J. S. Leventhal, D)
New Mexico (D):
Acoma area (C. H. Maxwell)
Church Rock-Smith Lake (C. T. Pierson)
Crownpoint uranium studies (J. F. Robertson)
North Church Rock (A. R. Kirk)
San Juan Basin uranium (M. W. Green)
Sanostee (A. C. Huffman, Jr.)
Thoreau uranium studies, New Mexico (J. F. Robertson)
South Dakota-Wyoming, Uranium-bearing pipes (C. G. Bowles, D)
Texas:
Coastal plain, geophysical and geological studies (D. H. Eargle, Austin)
Tilden-Loma Alta area (K. A. Dickinson, D)
Uranium disequilibrium studies (F. E. Senftle, NC)
Texas-Wyoming, Roll-type deposits (E. N. Harshman, D)
Utah-Colorado (D):
Moab quadrangle (A. P. Butler, Jr.)
Uinta and Piceance Creek basin (L. C. Craig)
Washington, Midnite uranium mine (J. T. Nash, D)
Wyoming (D):
Badwater Creek (R. E. Thaden)
Crooks Peak quadrangle (L. J. Schmitt, Jr.)
Granite as a source rock of uranium (J. S. Stuckless)

Uranium—Continued
States—Continued
Wyoming (D)—Continued
Northeastern Great Divide Basin (L. J. Schmitt, Jr.)
Powder River Basin (E. S. Santos)
Sagebrush Park quadrangle (L. J. Schmitt, Jr.)
Stratigraphic analysis of Tertiary uranium basins of Wyoming (D. A. Seeland)
Stratigraphic analysis of Western Interior Cretaceous uranium basins (H. W. Dodge, Jr.)

Urban geology:
States:
Arizona, Phoenix-Tucson region resources (T. G. Theodore, M)
California (M, except as otherwise noted):
Coastal geologic processes (K. R. Lajoie)
Flatlands materials and their land use significance (E. J. Helley)
Geologic factors in open space (R. M Gulliver)
Hillside materials and their land use significance (C. M. Wentworth, Jr.)
Pacific Palisades landslide area, Los Angeles (J. T. McGill, D)
Palo Alto, San Mateo, and Montara Mountain quadrangles (E. H. Pampeyan)
Quaternary framework for earthquake studies, Los Angeles Basin (J. C. Tinsley III)
Regional slope stability (T. H. Nilsen)
San Francisco Bay region, environment and resources planning study:
Bedrock geology (M. C. Blake)
Marine geology (D. S. McCulloch)
Open space (C. S. Danielson)
San Andreas fault:
Basement studies (D. C. Ross)
Basin studies (J. A. Bartow)
Regional framework (E. E. Brabb)
Tectonic framework (R. D. Brown)
San Mateo County cooperative (H. D. Gower)
Sargent-Berrocal fault zone (R. J. McLaughlin, D. H. Sorg)
Seismicity and ground motion (W. B. Joyner)
Southern:
Eastern part (D. M. Morton, Riverside)
Western part (R. F. Yerkes)
Colorado, Denver urban area, regional geochemistry (H. A. Tourtelot, D)
Massachusetts, Boston and vicinity (C. A. Kaye, Boston)
Montana, geology for planning, Helena region (R. G. Schmidt, NC)
New York, Engineering geology of New York City (C. A. Baskerville, NC)
Pennsylvania (NC, except as otherwise noted):
Geochemistry of Pittsburgh urban area (H. A. Tourtelot, D)
Susceptibility to landsliding:
Allegheny County (J. S. Pomeroy)
Beaver, Butler, and Washington Counties (J. S. Pomeroy)
Utah:
Salt Lake City and vicinity (Richard VanHorn, D)
Wasatch Front surficial geology (R. D. Miller, D)
Virginia, Geohydrologic mapping of Fairfax County (A. J. Froelich, NC)

Urban hydrology:
Analysis of urban flood data in United States (V. B. Sauer, w, Atlanta, Ga.)
Geohydrology, urban planning (H. G. O'Connor, w, Lawrence, Kans.)
Urban runoff networks (H. H. Barnes, Jr., w, NC)
Urban sedimentology (H. P. Guy, w, NC)
States:
Alaska, Anchorage geohydrology (Derrill Cowing, w, Anchorage)
Colorado:
Flood frequency, urban areas (C. V. Reeter, w, D)
Front Range urban corridor (D. E. Hillier, w, D)
Storm runoff quality, Denver (S. R. Ellis, w, D)
Urban runoff (S. R. Ellis, w, D)
Connecticut:
Connecticut valley urban pilot study (R. L. Melvin, w, Hartford)
Urbanization effect, small streams (L. A. Weiss, w, Hartford)
Florida:
Bay Lake area (E. R. German, w, Orlando)
Leon County (R. P. Rumenik, w, Tallahasse)
Stormwater data modeling (R. A. Miller, w, Orlando)
Stormwater quality, south Florida (H. C. Mattraw, w, Miami)
Tampa Bay region (M. A. Lopez, w, Tampa)
Hawaii, hydrology, sediment in Mauna Loa (C. J. Ewart, w, Honolulu)
Illinois, Effects of detention ponds on water quality (R. G. Striegl, w, DeKalb)
Indiana, Indianapolis Water Company canal study (William Meyer, w, Indianapolis)
Kansas:
Urban runoff, Wichita (D. B. Richards, w, Lawrence)
Urban stormwater quality (L. M. Pope, w, Lawrence)
Kentucky, Northern Kentucky urban hydrology (R. W. Davis, w, Louisville)
Maryland, Rock Creek—Anacostia River (T. W. Yorke, w, Towson)
Minnesota:
Quality of runoff, Twin Cities area (M. A. Ayers, w, St. Paul)
Water quality assessment, Coon Creek watershed (A. D. Arntson, w, St. Paul)
Missouri, stream hydrology, St. Louis (T. W. Alexander, w, Rolla)
New Mexico, urban flood hydrology, Albuquerque (J. P. Borland, w, Albuquerque)
New York:
Nonpoint pollution, Irondequoit Bay (D. E. Troutman, w, Albany)
Planning study, Long Island urban runoff (D. J. Sulam, w, Syosset)
Solid waste sites, Suffolk (G. E. Kimmel, w, Mineola)
Urban hydrology of Long Island (H. F. Ku, w, Syosset)
Ohio (R. P. Hawkinson, w, Columbus)
Oregon (w, Portland):
Bear Creek water-quality study (S. W. McKenzie)
Portland rainfall-runoff study (Antonius Laenen)
Salem storm-water quality (T. L. Miller)
Salem urban runoff (Antonius Laenen)
Pennsylvania (w, Malvern):
Philadelphia (T. G. Ross)
Storm-water measurements (T. G. Ross)
Urban hydrology, Warminster Township (R. A. Sloto)

Urban hydrology—Continued
States—Continued
Tennessee:
Effects of urbanization on floods and quality of water (F. N. Lee, w, Nashville)
Memphis urban flood frequency (B. L. Neely, w, Memphis)
Texas (w, Fort Worth, except as otherwise noted):
Austin (M. L. Maderak, w, Austin)
Dallas urban study (B. B. Hampton)
Fort Worth urban study (R. M. Slade, Jr.)
Houston urban study (Fred Liscum, w, Houston)
San Antonio urban study (Lynn Harinsen, w, San Antonio)
Utah, Salt Lake County urban runoff study (T. Arnow, w, Salt Lake City)
Washington, Bellevue urban runoff study (W. L. Haushild, w, Tacoma)
Wisconsin:
Simulation of urban runoff (R. S. Grant, w, Madison)
Urban nonpoint, southeast Wisconsin (P. E. Hughes, w, Madison)

Vegetation:
Element availability:
Soils (R. C. Severson, D)
Vegetation (L. P. Gough, D)
Elements in organic-rich material (F. N. Ward, D)
Plant geochemistry, urban areas (H. A. Tourtelot, D)
Western coal regions, geochemical survey of vegetation (J. A. Erdman, D)
See also Plant ecology.

Volcanic-terrane hydrology. *See* Artificial recharge.

Volcanology:
Caldron and ash-flow studies (R. L. Smith, NC)
Cascade volcanoes, geodimeter studies (D. A. Swanson, M)
Columbia River basalt (D. A. Swanson, M)
Kimberlites (B. C. Hearn, Jr.)
Regional volcanology (R. L. Smith, NC)
Tephra hazards from Cascade Range volcanoes (D. R. Mullineaux, D)
Volcanic-ash chronology (R. E. Wilcox, D)
Volcanic hazards (D. R. Crandell, D)
States:
Arizona, San Francisco volcanic field (J. F. McCauley, M)
Hawaii:
Hawaiian Volcano Observatory (Hawaii National Park)
Seismic studies (P. L. Ward, M)
Submarine volcanic rocks (J. G. Moore, M)
Idaho (D):
Central Snake River Plain, volcanic petrology (H. E. Malde)
Eastern Snake River Plain region (M. A. Kuntz, H. R. Covington)
Montana, Wolf Creek area, petrology (R. G. Schmidt, NC)
New Mexico, Valles Mountains, petrology (R. L. Smith, NC)
Wyoming, deposition of volcanic ash in the Mowry Shale and Frontier Formation (G. P. Eaton, D)

Water budget:
Hydrologic reconnaissance, west-central Utah (J. S. Gates, w, Salt Lake City, Utah)
Water budget, Eagle Lake (C. F. Myette, w, St. Paul, Minn.)

Water resources:
Central region field coordination (H. H. Hudson, w, D)
Clinker-water interaction (J. R. Herring, D)
Columbia-North Pacific ground water (B. L. Foxworthy, w, Tacoma, Wash.)
Comprehensive studies, Pacific Northwest (L. E. Newcomb, w, M)

Water resources—Continued
Computational hydraulics (V. C. Lai, w, NC)
Dams, weirs, and flumes (H. J. Tracy, w, Atlanta, Ga.)
Data coordination, acquisition, and storage:
NAWDEX Project (M. D. Edwards, w, NC)
Water Data Coordination (R. H. Langford, w, NC)
East Triassic waste-disposal study (G. L. Bain, w, Raleigh, NC)
Evaluation of land treatment (R. F. Hadley, w, D)
Foreign assistance:
PL 80-402 (J. R. Jones, w, NC)
Section 607 (J. R. Jones, w, NC)
Foreign countries, Saudi Arabia, Saudi Arabian advisory services (G. C. Tibbits, Jr., w, NC)
General hydrologic research (R. L. Nace, w, Raleigh, N.C.)
Ground water, Missouri Basin (O. J. Taylor, w, D)
Ground-water appraisal, New England region (Allen Sinnott, w, Trenton, N.J.)
Hydrology of land use change (D. J. Lystrom, w, NC)
Intensive river-quality assessment (D. A. Rickert, w, Portland, Oreg.)
Intermediate-depth drilling (L. C. Dutcher, w, M)
International activities (J. R. Jones, w, NC)
Monitoring design, coal regions (H. H. Hudson, w, D)
Modeling principles (J. P. Bennett, w, NC)
National assessment (D. W. Moody, w, NC)
Network design (M. E. Moss, w, NC)
Northeastern region field coordination (P. E. Ward, w, NC)
Northwest water-resources data center (N. A. Kallio, w, Portland, Oreg.)
Off-road vehicle use (C. T. Snyder, w, M)
Polaris operations (T. T. Conomos, w, M)
Powell arid lands centennial (R. F. Hadley, w, D)
Quality of clinker aquifer (J. R. Herring, D)
Quality-of-water accounting network (R. J. Pickering, w, NC)
Rehabilitation potential, energy lands (L. M. Shown, w, D)
Reservoir bank storage study (T. H. Thompson, w, M)
Southeastern region field coordination (C. L. Holt, w, Atlanta, Ga.)
Southeast sand aquifer study (H. B. Counts, w, Atlanta, Ga.)
State aid, miscellaneous (J. R. Jones, w, NC)
Water for coal conversion, Upper Missouri River basin (O. O. Taylor, w, D)
Water-resource activities (J. P. Monis, w, D)
Waterway treaty engineering studies (J. A. Bettendorf, w, NC)
Western Region field coordination (L. E. Newcomb, w, M)
States and territories:
Alabama:
Drainage areas (J. C. Scott, w, Montgomery)
Plans, reports, and information (W. J. Powell, w, Tuscaloosa)
Alaska (w, Anchorage, except as otherwise noted):
Arctic resources (J. M. Childers)
Coal resources study (D. R. Scully)
Collection of basic records analysis (D. R. Lamke)
Geohydrology, Delta-Clearwater area (D. E. Wilcox)
National Petroleum Reserve hydrology (C. E. Sloan)
North Star project (A. P. Krumbardt, w, Fairbanks)
Northwest Alaska gas pipeline (C. E. Sloan)
St. Paul Island (A. N. Feulner)
Arizona:
Black Mesa hydrologic study (C. K. Bell, w. Tucson)
Black Mesa monitoring program (C. K. Bell, w. Flagstaff)
Sedona ground-water availability (G. W. Levings, w, Flagstaff)

Water resources—Continued
States and territories—Continued
Arizona—Continued
Verde Valley water resources (S. J. Owen, w, Tucson)
Water resources of the Papago Reservation (L. J. Mann, w, Tucson)
Arkansas (w, Little Rock):
Cache River aquifer-stream system (M. E. Broom)
Characteristics of streams (M. S. Hines)
Investigations and hydrologic information (R. T. Sniegocki)
Lignite hydrology (J. E. Terry, w, Little Rock)
Lignite water resources (J. E. Terry)
Time-of-travel study (T. E. Lamb)
California:
Ground water:
Joshua Tree (D. J. Downing, w, Laguna Niguel)
Madera area, ground-water model (C. J. Landquist w, Sacramento)
Santa Cruz (K. S. Muir, w, M)
San Antonio Creek ground water appraisal (M. J. Mallory, w, Laguna Niguel)
Surface water network study (J. R. Crippen, w, M)
Water, Redwood National Park (S. H. Hofford, w, M)
Water resources, California desert (J. H. Koehler, w, Laguna Niguel)
Colorado (w, D, except as otherwise noted):
Areawide water-quality inventory (L. J. Britton)
Ground water:
Potentiometric surface mapping (F. A. Welder)
U.S. Bureau of Mines prototype mine (J. B. Weeks)
Hydrology:
El Paso County (P. J. Emmons, w, Pueblo)
Naval Oil Shale Reserve No. 1 (D. L. Collins)
Parachute-Roan Creek Basin (O. B. Adams, w, Grand Junction)
San Luis Valley (J. L. Hughes, w, Pueblo)
South Platte Valley (D. C. Hall)
Intensive monitoring, Raton, Colorado (D. P. Bauer)
Larimer-Weld hydrology (R. K. Livingston)
Quality of water:
Boulder County (D. C. Hall)
Geochemical investigations (S. G. Robson)
Regional monitoring (Gerhard Kuhn)
Regional monitoring, Raton Mesa (A. P. Hall, w, Pueblo)
Rio Grande Compact Commission (J. F. Blakey)
Sediment yield, Piceance Basin (V. C. Norman)
Southwest alluvial valleys—Upper Rio Grande (T. M. Crouch, w, Pueblo)
Spring hydraulics (R. L. Tobin)
Warm-water sloughs (A. W. Burns)
Water monitoring—coal mining, Colorado (T. R. Dosch, w, D)
Water resources, Park-Teller County (K. E. Goddard, w, D)
Yampa River basin assessment (T. D. Steele)
Connecticut (w, Hartford):
Ground water, Southbury-Woodbury (D. L. Mazzaferro)
Hydrogeology, south-central Connecticut (F. P. Haeni)
Integrated hydrologic network (R. L. Melvin)
Part 7, Upper Connecticut River basin (R. B. Ryder)
Part 9, Farmington River basin (F. P. Haeni)
Part 10, Lower Connecticut River basin (L. A. Weiss)
Short-term studies (C. E. Thomas, Jr.)

Water resources—Continued
States and territories—Continued
Florida:
Annual hydrologic report, southwestern Florida (H. C. Rollins, w, Tampa)
Broward County (W. J. Haire, Jr., w, Miami)
Caloosahatchee River study (B. F. McPerson, w, Miami)
City of Sarasota, monitoring (H. R. Sutcliffe, w, Sarasota)
East Boundary area investigation (B. G. Waller, w, Miami)
Ground water:
Hallandale area (W. J. Haire, w, Miami)
Hollywood area (W. J. Haire, w, Miami)
Hydrogeology, middle Peace Basin (W. E. Wilson III, w, Tampa)
Hydrology,Manatee County (D. P. Brown, w, Sarasota)
Ochlockonee River basin investigation (C. A. Pascale, w, Tallahassee)
Potentiometric surface, St. Petersburg-Tampa (R. M. Wolansky, w, Tampa)
Sand-gravel aquifer, Pensacola (Henry Trapp, w, Tallahassee)
Santa Fe River basin (J. D. Hunn, w, Tallahassee)
Sewage effluent disposal, irrigation (M. C. Yurewics, Tallahassee)
Technical assistance, south Florida (W. J. Haire, w, Miami)
Water resources:
Duval and Nassau counties (E. C. Hayes, w, Jacksonville)
Tequesta (G. W. Hill, w, Miami)
Hydrogeologic maps, Seminole County (W. D. Wood, w, Winter Park)
Hydrogeology, Osceola Forest (P. R. Seaber, w, Tallahassee)
Landfill and sewage effluent (M. R. Fernandez, w, Tampa)
Lee County (D. H. Boggess, w, Ft. Myers)
Loxahatchee River assessment (G. W. Hill, w, Miami)
Palm Beach County (J. N. Fischer, w, Miami)
Quality of water:
Estuarine hydrology, Tampa Bay (C. R. Goodwin, w, Tampa)
Solid waste, Hillsborough County (Mario Fernandez, Jr., w, Tampa)
Special studies, technical assistance (John Vecchioli, w, Tallahassee)
Surface water, Lakes in southwest Florida (K. M. Hammett, w, Tampa)
Technical assistance, Suwanee River Water Management District (J. C. Rosenau, w, Tallahassee)
Water Atlas (S. D. Leach, w, Tallahassee)
Water resources, Hendry County (J. E. Fish, w, Miami)
Water resources of Manasota Basin (D. P. Brown, w, Tampa)
Water resources, Orange County (C. H. Tibbals, w, Winter Park)
Western Collier County (W. J. Haire, w, Miami)
Georgia (w, Doraville):
Cretaceous (L. D. Pollard)
Hydrology of the Albany area (D. W. Hicks)
Streamflow network evaluation (R. F. Carter)
Water resources information system (J. R. George)
Hawaii (w, Honolulu):
Biology-morphology, Wailuku River (J. J. S. Yee)
Data management, Guam (C. J. Huxel, Jr.)
Topical studies (F. T. Hidaka)

Water resources—Continued

States and territories—Continued

Idaho (w, Boise):
- Flow in Silver Creek, Idaho (J. A. Moreland)
- Ground-water-quality assessment (H. R. Seitz)
- Kootenai Board—WWT (E. F. Hubbard)
- Special studies (C. A. Thomas)
- Streamflow evaluation, Upper Snake River (C. A. Thomas)

Indiana, Ground water near Fort Wayne (Michael Planert, w, Indianapolis)

Iowa (w, Iowa City):
- Bedrock mapping (R. E. Hansen)
- Low flow, Iowa streams (O. G. Lara)

Kansas (w, Lawrence, except as otherwise noted):
- Geohydrology Arkansas River valley southwest Kansas (R. A. Barker, w, Garden City)
- Glacial deposits (J. E. Denne)
- Regional precipitation variability study plan (C. A. Perry)
- Saline water Wellington Formation (A. J. Gogel)
- Special hydrologic investigations (H. G. O'Conner)
- Water supply in droughts (H. G. O'Conner)

Kentucky (w, Louisville):
- Ground water, Ohio River valley (J. M. Kernodle)
- Somerset hydrology (R. W. Davis)

Louisiana (w, Baton Rouge):
- Baton Rouge area (C. D. Whiteman, Jr.)
- Lignite hydrology (J. L. Snider, w, Alexandria)
- Ground water:
  - Grammercy area (D. C. Dial)
  - Kisatchie Forest area (J. E. Rogers, w, Alexandria)
  - Terrace aquifer, central Louisiana (J. L. Snider)
- New Orleans area (D. C. Dial)
- Reports on special topics (M. J. Forbes)
- Site studies (J. E. Rogers)
- Surface water:
  - Flood hydraulics and hydrology (A. J. Calandro)
  - Velocity of Louisiana streams (A. J. Calandro)

Maine, public inquiries (J. T. Armbruster w, Boston, Mass.)

Massachusetts, Public inquiries (M. R. Frimpter, w, Boston)

Michigan (w, Lansing, except as otherwise noted):
- Construction of wells (F. R. Twenter)
- Erosion in St. Joseph Basin (T. R. Cummings)
- Geohydrology, environmental planning (F. R. Twenter)
- Ground water:
  - Models, Muskegon County (W. B. Fleck)
  - West Uppir Peninsula (C. J. Doonan)
- Water resources of Pictured Rocks (A. H. Handy)
- Water resources of Sleeping Bear Dunes (A. H. Handy)

Minnesota (w, St. Paul):
- Impact of copper-nickel mining (P. G. Olcott)
- Twin Cities ground-water study (J. H. Guswa)

Mississippi (w, Jackson):
- Bridge site investigations (K. V. Wilson)
- Salt Dome hydrology in Mississippi (C. A. Spiers)
- Water assimilation (G. A. Bednar)

Missouri:
- Irrigation water, Audrian County (L. F. Emmett, w, Rolla)
- Water in northwestern Missouri (John Skelton, w, Rolla)

Montana (w, Helena, except as otherwise noted):
- Ground water, Fort Belknap (R. D. Feltis, w, Billings)
- Hydrology, lower Flathead (A. J. Boettche)
- Special investigations (J. A. Moreland)

Nebraska, Time-of-travel data (L. R. Petri, w, Lincoln)

Water resources—Continued

States and territories—Continued

Nevada (w, Carson City):
- Aquifers in the Fallon area (P. A. Glancy)
- Surface water network evaluation (Otto Moosburner)
- Topical studies (P. A. Glancy)
- Water supply:
  - Cold Spring Valley (A. S. Van Denburgh)
  - Mining districts (H. A. Shamberger)

New Hampshire, Public inquiries (R. E. Hammond, w, Concord)

New Jersey (w, Trenton):
- Problem river studies (J. C. Schornick, Jr.)
- Quantification nonpoint pollution (J. C. Schornick, Jr.)
- Short-term studies (C. L. Tilley-Groaan)
- Geophysical logging (R. L. Walker)
- Water resources, Wharton Tract (A. W. Harbaugh)

New Mexico (w, Albuquerque):
- Bureau of Indian Affairs water-supply investigations (F. P. Lyford)
- Coal-lease areas, northwest New Mexico (J. R. Hejl)
- Ground water:
  - Capitan Limestone (W. L. Hiss)
  - Harding County (F. D. Trauger)
  - Miscellaneous activities, State Engineering (W. A. Mourant)
  - White Sands Missile Range, water levels and pumpage (H. D. Hudson)
- Liaison—U.S. Geological Survey-Bureau of Land Management (Kim Ong)
- Pojoaque River analyses (G. A. Hearne)
- Southwest alluvial valleys (east) (D. W. Wilkins)
- Water resources, Acoma and Laguna Reservations (F. P. Lyford)
- Water resources, Mimbres Basin (J. S. McLean)

New York (w, Syosset, except as otherwise noted):
- Basin recharge with sewage effluent (R. C. Prill)
- Hydrogeology of Nassau County (Chabot Kilburn)
- Hydrogeology—upstate New York (R. M. Waller, w, Albany)
- Long Island water quality (B. G. Katz)
- Nassau County, ground-water (Chabot Kilburn)
- Short-term studies (L. A. Martens, w, Albany)
- Suffolk County, water-quality observation well program (Julian Soren)
- Water resources, South Fork, Long Island (Bronius Nemickas)

North Carolina (w, Raleigh):
- Hydrology of Albermarle-Pamlico area (C. C. Daniel)
- Public water supplies (T. M. Robison)
- Surface water, Requests for data (H. N Jackson)

North Dakota (w, Bismarck, except as otherwise noted):
- Ground water:
  - Billings-Golden Valley Slope (L. O. Anna)
  - Dickey-Lamoure (J. S. Downey)
  - Hydrologic changes due to mining (W. F. Horak)
  - Ransom-Sargent (C. A. Armstrong)
  - Special investigations (K. F. Brinster)
- Rattlesnake Butte area hydrology (W. F. Horak)
- Wibaux-Beach deposit hydrology (W. F. Horak, Jr.)

Northern Mariana Islands, Water resources information—Northern Marianas (D. A. Davis, w, Honolulu, Hawaii)

Oklahoma (w, Oklahoma City):
- Ground water, Antlers Sand (D. L. Hart, Jr.)
- Monitor Oklahoma coal field (R. K. Corley)

Water resources—Continued
States and territories—Continued
Oklahoma (w, Oklahoma City)—Continued
Requests, special investigations (J. H. Irwin)
Pennsylvania (w, Harrisburg, except as otherwise noted):
Chemistry of precipitation (T. G. Ross, w, Malvern)
Gaging network (H. N. Flippo, Jr.)
Ground-water resources of Monroe County (L. D. Carswell, w, Philadelphia)
Ground water:
Chester County (L. J. McGreevy, w, West Chester)
Cumberland Valley (A. E. Beecher)
Ground-water resources of the Williamsport area (O. B. Lloyd)
Quality of water, highway construction effects on streams (J. F. Truhlar, Jr.)
Western Pennsylvania (G. R. Schiner)
Puerto Rico (w, San Juan):
Contingent requests (E. D. Cobb)
Geohydrology of landfills, (Fernando Gomez-Gomez)
St. Thomas water-resources appraisal (H. J. McCoy)
Rhode Island, Public inquiries (H. E. Johnston, w, Providence)
South Carolina (w, Columbia):
Cooper River rediversion (P. W. Johnson)
Reconnaissance of estuaries (F. A. Johnson)
South Dakota (w, Huron, except as otherwise noted):
Cheyenne and Standing Rock Indian Reservations (L. W. Howells)
Clark County (L. J. Hamilton)
Deuel and Hamlin Counties (Jack Kume, w, Vermillion)
Water resources:
Aurora and Jerauld Counties (L. J. Hamilton)
Davison-Hanson Counties (J. E. Powell, E. F. Le Roux)
Miner County (S. D. McGarvie, w, Vermillion)
Yankton County (J. E. Powell)
Tennessee, Plan for lignite hydrology studies (W. S. Parks, w, Memphis)
Texas:
Edwards aquifer, Austin area (M. L. Maderak, w, Austin)
Ground water:
El Paso (D. E. White, w, El Paso)
Houston (R. K. Gabrysch, w, Houston)
Model study, Chicot and Evangeline aquifers (W. R. Meyer, w, Houston)
Orange County (G. W. Bonnet, w, Houston)
San Antonio (R. D. Reeves, w, San Antonio)
Hydrology of lignite mining (M. L. Maderak, w, Austin)
Quality of water, bays and estuaries (D. C. Hahl, w, Houston)
Trust territory, water-resource information (D. A. Davis, w, Honolulu, Hawaii)
Utah (w, Salt Lake City, except as otherwise noted):
Central Wasatch Plateau (C. T. Sumsion)
Ground water:
Oil-shale hydrology (K. L. Lindskov)
Statewide ground-water conditions (J. C. Stephens)
Navajo Sandstone, east-central Utah (J. W. Hood)
Program enhancement (Theodore Arnow)
Quality of water, Flamingo Gorge Reservoir (E. L. Bolke)
Surface water:
Canal-loss studies (R. W. Cruff)
Inflow to Great Salt Lake (J. C. Mundorff)
Vermont, Water quality, Black River (K. W. Toppin, w, Boston, Mass.)

Water resources—Continued
States and territories—Continued
Virginia (w, Richmond):
Ground water:
Geohydrologic data (H. T. Hopkins)
Hydrology of Prince William Forest Park (H. T. Hopkins)
Hydrology of the Great Dismal Swamp (J. F. Harsh)
Planning study of low flow (B. J. Prugh)
Project planning and public inquiries (P. M. Frye)
Washington (w, Tacoma):
Bonaparte Creek ground-water study (F. A. Packard)
Ground water:
Special hydrologic problems (William Meyer)
Test drillings (E. L. Bolke)
Inquiries (J. R. Williams)
Model simulation for water management (J. A. Skrivan)
Quileute project (L. M. Nelson)
Real-time data collection (R. R. Adsit)
West Virginia (w, Charleston):
Saline ground water (J. B. Foster)
Studies for unforeseen needs (G. G. Wyrick)
Wisconsin (w, Madison):
Ground water, Columbia County (C. A Harr)
Ground-water-quality monitoring (S. M. Hindall)
Menomonee River sediment study (E. R. Zuehls)
Wyoming (w, Cheyenne):
Effluent monitor, national parks (E. R. Cox)
Green River basin water supply (H. W. Lowham)
Water resources, Powder River Basin (M. E. Lowry)

Water use:
National water use data program (J. R. Ruggles, w, NC)
States and territories:
Alabama, Water use (M. E. Davis, w, University)
Alaska, Water use (L. D. Patrick, w, Anchorage)
Arizona, Water use (S. G. Brown, w, Tucson)
Arkansas, Water use (A. H. Ludwig, w, Little Rock)
California, Water use (J. R. Crippen, w, M)
Colorado, Water use (R. R. Hurr, w, D)
Connecticut, Water use (F. P. Haeni, w, Hartford)
Florida, Water use, (S. D. Leach, w, Tallahassee)
Georgia, Water use (H. R. Stiles, w, Doraville)
Hawaii, Water use (R. H. Nakahara, w, Honolulu)
Idaho, Water use (H. A. Ray, w, Boise)
Illinois, Water use (W. G. Curtis, w, Champaign)
Iowa, Water use (O. G. Lara, w, Iowa City)
Kansas:
Estimating ground-water withdrawals (C. H. Baker, Jr., w, Lawrence)
Water use (C. H. Baker, Jr., w, Lawrence)
Kentucky, Water use (R. J. Faust, w, Louisville)
Louisiana, Water use (W. H. Walter, w, Baton Rouge)
Maryland, Water use (F. K. Mack, w, Towson)
Massachusetts, Water use (J. A. Baker, w, Boston)
Michigan, Water use (F. R. Twenter, w, Lansing)
Minnesota, Water use (E. L. Madsen, w, St. Paul)
Mississippi, Water use (J. A. Callahan, w, Jackson)
Missouri, Water use (L. D. Hauth, w, Rolla)
Montana, Water use (Charles Parrett, w, Helena)
Nebraska, Water use (D. R. Lawton, w, Lincoln)
Nevada, Water use (C. V. Schroer, w, Carson City)
New Jersey, Water use (A. A. Vickers, w, Trenton)
New Mexico, Water use (W. K. Dein, w, Santa Fe)
New York, Water use (B. B. Eissler, w, Albany)

Water use—Continued
States and territories—Continued
North Carolina, Water use (N. M. Jackson, Jr., w, Raleigh)
North Dakota, Water use (Dale Frink, w, Bismarck)
Ohio, Water use (R. M. Hathaway, w, Columbus)
Oklahoma, Water use (J. D. Stoner, w, Oklahoma City)
Oregon, Water use (L. E. Hubbard, w, Portland)
Pennsylvania, Water use (A. E. Becher, w, Harrisburg)
Puerto Rico, Water use (Fernando Gomez-Gomez, w, San Juan)
Rhode Island, Water use (H. E. Johnston, w, Providence)
South Carolina, Water use (A. L. Putnam, w, Columbia)
South Dakota, Water use (E. F. LeRoux, w, Huron)
Tennessee, Water use (V. J. May, w, Nashville)
Texas, Water use (E. T. Baker, w, Austin)
Utah, Water use (R. W. Cruff, w, Salt Lake City)
Vermont, Water use (J. A. Baker, w, Boston, Mass.)
Virginia, Water use (H. T. Hopkins, w, Richmond)
Washington, Water use (E. H. Gavock, w, Tacoma)
West Virginia, Water use (G. G. Wyrick, w, Charleston)
Wisconsin, Water use (R. S. McLeod, w, Madison)
Waterpower classification:
States:
California (c, Sacramento):
Kings River basin, examination of pumped storage sites (W. T. Smith)
Waterpower—Continued
States—Continued
California—Continued
Mokelumne River basin, examination of pumped storage sites (D. E. Wilson)
Review of withdrawals, Owens River basin Westside tributaries (R. D. Morgan)
Upper San Joaquin River basin, examination of pumped storage sites (W. T. Smith)
Westside tributaries (R. D. Morgan)
Idaho, Pahsimeroi River, reservoir and dam site (K. J. St. Mary, c, Portland, Oreg.)
Oregon, Review of withdrawals (c, Portland):
Clackamas River basin (L. O. Moe)
Coquille River basin (S. R. Osborne)
Nestucca River basin (K. J. St. Mary)
South Umpqua River (L. O. Moe)
Wilderness Program. *See* Primitive and Wilderness Areas *under* Mineral and fuel resources—compilations and topical studies, mineral-resources surveys.
Zeolites:
California (southeastern), Oregon, and Arizona (R. A. Sheppard, D)
Zinc. *See* Lead, zinc, and silver.

SUBJECT INDEX

A

absolute age *see also* geochronology; isotopes

absolute age—dates

augen gneiss: Proterozoic material in the Yukon-Tanana Upland, central Alaska 206

corals: Quaternary climates, eustacy, and tectonism, southeastern United States 231

gneisses: "Monson Gneiss", eastern Connecticut 61

— Two generations of Archean gneiss in the Big Horn Mountains 207

granites: Rejuvenation of an ancient craton 208

greenstone: Upper Triassic sedimentary copper deposit in the western Clearwater Mountains 110-111

metamorphic rocks: Paleozoic events in the Piedmont near Fredericksburg, Virginia 207-208

metaplutonic rocks: Paleozoic events in the Piedmont near Fredericksburg, Virginia 71

minerals: Ordovician plutonism in Idaho and Montana 84

norite: Samarium-neodymium age of the Stillwater Complex, Montana 205

opal: Use of uranium-lead isotope systematics to date uraniferous opals 54

peat: Records of past climates in Clear Lake sediments 221

shells: Bootlegger Cove Clay; geographic and stratigraphic mollusk occurrences 111

— Dating Arctic Quaternary raised marine deposits by uranium series and amino acids ratios 205-206

— Persistent low level of Lake Bonneville during last 10,000 years 91-92

— Temperature aspects of late Quaternary marine molluscan faunas 231

volcanic rocks: Age of uranium host rocks in the Date Creek basin, west-central Arizona 50

— Cretaceous volcanism, southwestern Nevada 91

— Extensional volcanism in the Matanuska Valley region 111

— Geologic framework along the Idaho Falls-Blackfoot corridor, east flank of the Snake River Plain, Idaho 83

— Stratigraphy of the Naches Formation 94

— Volcanic rocks of Eocene age from the Pioneer Mountains, Montana 80

wood: Pleistocene and Holocene valley fill in coastal plain streams, eastern Alabama 69

zircon: Age of Yellowjacket Formation, Idaho 81

— Ordovician age of the Quantico Formation reaffirmed 72-73

— Proterozoic cataclastic augen gneiss in the Big Delta quadrangle 108

absolute age—interpretation

deglaciation: End of Pinedale Glaciation, north-central Colorado 222-223

igneous activity: Two Cenozoic igneous events on the Alaska Peninsula 110

intrusions: Lead isotopes in ores and rocks of southwest New Mexico 204

isochrons: Lead isotopes indicate tectonic division in Saudi Arabia 206

— Lead isotopes, southwest New Mexico 206

mantle: Samarium-neodymium study regarding evolution of the Earth's mantle 204

overprinting: Episodic plutonism in the Coast batholith of southeastern Alaska 199

uranium disequilibrium: Application of radiometry to coastal plain formations 70

absolute age—methods

Ar/Ar: Irradiation of samples for $^{40}Ar/^{39}Ar$ dating using the Geological Survey TRIGA Reactor 208

C-14: Radiocarbon dating of pre-Holocene carbonate deposits 205

acoustical surveys *see under* geophysical surveys *under* Massachusetts

activation analysis *see under* methods *under* chemical analysis

aeromagnetic surveys *see* magnetic surveys *under* geophysical surveys *under* Alaska; California; Georgia; Hawaii; Idaho; Montana; New York; North Carolina; Oregon; South Carolina; United States; Vermont

Alabama—areal geology

regional: South Carolina, Georgia, and Alabama 68-70

Alabama—economic geology

water resources: Alabama 126-127

Alabama—environmental geology

geologic hazards: Flood of April 1979 127

— Hurricane Frederick 126-127

pollution: Limnology of West Point Reservoir, Georgia and Alabama 235

Alabama—geochronology

Quaternary: Pleistocene and Holocene valley fill in coastal plain streams, eastern Alabama 69

Alabama—hydrogeology

hydrology: Baseline hydrology in coal areas 127

Alabama—stratigraphy

Carboniferous: Geology of the Mississippian and Pennsylvanian of north-central Alabama 69-70

Cretaceous: Upper Cretaceous geology of the Tombigbee River, Alabama and Mississippi 230

Paleocene: Dinoflagellates and increased biostratigraphic resolution 230

Tertiary: Tertiary stratigraphy, eastern Alabama and western Georgia 68-69

Alaska—areal geology

regional: Alaska 102-113

— East-central 106-109

— Northern 104-105

— Southeastern 111-113

— Southern 109-110

— Southwestern 110-111

— Statewide 102-104

— West-central 106
Alaska—economic geology
barite deposits: Gravity measurement of approximate tonnage of a Brooks Range barite deposit 104-105
bibliography: Alaskan mineral resources 104
coal: Northern Alaskan coals 28
— Western and Alaskan coals 26-28
copper ores: Bornite deposit, Cosmos Hills, northwest arctic Alaska 105
— Metallogenic and tectonic significance of isotopic data from the Nikolai Greenstone, McCarthy quadrangle 109-110
— Two Cenozoic igneous events on the Alaska Peninsula 110
— Upper Triassic sedimentary copper deposit in the western Clearwater Mountains 110-111
fuel resources: Rock units of the eastern Gulf of Alaska Outer Continental Shelf 161
geothermal energy: Alaska Peninsula volcanoes 60
gold ores: Geologic map of the Fairbanks gold belt 107
— Gold placers in the Mount Hayes quandrangle 109
maps: Geologic map of the Fairbanks gold belt 107
metal ores: Geochemical definition of mineral province, Alaska Range, Alaska 14
— Geochemical definition of mineral province, Brooks Range, Alaska 14
— Geochemical definition of mineral provinces in the Alaska Range and Brooks Range 103-104
— Metallic mineral occurrences near the plutonic complex sill in the Coast Range 112
— Metalliferous mineral resource potential of the Big Delta quadrangle 108
— Upper Triassic massive sulfide deposits near Wrangell 112-113
mineral resources: Alaskan mineral resources 104
— AMRAP levels III and IV program highlights 103
— Levels II, III, and IV mineral resource appraisals of Alaska 102-103
— Selected highlights of RAMRAP level II program 103
petroleum: Depositional history and reservoir development of Nanushuk Group 31
— Geochemical prospecting for petroleum, Simpson Peninsula 32
— High-frequency aeromagnetic anomalies associated with hydrocarbon microseepage 32
— National Petroleum Reserve in Alaska 31-32
— Offshore Alaska 32
— Petroleum potential of Norton basin, Outer Continental Shelf 32
— Petroleum potential of Upper Cretaceous rocks, Cook Inlet 32
— Two types of oil in North Slope 31-32
phosphate deposits: Uraniferous phosphate occurrence on Kupreanof Island, southeast Alaska 51
polymetallic ores: Geochemical evidence for mineral deposits, Petersburg and Port Alexander quadrangles, Alaska 14-15
uranium ores: Uraniferous phosphate occurrence on Kupreanof Island, southeast Alaska 51
— Uranium studies in Alaska 44
Alaska—engineering geology
geologic hazards: Gas-charged sediments and associated features of the Alaskan Continental Shelf 157-158
permafrost: Permafrost distribution model 104
Alaska—environmental geology
land use: Levels II, III, and IV mineral resource appraisals of Alaska 102-103
Alaska—geochronology
Cenozoic: Two Cenozoic igneous events on the Alaska Peninsula 110
Eocene: Extensional volcanism in the Matanuska Valley region 111
Pleistocene: Bootlegger Cove Clay; geographic and stratigraphic mollusk occurrences 111
Proterozoic: Proterozoic cataclastic augen gneiss in the Big Delta quadrangle 108
— Proterozoic material in the Yukon-Tanana Upland, central Alaska 206
Triassic: Metallogenic and tectonic significance of isotopic data from the Nikolai Greenstone, McCarthy quadrangle 109-110
— Upper Triassic sedimentary copper deposit in the western Clearwater Mountains 110-111
Alaska—geomorphology
erosion features: Badlands on the north side of the Alaska Range 109-110
glacial geology: Glacial advances in the Yukon-Tanana upland 107
— Sliding speed of Black Rapids Glacier, Alaska 219
Alaska—geophysical surveys
electromagnetic surveys: Observation of induced electric currents in the Alaska oil pipeline 183
gravity surveys: Gravity measurement of approximate tonnage of a Brooks Range barite deposit 104-105
magnetic surveys: High-frequency aeromagnetic anomalies associated with hydrocarbon microseepage 32
— Tertiary volcanic centers on the Alaska Peninsula 111
surveys: Application of aeromagnetic and gravity data to the geological interpretation of the Tintina fault and the Circle quadrangle 107-108
Alaska—oceanography
continental shelf: Gas-charged sediments and associated features of the Alaskan Continental Shelf 157-158
— Quaternary sedimentary facies of the northeast Gulf of Alaska Continental Shelf 158-159
— Rock units of the eastern Gulf of Alaska Outer Continental Shelf 161
ocean circulation: Alaskan Continental Shelf sediment dynamics 156-157
Alaska—paleontology
foraminifera: Distribution of benthic foraminifers, Gulf of Alaska Continental Shelf 159
Alaska—petrology
intrusions: Episodic plutonism in the Coast batholith of southeastern Alaska 199
— Mount Juneau orthogneiss pluton 112
— Multiple intrusion of the La Perouse layered gabbro, Alaska 199
— Tertiary granite stock, southwestern Kupreanof Island 113
— The plutonic complex tonalite sill in the Coast Range 113
metamorphic rocks: Geologic terranes of the Circle quadrangle 107
volcanology: Holocene volcano on the Alaska Peninsula 110
Alaska—sedimentary petrology
sedimentation: Neogene sedimentation, southern Bering Sea 159
Alaska—seismology
crust: Crustal structure of the Aleutian Trench-Amlia fracture zone intersection 161-162
Alaska—stratigraphy
Carboniferous: Paleotectonic setting of the Carboniferous of Alaska 103
Cretaceous: Depositional history and reservoir development of Nanushuk Group 31
— Petroleum potential of Upper Cretaceous rocks, Cook Inlet 32
Devonian: Regional stratigraphy and depositional environment of the Kanayut Conglomerate 105
— Significance of Middle Devonian clastic rocks of the eastern Brooks Range 104
Ordovician: Identification of Ordovician rocks in Lake Minchumina area 106
Paleozoic: Collision-deformed Paleozoic continental margin of Alaska; foundation for microplate accretion 106-107
Permian: Paleomagnetism of Permian basalts 110
Quaternary: Quaternary sedimentary facies of the northeast Gulf of Alaska Continental Shelf 158-159
Alaska—structural geology
structural analysis: Structural analysis of plutonic and metamorphic rocks from an area east of Wrangell 113
tectonics: Alaska fragments 103
— Evidence for northwestward emplacement of Wrangellia terrane in the northern Talkeetna Mountains 109
— Newly recognized plutonic province displacement by the Chatham Strait fault 111

Alaska—tectonophysics
crust: Extensional volcanism in the Matanuska Valley region 111
plate tectonics: Alaska fragments 103
— Collision-deformed Paleozoic continental margin of Alaska; foundation for microplate accretion 106-107
— Crustal structure of the Aleutian Trench-Amlia fracture zone intersection 161-162
— Evidence for northwestward emplacement of Wrangellia terrane in the northern Talkeetna Mountains 109
— Metallic mineral occurrences near the plutonic complex sill in the Coast Range 112
— Metallogenic and tectonic significance of isotopic data from the Nikolai Greenstone, McCarthy quadrangle 109-110
— Northward movement of the Chugach terrane, Alaska 180
— Ophiolites of western Alaska 106
— Paleotectonic setting of the Carboniferous of Alaska 103
— Tertiary volcanic centers on the Alaska Peninsula 111

algae—Chrysophyta
paleoecology: Chrysomonad cysts as paleoenvironmental indicators 241

algae—diatoms
ecology: Simulation model of Skeletonema costatum population dynamics in northern San Francisco Bay 173
identification: Inverted microscope method for the identification and enumeration of periphytic diatoms 235

algae—ecology
lacustrine environment: Phosphorus and nitrogen as limiting nutrients in two arctic lakes 241

algal flora—biostratigraphy
Eocene: Coccolith correlation for Ardath Shale, San Diego County, California 230
Miocene: Three periods of intense high-latitude cooling in the middle to late Miocene 231

alluvium *see under* clastic sediments *under* sediments

angiosperms—ecology
floodplains: Flood rings in trees along the Potomac River 233
growth: Dendroclimatic investigations of hickory and oak 233

Antarctica—geophysical surveys
remote sensing: Polar ice remote-sensing satellite program 243

Appalachians—areal geology
regional: Appalachian Highlands and the Coastal Plains 66-74

Appalachians—economic geology
coal: Sulfur accumulation in coal 28-29
fuel resources: Appalachian Basin 38-40
— Distribution of organic matter in Devonian shale 38-39
— Origin of hydrocarbons in Devonian shale 38
— Surface joint patterns as a guide to fracture reservoirs 39
natural gas: Possible subsurface extension of Appalachian Basin natural gas province 39-40
— Potential siltstone and sandstone gas reservoirs in Devonian shale 39

Appalachians—engineering geology
slope stability: Evidence of modern slope movement in the Appalachian Mountains 234

Appalachians—geophysical surveys
seismic surveys: Possible subsurface extension of Appalachian Basin natural gas province 39-40

Appalachians—stratigraphy
Devonian: Middle and Late Devonian ashfall beds in Devonian shale 74

Appalachians—tectonophysics
plate tectonics: Study of diabase dikes 188-189

aquifers *see under* ground water

Arabian Peninsula *see also* Saudi Arabia

Arabian Peninsula—geochronology
Proterozoic: Lead isotopes indicate tectonic division in Saudi Arabia 206

Archean *see also under* geochronology *under* Montana; Wyoming

Arctic Ocean—engineering geology
permafrost: Permafrost distribution model 104

Arctic Ocean—geophysical surveys
remote sensing: Aircraft remote sensing of satellite Arctic program 242-243
— Passive microwave imagery time-lapse film of Arctic sea-ice variations 243
— Polar ice remote-sensing satellite program 243
— Sea-ice dynamics observed by radar imagery 243-244

Arizona—economic geology
arsenic ores: Arsenic, copper, and molybdenum, Baboquivari Mountains, Arizona 15
copper ores: Geochemical comparison of mineralized and barren stocks, Arizona 10
metal ores: A magnetic tectonic feature in southern Arizona 4
— Geochemical features, Pinaleno Mountains, Arizona 15
— Geochemical reconnaissance studies, Papago Indian Reservation, Arizona 15
— Regional geochemical studies, Patagonia Mountains, Arizona 13
mineral resources: Ajo 2° quadrangle, Arizona 17
— Mineral and energy resource system for Navajo Tribe 21
— Mineral resource assessment using aerial geophysical data 187
molybdenum ores: Arizona molybdenum mineral associations as keys to ore deposit metallogenic types 9
uranium ores: A model for sedimentation at the Anderson mine, west-central Arizona 50
— A possible relation between subsidence and uranium mineralization 57-58
— Age of uranium host rocks in the Date Creek basin, west-central Arizona 50
— Uranium mineralization in the Hopi Buttes of the Flagstaff and Gallup 1° x 2° quadrangles, Arizona 58
— Uranium occurrence at Pajaro Azul, east-central Arizona 42
water resources: Arizona 142-143

Arizona—engineering geology
land subsidence: Geophysical studies of earth fissures 188

Arizona—environmental geology
pollution: Arsenic concentrations in Verde Valley 142-143

Arizona—geochemistry
trace elements: Uranium mineralization in the Hopi Buttes of the Flagstaff and Gallup 1° x 2° quadrangles, Arizona 58

Arizona—geochronology
Tertiary: Age of uranium host rocks in the Date Creek basin, west-central Arizona 50

Arizona—geophysical surveys
gravity surveys: Gravity studies in the Sierra Ancha Wilderness Area, Gila County, Arizona 2
— Gravity studies of mineralized features, Silver City quadrangle, Arizona and New Mexico 5
remote sensing: Ajo 2° quadrangle, Arizona 17
surveys: Aerial radiometric and magnetic survey of the Sierra Ancha Wilderness Area and vicinity, Gila County, Arizona 2-3
— Geophysical studies of earth fissures 188

Arizona—hydrogeology
hydrology: Irrigation water available to Ak-Chin Indian Reservation 142
springs: Arsenic concentrations in Verde Valley 142-143

Arizona—petrology
igneous rocks: Basaltic rocks of the Springerville volcanic field, Arizona 79

Arizona—stratigraphy
Neogene: Cenozoic deformation, lower Colorado River area 91

Arizona—structural geology
neotectonics: Tectonism in the San Francisco volcanic field and southern Colorado Plateau, Arizona 82
tectonics: Easternmost metamorphic core complex, southern Arizona 90-91
— Metamorphic core complex, west-central Arizona 90
— Probable reactivated basement faults east of Defiance uplift 48

Arizona—tectonophysics
crust: Dike trends and stress directions in western Arizona 91

Arkansas—environmental geology
pollution: Benthic sediments and the dissolved-oxygen deficit in L'Anguille River basin, Arkansas 237

Arkansas—hydrogeology
ground water: Quality of water in the Wilcox aquifer 225
Arkansas—stratigraphy
Paleocene: Upland gravel, northeastern Arkansas 74-75
arsenic—abundance
ground water: Arsenic concentrations in Verde Valley 142-143
arsenic—analysis
spectroscopy: Atomic absorption method for arsenic 17
Asia *see also* Arabian Peninsula
Asia—geophysical surveys
remote sensing: Glacier surges monitored by satellite 219
Atlantic Coastal Plain—areal geology
Delmarva Peninsula: Delmarva Peninsula 67-68
regional: Appalachian Highlands and the Coastal Plains 66-74
— Southeast Coastal Plain 70-71
Atlantic Coastal Plain—environmental geology
ecology: Benthic fauna studies of the tidal Potomac River 168-169
— Damage to flood-plain forests along the Potomac River 233
— Flood rings in trees along the Potomac River 233
— Potomac Estuary Study 233
— Wetland studies of the Potomac River Estuary 169
pollution: Geochemistry of sediments and associated interstitial waters for the tidal Potomac River 167-168
— Interdisciplinary study of the Potomac River Estuary 166
— Seasonal distributions of oxygen, carbon, nitrogen, and silicon in the Potomac River 168
— Variations in nutrient and sediment concentrations in the Potomac River Estuary 167
— Water quality of major tributaries, Chesapeake Bay 234
Atlantic Coastal Plain—geochronology
absolute age: Application of radiometry to coastal plain formations 70
Pleistocene: Paleomagnetic investigation of Pleistocene sediments of the Delmarva Peninsula, central Atlantic Coastal Plain 67
Atlantic Coastal Plain—geophysical surveys
seismic surveys: Shallow stratigraphy of the Potomac River Estuary 167
Atlantic Coastal Plain—hydrogeology
ground water: Model insensitive to variations in transmissivity 225-226
Atlantic Coastal Plain—oceanography
marine geology: Atlantic and Gulf Coast 167-170
Atlantic Coastal Plain—stratigraphy
Cenozoic: Late Cenozoic marine deposition, Southeastern United States 70
changes of level: Quaternary climates, eustacy, and tectonism, southeastern United States 231
Atlantic Coastal Plain—structural geology
neotectonics: Quaternary climates, eustacy, and tectonism, southeastern United States 231
Atlantic Ocean *see also* Iceland
Atlantic Ocean—economic geology
petroleum: The ocean-continent transition zone off New Jersey 159-160
Atlantic Ocean—engineering geology
slope stability: Slope stability off the southeast Atlantic Coast 155
Atlantic Ocean—oceanography
sedimentation: Suspended matter in continental shelf and slope waters of the Georges Bank area 155
sediments: Discovery of upper Wisconsinan glacial till on the Continental Shelf off southeastern New England 66
Atlantic Ocean—stratigraphy
Pliocene: Extent of Northern Hemisphere Pliocene glaciation 231
Australasia *see also* New Zealand
Australia *see also* Northern Territory
Australia—economic geology
uranium ores: Canadian, Australian, and United States uranium deposits compared 45-46
automatic data processing—economic geology
coal: Coal resource model studies 20
— Computerization of the nation's resources 24
— National Coal Resources Data System 19-20
geothermal energy: Geothermal resources file 19
mercury ores: Production statistics applied to resource estimation 21
metal ores: Mineral-resource assessment 21-22
mineral exploration: Identification of geochemical anomalies 203
mineral resources: Computer applications of resource data files 20
— Computerized Resources Information Bank (CRIB) 19
— Dynamic modeling of mineral resources 20
— Mineral and energy resource system for Navajo Tribe 21
— Resource analysis 20-22
— Resource information systems 19-20
— Resource information systems and analysis 19-22
oil shale: Oil shale and saline mineral data system 20
petroleum: Petroleum resource appraisal and discovery process modeling 21
uranium ores: Porous media model computer and field studies of sandstone-type uranium deposits 51
— Uranium resource analysis 22
automatic data processing—engineering geology
geologic hazards: New techniques applied to studies of seafloor hazards and conditions 152-153
automatic data processing—general
information systems: Geologic Retrieval and Synopsis Program 20
maps: Geologic map data file 114
automatic data processing—geophysical surveys
gravity methods: Residual Bouguer gravity maps 18
remote sensing: Digital classification of Landsat data for identification of hydrothermal alteration 183
seismic methods: Improved methods for seismic refraction interpretation 60
well-logging: Computer programs for resistivity soundings over three vertical layers 186
— Simultaneous interpretation of geophysical well logs 19
automatic data processing—geophysics
magnetic field: Determination of K-indices by computer 182
automatic data processing—hydrogeology
hydrology: Data coordination, acquisition, and storage 146-148
— National Water Data Exchange 147-148
— New hydrologic instruments and techniques 242
— Office of Water Data Coordination 146-147
— Planning for conjunctive water-supply systems 239
— USGS-EPA urban studies 148
— Water Data Storage System 148
— Water use 150

B

Basin and Range Province—areal geology
regional: Basin and Range region 87-92
Basin and Range Province—economic geology
fluorspar: Fluorine, beryllium, and uranium mineralization in Thomas Range, western Utah 42-43
— Geochemical uranium, fluorite, and beryllium ore controls at Spor Mountain 54
maps: Geochemical maps of uranium, thorium, and thorium-uranium in granites of the Basin and Range province 56
mineral resources: Mineral-resource studies 87
uranium ores: Geochemical maps of uranium, thorium, and thorium-uranium in granites of the Basin and Range province 56
Basin and Range Province—geochronology
research: Geochronologic studies 91-92
Basin and Range Province—petrology
igneous rocks: Igneous rocks 91
Basin and Range Province—stratigraphy
Phanerozoic: Stratigraphic and structural studies 87-91

Basin and Range Province—structural geology
neotectonics: Controls of Pliocene and Pleistocene basaltic volcanism, southern Great Basin 89-90
tectonics: Stratigraphic and structural studies 87-91
batholiths *see under* intrusions
Bering Sea—economic geology
fuel resources: Geologic framework and hydrocarbon prospects of the eastern Bering Sea 162
Bering Sea—engineering geology
geologic hazards: Faults of the southern Bering Sea margin 158
— Seafloor erosion and deposition, northern Bering Sea 158
Bering Sea—geophysical surveys
seismic surveys: Petroleum potential of Norton basin, Outer Continental Shelf 32
Bering Sea—oceanography
continental shelf: Petrology of rocks from the Pribilof Islands region, southern Bering Sea shelf 162-163
ocean circulation: Seafloor erosion and deposition, northern Bering Sea 158
ocean floors: Geologic framework and hydrocarbon prospects of the eastern Bering Sea 162
sedimentation: Neogene sedimentation, southern Bering Sea 159
Bering Sea—structural geology
neotectonics: Faults of the southern Bering Sea margin 158
bibliography *see also under* economic geology *under* Alaska
bismuth—analysis
spectroscopy: Determination of nanogram amounts of bismuth in silicate rocks 244
brines *see also* bromine
bromine—analysis
chemical analysis: Automated colorimetric determination of bromide ions 245

C

cadmium—abundance
coal: Zinc and cadmium content of coal in the Interior coal province 28
California—areal geology
regional: California 96-102
California—economic geology
chromite ores: Chromite and nickel, western Cordillera 8-9
— Chromite in northern California 18
copper ores: Massive sulfide deposits in ophiolitic terrain, northern Klamath Mountains, Oregon and California 12
fuel resources: Diagenesis of reservoir rocks of the Monterey Shale, Santa Barbara coast, California 37
— Great Basin and California 37
geothermal energy: Complex stratigraphy at Medicine Lake Volcano 216
— Magma chamber in the Geysers-Clear Lake area 210
— Near-surface heat flow in Saline Valley, California 213
— Seismic velocity structure at Coso geothermal area 214
— Steam flow in the Larderello and The Geysers geothermal systems 211
— Upper crustal structure beneath the Coso Range, California 214
iron ores: Magnetite deposit, Minarets Wilderness Area, California 18
metal ores: Constraints placed upon location of the San Andreas fault by base and precious metal sulfide mineralization, Point Delgada, northern California 96-97
mineral resources: Interrelations among epithermal ore deposits and geothermal systems depositing mercury, gold and silver 209-210
petroleum: Porosity of Miocene siliceous shale, Midway-Sunset oil field, California 37
phosphate deposits: California phosphorite 22
uranium ores: Uranium in Monterey Formation 50-51
water resources: California 143-144
California—environmental geology
ecology: Effects of river discharge on phytoplankton biomass and species composition in the northern San Francisco Bay Estuary 173
— Heavy-metal distributions in mollusks of San Francisco Bay 174
— Plant distributions in the tidal wetlands of the Sacramento-San Joaquin River Delta 173-174
— Population dynamics of dominant bivalves in San Francisco Bay 174
— Sacramento-San Joaquin Delta wetlands, San Francisco Bay, California 167
— Simulation model of Skeletonema costatum population dynamics in northern San Francisco Bay 173
geologic hazards: December 1977 windstorm in San Joaquin Valley 220
— Southern California borderland; environmental geology 100
pollution: Biological-chemical consequences of a major sewage spill in South San Francisco Bay 173
— Functional and structural responses of a stream community to copper 240
— Heavy-metal distributions in mollusks of San Francisco Bay 174
— Russian River response to waste-water discharge and drought 143
— Water-quality monitoring for radioisotopes, California 236
California—geochemistry
organic materials: Anaerobic oxidation of acetylene by San Francisco Bay sediment slurries 171
— Distribution and stable-isotope composition of carbon in San Francisco Bay 172
— Hydrocarbon gases in surface sediments of San Francisco Bay 171-172
— Microbial formation of ethylene and ethane in San Francisco Bay sediments 171
California—geochronology
Pleistocene: Middle Wisconsinan marine platform at Point Delgada 96
— Zircon fission-track ages of a Pleistocene ash, California and Nevada 206-207
Quaternary: Records of past climates in Clear Lake sediments 221
— Tectonic uplift rates near Gaviota, California 231-232
California—geomorphology
shore features: Tidal wetland deposits of the Sacramento-San Joaquin Delta 170-171
California—geophysical surveys
heat flow: Near-surface heat flow in Saline Valley, California 213
magnetic surveys: Magnetite deposit, Minarets Wilderness Area, California 18
— New magnetic observatory near Fresno, California 181-182
magnetotelluric surveys: Field tests of real-time magnetotelluric systems 216
seismic surveys: Seismic study of a subsea gas accumulation off southern California 157
surveys: Chromite in northern California 18
California—hydrogeology
ground water: Ground water limited in north-central Santa Cruz County 143
— Ground-water recovery at Thousand Oaks 143
— Stable-isotope technique used to trace ground-water movement 227
hydrogeology: Appraisal data adequate for Owens Valley 144
hydrology: Water quality assessment of Merced River 143
maps: Classification of recharge in Santa Cruz area 143
California—mineralogy
sulfides: Alkali-iron sulfides from Coyote Peak, Humboldt County, California 192
California—oceanography
ocean circulation: A two-dimensional hydrodynamic model of San Francisco Bay 171
— California continental margin sediment dynamics 156
sea water: Seasonal distributions of water properties in San Francisco Bay 172
sedimentation: Coastal sedimentary processes off beaches 165
sediments: Gas within sediments of the northern California to Oregon Outer Continental Shelf 157
California—petrology
inclusions: Inclusions in upper Cenozoic volcanic rocks of the central Sierra Nevada, California 201

— Quenched mafic magma in rhyolite, Coso Range, California 196-197
intrusions: Batholithic rocks of southern California 203
— Mylonitic gneisses over a Cretaceous(?) pluton, Iron Mountains, southeastern California 100-101
— Tertiary hypabyssal intrusions, Sierra Nevada 98
metamorphic rocks: Volcanic greenschist in the subsurface of the southeastern San Joaquin Valley 99
California—sedimentary petrology
sedimentation: Sedimentology of the Neogene Little Sulphur Creek basins 97
— Source terrane for basement clasts of the Temblor Range 99
California—seismology
crust: Seismic velocity structure at Coso geothermal area 214
— Upper crustal structure beneath the Coso Range, California 214
California—stratigraphy
Cenozoic: Three-million-year record of climate in Searles Lake sediments 222
Devonian: Correlative Devonian eugeosynclinal rocks, California and Nevada 89
Eocene: Coccolith correlation for Ardath Shale, San Diego County, California 230
Miocene: California phosphorite 22
— Postmiddle Miocene accretion of Franciscan coastal belt rocks to northern California 97-98
Quaternary: A 100,000-year cave record of atmospheric temperatures 223
— Upper Quaternary stratigraphy and structure of the Antelope Valley and vicinity, California 100
California—structural geology
deformation: Fault creep in Mendocino County, California 98
neotectonics: Constraints placed upon location of the San Andreas fault by base and precious metal sulfide mineralization, Point Delgada, northern California 96-97
— Glacier snowlines and uplift of the San Bernardino Mountains 101-102
— Quaternary deformation in southern part of Elsinore fault zone 101
— Southern California borderland; environmental geology 100
— Southern Sierra Nevada uplift history 99
— Tectonic uplift rates near Gaviota, California 231-232
— Uplift and tilt of the Sierra Nevada 98-99
— Upper Quaternary stratigraphy and structure of the Antelope Valley and vicinity, California 100
tectonics: Correlative Devonian eugeosynclinal rocks, California and Nevada 89
— Postmiddle Miocene accretion of Franciscan coastal belt rocks to northern California 97-98
— Tectonic attenuation of Paleozoic rocks, southeastern California 101
— Tectonism and plutonism, northwestern Sierra Nevada 98
— Upper Mesozoic rocks of the Wilbur Springs antiform 97
California—tectonophysics
plate tectonics: Postmiddle Miocene accretion of Franciscan coastal belt rocks to northern California 97-98
— Southern California borderland; environmental geology 100
— Tectonism and plutonism, northwestern Sierra Nevada 98
Cambrian *see also under* stratigraphy *under* Montana; Virginia
Canada *see also* Appalachians; Atlantic Coastal Plain; Great Lakes; Great Lakes region; Great Plains; Northwest Territories; Ontario; Rocky Mountains; Saskatchewan
Canada—economic geology
uranium ores: Canadian, Australian, and United States uranium deposits compared 45-46
carbon—abundance
limestone: Organic carbon of seafloor middle Cretaceous limestones 163-164
carbon—isotopes
C-13/C-12: Distribution and stable-isotope composition of carbon in San Francisco Bay 172
carbonate rocks *see under* sedimentary rocks
Carboniferous *see also under* stratigraphy *under* Alabama; Alaska; Europe
catalogs—general
maps: Geologic map data file 114
Cenozoic *see also under* geochronology *under* Alaska; *see also under* stratigraphy *under* Atlantic Coastal Plain; California; Georgia
Cenozoic—paleontology
research: Mesozoic and Cenozoic studies 229-232
ceramic materials *see also under* economic geology *under* North Carolina
changes of level *see also under* geomorphology *under* Utah; *see also under* stratigraphy *under* Atlantic Coastal Plain
changes of level—correlation
paleoclimatology: Holocene sea-level change; a possible record of global climatic change 224
chemical analysis—methods
activation analysis: Trace elements in planetary materials by activation analysis 245
applications: Analytical methodology useful in geochemical exploration 17
chromatography: Ion chromatography 245
colorimetry: Automated colorimetric determination of bromide ions 245
research: Analytical chemistry 244-245
— Analytical methods 244-246
— Radiochemistry 244-245
spectroscopy: Atomic absorption method for arsenic 17
— Combined energy dispersive and wavelength dispersive analysis 191
— Determination of nanogram amounts of bismuth in silicate rocks 244
— Germanium concentrations in USGS rock standards as determined by electrothermal atomization atomic absorption spectrometry 244
— In situ capture gamma-ray analysis of coal in oversized boreholes 30-31
— Induction-coupled plasma spectroscopy 17
— Sensitive method for gold analysis 17
— X-ray spectroscopy 244
chemical analysis—techniques
applications: Analysis of water 245-246
sample preparation: Liquid ion exchange technique 17
— Methylation of humic and fulvic acids 246
chromatography *see under* methods *under* chemical analysis
clastic rocks *see under* sedimentary rocks
clastic sediments *see under* sediments
clay *see under* clastic sediments *under* sediments
clay mineralogy—areal studies
Idaho: Zonation of clay and zeolite minerals, Raft River geothermal boreholes, Idaho 209
Washington: Hydrothermal alteration at Mount Baker, Washington 198
clay mineralogy—experimental studies
adsorption: Uranium adsorption onto montmorillonite 53
kaolinite: Organic compounds on kaolinite 202
coal *see also under* economic geology *under* Alaska; Appalachians; automatic data processing; Eastern U.S.; Georgia; Illinois; Midwest; Montana; New Mexico; Pennsylvania; Rhode Island; United States; Utah; Virginia; West Virginia; Western Interior; Western U.S.; Wyoming; *see also under* organic residues *under* sedimentary rocks
coal—geochemistry
chalcophile elements: Chalcophile elements and uranium in coal 28
general: Geochemistry 28-30
mobilization: Mobilization of elements resulting from use of coal 29-30
oxidation: Electrolytic oxidation of coal 30
coal—properties
analysis: Application of automatic image analysis to coal petrography 30
— Laboratory and field analytical techniques 30-31
chemical properties: In situ capture gamma-ray analysis of coal in oversized boreholes 30-31
coal—resources
data bases: National Coal Resources Data System 19-20
evaluation: Coal resource model studies 20
global: Global studies 24-25

— World coal resources 24
Coelenterata—evolution
morphology: Evolution of the corals 232-233
Colorado—areal geology
maps: Geologic map of Colorado 114
Colorado—economic geology
copper ores: Stratabound Precambrian sulfide and gahnite deposits in the Pearl area, Colorado and Wyoming 10-11
geothermal energy: Travertine at Poncha Hot Springs, Chaffee County, Colorado 13
metal ores: Massive sulfide bodies in Colorado 18
— Stream sediment geochemical survey, southwestern Rawah Range, northern Colorado 10
thorium ores: Large thorium reserves in disseminated deposits 42
uranium ores: A regional disconformity in Jurassic rocks of the San Juan Basin 48
— Airborne geophysical survey for uranium 187
— Alkaline intrusive complexes, Wet Mountains, Colorado 42
— Colorado uranium deposits as ancient geothermal systems 59
— Early Permian depositional systems and paleogeography, Uncompahgre Basin 47
— Genetic geochemistry of Uravan mineral belt deposits; a new proposal 52
— Meeker uranium district projected 49
— Petrology and deformation of Leadville Dolomite, Pitch uranium mine 43
— Porous media model computer and field studies of sandstone-type uranium deposits 51
— Possible hot-spring origin for Front Range uranium veins 43-44
— Probable origin of uranium in the Browns Park Formation (Miocene) of the Sand Wash Basin, Moffat County, Colorado 49
— Radioactivity in water wells, Pueblo County, Colorado 56
— Salt Wash depositional environments and uranium 48
— Supergene uranium deposits in fracture zones associated with Laramide upthrusts 43
— Unconformity-related uranium occurrences in the Precambrian basement in the upper basin of the Arkansas River, Colorado 58-59
— Uranium in the Oligocene Antero Formation, Park County, Colorado 49-50
Colorado—geophysical surveys
electromagnetic surveys: Electromagnetic response of cultural features 186
surveys: Airborne geophysical survey for uranium 187
— Geophysical studies in the Never Summer Wilderness Area, Colorado 2
— Massive sulfide bodies in Colorado 18
well-logging: Nonlinear complex resistivity logging 185
Colorado—hydrogeology
hydrology: Evaluation of empirical water-quality prediction models in reservoirs 241
— Water quality studies 149
springs: Travertine at Poncha Hot Springs, Chaffee County, Colorado 13
thermal waters: Travertine at Poncha Hot Springs, Chaffee County, Colorado 13
Colorado—petrology
intrusions: Hoffman Park stock, Colorado, and its relation to the Mount Antero Granite 200-201
metamorphic rocks: Amphibolite facies mineral assemblages and the fractionation of CaO, U, and Th, Colorado 201
Colorado—soils
surveys: Helium and sulfur, Poorman fault, Colorado 16
Colorado—stratigraphy
Jurassic: Salt Wash depositional environments and uranium 48
Permian: Early Permian depositional systems and paleogeography, Uncompahgre Basin 47
Pleistocene: End of Pinedale Glaciation, north-central Colorado 222-223
— Late Pinedale Glaciation in the Northern Rocky Mountains 223
— Relation between late Pleistocene snowfields and "landslides" 223
Quaternary: Climatic influence on alluvial deposition, northwest Colorado 223-224
Colorado—structural geology
tectonics: Uplift studies in the Front Range, Colorado 82-83
Colorado Plateau—economic geology
uranium ores: Porous media model computer and field studies of sandstone-type uranium deposits 51
Colorado Plateau—structural geology
neotectonics: Cenozoic deformation, lower Colorado River area 91
— Tectonism in the San Francisco volcanic field and southern Colorado Plateau, Arizona 82
Columbia Plateau—hydrogeology
ground water: Simulation of ground-water flow in basalt aquifers underlying the Columbia Plateau 146
Columbia Plateau—petrology
igneous rocks: Columbia River Plateau studies 196
intrusions: Diatremes in the Grande Ronde graben 196
lava: Eastern extent of Picture Gorge Basalt 196
Columbia Plateau—structural geology
tectonics: Geometry and tectonic evolution of the Columbia Hills 96
— Left lateral strike-slip riedel shears in the Yakima ridges 95
colorimetry *see under* methods *under* chemical analysis
— Miocene deformation and canyon cutting at Graybach Mountain 95-96
— Tectonic evolution of the southeastern part of the Columbia Plateau 94-95
Connecticut—economic geology
water resources: Connecticut 117
Connecticut—geochemistry
trace elements: "Monson Gneiss", eastern Connecticut 61
Connecticut—geomorphology
glacial geology: Deglaciation, eastern Connecticut 63
— Deglaciation of central Connecticut and the "Middletown Readvance" 63
— Ice-shove structures in end moraines, northwest Connecticut 63
— Small glacial lakes in the Housatonic River valley 63
Connecticut—hydrogeology
ground water: Aquifer characteristics and organohalides in ground water, Southbury and Woodbury 117
— Estimating recharge areas for stratified drift aquifers, Connecticut 226
— Ground-water resources in southwestern Connecticut 117
Connecticut—petrology
metamorphic rocks: Correlation of Oakdale and Paxton Formations of east-central Massachusetts with stratigraphy in eastern Connecticut 62
Connecticut—sedimentary petrology
sediments: Saprolitic clay preserved in limestone selection depressions near East Canaan, Connecticut 63
Connecticut—structural geology
tectonics: Basement-cover rock relations, southeastern Connecticut 61
conodonts—biostratigraphy
Paleozoic: Extension of St. Clair bedding-plane thrust in Virginia 40
— Sedimentation rates and timing of Antler orogenic events determined from conodont zonation, Western United States 37
conservation *see also under* environmental geology *under* United States
conservation—natural resources
water resources: Waterpower classification; preservation of resource sites 176
continental shelf *see also under* oceanography *under* Alaska; Bering Sea; Massachusetts; United States
continental slope *see also under* oceanography *under* Louisiana; Texas
copper—abundance
surface water: Functional and structural responses of a stream community to copper 240
core—composition
experimental studies: Melting relations in the system Fe-S-O 191
Cretaceous *see also under* geochronology *under* Nevada; Washington; *see also under* stratigraphy *under* Alabama; Alaska; Mississippi; Montana; New Mexico; South Carolina; Utah; Western Interior; Wyoming

cross-bedding *see under* planar bedding structures *under* sedimentary structures
crust *see also under* seismology *under* Alaska; California; Idaho; Oregon; Utah; *see also under* tectonophysics *under* Alaska; Arizona; New Jersey
crust—properties
magnetic properties: Maghemitization of oceanic crust 181
— Random crustal magnetization and its effect on marine magnetic anomalies 181
crystal chemistry *see also* crystal growth; minerals
crystal chemistry—chlorides
tachyhydrite: Tachyhydrite 192
crystal chemistry—sulfides
copper sulfides: Copper-rich sulfides; low chalcocite and djurleite 191-192
crystal growth *see also* crystal chemistry; minerals
crystal growth—chain silicates, clinopyroxene
phase equilibria: Decomposition mechanism and kinetics in clinopyroxenes 190-191
crystal growth—oxides
manganese oxide: Rates of formation of manganese oxides 202-203
crystal structure *see also* crystal chemistry; minerals
crystal structure—chlorides
tachyhydrite: Tachyhydrite 192
crystal structure—sulfides
alkali-iron sulfides: Alkali-iron sulfides from Coyote Peak, Humboldt County, California 192
crystal structure—theoretical studies
lattice: Relations between lattice dynamics and thermodynamic properties of minerals 189-190
crystallography *see also* mineralogy

D

deformation *see also* geophysics; structural analysis
deformation—field studies
creep: Fault creep in Mendocino County, California 98
strain: Mylonitic gneisses over a Cretaceous(?) pluton, Iron Mountains, southeastern California 100-101
Delaware—economic geology
water resources: Delaware 117
Delaware—hydrogeology
ground water: Late Miocene aquifers 117
Devonian *see also under* stratigraphy *under* Alaska; Appalachians; California; Nevada; New Hampshire
diagenesis *see also* sedimentation
diagenesis—dolomitization
reservoir rocks: Distribution and diagenetic history of possible reservoir beds in Madison Group, disturbed belt, Montana 33
diagenesis—effects
porosity: Porosity of Miocene siliceous shale, Midway-Sunset oil field, California 37
reservoir properties: Mineralogy and diagenesis of gas-bearing reservoirs in Niobrara Chalk 36-37
— Petrology and reservoir characteristics of Mesaverde Group, Washakie Basin, Wyoming 36
— Reservoir characteristics of gas-bearing Eagle Sandstone, Bearpaw Mountains, Montana 33-34
— Reservoir characteristics of Sunniland Limestone (Lower Cretaceous), southern Florida 38
diagenesis—geochemistry
mobilization: Distribution and mobility of uranium in glassy and zeolitized tuff, Keg Mountain area, Utah 55
— Uranium leachability from freshly erupted volcanic ash of basaltic and dacitic composition 55-56
diagenesis—materials
reservoir rocks: Diagenesis of reservoir rocks of the Monterey Shale, Santa Barbara coast, California 37
diagenesis—processes
cementation: Reduction of sandstone permeability through shale dewatering 40-41
compaction: Production of hydrocarbons and alteration of sedimentary structures through compaction 41
diamonds *see also under* economic geology *under* Montana
diastrophism *see* orogeny
diatoms *see under* algae
diatremes *see under* intrusions
dikes *see under* intrusions
dolomitization *see under* diagenesis
dunes *see under* eolian features *under* geomorphology

E

Earth—magnetic field
declination: Magnetic declination measurements in Vermont 182
— New magnetic declination map of the United States 182
magnetic anomalies: Long wavelength magnetic anomalies 182-183
observations: Determination of K-indices by computer 182
— Geomagnetism 181-183
— New geomagnetic observatory instrumentation 182
— New magnetic observatory near Fresno, California 181-182
— Operation of the International Magnetospheric Study Network 182
spherical harmonic analysis: Rectangular harmonic analysis of magnetic fields 183
earthquakes *see also* engineering geology; seismology; *see also under* engineering geology *under* Washington; *see also under* seismology *under* Kentucky; Wyoming
Eastern Hemisphere *see also* Antarctica; Arctic Ocean; Asia; Atlantic Ocean; Europe; USSR
Eastern U.S.—economic geology
coal: Eastern coal 25-26
— Resources and quality 25-26
water resources: Northeastern region 116-126
— Southeastern region 126-133
Eastern U.S.—petrology
igneous rocks: Volcanic rocks in eastern United States 198-199
Eastern U.S.—stratigraphy
Pennsylvanian: Stratigraphy 25
Quaternary: Quaternary climates, eustacy, and tectonism, southeastern United States 231
echinoderms—biostratigraphy
Ordovician: Ordovician age of the Quantico Formation reaffirmed 72-73
ecology *see also under* environmental geology *under* Atlantic Coastal Plain; California; Florida; Texas; Washington
ecology—algae
lacustrine environment: Phosphorus and nitrogen as limiting nutrients in two arctic lakes 241
ecology—angiosperms
atmospheric precipitation: Dendroclimatic investigations of hickory and oak 233
ecology—Invertebrata
aquatic environment: Aquatic macroinvertebrates, Wyoming 235
ecology—Plantae
research: Plant ecology 233-234
elastic waves *see under* seismology
electrical logging *see* well-logging
electrical surveys *see under* geophysical surveys *under* Nevada; New Mexico; Oregon
electromagnetic surveys *see under* geophysical surveys *under* Alaska; Colorado; Michigan; South Carolina; Wisconsin
electron probe *see under* methods *under* spectroscopy
energy sources *see also* uranium; *see also under* economic geology *under* New Mexico; United States
engineering geology *see also* deformation; environmental geology; geophysical methods; ground water; mining geology; rock mechanics; soil mechanics
engineering geology—petroleum engineering
techniques: New exploration and production techniques 40-41
environmental geology *see also* engineering geology
environmental geology—general
research: Climate 219-224
environmental geology—surveys
Western Interior: Environmental geology 76-77
Eocene *see also under* geochronology *under* Alaska; Montana; Washington; *see also under* stratigraphy *under* California; Washington; Wyoming
eolian features *see under* geomorphology

epeirogeny *see also* orogeny
Europe *see also* the individual nations
Europe—stratigraphy
Carboniferous: Intercontinental correlation of the Pennsylvanian System 24-25
evaporite deposits—resources
data bases: Oil shale and saline mineral data system 20

F

faults—displacements
active faults: Earthquake localities and surficial and buried faults correspondence, Kentucky 75
— Fault creep in Mendocino County, California 98
— Holocene faulting, Toppenish Ridge 95
— Neotectonics in Kansas 84
— Quaternary deformation in southern part of Elsinore fault zone 101
— Seismic risk on the Rexburg fault, Idaho 76
— Upper Quaternary stratigraphy and structure of the Antelope Valley and vicinity, California 100
gravity faults: Gravity fault klippen of volcanic rocks, northwest Wyoming 87
overthrust faults: Pine Mountain-Russell Fork-Richlands overthrust fault system, Virginia 74
reactivation: Evidence for fossilized rifts and reactivation of basement faults 189
— Probable reactivated basement faults east of Defiance uplift 48
right-lateral faults: Newly recognized plutonic province displacement by the Chatham Strait fault 111
strike-slip faults: Basement controls on steep faults, southwestern Montana and east-central Idaho 84-85
thrust faults: Allochthonous Paleozoic sedimentary rocks, central Idaho 83
— Cretaceous thrust system, southern Nevada 90
— Eastern edge of the Sapphire thrust system, Montana 85
— Evidence for northwestward emplacement of Wrangellia terrane in the northern Talkeetna Mountains 109
— Extension of St. Clair bedding-plane thrust in Virginia 40
— Facies changes and structural belts in the Proterozoic Y rocks of Glacier National Park, Montana 85
— Southern extension of the Sapphire thrust system, Montana 86
— Tectonic shortening in late Alleghanian time 67
— Thrust plates in the Blue Ridge 68
— Thrusting faults in Belt terrane in Montana 85
— Upper Mesozoic rocks of the Wilbur Springs antiform 97
wrench faults: Southern California borderland; environmental geology 100
faults—distribution
age: Lineated granitic rocks mark early faults in the Beaver Creek Area, western St. Lawrence County, New York 6-7
continental margin: Faults of the southern Bering Sea margin 158
fault zones: Application of aeromagnetic and gravity data to the geological interpretation of the Tintina fault and the Circle quadrangle 107-108
— Controls of Pliocene and Pleistocene basaltic volcanism, southern Great Basin 89-90
— Geometry and tectonic evolution of the Columbia Hills 96
— Tectonism and plutonism, northwestern Sierra Nevada 98
metamorphic rocks: Easternmost metamorphic core complex, southern Arizona 90-91
— Metamorphic core complex, west-central Arizona 90
patterns: Concurrent regional faulting and silicic volcanism, Sangre de Cristo Mountains, New Mexico 86
faults—effects
shear zones: Left lateral strike-slip riedel shears in the Yakima ridges 95
— Physical characteristics of faults, northeastern Massachusetts 62
— Shear zones associated with the Kings Mountain belt in the Piedmont of the Carolinas 66
faults—extent
indicators: Constraints placed upon location of the San Andreas fault by base and precious metal sulfide mineralization, Point Delgada, northern California 96-97
— Middle Wisconsinan marine platform at Point Delgada 96
lineaments: Spotsylvania lineament of Virginia 73
faults—patterns
en echelon faults: Holocene faulting, central Nevada 88-89
faults—systems
block structures: Fault-basin origin of Boston Basin, Massachusetts 62
ferns—biostratigraphy
Pennsylvanian: Correlation of the Dunkard Group 232
fission-track dating *see under* geochronology
Florida—economic geology
fuel resources: Gulf of Mexico and Florida 37-38
— Reservoir characteristics of Sunniland Limestone (Lower Cretaceous), southern Florida 38
petroleum: Helium anomaly-possible indicator of petroleum in southern Florida 38
water resources: Florida 127-130
Florida—engineering geology
waste disposal: Subsurface storage of liquid wastes 127
waterways: Estuary quality affected by alterations in the Loxahatchee River basin 130
Florida—environmental geology
ecology: Trees of the Apalachicola River flood plain 234
geologic hazards: Rains cause flooding in Pinellas, Hillsborough, and Pasco counties 129
pollution: Appearance and water quality of turbidity plumes in Tampa Bay, Florida 169
— Methane-producing bacteria in deep aquifer 236
— Nutrient yield of the Apalachicola River 237
— Tampa Bay-Floridan aquifer interconnection study 169-170
Florida—geochemistry
sulfur: Distribution and genesis of primary pyrite in coal 29
Florida—geomorphology
solution features: Sinkhole development as a result of hydrologic changes in the Tampa area 128-129
Florida—hydrogeology
ground water: Evaluation of cavity-riddled sandstone aquifer 130
— Hydrogeology of the northern Gulf Coast area 128
— North Tampa ground-water flow model 129
— Position of saltwater-freshwater interface in southwest Florida 129
— Structure of shallow artesian aquifers 129
— Three-dimensional predictive model at Pensacola 128
hydrology: Hydrologic modeling 148
— Lake and aquifers relation verified 130
— Modifications to watershed model 127
— Use of "effective" impervious area in calibrating rainfall-runoff models for urban bains 127-128
— Water-budget analysis of Lake Jackson 128
— Water quality of Caloosahatchee River 130
— Water quality studies 149
maps: Hydrogeologic mapping, southwest Florida 179-130
fluid inclusions *see also* inclusions
fluid inclusions—analysis
methods: Novel heating-freezing fluid inclusion stage 190
fluid inclusions—geochemistry
isotopes: Light-stable isotopes and fluid inclusion study of the Thompson Creek and Little Boulder Creek deposits, Idaho 205
folds—displacements
thrust faults: Post-Early Triassic structures in the North Hansel Mountains, Idaho 83-84
folds—orientation
plunging folds: Geometry and tectonic evolution of the Columbia Hills 96

folds—style
antiform folds: Upper Mesozoic rocks of the Wilbur Springs antiform 97
isoclinal folds: Tectonic attenuation of Paleozoic rocks, southeastern California 101
foliation *see also* structural analysis
foraminifera—distribution
benthonic taxa: Distribution of benthic foraminifers, Gulf of Alaska Continental Shelf 159
foraminifers—biostratigraphy
Mississippian: Foraminiferal faunas at the Mississippian-Pennsylvanian boundary, south-central Idaho 232
Pliocene: Extent of Northern Hemisphere Pliocene glaciation 231
fossils *see* appropriate fossil group
foundations *see also* rock mechanics; soil mechanics
fractures—style
joints: Surface joint patterns as a guide to fracture reservoirs 39
fuel resources—exploration
techniques: New exploration and production techniques 40-41
fuel resources—resources
general: Other areas 40

G

gems *see also under* economic geology *under* Montana
genesis of ore deposits *see* mineral deposits, genesis
geochemical prospecting *see under* geochemical methods *under* mineral exploration
geochemistry—general
research: Experimental and theoretical geochemistry 189-191
— Geochemistry, mineralogy, and petrology 189-208
— Geochemistry of water and sediments 201-203
geochemistry—methods
graphic methods: Correct use of the rule of tangents and its petrologic applications 189
research: Analytical chemistry 244-245
— Analytical methods 244-246
statistical methods: R-mode and Q-mode factor analysis 203
— Statistical geochemistry and petrology 203
geochemistry—processes
adsorption: Organic compounds on kaolinite 202
— Uranium adsorption onto montmorillonite 53
oxidation: Anaerobic oxidation of acetylene by San Francisco Bay sediment slurries 171
— Electrolytic oxidation of coal 30
— Rates of formation of manganese oxides 202-203
precipitation: A precipitation mechanism for hydrothermal vein-type uranium deposits 56
reduction: Experimental studies on uranyl ion reduction by H_2O reveal a marked pH dependence 52
sorption: Uranium (VI) sorption by iron oxides 52
geochemistry—properties
solubility: Economic implications of the solubility of crude oil in methane 40
thermodynamic properties: Reevaluation of the thermodynamic properties of minerals in the system CaO-Al_2O_3-SiO_2-H_2O 190
— Relations between lattice dynamics and thermodynamic properties of minerals 189-190
— Thermodynamic properties of minerals 191
geochemistry—surveys
Basin and Range Province: Geochemical maps of uranium, thorium, and thorium-uranium in granites of the Basin and Range province 56
New England: Igneous rocks and geochemistry 61-62
geochronology *see also* absolute age
geochronology—fission-track dating
apatite: Uplift studies in the Front Range, Colorado 82-83
dates: Preliminary uplift ages from fission-track studies 94
volcanic rocks: Stratigraphy of the Naches Formation 94
zircon: Klinker dating 207
— Zircon fission-track ages of a Pleistocene ash, California and Nevada 206-207
geochronology—methods
research: Advances in geochronometry 205-208
soils: Quantitative pedology as a dating technique in the Western United States 92
geochronology—paleomagnetism
magnetostratigraphy: Paleomagnetic investigation of Pleistocene sediments of the Delmarva Peninsula, central Atlantic Coastal Plain 67
secular variations: Paleomagnetic correlation of volcanic rocks 181
geochronology—racemization
amino acids: Application of radiometry to coastal plain formations 70
sediments: Tectonic uplift rates near Gaviota, California 231-232
shells: Dating Arctic Quaternary raised marine deposits by uranium series and amino acids ratios 205-206
— Temperature aspects of late Quaternary marine molluscan faunas 231
geochronology—tephrochronology
Quaternary: Records of past climates in Clear Lake sediments 221
geochronology—tree rings
Holocene: End of "Little Ice Age" in Glacier National Park 222
geochronology—varves
Holocene: Records of past climates in Elk Lake sediments 221
geologic hazards *see also under* engineering geology *under* Alaska; automatic data processing; Bering Sea; *see also under* environmental geology *under* Alabama; California; Florida; Great Plains; Gulf Coastal Plain; Idaho; Illinois; Massachusetts; Texas; United States; Washington; Wyoming
geologic hazards—landslides
submarine environment: Significance of submarine slides on intercanyon continental margin slopes 41
geologic hazards—observations
technology: New techniques applied to studies of seafloor hazards and conditions 152-153
geology—research
general: Geologic and hydrologic principles, processes, and techniques 180-246
geomorphology *see also* glacial geology
geomorphology—eolian features
dunes: Ancient eolian deposits in western Great Plains 220-221
geomorphology—erosion features
badlands: Badlands on the north side of the Alaska Range 109-110
geomorphology—fluvial features
canyons: Miocene deformation and canyon cutting at Graybach Mountain 95-96
channels: Aggradation of Powder River valley during 1978 flood 218
— Channel morphology and sedimentation in Pheasant Branch near Middleton, Wisconsin 217-218
streams: Stream morphology 217-218
terraces: Pleistocene and Holocene valley fill in coastal plain streams, eastern Alabama 69
— Scarp degradation and morphological modification of fluvial terraces along the Rappahannock River, Virginia 73
geomorphology—lacustrine features
extinct lakes: Persistent low level of Lake Bonneville during last 10,000 years 91-92
lakes: Debris flows and turbidites filling the basin of Crater Lake 92
geomorphology—maps
altitude: Average elevation map of the conterminous United States 213
geomorphology—mass movements
block fields: Evidence of modern slope movement in the Appalachian Mountains 234
landslides: Relation between late Pleistocene snowfields and "landslides" 223
geomorphology—processes
sedimentation: Coastal sedimentary processes off beaches 165
geomorphology—shore features
deltas: Tidal wetland deposits of the Sacramento-San Joaquin Delta 170-171
marine platforms: Middle Wisconsinan marine platform at Point Delgada 96

terraces: Tectonic uplift rates near Gaviota, California 231-232
tidal flats: Migration of Oregon coastal dunes 165

geomorphology—solution features
sinkholes: Sinkhole development as a result of hydrologic changes in the Tampa area 128-129
speleothems: A 100,000-year cave record of atmospheric temperatures 223

geomorphology—volcanic features
cauldrons: Large caldron complex in central Idaho 197
volcanoes: Holocene volcano on the Alaska Peninsula 110

geophysical methods—electrical methods
interpretation: Inversion of self-potential data 186

geophysical methods—electromagnetic methods
interpretation: Electromagnetic response of cultural features 186
— New technique for electromagnetic modeling and inversion 186
techniques: Model study of experimental electromagnetic method 186

geophysical methods—methods
applications: Methodology in exploration geophysics 18-19
techniques: Applied geophysics 186-189
— Geochemical and geophysical techniques in resource assessments 13-19

geophysical methods—seismic methods
interpretation: Improved methods for seismic refraction interpretation 60
— Improved methods of seismic refraction interpretation 186
— Seismic models of stratigraphically controlled oil fields and gas fields in Rocky Mountain basins 33

geophysical surveys *see* acoustical surveys *under* geophysical surveys *under* Massachusetts; *see* electrical surveys *under* geophysical surveys *under* Nevada; New Mexico; Oregon; *see* electromagnetic surveys *under* geophysical surveys *under* Alaska; Colorado; Michigan; South Carolina; Wisconsin; *see* gravity surveys *under* geophysical surveys *under* Alaska; Arizona; Montana; Nevada; New Mexico; *see* magnetic surveys *under* geophysical surveys *under* Alaska; California; Georgia; Hawaii; Idaho; Montana; New York; North Carolina; Oregon; South Carolina; United States; Vermont; *see* magnetotelluric surveys *under* geophysical surveys *under* California; Oregon; *see* seismic surveys *under* geophysical surveys *under* Appalachians; Atlantic Coastal Plain; Bering Sea; California; Great Lakes; Gulf of Mexico; Idaho; New Jersey; New York; Oregon; Pennsylvania; *see* surveys *under* geophysical surveys *under* Alaska; Arizona; California; Colorado; Missouri; Montana; New Mexico; Oregon; *see also* geophysical methods

geophysics *see also* deformation; engineering geology

geophysics—experimental studies
melting: Melting relations in the system Fe-S-O 191

geophysics—general
research: Geophysics 180-189

Georgia—areal geology
regional: South Carolina, Georgia, and Alabama 68-70

Georgia—economic geology
coal: Exploitation of thin coals in Georgia 25-26
deposits: Kaolin in the Macon-Gordon district, Georgia 1
mineral resources: Mineral-resource assessment of the Big Frog Wilderness Study Area, Tennessee and Georgia 5-6
water resources: Georgia 130-131

Georgia—environmental geology
pollution: Deterministic models of surface-water systems 237
— Effects of agriculture on stream quality, southwestern Georgia 238
— Limnology of West Point Reservoir, Georgia and Alabama 235

Georgia—geochemistry
trace elements: Pre-Cretaceous subsurface volcanic rocks in Georgia 198

Georgia—geophysical surveys
magnetic surveys: Aeromagnetic study of subsurface pre-Cretaceous rocks, Georgia and South Carolina coastal plains 70-71

Georgia—hydrogeology
ground water: Interaquifer ground-water transfer through idle multiaquifer wells 131
— Regional coastal plain sand aquifer study 130-131
— Water levels and steady-state calibration of a two-dimensional flow model 131
hydrology: Time-trend errors in low-flow analysis of streams 131

Georgia—oceanography
sediments: Subsurface hypersaline brines 166

Georgia—stratigraphy
Cenozoic: Cenozoic tectonics and regional stratigraphy, Georgia 68
Paleocene: Dinoflagellates and increased biostratigraphic resolution 230
research: Stratigraphy of the Atlanta area, Georgia 69
Tertiary: Tertiary stratigraphy, eastern Alabama and western Georgia 68-69

Georgia—structural geology
neotectonics: Cenozoic tectonics and regional stratigraphy, Georgia 68
tectonics: Thrust plates in the Blue Ridge 68

geosynclines *see also* orogeny

geotechnics *see* engineering geology

geothermal energy *see also under* economic geology *under* Alaska; automatic data processing; California; Colorado; Idaho; Italy; Mexico; Nevada; Oregon; United States; Utah; Wyoming

geothermal energy—affinities
metal ores: Interrelations among epithermal ore deposits and geothermal systems depositing mercury, gold and silver 209-210

geothermal energy—properties
geologic thermometry: Revised Na/K geothermometer 211
— Three new gas geothermometers 211-212
geothermal systems: Geothermal systems 208-216
reservoir properties: Electrical properties of geothermal materials 184
— Properties of multiphase fluids and their influence on geothermal phenomena 210-211

geothermal energy—resources
data bases: Geothermal resources file 19
general: Chapter completed in Geothermal Source Book 213

germanium—analysis
spectroscopy: Germanium concentrations in USGS rock standards as determined by electrothermal atomization atomic absorption spectrometry 244

glacial geology *see also* geomorphology

glacial geology—general
research: Glaciology 219

glacial geology—glacial features
glacial lakes: Small glacial lakes in the Housatonic River valley 63
moraines: Ice-shove structures in end moraines, northwest Connecticut 63

glacial geology—glaciation
deglaciation: Deglaciation, eastern Connecticut 63
— Deglaciation, ice lobation, and marine incursion, eastern Massachusetts 63-64
— Deglaciation of central Connecticut and the "Middletown Readvance" 63
— Deglaciation of the Connecticut Valley, Massachusetts 64
— Deglaciation of the Westfield and Connecticut Valleys, Massachusetts 64-65
— End of Pinedale Glaciation, north-central Colorado 222-223
— First bare ground in western Massachusetts 65
deposition: Late Pinedale Glaciation in the Northern Rocky Mountains 223
extent: Discovery of upper Wisconsinan glacial till on the Continental Shelf off southeastern New England 66
— Evidence for icecap in West Pioneer Mountains, Montana 76
— Extent of Northern Hemisphere Pliocene glaciation 231
— Glacier snowlines and uplift of the San Bernardino Mountains 101-102
general: Glacial geology 63-66
ice movement: Glacial advances in the Yukon-Tanana upland 107
snowfields: Relation between late Pleistocene snowfields and "landslides" 223

glacial geology—glaciers
extent: End of "Little Ice Age" in Glacier National Park 222
ice movement: Glacier surges monitored by satellite 219
— Sliding speed of Black Rapids Glacier, Alaska 219

glaciation *see under* glacial geology

glaciers *see under* glacial geology

gold—analysis
spectroscopy: Sensitive method for gold analysis 17

gravel *see also under* clastic sediments *under* sediments

gravity surveys *see under* geophysical surveys *under* Alaska; Arizona; Montana; Nevada; New Mexico

Great Basin—economic geology
fuel resources: Great Basin and California 37

Great Basin—structural geology
neotectonics: Controls of Pliocene and Pleistocene basaltic volcanism, southern Great Basin 89-90

Great Lakes—geophysical surveys
seismic surveys: Lake sediments 166-167

Great Lakes region—economic geology
uranium ores: Lake Superior region favorable for quartz-pebble-type uranium deposits 45

Great Lakes region—structural geology
tectonics: Basement control of Proterozoic X Penokean orogen 75

Great Plains—areal geology
regional: Rocky Mountains and the Great Plains 76-87

Great Plains—economic geology
fuel resources: Rocky Mountains and Great Plains 33-37
mineral resources: Economic geology 76

Great Plains—environmental geology
geologic hazards: February 1977 windstorm in Great Plains 220
surveys: Environmental geology 76-77

Great Plains—geomorphology
eolian features: Ancient eolian deposits in western Great Plains 220-221

Great Plains—hydrogeology
maps: Geohydrology of Paleozoic rocks in the northern Great Plains 134-135

Great Plains—petrology
igneous rocks: Igneous rocks 79-81

Great Plains—stratigraphy
Phanerozoic: Stratigraphy 77-78
Precambrian: Precambrian rocks 81-82

Great Plains—structural geology
tectonics: Tectonics 82-87

ground water *see also* hydrogeology; hydrology

ground water—aquifers
models: Aquifer-model studies 225
— Perturbation solutions of water-table aquifer equations 227
— Porosity, permeability, distribution coefficients, and dispersivity 227

ground water—geochemistry
models: Ground-water geochemical models 202

ground water—hydrodynamics
models: Mathematical simulation of hydrogeologic systems 226

ground water—levels
effects: Influence of water-table mounds on seepage through lakebeds 239

ground water—models
mathematical models: Planning for conjunctive water-supply systems 239

ground water—movement
cycles: Relation between surface water and ground water 238-239
research: Ground-water hydrology 224-227

ground water—pollution
water quality: Chemical and biological quality of ground water 235-236
— Ground-water-quality models and processes 238

ground water—recharge
research: Recharge studies 226-227

ground water—surveys
Alabama: Baseline hydrology in coal areas 127
Arbuckle Aquifer: Geohydrology of the Arbuckle-Simpson aquifer in south-central Oklahoma 138
Arizona: Arsenic concentrations in Verde Valley 142-143
— Arsenic, copper, and molybdenum, Baboquivari Mountains, Arizona 15
— Irrigation water available to Ak-Chin Indian Reservation 142
Atlantic Coastal Plain: Model insensitive to variations in transmissivity 225-226
California: Appraisal data adequate for Owens Valley 144
— Classification of recharge in Santa Cruz area 143
— Ground water limited in north-central Santa Cruz County 143
— Ground-water recovery at Thousand Oaks 143
— Stable-isotope technique used to trace ground-water movement 227
— Water-quality monitoring for radioisotopes, California 236
Colorado: Radioactivity in water wells, Pueblo County, Colorado 56
Columbia Plateau: Simulation of groundwater flow in basalt aquifers underlying the Columbia Plateau 146
Connecticut: Aquifer characteristics and organohalides in ground water, Southbury and Woodbury 117
— Estimating recharge areas for stratified drift aquifers, Connecticut 226
— Ground-water resources in southwestern Connecticut 117
Delaware: Late Miocene aquifers 117
Edwards Aquifer: Effects of faults on the direction of flow in the Edwards aquifer 139-140
Florida: Evaluation of cavity-riddled sandstone aquifer 130
— Structure of shallow artesian aquifers 129
— Subsurface storage of liquid wastes 127
— Three-dimensional predictive model at Pensacola 128
Floridan Aquifer: Hydrogeologic mapping, southwest Florida 179-130
— Hydrogeology of the northern Gulf Coast area 128
— Lake and aquifers relation verified 130
— Methane-producing bacteria in deep aquifer 236
— North Tampa ground-water flow model 129
— Position of saltwater-freshwater interface in southwest Florida 129
— Sinkhole development as a result of hydrologic changes in the Tampa area 128-129
— Tampa Bay-Floridan aquifer interconnection study 169-170
— Water-budget analysis of Lake Jackson 128
Georgia: Interaquifer ground-water transfer through idle multiaquifer wells 131
— Regional coastal plain sand aquifer study 130-131
— Water levels and steady-state calibration of a two-dimensional flow model 131
Great Plains: Geohydrology of Paleozoic rocks in the northern Great Plains 134-135
Idaho: Analyses of return flows to Snake River 144
— Assessment of ground-water quality in east-central Idaho 144
— Hydrologic conditions in Rockland Valley 144
Illinois: Mine-spoil hydrology 226-227
— Potentiometric surface and chemical characteristics of shallow aquifers in McHenry County 118
— Testing deep wells in sandstone 118
Indiana: Evaluation of ground water in Elkhart County 118
— Irrigation and ground water in Newton and Jasper counties, Indiana 150
— Nature and extent of the unconsolidated aquifers underlying the Indiana Dunes National Lakeshore 118
— Results for initial model calibration 119
— Southwestern Indiana lineament study 118
— Water-level declines in Cambrian and Ordovician rocks in northwestern Indiana 118
Jasper Aquifer: Jasper aquifer overlain by effective confining layer 140
Kansas: Ground-water model, west-central Kansas 225
— Potentiometric-head relations, lower Paleozoics, Kansas 227
— Sandstone aquifers; potential source of water in southwestern Kansas 135

Kentucky: Chloroform concentration in alluvium at Louisville 131-132
Louisiana: Median concentrations of chemical constituents in aquifers, southwestern Louisiana 236
— Sand-and-gravel aquifer overlies lignite deposits in Bienville Parish 135-136
Maryland: Aquifer studies in western Montgomery County 119
Michigan: Hydrologic analysis of Sands Plain 119
— Model study of Michigan coal deposit 119-120
— Study of ground water contaminated by trichloroethylene 119
Midwest: Carbon dioxide and methane outgassing from ground-water samples 226
Minnesota: Appraisal of Cambrian and Ordovician aquifers in southeastern Minnesota 122
— Appraisal of ground water in central Minnesota 121
— Ground-water appraisal in Big Stone County 122
— Ground-water appraisal of sand-plain areas in central Minnesota 120-121
— Interaquifer flow through well bores 225
— Potentiometric data from deep test well 120
— Sensitivity analysis useful for planning data collection 121
Mississippi: Large water-level declines in Eutaw-McShan aquifer 132
Missouri: Ground water and water quality downstream from the proposed Prosperity Reservoir in Center Creek basin 136
— Irrigation from deep wells in Audrain County, Missouri 150
Montana: Appraisal of aquifers in northern Cascade County 136
— Continued hydrologic studies of energy minerals rehabilitation inventory and analysis areas 136
— Shallow alluvial aquifers evaluated in Helena Valley 136-137
Navajo Sandstone: Navajo Sandstone; a source of ground water for future energy-related development in the northern San Rafael Swell area 140
Nebraska: Artificial recharge of ground water 226
Nevada: Geophysical investigations in Lemmon Valley 144-145
— Ground water studies in Las Vegas area 144
New Jersey: Ground-water use in the coastal-plain aquifer system of New Jersey 150
New Mexico: Assessment of ground-water resources in Santa Fe County 137
— Assessment of ground-water resources on the Zuni Indian Reservation 137
— Hydrologic properties of the Gallup Sandstone in McKinley County 137
— Resistivity study of the San Augustine aquifers, New Mexico 187
— Thinning of aquifer by solution 227
New York: Development of a Galerkin finite-element flow model for the transient response of a radially symmetric aquifer 123
— Ground-water quality of a postglacial sand-dune environment 123
— Organic pollutants in ground water 123
— Preliminary hydrogeology of an artificial-recharge site 122
— Pumping test in southern Nassau County, Long Island 122
— Streamflow augmentation with ground water 239
— Surficial geology and well guides in Oswego County 122
— Utilization of a regional ground-water-flow model to evaluate boundary conditions for a subregional model 123
North Dakota: Aquifer evaluations, North Dakota 227
— Buried-valley aquifers, McKenzie County 137
— Hydrology of prairie wetlands 239
— Surficial outwash aquifer in Logan County 137-138
— Test drilling and aquifer evaluation in Rattlesnake Butte area 137
Ogallala Aquifer: High Plains regional aquifer study 138
— Tertiary bedrock outliers and preglacial channels of western origin in Yankton County 139
Ohio: Subsurface mines as a water source 124
Oregon: Digital simulation of a multilayer aquifer system near Portland 145
— Improvement in ground-water conditions near The Dalles 145-146
Pennsylvania: Seismic-refraction exploration, northwestern Pennsylvania 225
— Water-supply capability of carbonate rock, south-central Pennsylvania 124
Rhode Island: Hydraulic properties of an anisotropic water-table aquifer in the Chipuxet River basin 124
South Dakota: Aquifer test of a glacial-outwash aquifer in central South Dakota 139
Spokane Aquifer: Digital-model simulation of the Spokane aquifer 225
— Solute transport in the Spokane aquifer 225
Tennessee: Ground water related to weathering products of facies of Fort Payne Formation 132-133
— Strontium-90 transport through solution cavities in limestone 133
Texas: Helium detection for uranium exploration 57
United States: Regional aquifer-system analysis program 150-151
Virginia: Ground-water resources in James City County evaluated 125
— Hydrogeology of the Culpeper Basin 125
— Hydrologic data collection, Great Dismal Swamp 124-125
Washington: Ground-water levels affected by irrigation in Sequim Peninsula 146
— Map of principal aquifers and general yields of wells 146
— Water budget estimated for Gig Harbor Peninsula 146
Wellington Aquifer: Aquifer tests in the Wellington Aquifer near Salina 135
Wilcox Aquifer: Quality of water in the Wilcox aquifer 225
Wisconsin: Concentrations of heavy metals in ground water, Wisconsin 235-236
— Ground water in Dodge County 125
— Hydrogeology and ground-water quality in northeastern Waukesha County 126
— Summary of ground-water quality data, Wisconsin 236
— Water resources of Forest County 125
Wyoming: Digital flow model of Bates Creek alluvial aquifer 141
— Digital model of effects of ground-water withdrawals in Laramie County 141
— Warm water in artesian aquifers in Carbon County 141
— Water study of energy-minerals area 141-142

Gulf Coastal Plain—environmental geology
geologic hazards: Possible effects on coral growth of offshore petroleum drilling, Gulf of Mexico 37-38

Gulf Coastal Plain—hydrogeology
ground water: Hydrogeology of the northern Gulf Coast area 128

Gulf Coastal Plain—oceanography
marine geology: Atlantic and Gulf Coast 167-170

Gulf Coastal Plain—stratigraphy
Jurassic: Continental slope stratigraphy of Texas and Louisiana 160-161

Gulf of Mexico—economic geology
fuel resources: Gulf of Mexico and Florida 37-38
petroleum: Possible effects on coral growth of offshore petroleum drilling, Gulf of Mexico 37-38

Gulf of Mexico—geochemistry
trace elements: Correlation of trace elements between sediments and benthic fauna 166

Gulf of Mexico—geophysical surveys
seismic surveys: Continental slope stratigraphy of Texas and Louisiana 160-161

Gulf of Mexico—oceanography
reefs: Possible effects on coral growth of offshore petroleum drilling, Gulf of Mexico 37-38

Gulf of Mexico—structural geology
salt tectonics: Continental slope stratigraphy of Texas and Louisiana 160-161

H

halides *see under* minerals
Hawaii—geochemistry
isotopes: Lead and neodymium isotopes in Hawaiian volcanic rocks 204
Hawaii—geochronology
Holocene: Paleomagnetic correlation of volcanic rocks 181
Hawaii—geophysical surveys
magnetic surveys: Aeromagnetic anomalies on Kilauea's east rift zone, Hawaii 209
Hawaii—petrology
volcanology: Hawaiian volcano studies 192-195
Hawaii—volcanology
Kilauea: Activity at Kilauea Volcano in 1979 192-193
— Loihi Seamount; active submarine volcano 194
— Origin of Hawaiian tholeiitic basalt 194-195
— Pressurized fractures in hot rock 215-216
Mauna Loa: Mauna Loa rift zones 193-194
— Mauna Loa Volcano quiescent in 1979 193
heat flow *see also under* geophysical surveys *under* California; Idaho; Nevada; *see also under* tectonophysics *under* Wyoming
heavy minerals *see also* placers
helium—abundance
ground water: Helium detection for uranium exploration 57
soil gases: Geochemical prospecting for petroleum, Simpson Peninsula 32
soils: Helium and sulfur, Poorman fault, Colorado 16
Hemichordata—biostratigraphy
Ordovician: Identification of Ordovician rocks in Lake Minchumina area 106
Holocene *see also under* geochronology *under* Hawaii; Minnesota; Montana; Utah
Holocene—stratigraphy
paleoclimatology: Holocene sea-level change; a possible record of global climatic change 224
hydrocarbons *see under* organic materials
hydrogeology *see also* ground water; hydrology
hydrogeology—general
research: Ground-water hydrology 224-227
— Miscellaneous studies 225-226
hydrology *see also* ground water; hydrogeology
hydrology—cycles
evapotranspiration: Evaporation and transpiration 239-240
models: Precipitation-runoff modeling 227-228
research: Relation between surface water and ground water 238-239
hydrology—general
research: Geologic and hydrologic principles, processes, and techniques 180-246
— Ground-water hydrology 224-227
hydrology—instruments
research: Instrumentation 219
— New hydrologic instruments and techniques 242
samplers: Artificial substrate sampler with increased habitat complexity 240-241
— New large volume depth-integrating sampler 219
hydrology—limnology
arctic environment: Phosphorus and nitrogen as limiting nutrients in two arctic lakes 241
indicators: Chrysomonad cysts as paleoenvironmental indicators 241
methods: Inverted microscope method for the identification and enumeration of periphytic diatoms 235
research: Limnology and potamology 240-242
sedimentation: Lake sediments 166-167
water quality: Areawide chemical loading 238
— Chemical and biological quality of surface water 234-235
— Surface-water-quality models and processes 237
hydrology—methods
automatic data processing: Planning for conjunctive water-supply systems 239
statistical methods: Flood-frequency study 148-149
— Hydrologic studies 228-229
hydrology—rivers and streams
estuaries: Estuarine and coastal hydrology 167-174
hydraulics: Channel hydraulics 229
models: Flow modeling 228
pollution: Volatilization of priority pollutants from streams 237
research: Surface-water hydrology 227-229
sedimentation: Variability of sediments yields 217
tracer experiments: Lithium as a tracer 202
hydrology—seepage
lakes: Influence of water-table mounds on seepage through lakebeds 239
hydrology—surveys
Alabama: Baseline hydrology in coal areas 127
— Flood of April 1979 127
Apalachicola River: Nutrient yield of the Apalachicola River 237
Arizona: Irrigation water available to Ak-Chin Indian Reservation 142
Atlantic Coastal Plain: Atlantic and Gulf Coast 167-170
— Water quality of major tributaries, Chesapeake Bay 234
California: Appraisal data adequate for Owens Valley 144
— Functional and structural responses of a stream community to copper 240
Caloosahatchee River: Water quality of Caloosahatchee River 130
Chattahoochee River: Deterministic models of surface-water systems 237
Colorado: Evaluation of empirical water-quality prediction models in reservoirs 241
Colorado River: Source areas of salinity and trends of salt loads in streamflow in the upper Colorado River 140
Eagle Lake: Hydrologic budget of Eagle Lake in central Minnesota 121
Filson Creek: Effect of acid precipitation of water quality of the Filson Creek watershed in northeastern Minnesota 121
Florida: Hydrologic modeling 148
— Lake and aquifers relation verified 130
— Modifications to watershed model 127
— Rains cause flooding in Pinellas, Hillsborough, and Pasco counties 129
— Tampa Bay-Floridan aquifer interconnection study 169-170
— Use of "effective" impervious area in calibrating rainfall-runoff models for urban bains 127-128
Georgia: Effects of agriculture on stream quality, southwestern Georgia 238
— Limnology of West Point Reservoir, Georgia and Alabama 235
— Time-trend errors in low-flow analysis of streams 131
Hudson River: Hudson River Estuary flows 123
Idaho: Hydrologic conditions in Rockland Valley 144
Illinois River: Rating studies at Illinois River dam sites 117
Indiana: Irrigation and ground water in Newton and Jasper counties, Indiana 150
— Sediment yields in northeastern Indiana 217
Lake Eufaula: Water from Gaines Creek and Gaines Creek arm of Lake Eufaula suitable for public supply 139
Lake Jackson: Water-budget analysis of Lake Jackson 128
L'Anguille River basin: Benthic sediments and the dissolved-oxygen deficit in L'Anguille River basin, Arkansas 237
Loxahatchee River: Estuary quality affected by alterations in the Loxahatchee River basin 130
Merced River: Water quality assessment of Merced River 143
Michigan: Hydrologic analysis of Sands Plain 119
Minnesota: Baseline water quality established before highway construction 120
— Rainfall-runoff relations in the Coon Creek watershed, Anoka County 120
— Water-quality monitoring lakes in northeastern Minnesota 121
— Water quality of lakes in Eagan 120
Mississippi: Major flood on Pearl River at Jackson 132
— Transport and degradation of acetone in streams 237

Missouri: Ground water and water quality downstream from the proposed Prosperity Reservoir in Center Creek basin 136
— Irrigation from deep wells in Audrain County, Missouri 150
Mole Lake: Mole Lake hydrology 125
Montana: Limnology of reservoirs, eastern Montana 241-242
— Sediment-yield estimates for central Powder River Basin, Montana and Wyoming 217
Nebraska: Statistical analyses of surface-water quality, Nebraska 235
New Jersey: Drainage areas determined for New Jersey streams 122
New York: Streamflow augmentation with ground water 239
North Carolina: Improvement in water quality of some rivers 132
North Dakota: Hydrology of prairie wetlands 239
Oklahoma: Mine ponds, a hydrologic asset in eastern Oklahoma 138
— Model study of alluvial aquifer along the Beaver and the North Canadian rivers 138
— Streamflow and water-quality characteristics of Coal Creek basin near Lehigh 138-139
Oregon: Benthic oxygen demand in Portland Harbor 145
— Estimating effective impervious area with rural and urban rainfall-runoff models 145
Pecos River: Water use by saltcedar and by replacement vegetation in the flood plain of the Pecos River, New Mexico 240
Pennsylvania: Premining water quality in the Stony Fork drainage basin, Fayette County 124
Potomac River: Benthic fauna studies of the tidal Potomac River 168-169
— Geochemistry of sediments and associated interstitial waters for the tidal Potomac River 167-168
— Interdisciplinary study of the Potomac River Estuary 166
— Point-source discharge of phosphorus into the Potomac River 244
— Potomac Estuary Study 233
— Seasonal distributions of oxygen, carbon, nitrogen, and silicon in the Potomac River 168
— Shallow stratigraphy of the Potomac River Estuary 167
— Variations in nutrient and sediment concentrations in the Potomac River Estuary 167
Powder River basin: Aquatic macroinvertebrates, Wyoming 235
Red Lake: Effects of peat mining on hydrology in the Red Lake 121
Red River: Low heavy-metal concentration in the Red River, Louisiana 234
Russian River: Russian River response to waste-water discharge and drought 143
Saginaw River: Flow model of Saginaw River 119
Saint Croix River: Saint Croix River flood and water-quality data 126
Snake River: Analyses of return flows to Snake River 144
South Carolina: Water-supply supplement from Intercoastal waterway 132
United States: Coastal and limnological studies 164-167
— Water quality studies 149
Utah: Seepage and reservoir studies in the Price River basin 140
Virginia: Hydrologic data collection, Great Dismal Swamp 124-125
— Water monitoring of coal-mining areas, Virginia 234
Washington: Ground-water levels affected by irrigation in Sequim Peninsula 146
— Phosphorus loading of lake water related to land uses 238
— Water budget estimated for Gig Harbor Peninsula 146
Williams Lake: Hydrologic setting of Williams Lake in north-central Minnesota 121-122
Wisconsin: Storm sediment yield measured in Nederlo Creek basin, Wisconsin 217
Wyoming: Regression model of effects of streamflow diversions on surface-water salinity 141
— Source-area sediment model of Big Sandy River basin 141
— Water study of energy-minerals area 141-142
Yakima River: Simulation of unregulated-streamflow record for the Yakima River at Union Gap 146
— Yakima River basin streamflow and irrigation diversions for 1977 drought year and 1960-1976 146
hydrology—techniques
chemical analysis: Adenosine triphosphate in aquatic samples 245-246
— Analysis of water 245-246
— Automated colorimetric determination of bromide ions 245
— Ion chromatography 245
sample preparation: Transport of chemical constituents in urban storm water 149-150
hydrothermal alteration *see under* processes *under* metasomatism

I

Iceland—petrology
volcanology: Icelandic studies 195-196
Iceland—volcanology
Krafla: Hydrogen gas monitor at Krafla Volcano 196
Surtsey: Surtsey Volcano drill hole 195
Idaho—economic geology
geothermal energy: Geothermal resource of the eastern Snake River Plain 209
— P-wave delays at two geothermal areas 215
— Seismic reflection survey in Raft River Geothermal Area, Idaho 60
— Temperature distribution caused by flow up a fault 214
— Temperature survey in Raft River geothermal system 213
— Zonation of clay and zeolite minerals, Raft River geothermal boreholes, Idaho 209
metal ores: Deep exploration target at Red Mountain stockwork, Yellow Pine, Idaho 12-13
mineral resources: Mineral resource assessment using aerial geophysical data 187
molybdenum ores: Light-stable isotopes and fluid inclusion study of the Thompson Creek and Little Boulder Creek deposits, Idaho 205
uranium ores: Proterozoic quartzite and conglomerate of central and northern Idaho unfavorable for quartz-pebble-conglomerate-type uranium deposits 46
water resources: Idaho 144
Idaho—environmental geology
geologic hazards: Seismic risk on the Rexburg fault, Idaho 76
Idaho—geochronology
Neogene: Geologic framework along the Idaho Falls-Blackfoot corridor, east flank of the Snake River Plain, Idaho 83
Ordovician: Ordovician plutonism in Idaho and Montana 84
Proterozoic: Age of Yellowjacket Formation, Idaho 81
Idaho—geophysical surveys
heat flow: Temperature survey in Raft River geothermal system 213
magnetic surveys: Geomagnetic variation studies 188
— Magnetic studies in the Belt Basin, Montana and Idaho 5
seismic surveys: Seismic reflection survey in Raft River Geothermal Area, Idaho 60
Idaho—hydrogeology
ground water: Assessment of ground-water quality in east-central Idaho 144
hydrology: Analyses of return flows to Snake River 144
— Hydrologic conditions in Rockland Valley 144
thermal waters: Temperature distribution caused by flow up a fault 214
Idaho—petrology
igneous rocks: Buried Pliocene calderas of the eastern Snake River Plain, Idaho 79
intrusions: Plutonic rocks of the Ten Mile Creek RARE II Area, central Idaho 3-4
metamorphic rocks: Granodiorite augen gneiss-tonalite-metagabbro; the earliest magma series in the Cretaceous Idaho batholith 11
volcanology: Deep drill hole in buried caldera, Snake River Plain, Idaho 197
— Large caldron complex in central Idaho 197

Idaho—sedimentary petrology
sedimentation: Total sediment load, Snake and Clearwater Rivers near Lewiston, Idaho 218
Idaho—seismology
crust: P-wave delays at two geothermal areas 215
Idaho—stratigraphy
Paleozoic: Foraminiferal faunas at the Mississippian-Pennsylvanian boundary, south-central Idaho 232
Idaho—structural geology
neotectonics: Geologic framework along the Idaho Falls-Blackfoot corridor, east flank of the Snake River Plain, Idaho 83
tectonics: Allochthonous Paleozoic sedimentary rocks, central Idaho 83
— Basement controls on steep faults, southwestern Montana and east-central Idaho 84-85
— Ordovician plutonism in Idaho and Montana 84
— Post-Early Triassic structures in the North Hansel Mountains, Idaho 83-84
Idaho—tectonophysics
plate tectonics: Tectonic rotation of the Seven Devils Group, Oregon and Idaho 180
igneous rocks *see also* magmas; metamorphic rocks; metasomatism; phase equilibria
igneous rocks—alkali basalts
petrology: Petrology of rocks from the Pribilof Islands region, southern Bering Sea shelf 162-163
igneous rocks—basalts
genesis: Controls of Pliocene and Pleistocene basaltic volcanism, southern Great Basin 89-90
magnetic properties: Paleomagnetism of Permian basalts 110
petrology: Basaltic rocks of the Springerville volcanic field, Arizona 79
tholeiitic basalt: Origin of Hawaiian tholeiitic basalt 194-195
igneous rocks—diabase
petrology: Study of diabase dikes 188-189
igneous rocks—diorites
tonalite: The plutonic complex tonalite sill in the Coast Range 113
igneous rocks—gabbros
composition: Multiple intrusion of the La Perouse layered gabbro, Alaska 199
igneous rocks—geochemistry
isotopes: Strontium isotopes along the Uinta trend 203-204
igneous rocks—granites
composition: New data on magnetite and ilmenite from the granitoid rocks in White Pine County, Nevada 199-200
genesis: Petrogenetic possibilities for late-mica granites, Pioneer Mountains, Montana 79-80
— Two suites of Cretaceous granitic rocks from the Pioneer batholith, Montana 80
mechanical properties: Internal friction experiments in granite 212-213
petrology: Hoffman Park stock, Colorado, and its relation to the Mount Antero Granite 200-201
— Tertiary granite stock, southwestern Kupreanof Island 113
igneous rocks—hypabyssal rocks
genesis: Tertiary hypabyssal intrusions, Sierra Nevada 98
igneous rocks—petrology
research: Igneous rocks 79-81
— Igneous rocks 91
— Igneous rocks and geochemistry 61-62
igneous rocks—plutonic rocks
age: Basement-cover rock relations, southeastern Connecticut 61
genesis: Plutonic rocks and magmatic processes 199-201
geochemistry: Batholithic rocks of southern California 203
textures: Structural analysis of plutonic and metamorphic rocks from an area east of Wrangell 113
igneous rocks—pyroclastics
alteration: Uranium leachability from freshly erupted volcanic ash of basaltic and dacitic composition 55-56
ash-flow tuff: Buried Pliocene calderas of the eastern Snake River Plain, Idaho 79
— Caldera source of Miocene Osiris Tuff, southwestern Utah 81-82
— Large caldron complex in central Idaho 197
tuff: Distribution and mobility of uranium in glassy and zeolitized tuff, Keg Mountain area, Utah 55
igneous rocks—rhyolites
petrology: Quenched mafic magma in rhyolite, Coso Range, California 196-197
igneous rocks—syenites
geochemistry: Alkaline intrusive complexes, Wet Mountains, Colorado 42
igneous rocks—ultramafics
ophiolite: Massive sulfide deposits in ophiolitic terrain, northern Klamath Mountains, Oregon and California 12
— Ophiolites of western Alaska 106
igneous rocks—volcanic rocks
composition: Proterozoic Y zoned ash-flow sheet, Mount Rogers, Virginia 198-199
genesis: Volcanic rocks of Eocene age from the Pioneer Mountains, Montana 80
geochemistry: Isotopic modification of magma, Yellowstone caldera, Wyoming 197
— Lead and neodymium isotopes in Hawaiian volcanic rocks 204
— Pre-Cretaceous subsurface volcanic rocks in Georgia 198
mafic composition: Mafic flows in the Cedar Breaks-Panguitch Lake area, Utah 81
petrology: Columbia River Plateau studies 196
— Deep drill hole in buried caldera, Snake River Plain, Idaho 197
— Inclusions in upper Cenozoic volcanic rocks of the central Sierra Nevada, California 201
— Petrology and geochemistry of the Oliverian domes of New England 200
— Volcanic rocks and processes 192-199
— Volcanic rocks in eastern United States 198-199
Illinois—economic geology
coal: Worth of geophysical and geological data and mineral supply 20
thorium ores: Large thorium reserves in disseminated deposits 42
water resources: Illinois 117-118
Illinois—environmental geology
geologic hazards: Flood-frequency study 148-149
Illinois—hydrogeology
ground water: Mine-spoil hydrology 226-227
— Potentiometric surface and chemical characteristics of shallow aquifers in McHenry County 118
— Testing deep wells in sandstone 118
hydrology: Rating studies at Illinois River dam sites 117
inclusions *see also* fluid inclusions
inclusions—xenoliths
andesite: Quenched mafic magma in rhyolite, Coso Range, California 196-197
observations: Inclusions in upper Cenozoic volcanic rocks of the central Sierra Nevada, California 201
Indiana—economic geology
water resources: Indiana 118-119
Indiana—hydrogeology
ground water: Evaluation of ground water in Elkhart County 118
— Nature and extent of the unconsolidated aquifers underlying the Indiana Dunes National Lakeshore 118
— Results for initial model calibration 119
— Southwestern Indiana lineament study 118
— Water-level declines in Cambrian and Ordovician rocks in northwestern Indiana 118
hydrology: Irrigation and ground water in Newton and Jasper counties, Indiana 150
Indiana—sedimentary petrology
sedimentation: Sediment yields in northeastern Indiana 217
intrusions—age
absolute age: Lead isotopes in ores and rocks of southwest New Mexico 204
— Samarium-neodymium age of the Stillwater Complex, Montana 205
intrusions—batholiths
geochemistry: Batholithic rocks of southern California 203
intrusions—diatremes
geochemistry: Uranium mineralization in the Hopi Buttes of the Flagstaff and Gallup 1° x 2° quadrangles, Arizona 58
occurrence: Diatremes in the Grande Ronde graben 196
petrology: Diamond potential of Missouri Breaks diatremes, Montana 4

intrusions—dikes
emplacement: Dike trends and stress directions in western Arizona 91
orientation: Study of diabase dikes 188-189

intrusions—emplacement
mechanism: Pressurized fractures in hot rock 215-216

intrusions—evolution
periodicity: Episodic plutonism in the Coast batholith of southeastern Alaska 199

intrusions—genesis
emplacement: Tertiary hypabyssal intrusions, Sierra Nevada 98

intrusions—laccoliths
extent: Aeromagnetic studies of the Square Butte Wilderness Area, Choteau County, Montana 2

intrusions—layered intrusions
emplacement: Multiple intrusion of the La Perouse layered gabbro, Alaska 199

intrusions—petrology
domes: Petrology and geochemistry of the Oliverian domes of New England 200

intrusions—plutons
age: Ordovician plutonism in Idaho and Montana 84
— Paleozoic events in the Piedmont near Fredericksburg, Virginia 71
— Two Cenozoic igneous events on the Alaska Peninsula 110
distribution: Newly recognized plutonic province displacement by the Chatham Strait fault 111
emplacement: Cretaceous volcanism and plutonism, Montana 11
— Mount Juneau orthogneiss pluton 112
— Mylonitic gneisses over a Cretaceous(?) pluton, Iron Mountains, southeastern California 100-101
— Tectonic attenuation of Paleozoic rocks, southeastern California 101
— Tectonism and plutonism, northwestern Sierra Nevada 98
geochemistry: Trace-element patterns in spatially related plutonic differentiation suites 45
petrology: Plutonic rocks of the Ten Mile Creek RARE II Area, central Idaho 3-4
structure: Multiple intrusion of the Norridgewock pluton, Maine 61

intrusions—sills
metallogeny: Metallic mineral occurrences near the plutonic complex sill in the Coast Range 112
petrology: The plutonic complex tonalite sill in the Coast Range 113

intrusions—stocks
petrology: Hoffman Park stock, Colorado, and its relation to the Mount Antero Granite 200-201
— Tertiary granite stock, southwestern Kupreanof Island 113

intrusions—structure
magnetic anomalies: Big Craggies ultramafic body, Oregon 18-19

Invertebrata *see also* Coelenterata; foraminifera; Mollusca; worms

Invertebrata—ecology
aquatic environment: Aquatic macroinvertebrates, Wyoming 235

invertebrates—biostratigraphy
Pennsylvania: Correlation of the Middle Pennsylvanian Series 232

isotope dating *see* absolute age

isotopes *see also* absolute age; geochronology

isotopes—analysis
radioactive isotopes: Water-quality monitoring for radioisotopes, California 236
stable isotopes: Light-stable isotopes and fluid inclusion study of the Thompson Creek and Little Boulder Creek deposits, Idaho 205
— Stable-isotope technique used to trace ground-water movement 227
— Stable isotopes 205

isotopes—carbon
C-13/C-12: Distribution and stable-isotope composition of carbon in San Francisco Bay 172

isotopes—igneous rocks
volcanic rocks: Isotopic modification of magma, Yellowstone caldera, Wyoming 197
— Lead and neodymium isotopes in Hawaiian volcanic rocks 204

isotopes—lead
Pb-206/Pb-204: Lead isotopes in ores and rocks of southwest New Mexico 204

isotopes—neodymium
Nd-144/Nd-143: Samarium-neodymium study regarding evolution of the Earth's mantle 204

isotopes—oxygen
O-18/O-16: A 100,000-year cave record of atmospheric temperatures 223
— Metallogenic and tectonic significance of isotopic data from the Nikolai Greenstone, McCarthy quadrangle 109-110
— Oxygen isotope studies of uranium source rocks 53-54

isotopes—strontium
Sr-87/Sr-86: Alkaline intrusive complexes, Wet Mountains, Colorado 42
— Inclusions in upper Cenozoic volcanic rocks of the central Sierra Nevada, California 201
— Initial strontium ratios of plutonic rocks along the "Uinta trend," northwestern Utah 9
— Strontium isotopes along the Uinta trend 203-204

isotopes—sulfur
S-34/S-32: Massive copper sulfide deposit of syngenetic-epigenetic origin, north-central Nevada 9-10

isotopes—tracer experiments
research: Isotope tracer studies 203-204

Italy—economic geology
geothermal energy: Source of steam at Larderello geothermal system, Italy 211
— Steam flow in the Larderello and The Geysers geothermal systems 211

J

joints *see under* style *under* fractures

Jurassic *see also under* stratigraphy *under* Colorado; Gulf Coastal Plain; New Mexico; Utah

K

Kansas—economic geology
water resources: Kansas 135

Kansas—hydrogeology
ground water: Aquifer tests in the Wellington Aquifer near Salina 135
— Ground-water model, west-central Kansas 225
— Potentiometric-head relations, lower Paleozoics, Kansas 227
— Sandstone aquifers; potential source of water in southwestern Kansas 135

Kansas—structural geology
neotectonics: Neotectonics in Kansas 84

Kentucky—economic geology
water resources: Kentucky 131-132

Kentucky—environmental geology
pollution: Chloroform concentration in alluvium at Louisville 131-132

Kentucky—seismology
earthquakes: Earthquake localities and surficial and buried faults correspondence, Kentucky 75

Kentucky—stratigraphy
Pennsylvanian: Tectonic subsidence in eastern Kentucky 25

Kentucky—structural geology
tectonics: Tectonic subsidence in eastern Kentucky 25

L

laccoliths *see under* intrusions

lakes *see under* lacustrine features *under* geomorphology

land use *see also under* environmental geology *under* Alaska; Michigan; United States; Utah; Wyoming

land use—classification
coal: Coal resource occurrence/coal development potential reports 176
— Known recoverable coal resource areas 176
geothermal energy: Known geothermal resource areas 176
mineral resources: Classification and evaluation of mineral lands 175-176
— Classified land 177
— Known leasing areas for potassium, phosphate, and sodium 176
oil and gas fields: Known geologic structures of producing oil and gas fields 175-176
water resources: Waterpower classification; preservation of resource sites 176

land use—management
fuel resources: Management of oil and gas leases on the Outer Continental Shelf 178

— Onshore oil and gas lease sales 177
— Outer Continental Shelf lease sales for oil and gas 178
mineral resources: Management of mineral leases on Federal and Indian lands 177
natural resources: Cooperation with other Federal agencies 179
— Management of natural resources on Federal and Indian lands 175-179

landslides *see under* mass movements *under* geomorphology

lava *see also* igneous rocks; magmas

lava—alteration
maghemitization: Maghemitization of oceanic crust 181

lava—distribution
lava flows: Eastern extent of Picture Gorge Basalt 196
pillow lava: Lower to middle Eocene seamount chain, northwest Olympic Peninsula 92-93
thickness: Tectonic evolution of the southeastern part of the Columbia Plateau 94-95

lava—geochemistry
isotopes: Isotopic modification of magma, Yellowstone caldera, Wyoming 197
trace elements: Pre-Cretaceous subsurface volcanic rocks in Georgia 198

lava—petrology
alkali basalt: Petrology of rocks from the Pribilof Islands region, southern Bering Sea shelf 162-163
lava flows: Mafic flows in the Cedar Breaks-Panguitch Lake area, Utah 81

lava—properties
magnetic properties: Paleomagnetic correlation of volcanic rocks 181

lava—structure
ridges: Left lateral strike-slip riedel shears in the Yakima ridges 95

lead—isotopes
analysis: Lead and neodymium isotopes in Hawaiian volcanic rocks 204
Pb-206/Pb-204: Lead isotopes in ores and rocks of southwest New Mexico 204

Lesser Antilles—oceanography
marine geology: Investigations and mapping of insular shelves 164

lignite *see also under* economic geology *under* Montana

limestone *see also under* carbonate rocks *under* sedimentary rocks

limnology *see under* hydrology

lineation *see also* structural analysis

lithium—abundance
sediments: Lithium as a tracer 202

lithium ores—resources
evaluation: Lithium 22-23

Louisiana—economic geology
water resources: Louisiana 135-136

Louisiana—environmental geology
pollution: Low heavy-metal concentration in the Red River, Louisiana 234
— Median concentrations of chemical constituents in aquifers, southwestern Louisiana 236

Louisiana—hydrogeology
ground water: Digital model of the "2,000-foot" sand of the Baton Rouge area 135
— Sand-and-gravel aquifer overlies lignite deposits in Bienville Parish 135-136

Louisiana—oceanography
continental slope: Continental slope stratigraphy of Texas and Louisiana 160-161

M

magmas *see also* igneous rocks; intrusions; lava

magmas—differentiation
fractional crystallization: Proterozoic Y zoned ash-flow sheet, Mount Rogers, Virginia 198-199

magmas—evolution
differentiation: Quenched mafic magma in rhyolite, Coso Range, California 196-197
magma chambers: Evolution of silicic magma chambers 196-198
— Magma chamber in the Geysers-Clear Lake area 210
— Two suites of Cretaceous granitic rocks from the Pioneer batholith, Montana 80

magmas—genesis
melting: Origin of Hawaiian tholeiitic basalt 194-195
processes: Plutonic rocks and magmatic processes 199-201

magmas—geochemistry
isotopes: Isotopic modification of magma, Yellowstone caldera, Wyoming 197
trace elements: Study of diabase dikes 188-189

magmas—viscosity
emplacement: Pressurized fractures in hot rock 215-216

magnetic field *see under* Earth

magnetic surveys *see under* geophysical surveys *under* Alaska; California; Georgia; Hawaii; Idaho; Montana; New York; North Carolina; Oregon; South Carolina; United States; Vermont

magnetotelluric surveys *see under* geophysical surveys *under* California; Oregon

Maine—economic geology
peat: Peat resources in Maine 1

Maine—petrology
intrusions: Multiple intrusion of the Norridgewock pluton, Maine 61

mantle *see also under* seismology *under* Western U.S.

mantle—geochemistry
evolution: Samarium-neodymium study regarding evolution of the Earth's mantle 204
siderophile elements: Siderophile elements in the Earth's upper mantle 244

maps *see also under* areal geology *under* Colorado; *see also under* economic geology *under* Alaska; Basin and Range Province; *see also under* environmental geology *under* Utah; *see also under* general *under* automatic data processing; catalogs; *see also under* geomorphology *under* United States; *see also under* geophysical surveys *under* Missouri; United States; *see also under* hydrogeology *under* California; Florida; Great Plains; Washington; *see also under* structural geology *under* United States

maps—cartography
automatic data processing: Digital classification of Landsat data for identification of hydrothermal alteration 183
— Geologic map data file 114
geologic maps: Geologic maps 114
gravity survey maps: Residual Bouguer gravity maps 18

marine geology *see also* oceanography; *see also under* oceanography *under* Atlantic Coastal Plain; Gulf Coastal Plain; Lesser Antilles; Pacific Coast; Puerto Rico; United States

marine geology—observations
deep-sea environment: Deep sea geology and resources 163-164

Mars—composition
chemical composition: Chemical composition of Mars 245

Maryland—economic geology
water resources: Maryland 118

Maryland—environmental geology
pollution: Point-source discharge of phosphorus into the Potomac River 244

Maryland—hydrogeology
ground water: Aquifer studies in western Montgomery County 119

Maryland—paleobotany
angiosperms: Dendroclimatic investigations of hickory and oak 233

mass movements *see under* geomorphology

Massachusetts—environmental geology
geologic hazards: Potential geologic hazards on the inner Continental Shelf off southeastern Massachusetts 153-154

Massachusetts—geomorphology
glacial geology: Deglaciation, ice lobation, and marine incursion, eastern Massachusetts 63-64
— Deglaciation of the Connecticut Valley, Massachusetts 64
— Deglaciation of the Westfield and Connecticut Valleys, Massachusetts 64-65
— First bare ground in western Massachusetts 65

Massachusetts—geophysical surveys
acoustical surveys: Acoustic stratigraphy of Nantucket Sound, Massachusetts 154
— Sediments and bedforms of western Massachusetts Bay 154

Massachusetts—oceanography
continental shelf: Acoustic stratigraphy of Nantucket Sound, Massachusetts 154
— Potential geologic hazards on the inner Continental Shelf off southeastern Massachusetts 153-154
— Sediments and bedforms of western Massachusetts Bay 154
sedimentation: Coastal sedimentary processes off beaches 165

Massachusetts—petrology
metamorphic rocks: Correlation of Oakdale and Paxton Formations of east-central Massachusetts with stratigraphy in eastern Connecticut 62

Massachusetts—stratigraphy
Pleistocene: Glacial stratigraphy of Cape Cod, Nantucket, and Martha's Vineyard, Massachusetts 65-66
— Stratigraphy and structure of the Sankaty Head Cliffs, Nantucket Island 65

Massachusetts—structural geology
faults: Physical characteristics of faults, northeastern Massachusetts 62
tectonics: Fault-basin origin of Boston Basin, Massachusetts 62

mathematical geology *see also* automatic data processing

melange *see under* interpretation *under* structural analysis

mercury ores—resources
evaluation: Production statistics applied to resource estimation 21

Mesozoic—paleontology
research: Mesozoic and Cenozoic studies 229-232

metal ores—affinities
geothermal energy: Interrelations among epithermal ore deposits and geothermal systems depositing mercury, gold and silver 209-210

metal ores—exploration
geochemical methods: Geochemical processes 15
— Movement of trace elements in weathering environment 15

metal ores—resources
evaluation: Mineral-resource assessment 21-22

metals *see also* arsenic; bismuth; gold; lead; lithium; uranium; zinc

metals—abundance
ground water: Concentrations of heavy metals in ground water, Wisconsin 235-236
surface water: Low heavy-metal concentration in the Red River, Louisiana 234

metals—geochemistry
trace elements: Heavy-metal distributions in mollusks of San Francisco Bay 174

metamorphic rocks *see also* igneous rocks; metamorphism; metasomatism

metamorphic rocks—distribution
terrains: Geologic terranes of the Circle quadrangle 107

metamorphic rocks—gneisses
augen gneiss: Proterozoic cataclastic augen gneiss in the Big Delta quadrangle 108
geochemistry: "Monson Gneiss", eastern Connecticut 61
orthogneiss: Mount Juneau orthogneiss pluton 112
— Petrology and geochemistry of the Oliverian domes of New England 200
textures: Mylonitic gneisses over a Cretaceous(?) pluton, Iron Mountains, southeastern California 100-101

metamorphic rocks—lithostratigraphy
correlation: Correlation of Oakdale and Paxton Formations of east-central Massachusetts with stratigraphy in eastern Connecticut 62
Devonian: Stratigraphic modifications, eastern New Hampshire 62
Precambrian: Comparison of Precambrian rocks of the Hartville uplift, eastern Wyoming, and of the Black Hills, western South Dakota 81-82
— Newly recognized Precambrian metasedimentary and metavolcanic rocks in the Seminoe Mountains, Wyoming 82
research: Stratigraphy of the Atlanta area, Georgia 69

metamorphic rocks—metaigneous rocks
age: Granodiorite augen gneiss-tonalite-metagabbro; the earliest magma series in the Cretaceous Idaho batholith 11

metamorphic rocks—metasedimentary rocks
genesis: Turbidite beds in the Albemarle Group, Carolina slate belt 66
lithostratigraphy: Identification of Ordovician rocks in Lake Minchumina area 106
mineral assemblages: Amphibolite facies mineral assemblages and the fractionation of CaO, U, and Th, Colorado 201
— Diverse types of garnets in metasedimentary rocks of the Great Smoky Group, North Carolina and Tennessee 66-67

metamorphic rocks—petrology
general: Metamorphic rocks and processes 201

metamorphic rocks—schists
greenschist: Volcanic greenschist in the subsurface of the southeastern San Joaquin Valley 99

metamorphic rocks—textures
fabric: Metamorphic terrane in Pilot Range of Nevada and Utah 87-88
— Structural analysis of plutonic and metamorphic rocks from an area east of Wrangell 113

metamorphism—age
absolute age: Episodic plutonism in the Coast batholith of southeastern Alaska 199

metasomatism—experimental studies
indicators: Near-infrared spectroscopy determination of degree of serpentinization in ultramafic rocks 185

metasomatism—processes
hydrothermal alteration: Hydrothermal alteration at Mount Baker, Washington 198
— Hydrothermal alteration at Mount Hood, Oregon 59-60
— Hydrothermal alteration in Yellowstone geyser basins 59
— Vitrinite reflectance geothermometry in the Cerro Prieto geothermal system, Baja California, Mexico 60

meteorology—instruments
networks: Satellite relay meteorological stations to study wind erosion 220

meteorology—winds
storms: December 1977 windstorm in San Joaquin Valley 220
— February 1977 windstorm in Great Plains 220

Mexico *see also* Gulf Coastal Plain

Mexico—economic geology
geothermal energy: Origin of Cerro Prieto, Mexico, brines 212
— Production-induced changes in the aquifer of Cerro Prieto Geothermal Area, Mexico 212
— Vitrinite reflectance geothermometry in the Cerro Prieto geothermal system, Baja California, Mexico 60

Mexico—hydrogeology
thermal waters: Origin of Cerro Prieto, Mexico, brines 212
— Production-induced changes in the aquifer of Cerro Prieto Geothermal Area, Mexico 212

Michigan—economic geology
iron ores: Extension of Iron River-Crystal Falls basin, Michigan and Wisconsin 6
metal ores: Geochemical lineament, Iron River 2° quadrangle, Michigan and Wisconsin 15
uranium ores: Lake Superior region favorable for quartz-pebble-type uranium deposits 45
— Possible low-grade uranium resources in graphitic slate, northern Michigan 44-45
— Potential unconformity-type uranium deposits, northern Michigan 45
water resources: Michigan 119-120

Michigan—environmental geology
land use: Model study of Michigan coal deposit 119-120
pollution: Study of ground water contaminated by trichloroethylene 119

Michigan—geophysical surveys
electromagnetic surveys: Mineral geophysical surveys in Wisconsin and Michigan 187-188

Michigan—hydrogeology
hydrology: Flow model of Saginaw River 119
— Hydrologic analysis of Sands Plain 119

Midwest—areal geology
regional: Central region 74-76

Midwest—economic geology
coal: Zinc and coal recoverable from coal mine refuse 1-2
mineral resources: Mineral resources 76
water resources: Central Region 133-142
zinc ores: Zinc and coal recoverable from coal mine refuse 1-2

Midwest—geochemistry
trace elements: Zinc and cadmium content of coal in the Interior coal province 28

Midwest—hydrogeology
ground water: Carbon dioxide and methane outgassing from ground-water samples 226
Midwest—structural geology
tectonics: Tectonics and stratigraphy 74-75
mineral deposits, genesis—controls
geochemical controls: A precipitation mechanism for hydrothermal vein-type uranium deposits 56
— Dissolved free oxygen and the genesis of sandstone-type uranium deposits 52
— Experimental studies on uranyl ion reduction by H_2O reveal a marked pH dependence 52
— Genetic geochemistry of Uravan mineral belt deposits; a new proposal 52
— Geochemical studies of a tabular uranium ore body 53
— Geochemical uranium, fluorite, and beryllium ore controls at Spor Mountain 54
— Organic geochemistry and uranium in the Grants mineral belt 51
— Presence of ore-stage marcasite and formation of roll-type deposits 52-53
— Pyrite and marcasite in roll-type uranium deposits 53
— Uranium in the Oligocene Antero Formation, Park County, Colorado 49-50
— Uranium mineralization at the Dennison-Bunn claim, Sandoval County, New Mexico 49
— Uranium (VI) sorption by iron oxides 52
paleogeographic controls: Early Permian depositional systems and paleogeography, Uncompahgre Basin 47
— Salt Wash depositional environments and uranium 48
— Stratigraphic analysis of Western Interior Cretaceous uranium basins 50
stratigraphic controls: Geologic factors in evolution of unconformity-type uranium deposits 46-47
— Potential unconformity-type uranium deposits, northern Michigan 45
— Stratigraphic control of solutions that deposited uranium in Cretaceous rocks, Catron County, New Mexico 57
— Unconformity-related uranium occurrences in the Precambrian basement in the upper basin of the Arkansas River, Colorado 58-59
structural controls: Allochthonous Paleozoic sedimentary rocks, central Idaho 83
— Constraints placed upon location of the San Andreas fault by base and precious metal sulfide mineralization, Point Delgada, northern California 96-97
— Metallic mineral occurrences near the plutonic complex sill in the Coast Range 112
— Petrology and deformation of Leadville Dolomite, Pitch uranium mine 43
— Structural control of rhyolite volcanism associated with uranium deposits, Western United States 8
— Sulfides in the Duluth Complex, Minnesota 76
— Supergene uranium deposits in fracture zones associated with Laramide upthrusts 43
mineral deposits, genesis—copper ores
mineralization: Bornite deposit, Cosmos Hills, northwest arctic Alaska 105
— Geochemical comparison of mineralized and barren stocks, Arizona 10
ore-forming fluids: Metallogenic and tectonic significance of isotopic data from the Nikolai Greenstone, McCarthy quadrangle 109-110
mineral deposits, genesis—lithium ores
environment: Evaporative model of lithium brine generation 22-23
mineral deposits, genesis—metal ores
metallogenic provinces: Geochemical definition of mineral province, Alaska Range, Alaska 14
— Geochemical definition of mineral province, Brooks Range, Alaska 14
— Geochemical definition of mineral provinces in the Alaska Range and Brooks Range 103-104
— Upper Triassic massive sulfide deposits near Wrangell 112-113
mineral deposits, genesis—processes
exhalative processes: Deep sea geology and resources 163-164
— Hydrothermal activity and massive sulfides on the East Pacific Rise 163
hydrothermal processes: Colorado uranium deposits as ancient geothermal systems 59
— Mineralization in the Spirit Lake quadrangle, southern Cascade Range, Washington 8
— Model for the origin of hydrothermal uranium deposits near Marysvale, Utah 11
— Possible hot-spring origin for Front Range uranium veins 43-44
syngenesis: Massive copper sulfide deposit of syngenetic-epigenetic origin, north-central Nevada 9-10
mineral deposits, genesis—uranium ores
age: Age of uranium host rocks in the Date Creek basin, west-central Arizona 50
— Limitations on genesis of Midnite mine uranium ores 44
— Use of uranium-lead isotope systematics to date uraniferous opals 54
controls: A possible relation between subsidence and uranium mineralization 57-58
— Distribution and mobility of uranium in glassy and zeolitized tuff, Keg Mountain area, Utah 55
— Preservation of uranium deposits in the Mariano Lake mine, New Mexico 48-49
— Probable origin of uranium in the Browns Park Formation (Miocene) of the Sand Wash Basin, Moffat County, Colorado 49
environment: A model for sedimentation at the Anderson mine, west-central Arizona 50
experimental studies: Uraniferous silica; conditions of formation 55
— Uranium adsorption onto montmorillonite 53
— Uranium leachability from freshly erupted volcanic ash of basaltic and dacitic composition 55-56
interpretation: Formation of tabular uranium deposits in the Powder River Basin 50
ore sources: Oxygen isotope studies of uranium source rocks 53-54
— Source of the uranium-bearing sandstone of the southern Powder River Basin 59
mineral exploration—geobotanical methods
uranium ores: Uranium concentration by moss and algae from surface water 56-57
mineral exploration—geochemical methods
coatings: Iron and manganese oxides, Pinos Altos district, New Mexico 16-17
gases: Spectral investigation of sulfur dioxide 16
— Volatile gases useful in geochemical exploration 16
general: Geochemical processes 15
geochemical prospecting: Geochemical definition of mineral province, Alaska Range, Alaska 14
— Geochemical definition of mineral province, Brooks Range, Alaska 14
— Geochemical features, Pinaleno Mountains, Arizona 15
— Geochemical reconnaissance results 13-15
— Hydrogeochemical prospecting 15-16
helium: Helium and sulfur, Poorman fault, Colorado 16
— Helium detection for uranium exploration 57
isotopes: Initial strontium ratios of plutonic rocks along the "Uinta trend," northwestern Utah 9
sampling: Sample media useful in geochemical exploration 16-17
soil sampling: Geochemical lineament, Iron River 2° quadrangle, Michigan and Wisconsin 15
stream sediments: Geochemical definition of mineral provinces in the Alaska Range and Brooks Range 103-104
— Geochemical evidence for mineral deposits, Petersburg and Port Alexander quadrangles, Alaska 14-15
— Geochemical reconnaissance studies, Papago Indian Reservation, Arizona 15
— Regional geochemical studies, Patagonia Mountains, Arizona 13
— Stream sediment geochemical survey, southwestern Rawah Range, northern Colorado 10

techniques: Analytical methodology useful in geochemical exploration 17
— Atomic absorption method for arsenic 17
— Induction-coupled plasma spectroscopy 17
— Liquid ion exchange technique 17
— Sensitive method for gold analysis 17
trace elements: Movement of trace elements in weathering environment 15
— Possible hydrothermal signature in Belt stratabound copper deposits, Montana 12
— Trace-element patterns in spatially related plutonic differentiation suites 45
uranium ores: Geochemical maps of uranium, thorium, and thorium-uranium in granites of the Basin and Range province 56
— Geochemical uranium, fluorite, and beryllium ore controls at Spor Mountain 54
— Potential uranium mineralization, Mineral Mountains, Utah 13
— Radioactivity in water wells, Pueblo County, Colorado 56

mineral exploration—geological methods
copper ores: Subvolcanic hydrothermal mineral deposits in the Carolina volcanic slate belt 7
diamonds: Diamond potential of Missouri Breaks diatremes, Montana 4
lead ores: Ore bodies at Great Gossan Lead, Virginia 7
metal ores: Metalliferous mineral resource potential of the Big Delta quadrangle 108
mineral resources: Geologic studies of mineral districts and mineral-bearing regions 6-13
— Lineated granitic rocks mark early faults in the Beaver Creek Area, western St. Lawrence County, New York 6-7
— Mineral-resource assessment of the Charlotte 2° quadrangle, North Carolina and South Carolina 4-5
molybdenum ores: Hydrothermal alteration in the Pioneer Mountains, Beaverhead County, Montana 3
plutons: Plutonic rocks of the Ten Mile Creek RARE II Area, central Idaho 3-4
stockwork deposits: Deep exploration target at Red Mountain stockwork, Yellow Pine, Idaho 12-13
uranium ores: Lake Superior region favorable for quartz-pebble-type uranium deposits 45
— Potential unconformity-type uranium deposits, northern Michigan 45
— Sites of labile uranium in granitic rocks 54
— Unconformity-related uranium occurrences in the Precambrian basement in the upper basin of the Arkansas River, Colorado 58-59

mineral exploration—geophysical methods
anomalies: Geophysical studies in the Big Snowy Mountains Wilderness Area, Fergus and Golden Valley counties, Montana 2
chromite ores: Chromite and nickel, western Cordillera 8-9
— Chromite in northern California 18
electromagnetic methods: Gold in South Carolina 18
— Mineral geophysical surveys in Wisconsin and Michigan 187-188
— Model study of experimental electromagnetic method 186
general: Methodology in exploration geophysics 18-19
gravity methods: Extension of Iron River-Crystal Falls basin, Michigan and Wisconsin 6
— Gravity features related to location of mineral deposits in North Carolina 11-12
— Gravity measurement of approximate tonnage of a Brooks Range barite deposit 104-105
— Gravity studies in the Sierra Ancha Wilderness Area, Gila County, Arizona 2
— Gravity studies of mineralized features, Silver City quadrangle, Arizona and New Mexico 5
— Residual Bouguer gravity maps 18
intrusions: Geophysical studies in the Never Summer Wilderness Area, Colorado 2
magnetic methods: Big Craggies ultramafic body, Oregon 18-19
— Magnetic studies in the Belt Basin, Montana and Idaho 5
— Magnetite deposit, Minarets Wilderness Area, California 18
metal ores: Massive sulfide bodies in Colorado 18
mineral resources: Mineral resource assessment using aerial geophysical data 187
radioactivity methods: Aerial radiometric and magnetic survey of the Sierra Ancha Wilderness Area and vicinity, Gila County, Arizona 2-3
— Application of high resolution gamma-ray spectrometry to uranium prospecting 57
— Uranium mineralization in the Hopi Buttes of the Flagstaff and Gallup 1° x 2° quadrangles, Arizona 58
— Uranium occurrence in southern Wah Wah Range, Utah 57
uranium ores: Airborne geophysical survey for uranium 187
— Possible low-grade uranium resources in graphitic slate, northern Michigan 44-45
well-logging: Borehole measurements to differentiate sulfides and clays 186

mineral exploration—hydrological methods
ground water: Arsenic, copper, and molybdenum, Baboquivari Mountains, Arizona 15
surface water: Geochemical study of water and sediment, Rio Tanama district, Puerto Rico 16

mineral exploration—methods
applications: Geochemical and geophysical techniques in resource assessments 13-19
uranium ores: Proterozoic quartzite and conglomerate of central and northern Idaho unfavorable for quartz-pebble-conglomerate-type uranium deposits 46

mineral exploration—ore guides
asbestos deposits: Near-infrared spectroscopy determination of degree of serpentinization in ultramafic rocks 185
greenstone: Greenstone in the Havallah Formation, Nevada 9
metal ores: A magnetic tectonic feature in southern Arizona 4
molybdenum ores: Arizona molybdenum mineral associations as keys to ore deposit metallogenic types 9
mudstone: Mudstone as uranium exploration guide 47-48
nelsonite: Cumulate and supercumulate nelsonite, central Virginia 7
tourmaline: Tourmaline associated with New England massive sulfide deposits 7
zunyite: Massive zunyite rock in north-central Nevada 87

mineral exploration—programs
legislation: Domestic minerals exploration program 13, 14

mineral exploration—remote sensing
applications: Remote detection of geochemical soil anomalies 16
— Remote sensing applied to geochemical exploration 16
lineaments: Ajo 2° quadrangle, Arizona 17
— Analysis of linear features 17-18
— Powder River Basin, Wyoming 18
— Rio Grande Rift zone, central New Mexico 17
— Southern Utah 17-18
maps: Digital classification of Landsat data for identification of hydrothermal alteration 183

mineral exploration—statistical methods
automatic data processing: Identification of geochemical anomalies 203
uranium ores: Porous media model computer and field studies of sandstone-type uranium deposits 51

mineral prospecting *see* mineral exploration

mineral resources *see also under* economic geology *under* Alaska; Arizona; automatic data processing; Basin and Range Province; California; Georgia; Great Plains; Idaho; Midwest; Montana; Nevada; New Mexico; New York; New Zealand; Rocky Mountains; Tennessee; United States; Utah; Washington; Wisconsin

mineral resources—economics
models: Dynamic modeling of mineral resources 20

mineral resources—exploration
geological methods: Geologic studies of mineral districts and mineral-bearing regions 6-13
programs: Domestic minerals exploration program 13, 14
mineral resources—resources
chemical resources: Chemical resources 22-23
data analysis: Resource analysis 20-22
data bases: Computer applications of resource data files 20
— Computerized Resources Information Bank (CRIB) 19
evaluation: Mineral-resource assessments of land areas 1-6
global: United States and world mineral-resource assessments 1
information systems: Resource information systems 19-20
— Resource information systems and analysis 19-22
research: Mineral-resource investigations 1-23
mineralogy—general
research: Geochemistry, mineralogy, and petrology 189-208
— Mineralogic studies and crystal chemistry 191-192
minerals *see also* crystal chemistry; crystal growth; crystal structure
minerals—chain silicates, clinopyroxene
phase equilibria: Decomposition mechanism and kinetics in clinopyroxenes 190-191
minerals—chlorides
tachyhydrite: Tachyhydrite 192
minerals—halides
zunyite: Massive zunyite rock in north-central Nevada 87
minerals—mineral data
thermodynamic properties: Reevaluation of the thermodynamic properties of minerals in the system CaO-Al_2O_3-SiO_2-H_2O 190
— Relations between lattice dynamics and thermodynamic properties of minerals 189-190
— Thermodynamic properties of minerals 191
minerals—orthosilicates
zunyite: Massive zunyite rock in north-central Nevada 87
minerals—orthosilicates, garnet group
accessory minerals: Diverse types of garnets in metasedimentary rocks of the Great Smoky Group, North Carolina and Tennessee 66-67
minerals—oxides
magnetite: New data on magnetite and ilmenite from the granitoid rocks in White Pine County, Nevada 199-200
manganese oxide: Rates of formation of manganese oxides 202-203
minerals—silicates
occurrence: Zonation of clay and zeolite minerals, Raft River geothermal boreholes, Idaho 209
minerals—sulfides
alkali-iron sulfides: Alkali-iron sulfides from Coyote Peak, Humboldt County, California 192
copper sulfides: Copper-rich sulfides; low chalcocite and djurleite 191-192
pyrite: Distribution and genesis of primary pyrite in coal 29
mining geology—evaluation
coal: Coal resource model studies 20
— Worth of geophysical and geological data and mineral supply 20
mercury ores: Production statistics applied to resource estimation 21
metal ores: Mineral-resource assessment 21-22
mineral resources: Mineral and energy resource system for Navajo Tribe 21
phosphate deposits: Estimation of world phosphate resources 21
uranium ores: Uranium resource analysis 22
Minnesota—economic geology
metal ores: Sulfides in the Duluth Complex, Minnesota 76
water resources: Minnesota 120-122
Minnesota—geochronology
Holocene: Records of past climates in Elk Lake sediments 221
Precambrian: Rejuvenation of an ancient craton 208
Minnesota—hydrogeology
ground water: Appraisal of Cambrian and Ordovician aquifers in southeastern Minnesota 122
— Appraisal of ground water in central Minnesota 121
— Ground-water appraisal in Big Stone County 122
— Ground-water appraisal of sand-plain areas in central Minnesota 120-121
— Potentiometric data from deep test well 120
— Sensitivity analysis useful for planning data collection 121
hydrology: Baseline water quality established before highway construction 120
— Effect of acid precipitation of water quality of the Filson Creek watershed in northeastern Minnesota 121
— Effects of peat mining on hydrology in the Red Lake 121
— Hydrologic budget of Eagle Lake in central Minnesota 121
— Hydrologic setting of Williams Lake in north-central Minnesota 121-122
— Rainfall-runoff relations in the Coon Creek watershed, Anoka County 120
— Water-quality monitoring lakes in northeastern Minnesota 121
— Water quality of lakes in Eagan 120
surveys: Interaquifer flow through well bores 225
Miocene *see also under* stratigraphy *under* California; Nevada; Pacific Ocean
Mississippi—economic geology
water resources: Mississippi 132
Mississippi—environmental geology
geological hazards: Major flood on Pearl River at Jackson 132
pollution: Transport and degradation of acetone in streams 237
Mississippi—hydrogeology
ground water: Large water-level declines in Eutaw-McShan aquifer 132
Mississippi—stratigraphy
Cretaceous: Upper Cretaceous geology of the Tombigbee River, Alabama and Mississippi 230
Mississippi Valley—structural geology
tectonics: Tectonic features in southeastern Missouri from remote-sensing and geophysical data 185
Mississippian *see also under* stratigraphy *under* Nevada
Missouri—economic geology
water resources: Missouri 136
Missouri—geophysical surveys
maps: Tectonic features in southeastern Missouri from remote-sensing and geophysical data 185
remote sensing: Tectonic features in southeastern Missouri from remote-sensing and geophysical data 185
surveys: Gravity-magnetic surveys in southeast Missouri 188
Missouri—hydrogeology
hydrology: Ground water and water quality downstream from the proposed Prosperity Reservoir in Center Creek basin 136
— Irrigation from deep wells in Audrain County, Missouri 150
Mollusca—Bivalvia
ecology: Population dynamics of dominant bivalves in San Francisco Bay 174
Mollusca—ecology
communities: Long-term studies of benthic community structure in Puget Sound 170
estuarine environment: Heavy-metal distributions in mollusks of San Francisco Bay 174
mollusks—biostratigraphy
Cretaceous: First recognition of the molluscan Exogyra cancellata subzone, South Carolina 229
Pennsylvanian: Geology of the Mississippian and Pennsylvanian of north-central Alabama 69-70
Pleistocene: Bootlegger Cove Clay; geographic and stratigraphic mollusk occurrences 111
Quaternary: Temperature aspects of late Quaternary marine molluscan faunas 231
Montana—economic geology
coal: Coal in the Tongue River Member of the Fort Union Formation 27
copper ores: Possible hydrothermal signature in Belt stratabound copper deposits, Montana 12
diamonds: Diamond potential of Missouri Breaks diatremes, Montana 4

fuel resources: Gravity studies in Montana indicate hydrocarbon potential 1
gems: Gold and sapphires in Tertiary gravels, Sapphire Range, Montana 14
gold ores: Gold and sapphires in Tertiary gravels, Sapphire Range, Montana 14
gravel deposits: Pleistocene gravel in southeastern Montana 76
iron ores: Resource potential of bedded iron deposits in the Tobacco Root Mountains, Montana 7
lead-zinc deposits: Lead and zinc, Choteau 2° quadrangle, Montana 14
lignite: Lignite in the Fort Peck Indian Reservation 27
metal ores: Intrusion and mineralization in Moccasin Mountains, Montana 11
mineral resources: Structure, stratigraphy, and intrusive rocks of part of the Sapphire Wilderness Study Area, Montana 5
molybdenum ores: Hydrothermal alteration in the Pioneer Mountains, Beaverhead County, Montana 3
natural gas: Reservoir characteristics of gas-bearing Eagle Sandstone, Bearpaw Mountains, Montana 33-34
petroleum: Distribution and diagenetic history of possible reservoir beds in Madison Group, disturbed belt, Montana 33
— Paleogeography and petroleum resources of Tyler Formation, central Montana 34
— Potential petroleum reservoir rocks in southwestern Montana 34
uranium ores: Formation of tabular uranium deposits in the Powder River Basin 50
water resources: Montana 136-137

Montana—environmental geology
reclamation: Continued hydrologic studies of energy minerals rehabilitation inventory and analysis areas 136

Montana—geochronology
Archean: Samarium-neodymium age of the Stillwater Complex, Montana 205
Eocene: Volcanic rocks of Eocene age from the Pioneer Mountains, Montana 80
Holocene: End of "Little Ice Age" in Glacier National Park 222

Montana—geomorphology
fluvial features: Aggradation of Powder River valley during 1978 flood 218
glacial geology: Evidence for icecap in West Pioneer Mountains, Montana 76

Montana—geophysical surveys
gravity surveys: Gravity studies in Montana indicate hydrocarbon potential 1
magnetic surveys: Aeromagnetic studies of the Square Butte Wilderness Area, Choteau County, Montana 2
— Magnetic studies in the Belt Basin, Montana and Idaho 5
surveys: Geophysical studies in the Big Snowy Mountains Wilderness Area, Fergus and Golden Valley counties, Montana 2

Montana—hydrogeology
ground water: Appraisal of aquifers in northern Cascade County 136
— Shallow alluvial aquifers evaluated in Helena Valley 136-137
hydrology: Limnology of reservoirs, eastern Montana 241-242

Montana—petrology
igneous rocks: Petrogenetic possibilities for late-mica granites, Pioneer Mountains, Montana 79-80
— Two suites of Cretaceous granitic rocks from the Pioneer batholith, Montana 80
intrusions: Cretaceous volcanism and plutonism, Montana 11

Montana—sedimentary petrology
sedimentation: Sediment-yield estimates for central Powder River Basin, Montana and Wyoming 217

Montana—stratigraphy
Cambrian: Correlation of Cambrian formations in southwestern Montana 77
Cretaceous: Depositional environment of the Groat Sandstone Bed in the northern Black Hills, Montana 77-78
Ordovician: Ordovician plutonism in Idaho and Montana 84
Paleocene: Coal in the Tongue River Member of the Fort Union Formation 27
Pennsylvanian: Paleogeography and petroleum resources of Tyler Formation, central Montana 34
Proterozoic: Facies changes and structural belts in the Proterozoic Y rocks of Glacier National Park, Montana 85
— Thrusting faults in Belt terrane in Montana 85
Tertiary: Tertiary gravels, Little Belt Mountains, Montana 78

Montana—structural geology
tectonics: Basement controls on steep faults, southwestern Montana and east-central Idaho 84-85
— Eastern edge of the Sapphire thrust system, Montana 85
— Facies changes and structural belts in the Proterozoic Y rocks of Glacier National Park, Montana 85
— Ordovician plutonism in Idaho and Montana 84
— Southern extension of the Sapphire thrust system, Montana 86
— Thrusting faults in Belt terrane in Montana 85

mud volcanoes *see also* volcanology

N

natural gas *see also under* economic geology *under* Appalachians; Montana; Rocky Mountains; Western Interior; Wyoming

natural gas—exploration
techniques: New exploration and production techniques 40-41

natural resources *see under* conservation

Nebraska—environmental geology
pollution: Statistical analyses of surface-water quality, Nebraska 235

Nebraska—hydrogeology
ground water: Artificial recharge of ground water 226

neodymium—isotopes
analysis: Lead and neodymium isotopes in Hawaiian volcanic rocks 204
Nd-144/Nd-143: Samarium-neodymium study regarding evolution of the Earth's mantle 204

Neogene *see also under* geochronology *under* Idaho; *see also under* stratigraphy *under* Arizona

neotectonics *see also under* structural geology *under* Arizona; Atlantic Coastal Plain; Basin and Range Province; Bering Sea; California; Colorado Plateau; Georgia; Great Basin; Idaho; Kansas; Nevada; New Mexico; United States; Utah; Washington; Wyoming

Nevada—economic geology
copper ores: Massive copper sulfide deposit of syngenetic-epigenetic origin, north-central Nevada 9-10
geothermal energy: Heat flow in relation to hydrothermal activity in the southern Black Rock Desert, Nevada 213
— Reservoir processes at Steamboat Springs 212
lithium ores: Evaporative model of lithium brine generation 22-23
metal ores: Greenstone in the Havallah Formation, Nevada 9
mineral resources: Interrelations among epithermal ore deposits and geothermal systems depositing mercury, gold and silver 209-210
— Massive zunyite rock in north-central Nevada 87
uranium ores: Uranium potential of newly recognized caldera near Manhattan, Nevada 10
water resources: Nevada 144-145

Nevada—engineering geology
waste disposal: Electrical and magnetic borehole studies useful for defining nuclear waste repositories in volcanic rocks 183
— Resistivity sounding investigation in the Syncline Ridge area, Nevada 184

Nevada—geochronology
Cretaceous: Cretaceous volcanism, southwestern Nevada 91
Pleistocene: Zircon fission-track ages of a Pleistocene ash, California and Nevada 206-207

Nevada—geophysical surveys
electrical surveys: Resistivity sounding investigation in the Syncline Ridge area, Nevada 184
gravity surveys: Geophysical investigations in Lemmon Valley 144-145
heat flow: Heat flow in relation to hydrothermal activity in the southern Black Rock Desert, Nevada 213

Nevada—hydrogeology
ground water: Ground water studies in Las Vegas area 144
thermal waters: Heat flow in relation to hydrothermal activity in the southern Black Rock Desert, Nevada 213
— Reservoir processes at Steamboat Springs 212

Nevada—petrology
igneous rocks: New data on magnetite and ilmenite from the granitoid rocks in White Pine County, Nevada 199-200

Nevada—stratigraphy
Devonian: Correlative Devonian eugeosynclinal rocks, California and Nevada 89
Miocene: Westward streamflow in Miocene of west-central Nevada 89
Mississippian: Lower Paleozoic rock fragments in Antler flysch, northern Nevada 88

Nevada—structural geology
neotectonics: Holocene faulting, central Nevada 88-89
tectonics: Correlative Devonian eugeosynclinal rocks, California and Nevada 89
— Cretaceous thrust system, southern Nevada 90
— Metamorphic terrane in Pilot Range of Nevada and Utah 87-88

New England—areal geology
regional: New England 61-66

New England—economic geology
metal ores: Tourmaline associated with New England massive sulfide deposits 7

New England—geochemistry
trace elements: Petrology and geochemistry of the Oliverian domes of New England 200

New England—geomorphology
glacial geology: Discovery of upper Wisconsinan glacial till on the Continental Shelf off southeastern New England 66
— Glacial geology 63-66

New England—oceanography
sedimentation: Modern continental shelf sediment accumulation off southern New England 154-155

New England—petrology
igneous rocks: Igneous rocks and geochemistry 61-62

New England—structural geology
tectonics: Tectonics and stratigraphy 61-62

New Hampshire—economic geology
uranium ores: Trace-element patterns in spatially related plutonic differentiation suites 45

New Hampshire—stratigraphy
Devonian: Stratigraphic modifications, eastern New Hampshire 62

New Jersey—areal geology
regional: New Jersey 67

New Jersey—economic geology
uranium ores: Nature of uranium occurrences in the northern Reading Prong 46
water resources: New Jersey 122

New Jersey—geophysical surveys
seismic surveys: The ocean-continent transition zone off New Jersey 159-160

New Jersey—hydrogeology
ground water: Ground-water use in the coastal-plain aquifer system of New Jersey 150
hydrology: Drainage areas determined for New Jersey streams 122

New Jersey—structural geology
tectonics: Tectonic shortening in late Alleghanian time 67

New Jersey—tectonophysics
crust: The ocean-continent transition zone off New Jersey 159-160

New Mexico—economic geology
coal: Coal in the central and east-central part of the San Juan Basin 27
energy sources: Mineral and energy resource system for Navajo Tribe 21
metal ores: Iron and manganese oxides, Pinos Altos district, New Mexico 16-17
mineral resources: Rio Grande Rift zone, central New Mexico 17
uranium ores: Organic geochemistry and uranium in the Grants mineral belt 51
— Preservation of uranium deposits in the Mariano Lake mine, New Mexico 48-49
— Stratigraphic control of solutions that deposited uranium in Cretaceous rocks, Catron County, New Mexico 57
— Uranium mineralization at the Dennison-Bunn claim, Sandoval County, New Mexico 49
water resources: New Mexico 137

New Mexico—geochemistry
isotopes: Lead isotopes in ores and rocks of southwest New Mexico 204

New Mexico—geochronology
Proterozoic: Lead isotopes, southwest New Mexico 206

New Mexico—geophysical surveys
electrical surveys: Geoelectrical study of the Rio Grande Rift 208
— Resistivity study of the San Augustine aquifers, New Mexico 187
gravity surveys: Gravity studies of mineralized features, Silver City quadrangle, Arizona and New Mexico 5
remote sensing: Rio Grande Rift zone, central New Mexico 17
surveys: Geophysical studies of the Rio Grande Rift 188

New Mexico—hydrogeology
ground water: Assessment of ground-water resources in Santa Fe County 137
— Assessment of ground-water resources on the Zuni Indian Reservation 137
— Hydrologic properties of the Gallup Sandstone in McKinley County 137
— Thinning of aquifer by solution 227
hydrology: Water use by saltcedar and by replacement vegetation in the flood plain of the Pecos River, New Mexico 240

New Mexico—Pelycosauria
Pennsylvanian: Extension of age terrestrial vertebrates 232

New Mexico—petrology
intrusions: Pressurized fractures in hot rock 215-216

New Mexico—stratigraphy
Cretaceous: Coal in the central and east-central part of the San Juan Basin 27
Jurassic: A regional disconformity in Jurassic rocks of the San Juan Basin 48

New Mexico—structural geology
neotectonics: Concurrent regional faulting and silicic volcanism, Sangre de Cristo Mountains, New Mexico 86

New York—economic geology
mineral resources: Lineated granitic rocks mark early faults in the Beaver Creek Area, western St. Lawrence County, New York 6-7
uranium ores: Nature of uranium occurrences in the northern Reading Prong 46
water resources: New York 122-123

New York—environmental geology
pollution: Organic pollutants in ground water 123

New York—geophysical surveys
magnetic surveys: Evidence for fossilized rifts and reactivation of basement faults 189
seismic surveys: Lake sediments 166-167

New York—hydrogeology
ground water: Development of a Galerkin finite-element flow model for the transient response of a radially symmetric aquifer 123
— Ground-water quality of a postglacial sand-dune environment 123
— Preliminary hydrogeology of an artificial-recharge site 122
— Pumping test in southern Nassau County, Long Island 122
— Surficial geology and well guides in Oswego County 122
— Utilization of a regional ground-water-flow model to evaluate boundary conditions for a subregional model 123
hydrology: Hudson River Estuary flows 123
— Streamflow augmentation with ground water 239

New York—structural geology
tectonics: Evidence for fossilized rifts and reactivation of basement faults 189

New Zealand—economic geology
mineral resources: Interrelations among epithermal ore deposits and geothermal systems depositing mercury, gold and silver 209-210

nitrogen—abundance
surface water: Phosphorus and nitrogen as limiting nutrients in two arctic lakes 241

noble gases *see also* helium

nodules—manganese composition
composition: Compositional relations of manganese nodules and associated sediments 163

nonmetals *see also* sulfur

North America *see also* Appalachians; Atlantic Coastal Plain; Canada; Great Lakes; Great Lakes region; Great Plains; Gulf Coastal Plain; Mexico; Rocky Mountains; United States

North America—economic geology
uranium ores: Canadian, Australian, and United States uranium deposits compared 45-46

North America—stratigraphy
Ordovician: Early Paleozoic symmetry across southern North America 88
Paleozoic: Early Paleozoic symmetry across southern North America 88
Pennsylvanian: Intercontinental correlation of the Pennsylvanian System 24-25

North Carolina—areal geology
regional: Carolinas, Tennessee 66-67

North Carolina—economic geology
ceramic materials: Hypothetical submarginal kyanite resource, Craggy Mountain Wilderness Study Area, North Carolina 6
copper ores: Subvolcanic hydrothermal mineral deposits in the Carolina volcanic slate belt 7
metal ores: Cassiterite and columbite, Charlotte 2° quadrangle, North Carolina 14
— Gravity features related to location of mineral deposits in North Carolina 11-12
tin ores: Mineral-resource assessment of the Charlotte 2° quadrangle, North Carolina and South Carolina 4-5
water resources: North Carolina 132

North Carolina—geophysical surveys
magnetic surveys: Study of diabase dikes 188-189

North Carolina—hydrogeology
hydrology: Improvement in water quality of some rivers 132

North Carolina—petrology
metamorphic rocks: Diverse types of garnets in metasedimentary rocks of the Great Smoky Group, North Carolina and Tennessee 66-67
— Turbidite beds in the Albemarle Group, Carolina slate belt 66

North Carolina—structural geology
faults: Shear zones associated with the Kings Mountain belt in the Piedmont of the Carolinas 66

North Dakota—economic geology
water resources: North Dakota 137-138

North Dakota—hydrogeology
ground water: Aquifer evaluations, North Dakota 227
— Buried-valley aquifers, McKenzie County 137
— Surficial outwash aquifer in Logan County 137-138
— Test drilling and aquifer evaluation in Rattlesnake Butte area 137
hydrology: Hydrology of prairie wetlands 239

Northern Hemisphere *see also* Arctic Ocean; Asia; Atlantic Ocean; Europe; North America; Pacific Ocean; USSR

Northern Hemisphere—stratigraphy
Pliocene: Extent of Northern Hemisphere Pliocene glaciation 231

Northern Territory—economic geology
uranium ores: Geologic factors in evolution of unconformity-type uranium deposits 46-47

Northwest Territories—geochronology
Quaternary: Dating Arctic Quaternary raised marine deposits by uranium series and amino acids ratios 205-206

O

ocean circulation *see also under* oceanography *under* Alaska; Bering Sea; California; Texas

ocean circulation—patterns
monitoring: Ocean topography by radar altimetry for iceberg towing 243

ocean floors *see also under* oceanography *under* Bering Sea; Pacific Ocean; United States

ocean floors—bottom features
submarine fans: Submarine fans 164

ocean floors—exploration
mineral resources: Deep sea geology and resources 163-164

oceanography—sea ice
icebergs: Ocean topography by radar altimetry for iceberg towing 243
models: Sea-ice model 244
observations: Aircraft remote sensing of satellite Arctic program 242-243
— Passive microwave imagery time-lapse film of Arctic sea-ice variations 243
— Polar ice remote-sensing satellite program 243
— Sea-ice dynamics observed by radar imagery 243-244
research: Sea-ice studies 242-244

Ohio—economic geology
water resources: Ohio 124

Ohio—hydrogeology
ground water: Subsurface mines as a water source 124

oil and gas fields *see also under* economic geology *under* Rocky Mountains

oil shale *see also under* economic geology *under* automatic data processing

oil shale—resources
data bases: Oil shale and saline mineral data system 20

Oklahoma—economic geology
water resources: Oklahoma 138-139

Oklahoma—hydrogeology
ground water: Geohydrology of the Arbuckle-Simpson aquifer in south-central Oklahoma 138
— High Plains regional aquifer study 138
hydrology: Mine ponds, a hydrologic asset in eastern Oklahoma 138
— Model study of alluvial aquifer along the Beaver and the North Canadian rivers 138
— Streamflow and water-quality characteristics of Coal Creek basin near Lehigh 138-139
— Water from Gaines Creek and Gaines Creek arm of Lake Eufaula suitable for public supply 139

Ontario—economic geology
uranium ores: Lake Superior region favorable for quartz-pebble-type uranium deposits 45

ophiolite *see under* ultramafics *under* igneous rocks

Ordovician *see also under* geochronology *under* Idaho; *see also under* stratigraphy *under* Alaska; Montana; North America; Virginia

ore guides *see under* mineral exploration

Oregon—areal geology
regional: Oregon 92

Oregon—economic geology
geothermal energy: Hydrothermal alteration at Mount Hood, Oregon 59-60
— Upper crustal structure of the Mount Hood region, Oregon 214
iron ores: Massive sulfide deposits in ophiolitic terrain, northern Klamath Mountains, Oregon and California 12
nickel ores: Chromite and nickel, western Cordillera 8-9
uranium ores: Uranium in the Lakeview area, Oregon 43
water resources: Oregon 145-146

Oregon—geophysical surveys
electrical surveys: Extreme self-potential anomalies found on Mount Hood, Oregon 209
magnetic surveys: Big Craggies ultramafic body, Oregon 18-19
magnetotelluric surveys: Field tests of real-time magnetotelluric systems 216
seismic surveys: Lake sediments 166-167
— Upper crustal structure of the Mount Hood region, Oregon 214
surveys: Debris flows and turbidites filling the basin of Crater Lake 92

Oregon—hydrogeology
ground water: Digital simulation of a multilayer aquifer system near Portland 145
— Improvement in ground-water conditions near The Dalles 145-146
hydrology: Benthic oxygen demand in Portland Harbor 145
— Estimating effective impervious area with rural and urban rainfall-runoff models 145
springs: Chemical differences in Alvord Desert hot springs and cold springs 145

Oregon—oceanography
sedimentation: Heavy minerals of Tillamook Bay surface sediments 170
— Holocene sedimentation in the Tillamook embayment, Oregon 170

sediments: Gas within sediments of the northern California to Oregon Outer Continental Shelf 157

Oregon—petrology
volcanology: The climatic eruption of Mount Mazama, Oregon 198

Oregon—seismology
crust: Upper crustal structure of the Mount Hood region, Oregon 214

Oregon—tectonophysics
plate tectonics: Tectonic framework of the Oregon continental margin 161
— Tectonic rotation of the Seven Devils Group, Oregon and Idaho 180

organic materials—abundance
limestone: Organic carbon of seafloor middle Cretaceous limestones 163-164
sediments: Geochemistry of sediments and associated interstitial waters for the tidal Potomac River 167-168
— Pesticide partition between sediment and water 246
— Variations in nutrient and sediment concentrations in the Potomac River Estuary 167

organic materials—analysis
chemical analysis: Adenosine triphosphate in aquatic samples 245-246
— Methylation of humic and fulvic acids 246
— Organic compounds in bed sediment 246

organic materials—distribution
sediments: Distribution and stable-isotope composition of carbon in San Francisco Bay 172
shale: Distribution of organic matter in Devonian shale 38-39
uranium ores: Organic geochemistry and uranium in the Grants mineral belt 51

organic materials—experimental studies
volatilization: Volatilization of ketones from water 237
— Volatilization of priority pollutants from streams 237

organic materials—geochemistry
adsorption: Organic compounds on kaolinite 202

organic materials—humates
composition: Constitution of humic substances from aquatic and terrestrial sources 28

organic materials—hydrocarbons
distribution: Gas-charged sediments and associated features of the Alaskan Continental Shelf 157-158
— Gas within sediments of the northern California to Oregon Outer Continental Shelf 157
— Seismic study of a subsea gas accumulation off southern California 157
experimental studies: Anaerobic oxidation of acetylene by San Francisco Bay sediment slurries 171
genesis: Microbial formation of ethylene and ethane in San Francisco Bay sediments 171
— Production of hydrocarbons and alteration of sedimentary structures through compaction 41
methane: Methane-producing bacteria in deep aquifer 236
— Origin of hydrocarbons in Devonian shale 38
occurrence: Hydrocarbon gases in surface sediments of San Francisco Bay 171-172
properties: Economic implications of the solubility of crude oil in methane 40

orogeny—causes
Penokean Orogeny: Basement control of Proterozoic X Penokean orogen 75

orogeny—periodicity
Antler Orogeny: Sedimentation rates and timing of Antler orogenic events determined from conodont zonation, Western United States 37

orthosilicates *see under* minerals

ostracods—biostratigraphy
Pleistocene: Stratigraphy and structure of the Sankaty Head Cliffs, Nantucket Island 65

oxides *see under* minerals

oxygen—isotopes
O-18/O-16: A 100,000-year cave record of atmospheric temperatures 223
— Metallogenic and tectonic significance of isotopic data from the Nikolai Greenstone, McCarthy quadrangle 109-110
— Oxygen isotope studies of uranium source rocks 53-54

P

Pacific Coast—areal geology
regional: Pacific Coast region 92-102

Pacific Coast—economic geology
zinc ores: Massive sulfide deposits in ophiolitic terrain, northern Klamath Mountains, Oregon and California 12

Pacific Coast—geochronology
Paleogene: Preliminary uplift ages from fission-track studies 94

Pacific Coast—oceanography
marine geology: Pacific Coast 170-174
sediments: Shallow shelf and beach heavy-mineral concentrations 165

Pacific Coast—petrology
volcanology: Cascade volcanism 198

Pacific Coast—stratigraphy
Quaternary: Temperature aspects of late Quaternary marine molluscan faunas 231

Pacific Ocean *see also* Bering Sea

Pacific Ocean—geochemistry
organic materials: Organic carbon of seafloor middle Cretaceous limestones 163-164

Pacific Ocean—oceanography
ocean floors: Hydrothermal activity and massive sulfides on the East Pacific Rise 163
— Loihi Seamount; active submarine volcano 194

Pacific Ocean—stratigraphy
Miocene: Late Miocene Pacific correlation by Dictyocha neonautica Bukry 230-231
— Three periods of intense high-latitude cooling in the middle to late Miocene 231

Pacific Ocean—tectonophysics
sea-floor spreading: Hydrothermal activity and massive sulfides on the East Pacific Rise 163

Paleocene *see also under* stratigraphy *under* Alabama; Arkansas; Georgia; Montana

paleoclimatology—Cenozoic
California: Three-million-year record of climate in Searles Lake sediments 222

paleoclimatology—Holocene
Appalachians: Evidence of modern slope movement in the Appalachian Mountains 234
global: Holocene sea-level change; a possible record of global climatic change 224
Minnesota: Records of past climates in Elk Lake sediments 221
Montana: End of "Little Ice Age" in Glacier National Park 222

paleoclimatology—indicators
algae: Chrysomonad cysts as paleoenvironmental indicators 241

paleoclimatology—Miocene
Pacific Ocean: Three periods of intense high-latitude cooling in the middle to late Miocene 231

paleoclimatology—Pleistocene
Rocky Mountains: End of Pinedale Glaciation, north-central Colorado 222-223
— Late Pinedale Glaciation in the Northern Rocky Mountains 223
— Relation between late Pleistocene snowfields and "landslides" 223

paleoclimatology—Pliocene
Northern Hemisphere: Extent of Northern Hemisphere Pliocene glaciation 231

paleoclimatology—Quaternary
Atlantic Coastal Plain: Quaternary climates, eustacy, and tectonism, southeastern United States 231
California: A 100,000-year cave record of atmospheric temperatures 223
— Records of past climates in Clear Lake sediments 221
Pacific Coast: Temperature aspects of late Quaternary marine molluscan faunas 231
Rocky Mountains: Climatic influence on alluvial deposition, northwest Colorado 223-224
Wyoming: Records of past climates in lake sediments from Yellowstone Park area 221-222

paleoecology—indicators
lacustrine environment: Chrysomonad cysts as paleoenvironmental indicators 241

Paleogene *see also under* geochronology *under* Pacific Coast

paleogeography—Devonian
Alaska: Significance of Middle Devonian clastic rocks of the eastern Brooks Range 104

paleogeography—Eocene
Washington: Lower to middle Eocene seamount chain, northwest Olympic Peninsula 92-93
Wyoming: Early Eocene streams of the Bighorn Basin, Wyoming 78

paleogeography—Miocene
Nevada: Westward streamflow in Miocene of west-central Nevada 89

paleogeography—Paleozoic
Alaska: Collision-deformed Paleozoic continental margin of Alaska; foundation for microplate accretion 106-107

paleogeography—Pennsylvanian
Montana: Paleogeography and petroleum resources of Tyler Formation, central Montana 34

paleogeography—Permian
Colorado: Early Permian depositional systems and paleogeography, Uncompahgre Basin 47

paleomagnetism—experimental studies
magnetic properties: Maghemitization of oceanic crust 181

paleomagnetism—interpretation
magnetic anomalies: Random crustal magnetization and its effect on marine magnetic anomalies 181
rocks: Rock magnetism 180-181

paleomagnetism—Permian
Alaska: Paleomagnetism of Permian basalts 110

paleomagnetism—Pleistocene
Atlantic Coastal Plain: Paleomagnetic investigation of Pleistocene sediments of the Delmarva Peninsula, central Atlantic Coastal Plain 67

paleomagnetism—pole positions
rotation: Northward movement of the Chugach terrane, Alaska 180

paleomagnetism—Triassic
Oregon: Tectonic rotation of the Seven Devils Group, Oregon and Idaho 180

paleontology—general
research: Paleontology 229-233

Paleozoic *see also under* geochronology *under* Saudi Arabia; Virginia; *see also under* stratigraphy *under* Alaska; Idaho; North America

Paleozoic—paleontology
research: Paleozoic studies 232-233

palynomorphs—biostratigraphy
Paleocene: Dinoflagellates and increased biostratigraphic resolution 230

palynomorphs—miospores
Quaternary: Records of past climates in Clear Lake sediments 221
— Records of past climates in lake sediments from Yellowstone Park area 221-222

peat *see also under* economic geology *under* Maine; *see also under* organic residues *under* sediments

Pelecypoda *see* Bivalvia *under* Mollusca

Pennsylvania—areal geology
regional: Pennsylvania 67-68

Pennsylvania—economic geology
coal: Resources in Carbon County, Pennsylvania 25
water resources: Pennsylvania 124

Pennsylvania—geophysical surveys
seismic surveys: Seismic-refraction exploration, northwestern Pennsylvania 225

Pennsylvania—hydrogeology
ground water: Water-supply capability of carbonate rock, south-central Pennsylvania 124
hydrology: Premining water quality in the Stony Fork drainage basin, Fayette County 124

Pennsylvania—structural geology
tectonics: A plate tectonic model for the Hamburg klippe, eastern Pennsylvania 67-68

Pennsylvania—tectonophysics
plate tectonics: A plate tectonic model for the Hamburg klippe, eastern Pennsylvania 67-68

Pennsylvanian *see also under* stratigraphy *under* Eastern U.S.; Kentucky; Montana; North America; West Virginia

permafrost *see also under* engineering geology *under* Alaska; Arctic Ocean

Permian *see also under* stratigraphy *under* Alaska; Colorado

petroleum *see also under* economic geology *under* Alaska; Atlantic Ocean; automatic data processing; California; Florida; Gulf of Mexico; Montana; United States; USSR; Western U.S.; Wyoming

petroleum—exploration
reservoir rocks: Reduction of sandstone permeability through shale dewatering 40-41
— Significance of submarine slides on intercanyon continental margin slopes 41
techniques: New exploration and production techniques 40-41

petroleum—genesis
source rocks: Production of hydrocarbons and alteration of sedimentary structures through compaction 41

petroleum—production
reservoir rocks: Economic implications of the solubility of crude oil in methane 40

petroleum—resources
evaluation: Petroleum resource appraisal and discovery process modeling 21

petrology—general
research: Geochemistry, mineralogy, and petrology 189-208

petrology—methods
graphic methods: Correct use of the rule of tangents and its petrologic applications 189
statistical methods: R-mode and Q-mode factor analysis 203
— Statistical geochemistry and petrology 203

Phanerozoic *see also* Mesozoic; *see also under* stratigraphy *under* Basin and Range Province; Great Plains; Rocky Mountains

phase equilibria—chain silicates, clinopyroxene
experimental studies: Decomposition mechanism and kinetics in clinopyroxenes 190-191

phase equilibria—experimental studies
Fe-S-O: Melting relations in the system Fe-S-O 191

phase equilibria—minerals
CaO-Al_2O_3-SiO_2-H_2O: Reevaluation of the thermodynamic properties of minerals in the system CaO-Al_2O_3-SiO_2-H_2O 190
experimental studies: Thermodynamic properties of minerals 191
theoretical studies: Relations between lattice dynamics and thermodynamic properties of minerals 189-190

phase equilibria—silicates
MgO-FeO-SiO_2: Correct use of the rule of tangents and its petrologic applications 189

phosphate deposits—resources
evaluation: Estimation of world phosphate resources 21
— Phosphorite 22

phosphorus—abundance
surface water: Phosphorus and nitrogen as limiting nutrients in two arctic lakes 241
— Phosphorus loading of lake water related to land uses 238
— Point-source discharge of phosphorus into the Potomac River 244

placers—gold ores
Alaska: Gold placers in the Mount Hayes quandrangle 109
Wyoming: Gold in Oligocene conglomerate, southeast margin of Wind River Mountains, Wyoming 76

placers—heavy mineral deposits
North Carolina: Mineral-resource assessment of the Charlotte 2° quadrangle, North Carolina and South Carolina 4-5

planetology *see also* Mars

Plantae *see also* algae; angiosperms; palynomorphs; Protista

Plantae—biostratigraphy
Pennsylvanian: Extension of age terrestrial vertebrates 232
— Geology of the Mississippian and Pennsylvanian of north-central Alabama 69-70

Plantae—ecology
estuarine environment: Potomac Estuary Study 233
research: Plant ecology 233-234
wetlands: Plant distributions in the tidal wetlands of the Sacramento-San Joaquin River Delta 173-174
— Sacramento-San Joaquin Delta wetlands, San Francisco Bay, California 167

plate tectonics *see also under* tectonophysics *under* Alaska; Appalachians; California; Idaho; Oregon; Pennsylvania

Pleistocene *see also under* geochronology *under* Alaska; Atlantic Coastal Plain; California; Nevada; Wyoming; *see also under* stratigraphy *under* Colorado; Massachusetts; Rocky Mountains; Washington

Pliocene *see also under* stratigraphy *under* Atlantic Ocean; Northern Hemisphere

plutons *see under* intrusions

pollution *see also under* environmental geology *under* Alabama; Arizona; Arkansas; Atlantic Coastal Plain; California; Florida; Georgia; Kentucky; Louisiana; Maryland; Michigan; Mississippi; Nebraska; New York; Tennessee; Virginia; Washington; Wisconsin; Wyoming

pollution—detection
techniques: Organic compounds in bed sediment 246
tracers: Lithium as a tracer 202

pollution—pollutants
coal: Mobilization of elements resulting from use of coal 29-30
organic materials: Volatilization of ketones from water 237
— Volatilization of priority pollutants from streams 237
pesticides: Pesticide partition between sediment and water 246
transport: Solute transport in porous media 238

pollution—water
water quality: Areawide chemical loading 238
— Chemical and biological quality of ground water 235-236
— Chemical and biological quality of surface water 234-235
— Chemical, physical, and biological properties of water 234-238
— Ground-water-quality models and processes 238
— Surface-water-quality models and processes 237

polymetallic ores *see also* gold; *see also under* economic geology *under* Alaska

Precambrian *see also under* geochronology *under* Minnesota; *see also under* stratigraphy *under* Great Plains; Rocky Mountains; South Dakota; Wyoming

Proterozoic *see also under* geochronology *under* Alaska; Arabian Peninsula; Idaho; New Mexico; *see also under* stratigraphy *under* Montana

Protista—biostratigraphy
Miocene: Late Miocene Pacific correlation by Dictyocha neonautica Bukry 230-231

Protozoa *see* Protista

Puerto Rico—economic geology
copper ores: Geochemical study of water and sediment, Rio Tanama district, Puerto Rico 16

Puerto Rico—oceanography
marine geology: Investigations and mapping of insular shelves 164

Q

Quaternary *see also under* geochronology *under* Alabama; California; Northwest Territories; Western U.S.; *see also under* stratigraphy *under* Alaska; California; Colorado; Eastern U.S.; Pacific Coast; Rocky Mountains; Wyoming

R

radioactive dating *see* absolute age

rare earths *see also* neodymium

rare earths—abundance
gneisses: "Monson Gneiss", eastern Connecticut 61
granites: Geochemical comparison of mineralized and barren stocks, Arizona 10
— Trace-element patterns in spatially related plutonic differentiation suites 45
intrusive rocks: Alkaline intrusive complexes, Wet Mountains, Colorado 42

rare earths—geochemistry
marine sediments: Compositional relations of manganese nodules and associated sediments 163

reclamation *see also under* environmental geology *under* Montana; Southwestern U.S.; Western U.S.

reefs *see also under* oceanography *under* Gulf of Mexico

regional geology *see* areal geology under the appropriate area term

remote sensing *see also* geophysical methods; *see also under* geophysical surveys *under* Antarctica; Arctic Ocean; Arizona; Asia; automatic data processing; Missouri; New Mexico; USSR; Utah; Wyoming

remote sensing—applications
mineral exploration: Remote detection of geochemical soil anomalies 16
— Remote sensing applied to geochemical exploration 16
sea ice: Ocean topography by radar altimetry for iceberg towing 243

remote sensing—interpretation
lineaments: Analysis of linear features 17-18
spectral analysis: Spectral signatures in the 0.4- to 1.1-m range 183-184

Reptilia—Pelycosauria
Pennsylvanian: Extension of age terrestrial vertebrates 232

reservoirs *see also under* engineering geology *under* Utah

Rhode Island—economic geology
coal: Rank of coal in the Narragansett Basin, Rhode Island 25
water resources: Rhode Island 124

Rhode Island—hydrogeology
ground water: Hydraulic properties of an anisotropic water-table aquifer in the Chipuxet River basin 124

rock mechanics *see also* soil mechanics

rock mechanics—deformation
friction: Internal friction experiments in granite 212-213

rock mechanics—experimental studies
spectral analysis: Spectral signatures in the 0.4- to 1.1-m range 183-184

rock mechanics—materials, properties
electrical properties: Electrical properties of geothermal materials 184
physical properties: Porosity, permeability, distribution coefficients, and dispersivity 227
research: Petrophysics 183-185
reservoir properties: Rock units of the eastern Gulf of Alaska Outer Continental Shelf 161
thermal properties: Thermal properties of rocks 212

rock mechanics—methods
statistical methods: Physical property statistics and geologic noise 184

Rocky Mountains—areal geology
regional: Rocky Mountains and the Great Plains 76-87

Rocky Mountains—economic geology
fuel resources: Rocky Mountains and Great Plains 33-37
mineral resources: Economic geology 76
natural gas: Origin and accumulation of biogenic gas in the Rocky Mountains 33
oil and gas fields: Seismic models of stratigraphically controlled oil fields and gas fields in Rocky Mountain basins 33

Rocky Mountains—environmental geology
surveys: Environmental geology 76-77

Rocky Mountains—petrology
igneous rocks: Igneous rocks 79-81

Rocky Mountains—stratigraphy
Phanerozoic: Stratigraphy 77-78
Pleistocene: End of Pinedale Glaciation, north-central Colorado 222-223
— Late Pinedale Glaciation in the Northern Rocky Mountains 223
— Relation between late Pleistocene snowfields and "landslides" 223
Precambrian: Precambrian rocks 81-82
Quaternary: Climatic influence on alluvial deposition, northwest Colorado 223-224

Rocky Mountains—structural geology
tectonics: Tectonics 82-87

Russia *see* USSR

S

salt tectonics *see also under* structural geology *under* Gulf of Mexico; Utah

sandstone *see also under* clastic rocks *under* sedimentary rocks

Saskatchewan—economic geology
uranium ores: Geologic factors in evolution of unconformity-type uranium deposits 46-47

Saudi Arabia—geochronology
Paleozoic: Lead isotopes indicate tectonic division in Saudi Arabia 206

Saudi Arabia—structural geology
tectonics: Lead isotopes indicate tectonic division in Saudi Arabia 206

sea-floor spreading *see also under* tectonophysics *under* Pacific Ocean

sea water—composition
seasonal variations: Seasonal distributions of water properties in San Francisco Bay 172
suspended materials: Suspended matter in continental shelf and slope waters of the Georges Bank area 155

sedimentary petrology—general
research: Sedimentology 217-219

sedimentary petrology—instruments
research: Instrumentation 219
samplers: New large volume depth-integrating sampler 219

sedimentary rocks *see also* sedimentary structures; sedimentation; sediments

sedimentary rocks—carbonate rocks
limestone: Organic carbon of seafloor middle Cretaceous limestones 163-164
travertine: Travertine at Poncha Hot Springs, Chaffee County, Colorado 13

sedimentary rocks—clastic rocks
bentonite: Middle and Late Devonian ashfall beds in Devonian shale 74
black shale: Significance of Middle Devonian clastic rocks of the eastern Brooks Range 104
breccia: Lower to middle Eocene seamount chain, northwest Olympic Peninsula 92-93
conglomerate: Regional stratigraphy and depositional environment of the Kanayut Conglomerate 105
— Source terrane for basement clasts of the Temblor Range 99
flysch: Lower Paleozoic rock fragments in Antler flysch, northern Nevada 88
petrology: Petrology of rocks from the Pribilof Islands region, southern Bering Sea shelf 162-163
sandstone: Depositional environment of the Groat Sandstone Bed in the northern Black Hills, Montana 77-78
— Reduction of sandstone permeability through shale dewatering 40-41
shale: Porosity of Miocene siliceous shale, Midway-Sunset oil field, California 37

sedimentary rocks—lithostratigraphy
Ordovician: Identification of Ordovician rocks in Lake Minchumina area 106

sedimentary rocks—organic residues
coal: Application of automatic image analysis to coal petrography 30
— Chalcophile elements and uranium in coal 28
— Distribution and genesis of primary pyrite in coal 29
— Electrolytic oxidation of coal 30
— Geochemistry 28-30
— Laboratory and field analytical techniques 30-31
— Resin rods in Upper Pennsylvanian coal beds 25
— Sulfur accumulation in coal 28-29
— Zinc and cadmium content of coal in the Interior coal province 28
vitrinite: Vitrinite reflectance geothermometry in the Cerro Prieto geothermal system, Baja California, Mexico 60

sedimentary rocks—properties
reservoir properties: Rock units of the eastern Gulf of Alaska Outer Continental Shelf 161

sedimentary structures *see also* sedimentary rocks; sediments

sedimentary structures—interpretation
preservation: Production of hydrocarbons and alteration of sedimentary structures through compaction 41

sedimentary structures—planar bedding structures
cross-bedding: Early Eocene streams of the Bighorn Basin, Wyoming 78
cross-stratification: Westward streamflow in Miocene of west-central Nevada 89

sedimentation—controls
paleoclimatologic controls: Climatic influence on alluvial deposition, northwest Colorado 223-224
tectonic controls: Basin-fill deposits of Beaver Valley, southwestern Utah 78
— Neotectonics in Kansas 84
— Sedimentology of the Neogene Little Sulphur Creek basins 97
— Southern Sierra Nevada uplift history 99
— Tertiary gravels, Little Belt Mountains, Montana 78
— Upper Quaternary stratigraphy and structure of the Antelope Valley and vicinity, California 100

sedimentation—cyclic processes
lacustrine sedimentation: Records of past climates in Elk Lake sediments 221

sedimentation—environment
braided streams: Early Permian depositional systems and paleogeography, Uncompahgre Basin 47
— Salt Wash depositional environments and uranium 48
estuarine environment: Geochemistry of sediments and associated interstitial waters for the tidal Potomac River 167-168
— Variations in nutrient and sediment concentrations in the Potomac River Estuary 167
fluvial environment: Regional stratigraphy and depositional environment of the Kanayut Conglomerate 105
lacustrine environment: A model for sedimentation at the Anderson mine, west-central Arizona 50
— Three-million-year record of climate in Searles Lake sediments 222
marine environment: Late Cenozoic marine deposition, Southeastern United States 70
shelf environment: Depositional environment of the Groat Sandstone Bed in the northern Black Hills, Montana 77-78
submarine fans: Submarine fans 164

sedimentation—processes
deltaic sedimentation: Tidal wetland deposits of the Sacramento-San Joaquin Delta 170-171
erosion: Variability of sediments yields 217
estuarine sedimentation: Heavy minerals of Tillamook Bay surface sediments 170
— Holocene sedimentation in the Tillamook embayment, Oregon 170
— Interdisciplinary study of the Potomac River Estuary 166
— Shallow stratigraphy of the Potomac River Estuary 167
fluvial sedimentation: Early Eocene streams of the Bighorn Basin, Wyoming 78
— Pleistocene and Holocene valley fill in coastal plain streams, eastern Alabama 69
glaciomarine sedimentation: Quaternary sedimentary facies of the northeast Gulf of Alaska Continental Shelf 158-159
lacustrine sedimentation: Lake sediments 166-167
marine sedimentation: Modern continental shelf sediment accumulation off southern New England 154-155
— Neogene sedimentation, southern Bering Sea 159
— Surface turbidity and hydrographic variability on the South Texas Continental Shelf 155
— Suspended matter in continental shelf and slope waters of the Georges Bank area 155
nearshore sedimentation: Coastal sedimentary processes off beaches 165

sedimentation—provenance
conglomerate: Source terrane for basement clasts of the Temblor Range 99
flysch: Lower Paleozoic rock fragments in Antler flysch, northern Nevada 88
heavy minerals: Shallow shelf and beach heavy-mineral concentrations 165
paleocurrents: Westward streamflow in Miocene of west-central Nevada 89

sedimentation—rates
indicators: Sedimentation rates and timing of Antler orogenic events determined from conodont zonation, Western United States 37

sedimentation—transport
marine transport: Alaskan Continental Shelf sediment dynamics 156-157
— California continental margin sediment dynamics 156
— Coastal erosion and sediment transport, the Puget Sound region 94
— Seafloor erosion and deposition, northern Bering Sea 158
stream transport: Aggradation of Powder River valley during 1978 flood 218
— Bedload movement in East Fork River, Wyoming 218
— Channel morphology and sedimentation in Pheasant Branch near Middleton, Wisconsin 217-218

— Laboratory study of bedload-transport processes 219
— Sediment transport 218-219
— Sediment yields in northeastern Indiana 217
— Storm sediment yield measured in Nederlo Creek basin, Wisconsin 217
— Suspended-sediment discharge in northeastern Wyoming streams 218
— The nature of bedload-material transport, New River, Tennessee 218-219
— Total sediment load, Snake and Clearwater Rivers near Lewiston, Idaho 218
— Upland gravel, northeastern Arkansas 74-75
turbidity currents: Debris flows and turbidites filling the basin of Crater Lake 92
— Significance of submarine slides on intercanyon continental margin slopes 41
— Turbidite beds in the Albemarle Group, Carolina slate belt 66
wind transport: Ancient eolian deposits in western Great Plains 220-221
sediments *see also* sedimentary rocks; sedimentary structures; sedimentation
sediments—clastic sediments
alluvium: Climatic influence on alluvial deposition, northwest Colorado 223-224
clay: Bootlegger Cove Clay; geographic and stratigraphic mollusk occurrences 111
— Saprolitic clay preserved in limestone selection depressions near East Canaan, Connecticut 63
diamicton: Diamictons of the Strait of Juan de Fuca 93-94
drift: Stratigraphy and structure of the Sankaty Head Cliffs, Nantucket Island 65
gravel: Tertiary gravels, Little Belt Mountains, Montana 78
— Upland gravel, northeastern Arkansas 74-75
till: Discovery of upper Wisconsinan glacial till on the Continental Shelf off southeastern New England 66
sediments—composition
heavy minerals: Shallow shelf and beach heavy-mineral concentrations 165
organic materials: Organic compounds in bed sediment 246
— Pesticide partition between sediment and water 246
sediments—environmental analysis
deltaic environment: Tidal wetland deposits of the Sacramento-San Joaquin Delta 170-171
glaciomarine environment: Quaternary sedimentary facies of the northeast Gulf of Alaska Continental Shelf 158-159
sediments—geochemistry
organic materials: Anaerobic oxidation of acetylene by San Francisco Bay sediment slurries 171
— Distribution and stable-isotope composition of carbon in San Francisco Bay 172
— Hydrocarbon gases in surface sediments of San Francisco Bay 171-172
— Microbial formation of ethylene and ethane in San Francisco Bay sediments 171
pore water: Geochemistry of sediments and associated interstitial waters for the tidal Potomac River 167-168
trace elements: Interdisciplinary study of the Potomac River Estuary 166
sediments—lithostratigraphy
Pleistocene: Glacial stratigraphy of Cape Cod, Nantucket, and Martha's Vineyard, Massachusetts 65-66
sediments—marine sediments
distribution: Investigations and mapping of insular shelves 164
geochemistry: Compositional relations of manganese nodules and associated sediments 163
— Correlation of trace elements between sediments and benthic fauna 166
organic materials: Gas-charged sediments and associated features of the Alaskan Continental Shelf 157-158
— Gas within sediments of the northern California to Oregon Outer Continental Shelf 157
— Seismic study of a subsea gas accumulation off southern California 157
pore water: Subsurface hypersaline brines 166
sediments—organic residues
peat: Distribution and genesis of primary pyrite in coal 29
sediments—provenance
heavy minerals: Heavy minerals of Tillamook Bay surface sediments 170
seepage *see under* hydrology
seismic surveys *see under* geophysical surveys *under* Appalachians; Atlantic Coastal Plain; Bering Sea; California; Great Lakes; Gulf of Mexico; Idaho; New Jersey; New York; Oregon; Pennsylvania
seismology *see also* engineering geology
seismology—crust
velocity structure: Seismic velocity structure at Coso geothermal area 214
— Upper crustal structure beneath the Coso Range, California 214
— Upper crustal structure of the Mount Hood region, Oregon 214
seismology—earthquakes
seismic risk: Seismic zonation of geologic materials, Seattle area 93
seismology—elastic waves
P-waves: P-wave delays at two geothermal areas 215
seismology—seismicity
seismotectonics: Earthquake localities and surficial and buried faults correspondence, Kentucky 75
shale *see under* clastic rocks *under* sedimentary rocks
shear zones *see under* effects *under* faults
shore features *see under* geomorphology
shorelines *see also under* engineering geology *under* Washington
silicates *see under* minerals
sills *see under* intrusions
slope stability *see also* engineering geology; geomorphology; *see also under* engineering geology *under* Appalachians; Atlantic Ocean; United States; Washington
slope stability—failure
classification: New techniques applied to studies of seafloor hazards and conditions 152-153
soil mechanics *see also* rock mechanics
soil mechanics—materials, properties
regolith: Mineralogical, chemical, and physical properties of regolith over crystalline rocks, Fairfax County, Virginia 71
soils—erosion
wind erosion: Satellite relay meteorological stations to study wind erosion 220
soils—field studies
remote sensing: Remote detection of geochemical soil anomalies 16
soils—surveys
Colorado: Helium and sulfur, Poorman fault, Colorado 16
Georgia: Effects of agriculture on stream quality, southwestern Georgia 238
Virginia: Soil stratigraphy on fluvial terraces of the Potomac and Rappahannock Rivers, Virginia 73-74
Western U.S.: Quantitative pedology as a dating technique in the Western United States 92
soils—water regimes
movement: Solute transport in porous media 238
— Water flow in the saturated zone 238-239
solubility *see under* properties *under* geochemistry
South Carolina—areal geology
regional: Carolinas, Tennessee 66-67
— South Carolina, Georgia, and Alabama 68-70
South Carolina—economic geology
copper ores: Subvolcanic hydrothermal mineral deposits in the Carolina volcanic slate belt 7
gold ores: Gold in South Carolina 18
monazite deposits: Mineral-resource assessment of the Charlotte 2° quadrangle, North Carolina and South Carolina 4-5
water resources: South Carolina 132
South Carolina—geophysical surveys
electromagnetic surveys: Gold in South Carolina 18
magnetic surveys: Aeromagnetic study of subsurface pre-Cretaceous rocks, Georgia and South Carolina coastal plains 70-71
South Carolina—hydrogeology
hydrology: Water-supply supplement from Intercoastal waterway 132
South Carolina—stratigraphy
Cretaceous: First recognition of the molluscan Exogyra cancellata subzone, South Carolina 229

South Carolina—structural geology
faults: Shear zones associated with the Kings Mountain belt in the Piedmont of the Carolinas 66

South Dakota—economic geology
water resources: South Dakota 139

South Dakota—hydrogeology
ground water: Aquifer test of a glacial-outwash aquifer in central South Dakota 139
— Tertiary bedrock outliers and preglacial channels of western origin in Yankton County 139

South Dakota—stratigraphy
Precambrian: Comparison of Precambrian rocks of the Hartville uplift, eastern Wyoming, and of the Black Hills, western South Dakota 81-82

Southern Hemisphere *see also* Antarctica; Atlantic Ocean; Pacific Ocean

Southern U.S.—areal geology
regional: Central region 74-76

Southwestern U.S.—economic geology
lithium ores: Identification of domestic lithium resources 22

Southwestern U.S.—environmental geology
reclamation: Participation in the interagency Energy Minerals Rehabilitation Inventory and Analysis Program 24

Soviet Union *see* USSR

spectrometry *see* spectroscopy

spectroscopy—methods
atomic absorption: Atomic absorption method for arsenic 17
— Germanium concentrations in USGS rock standards as determined by electrothermal atomization atomic absorption spectrometry 244
— Sensitive method for gold analysis 17
electron probe: Combined energy dispersive and wavelength dispersive analysis 191
gamma-ray spectroscopy: Application of high resolution gamma-ray spectrometry to uranium prospecting 57
— In situ capture gamma-ray analysis of coal in oversized boreholes 30-31
infrared spectroscopy: Near-infrared spectroscopy determination of degree of serpentinization in ultramafic rocks 185
optical spectroscopy: Determination of nanogram amounts of bismuth in silicate rocks 244
— Induction-coupled plasma spectroscopy 17
— Optical spectroscopy 244
X-ray spectroscopy: X-ray spectroscopy 244

Spermatophyta—ecology
floodplains: Damage to flood-plain forests along the Potomac River 233
— Trees of the Apalachicola River flood plain 234

springs *see also* ground water; *see also under* hydrogeology *under* Arizona; Colorado; Oregon; Utah

standard materials—analysis
spectroscopy: Determination of nanogram amounts of bismuth in silicate rocks 244
— Germanium concentrations in USGS rock standards as determined by electrothermal atomization atomic absorption spectrometry 244

strontium—isotopes
Sr-87/Sr-86: Alkaline intrusive complexes, Wet Mountains, Colorado 42
— Inclusions in upper Cenozoic volcanic rocks of the central Sierra Nevada, California 201
— Initial strontium ratios of plutonic rocks along the "Uinta trend," northwestern Utah 9
— Strontium isotopes along the Uinta trend 203-204

structural analysis *see also* folds

structural analysis—fractures
joints: Surface joint patterns as a guide to fracture reservoirs 39

structural analysis—interpretation
melange: Tectonism and plutonism, northwestern Sierra Nevada 98
petrofabrics: Metamorphic terrane in Pilot Range of Nevada and Utah 87-88
— Mylonitic gneisses over a Cretaceous(?) pluton, Iron Mountains, southeastern California 100-101
— Upper Mesozoic rocks of the Wilbur Springs antiform 97
structural complexes: Structural analysis of plutonic and metamorphic rocks from an area east of Wrangell 113

structural petrology *see* structural analysis

sulfides *see under* minerals

sulfur—abundance
coal: Sulfur accumulation in coal 28-29
soils: Helium and sulfur, Poorman fault, Colorado 16

sulfur—geochemistry
peat: Distribution and genesis of primary pyrite in coal 29

sulfur—isotopes
S-34/S-32: Massive copper sulfide deposit of syngenetic-epigenetic origin, north-central Nevada 9-10

sulphur *see* Sulfur

survey organizations—current research
U. S. Geological Survey: Participation in the interagency Energy Minerals Rehabilitation Inventory and Analysis Program 24

surveys—current research
U. S. Geological Survey: USGS-EPA urban studies 148

T

tectonics *see also* faults; folds; orogeny; structural analysis; *see also under* structural geology *under* Alaska; Arizona; Basin and Range Province; California; Colorado; Columbia Plateau; Connecticut; Georgia; Great Lakes region; Great Plains; Idaho; Kentucky; Massachusetts; Midwest; Mississippi Valley; Montana; Nevada; New England; New Jersey; New York; Pennsylvania; Rocky Mountains; Saudi Arabia; Utah; Virginia; Washington; Western U.S.

Tennessee—areal geology
regional: Carolinas, Tennessee 66-67

Tennessee—economic geology
mineral resources: Mineral-resource assessment of the Big Frog Wilderness Study Area, Tennessee and Georgia 5-6
water resources: Tennessee 132-133

Tennessee—environmental geology
pollution: Strontium-90 transport through solution cavities in limestone 133

Tennessee—hydrogeology
ground water: Ground water related to weathering products of facies of Fort Payne Formation 132-133

Tennessee—petrology
metamorphic rocks: Diverse types of garnets in metasedimentary rocks of the Great Smoky Group, North Carolina and Tennessee 66-67

Tennessee—sedimentary petrology
sedimentation: The nature of bedload-material transport, New River, Tennessee 218-219

tephrochronology *see under* geochronology

Tertiary *see also under* geochronology *under* Arizona; *see also under* stratigraphy *under* Alabama; Georgia; Montana

Texas—economic geology
sulfur deposits: Estimation of sulfur reserves using borehole gravimetry 41
uranium ores: Helium detection for uranium exploration 57
— Presence of ore-stage marcasite and formation of roll-type deposits 52-53
water resources: Texas 139-140

Texas—environmental geology
ecology: Correlation of trace elements between sediments and benthic fauna 166
geologic hazards: Flood-frequency study 148-149

Texas—geomorphology
shore features: Migration of Oregon coastal dunes 165

Texas—hydrogeology
ground water: Effects of faults on the direction of flow in the Edwards aquifer 139-140
— Jasper aquifer overlain by effective confining layer 140
hydrology: Source areas of salinity and trends of salt loads in streamflow in the upper Colorado River 140

Texas—oceanography
continental slope: Continental slope stratigraphy of Texas and Louisiana 160-161
ocean circulation: Surface turbidity and hydrographic variability on the South Texas Continental Shelf 155

thermal waters *see also under* hydrogeology *under* Colorado; Idaho; Mexico; Nevada; Washington; Wyoming

thrust faults *see under* displacements *under* faults

titanium ores—possibilities
recovery: Recovering rutile from porphyry copper deposits 7-8
trace elements *see under* geochemical methods *under* mineral exploration; *see under* geochemistry *under* Arizona; Connecticut; Georgia; Gulf of Mexico; lava; magmas; metals; Midwest; New England; sediments
Triassic *see also under* geochronology *under* Alaska
trilobites—biostratigraphy
Cambrian: Correlation of Cambrian formations in southwestern Montana 77

U

underground water *see* ground water
United States *see also* the individual states and regions
United States—areal geology
regional: Regional geologic investigations 61-114
United States—economic geology
coal: Coal analysis 24-31
— Computerization of the nation's resources 24
energy sources: Nuclear-fuel resources 41-59
fuel resources: Oil and gas resources 31-41
geothermal energy: Geothermal resources 59-60
mineral resources: United States and world mineral-resource assessments 1
petroleum: Petroleum resources of Outer Continental Shelf area 40
uranium ores: Canadian, Australian, and United States uranium deposits compared 45-46
— Nuclear-fuel resources 41-59
water resources: Special water-resource programs 146-151
— Urban water programs 148-150
— Water-resource investigations 115-151
United States—engineering geology
slope stability: Mass movement potential on the United States continental margins 153
United States—environmental geology
conservation: Management of natural resources on Federal and Indian lands 175-179
geologic hazards: Continental margin hazards and geologic environment of the seafloor 152-159
— Mass movement potential on the United States continental margins 153
land use: Urban water programs 148-150
— USGS-EPA urban studies 148
United States—geomorphology
maps: Average elevation map of the conterminous United States 213
United States—geophysical surveys
magnetic surveys: New magnetic declination map of the United States 182
maps: New magnetic declination map of the United States 182
United States—hydrogeology
ground water: Regional aquifer-system analysis program 150-151
United States—oceanography
continental shelf: Petroleum resources of Outer Continental Shelf area 40
marine geology: Coastal and limnological studies 164-167
— Coastal and marine geology 152-167
— Continental margin geologic framework and resource studies 159-163
— Estuarine and coastal hydrology 167-174
— Marine geology and coastal hydrology 152-174
ocean floors: Continental margin hazards and geologic environment of the seafloor 152-159
United States—structural geology
maps: Maps of vertical movements during the past 10 million years, conterminous United States 114
neotectonics: Maps of vertical movements during the past 10 million years, conterminous United States 114
uranium—abundance
coal: Chalcophile elements and uranium in coal 28
uranium ores—exploration
geobotanical methods: Uranium concentration by moss and algae from surface water 56-57
radioactivity methods: Application of high resolution gamma-ray spectrometry to uranium prospecting 57
well-logging: Borehole measurements to differentiate sulfides and clays 186
uranium ores—genesis
experimental studies: Uraniferous silica; conditions of formation 55
— Uranium adsorption onto montmorillonite 53
— Uranium leachability from freshly erupted volcanic ash of basaltic and dacitic composition 55-56
geochemical controls: A precipitation mechanism for hydrothermal vein-type uranium deposits 56
— Dissolved free oxygen and the genesis of sandstone-type uranium deposits 52
— Experimental studies on uranyl ion reduction by H_2O reveal a marked pH dependence 52
— Pyrite and marcasite in roll-type uranium deposits 53
— Uranium (VI) sorption by iron oxides 52
uranium ores—resources
evaluation: Uranium resource analysis 22
USSR—economic geology
petroleum: Petroleum geology of Volga-Ural petroleum province 40
USSR—geophysical surveys
remote sensing: Glacier surges monitored by satellite 219
Utah—economic geology
beryllium ores: Fluorine, beryllium, and uranium mineralization in Thomas Range, western Utah 42-43
— Geochemical uranium, fluorite, and beryllium ore controls at Spor Mountain 54
coal: Alton and Kolob coal fields, Cedar City 1° x 2° quadrangle, Utah 76
— Predictive model for Cretaceous deltaic coals of Utah 26
— Wasatch Plateau coal field, Utah 26
geothermal energy: P-wave delays at two geothermal areas 215
metal ores: Initial strontium ratios of plutonic rocks along the "Uinta trend," northwestern Utah 9
mineral resources: Southern Utah 17-18
uranium ores: Distribution and mobility of uranium in glassy and zeolitized tuff, Keg Mountain area, Utah 55
— Fluorine, beryllium, and uranium mineralization in Thomas Range, western Utah 42-43
— Geochemical studies of a tabular uranium ore body 53
— Geochemical uranium, fluorite, and beryllium ore controls at Spor Mountain 54
— Model for the origin of hydrothermal uranium deposits near Marysvale, Utah 11
— Mudstone as uranium exploration guide 47-48
— Potential uranium mineralization, Mineral Mountains, Utah 13
— Uranium occurrence in southern Wah Wah Range, Utah 57
— Use of uranium-lead isotope systematics to date uraniferous opals 54
water resources: Utah 140
Utah—engineering geology
reservoirs: Seepage and reservoir studies in the Price River basin 140
Utah—environmental geology
land use: Geologic maps of possible sites for proposed coal-fired powerplants, central Utah 77
maps: Geologic maps of possible sites for proposed coal-fired powerplants, central Utah 77
Utah—geochemistry
isotopes: Strontium isotopes along the Uinta trend 203-204
Utah—geochronology
Holocene: Persistent low level of Lake Bonneville during last 10,000 years 91-92
Utah—geomorphology
changes of level: Persistent low level of Lake Bonneville during last 10,000 years 91-92
Utah—geophysical surveys
remote sensing: Southern Utah 17-18
Utah—hydrogeology
ground water: Navajo Sandstone; a source of ground water for future energy-related development in the northern San Rafael Swell area 140

springs: Seepage and reservoir studies in the Price River basin 140

Utah—petrology
igneous rocks: Caldera source of Miocene Osiris Tuff, southwestern Utah 81-82
lava: Mafic flows in the Cedar Breaks-Panguitch Lake area, Utah 81

Utah—seismology
crust: P-wave delays at two geothermal areas 215

Utah—stratigraphy
Cretaceous: Predictive model for Cretaceous deltaic coals of Utah 26
— Wasatch Plateau coal field, Utah 26
Jurassic: A regional disconformity in Jurassic rocks of the San Juan Basin 48

Utah—structural geology
neotectonics: Basin-fill deposits of Beaver Valley, southwestern Utah 78
salt tectonics: An alternative explanation for some "orogenies" in central Utah 86-87
tectonics: Metamorphic terrane in Pilot Range of Nevada and Utah 87-88

V

varves *see* lacustrine features *under* geomorphology; *see under* geochronology

Vermont—economic geology
metal ores: Tourmaline associated with New England massive sulfide deposits 7

Vermont—geophysical surveys
magnetic surveys: Magnetic declination measurements in Vermont 182

Vertebrata *see also* Reptilia

Virginia—areal geology
regional: Virginia 71-74

Virginia—economic geology
coal: Coal quality in the Pocahontas field, Virginia and West Virginia 25
lead ores: Ore bodies at Great Gossan Lead, Virginia 7
metal ores: Cumulate and supercumulate nelsonite, central Virginia 7
water resources: Virginia 124-125

Virginia—environmental geology
pollution: Water monitoring of coal-mining areas, Virginia 234

Virginia—geochronology
Paleozoic: Paleozoic events in the Piedmont near Fredericksburg, Virginia 71
— Paleozoic events in the Piedmont near Fredericksburg, Virginia 207-208

Virginia—geomorphology
fluvial features: Scarp degradation and morphological modification of fluvial terraces along the Rappahannock River, Virginia 73

Virginia—hydrogeology
ground water: Ground-water resources in James City County evaluated 125
— Hydrogeology of the Culpeper Basin 125
hydrology: Hydrologic data collection, Great Dismal Swamp 124-125

Virginia—petrology
igneous rocks: Proterozoic Y zoned ash-flow sheet, Mount Rogers, Virginia 198-199

Virginia—sedimentary petrology
weathering: Mineralogical, chemical, and physical properties of regolith over crystalline rocks, Fairfax County, Virginia 71

Virginia—soils
surveys: Soil stratigraphy on fluvial terraces of the Potomac and Rappahannock Rivers, Virginia 73-74

Virginia—stratigraphy
Cambrian: Structural and stratigraphic relations, Chopawamsic Formation and subjacent rocks 71-72
Ordovician: Ordovician age of the Quantico Formation reaffirmed 72-73

Virginia—structural geology
tectonics: Extension of St. Clair bedding-plane thrust in Virginia 40
— Pine Mountain-Russell Fork-Richlands overthrust fault system, Virginia 74
— Spotsylvania lineament of Virginia 73
— Structural and stratigraphic relations, Chopawamsic Formation and subjacent rocks 71-72

volcanic features *see under* geomorphology

volcanism *see under* volcanology

volcanoes *see under* volcanology

volcanology—volcanism
age: Cretaceous volcanism, southwestern Nevada 91
— Extensional volcanism in the Matanuska Valley region 111
— Two Cenozoic igneous events on the Alaska Peninsula 110
ash falls: Middle and Late Devonian ash-fall beds in Devonian shale 74
calderas: Buried Pliocene calderas of the eastern Snake River Plain, Idaho 79
— Caldera source of Miocene Osiris Tuff, southwestern Utah 81-82
— Concurrent regional faulting and silicic volcanism, Sangre de Cristo Mountains, New Mexico 86
— Deep drill hole in buried caldera, Snake River Plain, Idaho 197
cauldrons: Large caldron complex in central Idaho 197
controls: Controls of Pliocene and Pleistocene basaltic volcanism, southern Great Basin 89-90
— Cretaceous volcanism and plutonism, Montana 11
evolution: Stratigraphic relations and volcanic history of Eocene rocks, eastern Absaroka Range, Wyoming 78
lava flows: Eastern extent of Picture Gorge Basalt 196
petrology: Cascade volcanism 198
processes: Volcanic rocks and processes 192-199
pyroclastic flows: The climatic eruption of Mount Mazama, Oregon 198
volcanic centers: Tertiary volcanic centers on the Alaska Peninsula 111

volcanology—volcanoes
Alaska: Alaska Peninsula volcanoes 60
— Holocene volcano on the Alaska Peninsula 110
Hawaii: Hawaiian volcano studies 192-195
Iceland: Icelandic studies 195-196
Kilauea: Activity at Kilauea Volcano in 1979 192-193
— Aeromagnetic anomalies on Kilauea's east rift zone, Hawaii 209
— Loihi Seamount; active submarine volcano 194
— Paleomagnetic correlation of volcanic rocks 181
— Pressurized fractures in hot rock 215-216
Krafla: Hydrogen gas monitor at Krafla Volcano 196
Mauna Loa: Mauna Loa rift zones 193-194
— Mauna Loa Volcano quiescent in 1979 193
Medicine Lake Volcano: Complex stratigraphy at Medicine Lake Volcano 216
Mount Baker: Hydrothermal alteration at Mount Baker, Washington 198
Mount Hood: Hydrothermal alteration at Mount Hood, Oregon 59-60
Surtsey: Surtsey Volcano drill hole 195

W

Washington—areal geology
regional: Washington 92-96

Washington—economic geology
metal ores: Mineralization in the Spirit Lake quadrangle, southern Cascade Range, Washington 8
mineral resources: Mineral resource assessment using aerial geophysical data 187
uranium ores: Limitations on genesis of Midnite mine uranium ores 44
water resources: Washington 146

Washington—engineering geology
earthquakes: Seismic zonation of geologic materials, Seattle area 93
shorelines: Coastal erosion and sediment transport, the Puget Sound region 94
slope stability: Landslide deposits, eastern Puget lowland 94

Washington—environmental geology
ecology: Long-term studies of benthic community structure in Puget Sound 170
geologic hazards: Landslide deposits, eastern Puget lowland 94
— Seismic zonation of geologic materials, Seattle area 93
pollution: Phosphorus loading of lake water related to land uses 238

Washington—geochronology
Cretaceous: Preliminary uplift ages from fission-track studies 94
Eocene: Stratigraphy of the Naches Formation 94

Washington—hydrogeology
ground water: Digital-model simulation of the Spokane aquifer 225
— Simulation of ground-water flow in basalt aquifers underlying the Columbia Plateau 146
— Solute transport in the Spokane aquifer 225
hydrology: Ground-water levels affected by irrigation in Sequim Peninsula 146
— Simulation of unregulated-streamflow record for the Yakima River at Union Gap 146
— Water budget estimated for Gig Harbor Peninsula 146
— Water quality studies 149
— Yakima River basin streamflow and irrigation diversions for 1977 drought year and 1960-1976 146
maps: Map of principal aquifers and general yields of wells 146
thermal waters: Hydrothermal alteration at Mount Baker, Washington 198

Washington—stratigraphy
Eocene: Lower to middle Eocene seamount chain, northwest Olympic Peninsula 92-93
Pleistocene: Diamictons of the Strait of Juan de Fuca 93-94

Washington—structural geology
neotectonics: Holocene faulting, Toppenish Ridge 95
tectonics: Geometry and tectonic evolution of the Columbia Hills 96
— Miocene deformation and canyon cutting at Graybach Mountain 95-96

waste disposal *see also under* engineering geology *under* Florida; Nevada

waste disposal—radioactive waste
storage: Borehole geophysical technique to determine geologic inhomogeneities in nuclear waste storage sites 184-185

water resources *see also under* economic geology *under* Alabama; Arizona; California; Connecticut; Delaware; Eastern U.S.; Florida; Georgia; Idaho; Illinois; Indiana; Kansas; Kentucky; Louisiana; Maryland; Michigan; Midwest; Minnesota; Mississippi; Missouri; Montana; Nevada; New Jersey; New Mexico; New York; North Carolina; North Dakota; Ohio; Oklahoma; Oregon; Pennsylvania; Rhode Island; South Carolina; South Dakota; Tennessee; Texas; United States; Utah; Virginia; Washington; Western U.S.; Wisconsin; Wyoming

waterways *see also under* engineering geology *under* Florida

weathering *see also under* sedimentary petrology *under* Virginia

weathering—processes
chemical weathering: Ground-water geochemical models 202
— Movement of trace elements in weathering environment 15

well-logging—applications
sulfur deposits: Estimation of sulfur reserves using borehole gravimetry 41
waste disposal: Electrical and magnetic borehole studies useful for defining nuclear waste repositories in volcanic rocks 183

well-logging—electrical logging
resistivity: Borehole geophysical technique to determine geologic inhomogeneities in nuclear waste storage sites 184-185
— Borehole measurements to differentiate sulfides and clays 186
— Computer programs for resistivity soundings over three vertical layers 186
— Nonlinear complex resistivity logging 185

well-logging—interpretation
automatic data processing: Simultaneous interpretation of geophysical well logs 19
calderas: Deep drill hole in buried caldera, Snake River Plain, Idaho 197
permafrost: Permafrost distribution model 104
porosity: Porosity of oil reservoirs in Bighorn Basin, Wyoming 35
temperature: Temperature survey in Raft River geothermal system 213

well-logging—techniques
gamma-ray spectroscopy: In situ capture gamma-ray analysis of coal in oversized boreholes 30-31

West Indies *see also* Lesser Antilles; Puerto Rico

West Virginia—economic geology
coal: Coal quality in the Pocahontas field, Virginia and West Virginia 25

West Virginia—sedimentary petrology
sedimentary rocks: Resin rods in Upper Pennsylvanian coal beds 25

West Virginia—stratigraphy
Pennsylvania: Correlation of the Middle Pennsylvanian Series 232
Pennsylvanian: Correlation of the Dunkard Group 232

Western Hemisphere *see also* Atlantic Ocean; North America; Pacific Ocean

Western Interior—economic geology
coal: Zinc and cadmium content of coal in the Interior coal province 28
natural gas: Mineralogy and diagenesis of gas-bearing reservoirs in Niobrara Chalk 36-37

Western Interior—stratigraphy
Cretaceous: Stratigraphic analysis of Western Interior Cretaceous uranium basins 50

Western U.S.—areal geology
regional: Western United States 92

Western U.S.—economic geology
coal: Western and Alaskan coals 26-28
metal ores: Chromite and nickel, western Cordillera 8-9
petroleum: Sedimentation rates and timing of Antler orogenic events determined from conodont zonation, Western United States 37
uranium ores: Structural control of rhyolite volcanism associated with uranium deposits, Western United States 8
water resources: Western region 142-146

Western U.S.—environmental geology
reclamation: Participation in the interagency Energy Minerals Rehabilitation Inventory and Analysis Program 24

Western U.S.—geochronology
Quaternary: Quantitative pedology as a dating technique in the Western United States 92

Western U.S.—seismology
mantle: P-wave delays at two geothermal areas 215

Western U.S.—structural geology
tectonics: Sedimentation rates and timing of Antler orogenic events determined from conodont zonation, Western United States 37

Wisconsin—economic geology
iron ores: Extension of Iron River-Crystal Falls basin, Michigan and Wisconsin 6
metal ores: Geochemical lineament, Iron River 2° quadrangle, Michigan and Wisconsin 15
mineral resources: Mineral geophysical surveys in Wisconsin and Michigan 187-188
water resources: Wisconsin 125-126

Wisconsin—environmental geology
pollution: Concentrations of heavy metals in ground water, Wisconsin 235-236
— Summary of ground-water quality data, Wisconsin 236

Wisconsin—geomorphology
fluvial features: Channel morphology and sedimentation in Pheasant Branch near Middleton, Wisconsin 217-218

Wisconsin—geophysical surveys
electromagnetic surveys: Electromagnetic response of cultural features 186

Wisconsin—hydrogeology
ground water: Ground water in Dodge County 125
— Hydrogeology and ground-water quality in northeastern Waukesha County 126
— Water resources of Forest County 125
hydrology: Mole Lake hydrology 125
— Saint Croix River flood and water-quality data 126

Wisconsin—sedimentary petrology
sedimentation: Storm sediment yield measured in Nederlo Creek basin, Wisconsin 217

worms—Polychaetia
biochemistry: Correlation of trace elements between sediments and benthic fauna 166
ecology: Long-term studies of benthic community structure in Puget Sound 170

Wyoming—economic geology
coal: Coal in the Mesaverde Formation, Wind River Indian Reservation 26
— Development of thick coal beds in the eastern Powder River Basin 26-27
— The Aspen Shale-Frontier Formation contact 27

fuel resources: Petrology and reservoir characteristics of Mesaverde Group, Washakie Basin, Wyoming 36
— Source-rock potential of some Upper Cretaceous shale, northeastern Wyoming 34-35
geothermal energy: Hydrothermal alteration in Yellowstone geyser basins 59
gold ores: Gold in Oligocene conglomerate, southeast margin of Wind River Mountains, Wyoming 76
natural gas: Overpressuring and fracture development in low-permeability rocks, Green River Basin, Wyoming 36
petroleum: Biogeochemical and airborne geochemical prospecting of Recluse oil field, Wyoming 35
— Petroleum source rocks in Chesterian strata, northwestern Wyoming 35-36
— Porosity of oil reservoirs in Bighorn Basin, Wyoming 35
thorium ores: Large thorium reserves in disseminated deposits 42
uranium ores: Formation of tabular uranium deposits in the Powder River Basin 50
— Oxygen isotope studies of uranium source rocks 53-54
— Powder River Basin, Wyoming 18
— Presence of ore-stage marcasite and formation of roll-type deposits 52-53
— Sites of labile uranium in granitic rocks 54
— Source of the uranium-bearing sandstone of the southern Powder River Basin 59
— Stratigraphic analysis of Western Interior Cretaceous uranium basins 50
— Supergene uranium deposits in fracture zones associated with Laramide upthrusts 43
— Uranium, gold, and thorium potential of Sierra Madre and Medicine Bow Mountains, Wyoming 44
water resources: Wyoming 141-142
zinc ores: Stratabound Precambrian sulfide and gahnite deposits in the Pearl area, Colorado and Wyoming 10-11

Wyoming—environmental geology
geologic hazards: Radioactive rocks and water, Yellowstone National Park, Wyoming 77
land use: Water study of energy-minerals area 141-142
pollution: Aquatic macroinvertebrates, Wyoming 235

Wyoming—geochemistry
isotopes: Isotopic modification of magma, Yellowstone caldera, Wyoming 197

Wyoming—geochronology
Archean: Two generations of Archean gneiss in the Big Horn Mountains 207
Pleistocene: Klinker dating 207

Wyoming—geophysical surveys
remote sensing: Powder River Basin, Wyoming 18

Wyoming—hydrogeology
ground water: Digital flow model of Bates Creek alluvial aquifer 141
— Digital model of effects of ground-water withdrawals in Laramie County 141
hydrology: Regression model of effects of streamflow diversions on surface-water salinity 141
— Source-area sediment model of Big Sandy River basin 141
thermal waters: Earthquake-induced thermal changes at Yellowstone National Park, Wyoming 214
— Hydrothermal alteration in Yellowstone geyser basins 59
— Radioactive rocks and water, Yellowstone National Park, Wyoming 77
— Warm water in artesian aquifers in Carbon County 141

Wyoming—sedimentary petrology
sedimentation: Bedload movement in East Fork River, Wyoming 218
— Sediment-yield estimates for central Powder River Basin, Montana and Wyoming 217
— Suspended-sediment discharge in northeastern Wyoming streams 218

Wyoming—seismology
earthquakes: Earthquake-induced thermal changes at Yellowstone National Park, Wyoming 214

Wyoming—stratigraphy
Cretaceous: Coal in the Mesaverde Formation, Wind River Indian Reservation 26
— The Aspen Shale-Frontier Formation contact 27
Eocene: Early Eocene streams of the Bighorn Basin, Wyoming 78
— Stratigraphic relations and volcanic history of Eocene rocks, eastern Absaroka Range, Wyoming 78
Precambrian: Comparison of Precambrian rocks of the Hartville uplift, eastern Wyoming, and of the Black Hills, western South Dakota 81-82
— Newly recognized Precambrian metasedimentary and metavolcanic rocks in the Seminoe Mountains, Wyoming 82
Quaternary: Records of past climates in lake sediments from Yellowstone Park area 221-222

Wyoming—structural geology
neotectonics: Gravity fault klippen of volcanic rocks, northwest Wyoming 87

Wyoming—tectonophysics
heat flow: Earthquake-induced thermal changes at Yellowstone National Park, Wyoming 214

X

xenoliths *see under* inclusions

Z

zinc—abundance
coal: Zinc and cadmium content of coal in the Interior coal province 28

INVESTIGATOR INDEX

A

Ackerman, H. 186
Ackermann, H. D. 60
Adam, D. P. 221, 241
Ager, T. A. 231
Albers, J. P. 8
Aleinikoff, J. N. 108, 206
Alexander, C. C. 30
Alexander, Calvin 208
Alhadeff, S. J. 131
Alldredge, L. R. 183
Allen, H. E., Jr. 148
Allen, R. W. 40
Alley, W. M. 148, 149
Allmendinger, R. W. 83
Allord, G. J. 242
Alminas, H. V. 15
Alpha, T. R. 165
Altschuler, Z. S. 29
Anders, Edward 245
Anderson, J. J. 81
Anderson, J. L. 95, 96
Anderson, L. A. 184
Anderson, R. E. 78
Anderson, R. Y. 221
Anderson, W. L. 186
Andrews, G. W. 13
Andrews, Sarah 78
Antweiler, J. C. 14, 76
Arcement, G. J. 229
Arihood, L. D. 119
Armbrustmacher, T. J. 42
Armi, L. 156
Armin, R. A. 9
Armstrong, A. K. 105
Arndt, H. H. 27
Arntson, A. D. 120
Aronson, D. A. 122
Arth, J. G. 71, 80, 199, 207
Ashley, R. P. 8
Attanasi, E. D. 20
Atwater, B. F. 170, 173
Aubele, J. C. 79
Avanzino, R. J. 202
Ayers, M. A. 120

B

Bacon, C. R. 196, 198
Baird, A. K. 203
Baker, E. T., Jr. 140
Baker, R. G. 221
Barczak, V. J. 222
Bargar, K. E. 59
Barker, C. E. 60
Barker, Fred 207
Barnes, D. F. 104
Barr, Douglas 128
Barron, J. A. 159
Barron, J. B. 231
Barton, P. B., Jr. 190
Bartow, J. A. 99
Basco, D. R. 228
Bassler, R. S. 72
Batchelder, J. N. 83, 96
Batchelder, J. W. 205
Batten, W. G. 217
Bauer, D. P. 237
Becher, A. E. 124
Beeson, M. H. 59
Bejcek, R. M. 148
Bentley, R. D. 95, 96, 196
Berg, H. C. 102, 112
Berger, B. R. 3, 15
Bergeron, M. P. 150
Bethke, P. M. 190
Beutner, E. C. 97
Beverage, J. P. 219
Beyer, L. A. 35, 37
Bigelow, R. C. 16
Bingham, J. W. 117
Bingham, R. H. 126
Bischoff, J. L. 163
Bisdorf, R. J. 186, 187
Black, D. F. B. 75
Blackwelder, B. W. 70, 231
Blakely, R. J. 18, 181
Bliss, J. D. 21
Blumer, S. P. 138
Bobyarchick, A. R. 71, 72, 73
Bodnar, R. J. 190
Bohannon, R. G. 90
Bolke, E. L. 225
Bonilla, M. G. 93
Booth, J. S. 153
Borton, R. L. 240
Bostick, N. H. 60
Bothner, M. H. 66, 154, 155
Boucher, G. W. 157
Boudette, E. L. 45
Bouma, A. H. 156, 157
Bowen, R. W. 20
Bowles, C. G. 57
Bown, T. M. 78, 84, 87
Boyd, E. L. 125
Boynton, G. R. 30
Bradbury, J. P. 221
Breed, C. S. 220
Breger, I. A. 28
Brew, D. A. 112
Brindley, G. W. 53
Broadhead, R. F. 39
Brock, M. R. 42, 44, 45, 58
Bromfield, C. S. 42, 57
Brooks, P. K. 201
Brooks, W. E. 50
Broom, M. E. 225
Brosge, W. P. 104
Brown, C. E. 6
Brown, G. E. 192
Bryan, M. L. 243
Bryant, B. H. 82
Bryant, C. T. 237
Buel, G. R. 235
Bugliosi, E. F. 139
Bukry, J. D. 230
Burchett, C. R. 132
Burke, D. B. 100
Butman, Bradford 154
Butterfield, F. S. 18
Buxton, H. T. 123
Bybell, L. M. 230

C

Cacchione, D. A. 156
Cadigan, R. A. 54, 56
Cady, J. W. 107
Cain, J. C. 182
Calkins, J. A. 19
Callender, Edward 167
Cameron, C. C. 1
Camp, V. E. 94
Campbell, J. A. 47
Campbell, N. P. 95
Campbell, W. H. 183
Campbell, W. J. 242, 243, 244
Canney, F. C. 16
Cannon, M. R. 136
Cannon, W. F. 6, 19
Carey, M. A. 24
Carey, W. P. 218
Cargill, S. M. 21
Carlson, Christina 97
Carlson, P. R. 158, 159
Carpenter, D. J. 53
Carpenter, R. H. 16
Carr, M. R. 239
Carr, W. J. 89
Carrara, P. E. 222
Carter, Claire 106
Carter, M. D. 24
Carter, V. P. 169, 233
Casadevall, T. J. 196
Case, J. E. 110, 111
Cathcart, J. B. 51
Cathrall, J. B. 14, 103
Causseaux, K. W. 129
Cecil, C. B. 28
Chaffee, M. A. 13
Champion, D. E. 181
Chao, E. C. T. 30
Chao, T. T. 16, 17
Chapman, R. M. 106
Chase, H. B., Jr. 25
Cheney, R. E. 243
Cheng, R. T. 171, 173
Childs, J. R. 162
Chintu Lai 228
Christenson, S. C. 138
Christiansen, R. L. 197
Christopher, R. A. 68
Church, R. L. 143
Churkin, Michael, Jr. 106
Claassen, H. C. 202
Clark, J. R. 17, 192

Clarke, J. S. 130
Clarke, J. W. 40
Clarke, S. H., Jr. 100, 157
Claypool, G. E. 31, 34, 38, 159
Clements, R. L. 241
Cloern, J. E. 173
Clutsom, F. G. 35
Coakley, J. M. 98
Coates, D. A. 207
Coats, R. R. 87
Cobb, E. H. 104
Cobb, J. C. 1
Coffrant, Denis 205
Coleman, J. M. 152
Collier, K. R. 141
Collins, William 16
Colton, G. W. 39
Colton, R. B. 76
Condit, C. D. 79
Coney, P. J. 103
Connor, C. L. 110
Connor, J. J. 12
Conomos, T. J. 172
Consul, J. J. 87
Cook, H. E. 41
Cooley, R. L. 226
Cooper, A. K. 162
Copeland, C. W., Jr. 230
Coplen, Tyler 227
Cordell, L. E. 188
Corken, R. J. 48
Corwin, R. F. 186
Cory, R. L. 168
Coury, A. B. 40
Covington, H. R. 209
Cox, B. C. 101
Cox, D. P. 110
Craig, L. C. 49
Crawford, J. K. 132
Crawford, T. J. 25
Creasey, S. C. 10
Crim, W. D. 14, 103
Crist, M. A. 141
Croft, M. G. 137
Cronin, T. M. 65, 231
Crouch, T. M. 124
Crumpler, L. S. 79
Csejtey, Bela, Jr. 109, 110
Culbertson, C. W. 171
Cunningham, C. G. 81
Cunningham, K. I. 32
Curtin, G. C. 14, 103
Cushman, R. L. 240
Czamanske, G. K. 7, 192

D

D'Agostino, J. P. 4, 11
Dalrymple, G. B. 208
Dalziel, Mary 35
D'Amore, Franco 211
Daniels, D. L. 11, 70
Daniels, J. J. 19, 183, 184, 186
Davis, J. R. 22
Davis, R. E. 138
Davis, R. W. 131
Dean, W. E., Jr. 221
Delaney, P. T. 215
Delevaux, M. H. 204, 206
DeLong, L. L. 141
Demas, C. R. 234
Demere, Thomas 230
Derkey, R. E. 12
Detterman, R. L. 110, 111
Devaul, R. W. 125
DeWitt, K. C. 114
DeYoung, J. H., Jr. 21
Dickerman, D. C. 124
Dickinson, K. A. 49, 51
Diment, W. H. 213, 214
Dingler, J. R. 165
Dixon, H. R. 82
Dodge, F. C. 201
Dodge, H. W., Jr. 50
Dodge, J. E. 140
Doe, B. R. 80, 208
Doherty, D. J. 197
Dolton, G. L. 40
Donnelly, J. M. 210
Donnelly-Nolan, J. M. 216
Donovan, T. J. 32, 35
Doyle, W. H., Jr. 148
Drake, A. A., Jr. 67
Drake, D. E. 156
Dresler, P. V. 168
Drew, L. J. 21
Drost, B. W. 146
Druse, S. A. 229
Dunlap, L. E. 225
Durham, D. L. 50
Dusel-Bacon, Cynthia 108
Dutro, J. T., Jr. 103, 104
Duval, J. S. 2, 187
Dyar, T. R. 131

E

Earhart, R. L. 85
Ebbert, J. C. 149
Edwards, L. E. 230
Egbert, R. M. 32
Ehrlich, G. G. 236
Eittreim, S. L. 156
Ekren, E. B. 197
Elachi, Charles 243
Elder, J. F. 237
Ellis, S. R. 149
Elston, D. P. 86
Embree, G. F. 76
Emmett, L. F. 150
Emmett, W. W. 218
Engberg, R. A. 235
Erd, R. C. 192
Ethridge, F. G. 51
Evans, H. T. 192
Evans, H. T., Jr. 191, 192
Evans, J. R. 215
Evarts, R. C. 185

F

Fabiano, E. B. 182
Fairchild, R. W. 138
Farooqui, S. M. 95, 96
Farr, Thomas 243
Farrar, C. D. 236
Faye, R. E. 130
Felmlee, J. K. 56
Ferreira, R. F. 241
Field, M. E. 100, 157
Finkelman, R. B. 25, 28
Fisher, J. N. 130
Fisher, M. A. 161
Fishman, M. J. 245
Fiske, R. S. 194
Fitterman, D. V. 186, 188
Flanigan, V. J. 2, 187
Flores, R. M. 27
Foose, M. P. 19, 76
Force, E. R. 5, 7
Ford, A. B. 112
Forester, R. M. 91
Foster, H. L. 106, 107, 108
Fournier, R. O. 211
Fracasso, M. A. 232
Frank, D. G. 198
French, A. B. 85
French, J. J. 143
Fretwell, J. D. 129
Frezon, S. E. 40
Frizzell, V. A., Jr. 94
Frye, P. M. 234
Futa, Kiyoto 206

G

Gable, D. J. 114
Gair, J. E. 7
Galanis, S. P., Jr. 213
Gallaher, J. T. 225
Galloway, S. E. 240
Gammon, P. T. 233
Gardner, J. V. 156, 158, 159, 162
Garrison, L. E. 152
Garza, Sergio 140
Gautier, D. L. 33
Gazdik, G. C. 6
Gibson, T. G. 68
Gilbert, C. M. 89
Gillespie, J. B. 135
Gillespie, W. H. 24, 69, 232
Gillies, D. C. 118
Gilliom, R. J. 238
Gilluly, James 213
Glenn, J. L. 167, 170
Glick, E. E. 74
Gloersen, Per 243
Glover, K. C. 141
Godsy, E. M. 236
Goemaat, R. L. 138
Goff, F. E. 210
Gogel, A. J. 227
Goldberg, M. C. 242, 246
Goldhaber, M. B. 52, 53
Goldsmith, Richard 61, 63
Goodwin, C. R. 169
Gordon, Mackenzie, Jr. 69, 72, 232
Gottfried, David 198
Grady, S. J. 145
Granger, H. C. 52
Grannemann, N. G. 119
Grant, N. K. 61
Grantz, Arthur 111
Grauch, R. I. 45, 46
Greeman, T. K. 118
Green, R. G. 182

Greene, H. G. 100
Greenwood, W. R. 11
Griesbach, F. R. 32
Griffin, E. A. 97
Griffitts, W. R. 14
Grimes, D. J. 14
Grolier, M. J. 220
Gromme, C. S. 103, 180
Grosz, Andrew 5, 6, 66
Grow, J. A. 159
Guswa, Jack 120

H

Haas, J. L., Jr. 190
Haeni, F. P. 225
Hagstrum, J. T. 86
Hahn, S. S. 240
Hall, W. E. 83, 205
Halley, R. B. 38, 41
Hamilton, L. J. 139
Hamilton, W. B. 101
Hammarstrom, J. M. 200, 80
Hammett, K. M. 127, 128
Hampton, M. A. 156, 157
Handman, Elinor 226
Hanson, R. L. 138
Harden, J. W. 92
Hardt, W. F. 144
Hardyman, R. F. 197
Harned, D. A. 132
Harr, C. A. 235
Harrill, J. R. 144
Harris, L. D. 39
Harrison, J. E. 85
Harsh, J. F. 124, 125
Harsh, P. W. 98
Hatch, J. R. 28, 29
Hatch, N. L., Jr. 62
Hatcher, P. G. 28
Hatcher, R. D., Jr. 188
Haushild, W. L. 149
Hauth, L. D. 150
Have, M. R. 120
Havens, J. S. 138
Hayes, L. R. 128, 131
Healy, J. H. 214
Hearn, B. C., Jr. 4, 210
Hearn, P. P. 244
Hedge, C. E. 42, 203
Hedley, A. G. 245
Helgesen, J. O. 124
Hem, J. D. 202
Hemingway, B. S. 190, 191
Hendricks, J. D. 32
Henry, T. W. 69, 232
Herd, D. G. 101
Heropoulos, Chris 96, 209
Hertohen, Jan 245
Herz, Norman 7
Hess, G. R. 164
Hetherington, M. J. 94
Hickling, N. L. 26
Hicks, D. W. 131
Hietanen-Makela, A. M. 98
Higgins, M. W. 69
Hildreth, E. W. 197
Hill, G. W. 166
Hill, J. F. 233
Hill, R. H. 13
Hillhouse, J. W. 103, 180
Hills, F. A. 46
Himmelberg, G. R. 199
Hinkle, M. E. 16
Hoare, J. M. 110
Hobbs, S. W. 83
Hodges, A. L., Jr. 117
Holcomb, R. T. 181, 193
Holmes, C. W. 164
Holmes, M. L. 32
Holtschlag, D. J. 119
Holzer, T. L. 188
Honey, J. G. 84
Hood, J. W. 140, 240
Hooper, P. R. 94, 196
Hoover, D. B. 209
Hopkins, D. M. 104
Horak, W. F. 137, 227
Horn, M. A. 122
Horton, J. W., Jr. 66
House, L. B. 228
Houston, R. S. 44
Howard, K. A. 100
Hsi-Ping 212
Hubbell, D. W. 219
Huber, N. K. 98
Hudson, J. H. 37, 41
Huebner, J. S. 191
Huffman, A. C., Jr. 48
Hufschmidt, P. W. 234
Hult, M. F. 225
Hunt, G. R. 183, 185
Hunt, S. J. 113
Hunter, R. E. 165
Hupp, C. R. 234
Hutchinson, C. B. 129, 169
Hutton, C. T., Jr. 114

I

Imbrigiotta, T. E. 118
Isaacs, C. M. 37
Iyer, Mahadeva 215
Izett, G. A. 84

J

Jachens, R. C. 18, 188
Jacobsson, S. P. 195
James, H. L. 7
James, R. V. 238
Janik, C. J. 212
Jeffcoat, H. H. 127
Jennings, M. E. 148, 237
Jindal, M. C. 169
Jobson, H. E. 228
Johnson, M. J. 143
Johnston, H. E. 124
Jones, D. L. 103, 106, 110, 162
Jones, M. L. 218

K

Kalliokoski, J. O. 45
Kammerer, P. A., Jr. 217, 236, 242
Kane, J. S. 244
Karl, H. A. 156
Karl, S. M. 110
Karlo, J. F. 83
Karlstrom, K. E. 44
Karlstrom, T. N. V. 224
Kaye, C. A. 62
Keith, S. B. 9
Keith, T. E. C. 59
Kennedy, G. L. 231
Kennedy, V. C. 202
Kent, B. H. 26
Kepferle, R. C. 39
Ketelle, R. H. 5
Ketner, K. B. 88
Keuler, R. F. 94
Khan, A. S. 40
Kieffer, S. W. 189, 210
Kiilsgaard, T. H. 3
Kircher, J. E. 141
Kirk, A. R. 48
Kistler, R. W. 91, 201
Klausing, R. L. 137
Klein, D. P. 4, 181
Kleinkopf, M. D. 1, 2, 5
Klepper, M. R. 85
Kling, S. A. 97
Klitgord, K. D. 159
Knebel, H. J. 165, 166, 167
Knepper, D. H., Jr. 17, 18, 185
Koehler, R. L. 156
Kohler, W. M. 214
Kolesar, P. T. 209
Konnert, J. A. 191, 192
Koopman, F. C. 242
Koski, R. A. 12
Kouma, Edwin 226
Kraker, G. P., Jr. 208
Krause, R. E. 131, 225
Krimmel, R. M. 219
Krohelski, J. T. 118
Krug, W. R. 217, 228
Kuberry, R. W. 182
Kume, Jack 135, 225
Kuntz, M. A. 197
Kurklin, J. K. 139
Kvenvolden, K. A. 157

L

LaBaugh, J. W. 241
Laenen, Antonius 145
LaFrance, D. E. 146
Lajoie, K. R. 231
Lander, D. L. 161
Lang, D. J. 234
Langmuir, Donald 52
Lanphere, M. A. 208
Lantz, R. J. 32
Lapham, W. W. 119
LaRose, H. R. 130
Larsen, F. D. 64
Larson, J. D. 124
Larson, S. P. 131, 135, 225
Lash, G. G. 67
Law, B. E. 36
Learned, R. E. 16
Leavesley, G. H. 227
Lecaille, Alain 181

Lee, D. E. 56, 199
Lee, J. W. 156
Leinz, R. W. 14
Leitman, Helen 234
Leland, H. V. 240
Leo, G. W. 71, 200
Leonard, A. R. 145
Leonard, B. F., III 12
Leonard, Robert 136
Lesure, F. G. 6
Leventhal, J. S. 51
LeVeque, R. A. 96
Lian, N. C. 154
Liberl, Franz 243
Lichtler, W. F. 226
Lichty, R. W. 227
Liddicoat, J. C. 67, 222
Lidwin, R. A. 125
Lidz, B. H. 41
Lindholm, G. F. 120
Lindner, J. B. 122
Lindsey, D. A. 11, 42
Ling, C. H. 244
Lipin, B. R. 189
Lipman, P. W. 86, 193
Liscum, Fred 148
Lockwood, J. P. 193, 201
Lonay, R. A. 199
London, E. B. H. 63
Long, C. L. 2, 5
Lopez, M. A. 127
Love, J. D. 76
Lowham, H. W. 141, 228
Lucchitta, Ivo 90, 91
Ludwig, K. R. 44, 54
Luepke, Gretchen 165
Luft, S. J. 49
Luoma, S. N. 174
Lupe, R. D. 48
Lyons, P. C. 25
Lystrom, D. J. 148
Lyttle, P. T. 67

M

Machette, M. N. 78
MacKevett, E. M., Jr. 110
MacKinnon, D. J. 220
Maclay, R. W. 139
Mades, D. M. 117
Madole, R. F. 220, 222, 223
Magoon, L. B. 31, 32
Mamay, S. H. 232
Mancini, E. A. 230
Manheim, F. T. 166
Mankinen, E. A. 181
Mansue, L. J. 217
Marchand, D. E. 92
Marcher, M. V. 138
Markewich, Helaine W. 68, 69, 73
Markochick, D. J. 36
Marlow, M. S. 162
Marmo, Vladi 199
Marsh, J. G. 243
Marshall, S. G. 202
Martin, Angel, Jr. 118
Martin, E. A. 166
Martin, R. A. 181
Martin, R. G., Jr. 160
Martinson, H. A. 218
Marvin, R. F. 11, 50, 80, 84
Mase, C. W. 213
Massey, B. C. 148
Matthews, Alan 110
Matthews, E. W. 131
Mattick, R. E. 159
Mattraw, H. C., Jr. 237
Mattraw, Harold 149
Maughan, E. K. 34, 35
Maurer, D. K. 144
Mayo, L. R. 219
Mazzaferro, D. L. 117
McBroome, L. A. 197
McCallister, R. H. 190
McCallum, M. E. 10
McCammon, R. B. 22
McCarthy, J. H., Jr. 15
McCauley, J. F. 220
McClennen, C. E. 154
McClymonds, M. E. 136
McCoy, G. A. 241
McCulloh, T. H. 32
McDonald, M. G. 119
McDougall, K. A. 97
McGee, K. A. 196
McGetchin, T. R. 245
McKenzie, D. J. 127
McKenzie, Stuart 145
McLaughlin, R. J. 96, 97
McLean, J. S. 137
McNeal, J. M. 56
McPherson, B. F. 130
Meade, Daniel 117
Meade, R. H. 218
Medlin, A. L. 19
Medlin, J. H. 29
Mehnert, H. H. 81
Meier, A. L. 17
Meissner, C. R., Jr. 74
Menzie, W. D. 108
Menzie, W. D., II 21
Merewether, E. A. 34
Metz, Jenny 196
Meyer, C. E. 206
M'Gonigle, J. W. 27
Miesch, A. T. 203
Millard, H. T., Jr. 56
Miller, D. M. 87, 100
Miller, J. A. 127
Miller, J. E. 148, 237
Miller, J. W. 97
Miller, R. D. 91
Miller, R. E. 159
Miller, R. L. 74
Miller, R. T. 121
Miller, Robert 149
Miller, T. P. 44, 60
Miller, T. S. 122
Miller, W. R. 13
Miller, William R. 134
Milliman, J. D. 155
Milton, D. J. 66
Minard, J. P. 94
Minkin, J. A. 30
Mixon, R. B. 67
Mognard, N. M. 243
Molenaar, C. M. 31
Molenaar, Dee 146
Molnia, B. F. 156, 157, 158, 159
Moody, J. A. 218
Moore, J. G. 195
Moore, R. H. 203
Moore, W. J. 7, 9, 203
Moreland, Joe 136
Morgan, David 145
Morgan, J. W. 244, 245
Morris, E. E. 237
Morrison, S. D. 96
Morton, J. L. 96
Moss, M. E. 239
Motooka, J. M. 17
Moulton, G. F. 222
Mourant, W. A. 137
Mower, R. W. 240
Mozley, P. S. 93
Muir, K. S. 143, 227
Mullenders, William 221
Muller, E. H. 122
Mullineaux, D. R. 93
Munroe, R. J. 213
Muth, K. G. 71, 207
Myette, C. F. 121
Myrick, R. M. 218
Mytton, J. W. 27

N

Naeser, C. W. 11, 82, 94, 207
Nakata, J. K. 220
Nash, J. T. 43, 44, 46
Nathenson, Manuel 211, 214
Nealey, L. D. 82
Negus-de Wys, Jane 74
Nehring, N. L. 212
Neil, S. T. 87
Nelson, A. E. 68
Nelson, C. H. 92, 157, 158, 166
Newell, M. F. 71, 207
Newell, W. L. 73
Newton, J. G. 127
Nichols, F. H. 170, 174
Nichols, K. M. 33
Niem, W. A. 170
Nilsen, T. H. 97, 105
Nokleberg, W. J. 109
Nolan, T. B. 209
Nord, G. L., Jr. 190
Norman, M. B., II 96
Normark, W. R. 163, 164
Norton, J. J. 81
Novak, S. W. 198
Nowlan, G. A. 15
Nutt, C. J. 46
Nyman, D. J. 236

O

Obermeier, S. F. 71
O'Hara, C. J. 153, 154
Ohlin, H. N. 96, 97
Ojakangas, R. W. 45
Okulitch, A. V. 84
Oldale, R. N. 65, 153
Olhoeft, G. R. 184, 185
Oliver, H. W. 18

Oliver, W. A., Jr. ... 232
Olm, M. C. ... 186
Olson, A. C. ... 19
Olson, J. C. ... 42
O'Neil, J. R. ... 80, 197, 223
Oremland, R. S. ... 171
Orr, B. R. ... 137
Osberg, P. H. ... 61
Osmonson, L. M. ... 57
Otton, J. K. ... 50
Owen-Joyce, S. J. ... 142
Owens, J. P. ... 70, 229

P

Palacas, J. G. ... 38
Pampeyan, E. H. ... 98
Parkhurst, D. L. ... 167
Parliman, D. J. ... 144
Parmenter, C. M. ... 155
Parsley, R. L. ... 72
Pascale, C. A. ... 127
Pasch, A. D. ... 111
Patterson, D. J. ... 140
Patterson, G. L. ... 226
Patterson, S. H. ... 1
Patton, W. W., Jr. ... 106
Pavich, M. J. ... 71, 73
Pavlides, Louis ... 71, 72, 73, 207
Payne, G. A. ... 120, 121
Pearl, J. E. ... 92
Pearson, R. C. ... 3
Pease, M. H., Jr. ... 62
Peddie, N. W. ... 182
Peper, J. D. ... 63
Pereira, W. E. ... 246
Perry, W. J., Jr. ... 39, 40
Peselnick, Louis ... 212
Peterman, G. E. ... 81
Peterson, D. A. ... 235
Peterson, D. H. ... 168
Peterson, Fred ... 47
Peterson, J. A. ... 40
Pevear, D. R. ... 93
Pfefferkorn, H. W. ... 24 232
Phair, George ... 201
Philbin, P. W. ... 30
Phillips, J. D. ... 189
Phillips, R. L. ... 165
Pierson, C. T. ... 42, 57
Pike, R. S. ... 40
Pinckney, D. J. ... 246
Pinder, G. F. ... 131 135
Piper, D. Z. ... 163
Pitkin, J. A. ... 2, 187
Pitman, J. K. ... 20
Pitt, A. M. ... 214
Pojeta, John, Jr. ... 72
Pollard, D. D. ... 215
Pollastro, R. M. ... 36
Poole, F. G. ... 88, 89
Poore, R. Z. ... 97, 231
Popenoe, Peter ... 155
Posson, Douglas ... 145
Potter, P. E. ... 39
Potter, R. W., II ... 191
Powell, Jack ... 96
Powers, R. B. ... 40
Prevot, Michel ... 181
Price, Leigh C. ... 40
Prince, K. R. ... 239
Prostka, H. J. ... 79
Prowell, David C. ... 68
Prugh, B. J. ... 124
Prych, E. A. ... 227
Pryor, D. B. ... 152
Puente, Celso ... 127
Pyen, G. S. ... 245

Q

Quinterno, P. J. ... 159

R

Radtke, D. B. ... 235, 238
Ragland, R. C. ... 188
Raines, G. L. ... 16, 17, 18
Ramseier, R. O. ... 243
Ramsier, R. O. ... 243
Rankin, D. W. ... 198
Rasmussen, L. A. ... 244
Rathbun, R. E. ... 237
Rawson, Jack ... 140
Raymond, W. H. ... 10
Reasenberg, P. A. ... 214
Redden, G. D. ... 157
Redden, J. A. ... 81
Redmond, Ann ... 234
Reilly, T. E. ... 122, 123
Reimer, G. M. ... 57
Reinhardt, Juergen ... 66, 68, 72
Reiser, H. N. ... 104
Repetski, J. E. ... 40
Reynolds, M. W. ... 78, 89
Reynolds, R. L. ... 52, 53
Rice, Charles L. ... 25
Rice, D. D. ... 33
Richmond, G. M. ... 221
Ridgley, J. L. ... 49
Riggs, H. C. ... 228
Rinella, Joseph ... 149
Ringen, B. H. ... 218
Ripple, C. D. ... 238
Robb, J. M. ... 159
Robbin, D. M. ... 37, 41
Roberts, A. A. ... 32, 35, 38
Roberts, A. E. ... 22
Roberts, D. G. ... 152
Roberts, R. J. ... 9
Robertson, E. C. ... 212
Robertson, J. A. ... 45
Robertson, J. F. ... 48
Robie, R. A. ... 191
Robinson, G. R., Jr. ... 190
Robinson, Russell ... 215
Robinson, S. W. ... 205
Roehler, H. W. ... 28
Roen, J. B. ... 39, 74
Rollins, H. C. ... 129
Root, D. H. ... 21
Rose, Devon ... 137
Ross, D. C. ... 99
Ross, Duncan ... 243
Rowley, P. D. ... 81
Rubin, Jacob ... 238
Rubin, Meyer ... 111, 193
Ruhl, Jim ... 120
Rumen, L. L. ... 40
Ruppel, B. D. ... 32
Ruppel, E. T. ... 84
Ruppert, L. F. ... 244
Ryder, R. T. ... 33
Rye, R. O. ... 9
Ryer, T. A. ... 26
Rytuba, J. J. ... 8

S

Sagstad, S. R. ... 137
Saindon, L. G. ... 227
Sallenger, A. H., Jr. ... 165
Sanchez, J. D. ... 26
Sandberg, C. A. ... 37
Sangrey, D. A. ... 153
Santos, E. S. ... 50
Sanzolone, R. F. ... 16, 17
Sapik, D. B. ... 146
Sargent, K. A. ... 76, 81
Sarna-Wojcicki, A. M. ... 206
Sass, J. H. ... 213
Sato, Motoaki ... 196
Schaefer, D. H. ... 144
Schafer, J. P. ... 63
Schemel, L. E. ... 172
Schiller, J. J. ... 125, 126
Schlee, J. S. ... 159
Schlocker, Julias ... 93
Schmidt, R. G. ... 19, 183
Schmoker, J. W. ... 38, 41
Schmoll, H. R. ... 111
Schneider, G. B. ... 20
Schnepfe, M. M. ... 29, 244
Scholl, D. W. ... 161
Schram, C. W. ... 30
Schroeder, R. A. ... 123
Schultz, D. M. ... 159
Schweinfurth, S. P. ... 69
Scott, E. W. ... 40
Scott, J. C. ... 126
Scott, J. H. ... 185, 186
Scott, Jonathon ... 138
Seeland, D. A. ... 59, 78
Selverstone, J. E. ... 11
Senftle, F. E. ... 30, 57
Shaw, H. R. ... 194
Shawe, D. R. ... 10
Shedlock, R. J. ... 118
Sheldon, R. P. ... 21
Sheridan, D. M. ... 10
Sherrill, M. G. ... 118
Shiao, L. Y. ... 217
Shideler, G. L. ... 155
Shinn, E. A. ... 37, 41
Shown, L. M. ... 217
Shride, A. F. ... 62
Shultz, D. J. ... 237
Shurr, G. W. ... 77
Siegel, D. I. ... 121
Sigafoos, R. S. ... 234
Silber, C. C. ... 29
Silberling, N. J. ... 103, 110
Silberman, M. L. ... 110, 111

Silver, L. T. 101
Simon, J. A. 24
Sims, J. D. 221
Sims, P. K. 75
Sinclair, W. C. 128, 130
Singer, D. A. 21
Skinner, J. V. 219
Skipp, A. L. 34
Skipp, B. A. L. 232
Slack, J. F. 5, 7, 66
Slack, K. V. 240
Slade, M. E. 20
Small, T. A. 139
Smith, B. D. 18, 44, 187
Smith, D. B. 55
Smith, G. I. 222
Smith, J. G. 199
Smith, M. A. 159
Smith, P. E. 148
Smithe, C. C. 230
Smyth, J. R. 245
Snavely, D. S. 123
Snavely, P. D., Jr. 92, 161
Snider, J. L. 135
Snyder, G. L. 81
Sohl, N. F. 229
Sonnevil, R. A. 111
Sorensen, M. L. 9
Sorenson, S. K. 143
Sorg, D. H. 96
Sparkes, A. K. 132
Speed, R. C. 91
Spiker, E. C. 172, 193
Spinazola, J. M. 135
Spirakis, C. S. 56, 57
St. Aubin, D. R. 109, 110
Staatz, M. H. 42
Stacey, J. S. 204, 206
Stanley, W. D. 216
Stannard, D. I. 226
Stark, J. R. 119
Stedfast, D. A. 123
Steinheimer, T. R. 246
Stephens, D. W. 237, 245
Stern, T. W. 71, 199, 207
Steven, T. A. 11, 81
Stevens, H. H., Jr. 219
Stevens, Ken 226
Stewart, J. H. 89
Stone, B. D. 63
Stricker, G. D. 28
Stuckless, J. S. 53, 54
Stueber, A. M. 133
Stump, D. E., Jr. 124
Sunada, D. K. 51
Suneson, N. H. 50, 90, 91
Sutley, S. J. 13, 17
Swanson, D. A. 196
Swanson, J. A. 19
Swift, C. H. 146
Sylvester, M. A. 143
Szabo, B. J. 205, 223, 231

T

Tabor, R. W. 94
Tai, D. Y. 237
Tanner, A. B. 30
Tasker, G. D. 228
Tatsumoto, Mitsunobu 204, 205
Taubeneck, W. H. 196
Teleki, P. G. 152, 243
Terry, J. E. 237
Thaden, R. E. 48
Thomas, C. A. 144
Thomas, J. G. 225
Thompson, C. L. 30
Thompson, J. K. 174
Thompson, W. B. 63
Thor, D. R. 92, 157, 158, 166
Thormahlen, D. J. 97
Thorman, C. H. 90
Thorpe, A. N. 30
Tietjen, G. L. 203
Tilley, L. J. 240
Tilling, R. I. 194
Tinsley, J. C., III 223
Todd, V. R. 101
Torak, L. J. 135
Toulmin, Priestley, III 200
Towle, J. N. 208
Trabant, D. C. 219
Tracy, J. L. 135
Trapp, Henry 128
Trent, V. A. 25
Trescott, P. C. 131, 135, 225
Trexler, J. H., Jr. 106
Troutman, B. M. 227
Truesdell, A. H. 211, 212
Trumbull, J. V. A. 164
Tschudy, R. H. 47
Turner, J. F. 127
Tweto, O. L. 114
Twichell, D. C., Jr. 154

U

Ucok, H. 184
Ulrich, G. E. 82
Underwood, M. B. 159, 162
Updegraff, D. M. 52
Urban, T. C. 213, 214

V

Vaccaro, J. J. 225
Vallier, T. L. 158, 159, 161, 162
Van Loenen, R. E. 199
Van Loenen, S. D. 47
Vance, J. A. 94
Varnes, K. L. 40
Vecchioli, John 127
Veenhuis, J. E. 148
Velnich, A. J. 122
Viets, J. G. 17
Vine, J. D. 22
Vogel, T. M. 171
von Huene, R. E. 161
Vowinkel, E. F. 150

W

Waddell, K. M. 140
Wagner, H. C. 92, 161
Wahrhaftig, Clyde 98, 109
Walker, G. W. 43
Wallace, A. R. 43, 59
Wallace, C. A. 5, 11, 85, 86
Walters, R. A. 171
Wandless, G. A. 244
Ward, A. W., Jr. 220
Wardlaw, B. R. 83
Warlow, R. C. 26
Warren, C. R. 64, 65
Wasson, B. E. 132
Watterson, J. R. 13
Watts, K. C. 15
Weaver, C. S. 214
Webb, J. C. 36
Weber, F. R. 106, 107
Webster, D. A. 133
Weeks, E. P. 240
Wegener, S. S. 214
Welder, G. E. 227, 240
Wells, J. D. 85
Welsch, E. P. 17
Wendlandt, R. F. 191
Wenner, David 53
Wenrich-Verbeek, K. J. 56, 58
Werre, R. W., Jr. 190
Wershaw, R. L. 246
Whetten, J. T. 94
White, A. F. 202
White, D. E. 209
White, I. C. 232
Whitebread, D. H. 9
Whiteman, C. D., Jr. 135
Whitlow, J. W. 4, 11
Whitney, J. W. 223
Wier, K. E. 73
Wiggins, L. B. 66, 191
Wilke, K. R. 136
Williams, B. B. 6
Williams, D. L. 92
Williams, E. J. 76
Williams, P. L. 81
Williams, R. P. 144
Wilshire, H. G. 220
Wilson, D. M. 1, 2
Wilson, F. A. 11
Wilson, F. H. 110, 111
Wilson, K. V. 132
Wilson, L. R. 182
Wilson, R. P. 142
Wilson, W. E. 127
Wilt, J. C. 9
Windolph, J. F. 25
Windolph, J. F., Jr. 26
Winsor, H. C. 83
Winter, T. C. 121, 239
Wintsch, R. P. 61
Witkind, I. J. 77, 86
Wolansky, R. M. 129, 179
Wolfe, E. W. 82
Wolfe, J. A. 96
Wolff, R. G. 227
Wong, F. L. 162
Wood, G. H., Jr. 24, 25
Wood, J. D. 181
Woodward, D. G. 122
Woodward, M. J. 206
Wright, H. E., Jr. 221
Wright, N. A. 20
Wright, T. L. 194
Wynn, J. C. 5, 18, 186

Y

Yanosky, T. M. 233
Yeend, W. E. 106, 109
Yount, J. C. 93
Yount, M. E. 110

Z

Zablocki, C. J. 209
Zack, Allen 132
Zartman, R. E. 81
Zellweger, G. W. 202
Zen, E-an 76, 77, 79, 80
Zenone, Chester 125
Zielinski, R. A. 55
Zietz, Isidore 188
Zimmerman, E. A. 141
Zimmerman, R. A. 94
Zoback, M. L. 213
Zohdy, A. A. R. 186, 187
Zubovic, Peter 29
Zuehls, E. E. 126
Zuffa, G. G. 97
Zurawske, Ann 132
Zwally, H. J. 243

☆ U.S. GOVERNMENT PRINTING OFFICE: 1981 — 341-614/193